MCIC Report/June 1986

MCIC-86-50

Corrosion of Metals in Marine Environments

A State-of-the-Art Report

Metals and Ceramics Information Center

A Department of Defense Information Analysis Center
Battelle Columbus Division
505 King Avenue
Columbus, Ohio 43201

SECURITY CLASSIFICATION OF THIS PAGE

REPORT DOCUMENTATION PAGE

1a. REPORT SECURITY CLASSIFICATION Unclassified	1b. RESTRICTIVE MARKINGS
2a. SECURITY CLASSIFICATION AUTHORITY	3. DISTRIBUTION / AVAILABILITY OF REPORT Approved for public release; distribution unlimited
2b. DECLASSIFICATION / DOWNGRADING SCHEDULE	
4. PERFORMING ORGANIZATION REPORT NUMBER(S) MCIC-86-50	5. MONITORING ORGANIZATION REPORT NUMBER(S)
6a. NAME OF PERFORMING ORGANIZATION Metals & Ceramics Information Center Battelle Columbus Division	6b. OFFICE SYMBOL (If applicable)
6c. ADDRESS (City, State, and ZIP Code) 505 King Avenue Columbus, OH 43201-2693	7a. NAME OF MONITORING ORGANIZATION Office of Deputy Under Secretary of Defense Research and Advanced Technology
	7b. ADDRESS (City, State, and ZIP Code) Room 3D0189 Washington, DC 20301
8a. NAME OF FUNDING / SPONSORING ORGANIZATION Defense Logistics Agency	8b. OFFICE SYMBOL (If applicable) DTIC-DF
	9. PROCUREMENT INSTRUMENT IDENTIFICATION NUMBER DLA900-83-C-1744
8c. ADDRESS (City, State, and ZIP Code) Defense Technical Information Center Cameron Station Alexandria, VA 22304-6145	10. SOURCE OF FUNDING NUMBERS PROGRAM ELEMENT NO. / PROJECT NO. / TASK NO. / WORK UNIT ACCESSION NO.

11. TITLE (Include Security Classification)

(U) CORROSION OF METALS IN MARINE ENVIRONMENTS -- A State-of-the-Art Report

12. PERSONAL AUTHOR(S)
J. A. Beavers, G. H. Koch, W. E. Berry

13a. TYPE OF REPORT	13b. TIME COVERED	14. DATE OF REPORT (Year, Month, Day)	15. PAGE COUNT
State-of-the-Art	FROM _____ TO _____	July, 1986	745

16. SUPPLEMENTARY NOTATION
3.5% NaCl

17. COSATI CODES		
FIELD	GROUP	SUB-GROUP

18. SUBJECT TERMS (Continue on reverse if necessary and identify by block number)
*Sea Water Corrosion, *Stress Corrosion, *Sea Testing, *State of the Art, *Aluminum Alloys, *Titanium Alloys, *Nickel Alloys, *Copper Alloys, *Stainless Steel, *Carbon

19. ABSTRACT (Continue on reverse if necessary and identify by block number)

This report is based on a review of selected literature items, discussions with marine technologists, and information derived from Battelle's own research programs in the marine corrosion field. The majority of the data were obtained from actual ocean exposures since they provide the most reliable information, but data from exposures in aqueous 3.5 percent NaCl and in simulated seawater are included where the former data are limited. Similarly, the focus of this report is on actual exposure data, but results of electrochemical studies are presented selectively where they aid in the understanding or interpretation of the phenomena.

This report is organized according to alloy type (i.e., carbon and low-alloy steels, stainless steels, etc.), exposure phase (atmosphere, splash and tide, submerged, and mud), failure mode, and parametric effects. Because of the extensive nature of the subject, information on coatings for marine applications, materials for desalination, and corrosion fatigue have been excluded.

20. DISTRIBUTION / AVAILABILITY OF ABSTRACT	21. ABSTRACT SECURITY CLASSIFICATION
☐ UNCLASSIFIED/UNLIMITED ☒ SAME AS RPT. ☐ DTIC USERS	Unclassified

22a. NAME OF RESPONSIBLE INDIVIDUAL	22b. TELEPHONE (Include Area Code)	22c. OFFICE SYMBOL
Jerome Persh	(202) 695-9602	ODUSDR&AT

DD FORM 1473, 84 MAR — 83 APR edition may be used until exhausted. All other editions are obsolete.

SECURITY CLASSIFICATION OF THIS PAGE

18. Steels, Galvanic Corrosion, Cavitation Corrosion, Atmospheric Corrosion, Pitting, Erosion, Salt Spray Tests, Liquid Immersion Tests, Cracking(Fracturing), Sea Water, Splash, Tides, Cathodic Protection, Temperature, Water Flow, Salinity, Aluminum, Titanium, Cobalt, Copper, Magnesium, Superalloys, Marine Atmosphere, Beryllium, Ocean Environments, Low Alloy Steels, Tantalum, Zirconium, Niobium, Molybdenum, Tungsten, Vanadium, Hafnium, Chromium, Platinum, Palladium, Gold, Silver, Lead(Metal), Zinc, Cadmium, Tin.

AUTHOR WORKSHEET

1. Report Number: MCIC-86-50
2. Title: CORROSION OF METALS IN MARINE ENVIRONMENTS
3. Price: $300 each paper copy (looseleaf)
4. 800 pages, 727 references, 412 tables, 342 figures
5. Authors: J. Beavers, G. Koch, and W. Berry

   All are nationally recognized experts on corrosion of metals.

   See also attached sheets
6. Performing Organization:

   Battelle Columbus Division
   505 King Avenue
   Columbus, Ohio 43201
7. Abstract:

   This report promises to be a classic in the field of marine corrosion. The focus of this report is on actual exposure data in seawater, wherever possible, rather than simulated or theoretical experiments.

   An introductory chapter describes the types of corrosion, the ocean environments (atmosphere, splash zone, tide zone, immersion and mud), and the factors affecting corrosivity of seawater (oxygen, biological, temperature, velocity, salinity and pH).

   The latter 13 chapters deal with individual alloy systems. Each chapter has separate sections dealing with the various aspects of corrosion described in the introduction (atmosphere, splash, tide, immersion and mud). The emphasis is on metals most commonly used in marine applications such as copper, aluminum, carbon and low-alloy steels, stainless steels, titanium and superalloys (nickel- and cobalt-base). Overall, 25 alloy systems are covered. Each chapter has a list of references.
8. The Report provides:

   - Data that previously were available from a variety of sources
   - Comprehensive coverage of data from many sources
   - Easy-to-use compilations arranged by alloy systems
   - Primarily sea water corrosion data. Simulated seawater data is used to fill what otherwise would be a gap in the data
   - An easily updated presentation of data in loose-leaf format.
9. Who would buy this report?

   Metallurgists, designers of equipment or devices to be used in marine environments.
10. What type of industry would have needed for this information?

    Shipbuilders, designers, marine architects, designers of offshore drilling rigs, designers and manufacturers of military equipment.

AUTHOR WORKSHEET (Continued)

11. What associations/societies/etc. would have mailing lists - who is contact for same etc.?

American Society for Metals (ASM), American Society for Testing and Materials (ASTM), SAMPE, American Institute of Mining and Metallurgical Engineers (AIME), National Assocation of Corrosion Engineers (NACE).

12. Keywords:

Corrosion, seawater, aluminum and aluminum alloys, titanium and titanium alloys, stainless steels, nickel-base alloys, carbon and low-alloy steels, magnesium alloys, copper and copper-base alloys, cobalt and cobalt-base alloys, beryllium, refractory metals, tantalum, zirconium, niobium, molybdenum, tungsten, vanadium, hafnium and chromium, noble metals, platinum, palladium, gold and silver, lead, zinc, cadmium, and tin, cathodic protection.

13. NTIS Scope-Note Fields:

71g, j, n

JOHN A. BEAVERS

Associate Manager
Corrosion and Electrochemical Technology Section

Education

B.S., Metallurgical Engineering, University of Illinois
Ph.D., Metallurgical Engineering, University of Illinois

Qualifications

Dr. Beavers has directed or contributed to numerous research programs at Battelle on corrosion performance of structural materials. These programs have included failure analyses, literature surveys, and experimental and field evaluations of materials and have addressed most forms of aqueous corrosion. Dr. Beavers has utilized a variety of experimental techniques for evaluation of materials performance for these forms of corrosion. These include electrochemical techniques such as potentiodynamic polarization, polarization resistance, electrochemical impedance, and galvanic current measurements; surface analysis techniques such as Auger, EDAX, microprobe, XRD; TEM and SEM surface characterization techniques; metallographic techniques; fracture mechanics; dynamic mechanical loading techniques such as slow strain rate and low cycle fatigue. Recent relevant projects are described below.

Relevant Experience At Battelle

Corrosion of Metals in Marine Environments. Coauthor of a book on marine corrosion. Preparation of the book, which is sponsored by the DOD Information Analysis Center is currently being carried out. The program involves updating and rewriting the original publication which was issued in 1973. The book is organized into sections according to alloy type, environment (including atmospheric corrosion) and failure mode.

Failure Analyses. Dr. Beavers has conducted or contributed to numerous failure analyses of metallurgical components for utilities, other industrial sponsors and government sponsors. Typical examples of recently performed failure analyses are given below.

- Stress-corrosion cracking failure of admiralty brass condenser tubes in a PWR
- Corrosion failure of welds in the service water piping system of a PWR

- Pitting and erosion corrosion failure of a fan cooler for the containment vessel of a PWR
- Pitting and erosion/corrosion failure of copper-10 nickel heat exchanger tube in brackish river water
- Fatigue failure of Type 316 stainless steel safe-end in a PWR primary circuit piping
- Pitting and SCC failures of Type 304 stainless steel in a RAD waste concentrator in a PWR
- Stress-corrosion cracking failure of turbine disc in a PWR.

Construction Materials for Wet Scrubbers. EPRI RP982-14 (CS-1736). Contributed to a program in which the utility experience with materials of construction in full-scale lime/limestone FGD systems was documented. In this program, utility experience with construction materials was collected by site visits, and telephone and letter contacts. The data obtained were then critically evaluated with respect to failure modes, mechanisms, and locations. This work currently is being updated under EPRI 1871-3.

Service Water Piping. Utility. A laboratory program was carried out to aid in identification of the root cause of corrosion failures in a service water piping system and to evaluate remedial measures. Electrochemical and long term exposure tests were carried out on the pipe steel to evaluate the relative contribution of galvanic coupling, crevices, welds, metallurgy etc. on the accelerated attack of the welds which had occurred in service.

Test Method for Defining Susceptibility of Line Pipe Steels to Stress-Corrosion Cracking. Principal Investigator on a program in which a standardized test method for defining the SCC susceptibility of line pipe steels was developed. Previous studies had identified the optimum environmental conditions and specimen geometry for performing such an evaluation and the aim of the work is to identify the optimum loading conditions and test time.

Investigation of Line Pipe Steel That Are Highly Resistant to SCC. Principal Investigator on an on-going A.G.A. program in which the relationship between metallurgical characteristics of line pipe steel and SCC susceptibility is being investigated. The goal of this work is to understand the influence of processing parameters on those characteristics that control SCC susceptibility so that steels can be made consistently resistant to SCC.

Corrosion Resistant Alloys for Flue Gas Desulfurization Systems. EPRI RP1871-1. Program Manager for an EPRI program in which a survey of the state-of-the-art of current alloys and linings was examined and laboratory studies of these materials were initiated. The state-of-the-art was surveyed through a detailed examination of the published literature including EPRI reports such as 1736, and through telephone and letter contacts. It was concluded from the survey that the most severe corrosion and degradation problems are encountered in outlet ducts and stacks, and, accordingly, laboratory studies were performed on candidate alloys and linings under simulated outlet duct environments.

SCC of Pipeline Steels. Principal investigator on program to study the effects of loading parameters on the SCC of pipeline steels. In this program for the American Gas Association, the effect of R ratio and frequency on SCC is being investigated under low frequency cyclic loading.

Corrosion Related Failures in Power Plant Condensers. EPRI TPS 70-730 NP 4168. Project Manager on an EPRI program whose objective was to assess recent experience with corrosion failures in surface condensers. The information was obtained through a survey of the literature and telephone and letter contacts.

Long-Term Performance of Materials Used for High Level Waste Packaging. Principal Investigator of the overpack corrosion task on the ongoing NRC program on waste container performance in simulate terminal disposal environments. In this program, potential failure modes and aging mechanisms for the primary candidate materials are being performed to evaluate the performance of the overpack materials. These data are then being used to develop and refine mathematical models that will be used to predict system performance. Currently, SCC and pitting of low alloy steels are being studied.

Nuclear Fuel Reprocessing. Project Manager of a program to select and evaluate materials for use in LMFBR nuclear fuel reprocessing equipment. In this four year program for DOE, candidate materials were selected and potential failure modes were identified for each of the components in the system. The candidate materials, which included stainless steels, nickel-base alloys, zirconium alloys and C. P. titanium were then evaluated in the laboratory under simulated operating conditions.

Binary Weapons. Project Manager on a program to select and evaluate candidate canister materials for DF. In this ongoing program for the Army Armament Research and Development Command, candidate canister materials are being evaluated for potential failure modes by means of exposure tests, slow strain rate tests, as well as electrochemical techniques. Materials being studied include stainless steels, nickel-base alloys, and aluminum alloys.

JOHN A. BEAVERS (Continued)

Professional Recognition and Affiliations

Dr. Beavers is a member of the American Society for Metals (ASM) and the National Association of Corrosion Engineers (NACE). Currently, he is chairman of the NACE Unit Committee T-3E "SCC and Corrosion Fatigue".

Selected Publications

Dr. Beavers has authored or co-authored more than 20 technical publications.

Beavers, J. A., and Koch, G. H., "Review of Corrosion Related Failures in Flue Gas Desulfurization Systems", CORROSION/82, Houston, 1982, Paper 202.

Beavers, J. A., and Koch, G. H., "Review of Corrosion Related Failures in Flue Gas Desulfurization Systems", Materials Performance, Vol. 21, October, 1982, p. 13.

Beavers, J. A., Rosenberg, I. C., and Pugh, E. N., "The Role of Intergranular Attack in Stress-Corrosion Phenomena", Tri-Services Conference on Corrosion, Houston, Texas, p. 57 (1972).

Gabel, H., Beavers, J. A., Woodhouse, J. B., and Pugh, E. N., "The Structure and Composition of Thick Films on Alpha Phase Copper Alloys", Corrosion, 32, 253 (1976).

Nelson, J. L., and Beavers, J. A., "The Application of a Photogammetric Technique to the Determination of the Orientation of Stress-Corrosion Fractures", Metallurgical Transactions, 10, 658 (1979).

Beavers, J. A., and Pugh, E. N., "The Propagation of Transgranular Stress-Corrosion Cracks in Admiralty Metal", Metallurgical Transaction, 11, 809 (1980).

Beavers, J. A., Berry, W. E., and Boyd, W. K., "Selection and Evaluation of Materials for Advanced Fuel Reprocessing Equipment", ORNL/AFRP-78/1 (August, 1978).

Beavers, J. A., Boyd, W. K., and Berry, W. E., "Materials Performance in Nitric Acid Solutions Containing Fluoride", ORNL/CFRP-78/7 (January, 1979).

Beavers, J. A., Boyd, W. K., Griess, J. C., and Berry, W. E., "Selection of Materials for the Iodox Process", ORNL/Sub-79/77327/1 (December, 1979).

Beavers, J. A., Boyd, W. K., Griess, J. C., and Berry, W. E., "Materials Compatibility in Hydriodic Acid Solutions", ORNL/TM-7330 (July, 1980).

JOHN A. BEAVERS (Continued)

Beavers, J. A., Griess, J. C., and Boyd, W. K., "Stress-Corrosion Cracking of Zirconium in Nitric Acid", Corrosion/80, Paper No. 238, and Corrosion, 37 (5), 292 (May, 1981).

Beavers, J. A., Stiegelmeyer, W. N., and Berry, W. E., "Failure Analyses of Corrosion in RAD Waste Systems", Corrosion/80, Paper No. 261.

Beavers, J. A., and Diegle, R. B., "The Effect of Degradation of Glycols on Corrosion of Metals Used in Non-Concentrating Solar Collectors", Corrosion/81, Paper No. 207.

Beavers, J. A., Agrawal, A. K., and Berry, W. E., "Corrosion Related Failures in Power Plant Condensers", Corrosion/81, Paper No. 17, and Materials Performance, 20 (10), 19 (October, 1981).

Diegle, R. B., Beavers, J. A., and Clifford, J. E., "Corrosion Problems with Aqueous Coolants", DOE/CS/10510-T11 (1980), NTIS, Energy Res. Abstr. (1980) 5 (21), Abstr. No. 33516.

Griess, J. C., and Beavers, J. A., "Materials Compatibility in Selected Fuel Element Reprocessing Environments", Trans. American Nuclear Society, 39, 146, Winter Meeting, San Francisco, California (November 29 - December 3, 1981).

Beavers, J. A., Berry, W. E., and Griess, J. C., "Materials Performance in Off-Gas Systems Containing Iodine", ORNL/Sub-7327/11 (November, 1981).

Beavers, J. A., Berry, W. E., Griess, J. C., and White, R. R., "Corrosion Studies in Fuel Element Reprocessing Environments Containing Nitric Acid", ORNL/Sub-7237/13 (April, 1982).

Koch, G. H., and Beavers, J. A., "Materials Testing in Simulated Flue Gas Desulfurization Duct Environments", EPRI Report CS-2537, August, 1982.

Koch, G. H., Beavers, J. A., Thompson, N. G., and Berry, W. E., "Literature Review of FGD Construction Materials", EPRI Report CS-2533, August, 1982.

Koch, G. H., Beavers, J. A., and Syrett, B. C., "Experimental Evaluation of Alloys and Linings in Simulated Duct Environments for a Lime/Limestone Scrubber", CORROSION/82, Houston, 1982, Paper 197.

Dene, C. E., Syrett, B. C., Koch, G. H., and Beavers, J. A., "Alloys and Coatings for SO_2 Scrubbers", 1982 American Power Conference, Chicago, Illinois, April, 1982.

Koch, G. H., and Beavers, J. A., "Corrosion/Erosion Laboratory on Field Testing of Materials for Construction in Flue Gas Desulfurization Systems", 54th Annual Conference on Materials for Coal Conversion and Utilization, Gaithersburg, Maryland, October, 1981.

JOHN A. BEAVERS (Continued)

Koch, G. H., and Beavers, J. A., "Laboratory and Field Evaluation of Materials for Flue Gas Desulfurization Systems", Seventh Symposium on Flue Gas Desulfurization, Hollywood, Florida, June, 1982.

Koch, G. H., and Beavers, J. A., "Performance of Candidate Materials for Flue Gas Desulfurization Systems", Proceedings of the Seventh Annual Conference on Materials for Coal Conversion and Utilization, Gaithersburg, Maryland, October, 1982.

Koch, G. H., Whitman, L., and Beavers, J. A., "The Effect of Synthetic Scrubber Solution Chemistry on the Corrosion Behavior of Type 316L Stainless Steel and Titanium Grade 2", Proceedings of the Electrochemical Society Symposium on Corrosion of Fossil Fuel Systems, Detroit, Michigan, October, 1982. Submitted for publication in J. of Electrochem. Soc.

Koch, G. H., and Beavers, J. A., "The Influence of Scrubber Chemistry on the Corrosion of Alloys in Lime/Limestone Flue Gas Desulfurization Systems", Corrosion/83, Anaheim, California, Paper No. 186.

Beavers, J. A., Agrawal, A. K., Berry, W. E., "Corrosion Related Failures in Feedwater Heaters", Corrosion/84, New Orleans, Louisiana, Paper No. 169

Beavers, J. A., Berry, W. E., and Griess, J. C., "Materials Performance in Moist Iodine Vapors at Low Temperatures", Proceedings of 9th International Congress on Metallic Corrosion, Toronto, Canada, June 3 - 7, 1984.

Rosenberg, H. S., Koch, G. H., Kistler, C. W., Jr., and J. A. Beavers, "Performance of Duct and Stack Materials in Wet Scrubbers", Ninth Symposium on Flue Gas Desulfurization, Cincinnati, Ohio, June 4-7, 1985, No. 5B.

GERHARDUS H. KOCH

Associate Manager
Corrosion & Electrochemical Technology Section

Education

B.S., M.S., Aeronautical Engineering, University of Technology, Delft, The Netherlands
Ph.D., Metallurgical Engineering, University of Illinois

Qualifications

Dr. Koch has extensive management experience in various projects concerning materials degradation. He is currently serving as manager or principal investigator for four EPRI projects involving the corrosion chemistry of SO_2 scrubbers, materials failure causes in FGD systems, corrosion/erosion laboratory and field testing of candidate materials, and cyclic reheat studies in SO_2 scrubbers. Most of this work involves the coordination of field and laboratory studies that simulate the actual environments to understand the mechanism of failure and allows selection of materials most effective for application. Emphasis in these studies are placed on nickel-base and titanium alloys. Dr. Koch also manages a program for the Air Force to monitor corrosion at wing-to-pylon fittings and the fuselage of C-141 cargo planes using insitu monitors. Prior to joining Battelle, he was involved in the development of multiple-layer adhesive bonded aluminum and titanium structures and aluminum-fiber reinforced plastic laminates for improved strength and crack propagation properties. The studies of surface treatments and hybrid structures included extensive atmospheric testing using static testing sites and aircraft. Experimental techniques utilized during this work included scanning and transmission electron microscopy and surface analysis techniques such as Auger Electron Spectroscopy, and Secondary Ion Mass Spectroscopy (SIMS). Dr. Koch is coauthoring a book on the Corrosion of Metals in Marine Environments. Dr. Koch's Ph.D. theses topic was on stress-corrosion cracking and gaseous hydrogen embrittlement of alpha titanium alloys.

Relevant Experience at Battelle

Corrosion Metals in Marine Environments. Coauthor of a book on the effect of marine environments (immersion, splash and tide, and atmospheric) on the corrosion and stress-corrosion cracking of structural materials. These materials include aluminum alloys, titanium alloys, carbon steels, stainless steels, nickel-base alloys, and copper alloys.

Corrosion Resistant Alloys for Flue Gas Desulfurization Systems. EPRI RP1871-1. Contributed to EPRI program in which a survey of laboratory studies of the materials were initiated. The state-of-the-art was surveyed through a detailed examination of the published literature including EPRI reports such as

CS-1736 and through telephone and letter contacts. It was concluded from the survey that the most severe corrosion and degradation problems are encountered in stacks and outlet ducts, and accordingly, laboratory studies were performed on candidate alloys and linings under simulated duct environments.

Materials Failure Causes in FGD Systems. EPRI RP2248-3. Principal Investigator in a program to obtain information of component materials used in wet FGD systems. This is accomplished by site visits for field evaluations of the failures, laboratory studies of samples collected in the field and analysis of the data to establish the causes of failure.

Corrosion Chemistry of SO_2 Scrubbers. EPRI RP1871-6. Project Manager of an ongoing EPRI program to identify trace elements in FGD components and to investigate the effect of trace elements on the corrosion behavior of selected alloys. The single and interactive effects of trace elements in synthetic scrubber solution on the corrosion behavior is studied by potentiodynamic polarization and the results of these studies are being evaluated using various statistical approaches.

Professional Recognition and Affiliations

Dr. Koch is a member of the National Association of Corrosion Engineers. He is chairman of NACE's Technical Practices Committe T5F on Corrosion Problems Associated with Pollution Control.

Selected Publications

Dr. Koch has authored and coauthored a number of technical publications in the field of aqueous corrosion of alloys and environmental degradation of non-metallic materials.

Beavers, J. A., Koch, G. H., "Review of Corrosion Related Failures in Flue Gas Desulfurization Systems", Materials Performance, Vol. 21, October, 1982, p. 13.

Koch, G. H., Whitman, L., and Beavers, J. A., "The Effect of Synthetic Scrubber Solution Chemistry on the Corrosion Behavior of Type 316 Stainless Steel and Titanium Grade 2", Proceedings of the Symposium on Corrosion in Fossil Fuel Systems, The Electrochemical Society, Inc., V. 83-85, 1983, p. 328-338.

Koch, G. H., and Beavers, J. A., "The Influence of Scrubber Chemistry on the Corrosion of Alloys in Lime-Limestone Flue Gas Desulfurization Systems", CORROSION/83, Anaheim, California, Paper No. 186.

Koch, G. H., Thompson, N. G., and Means, J., "Trace Elements in Flue Gas Desulfurization Environments and Their Effects on the Corrosion of Alloys", CORROSION/84, New Orleans, La, April, 1984, Paper No. 297.

GERHARDUS H. KOCH (Continued)

Thompson, N. G., Koch, G. H., Spangler, J. M., and Syrett, B. C., "Determination of Solution Species that Significantly Affect Corrosion of Alloys in FGD Systems", Proceedings of 1984 Air Pollution Seminar on Solving Corrosion Problems in Air Pollution Control Equipment, Orlando, Florida, December, 1984.

Koch, G. H., and Thompson, N. G., "Localized Attack of Nickel-Containing Alloys in SO_2 Scrubber Environments", Proceedings of International Conference on Corrosion of Nickel-Base Alloys, ASM, Cincinnati, Ohio, October, 1984.

Thompson, N. G., Koch, G. H., and Syrett, B. C., "Effects of Trace Elements on the Polarization Behavior of Alloys in FGD Environments", CORROSION/85, Boston, Massachusetts, March, 1985.

Koch, G. H. and Syrett, B. C., "Progress in EPRI Research on Materials for Flue Gas Desulfurization Systems", Proc. of I. Corr. Conference on Dewpoint Corrosion, London, England, May 1985, Institution of Corrosion Science and Technology, England (1985).

Syrett, B.C., Koch, G.H., and Mansfeld, F., "Review of Corrosion in SO_2 Scrubbers", Proc. of the 4th Asian-Pacific Corrosion Control Conference, Tokyo, Japan, May, 1985.

Schutz, R.W., Graiman, J. S., Koch, G.H., and Smith, R.E., "Performance of Titanium in Aggressive Zones of a Closed-Loop FGD Scrubber", CORROSION/86, NACE, Houston, Texas.

Koch, G. H., Chakrapani, D. G., and Pugh, E. N., "On the Mechanism of SCC in a Mg-Al Alloy", Proceedings of the 6th International Corrosion Congress, Sydney, Australia (1975).

Koch, G. H., Bursle, A. J., and Pugh, E. N., "Gaseous Hydrogen Embrittlement on Ti-8Al-1V-1Mo", Proceedings of the 2nd International Congress on Hydrogen in Metals, Paris, France (1977).

Koch, G. H., Bursle, A. J., and Pugh, E. N., "Comparison and Interpretation of Fracture Surfaces Produced in Ti-8Al-1V-1Mo by Stress-Corrosion Cracking and Slow-Strain-Rate Hydrogen Embrittlement", Metallurgical Transactions, Vol. 9A, p. 129 (1978).

Koch, G. H., "Hydrogen Induced Fracture of a High Strength Aluminum Alloy", Corrosion Journal, Vol. 35, No. 2, p. 73 (1979).

Koch, G. H., "The Fracture Behavior of Multiple Layer Adhesive Bonded Aluminum Structures", Proceedings of the 24th National SAMPE Symposium, San Francisco, SAMPE Quarterly, Vol. 11, No. 1, p. 7 (1979).

GERHARDUS H. KOCH (Continued)

Koch, G. H., "Crack Propagation in Multiple Layer Adhesive Bonded Material", Proceedings of the 10th ICAF Symposium, Brussels (May 14-19, 1979).

Koch, G. H., and Kolijn, D. T., "The Heat Treatment of the Commercial Aluminum Alloy 7075", Journal of Heat Treating, Vol. 1, No. 2, p. 3 (December, 1979).

Koch, G. H., "The Environmental Durability of 2024-T3-Kevlar Fiber and 2024-T3-Carbon Fiber Laminates", Proceedings of the 26th National SAMPE Symposium, Los Angeles, California (April 20-30, 1981).

Koch, G. H., Bursle, A. J., Liu, R., and Pugh, E. N., "Comparison of Gaseous Hydrogen Embrittlement, Slow-Strain-Rate Hydrogen Embrittlement and Stress-Corrosion Cracking in Ti-8Al-1V-1Mo", Metallurgical Transactions 19, Vol. 12A, October, 1981, p. 1033.

WARREN E. BERRY

Research Leader
Corrosion and Electrochemical Technology Section

Education

B.S., Chemistry, Ohio University
Graduate Work at The Ohio State University

Qualifications

Since joining Battelle Mr. Berry has been actively engaged in corrosion research on a broad spectrum of problems ranging from automotive corrosion, liquid-metal corrosion, underground corrosion, aerospace corrosion, corrosion by food products, corrosion by natural waters, and corrosion in nuclear and conventional power plants. For the past 33 years he has directed research programs on the stress-corrosion of structural steels, high-strength steels, stainless steels, nickel-base alloys, and aluminum alloys in a wide range of environments ranging from soils and natural waters to treated primary and secondary coolants of nuclear reactors. He has conducted a number of failure analyses resulting from stress-corrosion in the transportation, chemical processing, aerospace, and nuclear industries. He currently is directing research on stress-corrosion cracking in high-temperature water in support of nuclear reactor applications.

Relevant Experience

Examples of research programs conducted by Mr. Berry that are relevant to the problem at hand include.

Corrosion by High-Temperature High-Pressure Aqueous Fluids in support of light water nuclear reactor materials development. The study encompassed coupon and electrochemical corrosion studies, galvanic couple tests, and constant load, slow strain rate, and cyclic load stress-corrosion tests in primary and secondary coolants and in highly corrosive alkaline and acid-chloride solutions that might develop in dry-out areas in steam generators. (G5100-5000, G6760, G5901-7200. G5901-7700, G5901-7300, G5000-3300, G5590, G5628, G6737, G6971, G6974 G-7030, G9571, G5200-6600, G5040-3500, N3318, K3568)

Corrosion in High-Temperature High-Pressure Brines saturated with H_2S and CO_2 as part of Battelle's Group Program on defining the limits for corrosion of materials in deep sour gas wells. General corrosion and stress-corrosion cracking studies are being carried out in 20 w/o brine solutions at 200 C and 2000 psi system pressure. Specially designed reference electrodes are being used to measure the corrosion potentials in these systems (N0920-0902).

Corrosion of structural materials by F_2, HF, Cl_2, or HCℓ in high-temperature developmental processes for decladding nuclear fuel elements. Metal wastage rates, metallurgical changes, and structural integrity were determined for nickel, nickel-base alloys, and highly alloyed stainless steels at temperatures to 500 C. The studies solved a grain-boundary-environment interaction that led to a loss in structural strength that was plaguing large scale pilot plants (G5119).

Evaluation of Condenser Corrosion Problems in several marine based nuclear power plants. The studies identified the seawater induced corrosion problems in the inlet screening, water tunnels, water boxes, tube sheets, and tubes, determined why some components corroded more readily than others, and recommended procedures for reducing corrosion which were later applied and found to be effective (NO624-0200, N-624-0400, N9358-0100).

Professional Recognition and Affiliations

Mr. Berry is an active member of the National Association of Corrosion Engineers, participating in committee work and technical symposia. Currently he is Chairman of the NACE Research Committee. He is past chairman of NACE Group Committee T-7, Corrosion by Water, Unit Committee T-7D, Corrosion in High-Purity and Power Plant Waters, and Unit Committee T-3E, Stress-Corrosion Cracking. He also is author of some 40 AEC project reports in corrosion, chapters in the Reactor Handbook, Handbook on Corrosion Testing (Nuclear Materials) and Corrosion Standards in the Nuclear Industry, as well as some 30 papers on various aspects of corrosion, mainly in high-temperature water. He was a delegate from the U.S.A. at the International Conference on Nuclear Corrosion Technology in Brussels, Belgium, in 1959, and an invited speaker at the Symposium on Corrosion of Cladding Materials sponsored by Chimie Industrielle in Paris in 1961, and the Symposium on High-Temperature High-Pressure Electrochemistry in Aqueous Solutions at Surrey, England in 1973.

Publications

His publications include a recent book on Corrosion in the Nuclear Industry for the Electrochemical Society Corrosion Monograph Series, and chapters in seven books relating to corrosion of reactor materials.

New Publications
Available in July 1986

Corrosion of Metals in Marine Environments

MCIC* Report 86-50, $300 U.S. ($600 Foreign)
800 pages; 727 references; 342 figures; 412 tables

This report promises to be a classic in the field of marine corrosion. The focus of this report is on actual exposure data in seawater, wherever possible, rather than simulated or theoretical experiments.

An introductory chapter describes the types of corrosion, the ocean environments (atmosphere, splash zone, tide zone, immersion and mud), and the factors affecting corrosivity of seawater (oxygen, biological, temperature, velocity, salinity and pH).

The latter 13 chapters deal with individual alloy systems. Each chapter has separate sections dealing with the various aspects of corrosion described in the introduction (atmosphere, splash, tide, immersion and mud). The emphasis is on metals most commonly used in marine applications such as copper, aluminum, carbon and low-alloy steels, stainless steels, titanium and superalloys (nickel- and cobalt-base). Overall, 25 alloy systems are covered. An abbreviated table of contents for the report is listed below.

Note: Each chapter has a list of references.

*The Metals and Ceramics Information Center (MCIC) is a Department of Defense Information Analysis Center.

MCIC Report/July 1986

MCIC-86-50

Corrosion of Metals in Marine Environments

by

J. A. Beavers, G. H. Koch, and W. E. Berry
Battelle Columbus Division
Columbus, Ohio 43201-2693

Approved for public release; distribution unlimited

METALS AND CERAMICS INFORMATION CENTER
A Department of Defense Information Analysis Center
Columbus, Ohio

ACKNOWLEDGMENTS

The authors would like to express their appreciation for the contributions of T. J. Barlo and W. K. Boyd. T. J. Barlo prepared the section on Cathodic Protection while W. K. Boyd assisted in the preparation of several of the chapters.

This document was prepared by the Metals and Ceramics Information Center (MCIC), Battelle Columbus Division, 505 King Avenue, Columbus, Ohio 43201-2693. MCIC's objective is to provide a comprehensive current resource of technical information on the development and utilization of advanced metal- or ceramic-base materials.

The Center is operated by Battelle-Columbus under Contract Number DLA900-83-C-1744 for the U.S. Defense Logistics Agency; technical operations are monitored by Mr. Jerome Persh of the Office of Deputy Under Secretary of Defense, Research and Advanced Technology. The support of these sponsor organizations is gratefully acknowledged.

TABLE OF CONTENTS

TABLE OF CONTENTS
(Continued)

TABLE OF CONTENTS
(Continued)

TABLE OF CONTENTS
(Continued)

TABLE OF CONTENTS
(Continued)

TABLE OF CONTENTS
(Continued)

TABLE OF CONTENTS
(Continued)

TABLE OF CONTENTS
(Continued)

CHAPTER 1
TABLE OF CONTENTS

CHAPTER 1
LIST OF TABLES

CHAPTER 1
LIST OF FIGURES

CHAPTER 1

INTRODUCTION, BACKGROUND, AND TEST METHODS

INTRODUCTION

This report is a second update of "Corrosion of Metals in Marine Environments" which was originally printed in 1970 as DMIC (now MCIC) Report 245, reprinted in 1975 as MCIC 75-245R and first updated in 1977 (MCIC-78-37).[1] These reports have been prepared in response to the large number of requests received by MCIC for assistance in the selection of materials for equipment or facilities to be used in marine environments. They are based on a review of selected literature items, discussions with marine technologists, and information derived from Battelle's own research programs in the marine corrosion field. The majority of the data were obtained from actual ocean exposures since they provide the most reliable information, but data from exposures in aqueous 3.5 percent NaCl and in simulated seawater are included where the former data are limited. Similarly, the focus of this report is on actual exposure data but results of electrochemical studies are presented selectively where they aid in our understanding or interpretation of the phenomena.

The report is organized according to alloy type (i.e., carbon and low-alloy steels, stainless steels, etc.) exposure phase (atmosphere, splash and tide, submerged, and mud), failure mode and parametric effects. Because of the extensive nature of the subject, information on coatings for marine applications, materials for desalination, and corrosion fatigue have been excluded. The latter topic is covered in a recent MCIC publication.[2]

Before reviewing the corrosion behavior of the individual materials, descriptions of corrosion failure modes, the ocean environment, and factors that control its corrosivity are presented.

CLASSIFICATION OF METALS AND ALLOYS

The common metallic materials can be divided into two classifications according to their corrosion behavior in marine environments: corrosion resistant materials and corrosion allowance materials. Most of the corrosion resistant materials depend upon the presence of a thin, tightly adherent passive oxide film to limit the rate of the corrosion (oxidation) reaction. Examples of these materials are aluminum, stainless steels, certain nickel-base alloys, and

titanium. The noble metals, platinum, gold and silver, also are corrosion resistant but owe their resistance, in part, to their inherent thermodynamic stability.

Corrosion allowance materials corrode at relatively high rates in marine environments and rates of attack are generally limited by the rate of the cathodic (reduction) reaction. Examples of these materials are steel and zinc. Copper-base alloys possess characteristics of both corrosion resistant and corrosion allowance materials. Rates of attack of virgin specimens in seawater are generally limited by the rate of oxygen reduction, but semi-protective passive films form on copper-base alloys with time.

Discussion of the forms of corrosion for these materials are given below.

FORMS OF CORROSION AND TEST TECHNIQUES

Aqueous corrosion generally is divided into eight common forms: uniform attack, pitting, crevice corrosion, galvanic corrosion, erosion-corrosion, environmentally assisted cracking, dealloying (selective leaching) and intergranular corrosion. These are discussed in detail elsewhere and are summarized below for completeness.

Uniform Attack

Uniform attack, as its name implies, is the general wastage of a metal. In aqueous environments, it is generally electrochemical in nature with two or more half cell reactions occurring simultaneously and randomly over the metal surface. The anodic reaction is metal oxidation while the cathodic reaction may be one or more of several reactions such as oxygen reduction, proton reduction, water reduction, metal ion reduction, or reduction of an oxidant such as nitrate or H_2O_2. In marine environments, the dominant reduction reaction generally is oxygen reduction. Although uniform attack represents the greatest destruction of metal on a tonnage basis, it is by far the least insidious form since rates of attack can be conservatively estimated and there are a variety of mitigation procedures.

Uniform corrosion is generally evaluated by measuring the weight loss of test specimens and subsequently calculating the corrosion rate in terms of a thickness loss per year, knowing the alloy density, surface area, and exposure time. The procedures are described in ASTM's Recommended Practice G1. Although the weight loss method can be very accurate, it gives only the integrated average corrosion rate over the test period. Moreover, if pitting and crevice corrosion are the primary modes of attack, uniform corrosion cannot be accurately determined from the weight loss measurement.

Alternative electrochemical methods include the Tafel extrapolation and polarization resistance test methods. The Tafel extrapolation method uses data from anodic and cathodic polarization measurements. (See ASTM G61 for more detailed discussion of polarization curves and the potentiodynamic polarization technique.) Extrapolation of the linear portions of the anodic and cathodic slopes to the free-corrosion potential provides the corrosion current density from which corrosion rates can be calculated, see Figure 1-1.

There are two polarization resistance techniques for calculating general corrosion rate; the two electrode or the three electrode technique. In the two electrode polarization resistance method, a potential of less than 15 mV is applied to two identical specimens. The ensuing current is measured, and the corrosion current at a given moment in time is calculated from the equation:(3)

$$i_{cor} = \left[\frac{\beta_a \cdot \beta_c}{2.3\,(\beta_a + \beta_c)}\right] \frac{\Delta i}{\Delta E} \quad \text{where} \quad \frac{\Delta i}{\Delta E} \equiv \frac{1}{PR}$$

where Δi is the measured current density, ΔE is one half the applied potential difference between the identical electrodes, and β_a and β_c are the Tafel slopes for the anodic and cathodic processes and PR = polarization resistance.

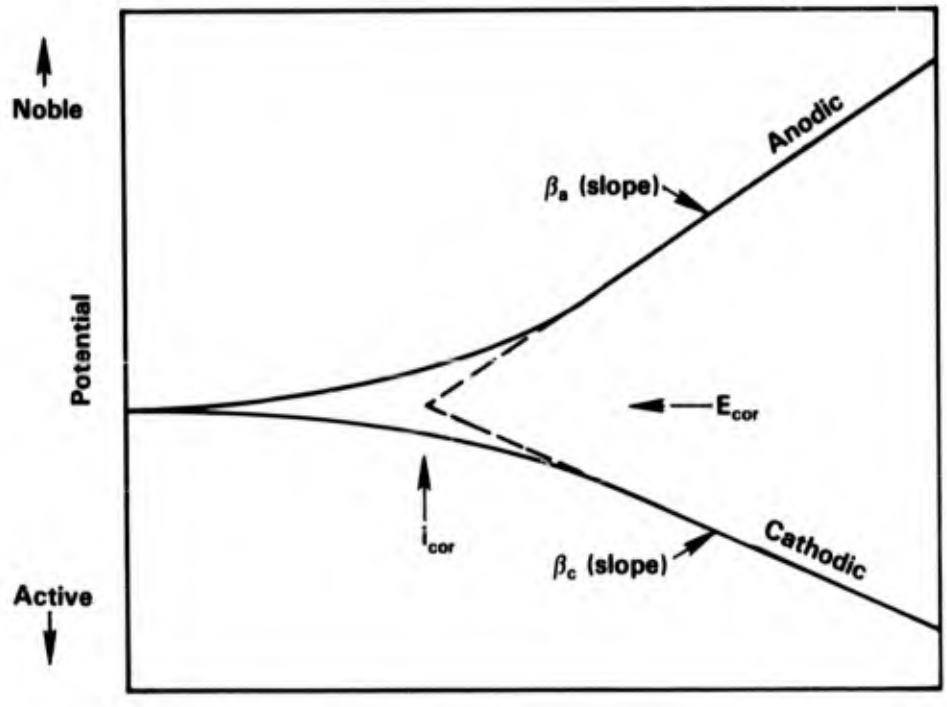

FIGURE 1-1. ANODIC AND CATHODIC POLARIZATION CURVE FOR AN ELECTRODE UNDERGOING ACTIVE CORROSION. EXTRAPOLATION ON THE LINEAR PORTION OF THE CURVES TO THE FREE CORROSION POTENTIAL PROVIDES AN ESTIMATION OF i_{cor}

Alternately, the polarization resistance can be calculated using three electrodes, consisting of one metal specimen, an inert (platinum or graphite) counter electrode, and a reference electrode (standard calomel or silver/silver chloride). With this technique, a polarization curve about the free-corrosion potential (±10 to 15 mV) is obtained by scanning the potential and measuring the ensuing current flow. The tangent to the plot of overpotential (applied potential - free corrosion potential) versus current density at the free corrosion potential, see Figure 1-2, is the value of the polarization resistance (PR) which is then converted to a corrosion current, i_{cor}, by means of the equation given above (see ASTM G59 for additional detail).

The advantages of the electrochemical techniques for corrosion rate measurements are that they are rapid and provide instantaneous measurements of the corrosion rates. On the other hand, these techniques may be inaccurate where redox reactions, other than corrosion, occur on the metal surface. Moreover, they, like weight loss measurements, provide a surface average corrosion rate and thus are inaccurate where pitting or crevice corrosion are occurring.

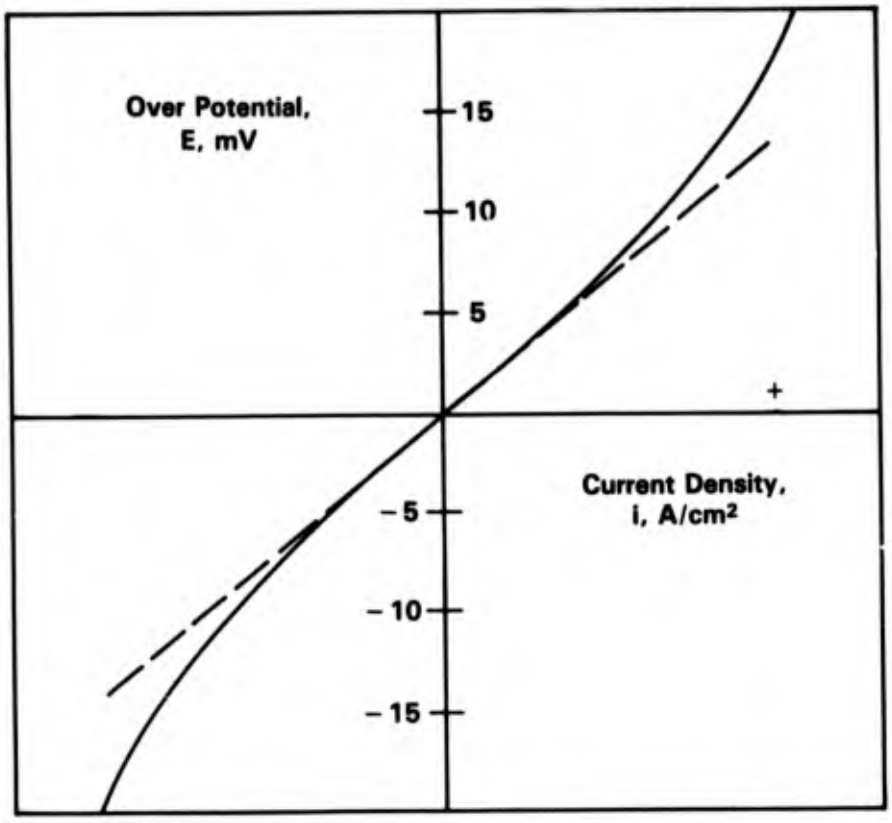

FIGURE 1-2. POLARIZATION CURVE NEAR THE FREE CORROSION POTENTIAL SHOWING THE TANGENT USED TO CALCULATE POLARIZATION RESISTANCE AT THE FREE CORROSION POTENTIAL

Pitting

In the corrosion literature, there are two common definitions of the term pitting; a morphological one and a mechanistic one. In the former, the mechanism by which the "pits" propagate may be anything from erosion-corrosion to differential cell corrosion. The most generally accepted mechanistic definition of pitting is localized corrosion that occurs on boldly exposed surfaces (no macro crevices) of passive metals under relatively stagnant conditions. Pitting may also occur on relatively film free metals at local metallurgical imperfections such as at inclusions. Although the mechanism of initiation is not well understood for either type of surface and may vary from one alloy system or environment to the next, it is generally considered that the mechanism of propagation of pitting is common to most systems. The propagation stage consists of metal oxidation within the pit, migration of anions into the pit to maintain charge neutrality, acidification in the region as a result of hydrolysis of the metal ions and oxidizer (oxygen) depletion once an occluded cell has formed. All of these processes tend to further destabilize the system; thus, pitting corrosion is autocatalytic in nature.

Metallurgical factors which favor pitting include any inhomogeneity in the material which can act as an initiation site such as inclusions, segregation, welds, scrapes, or heat tinted areas. Under submerged exposure, environmental factors which favor pitting include stagnant conditions, the presence of specific anions such as chloride, and heavy metal ions such as copper (in aluminum alloys), the presence of highly oxidizing conditions or local variation in the oxidizing strength of the environment.

Crevice Corrosion

Like pitting, crevice corrosion occurs in both passive metals and in relatively film free materials. The presence of a crevice or occluded cell is essential for initiation of crevice corrosion. The first step involves the depletion of an oxidizer (oxygen) within the crevice, resulting in the formation of a differential aeration cell and, on passive metals, a reduction in the stability of the passive films within the crevice. Once initiation has occurred, the processes associated with propagation of attack in crevices and pits are thought to be essentially identical in most systems.

The formation of the differential aeration cell produces crevice area/boldly exposed surface area relationships which are similar to those observed in galvanic couples. Thus, Ellis and LaQue[1] observed a straight line relationship between weight loss and external surface area for Type 430 stainless steel in flowing seawater, see Figure 1-3. A general rule of thumb

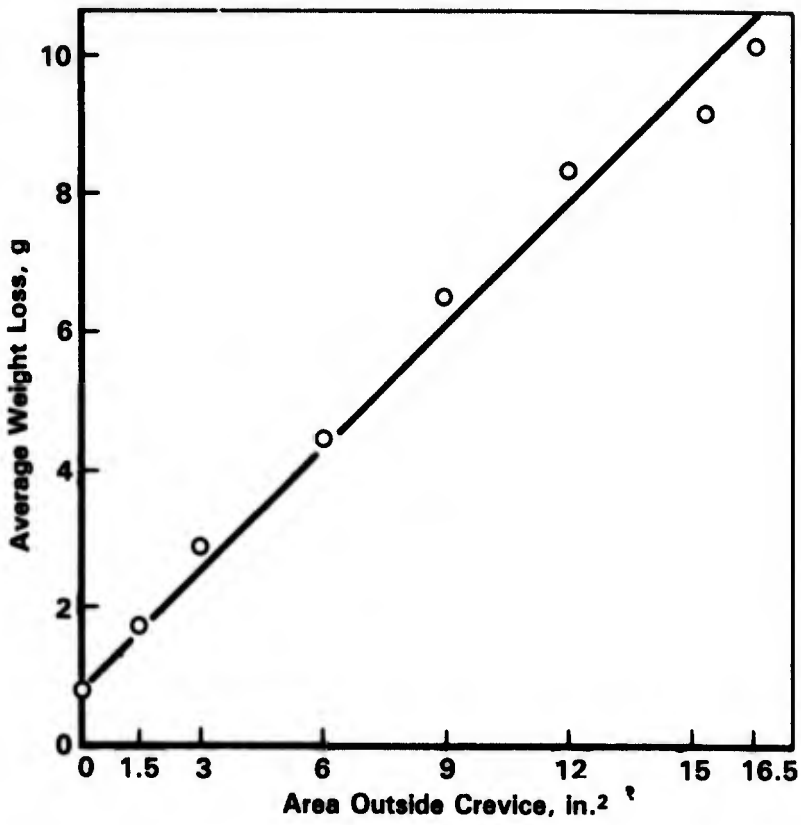

FIGURE 1-3. AVERAGE WEIGHT LOSS OF SPECIMENS AS RELATED TO AREA OF SPECIMEN OUTSIDE THE CREVICE[1]

is that above an area ratio of 10:1, further increases in the cathode area do not greatly affect the corrosion rate of the anode.

The common materials of construction are not uniformly susceptible to crevice corrosion in seawater as shown in Figure 1-4. The stainless steels and some aluminum alloys are highly sensitive whereas titanium and the high molybdenum nickel-base alloys are resistant.

The conditions that promote crevice corrosion include the presence of crevices, deposits, and fouling organisms. Common design features which promote crevice corrosion are the presence of gaskets, washers, and rivets. Crevice corrosion is generally more prevalent in the splash and tide zones, where there is a plentiful supply of oxygen, than under submerged conditions.

Pitting and crevice corrosion are generally evaluated by qualitative visual examination, or by a semi-quantitative measurement of pit depth or pit density. Electrochemical techniques also are used to evaluate pitting and crevice corrosion susceptibility. These have the advantage of being accelerated tests (e.g., potentiodynamic polarization), which provide pitting information even where pitting may not initiate under long term exposures. On the

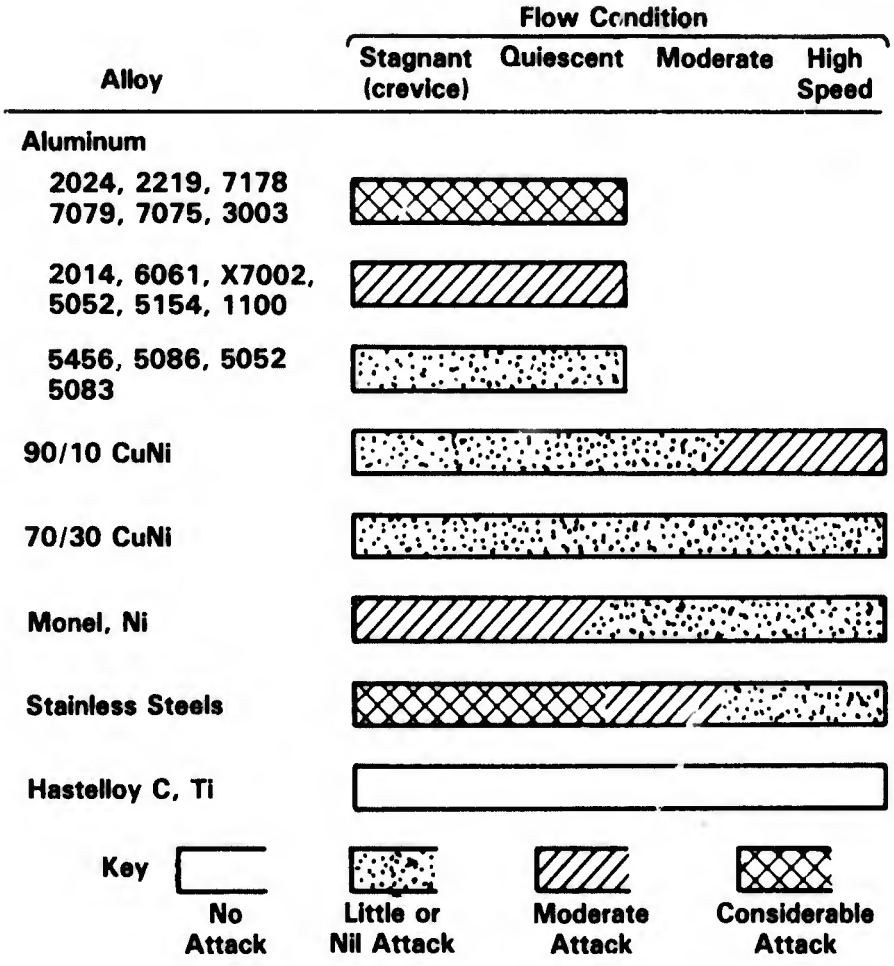

FIGURE 1-4. COMPARATIVE LOCALIZED ATTACK (CREVICE CORROSION AND PITTING) OF SOME IMPORTANT MARINE ALLOYS AS A FUNCTION OF SEAWATER FLOW CONDITIONS[1]

other hand, the behavior of an alloy in a short term (few hours) potentiodynamic polarization test generally is not indicative of its long term behavior in marine environments, especially where biofouling affects the corrosion behavior. Thus, a combination of long term exposures and short term potentiodynamic polarization tests generally provides the best understanding of a materials performance in marine environments.

Descriptions of potentiodynamic polarization techniques are given in ASTM Standards G3, G5, and G61. Figure 1-5 shows a schematic of a cyclic potentiodynamic polarization diagram. Hysteresis in the curve between the forward scan and the reverse scan is generally an indication of pitting/crevice corrosion. The important parameters which relate to pitting corrosion are: pitting potential (E_{pit}), protection potential (E_{prot}), and corrosion potential (E_{cor}).

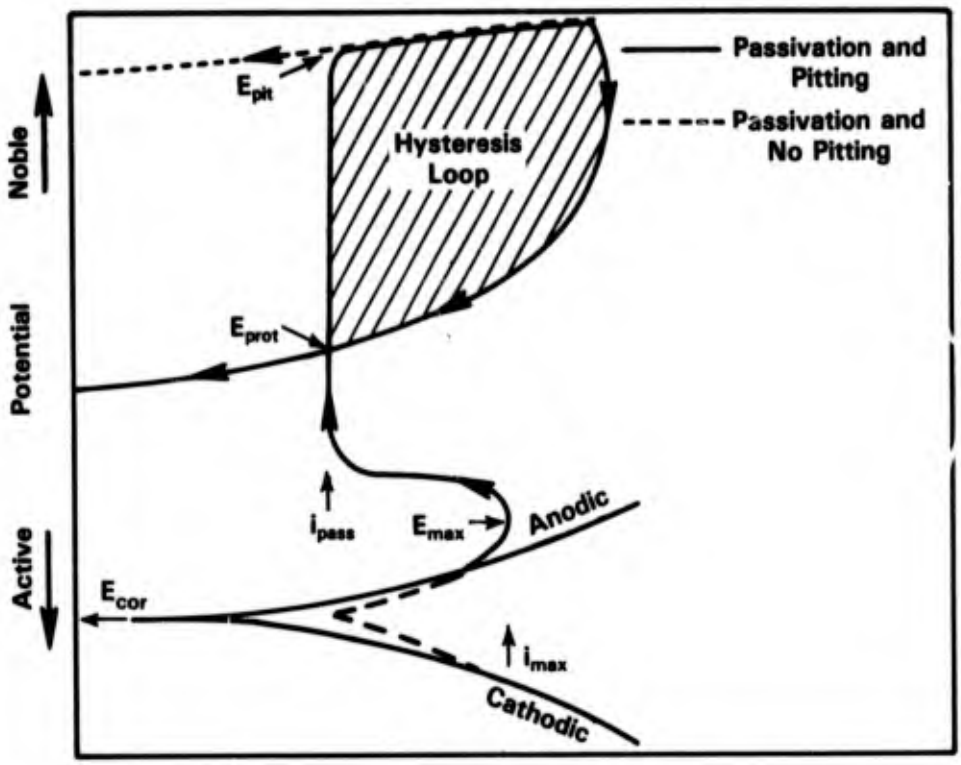

FIGURE 1-5. SCHEMATIC DIAGRAM OF TYPICAL POTENTIODYNAMIC POLARIZATION CURVES SHOWING IMPORTANT POLARIZATION PARAMETERS

E_{cor} = corrosion potential; E_{pit} = potential at which pits initiate on forward scan; E_{prot} = potential at which pits repassivate on reverse scan; i_{cor} = corrosion current density; i_{max} = current density at active peak; i_{pass} = current density in passive range.

Galvanic Corrosion

Galvanic corrosion is the accelerated attack of a metal when electrically coupled to a dissimilar metal and contacted with an electrolyte. Electrochemical potential differences between metallic materials which are immersed in the electrolyte provides the driving force for galvanic corrosion. A listing of these potentials in order of ascending or descending nobility, which is referred to as a galvanic series, is environment specific; a series in flowing seawater at 25 C is given in Table 1-1. When dissimilar metals are placed in electrical contact in the electrolyte, the corrosion rate of the more noble (electropositive material) will be decreased and the corrosion rate of the more active (electronegative material) will be increased. For this galvanic effect to occur, the dissimilar metals must be in electrical

TABLE 1-1. GALVANIC SERIES IN SEAWATER FLOWING AT 13 FPS (TEMPERATURE ABOUT 77 F)[1]

Material	Steady-State Electrode Potential, V(SCE)
Zinc	-1.03
Aluminum 3003-(H)	-0.79
Aluminum 6061-(T)	-0.76
Cast iron	-0.61
Carbon steel	-0.61
Stainless steel, Type 430, active	-0.57
Stainless steel, Type 304, active	-0.53
Stainless steel, Type 410, active	-0.52
Naval rolled brass	-0.40
Copper	-0.36
Red brass	-0.33
Bronze, Composition G	-0.31
Admiralty brass	-0.29
90Cu-10Ni, 0.82 Fe	-0.28
70Cu-30Ni, 0.47 Fe	-0.25
Stainless steel, Type 430, passive	-0.22
Bronze, Composition M	-0.23
Nickel	-0.20
Stainless steel, Type 410, passive	-0.15
Titanium[a]	-0.15
Silver	-0.13
Titanium[b]	-0.10
Hastelloy C	-0.08
Monel-400	-0.08
Stainless steel, Type 304, passive	-0.08
Stainless steel, Type 316, passive	-0.05
Zirconium[c]	-0.04
Platinum[c]	+0.15

(a) Prepared by powder-metallurgy techniques. Sheath-compacted powder, hot rolled, sheath removed, cold rolled in air.
(b) Prepared by iodide process.
(c) From other sources.

contact such that electron flow between the two metals can occur; close proximity in an ionic conducting media is not sufficient. However, in a complex structure or component, the path or paths of electrical conduction are not always readily apparent.

The severity of galvanic attack is dependent upon many variables, among them are the electrolyte conductance, the electrical contact conductance, the relative surface areas of the metals being coupled, the relative position of the metals in the galvanic series and the ease

with which the metals are polarized. Thus, copper will promote more severe galvanic attack of carbon steel than stainless steel or titanium because the latter two materials are more readily polarized than the copper.

It is found that, for a metal like carbon steel whose corrosion rate is usually controlled by the total cathodic area available, the ratio between the area of the cathode and the area of the anode is important. A small anode e.g., steel, coupled to a large cathode (e.g., copper) and immersed in seawater will result in a greatly increased rate of attack of the anode. The reverse situation of a small cathode coupled to a large anode will have only a minor influence on the rate of attack of the anode.

To control or prevent the accelerated attack as a result of galvanic coupling, certain principles should be observed. First, the possibility of breaking the electrical circuit by providing an insulating barrier at the junction between the two metals should be considered. Second, if dependable isolation is not feasible, the cathodic member of the couple should be covered with a nonconductive protective coating. By reducing this area, or eliminating the cathode entirely, enhanced corrosion of the anode material due to the couple is prevented in a safe manner. Under no circumstances should only the anode be painted. Any defect or "holiday" in the coating will result in the entire cathode area being coupled to a small area of anode material, and extremely high rates of penetration can be expected.

In the atmosphere, galvanic corrosion is confined to a short distance, usually a fraction of an inch, from the joint between the two metals because of the highly resistive nature of the condensed layer of moisture. On the other hand, galvanic corrosion may be significant over large distances in seawater because of its high conductivity. Some examples of couples and their corrosion behavior are given in Table 1-2.

Several test techniques are used to evaluate the galvanic corrosion behavior of metal couples. These include weight loss measurements and optical examination of galvanically coupled specimens following long term exposure in the corrosive environment. In these tests, parameters that are frequently varied are exposure time and the relative surface area ratio of the members of the couple.

Electrochemical techniques also are used to evaluate galvanic corrosion behavior. One commonly used technique is to electrically isolate the members of the couple in the electrolyte, but to electrically connect them through a zero resistance ammeter (ZRA). With this technique, the galvanic current flow can be measured as a function of time to provide an instantaneous estimate of the galvanic effect. Coupled and uncoupled potentials are frequently measured as a function of time, with respect to a reference electrode by periodically opening the electrical circuit through the ZRA to obtain an estimate of the amount of polarization of the electrode that is occurring as a result of the galvanic couple.

TABLE 1-2. EXAMPLES OF GALVANIC COUPLES IN SEAWATER[1]

Metal A	Metal B	Comments
	Couples That Usually Give Rise to Undesirable Results on One or Both Metals	
Magnesium	Low-alloy steel	Accelerated attack on A, danger of hydrogen damage on B.
Zinc[a]	Low-alloy steel	Accelerated corrosion of metal A, protection of metal B.
Bronze[a]	Low-alloy steel	Protection of metal A, possible fouling of metal A, accelerated corrosion of metal B.
Aluminum[a]	Low-alloy steel	Accelerated corrision of metal A, protection of metal B.
Stainless Steel	Low-alloy steel	Reduction in pitting of metal A, accelerated corrosion of metal B.
Aluminum	Copper	Accelerated pitting on A; ions from B attack A. Reduced corrosion on B may result in biofouling on B.
Bronze	Stainless steel	Increased pitting on A.
	Borderline, May Work, But Uncertain	
Copper	Solder	Soldered joint may be attacked but may have useful life.
Graphite	Titanium or Hastelloy C	
Monel-400	Type 316 SS	Both metals may pit.
	Generally Compatible	
Titanium	Inconel 625	
Lead	Cupronickel	

(a) Not contained in the original reference.

Where the anodic member of the couple is polarized more than about 50 mV from its free-corrosion potential, its corrosion rate is approximately equal to the current measured with the ZRA*; for polarization values less than 50 mV, the uncoupled corrosion rate of the electrode must also be considered.

Potentiodynamic polarization techniques also are used to estimate galvanic effects and interpret galvanic corrosion data. Since both potential and electrode-kinetics data are obtained, the potentiodynamic polarization data are much more useful than galvanic series data alone in estimating galvanic effects. As previously mentioned, caution must be exercised in applying electrochemical techniques to corrosion rate measurements because of the possible occurrence of spurious redox reactions and because short term tests may be inadequate for estimating long term corrosion behavior.

Erosion-Corrosion

Erosion-corrosion is an accelerated form of attack and is promoted by the relative movement between the corrosive media and the metal surface. Erosion-corrosion conditions can vary from relatively low velocity, lamellar flow to more severe impingement type attack where highly turbulent conditions exist. In all cases, the mechanisms are related to interaction of the corrosive media with a protective surface film. The relative movement of the solution may result in mechanical damage to the film or may replenish the electrolyte of aggressive species at the metal surface that, in turn, affects the protective nature of the passive film.

Erosion-corrosion is characterized by the presence of holes, grooves, or valleys which usually exhibit a directional pattern. A variety of adjectives has been used to describe erosion/corrosion such as horseshoe, star, crescent, and slot. Each is generally associated with a specific geometry. For example, horseshoe attack is associated with the erosion pattern around lodged obstructions in heat exchanger tubes.

Cavitation is a special form of erosion/corrosion which is caused by the formation and collapsing of vapor bubbles in a liquid near the metal surface. Cavitation occurs most commonly in rotating machinery such as pump impellers and ship propellers where high pressure drops are encountered. These pressure drops, if sufficiently large, can promote local

---

* Assuming spurious redox reactions (noncorrosion related) are not occurring in the electrolyte.

boiling. The vapor bubbles which form subsequently collapse, producing shock waves with very high pressures. These high pressures can produce plastic deformation of many metals. Thus cavitation damage is attributed to both corrosion and mechanical effects. The appearance of cavitation damage is similar to pitting except that the attacked areas are closely spaced, resulting in a roughened surface appearance.

Environmental factors that control erosion/corrosion include water velocity, oxygen content, water pH, temperature, flow geometry, and the presence of particulates in the water. Both the mechanical properties of the metal and the nature of the passive film on the metal affect the erosion/corrosion susceptibility. Stainless steels, nickel-base alloys and titanium are generally resistant to the various forms of erosion/corrosion whereas the copper-base alloys are usually more susceptible.

Several testing techniques are currently used to study erosion-corrosion. They fall into one of five categories: (1) simulated service tests; (2) rotating disc/spindle tests; (3) rotating drum tests; (4) multivelocity jet tests; or (5) jet impingement tests. In addition, high frequency vibratory equipment is used to study cavitation corrosion. The choice of a test technique is often dictated by what is convenient to the researcher. However, the data are usually reported as normalized weight loss of the material over a certain period of testing. The weight loss data also are supplemented by visual and microscopic descriptions of the nature of attack on the specimen. Electrochemical techniques, in conjunction with the other conventional techniques, are becoming increasingly popular for the study of the erosion-corrosion processes. Moreover, many investigators have used several of the above techniques simultaneously, in order to obtain complementary data to study the erosion-corrosion problem.

Environmentally Assisted Cracking

Environmentally assisted cracking (EAS) refers to the fracture or cracking of material by the conjoint action of an applied tensile stress and a specific corrosive medium. During EAS, the metal is unattacked over most of its surface but fine cracks progress through it. Depending upon the alloy-environment system and the specific form of the EAS, the cracking may be intergranular, transgranular or a mixed mode. Cracks may follow straight paths or branch in several directions.

EAS can be subdivided into three general categories, anodic stress-corrosion cracking, hydrogen stress cracking, and corrosion fatigue. Corrosion fatigue is not addressed further in this book. Anodic stress-corrosion cracking generally occurs where there is an appropriate balance between electrochemical activity of the advancing crack tip and passivity of the crack walls and the free surfaces. Cathodic protection is generally effective in preventing anodic

stress-corrosion cracking, but cathodic protection also accelerates hydrogen stress cracking by facilitating hydrogen entry. Other important variables that affect environmentally assisted cracking include metal composition, heat treatment, solution composition, temperature, and stress-related parameters such as the maximum stress or stress intensity and the presence of load cycling.

All engineering materials are susceptible to one or more forms of EAS under certain environmental and applied stress conditions. However, the environment that promotes cracking in one material may be completely harmless to another. For example, practically all copper-base alloys are susceptible to stress-corrosion cracking in ammoniacal environments whereas the austenitic stainless steels are immune in the same environment. On the other hand, copper-base alloys are generally considered to be immune to stress-corrosion cracking in seawater environments, but many stainless steels are extremely susceptible. Similarly, the high strength steels are susceptible to hydrogen stress cracking in chloride containing environments.

Several tests have been devised for studying the SCC susceptibility of an alloy in a given environment. Specimens of the alloy in the form of U-bend, C-ring, bent-beam, or tensile bar are stressed and then exposed to the environment. A specimen may be stressed either under constant load or constant strain. Exposed specimens are tested over a certain period of time or until failure occurs by cracking. Times to failure are recorded, and used for performance ranking of materials. After the test, specimens are usually examined metallographically to determine the mode of cracking and the depth of crack penetration. Descriptions of typical testing procedures are given in Reference 4 and in ASTM standards G30, G38, and G39.

Since SCC, like other forms of aqueous corrosion, is an electrochemical process, SCC tests are sometimes performed under controlled potential conditions. Controlled potential tests are conducted in order to simulate the oxidizing or reducing atmosphere that might prevail in the service environment, and also to obtain understanding of the processes involved in SCC.

Because constant load or constant strain tests require long exposures, an accelerated SCC test, namely, the slow strain rate technique, has gained popularity in the last few years. In this test, a tensile bar specimen of the alloy is slowly strained, at a strain rate typically between 10^{-5} and 10^{-7}/s. in the test environment until fracture. A reference test under identical conditions but in an inert atmosphere is made for comparison purposes. Reduction in the value of ultimate tensile strength or time to failure of the specimen in the environment, in relation to that in the reference test, indicates susceptibility to SCC. Little or no reduction in the above values in the environment suggests immunity from cracking. Other variables such as the occurrence of secondary cracking, a reduction in cross-sectional area or percentage

elongation of the specimen, can also be used for the evaluation. Details of the test technique and several examples are given in an ASTM publication ASTM STP 665, "Stress-Corrosion Cracking - The Slow Strain Rate Technique".[5]

Recently, it has been demonstrated that cycling the load on a specimen under a tensile stress can significantly increase susceptibility to SCC.[6] Such load cycles can occur in service as a result of thermally induced stresses or mechanical design. Accordingly, SCC tests that utilize load cycling increasingly have been used. Typically, the load cycles have a period of 1 to 10 minutes and amplitude variations between 50 and 100 percent of the yield stress. Evaluation for susceptibility is similar to that used for constant load or constant strain tests.

The use of precracked fracture mechanics type specimens also has been advocated for SCC tests in recent years.[7] The advantage of precracked specimens, over that of smooth specimens, is that the crack initiation (incubation) time in the test environment is reduced and the crack propagation rate in a susceptible alloy can be determined by following the crack advancement. The stress intensity factor, K_I, is the most common parameter used to describe the driving force for crack propagation, and is defined as $K_I = f\,\sigma\sqrt{\pi a}$, where a is the length of a crack or flaw, σ is the applied stress and f is a geometric parameter. Depending on the method of stressing and/or the geometry of the test specimen, see Figure 1-6, the stress intensity can be made to increase, decrease, or remain constant as the crack length increases. Further, threshold stress intensities (K_{Iscc}) below which a crack will not advance, can be determined. There are several types of fracture mechanics specimens in use today. Brown[7] has described the merits and drawbacks of these.

Dealloying

Dealloying is the selective removal of the more active element from a solid solution alloy by electrochemical processes. This phenomenon is also referred to as selective leaching. The most common example is the selective removal of zinc in brass alloys (dezincification). Similar processes occur in copper-aluminum alloys. Graphitic corrosion, a process in which iron is selectively removed from cast iron, leaving a graphite layer, is also considered to be a form of dealloying.

Dealloying failures in seawater applications are most common in copper-base alloys and generally are not observed in stainless steels or titanium. Two types of dealloying are observed in copper-base alloys, namely uniform or layer type, and plug type, in which the dealloyed region is localized on the metal surface.

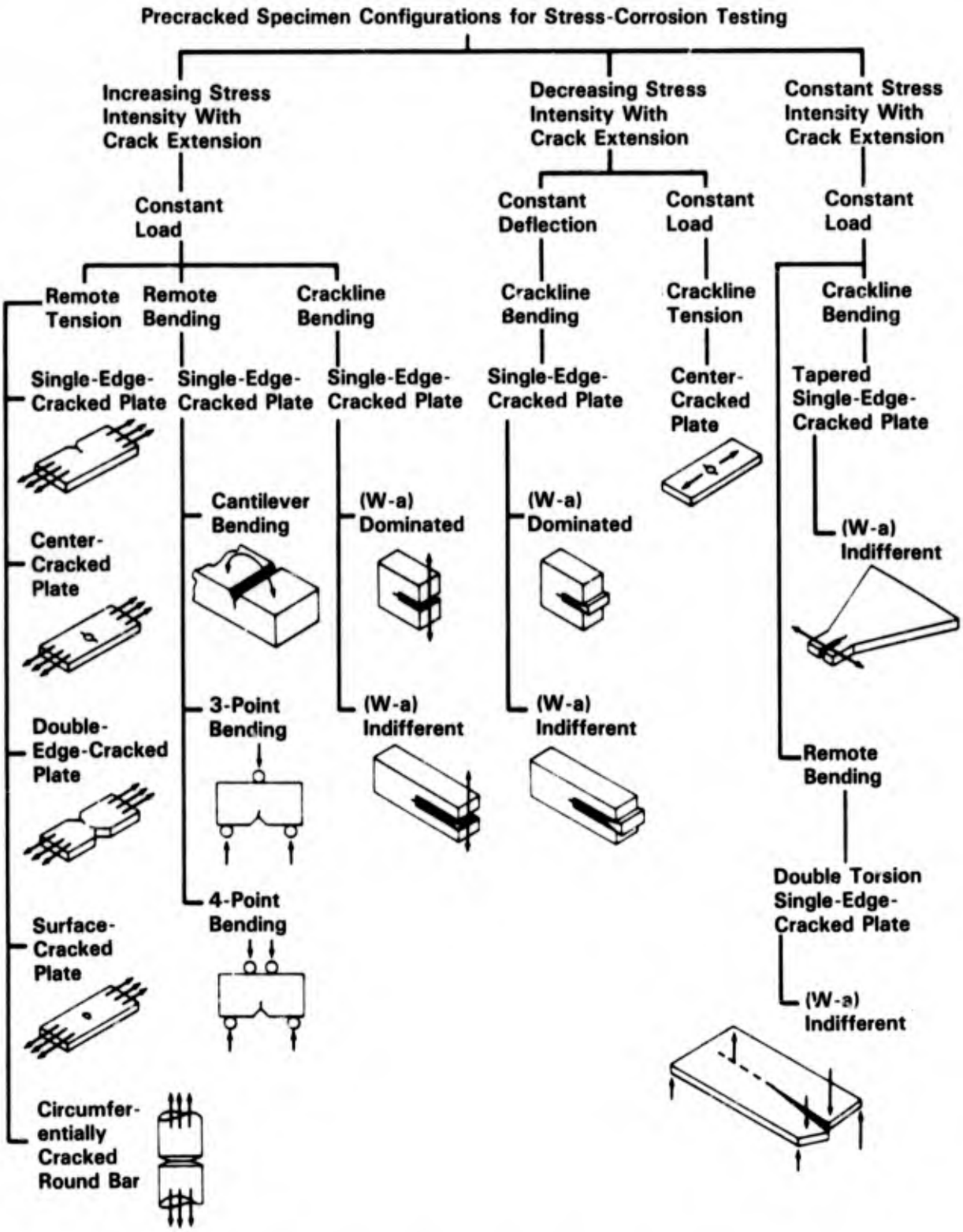

FIGURE 1-6. CLASSIFICATION OF PRECRACKED SPECIMENS FOR STRESS CORROSION TESTING[8]

Two mechanisms for dealloying have been proposed. One involves the co-dissolution of the two alloying elements and the deposition of the more noble material onto the metal surface. The other involves the surface or bulk diffusion and the selective dissolution of the active element.

The occurrence of dealloying is affected by the active elements present in the alloy as well as minor elemental additions such as tin and arsenic (in the case of dezincification). Other factors that affect the failure include heat treatment, solution composition, temperature, flow velocity, pH and electrochemical potential.

Intergranular Corrosion

Intergranular corrosion refers to localized attack of grain boundaries in certain aqueous environments. It can be caused by impurities at the grain boundaries, enrichment of one of the alloying elements, or depletion of one of these elements in the grain boundary areas. Intergranular corrosion is most commonly observed in austenitic stainless steels where the attack is related to heat treatment in the temperature range of 500 to 800 C. Heating the alloy in this temperature range promotes the precipitation of chromium carbides thereby removing the chromium from solid solution and resulting in a metal with lower chromium content than the adjacent areas.

Intergranular corrosion is also observed in susceptible aluminum alloys. Due to the strong directionality of the grains in plate materials, the intergranular corrosion is recognized by the formation of surface flakes and is therefore referred to as exfoliation corrosion.

Several methods are available to determine the susceptibility of materials to intergranular corrosion. Different intergranular corrosion tests standardized by the ASTM are listed in Table 1-3. These tests were developed primarily for detecting carbide sensitization of austenitic stainless steels, but also may find application for other stainless steels and nickel-base alloys.

In addition to the immersion tests, electrochemical techniques are used to distinguish between susceptible and resistant materials. Generally, the factors that are most affected by sensitization are i_{pass}, the active-passive transition current, and the potential, see Figure 1-5. A specific test is the electrochemical potentiokinetic reactivation (EPR) test which has been developed by Clarke and coworkers.[10,11] The test is based on the difference in activation behavior between sensitized and annealed materials and can be considered quantitative. A specimen is initially polarized in a specific solution (0.5M H_2SO_4 + 0.01M KSCN) in the noble direction into the passive region.

TABLE 1-3. STANDARD INTERGRANULAR CORROSION TESTS FOR STAINLESS STEEL[9]

ASTM Standard (Common Name)	Environment	Exposure	Evaluation	Species Attacked
A393* (Strauss)	15.7% H_2SO_4 + 5.7% $CuSO_4$, boiling	One 72 hr period	Appearance after bending	Chromium depleted area
A262, Practice A (Oxalic Etch)	10% $H_2C_2O_4$, anodic at 1 A/cm^2, ambient temperature	1.5 min	Type of attack	Various carbides
A262, Practice B (Streicher)	50% H_2SO_4 + 2.5% $Fe_2(SO_4)_3$, boiling	One 120 hr period	Weight loss per unit area	Chromium depleted area
A262, Practice C (Huey)	65% HNO_3, boiling	Five 48 hr periods, fresh solution each period	Average weight loss per unit area	Chromium depleted area sigma and carbides
A262, Practice D (Warren)	10% HNO_3 + 3% HF, 70 C	Two 2 hr periods	Weight loss per unit area	Chromium depleted area in Mo-bearing steels
A262, Practice E (Copper Accelerated) (Strauss)	15.7% H_2SO_4 + 5.7% $CuSO_4$, specimen in contact with copper, boiling	One 24 hr period	Appearance after bending	Chromium depleted area

* Discontinued in 1972.

During the subsequent reverse scan to the test potential, an annealed material will show no active corrosion. However, sensitized steel will not passivate sufficiently at the grain boundaries during the scan in the noble direction and during the reverse scan local film breakdown will result in increased current.

OCEAN ENVIRONMENTS

Seawater covers more than 70 percent of the earth's surface and is the most abundant naturally occurring electrolyte. Most of the common metals and alloys of construction are attacked by seawater or moisture-laden sea air. Since the behavior of materials may vary widely, depending on the exposure conditions, their performance is discussed according to the specific environmental zone involved, namely atmosphere, splash and tide, immersed, and mud. Characteristics of these zones and their influences on corrosion are briefly discussed below.

Atmosphere

Deposition of sea mist and sea salt occurs on materials exposed in marine atmospheres. The salts are deleterious to most common alloys, promoting localized attack; their hygroscopic nature and sea mist provide an electrolyte which is necessary for the attack to occur while the anions in the salt promote film breakdown on passive metal surfaces. The mere presence of the deposits also may promote the formation of differential aeration cells.

The salt deposition process is a function of many variables including wind and wave conditions, height above the sea, distance from the shore, panel orientation, degree of sheltering, and the amount and distribution of rain during a given time period. In general, those conditions which promote salt buildup and prevent rainfall from removing the salt promote the most severe corrosion. Thus, the bottom sides of panels or those panels which are sheltered from the rain generally are more severely attacked.

Fungi and mold also may deposit on metal surfaces in marine atmospheres. These organisms may promote corrosion by the formation of differential aeration cells and by holding moisture on the metal surface.

Splash Zone

Materials in the splash zone are almost continuously wetted with well aerated seawater and biofouling generally does not occur.

For materials such as carbon and low-alloy steels, which do not form thin, tenacious passive films, the splash zone is the most aggressive of the marine zones. In this region, there is an ample supply of oxygen and the entrained bubbles in the seawater are highly destructive toward the thick semi-protective films that form on some of these materials. A corrosion profile of a steel piling showing the relative corrosion rates of carbon steel in the various zones is given in Figure 1-7.

Metals which form tightly adhering passive films such as the stainless steels and titanium generally perform well in the splash zone because the well aerated conditions promote passivity.

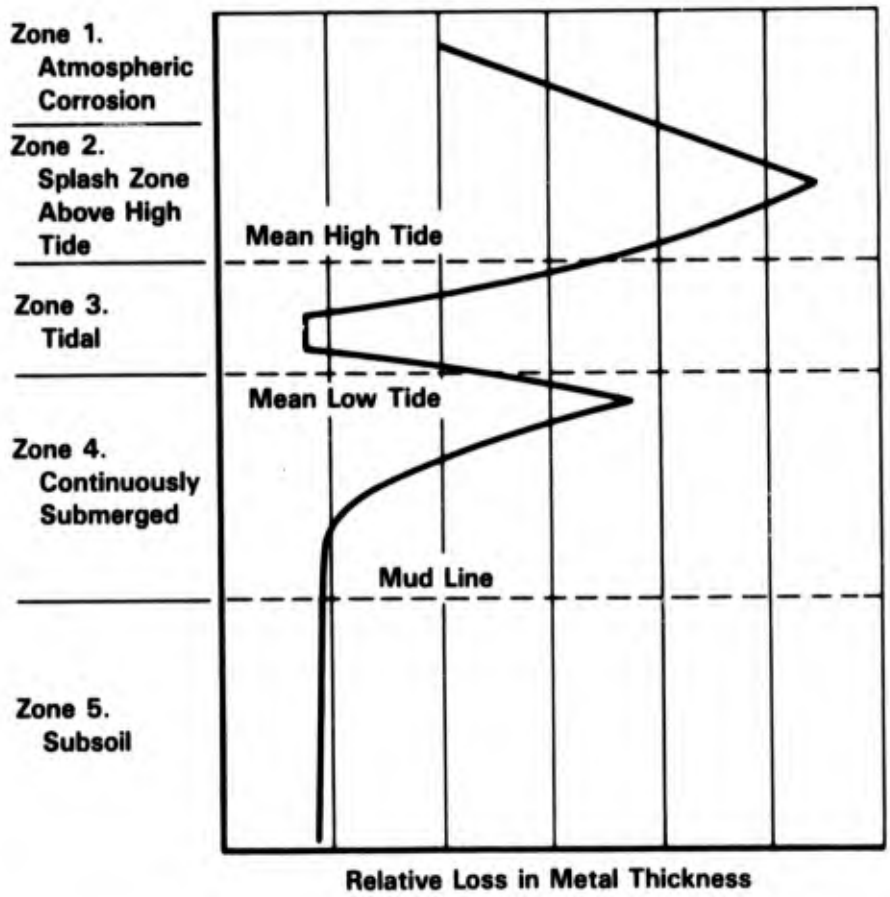

FIGURE 1-7. CORROSION PROFILE OF STEEL PILING AFTER 5 YEARS' EXPOSURE IN SEAWATER AT KURE BEACH, NC (INTERNATIONAL NICKEL CO.)[1]

Tide Zone

In the tide zone, a material alternates between fully immersed exposure and splash zone exposure; the relative amount of time under each exposure condition varies depending upon location within the zone. Thus, the tide zone is a transition region with a range of exposure conditions. For isolated test panels, upper tide zone exposure is similar to splash zone exposure, whereas lower tide zone exposure is similar to immersed conditions. In general, the aerated conditions within the tide zone promote rapid attack of metals such as steel whereas passive metals such as stainless steels and titanium are protected. However, fouling does occur in the tide zone and this may result in partial protection of steels or may promote localized attack of stainless steels.

One also has to differentiate between the behavior of isolated panels in the tide zone, and the typical case, occurring in practice, where a structure such as a pile extends from the atmosphere through the splash and tide zones into submerged and mud zones. For a continuous steel pile, rapid attack takes place on that part of the surface just below the water line, with the portion at the water line being the cathode which receives protection at the expense of the metal below, see Figure 1-7.

Immersion Zone

The major factors which affect the corrosivity of the immersion zone are: oxygen, biological activity, pollution, temperature, and velocity. The seawater pH and salinity also may influence corrosivity. A discussion of the relationships between these factors and corrosivity is given, in detail, in the next section. These factors are, in turn a function of location, the depth and the season.

Oceanographic data showing the variation in oxygen, temperature, pH, and salinity with depth for a site in the Pacific Ocean are shown in Figure 1-8. These data show that the oxygen concentration is the highest near the surface (approximately 6 ppm), reaches a minimum of about 0.2 ppm at about 2,000 feet in depth and increases slightly to about 1 ppm at about 6,000 feet in depth. Near the surface, photosynthesis and wave action oxygenate the seawater, whereas at intermediate depths, decomposition of organisms consumes the oxygen. The oxygen found at greater depths in the Pacific is attributed to supply of oxygenated arctic water by bottom currents.

On the other hand, analysis of seawater from various depths in the Atlantic, at the Navy's TOTO deep sea test site, indicate that the oxygen concentration does not vary appreciably with depth, see Table 1-4. The higher oxygen concentration at depths in the

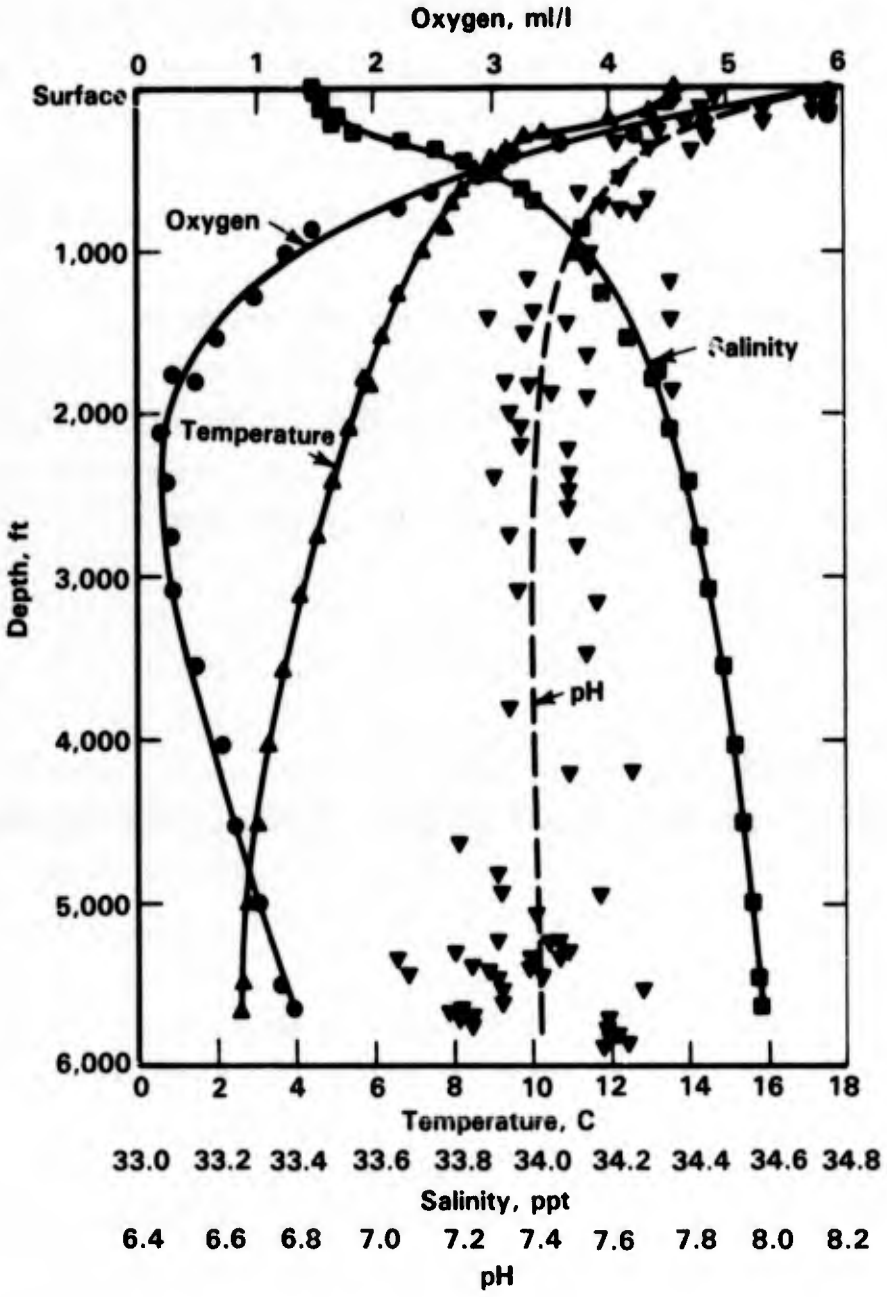

FIGURE 1-8. OCEANOGRAPHIC DATA TAKEN IN THE PACIFIC OCEAN AT A SITE WEST OF PORT HUENEME, CALIFORNIA[1]

TABLE 1-4. HYDROGRAPHIC ASPECTS OF TONGUE-OF-THE-OCEAN WATER (ATLANTIC OCEAN)[1]

Depth, ft	Temperature, C	Salinity, ppt	Oxygen, ml/l
Surface	24.08	36.79	4.59
33	--	36.73	4.58
66	24.09	36.72	4.61
164	24.14	36.73	4.26
249	24.13	36.78	4.42
331	24.14	36.79	4.42
495	23.92	36.74	4.15
663	22.35	36.70	4.15
820	19.27	36.56	4.13
1,158	17.31	36.36	3.92
1,654	13.78	35.82	3.46
1,985	11.73	35.55	3.19
2,316	10.03	35.33	3.11
2,648	8.09	--	3.59
3,310	--	35.04	4.96
4,967	4.18	35.00	5.73
5,100	4.12	35.00	5.26
19,567	4.0	--	5.73

Atlantic than in the Pacific has been attributed to the lower biological oxygen demand in the Atlantic. In other words, decaying organisms in the Atlantic do not exhaust the available oxygen supply.

The lower pH found in waters at great depth may be partially explained on thermodynamic grounds, since the pH is reduced by extreme pressures alone. However, it is also known that the carbon dioxide-calcium bicarbonate-calcium carbonate equilibrium tends to be shifted; that is, the dissolved calcium carbonate in the deep ocean tends to be slightly below saturation; while, conversely, it is frequently super saturated at the surface.[1] One would therefore expect that, in deep waters, there would be less tendency to form a protective mineral scale, as compared with surface waters. It has been observed, for example, that the consumption of sacrificial anodes for providing cathodic protection is significantly greater at extreme depths, e.g., 5000 feet than in surface waters.

Data showing the seasonal variation in the pH, oxygen concentration, temperature and concentration of sulfate-reducing bacteria for a polluted harbor and a pollution-free strait are given in Figure 1-9. These data show that pH values were seasonally independent and were about 1 unit lower in the polluted seawater than in the unpolluted seawater. Parameters other

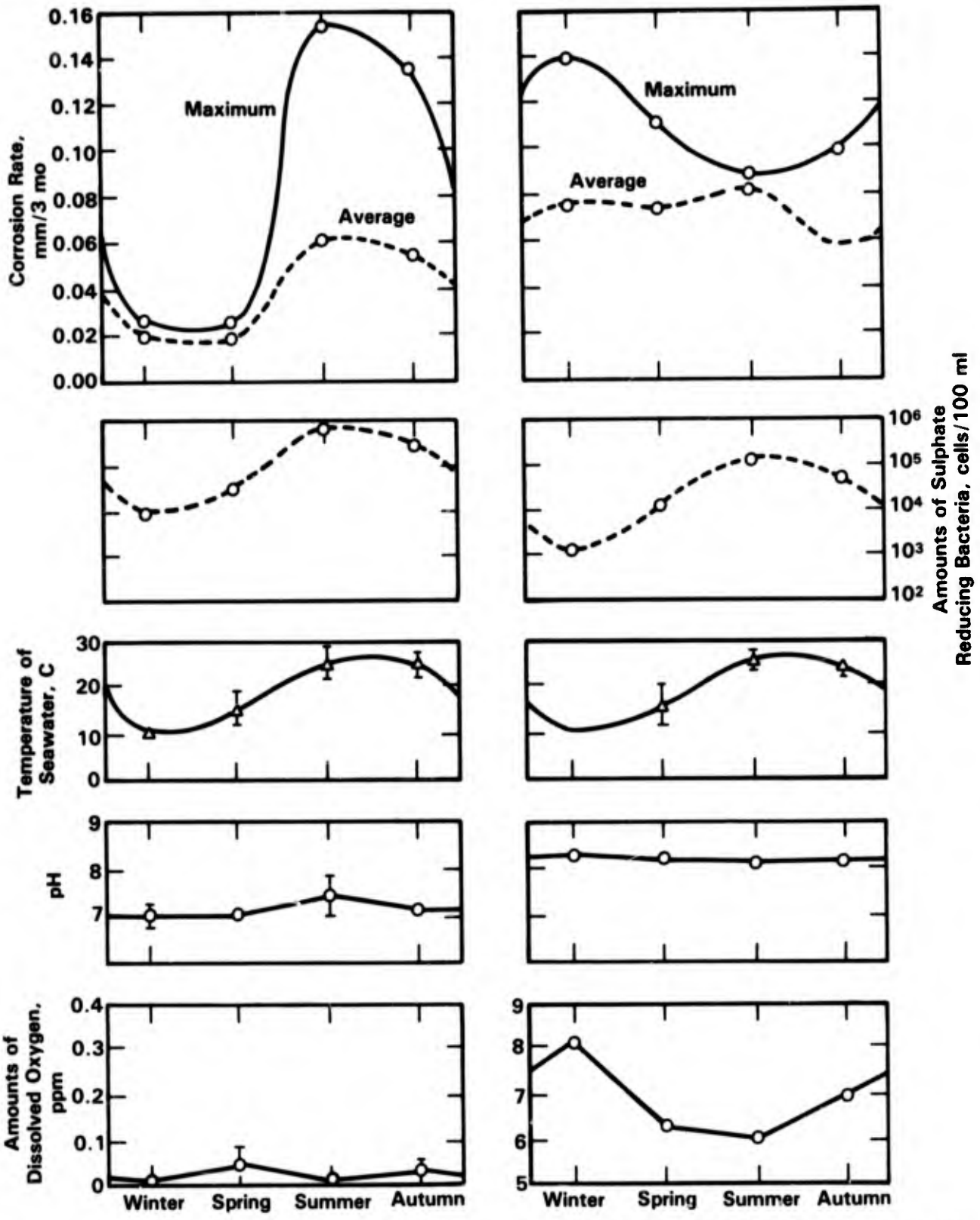

(a) The polluted sea area "Okudokai Harbor" (b) The pollution free sea area "Kammon Strait"

FIGURE 1-9. SEASONAL FACTORS INFLUENCING THE CORROSION BEHAVIOR OF NORMAL CARBON STEEL IN POLLUTED AND UNPOLLUTED SEA AREAS[12]

than pH exhibited seasonal variations which were different for the polluted and unpolluted seawater. For the polluted seawater, the oxygen content was low throughout the year (below 0.5 ppm) and was slightly higher in the spring and in the autumn. The temperature was the highest in the summer and autumn, as was the concentration of sulfate reducing bacteria. The overall effect of these parameters was to produce the most severe corrosion of carbon steel during the summer and autumn months.

For the unpolluted seawater, the temperature and the concentration of sulfate reducing bacteria were also the highest in the summer. However, the oxygen content peaked in the winter months as did the corrosion rate of the carbon steel.

Mud Zone

The environmental conditions within the mud zone are highly geographically dependent and have been well characterized in only a few instances. In general, there are opposing influences of the environment on corrosivity within the mud zone. The oxygen concentration is low, which is beneficial for materials such as steel and copper. On the other hand, sulfate reducing bacteria which are found in the mud zone produce sulfides that are highly detrimental to these materials. Practical experience from examination of off-shore structures and with experimental piles indicates that steel is often attacked more slowly in the mud zone than in the seawater above it.

FACTORS AFFECTING THE CORROSIVITY OF SEAWATER

The roles of oxygen, biological activity, temperature, velocity, salinity, and pH on the corrosivity of seawater are discussed below.

Oxygen

The oxygen concentration in seawater may range from as low as <0.2 ppm at great depths to up to 12 ppm near the surface. Photosynthesis of green plants, wave action, etc. increase the oxygen level whereas the biological oxygen demand of decomposing organisms will reduce it. The solubility of oxygen in seawater also increases with decreasing temperature. For a given location, seasonal variations in oxygen level resulting from the above actions will, in turn, influence corrosion behavior.

Oxygen affects the corrosion rate of metallic materials by providing a cathodic reaction ($O_2 + 2H_2O + 4\ e^- \rightarrow 4OH^-$) having a relatively noble equilibrium potential and rapid kinetics. For corrosion allowance materials such as steels, the presence of oxygen greatly accelerates rates of attack since the corrosion kinetics are limited, in many cases, by the rate of the reduction reaction. On the other hand, the presence of oxygen generally reduces rates of attack of corrosion resistant materials such as stainless steels and titanium by promoting passivation. However, where the oxygen supply to a passive metal surface is limited locally, such as at crevices, the presence of oxygen on the boldly exposed surfaces may promote localized attack.

For the corrosion allowance materials, the rate of the oxygen reduction reaction generally is limited by the rate of transport of oxygen to the metal surface. Thus, factors which influence the rate of transport such as the oxygen concentration of the seawater and velocity of the seawater also affect the corrosion rate.

Biological Activity

When a metal or other surface is first immersed in seawater, a biological slime tends to develop within a matter of hours. Subsequent to the formation of the biological slime film, embryonic sessile organisms become firmly attached. Once attached, they rapidly transform to the mature form. Clapp[8, p 433] lists the following most common forms of sessile fouling organisms:

- Organisms Which Build Hard Shells
  - Annelids
  - Barnacles
  - Encrusting Bryzoa
  - Mollusks
  - Corals
- Organisms Without Hard Shells
  - Marine Algae
  - Filamentous Bryzoa
  - Coelenterates or Hydroids
  - Tunicates
  - Calcareous and Silaceous Sponges.

The growth of sessile organisms, referred to as biofouling, is a major factor in the performance of metals in marine environments. For corrosion allowance materials, fouling may actually reduce rates of attack by limiting the supply of oxygen to the metal surface. However, the decay and by-products of marine organisms can be aggressive and promote

localized attack of both corrosion resistant and corrosion allowance materials. Moreover, the simple presence of the marine organisms can aid in the development of differential aeration cells. For heat exchanger applications, lodgement of organisms also promotes erosion-corrosion of susceptible materials such as copper-base alloys by increasing the seawater velocity in localized areas.

Temperature

The effect of temperature on the corrosion of metals is complicated by the interdependence of other relevant parameters and temperature. The kinetics of activation-controlled oxidation reactions and diffusion-controlled reduction reactions increase with increasing temperature. On the other hand, the passivation phenomenona is a complex function of temperature since the stability of the films and the rate of formation are affected. In addition, oxygen solubility in seawater decreases with increasing temperature and calcareous scales exhibit retrograde solubility, increasing the likelihood of precipitation of protective scales at elevated temperatures. Biological activity increases with increasing temperature over the temperature range near ambient, which can be either beneficial or deleterious. At higher temperatures, the marine organisms are actually killed, and thus biofouling does not occur. Thus, the overall influence of temperature on corrosion must be established for each unique set of conditions.

Velocity

The corrosion rate of corrosion allowance materials such as steels and copper-base alloys normally increases with increasing seawater velocity since rates of attack of these metals are frequently limited by the availability of oxygen at the metal surface. In addition, high velocities tend to erode barrier films which form on alloys such as the copper-base alloys. Passive metals such as titanium and stainless steels are highly resistant to flowing seawater. Indeed, pitting of stainless steels is less likely in flowing seawater than under stagnant conditions.

Salinity

The major oceans of the world are completely connected in the southern hemisphere and mixing is continuous. Not surprisingly, the relative proportion of salts does not vary appreciably in these interconnected seas; variations in salinity in open ocean surface waters

typically range from 3.2 to 3.75 percent. In this range, the corrosion of common metals is not appreciably affected. The composition of seawater for a salinity of 3.5 percent is given in Table 1-5.*

Large variations in salinity are found in more isolated seas, as shown in Table 1-6. These salinity variations are accompanied by other chemical changes in the seawater and thus the overall effect on corrosion behavior is difficult to predict. The concentration of aggressive ions such as chloride is lower in diluted seawater and in seawater having lower salinity, but the solubility of oxygen increases with decreasing salinity. Moreover, diluted seawater, as is found in the mouths of rivers, is usually unsaturated with respect to carbonate and thus is less likely to scale. Biofouling also is less likely in diluted seawater due to the reduced activity of marine organisms.

pH

The pH of seawater may vary slightly depending on the photosynthetic activity. Plant matter consumes carbon dioxide and affects the pH during daylight hours. Carbon dioxide content in seawater is influenced close to the surface by the exchange with carbon dioxide in the atmosphere. The daily shift in pH from, say, 8.0 to 8.2 has little direct effect on the corrosion behavior; however, it can be a factor in calcareous scale deposition, which in turn, influences corrosivity.

As pressure is increased, pH is reduced according to thermodynamic considerations. Thus, at great depths, there is some evidence of less tendency for protective carbonate type scales to form.

---

* Salinity is defined as the total weight in grams of solid matter dissolved in 1000 grams of water. Thus, a salinity of 3.5 percent indicates a solid matter content of 35 grams per 1000 grams of seawater or a solid content of 35,000 ppm. Salinity is usually determined by measuring the chlorinity (i.e., chloride-ion content in grams per 1000 grams of water) of the seawater, and then deriving from the relationship S o/oo = 1.805 Cl o/oo + 0.030.[14]

TABLE 1-5. COMPOSITION OF SEAWATER AND IONIC CONSTITUENTS[13]

Constituent	g/kg of Water of Salinity,[a] 35 o/oo	Cations, percent		Anions, percent	
Chloride	19.353	Na^+	1.056	Cl^-	1.898
Sodium	10.76	Mg^{++}	0.127	SO_4^-	0.265
Sulphate	2.712	Ca^{++}	0.040	HCO_3^-	0.014
Magnesium	1.294	K^+	0.038	Br^-	0.0065
Calcium	0.413	Sr^{++}	0.001	F^-	0.0001
Potassium	0.387				
Bicarbonate	0.142	Total	1.262	Total	2.184
Bromide	0.067				
Strontium	0.008				
Boron	0.004				
Fluoride	0.001				

(a) See footnote on page 1-28.

TABLE 1-6. TOTAL SOLIDS IN OCEAN WATERS[15]

Body of Water	Total Dissolved Solids, ppm
Baltic Sea	8,000
Black Sea	22,000
Atlantic Ocean	37,000
Mediterranean Sea	41,000
Caspian Sea	13,000
Irish Sea	32,500

REFERENCES FOR CHAPTER 1

1. Boyd, W. K. and Fink, F. W., "Corrosion of Metals in Marine Environments", Battelle Columbus Laboratories, Metals and Ceramics Information Center Report MCIC-78-37 (March, 1978).

2. Jaske, C. E., Payer, J. H., and Balint, V. S., "Corrosion Fatigue of Metals in Marine Environments", Battelle Columbus Laboratories, Metals and Ceramics Information Center Report MCIC 81-42 (July, 1981).

3. Stearns, M. and Geary, A. L., Journal of Electrochemical Society, 105, p 638 (1958).

4. Champion, F. A., Corrosion Testing Procedures, J. Wiley & Sons, New York (1964).

5. Ugiansky, G. M. and Payer, J. H., Stress-Corrosion Cracking, The Slow Strain Rate Technique, ASTM STP 665, American Society for Testing and Materials (1979).

6. Berry, W. E., White, E. L., and Payer, J. H., "Cyclic Load Stress-Corrosion Cracking of Sensitized Stainless Steels in Oxygenated High Temperature Water", Corrosion/80, Paper No. 236, NACE (1980).

7. Brown, B. F., Stress-Corrosion Cracking in High Strength Steels and in Titanium and Aluminum Alloys, Naval Research Laboratory, Washington, DC (1972).

8. The Corrosion Handbook, Edited by H. H. Uhlig, John Wiley & Sons, New York (1948).

9. Sedriks, A. J., Corrosion of Stainless Steels, J. Wiley & Sons, New York, p 139 (1979).

10. Clarke, W. L., Romero, V. M., and Danko, J. C., "Detection of Sensitization in Stainless Steel Using Electrochemical Techniques", Corrosion/77, Paper No. 180, NACE (1971).

11. Clarke, W. L., Cowan, R. L., and Walker, W. L., "Comparative Methods for Measuring Degree of Sensitization in Stainless Steels", Proceedings Symposium on Intergranular Corrosion of Stainless Steels, ASTM STP 656, ASTM, Toronto, Canada (May, 1978).

12. Shimada, H., Miida, K., and Yokooji, T., "Corrosion of Steels in Various Marine Environments" (A Joint Study with Maritime Safety Agency), Nippon Steel Technical Report, No. 8, pp 31-42 (May, 1976).

13. Lyman, J. and Abel, R. B., "Chemical Aspects of Physical Oceanography", J. Chemical Education, 35 (3), pp 113-115 (1958).

14. Chemical Oceanography, Vol. I, Edited by J. P. Riley and G. Skirrow, Academic Press, N.Y.C. and London, "The Physical Properties of Seawater" (R. A. Cox), Chapter 3 (1965).

15. Temperley, T. G., "Corrosion Phenomena in the Coastal Areas of the Persian Gulf", Corrosion Science, 5, pp 581-589 (1965).

CHAPTER 2
TABLE OF CONTENTS

CHAPTER 2
TABLE OF CONTENTS
(Continued)

CHAPTER 2
LIST OF TABLES

CHAPTER 2
LIST OF TABLES
(Continued)

CHAPTER 2
LIST OF FIGURES

CHAPTER 2
LIST OF FIGURES
(Continued)

CHAPTER 2
LIST OF FIGURES
(Continued)

CHAPTER 2
LIST OF FIGURES
(Continued)

CHAPTER 2
LIST OF FIGURES
(Continued)

CHAPTER 2

ALUMINUM AND ALUMINUM-BASE ALLOYS

Since the corrosion resistance of aluminum alloys depends on the presence of a passive oxide film, they are generally most resistant in well-aerated marine environments. Failure by localized attack such as pitting, crevice corrosion, exfoliation corrosion, or stress-corrosion cracking is characteristic of many alloys, in particular, the high strength alloys.

Table 2-1 briefly summarizes the aluminum alloy designation system. The seven principal series contain the major alloying elements shown and are either heat treatable or nonheat treatable, as indicated. The compositions of specific alloys are listed in Appendix B. The 5000 series aluminum alloys are widely used for marine applications. Examples are Alloys 5006, 5083, and 5456. If higher strength is required, alloys in the 6000 series such as 6061-T6 are often selected. High strength alloys in the 2000 and 7000 series are commonly used aerospace alloys, but have relatively poor performance in marine environments.

A discussion of the corrosion behavior of aluminum alloys in different types of marine environments is given in the following sections.

TABLE 2-1. ALUMINUM ALLOY DESIGNATION SYSTEM

Major Alloying Element	Alloy Series
None 99% +	1000(a)
Copper	2000(b)
Manganese	3000(a)
Silicon	4000(a)
Magnesium	5000(a)
Magnesium/Silicon	6000(b)
Zinc/Magnesium	7000(b)
Others	8000

(a) Nonheat treatable.
(b) Heat treatable.

ATMOSPHERE

General Corrosion

Aluminum and its alloys exhibit good resistance to general corrosion when exposed to marine atmospheres, particularly the 3000 and 5000 series aluminum alloys. In general, it has been reported that the corrosion rates of aluminum alloys in marine environments decrease with time. Figure 2-1 shows a continuing decrease in corrosion rates of Alloys 3004-H14 and 5152-H14 after up to 7 years' exposure at Kure Beach, 24 m (80 ft) from the shore line.[1] However, studies by Otero, et al.[2] indicated that, during a ten-year exposure at a coastal test site near Alicante, Spain (Mediterranean Coast), the weight losses of several aluminum alloys increased with the exposure time as a linear function, see Figure 2-2. It may be argued that in the latter case, pitting and crevice corrosion contributed to the weight loss, which would explain the apparent discrepancy between the two sets of results.

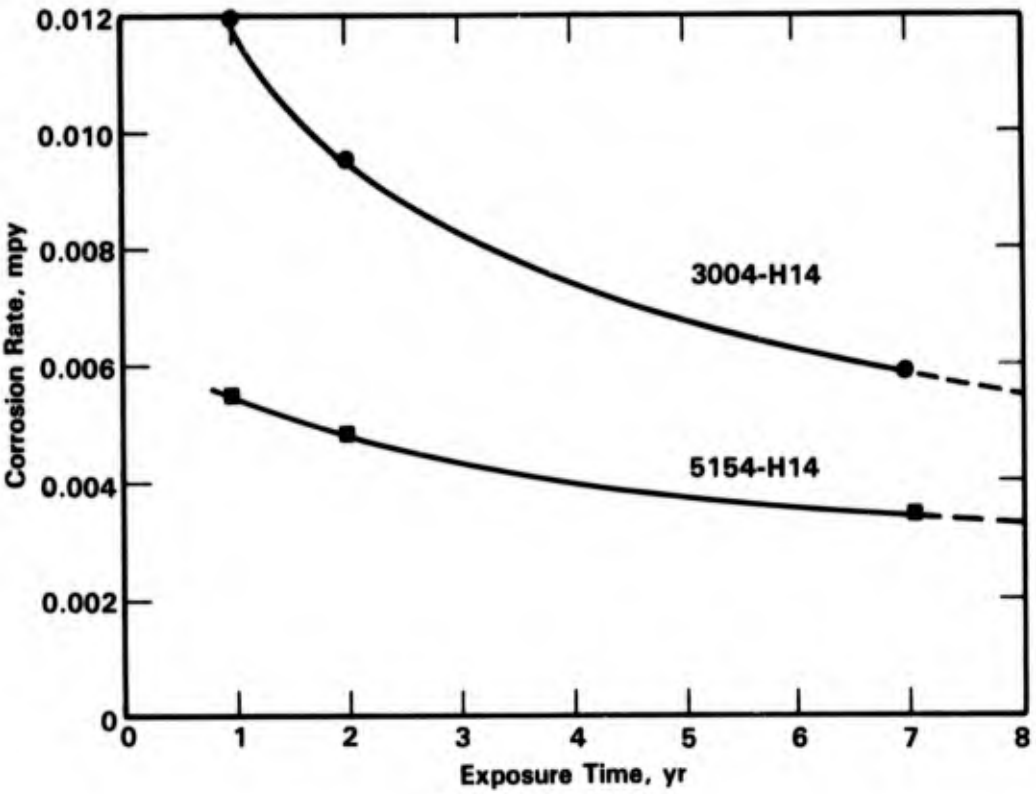

FIGURE 2-1. REDUCTION IN CORROSION RATES WITH TIME OF TWO ALUMINUM ALLOYS, EXPOSED TO MARINE ATMOSPHERE ON THE 24 m (80 ft) LOT AT KURE BEACH, NC[1]

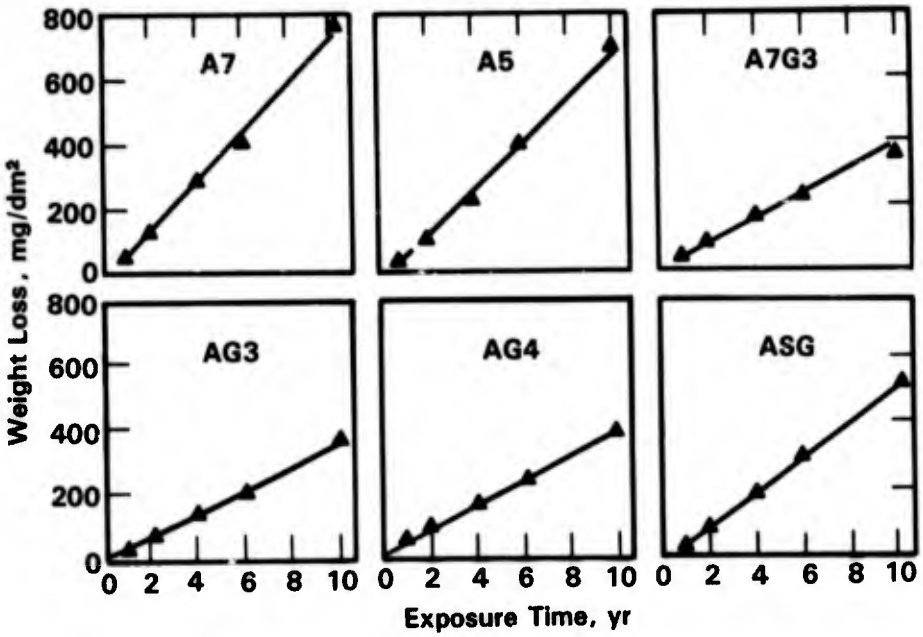

Composition of Aluminum Materials Tested

Designation	Chemical Analysis, weight percent					BHN
	Mg	Fe	Si	Mn	Cr	
A7	--	0.20	0.12	--	--	40
A5	--	0.33	0.14	--	--	36
A7G3	3.3	0.20	0.18	0.22	--	57
AG3	3.4	0.24	0.18	0.12	--	55
AG4	4.5	0.20	0.15	0.20	0.14	66
ASG	1.0	0.16	1.15	--	--	53

FIGURE 2-2. WEIGHT LOSS OF SIX ALUMINUM ALLOYS AS A FUNCTION OF TIME EXPOSED NEAR ALICANTE, SPAIN[2]

Table 2-2 summarizes the corrosion rates of various aluminum alloys exposed to three different marine sites. After 5 years, the highest corrosion rate observed was 0.025 mpy indicating the high corrosion resistance of the alloys with tne heat treatment indicated.

TABLE 2-2. CORROSION RATES OF DIFFERENT ALUMINUM ALLOYS AS CALCULATED FROM WEIGHT-LOSS DATA, EXPOSED AT THREE MARINE SITES[3]

	Corrosion Rate, mpy									
	Bohus-Malmon, Sweden			Arenzano, Italy[c]	Kure Beach, North Carolina					
					80-ft Lot			800-ft Lot		
Alloy	1 Yr	3.06 Yr[a]	5.12 Yr	1.75 Yr	1 Yr	2 Yr	5 Yr	1 Yr	2 Yr	5 Yr
1100-H14	0.009	0.002	0.010	0.035	0.027	0.028	0.018	0.021	0.022	0.009
1180-H14	0.008	0.003	0.006	0.024	0.024	0.023	0.025	0.020	0.018	0.009
3003-H14	0.009	0.003	0.009	0.036	0.037	0.027	0.018	0.022	0.021	0.009
5050-H34	0.009	0.003	0.007	0.023	0.026	0.022	0.015	0.020	0.014	0.007
5052-H34	0.008	0.006	0.007	0.020	0.028	0.021	0.010	0.018	0.014	0.009
5154-H34	0.009	0.004	0.007	0.023	0.023	0.020	0.013	0.018	0.014	0.007
5086-H34	0.007	0.001	0.007	0.023	0.023	0.019	0.010	0.018	0.013	0.010
6061-T6	0.011	(b)	0.012	0.041	0.033	0.027	0.019	0.034	0.021	0.011

(a) Values reflect insufficient cleaning after exposure.
(b) Increase in weight.
(c) Data not determined for 4.12 and 5 year panels.

In subsequent exposure studies by Ailor,[4] different aluminum alloys were exposed to marine atmospheres at four locations, see Table 2-3. The climatological conditions at these sites are described in Table 2-4. The results of the 7-year test indicate that the high strength 2000 and 7000 series aluminum alloys were the most susceptible to general corrosion, whereas the 1000, 3000, 5000, and 6000 series alloys were very resistant.

The results of a study of 5086, 5083, and 5456 aluminum alloys in H116 and H117 tempers exposed to a marine atmosphere 80 feet from the ocean at Wrightsville Beach, NC, again indicated extremely low corrosion rates after 2 years of exposure (see Table 2-5).

The corrosion rates for Alloys 1100 and 6061, exposed for 16 years at Cristobal, Canal Zone, are presented in Table 2-6. The attack in this environment was uniform with pits less than 5 mils deep, for the entire 16 years. The average corrosion rate for each alloy was 0.007 mpy.

TABLE 2-3. CORROSION RATES OF ALUMINUM ALLOYS AFTER SEVEN YEARS OF EXPOSURE ON FOUR DIFFERENT MARINE SITES[4]

Alloy	Corrosion Rate, mpy				
	Kure Beach, NC	Manila, Philippines	Denge Marsh, England	Aruba, Netherland Antilles	Average
1199-H14	0.002	0.002	0.006	0.008	0.005
2014-T3	0.014	0.011	0.039	0.699	0.191
3005	0.009	0.004	0.027	0.009	0.012
5052-H34	0.004	0.003	0.011	0.009	0.007
5086-H32	0.007	0.005	0.016	0.011	0.010
5456-H321	0.007	0.005	--	0.023	0.012
Al-7 Mg-O	0.007	0.023	0.041	0.016	0.022
6061-T6	0.008	0.004	--	0.034	0.012
Alclad 6061-T6	0.007	0.003	--	0.085	0.026
6062-T5	0.008	0.004	--	0.046	0.019
7075-T6	0.019(a)	0.012(a)	--	0.402(a)	0.144

(a) Intergranular attack.

TABLE 2-4. CLIMATOLOGICAL INFORMATION ON TEST SITES LISTED IN TABLE 2-3[4]

Location	Classification	Normal Daily Temperature Range, C		Prevailing Wind		Rainfall Annual Mean, mm	Driest Period	Wettest Period	Possible Sunshine, percent	Other Conditions	Racks Face
		Low	High	Direction	Mean Speed, mph						
Kure Beach, NC 80-ft lot	East Coast Marine	2.8	31.7	SW	9.3	1,270	October-November	July-September	68	Occasional hurricanes - snowfall rare. Located on the Cape Fear Peninsula, 17 miles SE of Wilmington, NC.	ESE
Manila, Philippines	Subtropical-Industrial	20.6	35.6	NE		82	January-March	July-August	--	Occasional typhoons. Located in the city of Manila, 7 miles east of Manila Bay.	SE
Denge Marsh, England	Marine	-7	22	SW	20	645	June	October-November	20	Occasional storms. Located on the English Channel - 200 ft from the water. Fog and sea mist 20% of time.	S
Aruba, Netherland Antilles	Tropical Marine	25.6	31.4	F	13.7	540	April-September	October-March	66	Located on the east coast of the island of Aruba (12°33'N latitude). Site is 100 ft from the Caribbean Sea. Panels receive frequent wettings by sea spray.	SE

TABLE 2-5. CORROSION TEST RESULTS FOR ALUMINUM ALLOYS IN MARINE ATMOSPHERE 80 FEET FROM OCEAN NEAR WRIGHTSVILLE BEACH, NC[5]

Alloy and Temper	Plate Thickness, in.	Corrosion Rate, mpy			Corrosion Description After 2 Years
		6 Months	1 Yr	2 Yr	
		As-Rolled Condition			
5086-H116	1/4	0.10	0.09	Nil	Scattered light pitting
5086-H117	1/4	0.10	0.13	Nil	Scattered light pitting
5083-H116	1/4	Nil	0.11	Nil	Scattered light pitting
5456-H116	1/4	0.10	0.11	Nil	Scattered light pitting
5456-H117	1/4	0.10	0.13	0.10	Scattered light pitting
5083-H116	1/2	0.30	0.13	0.10	Scattered light pitting
5456-H116	1/2	0.35	0.13	0.05	Scattered light pitting
5086-H116	3/4	0.50	0.12	0.10	Scattered light pitting
		Sensitized Condition			
5086-H116	1/4	Nil	0.17	Nil	Scattered light pitting
5086-H117	1/4	0.20	0.17	Nil	Scattered light pitting
5083-H116	1/4	Nil	0.33	Nil	Scattered light pitting
5456-H117	1/4	0.30	0.65	Nil	Moderate light blistering
5083-H116	1/2	0.40	0.31	0.05	Scattered light pitting
5456-H116	1/2	0.40	0.23	0.10	Scattered light pitting
5086-H116	3/4	0.50	0.26	0.10	Scattered light pitting

TABLE 2-6. CORROSION OF ALUMINUM ALLOYS EXPOSED 16 YEARS IN THREE TROPICAL ENVIRONMENTS IN THE PANAMA CANAL ZONE[6]

	Average Penetration[a], mils			Depth of Pitting[b], mils						Tensile Strength Loss %[c],	Type of Corrosion Attack[d],
				Average of 20 Deepest Pits			Deepest Pits				
	1 Yr	8 Yr	16 Yr	1 Yr	8 Yr	16 Yr	1 Yr	8 Yr	16 Yr	8 Yr	16 Yr
Alloy 1100											
Immersion											
Seawater	0.28	0.61	0.97	9 (13)	11	17	15	19	33	2	J
Mean Tide	0.06	0.31	0.53	11 (9)	14	39	29	37	67	1	J, Q
Atmospheric											
Marine	0.01	0.02	0.11	N	N	N	N	N	N	0	A
Alloy 6061											
Immersion											
Seawater	0.28	0.73	0.91	N	23	14	N	49	79	0	J
Mean Tide	0.04	0.13	0.29	N	N	17	N	N	41	0	J
Atmospheric											
Marine	0.03	0.03	0.11	N	N	N	N	N	N	1	A

(a) Calculated from weight loss and specific gravity.
(b) Represents depth of penetration from original surface; N - measurable pits; number in parentheses gives number of measurable pits when less than 20.
(c) Percent change in tensile strength calculated on basis of 1/4-inch-thick metal and average of four tests for underwater specimens, and 1/16-inch-thick metal and average of three tests for atmospheric specimens.
(d) A - uniform attack; J - marine fouling contact; Q - pitting attack (random).

In addition to the exposure tests described, various atmospheric testing in tropical environments[7-11] and cool, marine atmospheres[12-15] indicated equally low corrosion rates of aluminum alloys.

Because of its resistance to general corrosion, aluminum is often used without added surface protection. However, anodizing is used to enhance the resistance to corrosion. As a surface protection method for aluminum alloys, sulfuric acid anodizing is widely used. For architectural applications, standards are given by ASTM Standard B58. The coating thickness is considered the principal classification parameter. Sulfuric acid anodizing is also widely used for protection of high strength aluminum alloys of the 2000 and 7000 series in aircraft applications.[16] Additional protection can be achieved by sealing.

A typical anodizing layer consists of a dense barrier layer and an additional porous outer layer. Hot water sealing is generally considered to cause hydration of the porous aluminum oxide, assumed to be amorphous, to form a crystalline hydrate. As the hydrate forms, the pores close. Inhibitors are often added to the aqueous sealing solution to provide added corrosion resistance. Other types of anodizing treatments include chromic acid and phosphoric acid anodizing. These oxides are much thinner compared to the layer obtained in sulfuric acid anodizing, about 1 μm by phosphoric acid anodizing, 5-10 μm by chromic acid anodizing and about 20 μm by sulfuric acid anodizing. Because of their porous nature, unsealed anodizing layers are excellent substrates for protective organic coatings and a suitable marine formulation will provide long lasting additional protection.

Pitting

Since the corrosion resistance of aluminum alloys depends on the presence of a thin protective oxide film, many of these alloys tend to pit in marine environments. Five-year and seven-year results at various test sites of 1000, 2000, 3000, 5000, 6000, and 7000 series aluminum alloys are presented in Figure 2-3 and Table 2-7. In these comparisons, Alloy 6061 showed the best performance with a maximum pitting ranging from 3-7 mils. The Al-7Mg alloy with a trace of oxygen (Al-7Mg-O) showed the least resistance to pitting with an average pit depth after seven years of 12.0 mils. Figure 2-3 shows that the pitting rate decreases with time and in some cases pitting actually stops. Otero, et al.[2] who investigated pitting corrosion of various aluminum alloys during a 10-year exposure to a marine atmosphere in Alicante, Spain, also showed a decrease in pitting rate with time of exposure (see Figure 2-4). Figure 2-4 also indicates that position, upward versus downward facing, can have a significant effect on the pitting rate of some aluminum alloys. In general, the surface facing ground

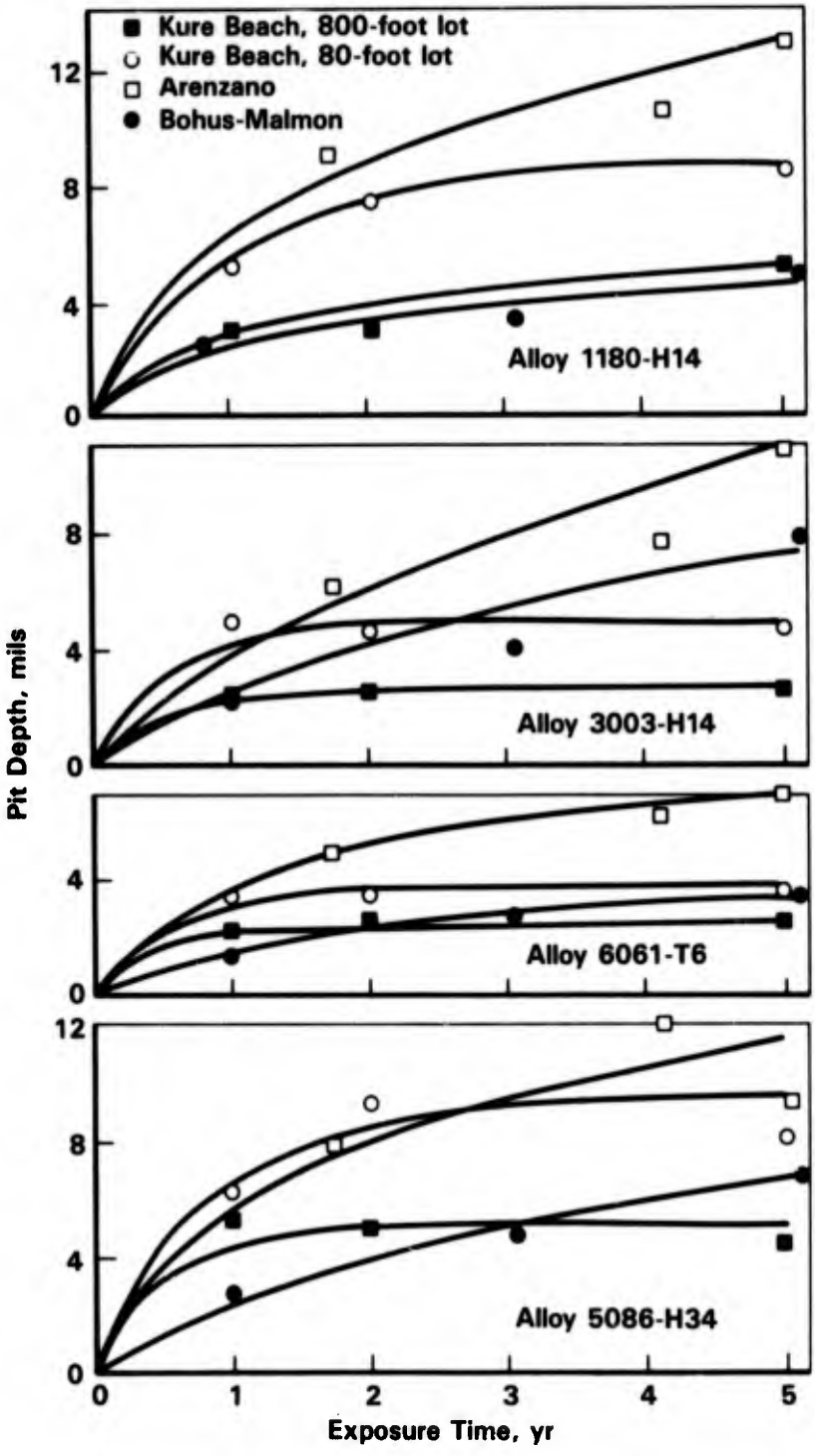

FIGURE 2-3. MAXIMUM MEASURED PIT DEPTHS OF FOUR ALUMINUM ALLOYS AS A FUNCTION OF TIME DURING EXPOSURE TO FOUR DIFFERENT MARINE SITES[3]

TABLE 2-7. MAXIMUM PIT DEPTHS FOR ALUMINUM ALLOYS MEASURED AFTER SEVEN YEARS' EXPOSURE TO FOUR DIFFERENT MARINE SITES[4]

Alloy	Depth, mils				
	Kure Beach, NC	Manila, Philippines	Denge Marsh, England	Aruba, Netherland Antilles	Average
1199-H14	4.3(a)	3.6(a)	6.7(a)	18.5	8.3
2014-T3	2.8	1.8	2.8	6.0	3.4
3005	4.3(a)	4.7(a)	7.3	7.0	5.8
5052-H34	2.8	5.0	5.0	10.3	5.8
5086-H32	2.6	4.6	5.1(a)	7.5	5.0
5456-H321	3.2(a)	2.4	4.7(a)	5.0	3.8
Al-7Mg-O	7.3(a)	7.0(a)	11.8	22.0	12.0
6061-T6	1.8	2.4(a)	--	3.7(a)	2.6
Alclad 6061-T6(b)	1.6(a)	2.4(a)	2.0	2.4	2.1
6062-T5	5.3(a)	5.6(a)	--	6.5(a)	4.4
7075-T6	2.2	1.8(a)	3.2	13.6(a)	5.2
Average	3.5	3.8	5.3	9.3	5.5

(a) Skyward side - all others for underside of panel.
(b) Average cladding thickness 0.0024 inches.

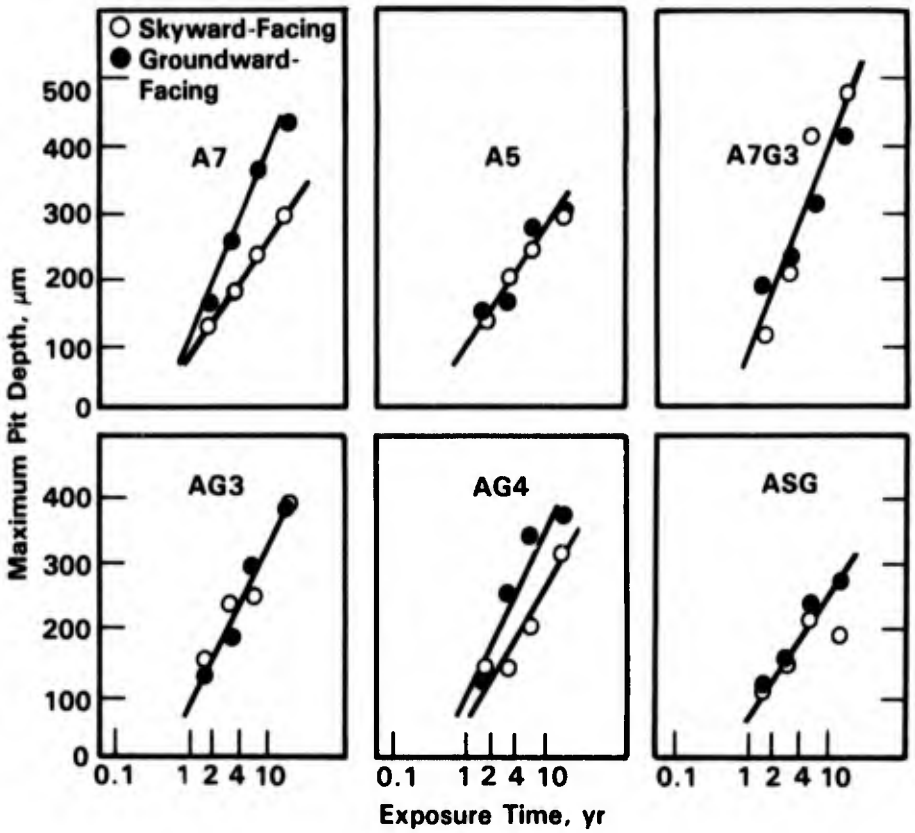

FIGURE 2-4. MAXIMUM MEASURED PIT DEPTH VERSUS PERIOD OF EXPOSURE OF SIX DIFFERENT ALUMINUM ALLOYS EXPOSED NEAR ALICANTE, SPAIN[2] (SEE FIGURE 2-2 FOR ALLOY DESIGNATION)

contained deeper pits than the surface facing the sky. This was attributed to rainwater washing over the surface facing the sky and to the fact that this surface dried more readily.

The metallurgical condition plays an important role in the pitting resistance of aluminum alloys. A thirty year study in Salins de Giraud by M. Lashermes, et al.[10] indicated that for nonheat-treatable alloys such as the 1000, 3000, and 5000 series aluminum alloys, the resistance to pitting corrosion increases with work hardening (see Figure 2-5). The annealed condition is designated by (0), the semi-hard conditon by (H14) and the fully hardened condition by (H18). In the work hardened condition (H14 and H18) resistance to pitting is similar for several alloys and the pit depth does not exceed 0.5 mm (see Alloy 1070-H14 in Figure 2-5). In the annealed (0) or slightly work hardened condition (H14) larger differences between the alloys were observed. The 3003 and 1199 alloys were more resistant than 5056, 1070, or 1200. The maximum pit depths measured were 0.2 mm for 3003-0 and 0.63 mm for 1070-0.

Characteristics of Aluminum Samples Exposed for Long Periods in Salins de Giraud, France (see Figure 2-5)[10]

Alloy	Condition	Composition, weight percent							Date Exposed	Years Exposed	Number of Samples for Each Condition
		Fe	Si	Cu	Mn	Mg	Zn	Ti			
1199	O[a]										
	H14[b]	0.002	0.002	0.005					1958	21	2
	H18[c]										
1070	O										
	H14	0.12	0.09	0.02	0.04	<0.001		0.004	1958	21	1
	H18										
1200	O										
	H14	0.5	0.12	0.003	0.013	<0.005			1958	21	2
	H18										
2014	T4[d]	0.38	0.88	4.15	0.9	0.5		0.15	1956	23	2
	T6[e]										
3003	O	0.57	0.17	0.2	1.2				1950	20	4
	H18										
5005	H14	0.4	0.15	0.05	0.07	0.62	0.02	0.07	1962	17	1
	H18										
5754	H18	0.3	0.17	0.1	0.38	2.8				25	1
5056 A	O										
	H12	0.18	0.08	0.026	0.39	5.2			1957	22	2
	H14	0.31	0.13	0.08	0.52	5.3			1954	25	1
6061	T4	0.17	0.53	0.31	0.1	0.98	0.27	0.09	1960	19	2
	T6										
6082	T4	0.32	1.07	<0.01	<0.1	0.95			1960	19	2
	T6										
6181	T4	0.32	1.07	<0.01	1.02	0.99			1960	19	3
	T6										

(a) Annealed.
(b) Half hardened.
(c) Fully hardened.
(d) Naturally aged temper.
(e) Artificially aged temper.

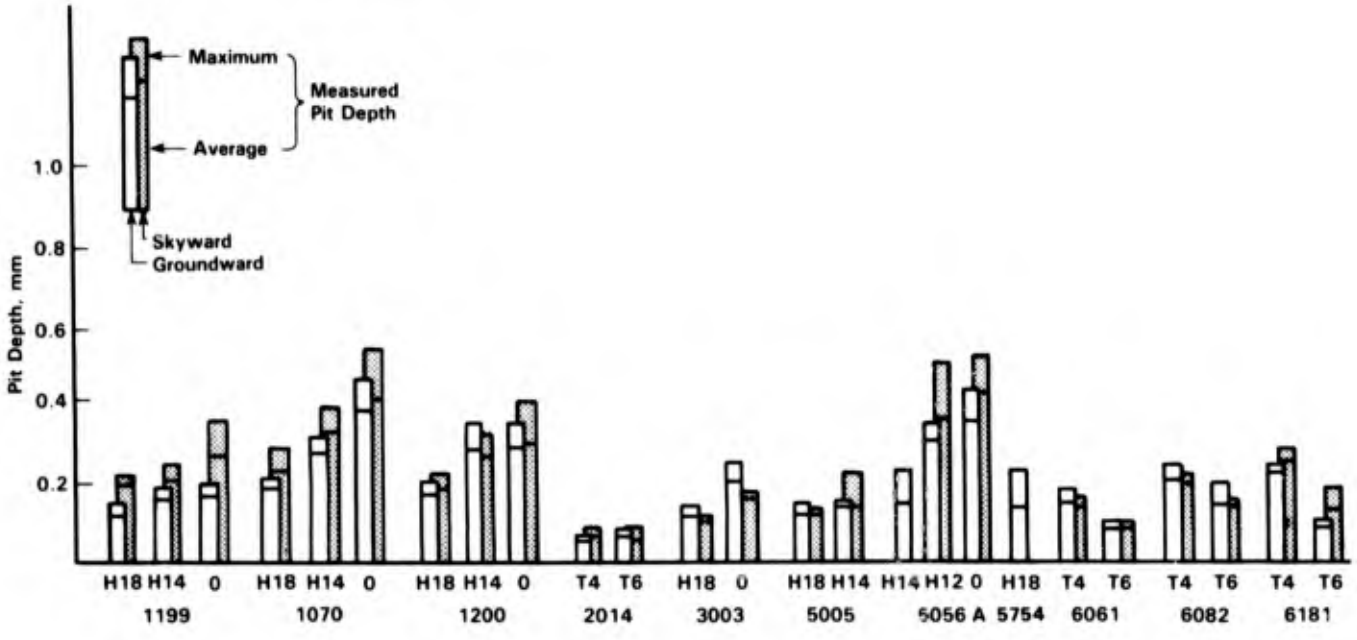

FIGURE 2-5. MAXIMUM AND AVERAGE DEPTHS OF PITS IN ALUMINUM ALLOYS EXPOSED IN SALINS DE GIRAUD, FRANCE, FOR UP TO TWENTY-FIVE YEARS[10]

Of the heat-treatable alloys, 2000 and 6000 series showed resistance to pitting comparable to that of the nonheat-treatable alloys. In particular, aluminum Alloy 2014 only showed very minor pitting. Figure 2-5 indicates that, in general, the T6 condition provides better pitting resistance than the T4 condition.

Galvanic Corrosion

Galvanic corrosion of aluminum alloys may occur when they are joined in metal-to-metal contact to other more noble materials. Table 2-8, which shows the galvanic series of a range of materials commonly used in marine environments, indicates that aluminum is active to most other materials.

Five year exposure tests of galvanic couples of 6061-T6 and 7075-T6 with various alloys were performed in a marine environment at the U.S. Army Tropical Testing Station, Panama Canal Zone.[18-20] The results, shown in Table 2-9, indicate very low corrosion rates of the aluminum alloys even when coupled to titanium. Fifteen year exposure tests were performed in a marine atmosphere at Bohus Malmon exposing different aluminum alloys (Al99.5, AlMn1, AlSiMg, AlCu4Mg1, AlMg2.5, AlSi12, and AlSi5Cu3) coupled with copper, steel, stainless steel, and zinc.[21] The results of the marine exposure tests after 1 and 15 years are compared with exposure to rural and urban environments in Table 2-10. Since the corrosion rates of the different aluminum alloys were very similar, Table 2-10 shows the average rates of the alloys. This long term test indicated a significant increase in corrosion rate of the aluminum alloys when coupled to more noble metals. In particular, coupling to Cu resulted initially in an order of magnitude increase in the corrosion rate of aluminum. However, in all cases, the corrosion rate decreased with time, likely as a result of the formation of corrosion product on the aluminum surface which would reduce the galvanic current. Zinc, which is more active than aluminum, provided effective cathodic protection. The low corrosion rate observed in the tropical marine environment in the Panama Canal Zone may be attributed to rapid initial formation of corrosion products which insulated the aluminum alloys from the more noble materials.

Advanced graphite epoxy (Gr/Ep) composites have become an important structural material for aerospace applications. Since contact between Gr/Ep composites and aluminum components is unavoidable, galvanic corrosion is of great concern. To secure the various Gr/Ep components such as wing skins to spars and ribs, thousands of fasteners are needed.[22-24] Exposure tests of aluminum fasteners (Al 2117) in intimate contact with Gr/Ep in a 5 percent salt spray environment resulted in rapid corrosion of the aluminum after only 24 hours.[23] Organic type paint coatings, zinc chromate primer followed by application of a

TABLE 2-8. GALVANIC SERIES IN FLOWING WATER (13 ft/sec) AT ABOUT 75 F (23.9 C)[17]

Material	Steady State Electrode Potential, V(SCE)
Graphite	+0.25
Platinum	+0.15
Zirconium	-0.04
Type 316 Stainless Steel (Passive)	-0.05
Type 304 Stainless Steel (Passive)	-0.08
Monel 400	-0.08
Hastelloy C	-0.08
Titanium	-0.10
Silver	-0.13
Type 410 Stainless Steel (Passive)	-0.15
Type 316 Stainless Steel (Active)	-0.18
Nickel	-0.20
Type 430 Stainless Steel (Passive)	-0.22
Copper Alloy 715 (70-30 Cupro-Nickel)	-0.25
Copper Alloy 706 (90-10 Cupro-Nickel)	-0.28
Copper Alloy 442 (Admiralty Brass)	-0.29
G Bronze	-0.31
Copper Alloy 687 (Aluminum Brass)	-0.32
Copper	-0.36
Alloy 464 (Naval Rolled Brass)	-0.40
Type 410 Stainless Steel (Active)	-0.52
Type 304 Stainless Steel (Active)	-0.53
Type 430 Stainless Steel (Active)	-0.57
Carbon Steel	-0.61
Cast Iron	-0.61
Aluminum 3003-H	-0.79
Zinc	-1.03

TABLE 2-9. ATMOSPHERIC EXPOSURE CORROSION RATES (mm/yr)[a] OF ALUMINUM ALLOYS 6061-T6 AND 7075-T6 COUPLED TO SEVERAL OTHER MATERIALS EXPOSED IN THE PANAMA CANAL ZONE[18]

Alloy	Exposure Time, months	Mg	Stainless Steel	Steel	6061Al	7075Al	Brass	Monel	Titanium
6061-T6 Aluminum	2	0.002	0.006	0.005	0.002	0.002	0.006	0.005	0.005
	4	0.001	0.002	0.006	0.002	0	0.004	0.002	0.002
	8	0.001	0.001	0.004	0.001	0.001	0.002	0.001	0.002
	15	0	0.002	0.006	0.001	0.001	0.003	0.003	0.003
	24	0	0.003	0.007	0.001	0.001	0.007	0.003	0.003
	36	0	0.002	0.007	0.001	0.001	0.004	0.004	0.002
7075-T6 Aluminum	2	0.003	0.007	0.009	0.005	0.003	0.010	0.007	0.007
	4	0.002	0.005	0.005	0.002	0.003	0.004	0.003	0.004
	8	0.001	0.003	0.004	0.001	0.001	0.003	0.003	0.003
	15	0	0.003	0.016	0.002	0.001	0.005	0.003	0.003
	24	0	0.003	0.012	0.002	0.001	0.010	0.003	0.004
	36	0.001	0.003	0.007	0.001	0.003	0.005	0.003	0.003

(a) Essentially zero corrosion rate for the 316 stainless steel, 400 Monel, and Titanium 6Al-4V specimens.

TABLE 2-10. ATMOSPHERIC CORROSION RATE OF ALUMINUM COUPLED TO DIFFERENT METALS IN THE THREE DIFFERENT ATMOSPHERES[21]

Al Coupled With Metals	Mean Corrosion Rate, mg/yr					
	Rural (Ryda, Sweden)		Urban (Stockholm, Sweden)		Marine (Smögen, Sweden)	
	1 Yr	15 Yr	1 Yr	15 Yr	1 Yr	16 Yr
Al (Normal Corrosion)	1.3	0.6	2.4	0.9	28	7.6
Cu	11	6.1	24	4.2	313	79
Fe	5.4	2.0	9.3	1.5	187	41
Stainless Steel	4.1	1.9	8.4	2.6	120	21
Zn	2.0	0.5	1.4	0.13	3	0.3

strontium chromate-epoxy polyamide primer silicone primer, followed by application of an appropriate organic top coat to a total thickness of 2 mils offered protection for aluminum fasteners.[23] No evidence of corrosion was found after 504 hours salt spray exposure.

Other applications include graphite/aluminum metal matrix composites (Gr/Al MMC) which are potential structural materials for aerospace needs. The materials combine low weight with increased strength and modulus. Again, galvanic corrosion as a result of the potential difference between the graphite fibers and the aluminum matrix is a reason for concern. Different types of composites are Gr/Ep skin-aluminum honeycomb sandwich,[24,25] graphite fiber/epoxy core with aluminum skin,[26,27] and composites where graphite fibers are embedded in an aluminum matrix.[26,28] Vassilaros[26] showed extensive corrosion of Gr/Al test panels after 6 and 12 week exposure to marine environments, which was attributed to galvanic corrosion of the core after penetration of aluminum surface foils. Also, extensive edge corrosion was observed. Figure 2-6 shows a schematic illustration of the different types of corrosion attack observed. It was concluded that appropriate surface treatment of surface foils was needed for the Gr/Al composite to be resistant to marine environments. Subsequent work by Aylor, et al.[28] indicated that sulfuric acid anodizing of the surface foil provided adequate corrosion protection whereas electroless nickel plating did not.

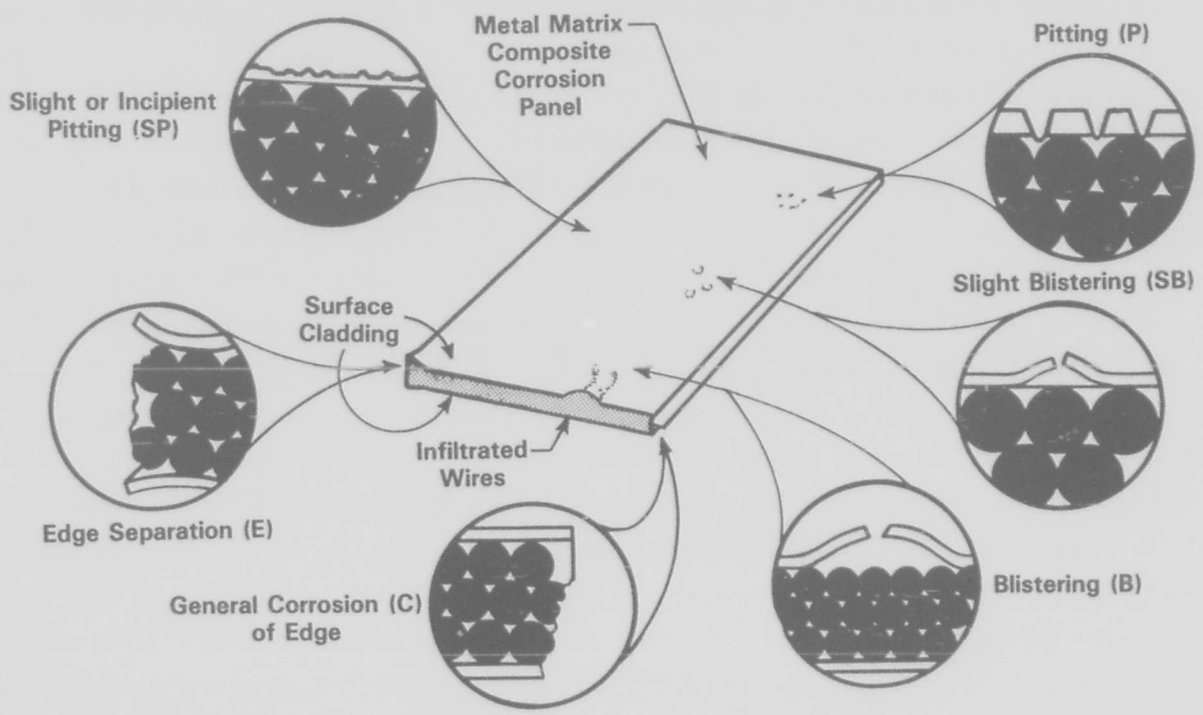

FIGURE 2-6. SCHEMATIC ILLUSTRATION OF TYPES OF CORROSION ATTACK OBSERVED IN GRAPHITE/ALUMINUM METAL MATRIX COMPOSITES[26]

Stress-Corrosion Cracking

Aluminum and its alloys can fail by cracking intergranularly when simultaneously exposed to marine environments and stresses of sufficient magnitude. Although stress-corrosion cracking (SCC) has occurred frequently in atmospheric environments, most information is obtained from exposures and experiments in aqueous environments. Therefore, the parameters which affect stress-corrosion cracking of aluminum alloys are discussed in the section on aqueous marine environments. Results of exposure tests in marine atmosphere are discussed in this section.

In marine environments, many aluminum alloys, in particular the high strength aluminum alloys, can fail at stresses far below the yield stress, due to SCC. Smooth SCC test specimens of various aluminum alloys have been exposed in stressed conditions to both marine and inland industrial atmospheres. Typical results are shown in Figure 2-7. Note that in the marine atmosphere, all the alloys listed seem to have the same smooth-specimen threshold stress of 7 ksi. However, in the inland industrial atmosphere, Alloy 7079-T6 cracked at the lowest stress levels, which is consistent with the service behavior of the alloy. The probability of failure of smooth SCC specimens in several environments is shown in Figure 2-8. Again, Alloy 7079-T6 showed a significant high percentage of failures in an industrial atmosphere when stressed to only 15 percent of the yield strength.

Typical results of a one year sea coast exposure of smooth tensile specimens of different high strength aluminum alloys are presented in Table 2-11. The tensile specimens were taken from the short transverse grain direction of the aluminum plate, which is the direction most susceptible to SCC, and stressed up to 100 percent of their yield strengths. Aluminum Alloys 2048-T851, 2214-T87, 7049-T7351, 7050-T73651, 7075-T7351, and 7475-T7351 exhibited very high resistance to SCC with no SCC failures at stresses of 75 or 100 percent of their short transverse yield strengths. Alloys 2024-T851 and 2124-T851 exhibited moderate resistance to SCC with failures occurring when stressed to 75 percent of their yield strengths, and 2024-T351 and 7075-T651 were highly susceptible to SCC.

Alternatively, the susceptibility to SCC can also be determined by crack propagation in precracked specimens. The important parameters in these studies are the threshold stress intensity factor (K_{Iscc}) and the crack velocity. Sprowls, et al.[31] studied the SCC susceptibility of aluminum alloy using fracture mechanics techniques. Table 2-12 shows the crack velocities in a sea coast environment (Point Judith, Rhode Island) of double cantilever beam (DCB) bolt specimens in the short transverse direction of aluminum alloys with low and high resistance to SCC.

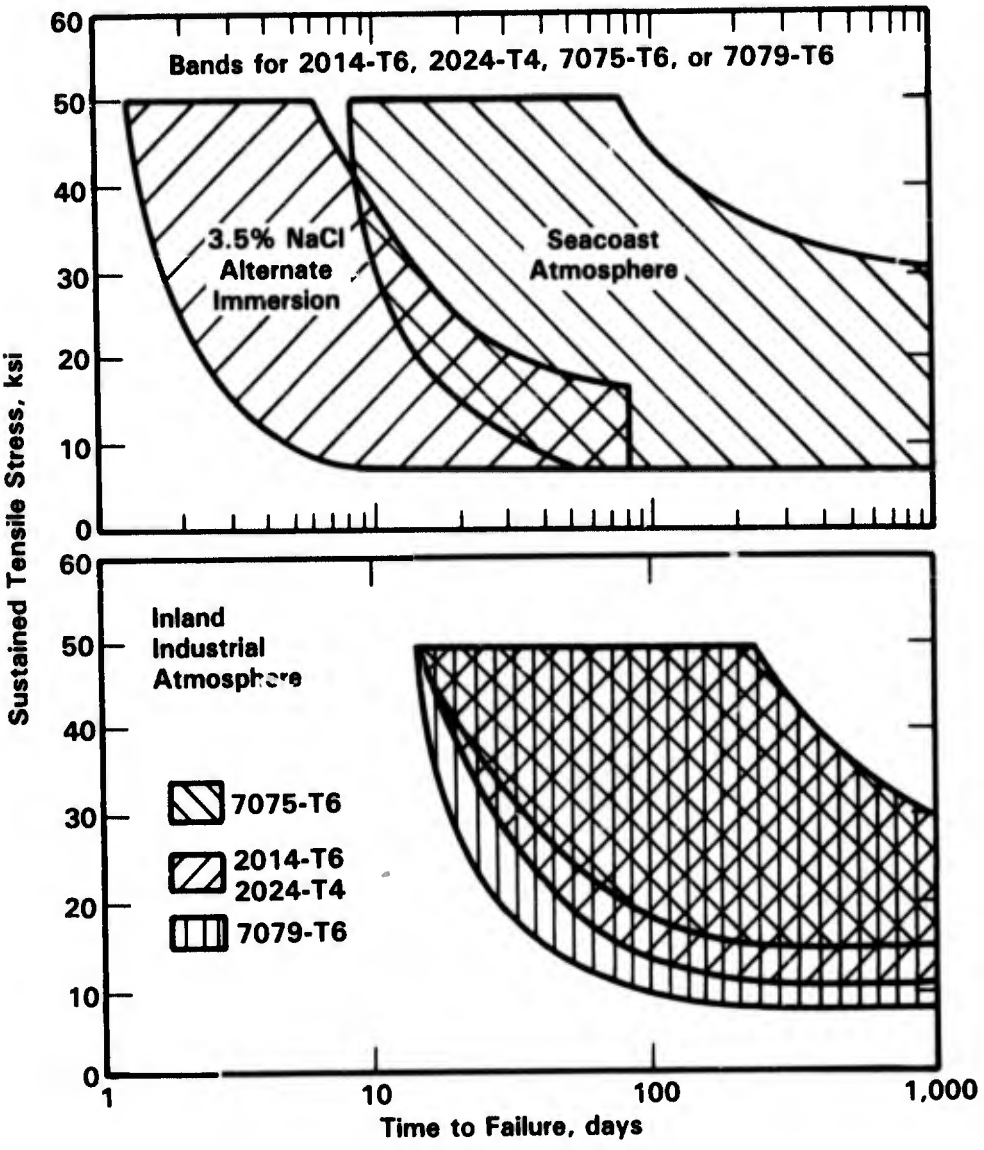

FIGURE 2-7. TIME TO FAILURE BY STRESS-CORROSION CRACKING OF SMOOTH SPECIMENS STRESSED IN THE SHORT TRANSVERSE DIRECTION AND EXPOSED TO THREE DIFFERENT ENVIRONMENTS[29]

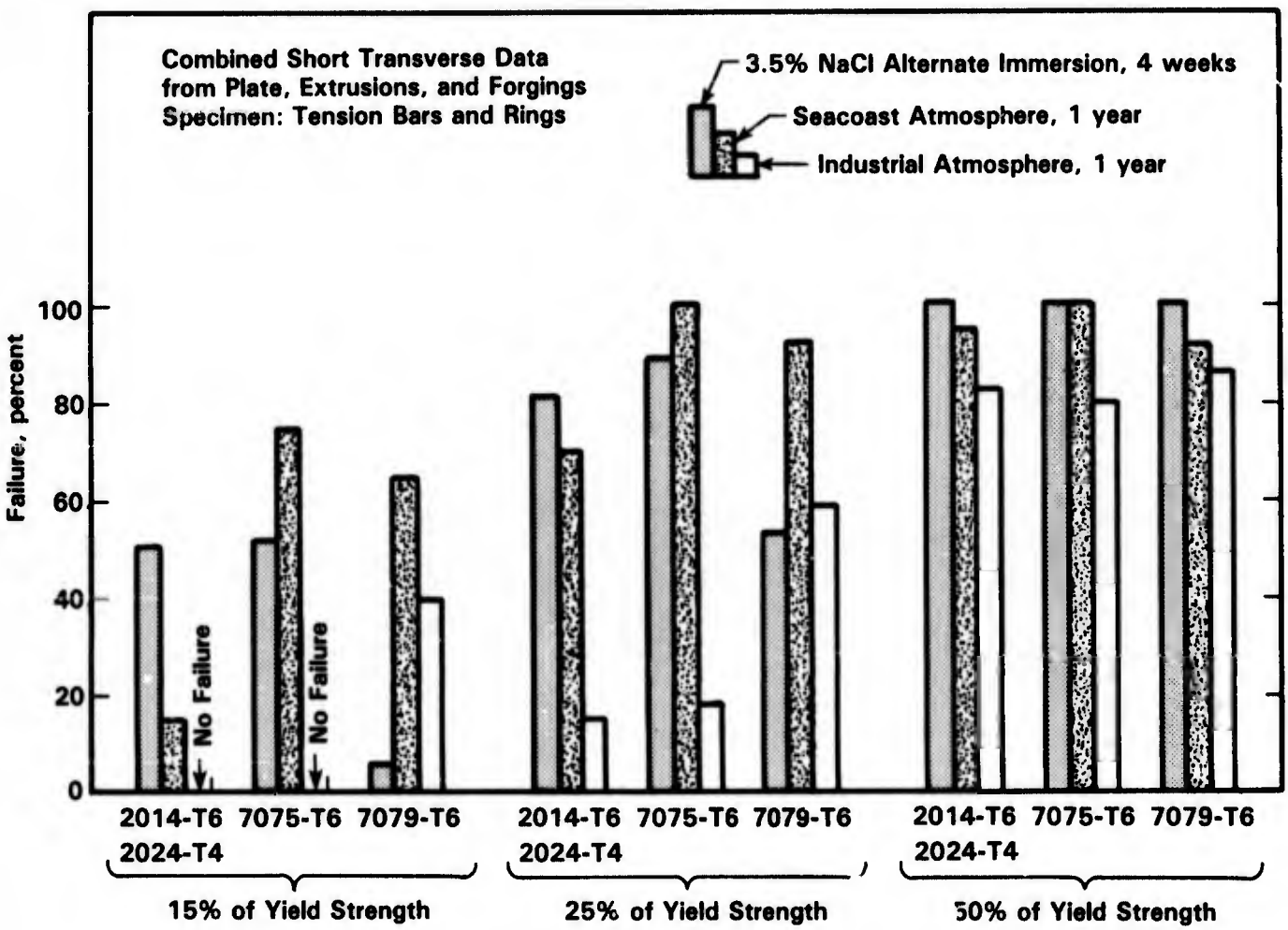

FIGURE 2-8. COMPARISON OF THE PROBABILITY OF FAILURE BY STRESS-CORROSION CRACKING OF SMOOTH SPECIMENS IN SEVERAL ENVIRONMENTS[29]

TABLE 2-11. COMPARISON OF SCC RESULTS OF ALUMINUM ALLOYS EXPOSED TO THE SEACOAST AND ALTERNATE IMMERSION IN SALT WATER AND SEAWATER[a][30]

Alloy Plate Thickness, cm (Source #)[b]	Applied Stress MPa	ksi	YS, percent	Seacoast (Kure Beach, NC) F/N[c]	Time, months	Salt Water F/N[c]	Time, months	Seawater F/N[c]	Time, months
2024-T351	75	11	25	4/5	0.1, 0.3, 12, 16	4/6	0.4, 0.8, 1.3, 1.5	3/3	0.1, 0.2, 1.2
10 cm	150	22	50	5/5	0.1(5)[e]	5/5	0.1(4), 0.8	3/3	0.1(3)
(MS)									
2024-T851	215	31	50	0/5		3/3	0.5, 0.7, 0.8	1/3	2.5
6.4 cm	320	46.5	75	5/5	4.5, 5, 10, 22	3/3	0.3, 0.5, 0.5	3/3	2.3, 2.3, 2.5
(KA)									
2124-T851	215	31	50	0/5		3/3	1.4, 2.6, 2.6	0/3	
5 cm	320	46.5	75	1/5	5	3/3	0.2, 0.9, 0.9	0/3	
(RM)									
2124-T851	205	29.5	50	0/4					
6.4 cm	305	44	75	4/5	4.5, 5, 12				
(KA)									
2124-T851	200	28.5	50	0/5					
10 cm	295	43	75	0/5		2/2	0.9, 1.0	0/3	
(KA)									
2048-T851	210	30.5	50	0/5		2/3	1.3, 3	0/3	
5 cm	315	46	75	3/5	27, 28, 29	3/3	0.4, 4.1, 4.1, 4	0/3	
(RM)									
2219-T87	275	40	75	2/5	25, 25	3/17[d]	0.7, 0.8, 0.9	0/4	
5 cm	365	53	100	5/5	5, 13, 14, 14, 14	0/6[d]		0/3[d]	
(MS)									
7049-T7351	205	29.5	50	0/8					
7.6 cm	305	44	75	3/8	28, 28, 30	2/3	1.7, 1.8	0/3	
(KA)	405	59	100	7/8	14, 16, 20(3), 36, 38	3/3	1.5, 1.6, 1.7	0/3	

TABLE 2-11. (Continued)

Alloy Plate Thickness, cm (Source #)[b]	Applied Stress MPa	ksi	YS, percent	Seacoast (Kure Beach, NC) F/N[c]	Time, months	Salt Water F/N[c]	Time, months	Seawater F/N[c]	Time, months
7075-T73651	210	30.5	50	0/8		0/3		0/3	
5 cm	315	46	75	0/8		2/3	2.9, 2.9	0/3	
(AC)	420	61	100	2/8	28, 34	3/3	2.9(3)	0/3	
7075-T73651	180	26	45	0/8					
7.6 cm	265	39	65	1/8	27	2/3	1.8, 2.1	0/3	
(KA)	345	50	85	0/8		3/3	1.8, 2.6, 2.6	0/3	
7075-T651	110	16	25	5/5	0.2(4), 0.6	9/9	0.1(3), 0.2(4), 0.5, 0.8	9/9	0.1(4), 0.2(4), 0.3
6.4 cm	220	32	50	4/4	0.1(4)	6/6	0.1(5), 0.2	6/6	0.1(6)
(MS)									
7075-T7351	205	29.5	50	0/8					
6.4 cm	305	44	75	0/8					
(AC)	405	59	100	2/7	25, 35				
7075-T7351	210	30.5	60	0/8					
7.6 cm	300	43	85	0/8		2/3	1.5, 2.1	0/3	
(KA)	350	51	100			1/3	2.8	0/3	
	405	59	115	0/8					
7475-T7351	305	44	75	0/5		1/3	2.9	0/3	
5 cm	405	59	100	0/5		2/3	1.7, 2.9	0/3	
(AC)									
7475-T7351	185	27	50	0/7					
7.6 cm	280	40.5	75	0/8		0/3		0/3	
(KA)	370	54	100	0/8		1/3	2.6	0/3	

(a) Total exposure was until failure or 38 months (18 months for 2024-T31 and 7075-T651) for seacoast and three months for Al in salt and seawater.
(b) AC - Alcoa, KA - Kaiser, MS - MSFC, RM - Reynolds.
(c) F/N - Ratio of number of specimens that failed to number exposed.
(d) Total exposure of one month.
(e) Number in parenthesis is the number of specimens that failed in the given time.

TABLE 2-12. STRESS-CORROSION CRACK VELOCITY IN ALUMINUM ALLOYS EXPOSED TO VARIOUS ENVIRONMENTS.[31] SHORT TRANSVERSE (ST) DOUBLE CANTILEVER BEAM SPECIMENS WERE BOLT LOADED TO POP-IN

	Average Initial Crack Velocity, in./hr	
	Outdoor Atmosphere[a]	
Alloy	Seacoast (Point Judith, RI)	Industrial
Alloys with High Resistance to Stress-Corrosion Cracking		
5456-H117	0	0
6061-T651	0	0
7075-T7351	0	0
2219-T87	4×10^{-5}[b]	1×10^{-5}[b]
2021-T81	7×10^{-5}[b]	2×10^{-5}[b]
2024-T851	1×10^{-5}[b]	4×10^{-6}[b]
Alloys with Low Resistance to Stress-Corrosion Cracking		
2014-T651	2×10^{-4}	2×10^{-4}
2024-T351	2×10^{-4}	2×10^{-4}
2219-T37	3×10^{-4}	3×10^{-4}
7075-T651	2×10^{-4}	1×10^{-4}
7039-T6351	2×10^{-4}	3×10^{-4}
7079-T651	4×10^{-4}	4×10^{-4}
5456-Sens.	5×10^{-4}	5×10^{-5}

(a) Based on the first six months of exposure.
(b) Transgranular mechanical fracture rather than intergranular SCC.

The table indicates that the performance of the resistant alloys was markedly superior to that of the low resistance alloys. No crack growth was observed on specimens of 5456-H117 and 6061-T651 after 24 months' exposure. The other 4 alloys showed small amounts of crack growth that initiated in 3 to 8 months. However, metallographic examination revealed the cracking to be intergranular SCC only in the case of 7075-T7351 and transgranular tensile fracture in the case of 2021-T81, 2024-T851, and 2219-T87.

It was further noticed that corrosion products formed in the cracks, which resulted in so-called self loading. This can significantly increase the stress-intensity factor at the crack tip

and be a potential driving force for SCC of moderately susceptible alloys. Studies by Dorward, et al.[32] of 2000 and 7000 series aluminum alloys at a marine-atmosphere exposure site near Daytona Beach, Florida, indicated that the self loading is enhanced by copper but is not limited to copper-bearing alloys. The copper-free Alloy 7039-T64, for example, showed self loading effects after 3 to 4 years exposure. Naturally aged 2000 series alloys and peak aged, copper containing 7000 series alloys were most sensitive to self loading, usually showing the effects within six months.

Intergranular Corrosion

Intergranular corrosion of aluminum alloys can seriously affect their strength. Susceptibility to intergranular corrosion, which is parallel to the susceptibility to stress-corrosion cracking, strongly depends on alloy composition, heat treatment, and grain orientation. A common form of intergranular corrosion is exfoliation which occurs in plates or forgings where intergranular attack occurs along elongated grains and subsequent formation of corrosion products lifts the metal surface. Some alloys are extremely prone to attack where machining occurs across the grain of the material.

The exfoliation performance of 7000 series alloys was evaluated at two sea coast locations, one at Point Judith, Rhode Island, and another at Daytona Beach, Florida.[33,34] After 11 years of exposure the 7075-T73 did not show, and 7075-T76, and 7178-T76 showed very little exfoliation corrosion. Relatively short term (3 years) exposure indicated similar excellent performance of the T76, T736, and T73 tempers of the newer Alloys 7049 and 7050.

Shipboard exposure tests by Jankowski, et al.[35,36] were performed to study the combined effect of stack gas exhaust and sea spray on the corrosion of aluminum alloys. Table 2-13 lists the different aluminum alloys and tempers in a range of expected resistance to exfoliation corrosion. The results of the tests presented in Table 2-14 indicated that the naturally aged type T3 temper of the 2124 plate was susceptible to exfoliation, whereas the artificially aged T8 temper was resistant. Further, it could be concluded from this work that an increase in ambient temperature resulted in more severe corrosion and that the environment of an aircraft carrier, however powered, was considerably more corrosive than sea coast or industrial environments (see Figure 2-9).

The aluminum-magnesium Alloys 5086, 5083, and 5456 are widely used for naval construction because of their resistance to marine corrosion, high strength-to-weight ratio, and weldability. The alloys have been used for light weight super structures and as primary structural metal for high-speed, high-performance ships and craft. The most desirable combination of properties is achieved in a mildly cold-worked temper designated as 5086-H32,

TABLE 2-13. ALUMINUM ALLOYS USED FOR SHIPBOARD EXFOLIATION TESTS ON THREE CARRIERS[36]

Alloy/Form	Temper	Thickness, mm (in.)	Expected Resistance to Exfoliation	Dimensions, mm (in.)
2124 Plate	T851	12.2 (0.5)	High	76 x 152 (3 x 6)
	T351		Intermediate	
	T351 + 0.5 hours at 375 F		Low[a]	
	T851	50.8 (2.0)	High	
	T351		Intermediate	
	T351 + 0.5 hours at 375 F		Low	
7075 Extrusion		12.2 (0.5)	High	76 x 76 (3 x 3)
			Intermediate	
			Low[a]	
7178 Sheet	T6	2.3 (.091)	Low	76 x 152 (3 x 6)
	T6 + 10 hours at 325 F		Intermediate	
	T6 + 11 hours at 325 F		High	

(a) Only these two materials were exposed on the third carrier.

TABLE 2-14. RESULTS OF EXFOLIATION TEST ACCORDING TO ASTM G34-79[a] ON THREE CARRIERS[36]

	Conventional Carrier Mediterranean (50-65 F)		Nuclear Carrier Indian Ocean (80-95 F),	Third Carrier (Conventional),
	4 Months	8 Months	10 Months	8 Months
2124, 0.5-inch Plate				
Low Resistance				
T/10	EA	ED	ED	ED
T/2	EA	EC	ED	ED
Intermediate Resistance				
T/10	EA	EC	ED	
T/2	P	P	EC	

TABLE 2-14. (Continued)

	Conventional Carrier Mediterranean (50-65 F)		Nuclear Carrier Indian Ocean (80-95 F),	Third Carrier (Conventional),
	4 Months	8 Months	10 Months	8 Months
High Resistance				
T/10	P	P	P	
T/2	P	P	P	
2124, 2-inch Plate				
Low Resistance				
T/10	EB	ED	ED	
T/4	EB	ED	ED	
T/2	EA	EC	ED	
Intermediate Resistance				
T/10	P	P	EB	
T/4	EA	EC	EC	
T/2	EA	EC	ED	
High Resistance				
T/10	P	P	P	
T/4	P	P	P	
T/2	P	P	P	
7075, 0.5-inch Extrusion				
Low Resistance				
T/10	EB	ED	ED	EC
T/2	EA	EB	EC	EB
Intermediate Resistance				
T/10	EA	EB	EB	
T/2	P	P	EA	
High Resistance				
T/10	P	P	P	
T/2	P	P	P	
7178, 0.091-inch Sheet				
Low Resistance				
T/10	EA	ED	ED	
Intermediate Resistance				
T/10	P	P	P, EB	
High Resistance				
T/10	P	P	P	

(a) P--Pitting; Exfoliation Ratings: EA--Slight, EB--Moderate, EC--Severe, ED--Very Severe.

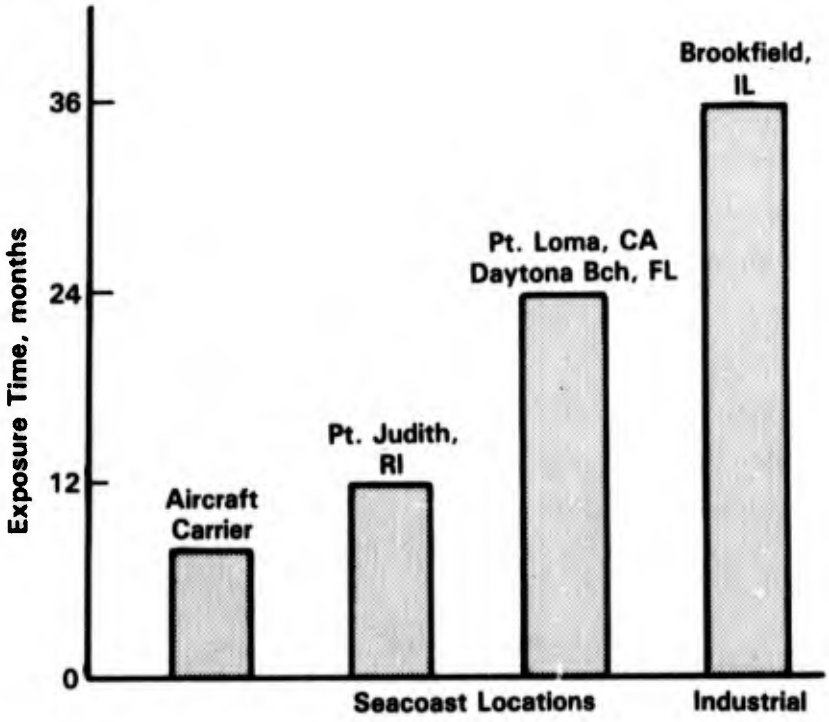

FIGURE 2-9. TIME REQUIRED AT VARIOUS MARINE AND INDUSTRIAL SITES TO PRODUCE SEVERE EXFOLIATION IN 0.5 INCH THICK ALUMINUM 2124 PLATE HEAT TREATED TO BE SUSCEPTIBLE TO EXFOLIATION[36]

5083-H321, and 5456-H321. However, under certain conditions, exfoliation corrosion problems have been experienced with the standard temper. To solve the exfoliation problem, the aluminum industry developed rolling procedures for tempers meeting the mechanical property requirements specified for the H32 and H321 tempers and having a structure which is resistant to exfoliation corrosion.[37,38] These tempers for sheet and plate 5000 series alloys are designated H116 (Reynold Metals Company), and H117 (Alcoa). Czyryca and Hack[39] performed studies exposing the exfoliation resistant tempers to three marine environments at Wrightsville Beach, NC, for periods of 6 months, 1 year, and 2 years. The results of 2 years of exposure to the marine environments (marine atmosphere, splash and spray, and fully submerged in seawater) indicated that Alloys 5086, 5083, and 5456 in the H116 and H117 tempers have good corrosion resistance. No exfoliation attack was evident on any of the test panels.

SPLASH AND TIDE

The weight loss for aluminum alloys under tide exposure levels tends to be intermediate between the low atmospheric weight loss and the somewhat higher values observed under fully immersed conditions. Data for 1, 8, and 16-year exposures of two aluminum alloys are given in Table 2-15. On the other hand, Table 2-15 shows that pit depths tend to be greater under tide exposure than those observed under either atmospheric or immersed exposure. Since the average penetration rates are calculated from weight loss, the majority of weight loss for a passive material such as aluminum can be attributed to pitting. Thus, one can interpret the data in Table 2-15 to suggest that initiation of pits in the tide zone is somewhat less likely than under submerged conditions, but once pits initiate, they propagate at higher rates in the tide zone. Comparison of the data in Table 2-15 for the two alloys studied, 6061 and 1100, indicates that the 6061 alloy is marginally more resistant to pitting attack than the 1100 alloy in the tide zone. These data are plotted in Figure 2-10.

IMMERSION

General Corrosion

Effect of Alloy Composition

Aluminum alloys usually have good resistance to general corrosion in seawater environments. In particular, Al-Mg (5000 series) and Al-Mg-Si (6000 series) are widely used for seawater application. Exposure studies by Reinhart and Jenkins[41] in the Pacific Ocean have shown that the corrosion rates of these alloys, based on weight loss, were less than 3 mpy. Figure 2-11 shows the average calculated corrosion rates of different 5000 series alloys tested in the Pacific Ocean.[41] It should be noted at this point that breakdown of the aluminum oxide film is usually local and corrosion in seawater is often in the form of pitting. Thus, the weight loss measured is, for the most part, due to pitting or crevice corrosion. However, the alloying elements discussed in this section have been shown to affect general corrosion as well as pitting.

A study by Beberdick[42] comparing Al-Mg alloys to 7075-T6 in a 3.5 percent NaCl environment indicated that the binary 8 percent Mg and 10 percent Mg alloys are highly resistant to general corrosion. Alloying with Cu (0.4 weight percent), and Cu and Mn (0.4 and 0.5 weight percent) to reduce the tendency to intergranular corrosion, was found to result in

TABLE 2-15. CORROSION OF ALUMINUM ALLOYS EXPOSED 16 YEARS IN THREE ENVIRONMENTS IN THE PANAMA CANAL ZONE[40]

	Average Penetration[a], mils			Depth of Pitting[b], mils						Tensile Strength Loss %[c],	Type of Corrosion Attack[d],
				Average of 20 Deepest Pits			Deepest Pits				
	1 Yr	8 Yr	16 Yr	1 Yr	8 Yr	16 Yr	1 Yr	8 Yr	16 Yr	8 Yr	16 Yr
Alloy 1100											
Immersion											
Seawater	0.8	0.61	0.97	9 (13)	11	17	15	19	33	2	J
Mean Tide	0.06	0.31	0.53	11 (9)	14	39	29	37	67	1	J, Q
Atmospheric											
Marine	0.01	0.02	0.11	N	N	N	N	N	N	0	A
Alloy 6061											
Immersion											
Seawater	0.28	0.73	0.91	N	23	14	N	49	79	0	J
Mean Tide	0.04	0.13	0.29	N	N	17	N	N	41	0	J
Atmospheric											
Marine	0.03	0.03	0.11	N	N	N	N	N	N	1	A

(a) Calculated from weight loss and specific gravity.
(b) Represents depth of penetration from original surface; N - measurable pits; number in parentheses gives number of measurable pits when less than 20.
(c) Percent change in tensile strength calculated on basis of 1/4-inch-thick metal and average of four tests for underwater specimens, and 1/16-inch-thick metal and average of three tests for atmospheric specimens.
(d) A - uniform attack; J - marine fouling contact; Q - pitting attack (random).

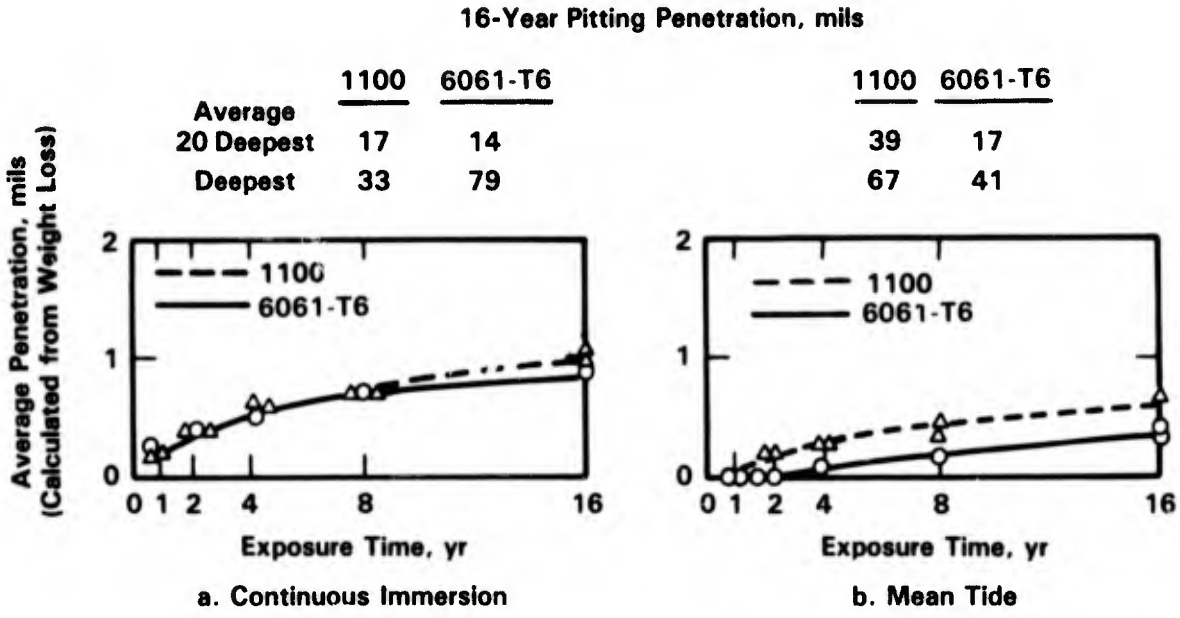

FIGURE 2-10. COMPARISON OF ALUMINUM ALLOY 6061-T6 WITH COMMERCIALLY PURE 1100 ALUMINUM FOR 16 YEARS OF EXPOSURE IN SEAWATER ENVIRONMENTS[40]

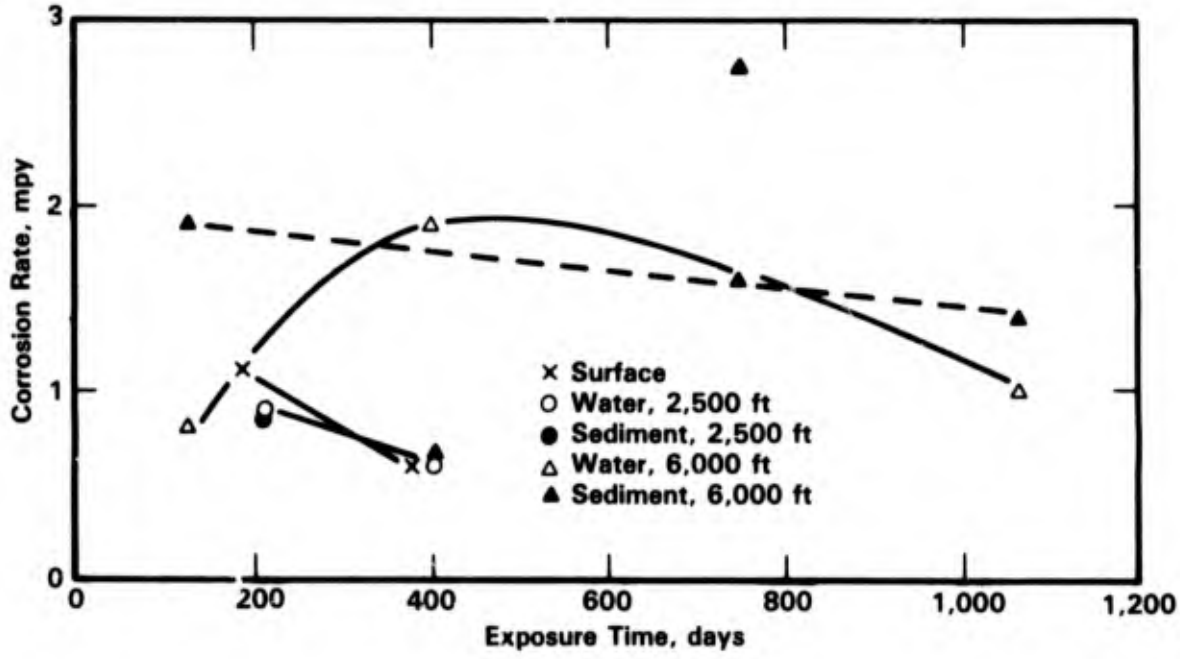

FIGURE 2-11. AVERAGE CORROSION RATES OF VARICUS 5000 SERIES ALUMINUM ALLOYS AT THE SURFACE AND AT DIFFERENT DEPTHS IN THE PACIFIC OCEAN NEAR PORT HUENEME, CA[41]

an increase in the weight loss over the binary alloys but the weight loss of the Cu and Mn containing alloys was less than that of 7075-T6 (see Figure 2-12).

On the other hand, Mondolfo[43] showed that addition of Cu to Al-Mg alloy at concentrations less than 0.2 weight percent improved general corrosion as well as pitting resistance. This apparent discrepancy may be explained in terms of the formation of an Al-Mg-Cu intermetallic phase which forms above a Cu concentration of 0.2 weight percent. It was hypothesized that this phase could render the alloy more susceptible to general corrosion.

Zinc additions to aluminum alloys decrease the tendency for localized attack and promote general corrosion.[44] Zinc is used as an alloy addition in aluminum Alloy 7072, which is used as a sacrificial anode. A successful application of this alloy is cladding over Al 3003 or 3004.

Zamin[45] showed that Fe had a detrimental and Mn had a beneficial effect on general corrosion as well as pitting of Al containing 0.4-1.2 percent Mn, 0.4-0.8 percent Fe, 0.15 percent Si, and a small amount of Mg. The beneficial effect of Mn was explained in terms of it reducing the difference in electrochemical potential between the matrix and the intermetallics.

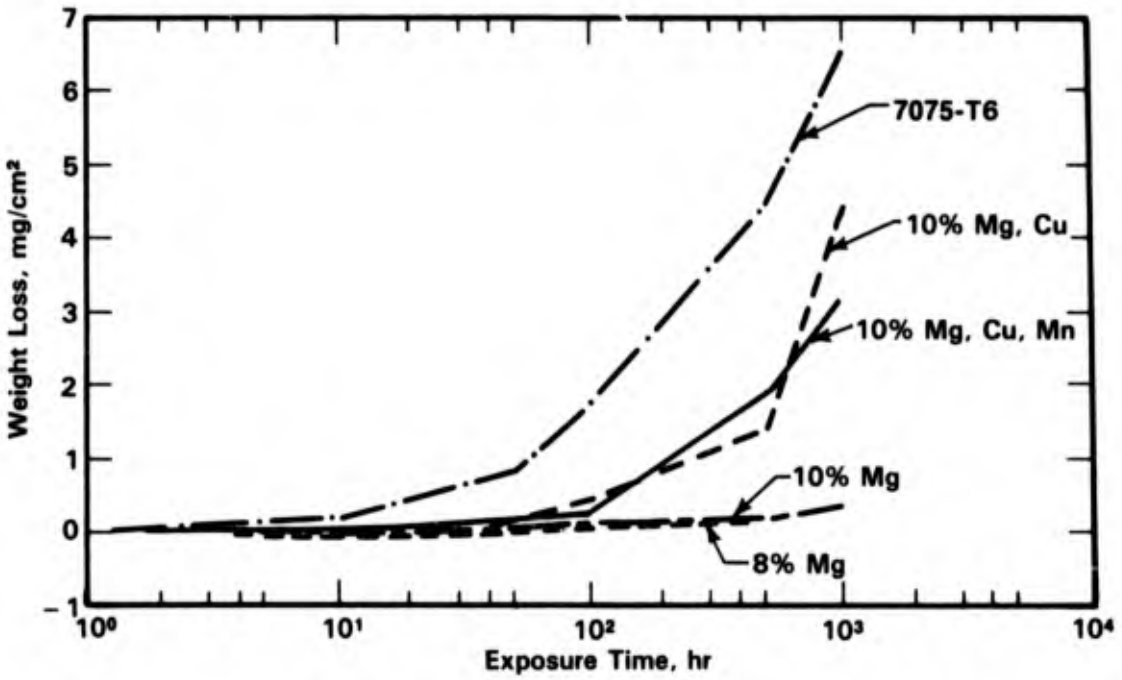

FIGURE 2-12. EFFECT OF Cu, Mn, AND Mg ALLOY ADDITIONS ON THE GENERAL CORROSION RATE OF ALUMINUM IN 3.5 PERCENT NaCl SPRAY[42]

Micro additions of Ti, Zr, and Cr (0.3 weight percent) were found to increase the resistance of Al-6Mg alloys[46] to general corrosion, see Table 2-16. At the aging temperatures investigated, the effect of Zr was the largest. This was attributed to a more even distribution of Mg_2Al_3 through the bulk of the alloy. Addition of 0.3 weight percent Ti or Cr increased the corrosion resistance of the alloy after quenching. However, addition of these elements promoted decomposition of the solid solution, which caused a more heterogeneous structure after aging at 150 to 200 C. This could have a detrimental effect on the corrosion resistance of the alloys.

Effect of Heat Treatment

Heat treatment of aluminum alloys can significantly affect their corrosion behavior. In the following section various heat treatments of aluminum alloys and their effect on general corrosion in seawater environments are discussed.

As discussed in the previous sections, the Al-Mg alloys (5000 series) are widely used in seawater environments. Commercial Al-Mg alloys are strengthened primarily by strain hardening, which is identified by the letter H in their temper designation. The first digit following the H indicates whether the alloy has been strain hardened only (H1), strain hardened and then partially annealed (H2), or strain hardened and then stabilized (H3). The digit following H1, H2, or H3 indicates the final degree of strain hardening. These digits range from 0 (annealed) to 8 (fully work hardened).

TABLE 2-16. EFFECT OF HEAT TREATMENT AND ALLOY ADDITION OF Zr AND Ti ON THE CORROSION RATE OF Al-6Mg ALLOY IN ARTIFICIAL SEAWATER[46]

Alloy	Corrosion Rate, $g/m^2/hr$		
	Quenched	Aged at 150 C	Aged at 200 C
Al-6Mg	1.2	1.6	1.8
Al-6Mg + Zr	0.8	0.8	0.93
Al-6Mg + Ti	0.53	1.0	1.5
Al-6Mg + Zr	0.97	1.0	1.43

Rapid cooling of Al-Mg alloys can result in a super saturated solid solution. However, no appreciable precipitation hardening occurs in these alloys, because the kinetics are slow at room temperature. The kinetics are accelerated by cold work, by exposure to elevated temperatures, and by a higher Mg content.

Results of exposure studies by Reinhart of various Al alloys in the Pacific Ocean[41] included corrosion rates of 5000 series alloys (see Table 2-17). In all cases, the corrosion rates, based on weight loss, of these alloys were low (<1 mpy) and appeared to be independent of heat treatment. The highest rate was found for Al 5052 in the annealed condition.

Aluminum-Mg-Si alloys (6000 series) are used in applications requiring strength and high corrosion resistance. These alloys are strengthened by precipitation hardening, which is identified by the letter T, and are used in the naturally aged (T4) and artificially aged (T6) condition. Table 2-17 showing results of exposure studies in the Pacific Ocean[41] indicates no effect of heat treatment on general corrosion of Al Alloy 6061.

TABLE 2-17. CORROSION RATES OF 5000 SERIES ALUMINUM ALLOYS IMMERSED IN THE PACIFIC OCEAN OFF PORT HUENEME, CA[41]

Alloy	Exposure		Corrosion Rate, mpy
	Days	Depth, ft	
5052-0	1064	5300	3.1
5052-H22	1064	5300	0.4
5052-H34	402	2370	0.2
5454-H32	197	2340	0.7
5454	402	2370	0.6
5456-H321	402	2370	1.1
5456-H32	402	2370	0.6
5456-H343	197	2340	0.4
5085	402	2370	0.5
5085-H113	402	2370	0.6
5086	402	2370	0.8
5086-H32	402	2370	0.4
5086-H34	402	2370	0.6
5086-H112	181	5	1.1

Aluminum-Cu-Mg alloys (2000 series) are heat-treatable, high strength aluminum alloys. These alloys derive their strength from precipitation hardening which is achieved by solution heat treatment, followed by rapid cooling and their natural aging at room temperature (T4 temper) or artificial aging at intermediate temperatures (T6 temper). Cold working after quenching further increases strength, resulting in the T3 temper and, when artificially aged, the T8 temper. Table 2-17 showing results of exposure studies of 2000 series alloys in the Pacific Ocean[41] does not indicate significant variations in corrosion rate as a result of standard heat treatments.

Effect of Temperature, pH, and Aeration

Studies by Reinhart, et al.[41,47] have shown that aluminum alloys tend to corrode at higher rates in the deep ocean than at the surface (see Figures 2-13 and 2-14). The rates that were reported for 1000, 3000, and 5000 series alloys at 6000 feet reached a maximum of about three times that of the alloys exposed to surface water. It has generally been assumed that the low dissolved oxygen concentration was responsible for the high corrosion rates. However, Dexter[35,48] argued that the decrease in corrosion rate could be explained in terms of a decrease in pH rather than a decrease in dissolved oxygen concentration. It can be concluded from these studies that, for reasons not fully understood, corrosion rates of aluminum alloys are higher at depth than near the surface.

Effect of Temperature

Studies on the effect of temperature have mainly been concerned with temperature ranges associated with seawater depth effects, 5 to 25 C, and 25 to 125 C, which is associated with desalination. In these studies it is often difficult to separate effects of temperature and the effects of seawater composition associated with temperature effects such as oxygen solubility and fouling.

Larsen-Basse[49] studied the effect of temperature on Alloys 3004, 5052, Alclad 3003, and Alclad 3004 and found a strong effect on uniform and pitting corrosion. Diagrams, as in Figure 2-15, show that in warm water (24.5-28 C) under free fouling conditions, weight loss was much higher than in cold water (9.5-10.5 C). Microscopic examination of the test specimens showed that, in the warm water, the metal loss was uniform and no pitting was observed. In contrast, examination of the cold water specimens showed that all the specimens corroded by pitting.

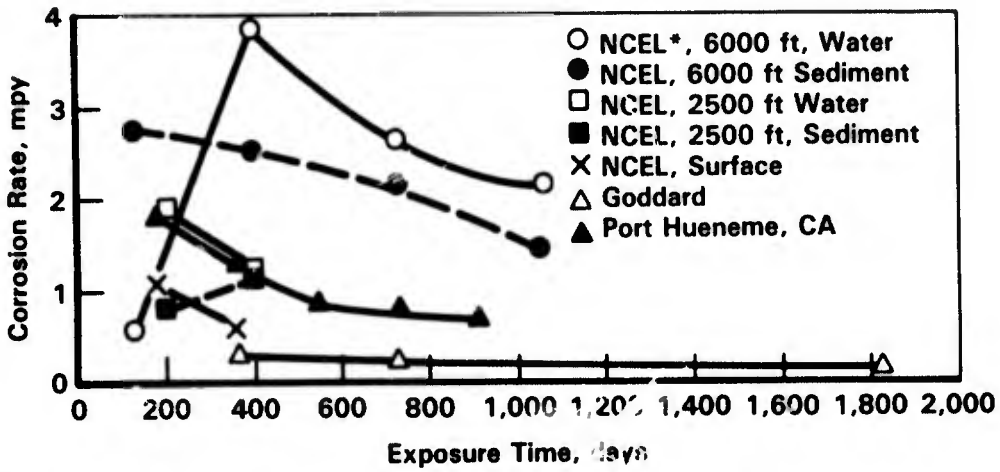

*NCEL–Naval Civil Engineering Laboratory of Port Hueneme, CA

FIGURE 2-13. CORROSION RATES OF 3003 ALLOY AT DIFFERENT DEPTHS AND SURFACE LOCATIONS IN DIFFERENT OCEAN ENVIRONMENTS[41]

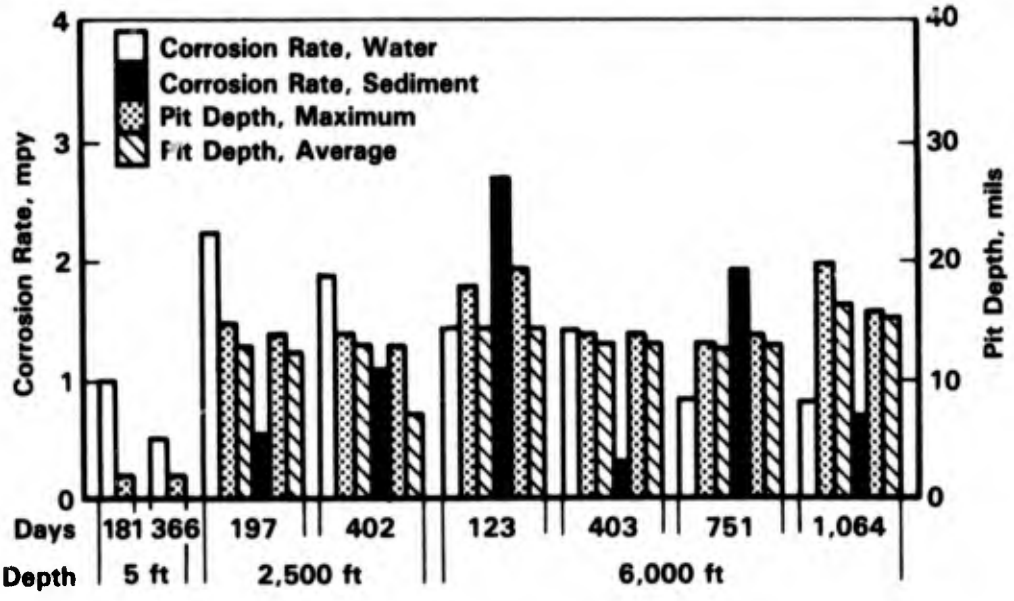

FIGURE 2-14. CORROSION RATES AND MAXIMUM AND AVERAGE PIT DEPTHS OF ALCLAD 3003 ALLOY AT VARIOUS DEPTHS IN THE PACIFIC OCEAN OFF PORT HUENEME, CA[41]

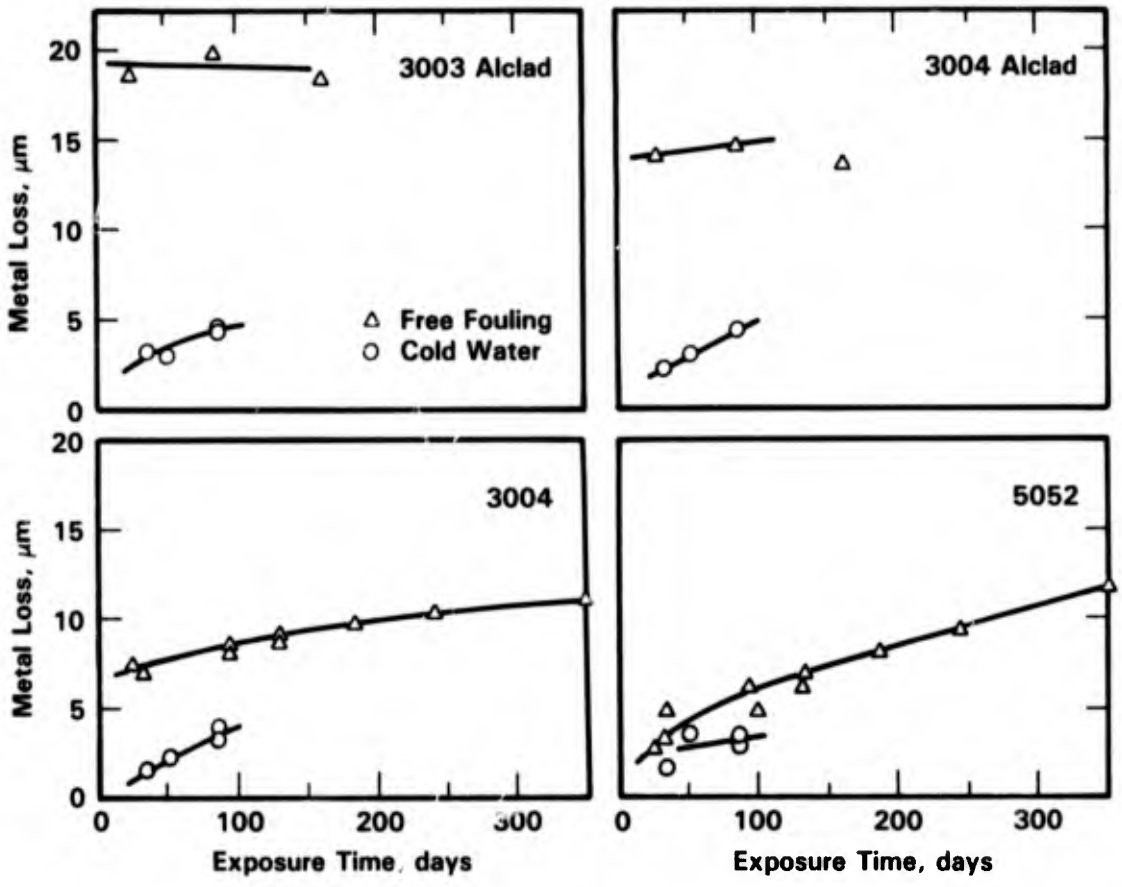

FIGURE 2-15. CORROSION RATE OF FOUR ALUMINUM ALLOYS EXPRESSED AS METAL LOSS IN DIFFERENT SEAWATER ENVIRONMENTS[49]

Russian workers[50,51] have observed an increase in corrosion rate of different aluminum alloys in synthetic Caspian Seawater with increasing temperature in the range of 20-120 C. Figure 2-16 shows the relationship between corrosion rate, temperature, and pH.[52] The increase in corrosion rate in the lower temperature range (20-60 C) was attributed to a decrease in oxygen solubility. The figure shows a relative minimum at 90 C at which temperature the aluminum oxide boehmite is the most stable. Near the boiling temperature the corrosion rate was found to increase sharply. Also, in the pH range investigated, the corrosion rate increased with increasing pH.

Pitting and Crevice Corrosion

It is well known that aluminum alloys pit in chloride containing solutions including seawater.[53-57] The various methods that are available to determine the susceptibility of materials to pitting and crevice corrosion are discussed in Chapter 1.

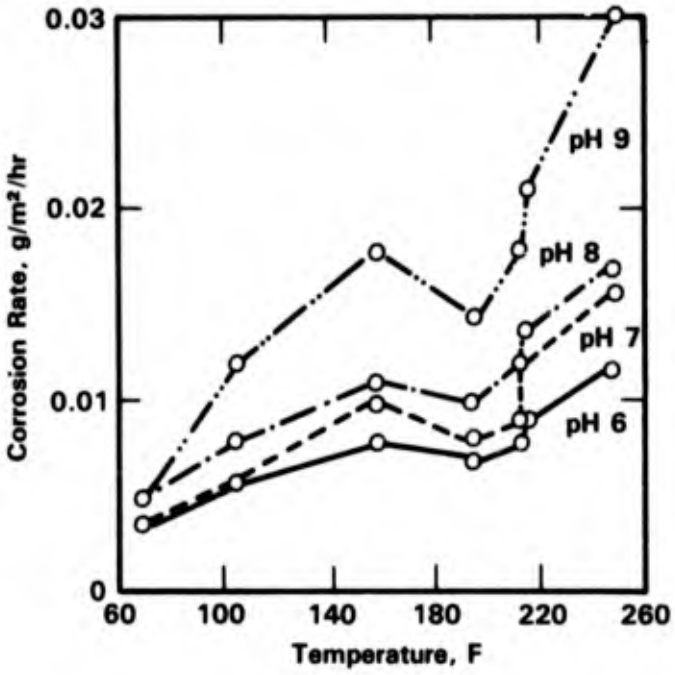

FIGURE 2-16. CORROSION OF ALLOY Al-3Mg IN SEAWATER AS FUNCTION OF TEMPERATURE AND pH (TEST DURATION 500 h)[52]

Effect of Alloy Composition

Alloy composition has a significant effect on the degree of susceptibility to pitting and crevice corrosion of aluminum alloys. In early studies by Godard and Booth[58] of 5 commercial aluminum alloys after 10 years' exposure at three marine sites, it was observed that Alloy 7075-T6 was very susceptible to pitting whereas Alloys 1100-H14 and 3003-H14 were somewhat more resistant. More extensive studies of various seawater environments confirmed this general behavior as illustrated in Tables 2-18 and 2-19 and Figure 2-17. The tables and figure indicate that Alclad and the 5000 (Al-Mg) series alloys were the least susceptible to pitting and crevice corrosion.

A common criterion for measuring pitting corrosion susceptibility is the pitting potential (E_{pit}) defined as the critical potential below which pits do not initiate. Zossi, et al.[59] showed the effect of Mg, Cu, and Zn alloy addition on the pitting potential (see Figure 2-18). The pitting potential was found to increase with increasing Cu content, suggesting a beneficial effect of Cu. Addition of Mg did not appear to affect the pitting potential, whereas addition of Zn resulted in a decrease in E_{pit}, suggesting that Zn would promote pitting and crevice corrosion. The effects of these elements on the pitting potential were confirmed by Muller

TABLE 2-18. MAXIMUM PITTING DURING 10-YEAR EXPOSURE OF PLATE SPECIMENS[62]

Alloy	Pitting Depth, mils		
	Harbor Island, NC	Halifax, N. S.	Equimalt, B. C.
1100-H14	40	32	30
3003-H14	21	22	20
6061-T4	14	33	50
6061-T6	95	54	116
7072-P[a]	56	150	26
7075-T6	66	P[a]	P[a]

(a) P = perforated.

TABLE 2-19. COMPARISON OF ATTACK OF SELECTED ALUMINUM ALLOYS TO CREVICE CORROSION AFTER 1-YEAR EXPOSURE TO SEAWATER AT KEY WEST, FL[40]

Alloy	Deepest Attack, mils			
	2	3-5	6-10	11-20
1100 F				X
1100-H14		X		
3003-H14				X
5050-H34		X		
5052-H32		X		
5052-H34		X		
5083-0	X			
5086-H32	X			
5086-H34	X			
5086-H112	X			
5154-H38		X		
5257-H25	X			
5456-H321	X			
6061-T6				X
6061-T651	X			
X7002-T6		X	X	
X7005-T63	X			
7075-T7351				X
7079-T6				X

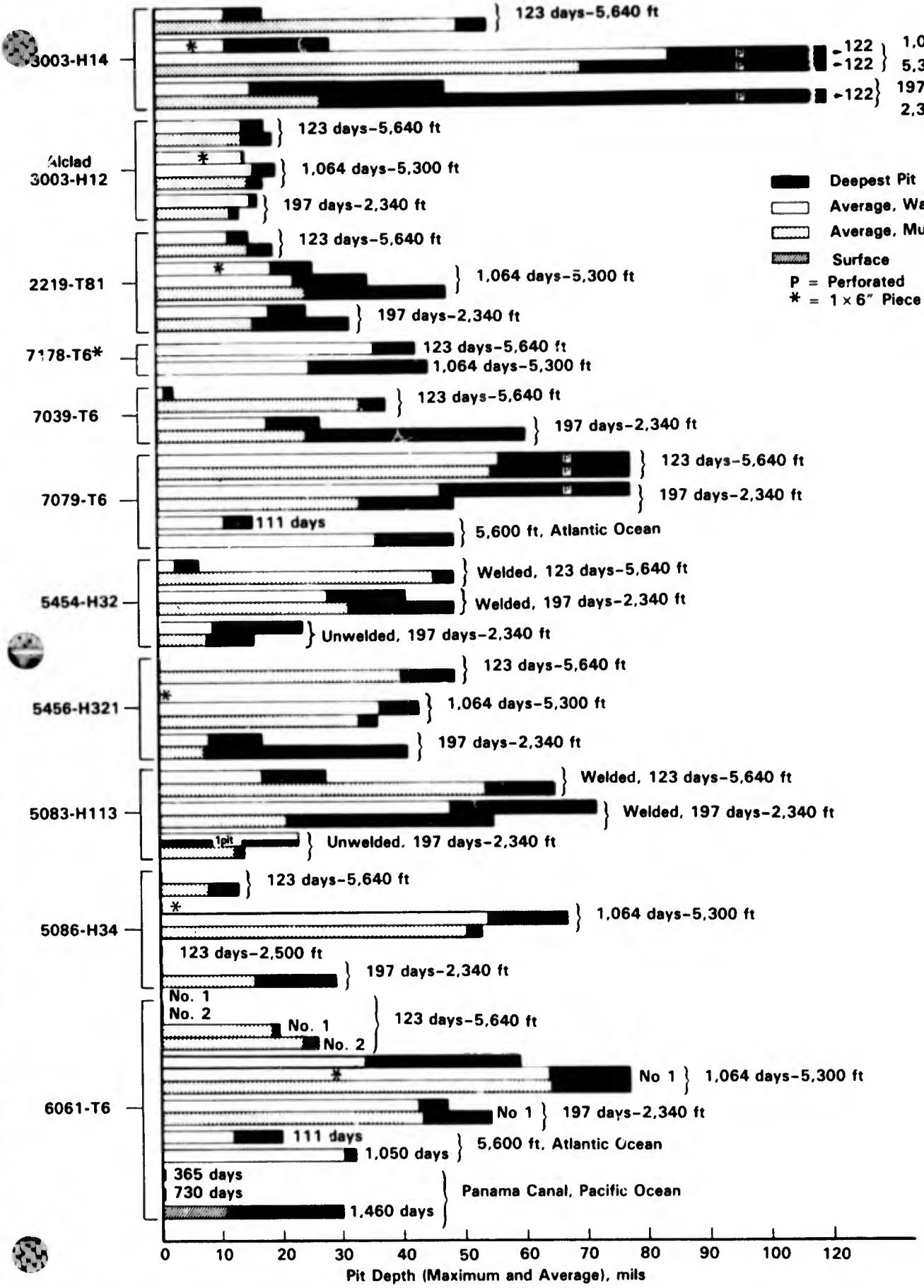

FIGURE 2-17. PITTING OF ALUMINUM ALLOYS IN THE PACIFIC OCEAN OFF PORT HUENEME, CA[67]

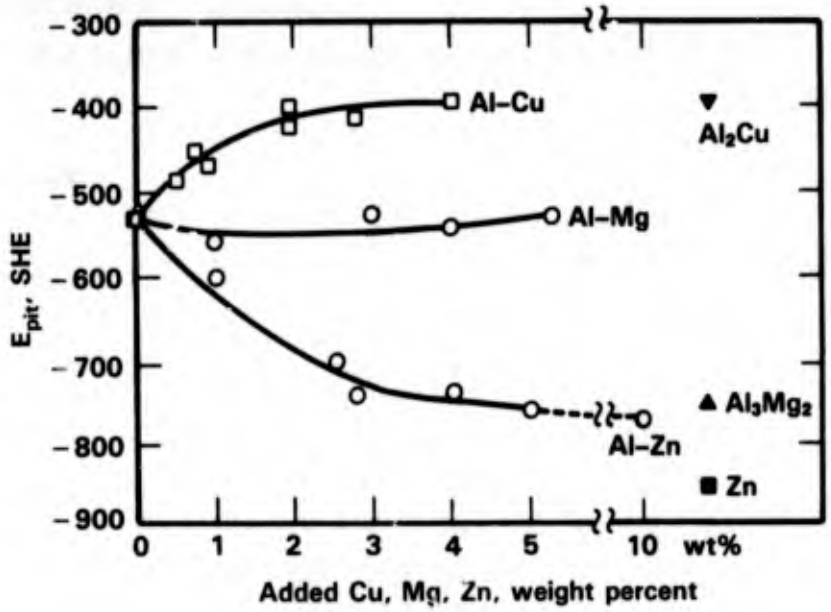

FIGURE 2-18. PITTING POTENTIAL (E_{pit}) VALUES AS A FUNCTION ALLOY ADDITIONS TO ALUMINUM ALLOYS, COMPARED WITH E_{pit} OF PHASES THAT ARE PRESENT IN ALUMINUM ALLOYS. THE CORROSION MEDIA WAS 1M NaCl FOR Al-Cu, Al-Mg, AND Al-Zn ALLOYS. FOR Al_3Mg_2 THE E_{pit} CORRESPONDS TO A SOLUTION 0.5M NaCl[59]

and Galvele.[60,61] Sujimoto, et al.[62] studied the pitting corrosion of several binary aluminum alloys in an aqueous NaCl solution. The pitting potentials of the binary aluminum alloys with 5 to 10 percent alloying elements were found to decrease in the order: Al-Cu > Al-Ni > Al-Fe, Al-Si > Al-V > Al-Mn, Al-Cr, Al-B > Al-Zn > Al-Ti > Al-Mg > Al-Be, suggesting an increase in susceptibility to pitting and crevice corrosion.

In a study by Holtan and Sigurdsson[63] of aluminum alloyed with about 3-5 percent Mg and small amounts of Cr, Mn, and Sb, it was found that the pitting potential was not much affected by these secondary alloying elements. It was found that the pitting potential increased with increasing amounts of Cr up to a certain point (see Figure 2-19), but that the Cr content seemed to be of less importance when Mn was present as well. The pitting potential increased with increasing amounts of Mn, reached a maximum and then decreased.

Niskanen, et al.[64,65] performed electrochemical tests on four aluminum-lithium alloys in 3.5 percent NaCl under several aging conditions. It was found that the anodic aluminum lithium phase formed in the alloy deleteriously affected pitting behavior. Data for aluminum lithium binary alloys are given in Table 2-20.[65] Alloying with either copper or magnesium retarded delta formation by tieing up lithium in transition phases and improved pitting performance.

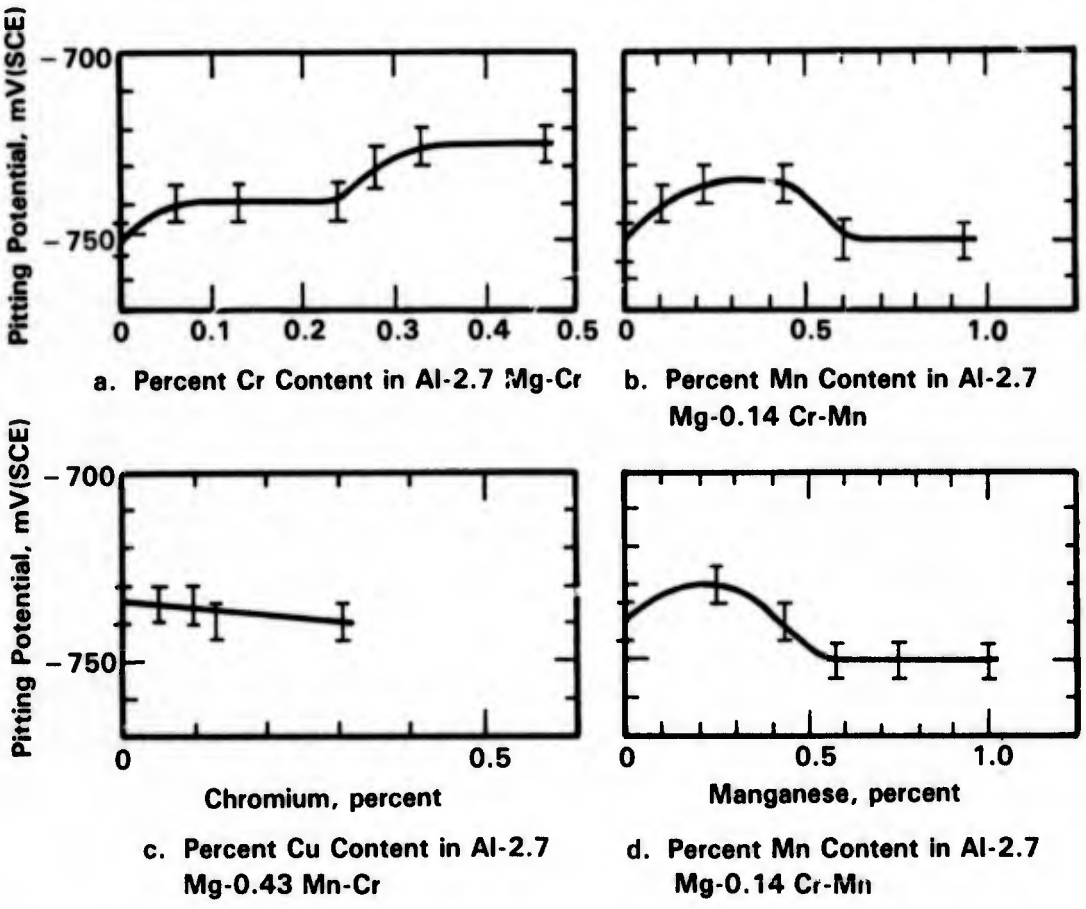

FIGURE 2-19. PITTING POTENTIAL OF ALUMINUM ALLOY AS A FUNCTION OF SECONDARY ALLOYING ELEMENTS(63)

TABLE 2-20. CORROSION DATA FOR Al-Li BINARY ALLOYS IN 3.5 PERCENT NaCl AT 25 C[65]

Alloy Composition	Aging Time, hours	Free Corrosion Potential[c], V(SCE)	Free Corrosion Potential[d], V(SCE)	Pitting Potential, V(SCE)	Passive Current Density, A/cm^2
Al-0.91Li		-0.736	-1.067	-0.727	2.8×10^{-6}
Al-2.85Li	0.25[a]	-0.739	-1.146	-0.692	3.5×10^{-6}
	12.0[a]	-0.782	-1.143	-0.725	1.95×10^{-6}
	24.0[a]	-0.762	-1.130	-0.698	4.0×10^{-6}
	168.0[b]	-1.597	-1.543	-0.755	34.0×10^{-6}
	336.0[a]	-1.469			
	336.0[b]	-1.347			

(a) Aged at 200 C.
(b) Aged at 250 C.
(c) After 24 hours.
(d) From potentiodynamic polarization curve.

Effect of Heat Treatment

Although no systematic studies on the effect of heat treatment on pitting are reported, some studies were performed that indicated an effect of heat treatment. Groover, et al.[66] compared the pitting and crevice attack behavior of aluminum Alloy 1100 in the T and H14 temper in surface water at Key West, FL (see Figure 2-20). Pitting was relatively minor for both heat treatments but the H14 heat was found to provide better resistance to crevice corrosion.

Early studies by Galvele and coworkes[61,68] on the pitting behavior of high purity Al-Cu alloys indicated that heat treatment of these alloys affected the pitting potential because of the formation of copper depleted zones in the aged alloys. Specifically, when an Al-4Cu alloy was aged to peak hardness, the pitting potential of the alloy in a 1M NaCl solution decreased, indicating a higher susceptibility to pitting corrosion, see Figure 2-21. Sujimoto, et al.[69] showed different pitting potentials for the matrix and grain boundary region in Al-4 percent Cu alloys as indicated in Figure 2-22. This difference in pitting potential was attributed to a copper depleted zone at the grain boundary. Similarly, Maitra and English[70] showed two pitting potentials in aluminum Alloy 7075-T6 whereas, for 7075-W, only one pitting potential was observed (see Figure 2-23). The more active pitting potential for 7075-T6 was attributed

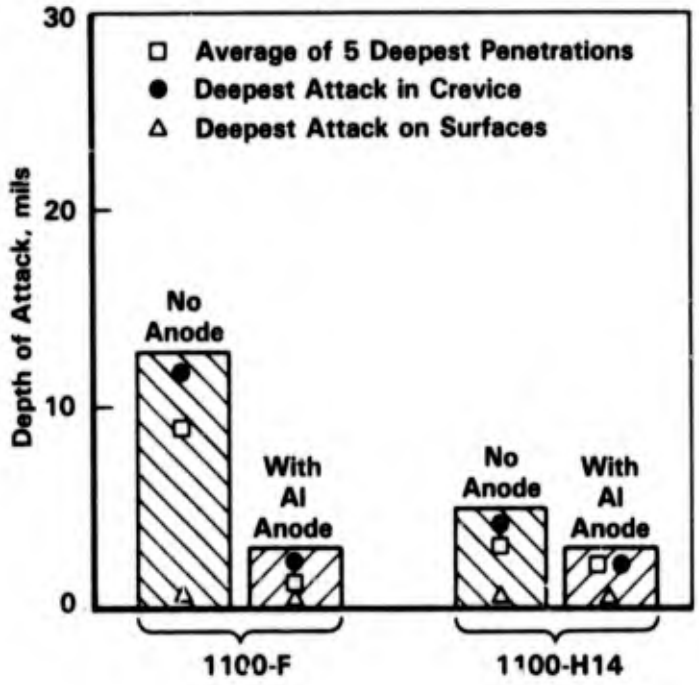

FIGURE 2-20. CORROSION AND EFFECT OF CATHODIC PROTECTION ON 1100-F AND 1100-H14 ALLOYS AFTER 368 DAYS' SEAWATER EXPOSURE AT KEY WEST, FL[66]

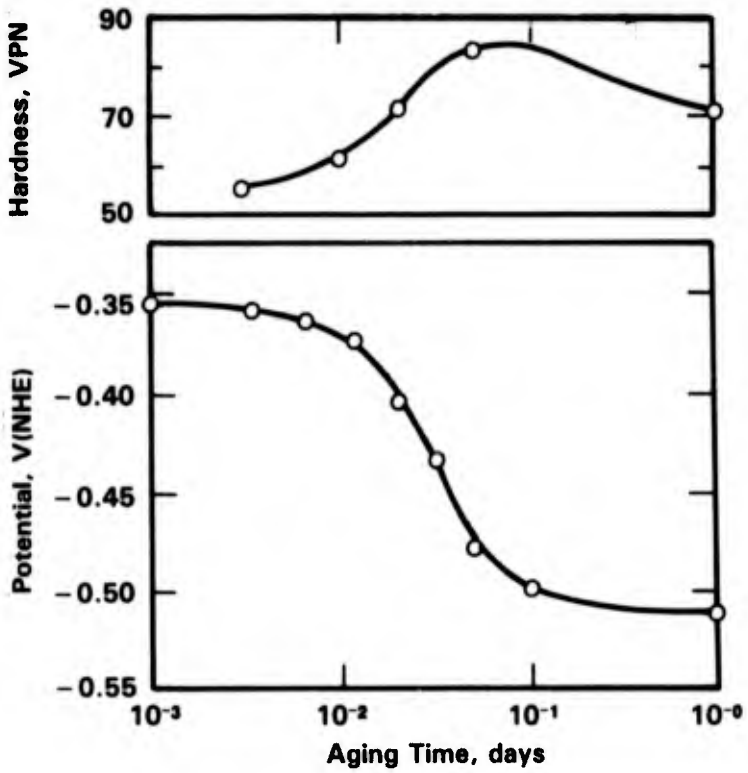

FIGURE 2-21. EFFECT OF AGING TIME ON PITTING POTENTIALS AND HARDNESS OF Al-4 PERCENT Cu AGED AT 240 C. DEAERATED 1M NaCl SOLUTION AT 25 C[68]

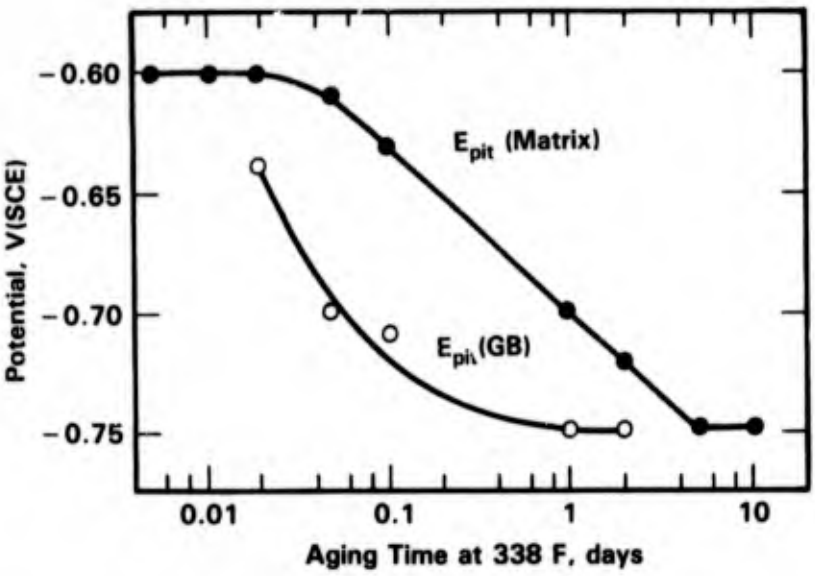

FIGURE 2-22. THE CHANGE IN PITTING POTENTIALS WITH AGING TIME AT 170 C FOR THE GRAIN BOUNDARIES, E_{pit} (GB), AND THE GRAINS, E_{pit} (MATRIX), OF Al-4 PERCENT Cu ALLOY IN A 1M AQUEOUS NaCl SOLUTION (pH 10.0)[69]

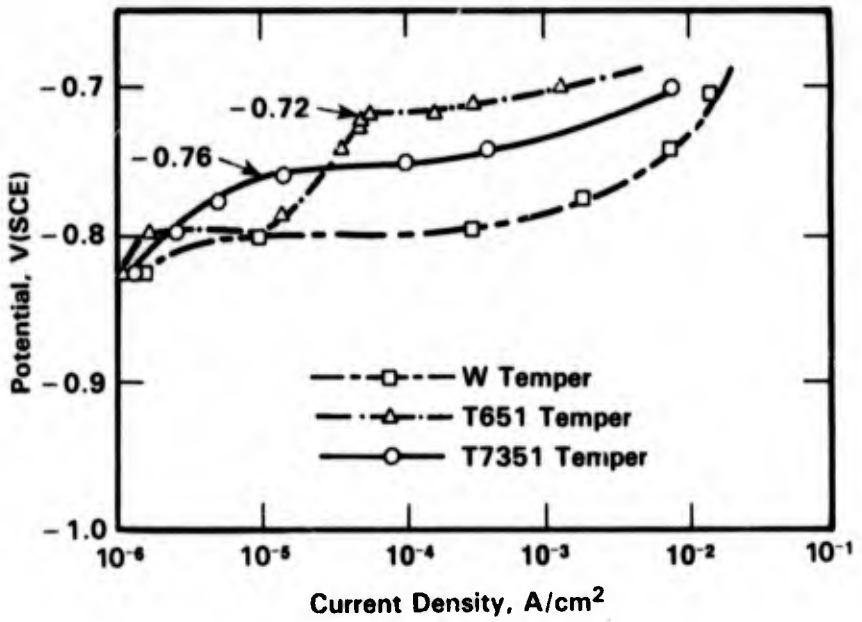

FIGURE 2-23. ANODIC POLARIZATION CURVES FOR Al 7075-W, T651, AND T7351 TEMPERS IN DEAERATED 3.5 PERCENT NaCl[70]

to pitting of the solute enriched grain boundary region and the more noble pitting potential was considered the result of pitting of the matrix. In the overaged condition for 7075-T73, only one pitting potential was observed which corresponded to pitting of the Cu depleted solid solution matrix.

Effect of Depth and Aeration

There is considerable controversy in the literature concerning the relationship between pitting of aluminum and depth and aeration. Work on the subject by Rynewicz,[71] Wheatfall,[72] and early data by Reinhart[41] indicated that the severity of pitting increased with increasing depth. This effect was attributed to a decrease in oxygen with increasing depth. Typical data for 5000 series aluminum alloys are given in Figure 2-24. On the other hand, results of electrochemical studies by Dexter[48,73] indicated that, when all other factors

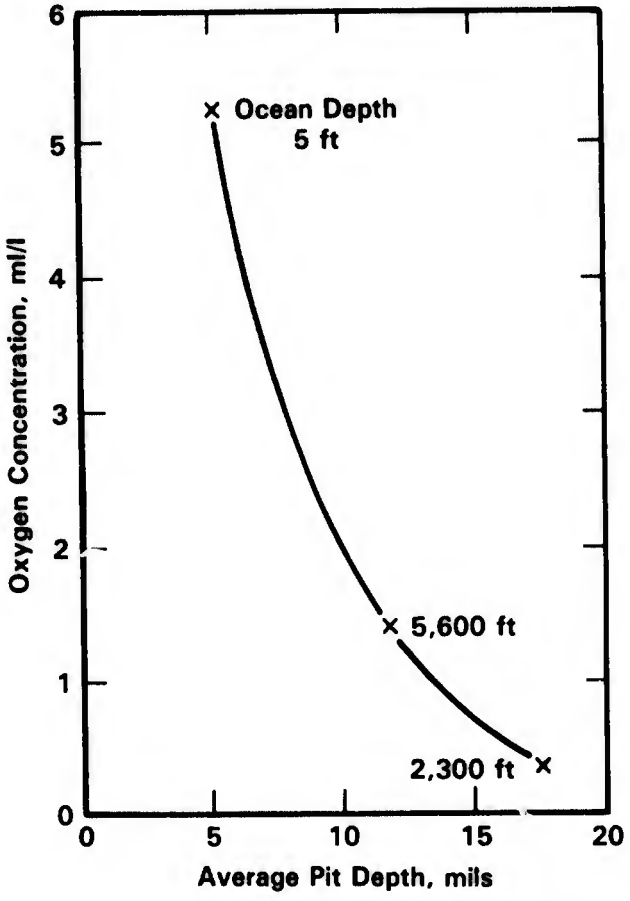

FIGURE 2-24. RELATION BETWEEN AVERAGE PIT DEPTHS OF ALUMINUM-MAGNESIUM ALLOYS (5000 SERIES) AND OXYGEN CONCENTRATION OF SEAWATER[41]

are held constant, a decrease in dissolved oxygen reduced the severity pitting and crevice corrosion. Thus, Dexter[73] attributed the variation in corrosion behavior of aluminum alloys with depth to the variation in pH, temperature, and oxygen concentration. He observed that combinations of low temperature, low pH, and high dissolved oxygen was most corrosive toward aluminum alloys. Based on the relationship between oxygen, temperature, pH, and depth for the Pacific Ocean test site (see Figure 2-25) Dexter predicted that the most

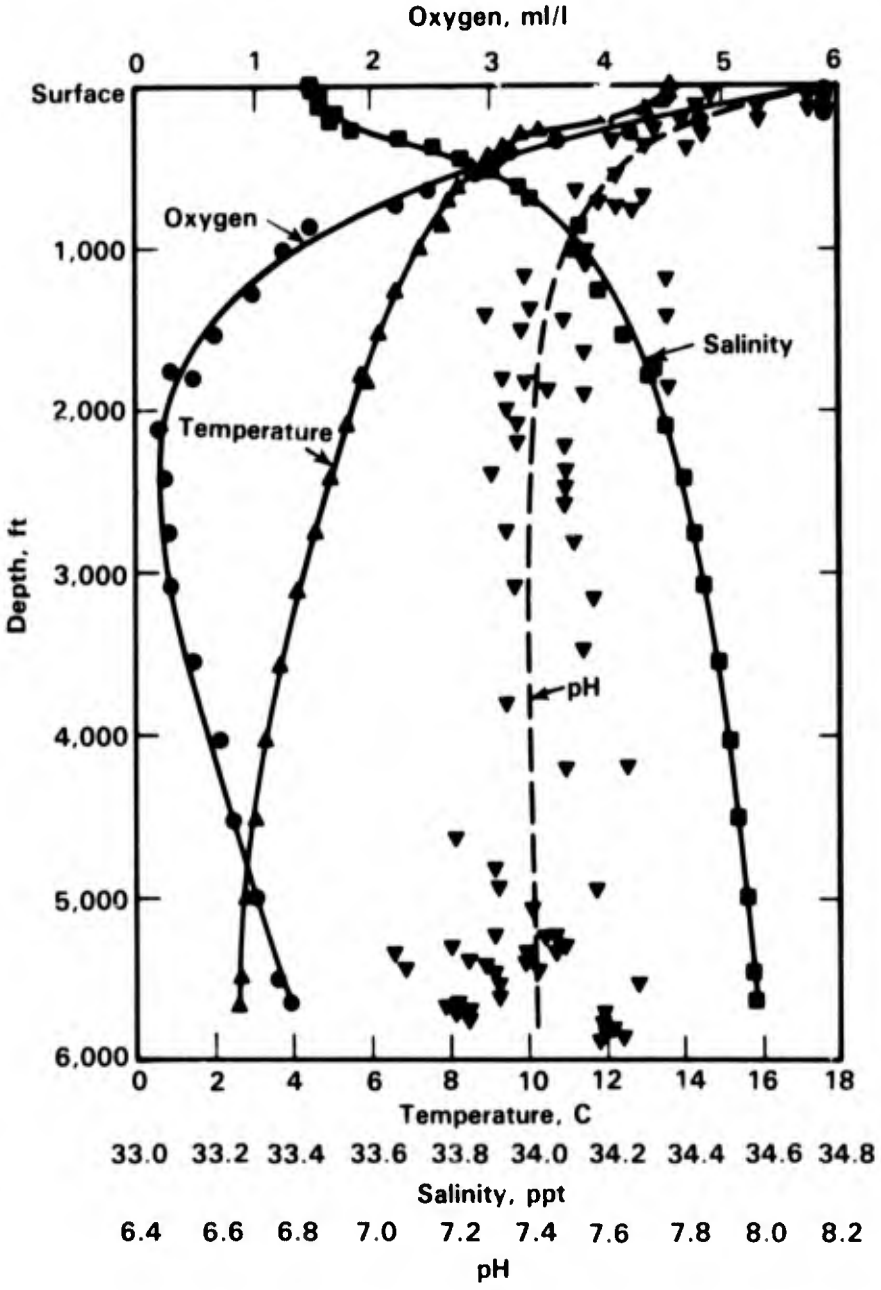

FIGURE 2-25. HYDROGRAPHIC DATA AS A FUNCTION OF DEPTH AT THE SITE FROM WHICH THE DEEP PACIFIC OCEAN CORROSION DATA WERE TAKEN[74]

corrosive condition will occur at intermediate depths, between 150 and 400 meters; while in the Atlantic Ocean, the most corrosive conditions may be found at greater depths due to the overall higher oxygen levels.

Results of more recent data by Reinhart and Jenkins[75] for a series of aluminum alloys at the Pacific Ocean test site near Port Hueneme are consistent with this hypothesis, at least for some of the alloys, see Figure 2-26. Data for 2024, 6061-T6, and 2219-T81 exhibit maximum pitting at an intermediate depth of 250 meters, while 5083-H113 and 5086-H34 exhibited a minimum in attack at this depth, and attack of 3003 H14 increased monotonically with increasing depth.

It can be concluded from all of the above studies taken together, that for reasons which are not fully understood, pitting of aluminum alloys is likely to be more severe at depth than at the surface and that the specific relationship between rates of pitting and depth is probably dependent upon the specific location and aluminum alloy being considered.

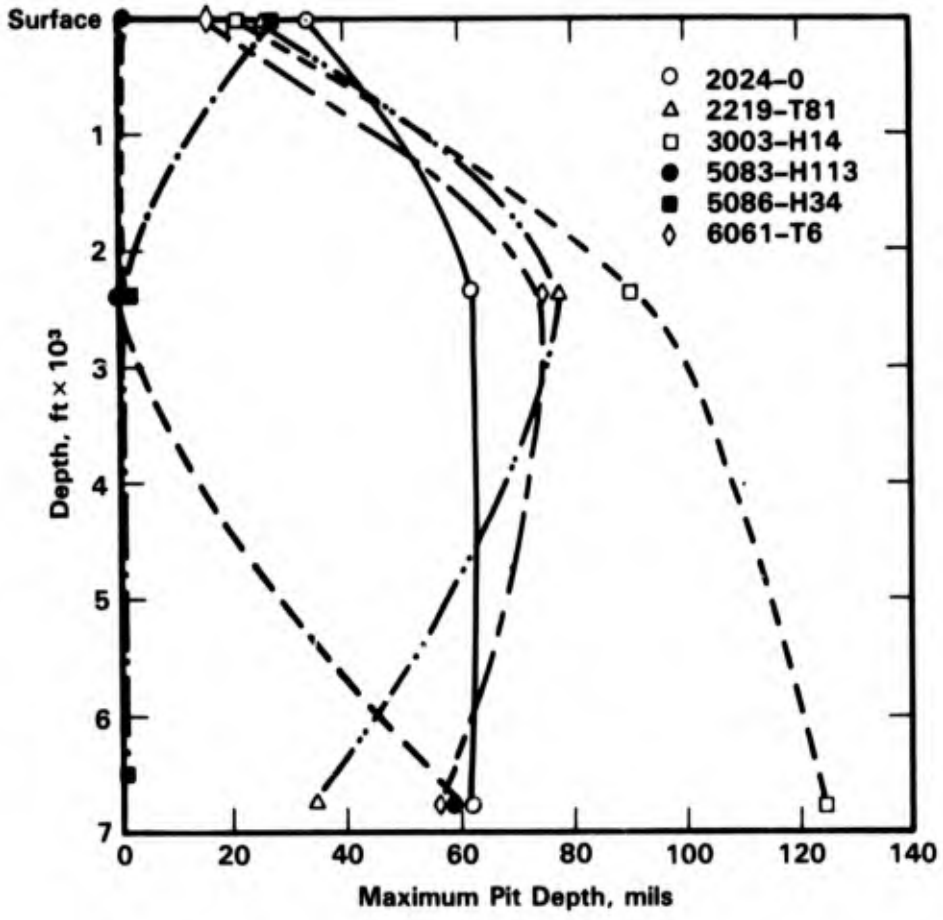

FIGURE 2-26. MAXIMUM DEPTHS OF PITS OF ALUMINUM ALLOYS VERSUS DEPTH AFTER 1 YEAR OF EXPOSURE IN THE PACIFIC OCEAN NEAR PORT HUENEME, CA[75]

Effect of Temperature

Studies of pitting of aluminum alloys have been concerned with two temperature ranges; 5 to 25 C, which is associated with seawater depth effects and 25 to 125 C, which is associated with desalination. In these studies, it is difficult to separate the effect of temperature on pitting from the influence that temperature has on seawater composition or from natural variation in seawater composition in seawater of varying temperatures. For example, both the temperature and the dissolved oxygen content of seawater vary with seawater depth. Nevertheless, the general concensus seems to exist in the literature concerning the "net" effect of temperature variation on pitting behavior of aluminum alloys. Dexter[48,73] studied the effect of oxygen, pH, and temperature on the electrochemical behavior of pure aluminum and 5052 aluminum in clean seawater. It was found that a decrease in water temperature promoted a noble shift in the corrosion potential, while not greatly influencing the pitting potential; thus, pitting is more likely at lower temperatures. Results of the deep ocean studies by Reinhart[41] and Reinhart and Jenkins[75] are essentially in agreement with Dexter's results although the authors differ in the interpretation of the data (see section on effect of depth). Reinhart and Reinhart and Jenkins observed more severe pitting of most aluminum alloys at depths where temperatures were colder rather than near the surface waters.

Ahmed[76] and Alier[51] studied the effect of temperature on pitting of aluminum alloys for desalination applications and both found that the propensity for pitting decreased with increasing temperature. Ahmed found that the pit density of 5052 aluminum decreased dramatically with increasing temperature from 82 to 108 C in flowing seawater. The general corrosion rate of this alloy did increase with increasing temperature. Aliev[51] found that the pitting potential of several Russian aluminum alloys increased more rapidly than the corrosion potential in Caspian seawater with an increase in temperature over the temperature range of 20 to 100 C. This behavior indicates a decreasing likelihood of pitting.

Effect of Time

Fundamental considerations of pit propagation predict that pitting will follow a power law,

$$d \propto t^b$$

where d is depth of pitting, t is time and b is an exponent, that is usually less than one. For example, b = 1/3 for a hemispherical pit.[77] Aluminum alloys frequently follow power law

behavior with exponents less than one, which is desirable since this indicates that rates of pitting decrease with time. Unfortunately, long term exposure data for aluminum alloys in seawater suggest that the exponent is greater than one. Data by Reinhart and Jenkins[75] for several aluminum alloys indicates that only Alclad 3003-H12 exhibited a decrease in the rate of pitting with time, see Figures 2-27 and 2-28. The authors attributed the good performance of the latter alloy to the sacrificial nature of the Alclad, which promoted lateral attack, rather than deep pitting.

Effect of Velocity

Limited data were found in the literature on the effect of velocity on the pitting of aluminum alloys in seawater and these data are somewhat contradictory in nature. Mansfeld and Kenkel[78] performed potentiodynamic polarization experiments on rotating cylinder electrodes of 6061 aluminum in ASTM ocean water and found that the pitting potential was between -0.71 V and -0.69 V(SCE) and did not vary systematically with rotation speed, for

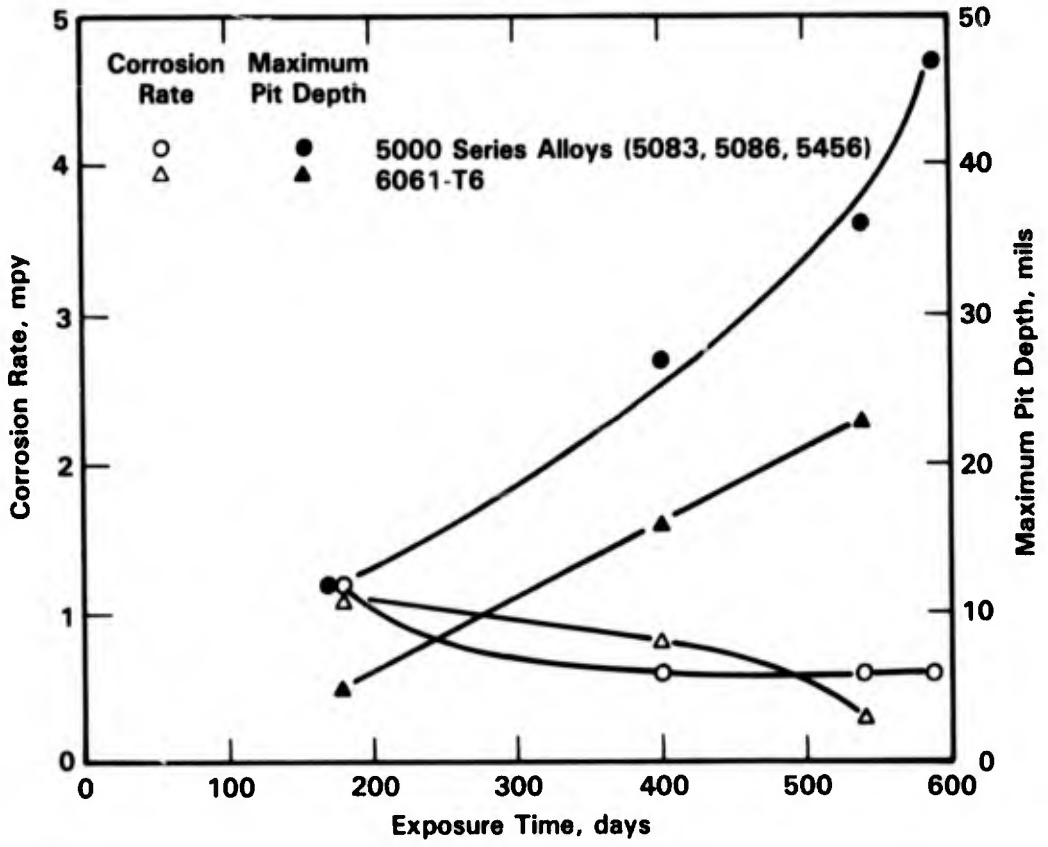

FIGURE 2-27. CORROSION RATES AND MAXIMUM DEPTHS OF PITS FOR ALUMINUM ALLOYS 5000 SERIES AND 6061-T6 VERSUS TIME OF EXPOSURE IN SURFACE SEAWATER[75]

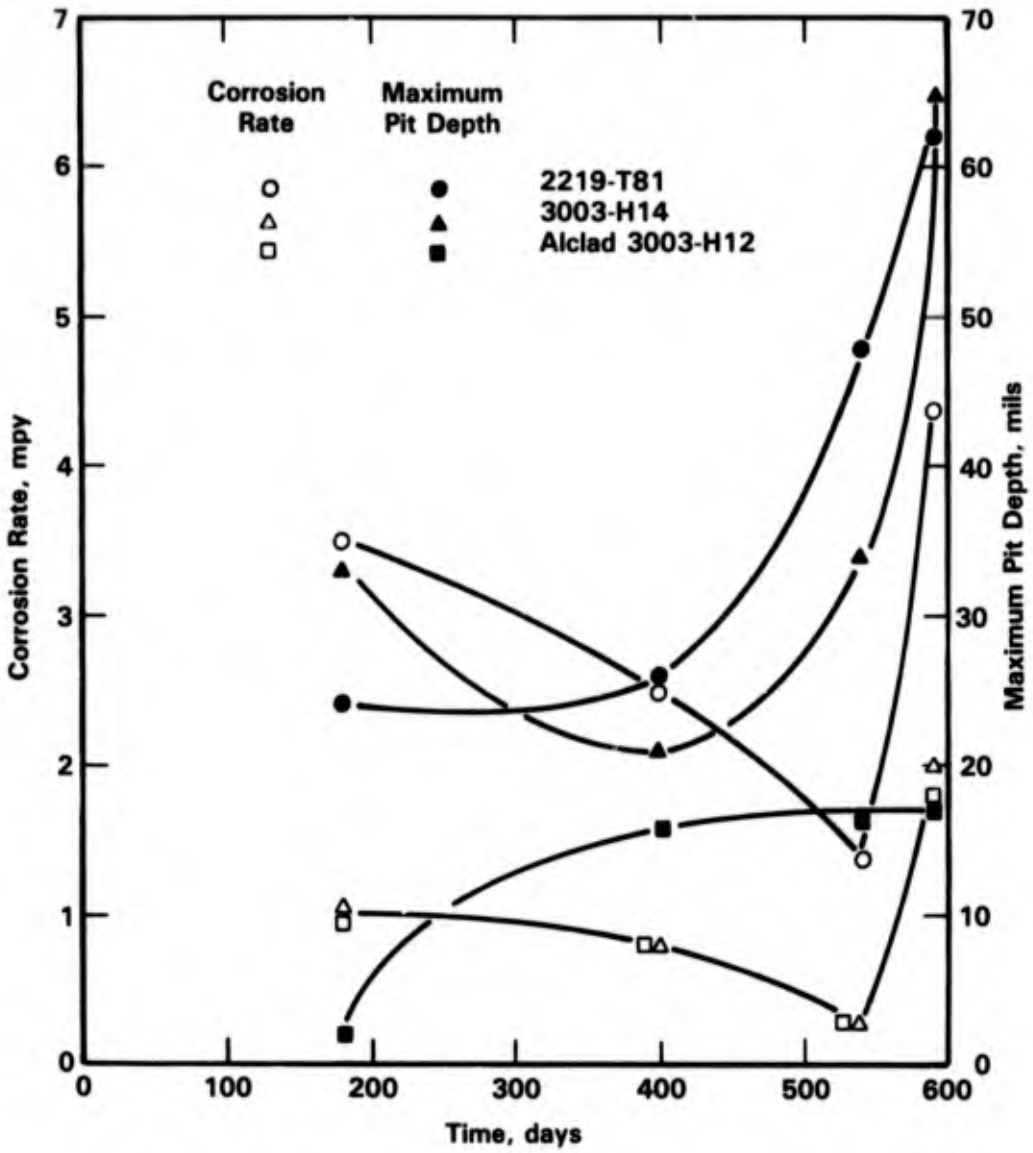

FIGURE 2-28. CORROSION RATES AND MAXIMUM DEPTHS OF PITS FOR ALUMINUM ALLOYS 2219-T81, 3003-H14, AND ALCLAD 3003-H12 VERSUS TIME OF EXPOSURE IN SURFACE SEAWATER[75]

speeds up to 2000 revolutions per minute. Similarly, Aliev and Freiman[51] reported no systematic effect of rotation speed on the corrosion potential, the pitting potential, or the protection potential for a disk electrode of an aluminum alloy (AMts) in Caspian seawater at 90 C. Franz and Novak[77] did report a slight noble shift (40 mV) in the pitting potential of rotating annuli of pure aluminum with increasing velocity (0-2000 RPMs) in a deaerated 0.1 normal NaCl solution at 25 C.

On the other hand, Davis, et al.[79] reported that the pitting potential, and corrosion potential of pure aluminum and 5456 aluminum in actual seawater decreased with increasing

velocity at 75 F, see Figure 2-29. However, these data are inconclusive since both the corrosion and pitting potentials decreased with increasing velocity. Results of potentiostatic exposure tests did show that the extent of pitting in these alloys decreased with increasing velocity for potentials more noble than the pitting potential.

Effect of Pollution

Little work has been done on the effect of seawater pollution on pitting and crevice corrosion of aluminum alloys. However, it is well known that various metallic ions in seawater such as copper, nickel, or lead can have a detrimental effect on the pitting resistance.[80] In particular, Herrigel[81] described the severe pitting of aluminum in a desalination plant as a result of the presence of copper in the feedwater. Raising the pH of the feedwater to about 7.5 and increasing the oxygen concentration to about 50 micrograms per liter eliminated the pitting attack.

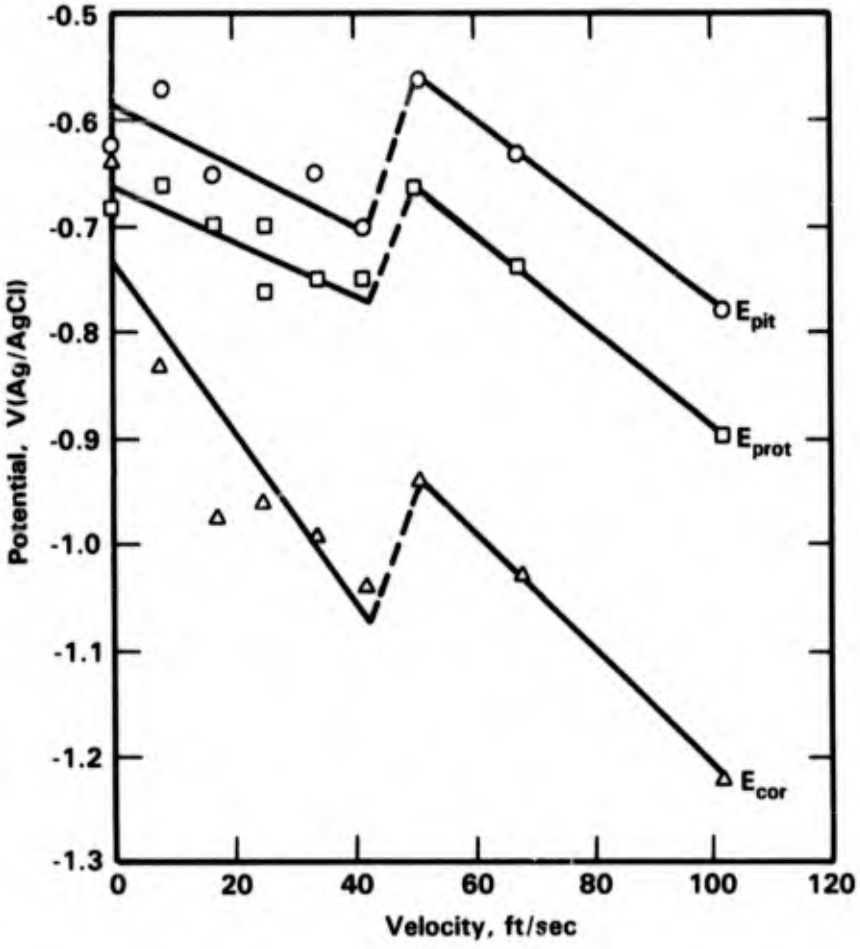

FIGURE 2-29. EFFECT OF VELOCITY ON E_{pit} (PITTING POTENTIAL), E_{prot} (PROTECTION POTENTIAL), AND E_{cor} (CORROSION POTENTIAL) ON PURE ALUMINUM IN SEAWATER[79]

The effect of hydrogen sulfide contamination of seawater on both uniform and pitting corrosion of pure aluminum and an Al-6Mg alloy was investigated by Russian workers.[82] The workers found that H_2S had a beneficial effect on both forms of corrosion.

Erosion-Corrosion

Aluminum alloys are generally resistant to erosion corrosion in low velocity seawater, below velocities of 20 fps.[81-85] However, at higher seawater velocities, considerable weight loss is experienced. Figure 2-30 which shows the weight loss of aluminum Alloys 5456-H343 and 6061-T6 as a function of seawater velocity after 30 days, indicates that at velocities of 10-20 fps depending on alloy and orientation, surface and weight loss increase significantly.

Davis and Gehring[86] studied the effect of time on the corrosion behavior of several alloys exposed to various seawater velocities for selection of these materials for high performance ships. Figure 2-31 shows that, in seawater at 20 knots, the corrosion rate of two 5000 series alloy decreased with time after an initial increase; the maximum corrosion rate at this water velocity was less than 5 mpy. At higher seawater velocity, the corrosion behavior of these alloys appeared to be different, see Figures 2-32 and 2-33. At a seawater velocity of 30 knots a slight decrease in corrosion rate of Alloy 5456-H117 was detected with increasing exposure time, whereas the corrosion rate of Alloy 5086-H117 showed a considerable increase with time. At 60 knots, the corrosion rates were constant with time between 12 and 14 mpy. Davis and Gehring hypothesized that pitting susceptibility of these alloys was reduced as the velocity increased from 0 to 10 knots by an increased supply of oxygen. Pitting susceptibility increased again at 20 knots as a result of a transition from laminar to turbulent flow and decreased at velocities above 30 knots by the highly turbulent boundary layer that prohibits the establishment of conditions required for pitting. However, the conditions that reduced pitting tended to increase general attack.

Later studies by Gehring and Peterson[87] and Ahmed on 5000 series alloys confirmed Gehring's earlier finding[86] that the rate of corrosion of specific aluminum alloys was strongly dependent on seawater velocity. It was concluded from the later studies that the basic mechanism for high velocity corrosion of a 5000 series alloy (5456-H117) involves film breakdown leading to enhanced micropitting near intermetallics.

Cavitation damage to aluminum can occur in the presence of turbulent liquid. During turbulence, voids form and collapse releasing bursts of energy. If this occurs at the metal surface, the protective oxide may break resulting in pit initiation. Pitting can be sufficiently dense to cause roughening of the surface. Although cavitation damage of aluminum has been

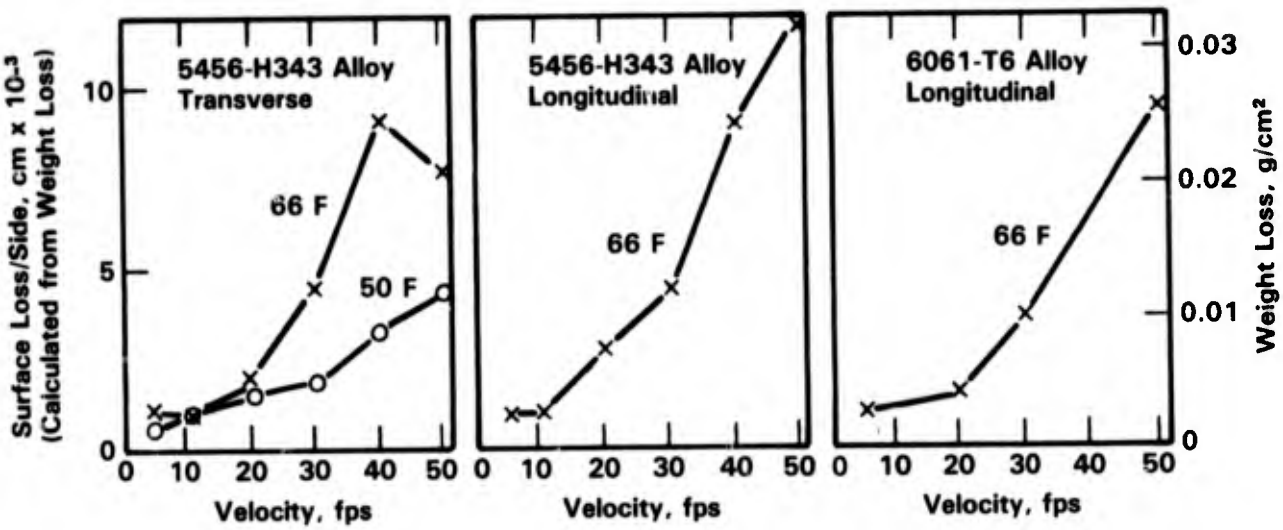

FIGURE 2-30. WEIGHT LOSS AND SURFACE RECESSION (CALCULATED FROM WEIGHT LOSS) AS A FUNCTION OF WATER VELOCITY FOR TWO ALUMINUM ALLOYS AFTER 30 DAYS IN SEAWATER[85]

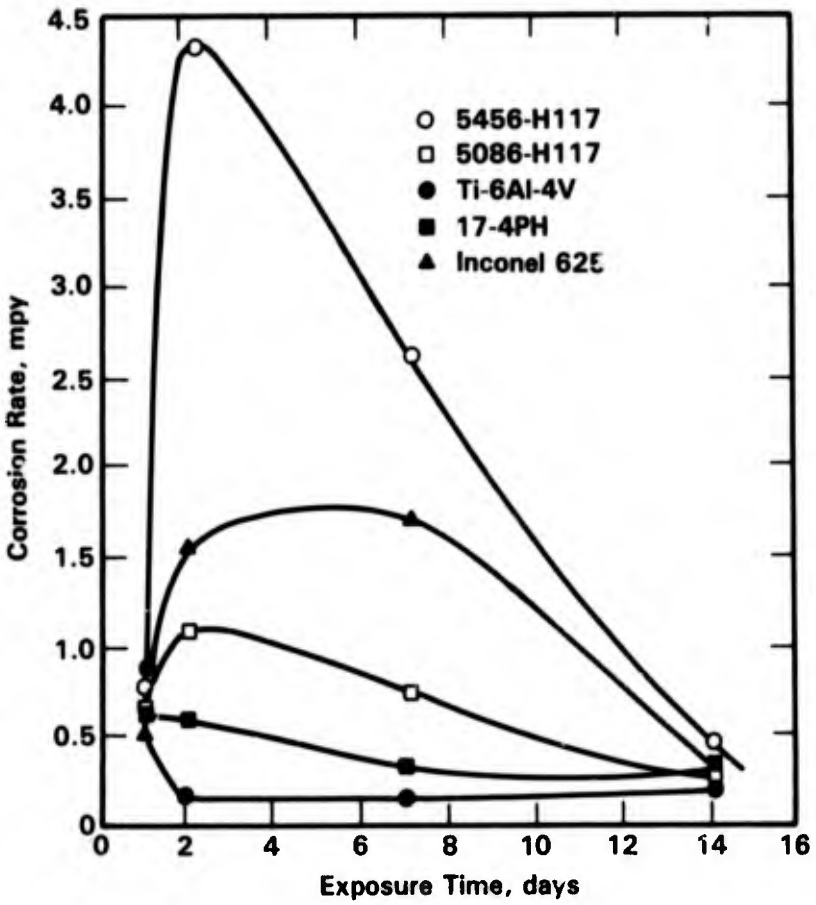

FIGURE 2-31. CORROSION RATE-TIME BEHAVIOR OF DIFFERENT ALLOYS AT 20 KNOTS IN SEAWATER[86]

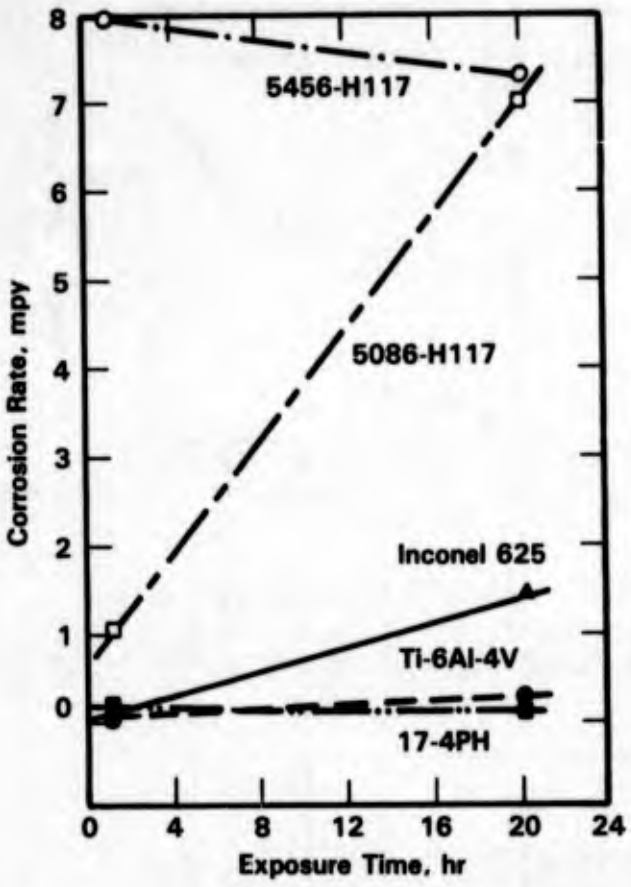

FIGURE 2-32. CORROSION RATE-TIME BEHAVIOR OF DIFFERENT ALLOYS AT 30 KNOTS IN SEAWATER(86)

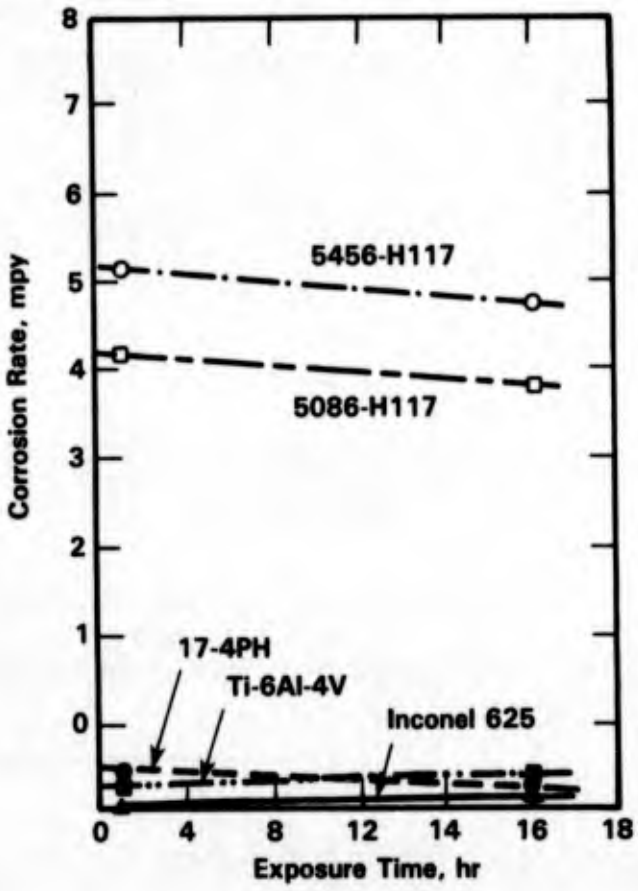

FIGURE 2-33. CORROSION RATE-TIME BEHAVIOR OF DIFFERENT ALLOYS AT 60 KNOTS IN SEAWATER(86)

reported, little quantitative work has been performed on cavitation of aluminum in actual or simulated seawater.

Galvanic Corrosion

Marine structures are usually designed with strength requirement as the primary parameter for selection of materials of construction. The use of more than one type of metal in a structure may be necessary to obtain the desired mechanical properties. Accelerated corrosion of aluminum alloys commonly occurs when these alloys are electrically coupled to other alloys such as stainless steel, titanium, and Monel. Usually, uncoupled materials are ranked in a galvanic series according to their corrosion potential in a specific environment, e.g., seawater, see Table 2-8. Although this type of classification could be useful as an

indication of general trends in galvanic corrosion, it cannot provide information on the extent of galvanic corrosion when dissimilar materials are electrically coupled. As pointed out by Mansfeld, et al.[88] the extent of galvanic corrosion does not only depend on potential difference between the dissimilar materials but also on kinetic parameters such as corrosion rates of the uncoupled materials and Tafel slopes as well as on area ratios.

Mansfeld[88] measured galvanic current densities of aluminum-dissimilar metal couples in an aerated 3.5 percent NaCl solution and found that they were in good agreement with the increase in dissolution rates due to galvanic coupling. Table 2-21 shows the galvanic series of various aluminum alloys coupled to dissimilar metals based on galvanic current densities. In general, galvanic corrosion of Al alloys coupled to dissimilar metals decreases in the order Ag > Cu > steel 4130 >> stainless steel - Ni > Inconel Alloy 718 >> Ti-6Al-4V-Haynes Alloy 188 > Sn > Cd. This ranking is different from the ranking according to the corrosion potential of uncoupled alloys (see Table 2-8). Mansfeld[88] ranked various alloys based on their compatibility with aluminum according to Table 2-21. These alloys were placed in three classes according to relative increases in dissolution rates.* Class I included rates below 5, Class II had rates between 5 and 15, and Class III rates were above 15 (see Table 2-22).

In a subsequent study, Reboul[89] compared couples made of aluminum Alloys 1050, 5086, 2024, and 7075 with other metals (carbon steel, Type 316 stainless steel, and titanium) in tapwater and artificial seawater (3 percent NaCl + PO_4HNa_2 0.019 percent + 0.125 percent BO_3H_3 + CO_3Na_2). Galvanic currents generated in tapwater, see Table 2-23, indicate that the lowest corrosion occurs when steel is coupled to copper free aluminum alloys. Although these couples generate the weakest galvanic currents, field experiments showed[89] that couples that have highest individual resistance to corrosion such as the stainless steel with a Cu-free aluminum alloy have the longest life. Moreover, Reboul[89] confirmed earlier work by Ulanovskii[90] that for a given couple the galvanic current decreases rapidly with time, stabilizing within a few days, see Figure 2-34.

Seawater exposure tests of galvanic couples of aluminum Alloys 6061-T6 and 7075-T6 with various alloys were performed in a seawater environment at the U.S. Army Tropical Testing Station, Panama Canal Zone.[18,19] The results in Table 2-24 indicate that coupling of the aluminum alloys with either active or noble metals tended to result in galvanic attack of the aluminum.

---

* The relative increases in dissolution rates are $\frac{r_A - r_o}{r_o} = k\,\bar{i}_g/i_{cor}$

where r_o is the uncoupled dissolution rate (mdd),
r_A is the galvanic dissolution rate (mdd),
i_{cor} is the uncoupled current density ($\mu A/cm^2$), and
$\bar{i}_g$ is the galvanic current density ($\mu A/cm^2$).

TABLE 2-21. GALVANIC SERIES FOR Al ALLOYS IN 3.5 PERCENT NaCl, BASED ON THE AVERAGE GALVANIC CURRENT DENSITY $\bar{i}_g$ AND THE DISSOLUTION RATE OF THE GALVANIC COUPLE r_A[88]

Overall Ranking	Couple	$\bar{i}_g$, $\mu A/cm^2$	r_A, mdd	Overall Ranking	Couple	$\bar{i}_g$, $\mu A/cm^2$	r_A, mdd
1	7075-Ag	63.8	68.8	49	7075-Haynes 188	8.9	6.9
2	6061-Ag	54.5	65.6	50	2219-PH13-8Mo	8.4	17.2
3	1100-Ag	53.8	55.3	51	7075-Ti-6-4	8.3	8.5
4	2024-Ag	50.6	64.3	52	1100-Ti-6-4	8.3	8.1
5	2219-Ag	47.4	69.4	53	6061-Inco 718	8.1	7.0
6	7075-Cu	45.0	58.8	54	1100-Haynes 188	6.1	7.1
7	6061-Cu	43.6	47.7	55	7075-Cd	5.9	5.9
8	2024-Cu	41.0	63.1	56	2024-Haynes 188	5.8	14.6
9	1100-Cu	39.8	40.4	57	7075-Sn	5.8	7.3
10	2219-Cu	36.3	49.6	58	2024-Ti-6-4	5.3	17.2
11	1100-4130	27.9	30.2	59	6061-Ti-6-4	5.2	8.3
12	7075-4130	25.0	26.0	60	6061-Haynes 188	5.0	7.7
13	2024-4130	24.5	38.1	61	2219-Sn	4.7	7.7
14	6061-4130	24.3	27.0	62	2219-Ti-6-4	4.4	18.4
15	7075-Ni	22.0	22.6	63	2219-Haynes 188	4.0	5.4
16	6061-Ni	21.9	29.7	64	7075-2219	3.8	4.2
17	2219-4130	20.3	34.6	65	1100-Sn	3.4	4.0
18	2024-Ni	18.0	29.0	66	6061-2219	3.1	-0.5
19	1100-PH13-8Mo	17.5	18.9	67	2024-2219	2.8	16.7
20	7075-A286	17.0	18.1	68	2024-Sn	2.75	13.1
21	7075-SS304L	17.0	16.1	69	7075-2024	2.6	-1.3
22	7075-SS347	16.8	16.2	70	2024-6061	1.95	18.5
23	1100-SS301	16.6	20.8	71	6061-2024	1.95	± 0
24	7075-PH13-8Mo	16.5	16.2	72	6061-Sn	1.59	5.9
25	6061-PH13-8Mo	16.0	19.8	73	1100-2219	1.20	3.1
26	7075-SS301	15.3	17.1	74	1100-2024	1.15	1.8
27	6061-A286	14.7	18.7	75	6061-1100	0.66	3.7
28	6061-SS347	14.1	21.2	76	7075-6061	0.66	-1.8
29	2219-SS347	13.9	25.0	77	6061-Cd	0.28	4.0
30	1100-Ni	13.9	15.9	78	1100-7075	0.26	4.1
31	1100-A286	13.8	14.5	79	7075-1100	-0.26	-2.3
32	2219-A286	13.4	22.0	80	1100-6061	-0.66	2.3
33	2024-SS301	13.2	30.4	81	6061-7075	-0.66	-1.4
34	2024-PH13-8Mo	12.9	21.0	82	1100-Cd	-0.90	1.3
35	2024-SS304L	12.8	26.5	83	2024-1100	-1.15	10.6
36	6061-SS301	12.4	17.3	84	2219-1100	-1.5	8.6
37	1100-SS304L	12.3	17.9	85	6061-Zn	-1.51	6.6
38	2219-SS304L	12.2	21.4	86	1100-Zn	-1.52	8.6
39	7075-Inco 718	12.2	11.6	87	2024-Cd	-1.54	5.9
40	1100-SS347	12.0	14.7	88	2219-Cd	-2.1	5.5
41	2219-Ni	11.3	30.4	89	2219-2024	-2.3	8.7
42	6061-SS304L	11.3	16.1	90	2024-7075	-2.6	9.0

TABLE 2-21. (Continued)

Overall Ranking	Couple	$\bar{i}_g$, $\mu A/cm^2$	r_A, mdd	Overall Ranking	Couple	$\bar{i}_g$, $\mu A/cm^2$	r_A, mdd
43	2219-SS301	11.0	18.6	91	2219-6061	-3.1	8.9
44	2024-SS347	10.5	24.2	92	7075-Zn	-3.4	4.0
45	2219-Inco 718	10.4	24.0	93	2219-7075	-3.8	11.4
46	1100-Inco 718	10.4	11.4	94	2024-Zn	-6.8	19.3
47	2024-A286	10.3	25.4	95	2219-Zn	-11.1	34.2
48	2024-Inco 718	9.3	20.4				

TABLE 2-22. COMPATIBILITY OF Al ALLOYS AND DISSIMILAR MATERIALS[88]

Class	Al 1100	Al 2024	Al 2219	Al 6061	Al 7075
I Compatible (<5)[a]	Cd	Cd, 7075, 1100, Sn, Haynes, 2219, Ti-6-4, 6061, Zn, Inco 718, PH13-8Mo, SS347, A286, SS304, Ni, SS301	Cd, 2024, 6061, 1100, Haynes, 7075, Zn, PH13-8Mo, SS301, SS304, A286, Inco 718, Ti-6-4, SS347	7075, 2219, 2024	1100, 6061, 2024, Zn 2219
II Borderline (5 to 15)[a]	2024, 6061, 2219	4130, Cu, Ag	Ni, Zn, 4130, Cu, Ag	1100, Cd, Sn, Inco 718, Zn, Haynes, Ti-6-4	Cd, Haynes, Sn, Ti-6-4, Inco 718
III Incompatible (>15)[a]	Sn, 7075, Haynes, Ti-6-4, Zn, Inco 718, A286, SS347, Ni, SS304, PH13-8Mo, SS301, 4130, Cu, Ag			SS304, SS301, A286, PH13-8Mo, SS347, 4130, Ni, Cu, Ag	SS304, SS347, PH13-8Mo, SS301, A286, Ni, 4130, Cu, Ag

(a) ( ) = relative increase in dissolution rate.

TABLE 2-23. CURRENTS GENERATED BY GALVANIC COUPLES IN TAPWATER[89]

Couples		Galvanic Current,	Weight Loss			Potential Coupled	Pits	
			Anode		Cathode			Maximum
Aluminum	Steel	$\mu A/cm^2 10^{-2}$	mdd[c]	$\mu A/cm^2 10^{-2}$	mdd	Anode	Number per dm^2	Depth, μm
1050[a]	Plain steel	6	0.46	37	15.8	-760	0	
5086	Plain steel	7.7	1.47	120	15.3	-750	0	
1050[b]	Stainless steel 316	21.7	0.50	40	0	-450	20	500
5086	Stainless steel 316	22.4	1.69	137	0	-440	11	500
Single Samples								
1050	Plain steel	Noncoupled	0.37	30	16.7			

(a) Average of 3 measurements.
(b) Average of 2 measurements.
(c) mdd = $mg/dm^2/day$, and 1 mdd (Al) ~1.23 $\mu A/cm^2$.

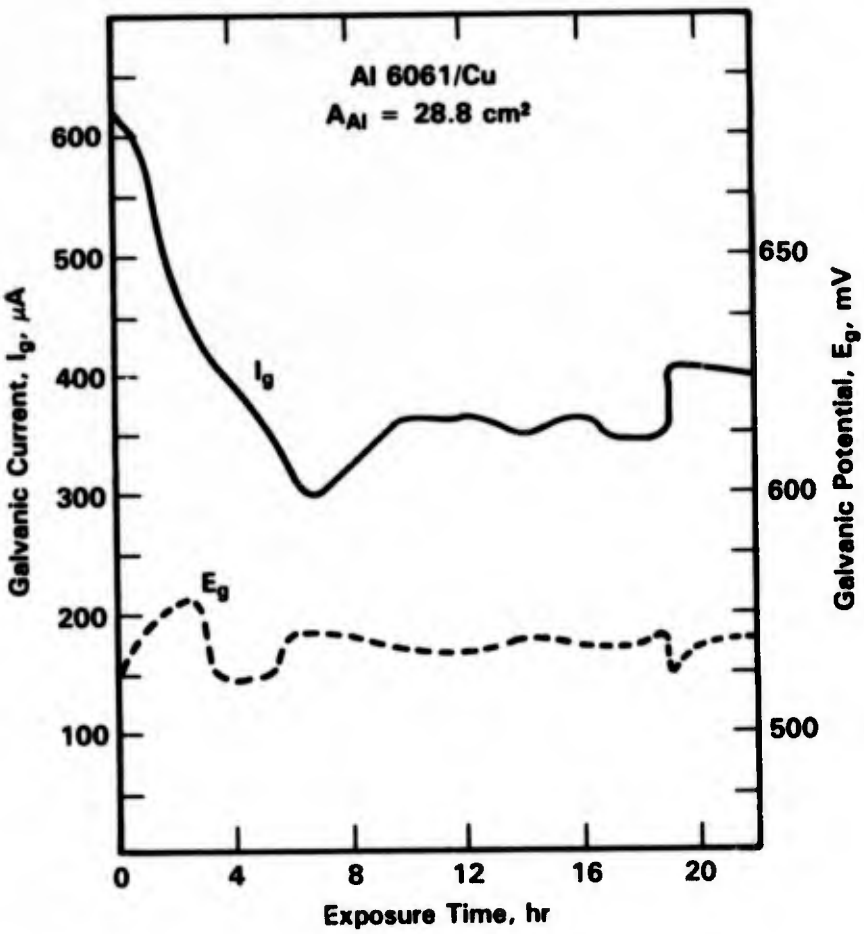

FIGURE 2-34. GALVANIC CURRENT (I_g) AND GALVANIC POTENTIAL (E_g) FOR AN Al 6061/Cu COUPLE IN A 3.5 PERCENT NaCl SOLUTION[91]

TABLE 2-24. CORROSION RATES FOR TWO ALUMINUM ALLOYS WHEN COUPLED TO THE METALS INDICATED AND EXPOSED FOR 2 AND 4 MONTHS TO SEAWATER AT THE U.S. ARMY TROPICAL TESTING STATION, PANAMA CANAL ZONE, 1:1 AREA RATIO[19]

Months	Corrosion Rate, mm/yr	
	6061 Aluminum	7075 Aluminum
	Magnesium	
2	0.445	5.162
4	0.786	4.158
	Stainless Steel	
2	0.380	0.467
4	0.276	0.305
	Steel	
2	0.251	0.340
4	0.176	0.189
	6061 Aluminum	
2	0.043	0.013
4	0.021	0.009
	7075 Aluminum	
2	0.050	0.040
4	0.024	0.030

Corrosion studies performed by Lennox, et al.[92] on 5086-H32 aluminum in quiescent seawater showed accelerated corrosion of the aluminum alloy when coupled to copper-nickel 10 percent, yellow brass, 304 stainless steel, or mild steel.

The accelerating effect of the cathode-anode area ratio is illustrated in Table 2-25. If the anodic area (aluminum) is small compared to the cathodic area, severe corrosion of the aluminum may result. The area ratio effects should be considered when galvanic corrosion is controlled by applying protective coatings. A coating should never be applied to the anode only. In that case, if the coating is damaged, the galvanic current will concentrate resulting in localized high corrosion rates. The cathodic surfaces should be coated and the anodic surface should be left bare.

TABLE 2-25. CALCULATED CORROSION RATE OF H30 ALUMINUM IN AERATED STATIC SEAWATER WHEN GALVANICALLY COUPLED AT THREE AREA RATIOS TO OTHER METALS FOR OVER 100 DAYS[93]

M[a]	Corrosion Rate, mm/yr M:Al[b] 10:1	1:1	1:10
Carbon	39	2 to 10	0.4
Titanium	--	--	--
Monel 400	2.2	0.12	--
EN58J	--	--	--
Copper	4.5	0.66	0.05
Silicon Bronze	2.0	0.6	--
NiAl Bronze	2.4	0.15	0.09
10 percent Al Bronze	2.4	0.6	--
CN30	1.7	0.1	--
LG4 Gunmetal	--	--	--
Lead	0.5	0.15	--
Tin	2.2	0.14	--
HY80	1.6	0.3	0.2
Ni Resist	0.7	0.06	--
Mild Steel	1.7	0.07	0.06
H30 Aluminum	0.09	0.01	0.001

(a) Cathodic member of couple.
(b) Anodic member of couple.

The effect of seawater velocity on galvanic corrosion of aluminum was investigated by Mansfeld and Kenkel[94] and Davis and Gehring.[95-97] In both cases it was found that the galvanic corrosion rate of aluminum increased with increasing velocity. Davis and Gehring[95] investigated the possibility of suppressing galvanic corrosion of aluminum Alloy 5456-H117 coupled to titanium Alloy Ti-6Al-4V, 17-4 pH stainless steel and Inconel Alloy 625 at seawater velocities of zero, 60, and 90 knots.

It was found that the galvanic corrosion rate could be suppressed electrochemically to the uncoupled corrosion rate when the measured galvanic corrosion current was zero or negative. Galvanic corrosion was accelerated above the uncoupled corrosion rate when the galvanic corrosion current was greater than the reduction current on the material to which the aluminum was coupled. In this work, a potential range for suppression of galvanic corrosion was estimated as a function of seawater velocity -0.95 to -1.115 V(Ag/AgCl) at zero velocity and -1.2 to -1.6 V(Ag/AgCl) at 60 and 90 knots.

As discussed in a previous section on galvanic corrosion in the atmosphere, graphite epoxy composites have become important structural materials for aerospace applications and galvanic corrosion of aluminum in contact with these composites is of great concern. Although most applications are not for immersed conditions, some research has been performed in actual and simulated seawater environments.[98-100] A study by Dull, et al.[99] on the corrosion behavior of an aluminum Alloy 6061/graphite composite in a 3.5 percent NaCl solution indicated that corrosion rates decreased with increasing time of exposure. Figure 2-35 shows the effect of time at different temperatures on the corrosion rates of aluminum Alloy 6061 and Al-Gr/Ep. It was observed that galvanic corrosion of composites was only slightly greater than that of the alloy and was definitely not as severe as suggested by thermodynamics. This was confirmed in a later study by Kendall and Dull.[98] This observation may be explained by area ratio effects where the anodic area (aluminum) exposed to the seawater is much greater than the cathodic area (graphite). The mechanism of galvanic corrosion of the composite was explained by Dull, et al.[99] as being crevice corrosion along the region of high carbon fiber density promoted by galvanic coupling.

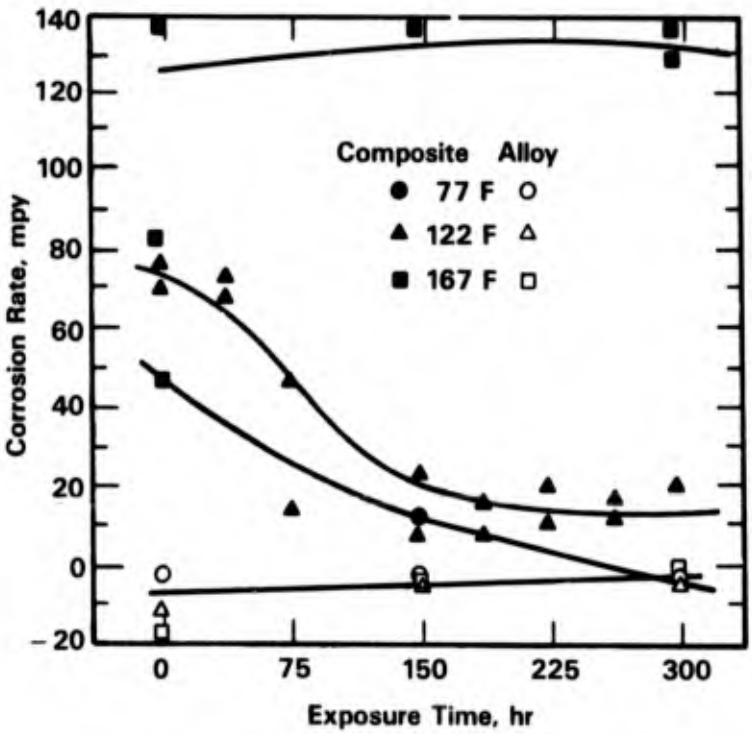

FIGURE 2-35. THE EFFECT OF EXPOSURE TIME ON THE CORROSION RATE OF 6061 ALUMINUM ALLOY-THORNEL 50 GRAPHITE COMPOSITE IN 3.5 PERCENT NaCl SOLUTION BETWEEN 298 K AND 348 K[99]

Stress-Corrosion Cracking

Many of the high strength aluminum alloys can, under certain conditions, fail in marine environments at stresses far below the yield strength due to intergranular SCC. The susceptibility of aluminum alloys to SCC greatly depends on alloy composition, microstructure, orientation, and heat treatment as well as on environmental variables such as pH and temperature. The effect of each of these variables on the SCC behavior of aluminum alloys is discussed in the following sections. The information on SCC is based on service experience, marine exposure of experimental panels, and laboratory testing in actual or simulated seawater. Several techniques have been used in laboratory testing, including testing of smooth and precracked specimens, constant strain and constant strain rate testing, and continuous and alternate immersion testing.

Effect of Alloy Composition

Metallurgical variables such as alloy composition and heat treatment have a strong effect on the SCC resistance of aluminum alloys. The major alloy systems for commercial application that have suffered SCC include, Al-Cu, Al-Cu-Mg, Al-Mg, Al-Mg-Zn, Al-Zn, Al-Zn-Mg-Cu, and Al-Mg-Si.

Speidel[101] listed some general rules for SCC of these alloys in aqueous environments. Pure aluminum is generally considered not susceptible to SCC and, for any given alloy system, the susceptibility to SCC tends to increase with increasing concentration of alloying elements that can be put in super saturated solid solution. SCC resistance of ternary or higher order systems is not only influenced by the sum but also by the ratios of the alloying elements. Minor alloy additions of Cr, Mn, Zr, Ti, V, Ni, and Li to the alloys mentioned above can increase the resistance to SCC. Below, the SCC behavior of specific commercial aluminum alloys in seawater environments is discussed.

5000 Series. Aluminum-Mg (5000 series) alloys containing more than 5 weight percent Mg are susceptible to SCC in seawater environments. At these concentrations, Mg preferentially precipitates along the grain boundaries in the form of a continuous film of Mg_2Al_3 phase. This phase is anodic with respect to the matrix and preferential dissolution of this phase is generally thought to be the mechanism of SCC in this alloy.[102] However, if the Mg content is kept at values less than 4 weight percent, no continuous precipitate can form along the grain boundaries and the alloy becomes resistant to SCC (see Figure 2-36). Various Mg containing commercial Al alloys, 5000 series alloys, have less than 4 percent Mg and are resistant to SCC. In Table 2-26 the various commercial 5000 series alloys are grouped by Mg

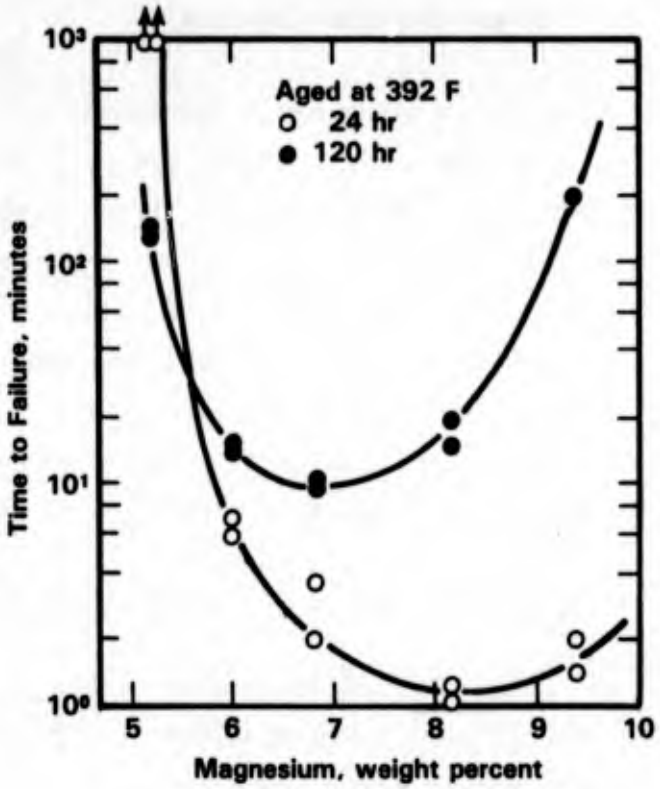

FIGURE 2-36. EFFECTS OF MAGNESIUM CONTENT ON STRESS-CORROSION IN A 3.5 PERCENT NaCl SOLUTION FOR Al-Mg ALLOYS AGED FOR 24 AND 120 HOURS AT 392 F[103]

TABLE 2-26. COMMERCIAL ALLOYS OF THE 5000 SERIES GROUPED BY MAGNESIUM CONTENT

Magnesium Content, weight percent	Alloy Designation
Maximum	
<3.5	5005, 5050, 5052, 5454, 5357, 5457, 5557
3.5-4.5	5154 (3.1 to 3.9 Mg, 0.1 maximum Mn)
	5086 (3.5 to 4.5 Mg, 0.2 to 0.7 Mn)
>4.5	5083 (4.0 to 4.9 Mg, 0.3 to 1.0 Mn)
	5155 (3.5 to 5.0 Mg, 0.2 to 0.6 Mn)
	5056 (4.5 to 5.6 Mg, 0.05 to .20 Mn)
	5356 (4.7 to 5.5 Mg, 0.05 to .20 Mn)
	5456 (4.7 to 5.5 Mg, 0.5 to 1.0 Mn)
Nominal	
3.5	5154
4	5086
4.5	5083
5	5356-5456

content. Table 2-27 shows the stress-corrosion behavior of various Al alloys exposed to the Pacific Ocean water near Port Hueneme at a depth of 2370 feet.[41] The table indicates that all of the 5000 series alloys are resistant to SCC. However, Figure 2-37 indicates that alloys with Mg concentration ranging from 4.0 to 5.5 weight percent (e.g., 5083 and 5456) can be susceptible to SCC in a 3.5 percent NaCl solution.[104] If the Mg concentration in Al-Mg is 4 to 8 weight percent, the resistance to SCC can be increased by a combination of heat treatment and cold working, which will be described in the following section.

In order to improve the resistance of Al alloys containing more than 5 percent Mg to SCC, the effects of additional alloying elements have been investigated. These elements are Bi,[105] B and Be,[106] and Cu and Zr.[107] Baba, et al.[105] found that additions of 0.2 to 0.4 weight percent Bi greatly improved the resistance to SCC of Al-6 percent Mg and Al-8 percent Mg in a 3.5 percent NaCl solution at room temperature (see Figure 2-38). Addition of Bi did not change tensile properties, grain size or aging characteristics. The effect of Bi was attributed to the formation of the insoluble compound Bi_2Mg_3 which may act as a sacrificial anode with respect to the base metal. Figure 2-38 also indicates that Cr and Zr have an additional beneficial effect. Also, Baba[107] showed the beneficial effect of Cu and Zr additions on the SCC resistance of Al-8 percent Mg in a 3.5 percent aqueous NaCl solution (see Figure 2-39).

The trace elements B and Be were found to have a beneficial effect on the SCC resistance of Al-Mg alloys containing 8 percent Mg.[106] Addition of 0.02 percent B and 0.02 percent Be were found to improve SCC resistance by promoting general precipitation inside the grains rather than at the grain boundaries. A 5000 series alloy was developed containing 6 to 8 percent Mg, 0.001 to 0.02 percent Be, and 0.001 to 0.05 percent B; this alloy was designated 5090 and showed excellent resistance to SCC and exfoliation corrosion in marine environments.[108]

6000 Series. Of the Al-Mg-Si (6000 series) alloys, 6061 is the most common alloy and, in a fully aged condition (T6 temper), the precipitate is present as small discrete particles and the alloy is resistant to SCC.

2000 Series. Aluminum-Cu and Al-Cu-Mg (2000 series) alloys are heat-treatable high strength aluminum alloys. Aluminum-Cu alloys derive their strength from precipitation hardening. Addition of Cu also increases the quench sensitivity of the alloy.[109]

Addition of trace amounts of Ti (0.2 percent) to a Al-5 percent Cu alloy was found to improve the resistance to SCC in a 1M NaCl solution.[110,111] The improved SCC behavior

TABLE 2-27. STRESS-CORROSION BEHAVIOR OF ALUMINUM ALLOYS EXPOSED IN THE PACIFIC OCEAN NEAR PORT HUENEME, CA, AT A DEPTH OF 2370 FEET[41]

Alloy	Stress, ksi	Strength, percent	Exposure, days	Depth, feet	Specimens	
					Exposed	Failed
1100-H14	7.5	50	402	2370	3	0
1100-H14	11.8	75	402	2370	3	0
1180	6.3	50	402	2370	3	0
1180	9.5	75	402	2370	3	0
2014-T6	30.8	50	402	2370	3	0
2014-T6	46.1	75	402	2370	3	0
2219-T81	25.0	50	402	2370	3	0
2219-T81	37.5	75	402	2370	3	0
2219-T87	25.3	50	402	2370	3	0
2219-T87	37.9	75	402	2370	3	3
3003-M14	6.1	50	402	2370	3	0
3003-M14	9.1	75	402	2370	3	0
5050-M34	11.0	50	402	2370	3	0
5050-M34	16.6	75	402	2370	3	0
5052-M34	14.9	50	402	2370	3	0
5052-M34	22.4	75	402	2370	3	0
5056-M32[a]	12.0	75	403	6750	2	0
5056-M32[a]	11.8	75	197	2340	3	0
5056-M32[a]	11.8	75	402	2370	3	0
5056-M32	20.2	50	402	2370	3	0
5056-M32	10.4	75	402	2370	3	0
5083-M113[a]	15.0	75	403	6750	2	0
5083-M113[a]	14.6	75	197	2340	3	0
5083-M113[a]	14.6	75	402	2370	3	0
5086-M12	15.1	50	402	2370	3	0
5086-M12	22.7	75	402	2370	3	0
X7002-T6	30.2	50	402	2370	3	0
X7002-T6	43.4	75	402	2370	3	0
Alclad X7002-T6	28.3	50	402	2370	3	0
Alclad X7002-T6	42.5	75	402	2370	3	0
7079-T6	23.6	50	402	2370	3	2
7079-T6	10.4	75	402	2370	3	3
Alclad 7079-T6	35.0	50	402	2370	3	1
Alclad 7079-T6	52.5	75	402	2370	3	2
7178-T6	40.7	50	402	2370	3	0
7178-T6	61.2	75	402	2370	3	3

(a) Welded.

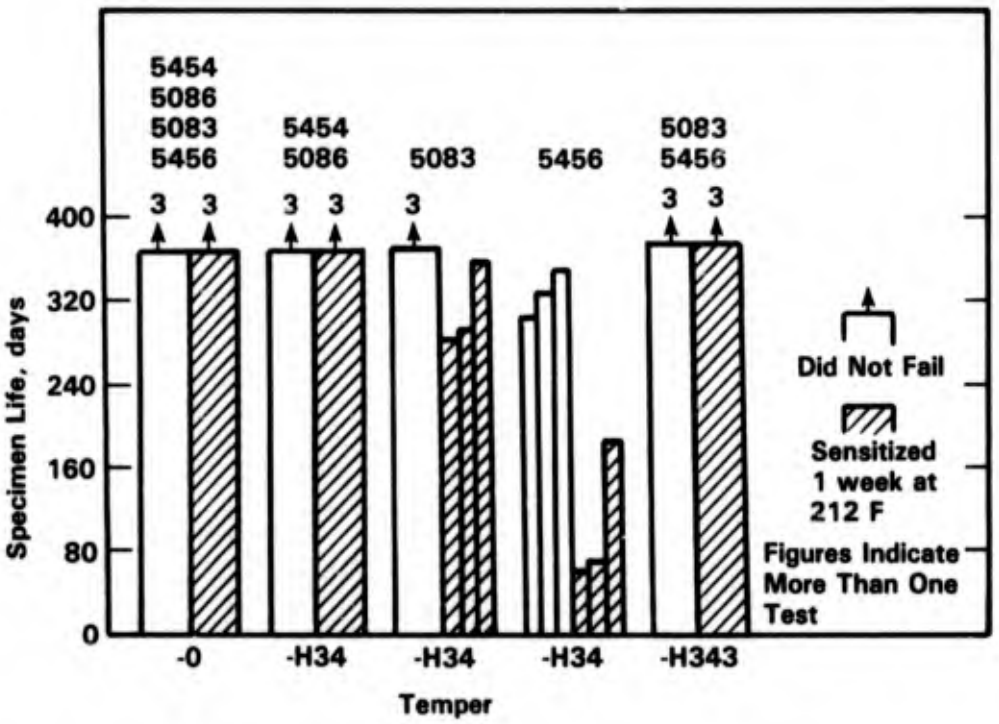

FIGURE 2-37. STRESS-CORROSION RESISTANCE OF STRESSED PREFORMED SPECIMENS OF SEVERAL ALLOYS OF Al-Mg-Mn ALLOY SHEET (0.064 INCH) EXPOSED TO 3.5 PERCENT NaCl SOLUTION BY ALTERNATE IMMERSION[104]

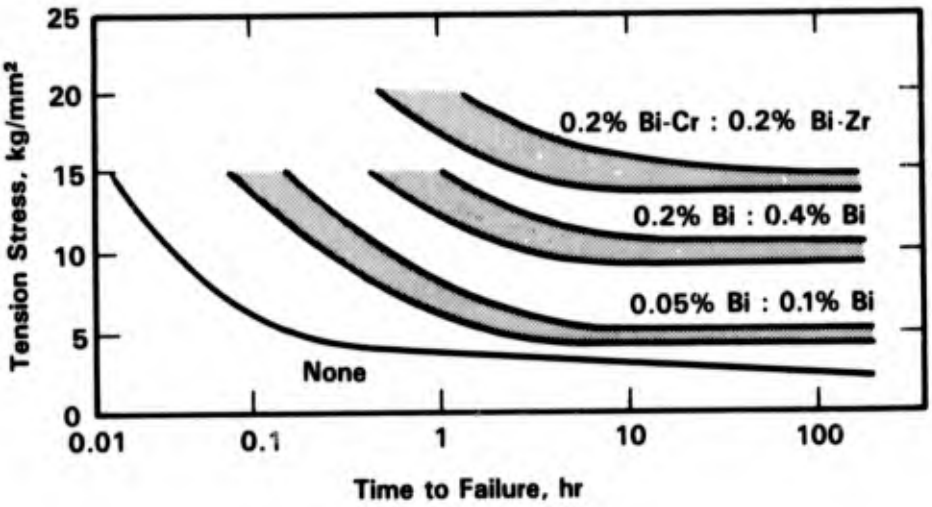

FIGURE 2-38. EFFECT OF ADDITION OF Bi, Cr, AND Zr ON STRESS-CORROSION CRACKING FOR Al-8 PERCENT Mg ALLOY (WATER-QUENCHED FROM 400 C AND SENSITIZED AT 130 C FOR 7 DAYS) IN 3.5 PERCENT NaCl SOLUTION AT ROOM TEMPERATURE[105]

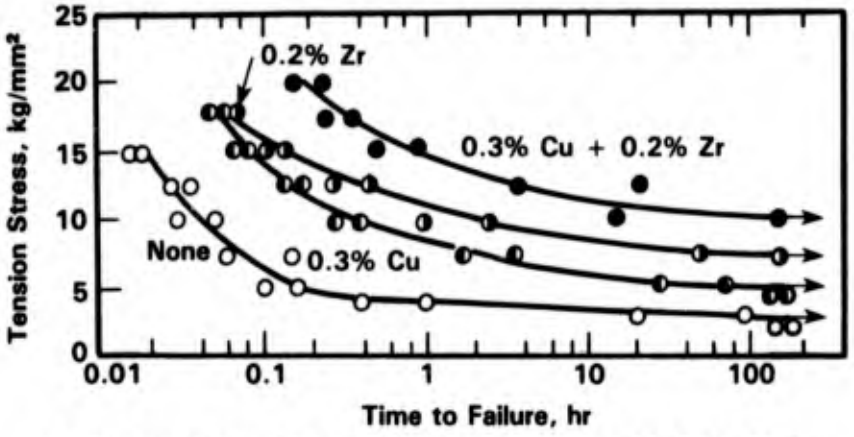

a. Water quenched from 750 F and aged at 265 F for 7 days

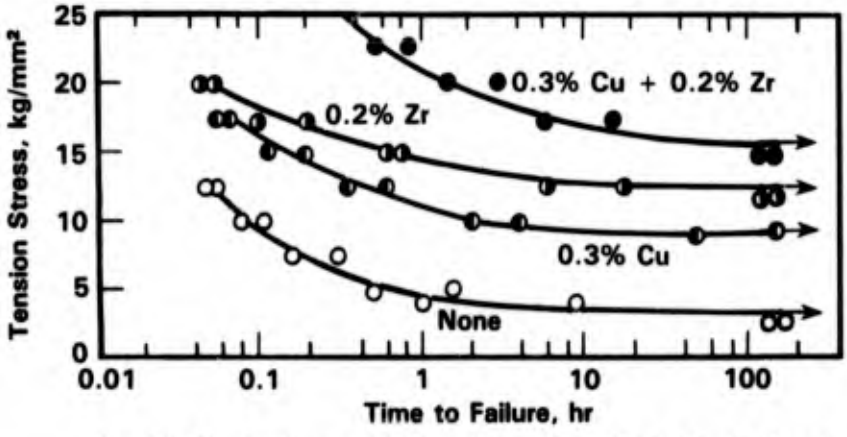

b. Air-Cooled from 750 F and aged at 265 F for 7 days

FIGURE 2-39. EFFECTS OF Cu AND Zr ON THE STRESS-CORROSION CRACKING OF Al-8 PERCENT Mg ALLOY TESTED BY THE CONSTANT LOAD METHOD IN 3.5 PERCENT NaCl ALTERNATE IMMERSION[107]

was attributed to a reduction in grain size which promoted general precipitation of an intermetallic phase.

The addition of Mg to Al-Cu alloys serves to improve the mechanical properties of the alloy. Commercial Al-Cu-Mg alloys are designated 2000 series alloys. The SCC resistance of common 2000 series alloys are summarized in Figure 2-40 which show the crack velocity as a function of stress intensity factor K_I during alternate immersion in 3.5 percent NaCl.[112] Three groups of alloys can be distinguished in the diagram. The alloys most susceptible to SCC are 2014-T451, 2219-T37, 2014-T651, and 2024-T351. These alloys formed cracks at very low levels of K, below 10 MN $m^{-3/2}$. The susceptibility of these alloys was also indicated by the low values of threshold stresses for SCC of smooth tensile specimens,[112,113] i.e., below 55 MN/m^2 (see Table 2-28). However, exposure of the Alloys 2014-T6 and 2219-T8 to actual seawater near Port Hueneme at a depth of 2370 feet did not show any SCC failures

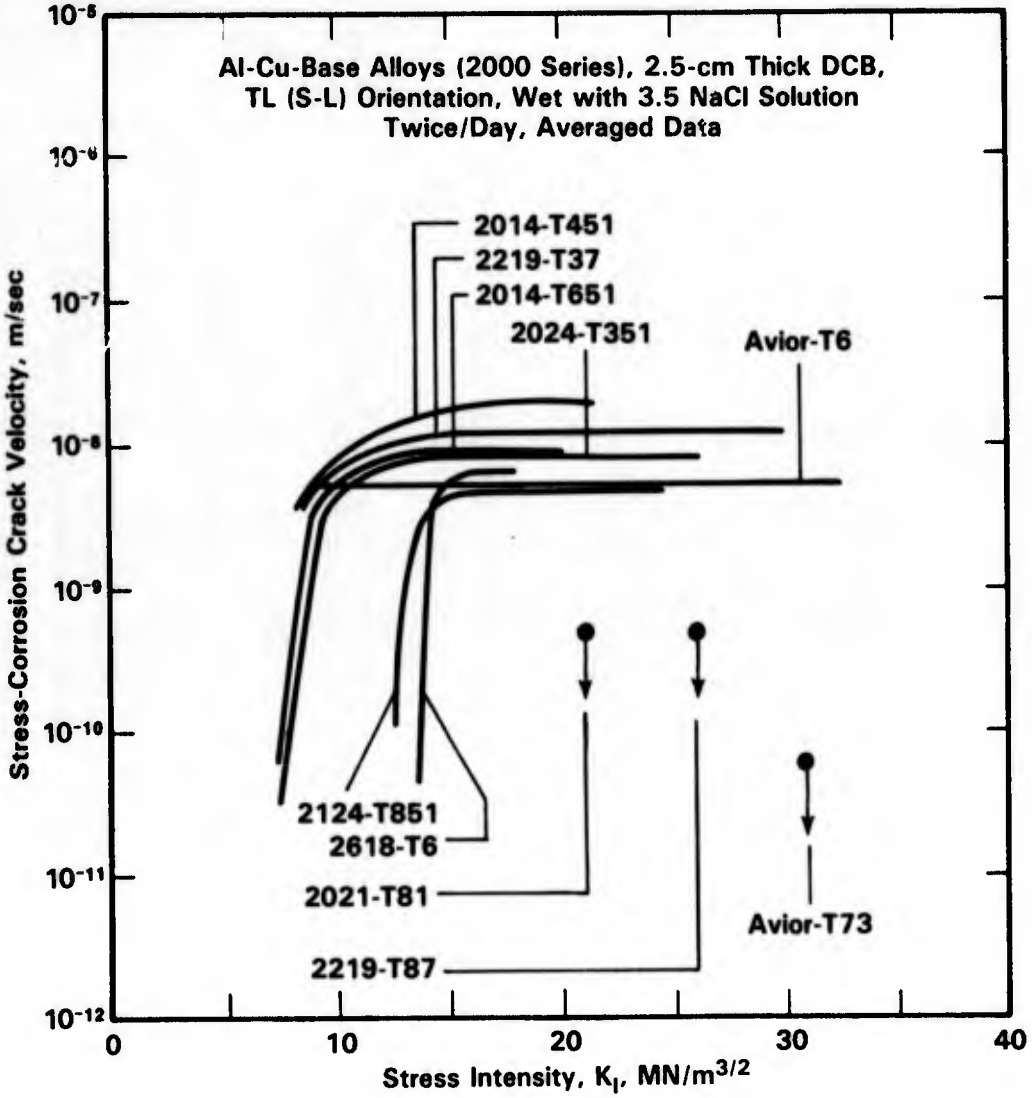

FIGURE 2-40. SUMMARY OF STRESS-CORROSION CRACK GROWTH RATES IN VARIOUS ALUMINUM ALLOYS BASED ON THE ALUMINUM-COPPER SYSTEM(112)

TABLE 2-28. ESTIMATE OF THE HIGHEST SUSTAINED TENSION STRESS AT WHICH TEST SPECIMENS OF DIFFERENT ORIENTATIONS TO THE GRAIN STRUCTURE WOULD NOT FAIL BY SCC IN A 3.5 PERCENT NaCl ALTERNATE IMMERSION TEST (84 DAYS) OR IN INLAND INDUSTRIAL ATMOSPHERE (1 YEAR), WHICHEVER IS LOWER[112,113]

Alloy and Temper	Direction of Applied Stress	Plates		Extrusions		Forgings	
		MN/m^2	ksi	MN/m^2	ksi	MN/m^2	ksi
2014-T6	L	310	45	310	45	210	30
	LT	210	30	150	22	170	25
	ST	<55	<8	<55	<8	<55	<8
2219-T87	L	>270	>40	>240	>35	>260	>38
	LT	>260	>38	>240	>35	>260	>38
	ST	>260	>38	>240	>35	>260	>38
2024-T3, T4	L	170	25	>340	>50		
	LT	140	20	120	18		
	ST	<55	<8	<55	<8		
2024-T8	L	>340	>50	>410	>60	290	43
	LT	>340	>50	>340	>50	290	43
	ST	200	30	>310	>45	100	15
7039-T64	L	>290	>42				
	LT	240	35				
	ST	<35	<5				
7075-T6	L	340	50	410	60	240	35
	LT	310	445	220	32	170	25
	ST	<55	<8	<55	<8	<55	<8
7075-T76	L	>340	>49	>360	>52		
	LT	>340	>49	>340	>49		
	ST	170	25	170	25		
7075-T73	L	>340	>50	>360	>53	>340	>50
	LT	>330	>48	>330	>48	>330	>48
	ST	>300	>43	>300	>43	>300	>43
7178-T6	L	380	55	450	65		
	LT	260	38	170	25		
	ST	<55	<8	<55	<8		
7178-T76	L	>360	>52	>380	>55		
	LT	>360	>52	>360	>52		
	ST	170	25	170	25		
7079-T6	L	>380	>55	>410	>60	>340	>50
	LT	270	40	240	35	210	30
	ST	<55	<8	<55	<8	<55	<8
7049-T73	ST					≈170	≈25
7059-T736	ST					>170?	>25?
7175-T736	ST					≈170	≈25

TABLE 2-28. (Continued)

Alloy and Temper	Direction of Applied Stress	Plates		Extrusions		Forgings	
		MN/m^2	ksi	MN/m^2	ksi	MN/m^2	ksi
RX 720	ST	>170	>25				
RR 58	L	>300	>44				
	ST	>270	>40				
DTD 3067	ST	140	20				
DT 3066	ST	140	20				
AZ 74	ST					310	45

(see Table 2-27). Although no explanation for this discrepancy can be offered, it may be possible that the stress level of the specimens exposed to the actual ocean environment were below the SCC threshold stress so that cracking would not occur.

The second group of alloys consists of those alloys which are susceptible to SCC but cracked at much higher stress intensity levels (between 13 and 15 MN $m^{-3/2}$). These alloys include Alloys 2124-T851 and 2618-T6 (RR58). The smooth specimen stress-corrosion threshold stresses of these alloys ranged from 100 to over 200 MN/m^2. The third group of alloys in the 2000 series are those which are highly resistant to stress-corrosion cracking. These alloys include 2021-T81 and 2219-T87.

The addition of trace amounts of Ag appears to have a beneficial effect on the SCC resistance of 2000 series alloys. As indicated in Figure 2-40, the high strength cast Ag containing aluminum alloy developed in France principally for aerospace application, Avior-T73, is very resistant to SCC as measured by passing an alternate immersion test for 30 days at 80 percent of the yield strength. It should be noted that, in the T6 condition, Avior belongs to the most susceptible alloys, whereas, in the T73 condition, the alloy has excellent resistance.

7000 Series. The highest strength aluminum alloys (7000 series) are based on Zn and Mg alloying additions. Exposure studies by Reinhart[41] in the Pacific Ocean near Port Hueneme showed several 7000 series alloys to be susceptible to SCC. Experimental studies by Miller and Scott performed in Synthetic seawater[114] showed that the susceptibility to SCC increased with increasing Mg content (2.5 to 3.0 weight percent) but was little affected by changing the Zn level (4.0 to 5.0 weight percent). Hence, the best combination of strength and SCC

resistance may be achieved by maintaining a high Zn content and keeping the Mg level to a minimum.

Quaternary additions of Cu were found to be beneficial for SCC resistance.[114-117] The SCC growth data of four Al-6Zn-2Mg-XCu alloys in the T651 condition tested in a 3.5 percent NaCl solution are presented in Figure 2-41 as a function of stress intensity factor.[117] An increase in Cu content up to 2.1 weight percent was found to significantly improve the resistance to SCC; in particular in the K independent region (region II).* It was speculated[117] that the improvement in the K dependent region (region I) was associated with a change in the deformation mode of the alloy, which decreased the stress concentration at the grain boundaries. The strong improvement in the region II SCC resistance was attributed to electrochemical factors. It was speculated that Cu enters the grain boundary precipitates making them less anodic.

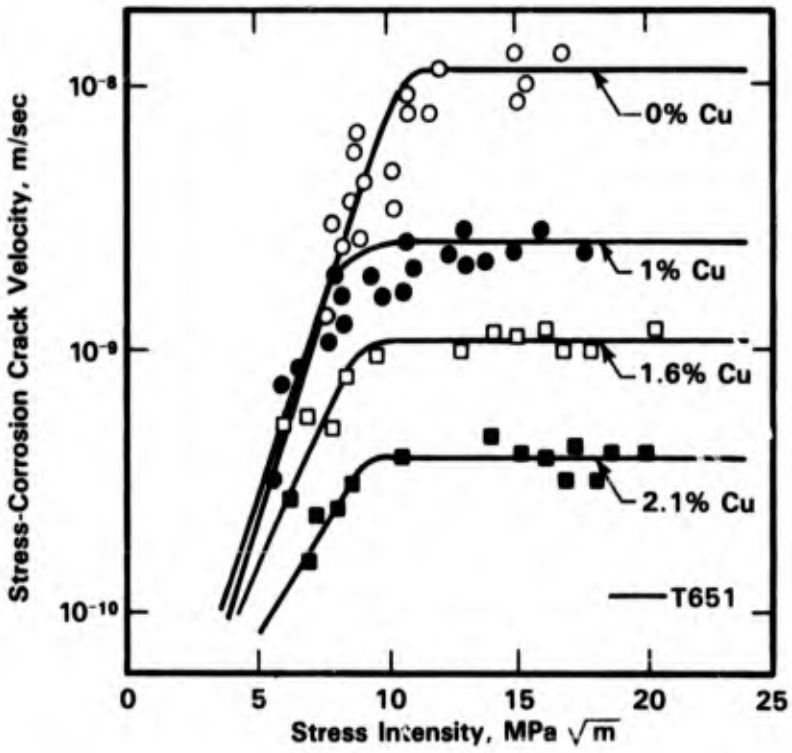

FIGURE 2-41. EFFECT OF STRESS INTENSITY ON STRESS-CORROSION CRACK VELOCITY OF THE Al-Zn-Mg ALLOY WITH VARYING COPPER CONTENTS IN 3.5 PERCENT NaCl[117]

---

* K versus da/dt curves generally consist of three distinct regions, region I at low K_I values which is strongly dependent on K_I, region II at intermediate K_I values which is independent of K_I, and region III at higher K_I values where rapid failure occurs.

Addition of minor alloying elements can also have a significant effect on the SCC resistance of Al-Mg-Zn alloys. The resistance to SCC of Al-Zn-Mg alloys in a 3.5 percent NaCl aqueous solution was improved significantly with the addition of small amounts of Ti. Chen and Judd[118,119] found that a significant improvement in the SCC resistance was obtained for the maximum strength condition in a Al-Zn-Mg alloy with a 0.041 weight percent Ti addition when compared to alloys without Ti. Increasing the Ti concentration to higher than 0.2 weight percent considerably lowered the SCC resistance. Chen and Judd[118] hypothesized that Ti acts as a grain refiner and retards the precipitation kinetics at the grain boundaries.

Some controversy exists on the effect of Ag on the SCC resistance of 7000 series alloys. On the one hand, Ag was shown to have a beneficial effect on the SCC resistance.[120-123] Table 2-29 indicates that addition of small amounts of Ag considerably increased the life of stressed sheet of Al-Zn-Mg alloys in a 3.5 percent NaCl solution.[121] As a result of this work one 7075 type alloy containing Ag is available commercially, i.e., the German Alloy AZ74.61.

However, other workers investigating Ag additions have found no significant increase in SCC resistance due to the presence of this element.[104,124] The confusion regarding the effect of Ag was eliminated when it was pointed out that much of the earlier work was carried out at high temperature aging conditions using thin products that could be heated up rapidly. It was shown[124] that, under these conditions, Ag containing alloys attained higher strength and resistance to SCC. Virtually the same effect could be achieved in Ag free alloys by using appropriate heat treatments.[124]

Chromium is added to Al-Zn-Mg alloys to suppress recrystallization. Commercial alloys containing Cr are 7049, 7075, 7175, 7178, and RX720. Chromium does not appear to have an effect on K_{Iscc} of 7000 series alloys but some effect is noted on the stress-corrosion crack velocities as indicated in Figure 2-42, which shows the crack growth rates of 7000 series alloys in a 3.5 percent NaCl solution as a function of the stress intensity factor.

Addition of Cr to 7000 series alloys increases the quench sensitivity of the alloys. To reduce the quench sensitivity Cr has been replaced by Mn or Zn in alloys which contain a Cu concentration greater than 2 weight percent. The effects of Mn and Zr on recrystallization and grain growth resemble those of Cr, but substantially more Mn than Cr is required to achieve the same results; whereas, the effect of Zr seems to be greater than Cr for a given weight percent.[124] Alloys with Cu concentrations greater than 2 weight percent containing either Zr or Mn (or both) to replace Cr show an improved stress-corrosion behavior over the Cr containing alloys.[124-138] Figure 2-43 shows the improved SCC resistance of an Al-5.4Zn-3Mg alloy containing 1.5 weight percent Mn and 0.2 percent Zr commercial 7000 series alloys.[128]

TABLE 2-29. THE INFLUENCE OF THE ADDITION OF SILVER TO AN Al-Zn-Mg ALLOY ON MECHANICAL AND STRESS-CORROSION LIFE IN A 3.5 PERCENT NaCl SOLUTION[121]

Alloy Composition, weight percent				Aging Treatment	0.1% PS, tons/in.^{2}	TS, tons/in.^{2}	Life, hours[a]
Zn	Mg	Cu	Ag				
5.43	2.36	--	--	16 h at 135 C	22.2	24.5	0.3, 8.7, 14.7, 25.4, 26
5.52	2.36	1.01	--	16 h at 135 C	26.2	28.9	25.2, 35, 206, 238U
5.40	2.47	--	0.30	16 h at 135 C	27.3	29.8	48.5, 91, 94, 332
5.40	2.44	1.01	0.31	16 h at 135 C	28.0	31.2	335, 212U, 238U
				2.5 h at 175 C	27.6	30.6	238U, 502U

(a) U = Specimen unbroken, test discontinued.

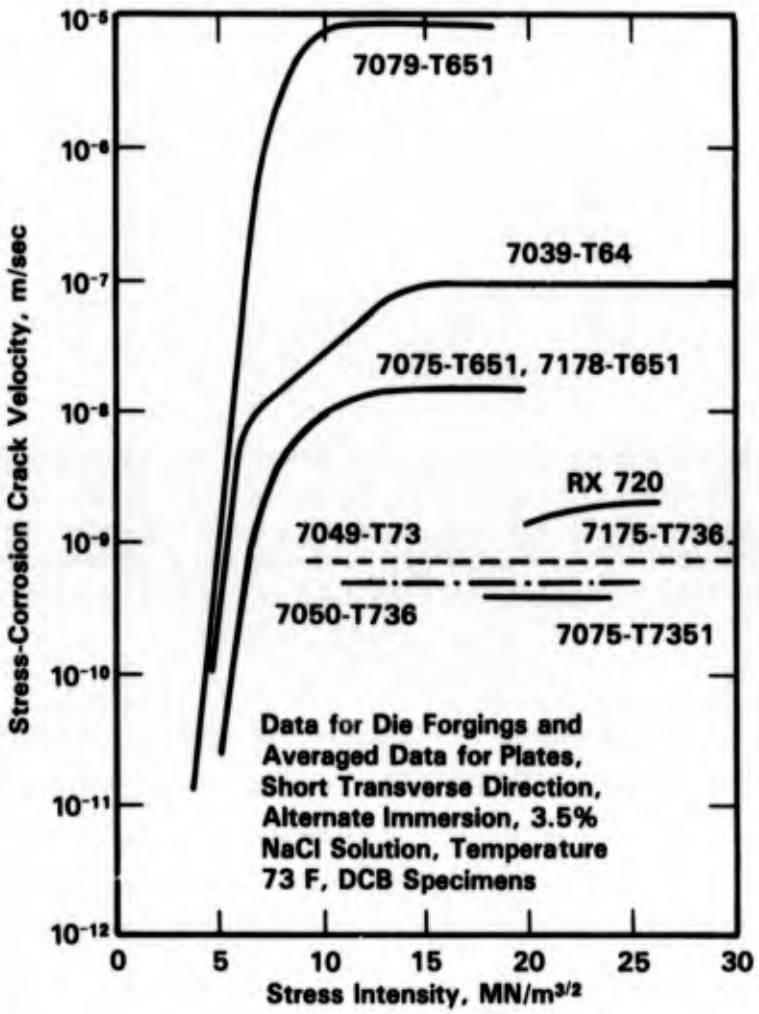

FIGURE 2-42. COMPARISON OF STRESS-CORROSION CRACK GROWTH RATES OF Al-Zn-Mg-Cu (7000 SERIES) ALLOYS IN 3.5 PERCENT NaCl SOLUTION[101]

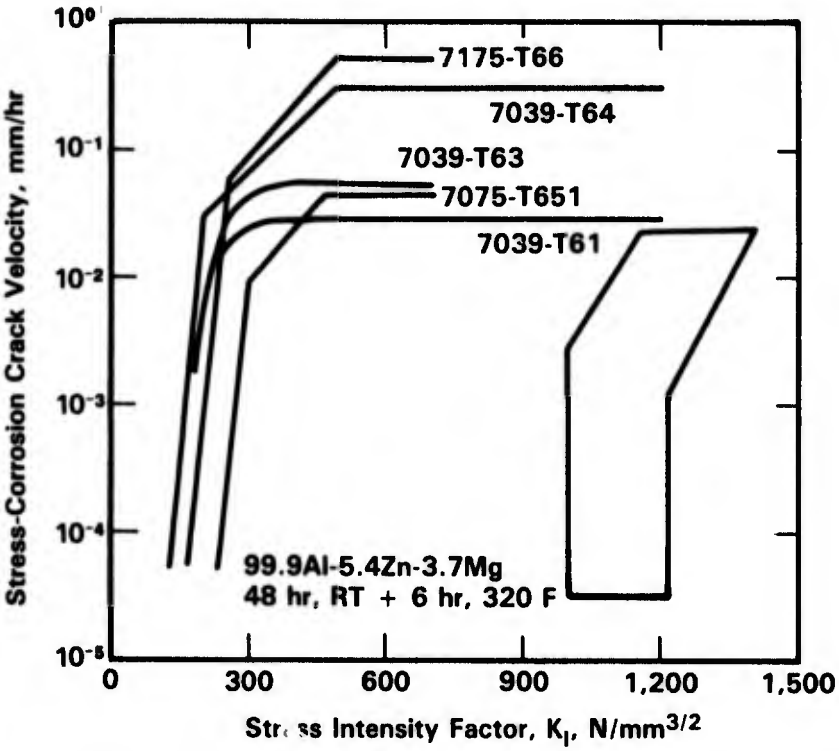

FIGURE 2-43. STRESS-CORROSION CRACK VELOCITY VERSUS STRESS INTENSITY FACTOR DIAGRAM SHOWING IMPROVED SCC BEHAVIOR OF Al-5.4Zn-3Mg WITH 1.5 WEIGHT PERCENT Mo AND 0.2 WEIGHT PERCENT Zn COMPARED TO COMMERCIAL 7000 SERIES ALLOYS (TEST SOLUTION: 3 PERCENT AQUEOUS NaCl SOLUTION, pH 4, 25 C)[128]

Aluminum alloys containing Li offer attractive characteristics. Lithium is the only element which, when added to Al, simultaneously increases strength and elastic modulus, and decreases the density. However, a major drawback of Al-Li alloys is low fracture toughness. Various trace elements such as Mn, Mg, Cr, Zr, and Cu have been added in an attempt to improve the toughness.[65] A study by Pizzo[129] on Al-Cr-Cu, Al-Li-Cu, and Al-Li-Cu-Mg indicated that the Al-Li alloys were less resistant to SCC as well. Figure 2-44 shows the results of the exposure of stressed tuning fork specimens (as suggested in ASTM STP 425) to 3.5 percent NaCl solution.[129]

Effect of Heat Treatment

Heat treatment has a significant effect on the SCC resistance of aluminum alloys in seawater environments. In the following sections the effect of heat treatment on different aluminum alloy groups are discussed: Al-Mg (5000 series alloys), Al-Mg-Si (6000 series alloys), Al-Cu (2000 series alloys), and Al-Zn and Al-Zn-Mg (7000 series alloys).

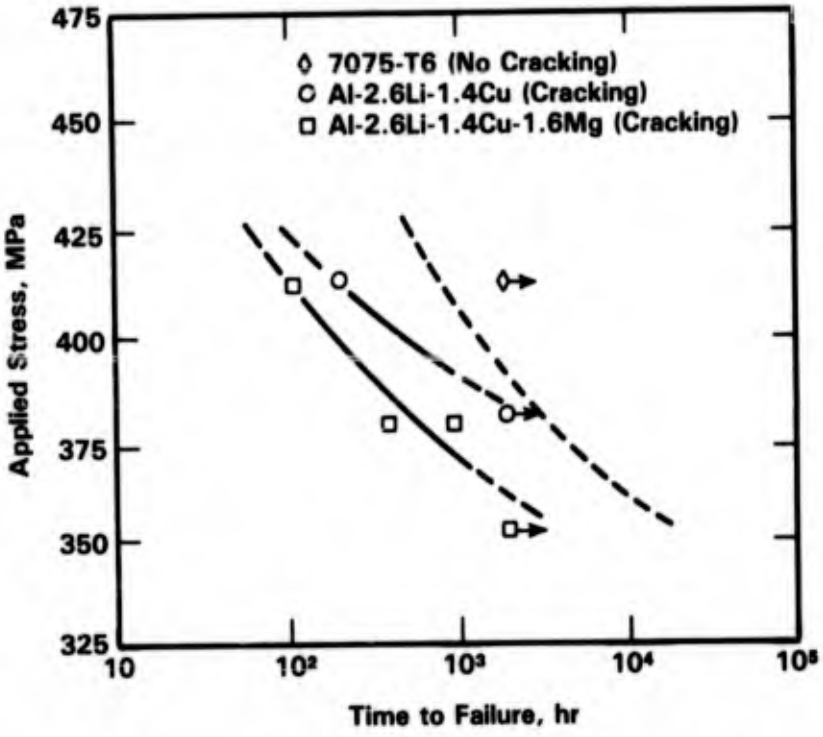

FIGURE 2-44. AQUEOUS CHLORIDE STRESS-CORROSION OF TWO Al-Li-Cu POWDER METALLURGY (P/M) ALLOYS IN 3.5 PERCENT NaCl SOLUTION[129]

5000 Series. The SCC behavior of Al-Mg (5000 series) alloys depends on the precipitation state of the alloy. In particular, the precipitation of Mg_2Al_3 along the grain boundaries strongly affects the susceptibility. The grain boundary precipitation reaction is sluggish and is accelerated by deformation, by exposure to elevated temperatures, and by higher Mg content. Following solution treatment, various aging treatments can be performed.

As indicated in Figure 2-45, SCC susceptibility is little affected by different solution treatment temperatures.[130]

However, aging time and temperature have a strong effect on the susceptibility to SCC as indicated by Figures 2-46 and 2-47. These figures show the effects of aging time and temperature on the susceptibility of various Al-Mg alloys to SCC in 3.5 percent NaCl solutions.[103,131] The diagrams indicate that different combinations of Mg concentration, aging time, and aging temperature can result in different susceptibilities to SCC. The increase in resistance to SCC at longer aging times and aging temperatures is likely due to resolutionizing of the Mg_2Al_3 precipitates.

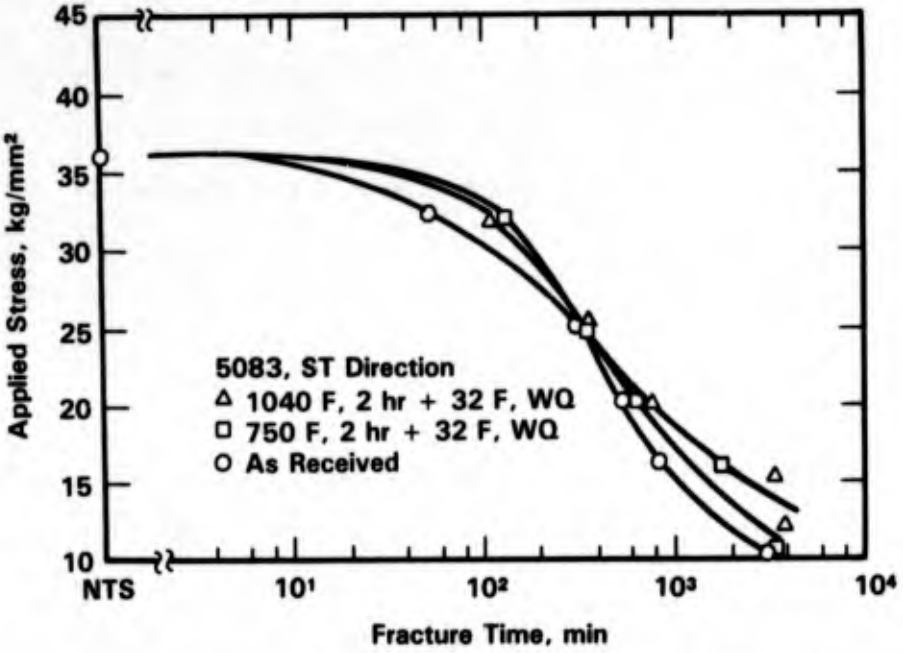

FIGURE 2-45. STRESS-CORROSION CRACKING CURVES IN 3.5 PERCENT NaCl + 0.5 PERCENT H_2O_2 SOLUTION FOR SHORT TRANSVERSE (ST) DIRECTION SPECIMENS OF 5083 ALUMINUM HEAT-TREATED AT VARIOUS SOLUTION TEMPERATURES(130)

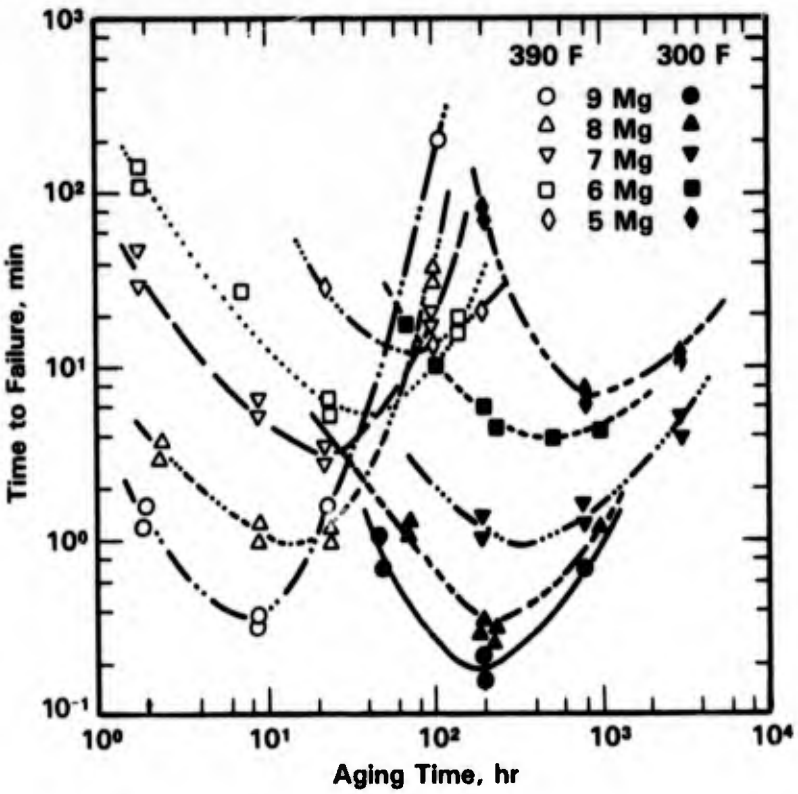

FIGURE 2-46. EFFECTS OF ISOTHERMAL AGING AT 390 AND 300 F ON STRESS-CORROSION OF Al-Mg ALLOYS IN A 3.5 PERCENT NaCl SOLUTION(103)

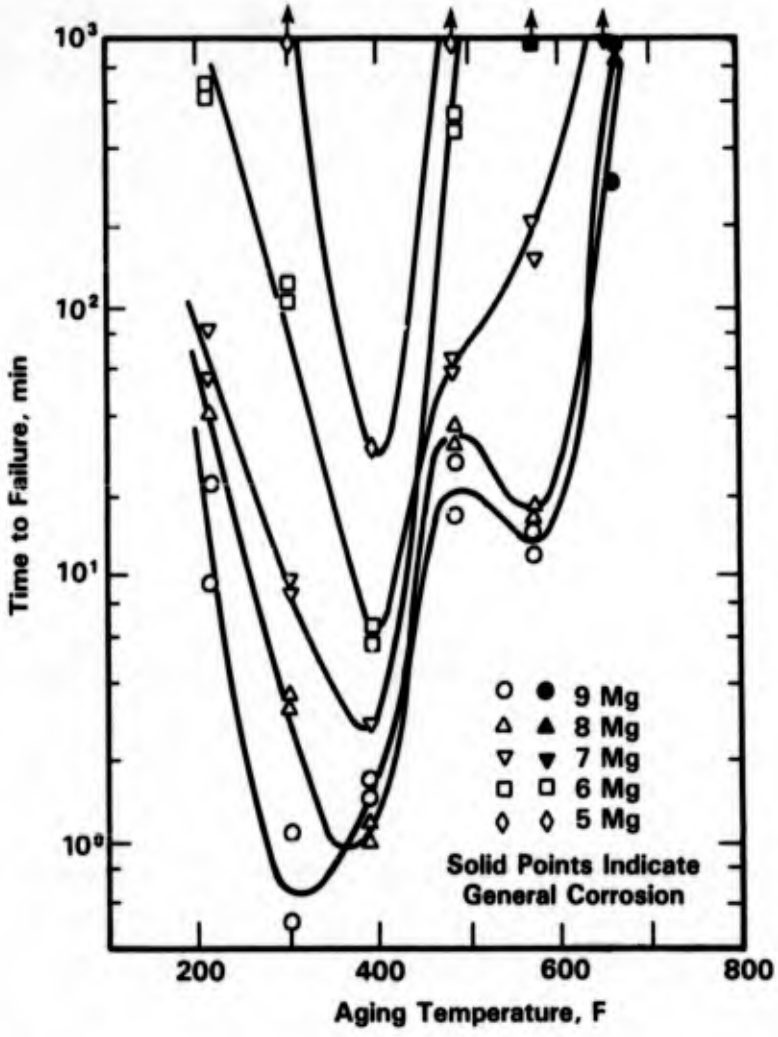

FIGURE 2-47. EFFECT OF AGING TEMPERATURE ON TIME TO FAILURE DUE TO STRESS-CORROSION CRACKING OF Al-Mg ALLOYS AGED FOR 24 HOURS IN A 3.5 PERCENT NaCl SOLUTION[131]

A study of the effect of nine different tempers of Alloy 5456 with and without sensitization (to simulate welding) on the SCC resistance in seawater near Wrightsville Beach, NC, was performed by Niederberger, et al.[132] Failures occurred with the H12, H16, H32, and H36 tempers, whereas no failures were detected in sensitized or unsensitized samples in the O, H22, H24, and H321 tempers. However, in studies by Reinhart[41] Alloy 5456-H32, as well as a series of other magnesium-bearing alloys, showed no signs of stress-corrosion failure after exposure for about 400 days in the deep ocean. Although no explanation can be offered for this discrepancy it may be argued that, in the studies by Reinhart, the stress was below the threshold for SCC or the alloys may have received a thermomechanical treatment such as is discussed in the following paragraph.

An alternative method to achieve a SCC resistant microstructure in Al-Mg alloys containing 4 to 9 weight percent Mg is a combination of heat treatment and working. Working is done after solution treatment and can be done at aging temperature (isothermal rolling)[42] or at room temperature prior to aging or between two aging treatments. An example of the latter thermomechanical treatment is shown in Figure 2-48. Figure 2-49 indicates the beneficial effects of the cold rolling during aging treatment on SCC of Al-8Mg in a 3.5 percent NaCl solution. These and other treatments provide tempers with increased SCC resistance. Examples are H321, H323, H343, H116, and H117 for the commercial Alloys 5083 and 5456.[38,134,135]

6000 Series. The commercial Al-Mg-Si alloys (6000 series) which are strengthened by precipitation hardening, are generally highly resistant to SCC.[104] Alloy 6061 is one of the commercial 6000 series alloys that can be made susceptible to SCC in the T4 heat treatment condition if a high heat treating temperature is followed by a slow quench.[104] In the fully aged condition, T6 temper, the precipitates are present as small discrete particles and the alloy is highly resistant to SCC.

Al-Cu-Mg Alloys. Al-Cu and Al-Cu-Mg alloys derive their strength from precipitation hardening, which is achieved by solution heat treatment, followed by rapid cooling and either natural aging at room temperature (T4 temper) or artificial aging at an intermediate temperature (T6 temper). Cold working after quenching further increases the strength, resulting in the T3 temper and when artificially aged, the T8 temper.

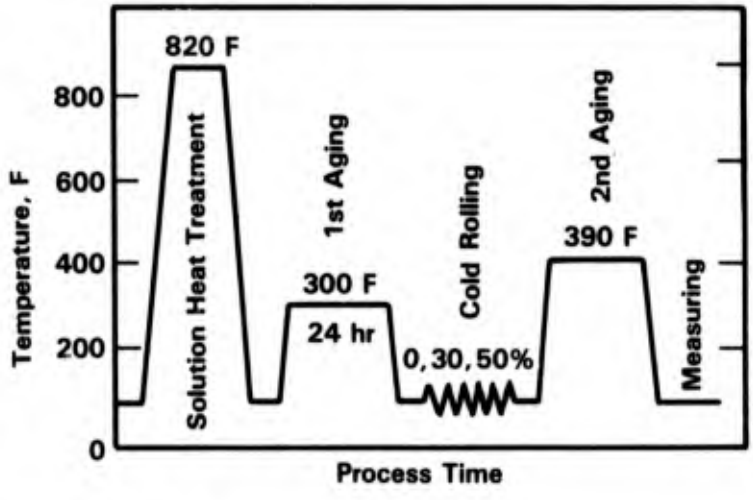

FIGURE 2-48. PROCESS DIAGRAM OF A TYPICAL THERMOMECHANICAL TREATMENT FOR ALUMINUM ALLOYS[133]

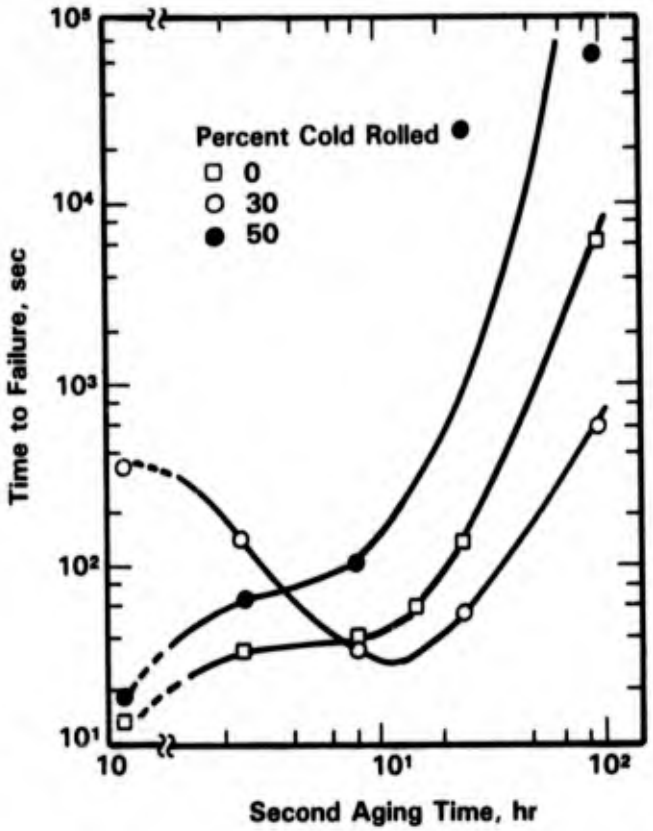

FIGURE 2-49. EFFECTS OF THERMOMECHANICAL TREATMENT (TMT) ON THE STRESS-CORROSION SUSCEPTIBILITY OF Al-8 PERCENT Mg ALLOY IN A 3.5 PERCENT NaCl SOLUTION[133]

Al-Cu-Mg alloys such as 2024, 2014, and 2219 in the naturally aged T3 and T4 tempers can be highly susceptible to SCC in seawater.[136] The susceptibility of Al-Cu and Al-Cu-Mg alloys to SCC is greatly affected by heat treatment. In particular, the susceptibility to SCC depends on the rate of quenching following solution treatment and aging conditions. The effect of quench rate on susceptibility to SCC is illustrated in Figure 2-50. The diagram in Figure 2-50 indicates that at quench rates faster than a certain rate (depending on alloy composition) the alloys are resistant to SCC. However, very fast quench rates may introduce stresses in relatively complex forgings. Therefore, controlled quenching with polyalkylene glycol has been used when quench distortion needs to be avoided or low residual stress combined with resistance to SCC is required.[137]

During aging following quenching, the susceptibility to SCC increases with aging time initially (the rate of increase depending on aging temperature) reaches a maximum and then decreases.[69,138,139] Figures 2-51 and 2-52 show the effect of aging time on the SCC susceptibility of an Al-4 percent Cu alloy and the commercial 2024 alloy. Figure 2-51 also

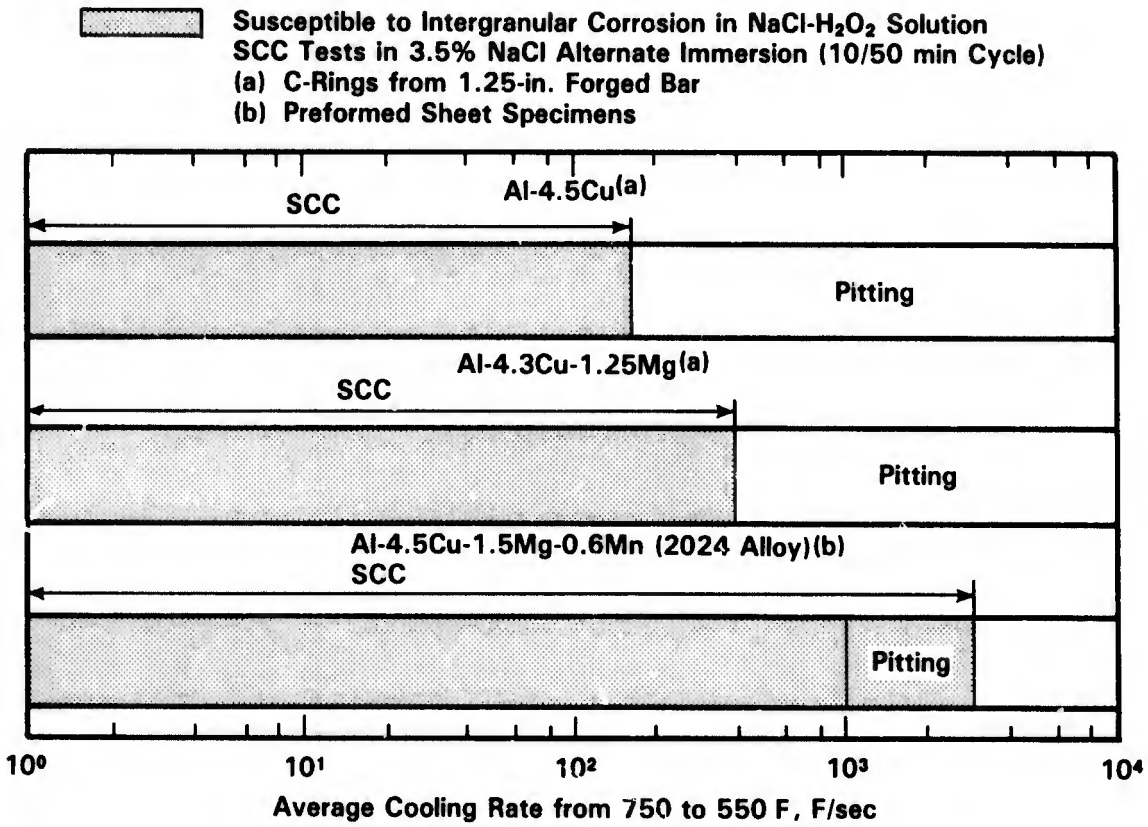

FIGURE 2-50. EFFECT OF QUENCHING RATE ON SUSCEPTIBILITY TO INTERGRANULAR CORROSION AND SCC FOR SOME 2000 SERIES ALLOYS[104]

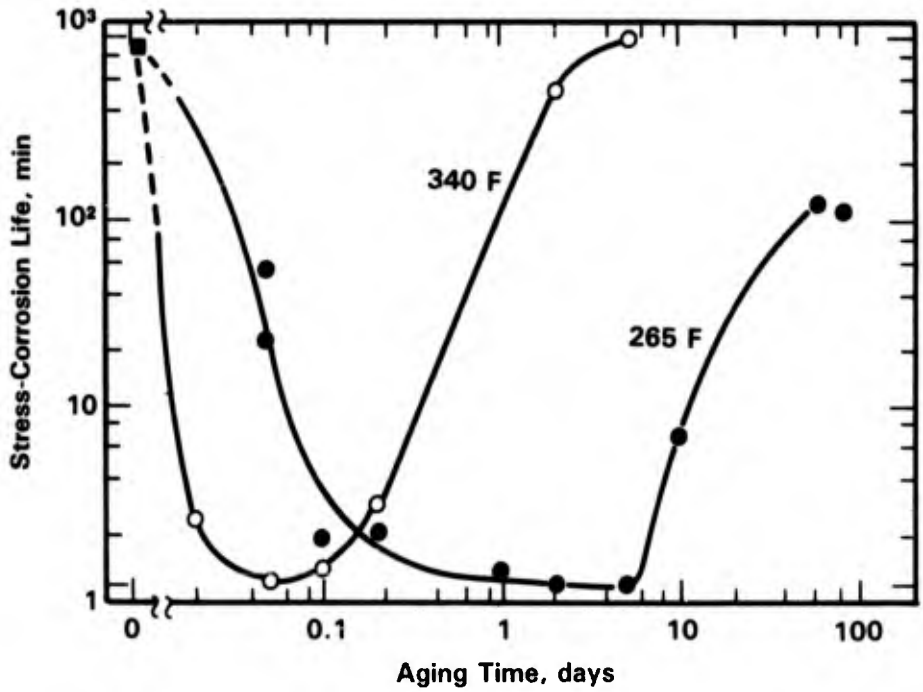

FIGURE 2-51. THE EFFECT OF AGING TIME AT 265 AND 340 F ON THE SCC LIFE FOR Al-4 PERCENT Cu ALLOY IN 1M NaCl + 1 WEIGHT PERCENT H_2O_2[69]

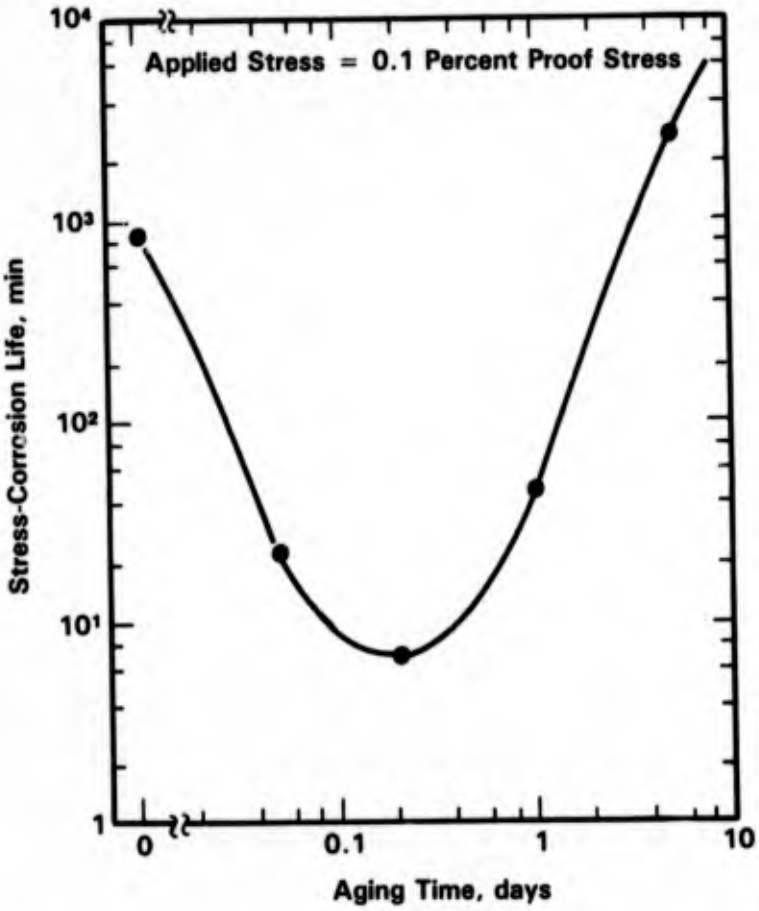

FIGURE 2-52. THE SCC LIFE-TIME OF 2024 ALLOY IN 1M NaCl + 1 WEIGHT PERCENT H_2O_2 AS A FUNCTION OF THE AGING TIME AT 340 F[139]

shows that shorter aging times are required for sensitization and overaging of the Al-Cu alloy. Figure 2-52 indicates that overaging can make a 2000 series alloy resistant to SCC. However, the aluminum Alloy 2014 in the artificially aged T6 temper was found to be highly susceptible to SCC in seawater.[140,141]

7000 Series. The resistance of Al-Zn-Mg and Al-Zn-Mg-Cu (7000 series) alloys to SCC in seawater strongly depends on heat treat parameters such as solution treatment temperature, quench rate, and aging temperature and time. In particular, the 7000 series alloys are highly susceptible to SCC when they are aged to peak strength (T6 temper).

The T6 temper can be achieved by different combinations of the above heat treat parameters. Shastry, et al.[142] showed that solution treatment temperature has a significant effect on the stress-corrosion resistance of 7075-T6. Figure 2-53 shows that the plateau velocity is the lowest and thus the resistance the highest at a solution treatment temperature of about 800 F. At higher temperatures, the susceptibility to SCC increases rapidly.

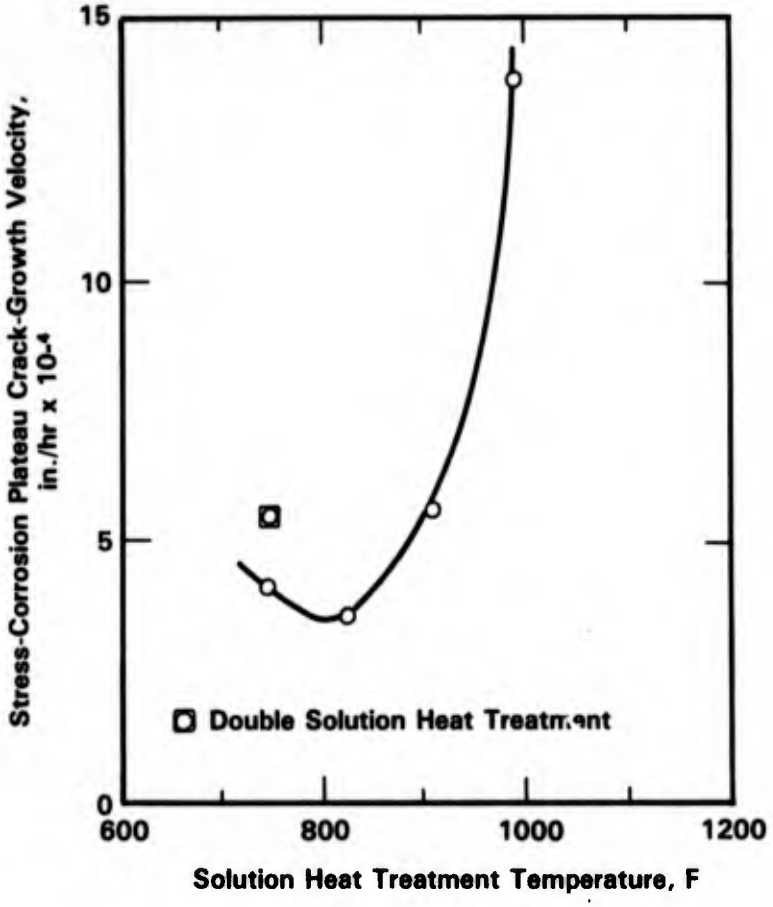

FIGURE 2-53. VARIATION OF STRESS-CORROSION PLATEAU VELOCITY WITH SOLUTION TREATMENT TEMPERATURE FOR ALUMINUM 7075-T6 ALLOY TESTED IN 3.5 PERCENT NEUTRAL NaCl SOLUTION(142)

As is the case of the 2000 series alloys, the resistance to SCC can be improved by increasing the quench rate. Rapid quenching (greater than 200 F/sec) was found to improve the SCC resistance of the Cu containing 7000 series Alloy 7075-T6 in the long transverse direction.(104) However, the beneficial effects of these high quenching rates on the resistance to SCC of 7075-T6 plate is nonexistant for plate and forgings where stressing in the short transverse direction is possible.

The resistance of Al-Zn-Mg alloys to SCC can be improved by aging at relatively high temperatures (325 to 350 F). A drawback of the aging treatment is that the increase in resistance to SCC is achieved at the expense of the strength of the alloys, as is illustrated in the schematic diagram in Figure 2-54.

A number of commercial overaging heat treatments has been developed for several high strength 7000 series aluminum alloys.(103,124,144-146) The commercially available tempers for these alloys are -T76 and -T73. Figure 2-55 shows the effect of overaging of the low Cu

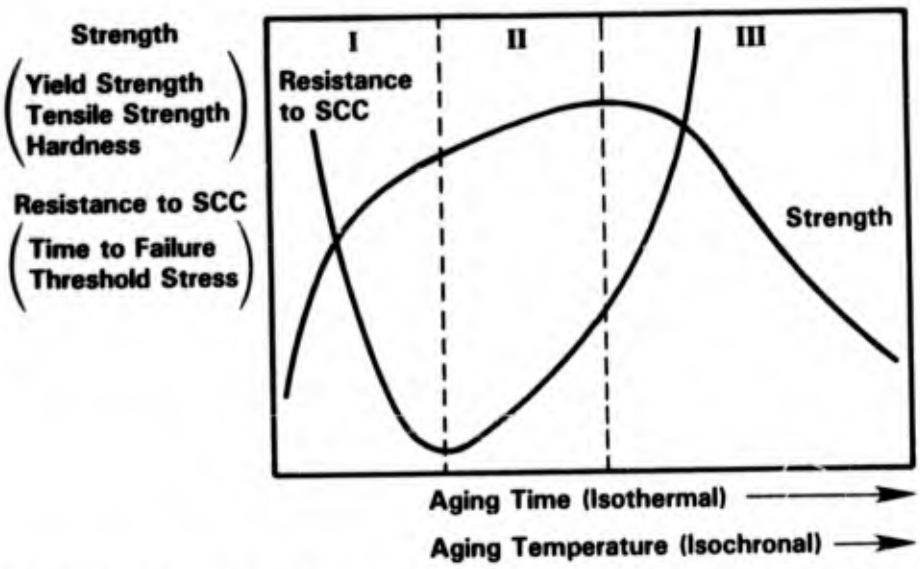

FIGURE 2-54. RELATIONSHIP BETWEEN STRENGTH AND STRESS-CORROSION RESISTANCE DURING AGING OF HIGH-STRENGTH, 7000 SERIES ALLOYS[143]

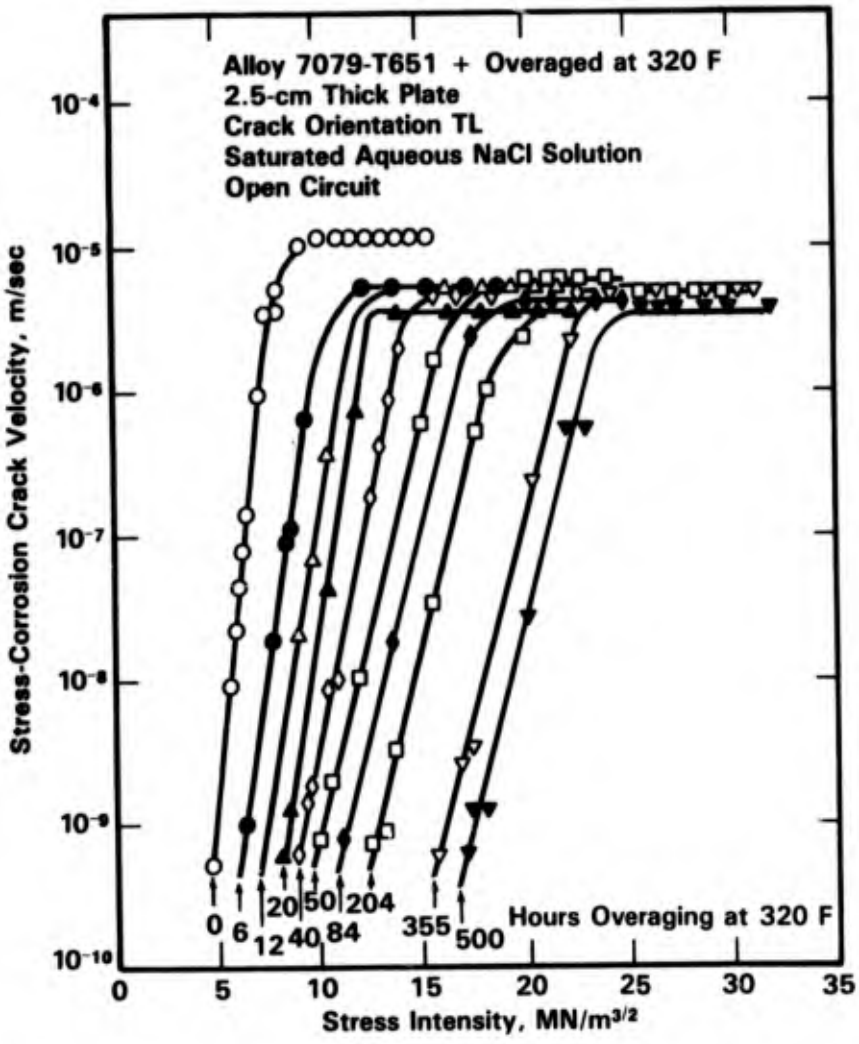

FIGURE 2-55. EFFECT OF OVERAGING (AGING TIME IN HOURS) ON STRESS-CORR CRACK VELOCITY OF HIGH STRENGTH ALUMINUM ALLOY 7079[10

Alloy 7079.[101] The diagram indicates that overaging has no effect on the plateau velocity but has a strong effect on K_{Iscc} after long aging times. Since these long aging times also result in a considerable decrease in tensile yield strength, overaging of this alloy is impractical. Similarly, for other low Cu alloys such as 7039 and 7007, overaging treatments are not practical.[101] On the other hand, in the Cu-rich Alloys 7075 and 7178, a considerable reduction in crack velocity was achieved after 15 hours at a temperature of 160 C (see Figure 2-56), which results in a T76 temper. Moreover, the decrease in strength as a result of overaging to the T76 temper is minimal. The overaging from T6 to T73 results in a moderate reduction in tensile yield strength of 10 to 15 percent[124] and a considerable improvement in fracture toughness.[147] Recently, alloys have been developed that combine the strength of the 7000 series T6 temper and the SCC resistance of the T73 temper.[101,148-151] These alloys are 7049-T73, 7175-T736, 7075-T736, and 7010-T736.

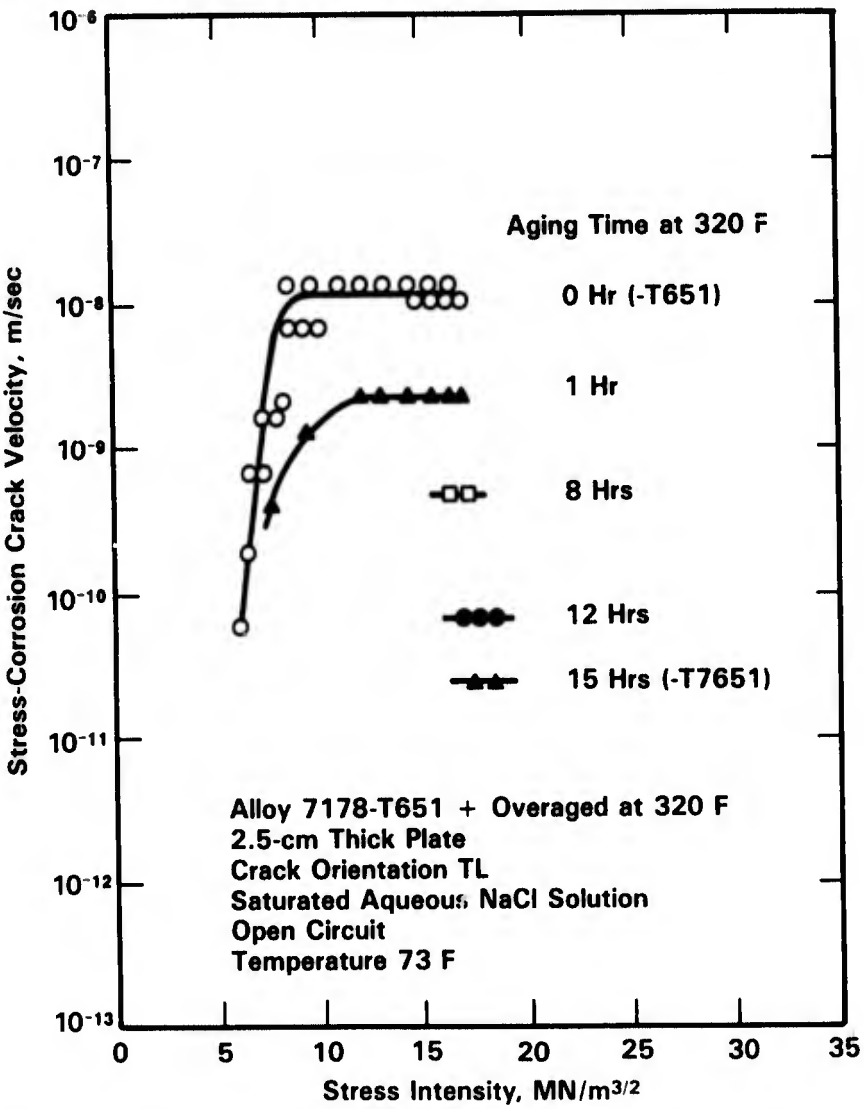

FIGURE 2-56. EFFECT OF OVERAGING ON STRESS-CORROSION CRACK VELOCITY IN ALUMINUM ALLOY 7178[101]

An alternative method to achieve a combination of high strength and SCC resistance includes thermomechanical treatments.[152,153] Reiman and Brisbane[152] showed that a combination of heat treatment and forming could improve the SCC resistance and increase the strength compared to the T6 temper (see Figure 2-57 and Table 2-30). The thermomechanical treatments developed in this study are: (a) 7075-TMT, solution treat at 465 C and water quench, age 1 hour at 100 C followed by 10 percent cold work, final age at 120 C for 16 hours, and (b) 7075-TMTII, as for (a) plus 6 hours at 165 C.

Geometric Effects

Since SCC in aluminum alloys is almost always intergranular, the resistance of these alloys to SCC is strongly related to the local grain shape and orientation with respect to the applied stress. The grain orientation in standard wrought forms are indicated schematically in Figure 2-58. Because of the importance to relate the grain orientation to the direction of the applied load, two index systems have been devised. In one system used in the absence of cracking, the three stressing directions are denoted by longitudinal (L), long transverse (LT), transverse (T), or short transverse (ST) as shown in Figure 2-58. The second system, which considers the presence of cracks, specifies both the cracking plane and the direction of crack propagation. It uses (L, T, W) to indicate the three perpendicular directions, L for the longitudinal direction, T for the thickness direction, and W for the width direction. The crack propagation is identified by the direction normal to the crack. The crack propagation direction is identified by one of the directions, L, T, or W, see Figure 2-59.

Aluminum alloys are most susceptible when the stress is applied in the ST direction (see Table 2-28), i.e., perpendicular to the grain flow. The important influence of grain orientation on SCC is illustrated in Figure 2-60, which shows the time-to-failure of smooth tensile specimens of Alloy 7075-T6 as a function of applied stress in a 3.5 percent NaCl solution. Note that both the time-to-failure and the threshold stress decreased as the stressing direction is changed from the longitudinal to the short transverse direction.

During forging, the grains are flattened in the parting plane, as indicated in Figure 2-61, and cracking may occur along that plane. Hyatt[154] showed that residual stresses in susceptible material can be sufficient to initiate cracks and can also play an important role in accelerating crack growth rates in artificial seawater. It was further shown that residual stresses in precracked specimens could easily be eliminated by plastically deforming the specimens after quenching.

Surface deformation of aluminum structural components also has a significant effect on stress-corrosion cracking initiation. Ratke[156] indicated that superficial plastic deformation

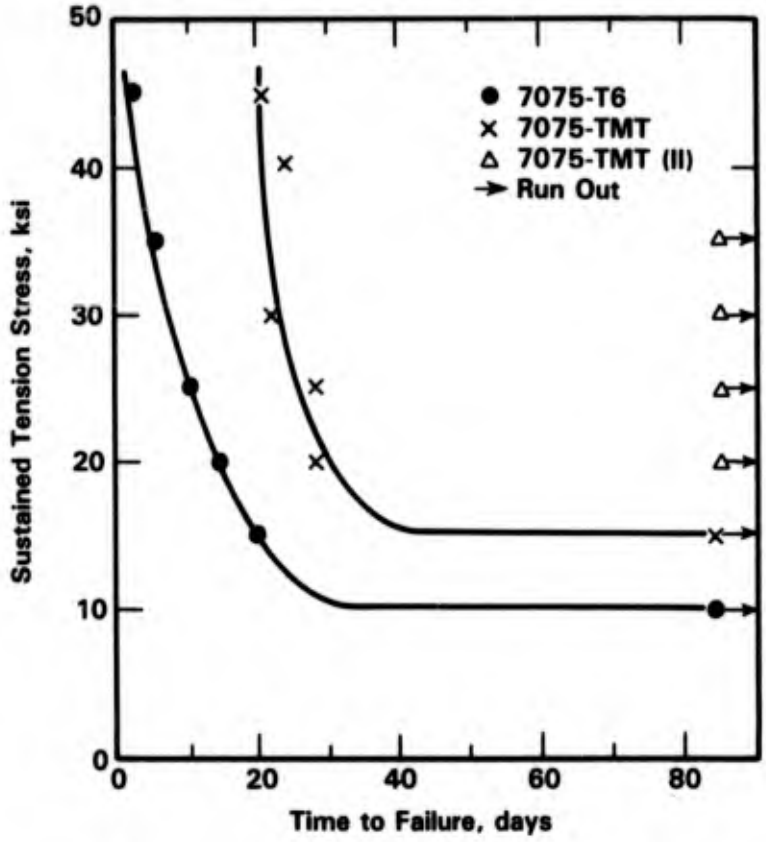

FIGURE 2-57. SHORT TRANSVERSE STRESS-CORROSION BEHAVIOR FOR THERMOMECHANICALLY TREATED (TMT) 7075. ALTERNATE IMMERSION IN 3.5 PERCENT NaCl[152]

TABLE 2-30. TENSILE PROPERTIES OF THERMOMECHANICALLY TREATED (TMT) 7075 COMPARED TO THOSE OF 7075T-651 BAR STOCK[152]

Temper	T-6	TMT	TMT II
0.2 percent yield strength, ksi	74.5	82.6	70.0
Ultimate tensile strength, ksi	83.1	87.1	79.3
Elongation, percent in 1 in.	16.5	14.6	19.0
Red. in area, percent	32.0	31.9	41.9

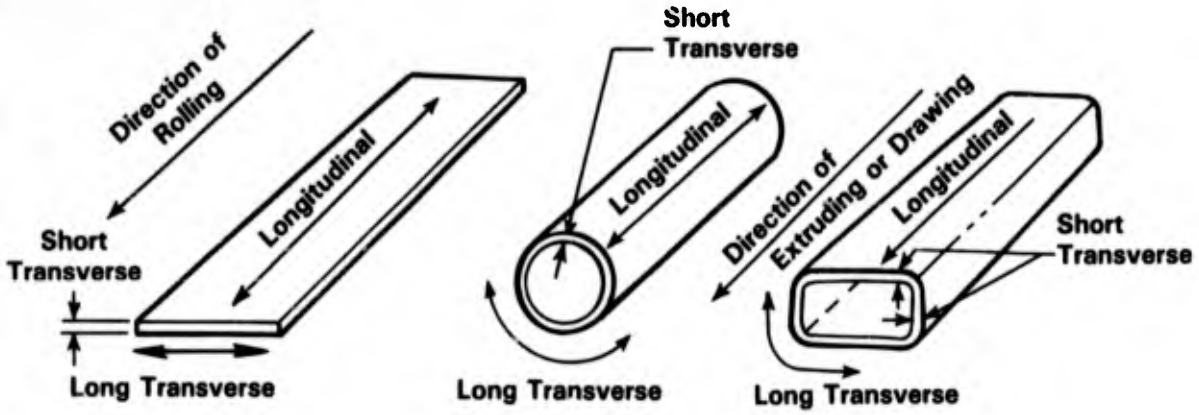

a. Sheet and Plate

b. Extruded and Drawn Tube

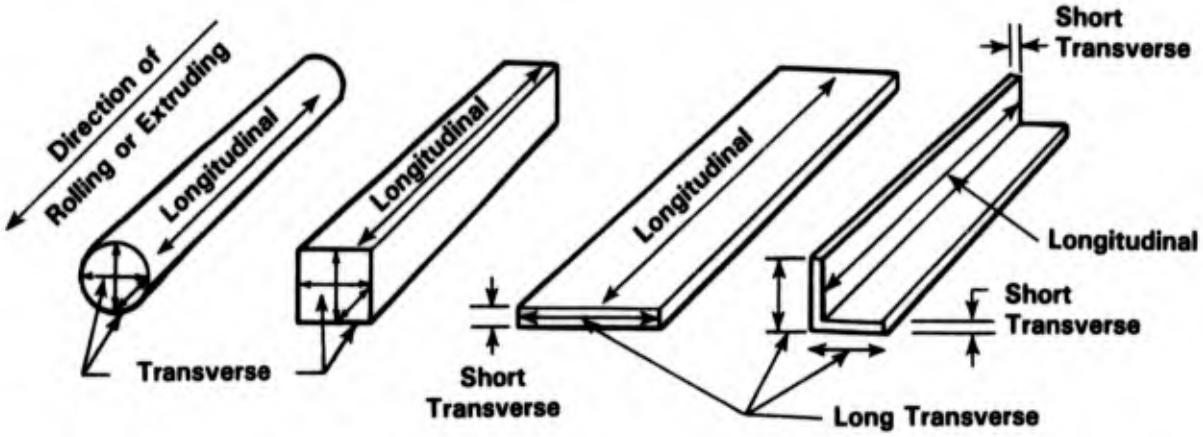

c. Rolled and Extruded Rod Bar and Thin Shapes (Hand Forgings Generally the Same)

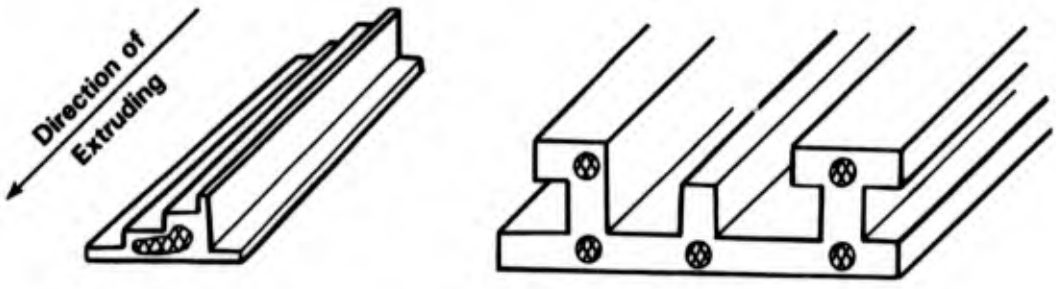

Crosshatched areas are transverse; other areas same as (c).

d. Extruded Thick and Complex Shapes

FIGURE 2-58. GRAIN ORIENTATIONS IN STANDARD WROUGHT FORMS[154]

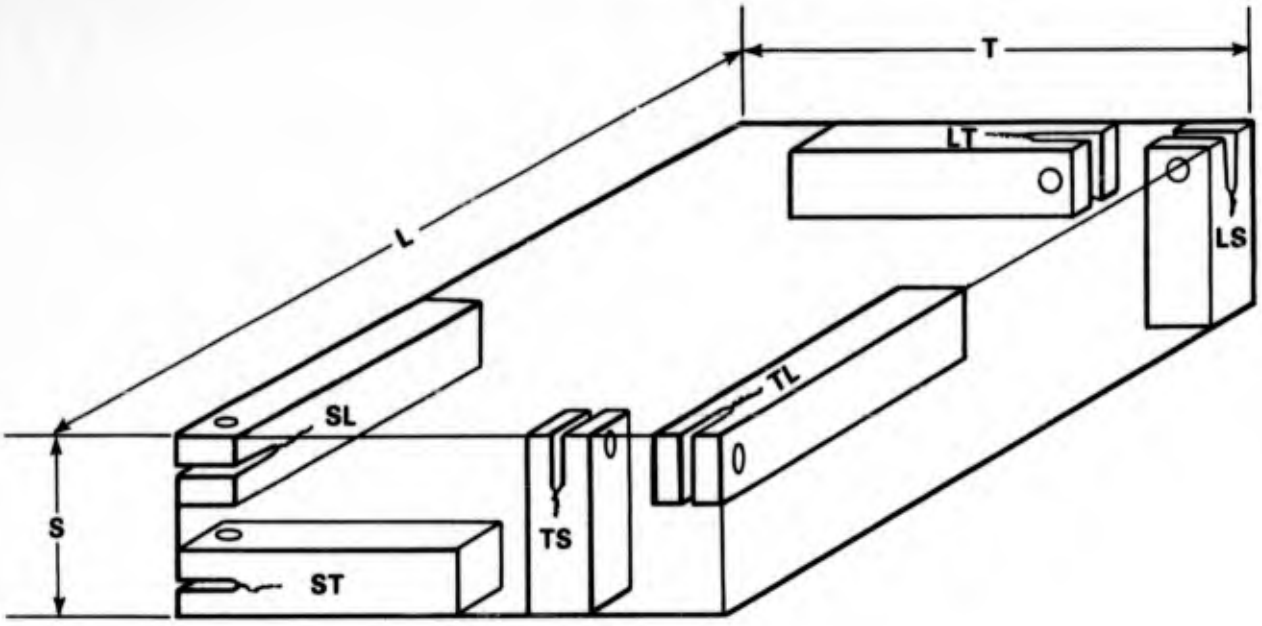

T = Long Transverse
L = Longitudinal (Rolling or Extrusion) Direction
S = Thickness
First Letter = Normal to the Fracture Plane
Second Letter = Direction of Propagation in Fracture Plane

FIGURE 2-59. SOME POSSIBLE DOUBLE-CANTILEVER-BEAM (DCB) SPECIMEN ORIENTATIONS IN PLATE MATERIAL(154)

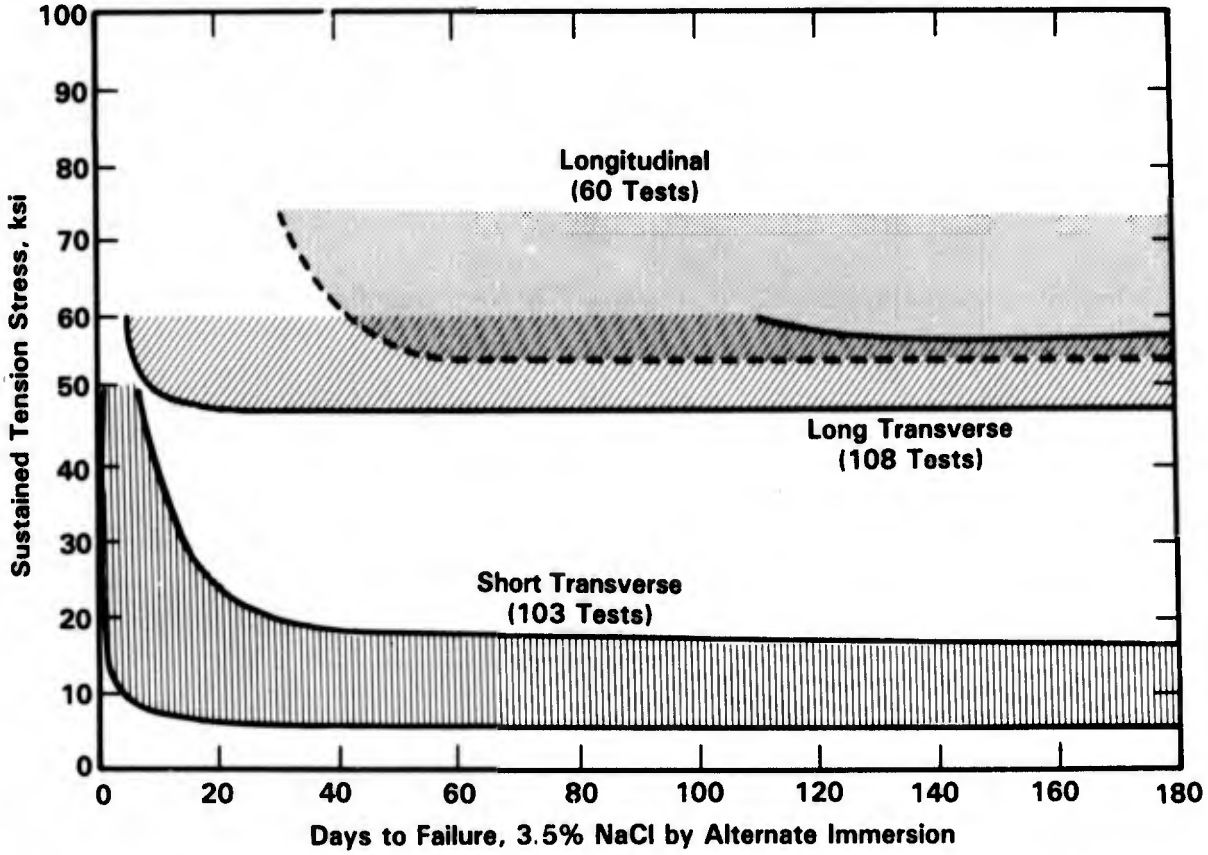

FIGURE 2-60. RESISTANCE TO STRESS-CORROSION CRACKING OF 7075-T6 PLATE AS INFLUENCED BY DIRECTION OF STRESSING(159)

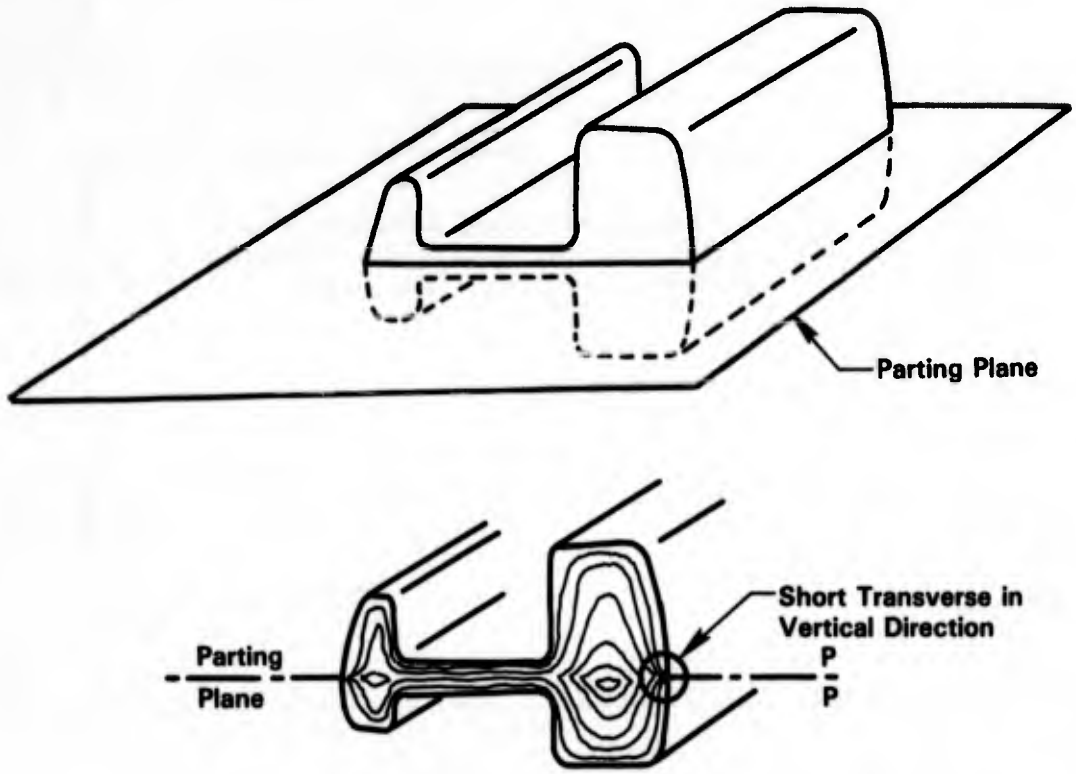

FIGURE 2-61. SCHEMATIC REPRESENTATION OF THE GRAIN FLOW IN A SECTION OF A TYPICAL DIE FORGING(154)

such as that produced by milling or drilling could increase the susceptibility to SCC and should be avoided. However, shot peening can greatly increase the SCC resistance.(156,157) In addition to introducing compressive stresses on the surface, shot peening results in smearing of the surface which greatly reduces the susceptibility to SCC. Further, the velocity of existing stress-corrosion cracks can be reduced significantly by applying stress overloads, which introduce crack tip residual compressive stresses.(158)

The grain shape resulting from forging can generally not be changed by subsequent aging because impurities which form at the grain boundaries prevent the grain boundaries from moving during heat treatment. Also in thin gauge material such as sheet, no stress can be applied in the ST direction (which is in the direction perpendicular to the plane of the sheet).

When a flaw or precrack is present in an actual part or test specimen, crack propagation is controlled by the stress intensity factor (K_I when plane-strain conditions apply). If stress-corrosion cracks propagate under a constant applied load, the K_I increases until the fracture toughness K_{Ic} is reached and rapid failure occurs. By plotting the time-to-failure as a function of K_I, the threshold stress intensity factor (K_{Iscc}) can be determined, see Figure 2-62. Stress-corrosion crack velocity as a function of K_I is used often to study the

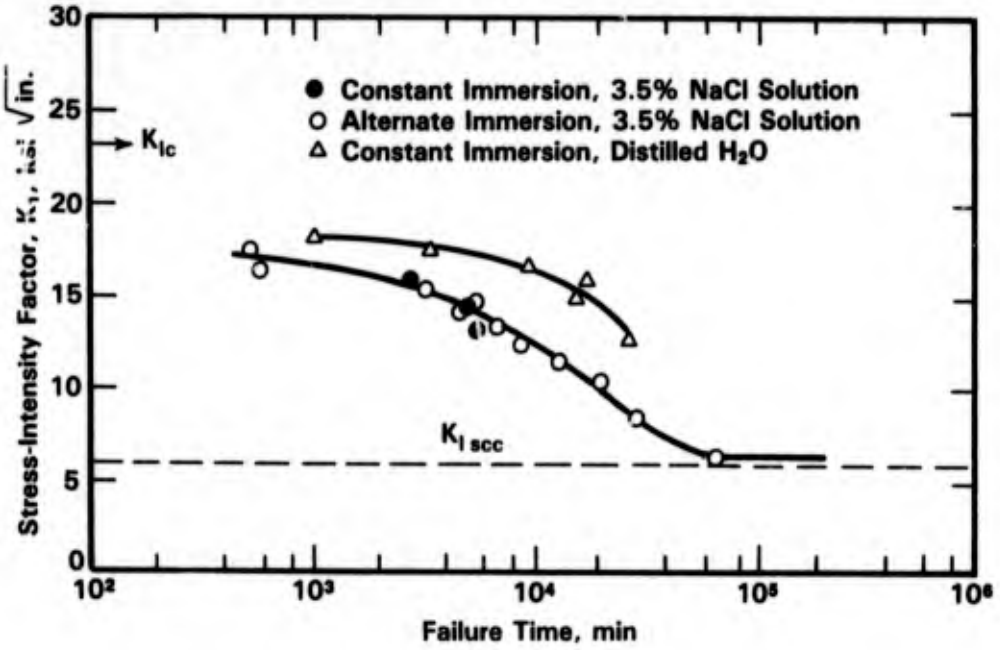

FIGURE 2-62. PRECRACKED-SPECIMEN STRESS-CORROSION DATA FOR SHORT TRANSVERSE 7075-T651 PLATE ILLUSTRATING THE TIME-TO-FAILURE METHOD OF OBTAINING K_{Iscc}. USING THIS TECHNIQUE, A K_{Iscc} OF ABOUT 6 KSI $\sqrt{IN.}$ IS OBTAINED.(160)

crack growth behavior of aluminum alloys, examples of which have been presented in previous sections.

Service stress-corrosion failures in susceptible aluminum alloys usually result from sustained unintentionally induced or residual tensile stresses in the short transverse or transverse direction. A typical source of unintentionally induced stresses results from assembly. This is illustrated in Figure 2-63. Residual stresses are usually induced by quenching after solution heat treatment.(155) An additional source of stress which is less common, results from the formation of voluminous corrosion products within an existing crack.

Macro-crack branching can be observed in some materials which failed by SCC.(168) The conditions under which macro-branching occurs were defined by Speidel.(168) The conditions are that the V-K curve must show a K_I independent region and that the crack-tip stress intensity at the point of branching must be at least 1.4 times the stress intensity at which region II begins.

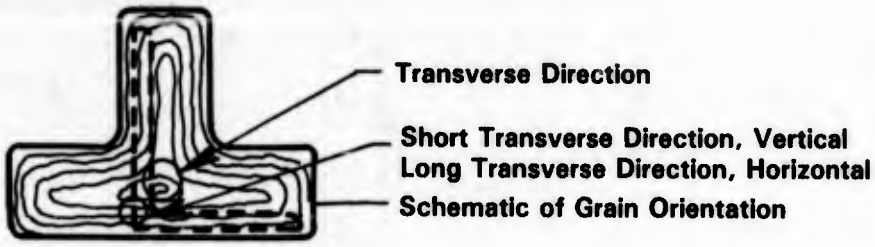

Location of machined angle with respect to transverse grain flow in thick tee

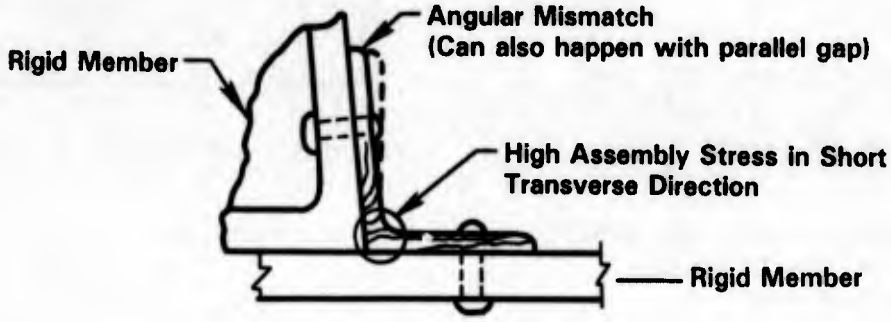

FIGURE 2-63. ILLUSTRATION OF LOCKED-IN SHORT TRANSVERSE STRESSES RESULTING FROM ASSEMBLY[155]

Strain Rate Effect

Loading procedures have a considerable effect on the SCC behavior of aluminum alloys. For instance, several researchers[140,163-165] showed a considerable increase in susceptibility to SCC with decreasing strain rate. Figures 2-64 and 2-65 show that, in a 3.5 percent NaCl solution, a minimum in ductility or minimum resistance to SCC exists at a specific strain rate. At higher strain rates the resistance to SCC increases sharply, and the percent reduction in area and elongation decreases significantly with increase in susceptibility, viz from T7351 to T6.

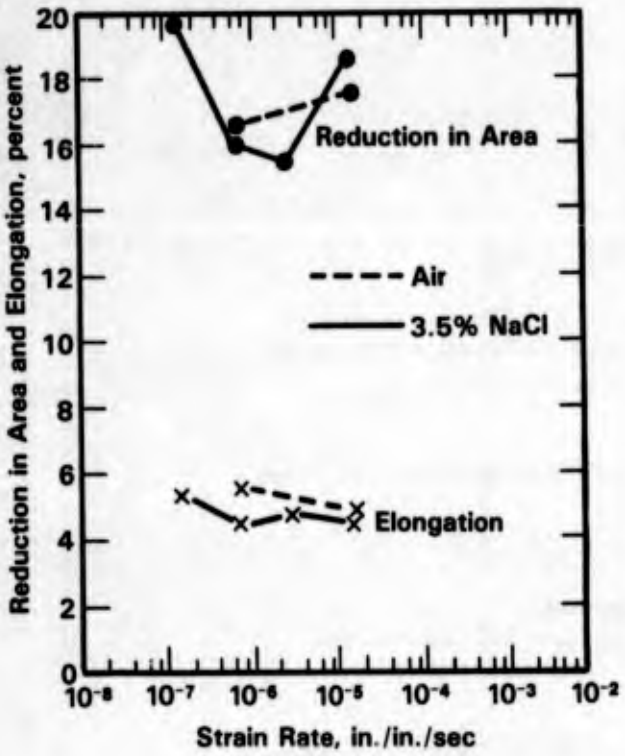

FIGURE 2-64. SLOW STRAIN RATE SCC TEST RESULTS FOR 7075-T7351[165]

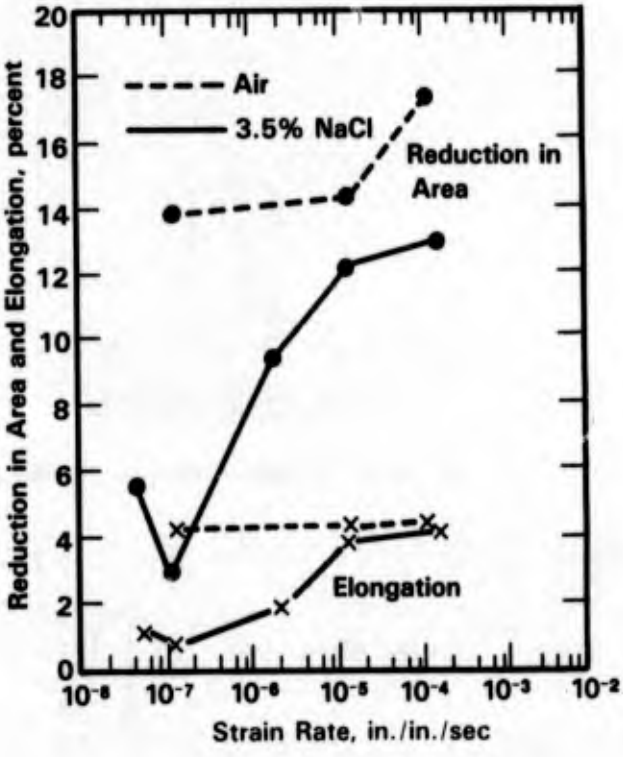

FIGURE 2-65. SLOW STRAIN RATE SCC TEST RESULTS FOR 7075-T6[165]

Effect of Potential

Stress-corrosion cracking of aluminum alloys is greatly affected by electrochemical potential. Figure 2-66 shows that application of cathodic potentials can reduce crack propagation by several orders of magnitude.[101] Thus, cathodic protection of aluminum alloys appears possible. However, Figure 2-67 shows that a minimum in susceptibility occurs between -1.3 and -1.4 V(SCE) and that, at potentials more negative than -1.4 V(SCE), stress corrosion crack velocities in 3 percent NaCl solution increase, parallel to an increasing hydrogen permeability. This would suggest that hydrogen could play a critical role in stress corrosion cracking at cathodic potentials.[123,167-169]

Thus, it is conceivable that an anodic dissolution mechanism operates at noble potentials whereas a hydrogen embrittlement mechanism operates at active potentials.

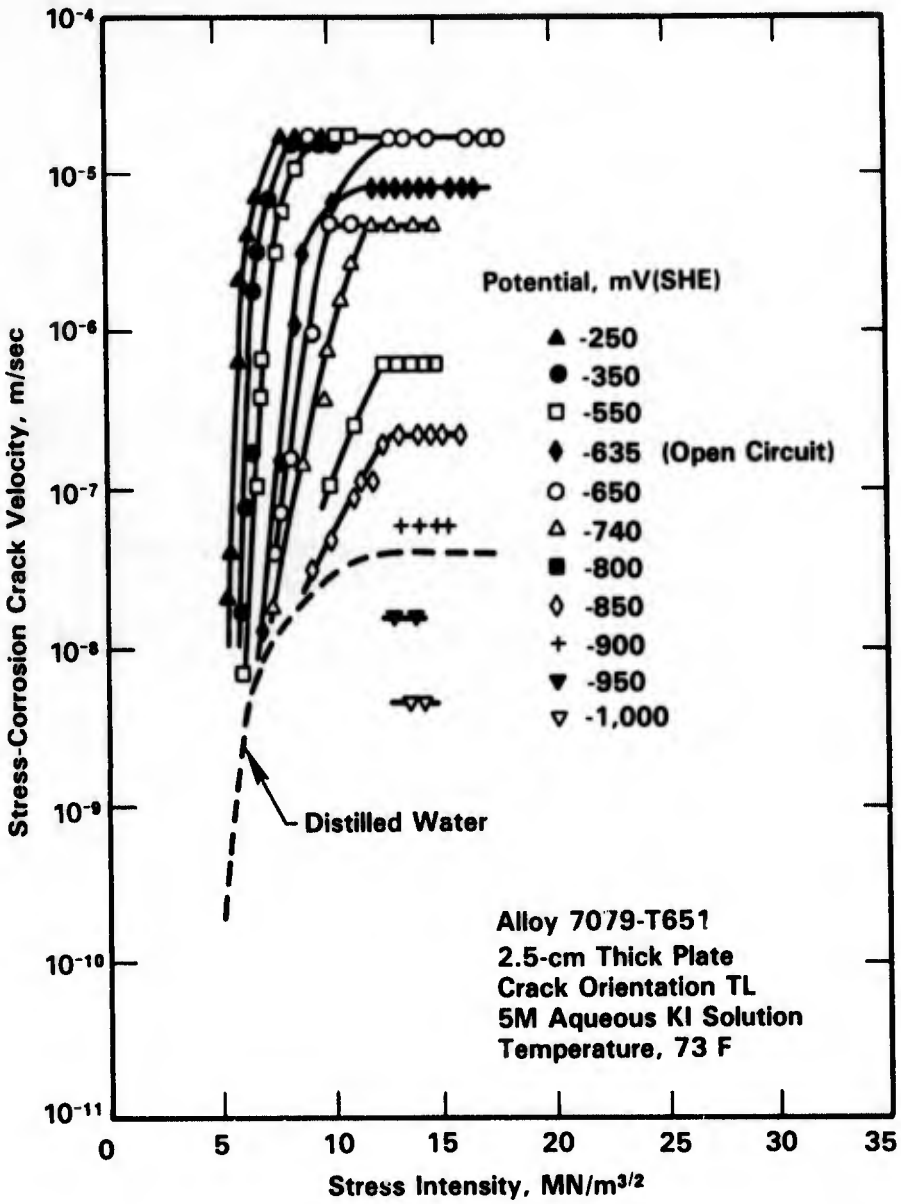

FIGURE 2-66. THE EFFECT OF ELECTROCHEMICAL POTENTIAL AND STRESS INTENSITY ON STRESS-CORROSION CRACK VELOCITY IN A HIGH STRENGTH ALUMINUM ALLOY(101)

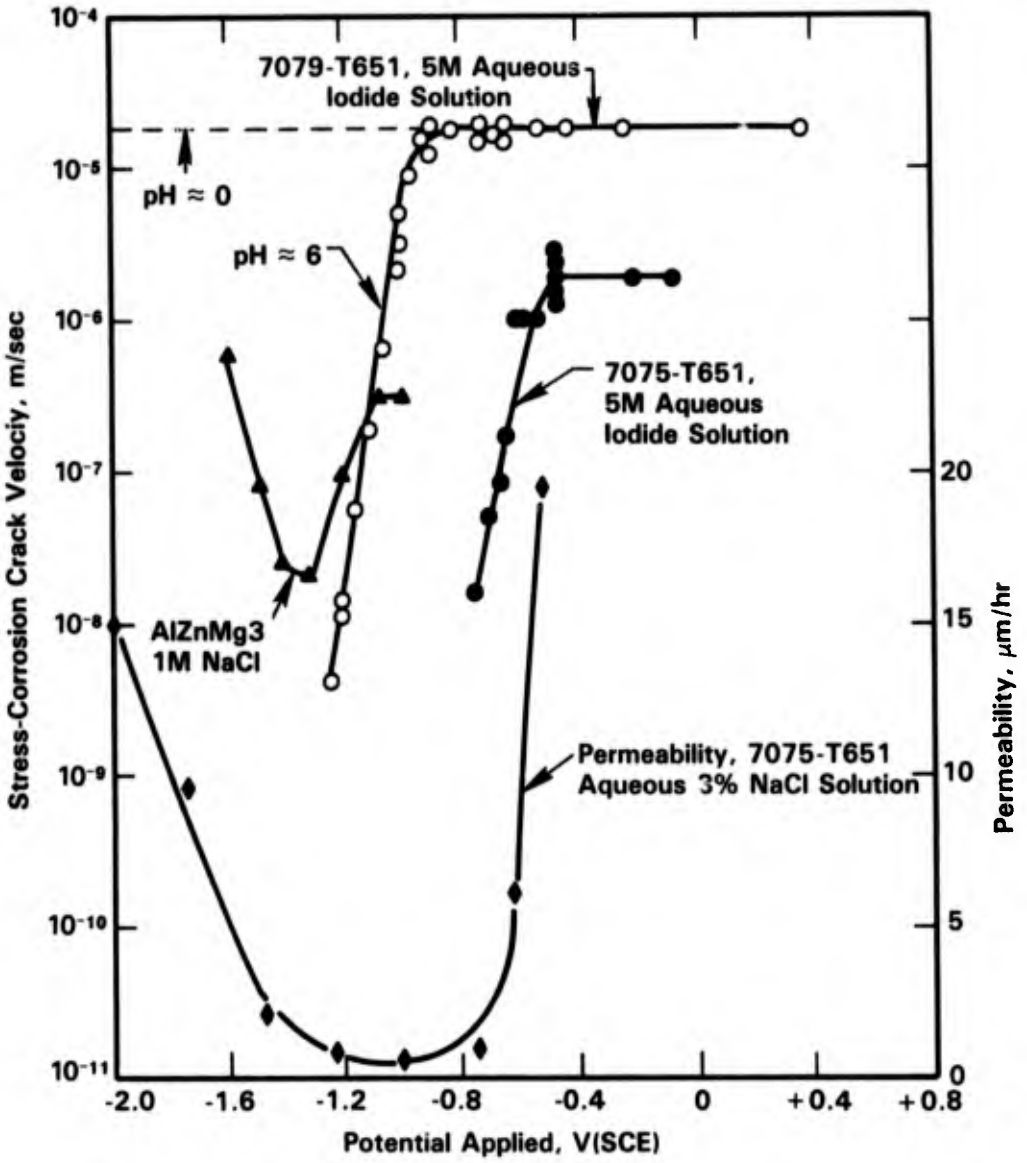

FIGURE 2-67. EFFECT OF ELECTROCHEMICAL POTENTIAL ON HYDROGEN PERMEABILITY AND STRESS-CORROSION CRACK VELOCITY IN Al ALLOYS[101]

Effect of Temperature

Although no field data are available on the effect of temperature on SCC, data obtained in simulated seawater have indicated that temperature has a significant effect on SCC resistance of aluminum alloys. Helfrich[170] showed that an increase of test temperature of a 3.5 percent NaCl solution decreased the time failure of the aluminum Alloy 7039-T64 (see Figure 2-68).

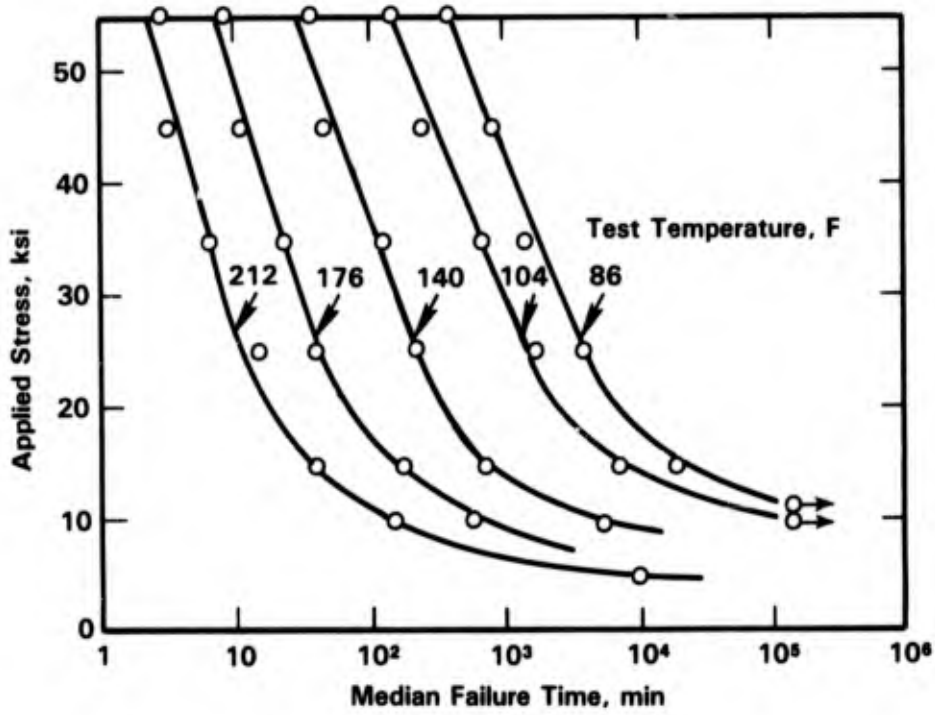

FIGURE 2-68. EFFECT OF STRESS AND TEMPERATURE ON TIME TO FAILURE BY SCC OF ALLOY 7039-T64 EXPOSED IN A 3.5 PERCENT AQUEOUS NaCl SOLUTION[170]

A study by Landkof of Alloy 7039 in 3.5 percent NaCl in a temperature range of 36.5 C to 52 C, indicated a strong effect of temperature on the plateau SCC crack velocity (see Figure 2-69). Similar observations were made by Speidel, et al.[101] who studied various aluminum alloys in a 3M KI solution at wide range of temperatures.

Hyatt and Quist[172] investigated the combined effect of temperature (at 250 F) and exposure time on the SCC growth rate of 2024-T351 in a 3.3 percent NaCl solution (see Figure 2-70). The figure shows an increase in crack velocity to a constant value with time of exposure at 250 F; this increase was attributed to aging of the alloy.

Effect of pH

Laboratory data obtained in simulated seawater solutions indicate that pH has a significant effect on stress-corrosion cracking of aluminum alloys. In general, the occurrence of SCC is markedly reduced with increasing pH.[104,173] Hyatt and Speidel[154] studied the

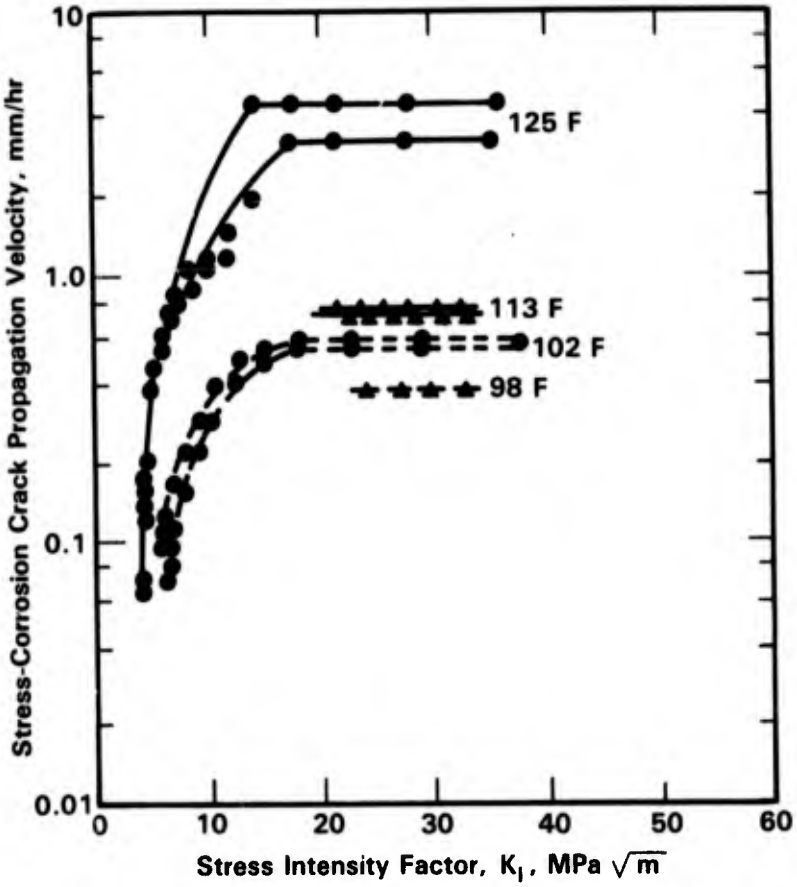

FIGURE 2-69. CRACK PROPAGATION VELOCITY VERSUS STRESS INTENSITY FACTOR IN 3.5 PERCENT NaCl AT VARIOUS TEMPERATURES[171]

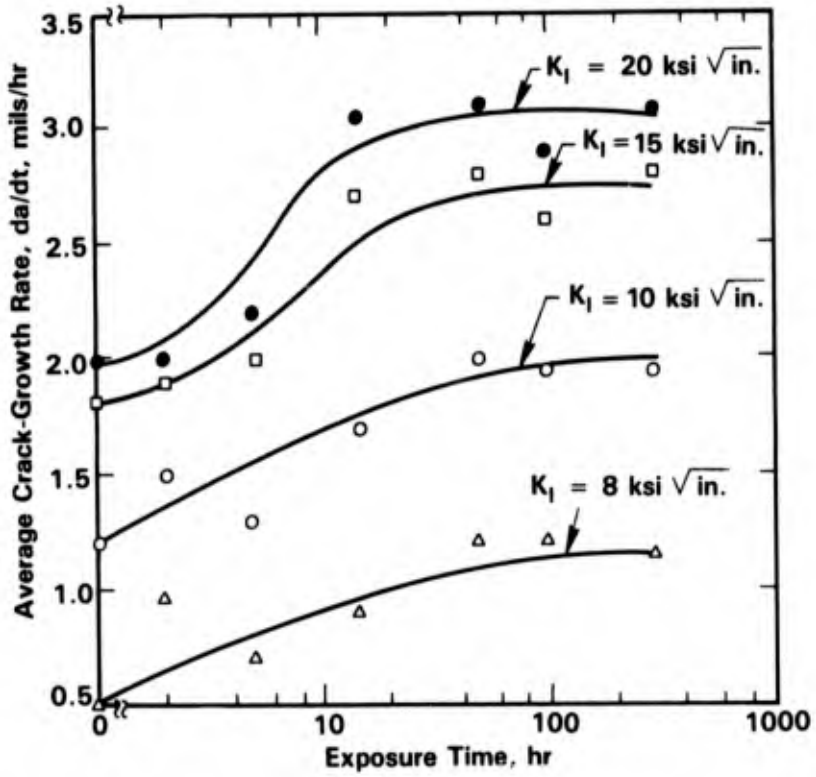

FIGURE 2-70. EFFECT OF EXPOSURE TIME AT 250 F ON STRESS-CORROSION CRACK GROWTH RATE AT VARIOUS K_I LEVELS IN DCB SPECIMENS FROM 2024-T351 PLATE[172]

effect of pH of aqueous halide solutions on the crack growth rate as a function of stress intensity. The results of these studies can be summarized as follows:

- In the stress independent region (II), crack velocity was found to be independent of pH between pH 1 and 11.
- The crack velocities in the stress dependent region (I) is displaced to lower stress intensities when the pH is reduced to values smaller than 3 but the crack velocities in region I were found to be independent of pH between pH values 3.5 and 11.

Effect of Depth and Aeration

Although no systematic studies were performed on the effect of depth and aeration on SCC of aluminum alloys, Reinhart and Jenkins have studied SCC behavior of structural materials including aluminum alloys in deep ocean environments.[41,47,75] These studies were performed in the Pacific Ocean near Port Hueneme at a depth of 2,340 feet for 402 days. The environment at this site was characterized and the oxygen concentration and pH at this depth were found as indicated in Figure 2-25. Stress-corrosion experiments were performed on Alloys 1100-H14, 1180, 2014-T6, 2219-T81, 2219-T87, 3303-H14, 5050-H34, 5083-H113, 5086-H12, 5454-H32, 7002-T6, Alclad 700X-T6, 7079-T6, Alclad 7079-T6, and 7178-T6. These alloys were stressed to stresses equivalent to 50 or 75 percent of their respective yield strengths in the transverse direction using four-point bending. Only Alloys 2219-T87, 7079-T6, Alclad 7079-T6, and 7178-T6 failed by stress-corrosion cracking at these depths. Reinhart's study indicated that SCC of susceptible aluminum alloys could occur in deep ocean environment. However, the study did not investigate whether a correlation exists between susceptibility and depth.

Intergranular Corrosion

Intergranular corrosion is selective attack of the grain boundary zone along the grain boundary with no appreciable attack of the matrix. The mechanism of attack is electrochemical and is the result of local cell action in the grain boundaries. Localized electrochemical cells are formed between precipitates along the grain boundary and the depleted aluminum solid solution from which the precipitates formed. In some alloys, such as the Al-Mg and Al-Zn-Mg-Cu alloys, the precipitates Mg_2Al_3, $MgZn_2$, and Al_X-Zn_X-Mg are more anodic than the adjacent matrix, whereas in other alloys such as Al-Cu, the precipitates $CuCl_2$ and Al_XCu_XMg are more cathodic than the adjacent matrix.

Exfoliation corrosion or layer corrosion is a form of intergranular attack that proceeds along multiple narrow paths parallel to the surface of the metal. Exfoliation, which occurs predominantly in relatively thin products with highly worked elongated grain structures, is characterized by leafing of relatively uncorroded metal and thicker layers of corrosion products. The layers of corrosion products cause the metal to appear to swell.

As in the case of intergranular stress-corrosion cracking, intergranular corrosion is strongly dependent on alloy composition and heat treatment. Alloys that do not form second-phase precipitates or those in which the precipitates have corrosion potentials similar to the matrix such as $MnAl_6$, are not susceptible to intergranular corrosion. Examples of alloys of this type are 1100, 3003, and 3004. Discussion of susceptible aluminum alloys are given below.

5000 Series Alloys

Aluminum-magnesium alloys containing less than 3 weight percent magnesium are resistant to intergranular corrosion in seawater environments. At higher Mg concentrations, the 5000 series alloys may become susceptible to intergranular attack depending upon the precipitation of Mg_2Al_3 along the grain boundary. The commercial 5000 series alloys (e.g., 5083, 5086, 5454, and 5456) generally show acceptable resistance to intergranular corrosion.[180,75] A study by Reinhart[41] where various aluminum alloys were exposed in the Pacific Ocean near Port Hueneme, CA, showed only intergranular attack in the heat-affected zone adjacent to welds in 5454-H32 and 5083-H113.[41]

A method to achieve resistance of Al-Mg alloys containing 4 to 9 weight percent Mg is a combination of heat treatment and cold working or thermomechanical treatment.[42]

Exfoliation has been observed in some highly worked 5000 series materials such as 5456-H321 boat hull plates.[34] These plates developed a highly elongated grain structure and selective grain boundary precipitation. Thus, special boat hull plate tempers H116 and H117, which have high resistance to exfoliation corrosion, were developed for these alloys.[174]

6000 Series Alloys

6000 series alloys (Al-Mg-Si) are usually resistant to intergranular corrosion.[175] However, when the alloy contains an excessive amount of Si, more than needed to form Mg_2Si, susceptibility to intergranular corrosion increases because of the strong cathodic nature of the insoluble Si constituent.

2000 Series Alloys

In 2000 series (Al-Cu) alloys, thermal treatments that cause selective grain boundary precipitation can lead to susceptibility to intergranular corrosion. Factors that affect the susceptibility are quenching rate, aging, and plastic deformation. It has been shown that rapid quenching during heat treatment, and subsequent aging to peak or slightly averaged strength results in high resistance to intergranular corrosion.(61) On the other hand, slow cooling from solution treatment temperatures results in susceptibility to intergranular corrosion. As-quenched or naturally-aged tempers (T3, T4) may be highly susceptible to SCC and exfoliation, but only slightly susceptible to intergranular corrosion.(176) However, when artificially aged (tempers T6, T8), without changing its susceptibility to other forms of intergranular corrosion, the same alloy may show a substantial increase in the resistance to both SCC and exfoliation. Examples of 2000 series alloys in T6 or T8 tempers that have been successfully used without exfoliation problems are 2024, 2048, 2124, and 2219.(34) A relatively new alloy in this series is 2048-T851, which was primarily developed to provide high toughness.(34)

On the other hand, exposure studies in the Pacific Ocean by Reinhart(41) showed intergranular corrosion in 2014-T6, 2024-T3, 2219-T81, and 2219-T87, and exfoliation in Alloy 2024-T3.

7000 Series Alloys

Intergranular corrosion and exfoliation corrosion in Al-Zn-Mg alloys can also be affected by thermal treatments. As in the case of 2000 series alloys rapid quenching from the solution, heat treat temperature and overaging will produce alloys resistant to intergranular corrosion. Addition of Cu generally increases the susceptibility to intergranular corrosion, which does not arise from preferential dissolution of grain boundary precipitates but from Cu depleted zones.(177) Of the commercial 7000 series alloys (Al-Zn-Mg-Cu), Alloys 7075-T73, 7075-T63, and 7178-T76 were found to provide very high resistance to intergranular corrosion.(34,178,179) The T76 temper designation is that which denotes the highest strength obtainable with high resistance to exfoliation corrosion. Also, recently developed Alloys 7050 and 7010 in the T73 temper(148) are resistant to exfoliation.

MUD

Results of experiments conducted in the Pacific Ocean off Port Hueneme for aluminum alloys are given in Figure 2-71 and Figure 2-17. These figures show that there was considerable variation in the data for the alloys examined but that, in many cases, weight loss and pit depths were greater for the mud exposure than for exposure of the same alloy under immersed condition at a similar depth. The poor performance of the aluminum alloys under mud exposure is not surprising; the presence of deposits and deaeration tends to promote local breakdown of passive films on the aluminum alloys. Since the composition of the ocean sediments varies, caution should be exercised in applying the data to other geological locations.

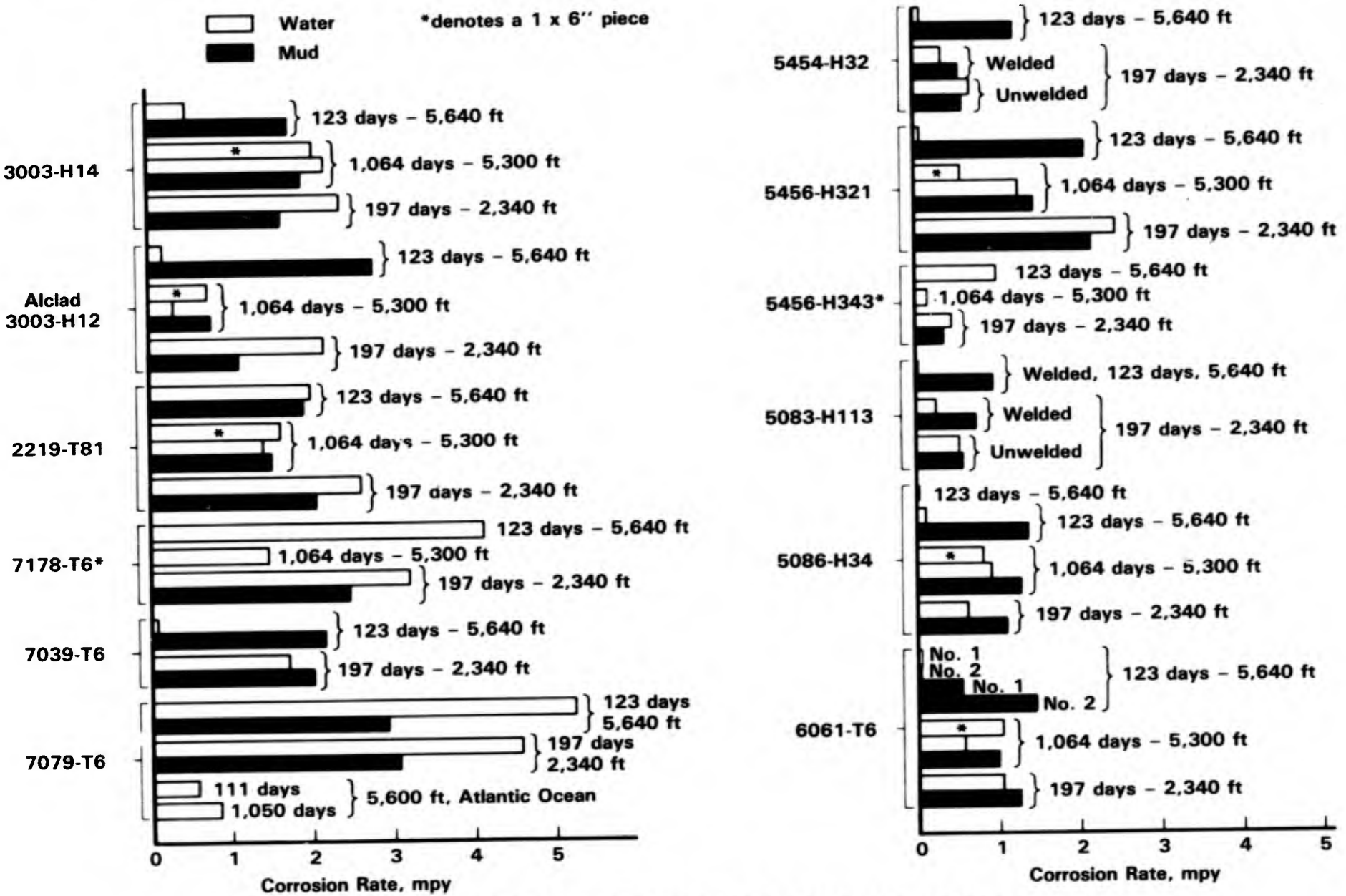

FIGURE 2-71. CORROSION RATES OF ALUMINUM ALLOYS IN THE DEEP OCEAN (THE PACIFIC OCEAN UNLESS OTHERWISE SPECIFIED)[47]

REFERENCES FOR CHAPTER 2

1. Barkman, E. F. and Lindberg, R. I., "Aluminum Alloys for Use in Heat Exchanger Tubing for OTEC Applications", OTEC Biof. and Corr. Symposium, WA, pp 305-318 (November, 1977).

2. Venkateswaran, G. and Galow, E., "Behavior of Some Modified Aluminum Alloys in Dynamic and Nearly Static Air Saturated North Seawater Systems", Bhabha at Res Centre, Bombay, India, GKSS-82/E-19, 55 pp (1982).

3. Ailor, W. H., "Five-Year Corrosion of Aluminum Alloys at Several Marine Sites", British Corrosion Journal, 18 (6), pp 237-243 (May, 1966).

4. Ailor, W. H., "Metal Exposures at Tropical and Marine Sites", 6th Annual Offshore Technology Conference, 1, pp 293-312 (May, 1974).

5. Czyryca, E. J. and Hack, H. P., "Corrosion of Aluminum in Exfoliation-Resistant Tempers Exposed to Marine Environments for 2 Years", Naval Ship Research and Development Center Report NSRDC-4423, p 23 (November, 1974).

6. Southwell, C. R., et al., "Corrosion of Metals in Tropical Environments, Aluminum and Magnesium", Materials Protection, 4 (2), pp 30-35 (1965).

7. Latimer, K. G. and Booth, F. F., "Atmospheric Exposure of Aluminum Alloys for Three Years in Nigeria", Metallurgia, 67 (2), pp 73-79 (1963).

8. Southwell, C. R. and Bultman, J. D., "Atmospheric Corrosion Testing in the Tropics", Atmospheric Corrosion, pp 943-967 (November, 1980).

9. Pelensk, M. A., et al., "Corrosion Investigations at Panama Canal Zone", Atmospheric Factors Affecting the Corrosion, ASTM-STP-646, pp 58-73 (1978).

10. Lashermes, M., et al., "Thirty Year Atmospheric Corrosion of Aluminum Alloys in France", Atmospheric Corrosion, pp 353-364 (November, 1980).

11. Batrakov, V. P., et al., "Corrosion Resistance of Alloy 1420 in Marine Climates", Protection of Metals, 17 (6), pp 505-514 (June, 1981).

12. Fahy, F. W., "Atmospheric Corrosion of Anodized Aluminum Exposed Over a Twelve Year Period in New Zealand", British Corrosion Journal, 15 (4), pp 203-207 (1980).

13. Ailor, W. H., "Seven-Year Exposure at Point Reyes, California", Corrosion in Natural Environments, ASTM-STP-558, pp 75-81 (1974).

14. Lindgren, S., et al., "Weldable Structural Al Alloys - Corrosion Resistance in Outdoor Atmosphere and in Water", 7th Scandinavian Corrosion Congress, Norway, pp 297-310 (1975).

15. Oelsner, G., "Atmospheric Corrosion Testing of Aluminum in Italy", Atmospheric Corrosion, pp 797-805 (October, 1980).

REFERENCES FOR CHAPTER 2
(Continued)

16. Wanamaker, J. L., et al., "Duplex Sealing of Anodized Aluminum", Materials Performance, 18 (12), pp 25-39 (December, 1979).

17. Cotton, J. B. and Downing, B. P., "Corrosion Resistance of Titanium to Seawater", Institute of Marine Engineers Transactions, 69 (8), pp 311-319 (1957).

18. Pelensky, M. A., et al., "Corrosion Investigations at Panama Canal Zone", Atmospheric Exposure Testing Symposium, pp 58-73 (May, 1978).

19. Pelensky, M. A., et al., "Air, Soil, and Sea Galvanic Corrosion Investigation at Panama Canal Zone", Galvanic and Pitting Corrosion ASTM-STP-576, pp 94-113 (1976).

20. Ebihara, W. T., "Tropical Exposure of Galvanically Coupled Metal Systems", Army Armament R&D, ARSCD-TR-79004, 18 pp (June, 1979).

21. Lage, K. and Sune, L., "Galvanic Corrosion of Seven Different Al Alloys in Contact With Copper, Steel, Stainless Steel, and Zinc-Field Tests in Outdoor Atmospheres", Corrosion and Corrosion Protection of Aluminum, pp 95-106 (1976).

22. Morris, A. W., "Electrochemical Screening of Fastener Materials for Carbon Composite Joint Applications", Corrosion '80, Chicago, IL, Paper 23, 9 pp (March, 1980).

23. Prince, D. E., "Corrosion Behavior of Metal Fasteners in Graphite-Epoxy Composites", Air Force Materials Laboratory Report AFML-TR-75-53, 22 pp (July, 1975).

24. Stifel, P. M., "Carrier Testing of Graphite Composites in Contact With Metals on F-4", McDonnell Aircraft, St. Louis, MO, 72 pp (July, 1980).

25. Askins, D. R. and Schwartz, H. S., "Effect of Salt Spray Exposure on Structural Integrity of Graphite/Epoxy Skin-Al Honeycomb Sandwich", Durability of Adhesive Bonded Structures, Wiley, New York, NY, pp 217-227 (1976).

26. Vassilaros, M. G., et al., "Marine Corrosion and Fatigue of Graphite/Aluminum Composites", Tri-Service Conference on Corrosion, AFWAL-TR-81-4019-V2, pp 21-53 (November, 1980).

27. Koch, G. H., "The Fracture Behavior of Multiplying Layer Adhesive Bonded Aluminum Structures", SAMPE Quarterly, 11 (1), p 7 (1970).

28. Aylor, D. M., et al., "Marine Corrosion and Protection for Graphite/Aluminum Metal Matrix Composites", Materials Performance, 23 (7), pp 32-38 (1984).

29. Sprowls, D. O. and Brown, R. H., "Resistance of Wrought High-Strength Aluminum Alloys to Stress-Corrosion", Technical Paper 17, Aluminum Co., New Kensington, PA (1962).

30. Humphries, T. S. and Nelson, E. E., "Seacoast Stress-Corrosion Cracking of Aluminum Alloys", NASA, Huntsville, AL, NASA-TM-82393, 29 pp (January, 1981).

REFERENCES FOR CHAPTER 2
(Continued)

31. Sprowls, D. O., et al., "Evaluation of Stress-Corrosion Cracking Susceptibility Using Fracture Mechanics Techniques", Alcoa, PA, NAS8-21487, 117 pp (May, 1973).

32. Dorward, R. C., et al., "Marine Atmosphere Stress-Corrosion Tests on Precracked Specimens From High Strength Aluminum Alloys: Effect of Corrosion-Product Wedging", Journal of Testing and Evaluation, 6 (4), pp 268-275 (July, 1978).

33. Sprowls, D. O., et al., "Exfoliation Corrosion Testing of 7075 and 7178 Aluminum Alloys - Interim Report on Atmospheric Exposure Tests", Corrosion in Natural Environments, ASTM-STP-558, pp 99-113 (1974).

34. Sprowls, D. O., "High Strength Aluminum Alloys With Improved Resistance to Corrosion and Stress-Corrosion Cracking", 1976 Tri-Service Conference on Corrosion, MCIC-77-33, pp 89-120 (October, 1976).

35. Jankowsky, E. J., et al., "Aircraft Carrier Exposure Tests of Aluminum Alloys", Naval Air Development Center, NADC-79251-60, 34 pp (November, 1979).

36. Ketcham, S. J. and Jankowsky, E. J., "Shipboard Exposure Tests of Aluminum Alloys", Proceedings of the 1980 Tri-Service Conference on Corrosion, AFWAL-TR-81-4019, (November 5-7, 1980).

37. Brooks, C. L., "Aluminum-Magnesium Alloys 5086 and 5456-H116", Naval Engineers Journal, 82 (4), pp 29-32 (1970).

38. Wood, C., Jr., "Selecting Wrought Aluminum Alloys for Marine Use", Alcoa (June, 1969).

39. Czyryca, E. J. and Hack, H. P., "Corrosion of Aluminum Alloys in Exfoliation-Resistant Tempers Exposed to Marine Environments for 2 Years", Proceeding of the 1974 Tri-Service Corrosion of Military Equipment Conference, AFML-TR-75-42 (September, 1975).

40. Boyd, W. K. and Fink, F. W., "Corrosion of Metals in Marine Environments", Battelle Columbus Laboratories Report MCIC-78-37, 103 pp (March, 1978).

41. Reinhart, F. M., "Corrosion of Materials in Hydrospace. Part V: Aluminum Alloys", Naval Civil Engineering Laboratory, NCEL-TN-N-1008, 89 pp (January, 1969).

42. Beberdick, L. E., "A Preliminary Investigation of the Corrosion and Stress-Corrosion Susceptibility of Thermomechanically Processed High Magnesium, Aluminum-Mg Alloys", Naval Postgrad School, Monterey, CA, 85 pp (September, 1981).

43. Mondolfo, L. F., Aluminum Alloys: Structure and Properties, Butterworth, Inc., pp 806-819 (1976).

44. Bonora, P. L., "The Anodic Dissolution of Aluminum Zinc Alloys in Seawater", Materials Chemistry, 2 (1), pp 35-49 (1977).

REFERENCES FOR CHAPTER 2
(Continued)

45. Zamin, M., "The Role of Manganese in the Corrosion Behavior of Al-Mn Alloys", Corrosion, 37 (11), pp 627-632 (November, 1981).

46. Klimko, A. F. and Mochalova, L. M., "Effect of Microalloying on Aging and Corrosion Resistance of AMg6 Alloys", Soviet Materials Science, 9 (1), pp 103-104 (February, 1973).

47. Reinhart, F. M., "Corrosion of Materials in Hydrospace", Naval Civil Engineering Laboratory, R-504, 118 pp (December, 1966).

48. Dexter, S. C., "Effect of Variations in Seawater Upon the Corrosion of Aluminum", Corrosion, 36 (8), pp 423-432 (August, 1980).

49. Larsen-Basse, J., "Corrosion of Aluminum Alloys in Ocean Thermal Energy Conversion Seawaters", Materials Performance, 23 (7), pp 16-21 (July, 1984).

50. Lee, T. S. and Tuthill, A. H., "Guidelines for the Use of Carbon Steel to Mitigate Crevice Corrosion of Stainless Steels in Seawater", Corrosion '82, Houston, TX, Paper 63, 21 pp (March, 1982).

51. Aliev, A. F. and Freiman, L. I., "Electrochemical Behavior of Aluminum Alloys in Connection With the Operating Conditions of a Seawater Thermal Desalination Plant", Protection of Metals, 12 (4), pp 351-356 (August, 1976).

52. Konstantinova, E. V. and Nazarova, N. P., "Investigations of the Possibilities of Using Aluminum Alloys as Structural Materials for Distillation Equipment", Protection of Metals, 12 (3), pp 279-281 (June, 1976).

53. Edeleanu, C. and Evans, U. R., "The Causes of the Localized Character of Corrosion on Aluminum", Transactions of the Faraday Society, 47, p 1121 (1951).

54. Richardson, J. A. and Wood, G. C., "A Study of the Pitting Corrosion of Al by Scanning Electron Microscopy", Corrosion Science, 10, pp 313-323 (1970).

55. Wood, G. C., et al., "The Mechanism of Pitting of Aluminum and Its Alloys", Localized Corrosion, National Association of Corrosion Engineers, pp 526-446 (1974).

56. Bogar, F. D. and Foley, R. T., "The Influence of Chloride Ions on the Pitting of Aluminum", Journal of the Electrochemical Society, 119, p 462 (1972).

57. Johnson, W. K., "Recent Developments in Pitting Corrosion of Aluminum", British Corrosion Journal, 6, p 782 (1971).

58. Godard, H. P. and Booth, F. F., "Corrosion Behavior of Aluminum Alloys in Seawater", International Congress of Marine Corrosion and Protection, Cannes, France, pp 37-52 (1964).

59. Zossi, A. M., et al., "Effect of Solidification Microstructure on Corrosion Behavior of the Chill Zone in Aluminum Binary Alloys", Metallurgical Transactions, 7A (10), pp 1489-1496 (October, 1976).

REFERENCES FOR CHAPTER 2
(Continued)

60. Muller, I. L. and Galvele, J. R., "Pitting Potential of High Purity Binary Aluminum Alloys. II: Al-Mg and Al-Zn Alloys", Corrosion Science, 17 (12), pp 995-1007 (1977).

61. Muller, I. L. and Galvele, J. R., "Pitting Potential of High Purity Binary Aluminum Alloys - Al-Cu Alloys Pitting and Intergranular Corrosion", Corrosion Science, 17 (3), pp 179-189 (1977).

62. Sujimoto, et al., Journal of Japanese Institute of Metals, 34, p 312 (1970).

63. Holtan, H. and Sigurdsson, H., "Pitting Potentials of Al Alloys", Werkstoffe und Korrosion, 28 (7), pp 475-477 (July, 1977).

64. Niskanen, P., et al., "Corrosion of Aluminum Alloys Containing Lithium", Corrosion Science, 22 (4), pp 283-304 (1982).

65. Niskanen, P., et al., "The Influence of Microstructure on the Corrosion of Al-Li, Al-Li-Mn, Al-Li-Mg, and Al-Li-Cu Alloys in 3.5 Percent NaCl Solution", First International Aluminum-Lithium Conference, Stone Mountain, GA, pp 347-376 (May, 1980).

66. Groover, R. E., et al., "Characterization of the Corrosion Behavior and Response to Cathodic Protection of Nineteen Aluminum Alloys in Seawater", Naval Research Laboratory, NRL Memo 1961 (January, 1969).

67. Ambler, H. R. and Bain, A.A.J., "Corrosion of Metals in the Tropics", Journal of Applied Chemistry, 5, pp 437-467 (September, 1955).

68. Galvele, J. R. and DeMicheli, S. M., "Mechanism of Intergranular Corrosion of Al-Cu Alloys", Corrosion Science, 10 (11), p 795 (1970).

69. Sugimoto, K., et al., "Stress-Corrosion Cracking of Aged Al-4 Percent Cu Alloy in NaCl Solution", Corrosion Science, 15 (11/12), pp 709-720 (December, 1975).

70. Maitra, S. and English, G. C., "Mechanism of Localized Corrosion of 7075 Alloy Plate", Metallurgical Transactions, 12A (3), pp 535-541 (March, 1981).

71. Rynewicz, J., "Corrosion in Deep Oceans", Ocean Engineering - Petroleum Engineer, 46 (13), pp 57-66 (November, 1974).

72. Wheatfall, W. L., "Metal Corrosion in Deep Ocean Environments", Navy Marine Engineering Laboratory, R-429/66, 23 pp (January, 1967).

73. Dexter, S. C., "Oxygen Temperature and pH Effects on Corrosion of Aluminum in Seawater", Sixth Ocean Thermal Energy Conversion Conference, 2 (CONF-790631), pp 12.4 to 1-11 (1979).

74. Reinhart, F. M. and Jenkins, J. F., "Corrosion of Alloys in Hydrospace - 189 Days at 5,900 Feet", Final Report NCEL-TN-1224, 41 pp (April, 1972).

REFERENCES FOR CHAPTER 2
(Continued)

75. Reinhart, F. M. and Jenkins, J. F., "Corrosion of Materials in Surface Seawater After 12 and 18 Months of Exposure", Final Report NCEL-TN-1213, 106 pp (January, 1972).

76. Ahmed, Z., "Corrosion and Corrosion Prevention of Aluminum Alloys in Desalination Plants - II", Anti-Corrosion Methods and Materials, 28 (7), pp 4-10 (July, 1981).

77. Franz, F. and Novak, P., "Effect of Rotation on the Pitting Corrosion of Aluminum Electrodes", Localized Corrosion, NACE, p 576 (1974).

78. Mansfeld, F. and Kenkel, J. V., "The Effect of Rotation on Pitting Behavior of Aluminum and Stainless Steel", Corrosion, 35 (1), pp 43-44 (January, 1979).

79. Davis, J. A., et al., "Pitting Behavior of Aluminum Alloys in High Velocity Seawater", Bell Aerospace Company Report N00014-75C-1087, 20 pp (June, 1976).

80. Schmitt, C. R., "Corrosion Behavior of Aluminum in Water", Reviews on Coatings and Corrosion, 4 (1), pp 95-112 (1979).

81. Herrigel, H. R., Materials Performance, 15, pp 43-45 (March, 1976).

82. Ulanovskii, I. B. and Sokolov, B. S., "Influence of Hydrogen Sulfide on Corrosion Susceptibility of Aluminum and Its Alloys in Seawater (Translation)", Protection of Metals, 16 (3), pp 254-255 (1980).

83. Ahmad, Z., "Effect of Velocity on the Corrosion Behavior of Al-Mg 3 in North Seawater", Metal Corrosion Industry, 57 (677), pp 11-26 (January, 1982).

84. Davis, J. A. and Gehring, G. A., Jr., "Effect of Velocity on the Seawater Corrosion Behavior of High Performance Ship Materials", Materials Performance, 14 (4), pp 32-39 (April, 1975).

85. Symonds, J., "Effect of Velocity on the Seawater Corrosion Resistance of Two Aluminum Alloys", 5th Ocean Thermal Energy Conversion Conference, 4, pp viii/222-230 (1978).

86. Davis, J. A. and Gehring, G. A., Jr., "Corrosion Behavior Variations With Time and Velocity in Seawater", Corrosion '75, Toronto, Ontario, Canada, Paper 123, 16 pp (April, 1975).

87. Gehring, G. A., Jr. and Peterson, M. H., "Corrosion of 5456-H117 Aluminum in High Velocity Seawater", Corrosion, 37 (4), pp 232-242 (1981).

88. Mansfeld, F., et al., "Galvanic Corrosion of Aluminum Alloys. I: Effect of Dissimilar Metal", Corrosion, 30 (10), pp 343-353 (October, 1974).

89. Reboul, M. C., "Galvanic Corrosion of Aluminum", Corrosion, 35 (9), pp 423-428 (September, 1979).

90. Ulanovskii, I. B., et al., "Corrosion of Steel, Titanium, and Copper at Various Depths in the Black Sea", Protection of Metals, 12 (4), pp 394-395 (July, 1976).

REFERENCES FOR CHAPTER 2
(Continued)

91. Mansfeld, F., "Results of Galvanic Corrosion Round Robin Testing", Corrosion, 33 (6), pp 224-226 (June, 1977).

92. Lennox, T. J., Jr., et al., "Corrosion and Cathodic Protection of 5086-H32 Al Coupled to Dissimilar Metals", Materials Performance, 13 (2), pp 31-36 (February, 1974).

93. Scholes, I. R., et al., "Bimetallic Corrosion in Seawater", European Congress on Metallic Corrosion, London, England, pp 161-169 (1977).

94. Mansfeld, F. and Kenkel, J. V., "Laboratory Studies of Galvanic Corrosion. III: Effect of Velocity in NaCl and Substitute Ocean Water", Corrosion, 33 (7), pp 236-240 (July, 1977).

95. Davis, J. A. and Gehring, G. A., Jr., "Galvanic Corrosion as a Function of Applied Potential in High Velocity Seawater", Corrosion '76, Houston, TX, Paper 75, 14 pp (March, 1976).

96. Davis, J. A. and Gehring, G. A., Jr., "The Effect of Velocity on the Seawater Corrosion Behavior of High Performance Ship Materials", Materials Performance, 14 (1975).

97. Davis, J. A. and Gehring, G. A., Jr., "Corrosion Behavior Variations With Time and Velocity in Seawater", Corrosion '75, Chicago, IL, Paper 123 (1975).

98. Kendall, E. and Dull, D. L., "Salt Water Corrosion Behavior of Aluminum-Graphite Composites", Aerospace Corporation Report SAMSO-TR-74-67, 20 pp (March, 1974).

99. Dull, D. L., et al., "The Corrosion of 6061 Aluminum Alloy - Thornel 50 Graphite Composite in Distilled Water and Sodium Chloride Solution", Aerospace Corporation Report AFML-TR-75-42, pp 399-409 (1974).

100. Miller, B. A. and Lee, S. G., "The Effect of Graphite-Epoxy Composites on the Galvanic Corrosion of Aerospace Alloys", WPAFB Report AFML-TR-76-121, 45 pp (September, 1976).

101. Speidel, M. O., "Stress-Corrosion Cracking of Aluminum Alloys", Metallurgical Transactions, 6A (4), pp 631-651 (April, 1975).

102. Holtyn, C. H., "The Age of Ships", Society of Naval Architects and Marine Engineers, preprint 9 (November, 1966).

103. Ohnishi, T., et al., "Effect of Microstructure of Stress-Corrosion Susceptibility", Journal of Japan Institute of Light Metals, 26 (1), pp 8-17 (January, 1976).

104. Sprowls, D. O. and Brown, R. H., "Stress-Corrosion Mechanisms for Aluminum Alloys", Proceeding of Conference on Fundamental Aspects of Stess Corrosion Cracking, NACE, p 466 (1969).

105. Baba, Y., et al., "Effect of Addition of Bi on Stress-Corrosion Cracking of Al-Mg Alloy", Sumitomo Light Metal Technical Reports, 14 (2), pp 1-6 (April, 1973).

REFERENCES FOR CHAPTER 2
(Continued)

106. Chandrashekar, R. and Vasu, K. I., "Morphology of Stress-Corrosion Cracks and Crack Branching in Aluminum-Magnesium Alloys", Metallography, 6 (5), pp 377-392 (October, 1973).

107. Baba, Y., "Effect of Additions of Cu and Zr on Stress-Corrosion Cracking of Al-Mg Alloys", Journal of Japan Institute of Metals, 36 (4), pp 341-346 (April, 1972).

108. Ford, J. A. and Pryor, M. J., "Corrosion Performance of MRL-ADJ", Olin Metals Research Laboratories Report MRL-70-PR-11 (February 19, 1970).

109. McMillan, J. C. and Hyatt, M. V., "Development of High-Strength Aluminum Alloys With Improved Stress-Corrosion Resistance. Phase II", Boeing Report AFML-TR-68-148, 142 pp (June, 1968).

110. Bhat, M. V. and Vasu, K. I., "Electrochemical Aspects of Stress-Corrosion Cracking in Aluminum-5 Percent Zinc and Aluminum-5 Percent Copper Alloys Containing Added Titanium", Journal of the Electrochemical Society of India, 32 (3), pp 245-251 (1983).

111. Bhat, M. V. and Vasu, K. I., "Relevance of Microstructure to Stress-Corrosion Cracking in Al-5 Percent Zn and Al-5 Percent Cu Alloys Containing Titanium", Practical Metallography, 20 (3), pp 130-137 (March, 1983).

112. Speidel, M. O. and Hyatt, M. V., Advances in Corrosion Science of Technology, Plenum Press, New York, NY, 2, pp 115-335 (1972).

113. Brown, R. H., et al., Stress-Corrosion Cracking of Metals, A State of the Art, ASTM-STP-518, ASTM, Philadelphia, PA, pp 87-118 (1972).

114. Miller, W. S. and Scott, V. D., "Effect of Composition on the Mechanical and Stress-Corrosion Behavior of Al-Zn-Mg Alloys", Metal Science, 12 (2), pp 95-101 (February, 1978).

115. Sarkar, B., "Stress-Corrosion Characteristics of Al-Zn-Mg Alloys With Copper Additions", Georgia Institute of Technology, Dissertation, 123 pp (August, 1979).

116. Izumi, Y., et al., "Effect of Microstructure and Corrosive Environments on Stress-Corrosion Cracking in Al-Zn-Mg Alloys", Journal of the Japan Institute of Metals, 43 (7), pp 671-679 (July, 1979).

117. Sarkar, B., et al., "The Effect of Copper Content and Heat Treatment on the Stress-Corrosion Characteristics of Al-6Zn-2Mg-xCu Alloys", Metallurgical Transactions, 12A (11), pp 1939-1943 (November, 1981).

118. Chen, C. and Judd, G., "Stress-Corrosion Cracking Susceptibility and Aging Characteristics of Al-Zn-Mg-Ti Alloys", Rensselaer Polytechnic Institute, Report TR-5, 22 pp (August, 1973).

REFERENCES FOR CHAPTER 2
(Continued)

119. Chen, C. and Judd, G., "Microstructural Characterization and Stress-Corrosion Cracking Susceptibility of Al-Zn-Mg-Ti Alloys", Rensselaer Polytechnic Institute, Report TR-6, 19 pp (September, 1974).

120. Evans, G. B., "The Choice of Materials", 29th Meeting of Structues and Materials Panel AGARD, Turkey, 10 pp (September, 1969).

121. Polmaer, I. J., "The Properties of Commercial Al-Zn-Mg Alloys, Practical Implications of Trace Additions of Silver", Journal of the Japan Institute of Metals, 89, pp 51-59 (1960-1961).

122. Rosenkranz, W., "Development of a High Strength, Stress-Corrosion Resistant Alloy of the Al-Zn-Mg Type. Part II: The Effect of the Chemical Composition of the Artificial Aging and Stress-Corrosion of High Strength Al-Zn-Mg-Cu Alloys", Aluminum, 39, pp 741-752 (December, 1963).

123. McMillan, J. C. and Hyatt, M. V., "Development of High-Strength Aluminum Alloys With Improved Stress-Corrosion Resistance, Boeing Company Report AFML-TR-67-180, 97 pp (June, 1967).

124. Staley, J. T., "Investigation to Improve the Stress-Corrosion Resistance of Aluminum Aircraft Alloys Through Alloy Additions and Specialized Heat Treatment", Alcoa Final Report N00019-68C0146, 199 pp (February, 1969).

125. Valikov, V. D. and Sinyarski, V. C., "A Study of the Corrosion Cracking of Al-Zn-Mg-Cu Alloys", Translation, D RIC-Trans-2682, 15 pp (March, 1972).

126. Shaffer, I. S., "Stress-Corrosion Resistance of a New High Strength Aluminum Alloy Developed for Use in Thick Sections", Naval Air Development Center Report NADC-MA-7168, 15 pp (November, 1971).

127. Pow, E. C., et al., "Analysis of Stress-Corrosion Crack-Tip Surface Chemistries in 7075 Type Aluminum Alloys", Scripta Metallurgica, 15 (1), pp 55-60 (January, 1981).

128. Althoff, J., et al., "New Weldable High-Strength Al-Zn-Mg Alloys Free From Susceptibility to Stress-Corrosion Cracking", Aluminum and Supplement in English, 52 (9), pp 1-3 (September, 1976).

129. Pizzo, P. P., "The Relative Stress-Corrosion Cracking Susceptibility of Candidate Aluminum-Lithium Alloys for Aerospace Applications", Advanced Research and Applications Corporation Report NASA-CR-3578, 126 pp (January, 1982).

130. Enjo, T., et al., "Effects of Relatively Insoluble Compounds and Beta Phase on Stress-Corrosion Cracking in 5083 Aluminum Alloy", Transactions of JWRI, 8 (1), pp 67-75 (1979).

131. Ohnishi, T. and Nakatani, Y., "Factors Affecting the Stress-Corrosion Susceptibility of Aluminum Magnesium Alloys", Journal of Japan Institute of Light Metals, 26 (1), pp 18-26 (January, 1976).

REFERENCES FOR CHAPTER 2
(Continued)

132. Niederberger, R. B., et al., "Corrosion and Stress-Corrosion of 5000 Series Al Alloys in Marine Environments", Corrosion, 22 (3), pp 68-73 (1966).

133. Ohnishi, T., et al., "Effect of Thermomechanical Treatment of Strength and Stress-Corrosion of Al-8 Percent Mg Alloy", Journal of Japan Institute of Light Metals, 27 (2), pp 63-70 (February, 1977).

134. Brook, C. L., "Aluminum-Magnesium Alloys 5086 and 5456-H116", Naval Engineering Journal, 82 (4), p 29 (August, 1970).

135. Dix, E. H., Jr., et al., "Development of Wrought Aluminum-Magnesium Alloys", Alcoa Research Laboratories, Technical Report 14 (1958).

136. Hayne, F. H. and Boyd, W. K., "Stress-Corrosion Cracking of Aluminum Alloys", DMIC Report 228, Battelle Memorial Institute (July, 1966).

137. Collins, J. F. and Maduell, C. E., "Polyalkylene Glycol Quenching of Aluminum Alloys", Materials Performance, 16 (7), pp 20-23 (July, 1977).

138. Izu, M., et al., "Stress-Corrosion Cracking and Intergranular Corrosion of 2017 Aluminum Alloy", Journal of Japan Institute of Light Metals, 33 (7), pp 386-391 (July, 1983).

139. Urushino, K. and Sugimoto, K., "Stress-Corrosion Cracking of Aged Al-Cu-Mg Alloys in NaCl Solution", Corrosion Science, 19 (4), pp 225-236 (1979).

140. Gray, J. A., "Stress-Corrosion Testing of AU4SG Aluminum Alloy in Plate Form", Royal Aircraft Establishment, Farnborough, England, RAE-TR-78054, 25 pp (May, 1978).

141. Kim, J. T. and Pyun, S., "Stress-Corrosion Cracking Behavior of the Alloy AlCuSiMn (2014) With and Without Deformation Structure", Aluminum and Supplement in English, 59 (6), pp 456-458 (June, 1983).

142. Shastry, C. R., et al., "The Effect of Solution Treatment Temperature on Stress-Corrosion Susceptibility of 7075 Aluminum Alloy", AMMRC, AMMRC-TR-82-31, 25 pp (January, 1981).

143. Speidel, M. O., "Interaction of Dislocations With Precipitates in High Strength Aluminum Alloys and Susceptibility to Stress-Corrosion Cracking", Proceedings of Conference on Fundamental Aspects of Stress-Corrosion Cracking, NACE, p 561 (1969).

144. Sprowls, D. O. and Nock, J. A., Jr., "Thermal Treatment of Aluminum-Base Alloy Article", U.S. Patent 3,198,676 (August 3, 1965).

145. Vaccari, J. A., "New Wright Aluminum Alloys Fight Corrosion", Material Engineering, 71, p 22 (June, 1970).

146. Doig, P., et al., "The Stress-Corrosion Susceptibility of 7075 Al-Zn-Mg-Cu Alloys Tempered From T6 to an Overaged T7X", Corrosion, 33 (6), pp 217-221 (June, 1977).

REFERENCES FOR CHAPTER 2
(Continued)

147. Koch, G. H. and Kolijn, D. T., "The Heat Treatment of Commercial Aluminum Alloy 7075", Journal of Heat Treating, 1 (3), pp 3-14 (1979).

148. Biggs, L. A., "Stress-Corrosion Resistance of 7010-T73651", Naval Air Development Center, NADC-80038-60, 13 pp (April, 1980).

149. Dorward, R. C. and Hasse, K. R., "Flaw Growth of 7075, 7050, and 7049 Aluminum Plate in Stress-Corrosion Environments", Kaiser Aluminum, NAS8-30890, 212 pp (October, 1976).

150. Shaffer, I. S., "Stress-Corrosion Resistance of Die Forged 7175-T736 Aluminum Alloy", Naval Air Development Center, NADC-MA-7055, 18 pp (September, 1970).

151. Staley, J. T. and Hunsicker, H. Y., "Investigation to Develop a High Strength Stress-Corrosion Resistant Aluminum Aircraft Alloy", Alcoa Final Report, 182 pp (January, 1970).

152. Reimann, W. H. and Brisbane, A. W., "Improved Fracture Resistance of 7075 Through Thermomechanical Processing", Engineering Fracture Mechanics, 5 (1), pp 67-78 (February, 1973).

153. Paton, N. E. and Sommer, A. W., "Influence of Thermomechanical Processing Treatments on Properties of Aluminum Alloys", 3rd International Conference on Strength of Metals and Alloys, 1 (21), pp 101-108 (August, 1973).

154. Hyatt, M. V. and Speidel, M. O., "High Strength Aluminum Alloys, Chapter 4", Stress-Corrosion Cracking in High Strength Steels and in Titanium and Aluminum Alloys, Edited by B. F. Brown, Naval Research Laboratory (1972).

155. Hyatt, M. V., "Effects of Residual Stresses on Stress-Corrosion Crack Growth Rates in Aluminum Alloys", Boeing Company, D6-24469, 23 pp (November, 1969).

156. Ratke, L., "Influence of Surface Deformation on the Stress-Corrosion Cracking Behavior of Age-Hardened AlZn5Mg3", Aluminum and Supplement in English, 58 (12), pp 715-718 (December, 1982).

157. Kohler, W., "Improvement of Stress-Corrosion Resistance of Aluminum Weldments by Shot Peening", 2nd International Conference on Aluminum Weldments, Munich, FRG, pp II: 7.1-7.8 (May, 1982).

158. Hanisch, A. H. and Burck, L. H., "Effects of Overloads on the Incubation Time for Stress-Corrosion Cracking of 7075 Aluminum", Corrosion, 38 (6), pp 330-335 (June, 1982).

159. Sprowls, D. O. and Brown, R. H., "What Every Engineer Should Know About Stress-Corrosion of Aluminum", Metal Progress, 81 (4), pp 79-85 (1962).

160. Mulherin, J. H., "Influence of Environment on Crack Propagation Characteristics of High Strength Aluminum Alloys", ASTM STP 425, p 66 (1967).

REFERENCES FOR CHAPTER 2
(Continued)

161. Chu, H. P. and Wacker, G. A., "Stress Testing of 7079-T6 Aluminum Alloy in Seawater Using Smooth and Precracked Specimens", Journal of Basic Engineering, 91 (4), pp 565-569 (December, 1969).

162. Speidel, M. O., "Branching of Stress-Corrosion Cracks in Aluminum Alloys", The Theory of Stress-Corrosion Cracking in Alloys, Edited by J. C. Scully, NATO Scientific Affairs Division, Brussels, pp 345-354 (1971).

163. Holroyd, N.J.H. and Hardie, D., "Strain-Rate Effects in the Environmentally Assisted Fracture of a Commercial High-Strength Aluminum Alloy (7049)", Corrosion Science, 21 (2), pp 129-144 (1981).

164. Gopalan, P., et al., "Stress-Corrosion Cracking of Aged Al-5Zn-4Mg Alloy in 3.5 Percent NaCl Solution", Journal of the Electrochemical Society of India, 32 (1), pp 17-21 (January, 1983).

165. Ugiansky, G. M., et al., "Slow Strain-Rate Stress-Corrosion Testing of Aluminum Alloys", Stress-Corrosion Cracking, The Flow Strain Rate Technique, ASTM-STP-665.

166. Nguyen, T. H., et al., "On the Nature of the Occluded Cell in the Stress-Corrosion Cracking of AA 7075-T651 - Effect of Potential, Composition, Morphology", Corrosion, 38 (6), pp 319-326 (June, 1982).

167. Gest, R. J. and Troiano, A. R., Corrosion, 30, p 274 (1974).

168. Speidel, M. O., Proceedings of Conference "Hydrogen in Metals", ASM, p 249 (1974).

169. Louthan, M. R., Jr. and Dexter, A. H., Metallurgical Transactions A, 6A, p 1655 (1975).

170. Helfrich, W. F., "Influence of Stress and Temperature on Short Transverse Stress-Corrosion Cracking of an Al-4.2Zn-2.5Mg Alloy", ASTM-STP-425 (1967).

171. Landkof, M. and Galor, L., "Stress-Corrosion Cracking of Al-Zn-Mg Alloy AA-7039", Corrosion, 36 (5), pp 241-246 (May, 1980).

172. Hyatt, M. V. and Quist, W. E., "Effect of Exposure Time at 250 F on Stress-Corrosion Crack Growth Rates in 2024-T351 Aluminum", Boeing Company, D6-25218, 20 pp (March, 1970).

173. McHardy, J. and Hollingsworth, E. H., "Investigation of the Mechanism of Stress-Corrosion of Aluminum Alloys", Alcoa Final Report on Contract No. 65-0327 (1966).

174. Czyryca, E. and Hack, H. P., "Corrosion of Aluminum Alloys in Exfoliation Resistant Tempers Exposed to Marine Environments for Two Years", Proceedings of the 1974 Transveric Corrosion of Military Equipment Conference, Technical Report AFML-TR-75-42 VII (September, 1975).

REFERENCES FOR CHAPTER 2
(Continued)

175. Lifka, B. W. and Sprowls, D. O., "Significance of Intergranular Corrosion in High Strength Aluminum Alloy Products, Localized Corrosion--Cause of Metal Failure", ASTM-STP-516, pp 120-144 (1972).

176. Rhodes, D. and Radon, J. C., "Fracture Analysis of Exfoliation in an Aluminum Alloy", Engineering Fracture Mechanics, 10 (4), pp 843-853 (1978).

177. Tohma, K., et al., "Effect of Cu Addition on Intergranular Corrosion of Al-5.5Zn-2.5Mg Alloy", Journal of the Japan Institute of Light Metals, 33 (7), pp 377-385 (July, 1983).

178. Staley, J. T., "Investigation to Develop a High Strength Stress-Corrosion Resistant Naval Aircraft Aluminum Alloy", Alcoa Final Report, 114 pp (November, 1970).

179. Waldron, L. J., et al., "Performance of Stainless Steel Galvanically Coupled to Other Metals", Naval Research Laboratories, NRL-MR-1388, 12 pp (January, 1963).

180. Summerson, T. J., "Aluminum Association Task Group Exfoliation and Stress-Corrosion Testing of Aluminum Alloys for Boat Stock", Tri-Service Corrosion of Military Equipment Conference, Dayton, OH (October, 1974).

CHAPTER 3
TABLE OF CONTENTS

CHAPTER 3
LIST OF TABLES

CHAPTER 3
LIST OF FIGURES

CHAPTER 3
LIST OF FIGURES
(Continued)

CHAPTER 3

TITANIUM AND TITANIUM-BASE ALLOYS

Titanium and its alloys are among the most corrosion resistant metallic materials to seawater. Although there are limited data available on atmospheric, splash and tide, and mud exposure, the data indicate that resistance to corrosion extends to these environments as well. Typical atmospheric corrosion data shown in Table 3-1 indicate titanium's high resistance to corrosion in marine atmospheres as compared to other structural alloys.

However, under specific conditions, titanium and its alloys may be susceptible to crevice corrosion and stress-corrosion cracking. Alloy modifications and heat treatment can effectively increase the resistance of titanium to these types of failure.* Discussions of the different corrosion modes are given below.

General Corrosion

Titanium and its alloys have excellent resistance to general corrosion in marine environments due to the presence of a strongly adherent oxide film. Typical data, given in Table 3-2, show very low corrosion rates of unalloyed titanium and Ti-6Al-4V after up to 3 years' exposure in ambient seawater. Similar low rates have been observed for other titanium alloys, such as Ti-5Al-2Sn, Ti-13V-11Cr-3Al, Ti-7Al-2Cb-1Ta, Ti-6Al-2Cb-1Ta-1Mo, and Ti-0.15Pd.[2-5] Of particular interest was the observation that a welded Ti-50A tube from a surface condenser did not show any evidence of corrosion after 16 years of service in polluted seawater.[6]

A comparison of corrosion rates of titanium with other selected materials in marine environments at Kure Beach, NC again illustrates the excellent resistance of titanium to general corrosion attack, in both seawater and marine atmospheres, see Table 3-3.

---

* The alloys mentioned in this chapter are listed in Appendix C, Table C-1.

TABLE 3-1. CORROSION RATE OF MATERIALS EXPOSED TO THE ATMOSPHERE FOR 5 YEARS AT KURE BEACH, NC[7]

Materials	Corrosion Rate[a], mpy	
	80-ft Lot	800-ft Lot
Titanium	Nil	Nil
Alclad 24S-T3	0.0197	0.0034
Alclad 75S-T6	0.0278	0.0034
Type 302 stainless	0.0009	Nil
Type 316 stainless	0.0013	Nil
Inconel 600	0.0014	0.0003

(a) Average corrosion rates from three specimens.

TABLE 3-2. CORROSION OF TITANIUM IN AMBIENT SEAWATER

Alloy	Ocean Depth, m	Corrosion Rate, mm/yr	Reference
Unalloyed	Shallow	0.8×10^{-6}	(7)
	720-2070	<0.00025	(3)
	1300-1370	<0.00025	(3)
	1.5-2070	0.0	(3)
	1720	0.00004	(9)
Ti-6Al-4V	1.5-2070	<0.00025	(3)
	1720	8×10^{-6}	(9)
	1720	$\leq$0.001	(13)

TABLE 3-3. MATERIALS IMMERSED 480 DAYS IN QUIET SEAWATER IN THE BASIN AT KURE BEACH, NC, AND IN MARINE ATMOSPHERES[7]

Material[a]	Immersed in Quiet Seawater			Corrosion Rate in Marine Atmosphere, mpy		
	Average Corrosion Rate[b], mpy	Max Face Pitting, in.	Max Edge Pitting, in.	5 Years in Shore Rack 80 ft from Breakers	5 Years in Main Lot 800 ft from Breakers	4 Years 11 Months in Bridgeport, Connecticut
Titanium	Nil	None	None	Nil	Nil	0.00008
24S-T3	2.24	0.054[c]	0.37	0.0256	0.0028	0.0154
Alclad 24S-T3	0.612	0.001	0.001	0.0197	0.0034	0.0122
52S-1/2H	0.96	0.065[c]	0.21	0.0139	0.0026	0.0135
Alclad 75S-T6	0.60	0.001	0.001	0.0278	0.0034	0.0140
302 Stainless	0.146	0.060	0.050	0.0009	Nil	0.0001
316 Stainless	0.24	0.060	1.50[d]	0.0013	Nil	0.0003
347 Stainless	1.43	0.067[c]	2.50[d]	0.0011	Nil	0.0003
Monel	1.38	0.039	0.20	0.0175	0.0107	0.0349
Inconel	0.49	0.034	4.75[d]	0.0014	0.0003	0.0094

(a) Six specimens of each.
(b) Average of three specimens.
(c) Specimens perforated.
(d) Maximum depth of crevice corrosion.

Pitting and Crevice Corrosion

Effect of Alloy Composition. Titanium is highly resistant to pitting and crevice corrosion in seawater. Immersion tests with titanium and its alloys have never shown pitting or crevice corrosion in ambient seawater.[3,7-9] However, in seawater and brines at temperatures above 70 C (158 F), crevice corrosion of unalloyed titanium has been observed.[10-12]

Griess[12] studied the crevice corrosion of titanium and its alloys in chloride solutions at elevated temperatures and found that the localized attack was associated with the development of low pH conditions. Palladium (Pd), Mo, and Ni alloy additions were found to be beneficial in inhibiting this crevice attack. Other researchers also have observed the

beneficial effects of these alloy additions. Shimose and Takamura[14] showed that, in hot concentrated solutions of magnesium and ammonium chloride, titanium underwent crevice attack whereas a 0.2 percent palladium alloy was immune. Feige and Kane[15] reported that titanium alloyed with either 2 percent molybdenum, 0.2 percent palladium or 2 percent nickel showed improved resistance to crevice corrosion. Kobayaski, et al.[17] showed that alloying with nickel significantly improved the resistance to crevice corrosion at a concentration of 0.75 weight percent, see Figure 3-1. Also, a 0.17 percent palladium addition was found to improve the resistance to crevice corrosion, see Table 3-4.

Commercial alloys Ti grade 7 (Ti-Pd) and Ti grade 12 (Ti-Ni-Mo) have been developed to make use of the beneficial effects of palladium, molybdenum, and nickel alloying elements in improving pitting and crevice corrosion. The Ti-Pd alloy contains up to 0.25 weight percent palladium whereas titanium grade 12, its low-cost alternative, contains 0.8 weight percent nickel and 0.3 percent molybdenum.

Depth and Aeration. Depth or aeration have not been found to influence the pitting or crevice corrosion of titanium at ambient temperature. Reinhart and Jenkins[5] exposed several titanium alloys to different depths, which corresponded to oxygen concentrations of 0.4, 1.35, and 5.75 milliliters/liter. The titanium alloys were not attacked by seawater under any of these conditions after one year of exposure. The alloys in this investigation were TiCP, Ti75A, Ti-0.15Pd, Ti-5Al-2.5Sn, Ti-6Al-4V, Ti-7Al-2Cb-1Ta, and Ti-13V-11Cr-3Al.

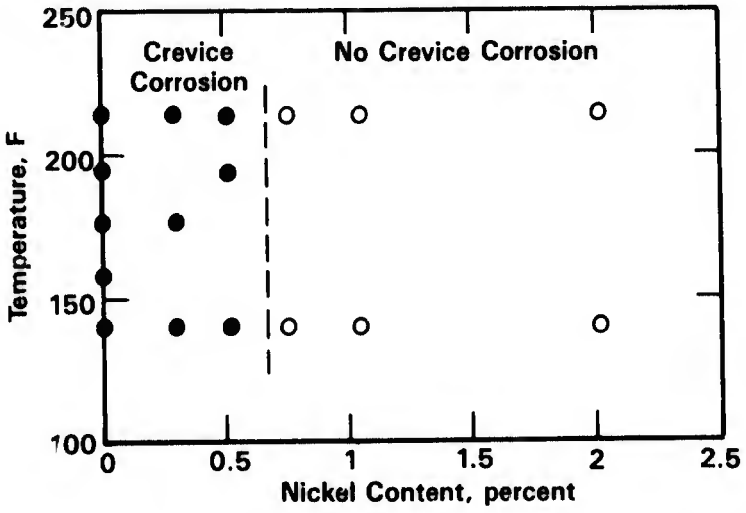

FIGURE 3-1. EFFECT OF THE Ni CONTENT ON THE CREVICE CORROSION RESISTANCE OF TITANIUM IN 6 PERCENT NaCl AQUEOUS SOLUTION AT VARIOUS TEMPERATURES[16]

TABLE 3-4. RESULTS OF CREVICE CORROSION TESTS OF VARIOUS BINARY TITANIUM ALLOYS IN BOILING 6 PERCENT NaCl AQUEOUS SOLUTION FOR 120 HOURS[16]

Alloying Element	Weight Percent	Crevice Corrosion
Ni	0.30	Occurred
	0.54	Occurred
	0.75	Not occurred
	1.05	Not occurred
	2.02	Not occurred
Pd	0.02	Occurred
	0.04	Occurred
	0.09	Occurred
	0.17	Not occurred
Ta	0.31	Occurred
	0.47	Occurred
	0.90	Occurred
	2.10	Occurred
Mo	0.31	Occurred
	0.52	Occurred
	1.08	Occurred
Sn	0.3	Occurred
	0.5	Occurred
	1	Occurred
	2	Occurred
	4	Occurred
	6	Occurred
Cu	0.3	Occurred
	0.5	Occurred
	1	Occurred
	2	Occurred

Temperature and pH. As discussed above, pitting or crevice corrosion of titanium have not been observed at temperatures below 70 C (158 F). Electrochemical studies performed by Griess[12] in aqueous chloride solutions showed that, with increasing temperature, the critical or maximum current density, i_{max}, and the passive current density, i_{pass}, increased, see Figure 3-2. Further, an increasing pH was found to decrease i_{max}[12] of titanium in aqueous chloride solutions. The boundary conditions for crevice corrosion for different

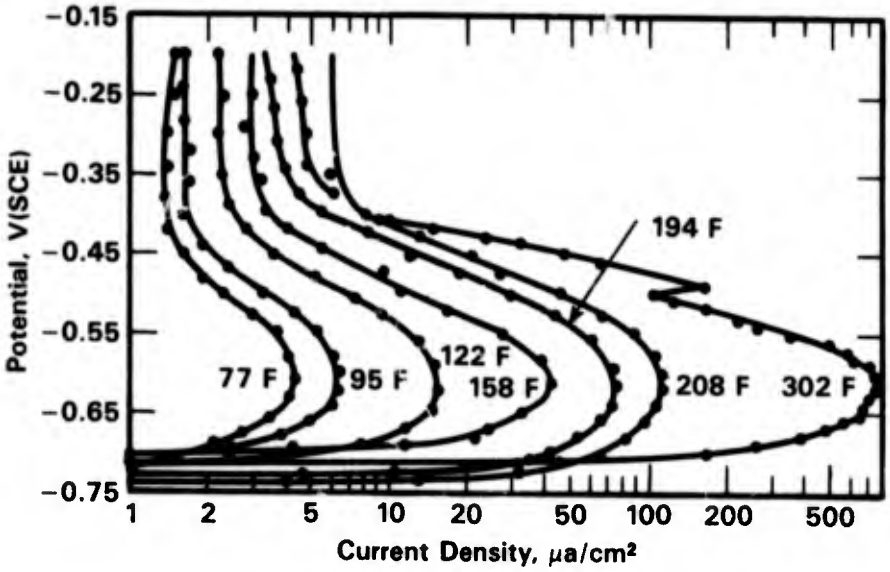

FIGURE 3-2. THE EFFECT OF TEMPERATURE ON THE ANODIC POLARIZATION OF TITANIUM IN 0.9M NaCl-0.1M HCl[12]

titanium alloys as a function of temperature and pH were obtained by immersion testing in saturated sodium chloride brines and are shown in Figure 3-3. The diagram indicates that, at neutral pH, no crevice corrosion occurs in commercial pure titanium below approximtely 120 C (250 F). Addition of nickel, molybdenum (grade 12) or palladium (grade 7) further extends the resistance of titanium to crevice corrosion to higher temperatures and lower pH.

The effect of temperature on the pitting behavior of titanium in aqueous chloride solutions was also demonstrated by Koizumi and Furuya[19] who showed a decrease in pitting potential in the temperature range of 20-150 C, see Figure 3-4. The effect of pH on the pitting potential was less dramatic, Figure 3-5, although at a temperature of 200 C, the pitting potential showed a shift in the active direction of about 0.2 V(SCE) from pH 7 to pH 1. It should be noted that the pitting potentials shown in Figures 3-4 and 3-5 are so noble that pitting is not expected to occur on boldly exposed surfaces in the absence of an applied potential.

Some controversial data exist on the effect of temperature on crevice corrosion of titanium. On the one hand, it was shown by different titanium alloy producers that the temperature at which crevice corrosion of titanium tube-to-tube plates could occur is sensitive to the chloride ion concentration, as is shown in Figure 3-6. However, Sato[20] did not find an effect of chloride concentration of crevice corrosion of titanium tubes in brines

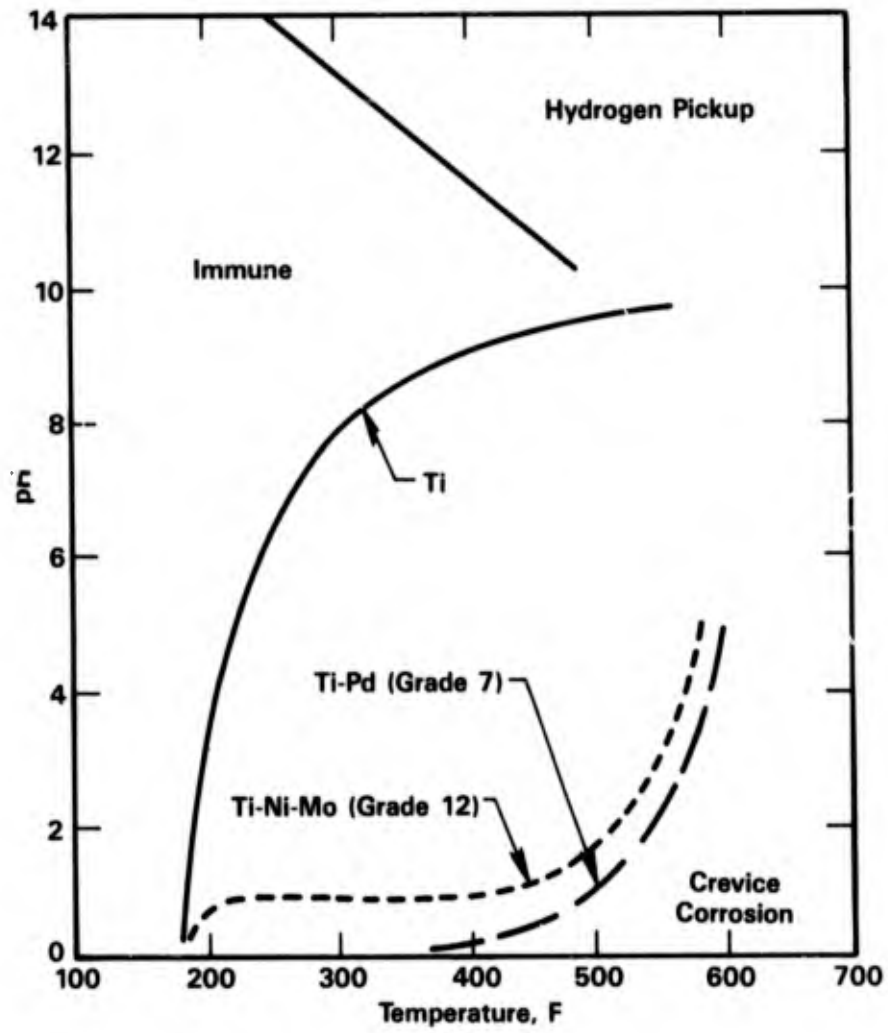

FIGURE 3-3. CORROSION RESISTANCE OF TITANIUM ALLOYS IN SATURATED NaCl BRINES[17,18]

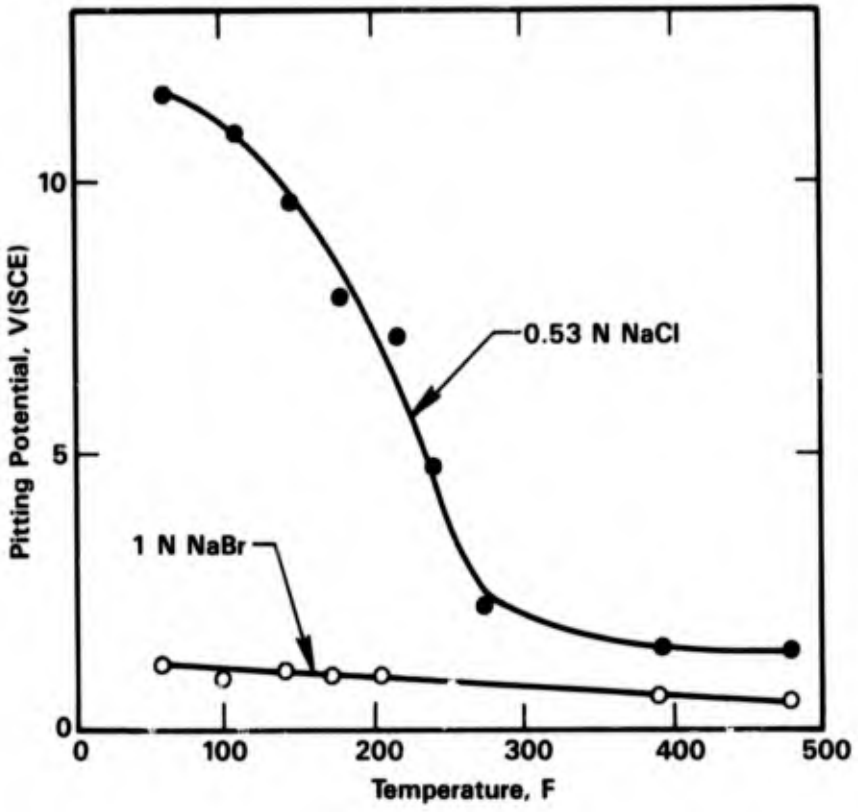

FIGURE 3-4. EFFECT OF TEMPERATURE ON PITTING POTENTIAL IN 0.53 N NaCl AND 1.0 N NaBr[19]

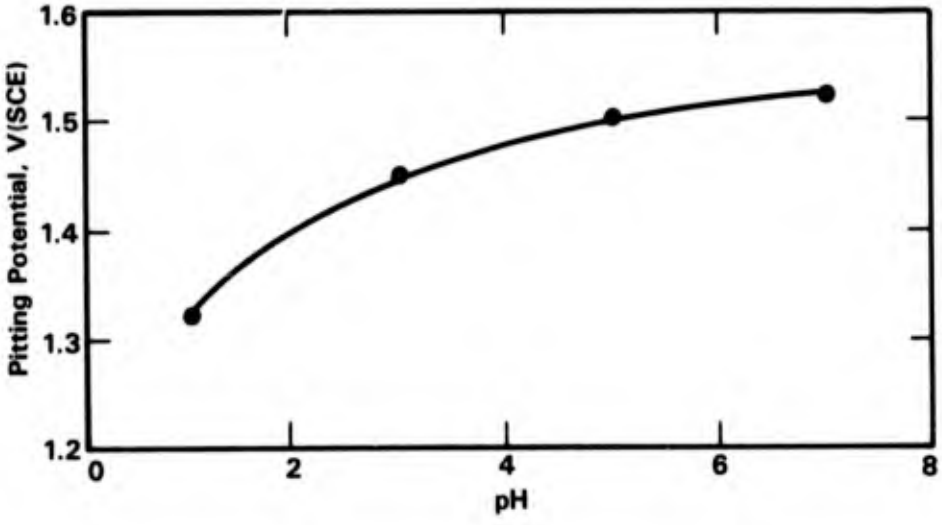

FIGURE 3-5. EFFECT OF pH ON PITTING POTENTIAL FOR PITTING IN 0.53 N NaCl AT 200 C[19]

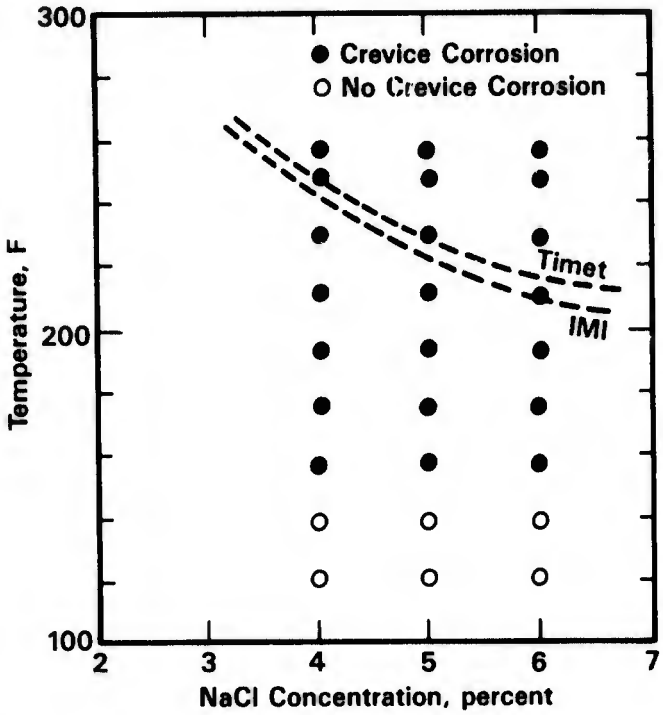

FIGURE 3-6. EFFECT OF TEMPERATURE AND SALT CONCENTRATION OF BRINE ON THE SUSCEPTIBILITY TO CREVICE CORROSION OF TITANIUM METAL AT THE CREVICE OF EXPANDED JOINTS OF TITANIUM TUBES TO TUBE PLATES[20]

and found the critical temperature for crevice corrosion to be approximately 70 C, see Figure 3-6. This value is much lower than those indicated by previous authors.

Effect of Time. Exposure tests in deep ocean environments in both the Pacific[7,21,22,25] and the Atlantic Ocean[24] have indicated that the duration of exposure does not affect the resistance of titanium alloys to pitting and crevice corrosion. Crevice corrosion tests at Kure Beach, NC,[7,25] in which glass fiber, zinc plated steel, and cadmium plated steel washers were bolted to titanium strips showed no crevice corrosion either after 360 days' immersion in seawater or after 4 years and 8 months of exposure on a shore rack.

Effect of Biofouling. Titanium is not toxic to marine organisms and therefore, biofouling can easily occur on titanium surfaces immersed in seawater.[6,25,26] Cotton and Downing reported extensive biofouling on titanium after 800 hours immersion in shallow seawater.[8]

However, the integrity of the corrosion resistant oxide film is fully maintained under marine deposits and no pitting or crevice corrosion has been observed. It has been shown that

biofouling on titanium heat exchanger tubes can be reduced by maintaining water velocities greater than 1.2 m/s[27]. Table 3-5, compiled by Franson and Covington,[6] indicates that titanium is also highly resistant to corrosion by chlorine and hypochlorite solutions which can be used to reduce biofouling. Finally, because of the high resistance of titanium to erosion corrosion, abrasive particles can be injected into seawater to control biofouling of titanium heat exchanger surfaces.

Potential. The pitting or breakdown potential of titanium in ambient seawater ranges between +2 and 10 V(SCE) depending on alloy composition.[28] Under ambient conditions, pitting does not normally occur because of the high breakdown potential, unless high noble potentials are applied. This sometimes occurs inadvertently by improper grounding of equipment during welding.

TABLE 3-5. CORROSION OF TITANIUM BY CHLORINE AND HYPOCHLORITES[6]

Environments	Temperature C	Temperature F	Corrosion Rate, mm/yr
Wet Cl_2	10-88	50-190	Nil-0.00051
Wet Cl_2	88	190	0.0009-0.0017[a]
River Water, Cl_2 saturated	93	200	0.0008
Water, Cl_2 saturated	75	167	0.0025
Water, Cl_2 saturated	97	207	0.069
Seawater, Cl_2 saturated	95	203	0.010
20% NaCl, Cl_2 saturated	88-96	190-205	Nil-0.0005
6% Sodium Hypochlorite	21	70	Nil
16% Sodium Hypochlorite	21	70	<0.0025[b]
2% Calcium Hypochlorite	100	212	0.0013
6% Calcium Hypochlorite	100	212	0.0013
18-20% Calcium Hypochlorite	21-24	70-75	Nil
1.5-4.0% NaOCl, 12-15% NaCl, 1% NaOH	66-93	150-200	0.0025
5% NaOCl, 2% NaCl, 4% NaOH	Boiling		0.06-0.07[c]

(a) TiCode-12 and Ti-50A, welded samples, respectively.
(b) No evidence of pitting.
(c) No corrosion in metal-to-metal or metal-to-Teflon crevices.

Another form of pitting has been observed in hot brine (about 160 F) when iron is embedded in the titanium surface as a result of scratching with an iron tool or the use of a steel wire brush.[29] It was speculated by Covington and Schutz[29] that, as a result of the potential difference between titanium and iron (approximately 0.5 V(SCE)) a local galvanic cell is set up in which the iron is consumed. As the iron is dissolved, a pit may initiate in the titanium surface and grow due to the acidic conditions that develop in the vicinity of the iron particle.

Velocity. Velocity does not normally affect the high pitting and crevice corrosion resistance of titanium alloys in seawater. As discussed previously, biofouling of titanium surfaces can occur at seawater velocities less than 1.2 m/sec.[27] However, no crevice corrosion has been observed under marine deposits. At velocities greater than 1.2 m/sec, the marine deposits can be removed and, only at a very high velocity (36 m/sec), some erosion corrosion of titanium has been observed.[30]

Erosion Corrosion

Titanium alloys have the ability to withstand high seawater velocities with negligible attack. Several investigators[7,8,25,30-36] have established that titanium alloys will withstand seawater at velocities that are of technical interest. Velocities as high as 36.5 m/sec (120 ft/sec) have been found to cause only minimal erosion rates in commercially pure titanium and Ti-6Al-4V, see Table 3-6. These high velocities are of importance for the selection of materials of construction of hydrofoils or craft operating at speeds of 60 knots (101 fps) or more.[31,35] In addition, high velocity information is important for other applications involving rapidly flowing seawater, e.g., high speed pumps and high velocity piping

TABLE 3-6. EFFECT OF SEAWATER VELOCITY ON CORROSION OF TITANIUM AND Ti-6Al-4V[30]

Seawater Velocity, m/sec	Corrosion Rate, mm/yr	
	Unalloyed Titanium	Ti-6Al-4V
0-0.6	Nil	--
7.6	Nil	--
36.5	0.007	0.011

systems where titanium is used to reduce size and weight of these components in deep diving submarines.[26] Comparison between the erosion behavior of commercially pure titanium, aluminum brass and a 70/30 cupro-nickel containing high iron and manganese again illustrates the high resistance of titanium to erosion in seawater, see Table 3-7.

Titanium also was shown to have excellent resistance to flowing seawater containing sand or silt, see Table 3-8. Titanium is at least twenty times more resistant to erosion by water containing sand than the copper-base materials, and metal loss under these conditions was equivalent to only 1×10^{-4} inches penetration per year. When using 10 mesh carborundum grit under similar test conditions, the erosion rate of titanium increased to 5×10^{-4} inches penetration per year, but the copper-base materials were much more severely eroded.

Titanium also has excellent resistance to impingement attack in seawater. Hohman[31] has reported jet erosion-corrosion rates of various materials in seawater moving at velocities of 90 knots for 30 days, see Figure 3-7. In this comparison, the titanium Alloys Ti-6Al-4V and Ti-8Al-2Cb-1Ta were superior to the other candidate materials.

Titanium also has an unusually high resistance to cavitation corrosion, which makes titanium an ideal material of construction for tube inlets.[25]

Galvanic Corrosion

The coupling of titanium with dissimilar metals usually does not accelerate the corrosion of titanium alloys. The exception is in reducing acidic environments where titanium does not passivate. Under these conditions, it has a potential similar to aluminum and will undergo accelerated corrosion when coupled to other more noble metals.[19] In aerated environments, however, titanium will accelerate the corrosion of less noble materials. Table 3-9 lists the galvanic series of various metals in flowing seawater.[8] This galvanic series does not greatly differ from galvanic series provided in the various handbooks[38,39] and those obtained in specific marine environments such as in Baltic Seawater.[40]

Because of its compatibility with graphite, titanium is frequently used for fasteners in graphite-epoxy composite materials.[41] An increasing number of carbon fiber reinforced epoxy matrix components are now being used in the construction of high performance aircraft to reduce weight.

The accelerating effect on the corrosion rate of various metals when they are galvanically connected to titanium in seawater is illustrated in Figure 3-8. The figure also indicates the significance of the anodic to cathodic area ratio effect on galvanic corrosion. The acceleration in corrosion of metals coupled to titanium as a result of cathode-anode area ratio also is illustrated in Table 3-10. If the cathodic area (titanium) exposed is small

TABLE 3-7. EROSION OF UNALLOYED TITANIUM IN SEAWATER LOCATIONS[37]

Location	Flow Rate, ft/sec (m/sec)	Duration, months	Corrosion Rate, mpy (mm/yr)			
			Grade 2 Titanium		70Cu-30Ni[a]	Aluminum
Brixham Sea	32.2 (9.8)	12	<0.098	(<0.0025)	11.8 (0.3)	39.4 (1.0)[b]
Kure Beach	3.3 (1)	54	3×10^{-5}	(0.75×10^{-6})	--	--
	27.9 (8.5)	2	4.9×10^{-3}	(0.000125)	1.9 (0.048)	--
	29.5 (9)	2	1.1×10^{-2}	(0.000275)	81.1 (2.06)	--
	23.6 (7.2 plus air)	1	0.020	(0.0005)	4.7 (0.12)	--
Wrightsville Beach	2.0-4.3 (0.6-1.3)	6	0.004	(0.0001)	0.9 (0.022)	--
	29.5 (9)	2	0.007	(0.000175)	--	--
Mediterranean Sea	23.6 (7.2 plus air)	0.5		0.5 mg/day	8.9 mg/day	19.3 mg/day
Dead Sea	23.6 (7.2 plus air)	0.5		0.2 mg/day	9.0 mg/day	6.7 mg/day

(a) High iron 70-30 cupron-nickel.
(b) Sample perforated.

TABLE 3-8. EROSION OF UNALLOYED TITANIUM IN SEAWATER CONTAINING SUSPENDED SOLIDS[37]

Flow Rate, ft/sec (m/sec)	Suspensed Matter in Seawater	Duration, hours	Corrosion/Erosion, mpy (mm/yr)		
			Grade 2 Titanium	70Cu-30Ni[a]	Aluminum Brass
23.6 (7.2)	None	10,000	Nil	Pitted	Pitted
6.6 (2)	40 g/l 60 mesh sand	2,000	0.1 (0.0025)	3.9 (0.10)	2.0 (0.05)
6.6 (2)	40 g/l 10 mesh emery	2,000	0.5 (0.0125)	Severe erosion	Severe erosion
11.5 (3.5)	1% 80 mesh emery	17.5	0.15 (0.0037)	1.1 (.028)	--
13.5 (4.1)	4% 80 mesh emery	17.5	3.3 (0.083)	2.6 (.065)	--
23.6 (7.2)	40% 80 mesh emery	1	59.1 (1.5)	78.7 (2.0)	--

(a) High iron, high manganese 70-30 cupron-nickel.

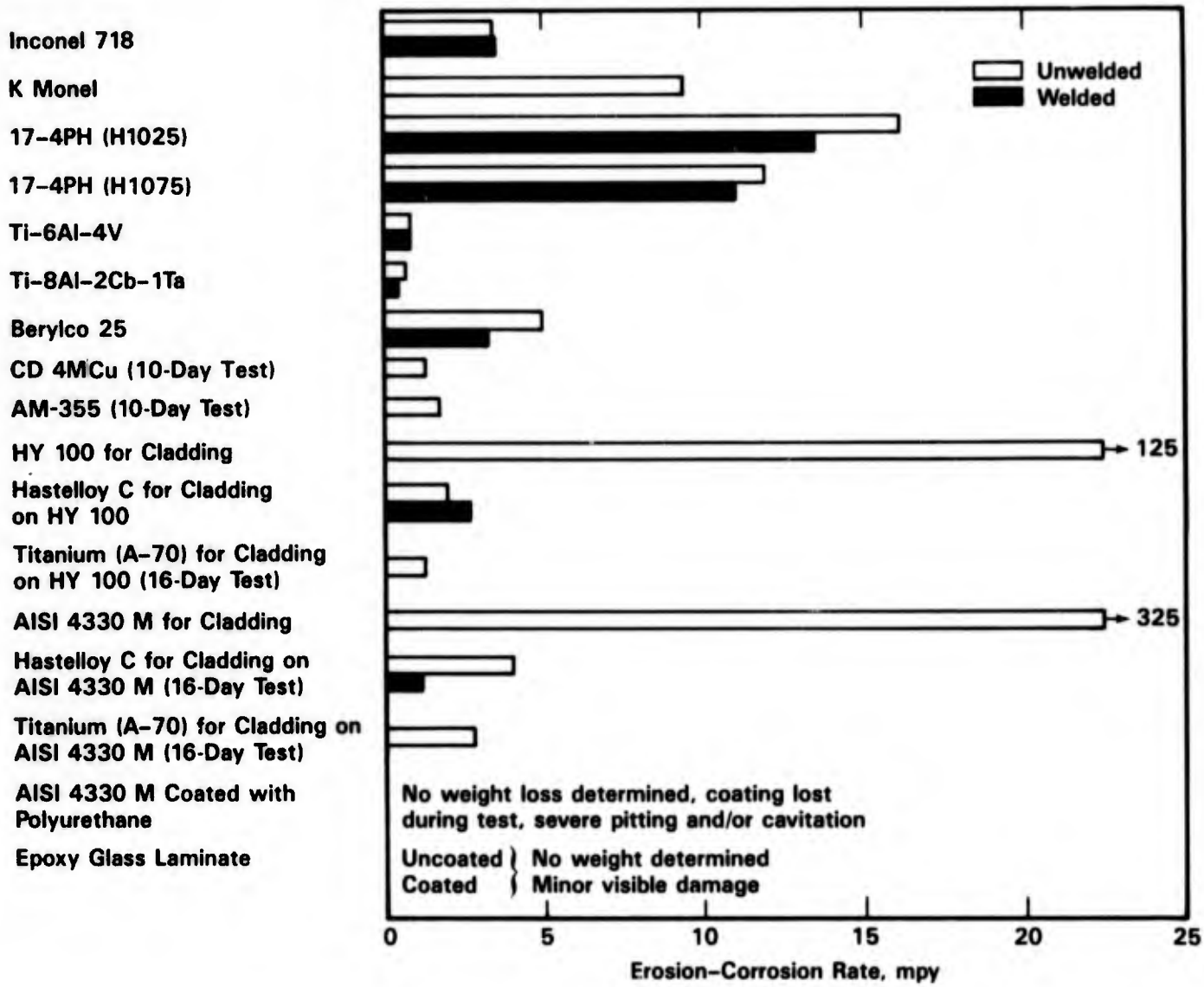

FIGURE 3-7. RATES FOR JET EROSION-CORROSION IN SEAWATER. EXPOSURE WAS FOR 30 DAYS AT 90 KNOTS[31]

TABLE 3-9. GALVANIC SERIES IN FLOWING WATER (13 FT/SEC AT ABOUT 75 F [23.9 C])[8]

Material	Steady State Electrode Potential, V(SCE)
Graphite	+0.25
Platinum	+0.15
Zirconium	-0.04
Type 316 Stainless Steel (Passive)	-0.05
Type 304 Stainless Steel (Passive)	-0.08
Monel 400	-0.08
Hastelloy C	-0.08
Titanium	-0.10
Silver	-0.13
Type 410 Stainless Steel (Passive)	-0.15
Type 316 Stainless Steel (Active)	-0.18
Nickel	-0.20
Type 430 Stainless Steel (Passive)	-0.22
Copper Alloy 715 (70-30 Cupro-Nickel)	-0.25
Copper Alloy 706 (90-10 Cupro-Nickel)	-0.28
Copper Alloy 442 (Admiralty Brass)	-0.29
G Bronze	-0.31
Copper Alloy 687 (Aluminum Brass)	-0.32
Copper	-0.36
Alloy 464 (Naval Rolled Brass)	-0.40
Type 410 Stainless Steel (Active)	-0.52
Type 404 Stainless Steel (Active)	-0.53
Type 430 Stainless STeel (Active)	-0.57
Carbon Steel	-0.61
Cast Iron	-0.61
Aluminum 3003-H	-0.79
Zinc	-1.03

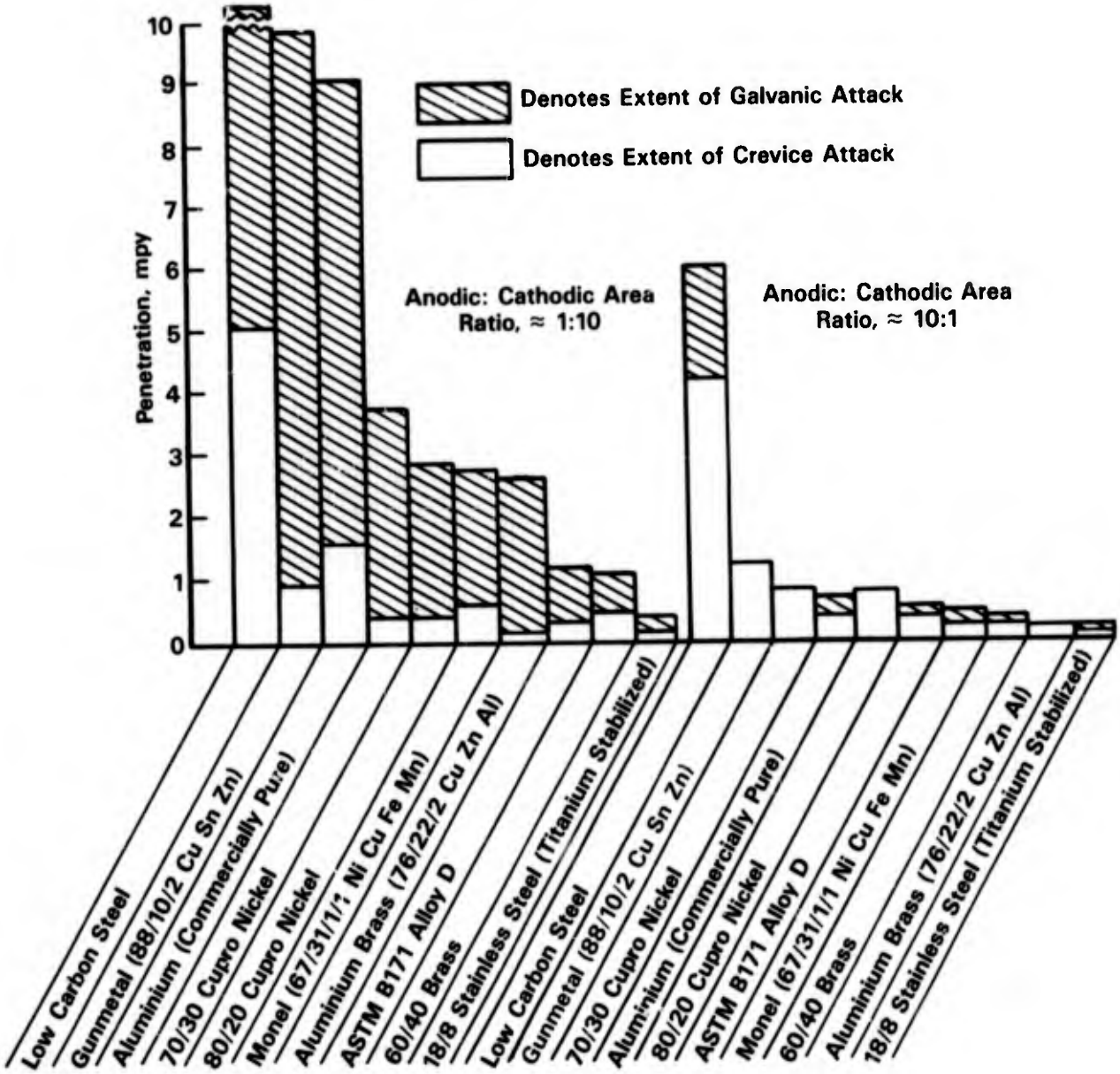

FIGURE 3-8. THE CORROSION BEHAVIOR OF VARIOUS METALS COUPLED TO TITANIUM AND IMMERSED IN AERATED SEAWATER FOR 2,500 HOURS[8]

TABLE 3-10. ACCELERATION FACTORS FOR CORROSION DUE TO DISSIMILAR METAL COUPLING IN FLOWING SEAWATER (ACCELERATION FACTOR FOR COUPLED MATERIAL UNLESS INDICATED BY SUFFIXES OF THE APPROPRIATE SYMBOL FOR THE OTHER MATERIAL)[42]

Coupled Material (M) (Materials in wrought form except cast form indicated by *)	Uncoupled Corrosion Rate, mm/year	Acceleration Factors[a] Titanium (Ti) 10:1 M	1:1 M	1:10 M
Zinc	0.05	35	4	2
SiC Aluminum	0.008	30	30	2
NS4 Aluminum	0.01	30	30	2
H30 Aluminum	0.008	30	30	2
Mild Steel	0.15	5	2	1
HY80 Steel	0.10	5	2	1
Ni-Resist (Type Aus 202 Spheroidal)*	0.05	3	2	1
Tin	0.03	2	1	1
Lead	0.01	3	1	1
Naval Brass[b]	0.04	8	4	1
Aluminum Brass	0.01	8	4	1
Aluminum Bronze (10% Al)[b]	0.02	4	2	1
Silicon Aluminum Bronze[b]	0.015	8	4	1
Nickel Aluminum Bronze[b]	0.015	2	1	1
Silicon Bronze	0.035	10	5	1
Copper	0.03	10	5	1
Phosphor Bronze (5% Sn)	0.02	10	5	1
Phosphor Bronze (10% Sn)*	0.02	8	4	1
Gun Metal LG4*	0.035	6	3	1
Hiduron 501*	0.02	6	3	1
90/10 Cupro-Nickel (1% Fe)	0.02	5	2	1
70/30 Cupro-Nickel (1% Fe)	0.02	5	1	1
CN-NS Cupro-Nickel	0.02	5	1	1
IN732 Cupro-Nickel	0.02	5	1	1
Inconel 625	<0.005	3	2	1
Monel 400[c]	0.005	15	2	1
Stainless Steel Type 316[c]	0.005	3	2	1
Ferralium 40V*[c]	0.005	3	2	1
Titanium	<0.001	1	1	1
Carbon (Acheson YAV Graphite)	--	1 Ti	1 Ti	2 Ti

(a) Results based on 100 hour tests for materials which can undergo polarity reversals.
(b) Acceleration factors subject to changes due to variable complex microstructure.
(c) These materials are subject to crevice corrosion.

compared to the anodic area, galvanic corrosion may be relatively low. However, if the cathodic area greatly exceeds the anodic area, severe corrosion of the anodic metal may result. These area-effect principles apply to efforts to control galvanic corrosion by applying protective coatings. Coatings should never be applied to the anode only. The cathodic surfaces should be coated as well or the anodic surfaces should be left bare. If only the anodic surfaces are coated, damaged areas will concentrate the galvanic current resulting in localized high corrosion rates.

Although the potential differences of the different materials are important in estimating the extent of galvanic corrosion of the anodic part of the couple, polarization characteristics of the couples play a significant role in galvanic corrosion. In galvanic corrosion, the cathodic reaction, oxygen reduction in seawater, is often the most important. Metals having high oxygen reduction overvoltages will have steeper cathodic polarization curves and cause less galvanic corrosion than metals with lower oxygen reduction overvoltages. This is illustrated by the polarization characteristics for titanium, steel, and copper-steel couples in Figure 3-9. Because of the polarization characteristics of titanium, coupling it to steel results in less galvanic corrosion of the steel than if the steel were coupled to copper, although the difference in the open-circuit potentials of steel and copper was approximately 200 mV less than that of steel and titanium. In this case, the weight loss of the steel was seven times greater when coupled to copper than when coupled to titanium.

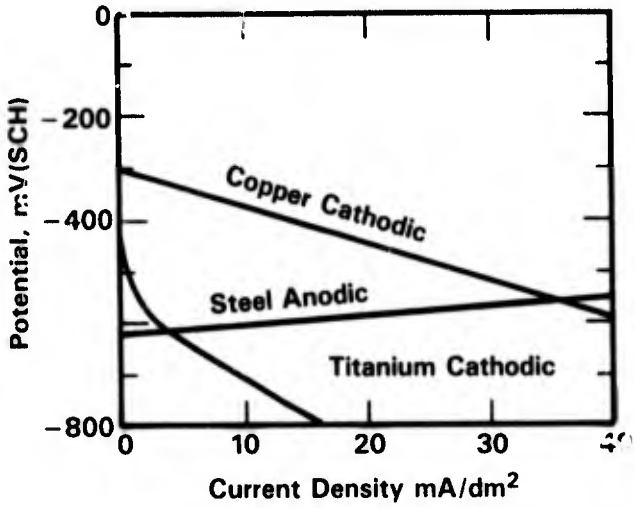

FIGURE 3-9. CATHODIC POLARIZATION OF COPPER AND TITANIUM AND THE ANODIC POLARIZATION OF STEEL IN SEAWATER[43]

Effect of Aeration and Temperature. Smith and Compton[44] studied the effect of temperature and aeration on the potential of Ti-6Al-4V in seawater, see Figure 3-10. The figure indicates somewhat surprisingly that below temperatures of 300 F the median potential of titanium in deaerated seawater is about 50 mV more positive than the median potential of titanium in aerated seawater. At high temperatures, the potentials in both aerated and deaerated water decreased, and the potential in deaerated seawater was more than 300 mV more negative than the potential in aerated seawater, as shown in Figure 3-10. Similar negative potential shifts have been observed for other materials such as various Cu-Ni alloys.[44]

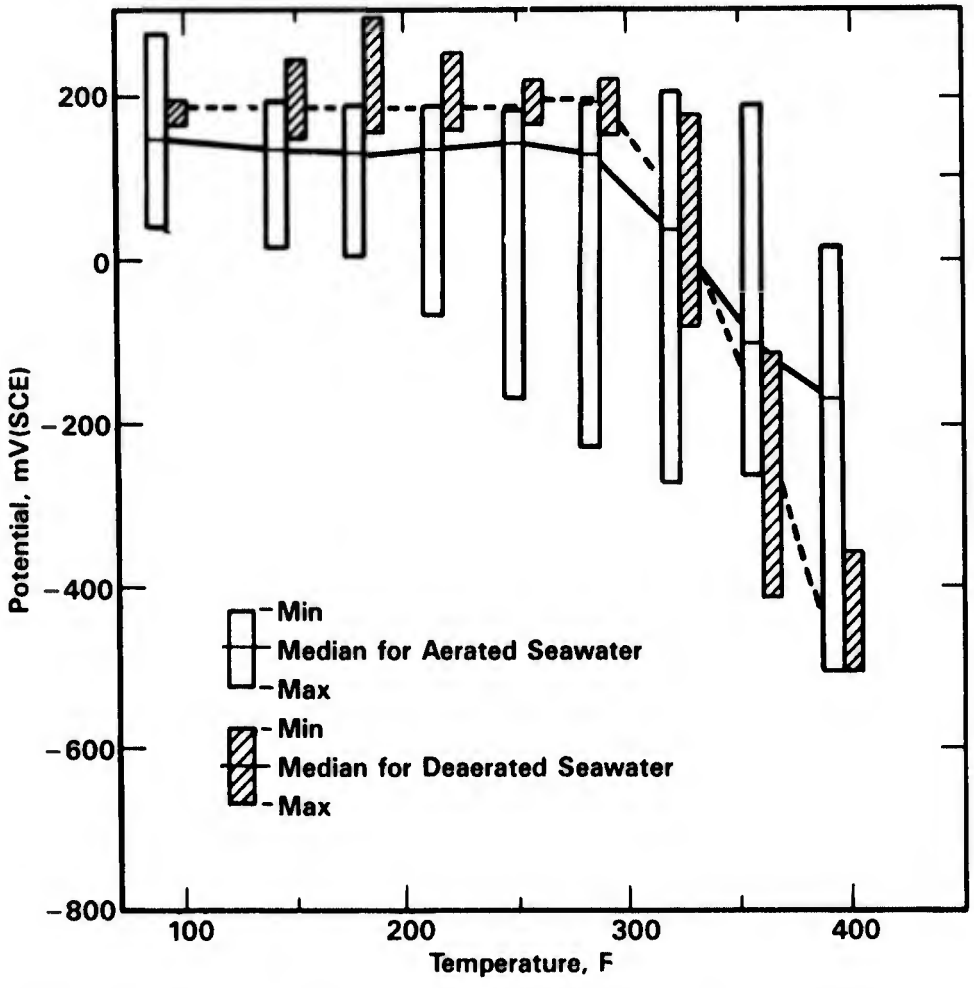

FIGURE 3-10. TEMPERATURE-GALVANIC POTENTIAL CURVE FOR Ti-6Al-4V IN AERATED AND DEAERATED SEAWATER[44]

Atmosphere. The extent to which galvanic corrosion will occur strongly depends on the conductivity and the volume of electrolyte. Galvanic corrosion will extend over a larger distance for a couple immersed in seawater than when exposed to marine atmospheric environments. Studies performed in the Panama Canal Zone exposing various couples to atmospheric, soil (burial), and seawater (immersion) environments[45] indeed showed that galvanic attack of metals coupled to titanium was the least severe in the atmospheric environment and the most severe during seawater immersion, see Table 3-11.

TABLE 3-11. CORROSION RATES CALCULATED FROM WEIGHT LOSS OF Ti-6Al-4V SPECIMENS COUPLED WITH VARIOUS METALS AND EXPOSED AT THE U.S. ARMY TROPICAL TESTING STATION, PANAMA CANAL ZONE[45]

Alloy Coupled to Ti-6Al-4V Alloy	Exposure Time, months	Corrosion Rate of Ti-6Al-4V Alloy, mm/yr
	Atmospheric Exposure[a]	
AZ31 Magnesium	2	0.063
	4	0.059
	8	0.055
	15	0.044
	24	0.045
	36	0.045
4340 Steel	2	0.072
	4	0.057
	8	0.037
	15	0.049
	24	0.047
	36	0.057
6061-T6 Aluminum	2	0.005
	4	0.002
	8	0.002
	15	0.003
	24	0.003
	36	0.002
7075-T6 Aluminum	2	0.007
	4	0.004
	8	0.003
	15	0.003
	24	0.004
	36	0.003

TABLE 3-11. (Continued)

Alloy Coupled to Ti-6Al-4V Alloy	Exposure Time, months	Corrosion Rate of Ti-6Al-4V Alloy, mm/yr
Atmospheric Exposure[a] (Continued)		
360 Brass	2	0.008
	4	0.003
	8	0.002
	15	0.001
	24	0.001
	36	0.001
Soil Burial Exposure[a]		
AZ31 Magnesium	2	1.021
	6	0.745
	12	0.562
	25	0.497
	36.7	0.329
4340 Steel	2	0.057
	6	0.091
	12	0.074
	25	0.062
	36.7	0.055
6061-T6 Aluminum	2	0.004
	6	0.008
	12	0.006
	25	0.005
	36.7	0.005
7075-T6 Aluminum	2	0.003
	6	0.018
	12	0.016
	25	0.013
	36.7	0.010
360 Brass	2	0.005
	6	0.011
	12	0.011
	25	0.007
	36.7	0.007
400 Monel	2	0
	6	0.009
	12	0.008
	25	0.005
	36.7	0.007

TABLE 3-11. (Continued)

Alloy Coupled to Ti-6Al-4V Alloy	Exposure Time, months	Corrosion Rate of Ti-6Al-4V Alloy, mm/yr
	Seawater Immersion	
AZ31 Magnesium	2	10.369
	4	9.893
	7	(b)
	12	(b)
	18	--
	28	(b)
316 Stainless Steel	2	0.088(c)
	4	0.017(c)
	7	0.028(c)
	12	0.015(c)
	18	0.265(c)
	28	0.011(c)
4340 Steel	2	1.015
	4	0.813
	7	0.725
	12	0.328
	18	0.582
	28	0.264
6061-T6 Aluminum	2	0.304
	4	0.196
	7	0.294
	12	0.153
	18	0.153
	28	0.103
7075 T-6 Aluminum	2	0.613
	4	0.306
	7	0.261
	12	0.173
	18	0.164
	28	0.099
360 Brass	2	0.179
	4	0.124
	7	0.133
	12	0.146
	18	0.111
	28	0.086

TABLE 3-11. (Continued)

Alloy Coupled to Ti-6Al-4V Alloy	Exposure Time, months	Corrosion Rate of Ti-6Al-4V Alloy, mm/yr
Seawater Immersion (Continued)		
400 Monel	2	0.010
	4	0.007
	7	0.010
	12	0.010
	18	0.025
	28	0.013

(a) Essentially zero corrosion rate for the 316 stainless steel and Ti-6Al-4V specimens.
(b) Total dissolution of magnesium presumed.
(c) Stainless steel attack - crevice pitting.

Stress-Corrosion Cracking

Early exposure test results which were based on smooth specimens indicated that titanium alloys were very resistant to stress-corrosion cracking in both seawater and marine atmosphere environments.[46] In actual field tests, titanium alloys were stressed to values equivalent to 35, 50, and 75 percent of their respective yield strength and exposed for different times at nominal depths of 2,500 and 6,000 ft in the Pacific Ocean near Port Hueneme, California.[47,48] Table 3-12 summarizes the stress-corrosion behavior of the titanium alloys. No stress-corrosion cracks were detected in most of the alloys, both in unwelded and butt welded specimens. However, the butt welded Ti-13V-11Cr-3Al alloys failed at stresses equivalent to 75 percent of the yield stress after 35, 77, and 135 days of exposure at the surface of the Pacific Ocean.

The resistance of titanium to stress-corrosion cracking was considered to be related to its resistance to pitting and crevice corrosion; these defects can create stress raisers and stimulate the formation of cracks in susceptible materials. Surface defects are often present in actual structures. Brown[46] considered this situation and first showed in 1964, the susceptibility of titanium alloys to cracking in aqueous sodium chloride solutions in the presence of a notch. Subsequently, a great amount of research has been devoted to

TABLE 3-12. STRESS-CORROSION OF TITANIUM ALLOYS EXPOSED IN THE PACIFIC OCEAN OFF PORT HUENEME, CA[3]

Alloy	Stress, ksi	Yield Strength, percent	Exposure Time, days	Depth, ft	Specimens Exposed	Specimens Failed
75A	24.5	35	403	6780	2	0
75A	24.5	35	197	2340	3	0
75A	35.0	50	403	6780	2	0
75A	35.0	50	197	2340	3	0
75A	35.0	50	402	2370	3	0
75A	52.6	75	403	6780	2	0
75A	52.6	75	197	2340	3	0
75A	52.6	75	402	2370	3	0
75A[a]	28.8	35	180	5	3	0
75A[a]	41.2	50	180	5	3	0
75A[a]	61.7	75	180	5	3	0
75A[b]	Welding stresses		181	5	4	0
Ti-0.15Pd[a]	23.8	35	180	5	3	0
Ti-0.15Pd[a]	33.9	50	180	5	3	0
Ti-0.15Pd[a]	50.8	75	180	5	3	0
Ti-0.15Pd[b]	Welding stresses		181	5	4	0
5Al-2.5Sn[a]	42.9	35	123	5640	3	0
5Al-2.5Sn[a]	42.9	35	403	6780	2	0
5Al-2.5Sn[a]	42.9	35	751	5640	3	0
5Al-2.5Sn[a]	42.9	35	197	2340	3	0
5Al-2.5Sn[a]	61.3	50	123	5640	3	0
5Al-2.5Sn[a]	61.3	50	403	6780	2	0
5Al-2.5Sn[a]	61.3	50	751	5640	3	0
5Al-2.5Sn[a]	61.3	50	197	2340	3	0
5Al-2.5Sn[a]	92.0	75	123	5640	3	0
5Al-2.5Sn[a]	92.0	75	403	6780	2	0
5Al-2.5Sn[a]	92.0	75	751	5640	3	0[c]
5Al-2.5Sn[a]	92.0	75	197	2340	3	0
5Al-2.5Sn[a]	43.3	35	180	5	3	0
5Al-2.5Sn[a]	61.8	50	180	5	3	0
5Al-2.5Sn[a]	92.7	75	180	5	3	0
5Al-2.5Sn[b]	Welding stresses		123	5640	2	0
5Al-2.5Sn[b]	Welding stresses		403	6780	2	0
5Al-2.5Sn[b]	Welding stresses		751	5640	2	0[d]
5Al-2.5Sn[b]	Welding stresses		197	2340	2	0
5Al-2.5Sn[b]	Welding stresses		402	2370	2	0
5Al-2.5Sn[b]	Welding stresses		181	5	4	0
7Al-2Cb-1Ta	110	100	102	4250	1	0
7Al-2Cb-1Ta, transverse weld	110	100	102	4250	1	0

TABLE 3-12. (Continued)

Alloy	Stress, ksi	Yield Strength, percent	Exposure Time, days	Depth, ft	Specimens Exposed	Specimens Failed
7Al-2Cb-1Ta, longitudinal weld	110	100	102	4250	1	0
7Al-2Cb-1Ta	110	100	199	4250	1	0
7Al-2Cb-1Ta, transverse weld	110	100	199	4250	1	0
7Al-2Cb-1Ta, longitudinal weld	110	100	199	4250	1	0
7Al-2Cb-1Ta[a]	34.9	35	180	5	3	0
7Al-2Cb-1Ta[a]	49.9	50	180	5	3	0
7Al-2Cb-1Ta[a]	74.9	75	180	5	3	0
7Al-2Cb-1Ta[b]	Welding stresses		181	5	4	0
6Al-4V	57.6	35	123	5640	3	0
6Al-4V[a]	48.8	35	123	5640	3	0
6Al-4V	47.6	35	403	6780	2	0
6Al-4V[a]	48.8	35	403	6780	2	0
6Al-4V	47.6	35	751	5640	3	0
6Al-4V[a]	48.8	35	751	5640	3	0
6Al-4V	47.6	35	197	2340	3	0
6Al-4V[a]	48.8	35	197	2340	3	0
6Al-4V	68.0	50	123	5640	3	0
6Al-4V[a]	69.7	50	123	5640	3	0
6Al-4V	68.0	50	403	6780	2	0
6Al-4V[a]	69.7	50	403	6780	2	0
6Al-4V	68.0	50	751	5640	3	0[e]
6Al-4V[a]	69.7	50	751	5640	3	0
6Al-4V	68.0	50	197	2340	3	0
6Al-4V[a]	69.7	50	197	2340	3	0
6Al-4V	68.0	50	402	2370	3	0
6Al-4V	102.0	75	123	5640	3	0
6Al-4V[a]	104.5	75	123	5640	3	0
6Al-4V	102.0	75	403	6780	2	0
6Al-4V[a]	104.5	75	403	6780	2	0
6Al-4V	102.0	75	751	5640	3	0[e]
6Al-4V[a]	104.5	75	751	5640	3	0[e]
6Al-4V	102.0	75	197	2340	3	0
6Al-4V[a]	104.5	75	197	2340	3	0
6Al-4V	102.0	75	402	2370	3	0
6Al-4V[a]	46.1	35	180	5	3	0
6Al-4V[a]	65.8	50	180	5	3	0
6Al-4V[a]	98.7	75	180	5	3	0
6Al-4V[b]	Welding stresses		123	5640	2	0
6Al-4V[b]	Welding stresses		403	6780	2	0
6Al-4V[b]	Welding stresses		751	5640	2	0[d]

TABLE 3-12. (Continued)

Alloy	Stress, ksi	Yield Strength, percent	Exposure Time, days	Depth, ft	Specimens Exposed	Specimens Failed
6Al-4V[b]	Welding stresses		197	2340	2	0
6Al-4V[b]	Welding stresses		402	2370	2	0
6Al-4V[b]	Welding stresses		181	5	4	0
13V-11Cr-3Al[a]	48.8	35	123	5640	3	0
13V-11Cr-3Al[a]	48.8	35	403	6780	2	0
13V-11Cr-3Al[a]	48.8	35	751	5640	3	0
13V-11Cr-3Al[a]	48.8	35	197	2340	3	0
13V-11Cr-3Al[a]	69.8	50	123	5640	3	0
13V-11Cr-3Al[a]	69.8	50	403	6780	2	0
13V-11Cr-3Al[a]	69.8	50	751	5640	3	0[d]
13V-11Cr-3Al[a]	69.8	50	197	2340	3	0
13V-11Cr-3Al[a]	104.6	75	123	5640	3	0
13V-11Cr-3Al[a]	104.6	75	403	6780	2	0
13V-11Cr-3Al[a]	104.6	75	751	5640	3	0
13V-11Cr-3Al[a]	104.6	75	197	2340	3	0
13V-11Cr-3Al[a]	44.2	35	180	5	3	0
13V-11Cr-3Al[a]	63.0	50	180	5	3	0
13V-11Cr-3Al[a]	94.5	75	180	5	3	3[f]
13V-11Cr-3Al[b]	Welding stresses		123	5640	2	0
13V-11Cr-3Al[b]	Welding stresses		403	6780	2	1[g]
13V-11Cr-3Al[b]	Welding stresses		751	5640	2	1[h]
13V-11Cr-3Al[b]	Welding stresses		197	2340	2	0
13V-11Cr-3Al[b]	Welding stresses		402	2370	2	1[g]
13V-11Cr-3Al[b]	Welding stresses		181	5	4	1[h,i]

(a) Transverse butt weld, unrelieved, across specimen at apex of bow.
(b) Circular weld 3 inches in diameter in center of specimen, unrelieved.
(c) Two specimens lost when structure was turned on its side and dragged along the bottom.
(d) One specimen lost when structure was turned on its side and dragged along the bottom.
(e) Three specimens lost when structure was turned on its side and dragged along the bottom.
(f) Specimens failed at edge of weld beads after 35, 77, and 105 days.
(g) Specimen partially embedded in bottom sediment cracked radially across the weld bead.
(h) Specimen in seawater cracked radially across the weld bead.
(i) Three specimens lost during a storm.

stress-corrosion cracking of titanium alloys in seawater and in aqueous sodium chloride solutions. Extensive research on these alloys has indicated that, in seawater and marine atmospheres, environmental factors do not play a dominant role in the susceptibility to stress-corrosion cracking. Thus, no difference has been found in cracking behavior of titanium alloys in seawater and in marine atmospheres. However, alloy composition, heat treatment and mechanical variables such as stress concentrators, stress state (plane strain or plane stress and strain rate) have a significant effect on stress-corrosion susceptibility. The effects of these variables on the stress-corrosion cracking behavior of titanium alloys is discussed below.

Effect of Alloy Composition. The composition of titanium alloys has a significant effect on the stress-corrosion cracking and hydrogen embrittlement resistance of these alloys. Titanium alloys can be grouped into three classes, based on alloy composition and microstructure, α, α + β, and β phase alloys. The α phase alloys have an hexagonal close packed (HCP) microstructure, whereas the β phase alloys have a body centered cubic (BCC) microstructure. The α alloys contain one or more of the α phase stabilizing elements, aluminum, oxygen, tin, or zirconium. So-called near α alloys such as Ti-6Al-5Zr-0.5Mo-0.2Si (IMI 685) or Ti-8Al-1V-1Mo contain a high proportion of α and little β phase stabilizer.

The stress-corrosion susceptibility of commercial α and α + β alloys in aqueous sodium chloride solutions and in seawater is summarized in Figure 3-11, and Tables 3-13 and 3-14. Figure 3-11 shows the K_{Iscc} values for various titanium alloys in aqueous sodium chloride solutions. Investigations performed on a wide spectrum of titanium alloys allowed separation of susceptible and resistant alloys, Tables 3-13 and 3-14.

In general, all α and near α alloys such as Ti-8Al-1Mo-1V, Ti-7Al-3Cb-2Sn and Ti-8Al-2Cl-1Ta are susceptible to SCC in seawater environments. The α + β Alloy Ti-6Al-4V with low oxygen concentration is considered the most resistant commercial titanium alloy for seawater service.

Aluminum, which is added to increase the strength by affecting slip,[52,53] has a significant influence on the stress-corrosion cracking behavior of titanium alloys.[47,48,54-57] It was found for binary Ti-Al alloys that a critical aluminum concentration of about 5 weight percent must be exceeded for SCC to occur in aqueous solutions. At higher aluminum concentrations, the intermediate α_2 phase (Ti_3Al) can form which both lowers the K_{Iscc} and increases the crack velocity.[58-60] Ti-Al-base alloys have been found to have K_{Iscc} values that vary from a high of more than 90 percent K_{Ic} to a low of 19 percent K_{Ic}.[60]

The effect of aluminum concentration on the commercial α + β alloys, is similar to that on the α alloys; only the α phase is susceptible to cracking. Figure 3-12, which shows the effect of aluminum concentration on the mechanical and stress-corrosion properties of a

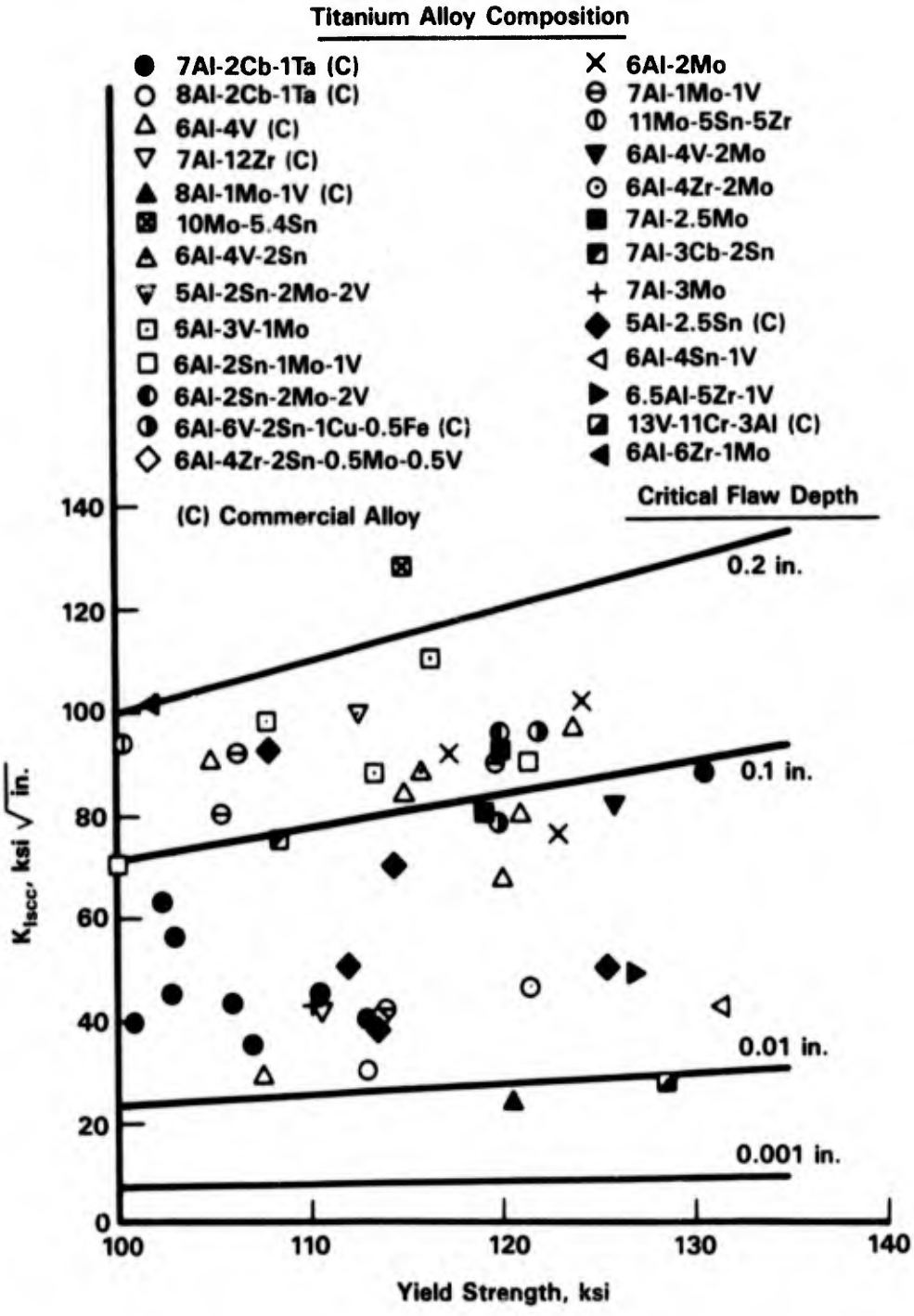

FIGURE 3-11. K_{Iscc} VALUES FOR VARIOUS TITANIUM ALLOYS IN SALT WATER. CRITICAL FLAW SIZE LINES ARE CALCULATED ASSUMING YIELD STRENGTH STRESSES AND LONG THIN SURFACE FLAWS.[49]

TABLE 3-13. TITANIUM ALLOYS WITH SCC SUSCEPTIBILITY IN SEAWATER AND AQUEOUS SODIUM CHLORIDE SOLUTIONS[50,51]

Ti with O >0.32 weight percent
Ti-8Mn
Ti-2.5Al-1Mo-11Sn-5Zr-0.2Si
Ti-3Al-11Cr-13V
Ti-4Al-4Mn
Ti-5Al-2.5Sn
Ti-6Al-2.5Sn
Ti-6Al-4V
Ti-6Al-3Cb-2Sn
Ti-6Al-4V-1Sn
Ti-6Al-4V-2Co
Ti-6Al-6V-2Sn
Ti-6Al-6V-2.5Sn
Ti-7Al-2Cb-1Ta
Ti-7Al-3Cb (as received and beta annealed)
Ti-7Al-3Mo
Ti-7Al-2Cr-1Ta
Ti-7Al-3Cb-2Sn
Ti-7Al-6V-2Sn
Ti-8Al-1Mo-1V
Ti-8Al-3Cb-2Sn
Ti-13V-11Cr-3Al

TABLE 3-14. TITANIUM ALLOYS WITH SCC RESISTANCE IN SEAWATER AND AQUEOUS SODIUM CHLORIDE SOLUTIONS[50,51]

Ti with O <0.3 weight percent
Ti-2Al-4Mo-4Zr
Ti-4Al-3Mo-1V
Ti-5Al-2Sn-2Mo-2V
Ti-6Al-2Mo
Ti-6Al-2Nb-Ta-0.8Mo
Ti-6Al-2Sn-1Mo-1V
Ti-6Al-2Sn-1Mo-3V
Ti-6.5Al-5Zr-1V
Ti-7Al-2.5Mo (as received and beta annealed + WQ + 1100 F age for 2h)
Ti-11.5Mo-6Zr-3.4Sn

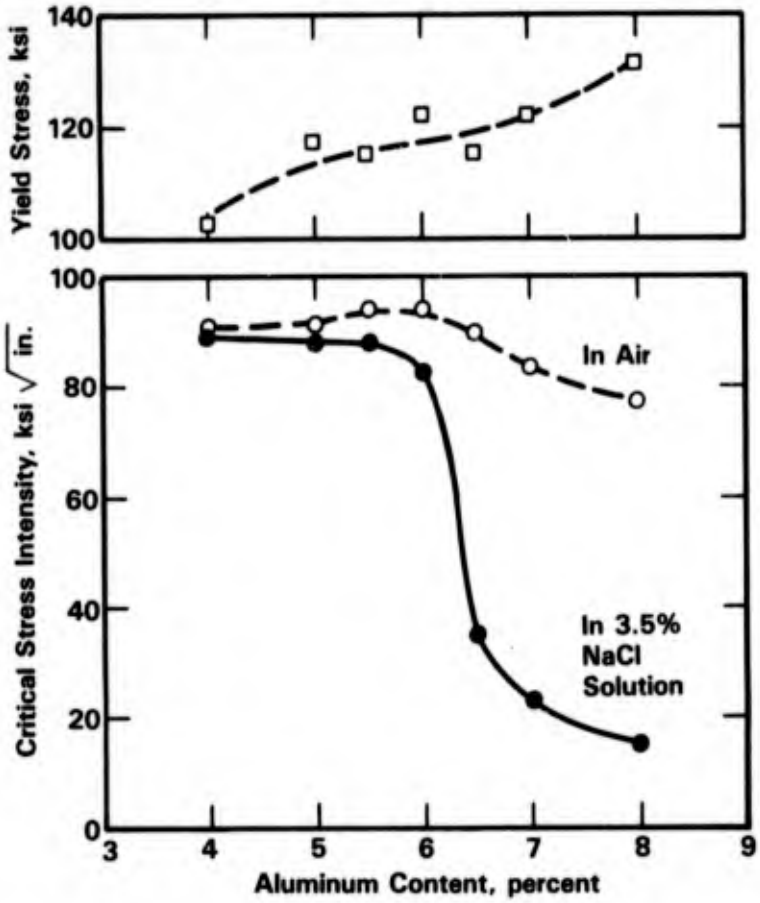

FIGURE 3-12. EFFECT OF ALUMINUM CONTENT ON THE STRENGTH, K_{Ic} AND K_{Iscc} OF A Ti-1.5Mo-5V-BASE ALLOY[48]

Ti-1.5Mo-5V-base alloy, illustrates the dramatic decrease in K_{Iscc} at aluminum concentrations between 5 and 6 weight percent.

Trace amounts of oxygen are deleterious to the stress-corrosion susceptibility of α alloys. In studies of binary Ti-O systems, it was shown that the critical oxygen concentration was in the range of 0.2 to 0.4 weight percent.[61] Similar results have been obtained on various grades of commercially pure titanium. For example, Ti-50A (0.12 weight percent O) shows a K_{Ic} and K_{Iscc} of approximately 60 ksi $\sqrt{\text{inch}}$, whereas Ti-70A (0.38 weight percent O) shows a K_{Ic} of 100 ksi $\sqrt{\text{inch}}$ and a K_{Iscc} as low as 30 ksi $\sqrt{\text{inch}}$.[62] In the case of commercial α phase alloys, the oxygen level below which SCC does not occur, decreases with increasing aluminum concentration. Systematic investigations performed by Wood, et al.[17] have shown for Ti-1.5Mo-0.5V-base alloys that material containing 4 weight percent aluminum was immune to SCC with oxygen concentrations less than 0.2 weight percent. At the same oxygen concentrations, the K_{Iscc} decreased from about 90 to 65 $MNm^{-2/3}$ at aluminum concentrations of 5 and 6 weight percent and to 20 $MNm^{-2/3}$ at aluminum concentration of 7 weight percent.

Oxygen is expected to have a deleterious effect on (α + β) alloys similar to that on α alloys. However, Sorkin, et al.[63] found for Ti-6Al-4V that oxygen concentrations ranging from 0.06 to 0.12 weight percent had no significant effect on the susceptibility to SCC in seawater while a decrease in fracture toughness with oxygen content was observed. At higher oxygen concentration, 0.18 weight percent,[61] 0.15 and 0.3 weight percent,[64] Ti-6Al-4V was found to be susceptible to SCC in aqueous salt solutions. Gastelow and Weaver[65] concluded that oxygen levels approaching 0.1 weight percent are damaging for many α + β alloys. This number is significant since an oxygen concentration of 0.15 weight percent is typical for U.S. and UK commercial alloys. U.S. materials used for deep submerged vessels specify a maximum oxygen content below 0.1 weight percent.

The effect of β phase stabilizers on the susceptibility to seawater SCC is not clear. Several investigators have shown that isomorphous β stabilizers such as molybdenum, vanadium, and niobium have a beneficial effect on the SCC resistance of titanium alloys.[55,57,62,66] However, studies by Boyd, et al.[47,48] have indicated that, in alloys with 7 and 8 weight percent aluminum, addition of a β stabilizer could be detrimental; whereas, in alloys with 6 weight percent aluminum, additions of the β stabilizer vanadium at concentrations greater than 2 weight percent could be beneficial. In titanium alloys containing large amounts of the β stabilizer manganese, cleavage of the β phase has been observed.[56,67] Further, α + β alloys containing silicon were also found to be susceptible to SCC.[63,68,69] These authors have suggested that addition of silicon, added to improve the creep strength, promotes the formation of Ti_3Si which effectively embrittles the β-phase.

Hydrogen has been found to have a considerable effect on the fracture behavior of a number of titanium alloys.[70-74] Most work has been concentrated on Ti-8Al-1V-1Mo and Ti-6Al-4V. In Ti-8Al-1Mo-1V, lowering the hydrogen content to below 5 g/m^3 (ppm) rendered the (α + β) equiaxed microstructure immune to SCC.[70] Howe and Good[71] showed that maintaining hydrogen levels at below 30 ppm raised the resistance to SCC in both β annealed and α + β alloys. Similar results were reported for Ti-6Al-4V.[71,73]

Effect of Heat Treatment. Heat treatment of α and (α + β) alloys has a marked effect on the stress-corrosion cracking behavior of these alloys in seawater. In α-phase alloys, the effect of heat treatment is to alter the morphology of the α-phase. Alpha annealing in the α-phase field produces an equiaxed grain structure irrespective of cooling rate. Heating α-phase alloys in the β-region reduces stress-corrosion cracking resistance by allowing grain growth to occur.[62,68] As discussed previously, low temperature aging of alloys with aluminum contents of 5 percent and above will lead to the formation of α_2 phase ($TiAl_3$) which results in an increase in stress-corrosion cracking susceptibility. Extended aging in the α + α_2 phase field

has been shown to produce a partial recovery of the resistance[54] which indicates an apparent dependency of SCC or the particle size of the α_2 precipitates.

The most common heat treatments for commercial (α + β) alloys are mill and duplex annealing.[75] Mill annealing for these alloys consists of (a) forming to size, (b) heating to a temperature below the (α + β) to β transus line for approximately 4 hours, and (c) furnace cooling to room temperature. A schematic drawing of this heat treatment is shown in Figure 3-13. Mill annealing generally produces a fine-grained equiaxed α + β microstructure. The furnace cooling causes the precipitation of α_2 in the α phase depending on the concentration of Al or Sn in the alloy.

Duplex annealing of (α + β) alloys consists of (a) forming to size, (b) heating to a temperature below the (α + β) -β transus line, (c) furnace cooling to room temperature, (d) heating to a lower temperature below the β transus, and (e) air cooling to room temperature, see schematic in Figure 3-14. Another common heat treatment for (α + β) alloys, β solution treating and aging, is shown in Figure 3-15. Beta solution treated and aged (β-STA) alloys are (a) formed to size at temperatures above the β transus, (b) water quenched, (c) heated to a temperature below the β transus (540 C or 675 C) for 4 hours, and (d) air cooled to room temperature. The microstructure resulting from this heat treatment is a coarse Widmanstätten (α + β)-phase structure. A variation to this heat treatment includes mechanical working.

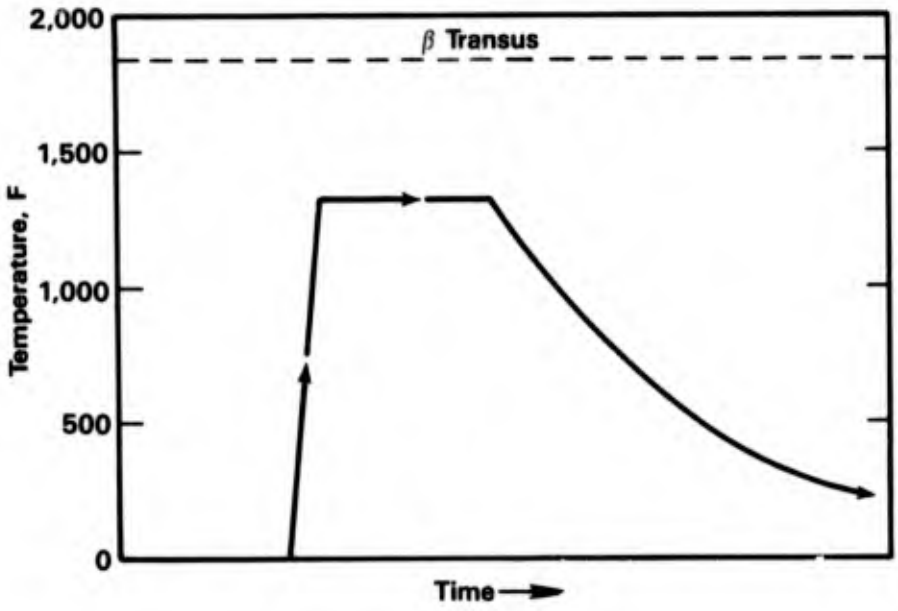

FIGURE 3-13. SCHEMATIC REPRESENTATION OF A MILL ANNEAL TREATMENT FOR Ti-6Al-4V[75]

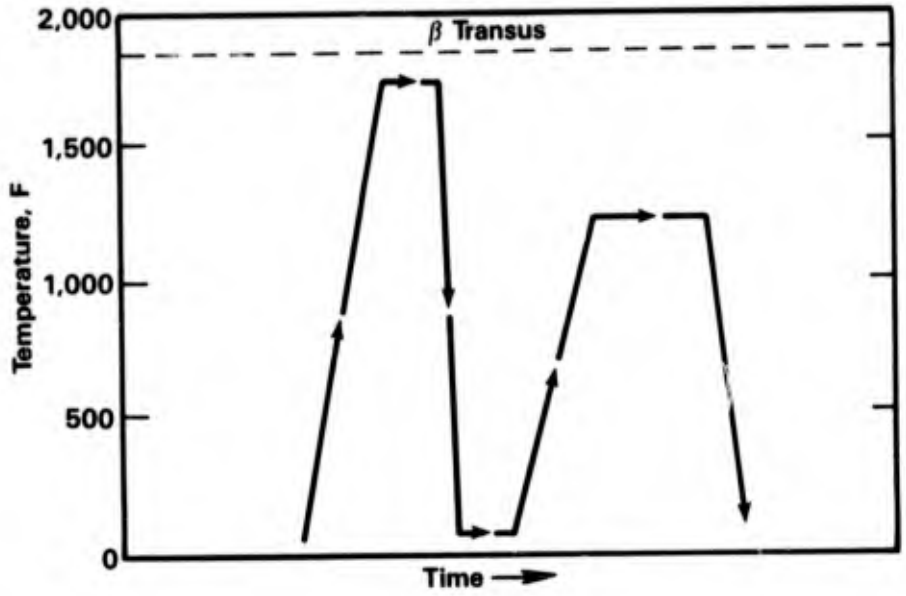

FIGURE 3-14. SCHEMATIC REPRESENTATION OF A DUPLEX ANNEAL TREATMENT FOR Ti-6Al-4V[75]

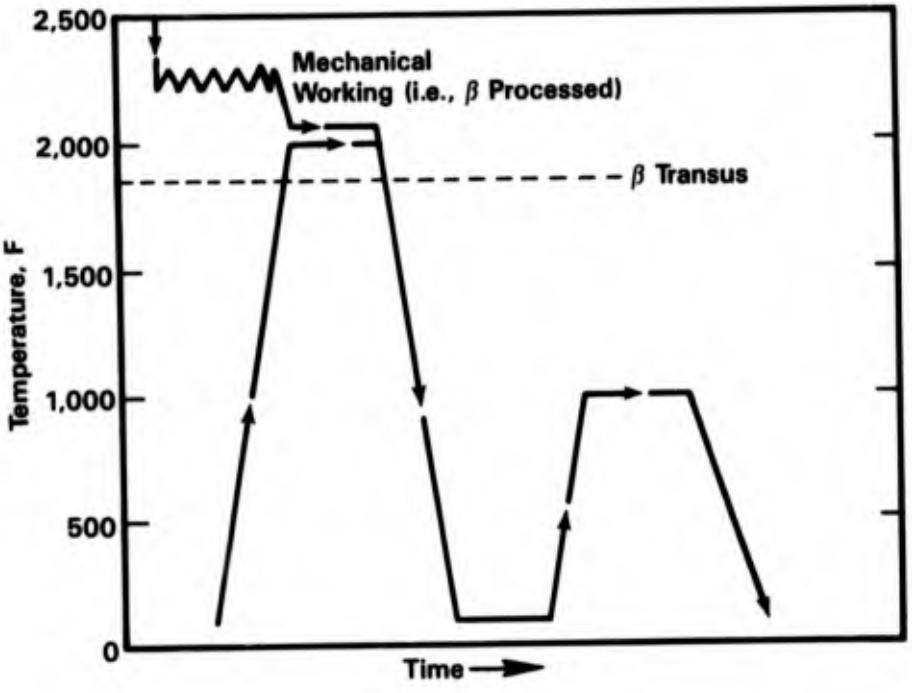

FIGURE 3-15. SCHEMATIC REPRESENTATION OF A βSTA HEAT TREATMENT FOR Ti-6Al-4V. NOTE THAT THE β-PROCESSING PROCEDURE IS ALSO INDICATED.[75]

In susceptible ($\alpha + \beta$) alloys such as Ti-8Al-1Mo-1V and Ti-7Al-2Mo-1V it has been observed that equiaxed microstructures are very sensitive to stress-corrosion cracking[47,62,76,77] whereas materials heated in the β phase field and rapidly quenched are immune. After aging in the $\alpha + \alpha_2$ phase field many of the advantages of the β solution heat treated and quenched material are lost. On the other hand, stress-corrosion resistant alloys such as Ti-4Al-3Mo-1V are not greatly affected by heat treatment. Processing at or just below the β transus to maximize strength with minimal grain growth produces the most desirable microstructure.[47,48] A summary of the effect of various heat treatments on the stress-corrosion cracking susceptibility of the ($\alpha + \beta$) Alloy Ti-6Al-4V in 3.5 percent NaCl is presented in Figure 3-16.

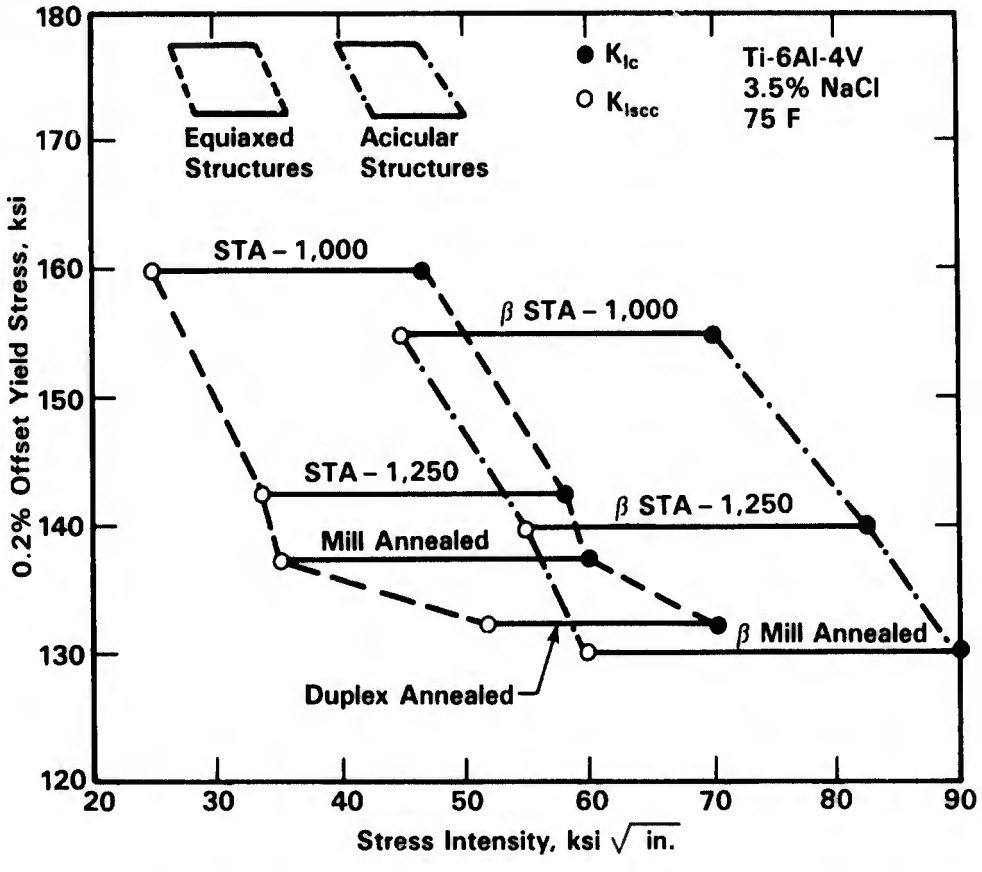

FIGURE 3-16. RELATIONSHIP BETWEEN YIELD STRESS, FRACTURE TOUGHNESS K_{Ic}, AND STRESS-CORROSION THRESHOLD K_{Iscc} FOR SEVERAL PHASE STRUCTURES AND MORPHOLOGIES IN Ti-6Al-4V TESTED IN 3.5 PERCENT NaCl[78]

Beta and (α + β) alloys may either be solution treated (β-ST) or solution treated and aged (β-STA). At the low aging temperatures the microstructure consists of fine Widmanstätten plates of α phase in a β phase matrix. The effect of β-phase on stress-corrosion susceptibility of titanium alloys in β-STA heat treatment condition in a 3.5 percent NaCl aqueous solution is shown in Figure 3-17. Metastable β-phase alloys are solution treated above the β transus and then either water cooled or water quenched. The ω phase, a finely dispersed intermetallic phase[79] might form on cooling from the aging temperature and cause embrittlement. The effect of heat treatment and time on the crack initiation load of the metastable Alloy Ti-8Mn in 0.6M KCl solution is shown in Figure 3-18.

Mechanical Variables. Titanium alloys that are susceptible to stress-corrosion cracking can be divided into two general groups.

- Those which experience stress-corrosion cracking without a stress concentration. These are mostly β alloys such as Ti-13V-11Cr-3Al and Ti-8Mn and very susceptible α and (α + β) alloys such as Ti-8Al-1Mo-1V.
- Those which will only experience stress-corrosion cracking in the presence of stress concentration such as a notch or a precrack.

An example of the effect of notch radius on the stress-corrosion cracking of Ti-7Al-2Cb-1Ta alloy (Ti-721) in seawater is shown in Figure 3-19. The diagram shows a dramatic decrease in fracture stress at very small notch radii.

Stress-corrosion cracking susceptibility was further shown to be dependent on specimen thickness.[55,68] Transition from resistance to susceptibility to stress-corrosion cracking is displayed by Ti-6Al-4V and Ti-8Al-1Mo-1V alloys with increasing thickness, see Figure 3-20. The increase in susceptibility to stress-corrosion cracking with increasing thickness can be attributed to plane strain conditions that develop as the result of increasing thickness. The transition from plane stress to plane strain may be affected by preferred orientation, straining rate and heat treatment.

As discussed above, titanium alloys fail in seawater transgranularly by a cleavage-like process, which suggests that stress-corrosion cracking susceptibility will depend on the orientation of the fracture plane with respect to the tensile stress. Such a preferred orientation effect is most pronounced in α and (α + β) alloys for which the cleavage plane is $(10\bar{1}7)$ which is about 15 degrees from the basal plane.[81-83] In β alloys, the cleavage plane is (100), and thus the anisotropy of properties is less pronounced. The influence of specimen orientation on the SCC susceptibility of Ti-8Al-1Mo-1V in a 3.5 percent NaCl aqueous solution is shown in Figure 3-21. The diagram shows that configurations where the cracking plane is parallel to the basal plane, exhibit the highest susceptibility, i.e., transverse direction.

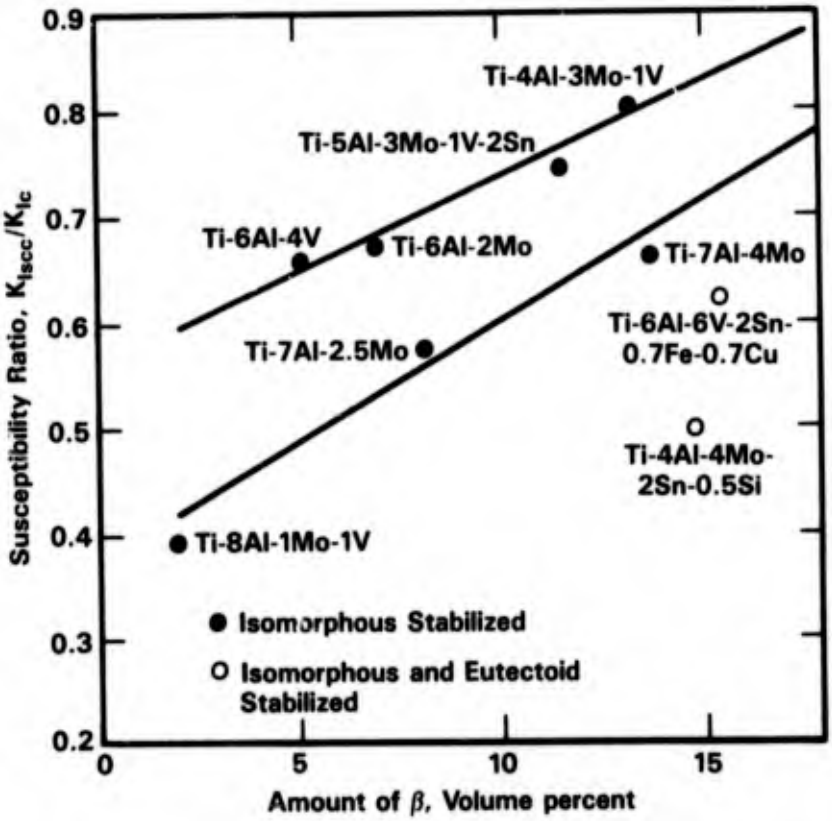

FIGURE 3-17. EFFECT OF β-PHASE ON STRESS-CORROSION SUSCEPTIBILITY OF TITANIUM ALLOYS IN A βSTA HEAT TREATMENT CONDITION(62)

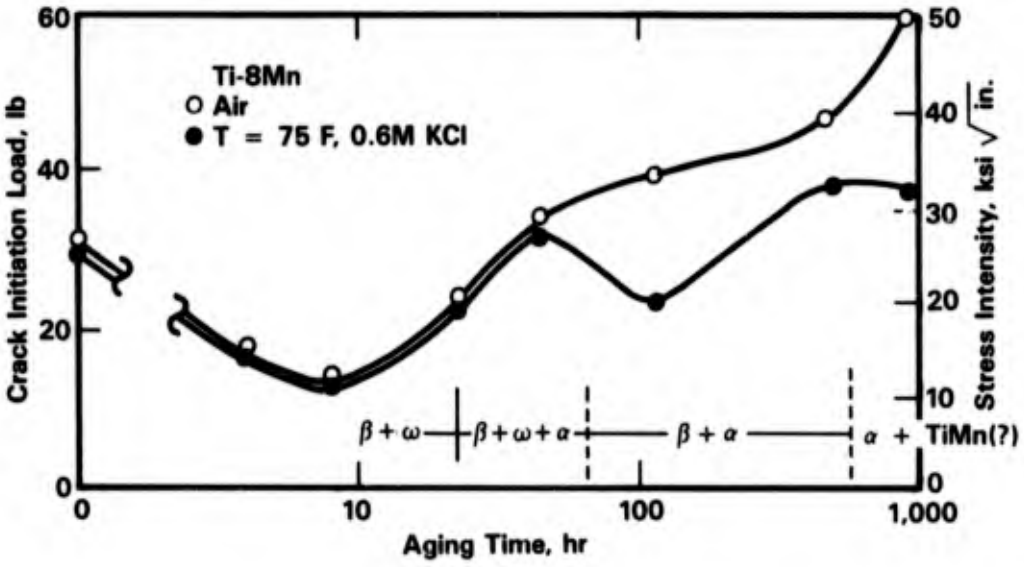

FIGURE 3-18. VARIATION OF CRACK-INITIATION LOAD FOR SPECIMENS OF Ti-8Mn QUENCHED FROM 1650 F AND AGED AT 750 F, TESTED IN AIR AND 0.6M KCl AT -500 mV. THE PHASE STRUCTURE OF THE ALLOY IS ALSO INDICATED(80)

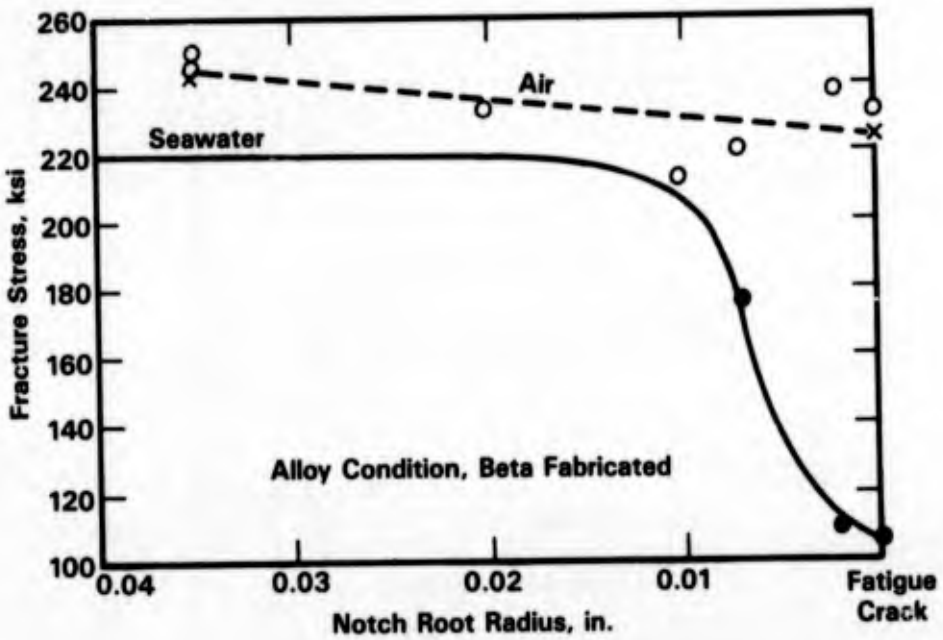

FIGURE 3-19. EFFECT OF NOTCH ACUITY ON NOMINAL BREAKING STRESS OF Ti-7Al-2Cb-1Ta[55]

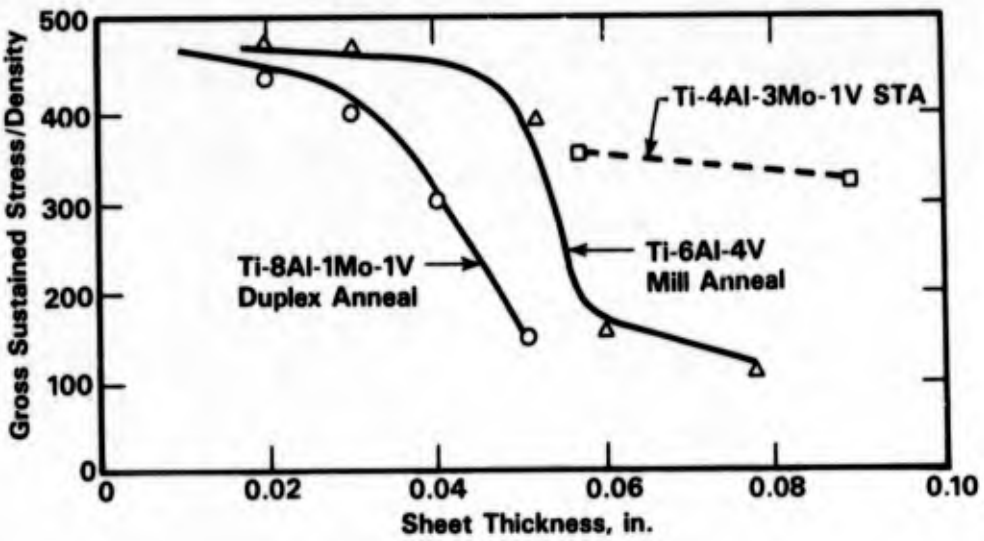

FIGURE 3-20. EFFECT OF SHEET THICKNESS ON STRESS-CORROSION SUSCEPTIBILITY IN SEAWATER[68]

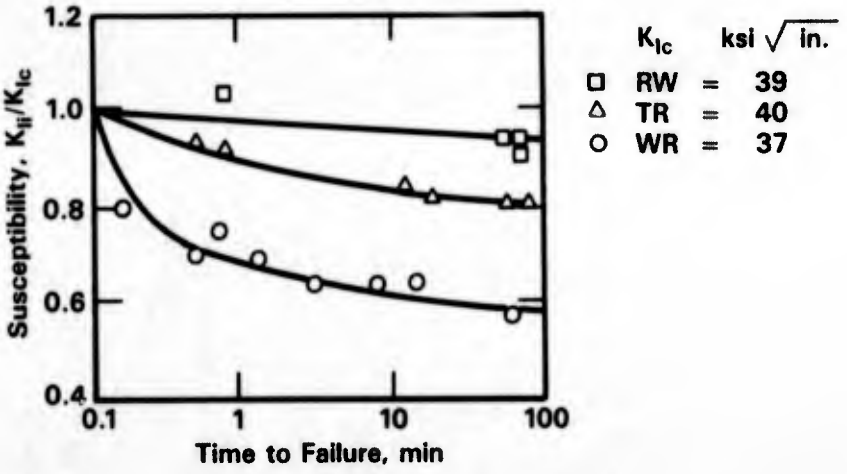

a. Stress Corrosion Susceptibility

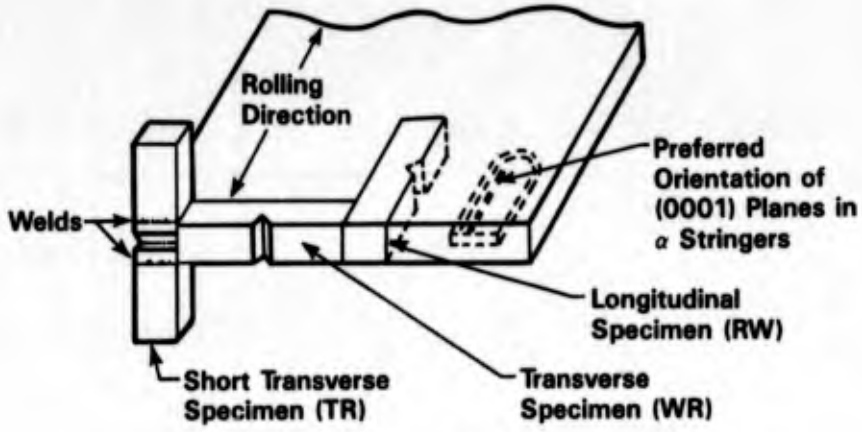

b. Specimen Orientation

FIGURE 3-21. STRESS-CORROSION SUSCEPTIBILITY AS A FUNCTION OF SPECIMEN ORIENTATION IN Ti-8Al-01Mo-1V 0.5-INCH ANNEALED PLATE (THREE-POINT-LOADED NOTCHED BEND SPECIMENS) EXPOSED TO A 3.5 PERCENT NaCl AQUEOUS SOLUTION[81]

Strain Rate Effect. Loading procedures have a considerable effect on stress-corrosion cracking behavior of titanium alloys. For example, it was shown[84] that the K_{Iscc} of Ti-6Al-4V could be increased by 30 percent by decreasing the rate of loading. Powell and Scully[85] showed that smooth specimens of Ti-5Al-2.5Sn tested in a 3 percent NaCl aqueous solution exhibited susceptibility to SCC in a narrow range of strain rates, Figure 3-22. A similar effect was observed by Beck, et al.[86] on precracked specimens of Ti-13V-11Cr-3Al tested in 0.6M KCl at -500 mV(SCE), see Figure 3-23. Further, the effect of loading rate was found to be strongly dependent upon alloy composition.[86]

Effect of Potential. The effect of potential is important since titanium alloys are often coupled to other metals when incorporated into a structure. Figure 3-24 shows fracture load of duplex annealed Ti-8Al-1Mo-1V in different halide solutions as a function of applied potential.[87] The minimum load at which fracture initiates in aqueous KCl solutions is around -500 mV(SCE), which is more noble than the free-corrosion potential of titanium alloys in 3.5 percent aqueous NaCl and seawater which is about -800 mV(SCE).

There is also a strong effect of potential on stress-corrosion crack velocities. Beck[87,88] showed an approximately linear relationship between potential and crack velocity which appears to be independent of the particular halide ion, see Figure 3-25.

Effect of Depth and Aeration. Reinhart and Jenkins have performed extensive studies of the corrosion of structural materials in deep ocean environments.[2,21] Included in this study were titanium alloys. The studies were performed at sites in the Pacific Ocean near Port Hueneme, CA, at depths of 6,000 ft, 2,500 ft, and near the surface. The environment at this site was characterized and the oxygen concentration solubility and pH were found as described in Figure 1-4 in the Introduction, Chapter 1. The stress-corrosion cracking results are given in Table 3-12. The specimens of the alloys were stressed to values equivalent to 35, 50, and 75 percent of their respective yield strength for different periods of time. With one exception, there were no stress-corrosion cracking failures of any of the alloys, both unwelded and welded. The unrelieved butt welded Ti-13V-11Cr-3Al alloy failed by stress-corrosion cracking when stressed at values equivalent to 75 percent of its yield strength after 35, 77, and 105 days of exposure at the surface at various depths, and in the bottom sediment of the Pacific Ocean. Apparently, this alloy is susceptible to SCC, and the depth or aeration does not appear to have a significant effect on stress-corrosion cracking. These results are confirmed by exposure tests in the Atlantic Ocean, near the Bahama Islands.[92] The difference in bottom conditions at the two exposure sites is given in Table 3-15.

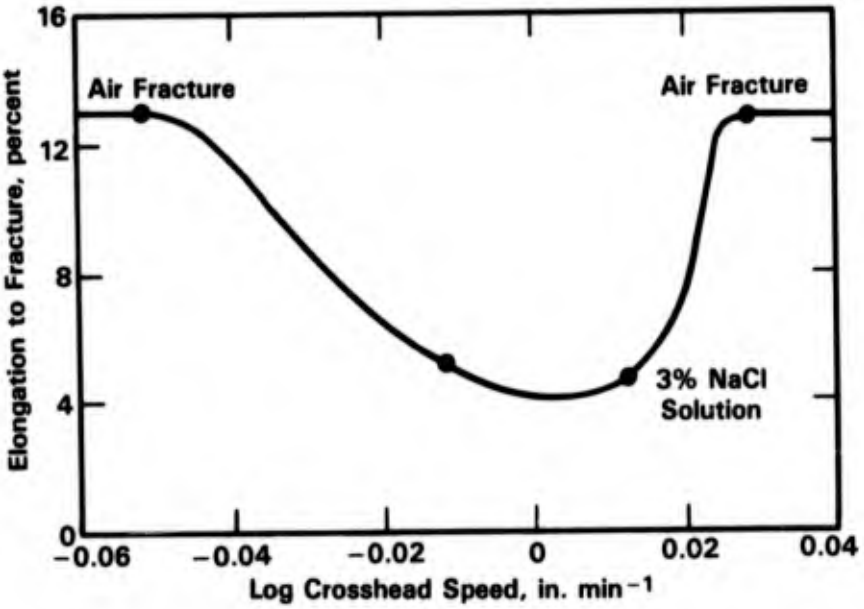

FIGURE 3-22. THE ELONGATION TO FRACTURE OF Ti-5Al-2.5Sn TENSILE SPECIMENS WITH A GAUGE LENGTH OF 1.18 INCHES IN 3 PERCENT AQUEOUS NaCl AS A FUNCTION OF INSTRON CROSSHEAD SPEED(85)

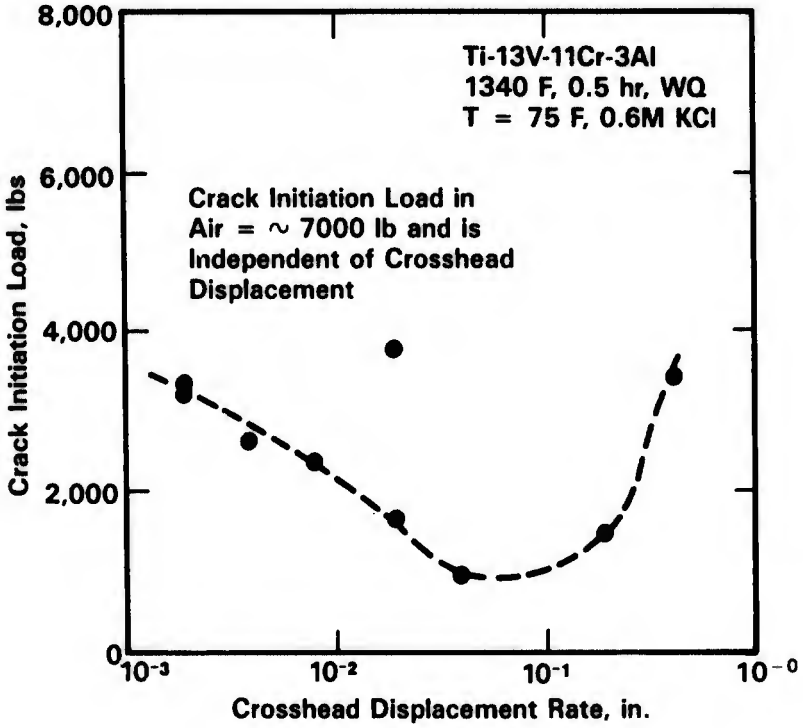

FIGURE 3-23. VARIATION OF CRACK INITIATION LOAD WITH CROSSHEAD DISPLACEMENT RATE IN Ti-13V-11Cr-3Al TESTED IN 0.6M KCl AT -500 mV(86)

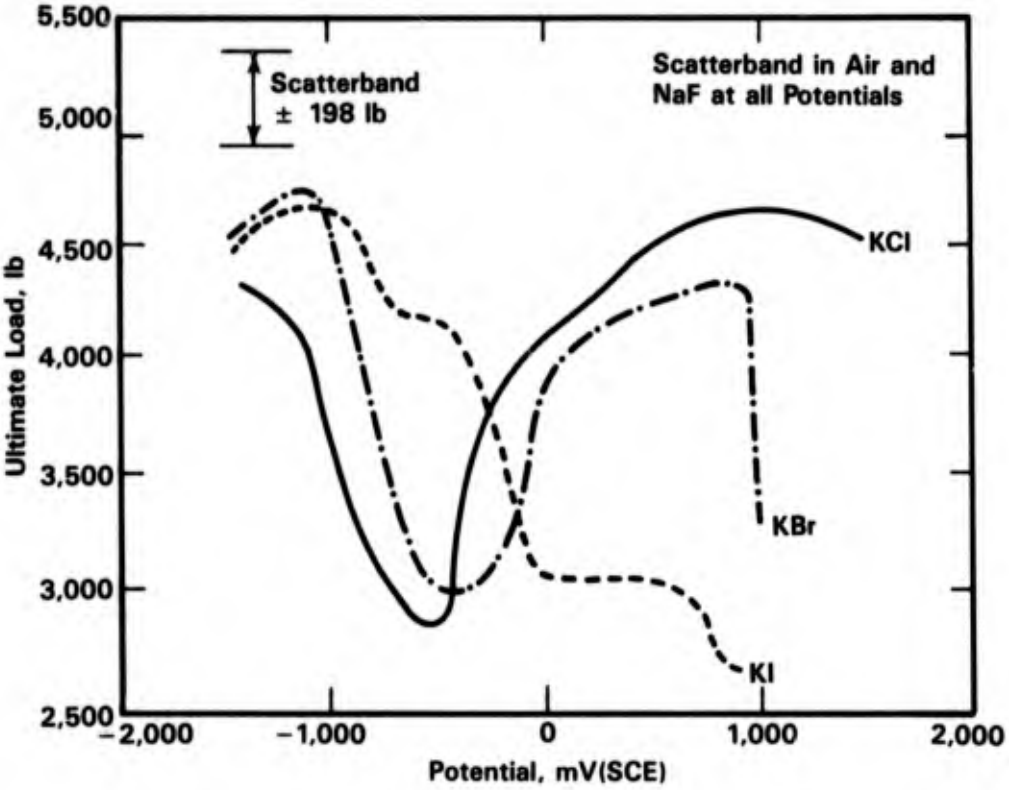

FIGURE 3-24. ULTIMATE FRACTURE LOAD OF 0.050-INCH-THICK DUPLEX ANNEALED Ti: 8-1-1 SPECIMENS IN 0.6M HALIDE SOLUTIONS UNDER POTENTIOSTATIC CONDITIONS[87]

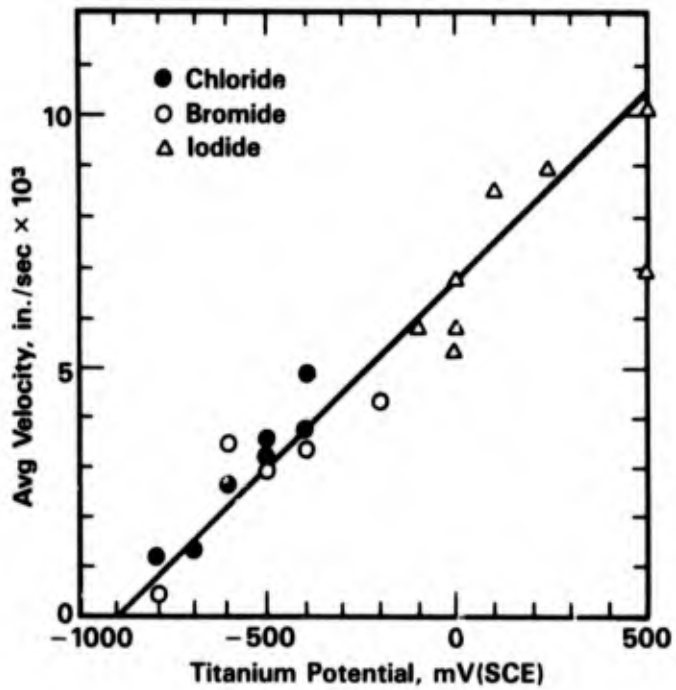

FIGURE 3-25. RELATION OF SCC VELOCITY TO POTENTIAL; Ti: 8-1-1 IN 0.6M NEUTRAL HALIDE SOLUTIONS[87]

TABLE 3-15. BOTTOM CONDITIONS - PACIFIC, ATLANTIC OCEANS[92]

	Atlantic	Pacific
Location	23 deg 52.12 min N 76 deg 46.60 min W	33 deg 51 min N 120 deg 35 min W
Depth	4,050	5,900
Temperature, C	4.56	2.3
Oxygen, ml/l	5.70	1.6
Salinity, ppt	34.98	34.6
Current, knots	0.5	0.03
pH	--	7.4

Effect of Temperature and pH. Although no field data are available on the effect of temperature on stress-corrosion cracking, some data have been generated in simulated seawater solutions. The critical stress intensity for crack initiation (K_{Iscc}) in Ti-8Al-1Mo-1V in a 3.5 percent NaCl aqueous solution does not vary with temperature.[93] However, crack velocity was found to be strongly temperature dependent, see Figure 3-26. The activation energies related to Stage II of the crack propagation are in a range of 13 to 21 KJ/mole.[93-95] It was further found[96] that, in the range of 0 to 85 C, the variation of the crack velocity of Ti-6Al-4V with temperature is not a single activated process, see Figure 3-27. In the crack velocity versus temperature curve, discontinuities were observed which were attributed to titanium hydride precipitation.

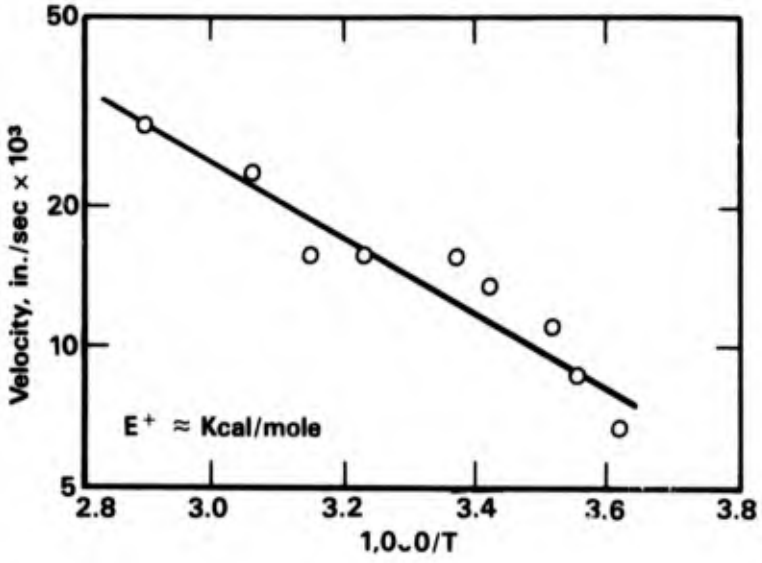

FIGURE 3-26. RELATION OF SCC VELOCITY TO TEMPERATURE; Ti: 8-1-1 IN 0.6M KCl AT -500 mV[95]

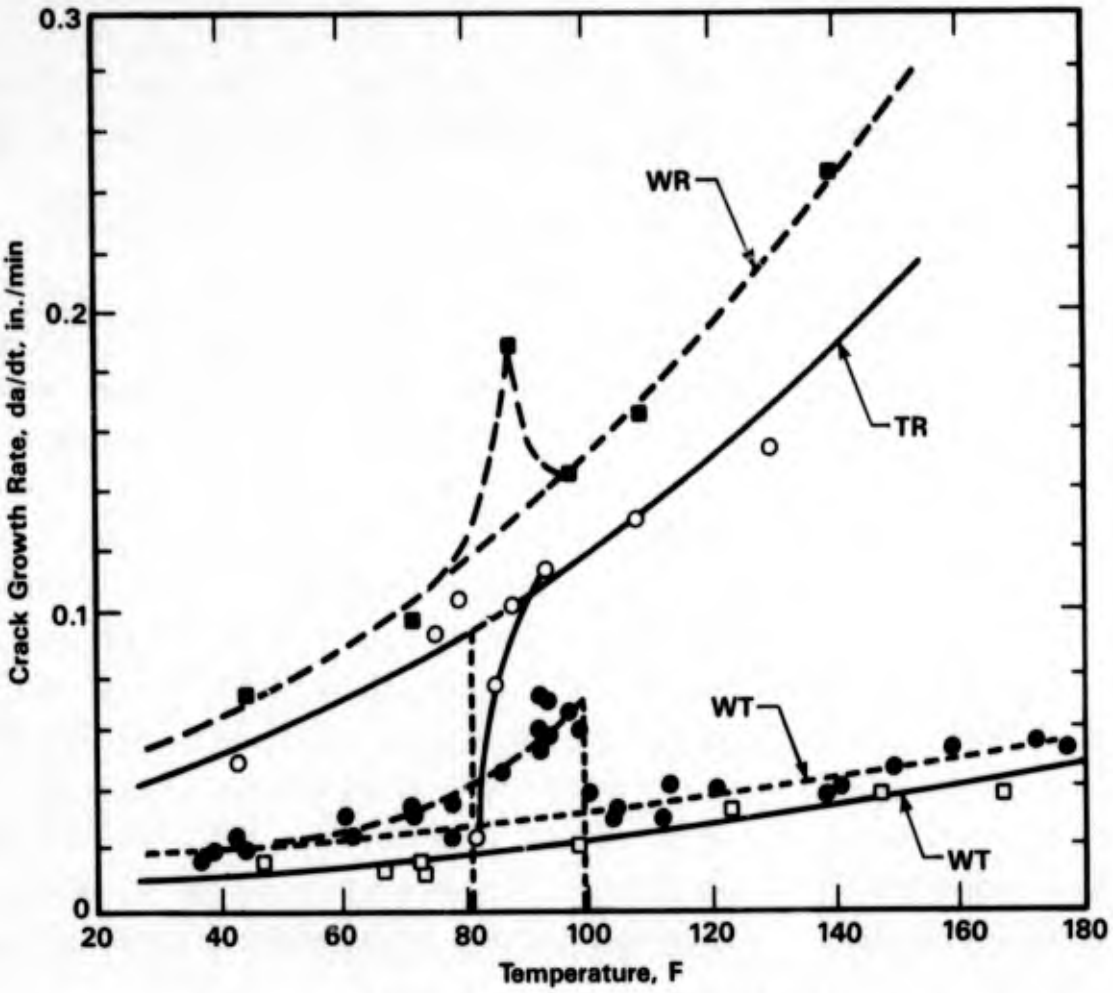

a. Crack Orientation Effects on Ti-6Al-4V

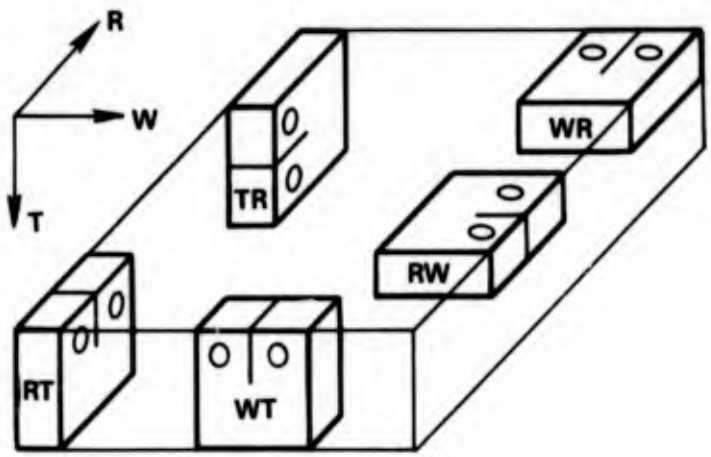

b. Crack Orientations of Tested Specimens

FIGURE 3-27. EFFECT OF CRACK ORIENTATION ON CRACK GROWTH RATE OF Ti-6Al-4V IN A 3 PERCENT AQUEOUS NaCl SOLUTION VERSUS TEMPERATURE[96]

Little work has been done to study the effect of pH on the stress-corrosion cracking of titanium alloys.[56,97] Figure 3-28 from work by Litoin and Hill[97] shows a distinct effect of pH on the fracture stress of Ti-7Al-2Cb-1Ta.

Hot Salt Stress Cracking

Hot salt stress-corrosion cracking of titanium alloys is of importance because of titanium's use for high temperature applications in jet aircraft. Although various laboratory investigations[98-101] have demonstrated that cracking can occur in titanium alloys stressed in contact with certain salts at elevated temperature, no service failures due to hot salt stress-corrosion cracking have been reported to date. Despite experimental difficulties, conditions have been identified under which cracking will occur readily.[101] Chloride salts, in particular NaCl, are correlated with the most severe attack of titanium alloys.[102,103] Further, most work has concluded that water is essential for cracking to occur.[104-106] However, some results indicate that water accelerated cracking but it is not essential[102] and also there is some evidence that water can actually retard cracking.[105] Further, an increase in stress and temperature will increase hot salt cracking, see Figure 3-29. Finally, unalloyed titanium is not susceptible to hot salt stress cracking, but all alloys exhibit some degree of susceptibility.[107]

The highly susceptible alloys are Ti-5Al-2.5Sn, Ti-7Al-12Zn, Ti-5Al-5Sn-5Zn, Ti-8Al-1Mo-1V and Ti-8Mn. The intermediately susceptible alloys are Ti-5Al-5Sn-5Zr-1Mo-1V, Ti-6Al-4V, Ti-6Al-6V-2Sn, Ti-5Al-2.75Cr-1.25Fe, and Ti-3Al-13V-11Cr. The most resistant alloys are Ti-4Al-3Mo-1V, Ti-2. 25Al-1Mo-11Sn-5Zr-0.25Si, and Ti-2Al-4Mo-4Zr. Also some of the β-phase alloys such as Ti-11.5Mo-6Zr-4.5Sn and Ti-8Mo-8V-3M-2Fe were found to relatively resistant to hot salt cracking.[100]

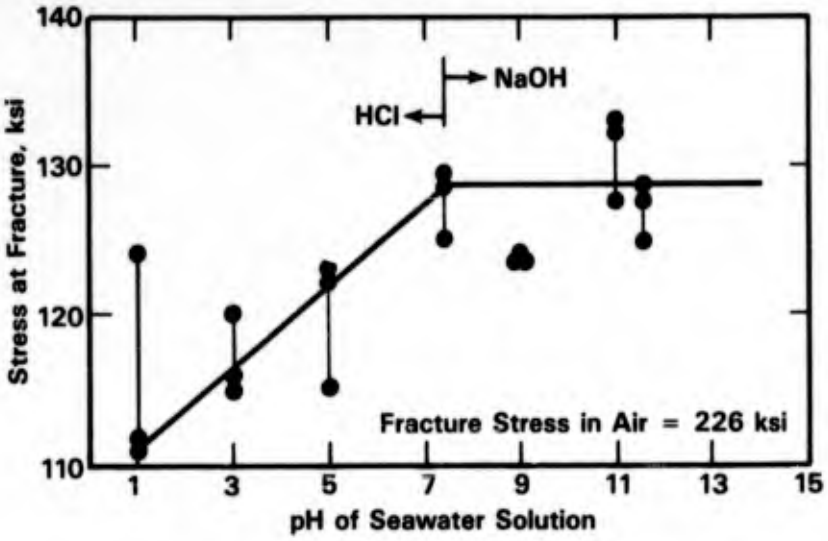

FIGURE 3-28. FRACTURE STRESS VERSUS pH FOR Ti-7Al-2Cb-1Ta IN SEAWATER. THE pH OF THE SEAWATER WAS ADJUSTED WITH HCl AND NaOH[97]

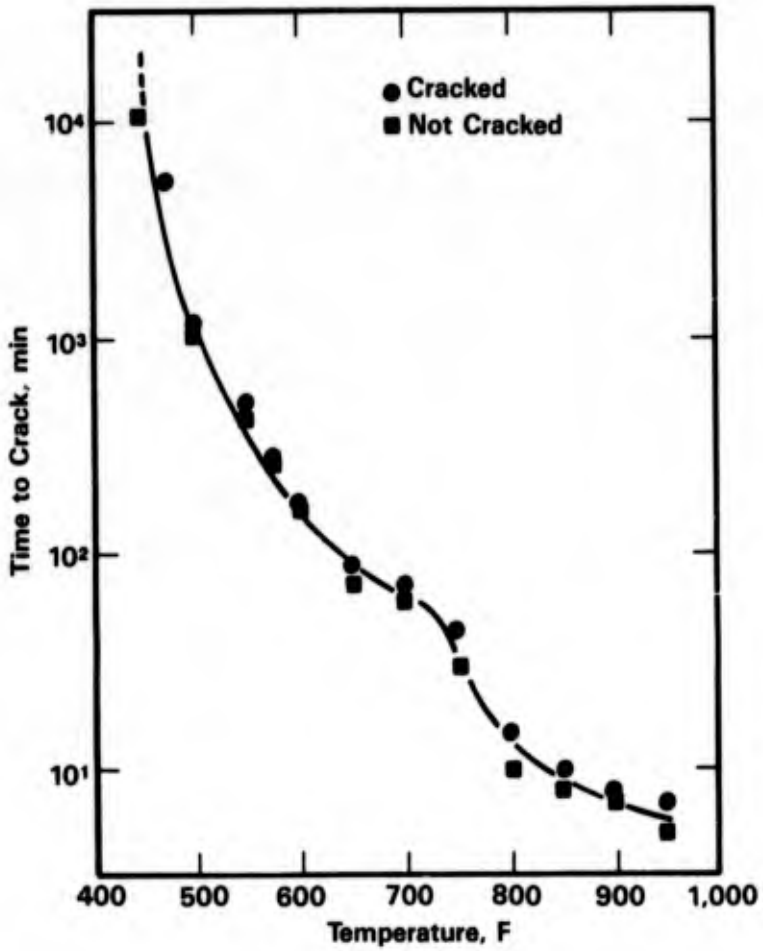

FIGURE 3-29. TIME TO INITIATE CRACKING BY NaCl IN Ti-8Al-1Mo-1V VERSUS TEMPERATURE[106]

REFERENCES FOR CHAPTER 3

1. Boyd, W. K. and Fink, F. W., "Corrosion of Metals in Marine Environments", Battelle Columbus Laboratories Report MCIC-78-37, 103 pp (March, 1978).

2. Reinhart, F. M., "Corrosion of Materials in Hydrospace", U.S. Naval Civil Engineering Laboratory (R-504), 118 pp (December, 1966).

3. Reinhart, F. M., "Corrosion of Materials in Hydrospace. III: Titanium and Titanium Alloys", U.S. Naval Civil Engineering Laboratory Report NCEL-TN-921, 30 pp (September, 1967).

4. Reinhart, F. M. and Jenkins, J. F., "Corrosion of Alloys in Hydrospace - 189 Days at 5,900 Feet", Final Report NCEL-TN-1224, 41 pp (April, 1972).

5. Reinhart, F. M. and Jenkins, J. F., "The Relationship Between the Concentration of Oxygen in Seawater and the Corrosion of Metals", U.S. Naval Civil Engineering Laboratory, pp 562-577 (1971).

6. Franson, I. A. and Covington, L. C., "Titanium and the OTEC Environment", Ocean Thermal Energy Conversion (OTEC) Symposium, pp 293-304 (October, 1977).

7. Bomberger, H. B., et al., "Corrosion Properties of Titanium in Marine Environments", Journal of the Electrochemical Society, 101 (9), pp 442-447 (September, 1954).

8. Cotton, J. B. and Downing, B. P., "Corrosion Resistance of Titanium to Seawater", Transactions of the Institute of Marine Engineers, 69, p 311 (1957).

9. Wheatfall, W. L., "Metal Corrosion in Deep-Ocean Environments", U.S. Navy Marine Engineering Laboratory, R&D Phase Report 4291166 (1967).

10. Feige, N. G. and Murphy, T. J., "Environmental Effects on Titanium Alloys", Corrosion, 22 (11), pp 320-324 (1966).

11. Fink, F. W., et al., "Investigation of Corrosion in Hot Seawater in an Experimental Loop Apparatus", Battelle Memorial Institute, U.S. Department of the Interior, OSW-PR-225 (December, 1966).

12. Griess, J. C., Jr., "Crevice Corrosion of Titanium in Aqueous Salt Solutions", Corrosion, 24 (4), pp 96-109 (April, 1968).

13. Pelensky, M. A., et al., "Air, Soil, and Sea Galvanic Corrosion Investigation at Panama Canal Zone", ASTM STP 576, p 94 (1973).

14. Shimose, T. and Takamura, A., Journal of Japan Institute of Metals, 29 (4), pp 416-421 (1965).

15. Feige, N. G. and Kane, R. L., Paper presented at the ASM Section of the National Metal Congress, Chicago, IL (October 31 - November 3, 1966).

16. Kobayashi, M., et al., "Study on Crevice Corrosion of Titanium", Titanium '80, 4, pp 2613-2622 (May, 1980).

REFERENCES FOR CHAPTER 3
(Continued)

17. Minkler, W. W., "Titanium for Chemical Processing Equipment", Metal Progress, 113, pp 27-31 (1978).

18. Covington, L. C., et al., "Selection of Titanium Alloys for Corrosion Resistance", Symposium on Selection of Materials, AIChE Annual Meeting, 42 pp (November, 1977).

19. Koizumi, T. and Furuya, S., "Pitting Corrosion of Titanium in High Temperature Halide Solutions", Titanium Science and Technology, 4, pp 2383-2393 (May, 1972).

20. Sato, S., "On the Materials for Desalination Plants and Their Problems - Particularly the Heat Exchanger Tube Materials", Sumitomo Light Metal Technical Report, 20 (1-2), pp 44-53 (January, 1979).

21. Reinhart, F. M. and Jenkins, J. F., "Corrosion of Materials in Surface Seawater After 12 and 18 Months of Exposure", U.S. Naval Civil Engineering Laboratory Final Report NCEL-TN-1213, 106 pp (January, 1972).

22. Ailor, W. H., Jr., "Metal Exposures at Tropical and Marine Sites", 6th Annual Offshore Technology Conference, 1, pp 293-312 (May, 1974).

23. Ambler, H. R. and Bain, A.A.J., "Corrosion of Metals in the Tropics", Journal of Applied Chemistry, 5, pp 437-467 (September, 1955).

24. Rynewicz, J., "Corrosion in Deep Oceans", Ocean Engineering - Petroleum Engineer, 46 (13), pp 57-66 (November, 1974).

25. Cox, B., "Titanium for Desalting Plants", Titanium for Energy and Industrial Applications, pp 123-142 (1981).

26. Crowe, C. R. and Hasson, D. F., "The Use of Titanium in Deep Sea Exploration", Titanium for Energy and Industrial Applications, pp 93-110 (1981).

27. Adamson, W. L., "Marine Fouling of Titanium Heat Exchangers", Report PAS-75-29, David W. Taylor Naval Ship R&D Center (March, 1976).

28. Posey, F. A. and Bohlmann, E. G., "Pitting of Titanium Alloys in Saline Waters", Desalination, 3, pp 269-279 (1967).

29. Covington, L. C. and Schutz, R. W., "The Effects of Iron on the Corrosion Resistance of Titanium", Paper presented at the 4th International Conference on Titanium, Kyoto, Japan (May 19-22, 1980).

30. Danek, G. J., Jr., "The Effect of Seawater Velocity on the Corrosion Behavior of Metals", Naval Engineers Journal, 78 (5), pp 763-769 (October, 1966).

31. Hohman, A. E. and Kennedy, W. L., "Corrosion and Materials Selection Problems on Hydrofoil Craft", Materials Protection, 2 (9), pp 56-68 (September, 1963).

REFERENCES FOR CHAPTER 3
(Continued)

32. Brennert, S. and Lindh, G., "Resistance to Corrosion of Metallic Material for Seawater Bearing Pipes", 7th Scandanavian Corrosion Congress, Trondheim, Norway, pp 346-355 (May, 1975).

33. "Properties and Applications of Titanium for Tubes", Pipes and Pipelines International, 22 (5), pp 11-15 (October, 1977).

34. Henrikson, S. and Knutsson, L., 'Corrosion Tests in Baltic Seawater on Heat Exchanger Tubes of Various Metallic Materials", British Corrosion Journal, 10 (3), pp 128-135 (1975).

35. Davis, J. A. and Gehring, G. A., Jr., "Effect of Velocity on the Seawater Corrosion Behavior of High Performance Ship Materials", Materials Performance, 14 (4), pp 32-39 (April, 1975).

36. Basil, J. L., "Corrosion of Materials in High Velocity Seawater", U.S. Naval Engineering Exp. Station Report 910160A, 9 pp (December, 1960).

37. "Titanium Heat Exchangers for Service in Seawater, Brine, and Other Natural Environments: The Corrosion Erosion and Galvanic Corrosion Characteristics of Titanium in Seawater, Polluted Inland Waters, and in Brines", Titanium Information Bulletin, Imperial Metal Industries (Kynoch) Limited (May, 1970).

38. Uhlig, H. H., Corrosion Handbook, Wiley, New York, NY, pp 420-425 (1958).

39. Fontana, M. G. and Greene, N. D., Corrosion Engineering, McGraw-Hill, New York, NY, p 32 (1978).

40. Little, B., et al., "Gulf of Mexico Study of Biofouling on OTEC Heat Exchanger Candidate Alloys", Materials Performance, 20 (8), pp 16-21 (August, 1981).

41. Morris, A. W., "Electrochemical Screening of Fastener Materials for Carbon Composite Joint Applications", Corrosion '80, Chicago, IL, Paper 23, 9 pp (March, 1980).

42. Scholes, I. R., et al., "Bimetallic Corrosion in Seawater", European Congress on Metal Corrosion, London, England, pp 161-169 (1977).

43. LaQue, F. L., "Galvanic Corrosion", The Encyclopedia of Electrochemistry, Edited by C. A. Hampel, Reinhold Publishing Corporation, New York, NY, pp 661-666 (1964).

44. Smith, C. A. and Compton, K. G., "Potentials of Selected Metal Alloys in Seawater at Elevated Temperatures", Corrosion, 31 (9), pp 320-326 (September, 1975).

45. Ebihara, W. T., "Tropical Exposure of Galvanically Coupled Metal Systems", Army Armament R&D Center Report ARSCD-TR-79004, 18 pp (June, 1979).

46. Brown, B. F., "A New Stress-Corrosion Cracking Test for High-Strength Alloys", Materials Research and Standards, 6 (3), pp 129-133 (1966).

REFERENCES FOR CHAPTER 3
(Continued)

47. Boyd, J. D., et al., "The Effect of Composition on the Mechanism of SCC of Titanium Alloys in Nitrogen Dioxide and Aqueous and Hot Salt Environments", NASA CR-1525 (1970).

48. Boyd, J. D., et al., "The Effect of Composition on the Mechanism of SCC of Titanium Alloys in Nitrogen Dioxide and Aqueous and Hot Salt Environments (Part 2)", NASA CR-1846 (1971).

49. Judy, R. W. and Goode, R. J., "Stress-Corrosion Cracking Characteristics of Alloys of Titanium in Salt Water", Naval Research Laboratory Report 6564 (July, 1967).

50. Craw, C. R. and Hasson, D. F., "The Use of Titanium in Deep Sea Exploration", Titanium for Energy and Industrial Applications, pp 93-110 (1981).

51. Boyd, W. K., "Stress-Corrosion Cracking of Titanium and Its Alloys", in "Titanium for the Chemical Engineer: Lectures Given at the AIChE Materials Conference, Philadelphia, PA, April 1, 1960", DMIC Memo 234, pp 35-44 (April, 1968).

52. Blackburn, M. J. and Williams, J. C., "Strength, Deformation Modes and Fracture in Titanium-Aluminum Alloy", Trans. Amer. Soc. Metals, 62, p 398 (1969).

53. Macky, T. L. and Tiner, N. A., "Stress-Corrosion Susceptibility of Titanium Alloys in Aqueous Environments", Metals Engineering Quarterly, 9 (4), pp 59-60 (1969).

54. Cavallaro, J. L. and Wilcox, R. C., "Embrittlement of Ti-7Al Binary Alloys in Seawater", Corrosion, 27 (4), pp 157-163 (1971).

55. Lane, I. R. and Cavallaro, J. L., "Metallurgical and Mechanical Aspects of the Seawater Stress-Corrosion of Titanium", Application Related Phenomena in Titanium Alloys, ASTM STP 432, pp 147-169 (1968).

56. Blackburn, M. J. and Cavallaro, J. L., "Metallurgical and Mechanical Aspects of the Stress-Corrosion Cracking of Titanium Alloys", Fundamental Aspects of Stress-Corrosion Cracking, Edited by R. W. Staehle, et al., NACE, p 620 (1969).

57. Crossley, F. A. and Carew, W. F., "Embrittlement of Ti-Al Alloys in the 6 to 10 Percent Aluminum Range", Journal of Metals, 209 (1) (1957).

58. Crossley, F. A., "Aircraft Application of Titanium: A Review of the Past and Potential for the Future", Journal of Aircraft, 18 (12), pp 993-1002 (December, 1981).

59. Williams, W. L., "Development of Structural Titanium Alloys for Marine Applications", Ocean Engineering, 1, pp 375-384 (1969).

60. Wood, R. A., et al., "The Effects of Alloy Composition on the Salt Water Stress-Corrosion Susceptibility of Titanium-Aluminum-Base Alloys", Titanium Science and Technology, 4, Plenum Press, New York, NY, pp 2639-2654 (1973).

REFERENCES FOR CHAPTER 3
(Continued)

61. Seagle, S. R., et al., "The Influence of Composition and Heat Treatment on the Aqueous Stress-Corrosion of Titanium", Application Related Phenomena in Titanium Alloys, ASTM STP 432, pp 170-188 (1968).

62. Curtis, R. E., et al., "Relationship Between Composition, Microstructure, and Stress-Corrosion Cracking (in Salt Solution) in Titanium Alloys", Transactions of ASM, 62, p 457 (1969).

63. Sorkin, G., et al., "Ti-6Al-4V for Marine Uses", Titanium and Titanium Alloys: Scientific and Technological Aspects, 3, Moscow, USSR, pp 2139-2147 (May, 1976).

64. Feeny, J. A. and Blackburn, M. J., "The Status of Stress-Corrosion and Hydrogen Embrittlement", Titanium Science and Technology, 4, Edited by R. I. Jaffee and H. M. Burte, pp 2517-2609 (1973).

65. Gastelow, C. R. and Weaver, M. J., "The Behavior of Titanium Alloys in Simulated Marine Gas Turbine Environments", National Gas Turbine Establishment Report 344 (March, 1977).

66. Shannon, J. L. and Brown, W. F., "A Review of Factors Influencing the Crack Tolerance of Titanium Alloys", Application Related Phenomenon Titanium Alloys, ASTM STP 432, pp 33-63 (1968).

67. Beck, T. R. and Blackburn, M. J., "Stress-Corrosion Cracking of Titanium Alloys: SCC of Titanium, 8 Percent Mn Alloy, Pitting Corrosion of Aluminum and Mass-Transport-Kinetic Model for SCC of Titanium" (April, 1968).

68. Piper, D. E., et al., "Corrosion Fatigue and Stress-Corrosion Cracking in Aqueous Environments", Metal Engineering Quarterly, 8 (3), pp 50-63 (1968).

69. Wanhill, R.J.H., "Fractographic Interpretation of Sub-Critical Cracking in a High Strength Titanium Alloy (IMI 550)", Corrosion, 29 (11), pp 435-441 (1973).

70. Onman, S. and Picton, G., "Role of Hydrogen in the Stress-Corrosion Cracking of Titanium Alloys", Corrosion Science, 14, pp 451-459 (1974).

71. Howe, D. G. and Goode, R. J., "Effect of Heat Treating Environmental Conditions on the Stress-Corrosion Cracking Resistance of Several Titanium Alloys", Applications Related Phenomena in Titanium Alloys, ASTM STP 432, pp 189-201 (1968).

72. Sandoz, G., "Subcritical Crack Propagation in Ti-8Al-1Mo-1V Alloy in Organic Environments, Salt Water, and Inert Environments", Fundamental Aspects of Stress-Corrosion Cracking, Edited by R. W. Staehle, et al., pp 684-690 (1969).

73. Meyn, D. A., "Effect of Hydrogen on Fracture and Inert Environment Sustained Load Cracking Resistance of Titanium Alloys", Metallurgical Transactions, 5 (11), pp 2405-2414 (1974).

REFERENCES FOR CHAPTER 3
(Continued)

74. Koch, G. H., et al., "A Comparison of Gaseous Hydrogen Embrittlement, Slow-Strain-Rate Hydrogen Embrittlement, and Stress-Corrosion Cracking in Ti-8Al-1Mo-1V", Metallurgical Transactions, 12A, pp 1833-1843 (1981).

75. Stress-Corrosion Cracking in High Strength Steels and in Titanium and Aluminum Alloys, Edited by B. F. Brown, Naval Research Laboratory (1972).

76. Lane, I. R. and Cavallaro, J. L., "Metallurgical Aspects of Stress-Corrosion Cracking of Titanium Alloys", Fundamental Aspects of Stress-Corrosion Cracking, Edited by R. W. Staehle, et al., NACE, p 620 (1969).

77. Mackay, T. L., "Stress-Corrosion Cracking of Titanium Alloys at Ambient Temperature in Aqueous Solutions", NASA CR-1464 (1969).

78. Finden, P., "Comparative Data - Titanium Alloy Screening Tests", Boeing Document D6-24541-TN.

79. Hickman, B. S., "The Formation of Omega Phase in Titanium and Zirconium: A Review", Journal of Material Science, 4, p 554 (1969).

80. Beck, T. R. and Blackburn, M. J., "Stress-Corrosion Cracking of Titanium Alloys: SCC of Titanium: 8 Percent Mn Alloy; Pitting Corrosion of Aluminum and Mass-Transport-Kinetic Model for SCC of Titanium", Progress Report 7, Contract NAS 7-489, The Boeing Company, Seattle, WA (April, 1968).

81. Fager, D. N. and Spurr, W. F., "Some Characteristics of Aqueous Stress-Corrosion in Titanium Alloys", Transactions ASM, 61, pp 283-292 (1968).

82. Meyn, D. A., "A Study of the Crystallographic Orientation of Cleavage Facets Produced by Stress-Corrosion Cracking of Ti-7Al-2Nb-1Ta in Water", NRL Progress Report (August, 1965).

83. Koch, G. H., et al., "Comparison and Interpretation of Fracture Surfaces Produced in Ti-8Al-1V-1Mo by Stress-Corrosion Cracking and Slow-Strain-Rate Hydrogen Embrittlement", Metallurgical Transactions, A, p 129 (1978).

84. "A Study of the Stress-Corrosion Cracking of Titanium Alloys in Seawater With Emphasis on the Ti-6Al-4V and Ti-8Al-1Mo-1V Alloys", Research Report R471, Project 93002, Research Metals, Inc. (October, 1965).

85. Powell, D. T. and Scully, J. C., "Stress-Corrosion Cracking of Alpha Titanium Alloys at Room Temperature", Corrosion, 24 (6), p 151 (1968).

86. Beck, T. R., et al., "Stress-Corrosion Cracking of Titanium Alloys", Boeing Research Laboratories, Seattle, WA, Contract NAS-7-489, Quarterly Progress Report 11 (1969).

87. Beck, T. R., "Stress-Corrosion Cracking of Titanium Alloys. I: Ti-8-1-1 Alloy in Aqueous Solutions", Journal of the Electrochemical Society, 114, pp 551-556 (1967).

REFERENCES FOR CHAPTER 3
(Continued)

88. Beck, T. R., "Stress-Corrosion Cracking of Titanium Alloys. II: An Electrochemical Mechanism", Journal of the Electrochemical Society, 115, pp 890-896 (1968).

89. Konoki, K., et al., "Application of New Stainless Steels to Seawater Heat Exchanger Tubes", Corrosion '81, Paper 125, Toronto, Ontario, 20 pp (April 1981).

90. Lee, T. S., "A Method for Quantifying the Initiation and Propagation Stages of Crevice Corrosion", Electrochemical Corrosion Testing, ASTM-STP-727, pp 43-68 (1981).

91. Corray, C. W., "Anodic Versus Cathodic Electrocoating", Plating and Surface Finishing, 67 (1), pp 18-20 (January, 1980).

92. Rynewicz, J., "Corrosion in Deep Oceans", Ocean Engineering - Petroleum Engineer, 46 (13), pp 57-66 (November, 1974).

93. Feeney, J. A. and Blackburn, M. J., "The Status of Stress-Corrosion Cracking of Titanium Alloys in Aqueous Solutions", The Theory of Stress-Corrosion Cracking in Alloys, Edited by J. C. Scully (1971).

94. Borsel, J. D., et al., NASA CR-1846 (October, 1971).

95. Beck, T. R., "Electrochemical Models for Stress-Corrosion Cracking of Titanium", The Theory of Stress-Corrosion Cracking in Alloys, Edited by J. C. Scully (1971).

96. Mankowski, G., et al., "Discontinuous Stress-Corrosion Cracking Behavior of Ti-6Al-4V in Synthetic Seawater With Temperature", Titanium '80, 4, Kyoto, Japan, pp 2605-2612 (May 19-22, 1980).

97. Litvin, D. A. and Hill, B., "Effect of pH on Seawater Stress-Corrosion Cracking Behavior of the Ti-7Al-2Cb-1Ta Alloy", Corrosion, 26 (3), pp 89-94 (March, 1970).

98. Jackson, J. D. and Boyd, W. K., "The Stress-Corrosion and Accelerated Crack Propagation Behavior of Titanium and Titanium Alloys", DMIC Technical Note, Battelle Columbus Laboratories (February, 1966).

99. Stress-Corrosion Crack of Titanium, ASTM-STP-397 (1966).

100. Peterson, V. C., "Hot Salt Stress-Corrosion of Titanium", Journal of Metals, 23, pp 40-47 (April, 1971).

101. Blackburn, M. J., et al., "Titanium Alloys", Stress-Corrosion Cracking in High Strength Steels and in Titanium and Aluminum Alloys, Edited by B. F. Brown, Naval Research Laboratory, p 293 (1971).

102. Logan, H. L., "Studies of Hot Salt Cracking of the Ti-8Al-1Mo-1V Alloy", Proceedings of Conference on Fundamental Aspects of Stress-Corrosion Cracking, Edited by R. W. Staehle, et al., NACE, p 662 (1969).

REFERENCES FOR CHAPTER 3
(Continued)

103. Rideout, S. P., et al., "Basic Mechanisms of Stress-Corrosion Cracking of Titanium", Stress-Corrosion Cracking of Titanium, ASTM STP 397, American Society for Testing of Materials, Philadelphia, PA, p 137 (1968).

104. Hatch, A. J., et al., "Effects of Environment on Cracking in Titanium Alloys", Stress-Corrosion Cracking of Titanium, ASTM STP 397, American Society for Testing of Materials, Philadelphia, PA, p 122 (1968).

105. Logan, H. L., et al., "Stress-Corrosion Cracking of Titanium", Stress-Corrosion Cracking of Titanium, ASTM STP 397, American Society for Testing of Materials, Philadelphia, PA, p 215 (1966).

106. Rideout, S. P., et al., "The Role of Moisture and Hydrogen in Hot Salt Cracking of Titanium Alloys", Proceedings of Conference on Fundamental Aspects of Stress-Corrosion Cracking, Edited by R. W. Staehle, et al., NACE, p 650 (1969).

107. Boyd, W. K., "Stress-Corrosion Cracking of Titanium and its Alloys", Proceedings of Conference on Fundamental Aspects of Stress-Corrosion Cracking, Edited by R. W. Staehle, et al., NACE, p 593 (1969).

CHAPTER 4
TABLE OF CONTENTS

CHAPTER 4
LIST OF TABLES

CHAPTER 4
LIST OF TABLES
(Continued)

CHAPTER 4
LIST OF TABLES
(Continued)

CHAPTER 4
LIST OF TABLES
(Continued)

CHAPTER 4
LIST OF TABLES
(Continued)

CHAPTER 4
LIST OF TABLES
(Continued)

CHAPTER 4
LIST OF FIGURES

CHAPTER 4
LIST OF FIGURES
(Continued)

CHAPTER 4
LIST OF FIGURES
(Continued)

CHAPTER 4
LIST OF FIGURES
(Continued)

CHAPTER 4
LIST OF FIGURES
(Continued)

CHAPTER 4

STAINLESS STEELS

Atmosphere

General Corrosion

As pointed out in the Introduction, corrosion in marine atmospheres is not so severe as in immersed or splash zone areas. Since resistance to pitting is not a major requirement in most atmospheric exposure applications, the high molybdenum ferritic and duplex stainless steels are not required. Thus, there are few quantitative corrosion data for these highly alloyed steels in marine atmospheres.

The conventional ferritic and austenitic stainless steels are used extensively in marine atmospheres. As pointed out by Larrabee[1] in his pioneer work on marine corrosion at the 800-foot lot at Kure Beach, NC, the stainless steels exhibit the following corrosion behavior in the marine atmosphere.

1. 12 percent Cr steel (Type 410) develops a red rust over part of its surface within a few months.

2. 17 percent Cr steel (Type 430) develops red rust over part of its surface after about one year, and on smooth surfaces the rust can be removed by polishing compound.

3. 18Cr-8Ni stainless steel (Type 304) initially becomes stained with a superficial yellowish substance over a small part of its surface. After a few years, this substance may be changed to red rust, but the latter can be removed by polishing compounds.

4. The addition of 2 to 3 percent Mo to the 18Cr-8Ni (Type 316) results in a marked increase in resistance to staining. Higher alloys such as 25-12 (Type 309) and 25-20 (Type 310) also are more resistant than Type 304 but the higher alloys are not so resistant as Type 316.

The effect of chromium content on resistance to atmospheric corrosion is shown dramatically in Figure 4-1. Note that the corrosion rate became negligible at $\geq$12 percent Cr in these 8-year exposures.

Long-term atmospheric corrosion data for stainless steels at Kure Beach, NC (15 years), and Cristobal, Panama, are summarized in Tables 4-1 and 4-2. Note the very low corrosion rates of $\leq$0.3 μm/yr (0.01 mpy) after 15 to 16 years of exposure.

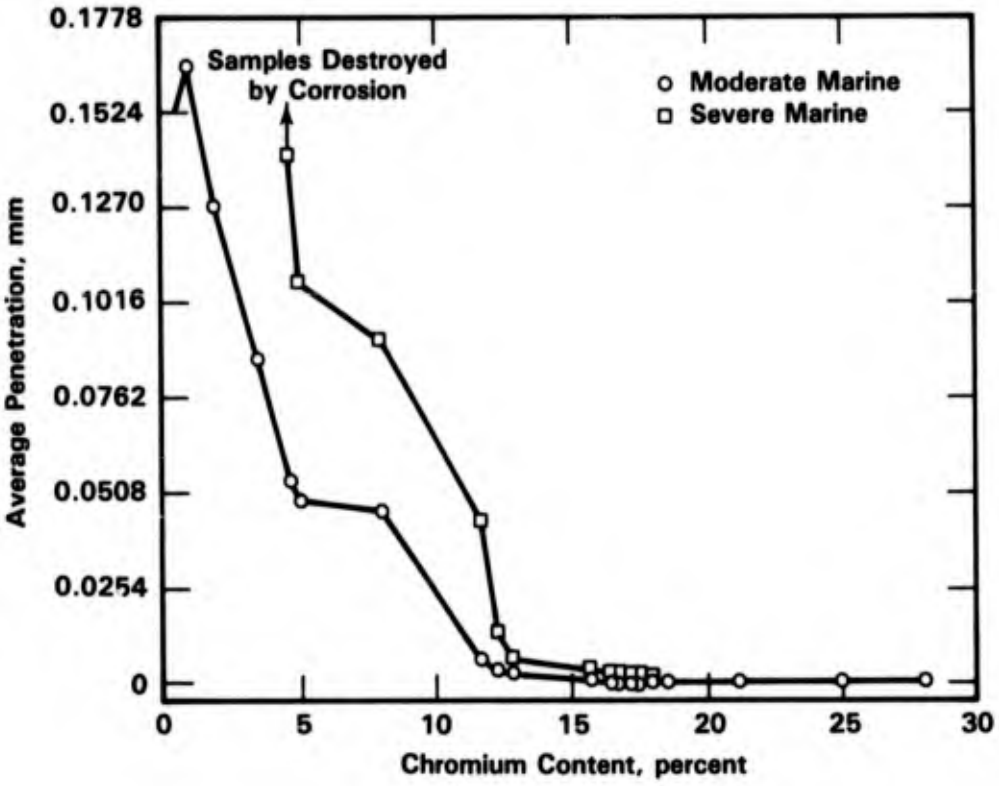

FIGURE 4-1. ATMOSPHERIC CORROSION OF CHROMIUM STEELS AFTER AN EIGHT-YEAR EXPOSURE[2]

TABLE 4-1. ATMOSPHERIC CORROSION OF SOME STAINLESS STEELS EXPOSED 15 YEARS TO A MARINE ENVIRONMENT (800-FOOT LOT AT KURE BEACH, NC)[2]

Type	Average Corrosion Rate, μm/yr	Average Depth of Pits, cm
301	<0.03	0.004
302	<0.03	0.003
304	<0.03	0.003
321	<0.03	0.007
347	0.03	0.009
316	<0.03	0.003
317	<0.03	0.003
308	<0.03	0.004
309	<0.03	0.003
310	<0.03	0.001

TABLE 4-2. CORROSION DATA FOR NONCOUPLED METAL PANELS EXPOSED AT NRL'S TROPICAL SEACOAST SITE AT CRISTOBAL, PANAMA[3]

Metal Type	General Corrosion: Average Penetration, μm[a] 1 Yr	2 Yr	4 Yr	8 Yr	16 Yr	General Corrosion: Final Rate,[b] μm/yr	Pitting: Average Deepest 20 pits,[c] μm 8 Yr	16 Yr	Pitting: Deepest Pit, μm	Tensile Strength, % Loss[d] 8 Yr	16 Yr
Stainless Steel											
410 (13Cr)	1.0	1.0	1.5	1.0	4.6	0.3	<125	<125	<125	<1	<1
430 (17Cr)	0.5	1.0	1.0	1.0	2.0	<0.3	<125	<125	<125	<1	<1
301 (17Cr, 7Ni)	0.3	<0.3	<0.3	0.3	0.5	0.3	<125	<125	<125	<1	<1
321 (17Cr, 10Ni, Ti)	<0.3	<0.3	<0.3	0.3	0.5	<0.3	<125	<125	<125	<1	<1
316 (18Cr, 13Ni, Mo)	<0.3	<0.3	<0.3	<0.3	<0.3	<0.3	<125	<125	<125	<1	<1

(a) Average penetration over a 4.23-dm^2 exposed area; calculations based on weight loss and density.
(b) Rate after time-corrosion relation had stabilized; slope of the linear portion of the curve, usually after two to eight years.
(c) Averages obtained by measuring the five deepest measurable (>125 μm) penetrations on each surface of duplicate panels.
(d) Percent loss in ultimate tensile strength for 1.59-mm (1/16-in.) thick metal.

Shorter term tests (1 to 5 years) have been conducted on the highly alloyed molybdenum-ferritic and duplex stainless steels. Qualitative results for these alloys are presented in Table 4-3. Note the absence of visible corrosion on these alloys as compared to rusting of the more conventional stainless steels. Thus, by comparison with the corrosion rates for the conventional alloys presented in Table 4-1, it is obvious that the general corrosion rates of the highly alloyed molybdenum stainless steels are infinitesimal in marine atmospheres.

Welding appears to have a negligible effect on the general corrosion rates of stainless steels in marine atmospheres. Das and Jena[4] have exposed welded Types 304 and 316 for 1 year in a marine atmosphere. Their results are summarized in Table 4-4. Note that welding increased the total amount of attack by $\leq$5 percent over that of the unwelded specimens (10 mg/m^2 = ~0.001 μm penetration).

TABLE 4-3. ATMOSPHERIC CORROSION OF STAINLESS STEELS EXPOSED AT THE 800-FOOT ATMOSPHERIC EXPOSURE SITE AT KURE BEACH, NC[2]

Group[a]	Alloy	Years Exposed	Composition, weight percent			Comments
			Cr	Mo	Other	
1	409	2	11	--	Ti	99% heavy rust spots
2	430	1	16	--	--	70% heavy rust spots
3	201	2	17	--	--	70% rust spots
	202	5	18	--	--	
	301	2	17	--	--	
	304	2	18	--	--	
	434	2	16	1	--	
	439	5	18	--	Ti	
4	321	1	18	--	Ti	70% light rust spots
	A-286	2	15	1.25	Ti	
5	316	2	18	2.5	--	60% very light rust spots
	444	1	18	2	Ti,Cb	
6	26-1S	2	26	1	Ti	5% very light rust spots
	E-Brite	2	26	1	--	
7	216	5	20	2.5	N	No corrosion
	Al-6X	5	20	6	--	
	Al-29-4	2	29	4	--	
	Al-29-4-2	2	29	4	--	

(a) Corrosion of alloys in each group was similar.

TABLE 4-4. LOSS IN WEIGHT AFTER 1 YEAR OF EXPOSURE AND VALUES OF n AND K OF DIFFERENT STEEL SAMPLES[4]

Nature of Samples	Weight Loss, V, mg/m^2	Value of n[a]	Value of K[a]
Type 304			
Gas welding	9.10	0.1	5.04
Arc welding	9.00	0.1	4.99
Without welding	8.80	0.1	8.80
Type 316			
Gas welding	8.20	0.1	4.55
Arc welding	8.00	0.1	4.43
Without welding	7.80	0.1	4.32

(a) From the corrosion rate equation $V = Kt^n$ where V = weight loss in mg/m^2; K = constant; and t = time of exposure in days.

Surface finish has an effect on the corrosion of stainless steels in a marine atmosphere. The effect has been summarized by Johnson and Pavlik[2] who conclude that the better the degree of surface finish, the less the tendency to form adherent rust. These conclusions are illustrated qualitatively in Table 4-5 from the work of Degerbeck, et al.[5] Note that for the three alloys studied, the polished surface was stain free on 18-2 Mo-Ti and Type 316 and only slightly stained on Type 304 after 5 years exposure, while the ground and pickled surfaces exhibited more attack (Types 304 and 316).

Pitting and Crevice Corrosion

As mentioned in the section on General Corrosion, the conventional steels exhibit little or no pitting in marine atmospheres. Karlsson and Olsson[6] report a pit depth of 0.16 mm (6 mils) in 13Cr stainless steel after 10 years exposure in a marine atmosphere. Ailor[7] found tiny superficial pits in Type 304 stainless steel exposed 7 years at Aruba. This test site was deemed to be extremely corrosive because the test panels were frequently wetted by seawater spray from waves breaking over the rocky shore.

Pitting data from long-term exposure tests are presented in Tables 4-1 and 4-2. Note that after 15 years' exposure at the Kure Beach 800-ft test lot, the average depths of pits on the 300 series stainless steels ranged from 10 to 90 μm (0.4 to 3.5 mils). Southwell and

TABLE 4-5. DEGREE OF CORROSION AFTER 1, 3, AND 5 YEARS' EXPOSURE IN A MARINE ATMOSPHERE[5]

Steel	Surface Condition	Mark After Number of Years[a]		
		1 Yr	3 Yr	5 Yr
18Cr-2Mo-Ti	Pickled	0	0	0
	Ground	0	0	0
	Polished	0	0	0
Type 316	Pickled	1	1	1
	Ground	1	1	1
	Polished	0	0	0
Type 304	Pickled	3	3	3-4
	Ground	4	5	5
	Polished	0	0-1	0-1

(a) Scale markings and corresponding surface conditions:

Mark	Appearance of Surface	Corroded or Stained Surface (% of Total Surface)
0	No rust or staining	0
1, 2, 3	Increased degree of staining--separate and small spots of rust	0-25
4, 5, 6	Discoloration and increased amount of rust	25-75
7, 8	Rust covering major part of surface	75-100

Bultman[3] indicated that the average deepest pit was less than 125 μm (5 mils) in both 300 and 400 series alloys exposed 16 years at Cristobal, Panama. Apparently, 125 μm was the limit of detection for the procedure used to measure the pit depth. In reporting another aspect of this same study, Southwell and Alexander[8] reported the <125 μm as 0 mil, thus indicating no pitting.

Khanna and Gnanamoorthy[9] have reported that sensitization produced pitting in 304 and 316 normal carbon and low carbon grades of stainless steel exposed in the Bengal Bay. Their results presented in Table 4-6 also indicate that pitting also occurred on some nonsensitized specimens. Apparently no metallographic examination was conducted on these specimens, and thus it is not known whether the pits were the result of intergranular attack in

TABLE 4-6. EVALUATIONS OF VARIOUS HEAT-TREATED SPECIMENS AFTER EXPOSURE[9]

Material	Sensitized	General Appearance of the Surface	Pit Density, (No./dm^2)
		Panel II, 3-Year Exposure Time	
316, 3.5 mm	Yes	Highly corroded--large pits all over the surface.	465
304, 6 mm	No	Light attack--surface covered nonuniformly with brown spots.	--
304, 6 mm	Yes	Large pits all over the surface.	155
304L, 1.6 mm	No	Surface covered nonuniformly with pits--more brown spots at corners.	733
316, 6 mm	No	No effect.	--
316L, 6 mm	Yes	Highly corroded--the surface fully covered with pits. Counting could not be performed.	--
304, 1.6 mm	Yes	Highly corroded--pits all over the surface.	310
316, 6 mm	Yes	Highly corroded--whole surface covered with brown spots.	248
304, 6 mm	No	Light brown spots, all over the surface--no deep pits were seen.	--

the sensitized microstructure or were more typical of the classical chloride pits in stainless steel.

Galvanic Corrosion

Galvanic corrosion is not as prevalent in the marine atmosphere as it is in seawater. Nevertheless, galvanic corrosion does occur, particularly over short distances where moist salt deposits serve as the conducting electrolyte. In studying the corrosion behavior of magnesium coupled to a number of alloys, Baboian[10] established an atmospheric galvanic corrosion series based on 22.6 years exposure at the Kure Beach 800-ft lot. The series is presented in

Table 4-7. Note that 304 stainless steel is at the noble end of the atmospheric galvanic series as it is in the seawater (immersed) galvanic series (see Figure 4-2).

Because stainless steel is noble to most alloys, it is attacked very little during atmospheric exposure and often promotes attack of the dissimilar metal in the galvanic couple. This accelerating corrosion effect of the stainless steel is demonstrated in the data in Tables 4-8 and 4-9. Ebihara[13] has tabulated galvanic corrosion rate data from an exposure site some 600 to 1250 m from the sea in Panama. Only minor galvanic corrosion effects were observed on magnesium and aluminum when coupled to 316 stainless steel. Apparently there was very little sea salt deposited on these specimens, because Baboian[10] reported an increase in the corrosion of magnesium alloys and a decrease in the corrosion of 304 stainless steel in his 304/Mg couple tests that ran 22.6 years at the 800-ft lot at Kure Beach.

However, there are materials which are more noble than stainless steel, and thus promote the corrosion of stainless steel in galvanic couples. Prince[14] found that A-286 metal fasteners corroded more rapidly in a 3.5 percent NaCl salt spray test when they were inserted in graphite-epoxy composites than when they were inserted in aluminum. In studies conducted in an acidified 3.5 percent NaCl spray, Morris[15] concluded that both A-286 and PH13-8Mo steel must be painted to protect them from corrosion when used in carbon fiber composites. It should be noted, however, that painting the anodic (corroding) member of a galvanic couple is not recommended in severely corrosive conditions, such as immersion in seawater.

TABLE 4-7. METALS ARRANGED ACCORDING TO INCREASING MAGNESIUM CORROSION IN GALVANIC COUPLE[10]

Kure Beach, 800-ft (245-m) Lot	
22.6 Years	2.48 Years
Al	Al
Zn	Zn
Zn Plated Steel	Zn Plated Steel
Cd Plated Steel	Cd Plated Steel
Steel	304 SS
85-15 Brass	85-15 Brass
304 SS	Monel
Monel	Nickel
Nickel	Steel

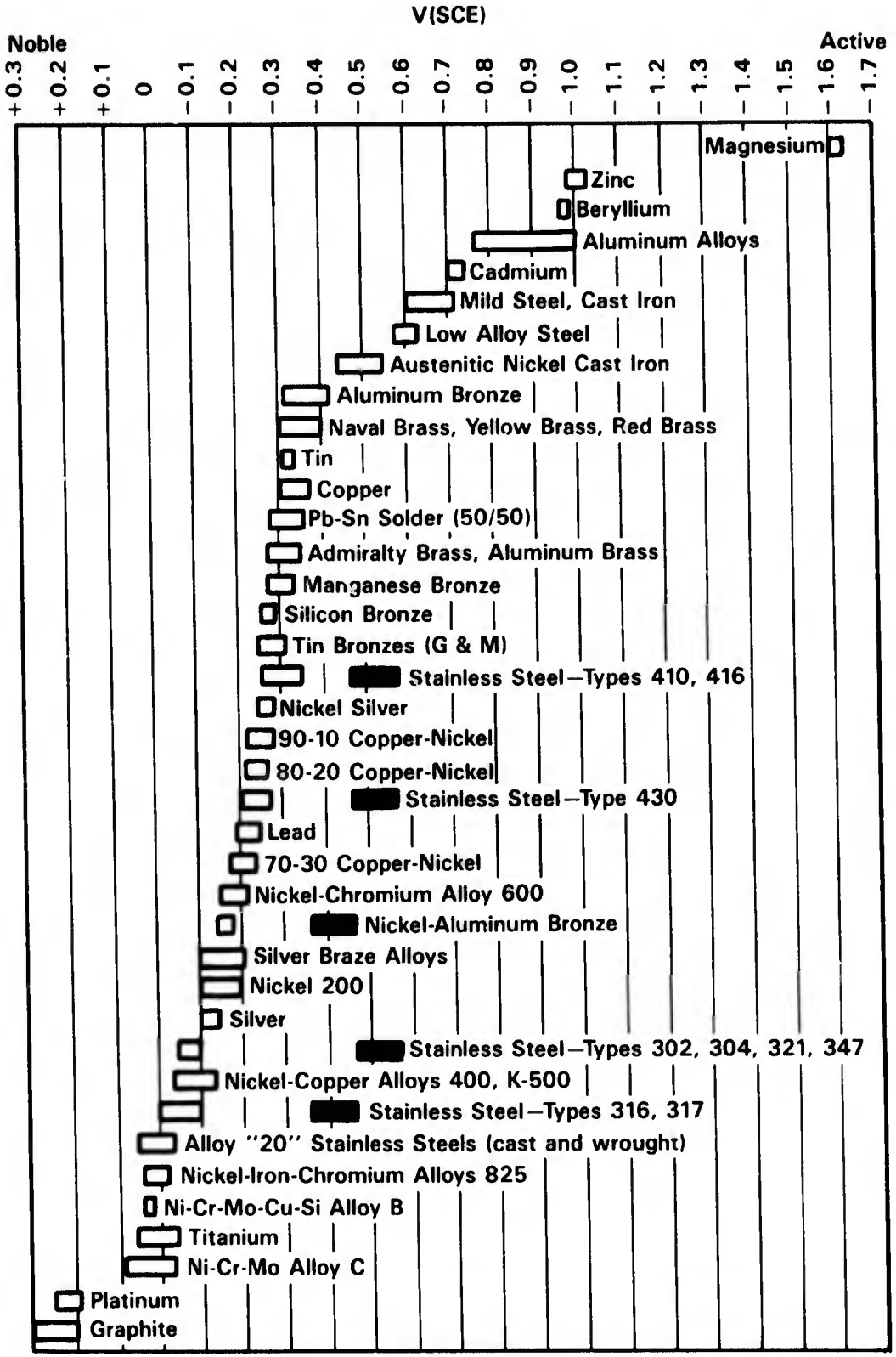

Alloys are listed in the order of the potential they exhibit in flowing seawater. Certain alloys indicated by the symbol: ■ in low-velocity or poorly aerated water, and at shielded areas, may become active and exhibit a potential near −0.5 volts.

FIGURE 4-2. CORROSION POTENTIALS OF VARIOUS MATERIALS IN FLOWING SEAWATER (2.5-4 MS^{-1}) AT TEMPERATURES IN RANGE 50-79 F; HATCHED SYMBOLS INDICATE POTENTIALS EXHIBITED BY STAINLESS STEELS IN ACIDIC WATER SUCH AS EXISTS IN CREVICES[11]

TABLE 4-8. CORROSION RATES OF MILD STEEL AND OTHER METALS WHEN COUPLED TOGETHER, AND WHEN COUPLED TO THEMSELVES, IN RYE (ENGLAND) MARINE ATMOSPHERE[12]

Couple	Corrosion Rates, $g/m^2/day$[a]		
		Other Metal	
	Mild Steel	Coupled to Mild Steel	Coupled to Itself
Hastelloy B	2.35	0.11	0.08
Incoloy 800	3.85	0.00	--
Incoloy 825	SD[b]	SD[b]	--
Inconel 600	2.91	0.00	--
Mild Steel	1.05		
Monel 400	SD[b]	SD[b]	--
Stainless Steel Type 410	1.95	0.03	0.08
Stainless Steel Type 304	2.35	0.01	0.02
Stainless Steel Type 316	SD[b]	SD[b]	0.01
Stainless Steel Type 430	1.80	0.02	0.03

(a) 1 $g/m^2/day$ = 0.456 mm/yr (18 mpy).
(b) SD = Specimen damaged.

TABLE 4-9. GALVANIC CORROSION OF METAL DISKS[a] EXPOSED AS BIMETALLIC COUPLES IN COASTAL AND INLAND TROPICAL ENVIRONMENTS IN PANAMA. BOTH METALS OF EACH COUPLE HAD THE SAME EXPOSED AREA (3.48 CM^2), AND THE DATA SHOW AVERAGE CORROSION PENETRATION OF EXPOSED SURFACES IN MICROMETERS[3]

Metal I	Metal II	Coastal-Cristobal				Inland-Miraflores			
		Metal I		Metal II		Metal I		Metal II	
		1 Yr	16 Yr	1 Yr	16 Yr	1 Yr	16 Yr	1 Yr	16 Yr
Selected Self-Couple Controls									
316 Stainless steel	316 Stainless steel	<1	7	<1	8	<1	4	<1	6
301 Stainless steel	301 Stainless steel	1	10	<1	8	1	2	<1	3
Bimetallic Couples									
316 Stainless steel	Carbon steel	2	12	194	930	<1	7	46	292
316 Stainless steel	Phosphor bronze	<1	6	22	151	<1	7	2	22
321 Stainless steel	Carbon steel	1	8	190	790	<1	9	49	281
301 Stainless steel	Carbon steel	<1	6	180	918	<1	3	44	291
301 Stainless steel	Phosphor bronze	<1	3	20	156	<1	3	2	20
430 Stainless steel	Carbon steel	2	21	167	707	<1	17	48	292
430 Stainless steel	Phosphor bronze	1	19	15	72	<1	18	2	22
410 Stainless steel	Carbon steel	3	26	155	715	1	21	52	314
410 Stainless steel	Phosphor bronze	9	34	10	63	<1	21	3	22

(a) ASTM-type bimetallic disk specimen.

Stainless steels appear to be compatible with titanium in galvanic couples. Bomberger, et al.[16] found no increased attack of 302 or 316 stainless steel when coupled to titanium and exposed 56 months at the Kure Beach 80-ft lot (see Table 4-10).

Stress-Corrosion Cracking

Stress-corrosion cracking (or hydrogen stress cracking) has often been a failure mode of stainless steels in marine atmospheres, particularly with those alloys that are heat treated to high strength levels. Stanley[17] has listed some of these failures in Table 4-11. Stanley[17] also has summarized the performance of stainless steels in marine atmospheres according to whether they have high resistance, intermediate resistance, or low resistance to SCC (see Tables 4-12, 4-13, and 4-14).

Austenitic Stainless Steels. In the mill annealed (or solution treated condition), the austenitic stainless steels are very resistant to stress-corrosion cracking in marine atmospheres. In Table 4-15, Money and Kirk[18] have summarized the results of 5 years of exposure at the Kure Beach 80-ft lot of U-bends of a number of austenitic alloys. Note that none of the annealed, cold worked or welded specimens failed by SCC. However, a high proportion of the sensitized specimens failed by SCC. As shown in Table 4-16 failures occurred in sensitized U-bends in as short a time as 35 days.

TABLE 4-10. ATMOSPHERIC GALVANIC-COUPLE (TITANIUM TO OTHER METAL) TESTS ON SHORE RACK, KURE BEACH (80 FT)[16]

Material Coupled to Titanium	360-Day Exposure			4 Years and 8 Months Exposure		
	Uncoupled Corrosion Rates,[a] mpy	Coupled Corrosion Rate, mpy		Uncoupled Corrosion Rates,[a] mpy	Coupled Corrosion Rate, mpy	
		7 x Ti Area[b]	1/7 x Ti Area[c]		7 x Ti Area[b]	1/7 x Ti Area[c]
Monel	Nil	0.020	0.032	0.0152	0.0197	0.0320
Inconel	0.011	0.006	0.003	0.0025	0.0029	0.0032
302 Stainless	Nil	0.009	0.023	0.0083	0.0091	0.0015
316 Stainless	0.004	0.004	0.003	0.0035	0.0029	0.0058

(a) Average of one 6 in. x 1.5 in. specimen and two 0.75 in. x 1.5 in. specimens.
(b) One 6 in. x 1.5 in. specimen.
(c) Average of two 0.75 in. x 1.5 in. specimens.

TABLE 4-11. FASTENER FAILURES ON THE TITAN III FAMILY OF VEHICLES[17]

Material	Hardness, UTS[a] and/or Heat Treatment	Application	Probable Failure Mode
15-7Mo	46 R_c	Shear tie bolt between solid and liquid cores	Stress-corrosion cracking
15-5PH	180 to 190 ksi	Solid rocket motor frangible bolt	Hydrogen stress cracking from galvanic coupling
17-4PH	H950	Fuel and oxidizer valve assemblies	Hydrogen stress cracking from galvanic coupling
440C	57 R_c	Actuator adjustable bolt	Stress-corrosion cracking
H-11	52 R_c; 260 ksi	Launch pad baseplate stems	Hydrogen stress cracking from galvanic coupling
431	180 ksi	Marman clamp on hot gas cooler	Stress-corrosion cracking
Unitemp 212	180 ksi	Solid rocket motor	Hydrogen stress cracking (?)
17-4PH	46 R_c; 1 hr, 900 F	Pressure valve	Stress-corrosion cracking
431	180 ksi	Solid rocket motor	Hydrogen stress cracking

(a) Hardness Rockwell C (R_c), ultimate tensile strength (UTS) ksi.

TABLE 4-12. MATERIALS WITH A HIGH RESISTANCE TO STRESS-CORROSION CRACKING[17]

Materials	Type	Heat Treatment*	Remarks
300 Series Stainless Types 303, 304, 316, 321, 347	Austenitic	Annealing	Stressed material can crack in chloride solutions. Annealed materials are not of high strength. Cold worked materials can develop high strength but they must be stress relieved.
17-4PH	Martensitic	H1000 and above	
17-7PH	Semi-austenitic	CH900	Strength is developed by cold work (60%) and aging (900 F).

TABLE 4-12. (Continued)

Materials	Type	Heat Treatment*	Remarks
PH13-8Mo	Martensitic	H1000 and above	
15-5PH	Martensitic	H1000 and above	
PH15-7Mo	Semi-austenitic	CH900	Strength is developed by cold work (60%) and aging (900 F).
PH14-8Mo	Semi-austenitic	CH900	As for PH15-7Mo.
AM-350	Semi-austenitic	SCT1000 and above	
AM-355	Semi-austenitic	SCT1000 and above	
Custom-455	Semi-austenitic	H1000 and above	
A-286	Austenitic	Solution treated and aged	
A-286 (CW and Aged)	Austenitic		High strength is developed by cold work (60%) and aging (1200 F).
Inconel 718	Face centered cubic	Solution treated and aged	
Inconel X-750	Face centered cubic	Solution treated and aged	
Rene-41	Face centered cubic	Solution treated and aged	
MP 35N	Face centered cubic	Solution treated and aged	Solution annealed and cold worked 60% and aged.
Waspaloy	Face centered	Solution treated and aged	
Low-Alloy Steels 4130, 4140, 4340, 8740	Martensitic	Quenched and tempered	High resistance to SCC if tempered to attain strength of 160 ksi or lower.
Maraging Steel	Martensitic	Solution treated and aged	High resistance if heat treated to 200 ksi or lower.

* For heat treatments refer to Aerospace Structural Metals Handbook, ASM Metals Handbook, or steel producer's literature.

TABLE 4-13. MATERIALS WITH A HIGH RESISTANCE TO STRESS-CORROSION CRACKING IF USED WITH CAUTION[17]

Materials	Type	Heat Treatment	Remarks
Low-Alloy Steels 4130, 4140, 4340, 8740, D6AC, HY-TUF	Martensitic	Quenched and tempered	Good resistance to SCC if tempered to about 160 to 180 ksi.
Maraging Steel	Martensitic	Solution treated and aged	All three grades; Maraging -200, -250, and -300.
400 Series Stainless 410, 416, 422, 431	Martensitic	Quenched and tempered	Not susceptible if tempered at 1100 F or higher.
15-5PH	Martensitic	H950 to H1000	
PH13-8Mo	Martensitic	H950 to H1000	
17-4PH	Martensitic	H950 to H1000	
AM-355	Semi-austenitic	SCT950 to H1000	

TABLE 4-14. MATERIALS WITH A LOW RESISTANCE TO STRESS-CORROSION CRACKING[17]

Materials	Type	Heat Treatment	Remarks
Low-Alloy Steels 4130, 4140, 4340, 8740, D6AC, HY-TUF	Martensitic	Quenched and tempered	Very susceptible to SCC if tempered to attain strengths of 180 ksi and higher.
H-11	Martensitic	Quenched and tempered	
17-7PH	Semi-austenitic	All heat treatments except CH900	
PH15-7Mo	Semi-austenitic	All heat treatments except CH900	
AM-355	Semi-austenitic	Heat treatments below SCT900	
400 Series Stainless 410, 416, 422, 431	Martensitic	Quenched and tempered	Very susceptible in the secondary hardening range, 500 to 1000 F.

TABLE 4-15. FIVE YEAR RESULTS OF THE SCC OF STAINLESS STEEL U-BENDS IN 80-FOOT LOT AT KURE BEACH[18]

Alloy/Heat	Ratio of Failures to Specimens Exposed					
	Annealed		As-Welded[b]		Cold Work 1/4 Hard	Sensitized at 1200 F, 1.5 hr + FC
	B[a]	S[a]	B	S	B	B
AISI 201/1	0/3	0/3	--	--	--	3/3
AISI 201/2	0/3	0/3	--	--	--	3/3
AISI 201/3	0/3	0/3	--	--	--	3/3
AISI 201/4	0/3[c]	0/3[c]	0/3[c]	0/3[c]	0/3[c]	3/3
AISI 201/5	0/3	0/3	0/3	0/3	0/3	3/3
AISI 301/1	0/3	0/3	--	--	--	3/3
AISI 301/2	0/3	0/3	--	--	--	3/3
AISI 301/3	0/3	0/3	--	--	--	3/3
AISI 301/4	0/3	0/3	0/3	0/3	0/3	3/3
AISI 301/5	0/3	0/3	0/3	0/3	0/3	3/3
AISI 301/6	0/3[c]	0/3[c]	0/3[c]	0/3[c]	0/3	1/3
AISI 301/7	0/3	0/3	--	--	--	3/3
AISI 302/4	0/3[c]	0/3[c]	0/3[c]	0/3[c]	0/3[c]	3/3
AISI 304/1	0/3	0/3	--	--	--	0/3
AISI 304/2	0/3	0/3	--	--	--	3/3
AISI 304/3	0/3	0/3	--	--	--	0/3
AISI 304/4	0/3[c]	0/3[c]	0/3[c]	0/3[c]	0/3[c]	3/3
AISI 304/5	0/3	0/3	0/3	0/3	0/3	3/3
AISI 304/6	0/3	0/3	--	--	--	0/3
AISI 304L/1	0/3	0/3	0/3	0/3	--	0/3
AISI 304L/2	0/3[c]	0/3[c]	0/3[c]	0/3[c]	0/3[c]	0/3
AISI 309/1	0/3[c]	0/3[c]	0/3[c]	0/3[c]	--	3/3
AISI 310/1	0/3[c]	0/3[c]	0/3[c]	0/3[c]	--	0/3
AISI 316/1	0/3	0/3	--	--	--	0/3
AISI 316/2	0/3[c]	0/3[c]	0/3	0/3[c]	0/3[c]	2/3
600/1	0/3[c]	0/3[c]	0/3[c]	0/3[c]	--	0/3
800/1	0/3[c]	0/3[c]	0/3[c]	0/3[c]	--	0/3
825/1	0/3[c]	0/3[c]	0/3[c]	0/3[c]	--	0/3
20Cb-3/1	0/3[c]	0/3[c]	0/3[c]	0/3[c]	--	0/3

(a) B = bold exposure, and S = sheltered exposure.
(b) Autogenous welding by TIG process. Weld beads were made on annealed material from Alloys 304L/1, 309, 310, 600, 800, and Cb3. Weld beads were made on 1/4 hard material for all other alloys.
(c) One specimen from each group examined metallographically for evidence of SCC.

TABLE 4-16. SCC OF STAINLESS STEELS IN MARINE ENVIRONMENTS[18]

(Bent-Beam Specimens--Exposure Time 5 Years)

Alloy AISI-Heat Number	Condition	Average Days to Failure of 3 Replicate Specimens at Stress Level[a] 50% YS	80% YS	U-bend
80-Foot Lot--Bold Exposure				
201-5	1/4 Hard	NF	NF	NF
	Sensitized	55	42	36
301-8	1/4 Hard	NF	NF	NF
	Sensitized	1826[b]	1826[b]	214
304-7	1/4 Hard	NF	NF	NF
	Sensitized	NF	NF	NF
80-Foot Lot--Sheltered Exposure				
201-5	1/4 Hard	NF	NF	NF
	Sensitized	38	36	35
301-8	1/4 Hard	NF	NF	NF
	Sensitized	1395	169	39
304-7	1/4 Hard	NF	NF	NF
	Sensitized	NF	NF	263
800-Foot Lot--Bold Exposure				
301-8	1/4 Hard	NF	NF	NF
	Sensitized	1826	1826	303
Under Deck of Wharf at FLLCL[c]				
301-8	1/4 Hard	NF	NF	NF
	Sensitized	197	94	52

(a) NF = No failure at 60 months.
(b) Confirmed by metallography.
(c) FLLCL = Frank L. LaQue Corrosion Laboratory.

Several of the austenitic stainless steels can be cold worked to high strength levels. Phelps[19] has exposed stressed specimens of some of these alloys for more than 6 years at the 80-ft lot at Kure Beach. His results, presented in Table 4-17, indicate that cold worked alloys with strength levels in excess of 225 ksi are resistant to SCC in marine atmospheres. Note in Table 4-17 that several of the alloys that were heat treated at 1100 F failed, possibly because they were sensitized by the heat treatment.

Martensitic and Precipitation Hardened Stainless Steels. As pointed out earlier, those stainless steels that can be heat treated to high strength levels often are susceptible to SCC (or hydrogen stress cracking). Long-term exposure results for stressed specimens of these types of alloys are presented in Tables 4-18, 4-19, 4-20, 4-21, 4-22, and 4-23. Note that susceptibility to SCC is highest for the heat treatments that produce maximum strength levels in the alloys. In general, susceptibility to SCC decreases with higher aging temperatures (lower strengths), but even some failures have been observed in overaged specimens.

TABLE 4-17. BEHAVIOR OF STRESSED COLD-ROLLED AUSTENITIC STAINLESS STEELS IN THE MARINE ATMOSPHERES[a][19]

Alloy	Cold Work, percent	Heat Treatment,[b] F	Yield Stress, ksi	Applied Stress		Exposure Time,[c] days
				ksi	Percent of Yield Strength	
Type 201	60	1100	188	141	75	702 F, 2226 F
	60	800	229	171	75	2460 NF
Type 202	60	1100	187	164	87.5	678 F
	60	800	215	161	75	2460 NF
Type 301	40	1100	151	126	83	2460 NF
	40	800	231	188	81	2460 NF
	60	800	238	178	75	240 NF
	Extra hard	750	271	190	70	347 F[d]
18Cr-15Mn[e]	60	1100	221	197	88	2460 NF
	60	800	239	179	75	2460 NF

(a) Bent-beam specimens exposed at the 80-foot lot, Kure Beach, NC.
(b) Heat treated for 2 hours at temperature indicated.
(c) F = failure; NF = no failure.
(d) One specimen out of eight failed; rest still OK at this time.
(e) Proprietary steel (USS Tenelon) containing small amounts of nickel and nitrogen.

TABLE 4-18. STRESS-CORROSION CRACKING RESULTS AT 80-FOOT LOT, KURE BEACH, FOR 17-4PH ALLOY IN VARIOUS CONDITIONS OF TREATMENT[20]

Alloy and Condition	Applied Stress		Number of Specimens		Average Time to Failure, days	Exposure of Unfailed Specimens, days
	ksi	Percent of Yield Strength	Exposed	Failed		
Not Welded						
17-4PH, H900	162.9	90	5	0	--	322
	135.8	75	5	0	--	322
17-4PH, H1025	139.9	90	5	0	--	322
	116.6	75	5	0	--	322
17-4PH, H1075	135.7	90	5	0	--	322
	113.1	75	5	0	--	322
17-4PH, H1150	101.9	90	5	0	--	322
	84.9	75	5	0	--	322
17-4PH, H900	--	90	5	3	322	560
17-4PH, H1150	--	90	5	0	--	560
Welded, Then Solution Treated and Aged						
17-4PH, H900	164.3	90	5	5	68	--
	137.0	75	5	4	114	322
17-4PH, H1025	143.6	90	5	0	--	322
	119.7	75	5	0	--	322
17-4PH, H1075	138.4	90	5	0	--	322
	115.4	75	5	0	--	322
17-4PH, H1150	117.4	90	5	0	--	322
	97.8	75	5	0	--	322
Solution Treated, Welded, and Aged						
17-4PH, H900	164.7	90	5	5	20	--
	137.3	75	5	5	31	--
17-4PH, H1025	144.7	90	5	0	--	322
	120.6	75	5	0	--	322
17-4PH, H1075	135.0	90	5	0	--	322
	112.5	75	5	0	--	322
17-4PH, H1150	103.9	90	5	0	--	322
	86.6	75	5	0	--	322

TABLE 4-19. STRESS-CORROSION CRACKING BEHAVIOR AT THE 80-FOOT RACK, KURE BEACH, NC, FOR SEMI-AUSTENITIC PRECIPITATION-HARDENING STAINLESS STEELS[20]

Alloy and Condition	Applied Stress		Number of Specimens		Average Time to Failure, days	Exposure Time of Unfailed Specimens, days	Direction
	ksi	Percent of Yield Strength	Exposed	Failed			
PH15-7Mo, TH1050	140	75	12	9	16	240	Longitudinal
	127	60	5	5	182	--	Transverse
	125	60	5	4	73	466	Transverse
	124	60	5	2	71	466	Transverse
	85	40	5	0	--	466	Transverse
	84	40	5	0	--	466	Transverse
	82	40	5	0	--	466	Transverse
PH15-7Mo, RH950	182	90	--	--	12 (a)	--	Longitudinal
	152	75	12	12	16	--	Longitudinal
	101	50	--	0(a)	--	175	Longitudinal
	131	60	5	5	28.2	--	Transverse
	132	60	5	5	22.2	--	Transverse
	131	60	5	5	19	--	Transverse
	87	40	5	4	173	466	Transverse
	88	40	5	4	74	466	Transverse
	87	40	5	1	82	466	Transverse
PH15-7Mo, RH1050	131	60	5	4	140	466	Transverse
	129	60	5	4	339	466	Transverse
	88	40	5	0	--	466	Transverse
	86	40	5	0	--	466	Transverse
PH15-7Mo, BCHT	140	60	5	5	24.2	--	Transverse
	140	60	5	5	44.2	--	Transverse
	93	40	5	5	49.6	--	Transverse
	94	40	5	5	61.6	--	Transverse

TABLE 4-19. (Continued)

Alloy and Condition	Applied Stress ksi	Applied Stress Percent of Yield Strength	Number of Specimens Exposed	Number of Specimens Failed	Average Time to Failure, days	Exposure Time of Unfailed Specimens, days	Direction
17-7PH, TH1050	110	75	27	7	21	320	Longitudinal
17-7PH, TH950	181	90	--	--	1 (a)	--	Longitudinal
	151	75	4	4	1	--	Longitudinal
	101	50	--	--	5 (a)	--	Longitudinal
17-7PH, RH950	183	90	--	--	2 (a)	--	Longitudinal
	152	75	30	21	5	380	Longitudinal
	102	50	--	--	16 (a)	--	Longitudinal
AM-355, CRT850	23.8	10	2	0	--	68	Longitudinal
	83.4	35	2	0	--	321	Longitudinal
	119.1	50	2	2	66	--	Longitudinal
	166.8	70	2	2	112	--	Longitudinal
	73.4	35	2	0	--	321	Longitudinal
	104.8	50	2	0	--	321	Longitudinal
	146.8	70	2	0	--	321	Longitudinal
AM-355, SCCRT850	30.4	10	2	0	--	68	Longitudinal
	106.4	35	2	0	--	461	Longitudinal
	152.0	50	2	1	319	461	Longitudinal
	212.8	70	2	2	21	--	Longitudinal

(a) Average of three or more specimens.

TABLE 4-20. STRESS-CORROSION CRACKING PERFORMANCE AT THE 800-FOOT RACK, KURE BEACH, NC, FOR SEMI-AUSTENITIC PRECIPITATION-HARDENING STAINLESS STEELS[20]

Alloy and Condition	Applied Stress		Number of Specimens		Average Time to Failure, days	Exposure Time of Unfailed Specimens, days	Direction
	ksi	Percent of Yield Strength	Exposed	Failed			
PH15-7Mo, TH1050	161	75	5	3	103	746	Transverse
	164	75	5	5	39.8	--	Transverse
	127	60	5	0	--	466	Transverse
	125	60	5	0	--	466	Transverse
	124	60	5	0	--	466	Transverse
	107	50	5	0	--	746	Transverse
	109	50	5	0	--	746	Transverse
	85	40	5	0	--	466	Transverse
	84	40	5	0	--	466	Transverse
	82	40	5	0	--	466	Transverse
PH15-7Mo, RH1050	131	60	5	0	--	466	Transverse
	129	60	5	0	--	466	Transverse
	88	40	5	0	--	466	Transverse
PH15-7Mo, RH950	174	75	5	5	68.8	--	Transverse
	175	75	5	5	14.2	--	Transverse
	131	60	5	4	179	466	Transverse
	132	60	5	4	126	466	Transverse
	131	60	5	4	164	466	Transverse
	116	50	5	5	169.4	--	Transverse
	117	50	5	5	98.8	--	Transverse
	87	40	5	1	346	466	Transverse
	88	40	5	0	--	466	Transverse
	87	40	5	0	--	466	Transverse
PH15-7Mo, BCHT	140	60	5	5	236.2	--	Transverse
	140	60	5	5	101.4	--	Transverse
	93	40	5	0	--	466	Transverse
	94	40	5	3	333	466	Transverse

TABLE 4-20. (Continued)

Alloy and Condition	Applied Stress ksi	Applied Stress Percent of Yield Strength	Number of Specimens Exposed	Number of Specimens Failed	Average Time to Failure, days	Exposure Time of Unfailed Specimens, days	Direction
PH15-7Mo, CH900	196	75	5	0	--	746	Transverse
	131	50	5	0	--	746	Transverse
17-7PH, TH1050	151	75	5	2	100	746	Transverse
	134	75	5	0	--	746	Transverse
	101	50	5	0	--	746	Transverse
	89	50	5	0	--	746	Transverse
17-7PH, RH950	168	75	5	5	7.4	--	Transverse
	165	75	5	5	51.6	--	Transverse
	112	50	5	5	30.2	--	Transverse
	110	50	5	1	116	746	Transverse
17-7PH, CH900	214	75	5	0	--	746	Transverse
	143	50	5	0	--	746	Transverse
AM-355, CRT850	23.8	10	2	0	--	68	Longitudinal
	83.4	35	2	0	--	321	Longitudinal
	119.1	50	2	0	--	321	Longitudinal
	166.8	70	2	2	152	--	Longitudinal
AM-355, CRT850	73.4	35	2	0	--	321	Longitudinal
	104.8	50	2	0	--	321	Longitudinal
	146.8	70	2	1	177	321	Longitudinal
AM-355, SCCRT850	30.4	10	2	0	--	68	Longitudinal
	106.4	35	2	0	--	461	Longitudinal
	152.0	50	2	0	--	461	Longitudinal
	212.8	70	2	0	--	461	Longitudinal

TABLE 4-21. HEAT TREATMENT OF THE SEMI-AUSTENITIC PRECIPITATION-HARDENABLE STAINLESS STEEL[20] IN TABLES 4-19 AND 4-20

Alloy	Condition	Austenite Conditioning		Transformation	Age or Temper	
		Temperature, F	Time, minutes		Temperature, F	Time, hours
17-7PH	TH1050	1400	90	Cool to 60 F within 1 hr, hold 30 min	1050	1-1/2
	TH950	1400	90	Cool to 60 F within 1 hr, hold 30 min	950	1-1/2
	RH950	1750	10	Hold 8 hr at -100 F	950	1
	TH1075	1400	90	Cool to 32-60 F within 1 hr, hold 30 min	1075	1-1/2
	TH1050	1400	90	Cool to 60 F within 1 hr, hold 30 min	1050	1-1/2
	RH950	1750	10	Hold 8 hr at -100 F	950	1
	CH900	--	--	Cold rolled at mill	900	1
PH15-7Mo	TH1050	1400	90	Cool to 60 F within 1 hr, hold 30 min	1050	1-1/2
	RH950	1750	10	Hold 8 hr at -100 F	950	1
	RH950	1750	20	Hold 5 hr at -110 F	950	1
	BCHT	1625	20	Cool to 1000 F in 45 min, air cool to room temp, 5 hr at -100 F	900	8
	TH1050	1400	90	Cool to 60 F within 1 hr, hold 30 min	1050	1-1/2
	RH950	1750	10	Hold 8 hr at -100 F	950	1
	CH900	--	--	Cold rolled at mill	900	1
	BCHT	1675	20	Cool to 1000 F in 45 min, cool to room temp, 8 hr at -100 F	900	24
AM-350	SCT850	1710	20	3 hr at -110 F	850	3
	BCHT	1675	20	Cool to 1000 F in 45 min, cool to room temp, 8 hr at -100 F	900	24
AM-355	SCT850	1710	20	3 hr at -110 F	850	3
	BCHT	1675	20	Cool to 1000 F in 45 min, cool to room temp, 8 hr at -100 F	900	24
	CRT850	--	--	Cold rolled	850	--
	SCCRT850	--	--	Subzero cooled, cold rolled	850	--

TABLE 4-22. STEEL ALLOY SMOOTH TENSILE SPECIMENS SCHEDULED FOR 4-YEARS EXPOSURE TO SEACOAST ATMOSPHERE[21]

Alloy	Temper	Test Direction[a]	Stress at 75% YS			Stress at 50% YS			Stress at 25% YS		
			Stress, ksi	Spec No.	Tf,[b] days	Stress, ksi	Spec No.	Tf,[b] days	Stress, ksi	Spec No.	Tf,[b] days
17-7PH	H1050	T	142.9	T15	141	95.3	T18				
				T16			T19				
				T17	141		T20				
PH15-7Mo	RH950	T	152.6	T15	41				50.9	T17	
				T16	41					T18	
PH15-7Mo	RH1050	T	146.3	T45	41	97.5	T48	41			
				T46	41		T49	41			
				T47	41		T50	73			
15-5PH	H1150M	T	69.8	T15		20.4	T18				
				T16			T19				
				T17			T20				
15-5PH	H900	T	128.4	T15					42.8	T17	
				T16						T18	
PH13-8Mo	H950	L	151.2	L15		100.8	L18				
				L16			L19				
				L17			L20				
PH13-8Mo	H950	T	147.5	T15		98.4	T18				
				T16			T19				
				T17			T20				
PH13-8Mo	H950	S	152.5	N15		101.7	N18				
				N16			N19				
				N17			N20				
PH13-8Mo	H1050	T	143.9	T45		89.3	T48				
				T46			T49				
				T47			T50				

TABLE 4-22. (Continued)

Alloy	Temper	Test Direction[a]	Stress at 75% YS			Stress at 50% YS			Stress at 25% YS		
			Stress, ksi	Spec No.	Tf,[b] days	Stress, ksi	Spec No.	Tf,[b] days	Stress, ksi	Spec No.	Tf,[b] days
431	HT200	L	124.1	L15					41.4	L17	
				L16						L18	
431	HT200	T	124.1	T15	141				41.4	T17	
				T16	561					T18	
431	HT200	S	115.3	N15					38.4	N17	
				N16						N18	
431	HT125	T	80.6	T45		53.7	T48				
				T46			T49				
				T47			T50				
AM-355	SCT850	T	114.4	T15					38.1	T17	
				T16						T18	
AM-355	SCT1000	T	127.3	T45		84.9	T48				
				T46			T49				
				T47			T50				
AM-355	SCT850	L	139.6	L15	41				46.5	L17	141
				L16	41					L18	141
AM-355	SCT850	T	142.7	T15	41				47.6	T17	141
				T16	41					T18	141
AM-355	SCT850	S	139.9	N15	41				46.7	N17	141
				N16	41					N18	499
AM-355	SCT1000	T	129.3	T45		86.2	T48				
				T46			T49				
				T47			T50				

(a) L = principal rolling or forging direction of product, T = width of product, and S = thickness of product.
(b) No entry in Tf (time to failure) column indicates specimen has not failed and is still in test.

TABLE 4-23. STRESS-CORROSION CRACKING RESULTS OF PH STAINLESS STEELS[a][22]

Alloy	Stress Direction	Temper	Applied Stress MPa	ksi	% YS	Salt Spray F/N[b]	Salt Spray Days	Seacoast F/N[b]	Seacoast Days
PH13-8Mo	ST	H1000	704	102	50	1/3	<180[d]	0/5	
			1056	153	75	0/3		2/5	82, 153
			1407	204	100	0/3		0/5	
	ST	H1050	631	92	50	0/3		0/5	
			947	137	75	0/3		0/5	
			1262	183	100	0/3		1/5	55
	LT	H1000	697	101	50	0/3		0/5	
			1045	152	75	1/3	<180[d]	0/5	
			1393	202	100	1/3	74[d]	0/5	
	LT	H1050	624	91	50	0/3		0/5	
			936	136	75	0/4		0/5	
			1248	181	100	0/3		0/4	
PH13-8Mo	Tr	H1000	693	101	50	0/3		0/5	
			1040	151	75	0/3		0/5	
			1386	201	100	0/3		0/5	
	Tr	H1050	624	91	50	0/3		0/5	
			936	136	75	0/3		0/5	
			1248	181	100	0/3		0/5	
PH13-8Mo	ST (C-Ring)	H1000	683	99	50	0/3		0/5	
			1024	149	75	0/3		0/5	
			1365	198	100	0/3		0/5	
	LT	H1000	683	99	50	0/3		0/5	
			1024	149	75	0/3		0/5	
			1365	198	100	0/3		0/5	
	LT	H1050	648	93	50	0/3		0/5	
			957	139	75	0/3		0/5	
			1276	185	100	0/3		0/5	
PH13-8Mo	ST	H1000	348	51	25			0/4	
			697	101	50	0/5		4/4	22, 34, 37, 91
			1045	152	75	2/5	35, 37	0/4	16, 55, 62, 336
			1393	202	100	2/5	35, 71		

TABLE 4-23. (Continued)

Alloy	Stress Direction	Temper	Applied Stress MPa	Applied Stress ksi	Applied Stress % YS	Salt Spray F/N[b]	Salt Spray Days	Seacoast F/N[b]	Seacoast Days
	ST	H1050	288	42	25			0/4	
			576	84	50	2/5	17, 86	0/4	
			863	125	75	0/5		0/4	
			1151	167	100	1/5	9		
	LT	H1000	697	101	50	1/3	32	3/3	13, 16, 82
			1045	152	75	0/3			
			1393	202	100	1/3	42		
	LT	H1050	291	42	25			0/3	
			583	85	50	1/3	28	0/3	
			874	127	75	1/3	15	0/3	
			1165	169	100	1/3	28		
PH13-8Mo	ST	H950	1024	149	75	2/3	7, 27	1/5	2
			1365	198	100	5/6	3, 10, 10, 13, 17	3/5	1, 5, 69
	LT	H950	1024	149	75	1/3	15		
			1365	198	100	0/3			
	LO	H950	1065	155	75	0/3			
			1420	206	100	0/3			
	ST	H1000	333	48	25	0/3		0/3	
			666	97	50	1/3	8	0/3	
			998	145	75	4/9	2, 7, 10, <180	2/5	2, 2
			1331	193	100	4/7	10, 10, 13, 27	0/5	
	ST (0.6 cm Dia)	H1000	333	48	25	0/3		0/5	
			666	97	50	3/3	7, 43, 139	3/5	16, 51[d], 106
			998	145	75	2/3	7, 7		
	ST (C-Ring)	H1000	666	193	50	0/3			
			998	145	75	0/3			
	LT	H1000	335	49	25			0/3	
			669	97	50	1/6	30	0/3	
			1004	146	75	2/6	13, 21		
			1338	194	100	0/3			
PH13-8Mo	LO	H1000	335	49	25			0/3	
			669	97	50	0/3		0/3	
			1004	146	75	0/3			
			1338	194	100	2/3	7, 7		

TABLE 4-23. (Continued)

Alloy	Stress Direction	Temper	Applied Stress MPa	Applied Stress ksi	Applied Stress % YS	Salt Spray F/N[b]	Salt Spray Days	Seacoast F/N[b]	Seacoast Days
	ST	H1050	307	45	25	0/3		0/3	
			614	89	50	1/3	44	0/3	
			921	134	75	2/3	7, 43		
	ST (C-Ring)	H1050	614	89	50	0/3			
			921	134	75	0/3			
	LT	H1050	290	42	25			0/3	
			579	84	50	0/3		0/3	
			869	126	75	1/3	45		
	LO	H1050	297	44	25			0/3	
			593	87	50	1/3	28	0/3	
			890	131	75	1/3	70		
PH13-8Mo	Tr	H950	1102	160	75	0/3			
			1469	213	100	0/3			
	Tr	H1000	1060	154	75	0/3			
			1413	205	100	1/3	13		
PH13-8Mo	Tr	H1000	342	50	25			0/4	
			683	99	50	0/4		0/4	
			1025	149	75	1/4	180		
	Tr	H1050	318	46	25			0/4	
			635	92	50	1/4	45	0/4	
			1053	138	75	1/4	24		
15-5PH	ST	H1000	565	80	50	0/4		0/5	
			848	120	75	0/3		0/5	
			1130	160	100	0/3		0/5	
15-5PH	ST	H1050	545	79	50	0/3		0/5	
			817	119	75	0/3		0/5	
			1089	158	100	0/3		0/5	
	LT	H1000	545	79	50	0/3		0/5	
			817	119	75	0/3		0/5	
			1089	158	100	0/3		0/5	

TABLE 4-23. (Continued)

Alloy	Stress Direction	Temper	Applied Stress MPa	Applied Stress ksi	Applied Stress % YS	Salt Spray F/N[b]	Salt Spray Days	Seacoast F/N[b]	Seacoast Days
	LT	H1050	538	78	50	0/3		0/5	
			807	117	75	0/3		0/5	
			1076	156	100	0/3		0/5	
15-5PH	Tr	H1000	566	82	50	0/3		0/5	
			848	123	75	0/3		0/4	
			1131	164	100	0/3		0/4	
	Tr	H1050	545	79	50	0/3		0/5	
			817	119	75	0/3		0/4	
			1089	158	100	0/3		0/4	
15-5PH	ST	H900	879	128	75			0/5	
			1172	170	100	1/2	<180	2/5	366, 384
	ST	H1000	797	116	75			0/5	
			1062	154	100	0/4		0/5	
17-4PH	ST	H1000	531	77	50	0/3		0/5	
			797	116	75	0/3		0/5	
			1062	154	100	1/3	23[d]	0/5	
	ST	H1050	527	77	50	0/3		0/5	
			791	115	75	0/3		0/5	
			1054	153	100	1/3	65[d]	0/5	
	LT	H1000	538	78	50	0/3		0/5	
			807	117	75	1/3	158[d]	0/5	
			1076	156	100	2/3	23[d], 26[d]	0/5	
	LT	H1050	521	76	50	0/3		0/5	
			781	113	75	0/3		0/5	
			1041	151	100	2/3	29[d], 58[d]	0/5	
15-5PH	LO	H1000	541	79	50	0/3			
			812	118	75	0/3			
			1082	157	100	0/3			

TABLE 4-23. (Continued)

Alloy	Stress Direction	Temper	Applied Stress MPa	Applied Stress ksi	Applied Stress % YS	Salt Spray F/N[b]	Salt Spray Days	Seacoast F/N[b]	Seacoast Days
17-4PH	Tr	H1000	521	76	50	0/3		0/5	
			781	113	75	1/3	24	1/5	76
			1041	151	100	2/3	16, 45	0/5	
	Tr	H1050	497	72	50	0/3		0/5	
			745	108	75	0/3		0/5	
			993	144	100	2/3	31, 36	1/5	13
17-4PH	ST	H900	869	126	75	2/3	6, 14	0/5	
			1158	168	100	3/3	2, 6, 35	0/5	
	ST	H1000	272	40	25	0/3		0/5	
			545	79	50	0/3		5/10	5, 7, 12, 68, 336
			817	119	75	3/6	7, 12, 16	8/10	5, 6, 7, 20, 40, 13, 57, 76
			1089	158	100	3/3	2, 6, 15		
	ST	H1050	264	39	25	0/3		1/5	82
			527	77	50	0/3		1/5	47
			791	116	75	3/3	7, 7, 8	3/5	43, 47, 55
	LT	H900	900	131	75	0/3			
			1200	174	100	1/3	139		
	LT	H1000	884	128	75	0/3			
			1179	171	100	0/3			
	LO	H900	931	135	75	0/3			
			1241	180	100	0/3			
	LO	H1000	833	121	75	0/3			
			1110	161	100	0/3			
	ST (C-Ring)	H900	869	126	75	0/3[c]			
			1158	168	100	0/2[c]			
	ST (C-Ring)	H1000	817	119	75	0/3[c]			
			1089	158	100	0/3[c]			
17-4PH[c]	Tr (C-Ring)	H900	1055	153	75	1/2	62		
			1407	204	100	2/3	62, 62		
	Tr (C-Ring)	H1000	848	123	75	0/3			
			1131	164	100	0/3			

TABLE 4-23. (Continued)

Alloy	Stress Direction	Temper	Applied Stress MPa	Applied Stress ksi	Applied Stress % YS	Salt Spray F/N[b]	Salt Spray Days	Seacoast F/N[b]	Seacoast Days
	LO	H900	1055	153	75	0/3			
			1407	204	100	0/3			
	LO	H1000	848	123	75	0/3			
			1131	164	100	0/3			
17-4PH[c]	Tr (C-Ring)	H900	900	131	75	0/3			
			1200	174	100	0/3			
	Tr (C-Ring)	H1000	822	119	75	0/3			
			1096	159	100	0/3			
	LO	H900	900	131	75	0/3			
			1200	174	100	0/3			
	LO	H1000	822	119	75	0/3			
			1096	159	100	0/3			
17-4PH[c]	ST (C-Ring)	H900	895	129	75	0/2			
			1193	173	100	0/3			
	ST (C-Ring)	H1000	817	119	75	0/2			
			1089	158	100	0/2			
	LT (C-Ring)	H900	895	129	75	0/2			
			1193	173	100	0/3			
	LT (C-Ring)	H1000	817	119	75	0/2			
			1089	158	100	0/2			
	LO	H900	895	129	75	0/2			
			1193	173	100	0/3			
	LO	H1000	817	119	75	0/2			
			1089	158	100	0/3			

(a) Test Data: Specimen was 0.3-cm diameter tensile unless noted otherwise and exposure time was until failure or 6 months for salt spray and 14 months for seacoast.
(b) F/N: ratio of failures to total number of specimens exposed.
(c) These C-rings and tensiles were exposed to alternate immersion for 6 months, and then they were unloaded, cleaned, vapor blasted, restressed, and exposed for 3 months to salt spray.
(d) Specimens broke under the coating or at coating-specimen interface; all others broke in reduced section.

The fracture toughness rating of several of the high strength stainless steels is summarized by Stanley in Table 4-24. Note that the stress intensity required to propagate a crack in the marine atmosphere (K_{Iscc}) is a function of the alloy and its heat treatment. Also note the low K_{Iscc} value for sensitized Type 304 stainless steel.

Splash and Tide Zones

General Corrosion and Pitting

Splash. The stainless steels, as a group, usually do well in the splash zone. The availability of well-aerated seawater tends to maintain the passivity of stainless steels without difficulty, provided crevices and shielded areas are avoided in the design. Since the splash zone is above the point at which marine life develops on the metal surface, biofouling is not a factor. As with atmospheric exposure, the austenitic grades are superior to the martensitic and ferritic grades.

The 300 series, particularly Types 304 and 316, have been used with success for small deck-mounted fittings for seagoing pleasure boats and other craft. Removal of sea-salt deposits by hosing with fresh water plus occasional polishing will keep such fittings in good condition. When salt deposits are allowed to accumulate, particularly at crevices, there is a tendency for local attack. This has been observed between the strands of stainless steel rope, in the threads of tensioning screws, and at the point where wire ropes enter swaged ferrules.

Anderson and Ross[23] have summarized in Table 4-25 the corrosion performance of stainless steel fasteners in Alloy 400 sheathing in the splash zone at Wrightsville Beach, NC. Since the electrochemical potentials of the stainless steels are very close to that of Alloy 400, galvanic corrosion effects can be neglected. Thus, the results in Table 4-25 indicate that even 12 Cr (Type 410) performs well in the splash zone, although its performance was not as good as that of 16 Cr or 18Cr-8Ni alloys.

Tide. Even though the tide zone is well aerated a large part of the time, there are factors present in this environmental zone that interfere with the maintenance of passivity. Marine animals, such as barnacles and mollusks, as well as other types of fouling settle in the tide zone (and below) and shield the surface from the oxygen needed for passivity. Crevice attack at areas of restricted access such as structural joints is more apt to take place in the tide zone, where, during the immersed portion of the day, relatively large areas outside the crevice are available to serve as cathodes.

TABLE 4-24. FRACTURE TOUGHNESS RATING OF ALLOYS AND HEAT TREATMENTS ON THEIR RESISTANCE TO SALT WATER ENVIRONMENTS[17]

Material[a]	Heat Treatment	Ultimate Tensile Strength, ksi	Seacoast Test		Accelerated Test[c]	
			K_{Iscc}	$\frac{K_{Iscc}}{K_{Ic}}$	K_{Iscc}	$\frac{K_{Iscc}}{K_{Ic}}$
Inconel 718[b]	1950 F, AC, 8 hr, 1350 F + FC to 1200 F for 24 hr	189.6	>106	0.87	130	0.98
17-4PH[b]	H1150	151.6	>93.9	0.77	110	0.89
AISI 304	Annealed	84.0	>53.5	0.77	59.7	0.86
4340	800 F temper	204.8	48.3	0.72	29.7	0.44
17-4PH	H900	202.4	<38.5	0.69	40.3	0.72
H-11 (AM)	1100 F temper	282.6	39.5	0.62	23.2	0.24
410[b]	1125 F temper	128.8	52.4	0.55	49.6	0.52
H-11 (AM)	1000 F temper	300.3	16.7	0.52	8.6	0.27
18Ni(250)Mar.	900 F	269.5	55.6	0.50	72.9	0.65
H-11 (VM)	1000 F temper		11.4	0.40	10.8	0.38
4340	475 F temper	267.2	13.3	0.29	11.1	0.24
AM-355 (FH)	SCT1000		33.1	0.28	50.3	0.42
AM-355	SCT1000	169.4	24.5	0.24	36.7	0.43
410	650 F temper	197.0	22.0	0.24	23.8	0.26
AM-355	SCT850	195.9	<10.7	<0.22	24.9	0.52
AM-355 (FH)	SCT850		<9.7	<0.15	~6.2	~0.10
AISI 304	Sensitized 100 hr at 1100 F	83.9	<8.5	<0.12	<15.2	<0.22

(a) Explanation of abbreviations: AM - Air Melt, VM - Vacuum Melt, FH - Fully Hardened.
(b) Plane strain conditions maintained only at low stress intensities. Therefore, values are approximate. True plane strain K_{Iscc} could not be obtained.
(c) 1000 hours in salt solution.

TABLE 4-25. SUMMARY OF SHEATHING FASTENERS EXPOSED IN THE SPLASH ZONE AT WRIGHTSVILLE BEACH, NC[23]

Alloy	Period, yr	Mechanical Properties	Corrosion Properties
Duranickel Alloy 301	15	OK	Excellent
Monel Ni-Cu Alloy 400	25	OK	Excellent
Monel Ni-Cu Alloy K-500	25	OK	Excellent
Type 305 SS	15	OK	Excellent
Type 316 SS	25	OK	Excellent
Type 410 SS	15	OK	Good
Type 431 SS	15	OK	Excellent
Inconel Alloy X-750	25	OK	Excellent

Thus, corrosion performance in the tide zone approaches that of full immersion. The conventional stainless steels exhibit pitting in the tide zone, and only the highly alloyed Cr-Mo and Cr-Ni-Mo alloys, that are resistant to pitting under submerged conditions, are resistant to pitting in the tide zone. Note in Tables 4-26 and 4-27 that after 16-year exposures in the tide zone, general corrosion rates of austenitic stainless steels are low at <1.0 mpy and the maximum depth pitting rates are relatively low at 2 to 7 mpy. Also note that the average of the 20 deepest pits did not increase between 8 and 16 years' exposure, thereby suggesting little propagation of attack after 8 years.

Galvanic Corrosion

Southwell, et al.[24] have examined the long term galvanic corrosion behavior in the tide zone of stainless steel coupled to several dissimilar metals. Their results for 16-year exposures are presented in Table 4-28. Note that where the stainless steel area was less than that of the dissimilar metal, there was little or no increased corrosion of either member of the couple which included stainless steel coupled to carbon steel, phosphor bronze, or naval brass.

TABLE 4-26. GENERAL CORROSION DATA FOR STAINLESS STEELS IN AQUEOUS ENVIRONMENTS[24]

Metals[a] Type	Exposure[b]	General Corrosion: Weight Loss, g/m^2 1 Yr	8 Yr	16 Yr	General Corrosion: Average Penetration, mils[c] 1 Yr	8 Yr	16 Yr	Final Steady State Rate,[d] mpy
410 Stainless	S	600	2810	4680	3.1[e]	14.3[e]	23.9[e]	(e)
steel (13Cr)	M	100	670	1260	0.5	3.4[e]	6.4[e]	(e)
	L	0	110	180	0.0	0.5	0.9[e]	(e)
302 Stainless	S	290	1100	1870	1.5[e]	5.5[e]	9.5[e]	(e)
steel	M	40	180	330	0.2	0.9	1.6	(e)
(18Cr-8Ni)	L	0	0	0	0.0	0.0	0.0	0.0
316 Stainless	S	120	410	160	0.6[e]	2.0[e]	0.8[e]	(e)
steel (18-13	M	10	40	20	0.1	0.2	0.1	(e)
+ Mo)	L	0	0	0	0.0	0.0	0.0	0.0
321 Stainless	S	230	1000	1460	1.2[e]	5.0[e]	7.3[e]	(e)
steel (17-10	M	30	130	230	0.1	0.7	1.1	(e)
+ Ti)	L	0	0	0	0.0	0.0	0.0	0.0

(a) As received, surface degreased before exposure.
(b) S = Seawater immersion; M = Seawater mean tide; L = Lake water immersion.
(c) Mils x 0.0254 = mm. Values calculated from weight losses.
(d) Slope of linear portion of time-corrosion curve, or if nonlinear, the slope of the tangent at 16 years.
(e) Deep local-action pitting; average penetration values not appropriate.

TABLE 4 '. PITTING DATA FOR STAINLESS STEELS IN AQUEOUS ENVIRONMENTS[24]

Metals[a] Type	Exposure[b]	Pitting Penetration, mils			
		Average 20 Deepest Pits[c]			
		1 Yr	8 Yr	16 Yr	Deepest Pit[d]
410 Stainless steel	S	61P[e]	161P[e]	212	p[e]
(13Cr)	M	46	67	107	p[e]
	L	<5	<5	94	p[e]
302 Stainless steel	S	70P[e]	140	151	p[e]
(18Cr-8Ni)	M	6	58	50	110
	L	<5	<5	<5	<5
316 Stainless steel	S	45P[e]	156P[e]	95	p[e]
(18-13 + Mo)	M	5	16	13	36
	L	<5	<5	<5	<5
321 Stainless steel	S	64	193P[e]	237	p[e]
(17-10 + Ti)	M	7	56	55	93
	L	<5	<5	<5	<5

(a) As received, surface degreased before exposure.
(b) S = Seawater immersion; M = Seawater mean tide; L = Lake water immersion.
(c) The twenty-pit average is determined from the five deepest pits on each surface of duplicate panels.
(d) The deepest single pit during the 16-year exposure.
(e) P = perforation.

TABLE 4-28. CORROSION DAMAGE DATA FOR METALS EXPOSED AS BIMETALLIC COUPLES IN AQUEOUS ENVIRONMENTS[24]

Couple		Average Strip Metal Penetration, mils[a]									Average Plate Metal Penetration, mils[a]								
		Seawater			Mean Tide			Fresh Water			Seawater			Mean Tide			Fresh Water		
Strip, 2 x 9 x 1/4 in.	Plate, 9 x 9 x 1/4 in.	1 Yr	8 Yr	16 Yr	1 Yr	8 Yr	16 Yr	1 Yr	8 Yr	16 Yr	1 Yr	8 Yr	16 Yr	1 Yr	8 Yr	16 Yr	1 Yr	8 Yr	16 Yr
316 Stainless steel (18-13 + Mo)	Carbon steel[b] (0.24% Cu)	0.0	0.0	0.1 2.0*[c]	0.1	0.0	0.1 0.2*	0.0	0.0	0.0 0.0*	7.9	28.3	49.5 48.1*	12.2	24.7	43.7 45.2*	8.0	25.1	32.4 26.0*
316 Stainless steel (18-13 + Mo)	Naval brass (39Zn-1Sn)	0.0	0.0	0.0 2.0*	0.0	0.0	0.0 0.2*	0.0	0.0	0.0 0.0*	3.9	9.3	16.2 12.4*	1.0	4.7	7.7 6.0*	0.4	2.0	2.5 1.9*
316 Stainless steel (18-13 + Mo)	Phosphor bronze (4Sn-0.25P)	0.0	0.0	0.0 2.0*	0.0	0.0	0.0 0.2*	0.0	0.0	0.0 0.0*	1.6	6.0	9.4 5.5*	0.7	3.4	6.1 3.5*	0.2	0.7	0.7 0.7*
316 Stainless steel (18-13 + Mo)	316 Stainless steel (18-13 + Mo)	0.0	0.3	3.1 2.0*	0.0	0.1	0.1 0.2*	0.0	0.0	0.0 0.0*	0.0	0.6	1.3 2.0*	0.0	0.0	0.1 0.2*	0.0	0.0	0.0 0.0*
302 Stainless steel (18Cr-8Ni)	Carbon steel (0.24% C)	0.0	0.0	0.2 9.3*	0.1	0.0	0.1 1.6*	0.0	0.0	0.0 0.0*	7.5	27.3	50.6 48.1*	11.7	23.0	47.2 45.2*	8.1	25.0	31.7 26.0*
302 Stainless steel (18Cr-8Ni)	302 Stainless steel (18Cr-8Ni)	0.1	5.7	8.2 9.3*	0.2	0.5	1.3 1.6*	0.0	0.1	0.1 0.0*	0.3	4.5	7.6 2.0*	0.1	0.7	1.2 0.2*	0.0	0.0	0.0 0.0*
Phosphor bronze (4Sn-0.25P)	410 Stainless steel (13% Cr)	0.5	0.4	0.7 5.5*	0.4	0.6	0.7 3.5*	0.2	0.7	0.9 0.7*	3.5	14.7	24.7 23.9*	0.6	4.2	8.8 6.4*	0.1	1.4	3.3 0.9*
Phosphor bronze (4Sn-0.25P)	302 Stainless steel (18Cr-8Ni)	7.8	16.3	21.9 5.5*	1.1	8.5	13.7 3.5*	0.5	4.1	3.8 0.7*	0.0	3.8	6.3 9.3*	0.1	0.4	1.0 1.1*	0.0	0.0	0.0 0.0*
Phosphor bronze (4Sn-0.25P)	316 Stainless steel (18-13 + Mo)	22.8	37.4	41.3 5.5*	3.2	21.9	29.8 3.5*	0.3	1.7	1.8 0.7*	0.0	0.2	0.2 2.0*	0.0	0.0	0.0 0.2*	0.0	0.0	0.0 0.0*
Carbon steel (0.24% C)	410 Stainless steel (13% Cr)	32.8	159.9 25.5*	M	22.2	73.7	178.4 45.2*	11.8	45.2	56.4 26.0*	0.2	0.1	9.2 23.9*	0.1	0.1	0.5 6.4*	0.0	0.0	0.0 0.9*
Carbon steel (0.24% C)	302 Stainless steel (18Cr-8Ni)	34.7	146.4 25.5*	M	22.7	88.9	175.6 45.2*	11.8	41.1	52.7 26.0*	0.0	0.0	0.8 9.5*	0.0	0.0	0.0 1.6*	0.0	0.0	0.0 0.0*
Carbon steel (0.24% C)	316 Stainless steel (18-13 + Mo)	34.7	140.6 25.5*	M	22.6	81.9	175.4 45.2*	10.5	33.3	44.4 26.0*	0.0	0.0	0.0 2.0*	0.0	0.0	0.0 0.1*	0.0	0.0	0.0 0.0*

(a) Mils x 0.0254 = mm. Values calculated from weight losses.
(b) A couple consisting of a strip of 316 stainless steel with an exposed area of 21.9 in.^{2} attached to a plate of carbon steel with an exposed area of 151.4 in.^{2} (area ratio = 1:6.9).
(c) Values marked with an asterisk (*) show the normal uncoupled corrosion loss.

However, when the area of the stainless steel was larger in the couple, there was increased attack (galvanic corrosion) of the dissimilar metals, carbon steel, and phosphor bronze. A practical guide for dissimilar metal couples has been compiled by Ballantine[25] and is presented in Table 4-29. Note that even in the area above the water line, only those metals with similar corrosion potentials can be safely coupled without undue corrosion. (See Figure 4-2 for the galvanic series in seawater.)

Stress-Corrosion Cracking

There appear to be no data on the SCC of stainless steels in the splash or tide zone. However, data have been obtained in salt spray tests and in 10-min in/50-min out alternate immersion tests in 3.5 percent NaCl solution. The latter probably more nearly simulates tide zone exposure while the salt spray test more nearly simulates the splash zone.

Few data are available for the austenitic alloys, but based on performance in the atmosphere and under submerged conditions, one would expect the low carbon grades and the mill annealed (solution treated) material for all carbon grades to be resistant to SCC. The sensitized normal carbon grade austenitic alloys would be expected to exhibit SCC in both the splash and tide zones. Humphries and Nelson[26] have exposed specimens stressed to 75 to 100 percent of yield for 6 months to the 3.5 percent NaCl alternate immersion test with the following results:

Alloy	Failures/Specimens
301	0/3
303	1/10
304	0/3
Armco 21-6-9	0/3

No explanation was given for the one failure in the tests with 303 stainless, but it is possible that it may have been sensitized.

Salt-spray tests results for a number of precipitation-hardened stainless steels are presented in Table 4-23. The results presented in this table suggest that the salt-spray test is more aggressive in producing SCC than is a marine atmosphere. These salt-spray test results also indicate that the higher strength alloys are more susceptible to SCC than are the overaged lower strength alloys, although there are exceptions.

TABLE 4-29. GUIDE FOR SELECTION OF FASTENER ALLOY FOR MARINE SERVICE ABOVE WATERLINE(25)[1]

Recommended Alloys are Listed in Order of Their Preference

Hull Superstructure or Base Plate Material	Trim Material to be Attached											
	Wood	Fiberglass	Rubber	Plastic (Nylon)	Aluminum	Steel	Steel (Galvanized)	Copper	Brass	Brass (Plated)	Nickel Stainless Steel	Monel Nickel-Copper Alloys
Wood	Monel 18-8 Stainless Steel Silicon Bronze	Monel 18-8 Stainless Steel Silicon Bronze	Monel 18-8 Stainless Steel Silicon Bronze	Monel 18-8 Stainless Steel Silicon Bronze	18-8 Stainless Steel Aluminum	Monel 18-8 Stainless Steel Silicon Bronze	Monel 18-8 Stainless Steel Silicon Bronze	Silicon Bronze 18-8 Stainless Steel Monel	Silicon Bronze 18-8 Stainless Steel Monel	18-8 Stainless Steel Monel	18-8 Stainless Steel Monel	Monel 18-8 Stainless Steel
Fiberglass	Monel 18-8 Stainless Steel Silicon Bronze	Monel 18-8 Stainless Steel Silicon Bronze	Monel 18-8 Stainless Steel Silicon Bronze	Monel 18-8 Stainless Steel Silicon Bronze	18-8 Stainless Steel Aluminum	Monel 18-8 Stainless Steel Silicon Bronze	Monel 18-8 Stainless Steel Silicon Bronze	Silicon Bronze 18-8 Stainless Steel Monel	Silicon Bronze 18-8 Stainless Steel Monel	18-8 Stainless Steel Monel	18-8 Stainless Steel Monel	Monel 18-8 Stainless Steel
Rubber	Monel 18-8 Stainless Steel Silicon Bronze	Monel 18-8 Stainless Steel Silicon Bronze	Monel 18-8 Stainless Steel Silicon Bronze	Monel 18-8 Stainless Steel Silicon Bronze	18-8 Stainless Steel Aluminum	Monel 18-8 Stainless Steel Silicon Bronze	Monel 18-8 Stainless Steel Silicon Bronze	Silicon Bronze 18-8 Stainless Steel Monel	Silicon Bronze 18-8 Stainless Steel Monel	18-8 Stainless Steel Monel	18-8 Stainless Steel Monel	Monel 18-8 Stainless Steel
Plastic (Nylon)	Monel 18-8 Stainless Steel Silicon Bronze	Monel 18-8 Stainless Steel Silicon Bronze	Monel 18-8 Stainless Steel Silicon Bronze	Monel 18-8 Stainless Steel Silicon Bronze	18-8 Stainless Steel Aluminum	Monel 18-8 Stainless Steel Silicon Bronze	Monel 18-8 Stainless Steel Silicon Bronze	Silicon Bronze 18-8 Stainless Steel Monel	Silicon Bronze 18-8 Stainless Steel Monel	18-8 Stainless Steel Monel	18-8 Stainless Steel Monel	Avoid
Aluminum	18-8 Stainless Steel Aluminum	18-8 Stainless Steel Aluminum	18-8 Stainless Steel Aluminum	18-8 Stainless Steel Aluminum	18-8 Stainless Steel Aluminum	18-8 Stainless Steel Aluminum	18-8 Stainless Steel Aluminum	Avoid	Avoid	Avoid	18-8 Stainless Steel	Avoid
Steel	Monel 18-8 Stainless Steel	Monel 18-8 Stainless Steel	Monel 18-8 Stainless Steel	Monel 18-8 Stainless Steel	18-8 Stainless Steel Aluminum	Monel 18-8 Stainless Steel Silicon Bronze	Monel 18-8 Stainless Steel Silicon Bronze	Silicon Bronze 18-8 Stainless Steel Monel	Silicon Bronze 18-8 Stainless Steel Monel	18-8 Stainless Steel Monel	18-8 Stainless Steel Monel	Monel 18-8 Stainless Steel
Steel (Galvanized)	Silicon Bronze	Silicon Bronze	Silicon Bronze	Silicon Bronze	Avoid	Monel 18-8 Stainless Steel Silicon Bronze	Monel 18-8 Stainless Steel Silicon Bronze	Silicon Bronze 18-8 Stainless Steel Monel	Silicon Bronze 18-8 Stainless Steel Monel	18-8 Stainless Steel Monel	18-8 Stainless Steel Monel	Monel 18-8 Stainless Steel
Copper	Silicon Bronze 18-8 Stainless Steel	Silicon Bronze 18-8 Stainless Steel	Silicon Bronze 18-8 Stainless Steel	Silicon Bronze 18-8 Stainless Steel	Avoid	Silicon Bronze 18-8 Stainless Steel Monel	Silicon Bronze 18-8 Stainless Steel Monel	Silicon Bronze 18-8 Stainless Steel Monel	Silicon Bronze 18-8 Stainless Steel Monel	18-8 Stainless Steel Monel	18-8 Stainless Steel Monel	18-8 Stainless Steel
Brass	Monel	Monel	Monel	Monel	Avoid	Silicon Bronze 18-8 Stainless Steel Monel	Silicon Bronze 18-8 Stainless Steel Monel	Silicon Bronze 18-8 Stainless Steel Monel	Silicon Bronze 18-8 Stainless Steel Monel	18-8 Stainless Steel Monel	18-8 Stainless Steel Monel	18-8 Stainless Steel Monel
Brass (Plated)	18-8 Stainless Steel Monel	18-8 Stainless Steel Monel	18-8 Stainless Steel Monel	18-8 Stainless Steel Monel	Avoid	18-8 Stainless Steel Monel	18-8 Stainless Steel Monel	18-8 Stainless Steel Monel	18-8 Stainless Steel Monel	18-8 Stainless Steel Monel	18-8 Stainless Steel Monel	Avoid
Nickel Stainless Steel	18-8 Stainless Steel Monel	18-8 Stainless Steel Monel	18-8 Stainless Steel Monel	18-8 Stainless Steel Monel	18-8 Stainless Steel	18-8 Stainless Steel Monel	18-8 Stainless Steel Monel	18-8 Stainless Steel Monel	18-8 Stainless Steel Monel	18-8 Stainless Steel Monel	18-8 Stainless Steel	Monel 18-8 Stainless Steel
Monel Nickel-Copper Alloys	Monel 18-8 Stainless Steel	Monel 18-8 Stainless Steel	Monel 18-8 Stainless Steel	Monel 18-8 Stainless Steel	Avoid	Monel 18-8 Stainless Steel	Monel 18-8 Stainless Steel	Monel 18-8 Stainless Steel	Monel 18-8 Stainless Steel	Monel 18-8 Stainless Steel	Monel 18-8 Stainless Steel	Monel

Effects of corrosion action on fastener alloys: Monel—develops grey-green corrosion film; 18-8 stainless steel—develops light brown corrosion film and heavier scaling in crevices, i.e., threads and under boltheads, some bleeding; silicon bronze—develops heavy green-brown corrosion film, bleeds; and aluminum—develops white powdery corrosion film interspersed with pits unless specially protected, limited usefulness.

The results of alternate immersion tests in 3.5 percent NaCl solution conducted by Sprowls, et al.[21] are summarized below. These tests were conducted for 205 days.

Alloy	Temper	Direction	% YS	Failure/Number	Failure, days
PH15-7Mo	RH950	T	75	2/3	1, 1
PH15-7Mo	RH1050	T	75	5/5	1, 1, 1, 1, 1
PH15-7Mo	RH1050	T	50	3/3	1, 2, 4
431	HT200	S	75	1/4	5
AM-355 Bar	SCT850	L	75	2/4	4, 4
AM-355 Bar	SCT850	T	75	1/4	7
AM-355 Bar	SCT850	S	75	2/4	3, 7
AM-355 Bar	SCT1000	T	75	1/5	138

Note that SCC failures were observed for all alloys within 7 days except for AM-355 SCT1000 where 1 specimen failed in 138 days and the other 4 specimens survived 205-days' exposure. In these same tests, no specimens of 17-7PH RH1050 failed in 205 days of exposure. Several other investigators also have observed no failures of PH alloys in the alternate immersion test, namely:

Deel and Mindlin[27] (7 Specimens, 1000-hr Exposure, 80% YS, 3.5% NaCl)

15-5PH	H1025	No SCC
PH13-8Mo	H1000	No SCC

Deel and Mindlin[28] (Same Conditions as Above)

17-7PH	H900	No SCC

Hatfield and Slavick[29] (90% YS, 90 Days in Synthetic Seawater)

PH14-8Mo	SRH1050	No SCC
PH14-8Mo	SRH900	No SCC
17-7PH	TH1050	No SCC

Immersion

General Corrosion

The general corrosion rates of stainless steels in seawater are so low that metal loss rates are of no consequence to structural integrity. From Table 4-30 which summarizes the corrosion behavior of the conventional stainless steels, it can be seen that pitting and crevice corrosion are the most usual forms of attack. These failure modes will be discussed in detail in the next section, and where available, data for general corrosion rates will be reported. However, it should be remembered, that the general corrosion rate data may include weight changes due to pitting, and thus the reported values may be much higher than the actual rates of general attack.

TABLE 4-30. SUMMARY OF THE BEHAVIOR OF REPRESENTATIVE STAINLESS STEELS IN SURFACE SEAWATER[30]

Stainless Steel	Pitting and Crevice Attack	Cathodic Protection	High Velocity	Comments
Type 410 (martensitic)	Very susceptible	Not applicable (hydrogen damage)	Not used	Not suitable for immersed service
Type 430 (ferritic)	Susceptible, but longer induction period than Type 410	Not applicable (hydrogen damage)	Not used	Not suitable for immersed service
17-4PH (martensitic precipitation hardening)	Susceptible	Effective for control of crevice and pitting	Good performance	
Type 304 (austenitic)	Susceptible	Effective for control of crevice and pitting	Good performance	Velocity must be continuous at approximately 5 fps or more to maintain passivation
Type 316 (austenitic)	Susceptible; pit initiation may be retarded, but attack, once started, often equals that for Type 304	Effective for control of crevice and pitting	Excellent performance	
Alloy 20 Cb (austenitic)	Less susceptible	Effective for control of crevice and pitting	Excellent performance	

Pitting and Crevice Corrosion

The principal failure modes of most stainless steels immersed in seawater are pitting or crevice corrosion. As will be discussed later, certain alloys that contain molybdenum are resistant to these forms of failure.

The chromium ferritic and martensitic alloys, as well as the common austenitic alloys (including Type 316), will pit in low velocity seawater (<5 fps) in part, because suspended matter settles on, or marine life becomes attached to, the surface. The areas beneath these deposits/marine growth become anodic because of oxygen depletion, and localized attack results. On freely exposed surfaces, velocities in excess of 5 fps are usually sufficient to prevent deposits/growths, and pitting does not occur. However, even at high water velocities, attack may occur in crevices (overlapping joints, gaskets, washers, etc.). Experience with crevice corrosion in service equipment has been summarized by Sedriks[31] (see Table 4-31).

TABLE 4-31. EXPERIENCE WITH CREVICE CORROSION IN SERVICE EQUIPMENT[31]

Frequent Problems	Infrequent Problems
Metal-to-Metal Crevices	
Bolt head to washer	Sleeve to pump shaft
Washer to baseplate	Tube to tube sheet
Bolt thread to nut thread	
Wire rope	
Root pass of pipe welds with incomplete fusion	
Attachment pads to vessel wall	
Fillet-welded rib to deck	
Metal-to-Nonmetal Crevices	
O-ring to polished surface	Valve-stem packing
Gasket to flange face	Pump-shaft packing
Teflon to metal	Dirt deposits
Polyethylene tape to metal	Rubber gasket to metal plate in plate-type heat exchangers
Barnacle to metal	
Silicone to metal	Sand or mud deposits
Molybdenum disulfide to metal	
Graphite-lubricated gasket to metal	

Effect of Alloy Composition. The pitting susceptibility of the common stainless steels was demonstrated as early as 1945 in long-term tests at Kure Beach, NC, reported by Larrabee in Table 4-32. Other long term results have been reported by Alexander, et al. for exposure in the Panama Canal Zone (Figure 4-3); Reinhart for deep ocean exposure west of Port Hueneme, CA (Table 4-33); Lawson, et al. in the 110 F to 200 F heat recovery portion at a desalination plant in Freeport, Texas (Figure 4-4); Garner (Table 4-34) at several locations; and Kowaka, et al. for crevice tests conducted in Japan (Figure 4-5). Note that the data in the latter figure are reported as loss per unit area and thus are qualitative for rating depth of attack. Also note from the data presented that even Type 316 stainless steel (2 to 3 percent Mo) is susceptible to pitting and crevice corrosion. As noted in Figure 4-3, perforations were observed in 245-mil thick Type 316 coupons after one year of exposure in the tropical waters of the Panama Canal Zone.

Comparable results have been observed in condenser tubes exposed under service conditions. Baker, et al.[37] report that tubes at one particular site in England started to leak at 8 months, and all tubes had leaked by 11 months with an overall ranking of pitting resistance of 316L > 316 > 304L > 304. At another site these same authors reported perforation of 304 and 304L tubes, but no perforations of 316 and 316L tubes after 2 years of condenser operations (25.4 mm OD tubing by 1.2 mm wall thickness). Hoskinson and Kuester[38] also report that the service performance of Type 316 condenser tubes has been variable, with 8 reported failures within 2 years at one power plant and only slight pitting with no service failures at another.

TABLE 4-32. CORROSION TESTS IN SEAWATER AT KURE BEACH, NC[1]

Composition				Duration,	Corrosion Rate,		Maximum Pitting,	
Cr	Ni	Mo	C	yr	mg/dm^2/day	in./yr	mm	in.
13.15	--	--	0.08	1.56	12	0.0022	1.48	0.058
17.3	--	--	0.10	1.56	9	0.0017	2.74	0.108
18.5	9.0	--	0.05	1.88	0.5	0.0009	3.3	0.130
18.8	10.2	2.7	0.05	5.26	0.4	0.0008	0.94	0.037
24.0	21.0	--	0.12	2.71	0.7	0.0013	0.48	0.019

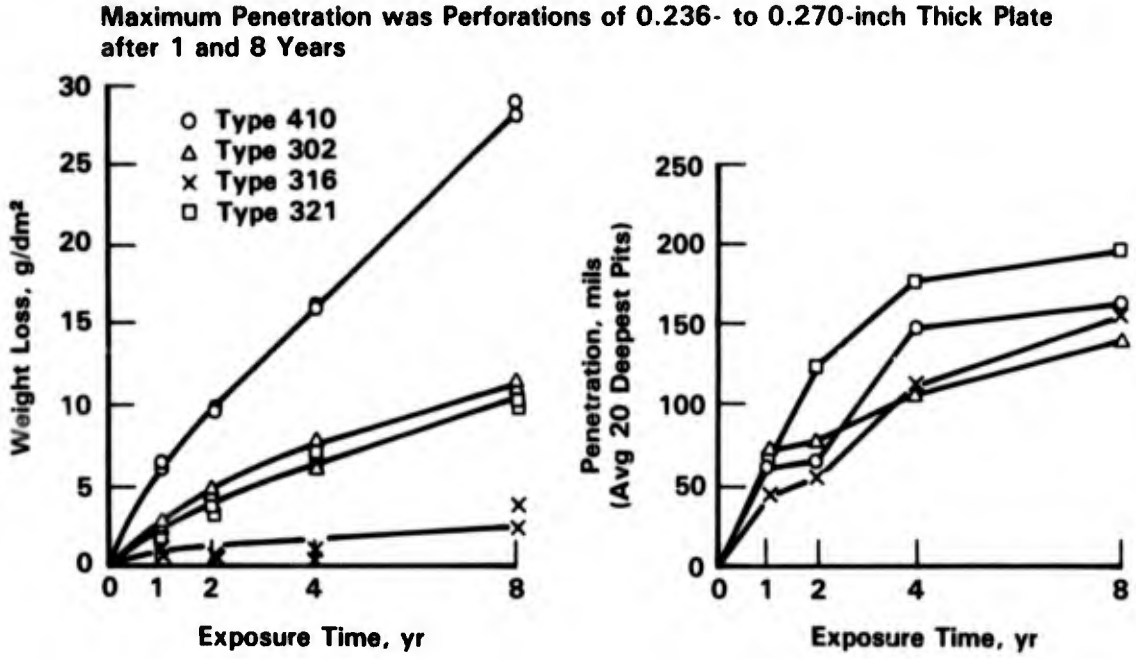

FIGURE 4-3. COMPARATIVE CORROSION OF VARIOUS STAINLESS STEEL ALLOYS CONTINUOUSLY IMMERSED IN TROPICAL SEAWATER[32]

TABLE 4-33. DEEP-OCEAN BEHAVIOR OF STAINLESS STEELS[33]

Type	Depth,[a] ft	Exposure Time, days	Crevice Attack, mils		Local Corrosion
			Water	Mud	
410	2,340	197	10	15	Edge and tunnel attack
	5,640	123	Slight	Slight	Severe tunnel
430	2,340	197	17	19	Tunnel
	5,300	1,064	25, 97	40	Severe tunnel
304	2,340	197	11	Slight	Edge, tunnel
	5,300	1,064	21	29	None in water; tunnel in mud
304L	2,340	197	8	18	Tunnel
	5,300	1,064	27, perforated	0	Severe tunnel
316	2,340	197	0	0	None visible
	5,300	1,064	21, 12	0	None
	5,640	123	0	0	Slight edge
316L	2,340	197	18	12	None visible
	5,300	1,064	25, 8	20	None visible
	5,640	123	Slight	Slight	None visible
Alloy 20 Cb	2,340	197	Slight	Slight	None visible; attack at wall of bolt hole
	5,300	1,064	0	--	None visible
	5,640	123	0	0	None visible

(a) Oxygen level at 2,340 feet is 0.60 ppm; that at 5,300 feet is about 1.70 ppm.

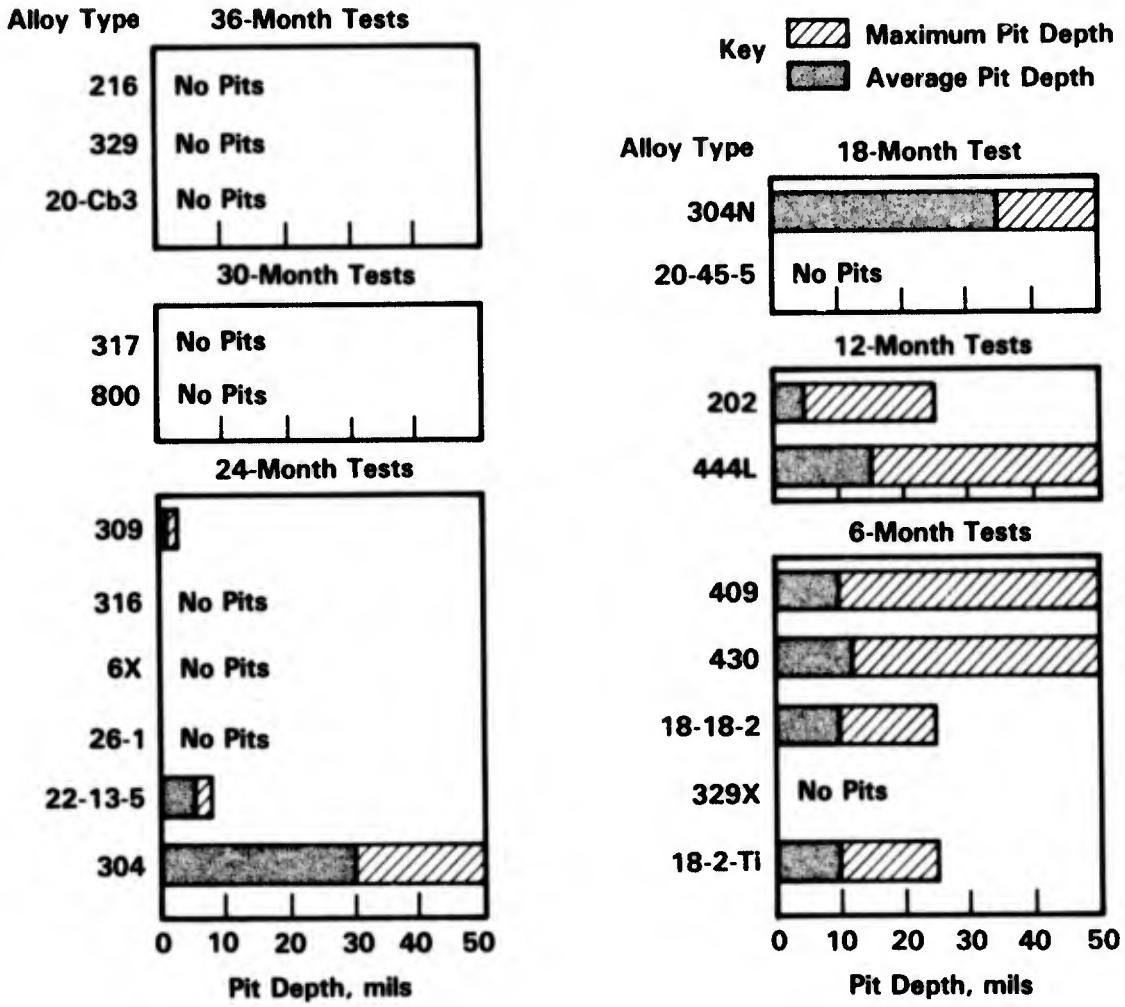

FIGURE 4-4. PITTING EVALUATION FOR STAINLESS STEELS FROM THE HEAT RECOVERY SECTION OF A DESALINATION PLANT IN FREEPORT, TX[34]

TABLE 4-34. RELATIVE EVALUATION[a] OF SEAWATER EXPOSURE RESULTS FOR CREVICE CORROSION STUDIES AT SEVERAL LOCATIONS[35]

Alloy	2 Year Key West, FL ≤32.5 C		2 Year Wrightsville Beach, NC ≤30 C		2 Year Esquimalt Harbor, B.C. Canada ≤10.5 C		1 Year Devon Island, N.W.T. Canada ≤0 C,
	No Weld	Welded	No Weld	Welded	No Weld	Welded	No Weld
Commercial Alloys							
304L		3		3		3	3
316L	1	1	3	2	3	3	3
317L	1	1	3	3	2	3	
Uddeholm 904L	0	0	1	2	1	1	
Jessop JS700	1	0	2	2	0	2	
Haynes H20M	0	0	1	0	2	2	
Al-6X	0	1	0	0	0	0	
Experimental Alloys							
316L/317L Type							
316L	1	3	2	3	3	2	
317L	1	0	3	3	3	1	
317L	1	0	0	3	2	2	
316L/317L Type + Nitrogen							
316L-0.23N	2	1	1	3	3	2	
317L-0.23N	1	1	3	2	0	1	
317L-0.26N	0	1	2	3	0	0	
6X Type + Nitrogen							
0.12N	0	0	1	0	0	0	
0.16N	0	0	0	0	0	0	
0.13N	0	0	0	0	0	0	
0.22N	0	0	0	0	0	0	
0.22N	0	0	0	0	0	0	
0.21N	0	0	0	0	0	0	
Mn Substituted							
20Cr-10Ni-9Mn-3Mo		0		1		0	
20Cr-10Ni-9Mn-4Mo		0		0		0	
20Cr-10Ni-9Mn-5.5Mo		0		0		0	

(a) 0 = No attack; 1 = Slight crevice corrosion <1 mil; 2 = Moderate crevice corrosion ≥1 to <5 mil; and 3 = Severe crevice corrosion ≥5 mil.

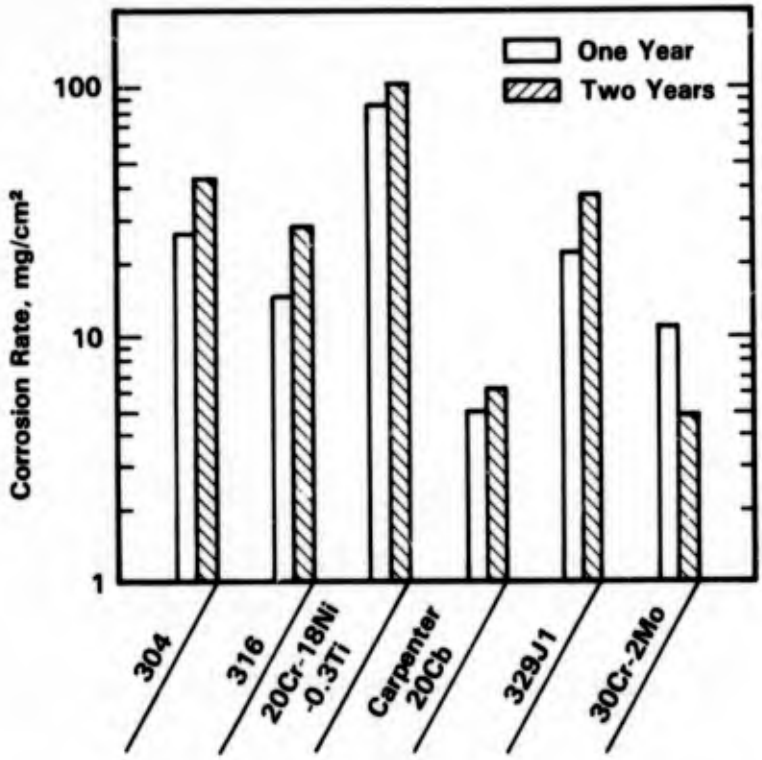

FIGURE 4-5. IMMERSION TEST RESULTS OF STAINLESS STEELS IN SEAWATER[36]

The critical alloying elements that prevent pitting in the stainless steels are chromium and molybdenum. Hack,[39] in 30-day tests with some 45 alloys at Wrightsville Beach, NC, concluded that at least 8 percent molybdenum is needed in austenitic steels and approximately 25Cr and 3.5Mo are needed in ferritic steels to prevent pitting and crevice corrosion. Qualitative long-term performance data for these types of alloys are presented in Table 4-35 by Fukuzuka, et al.; Table 4-36 by Hodgkiess and Rigas; Table 4-37 by Bond, et al.; Table 4-34 by Garner; Table 4-38 by Bond and Dundas; and Tables 4-39 and 4-40 by Kovach, et al. In addition, Brigham and Tozer[45] report no crevice corrosion for a 19Cr-10Ni-10Mn-3Mo alloy after 2-1/2 years in Halifax Harbor; Deverell and Maurer[46] reported no attack of Al-6X (20Cr-24Ni-6.5Mo) after 6-year exposures to full flow velocity in condenser tubes at a Florida utility; and Baroux, et al.[47] reported no crevice corrosion of a 17Cr-16Ni-5.5Mo-3Cu alloy after 5-year exposures in natural seawater at Brest.

TABLE 4-35. SUMMARY OF EVALUATIONS WITH MODEL SEAWATER HEAT EXCHANGER (ONE-YEAR TESTS)[40]

Steels	Existence of Crevice Corrosion: Temperature of Shell Side Seawater Velocity					
	50 C			80 C,	100 C,	140 C,
	0.5 m/s	1.0 m/s	1.5 m/s	1.0 m/s	1.0 m/s	1.0 m/s
20Cr-22Ni-5Mo-0.1N	No	No	No	No	No	No
20Cr-22Ni-5Mo-0.2N	No	No	No	No	No	No
20-Cr-24Ni-6.5Mo-0.02N	No	No	No	No	No	No
20Cr-22Ni-5Mo-0.02N	No	No	No	No	Yes	Yes
19Cr-25Ni-4.5Mo-0.02N	No	No	No	Yes	Yes	Yes
24Cr-5.5Ni-1.5Mo-0.02N (SUS329J1)	Yes	Yes	No	Yes	Yes	Yes
16.5Cr-13Ni-2.5Mo-0.02N (SUS316L)	Yes	Yes	Yes	Yes	Yes	Yes
19Cr-9Ni-0.02N (SUS304)	Yes	Yes	Yes	Yes	Yes	Yes

TABLE 4-36. OBSERVATIONS ON SPECIMENS SUBMERGED IN SEAWATER AERATED AT 25 AND 60 C, AND NONAERATED AT 100 C[41]

Material	Test Conditions[a]		
	25 C Aerated	60 C Aerated Submerged	100 C
Type 316L	C	C	C*
17Cr-13Ni-4Mo Steel	A	C	C
25Cr-6Ni-1.5Mo Steel	C	C	C
25Cr-4Ni-4Mo Steel	A	A	C
28Cr-3Mo Steel	A	A	A
Incoloy 825	A	A	C

(a) Test durations: 25 C, total of 31 weeks with examination after 10 and 19 weeks; 60 C, total of 31 weeks with examination after 10 and 21 weeks; and 100 C, total of 20 weeks with examination after 8 weeks.
A = Crevice corrosion absent.
C = Crevice corrosion observed.
C* = Crevice corrosion observed in one specimen out of four.

TABLE 4-37. CREVICE CORROSION BEHAVIOR OF STAINLESS STEELS IN LOW VELOCITY SEAWATER AT AMBIENT TEMPERATURE[a][42]

Nominal Composition, weight percent			Probability of Initiation, percent		Maximum Depth of Crevice Corrosion			
					61 Days		272 Days	
Cr	Mo	Ni	61 Days	272 Days	mm	in.	mm	in.
18	2	--	13	--	0.64[b]	0.025[b]	--	--
26	1	--	0	--	0	--	--	--
26	1	--	3	--	0.43	0.017	--	--
21	3	--	0	0	0	0	--	--
28	2	--	0	0.8	0	0	0.14 (1.1)[d]	0.006 (0.043)[d]
28	2	4	0	7.5	0	0	0.2	0.008
25	3.5	--	0	0	0	0	0	0
25	3.5	2	--	0 [c]	--	--	0 [c]	0 [c]
25	3.5	4	0	0	0	0	0	0
28	4	--	0	--	0	0	--	--
29	4	--	0	0	0	0	0	0
29	4	2	1.4	0	<0.02	<0.0008	0	0
27	1.5	4	18	--	0.15	0.006	--	--
18	--	9	10.5	--	1.47[b]	0.058[b]	--	--
18	2	11	7.2	--	0.23	0.009	--	--
18	3	13	8.0	--	--	--	--	--
17	4	14	16.3	--	1.13	0.044	--	--
18	4.3	13	--	10.8	--	--	0.17 (0.12)[d]	0.007 (0.005)[d]
19	4.3	25	--	1.7	0	0	0.006	0.002
21	4.4	25	0	5.0	0	0	0.009	0.004
20	6.1	18	--	0 [c]	--	--	0 [c]	0 [c]
20	6.5	24	0	0.8	0	0	0.01 (0.02)[d]	0.0004 (0.0008)[d]

(a) For the 61-day test the temperature range was 15.6-25 C (60-77 F); for the 272-day test the temperature range was 5-31 C (41-88 F).
(b) Perforated.
(c) 186 days.
(d) Attack at fouling sites.

TABLE 4-38. RESULTS OF CREVICE CORROSION TESTS IN AMBIENT FLOWING SEAWATER AND IN FILTERED SEAWATER AT 25 C[43]

Alloy			Fraction of Creviced Area Attack, %				Maximum Penetration, mm			
			Ambient Seawater			Filtered Seawater,	Ambient Seawater			Filtered Seawater,
Cr	Ni	Mo	2 m/s[a]	9 m/s[b]	24 m/s[a]	2 m/s	2 m/s[a]	9 m/s[b]	24 m/s[b]	2 m/s
20	--	5	0	--	--	1.7	0	--	--	0.38
26	--	1	0	0	0	21.6	0	0	0	0.30
25	--	3.5	0	0	1.7	0	0	0	0.02	0
25	2	3.5	--	0	0	0	--	0	0	0
25	4	3.5	0	0	0	0	0	0	0	0
29	--	4	0	0	0	0	0	0	0	0
29	2	4	1.7	0	0	0	<0.02	0	0	0
18	11	2.4	7.2	--	--	100	0.23	--	--	1.41
20	25	4	0	5	5	5.8	0	0.09	0.11	1.49
20	25	4	0	1.7	0.8	99.2	0	0.06	0.05 (0.08)[c]	0.83
20	25	6	0	0.8	0.8	0.8	0	0.01 (0.02)[c]	0.02	0.23
20	18	6	--	0	0	0	0	0	0	0

(a) The temperature range was 15.6 to 25 C.
(b) The temperature range was 5 to 31 C.
(c) Attack at fouling sites.

TABLE 4-39. NATURAL SEAWATER CREVICE CORROSION PERFORMANCE OF SC-1 STAINLESS STEEL[44]

Alloy	6-Months Exposure (14-Months Exposure)		
	Percent of Sites Attacked	Depth of Attack, in.	
		Range	Average
Type 316	50 (8)	0.009-0.036 (0.005-0.016)	0.022 (0.010)
26-1S	0 (2)	0 (0.0024)	0 (0.0024)
Cru-6M[a]	0	0	0
Cru-SC-1[b]	0	0	0

(a) 20Cr-25Ni-6Mo.
(b) 25Cr-2.5Ni-3Mo.

Exposure in slow flowing seawater at Wrightsville Beach, NC.
Water velocity 0.6 m/sec (1.0 ft/sec) at 15-25 C (60-77 F).
Serrated plastic washer crevices with 15 to 1 bold to crevice area ratio.

TABLE 4-40. CRUCIBLE SC-1* (SEA-CURE) CONDENSER TUBING FIELD TEST PERFORMANCE[44]

Site	Test Conditions			Duration, Months	Test Results		
	Velocity, m/sec (ft/sec)	Temperature, C (F)	Chloride, 1,000 ppm		Surface Fouling	Pitting Corrosion	Crevice Corrosion
Chesapeake Bay	0-2.3 (0-7.5)	32 (90)	8-10	9	Severe	None	None
Mystic River	1.1-1.8 (3.6-5.9)	10-32 (50-90)	17	10	Moderate	None	None
Tampa Bay	1.4 (4.5)	25-29 (77-85)	13-18	11	Moderate	None	None
Tampa Bay	3.2 (10.8)	18-38 (64-100)	4-40	14	Light	None	None
Nueces Bay	2.0 (6.5)	10-40 (50-104)	16	9	Moderate	None	None
Chesapeake Bay	2.1 (7.0)	18-43 (65-110)	10	13	Light	None	None
Chesapeake Bay	0-2.3 (0-7.5)	32 (90)	8-10	20	Severe	None	None
Cedar Bayou	2.2 (7.1)	31-36 (87-97)	20	12	Light	None	None

* 25Cr-2.5Ni-3Mo.

Welding and Heat Treatment. Welding can sensitize stainless steels to grain boundary attack in many corrosive environments. In the common austenitic stainless steels, the normal carbon grades (0.04 to 0.08C) will sensitize adjacent to welds in the so-called heat-affected zone (HAZ). In an exhaustive study, Samans[48] showed, as early as 1964, the time-temperature relationships that produce sensitization in these alloys. When heated in the temperature range of about 500 to 800 C, chromium carbides precipitate at the grain boundaries. This precipitation depletes the adjacent area of chromium to the extent that the chromium level is below that required for stainless steel (12 percent) and hence, these narrow zones become sensitized to intergranular corrosion. During welding, an area on either side of the molten weld bead is heated into this critical temperature range, which then results in sensitization in the heat affected zones.

The "L" grades of stainless steel contain $\leq$0.03 percent carbon and do not sensitize during normal welding operations. However, long-term (>12 hr) exposure in the 500 to 800 C temperature range can sensitize the "L" grades.

The austenitic alloys that contain molybdenum or very high chromium contents also can be sensitized by the precipitation of an Fe-Cr phase (sigma phase) at grain boundaries. As noted by Sedriks[31] sigma phase formation is possible at temperatures between 565 and 925 C in austenitic stainless steels containing more than 16 percent Cr and <32 percent nickel. This effect is demonstrated in Table 4-41 for alloys exposed 1 year in ambient seawater at Wrightsville Beach, NC. Note that no attack occurred in as-welded 316 and 317 stainless steel components. Intergranular attack (IGA) occurred only when specimens were heat treated to produce the sigma phase.

As pointed out by Steigerwald,[49] the ferritic stainless steels also exhibit intergranular corrosion because of chromium carbide and chromium nitride precipitation at grain boundaries. However, nitrides are more of a problem than carbides in the ferritics, and the heat treatments that lead to sensitization are different for the ferritics than for the austenitics.

Despite sensitization, the performance of welded stainless steel components in condensers and desalination equipment has generally been as good as that of nonwelded components. This has been shown by Baker, et al.[37] with welded 304, 304L, 316, and 316L condenser tubes in 8-month to 2-year exposures in seawater in England where perforations were observed, but no more so at welds than elsewhere; by Korovin and Ulanovskii[50] with 18-8, 21-5, and 21-6-2Mo in 2-year tests in the Baltic Sea; by Garner as shown in Table 4-34 where welded components of a number of stainless steels performed in crevice tests as well as their unwelded counterparts; by Reinhart[33] in his deep ocean tests where no unusual attack was reported for welded and for heat treated 15-7, 17-4, and 17-7PH alloys; by Maurer[51] who states that as-welded Al-6X condenser tubes have exhibited excellent corrosion resistance in

TABLE 4-41. RESULTS OF SEAWATER EXPOSURE FOR VARIOUS STAINLESS STEELS IN SEVERAL CONDITIONS OF HEAT TREATMENT: SPECIMENS EXPOSED FOR 1 YEAR IN AMBIENT TEMPERATURE SEAWATER UNDER TIDAL FLOW CONDITIONS AT WRIGHTSVILLE BEACH, NC[31]

Type	Condition[a]	Intergranular Attack[b]
316L	Annealed	No
	1 hr, 675 C, AC	No
	4 hr, 870 C, AC + 1 hr, 675 C, AC	Yes[c]
	As welded, matching filler	No
	Welded + 1 hr, 705 C, AC	No
	Welded + 1 hr, 870 C, AC	Yes[c]
316	Annealed	No
	2 hr, 620 C, AC	No
	1 hr, 675 C, AC	No
	As welded, matching filler	No
	Welded + 1 hr, 870 C, AC	Yes
317	Annealed	No
	4 hr, 595 C, AC	No
	1 hr, 675 C, AC	Yes
	As welded, matching filler	No
	Welded, 1 hr, 705 C, AC	Yes

(a) AC air cooled following indicated heat treatment.
(b) Attack often initiated in the creviced area of the mounting hole before spreading along grain boundaries.
(c) σ may form at 870 C in Type 316L.

seawater; by Hodgkiess, et al.[52] who report no attack on welded Type 316 after 21 weeks in aerated 60 C seawater in Scotland; and by Hodgkiess, et al.[53] who found no attack in welded Type 316 after 15 months of service in three desalination plants.

Evidence of selective attack (IGA) has been reported by Reinhart[33] in an annealed and pickled Type 405 (12Cr) alloy after 123-day exposures at the 5,640 feet depth in the Pacific and by Henrikson, et al.[54] who reported attack at welds in loop tests in 3,200 to 3,700 ppm Cl^- in Sweden, but who attributed this attack to oxides and defects in the welds that caused crevice attack. Selective attack in other chloride-type environments has been reported by Stefec, et al.[55] who found that the pitting resistance of 17Cr-12Ni-2.5Mo, based on pitting potential measurements in 0.1M NaCl was adversely affected by heat treatments of 1 to 100 hours at 550 to 750 C; and by Redmerski and Moskowitz[56] who reported that the effect of welding 430, 434, and 301 was to enrich Cr in the oxide layer and deplete it at the metal

surface which promoted attack in $FeCl_3$ tests. On the other hand, Hulquist and Leygraf[57] found that vacuum annealing or oxidation at low O_2 pressures produced thin Cr-and Ni-rich films on Type 316 that increased its resistance to crevice corrosion in 0.5M NaCl.

Thus, the available data tend to indicate that welding per se does not adversely affect the performance of stainless steels in seawater. However, elevated temperatures or higher chloride solutions might be more aggressive. Heat treatments that produce sigma phase are harmful, and as pointed out by Sedriks[31] it seems prudent to avoid sensitization in the welding of Fe-Cr-Ni and Fe-Cr-Ni-Mo alloys.

Effect of Temperature. In general, an increase in temperature in the range of 10 to 60 C would be expected to increase the severity of pitting and crevice corrosion in seawater; but this has not been true in most exposure tests. Data obtained by Lee[58] as shown in Figures 4-6 and 4-7 indicate that a maximum in pit depth is observed for Types 304 and 316 at

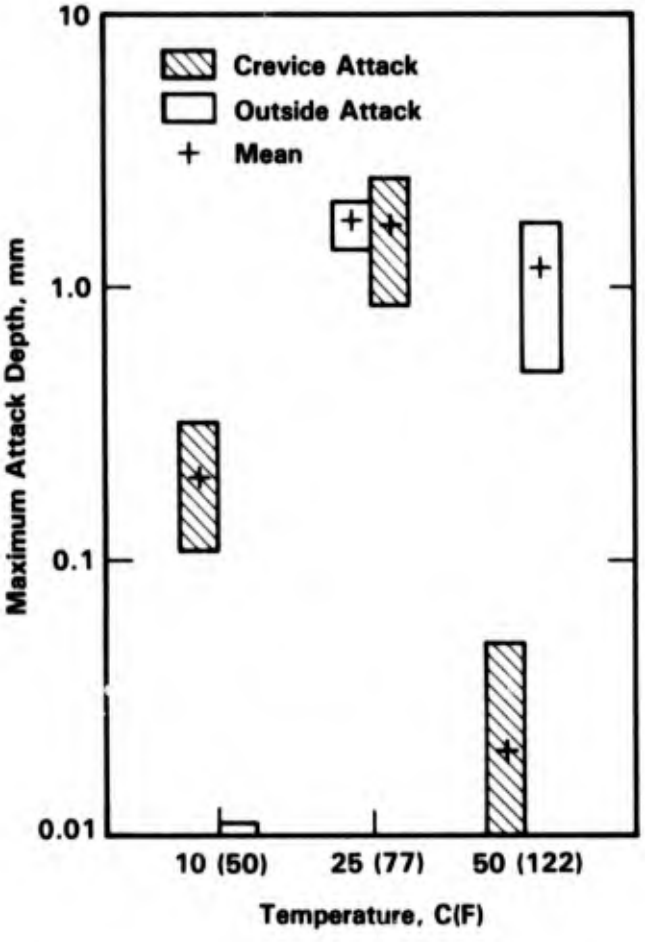

FIGURE 4-6. MAXIMUM DEPTH OF ATTACK FOR 5 SPECIMENS OF TYPE 304 STAINLESS STEEL AFTER 28 DAYS IN SEAWATER[58]

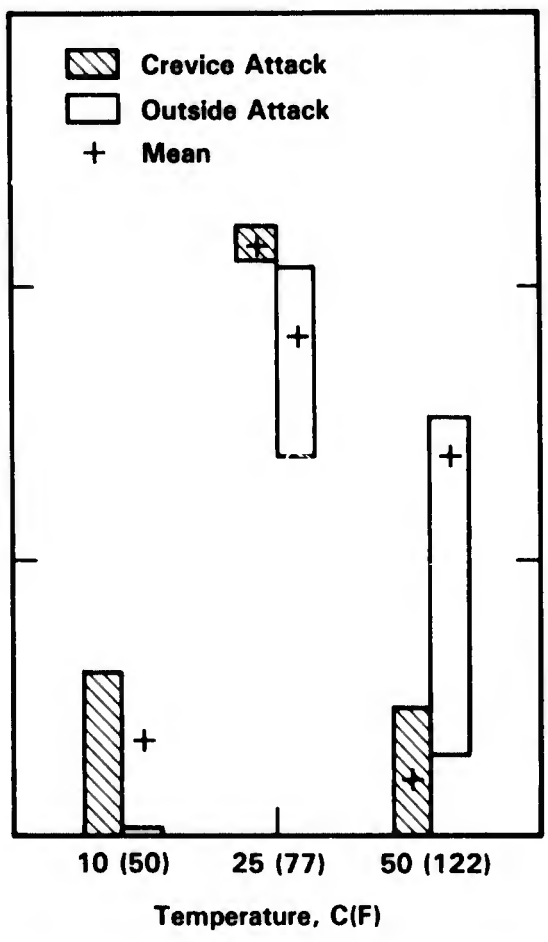

FIGURE 4-7. MAXIMUM DEPTH OF ATTACK FOR 5 SPECIMENS OF TYPE 316 STAINLESS STEEL AFTER 28 DAYS IN SEAWATER[58]

25 C as compared to 10 and 50 C. Similar, but not so striking, trends also have been observed by Asphahani, et al.[59] in almost identical tests as summarized in Table 4-42. The effect of temperature also is inferred from the depth of exposure in tests by Ulanovskii, et al.[60] reported in Table 4-43 where they find an increased rate of pitting attack and general corrosion as the temperature increased from 9 to a maximum of 25 C. Long term data summarized by Garner[35] in Table 4-34 indicate little effect of temperature on crevice corrosion at four exposure sites ranging in temperature from 0 to a maximum of 32.5 C.

Service experience with the high molybdenum alloys reveal that they have not pitted at temperatures to 40 C (Kovach, et al.[44] and 25Cr-2Ni-3Mo alloy in Table 4-40) and to 65 C (Eden[61] with 20Cr-25Ni-4.5Mo in Table 4-44).

The maximum in pitting and crevice attack at 25 C, or results that show little or no effect of temperature, are somewhat surprising in light of pitting potentials that have been obtained by a number of investigators in chloride environments other than seawater. As shown in Figures 4-8, 4-9, 4-10, 4-11, 4-12, 4-13, 4-14, and 4-15, the pitting potentials in chloride environments for most alloys studied become more negative as the temperature is increased. Thus, it would appear that pits should initiate more readily at the higher temperatures. Lizlovs[69] also has found that increasing temperature in the range 20 to 60 C increases susceptibility to crevice corrosion in controlled potential tests in 1 N NaCl (see Table 4-45).

It should be noted that the effects of temperature are complex. An increase in temperature would be expected to increase the rate of corrosion and pitting. However, this may be counterbalanced at the higher temperatures by a decrease in oxygen solubility and the killing of microorganisms, both of which would be expected to reduce the rate of corrosion attack.

Mechanical Effects. Mechanical effects on the pitting behavior of stainless steels can be related to two sources; cold work in the alloy itself and applied stress from an external source. Neither of these sources has been studied systematically, and thus only general trends can be inferred.

Gutman, et al.[70] cite German and Soviet literature which report that plastic deformation increases the susceptibility of stainless steels to pitting in chloride solutions. This effect has been substantiated by several investigators in chloride solutions other than seawater. Mazza, et al.[71] working with 3.5 percent NaCl at pH 2, 7, and 9 found that the pitting potentials of 304L and 316L became more negative as the amount of cold work was increased through 50 percent. This effect was less pronounced in the longitudinal direction than the long transverse or short transverse directions. Stefec and Franz,[72] in short time (30 minute) tests with 316 in 0.1M NaCl, found that the number and area of pits increased with

TABLE 4-42. CREVICE ATTACK IN 30-DAY TESTS AT WRIGHTSVILLE BEACH, NC[59]

Alloy	Depth of Attack, mm		
	12 C	28 C	50 C
304	0.51-0.56	0-0.81	0.05-0.12
316	0.09-0.34	0-0.57	0.03-0.05
Alloy 20 (Mod)	0-0.18	0-0.20	0

TABLE 4-43. CORROSION BEHAVIOR OF 18Cr-9Ni STAINLESS STEEL EXPOSED 21 MONTHS IN THE BLACK SEA[60]

Depth, m	Temperature, C	Crevice Specimens Maximum Pit Depth, mm	Corrosion Rate, $mg/dm^2/day$
7	9 to 25*	2.8	1.70
27	9 to 14	1.3	1.15
42	9 to 10	1.1	1.03
80	8 to 9	0.04	0.02

* Seasonal extremes.

TABLE 4-44. EXPERIENCE WITH SANDVIK 2RK65 (20Cr-25Ni-4.5Mo) IN SEAWATER COOLING[61]

	Application	Country	Tube Size, mm	Service Conditions	Performance of 2RK65
1.	Piping system blast furnace cooling	Italy	21.3 x 2.6 to 114.3 x 8	Polluted Mediterranean seawater; Cl^- = 2.5%, lots of solids, pH = 7.9, no H_2S, maximum service temperature 45 C.	In service since 1969 without failure.
2.	Transfer pipe line	Denmark	153 x 1.5	Seawater mixed with fatty acids. Maximum service temperature 50 C.	In service since 1969, no problems.
3.	Condensers in distillation for solvents	Portugal	25 x 2 30 x 2	Tube side: polluted harbor salt water, maximum service temperature 65 C (70 C). Shell side: butanol, methanol, and butyl-acetate.	In service since 1969 without failure.
4.	Conveying line in styrene plant	Sweden	204 x 1.5	Tube side: seawater, 1 m/s, maximum service temperature 25 C.	In service since 1970, no problems.
5.	H_2SO_4-cooler in chlorine plant	Italy	21.3 x 2	Tube side: 96-98% H_2SO_4, some chlorides, t_{in} = 60 C. Shell side: seawater.	In service since 1970 without problem.
6.	Catalytic cracking overhead condenser after reactor	Portugal	19.05 x 1.65	Tube side: seawater maximum service temperature 80 C (90 C). Shell side: gas/steam/condensate, H_2S and H_2O, t_{in} = 180 C, t_{est} = 40 C.	In service since 1970, good results.
7.	Heat exchanger in styrene plant	Holland	19.05 x 1.65	Tube side: brackish water, 1.8% Cl^-, maximum temperature 50 C (55 C). Shell side: hydrocarbons, temperature 260 C.	In service since 1971, good performance.
8.	Lube oil cooler on a ferry	Sweden	14 x 1	Tube side: lube oil for engine, t_{max} = 50 C. Shell side: often polluted harbor seawater with sulfides.	In service for 5-1/2 years, no problems.
9.	Coolers in ammonia plant	Brazil	31.75 x 1.25	Tube side: seawater t_{in} = 32 C, t_{out} = maximum 65 C, maximum service temperature 80 C (83 C). Shell side: ammonia temperature = 177 C.	In service for 3 years, good results.
10.	Condenser in MEA-stripper	Italy	19.05 x 1.65	Tube side: seawater maximum service temperature 55 C (60 C). Shell side: H_2S, CO, t_{in} = 110 C, t_{out} = 40 C.	In service for about 4 years, no problems.
11.	Coolers in ammonia plant	United Kingdom	19.05 x 1.65	Tube side: seawater maximum service temperature 45 C (48 C). Shell side: liquid gas/ammonia, 27 to 70 C.	In service for 4-1/2 years without any problems.
12.	Turbine steam condenser in ammonia plant	Japan	19.05 x 1.65	Tube side: seawater maximum service temperature 45 C (50 C). Shell side: steam.	In service more than 3 years without problems.

Figures within parentheses show estimated temperature if fouling (20 percent of total heat transfer resistance) on waterside is considered.

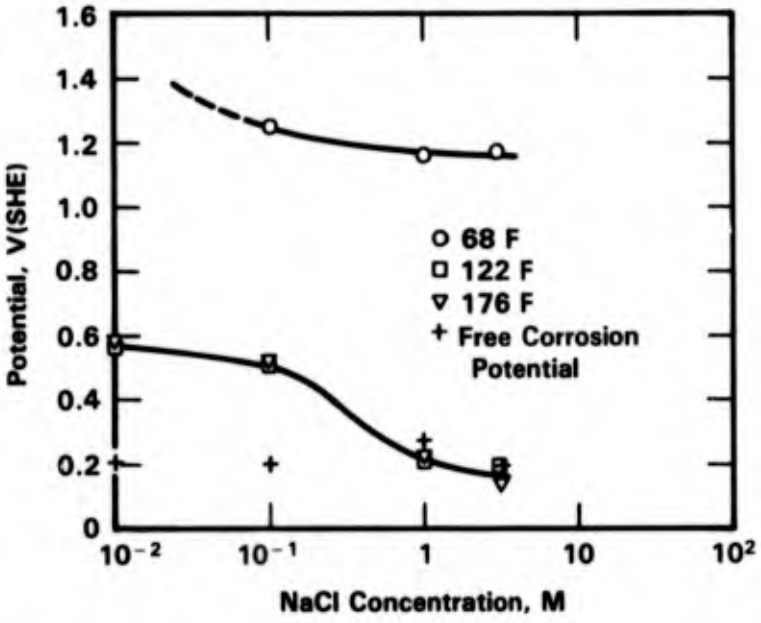

FIGURE 4-8. EFFECT OF TEMPERATURE AND NaCl CONCENTRATION ON PITTING POTENTIALS OF 22Cr-5.5Ni-3Mo IN AQUEOUS NaCl SOLUTIONS[62]

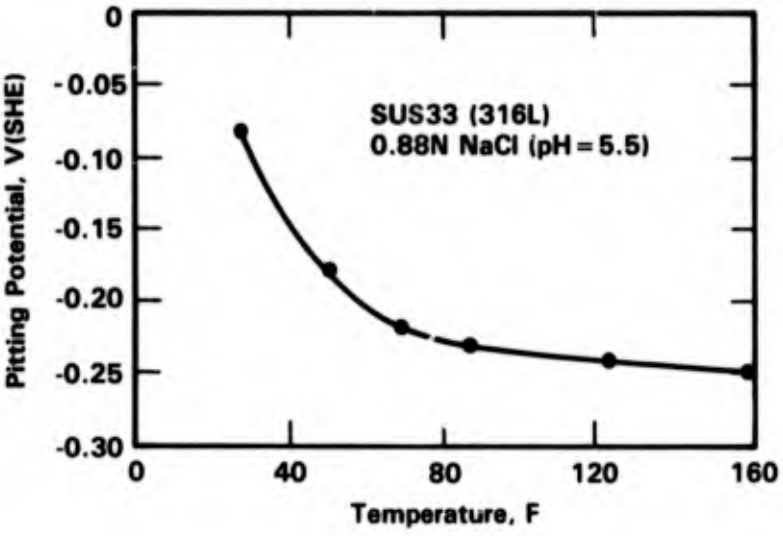

FIGURE 4-9. EFFECT OF TEMPERATURE ON CRITICAL POTENTIAL FOR PIT GROWTH OF TYPE 316L[63]

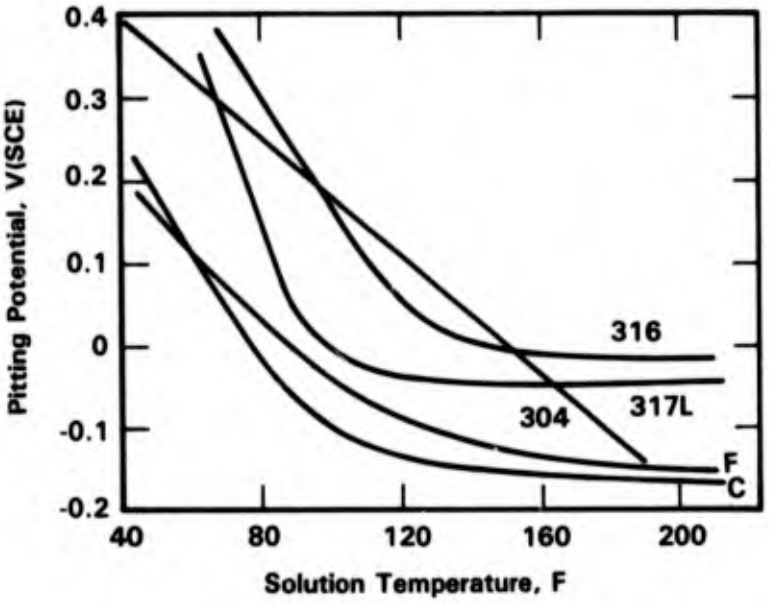

FIGURE 4-10. EFFECT OF TEMPERATURE ON THE PITTING POTENTIAL OF STEELS IN 3 PERCENT NaCl SOLUTION(64)

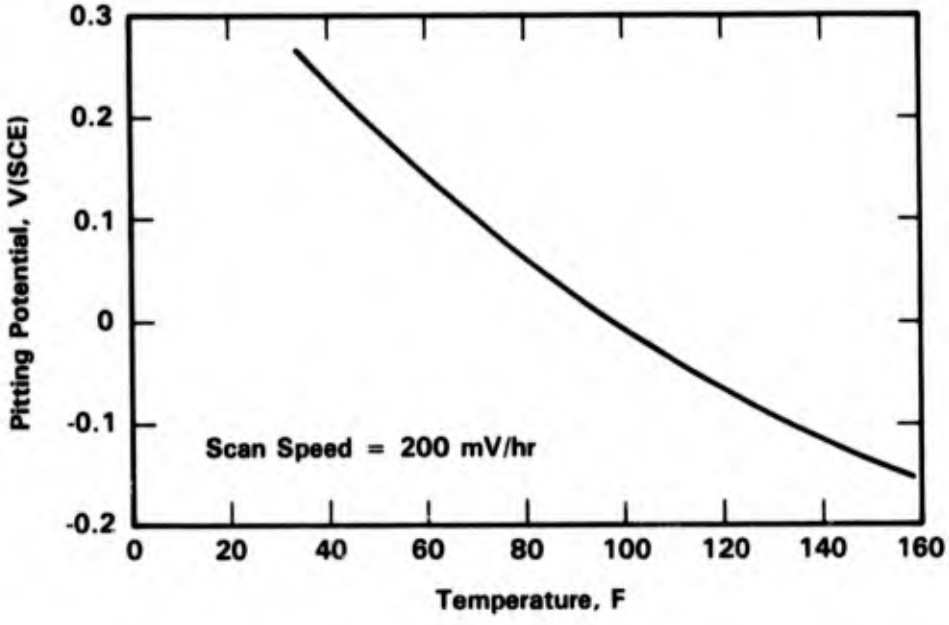

FIGURE 4-11. PITTING POTENTIALS OBTAINED FROM POTENTIODYNAMIC POLARIZATION SCANS IN NITROGEN SATURATED 1.0M NaCl FOR MODIFIED TYPE 430 STAINLESS STEEL(65)

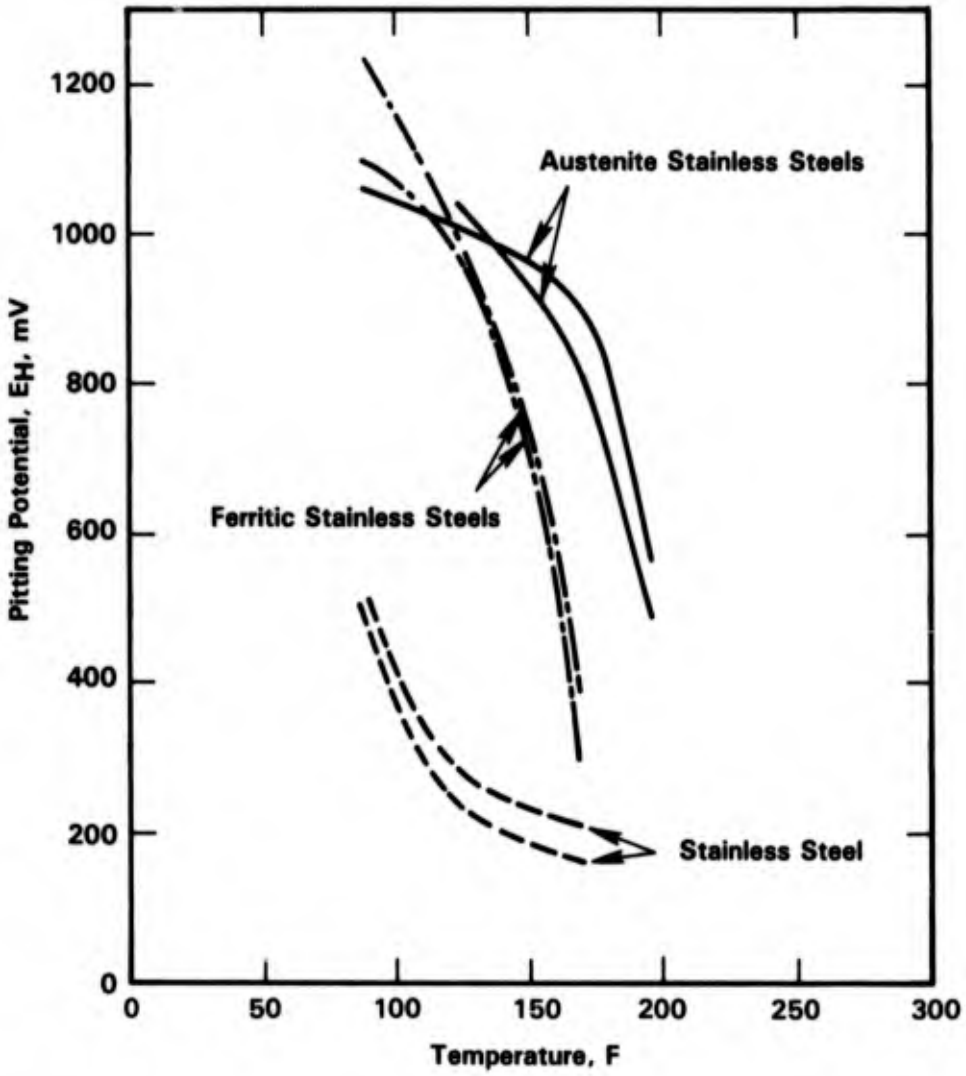

FIGURE 4-12. PITTING POTENTIAL AS A FUNCTION OF TEMPERATURE FOR SUPERFERRITIC AND AUSTENITIC STAINLESS STEELS IN ARTIFICIAL (ASTM) SEAWATER, AIR BUBBLED, STIRRED[66]

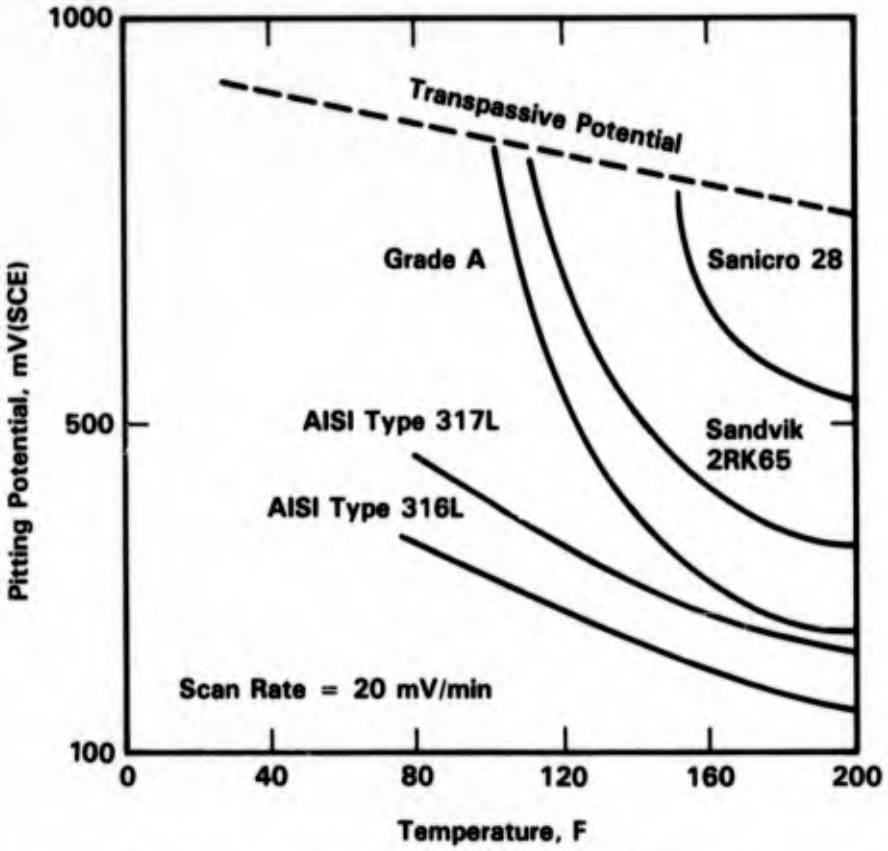

FIGURE 4-13. PITTING POTENTIALS OF STAINLESS STEELS IN 3 PERCENT SODIUM CHLORIDE AS A FUNCTION OF TEMPERATURE[67]

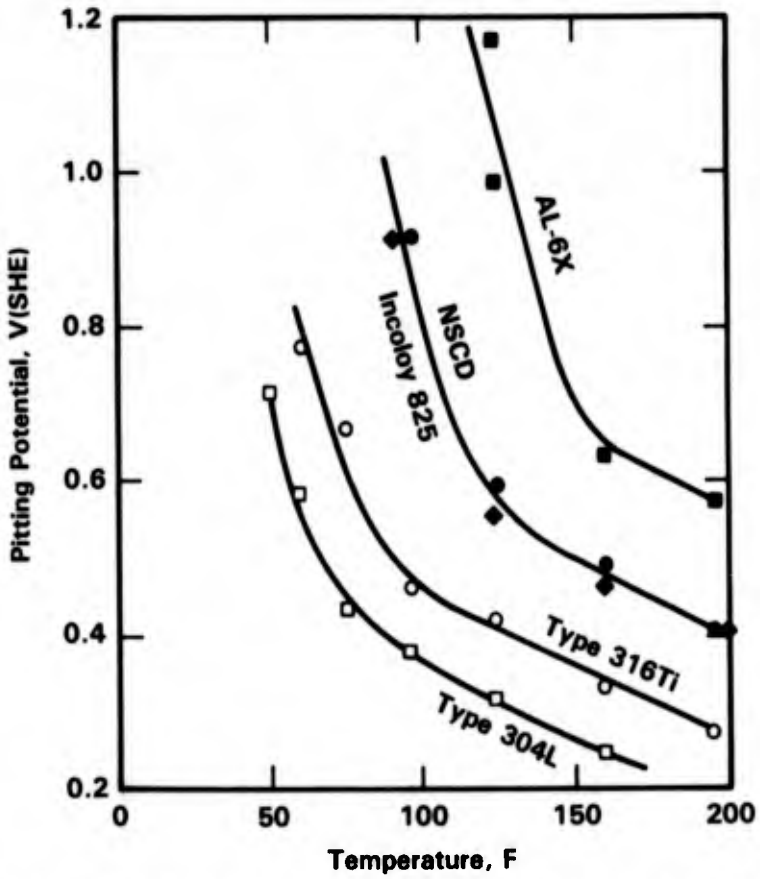

FIGURE 4-14. PITTING POTENTIAL CURVES FOR STAINLESS STEELS IN 0.5M SODIUM CHLORIDE, pH = 6.6 (SIMULATED SEAWATER)[47]

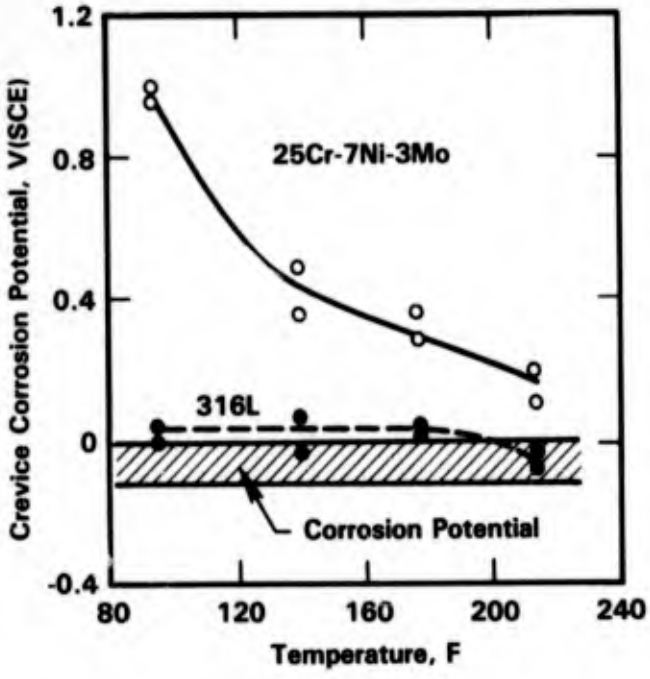

FIGURE 4-15. CREVICE CORROSION POTENTIALS FOR STAINLESS STEELS AS A FUNCTION OF TEMPERATURE (3 PERCENT NaCl + 1/20M Na_2SO_4 SOLUTION)[68]

TABLE 4-45. RESULTS OF CONTROLLED POTENTIAL CREVICE CORROSION TEST IN 1 N NaCl CELL ON FERRITIC STAINLESS STEELS[69]

Steel Type	Presence of Crevice Corrosion at Indicated Test Temperature				
	21 to 22 C	30 C	40 C	50 C	60 C
20Cr-2Mo	Yes	--	--	--	--
22.5Cr-2Mo	Yes	--	--	--	--
25Cr	Yes	--	--	--	--
26Cr-1Mo	No	Yes	Yes	--	--
25Cr-2Mo	No	Yes	Yes	--	--
28Cr-2Mo	No	No	No	Yes	--
25Cr-3.5Mo	No	No	No	Yes	--
25-Cr-5Mo	No	No	No	No	Yes

cold work through 30 percent, but the pit growth rate did not increase appreciably beyond 1 percent cold work. El-Sayed, et al.[73] found that the corrosion rate of a 17Cr-10Ni steel increased with cold work (66, 73, 83 percent) in 3 percent NaCl at 70 to 90 C and the corrosion potential became more negative with increasing amounts of cold work. On the other hand, Rowlands[74] conducted one-year crevice tests on 316 stainless steel in Langston and Chichester harbors and found that, in natural seawater, cold rolled material exhibited a crevice corrosion rate of 0.002 to 0.046 g/m^2/day whereas the rate for annealed material ranged from 0.06 to 0.54 g/m^2/day.

Effect of Heat Transfer. Reported data are sparse on the effect of heat transfer on the general and localized corrosion behavior of stainless steel. As reported in the section on Alloys, a number of field tests have been conducted in condensers and other heat exchangers that demonstrated the severe pitting tendencies of the conventional stainless steels and the good pitting resistance of the high Mo (>3.5 percent) stainless steels. However, no systematic studies appear to have been made on the effect of heat transfer per se. In lieu of such studies, it can be generalized that the major effect of heat transfer would be to elevate the surface temperature (see section on Effects of Temperature).

In OTEC heat exchanger tube tests at Freeport, Texas, Grimes and Schrieber[75] report that the corrosion rate of Al-6X was <0.0005 mm in 90 days. This value extrapolates to <0.002 mm/yr (<0.08 mil/yr). In other OTEC heat exchanger tests off Hawaii, Liebert, et al.[76] report that Al-6X exhibited no attack after 10 months' exposure. Periodic cleaning was required to restore heat transfer coefficients, but they never regained the clean tube values. This effect was attributed to the buildup of a tenacious film similar in appearance to dental plaque on teeth.

Schrieber[77] conducted heat transfer coefficient tests in the Office of Saline Water (OSW) units at Freeport, Texas. As shown in Figure 4-16, the heat transfer coefficient for Type 316 started out low, but did not change appreciably with acid cleaning and subsequent exposure to corrosive (300 ppb oxygen) conditions.

Biofouling. Biofouling produces slimes and deposits that can lead to pitting of the conventional stainless steels. This can occur by oxygen depletion under the deposit as in conventional crevice attack; or as pointed out by Liebert, et al.,[76] filamentous growths can trap water and result in high surface temperatures which would further aggravate corrosion in heat transfer systems.

The buildup of a deposit appears to be critical. For example, Willingham[78] found no pitting of fully exposed Type 316 when exposed 90 days at 20 C in a seawater medium that

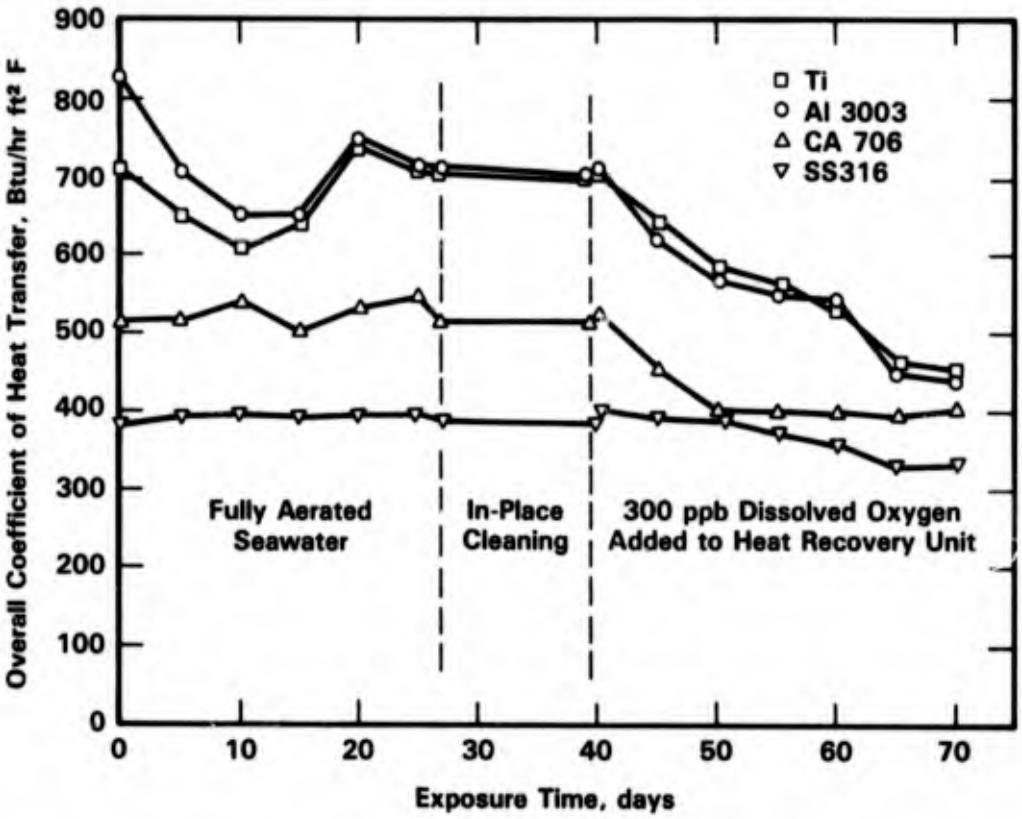

FIGURE 4-16. OVERALL COEFFICIENT OF HEAT TRANSFER VERSUS TIME AND ENVIRONMENT FOR FOUR ALLOYS AT 130 F EXIT TEMPERATURE (HEAT RECOVERY NO. 1)[77]

contained three types of sulfate-reducing bacteria. Lendvai-Lintnor, et al.[79] state that in the absence of antifoulants, corrosion inhibitors are not effective in preventing pitting in high chloride recirculating cooling water systems. Walston[80] observed that Type 316 performed well in cooling tower systems located world wide if the waters were aerated, but experienced localized corrosion in crevices with poor microbiological control. LaQue[81] attributes differences in the corrosion behavior of Type 304 exposed to synthetic seawater and natural seawater to microorganisms in the latter based on the following crevice tests:

	30 C		50 C	
Seawater	Area Attacked, percent	Maximum Depth, mm	Area Attacked, percent	Maximum Depth, mm
Natural	42	2.9	42	0.14
Synthetic	31	0.1	31	0.1

The reduced depth of attack in natural seawater at 50 C may be attributed to the killing of the bacteria in the water at the higher temperature.

Brennert and Lindh[82] conclude from a survey in Sweden that fouling by microorganisms can be minimized by treating with chlorine or hypochlorite at dose levels of 1 ppm chlorine several times every 24 hours.

The high Mo stainless steels appear to be resistant to pitting by biofouling presumably because they are resistant to crevice corrosion in seawater, as has been extensively discussed in preceding sections. The results of Brennert and Lindh's[82] questionnaire revealed that at least 3.5 percent Mo was required in stainless steel to ensure resistance to corrosion by microorganisms. In biofouling tests of OTEC heat exchanger alloys in the Gulf of Mexico, Little, et al.[83] found that Al-6X exhibited patchy colonization by microorganisms, but minimal corrosion after 90 days exposure at a velocity of 1.8 m/sec.

Potential. When a metal is immersed in an electrolyte it assumes an electrochemical potential which depends on both the alloy and the electrolyte. This potential is referred to as the corrosion potential (E_{cor}). Other electrochemical parameters of interest are the pitting potential (E_{pit}) and the protection potential (E_{prot}).

Lennox and Peterson[84] have measured the long-term corrosion potentials of boldly-exposed stainless steels in seawater. Their results, summarized in Table 4-46, revealed that the potentials varied somewhat with time, but the mean potentials were more positive for

TABLE 4-46. MEAN POTENTIALS AND RANGE OF POTENTIALS FOR STAINLESS STEELS IN SEAWATER, WITH AND WITHOUT CATHODIC PROTECTION[84]

Stainless Steel Alloy	Exposure Time, days	Exposure Condition	Potential, V(Ag/AgCl) Pier Mean	Pier Range	Cell Mean	Cell Range
24Ni-20Cr-6.5Mo	218	No CP	+0.023	+0.217 to -0.187	+0.038	+0.296 to -0.415
	552	No CP	+0.152	+0.269 to -0.057	+0.256	+0.320 to -0.148
26Cr-5Mo	218	No CP	-0.154	-0.006 to -0.235	-0.047	+0.075 to -0.228
	552	No CP	-0.098	+0.017 to -0.222	-0.035	+0.173 to -0.193
22Cr-13Ni-5Mn	176	No CP	-0.094	-0.023 to -0.180	-0.004	+0.053 to -0.117
	531	No CP	-0.065	+0.079 to -0.230	-0.085	+0.031 to -0.117
Type 216	546	No CP	-0.136	-0.007 to -0.440	-0.047	+0.155 to -0.297

those alloys that are more resistant to pitting. Lee[58] conducted controlled potential tests in seawater and, based on 20 to 30 days' exposure, found that crevice corrosion occurred at potentials -100 mV(Ag/AgCl) (SCE and Ag/AgCl are close and both are approximately +240 mV on the SHE scale). Lula[85] working in synthetic seawater obtained a pitting potential of +260 mV(SCE) for Type 316 which would be expected based on the value of -100 mV for 304 in natural seawater. Pitting potentials were much more noble for the high Mo alloys as shown in Table 4-47 from Lula.

Wilde[86] believes that a significant value in pitting is the difference between the pitting (E_{pit}) and pit protection (E_{prot}) potentials. In Figure 4-17 and Table 4-48, he has correlated this difference with weight loss for several stainless steels exposed 4.25 years in seawater. Note that weight losses increased as the difference between the pitting and pit protection potentials increased. Kain[87] has correlated the occurrence of hysteresis with crevice corrosion in seawater and has found reasonable, but not one-to-one correlation, see Table 4-49.

A number of investigators have examined the pitting behavior of stainless steels in NaCl solutions. Their results indicate that pitting potentials are more positive with increasing Mo content in the alloy, decreasing NaCl concentration, and decreasing temperature. These effects are illustrated in Figures 4-18 and 4-19, and Table 4-50.

It is interesting to note that Manning, et al.[92] were able to correlate pitting potentials with features in 304L austenitic (wrought) and duplex (weld bead) microstructures. They found that pitting potentials were more negative on the edges of 304L specimens because of sulfide inclusions. The pitting potential could be raised by passivating the edges or spherodizing the sulfides by heating 8 hours at 1300 C. They also found that pitting potentials of the wrought

TABLE 4-47. ELECTROCHEMICAL CREVICE CORROSION DATA IN ARTIFICIAL SEAWATER AT ROOM TEMPERATURE[85]

Alloy Designation	E_{pit}, SCE	E_{prot}, SCE	E_{pit}-E_{prot}, mV
Type 316	+0.26	-0.07	0.33
6X	+1.05	+1.02	0.03
29Cr-4Mo	+0.90	+0.85	0.05
Hastelloy C	+0.81	+0.75	0.06

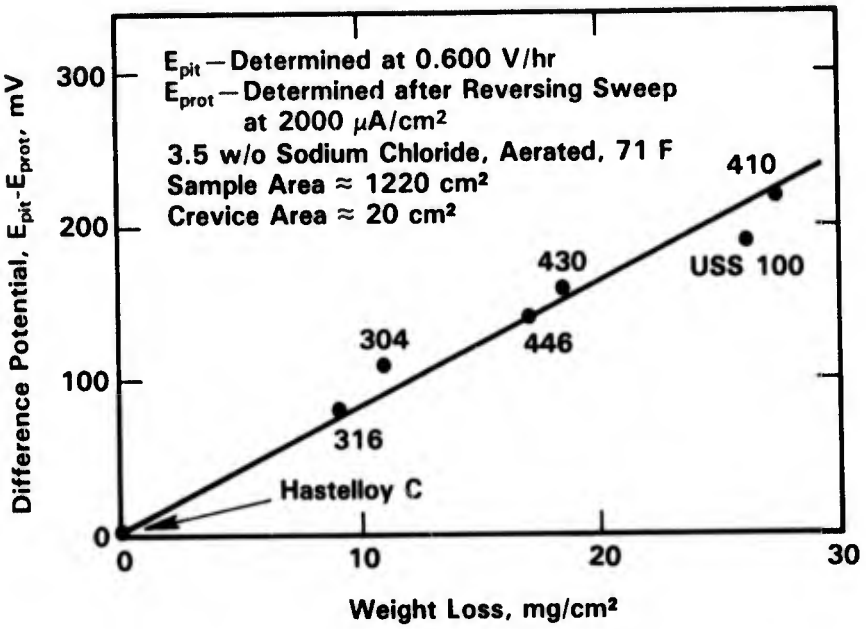

FIGURE 4-17. CORRELATION BETWEEN DIFFERENCE POTENTIAL AND CORROSION WEIGHT LOSS OF STAINLESS ALLOYS EXPOSED IN SEAWATER FOR 4.25 YEARS[86]

TABLE 4-48. ELECTROCHEMICAL AND CREVICE CORROSION DATA FOR SEVERAL STAINLESS ALLOYS IN AERATED 3.5 WEIGHT PERCENT NaCl AT 77 F AND SEAWATER[86]

Alloy Designation	E_{cor} (After 500 Hours), V(SCE)	E_{pit} V(SCE)	E_{prot}[(a)] V(SCE)	Crevice Corrosion Weight Loss After 4.25 years in Seawater, mg/cm²
Hastelloy C	+0.220	+0.970	+0.970	0.25
AISI Type 316	+0.088	+0.100	-0.020	9.16
AISI Type 304	+0.085	0.0	-0.110	10.80
AISI Type 446	+0.240	-0.050	-0.200	17.4
AISI Type 430	-0.040	-0.100	-0.260	18.90
USS 100	+0.012	-0.150	-0.340	25.80
AISI Type 410	-0.100	-0.200	-0.420	26.70

(a) Determined by reversing the sweep at an applied current of 2 mA/cm².

TABLE 4-49. COMPARISON OF THE OCCURRENCE OF HYSTERESIS FROM CYCLIC POLARIZATION TESTS WITH OCCURRENCE OF LOCALIZED ATTACK IN MULTIPLE CREVICE TESTS[87]

Alloy	12 C		28 C		50 C	
	Hysteresis	Crevice Corrosion*	Hysteresis	Crevice Corrosion*	Hysteresis	Crevice Corrosion*
Type 304 Stainless	Yes	Yes	Yes	Yes	Yes	Yes
Carpenter Alloy 20Cb-3	No	Yes	Yes	Yes	Yes	Yes
Incoloy Alloy 825	No	Yes	Yes	Yes	Yes	Yes
Hastelloy Alloy G	No	Yes	No	Yes	Yes	No
Inconel Alloy 625	No	No	No	No	No	No

* Attack at multiple crevice sites.

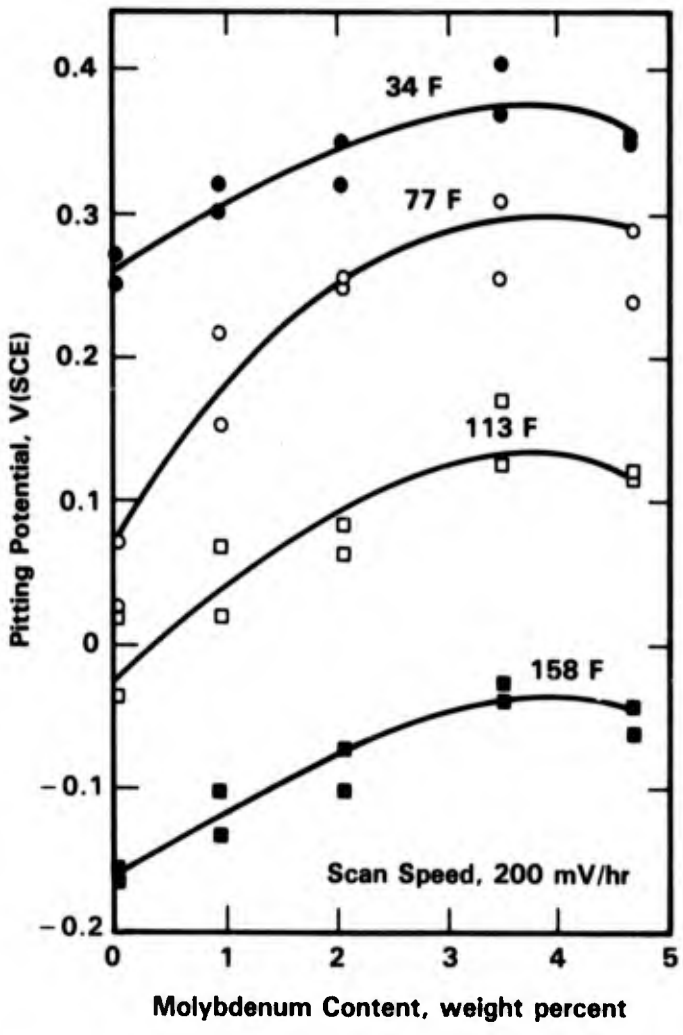

FIGURE 4-18. PITTING POTENTIALS OBTAINED FROM POTENTIODYNAMIC POLARIZATION SCANS IN NITROGEN-SATURATED 1.0M NaCl[65]

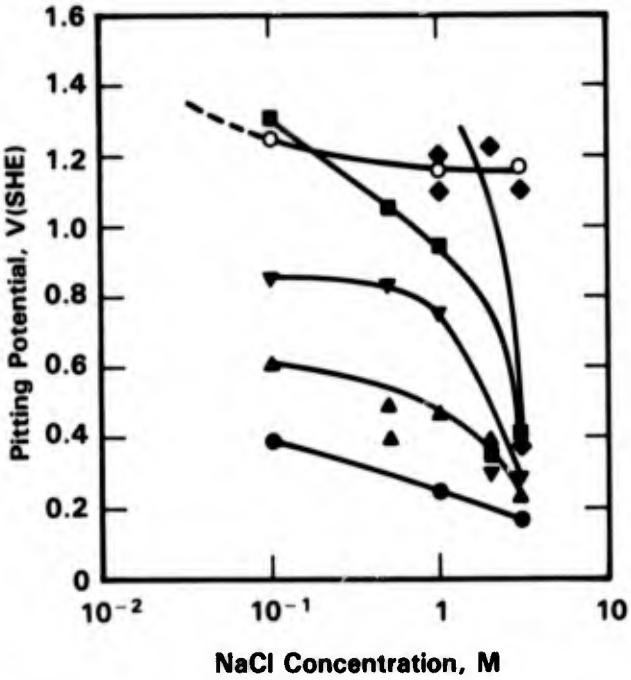

Steel	Mo, wt %	Key
X 5 CrNi 18 9	0.28	●
X 5 CrNiMo 18 10	2.16	▲
X 2 CrNiMo 18 12	2.69	▼
X 2 CrNiMo 18 16	3.20	■
X 5 CrNiMo 17 13	4.16	◆
AF 22 CrNiMo 22 5.5	2.78	○

FIGURE 4-19. PITTING POTENTIALS OF VARIOUS AUSTENITIC STEELS WITH DIFFERENT Mo CONTENT AND AUSTENITIC-FERRITIC STEEL AF 22 AT 68 F VERSUS NaCl CONCENTRATION[62]

TABLE 4-50. PITTING POTENTIALS AND ELECTROCHEMICAL PARAMETERS IN 0.1M NaCl[93]

Specimens	E_{cor}, V(SCE)*	E_{pit}, V(SCE)*	E_{prot}, V(SCE)*	i_{pit}, mA/cm^2	i_{prot}, mA/cm^2
SUS 403	-0.72	-0.375	-0.475	0.120	0.120
	-0.64	-0.370	--	0.150	0.150
SUS 430	-0.545	-0.310	-0.50	0.043	0.027
	-0.535	-0.400	-0.50	0.040	--
25Cr-5Ni-2Mo	-0.485	+0.020	-0.015	0.136	0.060
	-0.490	+0.025	-0.013	0.100	0.020
23Cr-5Ni	-0.495	-0.065	-0.090	0.046	0.016
	-0.520	-0.075	-0.115	0.107	0.060
SUS 304	-0.550	-0.075	-0.125	0.043	0.019
	-0.550	-0.080	-0.150	0.040	0.014
SUS 316	-0.500	-0.040	-0.180	0.046	0.023
	-0.510	-0.050	--	0.050	0.026
Incoloy 800	-0.515	-0.160	-0.160	0.057	0.025
	-0.490	-0.170	-0.17	0.053	0.030
Inconel 600	-0.465	-0.095	-0.165	0.032	0.011
	-0.425	-0.025	-0.140	0.057	0.024

* All potentials are referred to a saturated calomel electrode at room temperature.

metal decreased (became more negative) with increasing surface roughness (higher density of sulfides). Neither the edge exposure nor surface roughness affected the duplex (cast structure). Detailed examination revealed that pits initiated at the austenite/sulfide interface in the wrought 304L and at the δ/γ interface in the duplex material.

Geometry Effects. The geometry of crevices, exposure conditions, microstructure, and surface condition affect pitting and crevice corrosion. Mankowski, et al.[98] found that pits in 18Cr-12Ni-2Mo-Ti stainless grew more slowly if the specimen was facing up than if it was facing down. They attributed this effect to a higher chloride ion concentration in the upward facing pits which slowed diffusion processes.

Scotto, et al.[99] have investigated the effects of fabrication orientation on the pitting of 18Cr-9Ni and 17Cr-11Ni-2Mo in 3 percent NaCl. They found that pits occurred more readily on transverse than on longitudinal sections because of the more unfavorable sulfide inclusion shapes in that direction. Eklund[100] and Brennert and Eklund[101] believe that the prime cause of crevice corrosion in stainless steel is the electrochemical dissolution of sulfide inclusions, the formation of acid conditions, and the resulting exposure of bare active metal. This effect tends to be confirmed by Sydberger[102] who found that pickling ground surfaces improved the crevice corrosion resistance of 304, 316, and 329 presumably because of the removal of MnS inclusions from the metal surface.

Several investigators have attempted to quantify the effects of crevice dimensions on the crevice corrosion of stainless steels. Most have used a multiple crevice assembly (MCA) which consists of 20 grooves and plateaus machined in a plastic washer type specimen.[103] Susceptibility to attack has been related to both crevice depth and crevice gap (see Figure 4-20). In general, crevice corrosion has been found to increase as depth increases and gap decreases. Kain[104] demonstrated this effect for cast stainless steels where the MCA was torqued to 8.5 Nm and 2.5 Nm (see Table 4-51). The corresponding gaps for these torque levels were 0.1 μm for 8.5 Nm and 10 μm for 2.5 Nm. More detailed results are presented in Table 4-52. Based on a mathematical model, Kain predicted hours to initiation of attack in these cast alloys for several crevice gaps and depths as shown in Table 4-53. Kain also has made similar predictions for Type 304 and Type 316 stainless steels as shown in Figures 4-21 and 4-22. Kain states that only limited agreement has been realized between crevice gaps assumed for modeling purposes and gaps in actual nonmetal to metal crevices, presumably because of the difficulty in measuring actual crevice gaps. The LaQue Center also has determined the effect of gap size on the time to crevice corrosion initiation for a number of wrought alloys at crevice depths of 1 and 3.5 mm as shown in Figures 4-23 and 4-24.

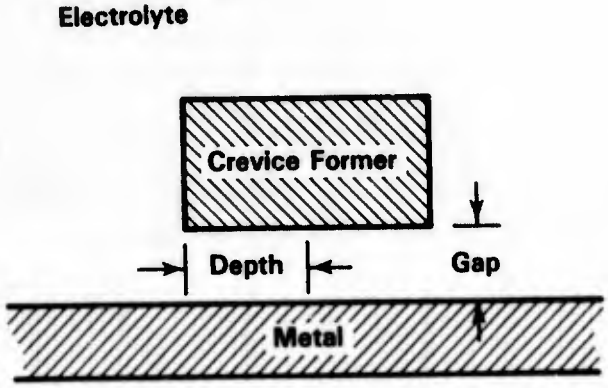

FIGURE 4-20. SCHEMATIC REPRESENTATION OF CREVICE GEOMETRY FACTORS, GAP AND DEPTH[103]

TABLE 4-51. OBSERVED TIMES TO INITIATION IN MULTIPLE CREVICE TESTS CONDUCTED IN 30 C SEAWATER*[104]

Test Conditions		Time, hr CF8M	CN7M	CN7MS	IN-862
8.5 Nm - 30 days	Earliest	87	87	87	87
	Average	87	87	87	145
	Deviation (n)	0 (5)	0(5)	0 (6)	59(2)
- 60 days	Earliest				109
	Average				162
	Deviation (n)				36(4)
Combined (8.5 Nm)	Earliest				87
	Average				157
	Deviation (n)				45(6)
2.8 Nm - 30 days	Earliest	36	109	109	
	Average	97	321	109	
	Deviation (n)	27 (6)	141(4)	0 (6)	
- 60 days	Earliest	109	109	36	109
	Average	109	302	113	230
	Deviation (n)	0 (6)	193(4)	40 (6)	158(4)
Combined (2.8 Nm)	Earliest	36	109	36	
	Average	103	312	111	
	Deviation (n)	19(12)	169(8)	28(12)	

(n) = Number of observations.

* No evidence of crevice corrosion found on any of the cast Alloy 625 and CW-12M-2 in test lasting up to 90 days at 8.5 Nm torque level.

TABLE 4-52. EXPANDED MATRIX-MULTIPLE CREVICE TEST RESULTS FOR SEVERAL CAST ALLOYS*[104]

Alloy	Test Conditions	Number of Sites Initiated		Penetration Range, mm	
		Side 1	Side 2	Side 1	Side 2
IN-862	30 day-8.5 Nm	3	1	0.12 to 0.22	0.29
		9	13	0.24 to 0.72	0.18 to 0.91
		16	10	0.18 to 1.17	0.12 to 1.22
	60 day-8.5 Nm	6	7	0.20 to 1.75	0.25 to 0.68
		4	14	0.24 to 0.72	0.23 to 1.05
	60 day-2.8 Nm	7	8	0.17 to 0.99	0.30 to 0.68
		7	2	0.08 to 4.31	0.13 to 0.26
		7	8	0.15 to 1.23	0.15 to 0.86
CN7M	30 day-8.5 Nm	14	17	0.18 to 0.76	0.28 to 2.33
		18	18	0.29 to 1.03	0.22 to 0.91
		17	13	0.18 to 1.17	0.15 to 0.70
	30 day-2.8 Nm	17	17	0.04 to 1.27	0.28 to 1.95
		18	16	0.16 to 2.24	0.08 to 1.89
	60 day-2.8 Nm	15	1	0.20 to 2.00	0.42
		19	20	0.17 to 0.97	0.08 to 2.93
CN7MS	30 day-8.5 Nm	16	19	0.18 to 2.34	0.26 to 2.06
		19	14	0.14 to 3.82	0.17 to 1.46
		14	20	0.08 to 2.47	0.12 to 2.95
	30 day-2.8 Nm	15	19	0.10 to 3.01	0.15 to 2.37
		16	18	0.13 to 2.71	0.13 to 2.72
		20	18	0.20 to 3.18	0.13 to 2.20
	60 day-2.8 Nm	19	13	0.06 to 1.73	0.21 to 2.17
		20	19	0.10 to 3.53	0.11 to 2.67
		11	19	0.10 to 2.16	0.11 to 2.29
CF8M	30 day-8.5 Nm	12	14	0.19 to 0.69	0.16 to 3.06
		17	4	0.45 to 3.77	0.45 to 0.83
		17	10	0.27 to 3.13	0.33 to 2.28
	30 day-2.8 Nm	19	12	0.18 to 3.92	0.10 to 4.04
		20	12	0.23 to 3.22	0.24 to 3.59
		18	20	0.07 to 2.86	0.10 to 3.93
	60 day-2.8 Nm	15	18	0.06 to 2.03	0.17 to 3.08
		15	13	0.14 to 1.55	0.15 to 2.24
		15	12	0.13 to 3.59	0.07 to 1.31

* 30 day-8.5 Nm test results from initial investigation (after Hack).

TABLE 4-53. EFFECT OF CREVICE GEOMETRY ON THE PREDICTED TIME TO BREAKDOWN FOR SEVERAL CAST ALLOYS IN SEAWATER[104]

Alloy	Crevice Depth, cm	Predicted Hours to Breakdown in Nonmetal to Metal Crevice Gap*			
		0.125 μm	0.250 μm	0.500 μm	1.250 μm
CW-12M2	0.5	791	NB	NB	NB
	1.0	191	465	NB	NB
Alloy 625	0.5	284	NB	NB	NB
	1.0	149	342	NB	NB
IN-862	0.5	147	NB	NB	NB
	1.0	106	232	590	NB
CN7MS	0.5	83	254	NB	NB
	1.0	70	147	333	NB
CN7M	0.5	80	238	NB	NB
	1.0	68	143	322	NB
CF8M	0.5	85	261	NB	NB
	1.0	71	149	338	NB

* NB = No breakdown.

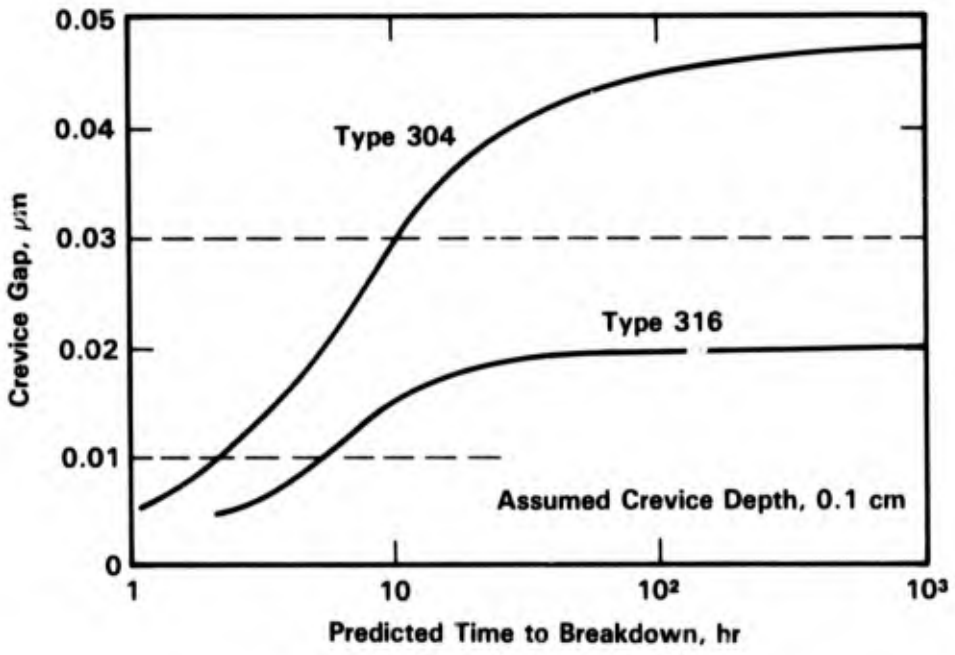

FIGURE 4-21. MODEL PREDICTION FOR EFFECT OF CREVICE DEPTH ON THE TIME TO BREAKDOWN FOR AISI TYPE 304 AND TYPE 316 STAINLESS STEEL IN SEAWATER[103]

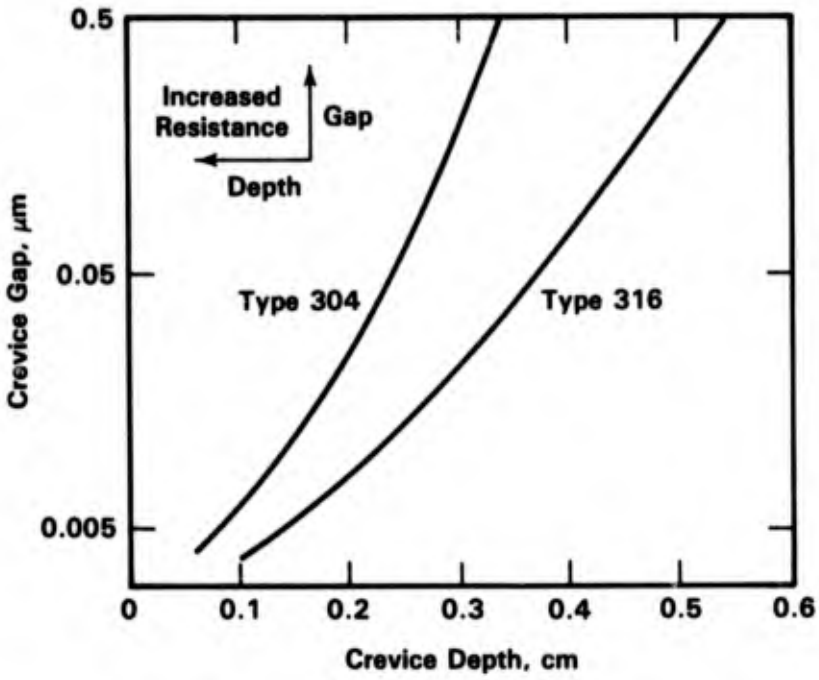

FIGURE 4-22. MODEL PREDICTION OF GEOMETRIC LIMITATIONS FOR RESISTANCE OF AISI TYPE 304 AND TYPE 316 STAINLESS STEEL TO CREVICE ATTACK IN SEAWATER[103]

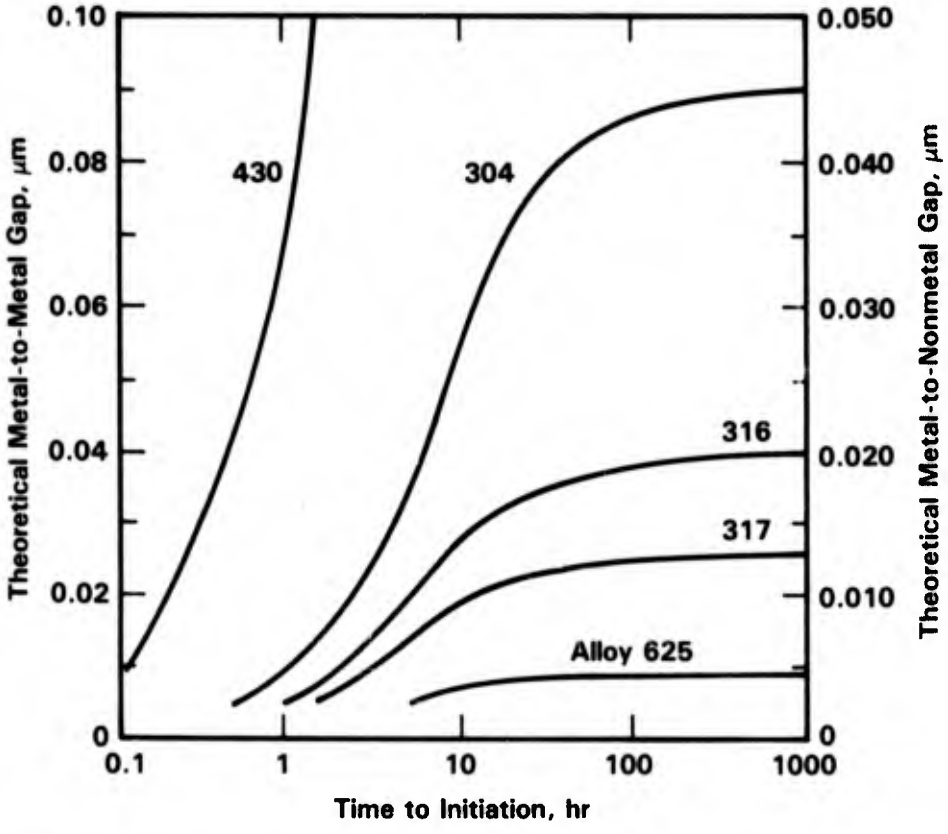

FIGURE 4-23. EFFECT OF CREVICE GAP ON TIME TO CREVICE-CORROSION INITIATION FOR VARIOUS ALLOYS IN AMBIENT TEMPERATURE SEAWATER AT CREVICE DEPTH OF 1 MM[31]

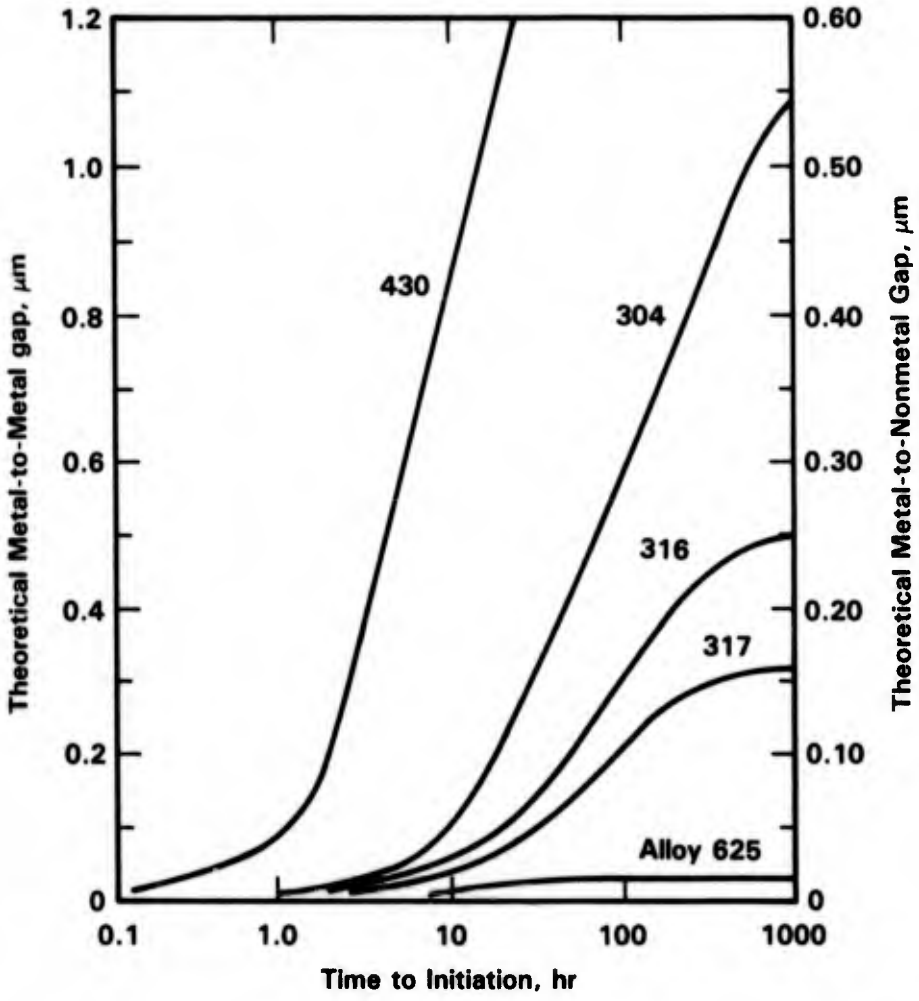

FIGURE 4-24. EFFECT OF CREVICE GAP ON TIME TO CREVICE-CORROSION INITIATION FOR VARIOUS ALLOYS IN AMBIENT TEMPERATURE SEAWATER AT CREVICE DEPTH OF 3.5 MM[31]

Oldfield and Sutton[105] also have used mathematical models to predict crevice corrosion. As shown in Table 4-54, they have devised minimum crevice corrosion resistance values which they correlate with alloy performance and with initiation of crevice attack as a function of gap size. Kain[106] has run MCA and "O" ring-on-tube crevice tests with 316 in seawater and obtained similar results for both types of crevice assemblies.

Wheatfall[107] has correlated the amount of area outside the crevice with amount and depth of crevice attack for several depths of exposure in the ocean. The results are summarized in Figure 4-25 and show an increase in attack as the area outside the crevice is increased by a factor of five. The amount of attack was greatest and the percent increase in attack was least in surface waters. This would be expected because the higher oxygen content

TABLE 4-54. MINIMUM CREVICE CORROSION RESISTANCE (CCR) VALUES REQUIRED FOR AN INFINITE TIME TO BREAKDOWN AS A FUNCTION OF CREVICE GAP FOR A CREVICE DEPTH OF 5 MM[105]

Metal-to-Nonmetal Crevice Gap, μm	Minimum CCR* Value Required for an Infinite Time to Breakdown
0.10	1600
0.25	500
0.50	360
1.0	185
2.5	80
5.0	40
10.0	25
25.0	8

* CCR numbers = are arbitrary values obtained from a predictive equation which at 1 μm crevice gap depth and 5 mm crevice depth predicts CCR numbers of ~50 for AISI Type 430, 200 for Type 304, 400 for Type 316, 1000 for IN-718, and 1800 for Inconel Alloy 625.

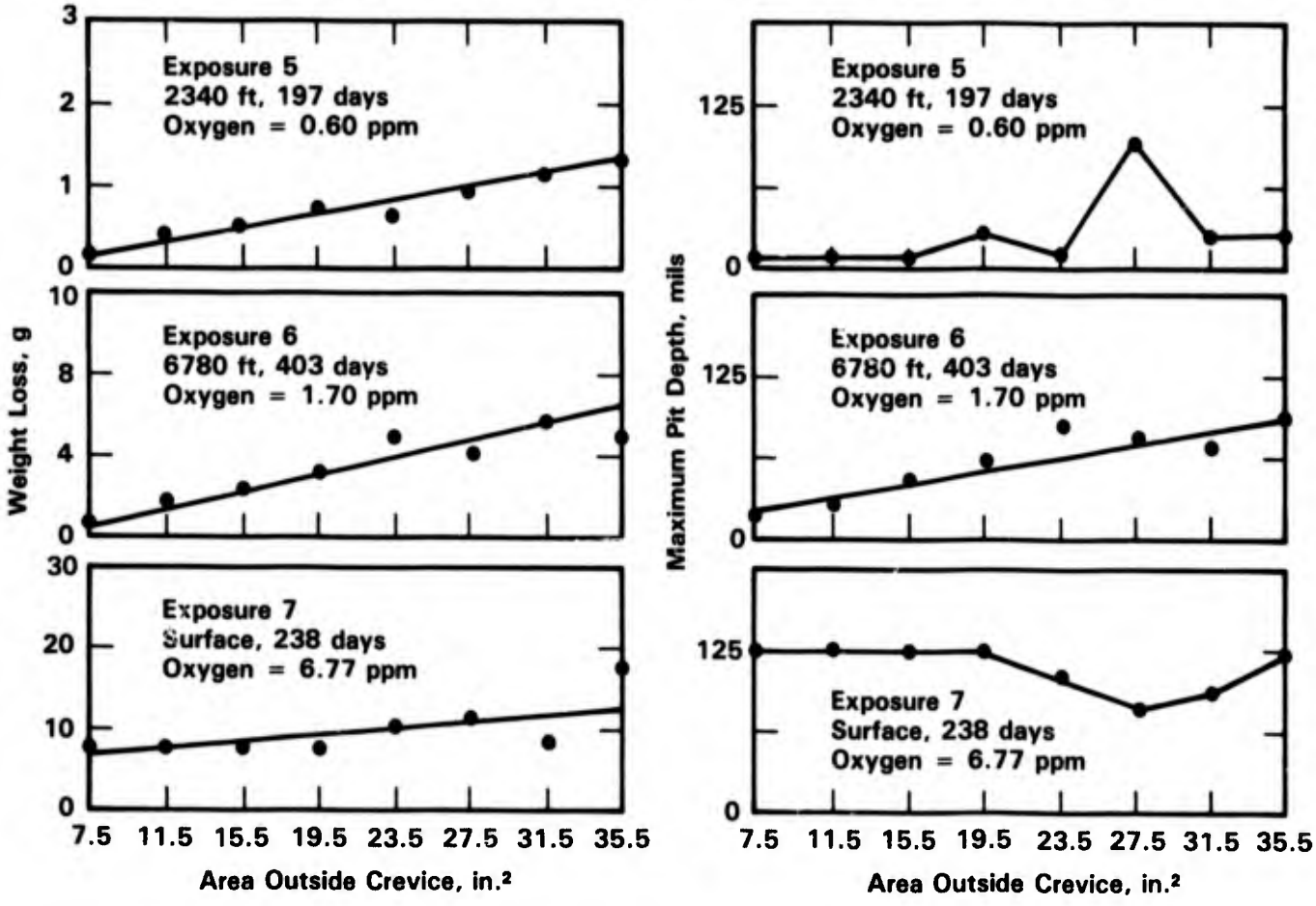

FIGURE 4-25. RELATION OF WEIGHT LOSS AND MAXIMUM PIT DEPTH IN THE CREVICE TO AREA OF SPECIMEN OUTSIDE THE CREVICE FOR TYPE 304 STAINLESS STEEL AT VARIOUS DEPTHS[107]

(Note: Specimen perforated at maximum pit depth = 0.125 in.)

would provide a larger driving force for the concentration cell corrosion, and would tend to be as effective on a small external surface area as on a large one.

Velocity. As pointed out earlier, the conventional stainless steels tend to pit in low velocity seawater. However, as a general rule of thumb, velocities greater than 1.5 to 2 m/s are sufficient to prevent pitting on boldly exposed surfaces. This critical velocity is believed to be sufficiently fast to prevent the deposition of suspended material from natural seawater. Thus, deposits do not build up, and crevice-type attack does not take place beyond the critical velocity.

Obviously, few deposits will occur from very clean seawater, and thus there are exceptions to the >1.5 m/s criterion. As shown by Henrikson, et al.[54] in Table 4-55, even 18Cr-11Ni stainless steel was resistant to 50 C seawater at velocities as low as 0.13 m/s. Note, however, that in these same tests, 13Cr-1Mo stainless steel was not resistant to pitting until the seawater velocity exceeded 5 m/s. Moller[108] reports that 310 and 316 did not pit in long-term tests at velocities of 4 fps (1.3 m/s) (see Table 4-56). On the other hand, as shown in Table 4-57, Bomberger, et al.[16] in long-term tests conducted at Kure Beach, NC, report that 302, 316, and 347 pitted to depths of 65 mils after 4-1/2 years exposure at 3 fps (1 m/s) velocity.

As would be expected, the Mo-containing stainless steels are resistant to pitting at velocities <1.5 m/s. Kovach, et al.[44] have shown in Table 4-40 that a 25Cr-2.5Ni-3Mo alloy exhibited no pitting or crevice corrosion in condenser tube tests conducted at velocities of 0 to 3.2 m/s at a number of U.S.A. coastal sites. Liebert, et al.[76] did not find any attack on Al-6X during a 10-month test at approximately 2 m/s near Hawaii, even though the test had frequent shutdowns. At higher temperatures (50 C), Fukuzuka, et al.[40] found that 304, 316L, and 329 exhibited crevice attack at velocities up to 1.5 m/s, but that alloys with 4.5 to 6.5 Mo did not exhibit crevice attack under these same conditions (see Table 4-35).

In general, the stainless steels are very resistant at very high seawater velocities. Weber[109] states that attack rates are very low for velocities through 55 m/s. As shown in Figure 4-26, the rates for stainless steel at 40 m/s are very low, and are about 3 orders of magnitude lower than those for carbon steel at the same velocity. Weber also has shown that velocity does increase the rate of attack on stainless steels in H_2S-contaminated chloride media, and, as shown in Figure 4-27, the rate of attack was in the following order:

Ferritic Cr > Austenitic-Ferritic > Austenitic Manganese > Austenitics > Special Austenitics (Mo)

TABLE 4-55. RESULTS OF 13-MONTH EXPOSURES OF UNWELDED TUBES IN BALTIC SEAWATER AT 50 C[54]

Stainless Steel	Seawater Velocity, m/s	Results
13Cr-1Mo	0.13	4 severe, 4 small pits
	1.25	1 severe, 4 small pits
	0.5	1 severe, 3 small pits
	5.	5 small pits
	10.	No pits
18Cr-11Ni	0.13 to 10.	No pits
17Cr-11Ni-1.5Mo	0.13 to 10.	No pits
17Cr-12.5Ni-2.5Mo	0.13 to 10.	No pits
17Cr-15Ni-4Mo	0.13 to 10.	No pits
19Cr-16Ni-1.4Mo	0.13 to 10.	No pits
21Cr-25Ni-2.7Mo	0.13 to 10.	No pits
26Cr-5Ni-1.5Mo	0.13 to 10.	No pits

TABLE 4-56. EFFECT OF SEAWATER VELOCITY ON PITTING OF WELDED TYPES 316 AND 310 STAINLESS STEELS (1,257 DAYS IN TEST)[108]

	In Flume at 4 Ft/Sec			In Basin at 0 Ft/Sec		
Material	Number of Pits	Maximum Depth, mils	Average Depth,[a] mils	Number of Pits	Maximum Depth, mils	Average Depth,[a] mils
Type 316 plate[b]	0	0	0	87	78	38
Type 316 weld	0	0	0	47	130	76
Type 310 te	0	0	0	19	110	38
Type 310 weld	0	0	0	23	>250[c]	120

(a) Average of 10 deepest pits.
(b) Test coupons--12 in. x 8 in. x 1/4-in.-thick with 11 lineal in. of SMA weldment in "t" pattern.
(c) Perforated from one side (thickness of specimen = 0.25 in.).

TABLE 4-57. MATERIALS IMMERSED IN SEAWATER FLOWING AT 3 FT/SEC IN TROUGH AT KURE BEACH, NC[16]

Material[a]	483 Days			618 Days			4-1/2 Years		
	Corrosion Rate, mpy	Maximum Face Pitting, in.	Maximum Edge Pitting, in.	Corrosion Rate, mpy	Maximum Face Pitting, in.	Maximum Edge Pitting, in.	Corrosion Rate, mpy	Maximum Face Pitting, in.	Maximum Edge Pitting, in.
302 Stainless	0.08	0.031	0.060	--	--	--	0.088	0.060	0.20
316 Stainless	0.16	0.020	0.10	--	--	--	0.061	0.050	0.10
347 Stainless	0.28	0.068[b]	1.5[c]	3.57	0.068[b]	1.5[c]	--	--	--

(a) Three specimens of each.
(b) Specimens perforate with pits.
(c) Maximum depth of crevice corrosion.

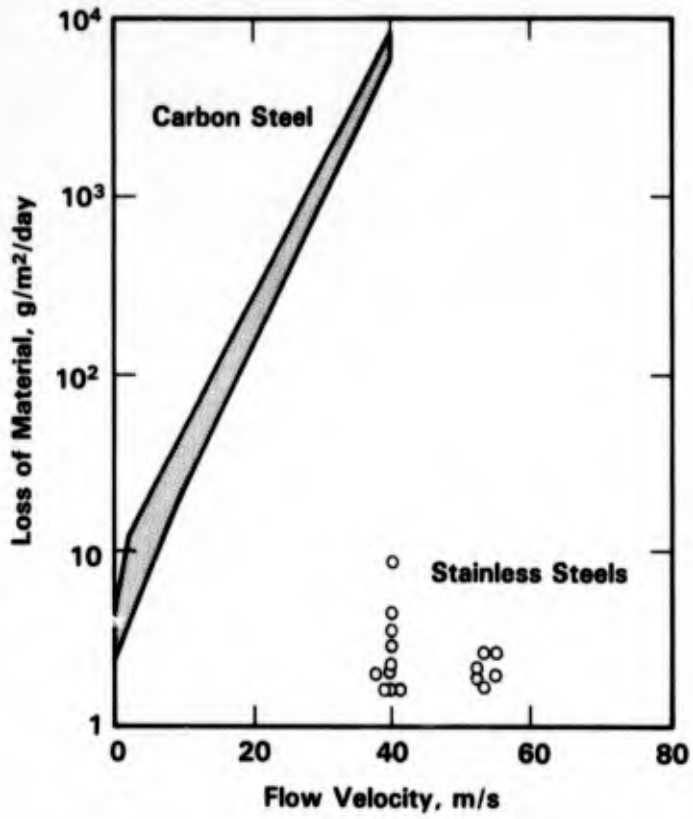

FIGURE 4-26. WEIGHT LOSS OF DIFFERENT MATERIALS IN CLEAN SEAWATER AS A FUNCTION OF FLOW VELOCITY[109]

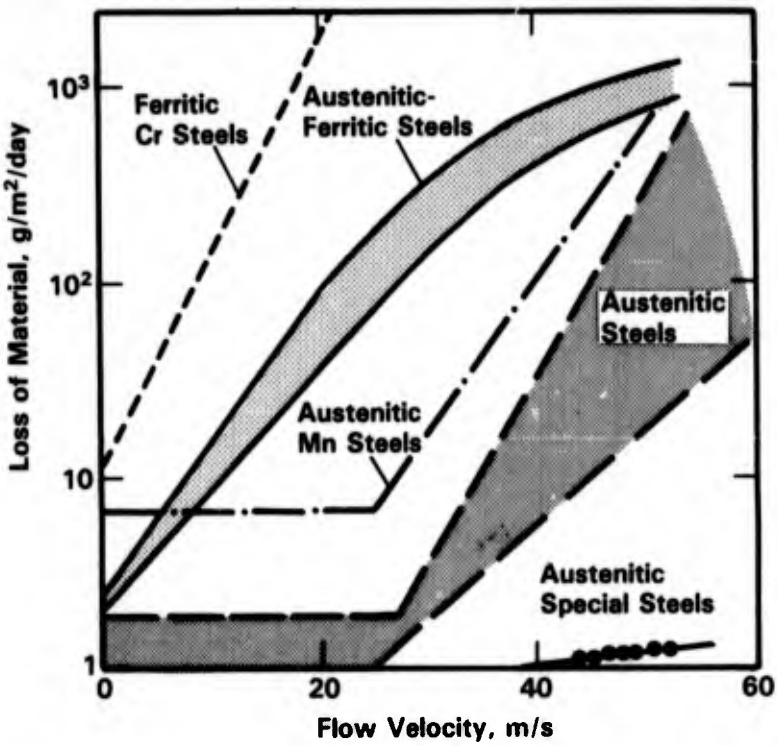

FIGURE 4-27. INFLUENCE OF FLOW VELOCITY ON WEIGHT LOSS OF DIFFERENT MATERIALS IN MEDIA WITH HIGH H_2S CONTENT (500 PPM) AND LOW pH VALUES (pH 4.5)[109]

Rates of attack for a number of stainless steels at velocities to 142 fps (43 m/s) are shown in Table 4-58 and Table 4-59. Note the very low corrosion rates even for those alloys that contain no Mo. It should be pointed out, however, that cavitation (rapid bubble collapse) can cause very high rates of attack in stainless steels. Hohman and Kennedy[111] report cavitation rates of the order of 1 to 2 in./yr (2.5 to 5 cm/yr) for 17-4PH, AM-355, and CD4MCu in seawater.

Time. The effect of exposure time on pitting has not been studied extensively. As pointed out by Reinhart,[33,112] pitting and crevice corrosion are highly variable and are difficult to quantify on a weight loss basis, see Tables 4-60 to 4-64. In many exposures, the susceptible alloys will perforate within the first year of exposure, whereas the resistant alloys will exhibit no pitting attack for the full exposure time of upwards of 8 to 10 years.

The variable nature of pitting and crevice corrosion is shown in Figure 4-28 from Lennox, et al.[113] Note that pitting and crevice corrosion were greater at 490 days' exposure than at 649 days. Similar anomalous behavior was observed for 20Cb-3 (Figure 4-29), but crevice corrosion was greater at 649 days than at 490 days.

Kowaka, et al.[36] showed a slight increase in attack between one and two years as shown in Figure 4-5. Bomberger, et al.[16] also showed an increase in pitting attack between 1-1/3 and 4-1/2 years' exposure of 302 and 316 (see Table 4-57). As shown in Figure 4-3, Alexander, et al.[32] found a decreasing pitting rate with time in tropical seawater. Note that all of their alloy specimens perforated in the first year of exposure. Since their data are for the average of the 20 deepest pits, it is obvious that pits propagated at different rates, or else some stopped propagating altogether. Otherwise, if all penetration rates were equal, the nonperforated pits at 1 year exposure would be those that initiated later and they would be expected to perforate before the end of 2 years' exposure.

It should also be noted that the pitting rate probably varies erratically during exposure. This can be inferred from Lennox and Peterson's[84] long term (560 days) potential tests where considerable day-to-day variation in the corrosion potential was observed.

Effect of pH. Most of the reported data for the effect of pH have been on effects on electrochemical behavior. However, as shown in Figure 4-30, Kowaka, et al.[36] have found that increasing the pH (pH 1 to 5) results in a decrease in crevice corrosion in 3 percent NaCl solution.

The pH/potential relationship has been studied by a number of investigators including Schrieber and Coley,[114] Ulanovskii and Korovin,[115] Mar, et al.,[116] Kowaka, et al.,[36] Oldfield and Sutton,[117] Roy,[118] Suzuki and Kitamura,[63] Mazza, et al.,[71]

TABLE 4-58. CORROSION BEHAVIOR AS A FUNCTION OF SEAWATER VELOCITY[110]

Alloy Designation	Composition Cr	Ni	Mn	Mo	Cu	High Velocity, 120 fps Corrosion Rate, mdd	Intermediate Velocity, 25 fps Corrosion Rate, mdd	Low Velocity (0-2 fps) (Crevice Attack) Maximum Penetration, in.	Remarks
S-1	17.0	4.5	6.5	--	--			0.625[a]	Inside crevice.
S-2	18.0	5.0	9.0	--	--			0.625[a]	Inside crevice.
S-3	17.0	7.0	2.0 Max	--	--			0.625[a]	Inside crevice.
S-4	19.0	10.0	2.0 Max	--	--	1.4		0.625 and 0.125[a](2)	Inside crevice. Inside crevice.
S-5	17.0	12.0	2.0 Max	2.5	--				
S-6	18.0	11.0	2.0 Max	--	--	1.8		0.03	
S-7	17.0	4.0	0.7	3.0	--	0.9			
S-8	16.5	4.0	--	--	4.0	2.6			
S-9	17.0	7.0	1.0 Max	--	--	1.0			
S-10	20.0	9.0	1.0 Max	4.0	--	0.6	14	0.16 (2)	Inside crevice, pitting on bold surface to 0.008.
S-11	20.0	29.0	--	3.0	4.0	2.0 (2)	1.1	0.11 (2)	Inside crevice, pitting on bold surface to 0.01.
S-12	50.0	28.0	1.3	8.5	5.5	0.4	0.9	0.04 (2)	Inside crevice, pitting on bold surface to 0.004.
S-13	55.0	28.0	1.3	8.5	5.5	0.5	1.1	0.20 (2)	Inside crevice, pitting on bold surface to 0.002.
S-14	24.0	13.0	2.5	--	--	1.3	24	0.08 (2)	Inside crevice, pitting on bold surface to 0.008.
S-15	28.0	10.0	1.5	--	--	4.6	39	0.13 (2)	Inside crevice, pitting on bold surface to 0.04.
S-16	26.0	5.0	--	2.0	3.0	0.6	2.1	0.18 (2)	Inside crevice, pitting on bold surface to 0.09.

(a) Specimens perforated.

General Notes:

- All are stainless alloys and have excellent corrosion resistance at high and intermediate velocities; severe local attack at low velocity and in crevices.
- All data are single tests unless otherwise noted by numbers in parentheses. Multiple test values may represent more than one heat, heat treatment, or form (cast versus wrought).
- Test description: high velocity: jet apparatus, generally 30-days duration; intermediate velocity: rotating rectangular bars, generally 60-days duration; and low velocity: quiet seawater or trough exposure, generally 1-year duration.
- Corrosion rate expressed as milligrams/square decimeter/day (mdd).

TABLE 4-59. SUMMARY OF CORROSION DATA FOR MATERIALS TESTED IN HIGH-VELOCITY JET APPARATUS[108]

Duration of Tests: 30 days
Exposed Area of Specimens: 3.5 $in.^2$

Material	Weight Loss, g	Corrosion Rate, mpy	Average Seawater Temperature, C	Seawater Velocity, ft/sec
AISI 304	0.008	0.2	10	142
AISI 316	0.008	0.2	10	142
Incoloy Alloy 825*	0.011	0.3	11	141
17-4PH**	0.012	0.3	10	142

Trademarks: * Huntington Alloys, Inc.
** Armco Steel Corporation.

TABLE 4-60. CORROSION OF 200 SERIES STAINLESS STEELS IN SEAWATER[112]

Alloy[c]	Exposure Days	Exposure Depth, ft	Dissolved O_2, ppm	Corrosion Rate, mpy[a]	Maximum Pit Depth, mils[b]	Corrosion, Crevice Depth, mils[b]	Corrosion Type[b]
201	366	5	3.9-6.6	0.6	--	--	SE
201	402	2,370	0.4	<0.1	0	I	C
201	403	6,780	1.6	<0.1	0	I	C
202	366	5	3.9-6.6	0.5	50 (PR)	50 (PR)	CP
202	402	2,370	0.4	<0.1	0	17	C
202	403	6,780	1.6	<0.1	0	I	C

(a) mpy - mils penetration per year calculated from weight loss.
(b) Symbols for types of corrosion: C - crevice; E - edge; I - incipient; P - pitting; PR - perforated; and S - severe.
(c) AISI Type.

TABLE 4-61. CORROSION OF 300 SERIES STAINLESS STEELS IN SEAWATER[112]

Alloy[a]	Exposure Days	Exposure Depth, ft	Dissolved O_2, ppm	Corrosion Rate, mpy[b]	Maximum Pit Depth, mils[c]	Corrosion, Crevice Depth, mils[c]	Corrosion Tunnel, Maximum Length, mils[c]	Corrosion Type[c]
301	398	5	3.9-6.6	2.3	103 (PR)	0	1150	TP
301	402	2,370	0.4	0.5	103 (PR)	0	2500	TP
301	403	6,780	1.6	1.4	103 (PR)	15	2450	CTP
301	588	5	3.9-6.6	1.7	103 (PR)	50	1500	CTP
302	366	5	3.9-6.6	<0.1	I	I	--	CP
302	398	5	3.9-6.6	0.4	53 (PR)	53 (PR)	5400	CETP
302	402	2,370	0.4	<0.1	0	I	--	C
302	402	2,370	0.4	<0.1	0	18	6000	CT
302	403	6,780	1.6	<0.1	0	I	--	C
302	403	6,780	1.6	<0.1	0	18	0	C
302	588	5	3.9-6.6	0.5	52 (PR)	52 (PR)	5500	CPT
304	366	5	3.9-6.6	0.4	34	33	--	CP
304	402	2,370	0.4	0.4	210 (PR)	0	2000	ETP
304	402	2,370	0.4	<0.1	0	13	--	C
304	403	6,780	1.6	0.5	210 (PR)	0	2000	ETP
304	403	6,780	1.6	<0.1	0	I	--	C
304	540	5	3.9-6.6	0.7	42	103	183	CPT
304	588	5	3.9-6.6	0.5	0	138	113	CT
304[d]	366	5	3.9-6.6	1.2	50 (PR)	50 (PR)	--	CP
304[d]	402	2,370	0.4	0.3	0	50 (PR)	--	C
304[d]	403	6,780	1.6	0.7	0	50 (PR)	--	C
304L	366	5	3.9-6.6	0.5	50 (PR)	0	--	P
304L	398	5	3.9-6.6	1.0	115 (PR)	0	1100	ETP
304L	402	2,370	0.4	<0.1	0	I	--	C
304L	402	2,370	0.4	0.4	115 (PR)	0	3000	TP
304L	403	6,780	1.6	<0.1	0	I	--	C
304L	403	6,780	1.6	<0.1	115 (PR)	12	4850	CETP
304L	540	5	3.9-6.6	0.7	115 (PR)	115 (PR)	1500	CETP
309	366	5	3.9-6.6	<0.1	0	I	--	C
309	402	2,370	0.4	<0.1	0	I	--	C
309	403	6,780	1.6	<0.1	0	I	--	C
310	366	5	3.9-6.6	<0.1	0	50 (PR)	--	C
310	402	2,370	0.4	<0.1	0	14	--	C
310	403	6,780	1.6	<0.1	0	I	--	C
311	366	5	3.9-6.6	<0.1	I	I	--	CP
311	402	2,370	0.4	<0.1	0	6	--	C
311	403	6,780	1.6	<0.1	0	I	--	C
316	366	5	3.9-6.6	<0.1	0	0	--	NC
316	398	5	3.9-6.6	0.4	154	20	1350	CETP

TABLE 4-61. (Continued)

Alloy[a]	Exposure Days	Exposure Depth, ft	Dissolved O_2, ppm	Corrosion Rate, mpy[b]	Maximum Pit Depth, mils[c]	Corrosion, Crevice Depth, mils[c]	Corrosion Tunnel, Maximum Length, mils[c]	Corrosion Type[c]
316	402	2,370	0.4	<0.1	0	I	--	C
316	402	2,370	0.4	0.1	230 (PR)	0	500	ETP
316	403	6,780	1.6	<0.1	0	I	--	C
316	403	6,780	1.6	<0.1	0	0	0	NC
316	540	5	3.9-6.6	0.3	0	63	70	CT
316	588	5	3.9-6.6	0.2	0	130	1500 (PR)	CP
316[d]	366	5	3.9-6.6	0.6	50 (PR)	50 (PR)	--	CP
316[d]	402	2,370	0.4	<0.1	0	8	--	C
316[d]	403	6,780	1.6	<0.1	0	I	--	C
316L	366	5	3.9-6.6	<0.1	0	I	--	C
316L	398	5	3.9-6.6	<0.1	0	0	0	SLE
316L	402	2,370	0.4	<0.1	0	I	--	C
316L	402	2,370	0.4	<0.1	0	0	0	NC
316L	403	6,780	1.6	<0.1	0	I	--	C
316L	403	6,780	1.6	<0.1	0	0	0	NC
317	366	5	3.9-6.6	<0.1	0	I	--	C
317	402	2,370	0.4	<0.1	0	I	--	C
317	403	6,780	1.6	<0.1	0	I	--	C
321	366	5	3.9-6.6	<0.1	22	0	--	P
321	402	2,370	0.4	0.2	0	30 (PR)	--	C
321	403	6,780	1.6	<0.1	0	I	--	C
325	366	5	3.9-6.6		16	12	--	CP
325	402	2,370	0.4	1.9	0	0	--	
325	403	6,780	1.6		0	0	--	P
329	366	5	3.9-6.6	<0.1	0	I	--	
329	402	2,370	0.4	<0.1	0	0	--	
329	403	6,780	1.6	<0.1	0	0	--	
330	366	5	3.9-6.6	0.4	50 (PR)	0	--	P
330	402	2,370	0.4	<0.1	0	30 (PR)	--	C
330	403	6,780	1.6	<0.1	0	I	--	C
347	366	5	3.9-6.6	0.7	50 (PR)	50 (PR)	--	CP
347	402	2,370	0.4	<0.1	0	I	--	C
347	403	6,780	1.6	<0.1	0	I	--	C

(a) AISI Type.
(b) mpy - mils penetration per year calculated from weight loss.
(c) Symbols for types of corrosion: C - crevice; E - edge; G - general; NC - no visible corrosion; P - pitting; PR - perforated; SL - slight; and T - tunnel.
(d) S - sensitized by heating to 1200 F for 1 hour and cooling in air.

TABLE 4-62. CORROSION OF 400 SERIES STAINLESS STEELS IN SEAWATER[112]

Alloy[a]	Exposure Days	Exposure Depth, ft	Dissolved O_2, ppm	Corrosion Rate, mpy[b]	Maximum Pit Depth, mils[c]	Corrosion, Crevice Depth, mils[c]	Corrosion Tunnel, Maximum Length, mils[c]	Corrosion Type[c]
405	402	2,370	0.4	1.8	40	15	0	CP
405	403	6,780	1.6	3.9	0	0	2000 (PR)	ET
405	588	5	3.9-6.6	4.5	124	250 (PR)	0	CP
410	366	5	3.9-6.6	3.0	50 (PR)	50 (PR)	--	CP
410	402	2,370	0.4	0.8	50 (PR)	50 (PR)	--	CP
410	402	2,370	0.4	0.5	40 (PR)	40 (PR)	6400	CTP
410	403	6,780	1.6	1.9	50 (PR)	50 (PR)	--	CP
410	403	6,780	1.6	0.2	40 (PR)	40 (PR)	6000	CTP
430	366	5	3.9-6.6	1.1	50 (PR)	50 (PR)	--	CP
430	402	2,370	0.4	0.8	30 (PR)	30 (PR)	--	CP
430	402	2,370	0.4	0.6	137 (PR)	20	6000	CETP
430	403	6,780	1.6	<0.1	0	I	--	C
430	403	6,780	1.6	0.2	137 (PR)	30	3750	CTP
430	540	5	3.9-6.6	0.7	50 (PR)	50 (PR)	4450	CTP
430	588	5	3.9-6.6	0.9	50 (PR)	50 (PR)	3900	CTP
446	366	5	3.9-6.6	0.6	50 (PR)	50 (PR)	--	CP
446	402	2,370	0.4	<0.1	0	I	--	C
446	403	6,780	1.6	<0.1	0	0	--	NC

(a) AISI Type.
(b) mpy - mils penetration per year calculated from weight loss.
(c) Symbols for types of corrosion: C - crevice; E - edge; NC - no visible corrosion; P - pitting; PR - perforated; T - tunnel.

TABLE 4-63. CORROSION OF 600 SERIES PRECIPITATION HARDENING STAINLESS STEELS[112]

Alloy	Exposure Days	Exposure Depth, ft	Dissolved O_2, ppm	Corrosion Rate, mpy[a]	Maximum Pit Depth, mils[b]	Corrosion, Crevice Depth, mils[b]	Corrosion Tunnel, Maximum Length, mils	Corrosion Type[b]	Corrosion Weld[b][c]
AISI 630, H925[e]	398	5	3.9-6.6	1.4	112 (PR)	112 (PR)	0	CEP	TPR (WB & HAZ)
AISI 630, H925[e]	402	2,370	0.4	<0.1	0	0	0	NC	NC
AISI 630, H925[e]	403	6,780	1.6	<0.1	0	0	0	NC	TPR (WB)
AISI 631, TH1050[d]	398	5	3.9-6.6	1.9	125 (PR)	125 (PR)	2600	CTP	SCC
AISI 631, TH1050[d]	402	2,370	0.4	0.4	125 (PR)	0	3750	ETP	IP
AISI 631, TH1050[d]	403	6,780	1.6	0.2	0	0	1750	ET	NC
AISI 632, RH1100[e]	398	5	3.9-6.6	1.8	125 (PR)	125 (PR)	750	CTP	NC
AISI 632, RH1100[e]	402	2,379	0.4	0.7	125 (PR)	0	1000	TP	NC
AISI 632, RH1100[e]	403	6,780	1.6	1.5	125 (PR)	125 (PR)	2000	CTP	NC
AISI 633	366	5	3.9-6.6	<0.1	0	I	--	C	--
AISI 633	402	2,370	0.4	<0.1	0	I	--	C	--
AISI 633	403	6,780	1.6	<0.1	0	I	--	C	--
AISI 635	398	5	3.9-6.6	0.6	40	40	1200	CETP	--
AISI 635	402	2,370	0.4	0.3	0	275 (PR)	1200	CT	--
AISI 635	403	6,780	1.6	0.2	0	20	0	C	--
AISI 635	588	5	3.9-6.6	0.5	275 (PR)	275 (PR)	500	CTP	--
17-14-Cu-Mo	366	5	3.9-6.6	<0.1	0	I	--	C	--
17-14-Cu-Mo	402	2,370	0.4	<0.1	0	I	--	C	--
17-14-Cu-Mo	403	6,780	1.6	<0.1	0	I	--	C	--

(a) mpy - mils penetration per year calculated from weight loss.
(b) Symbols for types of corrosion: C - crevice; E - edge; HAZ - heat affected zone along weld; I - incipient; NC - no visible corrosion; P - pitting; PR - perforated; SCC - stress-corrosion cracking T - tunnel; and WB - weld bead.
(c) Applies only to weld bead and adjacent heat affected zones.
(d) Three-inch diameter weld in center of specimens.
(e) Transverse butt weld across center of specimen.

TABLE 4-64. CORROSION OF MISCELLANEOUS CAST AND WROUGHT STAINLESS STEELS[112]

Alloy	Exposure Days	Exposure Depth, ft	Dissolved O_2, ppm	Corrosion Rate, mpy[a]	Maximum Pit Depth, mils[b]	Corrosion, Crevice Depth, mils[b]	Corrosion Tunnel, Maximum Length, mils[b]	Corrosion Type[b]
20Cb	398	5	3.9-6.6	<0.1	14	0	0	SLEP
20Cb	402	2,370	0.4	<0.1	0	0	0	NC
20Cb	403	6,780	1.6	0.0	0	0	0	NC
20Cb	540	5	3.9-6.6	<0.1	24	0	0	P
20Cb	488	5	3.9-6.6	<0.0	0	21	0	C
20Cb-3	366	5	3.9-6.6	<0.1	0	0	--	NC
20Cb-3	402	2,370	0.4	<0.1	I	0	--	P
20Cb-3	403	6,780	1.6	<0.1	0	I	--	C
Ni-Cr-Cu-Mo #1	366	5	3.9-6.6	<0.1	0	I	--	C
Ni-Cr-Cu-Mo #1	402	2,370	0.4	<0.1	0	8	--	C
Ni-Cr-Cu-Mo #1	403	6,780	1.6	<0.1	0	0	--	NC
Ni-Cr-Cu-Mo #2	366	5	3.9-6.6	0.1	0	27	--	C
Ni-Cr-Cu-Mo #2	402	2,370	0.4	0.2	3	0	--	P
Ni-Cr-Cu-Mo #2	403	6,780	1.6	<0.1	0	0	--	NC
Ni-Cr-Mo	366	5	3.9-6.6	<0.1	0	0	--	NC
Ni-Cr-Mo	402	2,370	0.4	<0.1	0	1	--	C
Ni-Cr-Mo	403	6,780	1.6	<0.1	0	I	--	C
Ni-Cr-Mo-Si	366	5	3.9-6.6	<0.1	0	0	--	NC
Ni-Cr-Mo-Si	402	2,370	0.4	<0.1	0	0	--	NC
Ni-Cr-Mo-Si	403	6,780	1.6	<0.1	0	0	--	NC
18Cr-14Mn-0.5N	366	5	3.9-6.6	2.6	50 (PR)	50 (PR)	--	CP
18Cr-14Mn-0.5N	402	2,370	0.4	1.1	0	62 (PR)	--	C
18Cr-14Mn-0.5N	402	2,370	0.4	0.8	115 (PR)	0	2000	TP
18Cr-14Mn-0.5N	403	6,780	1.6	<0.1	0	I	--	C
18Cr-14Mn-0.5N	403	6,780	1.6	0.5	115 (PR)	0	2750	TP
18Cr-14Mn-0.5N	588	5	3.9-6.6	1.6	0	34	2900 (PR)	CT
18Cr-14Mn-0.5N	608	5	3.9-6.6	1.8	0	115 (PR)	600 (PR)	CT

(a) mpy - mils penetration per year calculated from weight loss.
(b) Symbols for types of corrosion: C - crevice; E - edge; I - incipient; NC - no visible corrosion; P - pitting; PR - perforated; SL - slight; and T - tunnel.

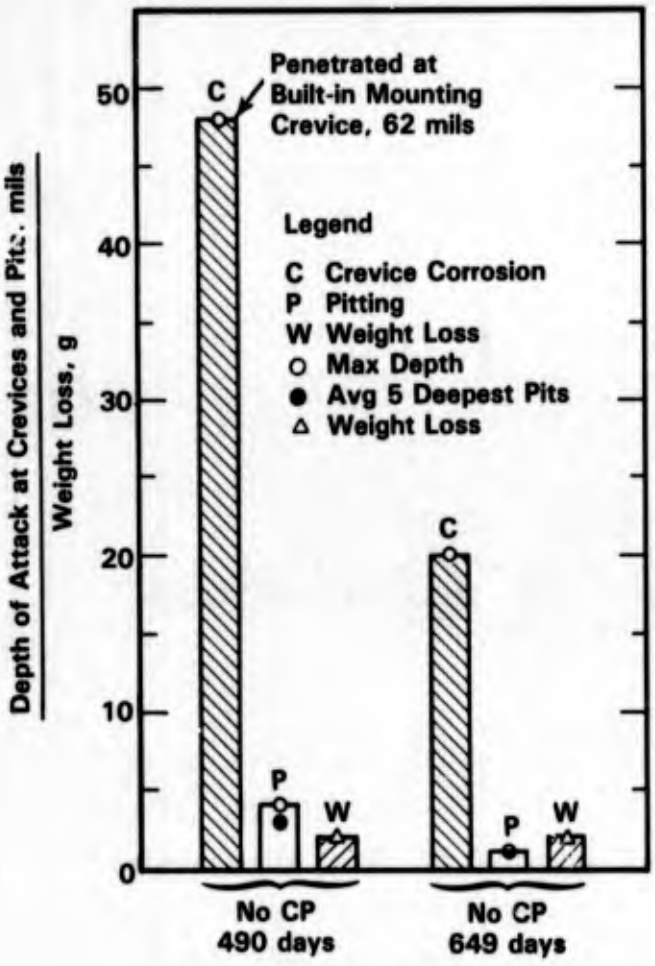

FIGURE 4-28. DEPTH OF ATTACK AND WEIGHT LOSS DATA ON 304 STAINLESS STEEL IN SEAWATER AT KEY WEST, FL, WITHOUT CATHODIC PROTECTION(113)

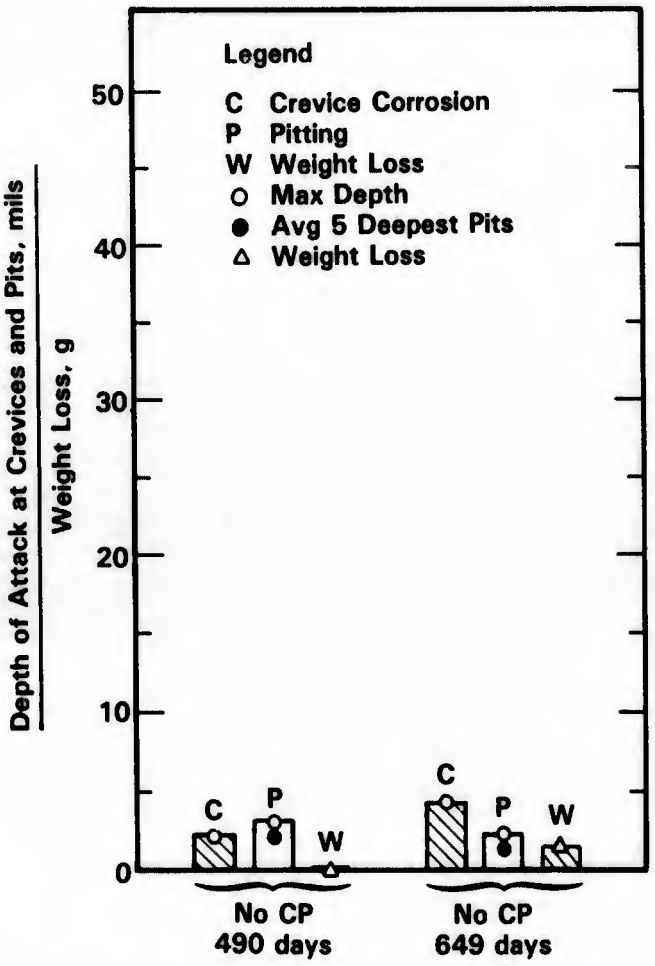

FIGURE 4-29. DEPTH OF ATTACK AND WEIGHT LOSS DATA ON STAINLESS STEEL No. 20Cb-3 IN SEAWATER AT KEY WEST, FL, WITHOUT CATHODIC PROTECTION(113)

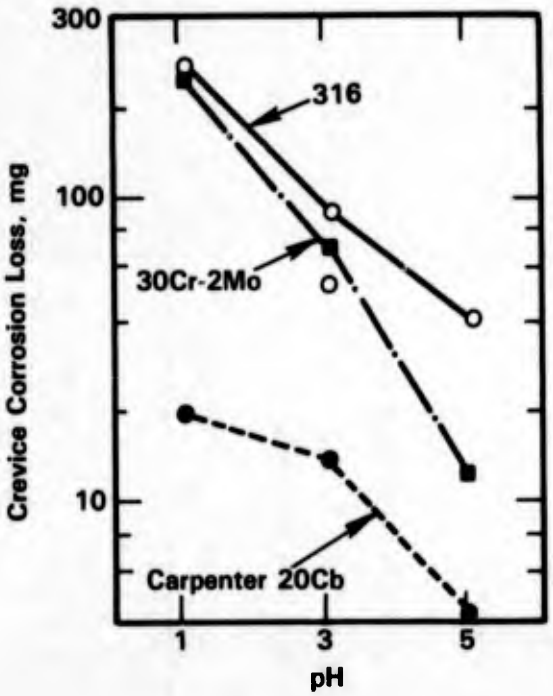

FIGURE 4-30. EFFECT OF pH ON CREVICE CORROSION OF STAINLESS STEELS IN THE SOLUTION OF 3 PERCENT NaCl + 1/20M Na_2SO_4 + ACTIVATED CARBON AT 35 C[36]

Manning, et al.,[119] and Scotto, et al.[99] Most of these studies have been conducted in NaCl solutions, although Schrieber and Coley[114] have measured corrosion, pitting, and pitting protection potentials of Type 304 in seawater as a function of pH, albeit the seawater was deaerated and at 250 F (see Figures 4-31 and 4-32). Note that the corrosion potential did not become more negative than the pitting protection potential until the pH exceeded 7 to 8.

As shown in Figure 4-33, the pitting potentials for conventional stainless steels in NaCl tend to become more negative and corrosion currents tend to become larger as the pH is decreased. This trend in the pitting potentials is evident in data reported by Manning, et al.[119] in Figure 4-34 although, they show a sharp increase in pitting potential at pH >8 to 9. On the other hand, Suzuki and Kitamura[63] have found that the critical potential for pit growth in Type 316L in 0.88 N NaCl at 70 C was approximately -0.255 V(SCE) and did not change with pH over the range 3 to 12. Manning, et al.[119] believe that the pitting potentials in their tests were a function of the morphology of sulfide inclusions in the microstructure which might account for the difference in pH effects between their results and those of Suzuki and Kitamura.[63]

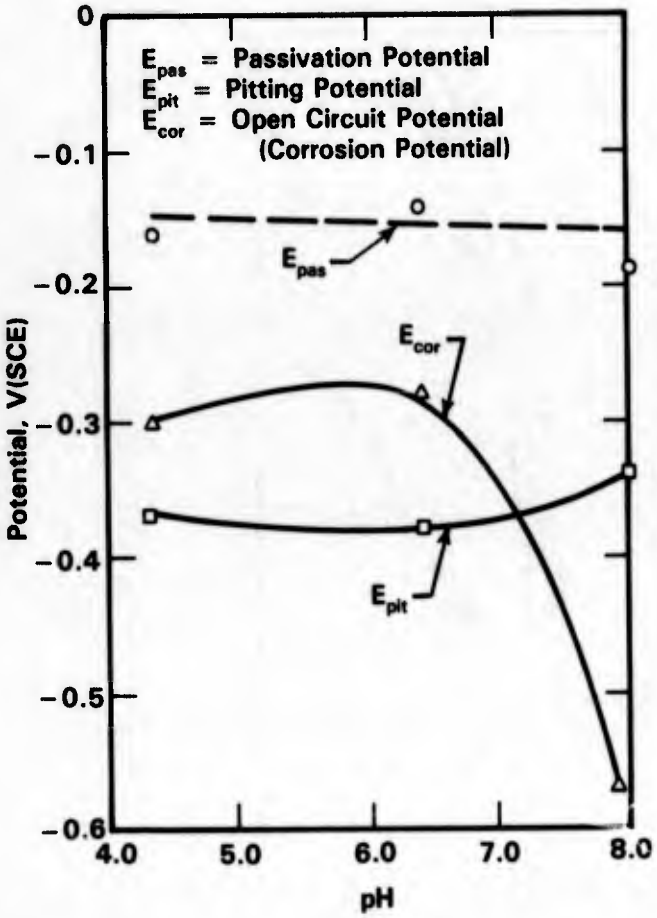

FIGURE 4-31. COMPILED POTENTIALS FOR AISI 304 STAINLESS STEEL IN DEAERATED SEAWATER WITH RUBBER O-RING CREVICE[114]

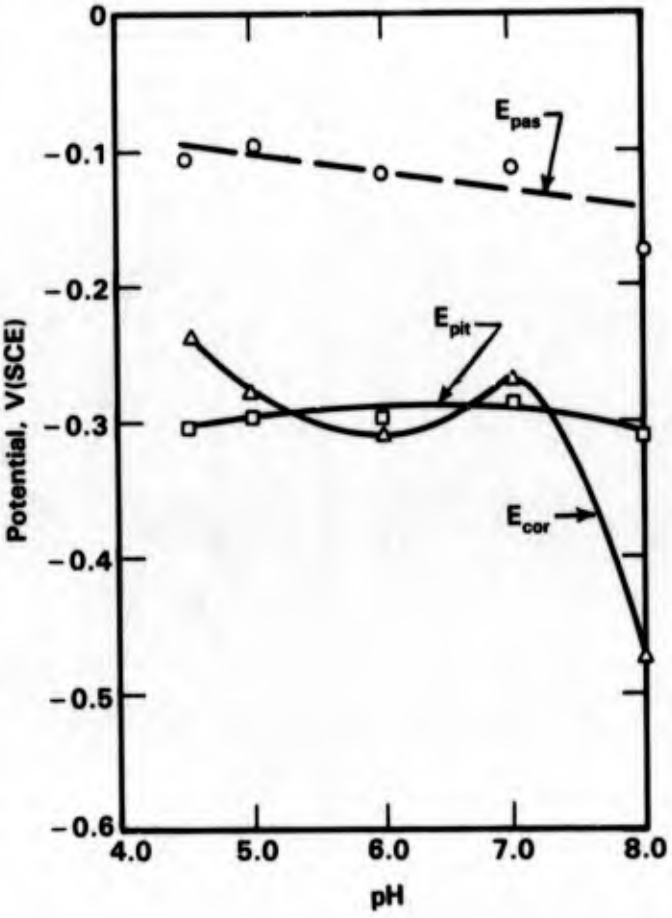

FIGURE 4-32. COMPILED POTENTIALS FOR AISI 304 STAINLESS STEEL IN DEAERATED SEAWATER WITHOUT ARTIFICIAL CREVICE[114]

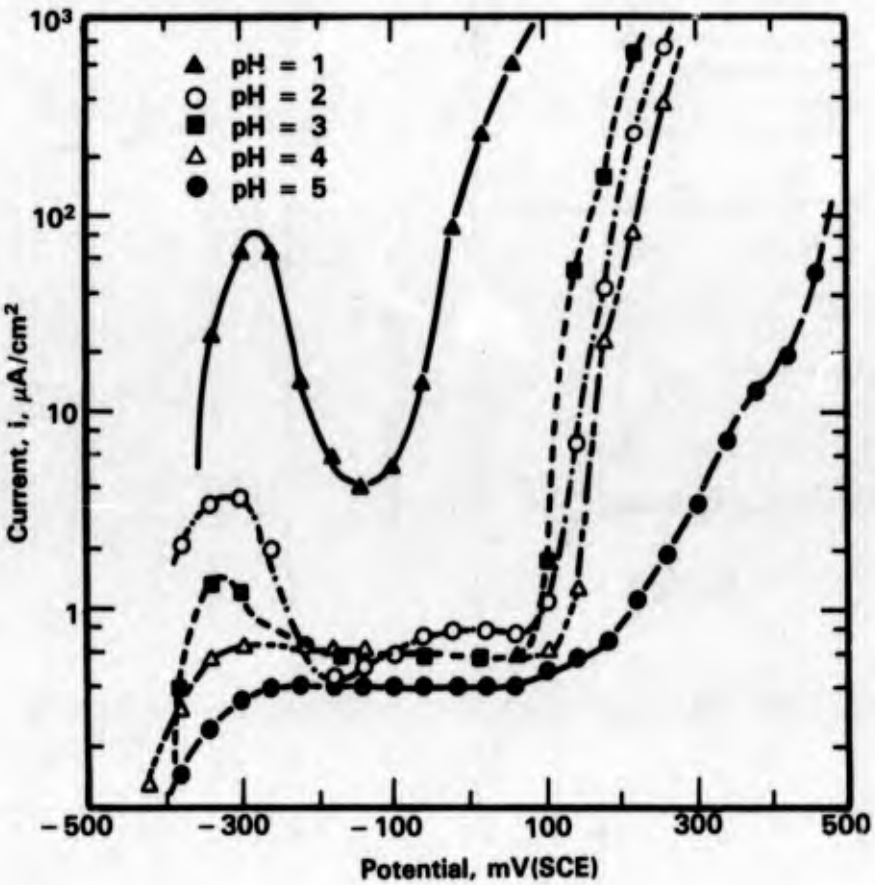

FIGURE 4-33. POTENTIOSTATIC POLARIZATION CURVES OF AISI 316 IN DEAERATED 3 PERCENT NaCl AT DIFFERENT pH VALUES[99]

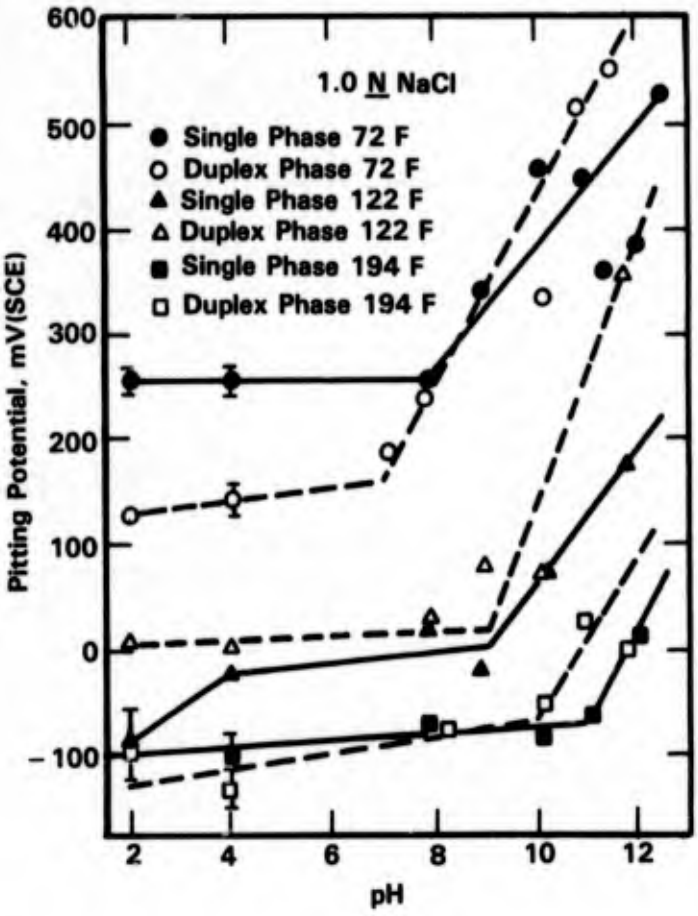

FIGURE 4-34. PITTING POTENTIALS OF SINGLE PHASE AND DUPLEX TYPE 304L AS A FUNCTION OF pH AT SEVERAL TEMPERATURES IN 1 N NaCl[119]

Several authors have determined the critical pH in crevices at which passivity breakdown and corrosion ensues. In studying this relationship with Type 316 in 0.5M NaCl, Oldfield and Sutton[117] showed that at pH <3, the chloride, iron, chromium, nickel, and molybdenum content increased (in decreasing order) in the crevice solution, (see Figure 4-35). Oldfield and Sutton[105] also have determined the critical pH and chloride levels in crevice solutions that cause crevice attack (sharp increase in the passive current) of several stainless steels, (see Table 4-65).

Pollutants. Despite the fact that stainless steels are widely recommended where corrosion problems are encountered in polluted seawater, only limited data are available from laboratory or field studies. Larrabee[1] mentioned that stainless steel pump impellers have been used successfully in polluted seawater, and Todd[120] quotes LaQue that Type 316 has performed well in polluted seawater. In Table 4-44 Eden indicates that 20Cr-25Ni-4.5Mo has

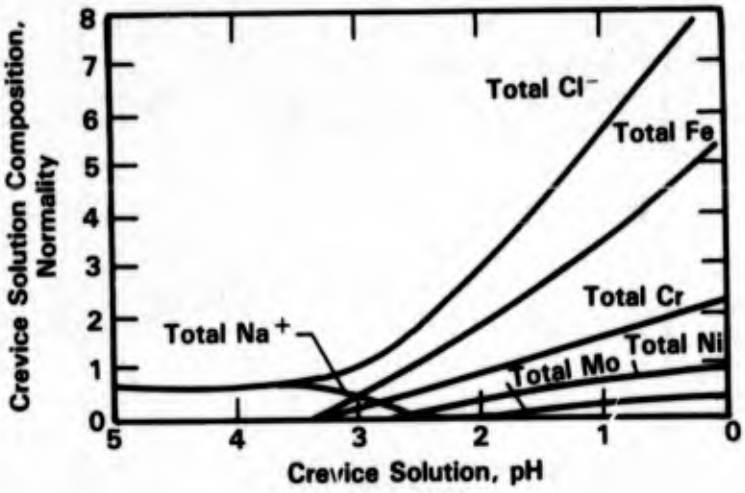

FIGURE 4-35. PREDICTED CHANGES IN CREVICE SOLUTION COMPOSITION AS pH FALLS: 18Cr-10Ni-2.5Mo IN 0.5M NaCl AT AMBIENT TEMPERATURE[117]

TABLE 4-65. CRITICAL CREVICE SOLUTION VALUES (CCS)[105]

Alloy	CCS	
	$(Cl^-)M$	pH
1. AISI 430	1.0	2.90
2. AISI 304	2.5	2.10
3. AISI 316	4.0	1.65
4. 20Cr-25Ni-4.5Mo-1.5Cu	4.0	1.25
5. IN-748	6.0	0.70
6. INCONEL* Alloy 625	6.0	0.00

* INCO Trade Mark.

been used successfully for at least 10 years in heat exchangers that handled polluted seawater. Hack[121] has conducted 120 day tests in flowing (2.4 m/s) seawater contaminated with 0 to 0.2 ppm sulfide, and observed only minor attack of approximately 0.1 mm depth and only at the 0.01 ppm sulfide level. Deverell and Davis[122] have conducted 100-hour tests in Na_2S-contaminated synthetic seawater and observed only minor attack (<0.0009 mm/yr) on Type 304, 26-1, and 29-4 stainless steels (see Table 4-66). Types 316, 29-4-2, and Al-6X exhibited no attack in these short term tests.

Weber[109] has summarized the effects of velocity in high H_2S-chloride media for the several classes of stainless steels as shown in Figure 4-27. Note that the conventional austenitics performed well at velocities in excess of 20 m/s, and the highly alloyed austenitics were resistant to the H_2S contaminated media at 50 m/s velocity. Vasilenko, et al.[123] have conducted 300 hour tests on 12Cr martensitic stainless steel in H_2S-saturated 3 percent NaCl and report a corrosion rate of 8 mg/m^2-hr (approximately 0.01 mm/yr).

Pitting potential measurements have been reported by Herbsleb and Popperling[62] and by Deverell and Davis.[122] Note in Figure 4-36 that the pitting potential for 22Cr-5.5Ni-3Mo decreased with increasing temperature and increasing chloride content in H_2S-saturated NaCl solutions. Comparing the data in Figure 4-36 with comparable data in Figure 4-19, it appears that the effect of H_2S in this study was to make the pitting potential about 100 mV more negative than in the absence of H_2S. The electrochemical behavior of a number of stainless alloys in Na_2S-contaminated synthetic seawater is summarized by Deverell and Davis[122] in Table 4-67. Note that the corrosion potentials were about the same for all alloys with or without Na_2S. The presence of Na_2S made the critical pitting potential and the pitting protection potential more negative for Type 304, but had no effect on these same potentials for 316, 18-2, 26-1, 29-4, 29-4-2, and Al-6X.

Effect of Aeration. Most of the studies on the effect of aeration (dissolved oxygen) have been done in connection with desalination or exposure in the deep ocean. In many experiments, both temperature and oxygen content varied. Hodgkiess and Rigas[41] compared oxygen levels at 25 C and 60 C in seawater tests conducted in Scotland. The crevice corrosion behavior of several alloys under aerated conditions (7 to 8 ppm O_2 at 25 C, 3.5 to 4.5 ppm O_2 at 60 C, and 1.3 to 1.6 ppm O_2 at 100 C) is summarized in Table 4-36. Note that under aerated conditions, the initiation of crevice attack appeared to be related to increasing temperature since it is unlikely that decreasing oxygen would produce an increased rate of attack. Oxygen did have a marked effect at a given temperature as demonstrated by these authors where these same alloys were exposed under deaerated conditions (0.3 to 0.6 ppm O_2) at 25 and 60 C. After 25 weeks' exposure, no crevice attack was observed on any specimen in

TABLE 4-66. CORROSION RATES IN AERATED SYNTHETIC SEAWATER WITH AND WITHOUT SULFIDE ADDITIONS[122]

Material	Corrosion Rate, mm/yr	
	Synthetic Seawater	Synthetic Seawater + 10 ppm Na_2S
Type 304	0	0.0003(a)
Type 316	0	0
E-Brite 26-1	0	0.0009
Type 29-4	0	0.0003
Type 29-4-2	0	0
Al-6X	0	0

(a) Rust staining.

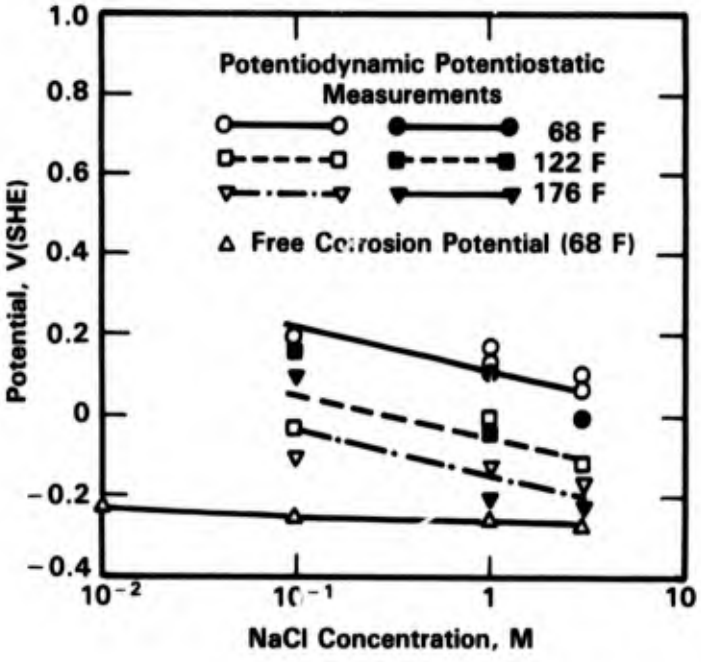

FIGURE 4-36. EFFECT OF TEMPERATURE AND NaCl CONCENTRATION ON PITTING POTENTIALS OF AF 22 (22Cr-5.5Ni-3Mo) IN AQUEOUS NaCl SOLUTIONS CONTAINING H_2S[62]

TABLE 4-67. RAPID SCAN POTENTIODYNAMIC ANODIC POLARIZATION RESULTS ON STAINLESS STEELS EXPOSED TO AERATED SYNTHETIC SEAWATER[122]

Material	Potentials	Potentials, V(SCE)	
		Synthetic Seawater	Synthetic Seawater + 10 ppm Na_2S
Type 304	E_{cor}	-0.30	-0.30
	E_{pit}	0.35	0.28
	E_{prot}	0.28	0.17
Type 316	E_{cor}	-0.32	-0.32
	E_{pit}	0.54	0.54
	E_{prot}	0.30	0.30
Type 18-2	E_{cor}	-0.34	-0.34
	E_{pit}	>0.80	>0.80
	E_{prot}	>0.80	>0.80
E-Brite 26-1	E_{cor}	-0.36	-0.36
	E_{pit}	>0.80	>0.80
	E_{prot}	>0.80	>0.80
Type 29-4	E_{cor}	-0.36	-0.37
	E_{pit}	>0.80	>0.80
	E_{prot}	>0.80	>0.80
Type 29-4-2	E_{cor}	-0.33	-0.31
	E_{pit}	>0.80	>0.80
	E_{prot}	>0.80	>0.80
Al-6X	E_{cor}	-0.33	-0.33
	E_{pit}	>0.80	>0.80
	E_{prot}	>0.80	>0.80

25 C seawater, and only 316L and Alloy 825 showed a slight indication of crevice attack in 60 C seawater.

Kain[106] in 30-day tests at Wrightsville Beach, NC, found a maximum in crevice attack for several stainless steels at 28 C (approximately 5.6 ppm O_2) compared to 12 C (approximately 7.8 ppm O_2) and 50 C (approximately 4.3 ppm O_2), (see Figure 4-37). He was not sure whether this effect could be attributed to oxygen alone. On the other hand, Roy[118] conducted tests in 0.6M NaCl and found that the corrosion potential of Type 304 varied only

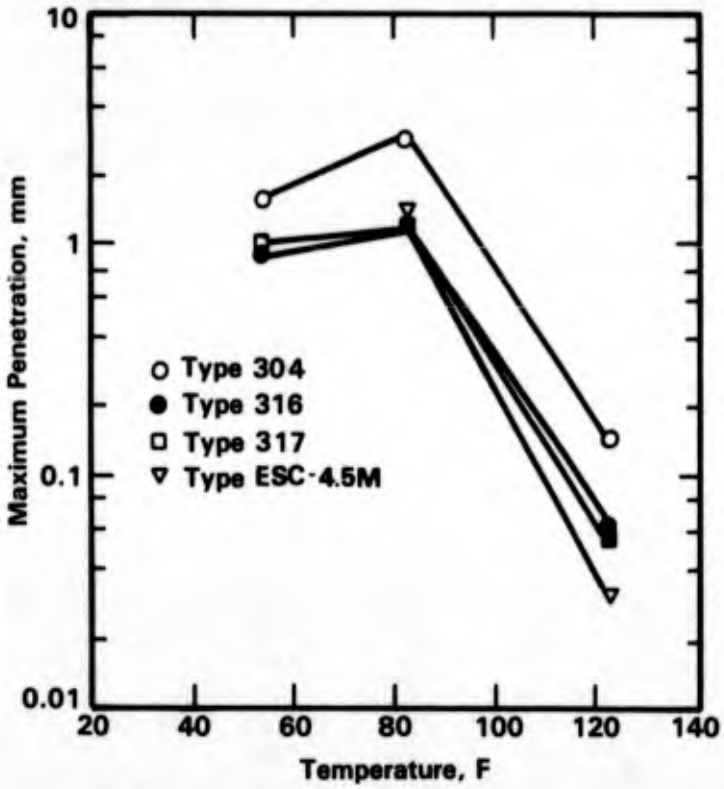

FIGURE 4-37. EFFECT OF SEAWATER TEMPERATURE ON MAXIMUM DEPTH OF CREVICE CORROSION IN A 30-DAY TEST[106]

about 25 mV (approximately 50 to 100 mV(SCE)) over the range 1 to 13 ppm dissolved O_2, but increased by 200 mV (approximately 250 to 300 mV(SCE)) when the oxygen level was increased to 40 ppm.

Oldfield and Todd[124] have compared the pitting behavior of Type 316 in aerated ambient seawater with deaerated (25 ppb O_2) 105 C seawater conditions in a desalination plant (see Table 4-68). Note that in ambient temperature air-saturated seawater, the maximum depth of pitting was 2.4 mm in 16 months' exposure; whereas, in the hot (105 C), but deaerated, seawater the pitting depth was only 0.12 mm after 18 months' exposure.

Reinhart and Jenkins[112,125] have attempted to relate corrosion behavior with oxygen content at various depths in the ocean. Despite the fact that Figures 4-38, 4-39, and 4-40 from their report indicate that the general corrosion rates of most stainless steels tend to increase with dissolved oxygen content, they were not able to make a good correlation between O_2 content and susceptibility to pitting or crevice corrosion, see Tables 4-60 to 4-64.

TABLE 4-68. PITTING OF TYPES 304 AND 316 STAINLESS STEELS IN MARINE ENVIRONMENTS[124]

Test	Grade of Steel	Seawater	Exposure Time, days	Maximum Depth of Pitting, mm
INCO	Type 316	Natural Atlantic Ocean	486	2.4
AISI	Type 316	Deaerated, 105 C, 25 ppb O_2	547	0.12
AISI	Type 304	Deaerated, 105 C, 25 ppb O_2	547	0.60

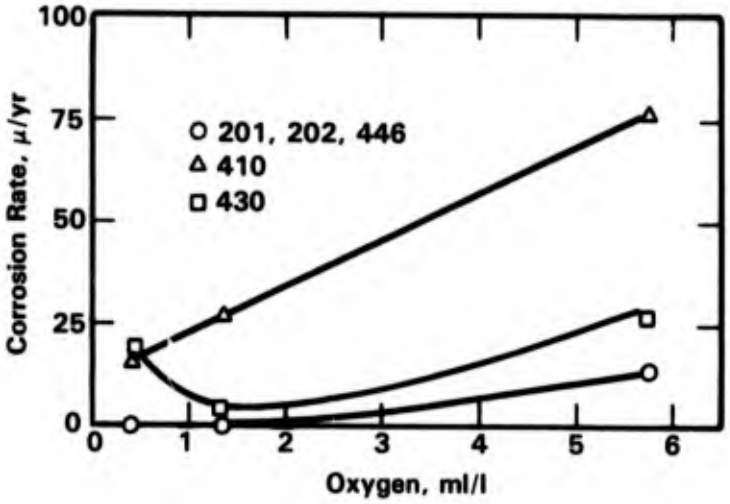

FIGURE 4-38. EFFECT OF OXYGEN CONCENTRATION OF SEAWATER ON THE CORROSION OF 200 AND 400 SERIES STAINLESS STEELS AFTER 1-YEAR EXPOSURE[125]

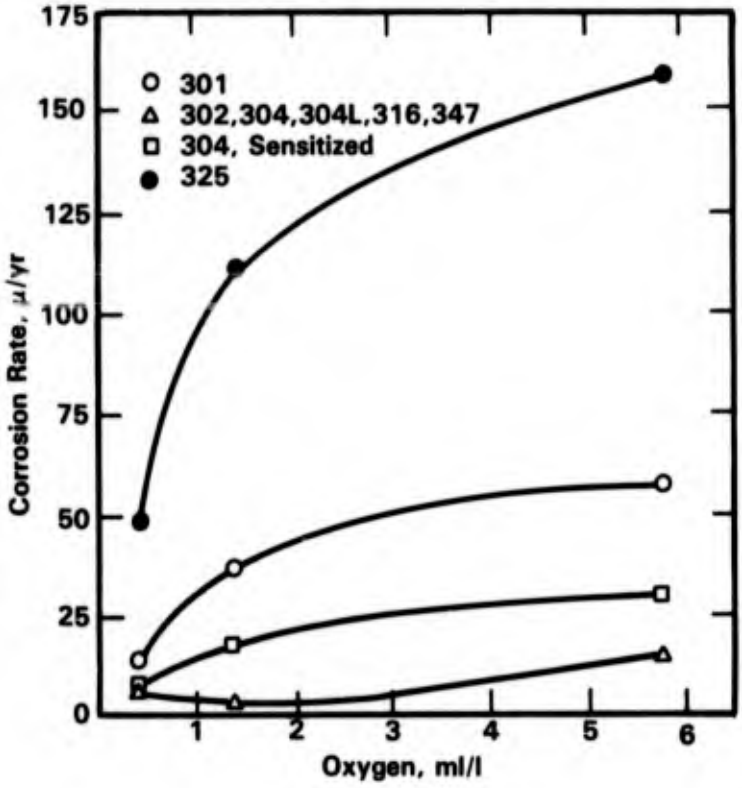

FIGURE 4-39. EFFECT OF OXYGEN CONCENTRATION OF SEAWATER ON THE CORROSION OF 300 SERIES STAINLESS STEELS AFTER 1-YEAR EXPOSURE[125]

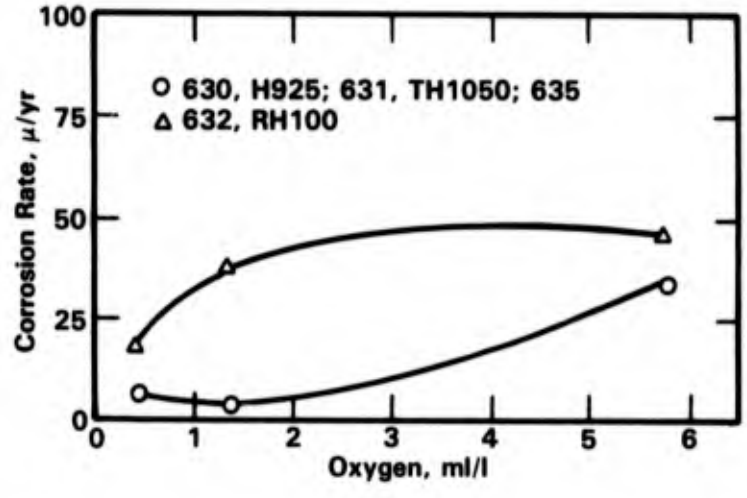

FIGURE 4-40. EFFECT OF OXYGEN CONCENTRATION OF SEAWATER ON THE CORROSION OF 600 SERIES STAINLESS STEELS AFTER 1-YEAR EXPOSURE[125]

Depth of Exposure. As pointed out in the section on Aeration, the principal effect of depth of exposure is to affect the oxygen content of the seawater. As shown in Figure 4-41, the dissolved oxygen content in the Pacific Ocean is at a maximum at the surface (approximately 5.6 ml/l), drops off dramatically in the first 1,000 feet, reaches a minimum of approximately 0.3 ml/l at approximately 2,000 feet, and slowly rises to approximately 1.6 ml/l at approximately 7,000 feet. As shown in Figures 4-41, 4-42, 4-43 and 4-38, 4-39, and 4-40 from Reinhart and Jenkins,[112,125] the corrosion rates of stainless steels tend to increase as the oxygen content of the seawater increases. As pointed out by Reinhart[33] the corrosion rates do not necessarily correlate with pitting depths. Pitting depths are presented in Tables 4-60 to 4-64.

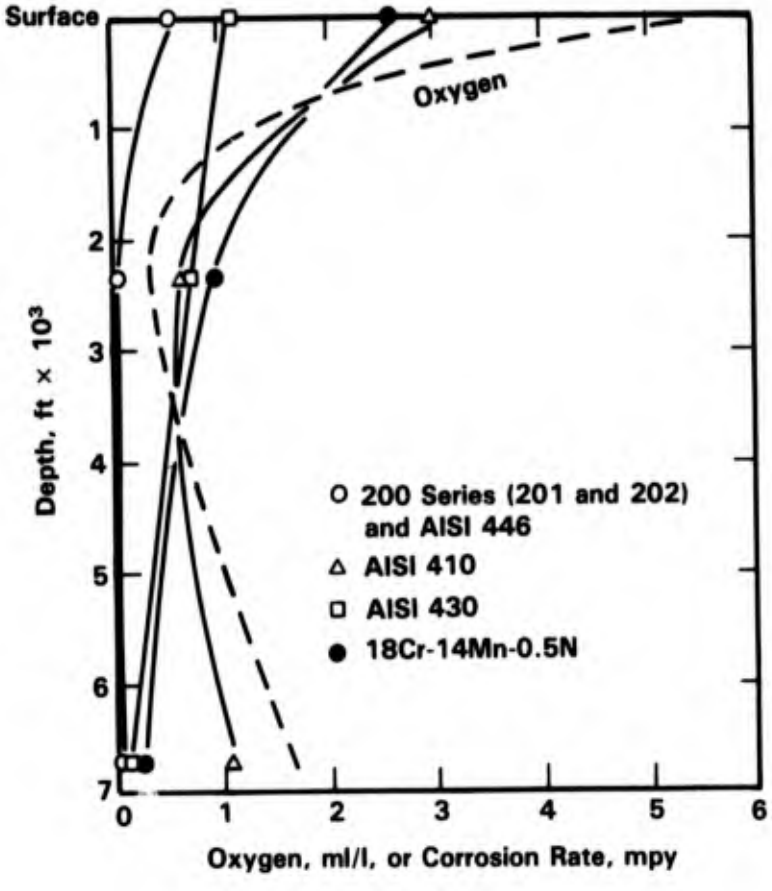

FIGURE 4-41. CORROSION OF 200 AND 400 SERIES STAINLESS STEELS VERSUS DEPTH AFTER 1 YEAR OF EXPOSURE[112]

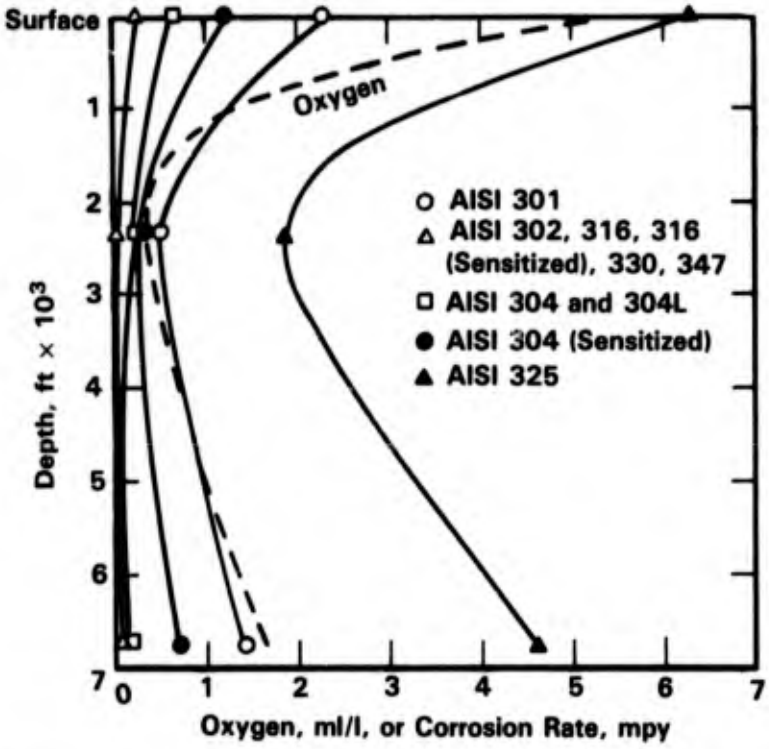

FIGURE 4-42. CORROSION OF 300 SERIES STAINLESS STEELS VERSUS DEPTH AFTER 1 YEAR OF EXPOSURE[112]

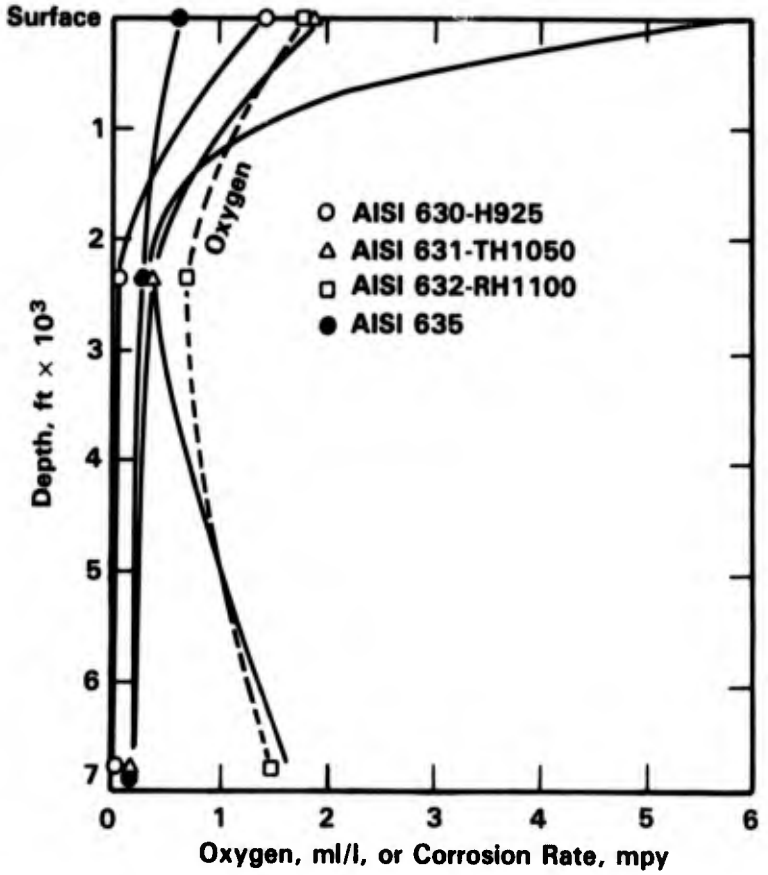

FIGURE 4-43. CORROSION OF 600 SERIES STAINLESS STEELS VERSUS DEPTH AFTER 1 YEAR OF EXPOSURE[112]

Wheatfall[107] showed some correlation between pit depth and oxygen content as a function of depth of exposure in his study on the effect of the exposed area outside the crevice. As shown in Figure 4-25, the maximum pit depth in Type 304 stainless steel increased from approximately 10 mils in 0.6 ppm oxygen water at 2,340 feet to >125 mils in 6.77 ppm oxygen at the surface in tests of approximately 200 days' duration. Rynewicz[126] observed crevice attack to a depth of 125 mils in precipitation hardened stainless steel exposed 4 years at 4,050 feet depth in the Atlantic Ocean and >50 mils pitting in specimens exposed 6 months at 5,900 feet depth in the Pacific Ocean, (see Table 4-69).

Seawater Composition. The constituents of seawater that usually vary, or are varied, are salinity (Cl^- ion), oxygen content, pH, pollutants, and biological activity (biofouling). The effect of the last four of these on the pitting of stainless steel have already been discussed in prior sections. The general trend has been that pitting/crevice corrosion susceptibility

TABLE 4-69. PERFORMANCE OF UNCOATED STAINLESS STEELS[126]

	Atlantic Ocean - 4 Years, 4,030 feet	Pacific Ocean - 6 Months, 5,900 feet
Almar 362 (15Cr-7Ni-1Ti)		
6 x 12 in.	Incipient pitting of 0.002-in. depth to severe crevice attack of 0.125 in. depth.	Incipient pitting of 0.002 in.
6 x 12 in. (stressed)	--	Incipient pitting of 0.002- to 0.050-in. depth (perforation).
1 x 6 in. (stressed)	--	No cracking; crevice from 0.002- to 0.03-in. deep.
Carpenter 455 (12Cr-9Ni-2.25Cu-1Ti)		
6 x 12 in.	Crevice corrosion to 0.040-in. deep.	Incipient pitting of 0.002 to crevice corrosion 0.10-in. deep.
6 x 12 in. (stressed)	--	Incipient pitting of 0.002 to 0.005 in.
1 by 6 in. (stressed)	--	One of three specimens cracked at bolt-hole.

increases, and pitting potentials decrease (become more negative) with increasing oxygen, decreasing pH, increasing H_2S (pollutant), increased biofouling, and increasing chloride concentration. The effect of salinity has been alluded to in several of these sections and additional information is provided in this section.

Based on laboratory tests and field experience, Kovach, et al.[44] have determined the critical chloride levels for crevice corrosion of Types 304, 316, and Crucible SC-1 (25Cr-2.25Ni-3Mo). Their results are presented in Figures 4-44, 4-45, and 4-46 and indicate that Types 304 and 316 exhibit crevice corrosion at approximately 1,000 ppm chloride (seawater contains approximately 19,000 ppm Cl^-). Kain[103] exposed 304 and 316 to diluted seawater, and as indicated in Tables 4-70 and 4-71 observed 0.05 to 0.1 mm (2 to 4 mils) crevice

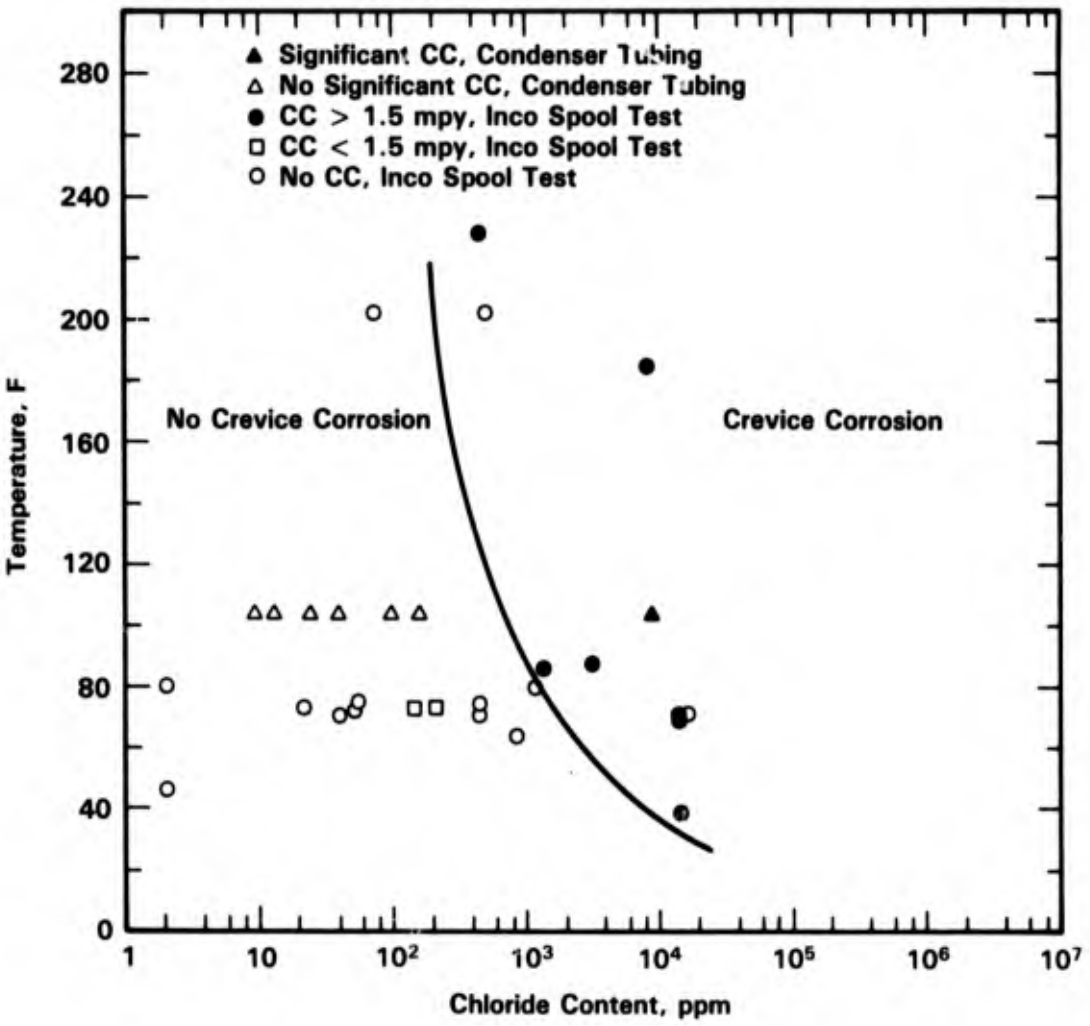

FIGURE 4-44. FIELD CREVICE CORROSION PERFORMANCE OF TYPE 304 STAINLESS STEEL IN HIGH TEMPERATURE-CHLORIDE WATERS[44]

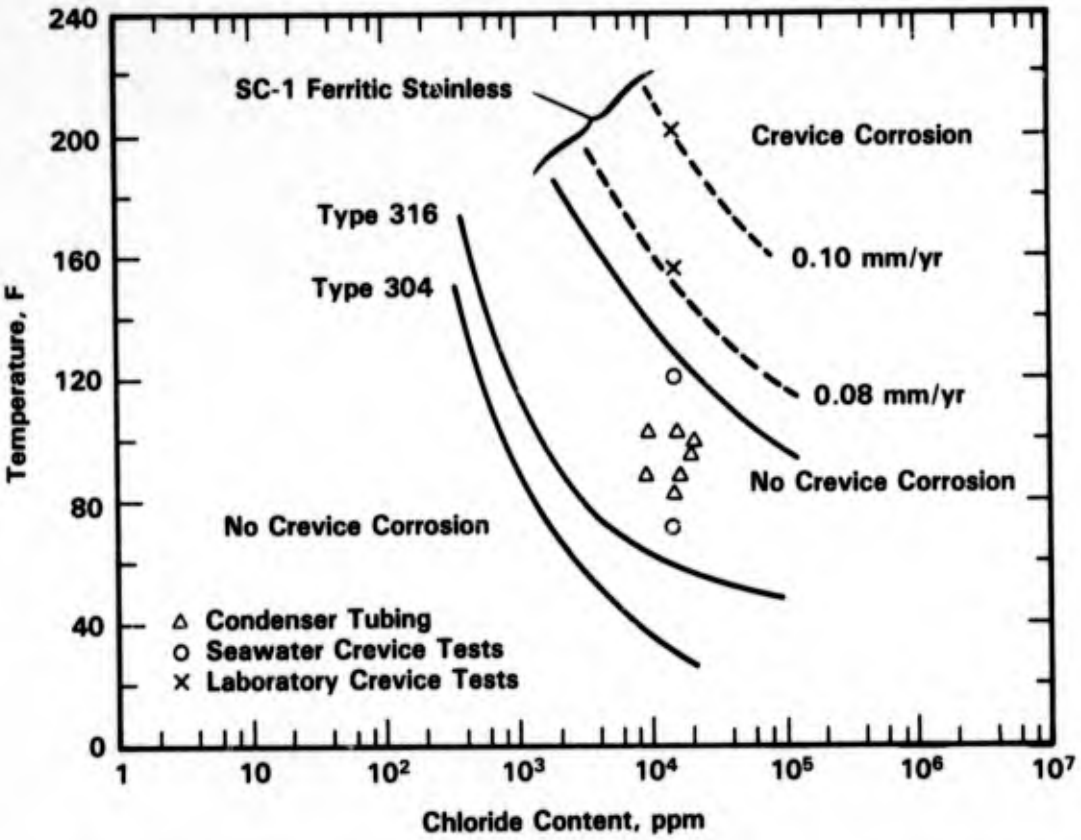

FIGURE 4-45. FIELD CREVICE CORROSION PERFORMANCE OF CRUCIBLE SC-1 FERRITIC STAINLESS IN HIGH TEMPERATURE-CHLORIDE WATERS[44]

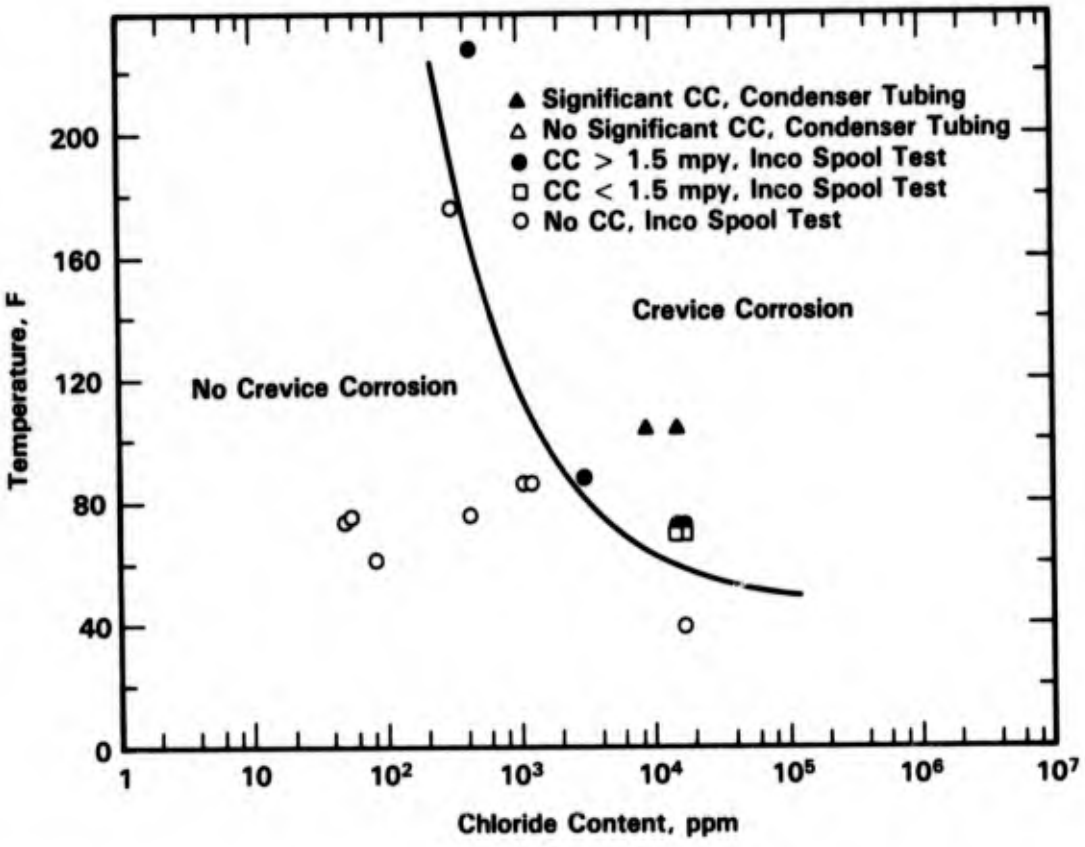

FIGURE 4-46. FIELD CREVICE CORROSION PERFORMANCE OF TYPE 316 AND OTHER STAINLESS STEELS IN HIGH TEMPERATURE-CHLORIDE WATERS[44]

TABLE 4-70. RESULTS OF 90 DAY MULTIPLE CREVICE TESTING OF TYPE 304 STAINLESS STEEL IN DILUTED SEAWATER AT 35 C[103]

Chloride Level	No. of Attacked Sites		Penetration Range, mm[a]	
	Side 1	Side 2	Side 1	Side 2
10,000 mg/l	4	0	0.06-0.09	None
	4	1	0.06-0.09	0.06
	3	0	0.06-0.06	None
5,000 mg/l	1	4	0.09	0.06-0.10
	4	4	0.05-0.09	0.02-0.11
	2	2	0.06, 0.10	0.04, 0.14
3,000 mg/l	3	8	0.02-0.07	0.06-0.19
	6	9	0.02-0.19	0.06-0.16
	0	6	None	0.03-0.11
1,000 mg/l	6	1	0.01-0.05	0.02
	8	3	<0.01-0.13	0.02-0.12
	0	0	None	None

(a) Maximum depth for individual sites.

TABLE 4-71. RESULTS OF 90 DAY MULTIPLE CREVICE TESTING OF TYPE 316 STAINLESS STEEL IN DILUTED SEAWATER AT 35 C[103]

Chloride Level	No. of Attacked Sites		Penetration Range, mm[a]	
	Side 1	Side 2	Side 1	Side 2
10,000 mg/l	0	1	None	0.04
	2	0	0.03, 0.04	None
	0	3	None	0.04-0.06
5,000 mg/l	0	3	None	0.01-0.05
	2	1	0.03, 0.05	0.05
	1	2	0.12	0.03, 0.04
3,000 mg/l	3	4	0.02-0.07	0.02-0.07
	4	0	0.05-0.11	None
	0	4	None	0.05-0.08
1,000 mg/l	4	0	<0.01-0.06	None
	0	1	None	0.05
	0	2	None	<0.01, 0.05

(a) Maximum depth for individual sites.

corrosion in 90 days at the 1,000 ppm Cl^- level. Kain[103] also predicted time to breakdown of Type 316 in a crevice as a function of crevice depth and chloride content. His curves presented in Figure 4-47 predict crevice attack after approximately 100 hours if crevice depths exceed 0.4 cm (with a crevice gap of 0.01 μm), although as described earlier only limited agreement has been obtained between predicted and actual results.

The corrosion performance of several stainless steels in a pilot plant cooling water (35,000 ppm Cl, 35 C) has been reported by Suciu and Wikoff[127] (see Table 4-72). Note that only the high Cr-Mo ferritics were resistant to pitting and crevice corrosion. However, tests conducted by these same authors in aerated geothermal brine (as shown in Figure 4-48) revealed that the 26Cr-3Mo corroded to a greater extent than Al-6X, and all alloys appeared to exhibit a maximum rate of attack at 50,000 ppm Cl^-, but little or no attack at 100,000 ppm Cl^-.

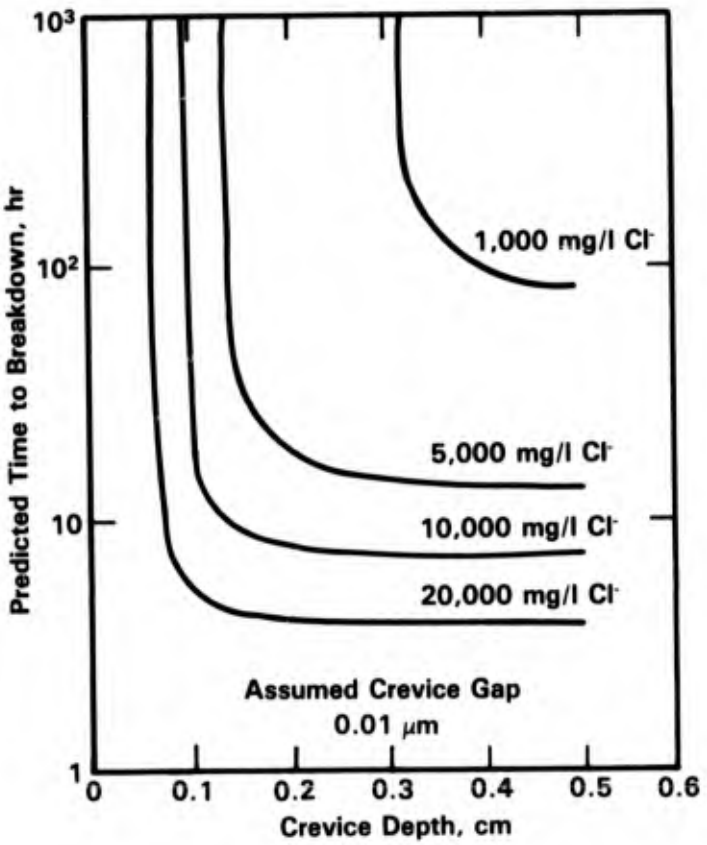

FIGURE 4-47. MODEL PREDICTION FOR EFFECT OF CREVICE DEPTH ON TIME TO BREAKDOWN FOR AISI TYPE 316 STAINLESS STEEL IN A SERIES OF CHLORIDE CONTAINING WATERS[103]

TABLE 4-72. RESULTS OF PILOT COOLING TOWER TESTS (35,000 ppm Cl Brine, 35 C Maximum)[127]

Alloy	Duration, months	Corrosion Rate mdd[a]	Corrosion Rate mpy	Comments
Sea-Cure (26Cr-3Mo)	10	0.93	0.17	No pitting or crevice corrosion.
12 Cr	6	9.57	1.76	Crevice and pitting corrosion.
Allegheny 6X	4	3.39	0.60	Pitting corrosion.
29-4-C	4	1.59	0.29	No pitting or crevice corrosion.
Monel 400	4	3.88	0.63	Pitting corrosion.
Ferralium 255 (26Cr-5.5Ni-3Mo)	2	2.66	0.49	No pitting or crevice corrosion.

(a) mdd = $mg/dm^2/day$.

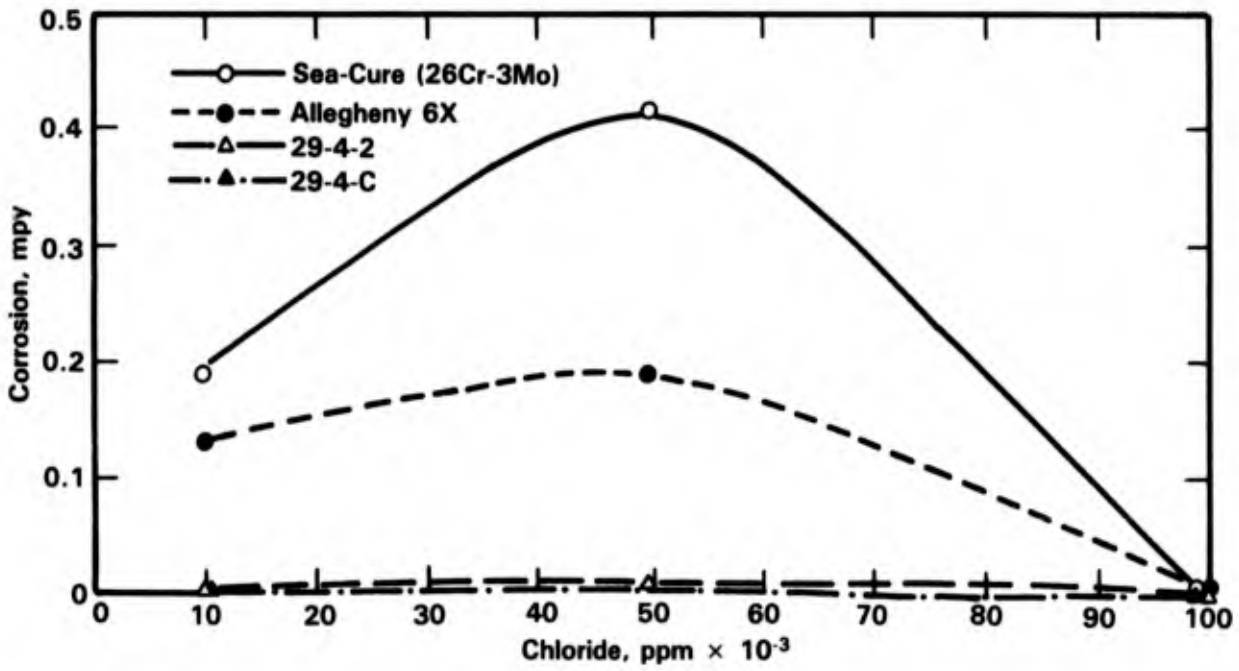

FIGURE 4-48. CORROSION AS A FUNCTION OF CHLORIDE CONCENTRATION LEVEL IN AERATED GEOTHERMAL BRINE, 35 C[127]

At 90 C, Dundas and Bond[128] observed crevice attack of ferritic steels with as little as 40 ppm Cl^- in deionized water. Their results, presented in Table 4-73, revealed that, at equivalent Cl^- concentrations of 1,000 to 2,000 ppm, deionized water was more aggressive in producing crevice attack than were a municipal water or a simulated well water. Results have been obtained by Cramer and Carter[129] for high chloride brines at 105 C. The results presented in Table 4-74 revealed that a 140,000 ppm Cl^- brine was much more corrosive than a 15,000 ppm Cl^- brine.

The effects of Cl^- concentration on pitting potentials are shown in Figures 4-49, 4-50, and 4-51. Note that the pitting potentials became more negative with increasing Cl^- content up to 1M, and in neutral NaCl were 100 to 200 mV(SCE) for Type 304 in 1M solution. As shown in Figure 4-49, the pitting potentials for 304, 316, and 317L did not change between 1.5 and 3M chloride.

Stress-Corrosion Cracking (SCC)

Effect of Alloy Composition. Stress-corrosion cracking has not been a problem with the unsensitized austenitic and ferritic stainless steels in ambient temperature seawater. On the other hand, SCC in seawater could be a problem with the martensitic and precipitation-hardened stainless steels based on their performance in marine atmospheres. Reinhart[33] exposed 15-7, 17-4, 17-7, and 14-8PH-type alloys in the deep ocean and observed SCC in only four conditions from a variety of heat treatments. The SCC failures were:

15-7 AMV RH950, 4-point loaded beams, 123 days at 5,640 ft depth and 197 days at 2,340 depth

15-7 AMV RH1150, 4-point loaded beams, 197 days at 2,340 ft depth

15-7 AMV RH1150, at a drilled hole, 1,064 days at 5,300 ft depth

17-7PH RH1050, heat-affected zone on a welded specimen, 197 days at 2,340 ft depth.

Veingarten, et al.[130] have exposed welded specimens of 17-7PH (103 ksi YS), 15Cr-3Ni (91 ksi YS), and 17-6, Ti (131 ksi YS) to Baltic seawater for 1,000 hours and observed no SCC.

Stress-corrosion cracking of the austenitic grades becomes more of a problem as the temperature of the seawater is increased to greater than 60 C. Sedriks[11] reports no SCC of U-bends of Type 316 or 2RK65 after 3 months' exposure in boiling seawater, but he noted that 316 has cracked in the vapors above boiling seawater. The effect of molybdenum on SCC behavior in strong NaCl solutions at approximately 105 C has been summarized by Sedriks[31]

TABLE 4-73. CREVICE CORROSION RESISTANCE OF SURFACE GROUND ALLOYS WITH A METAL-TO-METAL CREVICE IN O_2 SATURATED WATERS AT 90 C AFTER 45 DAYS' EXPOSURE[128]

Alloy	Chloride Content, ppm								
	Deionized H_2O[a]					Ann Arbor H_2O[b]		Simulated Well H_2O[c]	
	40	200	500	1000	2000	1000	2000	1000	2000
18Cr-Ti	0.070[d] (1)[e]	0.100 (1)	0.100 (1)						
18Cr-1.9Mo-Ti		NC[f] (1)	0.015 (1)	0.025 (1)		NC (3)	0.060 (1)	NC (1)	NC (1)
18Cr-2.1Mo-Ti	NC (4)	0.040 (1) NC (3)	0.030 (1) NC (3)	0.035 (1)		NC (2)	NC (1)	NC (2)	NC (2)
18Cr-2.2Mo-Ti	NC (4)	0.020 (1) NC (3)	0.040 (1) NC (2)	0.125 (1) 0.045 (1)	0.130 (1)	NC (2)	NC (2)	NC (1)	NC (1)
18Cr-2.3Mo-Ti			NC (4)	0.025 (1) NC (2)	0.040 (1) NC (1)	NC (2)	NC (1)	NC (1)	NC (1)
18Cr-2.7Mo-Ti			NC (4)	0.140 (1) NC (1)	0.160 (1)	NC (3)	NC (1)	NC (1)	NC (3)
21Cr-3.1Mo-Ti			NC (4)	NC (4)	0.020 (1) NC (1)	NC (2)	NC (2)	NC (4)	NC (4)

(a) pH 5-6.
(b) pH 9-10.
(c) Also 24 ppm NO_3^- + 14 ppm $SO_4^=$ + 180 ppm HCO_3^- at pH 8.3.
(d) Maximum penetration in millimeters.
(e) Number of specimens in parentheses.
(f) No crevice corrosion.

TABLE 4-74. CORROSION TESTS AT 105 C, AND 1 ATM, 15-DAY EXPOSURE[129]

Alloy	East Mesa Brine (MESA 6-1), 15,000 ppm Cl				Salton Sea Brine, 140,000 ppm Cl			
	General Corrosion, mpy		Crevice Corrosion[a]		General Corrosion, mpy		Crevice Corrosion[a]	
	D[b]	A[c]	D[b]	A[c]	D[b]	A[c]	D[b]	A[c]
Iron-Base:								
Sandvik 3RE60	0.1	0.6	0	2	0.0	0.9	1	5
E-Brite 26-1	0.0	0.0	0	0	0.0	3.6	0	0
304 Stainless	0.0	0.1	0	1	(d)	(d)	(d)	(d)
316L Stainless	0.0	0.0	1	1	0.0	4.0	1	5
Carpenter 20	0.1	0.2	0	0	0.0	2.2	1	4
Nickel-Base:								
Monel 400	0.2	2.5	0	3	2.8	3.7	3	4
Inconel X-750	0.0	0.1	(d)	(d)	0.0	3.4	2	4
Inconel 625	0.0	0.0	0	0	0.0	0.0	0	0
Hastelloy S	0.1	0.1	0	0	0.0	0.0	0	0
Hastelloy G	0.1	0.1	0	0	0.0	0.1	0	3
Hastelloy C-276	0.1	0.1	0	0	0.0	0.0	0	0

(a) Numbers indicate extent of crevice corrosion as follows: 0 = not detected; 3 = moderate (>1 mpy but <5 mpy); 4 = severe (>5 mpy but <50 mpy); 5 = very severe >50 mpy).
(b) Deaerated.
(c) Aerated.
(d) Alloy not tested.

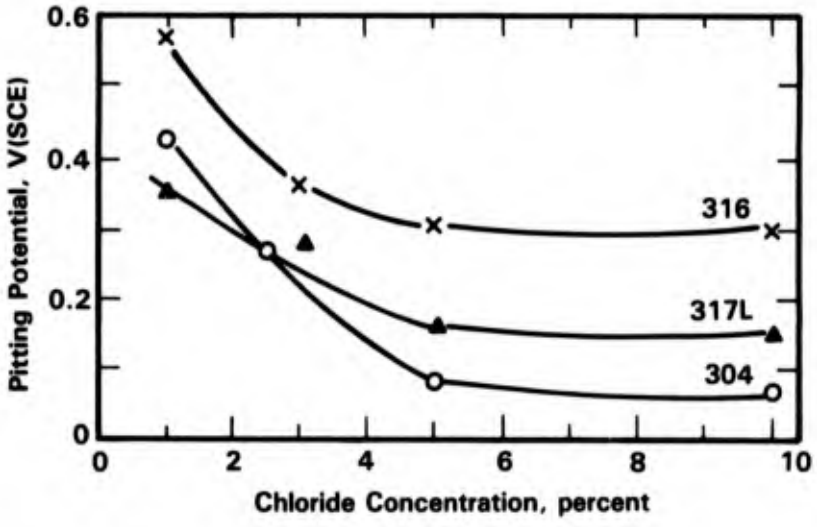

FIGURE 4-49. EFFECT OF CHLORIDE CONCENTRATIONS (PERCENT) ON THE PITTING POTENTIALS OF STAINLESS STEELS AT 20 C[64]

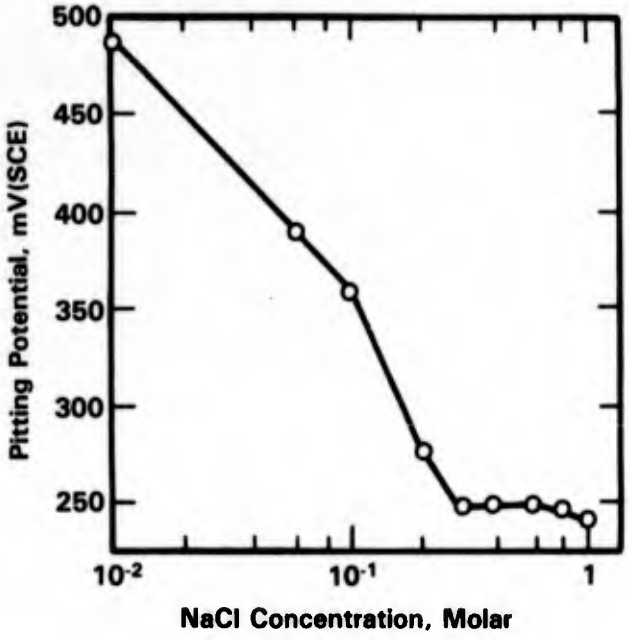

FIGURE 4-50. EFFECT OF CHLORIDE ION CONCENTRATION ON CRITICAL POTENTIAL FOR PITTING OF TYPE 304 STAINLESS STEEL[118]

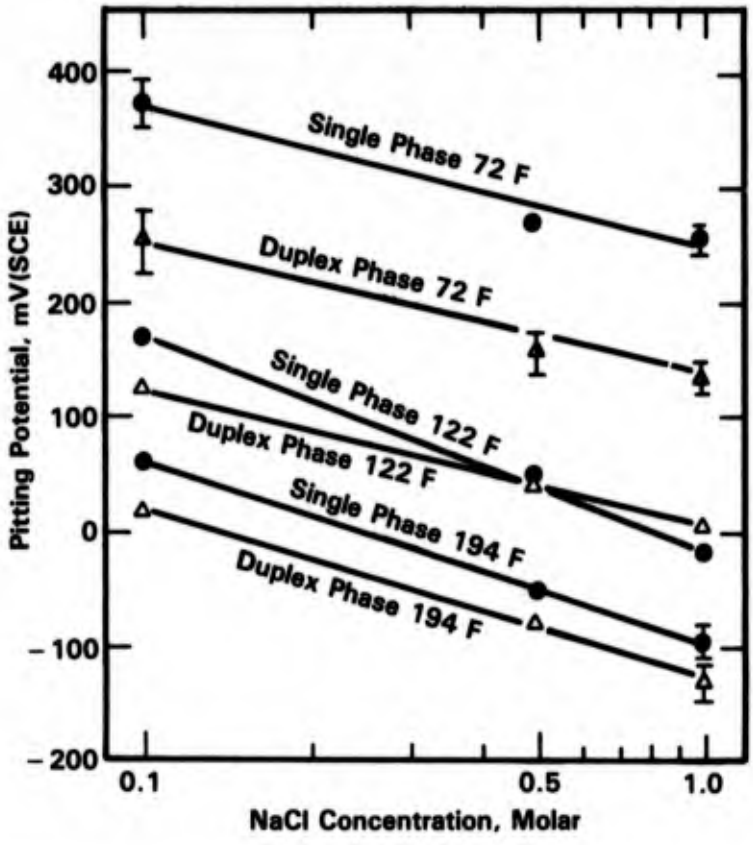

FIGURE 4-51. PITTING POTENTIALS OF SINGLE PHASE AND DUPLEX TYPE 304L AS A FUNCTION OF NaCl CONCENTRATION AT SEVERAL TEMPERATURES WITH A CONSTANT pH of 4[119]

in Figure 4-52 and by Dundas and Bond[131] in Table 4-75. Although one-to-one comparisons may not be possible between NaCl and seawater, note that the resistance to cracking increased as the Mo level increased, particularly at >2 percent Mo. Redmond and Miska[132] also have observed a similar beneficial effect of Mo as shown in Table 4-76. The effect of nickel on SCC susceptibility in aerated 22 percent NaCl at 105 C has been summarized by Speidel[133] as shown in Figure 4-53. Note that susceptibility to SCC increased in the range 0 to 20 percent nickel, but that resistance was restored at nickel levels >35 percent.

The ferritic molybdenum steels are resistant to SCC in most high-temperature chloride solutions as illustrated in Table 4-77 by Cramer and Carter[129] where E-Brite 26-1 was resistant to Salton Sea geothermal brine (155,000 ppm Cl^-) whereas several austenitics and Type 430 exhibited SCC even under deaerated conditions.

The boiling 42 percent $MgCl_2$ test has been used to rank SCC susceptibility in chloride environments as shown in Tables 4-76 and 4-78. However, the results from these tests are not strictly relatable to performance in seawater or even in neutral chloride solutions since the boiling 42 percent $MgCl_2$ test shows an increased susceptibility to SCC in the range of 0.5 to >4 percent Mo, (see Figure 4-54).

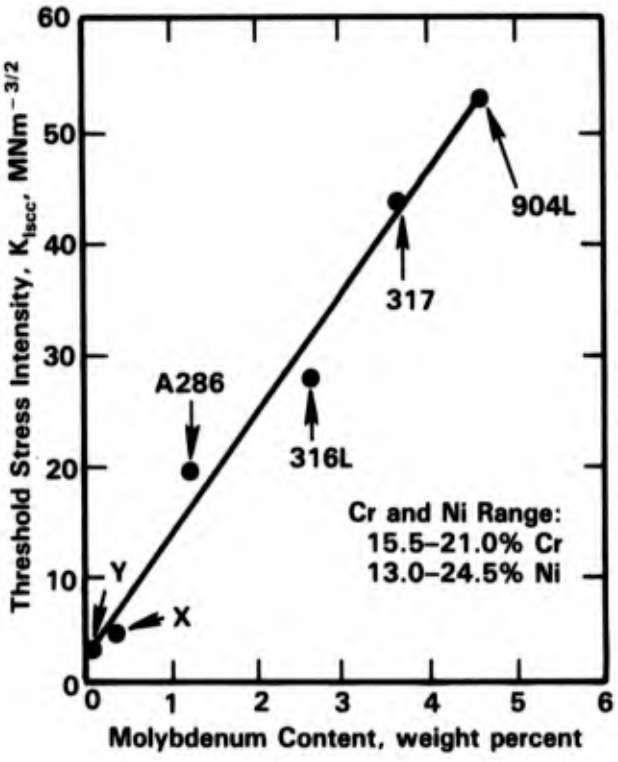

FIGURE 4-52. EFFECT OF Mo CONTENT ON STRESS-CORROSION THRESHOLD STRESS INTENSITY OF Fe-Cr-Ni-Mo ALLOYS IN AERATED AQUEOUS 22% NaCl SOLUTION AT 105 C; ALLOYS X AND Y ARE GERMAN HEAT-RESISTANT GRADES[31]

TABLE 4-75. EFFECT OF MOLYBDENUM ON STRESS-CORROSION CRACKING OF AUSTENITIC STAINLESS STEELS CONTAINING LESS THAN 0.07% NITROGEN IN BOILING ACIDIFIED 25% NaCl[131]

Steel	Mo, weight percent	N, weight percent	Cracking Time at Indicated pH, hr[a] pH 1.5	pH 4.0
18Cr-9Ni				
3[b]	0.3		7-23, 7-23	
18Cr-11 to 14Ni				
1A	0.0	0.04	168-188, 120-144	
1B	0.5	0.04	120-144, 452-500	
1D	1.4	0.04	120-144, 452-500	
2A	2.0	0.03	120-144, 452-624	
4	2.2	0.05	68-144, 68-117	
5	3.1	0.07	NC (1296), NC (1296) NC (1440), NC (1440)	NC (840), NC (840)
1E	4.2	0.04	NC (1296), NC (1296) NC (1320), NC (1320)	
12	4.3	0.02	NC (1440), NC (1440)	NC (1488), NC (1488)
20Cr-24Ni				
14	4.3	0.06	NC	(1632), NC (1632)
15	4.4	0.03	NC	(1416), NC (1416)
16	6.5	0.03	NC	(1416), NC (1416)

(a) NC = No cracking.
(b) Heat number indicated.

TABLE 4-76. TESTS INDICATE HOW THE SEAWATER STAINLESS STEELS WITHSTAND CHLORIDE STRESS-CORROSION CRACKING[132]

Stainless Steel	Stress-Corrosion Cracking Test[a] Boiling 42% $MgCl_2$	Wick Test	Boiling 25% NaCl, pH = 7
Sea-Cure	F	P	P
Al29-4-2	F	P	P
Al29-4C	P	P	P
Monit	F	P	P
Al-6X	F	P	P
254 SMO	F	P	P
Ferralium Alloy 255	F	N	P
Type 304	F	F	F
Type 316	F	F	F

(a) P = passed, F = failed, and N = not tested.

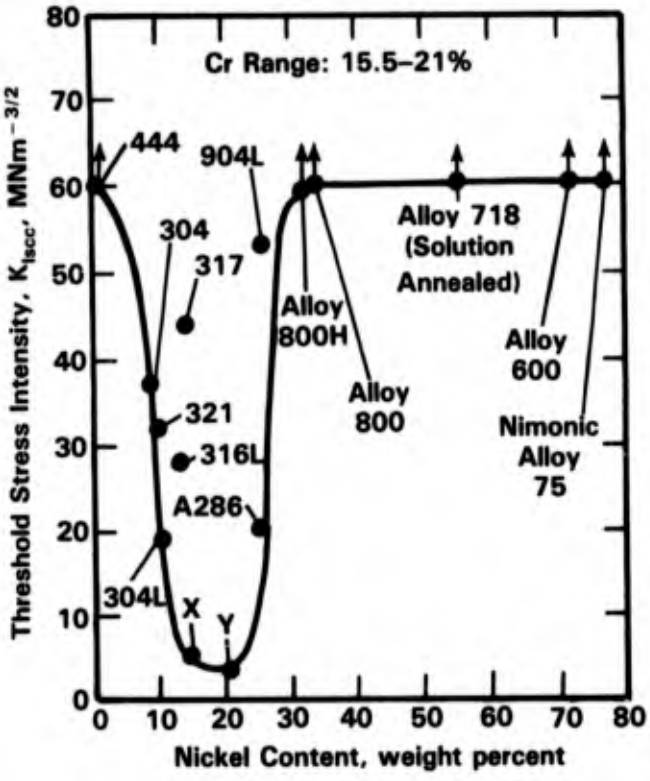

FIGURE 4-53. EFFECT OF Ni CONTENT ON STRESS-CORROSION THRESHOLD STRESS INTENSITY OF VARIOUS ALLOYS IN AERATED AQUEOUS 22% NaCl SOLUTION AT 105 C; ALLOYS X AND Y ARE GERMAN HEAT-RESISTANT GRADES[133]

TABLE 4-77. STRESS-CORROSION CRACKING IN SALTON SEA TYPE BRINE AT 232 C, 15-DAY EXPOSURE[a][129]

Alloy	Deaerated	100 ppm O_2[b]	100 ppm CH_4	250 ppm CO_2
Iron-Base:				
Sandvik 3RE60	D	(c)	(c)	(c)
E-Brite 26-1	--	--	--	--
316L Stainless	D	D	D	D
430 Stainless	D	D	D	D
Carpenter 20	D	(c)	(c)	(c)

(a) Stress-corrosion cracking indicated by: D = detected, -- = not detected.
(b) Stress-corrosion cracking of 316 stainless steel autoclaves terminated exposure at 5 to 7 days for samples in brine containing dissolved oxygen.
(c) Alloy not tested.

TABLE 4-78. STRESS-CORROSION CRACKING OF STAINLESS STEELS "U" BENDS IN BOILING 42 PERCENT $MgCl_2$[49]

Alloy	Time to Failure, hr
Type 304	8
Type 316	48
Type 430	624 NF
Type 434	1800 NF
18Cr-2Mo	1704 NF
26Cr-1Mo	1200 NF
26Cr-1Mo-Ti	516 NF(b)
21Cr-3Mo-Ti(a)	2000 NF
28Cr-4Mo	2400 NF(b)

(a) Specimen was a stressed bolt.
(b) Nominal 45% $MgCl_2$, NF = no failure.

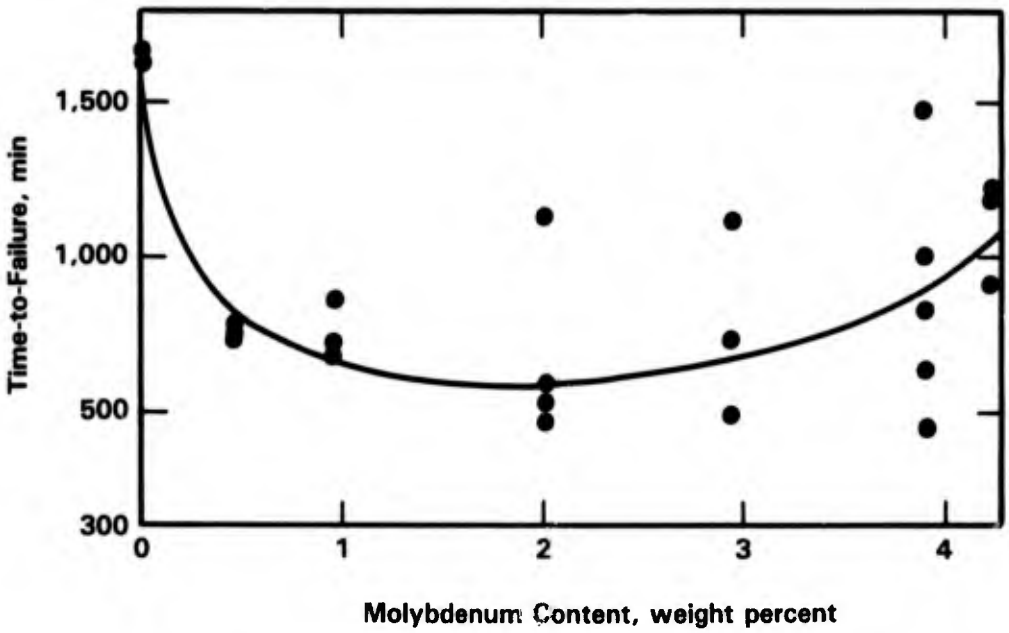

FIGURE 4-54. RESULTS OBTAINED ON 18Cr-14Ni-O to 4.2Mo STEELS STRESSED AT 75 PERCENT OF ROOM-TEMPERATURE YIELD STRENGTH IN BOILING MAGNESIUM CHLORIDE [140 C (284 F)][131]

Heat Treatment and Welding. Heat treatment and/or welding can affect the SCC susceptibility of stainless steels by varying the strength levels in martensitic and precipitation hardening grades or causing grain boundary sensitization (usually in the austenitic grades). The cracking of 15-7 and 17-7 in the deep ocean has already been alluded to in the section on effects of alloy composition. In this series of tests reported by Reinhart,[33] the heat treated conditions for the several alloys were as follows.

Alloy	HT	YS, ksi
15-7 AMV	Annealed	59
	RH1150	158
	RH950	220
PH15-7Mo	RH1100 (welded)	183
PH14-8	SRH950 (welded)	214
17-4PH	925 (welded)	185
17-7PH	TH1050 (welded)	188
	RH1050 (welded)	197

SCC was observed only in specimens of the 15-7 AMV RH950 and RH1150 heat treatments and in the 17-7PH RH1050. Thus, based on strength level alone, the results were not consistent since a relatively low strength material 15-7 AMV RH1150 failed while several higher strength materials, in particular the PH14-8 SRH950, did not fail.

Fujii[134] obtained similar inconsistent results in his fracture mechanics studies with 17-4PH in 3.5 percent NaCl. (In this type of high strength alloy, SCC results should be similar for NaCl and seawater.) Note in Table 4-79 that the difference between $K_{Ix(Air)}$ and K_{Iscc} did not decrease as the strength level decreased as the result of heat treatment. However, K_{Iscc} did increase as strength level decreased as one would expect. Sprowls, et al.[21] have observed a good correlation in 20 percent NaCl between K_{Ic} and K_{Iscc} for 17-7PH, PH15-7Mo, 15-5PH, PH13-8Mo AM-355, and 431 as shown in Table 4-80. Gouda and El-Sayed[135] also found a good correlation between the strength level and time to failure of Type 410 in 3 percent NaCl, see Figure 4-55.

There is an apparent gap in the data for the SCC behavior of welded or sensitized austenitic stainless steels in seawater. There are a number of reported incidences of intergranular SCC in sensitized stainless steels that have been exposed to marine atmospheres or to even dilute (>20 ppm) chloride solutions at pH 3.5 to 5.0. But only limited experience has been reported for immersion in seawater. Sedriks[11] reports that some unstressed sensitized

TABLE 4-79. SCC PROPERTIES OF 17-4PH STEEL[a][134]

Temper	σ_y, ksi	K_{Ix}, ksi $\sqrt{in.}$ Air	K_{Iscc}, ksi $\sqrt{in.}$ FC,[b] -0.3 V[c]	5086 Al, -0.8 V	Zn, -1.0 V	Mg, -1.3 V	IP,[d] -1.3 V
H900	177	113	79	54	30	26	28
H975	162	146	102	76	45	32	30
H1025	157	157	111	89	53	35	36
H1075	151	166	123	103	65	40	39
H1150	120	170	130	116	77	44	41
H1150M	91	118	97	93	100	90	--

(a) Corrodent: 3.5 percent NaCl solution.
(b) FC = freely corroding.
(c) Potential as measured against Ag/AgCl reference electrode.
(d) IP = instrumentally potentiostated.

TABLE 4-80. SUMMARY OF LONG-TRANSVERSE (T-L) TESTS OF COMPACT TENSION SPECIMENS OF STAINLESS STEEL ALLOYS FATIGUE PRECRACKED AND BOLT LOADED TO 95 PERCENT K_{Ic}[21]

Alloy & Temper		K_{Ic}, ksi $\sqrt{in.}$	20% NaCl Solution: Incubation, months	K_{Iscc}, ksi $\sqrt{in.}$	Average Initial Crack Velocity, in./hr
17-7PH	RH1050	47	0	<18	4×10^{-1}
PH15-7Mo	RH950	31	0	<15	5×10^{-2}
	RH1050	40	0	<20	4×10^{-2}
15-5PH	H900	72	0.5	33	2×10^{-3}
	H1150M	76[a]	>6.7	>72	--
PH13-8Mo	H950	62	0	<46	2×10^{-2}
	H1050	88	0	<65	2×10^{-2}
431	HT200	79	0	12	8×10^{-3}
	HT125	76[a]	1.2	43	2×10^{-3}
AM-355 (Plate)	SCT850	48	>6.7	8	9×10^{-3}
	SCT1000	105	0.5	37	6×10^{-3}
AM-355	SCT850	37	0	6	1×10^{-2}
	SCT1000	70	>6.7	28	1×10^{-2}

(a) Not valid per ASTM E399 criteria for K_{Ic}.

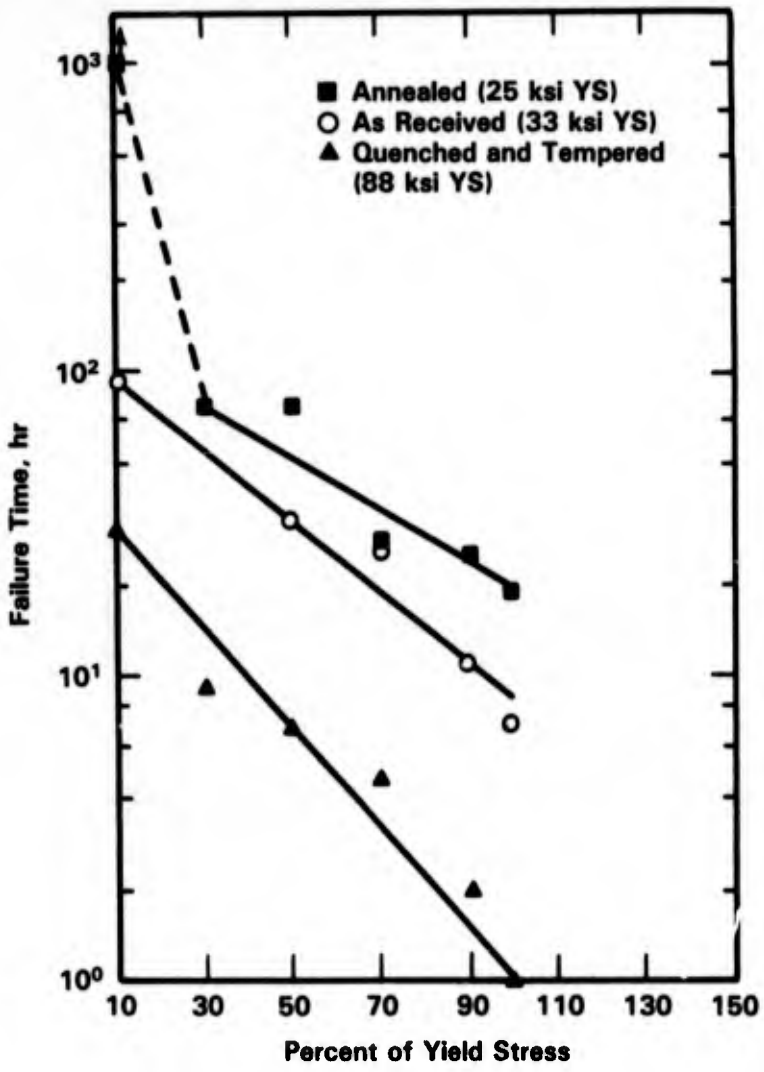

FIGURE 4-55. THE EFFECT OF STRESS ON THE TIME TO FAILURE OF 410 STAINLESS STEEL in 3 PERCENT NaCl SOLUTION[135]

specimens of Types 316, 316L, and 317 exhibited intergranular attack in a one-year exposure at Wrightsville Beach. Speidel[133] has reported that furnace sensitization produced a strong decrease in SCC resistance in Type 304 in 22 percent NaCl solution, see Figure 4-56, but no definitive data have been found for seawater immersion of stressed sensitized austenitic stainless steels. Until definitive data are developed, it would appear to be prudent to avoid sensitization of any form in austenitic alloys that are to be immersed in seawater or chloride solutions.

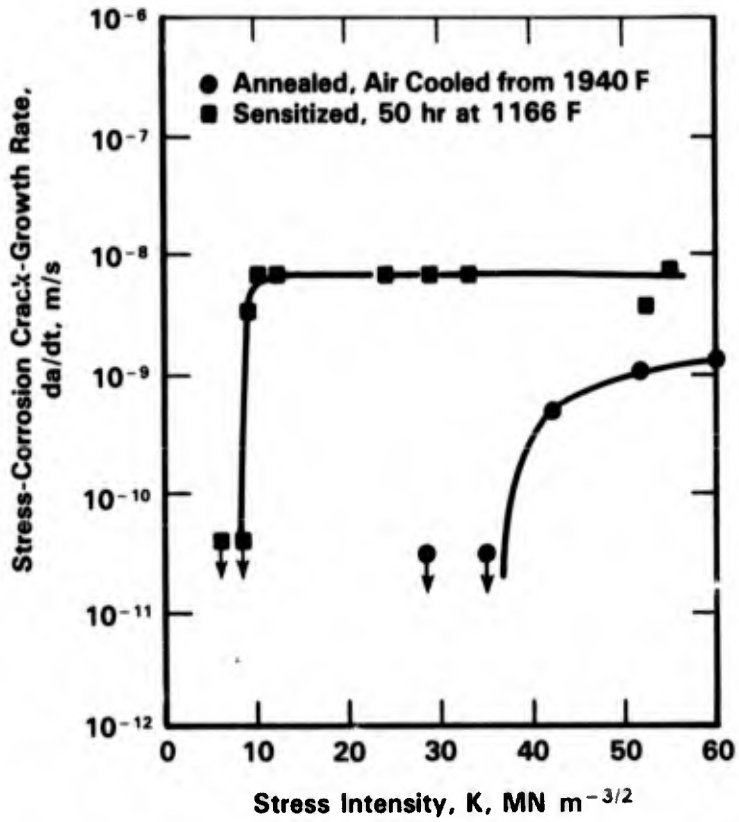

FIGURE 4-56. EFFECT OF FURNACE SENSITIZATION HEAT TREATMENT ON THE SCC RESISTANCE OF AUSTENITIC STAINLESS STEEL TYPE 304 IN 22 PERCENT NaCl AT 105 C[133]

Effect of Temperature. No evidence has been found for systematic studies of the effect of temperature on the SCC of stainless steels in seawater. Some studies have been conducted in NaCl solutions which at equivalent chloride levels would be expected to produce results similar to those for seawater. Truman[136] has studied the effect of temperature on the SCC of welded Type 304 tubing as a function of Cl^- content (100 to 100,000 ppm) and pH (2 to 12). His results are summarized in Table 4-81 and Figures 4-57, 4-58, and 4-59. Note that cracking occurred at $\geq$80 C in neutral chloride solutions containing 1,000 to 100,000 ppm Cl^-.

Herbsleb and Popperling[62] have conducted limited temperature studies on 22.5Cr-5.5Ni-3Mo alloy specimens uniaxially loaded to 90 percent of yield strength in 4.3M NaCl (approximately 150,000 ppm Cl^-). Their results, presented in Table 4-82, revealed no SCC in this alloy after exposure of approximately 1,000 hours at temperatures to 90 C.

Lin, et al.[137] have investigated the SCC susceptibility of sensitized Type 304 in 0.01M NaCl (approximately 350 ppm Cl^-) at temperatures $\geq$100 C. Their results, presented in Figure 4-60, indicate that SCC occurs at more negative potentials as the temperature is increased.

TABLE 4-81. TIMES (h) TO ONSET OF CRACKING OF TYPE 304 STAINLESS STEEL TUBING (EXPOSURE TIMES 13,500 h UNLESS OTHERWISE STATED)[136]

Salt	Temperature	Initial pH	Chloride Concentration, ppm*				
			10^5	10^4	10^3	5×10^2	10^2
NaCl	b.p.	2	144-168	NC T 6864	168-456	2616-3336	848-1008
NaCl	80 C	2	2208-2928	NT	NC T 6184	2304-3024	NC
NaCl	60 C	2	NC T 3008	620-890	NC	NT	NT
NaCl	b.p.	7	2	8-24	456-624	48-72	NC
NaCl	80 C	7	24-48	NC T 12,410	NC	NC	NC
NaCl	b.p.	12	240-408	158-216	9700-10,500	NC T 6000	NT
NaCl	80 C	12	NC	NC	NC	NC	NT
$MgCl_2$	b.p.	7	2	8-24	1512-2232	1440-2160	NC T 5000
$MgCl_2$	80 C	7	744-912	NC	NC	NC	NC
$CaCl_2$	b.p.	7	24-28	460-528	NC T 13,000	NT	NT
$CaCl_2$	80 C	7	2208-2928	NC	NC	NC	NC
$ZnCl_2$	b.p.	7	144-168	NC T 4008	1380-1548	2831-3552	NC T 5000
$ZnCl_2$	80 C	7	NC T 6048	NC T 5204	NC	NC	NT

* NC = no cracks; NT = not tested; and T = terminated after time indicated.

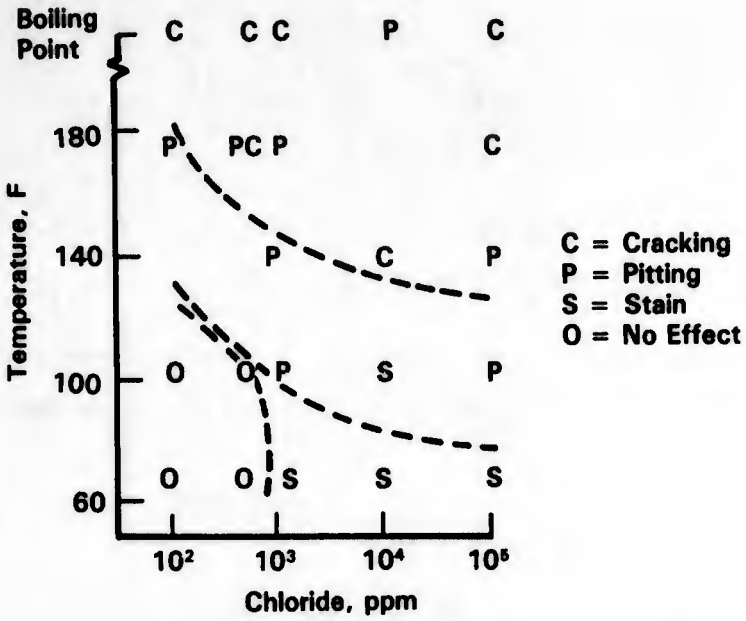

FIGURE 4-57. EFFECT OF CHLORIDE CONTENT AND TEMPERATURE ON TYPE OF CORROSION OF TYPE 304 IN SODIUM CHLORIDE SOLUTIONS: INITIAL pH 2[136]

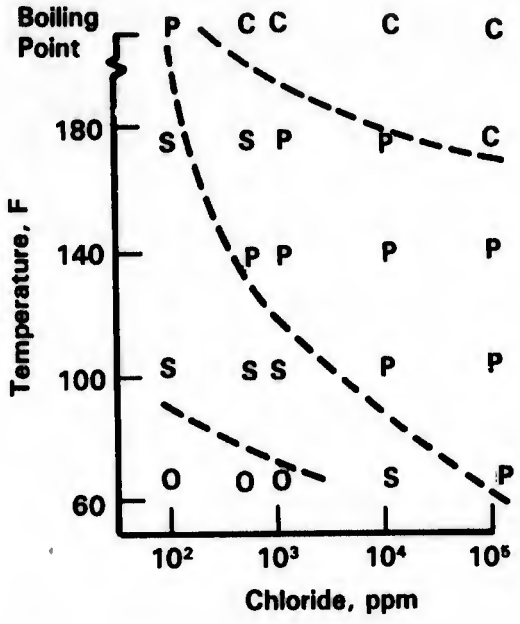

FIGURE 4-58. EFFECT OF CHLORIDE CONTENT AND TEMPERATURE ON TYPE OF CORROSION OF TYPE 304 IN SODIUM CHLORIDE SOLUTION: INITIAL pH 7[136]

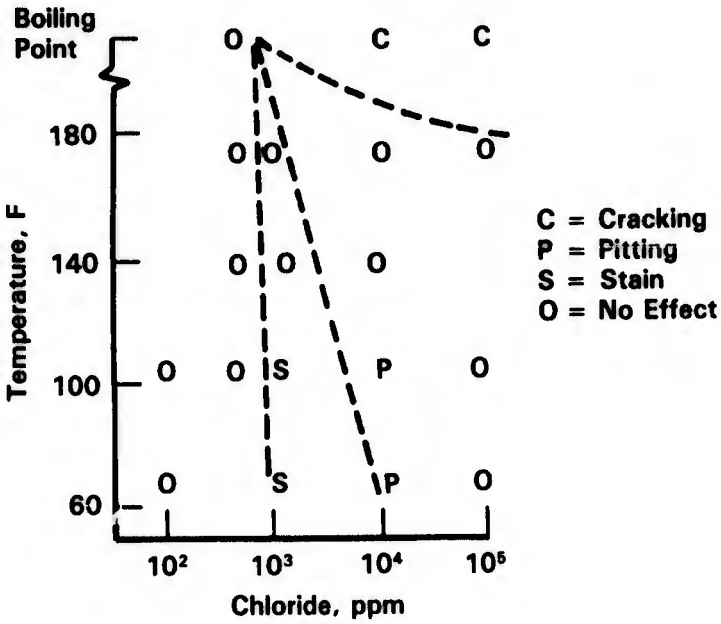

FIGURE 4-59. EFFECT OF CHLORIDE CONTENT AND TEMPERATURE ON TYPE OF CORROSION OF TYPE 304 IN SODIUM CHLORIDE SOLUTION: INITIAL pH 12[136]

TABLE 4-82. SCC EXPERIMENTS UNDER FREE CORROSION CONDITIONS; 22.4Cr-5.5Ni-3Mo IN 4.3M NaCl; σ = 0.9 YS[62]

Direction of Specimen	Temperature, C	Corrosion Potential, V(SHE)	Testing Time, hours	Remarks
Longitudinal	50	-0.11	1007, not cracked	No attack
Longitudinal	70	-0.12	1007, not cracked	No attack
Longitudinal	90	-0.11	1006, not cracked	No attack
Transverse	50	-0.11	1005, not cracked	Slight attack
Transverse	70	-0.12	1005, not cracked	Slight pitting
Transverse	90	-0.12	1268, not cracked	Slight pitting

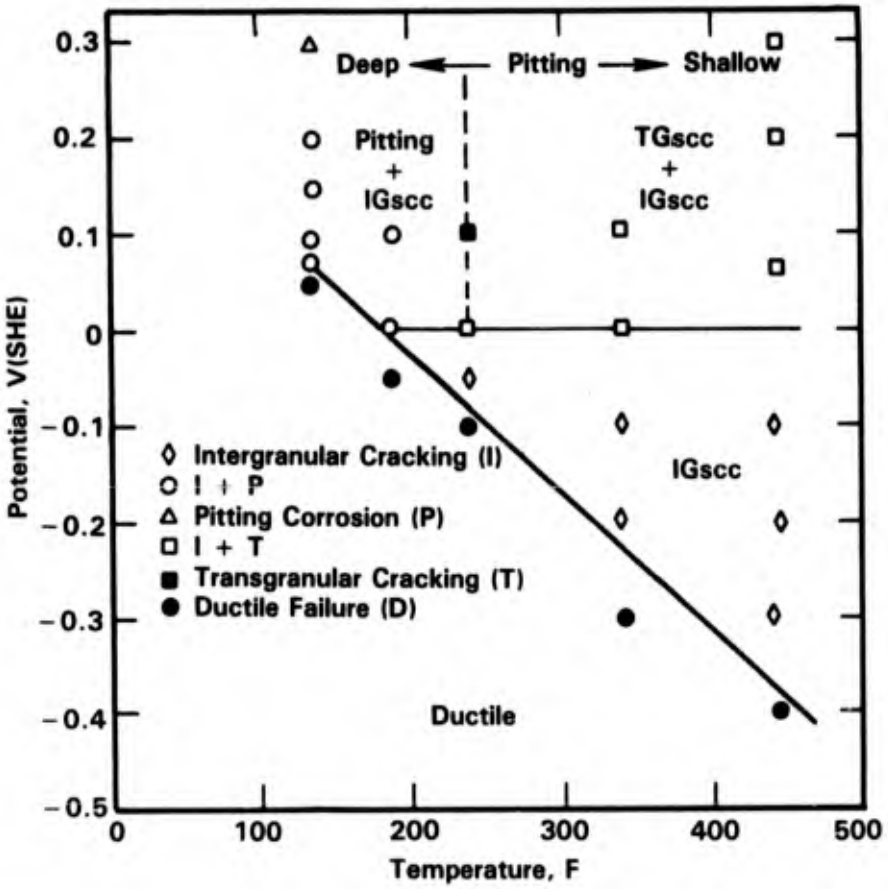

FIGURE 4-60. POTENTIAL-TEMPERATURE DIAGRAM SHOWING REGIONS OF DIFFERENT FAILURE MODES FOR TYPE 304 IN 0.01M NaCl[137]

Effect of Aeration. Data are sparse on the effect of aeration on the stress-corrosion cracking of stainless steels in seawater. For the austenitic alloys, this paucity of data is probably due to the absence of SCC below 80 C and the relatively low solubility of air (oxygen) at temperatures above 80 C. Isolated examples of the effects of aeration on SCC at higher temperatures have been reported for desalination and geothermal studies. Oldfield and Todd[124] cite data for 316L that indicate cracking in 126 C seawater that contained 600 ppb dissolved oxygen but no cracking in the same environment with 30 ppb dissolved oxygen. Cramer and Carter[129] summarized results in 232 C Salton Sea geothermal brine (see Table 4-77), but added in their text that the effect of adding oxygen was to increase the severity of SCC in 316L and initiate SCC in Inconel 625 and Hastelloy C-276. Similar effects would be expected with aerated seawater at these high temperatures. Note in Table 4-77 that Sandvik 3RE60, 316L, 430, and Alloy 20 exhibited SCC even under deaerated conditions (initial oxygen concentration <100 ppb).

Data on the effect of aeration on the SCC of martensitic and precipitation hardened steels are also sparse. One can infer from Reinhart's[33] deep ocean studies that SCC of the precipitation hardened alloys occurred most readily at the depths with the lowest oxygen levels. Three of the four failures occurred at the 2,340 ft depth which corresponds to the lowest oxygen level (<1 ppm) in that part of the Pacific Ocean. This could be expected because the failure of the high-strength martensitic and precipitation hardened alloys is believed to be caused by atomic hydrogen and its rate of generation is high at more negative potentials (more deaerated conditions).

Effect of Velocity. No data have been found on the effect of velocity on the SCC of stainless steels in seawater. Weber[109] states that cases of SCC in stainless steel pumps handling seawater are almost unknown. He then explains that is probably due to the temperature rarely exceeding 65 C and pump materials are in the form of castings which are more resistant to SCC than wrought counterparts. It can be speculated that if the effect of velocity is to bring a greater flux of aerated seawater (oxygen) to the component surface, then increased velocity should be beneficial to high-strength martensitic and PH steels (where hydrogen contributes to cracking) and should be detrimental to austenitic alloys at higher temperatures where oxygen increases the susceptibility to SCC. On the other hand, where pits act as sites of SCC initiation, high velocities may be beneficial.

Effect of Biofouling. No data have been found for the effect of biofouling on the SCC of stainless steels in seawater. Since SCC of the mill annealed austenitic alloys does not occur until temperatures exceed about 80 C, biofouling should not be a problem because most

organisms would not survive this temperature. On the other hand, if sulfate-reducing or hydrogen-producing bacteria were involved, SCC of martensitic and PH stainless steels could be enhanced.

Effect of Particulates. No data have been found on the effect of particulates on the SCC of stainless steels in seawater. It would be expected that any effect of particulates would be to settle out and produce a crevice effect, or act as an abrasive to erode the protective oxide film. The crevice-effect could conceivably promote SCC. The erosion effect would produce an actively corroding surface and would not be expected to promote SCC.

Mechanical Effects. Somewhat surprisingly, few data have been found for the effects of mechanical treatments on the SCC of stainless steels in seawater. As with other variables, this lack of data is probably related to the good resistance of the austenitic alloys to SCC at temperatures <80 C. Since many stainless steels with some degree of cold work are being used in seawater, it must be concluded that cold work does not have a strong adverse effect, at least at temperatures <80 C. This conclusion tends to be borne out by the results of Radhakrishnan and Iyer.[138] Working in a chloride medium, they found no effect of plastic strain (in the range of 0 to 24 percent) on the mechanical properties of stainless steel (hence no SCC) after 60 days exposure in 3.5 percent NaCl. They did not give the composition of the stainless steel.

Geometry Effects. The very limited data on the effects of geometry on SCC of stainless steels have been obtained in NaCl solutions instead of seawater. As mentioned in several previous sections, a crevice in conjunction with stress tends to increase the tendency for SCC. Gurevich[139] has examined the effects of preexisting fatigue cracks on the SCC of 15Cr-8Ni-3Mo in 3 percent NaCl and concluded that the plastic zone at the crack tip reduced the crack propagation rate by a factor of 2. However, the crack propagation rates in his 3-point loaded bent beams were inordinately high at 10^{-2} mm/sec.

Daniels[140] cautions that more than one type of test is needed to determine the SCC susceptibility of stainless steel. He studied 304 stainless steel in 1 to 20 percent NaCl at 100 C and found that SCC occurred at slower strain rates in slow strain rate tests (SSRT) as the chloride concentration decreased; and that SCC occurred at the free-corrosion potential and at both anodic and cathodic potentials in SSRT and U-bends, but did not occur at cathodic potentials in constant load tests.

Effect of Heat Transfer. No data have been found on the effect of heat transfer on the SCC of stainless steels in seawater. It can be anticipated that the major effects of heat transfer would be to elevate the temperature at the metal surface, and possibly to cause scale buildup. Increasing the surface temperature locally to >80 C could promote SCC as discussed in the Temperature Effects Section. A scale buildup could result in crevice corrosion which might increase the likelihood of SCC, particularly for sensitized austenitic alloys and the high strength martensitic and precipitation hardened alloys.

Effect of Potential. No data have been located for the effect of potential on the SCC of stainless steels in seawater. Some data have been obtained in NaCl solutions. These results cannot be correlated directly with seawater exposure but trends can be shown. Herbsleb and Popperling[62] and Gouda and El-Sayed[135] have found that the SCC susceptibility of 22Cr-5.5Ni-3Mo and Type 410 increased as the potential was made anodic (see Table 4-83 and Figure 4-61). On the other hand, Suery[141] and Fujii[134] have found that cathodic polarization increased SCC susceptibility of martensitic 12Cr-4Ni and precipitation hardened 17-4PH (see Table 4-79 and Figure 4-62). This suggests that these alloys probably fail by hydrogen stress cracking rather than SCC.

Figure 4-60 from Lin, et al.[137] shows that, as the temperature of 0.01M NaCl solution was increased, the potentials at which sensitized Type 304 exhibited IGSCC decreased (became more negative).

TABLE 4-83. EFFECT OF POTENTIAL AND TEMPERATURE ON TIME-TO-FAILURE OF 22Cr-5.5Ni-3Mo STRESSED TENSILE SPECIMENS IN H_2S-SATURATED 4.3M NaCl (pH 4)[62]

Temperature, C	Free Corrosion Potential, V(SHE)	Potential, V(SHE)	Time-to-Failure or Testing Time, hours
Ambient	Not measured	Free corrosion (E_{cor})	38
40	Not measured	Free corrosion (E_{cor})	48
60	Not measured	Free corrosion (E_{cor})	4
Ambient	-0.16	E_{cor} + 0.10	12
Ambient	-0.17	E_{cor} - 0.10	1195, not cracked
Ambient	-0.23	E_{cor} - 0.30	1030, not cracked
60	-0.23	E_{cor} + 0.05	9
60	-0.23	E_{cor} + 0.10	4
60	-0.23	E_{cor} + 0.20	2
60	-0.18	E_{cor} - 0.10	1097, not cracked

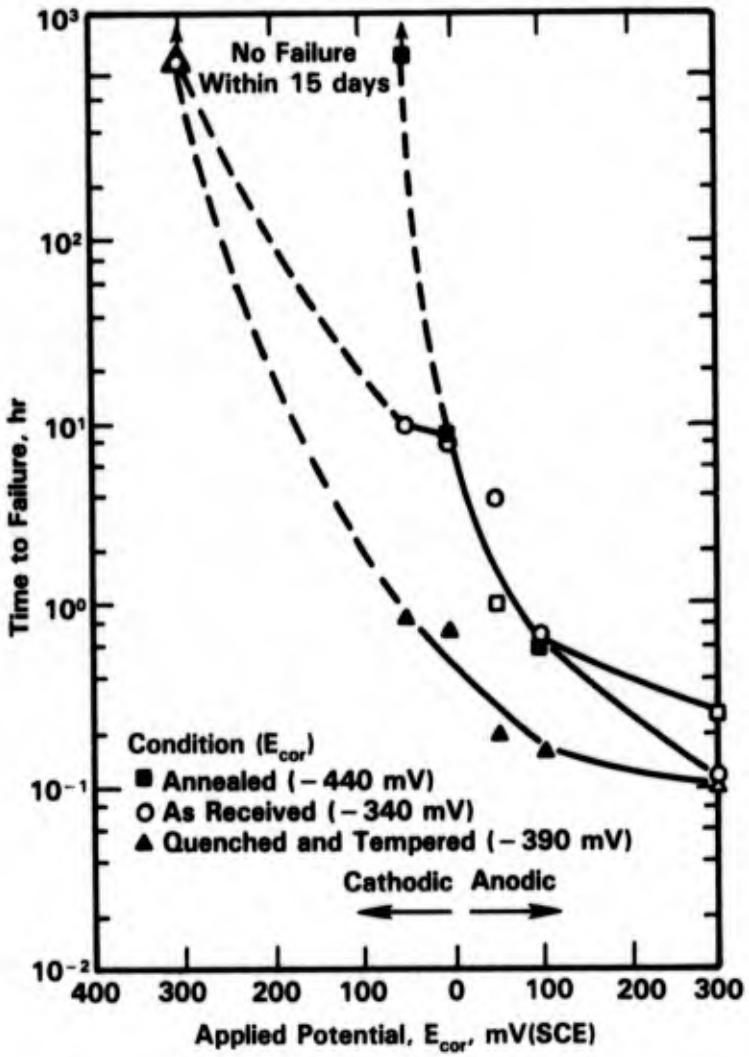

FIGURE 4-61. TIME TO FAILURE AS A FUNCTION OF APPLIED POLARIZATION POTENTIALS RELATIVE TO THE CORROSION POTENTIAL FOR STRESSED 410 STAINLESS STEEL IN 3 PERCENT NaCl SOLUTION(135)

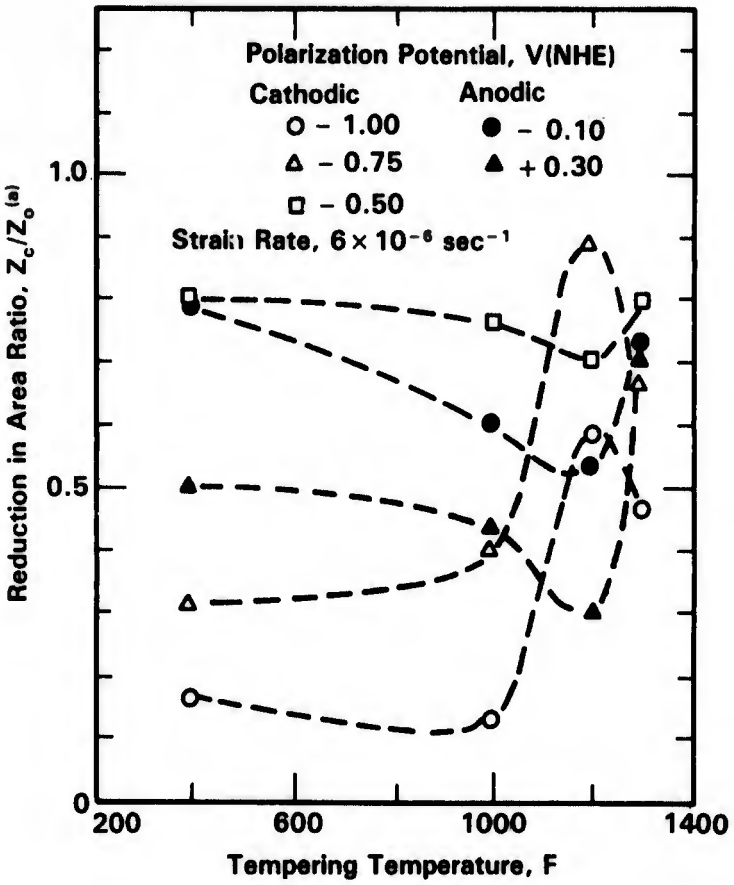

FIGURE 4-62. INFLUENCE OF TEMPERING TEMPERATURE AND POLARIZATION ON REDUCTION IN AREA OF 12Cr-4Ni CAST MARTENSITIC STAINLESS STEEL IN 3 PERCENT NaCl SOLUTION CORROSION POTENTIAL ~ -0.25 V(NHE)[141]

(a) Z_c = Reduction in Area in Corrodent
Z_o = Reduction in Area in Air

Effect of pH. No data have been found on the effects of pH on the SCC of stainless steels in seawater. Only limited data have been found for SCC in NaCl solutions. Truman[136] exposed welded tubes of Type 304 to a range of NaCl concentrations at pH 2, 7, and 12. His results are presented in Table 4-81. He concluded that the role of pH in producing SCC is complex, but that, in general, solutions of high alkalinity are less likely to give rise to SCC. The work of Kurov and co-workers[142,143] on crack tip chemistry in a neutral 3 percent NaCl solution tends to support this conclusion. They found that the pH at a SCC crack tip in an 18Cr-8Ni alloy fell from 6.5 to about 1 within 24 to 30 hours and then slowly rose to about pH 3 at 100 hours. Thus, in highly alkaline solutions, one might expect the pH at a crack tip to drop more slowly and perhaps never reach a low value where SCC is sustained.

Effect of Pollution. H_2S is the principal agent of pollution that affects corrosion behavior. No data have been found for the effects of H_2S in seawater on the SCC of stainless steels. However, several studies have been conducted in NaCl solutions that indicate trends. Herbsleb and Popperling[62] exposed a 22Cr-5.5Ni-3Mo duplex alloy to H_2S-contaminated and noncontaminated 4.3M NaCl solution at 50, 70, and 90 C. No SCC was observed in specimens exposed at 0.9 yield strength for 1,000 hours in noncontaminated solution. However, as shown in Table 4-84, SCC was observed at high H_2S concentrations at both ambient temperature and 60 C. SCC was observed at the 100 ppm H_2S level at ambient temperature, which is probably an upper limit for H_2S associated with pollution. The absence of SCC at the 100 ppm H_2S level at 60 C suggests a hydrogen stress cracking mode of failure since it is known that increasing temperature decreases the propensity for this type of failure.

McGuire, et al.[144] observed a similar effect of temperature on the SCC of Type 410 U-bends in 3 percent NaCl that contained 0.25 g/l H_2S (approximately 250 ppm). At 25 C, specimens with yield strength $\geq$120,000 psi exhibited cracking, whereas at 100 C, only those specimens with yield strength $\geq$175,000 psi failed.

Effect of Depth. The only data found on the effect of depth on the SCC of stainless steels in seawater have been those of Reinhart.[33] As mentioned in the section on aeration, three of the four failures observed in the precipitation hardened steels in his study occurred at the 2,340 ft depth. (Also see section on Alloy Composition.) The other failure occurred at 5,300 feet. The 2,340 ft depth corresponds to the lowest dissolved oxygen level in these tests

TABLE 4-84. EFFECT OF H_2S CONCENTRATION ON TIME-TO-FAILURE OF TENSILE SPECIMENS OF 22Cr-5.5Ni-3Mo (σ = 0.9 YS) IN 4.3M NaCl (pH 4) UNDER FREE CORROSION CONDITIONS[62]

Temperature, C	H_2S Concentration, g/l	Time-to-Failure, hours
Ambient	Saturated ($\approx$1.8)	38
Ambient	1.0	58
Ambient	0.1	471
60	Saturated ($\approx$1.8)	38
60	1.0	58
60	0.1	1007, not cracked

and the 5,300 ft depth also represents a low oxygen level. Since the high-strength precipitation hardened stainless steels are generally believed to fail by hydrogen stress cracking, it follows that susceptibility to SCC would be greatest where oxygen levels are low. Thus, the principal effect of depth on SCC of the high strength alloys appears to be related to the dissolved oxygen content at any given depth.

Effect of Seawater Composition. Few data have been found on the effect of seawater composition on the SCC behavior of stainless steels. As with other variables, this probably is the result of the resistance to SCC of the austenitic grades at temperatures $\leq$60 C. The effect of H_2S as a pollutant already has been discussed. Lee, et al.[145] have observed SCC of Type 316L in the piping and heat exchanger shells of the venting systems in desalination plants. They found a relatively high percentage (3.3 percent) of bromine in the corrosion product, and attributed the SCC to bromine. The bromides apparently reacted with ammonia in the seawater to form bromamines which were then evolved into the venting system.

Although the results are not correlatable one-to-one with those in seawater, several studies have been made on the effect on SCC of chloride content and type of chloride salt. The effect of chloride concentration (as NaCl) and acidity on the SCC of Type 304 has been reported by Torchio[146] (see Figure 4-63). He found a range of NaCl and HCl concentrations that produced SCC which lay between the conditions that produced pitting and uneven general attack. Truman[136] found that high chloride concentrations favored SCC and that the order of aggressiveness of the cations in producing SCC was Na>Mg>Ca>Zn. His results are summarized in Table 4-81. Gouda and El-Sayed[135] found that Type 410 (to 88 ksi YS) was more susceptible to SCC in boiling 3 percent NH_4Cl than it was in boiling 3 percent NaCl.

Erosion/Cavitation

There is a moderate amount of information on the erosion corrosion and cavitation of stainless steels in seawater. The two deterioration processes are quite different. The erosion data are for clean seawater where the shear stresses from the high velocity fluid remove a portion of the protective film and thereby increase the corrosion rate of the stainless steel. Erosion effects may be general over a broad area, or may be local such as at sharp changes in direction or at reduced cross sections. On the other hand, cavitation is the result of bubble collapse in the fluid as the result of rapid movement or vibration of the component or rapid pulsations in the fluid. The usual effect of the high implosive force of the collapsing bubbles is to rupture the protective oxide film on the stainless steel and, in severe cases, to damage the

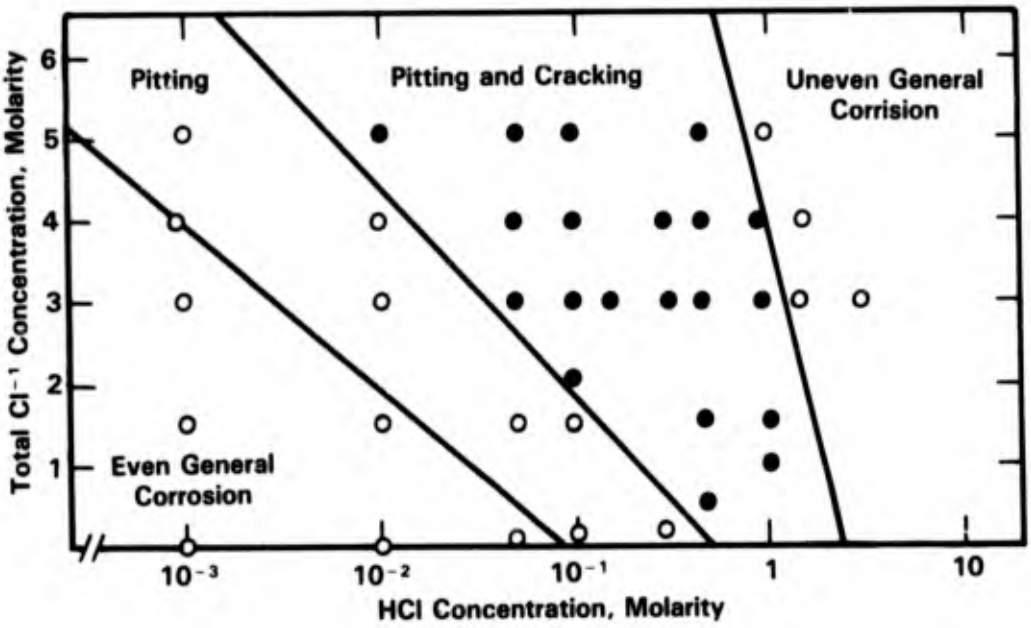

FIGURE 4-63. MORPHOLOGY OF THE CORROSION PROCESSES ON TYPE 304 STAINLESS STEEL AS A FUNCTION OF ACIDITY AND TOTAL CHLORIDE CONTENT[146]

metal itself. Cavitation is almost universally restricted to small areas, and is often found in pumps and high velocity systems.

Erosion. Erosion effects have been observed in high velocity pumping systems and in high velocity surface ships (hydrofoils). As noted in the section on Pitting, the conventional stainless steels pit at seawater velocities <5 fps, but are resistant to corrosion at velocities ≥5 fps through upwards of 100 fps. At very high velocities, the corrosion rate increases as the protective film is removed by the high velocity fluid. There are conflicting data on the upper limit of velocity. As shown in Tables 4-58, 4-59, 4-85, and 4-86, and Figures 4-26 and 4-27, the stainless steels appear to be relatively resistant to flowing seawater at velocities up to 150 fps. On the other hand, Pini and Weber[149] indicate that Type 316 and the conventional stainless steels exhibit increased attack at seawater velocities >70 fps, (see Figure 4-27). Hohman and Kennedy[111] report that 17-4PH corrodes at a rate of 10 to 15 mils/year in seawater at 90 knots (about 150 fps) as shown in Figure 4-64. Werchniak and Gudas (Table 4-86) have observed corrosion rates of <0.2 mil/year for 17-4PH at a lower velocity of 100 fps, and Davis and Gehring[150] report <2 mpy corrosion rates for 17-4PH after a short time (20 hours) test at 150 fps.

TABLE 4-85. RESULTS OF 30-DAY CORROSION TESTS IN HIGH VELOCITY SEAWATER[147]

Materials	Specimen Number	Weight Loss, gm	Corrosion Rate mdd	Corrosion Rate ipy[a]	Relative Corrosion Rate[b]	Test Run
Nickel Alloys	A1	0.0235	3.5	0.0006	0.013	1st
	A2	0.0203	3.0	0.0005	0.010	1st
	A3	0.0149	2.2	0.0004	0.008	1st
	A4	0.0100	1.5	0.0002	0.004	5th
	A5	0.0080	1.2	0.0002	0.004	5th
	A6	0.0070	1.0	0.0002	0.004	5th
Stainless Steels	B1	0.0126	1.8	0.0003	0.006	2nd
	B2	0.0094	1.4	0.0002	0.004	2nd
	B3	0.0063	0.9	0.0002	0.004	2nd
	B4	0.0173	2.6	0.0005	0.010	2nd
	B5	0.0070	1.0	0.0002	0.004	5th
	B6	0.0220	3.2	0.0006	0.013	5th
Titanium Alloys	C1	0.0062	0.9	0.0003	0.006	3rd
	C2	0.0093	1.4	0.0004	0.003	3rd
	C3	0.0079	1.2	0.0004	0.008	3rd
Copper Alloys	D1	1.2338	182	0.034	0.71	1st
	D2	1.2072	177	0.034	0.71	1st
	D3-1	2.0299	299	0.048	1.00	1st
	D3-2	1.5172	223	0.036	0.75	2nd
	D3-3	1.9481	286	0.046	0.94	3rd
	D3-4	2.2810	336	0.054	1.12	4th
	D3-5	2.3160	340	0.055	1.14	5th
Aluminum Alloys	E1	0.8572	126	0.067	1.40	4th
	E2	1.0488	155	0.083	1.73	4th
	E3	0.8396	123	0.068	1.42	4th
Carbon and Low-Alloy Steels	F1	2.114	311	0.057	1.19	3rd
	F2	8.164	1203	0.219	4.56	4th
	F3-2	4.412	651	0.118	2.46	2nd
	F3-3	3.639	536	0.09[illegible]	2.04	3rd
	F3-4	6.527	962	0.17[illegible]	3.64	4th

(a) $ipy = mdd \times \frac{0.001437}{d}$ where d = density, g/cc.

(b) $\frac{\text{Column 4}}{0.048}$ where 0.048 ipy = average rate for D3.

Note: Water velocity - 133 to 138 fps (79 to 82 knots)
Exposed specimen area - 3.5 sq. in. (0.23 dm^2)
Duration of Test - 30 days.

TABLE 4-86. RESULTS OF CORROSION-EROSION TESTS IN FLOWING SEAWATER[a][148]

Material	Duration of Test, day	Average Temperature, C	Weight Loss, gm	Corrosion Rate, μm/yr	Maximum Depth of Attack on Boldly Exposed Surfaces, mm
CA-6NM (12Cr-4Ni)	35	21	0.015	2.2	ND[b]
			0.005	0.7	ND
			0.010	1.5	ND
17-4PH	32	27.7	0.022	3.7	<0.02
			0.015	2.5	<0.02
			0.034	5.7	<0.02
Illium-PD	32	27.7	0.014	2.3	<0.02
			0.006	0.9	<0.02
			0.008	1.3	<0.02
Ti-6Al-4V	35	21	0.004	0.1	ND
			0.001	0.3	ND
			0.001	0.3	ND
IN-625	32	27.7	0.010	1.6	<0.02
			0.014	2.2	<0.02
			0.014	2.2	<0.02

(a) Velocity = 30 m/s.
(b) ND = nondetectable.

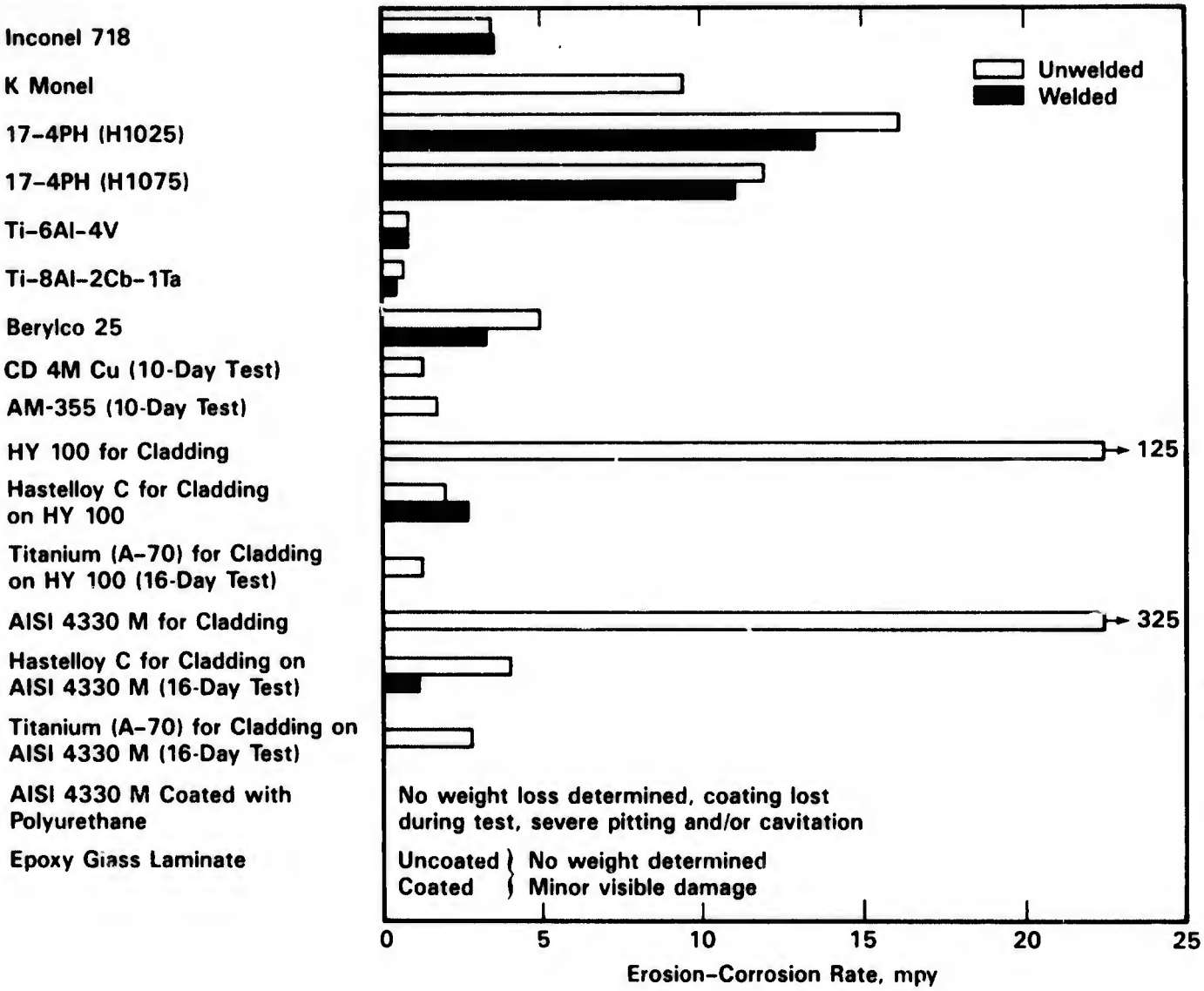

FIGURE 4-64. RATES FOR JET EROSION-CORROSION IN SEAWATER EXPOSURE FOR 30 DAYS AT 90 KNOTS[111]

Cavitation. Lee[151] has rated the austenitic and precipitation hardened stainless steels among the most resistant to cavitation attack in seawater (see Table 4-87). This ranking appears to be confirmed by studies conducted by Weber (Figure 4-65). Hohman and Kennedy[111] (Figure 4-66), and Werchniak and Gudas[148] (Table 4-88). Note that the data reported from these sources indicate a moderate amount of attack, but it must be remembered that laboratory cavitation tests are designed to accelerate attack to permit relative rankings of materials.

TABLE 4-87. MATERIALS OF VARIOUS RESISTANCE TO CAVITATION DAMAGE IN SEAWATER[151]

Resistance to Cavitation Damage Rating	Metals
Group I - Most resistant. Little or no damage. Useful under highly cavitating conditions.	Cobalt-base hardfacing alloys Titanium alloys Austenitic (series 300) and precipitation hardening stainless steels Nickel-chromium alloys such as Alloy 718 Nickel-chromium-molybdenum alloys such as Alloys 625 and C-276
Group II - These metals are commonly utilized where a high degree of resistance to cavitation damage is required but where some metal loss under the most severe conditions of cavitation is acceptable.	Nickel-copper-aluminum Alloy K-500 Nickel-copper Alloy 400 Nickel-aluminum bronze Nickel-aluminum-manganese bronze
Group III - These metals have some degree of cavitation resistance but are generally limited to low speed applications.	70/30 copper-nickel alloy Manganese bronze G Bronze and M Bronze Austenitic nickel cast irons
Group IV - These metals are normally not used in applications where cavitation damage may occur.	Carbon and low-alloy steels Cast irons Aluminum and aluminum alloys

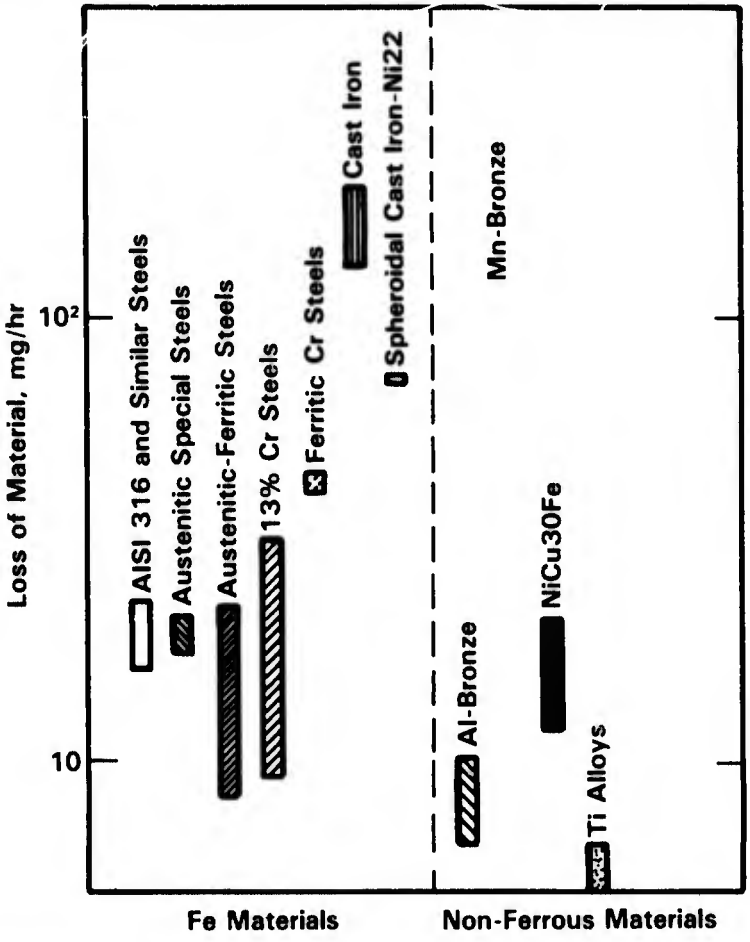

FIGURE 4-65. WEIGHT LOSS OF DIFFERENT MATERIALS DUE TO CAVITATION IN SEAWATER[109]

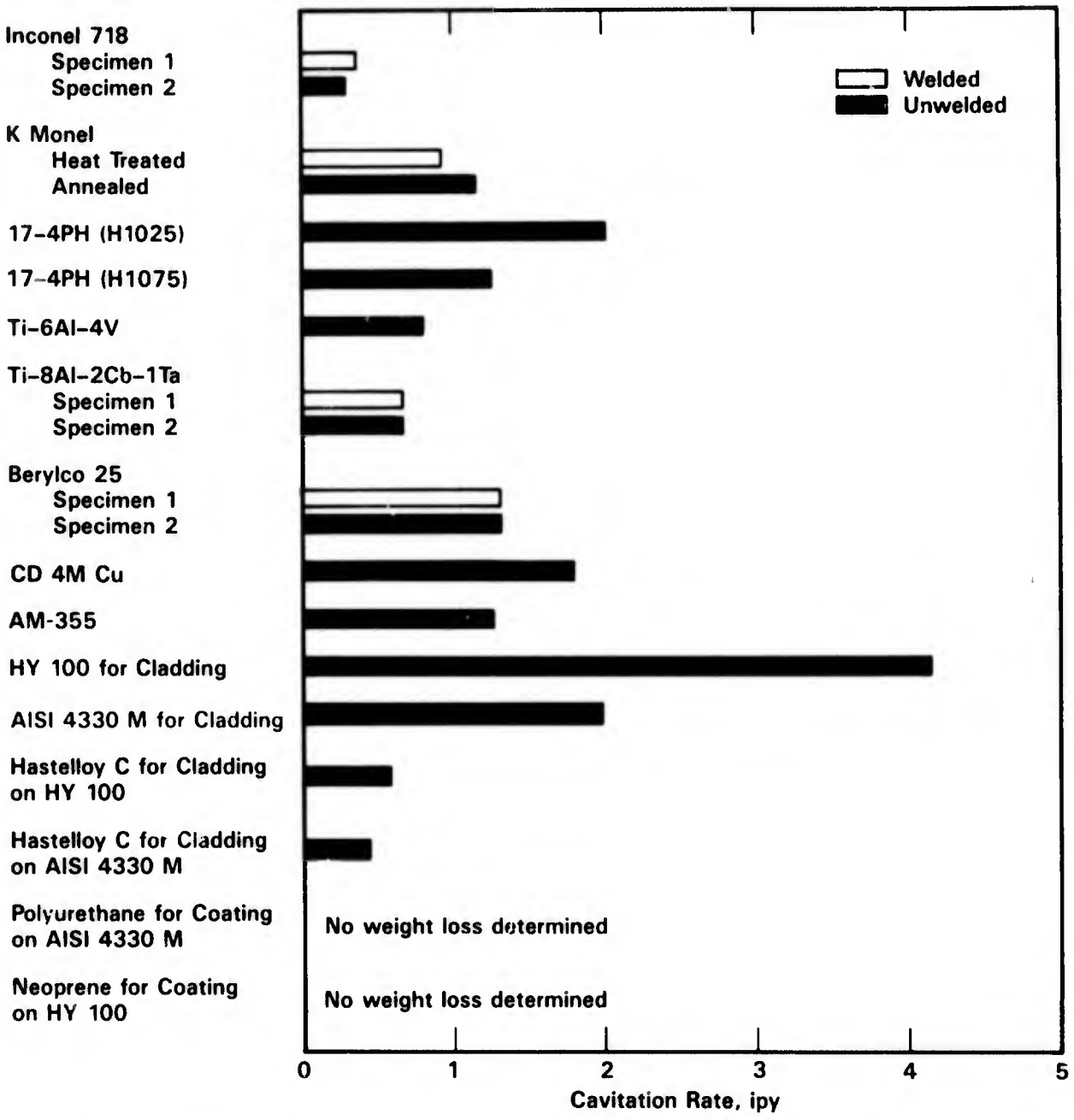

FIGURE 4-66. CAVITATION RATES IN SEAWATER: DOUBLE AMPLITUDE 0.001 INCH, FREQUENCY 22,000 CYCLES/SECOND[111]

TABLE 4-88. RESULTS OF CAVITATION-EROSION TESTS IN FLOWING SEAWATER[a](148)

Material	Duration of Test, day	Average Temperature, C	Maximum Depth of Attack, mm (downstream from the hole)
CA-6NM	31	27	0.58 0.25 0.10
17-4PH	30	26.6	0.27 0.24 0.02
Illium-PD	30	26.6	-- 0.09 0.20
Ti-6Al-4V	31	27	0.30 0.15 0.30
IN-625	30	26.6	0.15 0.13 0.06

(a) Velocity = 30 m/s.

Corrosivity of the environment is a factor in cavitation. As shown by Simoneau, et al. in Figure 4-67, cavitation loss for Type 304 is about twice as great in 3 percent NaCl solution as in distilled water in tests conducted at 20 KHz and 17 μm amplitude. Simoneau, et al.(152) also report that the application of cathodic protection decreases the damage due to cavitation which further indicates a contribution of corrosion to cavitation damage.

Intergranular Attack (IGA)

As discussed in the section on stress-corrosion cracking, the welding or heat treatment of the conventional stainless steels can lead to chromium carbide precipitation at grain boundaries, with a lowering of the chromium concentration adjacent to the grain boundaries and a resultant sensitization to intergranular attack (IGA). The critical temperature range for

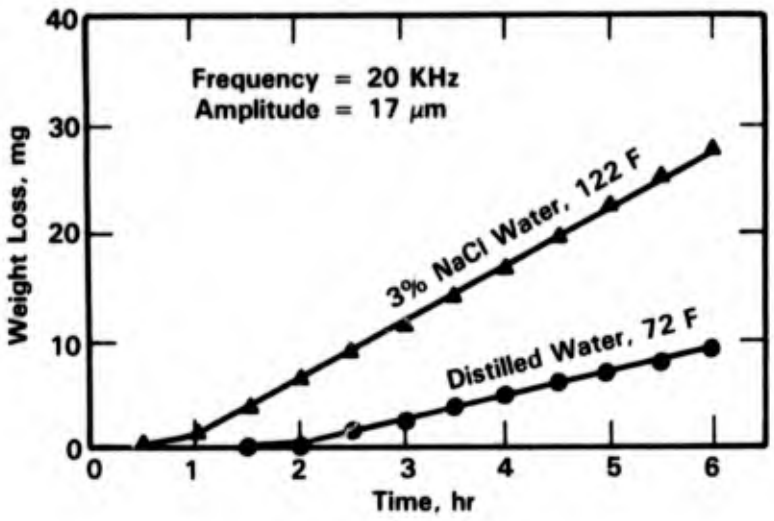

FIGURE 4-67. WEIGHT LOSS RESULTS FOR 304 STAINLESS STEEL IN CAVITATION TESTS[152]

sensitization is 500 to 800 C. Ozhiganov, et al.,[153] Sedriks,[11] and Speidel[133] have reported on the intergranular stress-corrosion cracking of sensitized stainless steel in seawater and chloride solutions. Sedriks also cites data that indicate that sensitized 316, 316L, and 317 exhibit IGA in long-term exposure (1 year) in seawater (see Table 4-41). Note that sigma phase, which also promotes IGA in seawater, may have been present in several of the heat treated specimens in Table 4-41. Shul'te, et al.[154] found IGA adjacent to a weld in 17-6 austenitic/martensitic stainless steel that was welded to 18-10 stainless steel. However, the 6-month exposure in seawater did not produce IGA in the heat affected zone of the 18-10 stainless steel.

Carter, et al.[155] and Carter and McCawley[156] have reported IGA in 316L stainless steel exposed 15 to 45 days in Salton Sea geothermal brine at about 235 C. The IGA apparently occurred at cold worked areas in the mill annealed material. Close examination of their photomicrographs reveals that the IGA was less than one grain deep. Companion specimens of 430, 26-1, 29-4, and 6X did not exhibit IGA under these same exposure conditions.

Thus, there are indications that sensitized austenitic stainless steels can exhibit IGA in seawater. On the other hand, welded stainless steel has been used extensively in seawater applications with few problems. Until definitive data become available, it would appear that welded normal carbon grades or sensitized austenitic stainless steels should be used with caution in seawater.

Galvanic Corrosion

Considerable information is available relative to the galvanic corrosion of stainless steel in seawater and sodium chloride environments. The information falls into four broad categories: (1) cathodic protection to prevent crevice corrosion of stainless steels; (2) galvanic series in seawater; (3) galvanic corrosion of the dissimilar metal of the couple; and (4) galvanic corrosion of the stainless steel member of the couple. Cathodic protection is described in detail in another section of this report and will not be discussed here except in passing to note that Lee and Tuthill,[157] and others have found that galvanic coupling to carbon steel prevents seawater crevice corrosion in the conventional 300 series stainless steel.

Galvanic Series. Several galvanic series have been developed based on the corrosion potentials of the various metals and alloys in seawater. One such series compiled by INCO is shown in Figure 4-2. Note that the stainless steels are very noble (positive) and thus would be expected to cause galvanic corrosion on the large group of alloys that exhibit more negative potentials. In turn, stainless steels would be expected to experience galvanic corrosion when coupled to the few metals that exhibit more positive corrosion potentials. Also note that the corrosion potentials in stainless steel crevices may be several hundred millivolts more negative than those for fully exposed surfaces which accounts for the driving force for crevice corrosion.

The effect of velocity on the corrosion potentials is summarized in Figure 4-68. Note that velocity in the range of 3 to 15 m/s has only a minor effect on corrosion potential and thus does not create a major change in ranking in the galvanic series. A galvanic series also has been developed by Henrikson and Asberg[158] for Baltic seawater which is lower in salinity than most ocean waters. Their results, presented in Table 4-89, reveal that Type 317 stainless steel was more noble than titanium in the Baltic seawater.

Smith and Compton[159] have determined galvanic series as a function of temperature (30, 100, 160, and 200 C). They found that the effect of increased temperature for most metals was to make the potential more negative and to reduce the spread of the values. Median potential values for Type 316 in aerated seawater were as follows:

Temperature, C	V(SCE)
30	-100
100	-180
160	-200
200	-300

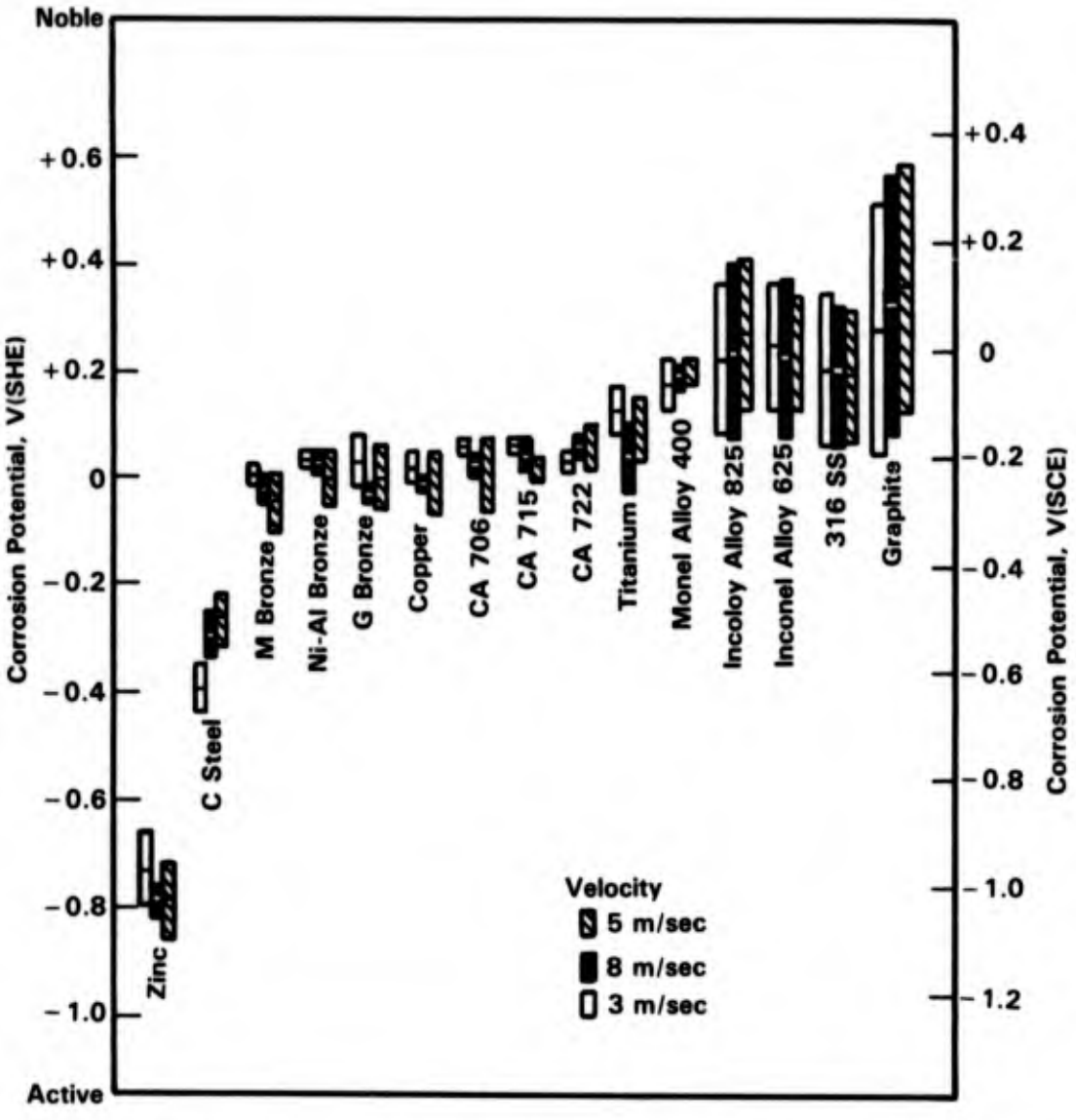

FIGURE 4-68. CORROSION POTENTIALS AS FUNCTION OF SEAWATER VELOCITY FOR 30 DAY EXPOSURES AT 25 C[11]

TABLE 4-89. GALVANIC SERIES BASED ON THE MEAN CORROSION POTENTIAL MEASURED OVER 60 DAYS IN BALTIC SEAWATER[158]

Material	Corrosion Potential mV(SCE)	Corrosion Potential mV(NHE)
Stainless steel 317	+78	+305
Titanium	+67	+294
Stainless steel 316	+64	+291
Stainless steel 317, creviced	+37	+264
Stainless steel 316, creviced	+16	+243
Hastelloy C-276	-23	+204
Gun metal	-41	+186
CuNi 90/10	-43	+184
Al-brass	-50	+177
Armature brass 2	-117	+110
Armature brass 1	-127	+100
Nickel-plated carbon steel	-136	+91
Stainless steel (26Cr-5Ni-1.5Mo)	-143	+84
Armature brass 3	-170	+57
Stainless steel (26Cr-5Ni-1.5Mo), creviced	-187	+40
Muntz metal	-302	-75
Lead	-425	-198
Cast iron (grey iron)	-720	-493
Carbon steel	-725	-498
Cast iron (ductile)	-728	-501
Al 2.5 Mg	-1067	-840

Dissimilar Metal Corrosion. A practical guide for coupling dissimilar metals to stainless steel is given in Table 4-90. Note that, in all applications, 3 or fewer metals are all that can be safely galvanically coupled to stainless steel without experiencing excessive galvanic attack.

The corrosion effects of galvanically coupling Types 304 and 316 to a number of dissimilar alloys in seawater are presented in Tables 4-91 and 4-92. Note in Table 4-91 that coupling to stainless steel increased the amount of attack on steel and 6061 and 7075 aluminum. Negligible, if any, increase in attack was observed for 360 brass, Monel 400, or titanium when coupled to Type 316. Similar results are noted in Table 4-92.

Several galvanic corrosion studies have been conducted with the high molybdenum ferritic and duplex stainless steels. Gehring and Maurer[161] report considerable galvanic attack of copper tube sheet materials when coupled to Al-6X tube material (see Table 4-93). The galvanic attack was more severe on Muntz metal than it was on aluminum bronze. Gehring and Kyle[162] reported somewhat similar galvanic effects (see Table 4-94), but noted a marked decrease in galvanic attack when the seawater temperature was reduced from 22 to 6 C.

Couples between stainless steels and dissimilar metals also have been studied for:

Aluminum: References 163-170
Steel: References 163-165
Copper Alloys: References 8, 163-165
Nickel Alloys: References 8, 163, 164
Titanium: References 16, 163, 164.

Galvanic Corrosion of Stainless Steels. In most galvanic couples, stainless steel is noble to the dissimilar metal and thus is protected from corrosion. However, Types 304 and 316 are attacked in some galvanic couples. As shown in Table 4-91, Ebihara[13] found a slight increase in attack in some of his 316 specimens that were coupled to Monel 400 and Ti-6Al-4V in seawater in the Panama Canal Zone. Pelensky, et al.[163] did not observe increased attack of Type 316 when coupled to Monel. Bomberger[16] found no effect on 316 coupled to titanium (see Table 4-95). Only a slight increase in attack was observed for Type 302 coupled to titanium in these same tests. Pelensky, et al.[163] and Charlot, et al.[164] also found no increased attack on Type 316 when coupled to titanium in seawater.

Miller and Lee[166] coupled several stainless steels to graphite-epoxy composites and exposed them to 3.5 percent NaCl solution. Their results, shown in Table 4-96, indicate that

TABLE 4-90. GUIDE FOR SELECTION OF FASTENER ALLOY FOR MARINE SERVICE BELOW WATERLINE[25]

Recommended Alloys are Listed in Order of Their Preference

Hull Superstructure or Base Plate Material	Trim Material to be Attached											
	Wood	Fiberglass	Rubber	Plastic (Nylon)	Aluminum	Steel	Steel (Galvanized)	Copper	Brass	Brass (Plated)	Nickel Stainless Stee.	Monel Nickel-Copper Alloys
Wood	Monel Silicon Bronze	Monel Silicon Bronze	Monel Silicon Bronze	Monel Silicon Bronze	Not Recommended	Monel Silicon Bronze 18-8 Stainless Steel	Monel Silicon Bronze 18-8 Stainless Steel	Monel Silicon Bronze 18-8 Stainless Steel	Monel Silicon Bronze 18-8 Stainless Steel	Monel Silicon Bronze 18-8 Stainless Steel	T-316 Stainless Steel[b]	Monel
Fiberglass	Monel Silicon Bronze	Monel Silicon Bronze	Monel Silicon Bronze	Monel Silicon Bronze	Not Recommended	Monel Silicon Bronze 18-8 Stainless Steel	Monel Silicon Bronze 18-8 Stainless Steel	Monel Silicon Bronze 18-8 Stainless Steel	Monel Silicon Bronze 18-8 Stainless Steel	Monel Silicon Bronze 18-8 Stainless Steel	T-316 Stainless Steel	Monel
Rubber	Monel Silicon Bronze	Monel Silicon Bronze	Monel Silicon Bronze	Monel Silicon Bronze	Not Recommended	Monel Silicon Bronze 18-8 Stainless Steel	Monel Silicon Bronze 18-8 Stainless Steel	Monel Silicon Bronze 18-8 Stainless Steel	Monel Silicon Bronze 18-8 Stainless Steel	Monel Silicon Bronze 18-8 Stainless Steel	T-316 Stainless Steel	Monel
Plastic (Nylon)	Monel Silicon Bronze	Monel Silicon Bronze	Monel Silicon Bronze	Monel Silicon Bronze	Not Recommended	Monel Silicon Bronze 18-8 Stainless Steel	Monel Silicon Bronze 18-8 Stainless Steel	Monel Silicon Bronze 18-8 Stainless Steel	Monel Silicon Bronze 18-8 Stainless Steel	Monel Silicon Bronze 18-8 Stainless Steel	T-316 Stainless Steel	Monel
Aluminum	18-8 Stainless Steel Aluminum	18-8 Stainless Steel Aluminum	18-8 Stainless Steel Aluminum	18-8 Stainless Steel Aluminum	T-316 Stainless Steel Aluminum	Not Recommended	Not Recommended	Not Recommended	Not Recommended	Not Recommended	T-316 Stainless Steel	Not Recommended
Steel	Monel Silicon Bronze 18-8 Stainless Steel	Monel Silicon Bronze 18-8 Stainless Steel	Monel Silicon Bronze 18-8 Stainless Steel	Monel Silicon Bronze 18-8 Stainless Steel	Not Recommended[a]	Monel Silicon Bronze 18-8 Stainless Steel	Monel Silicon Bronze 18-8 Stainless Steel	Monel Silicon Bronze 18-8 Stainless Steel	Monel Silicon Bronze 18-8 Stainless Steel	Monel Silicon Bronze 18-8 Stainless Steel	T-316 Stainless Steel	Monel
Steel (Galvanized)	Monel Silicon Bronze 18-8 Stainless Steel	Monel Silicon Bronze 18-8 Stainless Steel	Monel Silicon Bronze 18-8 Stainless Steel	Monel Silicon Bronze 18-8 Stainless Steel	Not Recommended	Monel Silicon Bronze 18-8 Stainless Steel	Monel Silicon Bronze 18-8 Stainless Steel	Monel Silicon Bronze 18-8 Stainless Steel	Monel Silicon Bronze 18-8 Stainless Steel	Monel Silicon Bronze 18-8 Stainless Steel	T-316 Stainless Steel	Monel
Copper	Monel Silicon Bronze 18-8 Stainless Steel	Monel Silicon Bronze 18-8 Stainless Steel	Monel Silicon Bronze 18-8 Stainless Steel	Monel Silicon Bronze 18-8 Stainless Steel	Not Recommended	Monel Silicon Bronze 18-8 Stainless Steel	Monel Silicon Bronze 18-8 Stainless Steel	Monel Silicon Bronze 18-8 Stainless Steel	Monel Silicon Bronze 18-8 Stainless Steel	Monel Silicon Bronze 18-8 Stainless Steel	T-316 Stainless Steel	Monel
Brass	Monel Silicon Bronze 18-8 Stainless Steel	Monel Silicon Bronze 18-8 Stainless Steel	Monel Silicon Bronze 18-8 Stainless Steel	Monel Silicon Bronze 18-8 Stainless Steel	Not Recommended	Monel Silicon Bronze 18-8 Stainless Steel	Monel Silicon Bronze 18-8 Stainless Steel	Monel Silicon Bronze 18-8 Stainless Steel	Monel Silicon Bronze 18-8 Stainless Steel	Monel Silicon Bronze 18-8 Stainless Steel	T-316 Stainless Steel	Monel
Brass (Plated)	Monel Silicon Bronze 18-8 Stainless Steel	Monel Silicon Bronze 18-8 Stainless Steel	Monel Silicon Bronze 18-8 Stainless Steel	Monel Silicon Bronze 18-8 Stainless Steel	Not Recommended	Monel Silicon Bronze 18-8 Stainless Steel	Monel Silicon Bronze 18-8 Stainless Steel	Monel Silicon Bronze 18-8 Stainless Steel	Monel Silicon Bronze 18-8 Stainless Steel	Monel Silicon Bronze 18-8 Stainless Steel	T-316 Stainless Steel	Monel
Nickel Stainless Steel	T-316 Stainless Steel[b]	T-316 Stainless Steel[b]	T-316 Stainless Steel[b]	T-316 Stainless Steel[b]	T-316 Stainless Steel[b]	T-316 Stainless Steel	T-316 Stainless Steel	T-316 Stainless Steel	T-316 Stainless Steel	T-316 Stainless Steel	Monel[c]	Monel[c]
Monel Nickel-Copper Alloys	Monel	Monel	Monel	Monel	Not Recommended	Monel	Monel	Monel	Monel	Monel	Monel[c]	Monel

Effects of corrosive action on fastener alloys: Monel—develops grey-green corrosion film; 18-8 stainless steel—develops light brown corrosion film and heavier scaling in crevices, i.e., threads and under boltheads, some bleeding; silicon bronze—develops heavy green-brown corrosion film, bleeds; and aluminum—develops white powdery corrosion film interspersed with pits unless specially protected, limited usefulness.

(a) No recommendation. These metal combinations are subject to severe galvanic effects when immersed in seawater and can be expected to give poor performance.
(b) Crevice corrosion can lead to early failure and high replacement rate of stainless fasteners for these combinations. Other fastener materials are subject to adverse galvanic corrosion.
(c) For stainless to stainless, a Monel fastener carefully insulated from stainless should give satisfactory service.

TABLE 4-91. SEAWATER IMMERSION CORROSION RATES[13]

Alloy	Exposure, months	Corrosion Rate, mm/yr							
		Mg	Stainless Steel	Steel	6061 Al	7075 Al	Brass	Monel	Titanium
316 Stainless Steel	2	0	0.097[b]	0	0	0	0	0.105[b]	0.088[b]
	4	0	0.034[b]	0	0	0	0	0.033[b]	0.017[b]
	7	0	0.036[b]	0	0	0	0	0.061[b]	0.028[b]
	12	0	0.013[b]	0	0	0	0	0.028[b]	0.015[b]
	18	0.003	0.030[b]	0	0	0	0	0.068[b]	0.265[b]
	28	0	0.014	0	0	0	0	0.038[b]	0.011[b]
AZ31 Mg	2	1.581	(a)						
	4	1.293							
	7	1.021							
	12	0.811							
	18	(c)							
	28	0.579							
4340 Steel	2		1.143	0.635					
	4		0.831	0.468					
	7		0.770	0.612					
	12		0.436	0.289					
	18		0.596	0.338					
	28		0.238	0.158					
6061-T6 Al	2		0.378		0.043				
	4		0.275		0.021				
	7		0.302		0.017				
	12		0.171		0.007				
	18		0.139		0.006				
	28		0.126		0.004				
7075-T6 Al	2		0.465			0.040			
	4		0.303			0.029			
	7		0.297			0.023			
	12		0.212			0.014			
	18		0.086			0.049			
	28		0.118			0.026			
360 Brass	2		0.339				0.124		
	4		0.184				0.106		
	7		0.159				0.190		
	12		0.130				0.139		
	18		0.110				0.115		
	28		0.095				0.085		

TABLE 4-91. (Continued)

Alloy	Exposure, months	Corrosion Rate, mm/yr							
		Mg	Stainless Steel	Steel	6061 Al	7075 Al	Brass	Monel	Titanium
400 Monel	2		0.011					0.034	
	4		0.015					0.006	
	7		0.009					0.008	
	12		0.006					0.007	
	18		0.015					0.027	
	28		0.006					0.011	

(a) Total dissolution of magnesium presumed.
(b) Stainless steel attack-crevice pitting.
(c) Specimens missing.

TABLE 4-92. RESULTS OF 4-MONTH GALVANIC EXPOSURE IN SEAWATER FOR GALVANIC COUPLES OF TYPE 316 STAINLESS STEEL (6"-DIAMETER DISKS) AND THE MATERIALS INDICATED(160)

	Weight Loss, grams				
	2-1/4"-Diameter Disks		6"-Diameter 316 Stainless Disk	Uncoupled Control	Appearance of Disks
	1	2			
USST-1	3.3	2.7	0.1	2.1	316 protected - slight staining of stainless from steel.
	4.1	3.3	0.0	1.9	Steel corroded.
1010 Steel	3.3	4.7	0.0	1.8	316 protected - slight staining of stainless from steel.
	3.8	3.6	0.0	1.7	Steel corroded.
Lead	0.5	0.9	0.2	0.5	Very slight crevice corrosion of 316.
	0.5	1.3	0.2	0.9	Lead corroded.
304 SS	0.4	0.4	0.1	0.2	Staining of 316. Bad crevice corrosion of 304.
	0.5	0.2	0.2	0.1	Staining of 316. Bad crevice corrosion of 304.

TABLE 4-92. (Continued)

	Weight Loss, grams				
	2-1/4"-Diameter Disks		6"-Diameter 316 Stainless Disk	Uncoupled Control	Appearance of Disks
	1	2			
Alloy M	0.1	0.1	0.1	0.0	Stainless ok. Alloy M stained and very slight corrosion.
	0.1	0.1	0.1	0.0	Stainless ok. Alloy M stained and very slight corrosion.
316L	0.2	0.0	0.0	0.1	Crevice corrosion on small 316L disk.
	0.2	0.1	0.0	0.3	316 ok.
410 SS	2.7	0.7	0.1	0.6	Staining of 316 under small disk.
	1.1	2.3	0.1	0.8	410 badly corroded at edges.
316 SS	0.6	0.2	0.1	0.3	Bad crevice corrosion of small 316 disk & control.
	0.9	0.5	0.0	0.2	Staining & slight crevice corrosion of 6" 316.
Mn Bronze	1.9	1.5	0.0	0.2	Stainless protected.
	1.6	1.5	0.0	0.5	Slight corrosion of small disks.
Naval Brass	1.0	0.8	0.0	1.0	Stainless protected.
	1.0	0.9	0.1	1.0	Slight corrosion of small disks.
Copper	0.4	0.3	0.1	0.5	Stainless protected.
	0.3	0.3	0.2	0.6	Slight corrosion of small disks.
Muntz Metal	2.0	1.9	0.1	0.9	Stainless protected.
	2.2	1.5	0.0	0.8	Slight corrosion of small disks.
Al Bronze	0.3	0.5	0.0	0.1	Stainless protected.
	0.3	0.4	0.0	0.1	Slight corrosion of small disks.

TABLE 4-92. (Continued)

	Weight Loss, grams				
	2-1/4"-Diameter Disks		6"-Diameter 316 Stainless Disk	Uncoupled Control	Appearance of Disks
	1	2			
Phos. Bronze	0.6	0.7	0.0	0.5	Stainless protected.
	0.5	0.8	0.0	0.4	Slight corrosion of small disks.
Si Bronze	0.6	0.4	0.0	0.9	Stainless protected.
	1.0	0.6	0.0	1.1	Slight corrosion of small disks.
1100 Al	1.1	1.1	0.0	0.1	
	1.1	1.2	0.0	0.1	
2024 Al	1.4	1.1	0.0	0.0	In all these couples stainless was protected and suffered no corrosion whatsoever, all small aluminum disks badly corroded.
	1.7	1.2	0.0	0.0	
5052 Al	1.1	1.1	0.0	0.0	
	1.1	1.0	0.0	0.0	
5086 Al	1.3	0.8	0.0	0.1	
	1.4	0.9	0.0	0.1	
6061 Al	1.4	1.3	0.0	0.0	In all these couples stainless was protected and suffered no corrosion whatsoever, all small aluminum disks badly corroded.
	1.0	1.1	0.0	0.0	
7075 Al	1.3	1.1	0.0	0.0	
	1.4	1.4	0.0	0.1	
XB605	+0.1	+0.1	0.1	0.2	
	+0.2	+0.2	0.1	--	
Zinc	1.9	1.4	0.2	0.5	316 fully protected.
	2.0	1.5	0.1	0.5	Zinc corroded.
Magnesium	Missing		0.2	*	316 slightly etched at crevice.
	Missing		0.1	*	316 slightly etched at crevice.

* Original weight = 8.5 grams.

TABLE 4-93. COMPARISON OF CORROSION RATES DETERMINED BY WEIGHT LOSS VERSUS ZERO-RESISTANCE AMMETER (ZRA) MEASUREMENTS[161]

Couple	Tube End	Corrosion Rate, mm/yr (weight loss)	Corrosion Rate[a], (ZRA)
Al-4X/Al-6X	Inlet	0.00864	0.00229
	Outlet	0.386	0.348
Muntz/Al-6X	Inlet	2.80	2.64
	Outlet	2.31	2.24
Al Bronze/Al-6X	Inlet	1.07	0.573
	Outlet	0.949	0.432
Muntz/Ti 50A	Inlet	6.96	6.38
	Outlet	6.99	6.89
Al Bronze/Ti 50A	Inlet	3.20	2.34
	Outlet	1.42	0.960
Muntz/90-10 CuNi	Inlet	0.846	0.451
	Outlet	0.279	0.334

(a) Galvanic corrosion rates determined from zero resistance ammeter measurements for 206-day average.

TABLE 4-94. CORROSION RATES FOR TUBESHEET/TUBE COUPLES EXPOSED UNDER SIMULATED CONDENSER CONDITIONS[162]

Couple	Tube End	Galvanic Corrosion Rates,[a] mm/yr			
		Seawater at 22 C	Brackish Water at 22 C	Seawater at 6 C	Brackish Water at 11 C
Al Bronze/Al-6X	Inlet	0.633	0.117	0.048	0.0965
	Outlet	0.634	0.150	0.0869	0.224
Al Bronze/Ti 50A	Inlet	1.86	0.201	0.0589	0.201
	Outlet	3.03	0.373	0.049	0.226
Muntz/Al-6X	Inlet	3.97	1.62	0.700	0.705
	Outlet	3.79	0.979	0.356	0.365
Muntz/Ti 50A	Inlet	9.17	2.25	0.758	0.627
	Outlet	6.32	0.825	0.363	1.00
Muntz/Al-6X[b]	Inlet	0.828	0.207	0.401	0.145
	Outlet	0.516	0.240	0.131	0.0693

(a) Corrosion rates determined by weight loss (5 months' exposure).
(b) Tubesheet/tube couple under cathodic protection.

TABLE 4-95. SEAWATER GALVANIC COUPLE TESTS IN BASIN AT HALF TIDE AT KURE BEACH[16]

Materials	193-Day Exposure			369-Day Exposure		
	Uncoupled Corrosion Rates,[a] mpy	Coupled Corrosion Rate, mpy		Uncoupled Corrosion Rates,[a] mpy	Coupled Corrosion Rate, mpy	
		7 x Ti Area[b]	1/7 x Ti Area[c]		7 x Ti Area[b]	1/7 x Ti Area[c]
Monel	0.071	0.060	0.130	0.073	0.06	0.130
Inconel	0.002	Nil	0.002	Nil	Nil	Nil
302 Stainless	0.058	0.010	0.120	0.004	0.008	0.096
316 Stainless	Nil	Nil	Nil	Nil	Nil	Nil

(a) Average of one 6 in. x 1.5 in. specimen and two 0.75 in. x 1.5 in. specimens.
(b) One 6 in. x 1.5 in. specimen. Metal area 7 x Ti area.
(c) Average of two 0.75 in. x 1.5 in. specimens. Metal area 1/7 x Ti area.

TABLE 4-96. GALVANIC SERIES FOR GRAPHITE EPOXY COMPOSITE MATERIALS (GECM) COUPLED WITH STAINLESS STEELS IN 3.5 PERCENT NaCl[165]

Coupled to	$\bar{i}_g$, $\mu A/cm^2$	r_g, mdd	r_g, mpy	r_A, mpy	$\Delta\phi^s_{cor}$, mV
SS-440C[a]	8.18	19.0	3.54	19.87	-298
SS-301	2.24	5.34	0.98	1.16	-200
SS-304	1.40	3.26	0.59	Nil	-240
PH17-7	1.05	2.36	0.44	Nil	-233
AFC-77	1.03	2.32	0.42	Nil	-309

(a) Severe pitting occurred on specimen surface.

Notes:

$\bar{i}_g$ = galvanic current
r_g = galvanic corrosion rate
r_A = weight loss corrosion rate
$\Delta\phi^s$ = potential difference between (GECM) and an alloy

only Type 440C experienced increased corrosion as the result of the galvanic couple, whereas 301, 304, PH17-7, and AFC-77 were compatible with the graphite-epoxy.

Mud

General Corrosion and Pitting

Corrosion data are limited for stainless steels exposed to the mud zone in the ocean. Bottom sediments vary somewhat in composition and in marine activity. Sulfate-reducing bacteria have been identified in the mud zone. Since oxidizing agents are absent, one would expect stainless steels to lose passivity at local sites and, as a result, to undergo pitting and crevice attack. Such is actually the case. However, in most cases, the corrosion behavior in the mud zone (Pacific off California) is similar to that observed for the same alloy in the water just above the ocean bottom.

Thus, pitting and crevice corrosion occurs in the mud zone in the conventional ferritic and austenitic alloys, and only the high molybdenum ferritics and duplex alloys are resistant to this type of attack. General corrosion rates are low for all the stainless steels except that pitting may be the primary failure mode.

The results of mud zone exposure of stainless steels at depths in the Pacific Ocean are summarized by Reinhart[33] in Table 4-97. From these data, Reinhart concluded that the corrosivity of the mud zone was about the same as that of the seawater just above the ocean floor. However, in his study, there was less pitting and crevice corrosion in the mud zone at the 2,300 foot depth than at other depths. This behavior can be attributed to the lower oxygen level in the water at the 2,000 foot depth than elsewhere, and in this respect, the behavior parallels that observed for stainless steels in the seawater itself.

TABLE 4-97. CORROSION RATES OF STAINLESS STEELS IN THE DEEP OCEAN[33]

Alloy	Thickness, in.	Environment[a]	Exposure, days	Depth, ft	Corrosion Rates[b] mdd	mpy	Crevice Corrosion Depth, mils	Type of Corrosion
AISI type 405[c]	0.123	W	1,064	5,300	9.0	1.7	Perforated	Edge, tunnel to perforation
AISI type 405	0.123	W	1,064	5,300	6.4	1.2	47	Edge, tunnel to perforation
AISI type 405	0.123	M	1,064	5,300	5.8	1.1	Perforated	Edge, tunnel to perforation
AISI type 405	0.262	W	123	5,640	12.7	2.4	0	Edge, tunnel
AISI type 405	0.262	M	123	5,640	10.8	2.0	0	Edge, tunnel
AISI type 405	0.262	W	197	2,340	11.1	2.1	0	Edge, tunnel
AISI type 405	0.262	M	197	2,340	7.8	1.4	0	Edge, tunnel
AISI type 410	0.040	W	123	5,640	1.0	0.2	Slight	Tunnel to perforation
AISI type 410	0.040	M	123	5,640	2.8	0.5	Slight	Tunnel to perforation
AISI type 410	0.040	W	197	2,340	1.0	0.2	10	Edge, tunnel
AISI type 410	0.040	M	197	2,340	1.2	0.2	15	Edge, tunnel
AISI type 430[c]	0.137	W	1,064	5,300	7.2	1.3	97	Edge, tunnel to perforation
AISI type 430	0.137	W	1,064	5,300	2.7	0.5	25	Tunnel to perforation
AISI type 430	0.137	M	1,064	5,300	3.9	0.7	40	Tunnel, one end gone
AISI type 430	0.137	W	123	5,640	2.6	0.5	10	Edge, tunnel
AISI type 430	0.137	M	123	5,640	0.9	0.2	10	Edge, tunnel
AISI type 430	0.137	W	123	2,500	0.0	0.0	0	Slight edge attack
AISI type 430	0.050	W	123	5,640	0.0	0.0	0	No visible corrosion
AISI type 430	0.050	M	123	5,640	0.0	0.0	0	No visible corrosion
AISI type 430	0.137	W	197	2,340	1.6	0.3	17	Tunnel
AISI type 430	0.137	M	197	2,340	2.1	0.4	19	Tunnel
AISI type 301	0.103	W	1,064	5,300	2.4	0.4	0	Tunnel to perforation
AISI type 301	0.103	M	1,064	5,300	5.4	1.0	0	Edge, tunnel to perforation
AISI type 301	0.103	W	123	5,640	1.8	0.3	Slight	Tunnel
AISI type 301	0.103	M	123	5,640	3.7	0.7	Slight	Tunnel
AISI type 301	0.103	W	197	2,340	1.7	0.3	Slight	Tunnel
AISI type 301	0.103	M	197	2,340	1.5	0.3	Slight	Tunnel
AISI type 302	0.050	W	123	5,640	0.0	0.0	Slight	No visible corrosion
AISI type 302	0.050	M	123	5,640	0.0	0.0	Slight	No visible corrosion
AISI type 302	0.050	W	197	2,340	0.0	0.0	Perforated, pin hole	Slight tunnel
AISI type 302	0.050	M	197	2,340	0.0	0.0	20	Slight tunnel
AISI type 304[c]	0.195	W	1,064	5,300	0.06	0.01	18	No visible corrosion
AISI type 304	0.195	W	1,064	5,300	0.19	0.03	74	Edge
AISI type 304	0.195	M	1,064	5,300	0.01	0.001	0	Edge, slight tunnel
AISI type 304[c]	0.214	W	1,064	5,300	0.06	0.01	0	13 mils maximum pit depth on one specimen of five
AISI type 304	0.214	W	1,064	5,300	0.22	0.04	21	No visible corrosion

TABLE 4-97. (Continued)

Alloy	Thickness, in.	Environment[a]	Exposure, days	Depth, ft	Corrosion Rates[b] mdd	Corrosion Rates[b] mpy	Crevice Corrosion Depth, mils	Type of Corrosion
AISI type 304	0.214	M	1,064	5,300	0.16	0.03	29	Tunnel
AISI type 304	0.214	W	123	5,640	0.25	0.04	0	Tunnel
AISI type 304	0.214	M	123	5,640	0.04	0.01	0	Tunnel
AISI type 304	0.214	W	197	2,340	1.3	0.24	11	Edge tunnel
AISI type 304	0.214	M	197	2,340	0.16	0.03	Slight	Edge tunnel
AISI type 304L[c]	0.117	W	1,064	5,300	0.5	0.09	Perforated	Edge tunnel
AISI type 304L	0.117	W	1,064	5,300	1.4	0.25	27	Tunnel to perforation
AISI type 304L	0.117	M	1,064	5,300	0.5	0.09	0	Tunnel to perforation
AISI type 304L	0.117	W	123	5,640	1.0	0.18	Slight	Tunnel
AISI type 304L	0.117	M	123	5,640	0.25	0.05	Slight	Tunnel
AISI type 304L	0.117	W	123	2,500	0.00	0.00	0	No visible corrosion
AISI type 304L	0.117	W	197	2,340	1.3	0.23	8	Tunnel
AISI type 304L	0.117	M	197	2,340	0.42	0.08	18	Tunnel
AISI type 316[c]	0.230	W	1,064	5,300	0.13	0.02	21	No visible corrosion
AISI type 316	0.230	W	1,064	5,300	0.00	0.00	12	No visible corrosion
AISI type 316	0.230	M	1,064	5,300	0.01	0.001	0	No visible corrosion
AISI type 316	0.230	W	123	5,640	0.21	0.04	0	Slight edge
AISI type 316	0.230	M	123	5,640	0.12	0.02	0	Slight edge
AISI type 316	0.230	W	197	2,340	0.38	0.07	0	No visible corrosion
AISI type 316	0.230	M	197	2,340	0.08	0.01	0	No visible corrosion
AISI type 316L[c]	0.121	W	1,064	5,300	0.20	0.03	25	No visible corrosion
AISI type 316L	0.121	W	1,064	5,300	0.003	0.001	8	No visible corrosion
AISI type 316L	0.121	M	1,064	5,300	0.000	0.000	20	No visible corrosion
AISI type 316L	0.121	W	123	5,640	0.000	0.000	Slight	No visible corrosion
AISI type 316L	0.121	M	123	5,640	0.000	0.000	Slight	No visible corrosion
AISI type 316L	0.121	W	123	2,500	0.000	0.000	0	No visible corrosion
AISI type 316L	0.121	W	197	2,340	0.000	0.000	18	No visible corrosion
AISI type 316L	0.121	M	197	2,340	0.000	0.000	12	No visible corrosion
18Cr-14Mn-0.5N[c]	0.115	W	1,064	5,300	0.9	0.2	0	No visible corrosion
18Cr-14Mn-0.5N	0.115	W	1,064	5,300	0.7	0.1	0	Tunnel to perforation
18Cr-14Mn-0.5N	0.115	M	1,064	5,300	2.2	0.4	0	Tunnel to perforation
18Cr-14Mn-0.5N	0.115	W	123	5,640	0.00	0.00	0	No visible corrosion
18Cr-14Mn-0.5N	0.115	M	123	5,640	2.1	0.4	Perforated	Tunnel
18Cr-14Mn-0.5N	0.115	W	197	2,340	3.8	0.7	109	Tunnel
18Cr-14Mn-0.5N	0.115	M	197	2,340	3.5	0.7	21	Tunnel
20-Cb	0.123	W	1,064	5,300	0.00	0.00	0	No visible corrosion
20-Cb	0.123	W	123	5,640	0.00	0.00	0	No visible corrosion

TABLE 4-97. (Continued)

Alloy	Thickness, in.	Environment[a]	Exposure, days	Depth, ft	Corrosion Rates[b] mdd	Corrosion Rates[b] mpy	Crevice Corrosion Depth, mils	Type of Corrosion
20-Cb	0.123	M	123	5,640	0.00	0.00	0	No visible corrosion
20-Cb	0.123	W	197	2,340	0.05	0.01	Slight	No visible corrosion, crevice corrosion at wall of bolt hole
20-Cb	0.123	M	197	2,340	0.84	0.15	Slight	No visible corrosion, crevice corrosion at wall of bolt hole
17Cr-7Ni-0.7Ti-0.2Al[c]	0.115	W	1,064	5,300	0.13	0.02	50	No visible corrosion
17Cr-7Ni-0.7Ti-0.2Al	0.115	W	1,064	5,300	0.000	0.000	16	No visible corrosion
17Cr-7Ni-0.7Ti-0.2Al	0.115	M	1,064	5,300	0.000	0.000	0	No visible corrosion
17Cr-7Ni-0.7Ti-0.2Al	0.275	W	123	5,640	0.000	0.000	Slight	No visible corrosion
17Cr-7Ni-0.7Ti-0.2Al	0.275	M	123	5,640	0.000	0.000	0	No visible corrosion
17Cr-7Ni-0.7Ti-0.2Al	0.275	W	197	2,340	0.000	0.000	0	No visible corrosion
17Cr-7Ni-0.7Ti-0.2Al	0.275	M	197	2,340	0.000	0.000	0	No visible corrosion
15-7 AMV-annealed	0.048	W	123	5,640	0.11	0.02	Perforated	Tunnel to perforation
15-7 AMV-annealed	0.048	M	123	5,640	2.7	0.5	Perforated	Tunnel to perforation
15-7 AMV-annealed	0.048	W	197	2,340	2.1	0.4	Perforated	Edge, tunnel to perforation, parts of specimens missing
15-7 AMV-annealed	0.048	M	197	2,340	1.8	0.3	Perforated	Edge, tunnel to perforation, parts of specimens missing
15-7 AMV RH1150[c]	0.045	W	1,064	5,300	6.2	1.2	Perforated	Tunnel to perforation
15-7 AMV RH1150	0.045	W	1,064	5,300	6.4	1.2	Perforated	Tunnel to perforation, 11-sq-in. hole
15-7 AMV RH1150	0.045	M	1,064	5,300	4.2	0.8	Perforated	Tunnel to perforation, 12-sq-in. hole
15-7 AMV RH1150	0.045	W	123	5,640	0.5	0.1	Perforated	Tunnel to perforation
15-7 AMV RH1150	0.045	M	123	5,640	0.6	0.1	Perforated	Tunnel to perforation
15-7 AMV RH1150	0.045	W	197	2,340	2.1	0.4	Perforated	Tunnel to perforation, parts of specimens missing
15-7 AMV RH1150	0.045	M	197	2,340	1.8	0.3	Perforated	Tunnel to perforation, parts of specimens missing
15-7 AMV RH950[c]	0.048	W	1,064	5,300	10.5	2.0	Perforated	Tunnel to perforation
15-7 AMV RH950	0.048	W	1,064	5,300	4.9	0.9	Perforated	Tunnel to perforation, stress corrosion cracks at drilled hole
15-7 AMV RH950	0.048	M	1,064	5,300	4.7	0.9	Perforated	Tunnel to perforation
15-7 AMV RH950	0.048	W	123	5,640	2.1	0.4	Perforated	Tunnel, pitting
15-7 AMV RH950	0.048	M	123	5,640	5.4	1.0	Perforated	Parts of specimens missing
15-7 AMV RH950	0.048	W	123	2,600	3.4	0.7	Slight	Pitting
15-7 AMV RH950	0.048	W	197	2,340	3.2	0.6	Perforated	Edge, tunnel to perforation
15-7 AMV RH950	0.048	M	197	2,340	2.5	0.5	Perforated	Edge, tunnel to perforation

TABLE 4-97. (Continued)

Alloy	Thickness, in.	Environment[a]	Exposure, days	Depth, ft	Corrosion Rates[b] mdd	Corrosion Rates[b] mpy	Crevice Corrosion Depth, mils	Type of Corrosion
AM-355 CRT[c]	0.040	W	123	5,640	0.04	0.007	0	No visible corrosion
AM-355 CRT[c]	0.040	W	197	2,340	1.2	0.2	Slight	Pitting
AM-355 CRT[c]	0.040	M	197	2,340	0.4	0.08	0	Slight pitting
17-4PH H925, C weld[d]	0.112	W	197	2,340	0.05	0.01	--	No visible corrosion
17-4PH H925, C weld	0.112	M	197	2,340	1.1	0.2	--	Weld bead attack
17-4PH H925, B weld	0.112	W	197	2,340	0.11	0.02	--	No visible corrosion
17-4PH H925, B weld	0.112	M	197	2,340	0.90	0.2	--	Tunnel 1-1/2 in. long
17-7PH TH1050, C weld	0.126	W	197	2,340	2.0	0.4	--	Crevice corrosion and tunneling at separator contact
17-7PH TH1050, C weld	0.126	M	197	2,340	1.5	0.3	--	Crevice corrosion and tunneling at separator contact
17-7PH TH1050, B weld	0.126	W	197	2,340	0.8	0.2	--	Crevice corrosion and tunneling at separator contact
17-7PH TH1050, B weld	0.126	M	197	2,340	0.4	0.07	--	Many pits in one area, 0.5 in. diameter
17-7PH RH1050, C weld	0.126	W	97	2,340	1.7	0.3	--	Stress-corrosion cracked in heat-affected zone
17-7PH RH1050, C weld	0.126	M	197	2,340	3.4	0.6	--	Crevice corrosion and tunneling at separator contact
17-7PH RH1050, B weld	0.126	W	197	2,340	3.1	0.6	--	Tunnel 1-1/2 in. long, 1/2 in. from and parallel to weld bead
17-7PH RH1050, B weld	0.126	M	197	2,340	1.5	0.3	--	Tunnel starting at edge 1 in. long x 1/2 in. wide
PH15-7Mo RH1100, C weld	0.124	W	197	2,340	3.0	0.6	--	Crevice corrosion and tunneling at separator contact
PH15-7Mo RH1100, C weld	0.124	M	197	2,340	2.4	0.5	--	Tunnel starting at edge 1 in. long x 3/4 in. wide
PH15-7Mo RH1100, B weld	0.124	W	197	2,340	1.0	0.2	--	Tunneling at one corner
PH15-7Mo RH1100, B weld	0.124	M	197	2,340	1.6	0.3	--	Tunneling at one corner
PH14-8Mo SRH950, C weld	0.120	W	197	2,340	1.2	0.4	--	Crevice corrosion at separator contact and tunneling on one edge
PH14-8Mo SRH950, C weld	0.120	M	197	2,340	0.21	0.04	--	No visible corrosion
PH14-8Mo SRH950, B weld	0.120	W	197	2,340	0.11	0.02	--	Incipient pits and tunneling
PH14-8Mo SRH950, B weld	0.120	M	197	2,340	0.05	0.01	--	No visible corrosion

(a) W = specimens exposed on side of STU in water; M = specimens exposed in base of STU, partially embedded in bottom sediment.
(b) mdd = milligrams per square decimeter per day; mpy = mils penetration per year.
(c) Specimen size, 1 x 6 inches; all others 6 x 12 inches.
(d) C weld = 3-inch-diameter weld ring in center of 6 x 12-inch specimens; B weld = transverse butt weld 6 inches long in 6 x 12-inch specimens.

REFERENCES FOR CHAPTER 4

1. Larrabee, C. P., "Corrosion of Steels in Marine Atmospheres and in Seawater", Transactions of the Electrochemical Society, 87, pp 171-182 (1945).

2. Johnson, M. J. and Pavlik, P. J., "Atmospheric Corrosion of Stainless Steel", Atmospheric Corrosion, Hollywood, FL, pp 461-473 (October, 1980).

3. Southwell, C. R. and Bultman, J. D., "Atmospheric Corrosion Testing in the Tropics", Atmospheric Corrosion, Hollywood, FL, pp 943-967 (October, 1980).

4. Das, C. R. and Jena, P. K., "A Study of Corrosion of Welded Steel Specimens in a Marine Atmosphere With and Without Protective Coatings", Corrosion Science, 23 (11), pp 1135-1140 (1983).

5. Degerbeck, J., Karlsson, A., and Berlund, G., "Atmospheric Corrosion of Stainless Steel of Type 18Cr-2Mo-Ti", British Corrosion Journal, 14 (4), pp 220-222 (1979).

6. Karlsson, A. and Olsson, J., "Atmospheric Corrosion of Stainless Steels", 7th Scandinavian Corrosion Conference, University Troldheim, Norway, pp 71-86 (1975).

7. Ailor, W. H., Jr., "Metal Exposures at Tropical and Marine Sites", 6th Annual Offshore Technology Conference, 1, pp 293-312 (May, 1974).

8. Southwell, C. R. and Alexander, A. L., "Corrosion of Metals in Tropical Environments - Nickel and Nickel-Copper Alloys", Materials Protection, 8 (3), pp 39-44 (March, 1969).

9. Khanna, A. S. and Gnanamoorthy, J. B., "Atmospheric Corrosion Studies on Stainless Steels and a Low-Alloy Steel in a Marine Atmosphere", Atmospheric Corrosion, Hollywood, FL, pp 489-499 (October, 1980).

10. Baboian, R., "Final Report on the ASTM Study: Atmospheric Galvanic Corrosion of Magnesium Coupled to Other Metals", Atmospheric Factors Affecting the Corrosion of Engineering Materials, ASTM-STP-646, pp 17-29 (1978).

11. Sedriks, A. J., "Corrosion Resistance of Austenitic Fe-Cr-Ni-Mo Alloys in Marine Environments", International Metals Reviews, 27 (6), pp 321-353 (1982).

12. Johnson, K. E. and Abbott, J. S., "Bimetallic Corrosion Effects on Mild Steel in Natural Environments", British Corrosion Journal, 9 (3), pp 171-176 (1974).

13. Ebihara, W. T., "Tropical Exposure of Galvanically Coupled Metal Systems", Army Armament R&D, Dover, NJ, ADBO39047-Limited, ARSCD-TR-79004, p 18 (June, 1979).

14. Prince, D. E., "Corrosion Behavior of Metal Fasteners in Graphite-Epoxy Composites", AFML, Wright-Patterson AFB, OH, AFML-TR-75-53, Final, ADBOO6394-Limited (July, 1975).

15. Morris, A. W., "Electrochemical Screening of Fastener Materials for Carbon Composite Joint Applications", Corrosion '80, Chicago, IL, Paper 23 (March, 1980).

REFERENCES FOR CHAPTER 4
(Continued)

16. Bomberger, H. B., Cambourelis, P. J., and Hutchinson, G. E., "Corrosion Properties of Titanium in Marine Environments", Journal of the Electrochemical Society, 101 (9), pp 442-447 (September, 1954).

17. Stanley, J. K., "The Current Situation on the Stress-Corrosion Cracking and Hydrogen Embrittlement of High Strength Fasteners", 13th Structures, Structural Dynamics, Materials Conference, TX (April, 1972).

18. Money, K. L. and Kirk, W. W., "Stress-Corrosion Cracking Behavior of Wrought Fe-Cr-Ni Alloys in Marine Atmosphere", Materials Performance, 17 (7), pp 28-36 (July, 1978).

19. Phelps, E. H., "Stress-Corrosion Behavior of High Yield-Strength Steels", Seventh World Petroleum Congress, 9, pp 201-209 (1967).

20. Slunder, C. J., "Stress-Corrosion Cracking of High-Strength Stainless Steels in Atmospheric Environments", DMIC Report 158 (September 15, 1961).

21. Sprowls, D. O., Shumaker, M. B., and Walsh, J. D., "Evaluation of Stress-Corrosion Cracking Susceptibility Using Fracture Mechanics Techniques", Alcoa, PA, Final - Part I, NASA, NAS8-21487 (May, 1973).

22. Humphries, T. S. and Nelson, E. E., "Stress-Corrosion Cracking Evaluation of Martensitic Precipitation Hardening Stainless Steels", NASA, Marshall Space Flight Center, AL, N80-16142, NASA-TM-78257 (January, 1980).

23. Anderson, D. B. and Ross, R. W., Jr., "Protection of Steel Piling in Marine Splash and Spray Zones - Metallic Sheathing Concept", 4th International Congress on Marine Corrosion and Fouling, Boulogne, France, pp 461-473 (1976).

24. Southwell, C. R., Bultman, J. D., and Alexander, A. L., "Corrosion of Metals in Tropical Environments - Final Report of 16-Year Exposures", Materials Performance, 15 (7), pp 9-26 (July, 1976).

25. Ballantine, W., "Choosing Corrosion-Resistant Fasteners for Marine Applications", Sea Technology, 17 (2), pp 8-10 (February, 1976).

26. Humphries, T. S. and Nelson, E. E., "Stress-Corrosion Cracking Evaluation of Several Ferrous and Metal Alloys", NASA Technical Memorandum TMX 64511 (April, 1970).

27. Deel, O. L. and Mindlin, H., "Engineering Data on New Aerospace Structural Materials", Battelle, Columbus, OH, Final AFML-TR-72-196-V1, AD755407 (September, 1972).

28. Deel, O. L. and Mindlin, H., "Engineering Data on New Aerospace Structural Materials", Battelle, Columbus, OH, Final, AFML-TR-72-196-V2, AD755408 (September, 1972).

29. Hatfield, D. C. and Slavick, J. J., "Evaluation of Mechanical Properties and Stress-Corrosion Resistance of Armco PH14-8Mo (Vacuum Melted)", McDonnell, St. Louis, MO, MAC-513-852, AD9206035L, GIDEP (April, 1970).

REFERENCES FOR CHAPTER 4
(Continued)

30. Boyd, W. K. and Fink, F. W., "Corrosion of Metals in Marine Environments", Battelle Columbus Laboratories, Metal and Ceramics Information Center Report, MCIC-78-37 (March, 1978).

31. Sedriks, A. J., "Corrosion Resistance of Austenitic Fe-Cr-Ni-Mo Alloys in Marine Environments", International Metals Reviews, 27 (6), pp 321-353 (1982).

32. Alexander, A. L., Southwell, C. R., and Forgeson, B. W., "Corrosion of Metals in Tropical Environments, Part 5 - Stainless Steel", Corrosion, 17 (7), pp 345t-353t (1961).

33. Reinhart, F. M., "Corrosion of Materials in Hydrospace", U.S. Naval Civil Engineering Laboratory, R-504, AD644473 (December, 1966).

34. Lawson, H. H., Doughty, S. E., and Jones, R. T., "Evaluating Material Performance in a 3000-GPD Stainless Steel Desalination Test Plant", Materials Performance, 13 (3), pp 11-16 (March, 1974).

35. Garner, A., "Crevice Corrosion of Stainless Steel in Seawater: Correlation of Field and Laboratory Tests", Corrosion '80, Chicago, IL, Paper 35 (March, 1980).

36. Kowaka, M., Nagano, H., and Suzuki, E., "Crevice Corrosion Test Method for Stainless Steel", The Sumitomo Search, 27, pp 9-21 (December, 1982).

37. Baker, D.W.C., Heaton, W. E., and Patient, B. C., "Evaluation of Stainless Steels for Condenser Tube Nest Construction", Corrosion Science, 12 (3), pp 247-264 (March, 1972).

38. Hoskinson, D. W. and Kuester, C. W., "Operating Experiences With Stainless Steel Condenser Tubes in Central Stations", Journal of Engineering for Power, 87 (4), Transactions of the ASME, Series A, pp 401-404 (October, 1965).

39. Hack, H. P., "Crevice Corrosion Behavior of 45 Molybdenum-Containing Stainless Steels in Seawater", Corrosion '82, Houston, TX, Paper 65 (March, 1982).

40. Fukuzuka, T., Shimogori, K., Fujiwara, K., and Sugie, K., "Corrosion Resistance of High Molybdenum Stainless Steel (20Cr-22Ni-5Mo-0.2N) to Seawater", Transactions of Iron and Steel Institute of Japan, 20 (9), p B403 (1980).

41. Hodgkiess, T. and Rigas, S., "A Comparison of the Corrosion Resistance of Some Higher-Alloy Stainless Steels in Seawater at 20-100 C", Desalination, 44, pp 283-294 (May, 1983).

42. Bond, A. P., Bertoli, C., and Dundas, H. J., "Corrosion Resistance of Stainless Steels in Seawater", Advance Stainless Steels for Seawater Applications, Piacenza, Italy, pp 1-10 (February, 1980).

43. Bond, A. P. and Dundas, H. J., "Resistance of Stainless Steels to Crevice Corrosion in Seawater", Materials Performance, 23 (7), pp 39-43 (July, 1984).

REFERENCES FOR CHAPTER 4
(Continued)

44. Kovach, C. W., Redmerski, L. S., and Kurtz, H. D., "Crevice Corrosion Performance of a Ferritic Stainless Steel Designed for Saline Water Condenser and Heat Exchanger Applications", Corrosion '80, Chicago, IL, Paper 95 (March, 1980).

45. Brigham, R. J. and Tozer, E. W., "Localized Corrosion Resistance of Mn-Substituted Austenitic Stainless Steels: Effect of Molybdenum and Chromium", Corrosion, 32 (7), pp 274-276 (July, 1976).

46. Deverell, H. E. and Maurer, J. R., "Stainless Steels in Seawater", Materials Performance, 17 (3), pp 15-20 (March, 1978).

47. Baroux, B., Maitrepierre, P., and Decleity, P., "The Behavior of Ugine NSCD in Seawater", Advance Stainless Steels for Seawater Application, Piacenza, Italy, pp 103-112 (February, 1980).

48. Samans, C. H., "Stress-Corrosion Cracking Susceptibility of Stainless Steels and Nickel-Base Alloys in Polythionic Acids and Acid Copper Sulfate Solution", Corrosion, 20 (8), pp 256t-261t (August, 1964).

49. Steigerwald, R. F., "New Molybdenum Stainless Steels for Corrosion Resistance: A Review of Recent Developments", Materials Performance, 13 (9), pp 9-16 (September, 1974).

50. Korovin, Y. M. and Ulanovskii, I. B., "The Corrosion Resistance of Chrome-Nickel Steels of the Type Kh21N5 in Seawater", Protection of Metals, 10 (5), pp 519-520 (October, 1974).

51. Maurer, J. R., "Controlling Corrosion Problems With the New High Technology Stainless Steels", Journal Materials for Energy Systems, 1 (1), pp 41-51 (June, 1979).

52. Hodgkiess, T., Eid, N., and Hanbury, W. T., "Corrosion of Welds in Seawater", Desalination, 27 (2), pp 129-136 (November, 1978).

53. Hodgkiess, T., Hanbury, W. T., and Hejazian, M. H., "Corrosion Tests of a Range of Materials in Three M. S. F. Plants", Desalination, 44, pp 223-242 (April, 1983).

54. Henrikson, S., Olsson, J., and Arvesen, J., "Corrosion Tests of Stainless Steels in Flowing Baltic Seawater", 6th Scandinavian Corrosion Congress, Gothenburg, Sweden, CONF-710520-1 (May, 1981).

55. Stefec, R., Franz, F., and Holecek, A., "Effect of Heat Treatment on Pitting Corrosion of Austenitic Chromium-Nickel-Molybdenum Steels in Sodium Chloride Solution", Werkstoffe und Korrosion, 30 (3), pp 189-197 (March, 1979).

56. Redmerski, L. S. and Moskowitz, A., "Effects of Surface Treatment on Corrosion Resistance of Stainless Steels", Transactions of Metallurgical Society of AIME, 245 (8), pp 2165-2173 (October, 1969).

REFERENCES FOR CHAPTER 4
(Continued)

57. Hulquist, G. and Leygraf, C., "Thermal Passivation of AISI 316 Stainless Steel in Controlled Vacuum", Journal of Vacuum Science and Technology, 17 (1), pp 85-88 (February, 1980).

58. Lee, T. S., "A Method for Quantifying the Initiation and Propagation Stages of Crevice Corrosion", Electrochemical Corrosion Testing, ASTM-STP-727, pp 43-68 (1981).

59. Asphahani, A. I., Manning, P. E., Silence, W. L., and Hodge, F. G., "Highly Alloyed Stainless Materials for Seawater Applications", Corrosion '80, Chicago, IL, Paper 29 (March, 1980).

60. Ulanovskii, I. B., Egorova, V. A., and Kakasheva, T. A., "Corrosion of Steel, Titanium, and Copper at Various Depths in the Black Sea", Protection of Metals, 12 (4), pp 394-395 (July, 1976).

61. Eden, A., "Recent Advances in the Use of Stainless Steel for Offshore and Seawater Applications", Anti-Corrosion Methods and Materials, 26 (11), pp 7, 9-13 (November, 1979).

62. Herbsleb, G. and Popperling, R. K., "Corrosion Properties of Austenitic-Ferritic Duplex Steel AF 22 in Chloride and Sulfide Containing Environments", Corrosion '80, Chicago, IL, Paper 13 (March, 1980).

63. Suzuki, T. and Kitamura, Y., "Critical Potential for Growth of Localized Corrosion of Stainless Steel in Chloride Media", Corrosion, 28 (1), pp 1-6 (January, 1972).

64. Man, H. C. and Gabe, D. R., "A Study of Pitting Potentials for Some Austenitic Stainless Steels Using a Potentiodynamic Technique", Corrosion Science, 21 (9/10), pp 713-721 (1981).

65. Bond, A. P., "Effects of Molybdenum on the Pitting Potentials of Ferritic Stainless Steels at Various Temperatures", Journal of Electrochemical Society, 120 (5), pp 603-606 (May, 1973).

66. Potzschke, M. and Rocke, M. B., "Corrosion Resistance of Stainless Steels and Nickel Alloys in Artificial Seawater", Desalination, 44, pp 295-305 (May, 1983).

67. Bernhardsson, S. O., Mellstrom, R., and Tynell, M., "Sandvik 2RK65: A High Alloy Stainless Steel for Seawater", Advance Stainless Steels for Seawater Applications, Piancenza, Italy, pp 45-58 (February, 1980).

68. Takano, M. and Staehle, R. W., "Effect of Electrochemical Potential on Stress-Corrosion Morphology of Type 304L Stainless Steel in Sulfuric Acid/Sodium Chloride Solutions at Room Temperature", Transactions of Japan Institute of Metals, 18 (11), pp 780-786 (1977).

69. Lizlovs, E. A., "Crevice Corrosion of Some High-Purity Ferritic Stainless Steels", Localized Corrosion - Cause of Metal Failure, ASTM-STP-516, pp 201-209 (1972).

REFERENCES FOR CHAPTER 4
(Continued)

70. Gutman, E. M., Budilova, E. V., and Lukin, B. Y., "Effect of Deformation on Pitting Corrosion of Steel 1Kh18N10T", Protection of Metals, 11 (6), pp 683-684 (December, 1975).

71. Mazza, B., Pedeferri, P., Sinigaglia, D., Cigada, A., and Mondora, G. A., "Pitting Resistance of Cold-Worked Commercial Austenitic Stainless Steels in Solution Simulating Seawater", Journal of the Electrochemical Society, 126 (12), pp 2075-2081 (December, 1979).

72. Stefec, R. and Franz, F., "A Study of the Pitting Corrosion of Cold-Worked Stainless Steel", Corrosion Science, 18 (1), pp 161-168 (1978).

73. El-Sayed, A. A., Morsy, S. M., and El-Raghy, S. M., "The Effect of Some Metallurgical Factors on the Corrosion Behavior of Austenitic Stainless Steels in 3 Percent NaCl Aqueous Solutions", Atomic Energy Est., Cairo, Egypt, AREAEE-231 (1979).

74. Rowlands, J. C., "Crevice Corrosion of Stainless Steels and Nickel Alloys Under Marine Conditions", British Corrosion Journal, 11 (4), pp 195-198 (1976).

75. Grimes, W. D. and Schrieber, C. F., "A Study of the Effects of Interleakage of Ammonia and Seawater on Corrosion and Scaling of Candidate Materials for OTEC Heat Exchangers", Corrosion '80, Chicago, IL, Paper 45 (March, 1980).

76. Liebert, B. E., Sethuramalingam, K., and Larsen-Basse, J., "Corrosion Effects in OTEC Heat Exchanger Materials", Materials Performance, 20 (8), pp 22-28 (August, 1981).

77. Schrieber, C. F., "Seawater Corrosion Test Program: Part Four", Dow Chemical, Midland, MI, OWRT/S-1976/II, PB-248672 (April, 1975).

78. Willingham, C. A., "Anaerobic Bacterial Corrosion of Metals in Seawater at Elevated Hydrostatic Pressures", Clapp Laboratories, Duxbury, MA, AD727221, Final, N00014-68C0365 (July, 1971).

79. Lendvai-Lintnor, E., et al., "An Innovative Approach to Controlling Salt Water Cooling Tower System Problems", Materials Performance, 17 (12), pp 16-22 (December, 1978).

80. Walston, K. R., "Materials Problems in Salt Water Cooling Towers", Materials Performance, 14 (6), pp 22-26 (June, 1975).

81. LaQue, F. L., "Topics for Research in Marine Corrosion", Materials Performance, 21 (4), pp 13-18 (April, 1982).

82. Brennert, S. and Lindh, B., "Resistance to Corrosion of Metallic Material for Seawater Bearing Pipes", 7th Scandinavian Corrosion Congress, Trandheim, Norway, pp 346-355 (May, 1975).

83. Little, B., Morse, J., Loeb, G., and Spiehler, F., "Gulf of Mexico Study of Biofouling on OTEC Heat Exchanger Candidate Alloys", Materials Performance, 20 (8), pp 16-21 (August, 1981).

REFERENCES FOR CHAPTER 4
(Continued)

84. Lennox, T. J., Jr. and Peterson, M. H., "Inherent Corrosion Resistance and Response to Cathodic Protection in Seawater of Recently Developed Stainless Steel Alloys", Naval Research Laboratory, Washington, DC, ADA029436, NRL-8016, Final (August, 1976).

85. Lula, R. A., "New Austenitic and Ferritic Stainless Steels for Seawater Applications", Sixth Annual Offshore Technology Conference, Dallas, TX, V1, OTC-1961, pp 283-292 (1974).

86. Wilde, B. E., "Critical Appraisal of Some Popular Laboratory Electrochemical Tests for Predicting the Localized Corrosion Resistance of Stainless Alloys in Seawater", Corrosion, 28 (8), pp 283-291 (August, 1972).

87. Kain, R. M., "Localized Corrosion Behavior in Natural Seawater: A Comparison of Electrochemical and Crevice Testing of Stainless Alloys", Corrosion '80, Chicago, IL, Paper 74 (March, 1980).

88. Defranoux, J. M., "A Mechanistic Study of the Effect of Molybdenum Additions on the Corrosion Resistance of Austenitic Stainless Steels", NASA, Washington, DC, NASA-TT-F-15950, N74-34934, Translation (October, 1974).

89. Chen, W.Y.C. and Stephens, R. J., "Anodic Polarization Behavior of Austenitic Stainless Steel Alloys With Lower Chromium Content", Corrosion, 35 (10), pp 443-451 (October, 1979).

90. Dundas, H. J. and Bond, A. P., "Effect of Variation of Cr, Mo, and Cu on Corrosion of Austenitic Stainless Steels", Corrosion '81, Toronto, Ontario, Canada, Paper 122 (April, 1981).

91. Herbsleb, G. and Schwenk, W., "Electrochemical Investigations of Pitting Corrosion", Corrosion Science, 13 (10), pp 739-746 (October, 1973).

92. Manning, P. E., Duquette, D. J., and Savage, W. F., "The Effect of Test Method and Surface Condition on Pitting Potential of Single and Duplex Phase 304L Stainless Steel", Corrosion, 35 (4), pp 151-157 (April, 1979).

93. Fujii, T., "Pitting Potentials of Stainless Steel in 0.1M Sodium-Chloride Solution at 280 C", Transactions of National Research Institute for Metals, 21 (1), pp 11-12 (March, 1979).

94. Azzerri, N., Mancia, F., and Tamba, A., "Electrochemical Prediction of Corrosion Behavior of Stainless Steels in Chloride-Containing Water", Corrosion Science, 22 (7), pp 675-687 (1982).

95. Truman, J. E. and Pirt, K. R., "The Resistance to Localized Corrosion of Some Stainless Steels", Corrosion Prevention and Control, 26 (6), pp 12-16, 22 (December, 1979).

96. Sugimoto, K. and Sawada, Y., "The Role of Alloyed Molybdenum in Austenitic Stainless Steels in the Inhibition of Pitting in Neutral Halide Solutions", Corrosion, 32 (9), pp 347-352 (September, 1976).

REFERENCES FOR CHAPTER 4
(Continued)

97. Kohl, H., Rabensteiner, G., and Hochoertler, G., "VEW A 963, A Stainless Steel With High Strength and High Corrosion Resistance", Advance Stainless Steels for Seawater Applications, Piacenza, Italy, pp 59-68 (February, 1980).

98. Mankowski, J., Szklarska Smialowska, Z., "The Effect of Specimen Position on the Shape of Corrosion Pits in an Austenitic Stainless Steel", Corrosion Science, 17 (9), pp 725-735 (September, 1977).

99. Scotto, V., Ventura, G., and Traverso, E., "The Influence of Nonmetallic Inclusion Nature and Shape on the Pitting Corrosion Susceptibility of 18Cr-9Ni and 17Cr-11Ni-2Mo Austenitic Stainless Steels", Corrosion Science, 19 (4), pp 237-250 (April, 1979).

100. Eklund, G. S., "On the Initiation of Crevice Corrosion on Stainless Steel", Journal of Electrochemical Society, 123 (2), pp 170-173 (February, 1976).

101. Brennert, S. and Eklund, G., "On the Mechanism of Pitting Corrosion of Stainless Steels in Chloride Solutions--Initiation", Scandinavian Journal of Metallurgy, 5 (2), pp 16-20 (1976).

102. Sydberger, T., "Influence of the Surface State on the Initiation of Crevice Corrosion on Stainless Steels", Materials and Corrosion, 32 (3), pp 119-128 (March, 1981).

103. Kain, R. M., "Crevice Corrosion of Stainless Steels in Seawater and Related Environments", Corrosion '81, Toronto, Ontario, Canada, Paper 200 (April, 1981).

104. Kain, R. M., "Crevice Corrosion Resistance of Several Iron and Nickel-Base Cast Alloys in Seawater", Corrosion '82, Houston, TX, Paper 66 (March, 1982).

105. Oldfield, J. W. and Sutton, W. H., "New Technique for Predicting the Performance of Stainless Steels in Seawater and Other Chloride-Containing Environments", British Corrosion Journal, 15 (1), pp 31-34 (1980).

106. Kain, R. M., "Crevice Corrosion Resistance of Austenitic Stainless Steels in Ambient and Elevated Temperature Seawater", Corrosion '79, Atlanta, GA, Paper 230 (March, 1979).

107. Wheatfall, W. L., "Metal Corrosion in Deep-Ocean Environments", U.S. Navy Marine Engineering Laboratory, Annapolis, MD, R-429/66 (January, 1967).

108. Moller, G. E., "The Successful Use of Austenitic Stainless Steels in Seawater", Society of Petroleum Engineers Journal, 17 (2), pp 101-110 (April, 1977).

109. Weber, J., "Materials for Handling Seawater at High Flow Velocities", Materials to Supply Energy Demand, Harrison, BC, ASM, pp 49-80 (1981).

110. Danek, G. J., Jr., "The Effect of Seawater Velocity on the Corrosion Behavior of Metals", Naval Engineers Journal, 78 (5), pp 763-769 (October, 1966).

111. Hohman, A. E. and Kennedy, W. L., "Corrosion and Materials Selection Problems on Hydrofoil Craft", Materials Protection, 2 (9), pp 56-68 (September, 1963).

REFERENCES FOR CHAPTER 4
(Continued)

112. Reinhart, F. M. and Jenkins, J. F., "Corrosion of Materials in Surface Seawater After 12 and 18 Months of Exposure", Final Report, NCEL-TN-1213, AD743872 (January, 1972).

113. Lennox, T. J., Jr., Groover, R. E., and Peterson, M. H., "How Effective is Cathodic Protection of Stainless Steels in Quiescent Seawater?", Materials Protection, 8 (5), pp 41-48 (May, 1969).

114. Schrieber, C. F. and Coley, F. H., "Behavior of Metals in Desalting Environments - Seventh Progress Report (Summary)", Materials Performance, 15 (7), pp 47-54 (July, 1976).

115. Ulanovskii, I. B. and Korovin, Y. M., "Accelerated Determination of the Relative Tendency of Stainless Steels Toward Crevice Corrosion in Seawater", Protection of Metals, 10 (4), pp 400-402 (July, 1974).

116. Mar, E. D., Scotto, V., and Mollica, A., "Contribution to the Discussion on Localized Corrosion of Stainless Steels in Natural Seawater", Werkstoffe und Korrosion, 31 (4), pp 281-285 (April, 1980).

117. Oldfield, J. W. and Sutton, W. H., "Crevice Corrosion of Stainless Steels. II: Experimental Studies", British Corrosion Journal, 13 (3), pp 104-111 (1978).

118. Roy, D. N., "Electrochemical Aspects of Pitting Corrosion of Stainless Steels in Chloride Media", Indian Journal of Technology, 17 (8), pp 304-307 (August, 1979).

119. Manning, P. E., Duquette, D. J., and Savage, W. F., "The Role of Sulfide Inclusion Morphology in Pit Initiation of Several Type 300 Series Stainless Steels", Corrosion, 36 (6), pp 313-319 (June, 1980).

120. Todd, B., "Nickel Containing Materials for Marine Applications", Anti-Corrosion, 25 (10), pp 4-7 (October, 1978).

121. Hack, H. P., "Susceptibility of 17 Machinery Alloys to Sulfide-Induced Corrosion in Seawater", Naval Ship R&D Center, Annapolis, MD, ADBO41334L, SME-79/56 (September, 1979).

122. Deverell, H. E. and Davis, J. A., "Effect of Sulfides and Other Pollutants on the Seawater Corrosion of Stainless Steels and Copper-Base Alloys", Corrosion '78, Houston, TX, Paper 27 (March, 1978).

123. Vasilenko, I. I., Alekseenko, M. F., Levitskaya, G. D., Radkevich, A. I., and Mukhina, Z. N., "Local Corrosion of Martensitic Stainless Steel in a Medium Containing Chloride Ions and Hydrogen Sulfide", Soviet Materials Science, 18 (6), pp 491-494 (December, 1982).

124. Oldfield, J. W. and Todd, B., "Corrosion Considerations in Selecting Metals for Flash Chambers", Desalination, 31 (1-3), pp 365-383 (October, 1979).

REFERENCES FOR CHAPTER 4
(Continued)

125. Reinhart, F. M. and Jenkins, J. F., "The Relationship Between the Concentration of Oxygen in Seawater and the Corrosion of Metals", U.S. Naval Civil Engineering Laboratory, Port Hueneme, CA, pp 562-577 (1971).

126. Rynewicz, J. F., "Evaluation of Paint Coatings Tested in the Deep Atlantic and Pacific Oceans", Corrosion in Natural Environments, ASTM-STP-558, pp 209-235 (1974).

127. Suciu, D. F. and Wikoff, P. M., "Evaluation of Materials for Systems Using Cooled, Treated Geothermal or High-Saline Brines", Idaho National Engineering Laboratory, EGG-2213, DE83000653 (September, 1982).

128. Dundas, H. J. and Bond, A. P., "Effect of Welding on Pitting and Crevice Corrosion Resistance of Ferritic Stainless Steel", Corrosion '82, Houston, TX, Paper 66 (March, 1982).

129. Cramer, S. D. and Carter, J. P., "Laboratory Corrosion Studies in Low- and High-Salinity Geobrines of the Imperial Valley, California", U.S. Bureau of Mines, Washington, DC Report of Investigation 8415 (1980).

130. Veingarten, A. M., Grinvald, I. I., and Laanson, G. A., "Stress-Corrosion Resistance of High-Strength Dispersion-Hardening Stainless Steels", Soviet Materials Science, 6 (4), pp 445-449 (July, 1979).

131. Dundas, J. F. and Bond, A. P., "Relation of Composition to Stress-Corrosion Cracking of Austenitic Stainless Steels", Corrosion '80, Chicago, IL, Paper 89 (March, 1980).

132. Redmond, J. D. and Miska, K. H., "High-Performance Stainless Steels for High-Chloride Service", Chemical Engineering, 90 (15), pp 93-96 (July, 1983).

133. Speidel, M. O., "Stress-Corrosion Cracking of Stainless Steels in NaCl Solutions", Metallurgical Transactions, 12A (5), pp 779-789 (May, 1981).

134. Fujii, C. T., "Stress-Corrosion Cracking Properties of 17-4PH Steel", Stress-Corrosion--New Approaches, ASTM-STP-610, pp 213-225 (1976).

135. Gouda, V. K. and El-Sayed, H. A., "Stress-Corrosion Cracking of 410 Stainless Steel in Aqueous Chloride Solutions", Surface Technology, 18 (4), pp 327-339 (April, 1983).

136. Truman, J. E., "Influence of Chloride Content, pH, and Temperature of Test Solution on the Occurrence of Stress-Corrosion Cracking (SCC) With Austenitic Stainless Steel", Corrosion Science, 17 (9), pp 737-746 (1977).

137. Lin, L. F., Cragnolino, G., Szklarska-Smialowska, A., and MacDonald, D. D., "Stress-Corrosion Cracking of Sensitized Type 304 Stainless Steel in High Temperature Chloride Solutions", Corrosion, 37 (11), pp 616-626 (November, 1981).

138. Radhakrishnan, V. R. and Iyer, S. R., "Stress-Corrosion Testing and Data Analysis", Werkstoffe und Korrosion, 30 (3), pp 185-189 (March, 1979).

REFERENCES FOR CHAPTER 4
(Continued)

139. Gurevich, S. E., "Investigation of the Stress-Corrosion Crack Growth Rates of Steel and Titanium Alloy in Artificial Seawater", Mechanical Behavior of Materials, 2, pp 457-462 (August, 1979).

140. Daniels, W. J., "Comparative Findings Using the Slow Strain-Rate, Constant Flow Stress, and U-Bend Stress-Corrosion Cracking Techniques", SCC--The Slow Strain-Rate Technique, ASTM-STP-665, pp 347-361 (1979).

141. Suery, P., "Detection of Heat Treatment Effects on Environmentally Induced Degradation of a Martensitic Stainless Steel and a Nickel-Base Alloy by the Slow Strain-Rate Technique", SCC--The Slow Strain-Rate Technique, ASTM-STP-665, pp 320-332 (1979).

142. Kurov, O. V., "Chloride Solution pH in Cracks During the Corrosion of Metals", Protection of Metals, 18 (4), pp 517-518 (July, 1982).

143. Kurov, O. V. and Melekhov, R. K., "Potential and pH at the Tip of a Developing Crack", Protection of Metals, 15 (3), pp 249-250 (June, 1979).

144. McGuire, M. F., Troiano, A. R., and Hehemann, R. F., "Stress-Corrosion of Ferritic and Martensitic Stainless Steels in Saline Solutions", Corrosion, 29 (7), pp 268-271 (July, 1973).

145. Lee, W.S.W., Oldfield, J. W., and Todd, B., "Corrosion Problems Caused by Bromine Formation in Additive Dosed MSF Desalination Plants", Desalination, 44, pp 209-221 (May, 1983).

146. Torchio, S., "Stress-Corrosion Cracking of Type AISI 304 Stainless Steel at Room Temperature, Influence of Chloride Content and Acidity", Corrosion Science, 20 (4), pp 555-561 (1980).

147. Basil, J. L., "Corrosion of Materials in High Velocity Seawater", U.S. Naval Engineering Exp. Station, Annapolis, MD, AD822264, 910160A (December, 1960).

148. Werchniak, W. and Gudas, J. P., "Seawater Corrosion and Corrosion Fatigue of High-Strength Cast Alloys for Propellers and Impellers", Corrosion '81, Toronto, Ontario, Canada, Paper 199 (April, 1981).

149. Pini, G. and Weber, J., "Materials for Pumping Seawater and Media With High Chloride Content", Sulzer Technical Review, 2, pp 69-80 (1979).

150. Davis, J. A. and Gehring, G. A., Jr., "Corrosion Behavior Variations With Time and Velocity in Seawater", Corrosion '75, Toronto, Ontario, Canada, Paper 123 (April, 1975).

151. Lee, T. S., "Seawater Velocity Effects on Corrosion Behavior of Materials", Sea Technology, 24 (11), pp 51, 53, 55-59 (November, 1983).

152. Simoneau, R., Fihey, J. L., and Roberge, R., "The Effect of Corrosion in Low-Intensity Cavitation Erosion", Cavitation Erosion in Fluid Systems, pp 71-81 (June, 1981).

REFERENCES FOR CHAPTER 4
(Continued)

153. Ozhiganov, Y. G., Goryachko, Y. S., Shevchenko, O. F., Litvinov, V. E., and Gubarev, M. K., "Influence of Fine Crystal Structure on the Susceptibility of Austenitic Steel to Corrosion Cracking in Seawater (Translation)", Protection of Metals, 14 (1), pp 68-70 (February, 1978).

154. Shul'te, A. Y., Silaev, I. I., Kholodyni, Vi. I., and Varanin, V. P., "Some Reasons for the Corrosion Damage of Weld Joints of Types 12Kh18N10T and 07Kh16N6 Stainless Steels", Soviet Materials Science, 18 (2), pp 186-189 (March, 1982).

155. Carter, J. P., Cramer, S. D., and Conrad, R. K., "Corrosion of Stainless Steels in the Geothermal Environments of the Salton Sea Known Geothermal Resource Area", Corrosion '81, Toronto, Canada, Paper 230 (April, 1981).

156. Carter, J. P. and McCawley, F. X., "In Situ Corrosion Tests in Salton Sea Geothermal Brine Environments", Journal of Metals, 30 (3), pp 11-15 (March, 1978).

157. Lee, T. S. and Tuthill, A. H., "Use of Carbon Steel to Mitigate Crevice Corrosion of Stainless Steels in Seawater", Materials Performance, 22 (1), pp 48-53 (January, 1983).

158. Henrikson, S. and Asberg, M., "Corrosion Potentials and Galvanic Corrosion Currents for Various Material Combinations in Baltic Seawater", 7th Scandinavian Corrosion Congress, Trandheim, Norway, pp 371-384 (May, 1975).

159. Smith, C. A. and Compton, K. G., "Potentials of Selected Metal Alloys in Seawater at Elevated Temperatures", Corrosion, 31 (9), pp 320-326 (September, 1975).

160. Waldron, L. J., Forgeson, B. W., Peterson, M. H., and Brown, B. F., "Performance of Stainless Steel Galvanically Coupled to Other Metals", NRL, Washington, DC, NRL-MR-1388, AD679659 (January, 1963).

161. Gehring, G. A., Jr. and Maurer, J. R., "Galvanic Corrosion of Selected Tubesheet/Tube Couples Under Simulated Seawater Condenser Conditions", Corrosion '81, Toronto, Ontario, Canada, Paper 202 (April, 1981).

162. Gehring, G. A., Jr. and Kyle, R. J., "Galvanic Corrosion in Steam Surface Condensers Tubed With Either Stainless Steel or Titanium", Corrosion '82, Houston, TX, Paper 60 (March, 1982).

163. Pelensky, M. A., Jaworski, J. J., and Gallaccio, A., "Air, Soil, and Sea Galvanic Corrosion Investigation at Panama Canal Zone", Galvanic and Pitting Corrosion, ASTM-STP-576, pp 94-113 (1976).

164. Charlot, L. A., Wong, C. M., and Gillam, W. S., "Investigation of Galvanically Induced Hydriding of Titanium in Saline Solutions", Battelle Northwest Laboratories, Richland, WA, RDPR-70-624, PB198639 (December, 1970).

165. Scholes, I. R., Astley, D. J., and Rowlands, J. C., "Bimetallic Corrosion in Seawater", EROCOR '77, European Congress on Metallic Corrosion, London, England, pp 161-169 (1977).

REFERENCES FOR CHAPTER 4
(Continued)

166. Miller, B. A. and Lee, S. G., "The Effect of Graphite-Epoxy Composites on the Galvanic Corrosion of Aerospace Alloys", Wright-Patterson AFB, Final, AFML-TR-76-121, ADA035029 (September, 1976).

167. Mansfeld, F., "Galvanic Corrosion of Al Alloys Coupled to Coated PH13-8Mo Stainless Steel", Corrosion, 29 (7), pp 276-281 (July, 1973).

168. Gurevich, L. Y., Lashchevskii, V. B., Batrakov, V. P., and Shvarts, M. M., "Investigation of the Corrosion Resistance of Welded Joints of Steel VN5-2", Protection of Metals, 9 (4), pp 364-368 (August, 1973).

169. Davis, J. A. and Gehring, G. A., "Galvanic Corrosion as a Function of Applied Potential in High Velocity Seawater", Corrosion '76, Houston, TX, Paper 75 (March, 1976).

170. Lennox, T. J., Jr., Peterson, M. H., Smith, J. A., and Groover, R. E., "Corrosion and Cathodic Protection of 5086-H32 Al Coupled to Dissimilar Metals", Materials Performance, 13 (2), pp 31-36 (February, 1974).

CHAPTER 5
TABLE OF CONTENTS

CHAPTER 5
LIST OF TABLES

CHAPTER 5
LIST OF TABLES
(Continued)

CHAPTER 5
LIST OF FIGURES

CHAPTER 5
LIST OF FIGURES
(Continued)

CHAPTER 5

NICKEL-BASE ALLOYS

The corrosion behavior of unalloyed nickel, high-nickel alloys, and Ni-Cr-Fe alloys with more than 30 percent nickel (such as Alloy 800) is discussed in this section. The reader is also referred to the section on Stainless Steels where data for several nickel alloys may be included with those presented for stainless steels. In particular, data for Alloys 625, 825, and C-276 are often included for comparison. The nominal composition of alloys discussed in this chapter are given in Appendix E.

Atmosphere

General Corrosion and Pitting

Unalloyed nickel and the nickel-base alloys have excellent resistance to corrosion in the marine atmosphere. As shown in Table 5-1 and Figure 5-1, unalloyed nickel and Alloy 400 exhibited no visible attack, no pitting, and weight loss penetration of <0.02 mpy after 16 years' of seacoast exposure in the Panama Canal Zone. As shown in Figure 5-1, the weight losses increased linearly with time over the 16-year exposure.

Miska[2] reports the following corrosion rates and pit depths for nickel-base alloys exposed 7 years at the Kure Beach, NC 25-m lot:

Alloy	Corrosion Rate, mpy	Maximum Pit Depth, mils
Unalloyed	0.01	--
600	0.0016	--
800	0.06	0.9
825	0.06	0.7

He also reports that Alloys F, G, 700, 718, Elgiloy, and Illium R also have excellent resistance to marine atmospheres, but the most resistant alloys are Alloy C, C-276, X-750, 625, MP35N, Chlorimet 3, and Rene' 41. Boyd and Fink[3] report that Alloy C was still bright and shiny after more than 20 years' exposure at Kure Beach.

TABLE 5-1. COMPREHENSIVE TABULATION OF CORROSION DAMAGE FOR NICKEL-COPPER ALLOYS AND COMPARISON METALS(1)

Symbol[a]	Metal	Exposure	Weight Loss, g/dm²					Average Penetration, mils					Depth of Pitting, mils: Average 20 Deepest[b]					Depth of Pitting, mils: Deepest Penetration					Tensile Strength Loss, %[c]	Type Corrosion Attack[d]
			1 Yr	2 Yr	4 Yr	8 Yr	16 Yr	1 Yr	2 Yr	4 Yr	8 Yr	16 Yr	1 Yr	2 Yr	4 Yr	8 Yr	16 Yr	1 Yr	2 Yr	4 Yr	8 Yr	16 Yr	16 Yr	16 Yr
A	Nickel 99%	Immersion																						
		Seawater	5.40	7.55	11.8	28.4	43.4	2.40	3.35	5.22	12.6	19.3	125	143	121	120	142	245	248	248	245	249	9	j, q, h, k
		Mean tide	0.78	1.30	2.99	5.77	9.89	0.35	0.58	1.33	2.56	4.39	(0)	37	47	65	61	0	56	105	103	121	2	j, q
		Fresh water	0.00	0.00	0.00	0.03	0.08	0.00	0.00	0.00	0.01	0.04	(0)	(0)	(0)	(0)	(0)	0	0	0	0	0	<1	k
		Atmospheric																						
		Marine	0.02	0.03	0.06	0.13	0.26	0.01	0.02	0.03	0.06	0.12	(0)	(0)	(0)	(0)	(0)	0	0	0	0	0	0	k
		Inland	0.01	0.04	0.06	0.09	0.21	0.01	0.02	0.03	0.04	0.09	(0)	(0)	(0)	(0)	(0)	0	0	0	0	0	0	k
B	Monel	Immersion																						
	(cold rolled)	Seawater	3.67	5.14	9.38	14.2	19.5	1.64	2.29	4.18	6.32	8.66	17	32	27	40	33	42	56	41	55	55	8	r, j
	67Ni-30Cu-1.4Fe	Mean tide	0.23	0.50	1.11	3.02	6.00	0.10	0.22	0.50	1.34	2.67	(0)	(0)	(0)	14	14	0	0	0	24	21	2	j, r
		Fresh water	0.00	0.20	0.03	0.25	1.36	0.00	0.09	0.01	0.11	0.61	8(1)	12(10)	19(15)	29(8)	30(11)	8	16	27	53	52	<1	r
		Atmospheric																						
		Marine	0.10	0.08	0.14	0.26	0.49	0.04	0.04	0.07	0.12	0.22	(0)	(0)	(0)	(0)	(0)	0	0	0	0	0	2	a, k
		Inland	0.02	0.05	0.08	0.14	0.30	0.01	0.03	0.04	0.06	0.12	(0)	(0)	(0)	(0)	(0)	0	0	0	0	0	1	k, a
C	Monel	Immersion																						
	(hot rolled)	Seawater	4.68	5.46	9.05	14.40	18.72	2.09	2.44	4.05	6.44	8.37	43	40	53	50	56	90	61	82	68	80	—	r, j
	67Ni-30Cu-2.1Fe	Mean tide	0.25	0.63	1.56	3.09	5.74	0.11	0.28	0.71	1.38	2.57	(0)	(0)	16(15)	17	24	0	0	20	25	36	—	j, r
D	Copper-nickel	Immersion																						
	30Ni-69Cu	Seawater	1.15	2.34	3.13	3.38	5.11	0.51	1.03	1.38	1.49	2.25	11(8)	12	24(10)	6(7)	7(.4)	15	18	37	8	10	<1	j, r
		Mean tide	0.19	0.31	0.61	0.97	1.71	0.08	0.14	0.27	0.43	0.75	(0)	(0)	(0)	(0)	(0)	0	0	0	0	0	<1	k, a
		Fresh water	0.38	0.60	1.20	2.18	2.96	0.17	0.26	0.53	0.96	1.31	(0)	(0)	(0)	(0)	(0)	0	0	0	0	0	<1	k
		Atmospheric																						
		Marine	0.08	0.14	0.27	0.52	0.93	0.03	0.06	0.12	0.23	0.41	(0)	(0)	(0)	2(2)	(0)	0	0	0	0	0	1	a, k
		Inland	0.04	0.11	0.18	0.30	0.62	0.02	0.05	0.08	0.13	0.27	(0)	(0)	(0)	3(1)	(0)	0	0	0	0	0	1	a, k
E	Nickel silver	Atmospheric																						
	18Ni-64Cu-17Zn	Marine	0.09	0.15	0.26	0.49	0.83	0.04	0.06	0.12	0.22	0.37	(0)	(0)	(0)	(0)	(0)	0	0	0	0	0	0	a, k
		Inland	0.04	0.09	0.16	0.29	0.63	0.02	0.04	0.07	0.13	0.28	(0)	(0)	(0)	(0)	(0)	0	0	0	0	0	0	a, k
F	Copper 99.9%	Immersion																						
		Seawater	2.74	5.03	5.95	12.1	13.6	1.21	2.22	2.62	5.33	6.02	27(15)	36(17)	16(11)	28	31	46	75	21	53	57	5	e, r
		Mean tide	1.47	1.85	4.30	2.45	2.99	0.65	0.82	1.90	1.08	1.32	9(2)	(0)	7(2)	10	(0)	11	0	8	23	0	1	e, r
		Fresh water	0.50	0.81	1.29	1.86	2.33	0.22	0.36	0.57	0.82	1.03	(0)	(0)	(0)	(0)	(0)	0	0	0	0	0	2	a
		Atmospheric																						
		Marine	0.37	0.52	0.86	1.29	1.73	0.17	0.23	0.38	0.57	0.77	(0)	(0)	(0)	(0)	(0)	0	0	0	0	0	4	a
		Inland	0.18	0.26	0.34	0.43	0.60	0.08	0.12	0.15	0.19	0.27	(0)	(0)	(0)	(0)	(0)	0	0	0	0	0	<1	a
		Immersion																						
G	Al-bronze	Seawater	0.39	0.75	1.25	1.58	2.62	0.19	0.36	0.60	0.76	1.26	(0)	(0)	(0)	14(3)	(0)	0	0	0	21	0	3	j, k
H	6061 Al	Seawater	0.19	0.33	0.39	0.50	0.63	0.28	0.48	0.56	0.73	0.92	(0)	(0)	13(10)	23	14	0	0	32	49	79	<1	j, a
J	Lead	Seawater	1.67	3.37	4.93	8.18	14.0	0.58	1.17	1.72	2.85	4.88	(0)	20	(0)	23	28	0	34	0	40	48	0	a, j, h
K	Zinc	Seawater	3.18	4.73	6.03	9.08	15.7	1.76	2.61	3.33	5.01	8.23	20(14)	36(17)	52	53	62	50	62	70	90	107	3	e, r, q

(a) Symbols refer to curves in Figure 5-1.
(b) Numbers in parentheses indicate number of measurable pits when less than 20. A measurable pit is >5 mils.
(c) Percent tensile losses are for samples of 1/4 in. thickness for immersion exposure and 1/16 in. thickness for atmospheric exposure.
(d) Corrosion types are described in detail in the appendix. Those referred to here are: a—uniform attack, e—local attack (uniformly distributed), r—local attack (randomly located), c—concentration cell, j—fouling contact, k—no visible attack, q—pitting (randomly distributed).

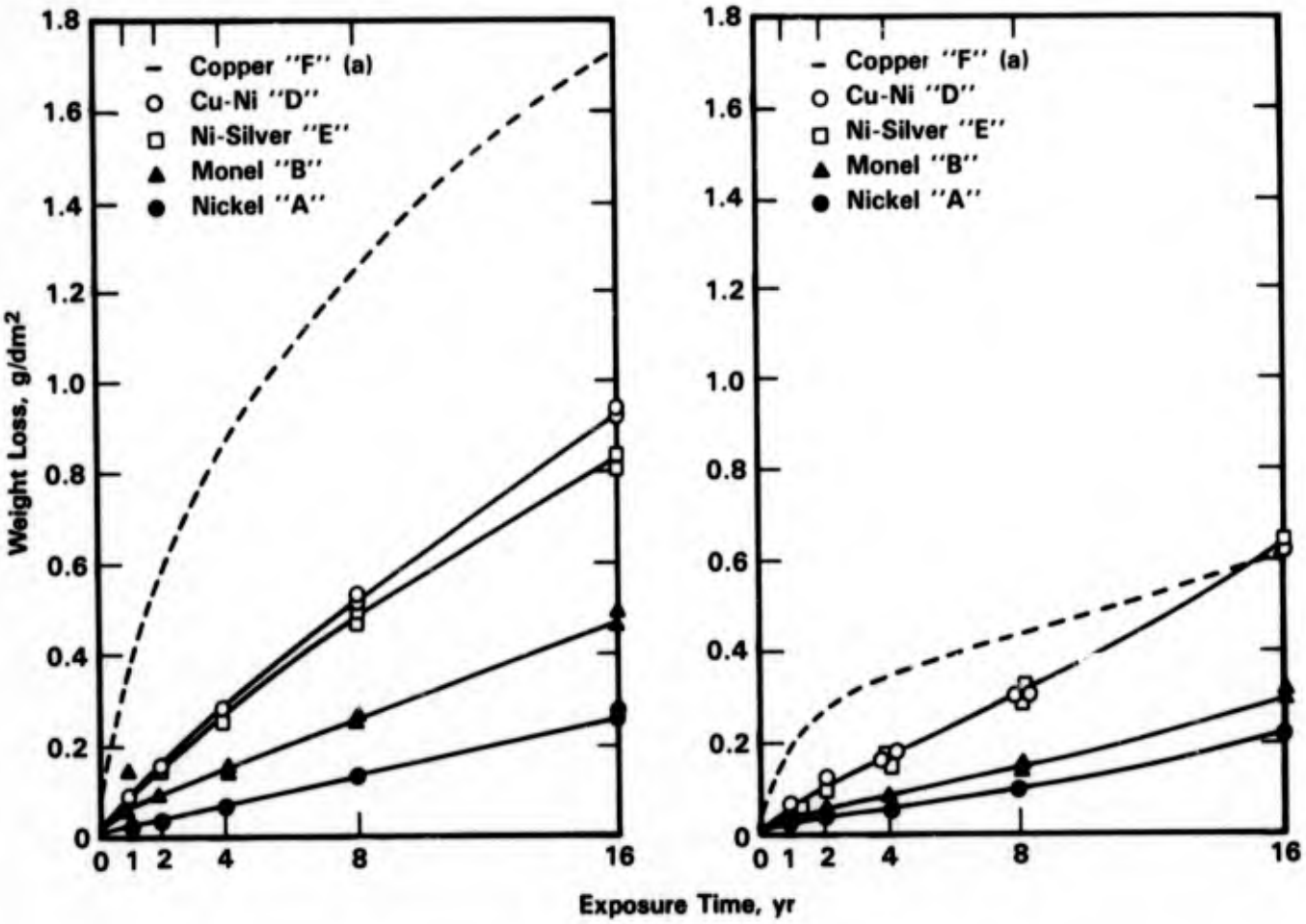

FIGURE 5-1. CORROSION OF NICKEL AND NICKEL-COPPER ALLOYS IN TROPICAL ATMOSPHERES[1]

(a) Symbols refer to alloys in Table 5-1.

Galvanic Corrosion

A type of galvanic series for alloys in a marine atmosphere has been prepared by Baboian (see Table 5-2). As in the galvanic series in seawater, the nickel-base alloys are at the noble end of the series. Southwell, et al.[5] in Table 5-3 report on galvanic couples between nickel/steel, Alloy 400/steel, and Alloy 400/phosphor bronze. In all cases, the nickel alloys were noble to the dissimilar metal, and their corrosion rates after 16 years of exposure at the seacoast in the Panama Canal Zone were <0.03 mpy.

Johnson and Abbott[6] exposed disk-type galvanic couples of steel to a number of nickel-base alloys in a marine atmosphere. The results presented in Table 5-4 show that Alloys 200,

TABLE 5-2. METALS ARRANGED ACCORDING TO INCREASING MAGNESIUM CORROSION IN GALVANIC COUPLE IN MARINE AND RURAL ATMOSPHERES[4]

Kure Beach, 800-ft Lot (Marine Atmosphere)			State College (Clean Rural Atmosphere)		
22.60 Yr	2.48 Yr	Corrosion of Mg	21.95 Yr	2.54 Yr	Corrosion of Mg
Al	Al	Least	Al	Zn PL steel	Least
Zn	Zn	↓	Zn	Al	↓
Zn PL steel	Zn PL steel		Zn PL steel	Zn	
Cd PL steel	Cd PL steel		Cd PL steel	304 SS	
Steel	304 SS		304 SS	85-15 brass	
85-15 brass	85-15 brass		85-15 brass	Nickel	
304 SS	Monel		Nickel	Monel	
Monel	Nickel		Monel	Cd PL steel	
Nickel	Steel	Most	Steel	Steel	Most

TABLE 5-3. CORROSION DAMAGE DATA FOR METALS EXPOSED AS BIMETALLIC COUPLED DISCS IN ATMOSPHERIC ENVIRONMENTS[5]

Couple				Metal A, g/m^2						Metal B, g/m^2					
				Coastal			Inland			Coastal			Inland		
Metal A			Metal B	1 Yr	4 Yr	16 Yr	1 Yr	4 Yr	16 Yr	1 Yr	4 Yr	16 Yr	1 Yr	4 Yr	16 Yr
Nickel (99% Ni)	(49)	= (35)	Carbon steel (0.24% C)	13	35	77	2	8	35	1087	2029	5204	315	759	1854
Nickel-copper (Monel: 70Ni-30Cu, cold rolled)	(47)	= (18)	Phosphor bronze (4Sn-0.25P)	16	38	92	4	14	53	86	192	638	15	63	187
Nickel-copper (Monel: 70Ni-30Cu, cold rolled)	(47)	= (35)	Carbon steel (0.24% C)	15	23	88	4	9	46	977	2127	4547	358	802	2026
Nickel-copper (Monel: 70Ni-30Cu, cold rolled)	(47)	= (47)	Nickel-copper (Monel: 70Ni-30Cu, cold rolled)	12	23	48	3	10	66	15	51	92	3	9	50

TABLE 5-4. CORROSION RATES OF MILD STEEL AND OTHER METALS WHEN COUPLED TOGETHER, AND WHEN COUPLED TO THEMSELVES, IN MARINE ATMOSPHERE[6]

Couple	Corrosion Rates, g/m^2, day		
	Mild Steel	Other Metal	
		Coupled to Mild Steel	Coupled to Itself
Mild steel-Hastelloy B	2.35	0.11	0.08
Mild steel-Incoloy 800	3.85	0.00	--
Mild steel-Incoloy 825	--	--	--
Mild steel-Inconel 600	2.91	0.00	--
Mild steel-Mild steel	1.05		
Mild steel-Monel 400	SD(a)	SD(a)	--
Mild steel-Nickel 200	2.12	0.07	--

(a) SD = specimen damaged.

400, 600, 800, 825, and B increased the rate of attack of the carbon steel as a result of the galvanic coupling.

Bomberger, et al.[7] coupled Alloys 400 and 600 to titanium in studies conducted at Kure Beach. Their results presented in Table 5-5, indicate that after more than four years' exposure, the attack on both alloys was negligible (penetration <0.03 mpy), but there was some slight increase in attack of the Alloy 400 when the Ti/400 area ratio was 7/1.

SCC and IGA

The results of stress-corrosion tests at Kure Beach on U-bends of annealed, welded, cold worked, or sensitized stainless steels and nickel-base alloys are included in Table 5-6. No SCC or IGA was observed for any of the alloys or conditions studied which included Alloys 600, 800, 825, and 20Cb3.

Splash and Tide

General Corrosion and Pitting

Miska[2] states that the corrosion resistance of nickel-base alloys in the splash zone is virtually as good as in the marine atmosphere, but may be reduced in tide zones. This is well

TABLE 5-5. ATMOSPHERIC GALVANIC-COUPLE TESTS ON SHORE RACK, KURE BEACH[7]

Material	360-Day Exposure			4.75-Yr Exposure		
	Uncoupled Corrosion Rates, mpy[a]	Coupled Corrosion Rates, mpy		Uncoupled Corrosion Rates, mpy[a]	Coupled Corrosion Rates, mpy	
		Metal Area 7 x Ti Area[b]	Metal Area 1/7 x Ti Area[c]		Metal Area 7 x Ti Area[b]	Metal Area 1/7 x Ti Area[b]
FS-1 Magnesium	1.26	2.50	5.5	0.88[d]	1.17[d]	3.52[d]
Alclad 24S-T3	0.06	0.277	0.86	0.0549	0.2130	0.291
52S-1/2H	0.05	0.056	0.199	0.0845	0.0362	0.0813
Alclad 75S-T6	0.10	0.460	0.99	0.0525	0.0786	0.393
Copper	0.12	0.022	0.42	0.0852	0.1350	0.241
Steel (low carbon)	6.13	9.82	Lost	--	--	--
Monel	Nil	0.020	0.032	0.0152	0.0197	0.0320
Inconel	0.011	0.006	0.003	0.0025	0.0029	0.0032
302 Stainless	Nil	0.009	0.023	0.0083	0.0091	0.0015
316 Stainless	0.004	0.004	0.003	0.0035	0.0029	0.0058

(a) Average of one 6 in. x 1.5 in. specimen and two 0.75 in. x 1.5 in. specimens.
(b) One 6 in. x 1.5 in. specimen.
(c) Average of two 0.75 in. x 1.5 in. specimens.
(d) Three years and 160 days' exposure.

TABLE 5-6. FIVE YEAR RESULTS OF THE SCC OF STAINLESS STEEL U-BENDS IN 82-FOOT LOT AT KURE BEACH[8]

Alloy/Heat	Ratio of Failures to Specimens Exposed					
	Annealed		As-Welded[b]		Cold Work 1/4 Hard	Sensitized at 1200 F, 1.5 Hr + FC
	B[a]	S[a]	B	S	B	B
AISI 201-1	0/3	0/3	--	--	--	3/3
AISI 201-2	0/3	0/3	--	--	--	3/3
AISI 201-3	0/3	0/3	--	--	--	3/3
AISI 201-4	0/3[c]	0/3[c]	0/3[c]	0/3[c]	0/3[c]	3/3
AISI 201-5	0/3	0/3	0/3	0/3	0/3	3/3
AISI 301-1	0/3	0/3	--	--	--	3/3
AISI 301-2	0/3	0/3	--	--	--	3/3
AISI 301-3	0/3	0/3	--	--	--	3/3
AISI 301-4	0/3	0/3	0/3	0/3	0/3	3/3

TABLE 5-6. (Continued)

Alloy/Heat	Ratio of Failures to Specimens Exposed					
	Annealed		As-Welded[b]		Cold Work 1/4 Hard	Sensitized at 1200 F, 1.5 Hr + FC
	B[a]	S[a]	B	S	B	B
AISI 301-5	0/3	0/3	0/3	0/3	0/3	3/3
AISI 301-6	0/3[c]	0/3[c]	0/3[c]	0/3[c]	0/3	1/3
AISI 301-7	0/3	0/3	--	--	--	3/3
AISI 302-4	0/3[c]	0/3[c]	0/3[c]	0/3[c]	0/3[c]	3/3
AISI 304-1	0/3	0/3	--	--	--	0/3
AISI 304-2	0/3	0/3	--	--	--	3/3
AISI 304-3	0/3	0/3	--	--	--	0/3
AISI 304-4	0/3[c]	0/3[c]	0/3[c]	0/3[c]	0/3[c]	3/3
AISI 304-5	0/3	0/3	0/3	0/3	0/3	3/3
AISI 304-6	0/3	0/3	--	--	--	0/3
AISI 304L-1	0/3	0/3	0/3	0/3	--	0/3
AISI 304L-2	0/3[c]	0/3[c]	0/3[c]	0/3[c]	0/3[c]	0/3
AISI 309-1	0/3[c]	0/3[c]	0/3[c]	0/3[c]	--	3/3
AISI 310-1	0/3[c]	0/3[c]	0/3[c]	0/3[c]	--	0/3
AISI 316-1	0/3	0/3	--	--	--	0/3
AISI 316-2	0/3[c]	0/3[c]	0/3	0/3[c]	0/3[c]	2/3
Inconel 600-1	0/3[c]	0/3[c]	0/3[c]	0/3[c]	--	0/3
Incoloy 800-1	0/3[c]	0/3[c]	0/3[c]	0/3[c]	--	0/3
Incoloy 825-1	0/3[c]	0/3[c]	0/3[c]	0/3[c]	--	0/3
Carpenter 20Cb-3-1	0/3[c]	0/3[c]	0/3[c]	0/3[c]	--	0/3

(a) B = bold exposure, and S = sheltered exposure.
(b) Autogenous welding by TIG process. Weld beads were made on annealed material from Alloys 304L-1, 309, 310, 600, 800, 825, and Cb3. Weld beads were made on 1/4 hard material for all other alloys.
(c) One specimen from each group examined metallographically for evidence of SCC.

illustrated in Table 5-1 and Figure 5-2 where after 16 years at mean tide in the Panama Canal Zone, the average penetration and maximum penetration for unalloyed nickel and Alloy 400 were 4.4 and 2.6 (average) and 121 and 36 mils, respectively. Corrosion was negligible for these same alloys after 16 years' exposure in the marine atmosphere.

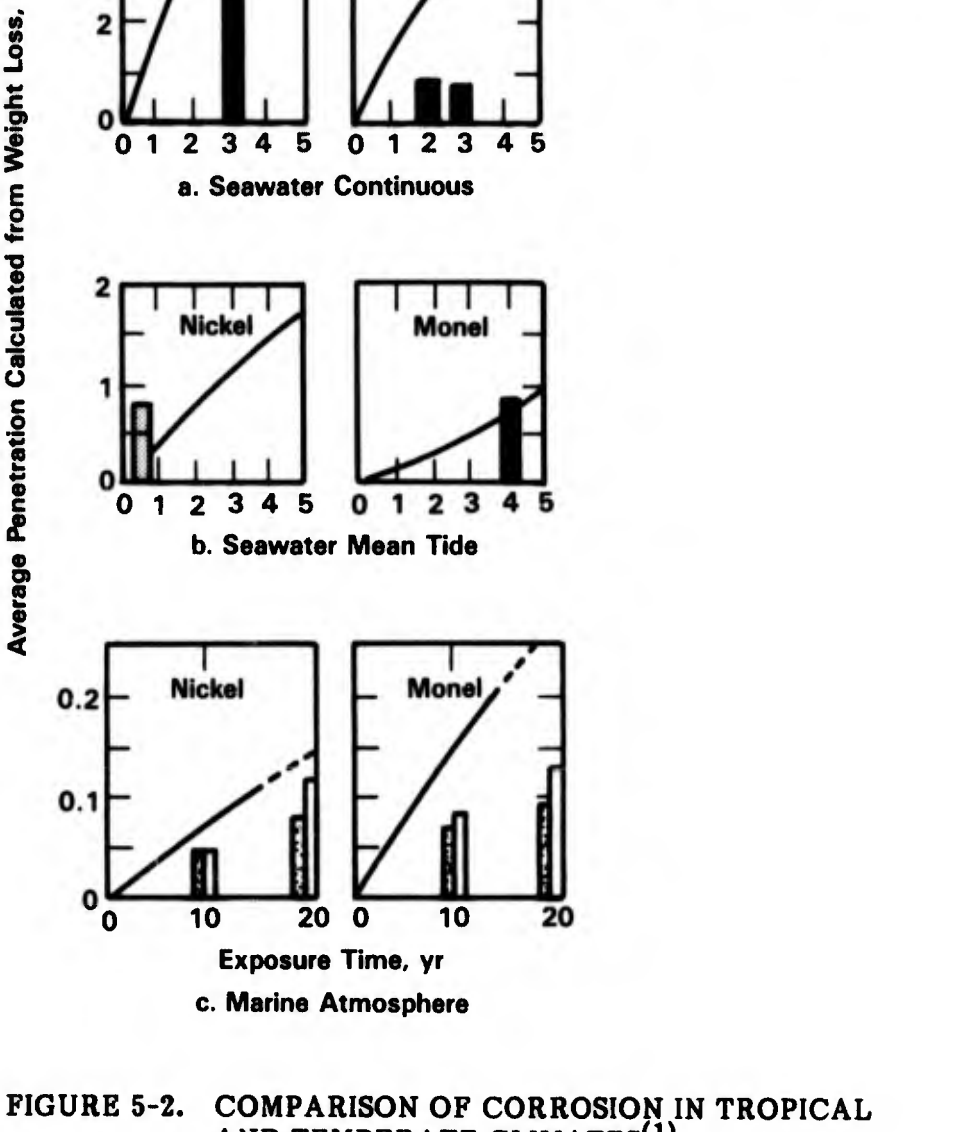

FIGURE 5-2. COMPARISON OF CORROSION IN TROPICAL AND TEMPERATE CLIMATES[1]

Galvanic Corrosion

Ballantine[9] has prepared a guide for galvanic coupling of fasteners in exposure above the water line. As shown in Table 5-7, only those materials close to the nickel alloys in the immersed and atmospheric galvanic series can be safely used without undue galvanic corrosion. In Table 5-8, Anderson and Ross[10] report that Alloys 301 400, 500, and X-750 were in excellent condition after 15 to 25 years' service as fasteners in Alloy 400 sheathing at Wrightsville Beach, North Carolina.

SCC and IGA

Alternate immersion tests have been conducted in 3.5 percent NaCl solution for several nickel-base alloys. Results are presented in Tables 5-9 and 5-10. Note that Alloys C, 718, and TDNICr were resistant to SCC in these tests. The low values for percentage of room temperature yield strength for several of the alloys in Table 5-9 were attributed to the notch effect of the precrack in these specimens.

Montano[13] reports no SCC of strengthened and aged MP35N exposed 180 days in the alternate immersion tests at loads of 50, 75, and 100 percent of yield strength. Deel and Mindlin[14,15] found no SCC of Alloys 702, 706, and 710 that were exposed 1000 hours to the alternate immersion test at loads of 80 percent of yield strength.

Immersion

As with the conventional stainless steels, the most frequent failure mode of the conventional nickel-base alloys in seawater is pitting or crevice corrosion rather than general attack. As a rule, the weight change from pitting attack is so low that corrosion rates obtained from calculations based on the entire surface area are very low and can be misleading as to the service life of the material. Since pitting and general corrosion are so intertwined in the reported literature, the general corrosion rates will be discussed in conjunction with pitting.

General, Pitting, and Crevice Corrosion

Alloy Composition. Unalloyed nickel exhibits a relatively low overall rate of attack in seawater with calculated penetration rates ranging from 0.05 to ~1 mpy. However, it does exhibit pitting in quiescent seawater. As shown in Table 5-11, a summary by Lennox,[16] this

TABLE 5-7. GUIDE FOR SELECTION OF FASTENER ALLOYS FOR MARINE SERVICE[9]

Recommended alloys are listed in order of their preference

ABOVE WATERLINE

Trim Material to be Attached

Hull Superstructure or Base Plate Material	Wood	Fiberglass	Rubber	Plastic (Nylon)	Aluminum	Steel	Steel (Galvanized)	Copper	Brass	Brass (Plated)	Nickel Stainless Steel	Monel Nickel-Copper Alloys
Wood	Monel 18-8 Stainless Steel Silicon Bronze	Monel 18-8 Stainless Steel Silicon Bronze	Monel 18-8 Stainless Steel Silicon Bronze	Monel 18-8 Stainless Steel Silicon Bronze	18-8 Stainless Steel Aluminum	Monel 18-8 Stainless Steel Silicon Bronze	Monel 18-8 Stainless Steel Silicon Bronze	Silicon Bronze 18-8 Stainless Steel Monel	Silicon Bronze 18-8 Stainless Steel Monel	18-8 Stainless Steel Monel	18-8 Stainless Steel Monel	Monel 18-8 Stainless Steel
Fiberglass	Monel 18-8 Stainless Steel Silicon Bronze	Monel 18-8 Stainless Steel Silicon Bronze	Monel 18-8 Stainless Steel Silicon Bronze	Monel 18-8 Stainless Steel Silicon Bronze	18-8 Stainless Steel Aluminum	Monel 18-8 Stainless Steel Silicon Bronze	Monel 18-8 Stainless Steel Silicon Bronze	Silicon Bronze 18-8 Stainless Steel Monel	Silicon Bronze 18-8 Stainless Steel Monel	18-8 Stainless Steel Monel	18-8 Stainless Steel Monel	Monel 18-8 Stainless Steel
Rubber	Monel 18-8 Stainless Steel Silicon Bronze	Monel 18-8 Stainless Steel Silicon Bronze	Monel 18-8 Stainless Steel Silicon Bronze	Monel 18-8 Stainless Steel Silicon Bronze	18-8 Stainless Steel Aluminum	Monel 18-8 Stainless Steel Silicon Bronze	Monel 18-8 Stainless Steel Silicon Bronze	Silicon Bronze 18-8 Stainless Steel Monel	Silicon Bronze 18-8 Stainless Steel Monel	18-8 Stainless Steel Monel	18-8 Stainless Steel Monel	Monel 18-8 Stainless Steel
Plastic (Nylon)	Monel 18-8 Stainless Steel Silicon Bronze	Monel 18-8 Stainless Steel Silicon Bronze	Monel 18-8 Stainless Steel Silicon Bronze	Monel 18-8 Stainless Steel Silicon Bronze	18-8 Stainless Steel Aluminum	Monel 18-8 Stainless Steel Silicon Bronze	Monel 18-8 Stainless Steel Silicon Bronze	Silicon Bronze 18-8 Stainless Steel Monel	Silicon Bronze 18-8 Stainless Steel Monel	18-8 Stainless Steel Monel	18-8 Stainless Steel Monel	AVOID
Aluminum	18-8 Stainless Steel Aluminum	18-8 Stainless Steel Aluminum	18-8 Stainless Steel Aluminum	18-8 Stainless Steel Aluminum	18-8 Stainless Steel Aluminum	18-8 Stainless Steel Aluminum	18-8 Stainless Steel Aluminum	AVOID	AVOID	AVOID	18-8 Stainless Steel	AVOID
Steel	Monel 18-8 Stainless Steel	Monel 18-8 Stainless Steel	Monel 18-8 Stainless Steel	Monel 18-8 Stainless Steel	18-8 Stainless Steel Aluminum	Monel 18-8 Stainless Steel Silicon Bronze	Monel 18-8 Stainless Steel Silicon Bronze	Silicon Bronze 18-8 Stainless Steel Monel	Silicon Bronze 18-8 Stainless Steel Monel	18-8 Stainless Steel Monel	18-8 Stainless Steel Monel	Monel 18-8 Stainless Steel
Steel (Galvanized)	Silicon Bronze	Silicon Bronze	Silicon Bronze	Silicon Bronze	AVOID	Monel 18-8 Stainless Steel Silicon Bronze	Monel 18-8 Stainless Steel Silicon Bronze	Silicon Bronze 18-8 Stainless Steel Monel	Silicon Bronze 18-8 Stainless Steel Monel	18-8 Stainless Steel Monel	18-8 Stainless Steel Monel	Monel 18-8 Stainless Steel
Copper	Silicon Bronze 18-8 Stainless Steel	Silicon Bronze 18-8 Stainless Steel	Silicon Bronze 18-8 Stainless Steel	Silicon Bronze 18-8 Stainless Steel	AVOID	Silicon Bronze 18-8 Stainless Steel Monel	Silicon Bronze 18-8 Stainless Steel Monel	Silicon Bronze 18-8 Stainless Steel Monel	Silicon Bronze 18-8 Stainless Steel Monel	18-8 Stainless Steel Monel	18-8 Stainless Steel Monel	18-8 Stainless Steel
Brass	Monel	Monel	Monel	Monel	AVOID	Silicon Bronze 18-8 Stainless Steel Monel	Silicon Bronze 18-8 Stainless Steel Monel	Silicon Bronze 18-8 Stainless Steel Monel	Silicon Bronze 18-8 Stainless Steel Monel	18-8 Stainless Steel Monel	18-8 Stainless Steel Monel	18-8 Stainless Steel Monel
Brass (Plated)	18-8 Stainless Steel Monel	18-8 Stainless Steel Monel	18-8 Stainless Steel Monel	18-8 Stainless Steel Monel	AVOID	18-8 Stainless Steel Monel	18-8 Stainless Steel Monel	18-8 Stainless Steel Monel	18-8 Stainless Steel Monel	18-8 Stainless Steel Monel	18-8 Stainless Steel Monel	AVOID
Nickel Stainless Steel	18-8 Stainless Steel Monel	18-8 Stainless Steel Monel	18-8 Stainless Steel Monel	18-8 Stainless Steel Monel	18-8 Stainless Steel	18-8 Stainless Steel Monel	18-8 Stainless Steel Monel	18-8 Stainless Steel Monel	18-8 Stainless Steel Monel	18-8 Stainless Steel Monel	18-8 Stainless Steel	Monel 18-8 Stainless Steel
Monel Nickel-Copper Alloys	Monel 18-8 Stainless Steel	Monel 18-8 Stainless Steel	Monel 18-8 Stainless Steel	Monel 18-8 Stainless Steel	AVOID	Monel 18-8 Stainless Steel	Monel 18-8 Stainless Steel	Monel 18-8 Stainless Steel	Monel 18-8 Stainless Steel	Monel 18-8 Stainless Steel	Monel 18-8 Stainless Steel	Monel

TABLE 5-7. (Continued)

BELOW WATERLINE

Trim Material to be Attached

Hull Superstructure or Base Plate Material	Wood	Fiberglass	Rubber	Plastic (Nylon)	Aluminum	Steel	Steel (Galvanized)	Copper	Brass	Brass (Plated)	Nickel Stainless Steel	Monel Nickel-Copper Alloys
Wood	Monel Silicon Bronze	Monel Silicon Bronze	Monel Silicon Bronze	Monel Silicon Bronze	NOT RECOMMENDED	Monel Silicon Bronze 18-8 Stainless Steel	Monel Silicon Bronze 18-8 Stainless Steel	Monel Silicon Bronze 18-8 Stainless Steel	Monel Silicon Bronze 18-8 Stainless Steel	Monel Silicon Bronze 18-8 Stainless Steel	T-316 Stainless Steel[a]	Monel
Fiberglass	Monel Silicon Bronze	Monel Silicon Bronze	Monel Silicon Bronze	Monel Silicon Bronze	NOT RECOMMENDED	Monel Silicon Bronze 18-8 Stainless Steel	Monel Silicon Bronze 18-8 Stainless Steel	Monel Silicon Bronze 18-8 Stainless Steel	Monel Silicon Bronze 18-8 Stainless Steel	Monel Silicon Bronze 18-8 Stainless Steel	T-316 Stainless Steel	Monel
Rubber	Monel Silicon Bronze	Monel Silicon Bronze	Monel Silicon Bronze	Monel Silicon Bronze	NOT RECOMMENDED	Monel Silicon Bronze 18-8 Stainless Steel	Monel Silicon Bronze 18-8 Stainless Steel	Monel Silicon Bronze 18-8 Stainless Steel	Monel Silicon Bronze 18-8 Stainless Steel	Monel Silicon Bronze 18-8 Stainless Steel	T-316 Stainless Steel	Monel
Plastic (Nylon)	Monel Silicon Bronze	Monel Silicon Bronze	Monel Silicon Bronze	Monel Silicon Bronze	NOT RECOMMENDED	Monel Silicon Bronze 18-8 Stainless Steel	Monel Silicon Bronze 18-8 Stainless Steel	Monel Silicon Bronze 18-8 Stainless Steel	Monel Silicon Bronze 18-8 Stainless Steel	Monel Silicon Bronze 18-8 Stainless Steel	T-316 Stainless Steel	Monel
Aluminum	18-8 Stainless Steel Aluminum	18-8 Stainless Steel Aluminum	18-8 Stainless Steel Aluminum	18-8 Stainless Steel Aluminum	T-316 Stainless Steel Aluminum	NOT RECOMMENDED	NOT RECOMMENDED	NOT RECOMMENDED	NOT RECOMMENDED	NOT RECOMMENDED	T-316 Stainless Steel	NOT RECOMMENDED
Steel	Monel Silicon Bronze 18-8 Stainless Steel	Monel Silicon Bronze 18-8 Stainless Steel	Monel Silicon Bronze 18-8 Stainless Steel	Monel Silicon Bronze 18-8 Stainless Steel	NOT RECOMMENDED	Monel Silicon Bronze 18-8 Stainless Steel	Monel Silicon Bronze 18-8 Stainless Steel	Monel Silicon Bronze 18-8 Stainless Steel	Monel Silicon Bronze 18-8 Stainless Steel	Monel Silicon Bronze 18-8 Stainless Steel	T-316 Stainless Steel	Monel
Steel (Galvanized)	Monel Silicon Bronze 18-8 Stainless Steel	Monel Silicon Bronze 18-8 Stainless Steel	Monel Silicon Bronze 18-8 Stainless Steel	Monel Silicon Bronze 18-8 Stainless Steel	NOT RECOMMENDED	Monel Silicon Bronze 18-8 Stainless Steel	Monel Silicon Bronze 18-8 Stainless Steel	Monel Silicon Bronze 18-8 Stainless Steel	Monel Silicon Bronze 18-8 Stainless Steel	Monel Silicon Bronze 18-8 Stainless Steel	T-316 Stainless Steel	Monel
Copper	Monel Silicon Bronze 18-8 Stainless Steel	Monel Silicon Bronze 18-8 Stainless Steel	Monel Silicon Bronze 18-8 Stainless Steel	Monel Silicon Bronze 18-8 Stainless Steel	NOT RECOMMENDED	Monel Silicon Bronze 18-8 Stainless Steel	Monel Silicon Bronze 18-8 Stainless Steel	Monel Silicon Bronze 18-8 Stainless Steel	Monel Silicon Bronze 18-8 Stainless Steel	Monel Silicon Bronze 18-8 Stainless Steel	T-316 Stainless Steel	Monel
Brass	Monel Silicon Bronze 18-8 Stainless Steel	Monel Silicon Bronze 18-8 Stainless Steel	Monel Silicon Bronze 18-8 Stainless Steel	Monel Silicon Bronze 18-8 Stainless Steel	NOT RECOMMENDED	Monel Silicon Bronze 18-8 Stainless Steel	Monel Silicon Bronze 18-8 Stainless Steel	Monel Silicon Bronze 18-8 Stainless Steel	Monel Silicon Bronze 18-8 Stainless Steel	Monel Silicon Bronze 18-8 Stainless Steel	T-316 Stainless Steel	Monel
Brass (Plated)	Monel Silicon Bronze 18-8 Stainless Steel	Monel Silicon Bronze 18-8 Stainless Steel	Monel Silicon Bronze 18-8 Stainless Steel	Monel Silicon Bronze 18-8 Stainless Steel	NOT RECOMMENDED	Monel Silicon Bronze 18-8 Stainless Steel	Monel Silicon Bronze 18-8 Stainless Steel	Monel Silicon Bronze 18-8 Stainless Steel	Monel Silicon Bronze 18-8 Stainless Steel	Monel Silicon Bronze 18-8 Stainless Steel	T-316 Stainless Steel	Monel
Nickel Stainless Steel	T-316 Stainless Steel[a]	T-316 Stainless Steel[a]	T-316 Stainless Steel[a]	T-316 Stainless Steel[a]	T-316 Stainless Steel[a]	T-316 Stainless Steel	T-316 Stainless Steel	T-316 Stainless Steel	T-316 Stainless Steel	T-316 Stainless Steel	Monel[b]	Monel[b]
Monel Nickel-Copper Alloys	Monel	Monel	Monel	Monel	NOT RECOMMENDED	Monel	Monel	Monel	Monel	Monel	Monel[b]	Monel

No recommendation. These metal combinations are subject to severe galvanic effects when immersed in seawater and can be expected to give poor performance.

(a) Crevice corrosion can lead to early failure and high replacement rate of stainless fasteners for these combinations. Other fasteners material are subject to adverse galvanic corrosion.

(b) For stainless to stainless, a Monel fastener carefully insulated from stainless should give satisfactory service.

Effects of corrosive action on fastener alloys: Monel - develops grey-green corrosion film. 18-8 Stainless Steel - develops light brown corrosion film and heavier scaling in crevices, i.e., threads and under boltheads. Some bleeding. Silicon bronze - develops heavy green-brown corrosion film. Bleeds. Aluminum - develops white powdery corrosion film interspersed with pits unless specially protected. Limited usefulness.

TABLE 5-8. SUMMARY OF SHEATHING FASTENERS[10]

Alloy	Period, years	Mechanical Properties	Corrosion Properties
Duranickel Alloy 301	15	OK	Excellent
Monel Ni-Cu Alloy 400	25	OK	Excellent
Monel Ni-Cu Alloy K-500	25	OK	Excellent
Type 305 SS	15	OK	Excellent
Type 316 SS	25	OK	Excellent
Type 410 SS	15	OK	Good
Type 431 SS	15	OK	Excellent
Inconel Alloy X-750	25	OK	Excellent

TABLE 5-9. EFFECT OF 60 DAYS OF ALTERNATE IMMERSION IN 3.5% NaCl ON THE TENSILE STRENGTH OF HIGH TEMPERATURE MATERIALS (PRECRACKED SPECIMENS)[11]

Alloy	Room Temperature, F_{tu}[a]		F_{tu}[a] After Alternate Immersion		Percent of Room Temperature Strength
	MN/m^2	ksi	MN/m^2	ksi	
Inconel 718	1369	198.7	1305	189.3	95
			1309	189.8	96
Rene' 41	1061	154	859.1	124.6	81
			885.3	128.4	83
L605	1001	145.3	620.6	90	62
			661.9	96	66
Haynes 188	923.9	134	732.3	106.2	79
			706.7	102.5	77
Hastelloy X	813.3	119	596.4	86.5	73
			597.1	86.6	73
TDNi Cr	725.5	105.3	660.5	95.8	91
			666.1	96.6	92

(a) F_{tu} = ultimate tensile strength.

TABLE 5-10. STRESS-CORROSION CRACKING TEST RESULTS[12]

Material Form	Condition	Stress Direction	Applied Stress ksi	Applied Stress % YS	Failure Ratio	Days to Failure	% Loss in TS
			Hastelloy C				
Sheet (0.063" thick)	Solution Treated	Long	43	75	0/3	--	--
	Solution Treated	Trans	43	75	0/3	--	--
Sheet (0.110" thick)	As Welded	--	0	0	--	--	7
		Face	60	50[b]	0/4	--	6
		Root	60	50[b]	0/4	--	10
Tube (1-1/4" dia x 0.058" wall)	Solution Treated	Trans (C-ring)[a]	30	50	0/3	--	--
			45	75	0/3	--	--
			60	100	0/3	--	--
			Inconel 718				
Bar (3/4" dia)	Aged 18 hours	Trans (C-ring)[a]	44	25	0/3	--	--
			88	50	0/3	--	--
			132	75	0/3	--	--
			175	100	0/3	--	--
Bar (1" dia)	Aged 19 hours	Long	103	75	0/3	--	N[c]
		Trans (C-ring)[a]	35	23	0/3	--	--
			69	50	0/3	--	--
			103	75	0/3	--	--
			138	100	0/3	--	--

(a) Load calculations were based on longitudinal rather than transverse yield strength.
(b) Load calculations were based on 50 percent of the weld tensile strength.
(c) N = negligible change in tensile properties.

TABLE 5-11. CORROSION OF NICKEL AND ITS ALLOYS[16]

Check indicates type of attack observed

Alloy			Seawater Total Immersion		Rate[c]		Maximum Depth[d]		Corrosion					Maximum Depth Rate /Year[d]	
									Principal Type						
Name	UNS	Source of Data[a]	Condition[b]	Time	mpy	um/y	mils	um	General	Pitting	Crevice	Outside Crevice	Edges	mils	um
Nickel 200	N02200	Key West, FL*	Quiescent	575 days	0.05	17	81	2057	—	—	✓	✓	Severe	51.4	1306
Nickel 200	N02200	Panama, Canal Zone**	Quiescent	16 yr	1.4	35.6	192P	4879	—	✓	—	—	—	12	305
Nickel 200	N02200	Harbor Island, NC***	Quiescent	?	13-60	330-1524	—	—	—	✓	—	—	—	60	1524
Nickel 200	N02200	Harbor Island, NC***	Quiescent	?	0-0.8	20.3	—	—	✓	—	—	—	—	—	—
Monel 400	N04400	Key West, FL*	Quiescent	575 days	0.07	2	17	432	—	—	✓	✓	—	10.8	274
Monel 400	N04400	Panama, Canal Zone**	Quiescent	16 yr	0.3	7.6	82	2083	—	✓	—	—	—	5.1	130
Monel 400	N04400	Harbor Island, NC***	Quiescent	?	0-18	0-457	—	—	—	✓	—	—	—	18	457
Monel 400	N04400	Harbor Island, NC***	Quiescent	?	0-1	0-25.4	—	—	✓	—	—	—	—	—	—
Monel K500	N05500	Key West, FL*	Quiescent	575 days	0.02	0.6	4	102	—	—	✓	✓	—	2.5	64
Inconel 600	N06600	Key West, FL*	Quiescent	575 days	0.25	6.4	18	452	—	—	Severe	✓	—	11.4	290
Inconel 617	—	Key West, FL*	Quiescent	575 days	0	0	0	0	—	—	—	—	—	0	0
Inconel 625	N06625	Key West, FL*	Quiescent	576 days	0.004	0.1	0	0	—	—	—	—	—	0	0
Inconel 706	N09706	Key West, FL*	Quiescent	575 days	0.63	16	50	1270	—	—	✓	—	✓	31.7	805
Inconel 718	N07718	Key West, FL*	Quiescent	575 days	0.15	3.7	32	813	—	—	✓	—	Slight	20.3	516
Alloy 20 Cb-3	N08020	Key West, FL*	Quiescent	575 days	0.04	1.1	12	305	—	—	✓	—	✓	7.6	193
Alloy 20 Cb-3	N08020	Harbor Island, NC***	?	?	0-10	0-254	—	—	—	✓	—	—	—	10	254
Incoloy 800	N08800	Key West, FL*	Quiescent	575 days	0.24	6.2	95P	2413P	—	—	✓	—	—	60.3	1532
Incoloy 825	N08825	Key West, FL*	Quiescent	575 days	0	0	9	229	—	—	✓	—	—	5.7	145
Incoloy 825	N08825	Harbor Island, NC***	Quiescent	?	0-10	0-254	—	—	—	✓	—	—	—	10	254
Hastelloy C276	N10276	Key West, FL*	Quiescent	576 days	0.004	0.1	0	0	—	—	—	—	—	0	0

TABLE 5-11. (Continued)

Alloy			Seawater Total Immersion		Corrosion										
					Rate[c]		Maximum Depth[d]		Principal Type					Maximum Depth Rate /Year[d]	
Name	UNS	Source of Data[a]	Condition[b]	Time	mpy	µm/y	mils	µm	General	Pitting	Crevice	Outside Crevice	Edges	mils	µm
Velocity Conditions:															
Nickel 200	N02200	Key West, FL*	0.75 fps (0.23 m/s)	574 days	2.7	67.8	108P	2743P	—	—	✓	✓	Very Severe	68.7	1745
Nickel 200	N02200	Harbor Island, NC***	20-120 fps (6.1-36.6 m/s)	?	0 to 1	0 to 25.4	—	—	✓	—	—	—	—	—	—
Monel 400	N04400	Key West, FL*	0.75 fps (0.23 m/s)	574 days	0.30	7.5	61P	1550P	—	—	✓	—	✓	38.8	986
Monel 400	N04400	Harbor Island, NC***	<3.0 fps (<0.93 m/s)	?	—	—	—	—	—	✓ Maybe	—	—	—	—	—
Monel 400	N04400	Harbor Island, NC***	6-15 fps (1.2-4.7 m/s)	?	<1	<25	—	—	✓	—	—	—	—	—	—
Monel 400	N04400	Harbor Island, NC***	20-120 fps (6.1-36.6 m/s)	?	0 to<1	0 to<25	—	—	✓	—	—	—	—	—	—
Monel K500	N05500	Key West, FL*	0.75 fps (0.23 m/s)	574 days	0.09	2.4	12	305	—	—	✓	✓	✓	7.6	193
Inconel 600	N06600	Key West, FL*	0.75 fps (0.23 m/s)	574 days	0.9	22.8	64P	1626P	—	—	✓	—	✓	40.7	1034
Inconel 617	—	Key West, FL*	0.75 fps (0.23 m/s)	574 days	0.008	0.2	7	178	—	—	✓	—	—	4.4	112
Inconel 625	N06625	Key West, FL*	0.75 fps (0.23 m/s)	574 days	0	0	2	51	—	—	—	✓	—	1.3	33
Inconel 706	N09706	Key West, FL*	0.75 fps (0.23 m/s)	574 days	1	25.4	62P	1575P	—	—	✓	✓	✓ & Tunneling	39.4	1001
Alloy 20 Cb-3	N08020	Key West, FL*	0.75 fps (0.23 m/s)	574 days	0.12	3.1	66	1676	—	—	✓	—	—	42	1067
Incoloy 800	N08800	Key West, FL*	0.75 fps (0.23 m/s)	574 days	0.68	17.2	95P	2413P	—	—	✓	—	—	60.4	1534
Incoloy 825	N08825	Key West, FL*	0.75 fps (0.23 m/s)	574 days	0.1	2.5	63	1600	—	—	✓	—	—	40	1016
Hastelloy C276	N10276	Key West, FL*	0.75 fps (0.23 m/s)	575 days	0.008	0.2	1	25	—	—	—	✓	—	<1	<25

(a) Source of data: *, T. J. Lennox, Jr. and M. H. Peterson, NRL, unpublished data; **, C. R. Southwell and J. D. Bultman, NRL Report 7834, January 2, 1975; and ***, F. L. LaQue, "Marine Corrosion", John Wiley & Sons, New York (1975).
(b) fps = feet per second; m/s = meters per second; and 1 ft = 0.305 meters.
(c) mpy = mils penetration per year; and µm/y = micrometers penetration per year.
(d) 1 mil = 0.001 inch = 25.4 µm.

pitting rate can range up to 50 mpy. However, as shown by Southwell and Alexander[1] in Figure 5-3 most of the deep pitting attack occurs within the first year or so, and the depth of penetration of the deepest pits increases very little during subsequent exposure.

Alloying improves the resistance of nickel to pitting. Alloy 400 (66Ni-32Cu-2Fe) is more resistant to pitting in seawater than is unalloyed nickel, although Alloy 400 (Monel B and C) does pit as shown in Figure 5-3. The major application of Alloy 400 is in the splash zone where it performs very well.

As with the stainless steels, the major alloying elements in nickel that impart resistance to pitting in seawater are chromium and molybdenum. And, as with the stainless steels, the chromium alloys are subject to pitting while the most resistant alloys are those that contain molybdenum in addition to chromium. Boyd and Fink[3] have ranked the relative seawater corrosion resistance of the nickel alloys in Table 5-12. This ranking is based on data such as

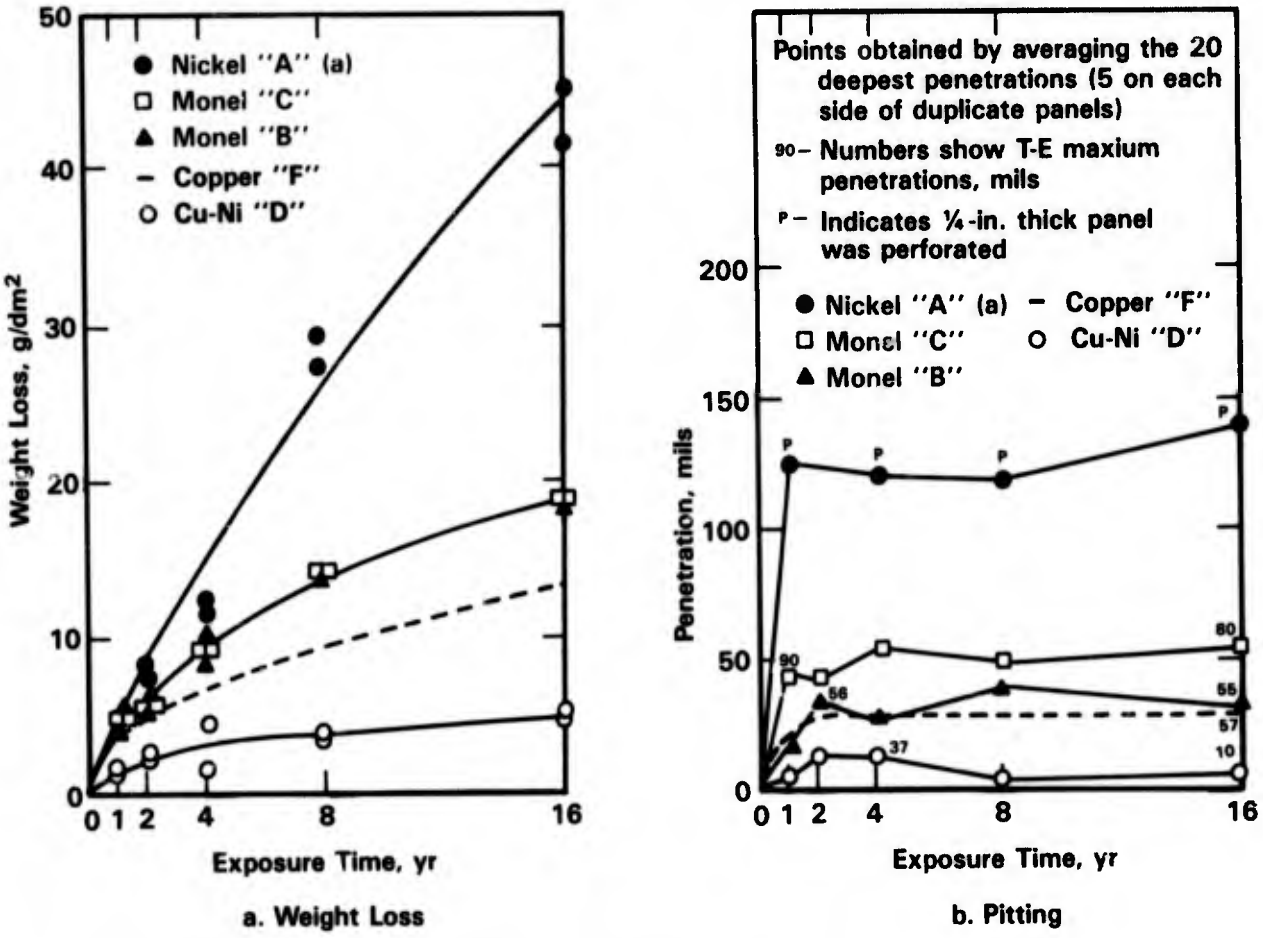

FIGURE 5-3. WEIGHT-LOSS AND PITTING AS A FUNCTION OF TIME FOR NICKEL AND NICKEL-COPPER ALLOYS CONTINUOUSLY IMMERSED IN TROPICAL SEAWATER[1]

(a) Symbols refer to alloys in Table 5-1.

TABLE 5-12. CLASSIFICATION OF NICKEL ALLOYS WHICH MAY FIND SPECIAL APPLICATION IN MARINE ENVIRONMENTS[3]

Alloy	Composition, weight percent	Remarks
	Class I: Most Resistant	
Hastelloy C	57Ni-16Cr-17Mo plus Fe, W, Co	Completely resistant except at welds.
Hastelloy C-276	57Ni-16Cr-17Mo plus Fe, W, Co	Low carbon (<0.02 C) can be welded.
Inconel 625	61Ni-22Cr-9Mo plus Fe, Cb	Approaches Hastelloy C in total resistance.
MP35N	35Ni-35Co-20Cr-10Mo	Excellent, so far, in preliminary experiments.
Chlorimet-3	60Ni-18Cr-18Mo plus Fe, Si	Cast alloy; excellent for pumps, etc.
Rene' 41	56Ni-11Co-19Cr-10Mo-3.1Ti	Good-to-excellent resistance to pitting.
Hastelloy X	52Ni-22Cr-9Mo-19Fe plus W, Co	Good-to-excellent resistance to pitting.
	Class II: Very Resistant	
Hastelloy F	46Ni-22Cr-7Mo-21Fe	
Hastelloy G	45Ni-21Cr-7Mo-20Fe-2Cu-25Co	Usually satisfactory; molybdenum content provides resistance to pitting.
Illium R	68Ni-21Cr-5Mo-3Cu	
Inconel 700	45Ni-28Co-15Cr-4Mo plus Ti, Al	
Elgiloy	15Ni-40Co-20Cr-7Mo-15Fe-2Mn	
Inconel 718	53Ni-19Cr-3Mo-18Fe plus Co, Ti, Al	
	Class III: Resistant, Some Pitting	
Inconel 600	76Ni-16Cr-7Fe	
Inconel X750	73Ni-15Cr-7Fe plus Cb, Ti, Al	
Incoloy 800	32Ni-21Cr-46Fe	May be some pitting at sites where seawater is stagnant.
Incoloy 825	42Ni-22Cr-30Fe-3Mo-2Cu	
Monel-400	66Ni-32Cu-2Fe	
Monel-K500	65Ni-30Cu-1Fe-3Al	

those presented in Tables 5-1, 5-11, 5-13, 5-14, and 5-15, and reflects the importance of increasing molybdenum content in the alloys on their resistance to pitting and crevice attack. Note in Table 5-13 that Alloys 600, 706, and 800, which do not contain molybdenum, exhibited deep crevice attack that ranged from 457 to 2,413 μm in 575 days' exposure at Key West, Florida; Alloys 718, 825, and 20Cb3, which contain 2 to 3 percent molybdenum, exhibited less crevice corrosion (229 to 813 μm) in these same exposures; whereas, Alloys 617, 625, and C-276 that contain 9 to 16 percent molybdenum exhibited no crevice attack in these tests. Kain[20] also observed no crevice attack in Alloy 625 or in an 18Cr-18Mo alloy in multiple crevice tests conducted for 90 days.

Temperature. As pointed out elsewhere, temperature can have different effects on corrosion, depending upon its effect on the environment. If it does not affect the environment, then the usual effect of increasing the temperature is to increase the rate of attack. However, increasing the temperature can reduce the amount of dissolved oxygen in the seawater, decompose bicarbonates to form insoluble carbonate scales, or kill biological species. All of these latter effects would tend to reduce the corrosion attack.

Tipton and Kain[21] have shown that weight losses for Alloy 400 in seawater reach a maximum at 30 C and drop to very low values at 50 C (see Figure 5-4); whereas in this same exposure, pit depths were greatest at 18 C and decreased to negligible values at 50 C (see Figure 5-5). Asphahani, et al.[22] report that Alloy G exhibits a maximum in depth of crevice attack at 28 C. In 30-day tests the average crevice attack for Alloy G was 0.03 mm at 12 C, 0.05 mm at 28 C, and 0 mm at 50 C.

In studying Alloy 825, Hodgkiess and Rigas[23] found no crevice corrosion after 31 weeks' exposure at 25 and 60 C, but did observe crevice corrosion after 20 weeks' exposure at 100 C. Temperature had no effect on crevice corrosion or general corrosion of C-276 in tests reported by Asphahani, et al.[22] Note in Table 5-16 that no crevice attack was observed in C-276 over the temperature range of 35 to 107 C; and in Table 5-17 that temperature had no effect on the corrosion rate over the range of 10 to 288 C.

Aeration. The principal studies on the effect of aeration have been conducted as part of the deep sea exposures by Reinhart and co-workers.[19,24,25] General corrosion rate results for a number of the nickel-base alloys are presented in Figures 5-6, 5-7, and 5-8. Note that for the conventional alloys, the general corrosion rate increases with increasing oxygen content in the seawater over the range of 0.4 to 5.8 ml O_2/l seawater. Also note that for most of the alloys, the general corrosion rates are <1 mpy even at the highest oxygen level of 5.8 ml/l. However, from the data presented in Table 5-15 it should be noted that several of

TABLE 5-13. NICKEL AND NICKEL ALLOYS; CORROSION DATA AND CHARACTERISTICS[17]

575 Days - Quiescent Seawater Immersion; Key West, FL

Alloy	Corrosion Depth, μm[a] Crevice Areas Maximum	Crevice Areas Mean	Other Areas Maximum	Other Areas Mean	Rate, μmpy[b]	Remarks
Unalloyed Nickel	2057	1099	457	152	16.6	Severe edge corrosion.
Monel 400	432	297	279	152	1.8	Edge corrosion.
Monel 500	51	38	102	61	0.6	Etched all surfaces.
Alloy 600	457	300	152	53	6.4	Entire crevice corroded.
Alloy 617	0	0	0	0	0	Light rust stain near crevice.
Alloy 625	0	0	0	0	0.1	Light rust stain near crevice.
Alloy 706	1270	892	0	0	16.0	Striated corrosion in crevice, edge corrosion, local etching.
Alloy 718	813	457	0	0	3.7	Light etch and edge corrosion.
20Cb3	305	191	0	0	1.1	Edge corrosion.
Alloy 800	2413 TP[c]	--	--	--	6.2	Etch pits outside crevice.
Alloy 825	229	110	76	45	0	Deepest crevice corrosion at nylon mounting nut.
C-276	0	0	0	0	0.1	Very light etch some areas.
304	1473 TP[c]	--	0	0	6.8	

(a) μm = micrometers; 1 μm ≈0.04 mils ≈0.00004 inches.
(b) μmpy = micrometers penetration per year; based on mass loss.
(c) TP = thickness penetrated.

TABLE 5-14. THE SUSCEPTIBILITY OF VARIOUS NICKEL ALLOYS TO PITTING CORROSION AFTER IMMERSION IN STAGNANT SEAWATER FOR 3 YEARS AT THE INCO TEST FACILITY AT HARBOR ISLAND, U.S.A.[18]

Material	Maximum Pit Depth After 3 Years, in.
Inconel Alloy 625	0.000
Incoloy Alloy 825	0.001
Monel Alloy K-500	0.034
Monel Alloy 400	0.042
Stainless steel Type EN58J	0.062
Mild steel	0.070

TABLE 5-15. CORROSION RATES AND TYPES OF CORROSION OF NICKEL ALLOYS IN THE PACIFIC OCEAN OFF PORT HUENEME, CA[19]

Alloy	Environment[a]	Exposure, days	Depth, feet	Corrosion Rate,[b] mpy	Corrosion Crevice, mils		Type of Corrosion[c]
Ni-Cr-Fe 600	W	123	5,640	<0.1	4		C
Ni-Cr-Fe 600	S	123	5,640	<0.1	3		C
Ni-Cr-Fe 600	W	403	6,780	0.1	23		C
Ni-Cr-Fe 600	S	403	6,780	0.3		--	I, C
Ni-Cr-Fe 600	W	751	5,640	<0.1	33		C
Ni-Cr-Fe 600	S	751	5,640	<0.1	4		C, P
Ni-Cr-Fe 600	W	1,064	5,300	0.1	35	(PR)[c]	C
Ni-Cr-Fe 600	S	1,064	5,300	<0.1	2		C
Ni-Cr-Fe 600	W	1,064	5,300	0.5	51		C, P
Ni-Cr-Fe 600	W	197	2,340	0.2	15		C
Ni-Cr-Fe 600	S	197	2,340	0.1	10		C
Ni-Cr-Fe 600	W	402	2,370	0.0		--	SL, ET
Ni-Cr-Fe 600	W	402	2,370	0.1	28		C
Ni-Cr-Fe 600	W	402	2,370	0.0		--	I, P
Ni-Cr-Fe 600, welded, 132 electrode	W	402	2,370	0.3		--	ET[f]
Ni-Cr-Fe 600, welded, 182 electrode	W	402	2,370	<0.1		--	ET
Ni-Cr-Fe 600, welded, 62 electrode	W	402	2,370	0.4		--	(g)
Ni-Cr-Fe 600, welded, 82 electrode	W	402	2,370	0.3		--	(h)
Ni-Cr-Fe 600	S	402	2,370	0.0		--	ET
Ni-Cr-Fe 600	S	402	2,370	0.1		--	T to PR, 125
Ni-Cr-Fe 600	S	402	2,370	<0.1		--	I, C
Cast, Ni-Cr-Fe 610	W	123	5,640	0.3	4		C
Cast, Ni-Cr-Fe 610	S	123	5,640	0.1	2		C
Cast, Ni-Cr-Fe 610	W	403	6,780	<0.1		--	I, C
Cast, Ni-Cr-Fe 610	S	403	6,780	0.1		--	I, C
Cast, Ni-Cr-Fe 610	W	751	5,640	0.6	83		C
Cast, Ni-Cr-Fe 610	S	751	5,640	0.3	5		C
Cast, Ni-Cr-Fe 610	W	1,064	5,300	0.9		--	I, P
Cast, Ni-Cr-Fe 610	S	1,064	5,300	<0.1	13		C
Cast, Ni-Cr-Fe 610	W	197	2,340	0.2	2		C
Cast, Ni-Cr-Fe 610	S	197	2,340	<0.1	3		C
Cast, Ni-Cr-Fe 610	W	402	2,370	0.3	18		C
Cast, Ni-Cr-Fe 610	S	402	2,370	<0.1		--	I, C
Ni-Cr-Fe X750	W	123	5,640	<0.1		--	NC
Ni-Cr-Fe X750	S	123	5,640	<0.1		--	NC
Ni-Cr-Fe X750	W	403	6,780	0.2	35	(PR)	C
Ni-Cr-Fe X750	S	403	6,780	<0.1	3		C

TABLE 5-15. (Continued)

Alloy	Environment[a]	Exposure, days	Depth, feet	Corrosion Rate,[b] mpy	Corrosion Crevice, mils	Type of Corrosion[c]
Ni-Cr-Fe X750	W	751	5,640	0.4	40 (PR)	C
Ni-Cr-Fe X750	S	751	5,640	<0.1	--	NC
Ni-Cr-Fe X750	W	1,064	5,300	0.1	40 (PR)	C, P to 25m
Ni-Cr-Fe X750	W	1,064	5,300	0.1	47	C
Ni-Cr-Fe X750	S	1,064	5,300	<0.1	9	C
Ni-Cr-Fe X750	W	197	2,340	0.4	18	C
Ni-Cr-Fe X750	S	197	2,340	<0.1	7	C
Ni-Cr-Fe X750	W	402	2,370	0.1	17	C
Ni-Cr-Fe X750	W	402	2,370	0.1	--	T
Ni-Cr-Fe X750, welded, 69 electrode	W	402	2,370	0.3	--	ET
Ni-Cr-Fe X750, welded, 718 electrode	W	403	2,370	0.2	--	(i)
Ni-Cr-Fe X750	S	402	2,370	<0.1	--	ET
Ni-Cr-Fe X750	S	402	2,370	<0.1	4	C
[illegible]i-Cr-Fe 718	W	402	2,370	<0.1	--	NC
Ni-Cr-Fe 718, welded, 718 electrode	W	402	2,370	0.0	--	NC
Ni-Cr-Fe 88	W	123	5,640	0.1	4	C
Ni-Cr-Fe 88	S	123	5,640	0.1	--	NC
Ni-Cr-Fe 88	W	403	6,780	<0.1	5	C
Ni-Cr-Fe 88	S	403	6,780	<0.1	--	NC
Ni-Cr-Fe 88	W	751	5,640	<0.1	--	I, C
Ni-Cr-Fe 88	S	751	5,640	1.3	--	(j)
Ni-Cr-Fe 88	W	1,064	5,300	<0.1	67	C
Ni-Cr-Fe 88	S	1,064	5,300	<0.1	5	C
Ni-Cr-Fe 88	W	197	2,340	0.3	17	C, P
Ni-Cr-Fe 88	S	197	2,340	<0.1	--	I, C
Ni-Cr-Fe 88	W	402	2,370	0.4	52	C, P
Ni-Cr-Fe 88	S	402	2,370	<0.1	--	I, C
Ni-Cr-Mo 3	W	123	5,640	<0.1	--	NC
Ni-Cr-Mo 3	S	123	5,640	<0.1	--	NC
Ni-Cr-Mo 3	W	403	6,780	<0.1	--	NC
Ni-Cr-Mo 3	S	403	6,780	<0.1	--	NC
Ni-Cr-Mo 3	W	751	5,640	<0.1	--	NC
Ni-Cr-Mo 3	S	751	5,640	<0.1	--	NC
Ni-Cr-Mo 3	W	1,064	5,300	<0.1	--	NC
Ni-Cr-Mo 3	S	1,064	5,300	<0.1	--	NC
[illegible]i-Cr-Mo 3	W	197	2,340	<0.1	--	NC
[illegible]i-Cr-Mo 3	S	197	2,340	<0.1	--	NC

TABLE 5-15. (Continued)

Alloy	Environment[a]	Exposure, days	Depth, feet	Corrosion Rate,[b] mpy	Corrosion Crevice, mils	Type of Corrosion[c]
Ni-Cr-Mo 3	W	402	2,370	<0.1	--	NC
Ni-Cr-Mo 3	S	402	2,370	<0.1	--	NC
Ni-Cr-Mo 625	W	402	2,370	<0.1	--	NC
Ni-Cr-Mo 625	S	402	2,370	<0.1	--	NC
Ni-Co-Cr 700	W	123	5,640	<0.1	--	NC
Ni-Co-Cr 700	S	123	5,640	<0.1	--	NC
Ni-Co-Cr 700	W	403	6,780	<0.1	--	NC
Ni-Co-Cr 700	S	403	6,780	<0.1	--	NC
Ni-Co-Cr 700	W	751	5,640	<0.1	--	NC
Ni-Co-Cr 700	S	751	5,640	<0.1	--	NC
Ni-Co-Cr 700	W	1,064	5,300	<0.1	--	NC
Ni-Co-Cr 700	S	1,064	5,300	<0.1	--	I, C
Ni-Co-Cr 700	W	197	2,340	<0.1	--	NC
Ni-Co-Cr 700	S	197	2,340	<0.1	--	NC
Ni-Co-Cr 700	W	402	2,370	<0.1	--	I, C
Ni-Co-Cr 700	S	402	2,370	<0.1	--	I, C
Ni-Fe-Cr 800	W	123	5,640	<0.1	--	NC
Ni-Fe-Cr 800	S	123	5,640	<0.1	--	NC
Ni-Fe-Cr 800	W	403	6,780	<0.1	--	NC
Ni-Fe-Cr 800	S	403	6,780	<0.1	1	C
Ni-Fe-Cr 800	W	751	5,640	<0.1	--	NC
Ni-Fe-Cr 800	S	751	5,640	<0.1	--	NC
Ni-Fe-Cr 800	W	1,064	5,300	<0.1	--	NC
Ni-Fe-Cr 800	S	1,064	5,300	<0.1	6	C
Ni-Fe-Cr 800	W	197	2,340	<0.1	--	NC
Ni-Fe-Cr 800	S	197	2,340	<0.1	--	NC
Ni-Fe-Cr 800	W	402	2,370	<0.1	--	NC
Ni-Fe-Cr 800	W	402	2,370	0.0	--	NC
Ni-Fe-Cr 800, welded, 82 electrode	W	402	2,370	<0.1	--	(k)
Ni-Fe-Cr 800, welded, 138 electrode	W	402	2,370	<0.1	--	(l)
Ni-Fe-Cr 800	S	402	2,370	<0.1	--	ET
Ni-Fe-Cr 800	S	402	2,370	<0.1	--	I, C
Ni-Fe-Cr 804	W	123	5,640	<0.1	--	NC
Ni-Fe-Cr 804	S	123	5,640	<0.1	--	NC
Ni-Fe-Cr 804	W	403	6,780	<0.1	--	I, C
Ni-Fe-Cr 804	S	403	6,780	<0.1	--	I, C

TABLE 5-15. (Continued)

Alloy	Environment[a]	Exposure, days	Depth, feet	Corrosion Rate,[b] mpy	Corrosion Crevice, mils	Type of Corrosion[c]
Ni-Fe-Cr 804	W	751	5,640	<0.1	--	NC
Ni-Fe-Cr 804	S	751	5,640	<0.1	--	I, C
Ni-Fe-Cr 804	W	1,064	5,300	<0.1	--	I, C
Ni-Fe-Cr 804	S	1,064	5,300	<0.1	--	I, C
Ni-Fe-Cr 804	W	197	2,340	<0.1	--	I, C
Ni-Fe-Cr 804	S	197	2,340	<0.1	--	I, C
Ni-Fe-Cr 804	W	402	2,370	<0.1	--	I, C
Ni-Fe-Cr 804	S	402	2,370	<0.1	--	I, C
Ni-Fe-Cr 825	W	123	5,640	0.0	--	NC
Ni-Fe-Cr 825	W	123	5,640	<0.1	--	NC
Ni-Fe-Cr 825	S	123	5,640	<0.1	--	NC
Ni-Fe-Cr 825	W	403	6,780	0.0	--	NC
Ni-Fe-Cr 825	W	403	6,780	<0.1	--	I, C
Ni-Fe-Cr 825	S	403	6,780	0.0	--	NC
Ni-Fe-Cr 825	S	403	6,780	<0.1	--	I, C
Ni-Fe-Cr 825	W	751	5,640	0.0	22	C
Ni-Fe-Cr 825	W	751	5,640	<0.1	--	NC
Ni-Fe-Cr 825	S	751	5,640	<0.1	--	NC
Ni-Fe-Cr 825	W	1,064	5,300	<0.1	--	I, C
Ni-Fe-Cr 825	S	1,064	5,300	<0.1	--	NC
Ni-Fe-Cr 825	W	197	2,340	0.0	--	NC
Ni-Fe-Cr 825	W	197	2,340	<0.1	--	I, C
Ni-Fe-Cr 825	S	197	2,340	0.0	8	C
Ni-Fe-Cr 825	S	197	2,340	<0.1	--	NC
Ni-Fe-Cr 825	W	402	2,370	<0.1	15	C
Ni-Fe-Cr 825	W	402	2,370	<0.1	--	ET; I, C
Ni-Fe-Cr 825, welded, 135 electrode	W	402	2,370	<0.1	--	(m)
Ni-Fe-Cr 825, welded, 65 electrode	W	402	2,370	<0.1	--	NC
Ni-Fe-Cr 825	S	402	2,370	0.0	8	C
Ni-Fe-Cr 825	S	402	2,370	<0.1	--	NC; I, C
Ni-Fe-Cr 825S[d]	W	123	5,640	<0.1	--	NC
Ni-Fe-Cr 825S	S	123	5,640	<0.1	--	NC
Ni-Fe-Cr 825S	W	403	6,780	<0.1	--	I, C
Ni-Fe-Cr 825S	S	403	6,780	<0.1	--	I, C
Ni-Fe-Cr 825S	W	751	5,640	<0.1	--	I, C
Ni-Fe-Cr 825S	S	751	5,640	<0.1	--	NC
Ni-Fe-Cr 825S	W	1,064	5,300	<0.1	--	NC
Ni-Fe-Cr 825S	S	1,064	5,300	<0.1	4	C

TABLE 5-15. (Continued)

Alloy	Environment[a]	Exposure, days	Depth, feet	Corrosion Rate,[b] mpy	Corrosion Crevice, mils	Type of Corrosion[c]
Ni-Fe-Cr 825S	W	197	2,340	<0.1	--	I, C; I, P
Ni-Fe-Cr 825S	S	197	2,340	<0.1	--	I, C; I, P
Ni-Fe-Cr 825S	W	402	2,370	<0.1	--	I, C; I, P
Ni-Fe-Cr 825S	S	402	2,370	<0.1	--	I, C; I, P
Ni-Fe-Cr 825Cb	W	123	5,640	<0.1	--	NC
Ni-Fe-Cr 825Cb	S	123	5,640	<0.1	--	NC
Ni-Fe-Cr 825Cb	W	403	6,780	<0.1	--	I, C
Ni-Fe-Cr 825Cb	S	403	6,780	<0.1	--	I, C
Ni-Fe-Cr 825Cb	W	751	5,640	<0.1	--	I, C
Ni-Fe-Cr 825Cb	S	751	5,640	<0.1	--	NC
Ni-Fe-Cr 825Cb	W	1,064	5,300	<0.1	--	NC
Ni-Fe-Cr 825Cb	S	1,064	5,300	<0.1	--	NC
Ni-Fe-Cr 825Cb	W	197	2,340	<0.1	--	NC
Ni-Fe-Cr 825Cb	S	197	2,340	<0.1	--	NC
Ni-Fe-Cr 825Cb	W	402	2,370	<0.1	--	NC
Ni-Fe-Cr 825Cb	S	402	2,370	<0.1	--	I, C
Ni-Fe-Cr 901	W	123	5,640	<0.1	--	NC
Ni-Fe-Cr 901	S	123	5,640	<0.1	--	NC
Ni-Fe-Cr 901	W	403	6,780	<0.1	--	I, C
Ni-Fe-Cr 901	S	403	6,780	<0.1	--	I, C
Ni-Fe-Cr 901	W	751	5,640	<0.1	--	NC
Ni-Fe-Cr 901	S	751	5,640	<0.1	--	I, C
Ni-Fe-Cr 901	W	1,064	5,300	<0.1	--	NC
Ni-Fe-Cr 901	S	1,064	5,300	<0.1	--	NC
Ni-Fe-Cr 901	W	197	2,340	<0.1	--	NC
Ni-Fe-Cr 901	S	197	2,340	<0.1	--	I, C
Ni-Fe-Cr 901	W	402	2,370	<0.1	--	I, C
Ni-Fe-Cr 901	S	402	2,370	<0.1	--	I, C
Ni-Fe-Cr 902[e]	W	402	2,370	1.4	35	C; I, P
Ni-Fe-Cr 902[e]	S	402	2,370	1.0	20	C; I, P
Ni-Cr-Fe-Mo F	W	123	5,640	<0.1	--	NC
Ni-Cr-Fe-Mo F	S	123	5,640	<0.1	--	NC
Ni-Cr-Fe-Mo F	W	403	6,780	<0.1	--	NC
Ni-Cr-Fe-Mo F	S	403	6,780	<0.1	--	NC
Ni-Cr-Fe-Mo F	W	751	5,640	<0.1	--	NC
Ni-Cr-Fe-Mo F	S	751	5,640	<0.1	--	NC
Ni-Cr-Fe-Mo F	W	1,064	5,300	<0.1	--	NC
Ni-Cr-Fe-Mo F	S	1,064	5,300	<0.1	--	NC

TABLE 5-15. (Continued)

Alloy	Environment[a]	Exposure, days	Depth, feet	Corrosion Rate,[b] mpy	Corrosion Crevice, mils	Type of Corrosion[c]
Ni-Cr-Fe-Mo F	W	197	2,340	<0.1	--	NC
Ni-Cr-Fe-Mo F	S	197	2,340	<0.1	--	NC
Ni-Cr-Fe-Mo F	W	402	2,370	<0.1	--	NC
Ni-Cr-Fe-Mo F	S	402	2,370	<0.1	--	NC
Ni-Cr-Fe-Mo G	W	402	2,370	<0.1	--	NC
Ni-Cr-Fe-Mo G	S	402	2,370	<0.1	--	NC
Ni-Cr-Fe-Mo X	W	123	5,640	<0.1	--	NC
Ni-Cr-Fe-Mo X	S	123	5,640	<0.1	--	NC
Ni-Cr-Fe-Mo X	W	403	6,780	<0.1	--	NC
Ni-Cr-Fe-Mo X	S	403	6,780	<0.1	--	NC
Ni-Cr-Fe-Mo X	W	751	5,640	<0.1	--	NC
Ni-Cr-Fe-Mo X	S	751	5,640	<0.1	--	NC
Ni-Cr-Fe-Mo X	W	1,064	5,300	<0.1	--	SL, ET
Ni-Cr-Fe-Mo X	S	1,064	5,300	<0.1	--	NC
Ni-Cr-Fe-Mo X	W	197	2,340	<0.1	--	NC
Ni-Cr-Fe-Mo X	S	197	2,340	<0.1	--	I, C
Ni-Cr-Fe-Mo X	W	402	2,370	<0.1	--	NC
Ni-Cr-Fe-Mo X	S	402	2,370	<0.1	--	NC
Ni-Cr-Co 41	W	1,064	5,300	0.0	--	NC
Ni-Mo-Fe B	W	123	5,640	2.3	--	U
Ni-Mo-Fe B	S	123	5,640	2.2	--	U
Ni-Mo-Fe B	W	403	6,780	4.0	--	U
Ni-Mo-Fe B	S	403	6,780	0.6	--	(n)
Ni-Mo-Fe B	W	751	5,640	2.9	--	G
Ni-Mo-Fe B	S	751	5,640	1.8	--	G
Ni-Mo-Fe B	W	1,064	5,300	1.5	--	G
Ni-Mo-Fe B	S	1,064	5,300	0.8	--	Nu
Ni-Mo-Fe B	W	197	2,340	<0.1	--	Nu, ET
Ni-Mo-Fe B	S	197	2,340	<0.1	--	I, C; I, P
Ni-Mo-Fe B	W	402	2,370	1.2	--	G
Ni-Mo-Fe B	S	402	2,370	0.2	--	U
Ni-Mo-Cr C	W	123	5,640	<0.1	--	NC
Ni-Mo-Cr C	S	123	5,640	<0.1	--	NC
Ni-Mo-Cr C	W	403	6,780	0.0	--	NC
Ni-Mo-Cr C	W	403	6,780	<0.1	--	NC
Ni-Mo-Cr C	S	403	6,780	0.0	--	NC
Ni-Mo-Cr C	S	403	6,780	<0.1	--	NC

TABLE 5-15. (Continued)

Alloy	Environment[a]	Exposure, days	Depth, feet	Corrosion Rate,[b] mpy	Corrosion Crevice, mils	Type of Corrosion[c]
Ni-Mo-Cr C	W	751	5,640	0.0	--	NC
Ni-Mo-Cr C	W	751	5,640	<0.1	--	NC
Ni-Mo-Cr C	S	751	5,640	0.0	--	NC
Ni-Mo-Cr C	S	751	5,640	<0.1	--	NC
Ni-Mo-Cr C	W	1,064	5,300	0.0	--	NC
Ni-Mo-Cr C	W	1,064	5,300	<0.1	--	NC
Ni-Mo-Cr C	S	1,064	5,300	0.0	--	NC
Ni-Mo-Cr C	S	1,064	5,300	<0.1	--	NC
Ni-Mo-Cr C	W	197	2,340	0.0	--	NC
Ni-Mo-Cr C	W	197	2,340	<0.1	--	NC
Ni-Mo-Cr C	S	197	2,340	0.0	--	NC
Ni-Mo-Cr C	S	197	2,340	<0.1	--	NC
Ni-Mo-Cr C	W	402	2,370	0.0	--	NC
Ni-Mo-Cr C	W	402	2,370	<0.1	--	NC
Ni-Mo-Cr C	S	402	2,370	0.0	--	NC
Ni-Mo-Cr C	S	402	2,370	<0.1	--	NC
Ni-Sn-Zn 23	W	123	5,640	2.6	25	C
Ni-Sn-Zn 23	S	123	5,640	1.8	14	C
Ni-Sn-Zn 23	W	403	6,780	8.4	36	C, P
Ni-Sn-Zn 23	S	403	6,780	<0.1	--	NC
Ni-Sn-Zn 23	W	751	5,640	3.5	56	C, P
Ni-Sn-Zn 23	S	751	5,640	2.1	52	C, P
Ni-Sn-Zn 23	W	1,064	5,300	1.7	50	C, P
Ni-Sn-Zn 23	S	1,064	5,300	1.0	--	P, 35m
Ni-Sn-Zn 23	W	197	2,340	0.5	15	C
Ni-Sn-Zn 23	S	197	2,340	<0.1	--	I, C
Ni-Sn-Zn 23	W	402	2,370	0.9	29	C
Ni-Sn-Zn 23	S	402	2,370	0.1	--	I, C
Ni-Be	W	402	2,370	1.1	--	(o)
Ni-Be	S	402	2,370	0.7	--	(p)
Ni-Cr 65-35	W	123	5,640	<0.1	--	NC
Ni-Cr 65-35	S	123	5,640	<0.1	--	NC
Ni-Cr 65-35	W	403	6,780	<0.1	35 (PR)	C
Ni-Cr 65-35	S	403	6,780	<0.1	--	I, C
Ni-Cr 65-35	W	751	5,640	<0.1	20	C
Ni-Cr 65-35	S	751	5,640	<0.1	--	I, C
Ni-Cr 65-35	W	1,064	5,300	<0.1	5	C
Ni-Cr 65-35	S	1,064	5,300	0.1	50 (PR)	C
Ni-Cr 65-35	W	197	2,340	0.3	24	C
Ni-Cr 65-35	S	197	2,340	<0.1	--	I, C

TABLE 5-15. (Continued)

Alloy	Environment[a]	Exposure, days	Depth, feet	Corrosion Rate,[b] mpy	Corrosion Crevice, mils	Type of Corrosion[c]
Ni-Cr 65-35	W	402	2,370	0.1	6	C
Ni-Cr 65-35	S	402	2,370	<0.1	--	I, C
Ni-Cr 75	W	123	5,640	<0.1	--	I, C
Ni-Cr 75	S	123	5,640	<0.1	--	NC
Ni-Cr 75	W	403	6,780	0.4	40 (PR)	C
Ni-Cr 75	S	403	6,780	<0.1	--	I, C
Ni-Cr 75	W	751	5,640	0.5	40 (PR)	C, P
Ni-Cr 75	S	751	5,640	<0.1	2	C
Ni-Cr 75	W	1,064	5,300	<0.1	--	I, C
Ni-Cr 75	S	1,064	5,300	<0.1	12	C
Ni-Cr 75	W	197	2,340	0.3	40 (PR)	C
Ni-Cr 75	S	197	2,340	<0.1	5	C
Ni-Cr 75	W	402	2,370	0.4	40 (PR)	C, P
Ni-Cr 75	S	402	2,370	<0.1	--	I, C
Ni-Cr 80-20	W	123	5,640	<0.1	2	C
Ni-Cr 80-20	S	123	5,640	<0.1	--	I, C
Ni-Cr 80-20	W	403	6,780	0.2	11	C
Ni-Cr 80-20	S	403	6,780	<0.1	--	I, C
Ni-Cr 80-20	W	751	5,640	0.4	32 (PR)	C
Ni-Cr 80-20	S	751	5,640	<0.1	--	I, C
Ni-Cr 80-20	W	1,064	5,300	<0.1	5	C
Ni-Cr 80-20	S	1,064	5,300	0.1	50 (PR)	C
Ni-Cr 80-20	W	197	2,340	0.2	32 (PR)	C
Ni-Cr 80-20	S	197	2,340	<0.1	--	I, C; E
Ni-Cr 80-20	W	402	2,370	0.2	18	C, P
Ni-Cr 80-20	S	402	2,370	<0.1	--	I, C
Ni-Mo 2	W	123	5,640	1.2	--	G
Ni-Mo 2	S	123	5,640	1.1	--	G
Ni-Mo 2	W	403	6,780	2.2	--	G
Ni-Mo 2	S	403	6,780	0.3	--	G
Ni-Mo 2	W	751	5,640	6.8	--	G
Ni-Mo 2	S	751	5,640	1.6	--	G
Ni-Mo 2	W	1,064	5,300	3.2	--	G
Ni-Mo 2	S	1,064	5,300	1.8	--	G
Ni-Mo 2	W	197	2,340	1.0	--	U
Ni-Mo 2	S	197	2,340	0.2	--	G
Ni-Mo 2	W	402	2,370	1.6	--	G
Ni-Mo 2	S	402	2,370	0.3	--	ET

TABLE 5-15. (Continued)

Alloy	Environment[a]	Exposure, days	Depth, feet	Corrosion Rate,[b] mpy	Corrosion Crevice, mils	Type of Corrosion[c]
Ni-Si D	W	123	5,640	1.3	12	C
Ni-Si D	S	123	5,640	1.4	10	C
Ni-Si D	W	403	6,780	2.4	5	C, P
Ni-Si D	S	403	6,780	1.4	14	C
Ni-Si D	W	751	5,640	1.7	29	C
Ni-Si D	S	751	5,640	1.5	6	C, P
Ni-Si D	W	1,064	5,300	1.6	42	C, P to 38m
Ni-Si D	S	1,064	5,300	1.1	25	C, P to 20m
Ni-Si D	W	197	2,340	0.2	--	I, C
Ni-Si D	S	197	2,340	<0.1	--	I, C
Ni-Si D	W	402	2,370	0.5	14	C
Ni-Si D	S	402	2,370	0.2	--	ET

(a) W = specimens exposed on sides of STU in seawater; S = specimens exposed in base of STU, partially embedded in bottom sediments.
(b) mpy = mils penetration per year calculated from weight loss.
(c) Symbols for type of corrosion: C = crevice; E = edge; ET = etched; G = general; I = incipient; NC = no visible corrosion; Nu = nonuniform; P = pitting; PR = perforation; SL = slight; T = tunneling; and U = uniform. Numbers indicate mils: i.e., 20m = 20 mils maximum; 14.6a = 14.6 mils average; and 20 = 20 mils.
(d) S = sensitized for 1 hour at 1200 F.
(e) 1" x 6" specimens.
(f) Weld bead perforated.
(g) Weld bead perforated, line corrosion at edge of weld bead.
(h) Weld bead perforated, line corrosion at edge of weld bead, tunneling to perforation in heat affected zone.
(i) Tunneling in heat affected zone parallel to weld bead (55 mils deep) and away from weld, perforated at edge of weld bead.
(j) Single pit to perforation, 180 mils.
(k) Edge penetration at weld.
(l) Line corrosion at edge of weld bead.
(m) One end of weld corroded.
(n) Groove at mud line, 4 mils.
(o) Surface of bars etched, pitting on ends to 17 mils.
(p) Surface of bars etched, pitting on ends to 8 mils.

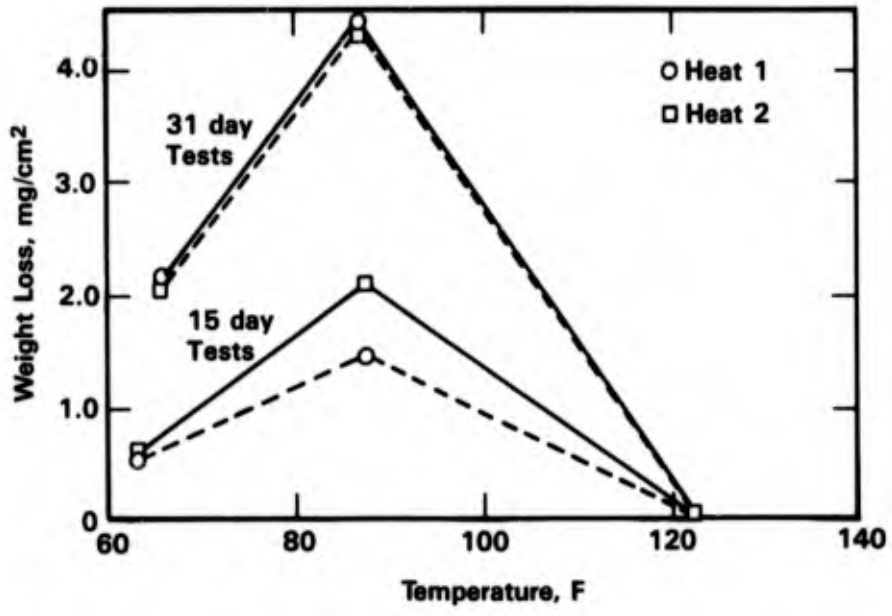

FIGURE 5-4. WEIGHT LOSS OF MONEL ALLOY 400 VERSUS SEAWATER TEMPERATURE[21]

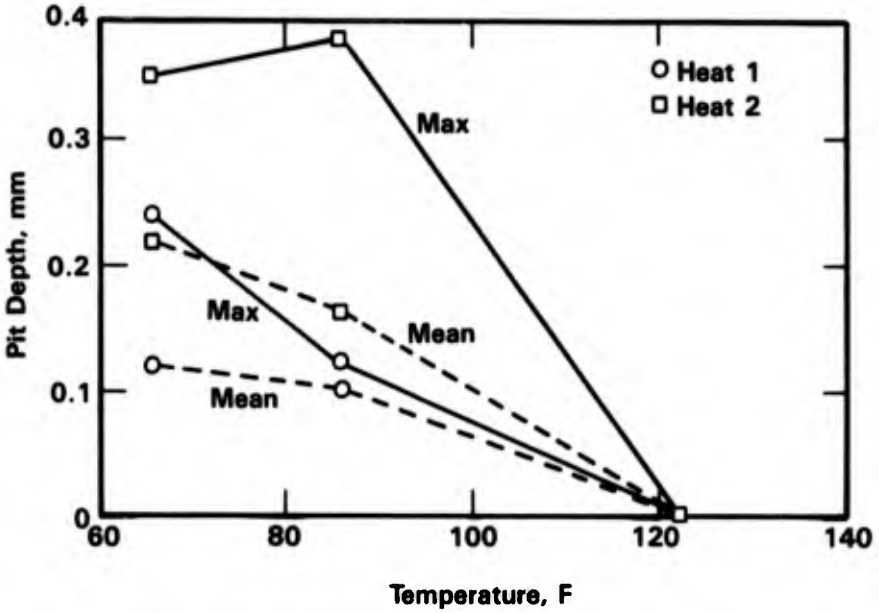

FIGURE 5-5. MAXIMUM AND MEAN DEPTH OF ATTACK OF MONEL ALLOY 400 AFTER 31 DAYS' EXPOSURE VERSUS SEAWATER TEMPERATURE[21]

TABLE 5-16. CORROSION RESISTANCE OF HASTELLOY ALLOY C-276 IN SEAWATER[22]

Temperature	pH	Dissolved O_2, ppb	Velocity, m/s	Crevice Attack	Test Duration
98.6 F	3.5	5,200	2.7	Not detected	112 days
95 F	3.5	28	2.7	Not detected	112 days
95 F	7.7	28	2.7	Not detected	112 days
145 F	7.7	28	1.4	Not detected	93 days
180 F	7.7	28	2.7	Not detected	112 days
225 F	7.7	28	2.7	Not detected	84 days

TABLE 5-17. CORROSION RESISTANCE OF HASTELLOY ALLOYS C/C-276 IN SEAWATER[22]

Temperature	Velocity, m/s	Corrosion Rate, mpy[a]	Test Duration
50 F	38	0.2	30 days
80 F	0.3	0.1	150 days
80 F	4	0.1	15 days
325 F	0.15	0.1	54 days
350 F	3	0.1	45 days
550 F	3.3	0.1	24 days

(a) Mils per year x 0.0254 = millimeters per year.

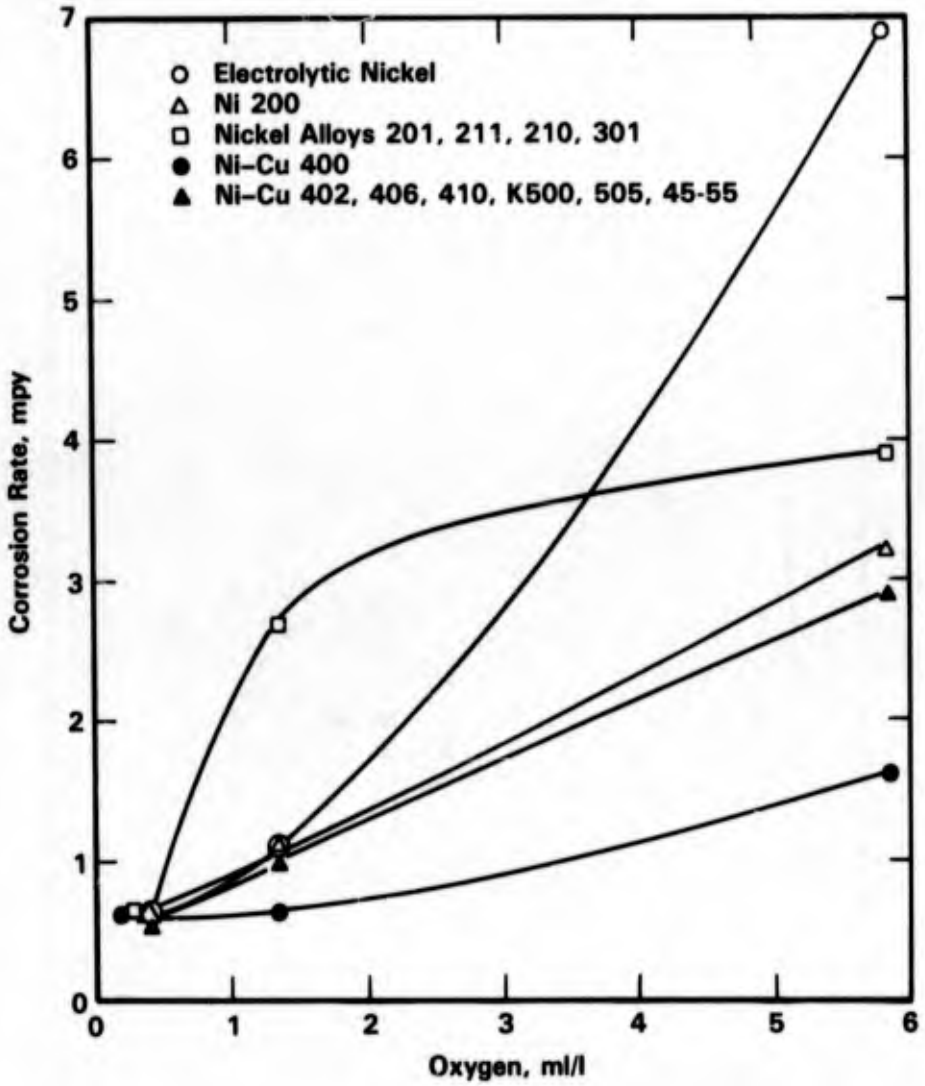

FIGURE 5-6. CORROSION OF NICKELS AND NICKEL-COPPER ALLOYS VERSUS OXYGEN CONTENT OF SEA-WATER AFTER 1 YEAR OF EXPOSURE[24]

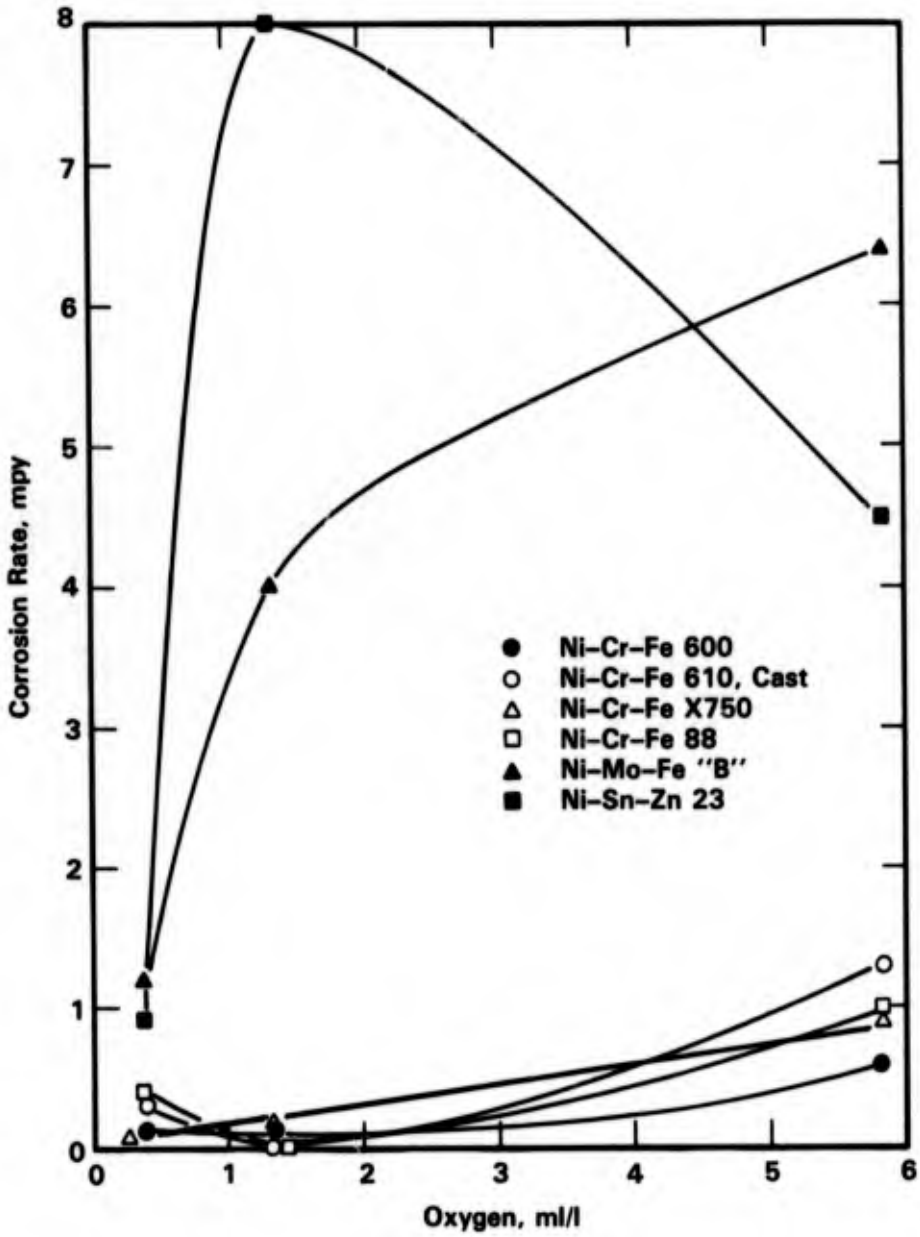

FIGURE 5-7. CORROSION OF NICKEL ALLOYS VERSUS OXYGEN CONTENT OF SEAWATER AFTER 1 YEAR OF EXPOSURE[24]

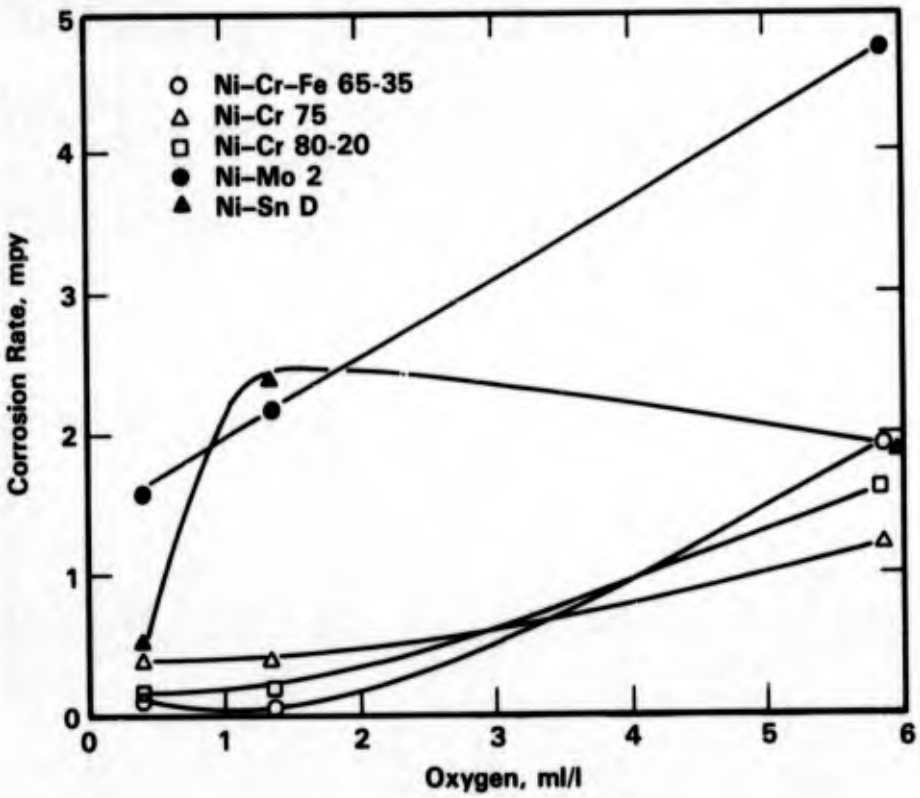

FIGURE 5-8. CORROSION OF NICKEL ALLOYS VERSUS OXYGEN CONTENT OF SEAWATER AFTER 1 YEAR OF EXPOSURE[24]

these alloys exhibited crevice attack even at the lowest oxygen level studied (0.4 ml/l), namely Alloy 600 to 28 mils, X-750 to 9 mils, and 825 to 15 mils after 402 days of exposure. It can also be seen in Table 5-15 that 625, 700, and a modified Alloy C did not exhibit crevice attack at any of the depths (O_2 levels) studied. Asphahani, et al.[22] also have observed no crevice attack in C-276 after 112 days' exposure to seawater containing 0.03 or 5.2 ppm dissolved oxygen at 35 to 37 C and pH 3.5.

Velocity. For the nickel alloys of interest, seawater velocities to 40 m/s do not have an adverse effect on corrosion behavior. In fact, as shown in Table 5-18, those alloys that exhibit crevice corrosion in stagnant seawater, such as 400, 600, and X-750, perform very well in high velocity seawater and exhibit corrosion rates <0.5 mpy at 120 fps velocity. Similar good corrosion resistance at 128 to 141 fps velocities also is shown in Tables 5-19, 5-20, 5-21, and 5-22.

TABLE 5-18. CORROSION BEHAVIOR AS A FUNCTION OF SEAWATER VELOCITY[26]

Alloy Designation	Nominal Composition											High Velocity, 120 fps Corrosion Rate, mdd	Intermediate Velocity, 25 fps Corrosion Rate, mdd	Low Velocity (0-2 fps) Crevice Attack	
	Ni	Cu	Fe	Mn	Si	Cr	Ti	Al	Cb	Mo	W			Maximum Penetration, inch	Remarks
N-1	Rem	31.5	1.4	1.0								3.0		1/16 spec. perforated (9)	Inside crevice, pitting on bold surface to 0.02
N-2	Rem	30.0	1.5	0.8	3.2							3.8		0.002 (2)	Inside crevice
N-3	Rem	29.0	2.0	0.8	4.0							6.5		0.006 (2)	Inside crevice, pitting on bold surface to 0.006
N-4	Rem	29.5	1.0	0.6			0.5	2.8				2.3 (2)		1/16 spec. perforated	Crevice boundary, pitting on bold surface to 0.03
N-5	Rem		7.2			15.8						1.5		0.01	Inside crevice, pitting on bold surface to 0.03
N-6	Rem		6.8	0.7		15.0	2.5	0.8	0.9			1.2		0.03	Inside crevice, pitting on bold surface to 0.03
N-7	Rem		18.0			19.0	0.8	0.6	5.2	3.0		1.0			
N-8	41.8	1.8	30.0	0.7		21.5	0.9			3.0		2.2		0.06	Crevice boundary
N-9	32.0		46.0	0.8		20.5								1/16 spec. perforated	Inside crevice
N-10	Rem		6.0	1.0 Max.	1.0 Max.	16.5				17.0	4.0				
N-11	55.0						45.0							0.02	Inside crevice, pitting on bold surface to 0.04
N-12	56.0						44.0							0.03	Inside crevice, pitting on bold surface to 0.09
N-13	56.0	6.5	6.5	1.3	0.7	22.5				6.4		0.5	1.2	0.04 (2)	Inside crevice

Notes:

- All are nickel alloys and have excellent corrosion resistance at high and intermediate velocities; severe local attack at low velocity and in crevices.
- All data are single tests unless otherwise noted by numbers in parentheses. Multiple test values may represent more than one heat, heat treatment, or form (cast versus wrought).
- Test description: high velocity: jet apparatus, generally 30-days duration; intermediate velocity: rotating rectangular bars, generally 60-days duration; and low velocity: quiet seawater or trough exposure, generally 1-year duration.
- Corrosion rate expressed as milligrams/square decimeter/day (mdd).

TABLE 5-19. SUMMARY OF CORROSION DATA FOR MATERIALS TESTED IN HIGH-VELOCITY JET APPARATUS[27]

Material	Weight Loss, gm	Corrosion Rate, mpy	Average Seawater Temperature, F	Seawater Velocity, ft/sec
Stellite 6B	0.003	0.1	54	126
Hastelloy C	0.010	0.2	54	128
AISI 304	0.008	0.2	50	142
AISI 316	0.008	0.2	50	142
Incoloy Alloy 825	0.011	0.3	52	141
17-4PH	0.012	0.3	50	142
Monel Alloy 400	0.016	0.4	52	141

TABLE 5-20. HIGH-VELOCITY SEAWATER IMPINGEMENT[3]

Data provided by The International Nickel Company, New York, NY.

Velocity 135 fps (91 mps)
Duration 30 days
Exposed Area 3.5 $in.^2$

Material	Weight Loss, grams	Corrosion Rate, mpy
Inconel 718	0.007	0.2
Inconel X-750	0.008	0.2
Inconel 600	0.010	0.3
Incoloy 825	0.011	0.3
Monel-400	0.016	0.4
Monel-K500	0.017	0.4
Ni-Al bronze	1.223	31
Naval brass	1.676	42
HY-80 steel	2.113	57
Medium C steel	6.518	176
High-tensile steel	8.167	220
Cast iron[a]	6.788	600

(a) In test only 10 days.

TABLE 5-21. EFFECT OF VELOCITY ON CORROSION RESISTANCE OF COPPER-NICKEL ALLOYS IN SEAWATER[28]

Alloy	Velocity 0-0.6 m/sec General Corrosion, mm/yr	Pitting, (Average of 20 Deepest) mm	5.5 m/sec BNF Jet Test 30 days, Depth of Attack, mm	30-40 m/sec General Corrosion, mm/yr
90/10 copper-nickel + 1.5% iron	0.015	Slight	0.060	0.5-1.3
70/30 copper-nickel + 0.6% iron	0.0065	0.12[a]	0.030	0.9-1.8
Monel Alloy 400 (70/30 nickel copper)	0.008[a]	0.85[a]	0	0.01

(a) After 16 years' exposure as reported by Southwell, et al., Materials Performance (July, 1976).

TABLE 5-22. CORROSION AS A RESULT OF IMPINGEMENT OF SEAWATER AT VELOCITIES UP TO 140 ft/sec[18]

Material	Corrosion/Erosion Rate, in./yr
Inconel Alloy 625	0.0000
Incoloy Alloy 825	0.0003
Monel Alloys 400 and K-500	0.0004
Nickel 200	0.0005
70/30 Cupro-nickel	0.0500
Carbon steel	0.1200

Boyd and Fink[3] have summarized in Table 5-23 the effect of velocity on the corrosion of Alloy C in seawater. Over the velocity range of 0.5 to 128 fps, Alloy C exhibited corrosion rates of <0.6 mpy. Asphahani, et al.[22] also reported a low corrosion rate for Alloy C276 of 0.2 mpy in 10 C seawater at 38 m/s (125 fps).

Geometrical Effect. Some data are available on the effect of crevice geometry on crevice attack. Wheatfall[29] observed that the depth of crevice attack in Alloy 400 increased monotonically with increasing area outside the crevice. His results presented in Figure 5-9 indicated this same trend for three exposure depths in the ocean that represented a range of dissolved oxygen concentration. Anderson[30] in Figure 5-10 also observed a more or less linear increase in depth of attack in Alloy 400 at bold/sheltered area ratios of 0.1/1 to 100/1, but at ratios above 100/1, the depth of attack increased sharply.

Kain[20] predicted hours to breakdown for two nickel alloys as a function of crevice gap and crevice depth as he did for stainless steels (see Stainless Steels, Immersion, Pitting and Crevice, Geometric Effect). His results presented in Table 5-24 indicate the high resistance of 625 and an 18Cr-18Mo alloy to crevice attack and show that the tendency for crevice attack decreases with increasing crevice gap and decreasing crevice depth.

Potential. Lennox, et al.[31] have measured the corrosion potentials of nickel alloys in seawater. Their results are presented in Table 5-25 and are illustrated graphically in Figure 5-11. Note the considerable range of potentials observed for any given alloy during the 575 days of exposure, the similarity of the mean corrosion potential for each alloy, and the effect of velocity in making the mean potential more positive for each of the alloys. Lennox, et al.[31] also correlated corrosion potentials with crevice corrosion depth (see Table 5-26); it was found that those alloys with high mean and high range of corrosion potentials exhibited little or no crevice corrosion.

Hodgkiess and Rigas[23] determined the corrosion, pitting, and protection potentials for Alloy 825 as a function of temperature with the following results:

	Potential, mV(SCE)		
Temperature, C	E_{cor}	E_{pit}	E_{prot}
20	-240	1050	1030
60	-280	230	0

TABLE 5-23. CORROSION OF HASTELLOY C IN SEAWATER ENVIRONMENTS[3]

Data taken from literature supplied by The International Nickel Company and Union Carbide Corporation.

Type of Test	Site	Seawater Conditions				Duration	Corrosion,[a] mpy	Notes
		Temperature, F	pH	Velocity, fps	Oxygen, ppm			
Spool	Curacao	82	6.6	(Pump suction)	3.5	3 yr	0.4	No pitting
Spool	--	325	--	0.5	--	3.3 yr	<0.1	
Coupon	Wrightsville Beach, NC	51	8.0±	128	Saturated	30 days	0.2	
Sandblasted plate	Wrightsville Beach, NC	Ambient	8.0±	Low	Saturated	10 yr	0.016	No pitting or crevice attack
Sheet tensile rotating in autoclave	Navy Laboratory at Annapolis, MD	350	--	10	--	1080 hr	(Weight gain)	
Navy erosion test	Wrightsville Beach, NC	86	8.0±	20	Saturated	60 days	0.63	

(a) Weight losses were so small that cleaning and weighing errors may be the major factor, especially for plate samples.

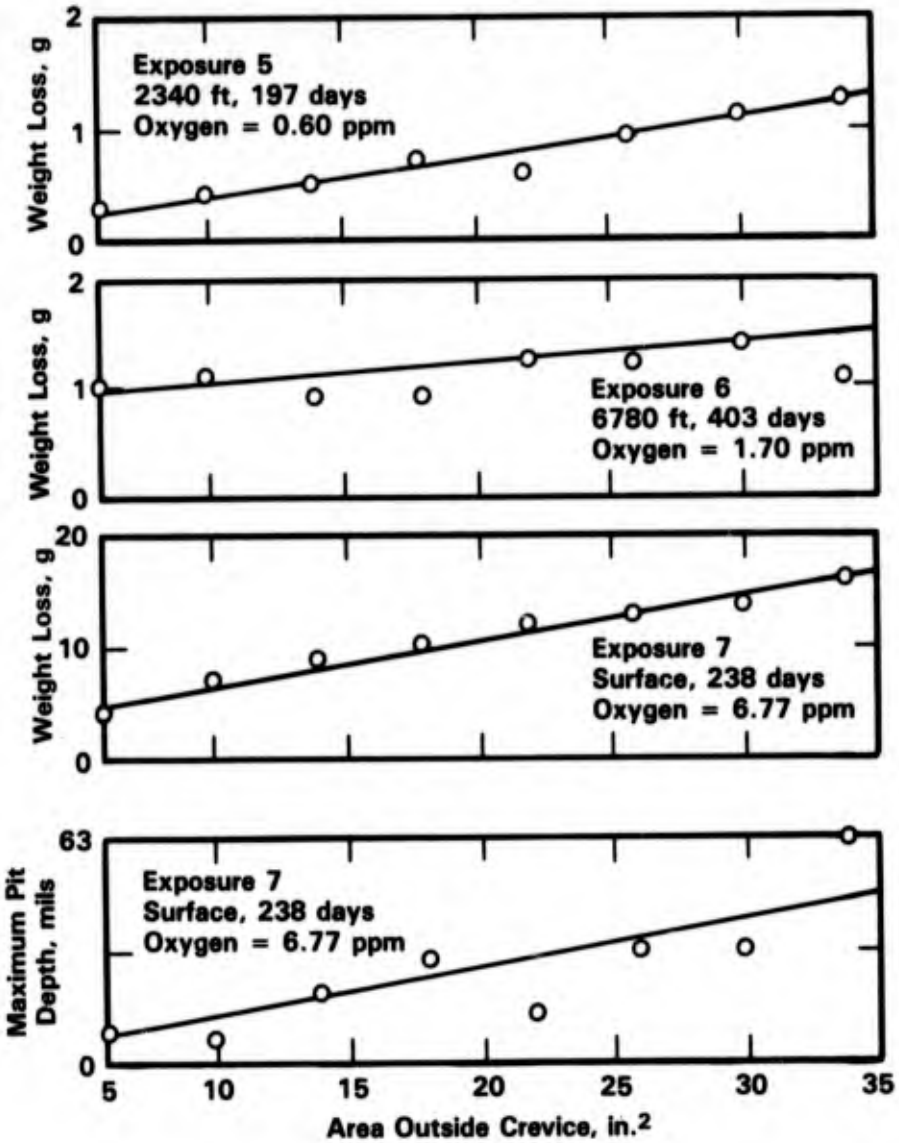

FIGURE 5-9. RELATION OF WEIGHT LOSS AND MAXIMUM PIT DEPTH IN THE CREVICE TO AREA OF SPECIMEN OUTSIDE THE CREVICE FOR MONEL 400 AT VARIOUS DEPTHS[29]

Specimen perforated at maximum pit depth = 63 mils

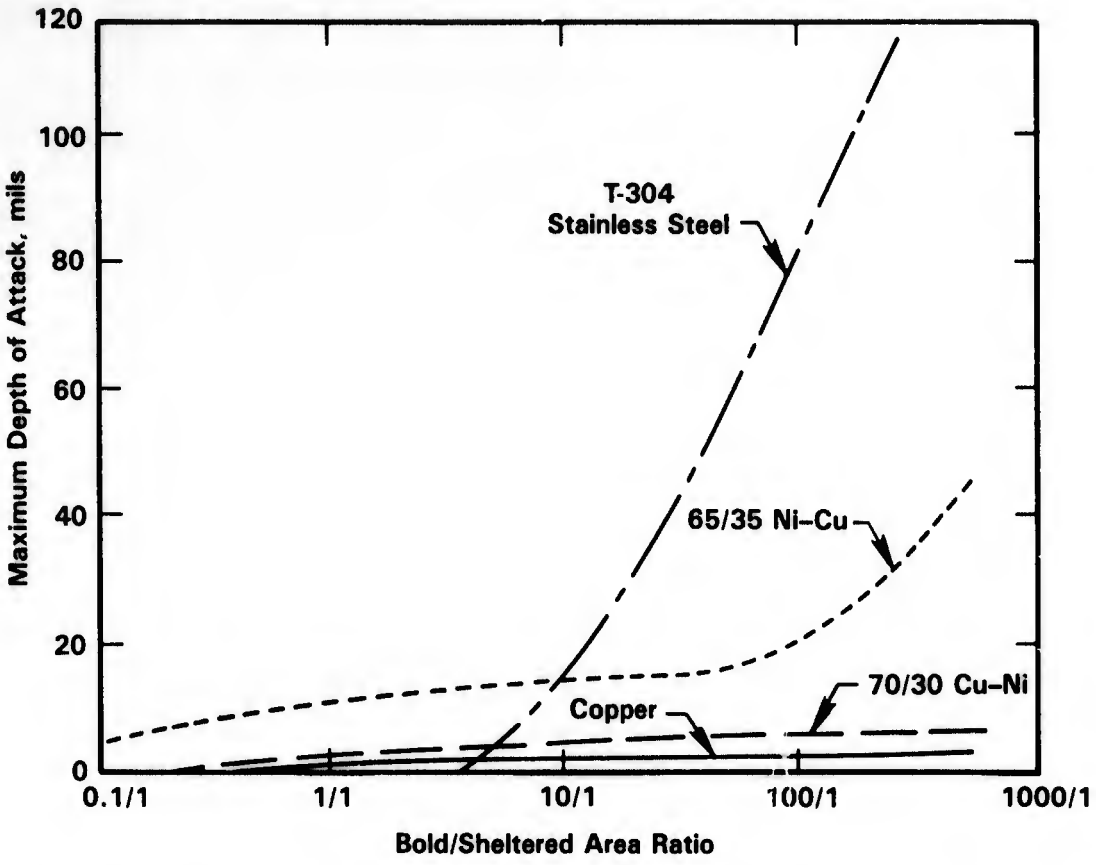

FIGURE 5-10. EFFECTS OF AREA RATIO ON THE DEPTH OF ATTACK IN TIGHT CREVICES AFTER THREE MONTHS OF EXPOSURE IN FLOWING SEAWATER[30]

TABLE 5-24. EFFECT OF CREVICE GEOMETRY ON THE PREDICTED TIME TO BREAKDOWN FOR SEVERAL CAST ALLOYS IN SEAWATER[20]

Alloy	Crevice Depth, cm	Predicted Hours to Breakdown in Nonmetal to Metal Crevice Gap*			
		0.125 μm	0.250 μm	0.500 μm	1.250 μm
Ni-18Cr-18Mo	0.5	791	NB	NB	NB
	1.0	191	465	NB	NB
Alloy 625	0.5	284	NB	NB	NB
	1.0	149	342	NB	NB

* NB = no breakdown.

TABLE 5-25. CORROSION POTENTIALS IN SEAWATER[a] (Ag/AgCl REFERENCE ELECTRODE)[31]

Common Alloy Designation	Quiescent (P)[b]		Flowing (F)[c]	
	Range	Mean	Range	Mean
Ni 200	-0.08 to -0.18	-0.12	+0.07 to -0.40	-0.14
Monel 400	-0.02 to -0.10	-0.07	-0.04 to -0.23	-0.08
Monel K-500	-0.04 to -0.19	-0.10	-0.03 to -0.13	-0.06
Inconel 600	+0.06 to -0.22	-0.10	+0.10 to -0.25	-0.04
Inconel 617	+0.25 to -0.04	-0.01	+0.29 to -0.27	+0.08
Inconel 625	+0.17 to -0.20	-0.06	+0.03 to -0.27	+0.16
Inconel 706	-0.06 to -0.28	-0.17	+0.08 to -0.21	-0.11
Inconel 718	-0.01 to -0.22	-0.10	+0.12 to -0.14	-0.03
Alloy 20	0.00 to -0.22	-0.09	+0.09 to -0.35	-0.06
Incoloy 800	+0.05 to -0.16	-0.06	+0.09 to -0.33	-0.09
Incoloy 825	+0.20 to -0.23	+0.07	+0.14 to -0.08	+0.06
Hastelloy C-276	+0.15 to -0.18	-0.09	+0.28 to -0.23	+0.15
MP 35N	+0.25 to -0.23	-0.07	+0.30 to -0.27	+0.17
Elgiloy	+0.05 to -0.24	-0.08	+0.25 to -0.11	+0.11
Ti-6Al-4V	+0.16 to -0.24	-0.01	+0.27 to -0.28	+0.14
AISI 304	-0.10 to -0.25	-0.16	-0.03 to -0.23	-0.12

(a) Period of measurements were up to 575 days.
(b) P = specimens immersed under pier.
(c) F = specimens immersed in flume.

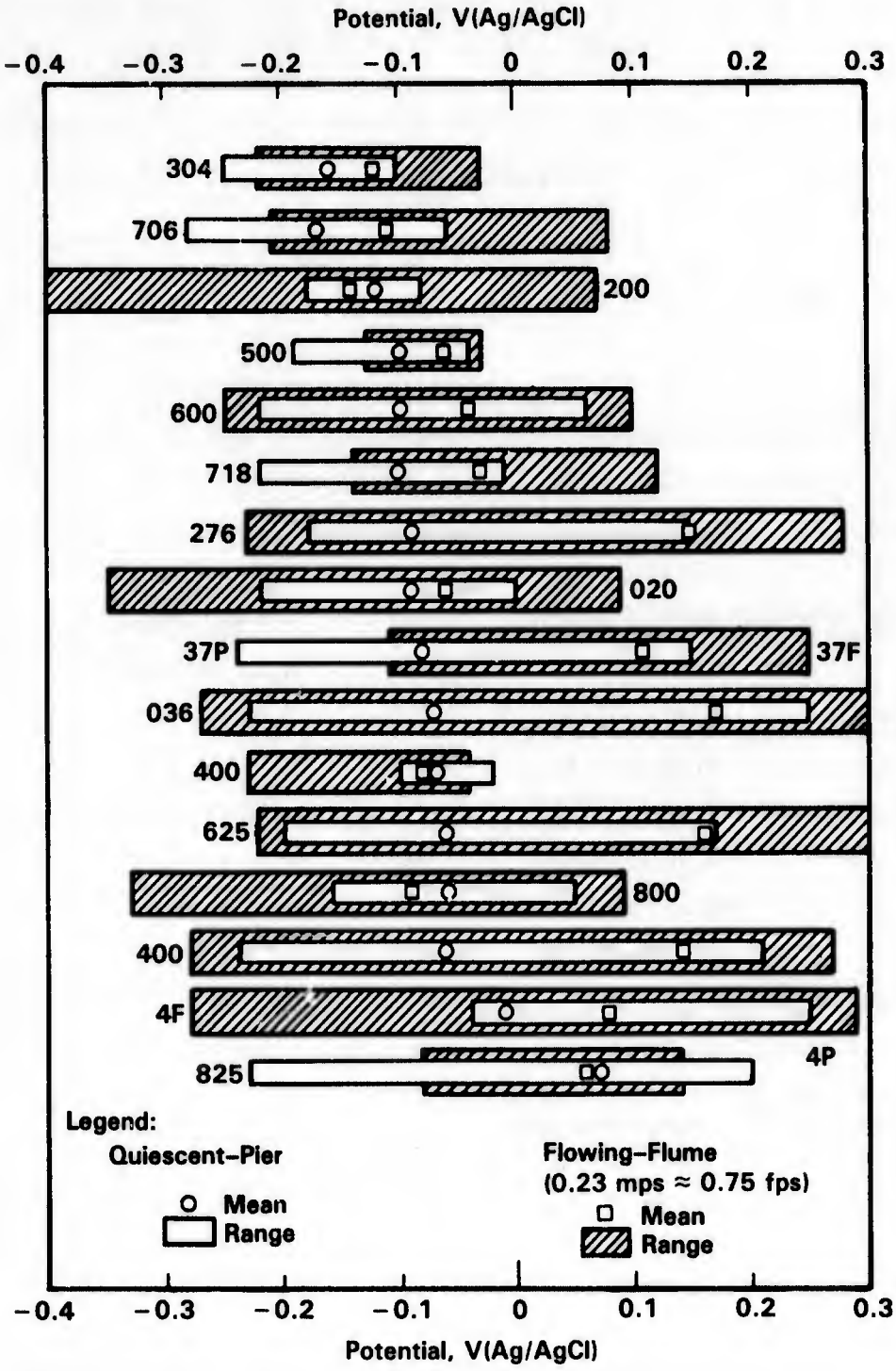

FIGURE 5-11. CORROSION POTENTIALS IN SEAWATER[31]

TABLE 5-26. CORROSION POTENTIALS VERSUS DEPTHS OF CREVICE CORROSION (FROM QUIESCENT AND FLOWING SPECIMENS)[31]

Common Alloy Designation	Potentials, V(Ag/AgCl)		Crevice Corrosion, μm	
	Spread of Means	Total Range	Average of Means	Average of Maxima
Nickel 200	0.02	0.47	1921	2400
Monel 400	0.01	0.21	924	991
Monel K-500	0.04	0.16	111	178
Inconel 600	0.06	0.35	963	1042
Inconel 617	0.09	0.56	74	89
Inconel 625	0.22	0.57	0	26
Inconel 706	0.06	0.36	1234	1423
Inconel 718	0.07	0.34	517	1181
Alloy 20	0.03	0.44	213	991
Incoloy 800	0.03	0.42	2413	2413
Incoloy 825	0.01	0.43	268	915
Hastelloy C-276	0.24	0.51	0	0
MP 35N	0.24	0.57	0	0
Elgiloy	0.19	0.49	125	125
Ti-6Al-4V	0.15	0.55	0	0
AISI 304 SS	0.04	0.22	1461	1461

Note that the effect of increasing temperature was to make all values more negative and to bring E_{pit} and E_{prot} much nearer to E_{cor} at 60 C. Tipton and Kain[32] observed a similar effect for Alloy 400 where E_{pit} and E_{prot} were +10 and -75 mV(SCE) at 19 C and were -20 and -120 mV(SCE) at 30 C.

Semino, et al.[33] determined pitting potentials for several nickel alloys as a function of Cl^- activity. Their results shown in Figure 5-12 indicate that pitting potentials become more negative as the Cl^- activity increases and that the ranking of pitting potentials is 800>600>400 (800 is more positive).

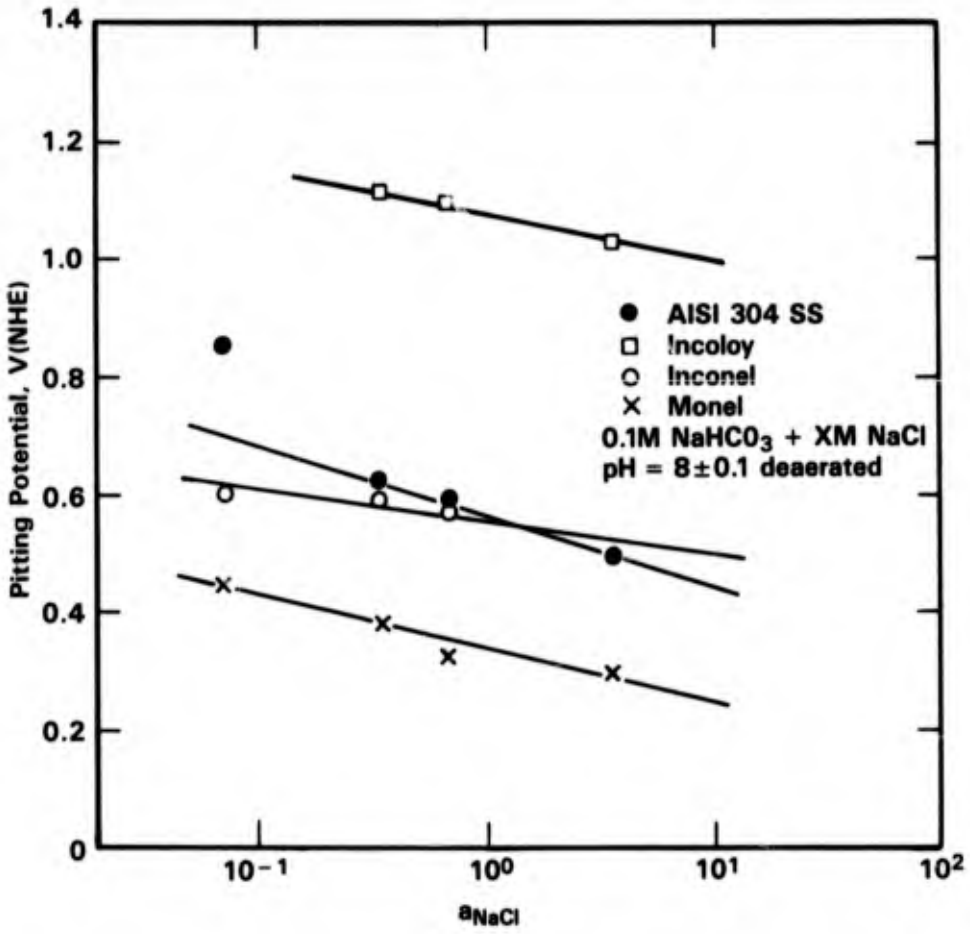

FIGURE 5-12. PITTING POTENTIALS VERSUS NaCl ACTIVITIES FOR TYPE 304 STAINLESS STEEL, INCOLOY, INCONEL 600, AND MONEL[33]

Time. As shown in Table 5-1, and Figures 5-1, 5-13, 5-14, and 5-15, the corrosion rates of all the nickel-base alloys tend to decrease with exposure time. This is a common characteristic of alloys that develop protective corrosion films. However, in many of these alloys, the reduced corrosion rates may have been the result of reduced pitting attack with time which would result in smaller weight changes at the longer exposures. The reduction in the pitting rate with time is shown for Alloy 400 in Figure 5-2 and Table 5-1 and to a lesser extent for the alloy in Table 5-15.

Pollution. Limited data obtained by Hack[34] show that Alloy 400 exhibits increased corrosion when the sulfide content of seawater increases from 0 to 5 mg/l (0 to 5 ppm). See the uncoupled data in Figure 5-16. The conventional nickel-chromium alloys are not subject to increased attack by sulfides in ambient seawater.

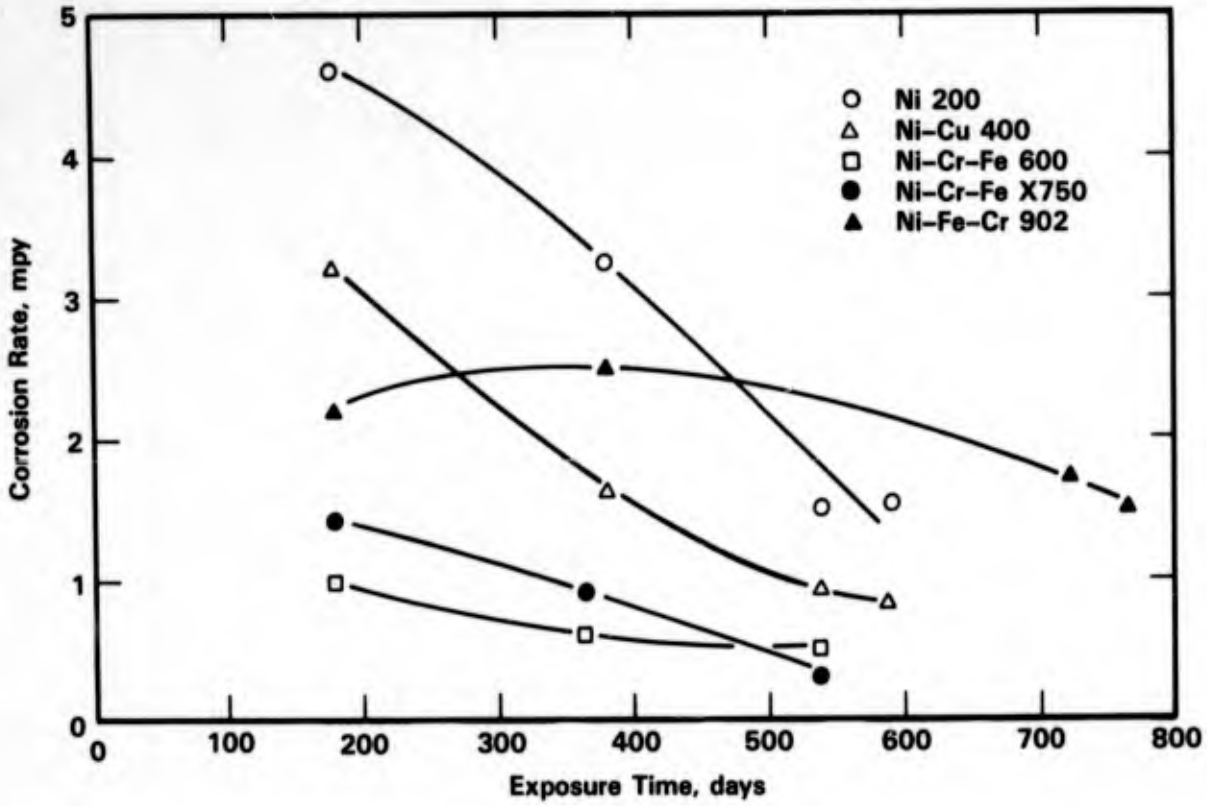

FIGURE 5-13. CORROSION OF NICKEL ALLOYS VERSUS TIME OF EXPOSURE AT THE SURFACE AT PORT HUENEME, CA[24]

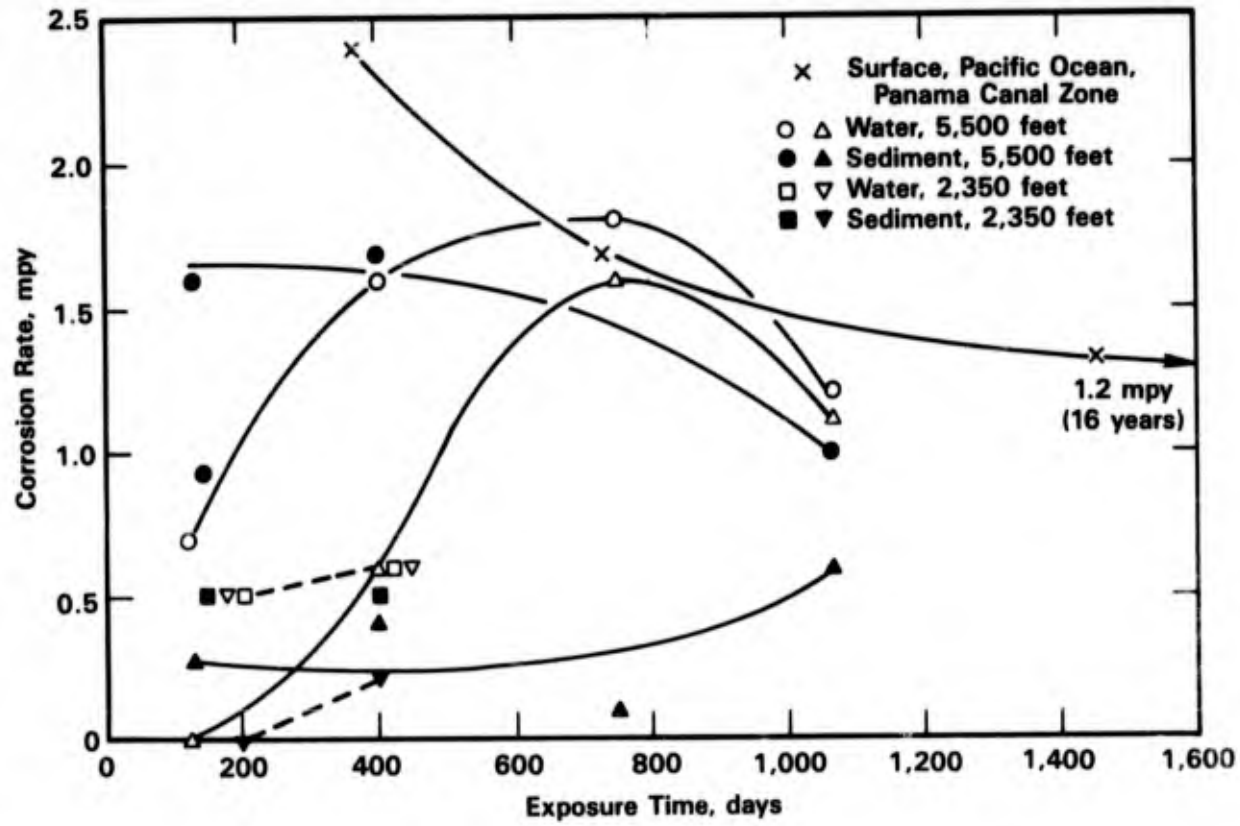

FIGURE 5-14. CORROSION OF NICKEL 200 IN SEAWATER[19]

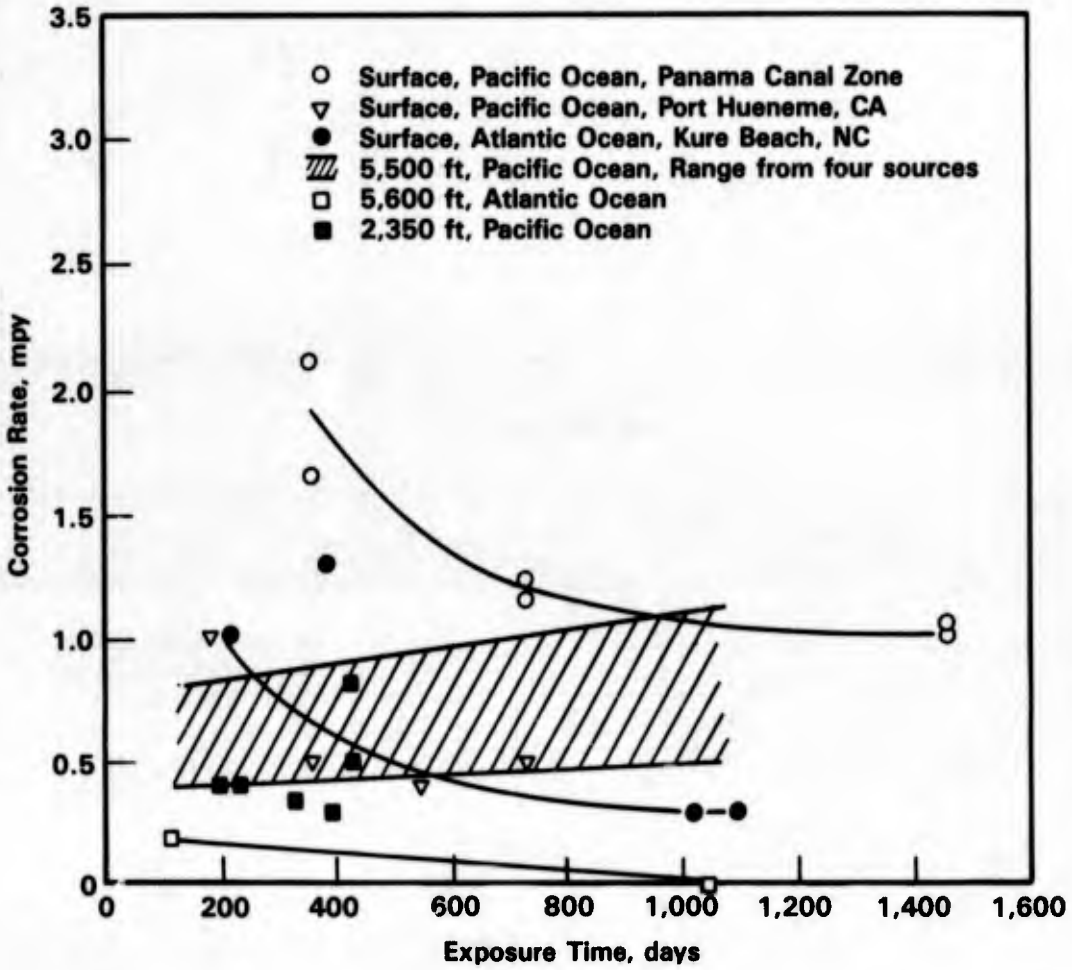

FIGURE 5-15. CORROSION OF NICKEL-COPPER ALLOY 400 IN SEAWATER[19]

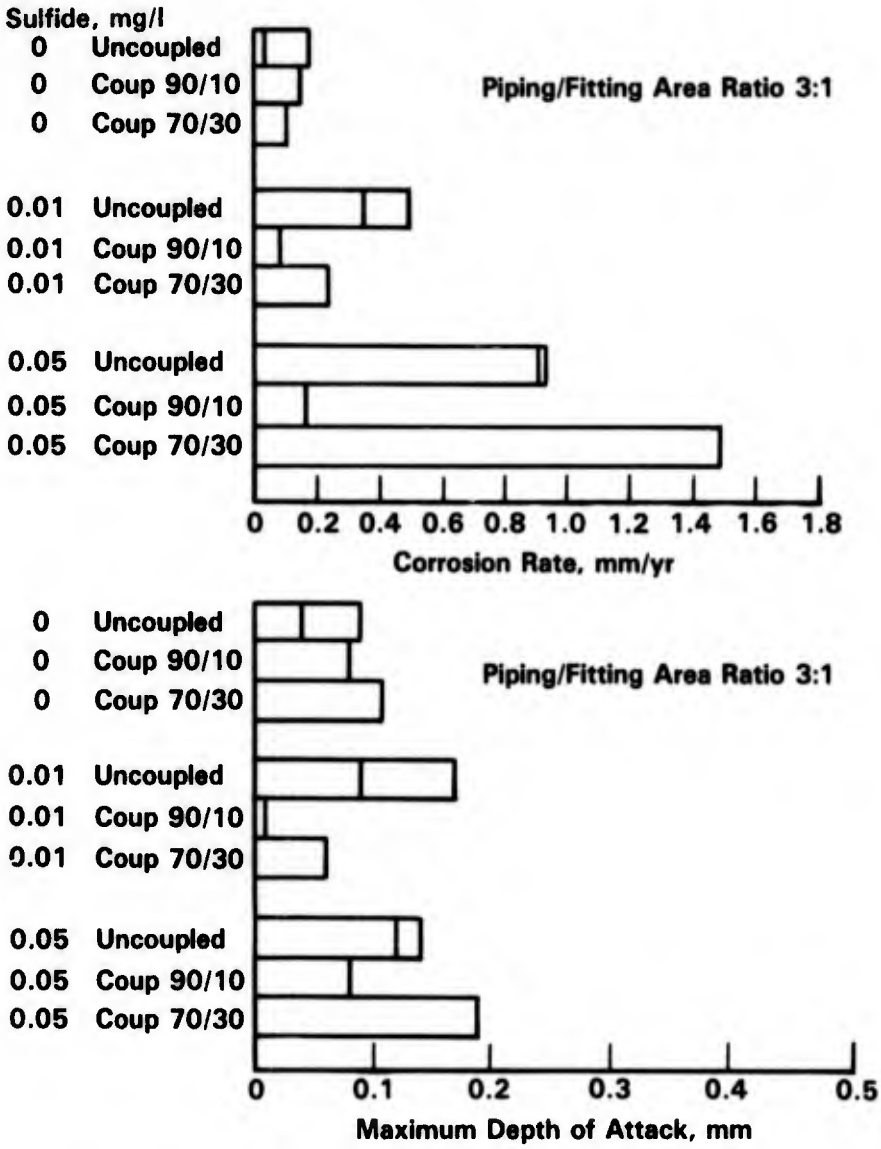

FIGURE 5-16. CORROSION OF MONEL COUPLED TO PIPING MATERIALS IN SULFIDE-CONTAINING SEAWATER[34]

Depth. The principal effect of depth of exposure on the corrosion of nickel-base alloys appears to be related to the dissolved oxygen content at various depths. As shown in Figures 5-17, 5-18, and 5-19, the general corrosion rate curves as a function of depth have nearly the same shape as does the oxygen content curve versus depth, i.e., corrosion rates are high at the surface where oxygen content is high and are lowest at about 2000 ft depth where oxygen contents are lowest. The tendency toward pitting also parallels the oxygen versus depth curve, although it can be seen from Reinhart's[19] Table 5-15 that 625, 700, and a modified Alloy C did not exhibit crevice attack at any of the depths studied.

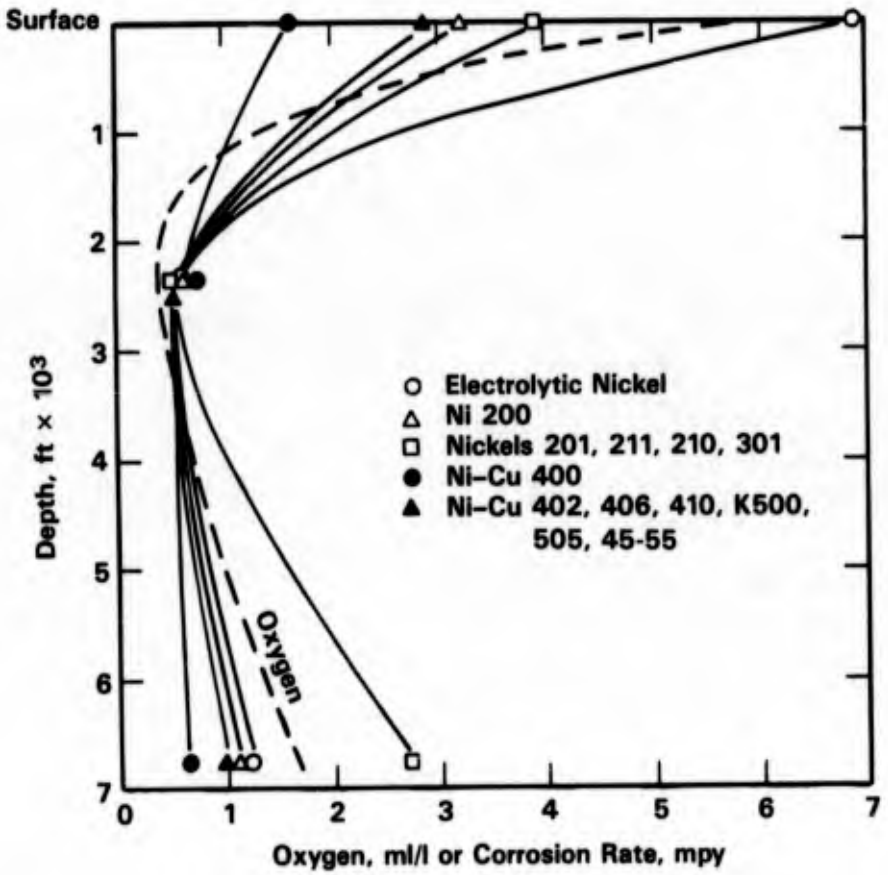

FIGURE 5-17. CORROSION OF NICKEL AND NICKEL-COPPER ALLOYS VERSUS DEPTH AFTER 1 YEAR OF EXPOSURE IN THE PACIFIC OCEAN[24]

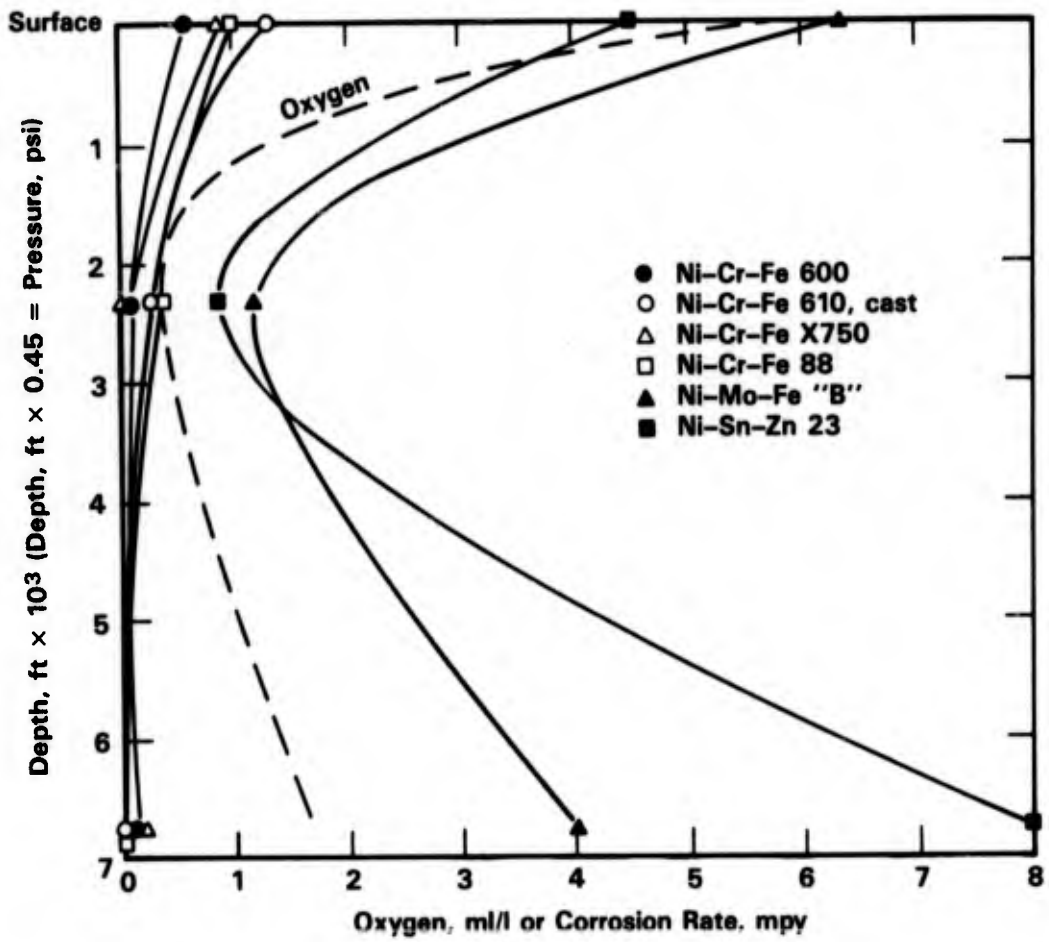

FIGURE 5-18. CORROSION OF NICKEL ALLOYS VERSUS DEPTH AFTER 1 YEAR OF EXPOSURE IN THE PACIFIC OCEAN[24]

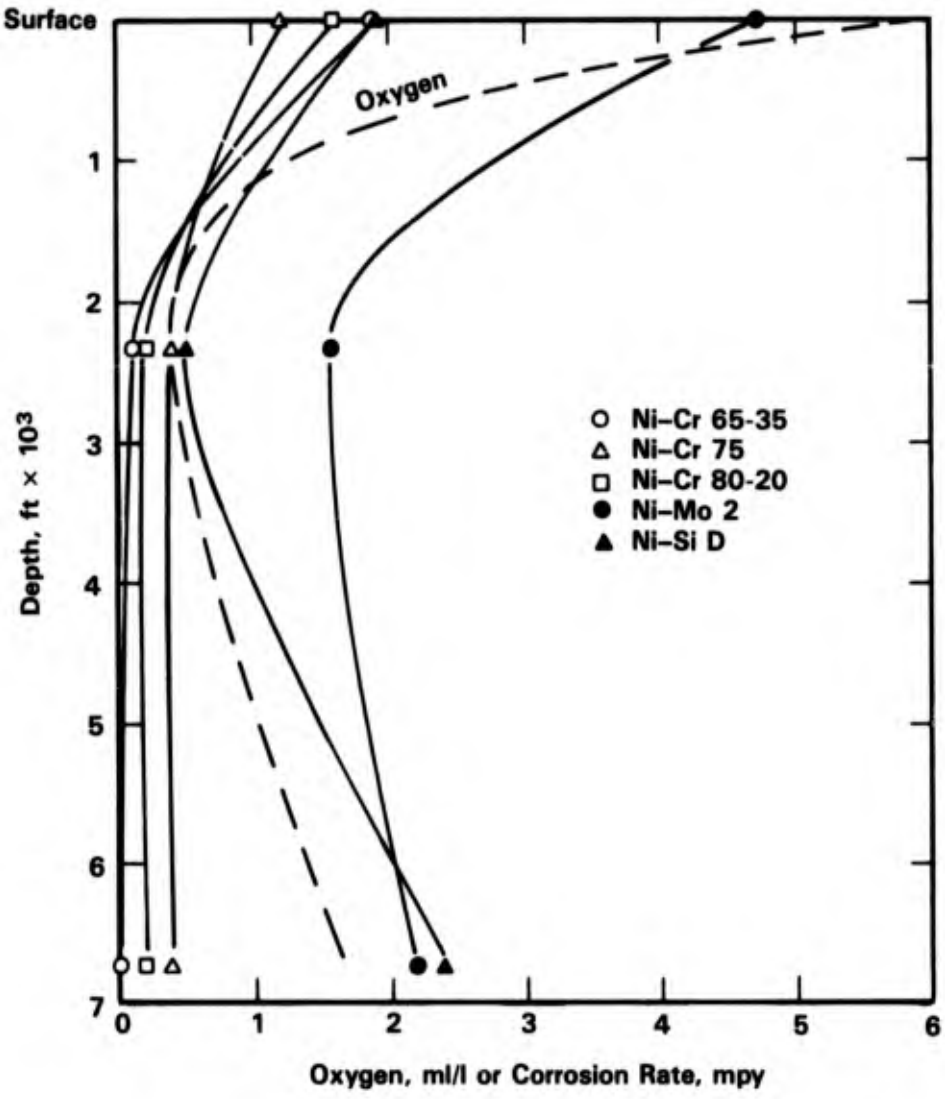

FIGURE 5-19. CORROSION OF NICKEL ALLOYS VERSUS DEPTH AFTER 1 YEAR OF EXPOSURE IN THE PACIFIC OCEAN[24]

Seawater Composition. Data pertinent to seawater composition have been reported by Semino[33] in Figure 5-12. Note that as chloride ion activity in NaCl increased from 10^{-1} to 10^{+1}, the pitting potentials became more negative for Alloys 400, 600, and 800. This indicates that the susceptibility to pitting increases with increasing chloride ion activity (concentration).

Erosion and Cavitation

As described in the section on Velocity, the nickel-chromium alloys are resistant to flowing seawater at velocities in excess of 140 fps (40 m/s). The results of jet erosion tests conducted by Hohman and Kennedy[35] for 30 days at 90 knots (152 fps, 46 m/s) are presented in Figure 5-20. The rates of attack for Alloys C and 718 were less than 4 mpy and welding appeared to have no adverse effect on the rate. Alloy 500 exhibited a 9 mpy rate of attack in these tests. Hohman and Kennedy[35] also conducted cavitation tests in seawater. Their results presented in Figure 5-21 show that the nickel alloys are more resistant to cavitation

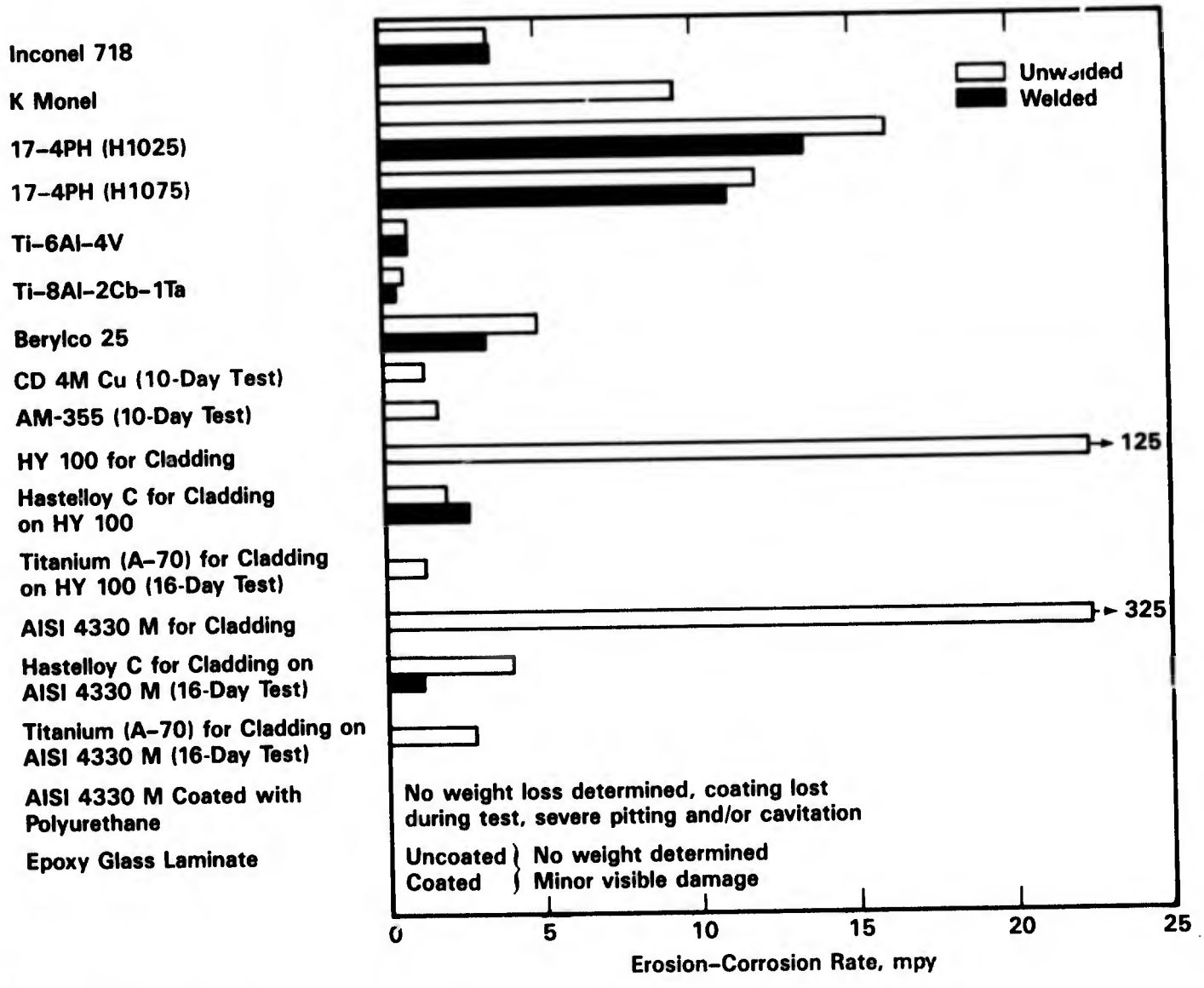

FIGURE 5-20. RATES FOR JET EROSION-CORROSION IN SEAWATER. EXPOSURE WAS FOR 30 DAYS AT 90 KNOTS[35]

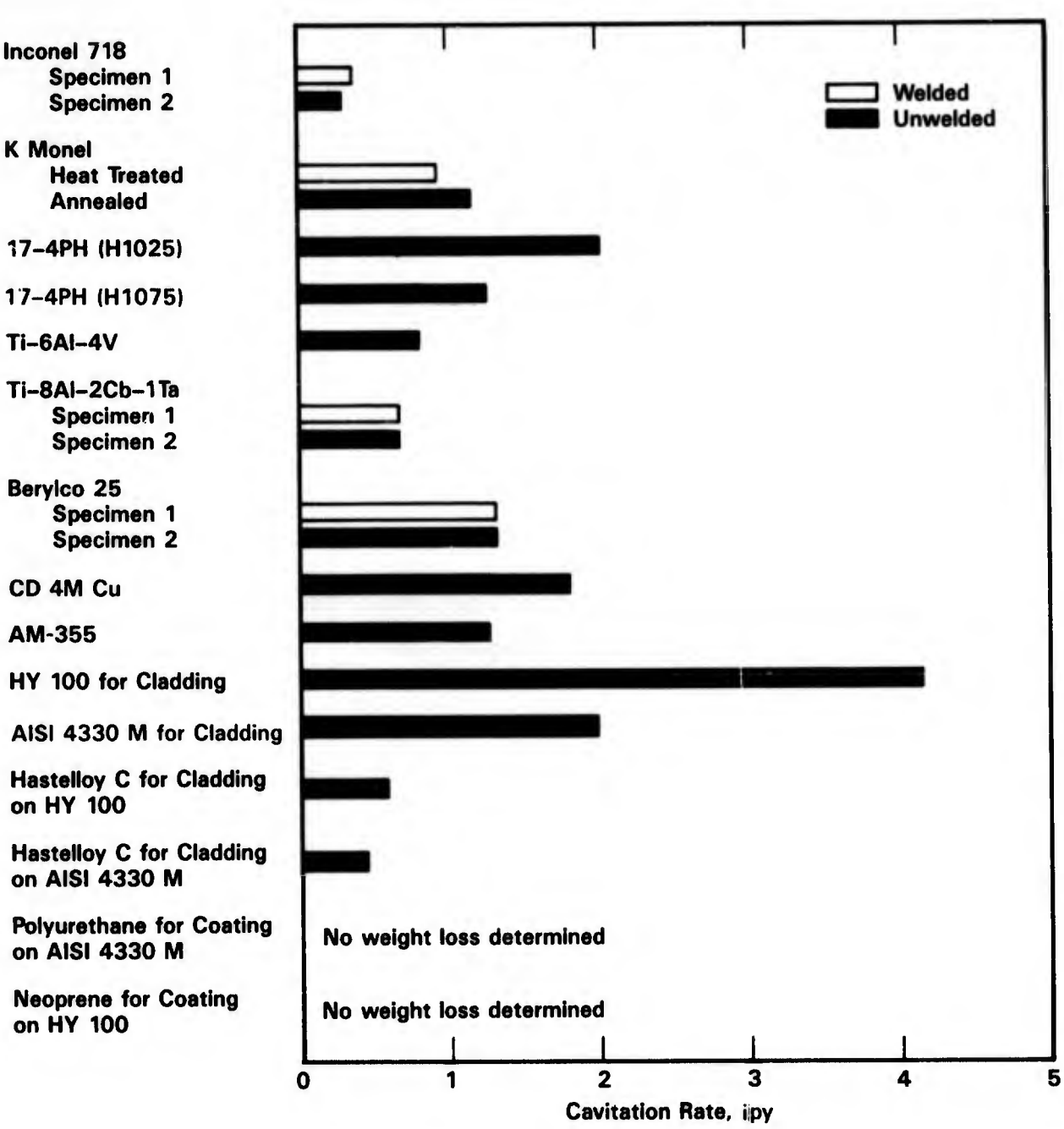

FIGURE 5-21. CAVITATION RATES IN SEAWATER. DOUBLE AMPLITUDE 0.001 INCH, FREQUENCY 22,000 CYCLES PER SECOND[35]

than most other alloy systems, even though, in these severe tests, Alloys C and 718 exhibited cavitation rates that approached 0.5 in./yr. The cavitation rate for Alloy 500 in these tests was about 1 in./yr with the annealed material having a slightly higher rate than the material heat treated to the strength needed for hydrofoil craft.

Galvanic Corrosion

Several nickel alloys are included in the galvanic series presented in Figure 5-22. Note that the more resistant nickel alloys are very noble. Thus, they would be expected to promote galvanic corrosion of those alloys that are more active, and experience little or no corrosion when coupled to the few alloys that are more noble; such is the case. Table 5-27 by Johnson and Abbott[6] shows that all the nickel alloys increase the corrosion of steel when galvanically coupled in seawater.

Ebihara[37] found that Alloy 400 promoted galvanic attack of A231 magnesium, 6061 and 7075 aluminum, 4340 steel, and 260 brass but had little or no effect on 316 stainless steel. Southwell, et al.[5] also report Alloy 400 produced galvanic attack on carbon steel as well as on phosphor bronze. As shown in Table 5-28 by Hack,[38] Alloy 400 also produces galvanic corrosion of 90-10 Cu-Ni and Ni-Al-bronze, but that Alloy 625 produces galvanic attack of Alloy 400.

Alloy 400 has been coupled to a number of alloys close to it in the galvanic series with little or no adverse effect. As shown in Table 5-29 by Vreeland,[39] Alloy 400 has little galvanic effect on a number of cobalt-base (Stellite) alloys. Anderson and Ross[10] report that the following fasteners were in excellent condition after being in Alloy 400 sheathing for 15 to 25 years: nickel 301, Alloy 400, Alloy K500, Alloy X-750, and Types 410, 431, 305, and 316 stainless steels.

Bomberger, et al.[7] have coupled Alloy 400 and 600 to titanium. Their results presented in Table 5-30 indicate no galvanic attack of Alloy 600 after one year of exposure at Ti/Alloy 600 ratios of 7/1. On the other hand, the Alloy 400 did exhibit some slight galvanic attack when the Ti/Alloy 400 ratio was 7/1, but not when the ratio was 1/7.

Velocity appears to have an effect on the corrosion of the anodic steel member of an Alloy 400/steel galvanic couple. As shown in Figure 5-23 by Perkins, et al.,[40] an increase in velocity from stagnant to 5 fps increased the rate of attack on the steel by a factor of ~3, but additional velocity increase did not increase the rate of attack any further.

According to Hack[34] 70/30 Cu/Ni promotes galvanic attack of Alloy 400 in sulfide polluted seawater, but 90/10 Cu/Ni affords galvanic protection, (see Figure 5-16).

Stress-Corrosion Cracking

The nickel-base alloys are known for their resistance to SCC in chloride-containing waters and are often used as alternative materials when stainless steels fail by chloride SCC.

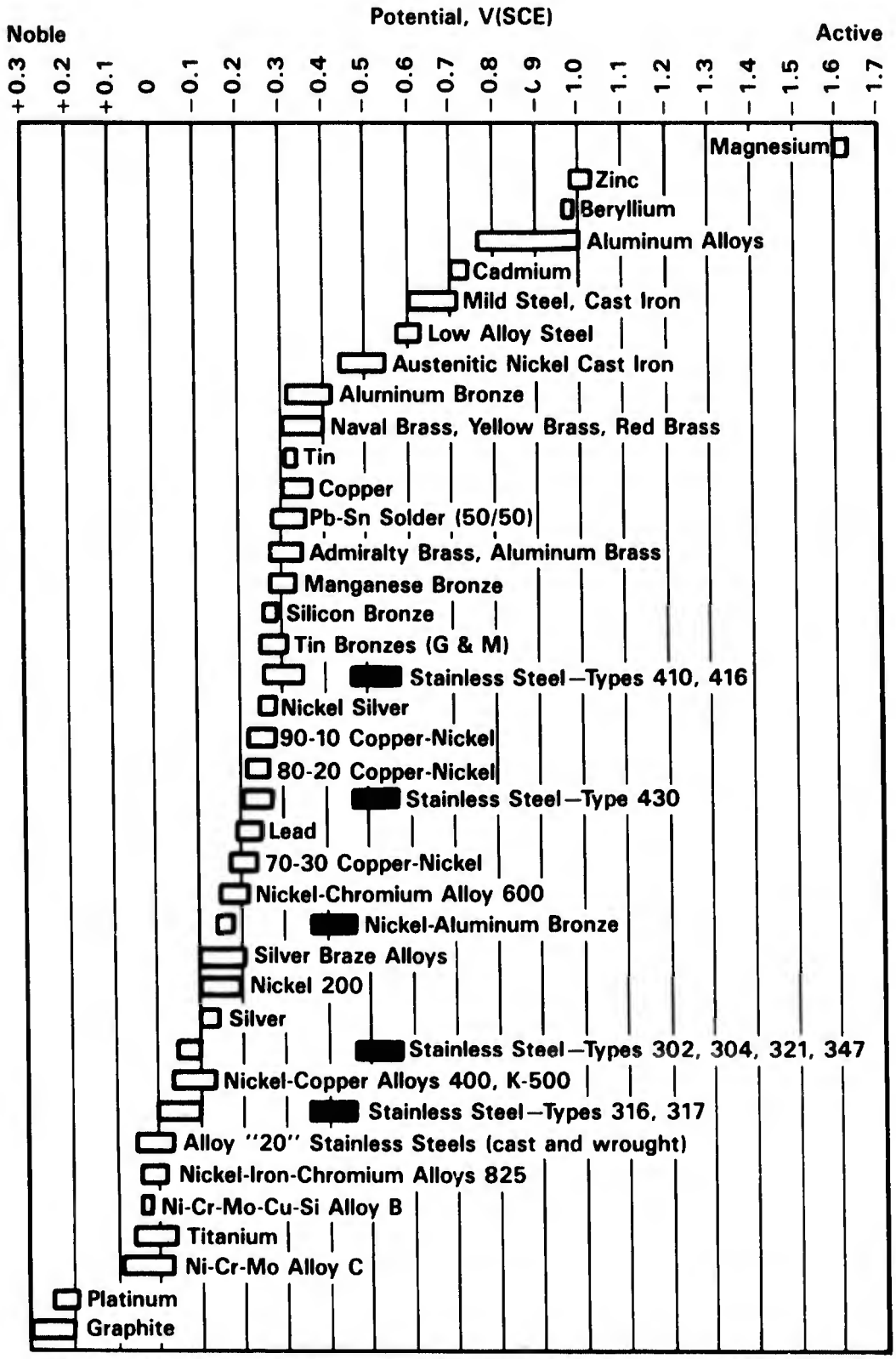

Alloys are listed in the order of the potential they exhibit in flowing seawater. Certain alloys indicated by the symbol: ■ in low-velocity or poorly aerated water, and at shielded areas, may become active and exhibit a potential near −0.5 volts.

FIGURE 5-22. GALVANIC SERIES IN SEAWATER[36]

TABLE 5-27. CORROSION RATES OF MILD STEEL AND OTHER METALS WHEN COUPLED TOGETHER, AND WHEN COUPLED TO THEMSELVES, IMMERSED IN CAERNARVON, N.W. WALES, SEAWATER[6]

Couple	Corrosion Rates, $g/m^2 \cdot day$		
	Mild Steel	Other Metal	
		Coupled to Mild Steel	Coupled to Itself
Mild steel-Hastelloy B	SD[a]	SD[a]	1.09
Mild steel-Incoloy 800	6.08	0.07	--
Mild steel-Incoloy 825	10.03	0.15	--
Mild steel-Inconel 600	8.66	0.16	--
Mild steel-Mild steel	5.67		
Mild steel-Monel 400	9.87	0.19	--
Mild steel-Nickel 200	8.16	0.15	--

(a) SD = specimen damaged.

TABLE 5-28. COMPARISON OF PREDICTED AND ACTUAL GALVANIC COUPLE PARAMETERS[38]

Material		Exposure Duration,	Current Density, μA/cm²		Couple Potential, mV		Anode Corrosion Rate, mm/yr	
Anode	Cathode	days	Predicted	Actual[a]	Predicted	Actual[a]	Predicted	Actual
HY-80 Steel	Ni-Al-Bronze	30	9.8	23	-630	-680	0.45	0.25, 0.15
		60	8.1	11	-635	-650	0.32	0.18, 0.32
		120	5.4	4.8	-640	-630	0.23	0.16, 0.24
90-10 Cu-Ni	Monel 400	30	6.0	1.4	-140	-110	1.2	0.04, 0.05
		60	7.8	4.8	-150	-120	1.1	0.13, 0.05
		120	7.0	3.4	-130	-140	2.0	0.03, 0.04
90-10 Cu-Ni	M Bronze	30	<0.16	0.02	-160	-150	0.03	0.02, 0.02
		60	<0.16	0.02	-160	-150	0.02	0.01, 0.02
		120	<0.16	0.02	-150	-130	0.02	0.01, 0.01
Monel 400	Inconel 625	30	<0.16 (12)[b]	7.9	-50	-40	0.06	0.09, 0.05
		60	<0.16 (6.2)[b]	5.7	-50	-40	0.05	0.09, 0.09
		120	<0.16	0.02	-50	-40	0.02	0.08, 0.04
Ni-Al-Bronze	Monel 400	30	16	9.5	-150	-160	0.20	0.07, 0.17
		60	16	5.0	-150	-210	0.20	0.14, 0.16
		120	16	11	-150	-200	0.20	0.13, 0.09
HY-80 Steel	Inconel 625	30	9.6	7.6	-635	-680	0.32	0.15, 0.13
		60	9.3	7.8	-635	-660	0.32	0.19, 0.19
		120	6.5	9.0	-640	-640	0.23	0.17, 0.19

(a) Average of two couples with current monitored differently.
(b) Based on anodic curve and observed couple potential.

TABLE 5-29. RESULTS OF CORROSION TESTS[39]

Material	Corrosion Rate of Test Metal, mpy		Rate Ratio, Coupled/Uncoupled
	Coupled to Monel	Uncoupled	
Tantung G	<0.1	--	--
Cobenium	<0.1	0.5	~0.2
Stellite 6K	<0.1	<0.1	~1
Stellite 6B	<0.1	<0.1	~1
Stellite 98M2	<0.1	<0.1	~1
Stellite 3	3.4	1.5	2.3
Stellite Star J	1.2	<0.1	12
Kennametal K162B	1.9	--	--
Kennametal K82	6.6	--	--
Kennametal K96	2.7	3.5	0.8
Kennametal K601	<0.1	1.2	0.1
Kennametal K701	4.6	2.6	1.8
Kennametal K801	3.6	2.8	1.3
Bearium Metal	18.1	2.4	7.5

TABLE 5-30. SEAWATER GALVANIC COUPLE TESTS OF TITANIUM AND VARIOUS METALS IN BASIN AT HALF TIDE AT KURE BEACH[7]

Material	193-Day Exposure			369-Day Exposure		
	Uncoupled Corrosion Rates, mpy[a]	Coupled Corrosion Rates, mpy		Uncoupled Corrosion Rates, mpy[a]	Coupled Corrosion Rates, mpy	
		Metal Area 7 x Ti Area[b]	Metal Area 1/7 x Ti Area[c]		Metal Area 7 x Ti Area[b]	Metal Area 1/7 x Ti Area[c]
Monel	0.071	0.060	0.130	0.073	0.06	0.130
Inconel	0.002	Nil	0.002	Nil	Nil	Nil
302 Stainless	0.058	0.010	0.120	0.004	0.008	0.096
316 Stainless	Nil	Nil	Nil	Nil	Nil	Nil

(a) Average of one 6 in. x 1.5 in. specimen and two 1.5 in. x 0.75 in. specimens.
(b) One 6 in. x 1.5 in. specimen.
(c) Average of two 0.75 in. x 1.5 in. specimens.

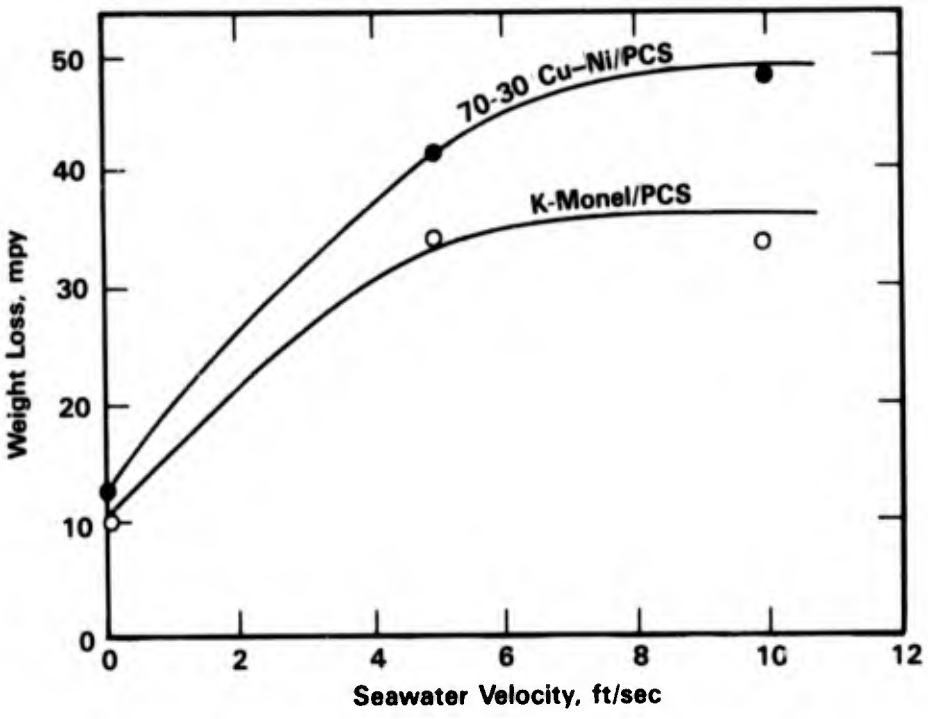

FIGURE 5-23. AVERAGE CORROSION RATE (IN 24 HOUR PERIOD) AS A FUNCTION OF VELOCITY FOR 70-30 CUPRONICKEL/PCS AND K-MONEL/PCS COUPLES (PCS = CARBON STEEL)[40]

However, there are few documented cases of the performance of stressed nickel-base alloys. Reinhart[19] included stressed Alloy C and 825 in his deep ocean tests. The results of his tests are presented in Table 5-31, and reveal no SCC in exposures to 731 days at stresses to 75 percent of yield strength. Sedriks[36] has reported no SCC of U-bends of 904L, G3, 625, and C276 after 300 to 550 hours' exposure in synthetic seawater at 35 and 80 C.

SCC may occur with nickel-base alloys in very high temperature chloride environments. Cramer and Carter[41] exposed Alloy 625 and C-276 to geothermal type brines at 232 C and detected SCC in both alloys in 7 to 30 day tests under deaerated conditions, and with 100 ppm dissolved oxygen. Cheng and Tymchyn[42] have conducted tilting autoclave tests with aerated synthetic seawater at 288 C and found SCC in Alloy X within 1 day and in Alloy C within 12 days. No SCC occurred in Alloy 600 after 39 days' exposure in these tests.

TABLE 5-31. STRESS-CORROSION TEST RESULTS FOR NICKEL-BASE ALLOYS IN A DEEP OCEAN ENVIRONMENT[19]

Alloy	Stress, ksi	Percent of YS	Exposure, days	Depth, ft	Number of Specimens	Number Failed
Ni-Mo-Cr Alloy C	21.0	35	123	5,640	3	0
Ni-Mo-Cr Alloy C	30.0	50	123	5,640	3	0
Ni-Mo-Cr Alloy C	45.0	75	123	5,640	3	0
Ni-Mo-Cr Alloy C	21.0	35	403	6,780	2	0
Ni-Mo-Cr Alloy C	30.0	50	403	6,780	2	0
Ni-Mo-Cr Alloy C	45.0	75	403	6,780	2	0
Ni-Mo-Cr Alloy C	21.0	35	751	5,640	3	0
Ni-Mo-Cr Alloy C	30.0	50	751	5,640	3	0
Ni-Mo-Cr Alloy C	45.0	75	751	5,640	3	0
Ni-Mo-Cr Alloy C	21.0	35	197	2,340	3	0
Ni-Mo-Cr Alloy C	30.0	50	197	2,340	3	0
Ni-Mo-Cr Alloy C	45.0	75	197	2,340	3	0
Ni-Mo-Cr Alloy C	30.0	50	402	2,370	3	0
Ni-Mo-Cr Alloy C	45.0	75	402	2,370	3	0
Ni-Mo-Cr Alloy 825	25.7	50	402	2,370	3	0
Ni-Mo-Cr Alloy 825	38.5	75	402	2,370	3	0

Intergranular Attack

Intergranular attack (IGA) has been reported to occur in heat-sensitized areas of welded Alloy C in heated seawater, and thus Alloy C276 is preferred if welded equipment is to be used under these conditions.[36] An extensive discussion of IGA of Fe-Cr-Ni alloys is given in the section on Stainless Steels.

Mud

Results of mud zone exposures in the deep ocean as reported by Reinhart[19] are included in Table 5-15. General corrosion rates for all alloys were low at <0.1 to 0.3 mpy whether exposed in the mud or in the seawater itself. However, for those alloys that exhibited crevice attack (Alloys 600, 610, X-750, 88, 825, and 902), the attack appeared to be deeper in the water than in the mud zone. In these tests, Alloys 625, 700, 804, 825S, 825Cb3, 901, B, G, F, X, and a modified G did not exhibit crevice attack in the mud zone.

REFERENCES FOR CHAPTER 5

1. Southwell, C. R. and Alexander, A. L., "Corrosion of Metals in Tropical Environments - Nickel and Nickel-Copper Alloys", Materials Protection, 8 (3), pp 39-44 (March, 1969).

2. Miska, K. H., "Most Nonferrous Metals and Alloys Weather Well", Materials Engineering, 79 (4), pp 64-66 (April, 1974).

3. Boyd, W. K. and Fink, F. W., "Corrosion of Metals in Marine Environments", Battelle Columbus Labs Report MCIC-78-37, 103 pp (March, 1978).

4. Baboian, R., "Final Report on the ASTM Study: Atmospheric Galvanic Corrosion of Magnesium Coupled to Other Metals", Atmospheric Factors Affecting Corrosion, ASTM-STP-646, pp 17-29 (1978).

5. Southwell, C. R., et al., "Corrosion of Metals in Tropical Environments - Aluminum and Magnesium", Materials Protection, 4 (12), pp 30 (December, 1965).

6. Johnson, K. E. and Abbott, J. S., "Bimetallic Corrosion Effects on Mild Steel in Natural Environments", British Corrosion Journal, 9 (3), pp 171-176 (1974).

7. Bomberger, H. B., et al., "Corrosion Properties of Titanium in Marine Environments", Journal of the Electrochemical Society, 101 (9), pp 442-447 (September, 1954).

8. Money, K. L. and Kirk, W. W., "Stress-Corrosion Cracking Behavior of Wrought Fe-Cr-Ni Alloys in Marine Atmosphere", Materials Performance, 17 (7), pp 28-36 (July, 1978).

9. Ballantine, W., "Choosing Corrosion-Resistant Fasteners for Marine Applications", Sea Technology, 17 (2), pp 8-10 (February, 1976).

10. Anderson, D. B. and Ross, R. W., Jr., "Protection of Steel Piling in Marine Splash and Spray Zones - Metallic Sheathing Concept", 4th International Congress on Marine Corrosion and Fouling, Boulogne, France, pp 461-473 (1976).

11. Davis, J. W., "Corrosion and Stress-Corrosion Susceptibility of Several High Temperature Materials", McDonnell Douglas, 3rd Quarterly, NAS8-27270, 34 pp (March, 1972).

12. Humphries, T. S. and Nelson, E. E., "Stress-Corrosion Cracking Evaluation of Several Ferrous and Nickel Alloys", NASA, NASA-TM-X-64511, 15 pp (April, 1970).

13. Montano, J. W., "A Mechanical Property and Stress-Corrosion Evaluation of MP35N Multiphase Alloy", NASA Report NASA-TM-X-64591, 25 pp (May, 1971).

14. Deel, O. L. and Mindlin, H., "Engineering Data on New Aerospace Structural Materials", Battelle, Columbus, OH, Final Report AFML-TR-72-196-V2, 168 pp (September, 1972).

15. Deel, O. L. and Mindlin, H., "Engineering Data on New Aerospace Structural Materials", Battelle, Columbus, OH, Final Report AFML-TR-72-196-V1, 118 pp (September, 1972).

16. Lennox, T. J., Jr., "Marine Electrochemical Corrosion and Control Systems", Naval Research Lab Final Report NRL-MR-3622, 66 pp (October, 1977).

REFERENCES FOR CHAPTER 5
(Continued)

17. Lennox, T. J., Jr., et al., "Corrosion Resistance and Response to Cathodic Protection of Advanced Alloys in Seawater", Corrosion '82, Houston, TX, (64) (March, 1982).

18. Maylor, J. B., "Corrosion Resistance of High Nickel Alloys in Seawater", Anti-Corrosion, 25 (7), pp 3, 5-9 (July, 1978).

19. Reinhart, F. M., "Corrosion of Materials in Hydrospace. Part II: Nickel and Nickel Alloys", Naval Civil Engineering Lab Report NCEL-TN-915, 65 pp (August, 1967).

20. Kain, R. M., "Crevice Corrosion Resistance of Several Iron and Nickel-Base Cast Alloys in Seawater", Corrosion '82, Houston, TX, (66), 25 pp (March, 1982).

21. Tipton, D. G. and Kain, R. M., "Effect of Temperature on the Resistance to Pitting of Monel Alloy 400 in Seawater", Corrosion '80, Chicago, IL, Paper 36, 13 pp (March, 1980).

22. Asphahani, A. I., et al., "Highly Alloyed Stainless Materials for Seawater Applications", Corrosion '80, Chicago, IL, Paper 29, 42 pp (March, 1980).

23. Hodgkiess, T. and Rigas, S., "A Comparison of the Corrosion Resistance of Some Higher-Alloy Stainless Steels in Seawater at 20-100 C", Desalination, 44, pp 283-294 (May, 1983).

24. Reinhart, F. M. and Jenkins, J. F., "Corrosion of Materials in Surface Seawater After 12 and 18 Months of Exposure", Final Report NCEL-TN-1213, 106 pp (January, 1972).

25. Reinhart, F. M. and Jenkins, J. F., "The Relationship Between the Concentration of Oxygen in Seawater and the Corrosion of Metals", U.S. Naval Civil Engineering Laboratory, pp 562-577 (1971).

26. Danek, G. J., Jr., "The Effect of Seawater Velocity on the Corrosion Behavior of Metals", Naval Engineers Journal, 78 (5), pp 763-769 (October, 1966).

27. Moller, G. E., "The Successful Use of Austenitic Stainless Steels in Seawater", Society of Petroleum Engineers Journal, 17 (2), pp 101-110 (April, 1977).

28. Todd, B., "Nickel Containing Materials for Marine Applications", Anti-Corrosion, 25 (10), pp 4-7 (October, 1978).

29. Wheatfall, W. L., "Metal Corrosion in Deep-Ocean Environments", U.S. Navy Marine Engineering Laboratory, R-429/66, 23 pp (January, 1967).

30. Anderson, D. B., "Statistical Aspects of Crevice Corrosion in Seawater", Galvanic and Pit Corr-Field and Lab Studies, ASTM-STP-576, pp 231-242 (1976).

31. Lennox, T. J., et al., "Corrosion Resistance and Response to Cathodic Protection on Advanced Alloys in Seawater", Materials Performance, 22 (6), pp 49-55 (June, 1983).

32. Tipton, D. G. and Kain, R. M., "Effect of Temperature on the Resistance to Pitting of Monel Alloy 400 in Seawater", Corrosion '80, Paper 36 (March, 1980).

REFERENCES FOR CHAPTER 5
(Continued)

33. Semino, C. J., et al., "The Localized Corrosion of Resistant Alloys in Chloride Solutions", Corrosion Science, 19 (12), pp 1069-1078 (1979).

34. Hack, H. P., "Galvanic Corrosion of Piping and Fitting Alloys in Sulfide Modified Seawater", Journal of Testing and Evaluation, JTEVA, 8 (2), pp 74-79 (March, 1980).

35. Hohman, A. E. and Kennedy, W. L., "Corrosion and Materials Selection Problems on Hydrofoil Craft", Materials Protection, 2 (9), pp 56-68 (September, 1963).

36. Sedriks, A. J., "Corrosion Resistance of Austenitic Fe-Cr-Ni-Mo Alloys in Marine Environments", International Metals Reviews, 27 (6), pp 321-353 (1982).

37. Ebihara, W. T., "Tropical Exposure of Galvanically Coupled Metal Systems", Army Armament R&D, ARSDC-TR-79004, 18 pp (June, 1979).

38. Hack, H. P., "Galvanic Corrosion Prediction Using Long-Term Potentiostatic Polarization Curves", Corrosion '83, Anaheim, CA, Paper 73, 15 pp (April, 1983).

39. Vreeland, D. C., "Galvanic Corrosion Behavior of Wear-Resistant Materials for Mechanical Shaft Seals", Navy Marine Engineering Laboratory, MEL-242/66, 13 pp (July, 1966).

40. Perkins, J., et al., "Flow Effects on Corrosion of Galvanic Couples in Seawater", Corrosion, 35 (1), pp 23-33 (January, 1979).

41. Cramer, S. D. and Carter, J. P., "Laboratory Corrosion Studies in Low and High Salinity Geobrines in the Imperial Valley, California", U.S. Bureau of Mines, Washington, DC, Report of Investigation 8415 (1980).

42. Cheng, C. F. and Tymchyn, H. L., "Stress-Corrosion of Inconel in 550 F Aerated Seawater", USAEC Report KAPL-M-CC-2 (February, 1961).

CHAPTER 6
TABLE OF CONTENTS

CHAPTER 6
LIST OF TABLES

CHAPTER 6
LIST OF TABLES
(Continued)

CHAPTER 6
LIST OF FIGURES

CHAPTER 6
LIST OF FIGURES
(Continued)

CHAPTER 6
LIST OF FIGURES
(Continued)

CHAPTER 6
LIST OF FIGURES
(Continued)

CHAPTER 6

CARBON AND LOW-ALLOY STEELS

Plain-carbon steel is the most important metal in marine service, and has been widely used for many years in marine construction. More recently, low-alloy steels of higher strength have been finding increasing application. Related ferrous materials such as cast irons, wrought iron, and ingot iron are sometimes used in special applications. Steels are selected for marine service because of such factors as availability, cost, ease of fabrication, design experience, and physical and mechanical properties.

The behavior of steel and other ferrous materials tends to show striking differences in the various exposure zones. Thus, one cannot apply the results from an atmospheric exposure to an application involving fully immersed conditions. The sections which follow give selected details of the corrosion of steel in each type of marine environment.

Atmospheric Corrosion

General and Pitting Corrosion

Carbon and low-alloy steels undergo general, pitting, and crevice corrosion in marine atmospheres. General corrosion rates, based on weight or average thickness losses, vary widely, between about 1 and 30 mils per year.[1] Similarly, pitting factors* vary widely. Typical data given in Table 6-1 indicate pitting factors between about 3 and 15. Both general and localized corrosion of carbon and low-alloy steels are greatly influenced by a number of parameters, which include geometrical factors, climate (both local and regional) and alloy composition. Discussions of these factors are given below.

Geometrical Factors. Larrabee[3] studied the effect of sheltering and facing direction (north, south, east, or west) on the corrosion of carbon steel on a lot 800 ft from the ocean at Kure Beach, NC. Specimens were mounted vertically in five horizontal rows on a sheltered test rack such that the upper two rows were completely sheltered from the rain. Results, given in Figure 6-1, show that the east exposure was most severe and that the higher, more

---

* Ratio of deepest measured penetration divided by the average penetration calculated from weight loss.

TABLE 6-1. COMPREHENSIVE EVALUATION OF CORROSION DAMAGE FOR TEN STRUCTURAL STEELS EXPOSED TO TROPICAL ATMOSPHERES IN THE PANAMA CANAL ZONE[2] (SEE APPENDIX F, TABLE F-1, FOR COMPOSITIONS OF STEELS)

Steel	Exposure	Weight Loss, g/dm²				Average Reduction in Thickness, mils[a]				Average 20 Deepest Pits, mils[b]				Deepest Pit, mils[b]				Pitting Factor[c]				Rank[d]
		1 Yr	2 Yr	4 Yr	8 Yr	1 Yr	2 Yr	4 Yr	8 Yr	1 Yr	2 Yr	4 Yr	8 Yr	1 Yr	2 Yr	4 Yr	8 Yr	1 Yr	2 Yr	4 Yr	8 Yr	
L	Marine	4.34	7.07	9.10	17.45	4.4	7.1	9.2	17.6	10	11	8	32	15	26	12	66(P)	7	7	3	8	5
	Inland	2.75	4.66	7.21	10.96	2.8	4.7	7.3	11.0	4	6	6	14	5	9	9	22	4	4	2	4	
M	Marine	3.07	3.92	5.05	7.48	3.1	4.0	5.1	7.5	13(5)	6	10	11	14	10	11	21	9	5	4	6	2
	Inland	1.84	2.94	4.27	5.65	1.9	3.0	4.3	5.7		4	9	11		6	12	15	0	4	5	5	
N	Marine	2.67	3.63	4.57	7.07	2.7	3.7	4.6	7.1	10(16)	9	8	11	15	15	11	13	11	8	5	4	2
	Inland	1.98	2.55	4.21	5.31	2.0	2.6	4.2	5.4	5(16)	0	7	10	9	0	9	16	9	0	4	6	
O	Marine	3.93	4.97	6.01	9.03	4.0	5.0	6.1	9.1	12	12	14	18	17	30	26	63(P)	9	12	9	14	4
	Inland	2.06	2.58	2.96	3.71	2.1	2.6	3.0	3.8	8(16)	6	8	11	16	13	9	18	2	10	6	10	
P	Marine	3.21	3.61	4.17	6.04	3.3	3.7	4.3	6.1	11	8	9	11	14	13	12	26	9	7	6	8	1
	Inland	1.58	1.88	1.98	2.29	1.6	1.9	2.0	2.4	0	0	0	5	0	0	0	9	0	0	0	8	
C	Marine	3.43	4.67	6.08	10.01	3.5	4.7	6.2	10.1	6	7	8	12	10	10	11	17	6	4	3	3	3
	Inland	2.23	3.43	4.94	6.84	2.3	3.5	5.0	6.9	0	4	6	11	0	6	8	14	0	3	2	4	
D	Marine	3.38	4.45	6.18	10.15	3.4	4.5	6.2	10.2	10	8	8	12	18	16	11	28	10	7	4	5	3
	Inland	1.96	2.96	4.26	5.77	2.0	3.0	4.3	5.8	0	6	7	10	0	7	8	17	0	5	4	6	
E	Marine	3.43	4.70	5.94	9.74	3.5	4.8	6.0	9.8	8	7	5	12	14	12	6	24	8	5	2	5	3
	Inland	2.09	3.51	5.08	6.86	2.2	3.6	5.1	6.9	0	5(10)	7	12	0	8	9	16	0	5	4	5	
F	Marine	3.33	4.46	5.58	8.98	3.4	4.5	5.6	9.0	7(10)	9	6	12	10	18	9	22	6	8	3	5	3
	Inland	2.29	3.46	4.80	6.36	2.3	3.5	4.8	6.4	0	6	7	13	0	8	9	18	0	4	4	6	
A	Marine	5.02	9.56	11.22	20.28	5.1	9.6	11.3	20.4	13	20	18	34	20	26	50	67	8	5	9	7	6
	Inland	2.73	5.09	8.28	12.58	2.8	5.1	8.3	12.6	0	9	10	17	0	19	15	27	0	7	4	4	
A	Marine	5.15	8.95	11.01	21.83	5.2	9.0	11.1	21.9	10	20	18	37	19	34	45	97	7	8	8	9	6
(millscale)	Inland	2.98	5.42	8.27	12.33	3.0	5.5	8.3	12.4	5(2)	8	7	17	6	13	9	27	4	5	2	4	

(a) Calculated from weight loss and specific gravity.
(b) Pit depths referred to the original surface of the metal either by measurement from an uncorroded surface or by calculation using the original and final average measured thickness of the same. Average of 20 deepest pits represents average of the 5 deepest pits measured on each side of duplicate specimens (area, 0.89 sq ft); values in parentheses indicate total number averaged when less than 20. Penetration of plate by deepest pit is indicated by "P".
(c) Ratio of the deepest measured penetration to the average calculated penetration.
(d) Visual inspection ranking based on observation of cleaned eight-year exposure panels. A total of eight surfaces were inspected (both sides of duplicate panels from the inland and marine exposures).

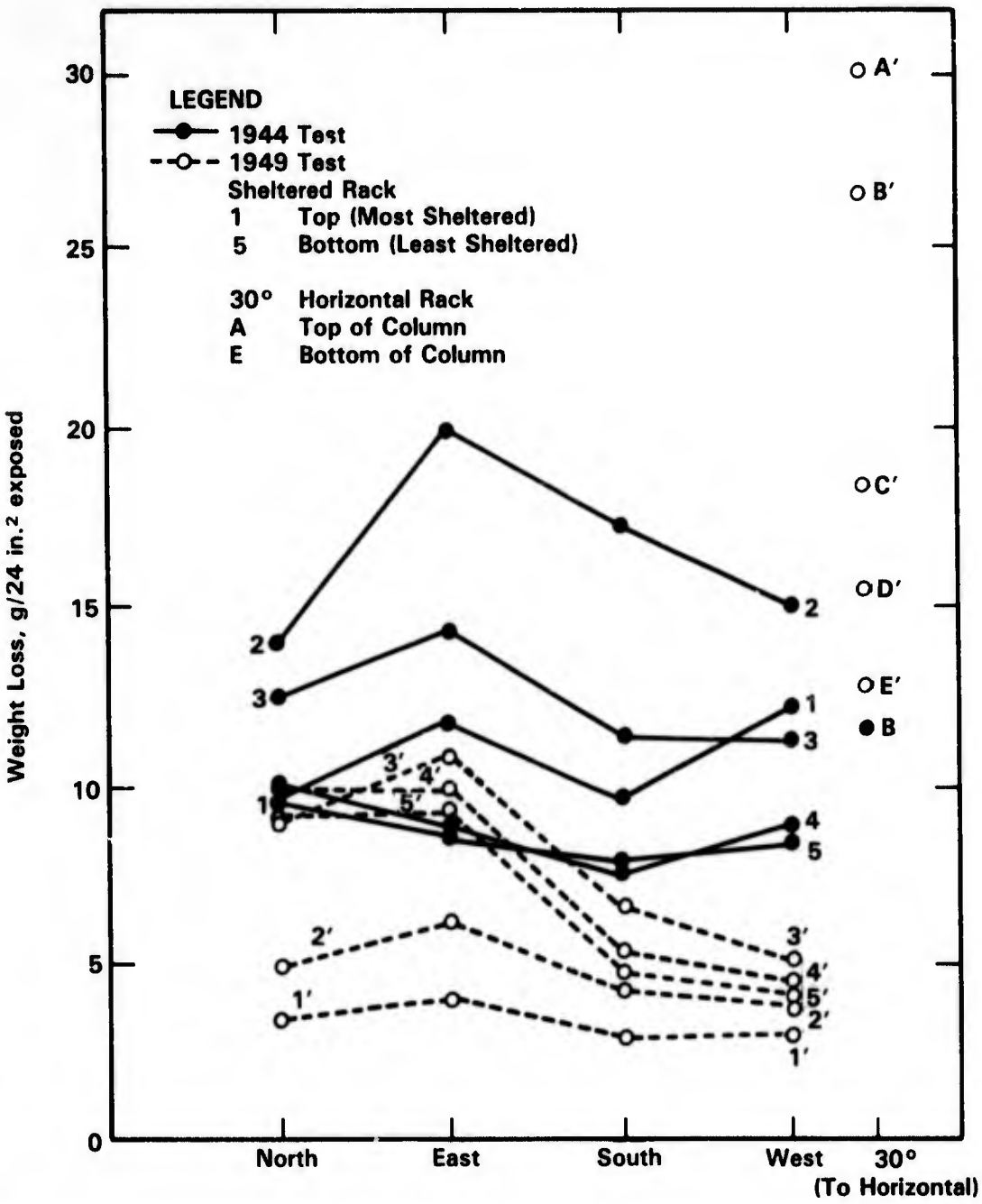

FIGURE 6-1. EFFECT OF AMOUNT OF SHELTER AND DIRECTION OF EXPOSURE ON CORROSION OF CARBON STEEL AFTER EXPOSURES IN MARINE ATMOSPHERE FOR TWO YEARS[3]

sheltered specimens generally exhibited the highest weight losses. This behavior was attributed to the deposition of sea salt on the specimens facing the ocean and the washing action of rain in removing the sea salt from the lower specimens.

Larrabee[3] also studied the corrosion of carbon steel specimens exposed at an angle of 30 degrees to the horizontal, one above the other, in an unsheltered south facing rack.

Results, also given in Figure 6-1, show that attack generally was greater in these exposures than in the sheltered exposures and was highest for the uppermost specimens. Corrosion of the skyward faces was mild and uniform whereas the downward faces underwent severe attack. Thus, it was concluded that rain washed the deposited salts from the top sides of the specimens and that the amount of salt deposited on the bottom sides of the specimens increased with increasing height above the ground.

Ambler and Bain[4] also studied the effect of orientation on the marine atmospheric corrosion of carbon steel. Results of these studies, summarized in Table 6-2, also show that the seaward exposed faces experience the highest corrosion rates. Analysis of the effect of skyward versus downward facing of the specimens on corrosion was confounded in this study by the fact that the specimens were oriented at 45 degree angle to the horizontal and the upper faces also were the seaward faces. Ambler and Bain[4] did observe that exposures at 20 ft above the ground were more severe than exposures at 5 ft above the ground, which is qualitatively in agreement with the results of Larrabee.[3] Ambler and Bain[4] also reported that the exposure height effect on corrosion rates was not observed away from the salt spray, see Table 6-3.

Ambler and Bain[4] also studied the effect of screening specimens from the prevailing wind on the corrosion rate of mild steel and other alloys. Results summarized in Table 6-4 show that specimens which were sheltered from the wind exhibited lower rates of attack than those which were not.

Effect of Climate. Considering the large effect that geometrical factors can have on corrosion rates of carbon steel in marine atmospheres, it is tenuous to compare, in detail, results of studies by different researchers where exposures were performed at different locations using varied test procedures. Nevertheless, several systematic studies of local climate and weather effects on corrosion have been performed. Ambler and Bain[4] studied the effect of location in Nigeria on the corrosion rates of carbon steel and correlated rates of attack with the salinity of the atmosphere, see Figure 6-2. Similarly, the 80-ft lot at Kure Beach, NC, has been shown to be much more aggressive than the 800-ft lot; typical data are shown in Table 6-5.

However, not all marine sites have been found to be highly corrosive. Southwell and Bultman[5] reported that exposures at Naos Island in the bay of Panama, only 2.5 m above high tide, produced corrosion rates which were only slightly higher than inland exposures in the Panama Canal Zone. The low corrosion rate observed on the Pacific island was attributed to frequert rain showers which rinsed the specimens and low wind velocities, which minimize salt spray.

TABLE 6-2. CORROSION ON FACES OF STEEL PANELS, VARIOUSLY ORIENTED IN LAGOS AND PORT HARCOURT, NIGERIA[4]

Site	Conditions of Exposure		Mean Corrosion, g/dm^2/month
Lagos, 50 yards from HWM*	Vertical; 5 ft above ground	Seaward face	5.3
		Landward face	2.2
Lagos, 200 yards from HWM	Vertical; 5 ft above ground	Seaward face	0.50
		Landward face	0.45
Lagos, 200 yards from HWM	45 degrees facing sea, 5 ft above ground		
		Upper and seaward face	0.79
		Lower and landward face	0.71
Lagos, 200 yards from HWM	45 degrees facing sea, 20 ft above ground		
		Upper and seaward face	1.07
		Lower and landward face	1.36
Lagos, 200 yards from HWM	Vertically, mounted on wind vane, 25 ft high		
		Windward face	1.80
		Leeward face	1.25
		Edge on	1.47
Port Harcourt	45 degrees	Upper (windward) face	0.22
		Lower (leeward) face	0.25

* HWM = high water mark.

TABLE 6-3. EFFECT OF HEIGHT ON CORROSION AT TWO MARINE SITES IN NIGERIA[4]

Site	Height Above Ground, ft	Corrosion, g/dm^2/month		
		Mild Steel	Brass	Aluminum
Bonny Island Lighthouse, about 2 miles from surf	5	0.35	—	—
	30	0.37	0.046	0.017
		0.27	0.045	0.016
	60	0.28	0.030	0.015
		0.43	0.030	0.018
	120	0.38	0.023	0.022
		0.31	0.025	0.020
Lighthouse Beach Lagos, 200 yards from HWM*	5	2.1	0.035	0.0135
	18	2.3	0.038	0.013
Lighthouse Beach Lagos, 400 yards from HWM	5	1.3	—	—
	75	2.2	—	—

* HWM = high water mark.

TABLE 6-4. EFFECT OF SHELTER (PANELS AT 45 DEGREES TO SEA) FROM SEA WIND ON CORROSION AT LAGOS, NIGERIA[4]

Site	Period, months	Conditions of Exposure	Corrosion, g/dm^2/month		
			Mild Steel	Brass	Aluminum
Lighthouse Beach 50 yards from HWM*	2	Behind low screen of palm thatch	1.09, 1.28	--	--
	4	Fully exposed	1.53, 1.16	--	--
		(average figure)	4.9	--	--
Lighthouse Beach 200 yards from HWM	4	In lee (N.E.) of building	0.45, 0.41	0.011, 0.010	0.004, 0.003
		Fully exposed (average figures)	2.8	0.016	0.01

* HWM = high water mark.

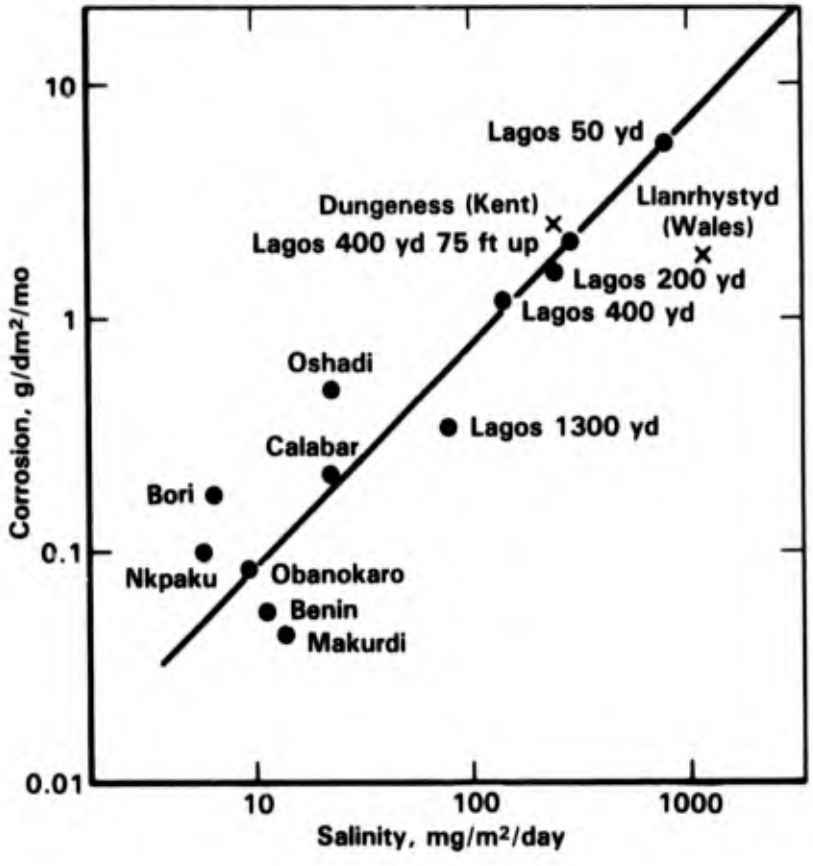

FIGURE 6-2. RELATION BETWEEN CORROSION OF MILD STEEL AND SALINITY AT EXPOSURE SITES IN NIGERIA AND ELSEWHERE[4]

TABLE 6-5. MARINE ATMOSPHERIC CORROSION BEHAVIOR OF FERROUS MATERIALS AT DIFFERENT MARINE SITES[1,4]

Site	Exposure Time, Years	Corrosion Rate, mpy (Calculated From Weight Loss) Open Hearth Iron	Carbon Steel	Wrought Iron[a]
Kure Beach, NC (80-foot lot)	1	31.5		--
	1.5 to 3.5		47	
Daytona Beach, FL (300-foot lot)	1	9.1		
Sandy Hook, NJ	1	3.3		
Kure Beach, NC (800-foot lot)	1	2.6		
	1.5	2.7[b]	1.6	--
	3.5		1.5	--
	7.5		1.3	--
Block Island, RI	1.1	8.6[b]	2.7	--
	3.3		2.6	--
Halifax, Nova Scotia	5	1.2	0.62	1.2
Auckland, New Zealand	5	3.3	1.37	2.2
Plymouth, England	5	8.2	2.03	4.7
Colombo, Ceylon	5	17.9	17.3	11.0
Cristobal, Panama Canal Zone (300-foot lot)	0 to 4		2.8	3.5
	4 to 8		2.3	2.1

(a) Exposed for same period as carbon steel panels.
(b) High-purity iron with 0.02 percent copper.

Annual variation in weather and climatic conditions at the same site also can greatly influence the corrosivity of the environment. Larrabee[3] reported on two identical experiments at the same test rack at Kure Beach, NC, and observed significantly different results, see Figure 6-1.

Effect of Alloying. It is well established that alloy additions to carbon steel are beneficial in improving corrosion resistance in marine atmospheric exposure. Data by

Larrabee[3] and by Copson[1] for a number of carbon and low-alloy steels are given in Figure 6-3 and Table 6-6. These data show that a wide range of compositions gave improved resistance to marine atmospheric corrosion. The most resistant steels appear to be those in groups 5, 7, 10, and 11 from the data by Copson.[1] It is interesting to note that the composition of group 5 alloys generally meets the specification of the widely used high strength low-alloy steel Corten*. When selected corrosion data from Table 6-6 are plotted as a function of the total concentration of elements added, the results suggest that a total alloy content of about 2 percent provides optimum performance, see Figure 6-4.

The effects of addition of individual alloying elements to carbon steel on corrosion in marine atmospheres also have been studied in some detail. Results of a study by Copson[1] on the effects of individual additions of Cu, Mn, Ni, and Cr on atmospheric corrosion at Kure Beach, NC, are given in Figure 6-5. These data show that additions of up to about 1 percent Cu are beneficial for high P (0.1 percent P) steels containing 0.030-0.06 percent S, but the

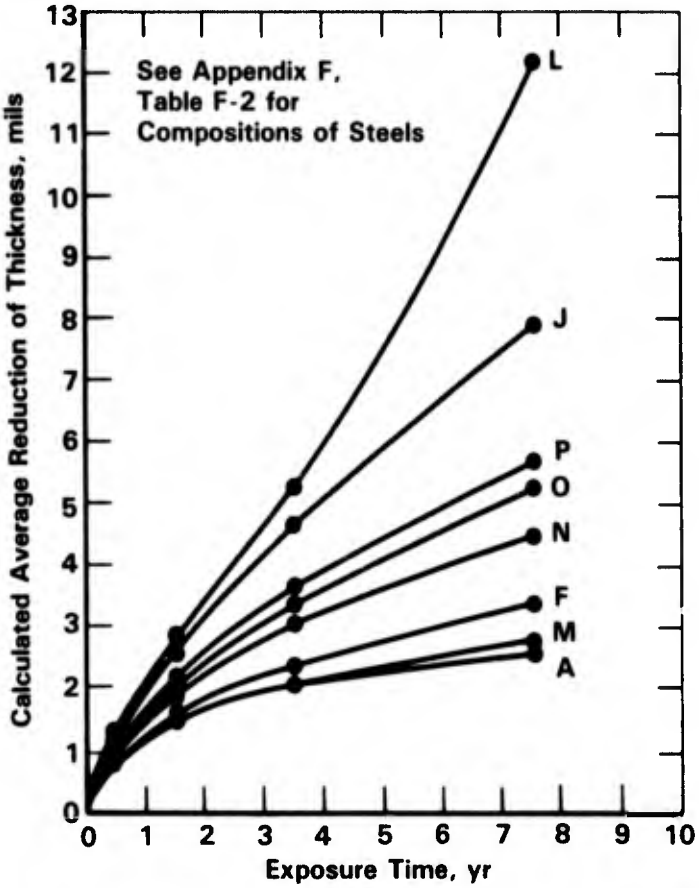

FIGURE 6-3. EFFECT OF EXPOSURE TIME ON CORROSION OF STEELS IN MARINE ATMOSPHERE AT KURE BEACH, NC[3]

* Corten is a registered trademark of U.S. Steel. Its composition is C, 0.12 max; Mn, 0.2-0.5; P, 0.07-0.15; S, 0.05 max; Si, 0.25-0.75; Cu, 0.25-0.55; Cr, 0.31-1.25; and Ni, 0.65 max.

TABLE 6-6. CORROSION OF LOW-ALLOY STEELS IN A MARINE ATMOSPHERE FOR 15.5 YEARS AT KURE BEACH, NC (800-FOOT LOT)[1]

Group, Description	Composition, percent									= Total Alloy Content, percent	Weight Loss[a], mg/dm^2
	C	Mn	Si	S	P	Ni	Cu	Cr	Mo		
1, High-purity iron plus copper	0.020	0.020	0.003	0.03	0.006	0.05	0.020	--	--		
	0.020	0.023	0.002	0.03	0.005	0.05	0.053	--	--	0.1	43
	0.02	0.07	0.01	0.03	0.003	0.18	0.10	--	--	0.4	29.8
2, Low-phosphorus steel, plus copper	0.040	0.39	0.005	0.02	0.007	0.004	1.03	0.06	--	1.5	17.3
3, High-phosphorus steel, plus copper	0.09	0.43	0.005	0.03	0.058	0.24	0.36	0.06	--	1.2	16.9
	0.095	0.41	0.007	0.05	0.104	0.002	0.51	0.02	--	1.0	16.5
4, High-manganese and -silicon steels, plus copper	0.17	0.67	0.23	0.03	0.012	0.05	0.29	0.14	--	1.4	16.6
5, Copper steel, plus chromium and silicon	0.072	0.27	0.83	0.02	0.140	0.03	0.46	1.19	--	2.9	6.3
6, Copper steel, plus molybdenum	0.17	0.89	0.05	0.03	0.075	0.16	0.47	--	0.28	1.9	11.8
7, Nickel steel	0.16	0.57	0.020	0.02	0.015	2.20	0.24	--	--	3.0	9.4
	0.19	0.53	0.009	0.02	0.016	3.23	0.07	--	--	3.9	9.2
	0.17	0.58	0.26	0.01	0.007	4.98	0.09	--	--	5.9	6.1
	0.13	0.23	0.07	0.01	0.007	4.99	0.03	0.05	--	5.4	7.5
8, Nickel steel, plus chromium	0.13	0.45	0.23	0.03	0.017	1.18	0.04	0.65	0.01	2.6	10.5
9, Nickel steel, plus molybdenum	0.16	0.53	0.25	0.01	0.013	1.84	0.03	0.09	0.24	3.0	9.8
10, Nickel steel, plus chromium and molybdenum	0.10	0.59	0.49	0.01	0.013	1.02	0.09	1.01	0.21	3.4	6.5
	0.08	0.57	0.33	0.01	0.015	1.34	0.19	0.74	0.25	3.4	7.6
11, Nickel-copper steel	0.12	0.57	0.17	0.02	0.01	1.00	1.05	--	--	2.8	10.6
	0.09	0.48	1.00	0.03	0.055	1.14	1.06	--	--	3.8	5.6
	0.11	0.43	0.18	0.02	0.012	1.52	1.09	--	--	3.2	10.0
12, Nickel-copper steel, plus chromium	0.11	0.65	0.13	0.02	0.086	0.29	0.57	0.66	--	2.4	10.5
	0.11	0.75	0.23	0.04	0.020	0.65	0.53	0.74	--	2.9	9.3
	0.08	0.37	0.29	0.03	0.089	0.47	0.39	0.75	--	2.4	9.1
13, Nickel-copper steel, plus molybdenum	0.03	0.16	0.01	0.03	0.009	0.29	0.53	--	0.08	1.1	18.2
	0.13	0.45	0.066	0.02	0.073	0.73	0.573	--	0.087	2.0	11.2

(a) A weight loss of 10 mg/dm^2/15.5 years = 0.32 mpy.

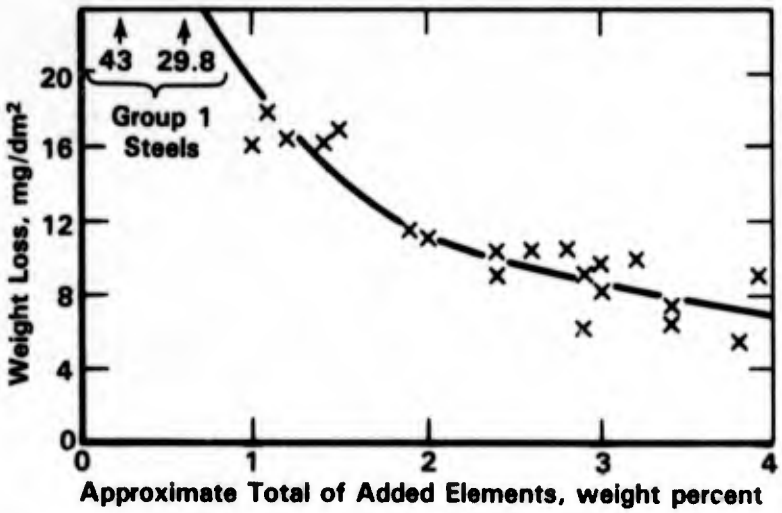

FIGURE 6-4. CORROSION OF SELECTED LOW-ALLOY STEEL PANELS EXPOSED IN MARINE ATMOSPHERE FOR 15.5 YEARS AT KURE BEACH, NC (800-FOOT LOT)[1]

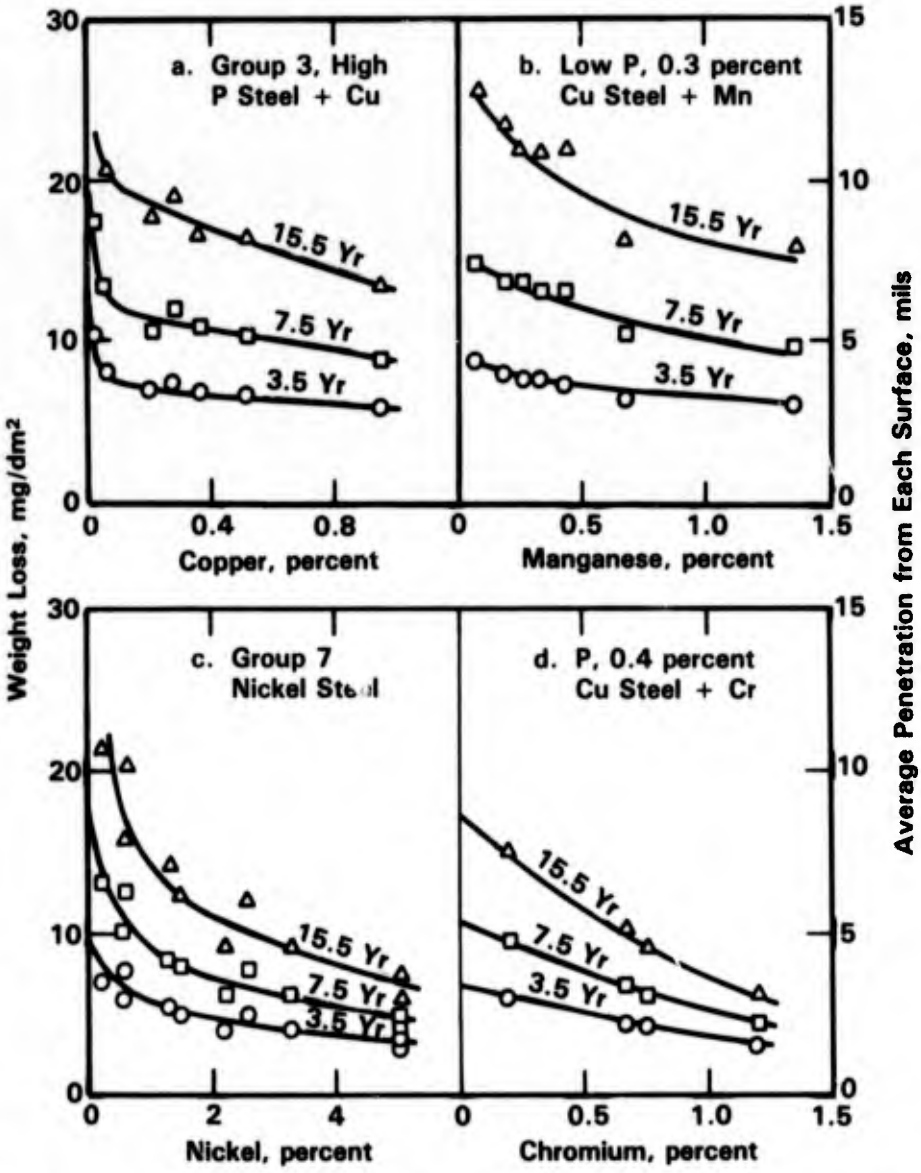

FIGURE 6-5. WEIGHT LOSS PLOTTED AGAINST COPPER, MANGANESE, NICKEL, OR CHROMIUM CONTENT OF CERTAIN STEELS AT KURE BEACH, NC (800-FOOT SITE)[1]

greatest benefit occurs with about the first 0.1 percent Cu addition. On the other hand, Fyfe, et al.[6] showed that the effect of Cu on corrosion of S free iron was negligible in marine exposures at Pilsey Island, Sussex, England. Thus, Fyfe, et al.[6] speculated that the beneficial effect of Cu in steels is related to the formation of insoluble copper sulfides. Much earlier, Buck[7] had speculated that ferrous sulfides are much more corrosive toward steels than copper sulfides.

The data in Figure 6-5 also show that Mn, Ni, and Cr additions are beneficial but larger percentage additions of Ni or Mn are required than Cu or Cr to impart the same degree of resistance. Copson[8] noted in an earlier study that Ni was beneficial in reducing pitting. On the other hand, the Cr bearing steels tended to have fewer but deeper pits than the other low-alloy steels.[8]

Phosphorus also is highly beneficial with regard to atmospheric corrosion resistance when added to Cu bearing steels. Larrabee and Coburn[9] studied the effect of Cu and P on the corrosion rates of low-alloy steels in 15.5 year exposures at Kure Beach, NC. Results of the study, given in Figure 6-6, show that the corrosion rates of the high P alloys (approximately 0.06 P) were consistently lower than those of the low P (<0.01 P) steels for all Cu contents studied.

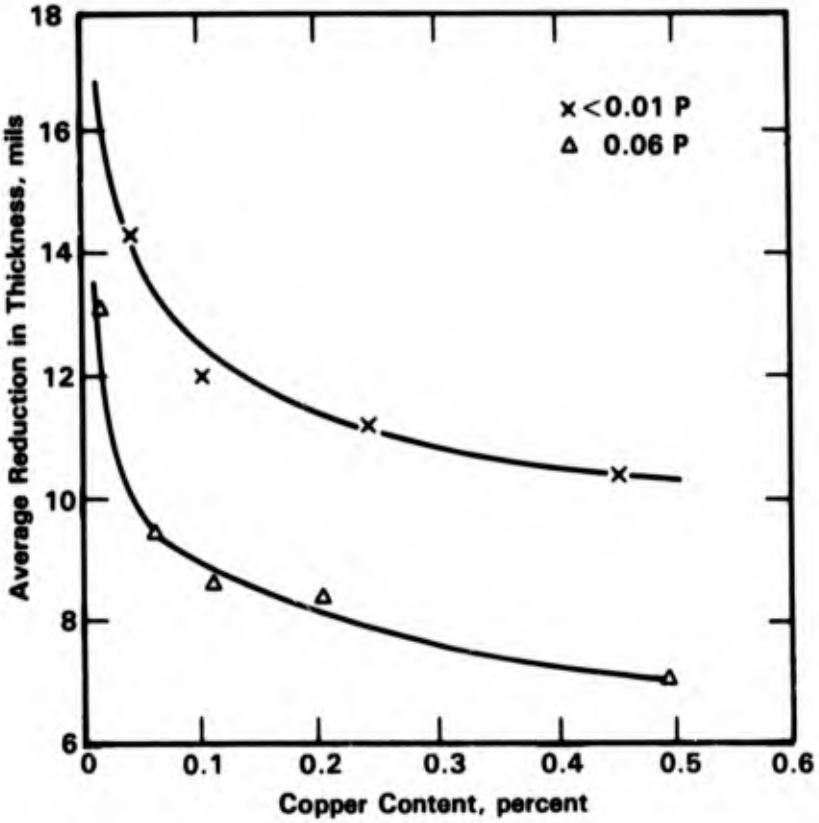

FIGURE 6-6. EFFECT OF Cu AND P ON THE THICKNESS LOSS OF LOW-ALLOY STEELS IN 15.5 YEAR EXPOSURES AT KURE BEACH, NC (800-FOOT LOT)[9]

Effect of Surface Condition. Southwell, et al.[2] studied the effect of surface preparation on the general and pitting corrosion of carbon steel. Specimens having pickled and mill-scaled surfaces were exposed for up to 8 years in marine and inland sites in the Panama Canal Zone. Results of this study, given in Figure 6-7, show that there was very little difference in the performance of the mill-scaled and pickled surfaces. This behavior is contrasted to that of submerged specimens where the presence of mill-scale was found to be highly detrimental (see section on immersed exposure).

Splash and Tide

The corrosion behavior of carbon and low-alloy steels in the splash and tidal zone has been investigated in some detail as a result of corrosion problems that have been encountered with pilings in seawater applications. A typical corrosion profile of a steel piling is given in Figure 6-8 where it can be seen that rates of attack in the splash zone (Zone 2) and in the continually immersed zone which is adjacent to the tidal zone (Zone 4) are much higher than corrosion rates elsewhere (i.e., atmosphere (Zone 1), mid tidal region (Zone 3), and deep submerged and mud (Zone 5)). Humble[10] has presented explanations to account for these wide variations in corrosion rates. He suggests that Zone 1 is wetted only infrequently and thus the corrosion rates in Zone 1 are similar to those observed for marine atmospheres.

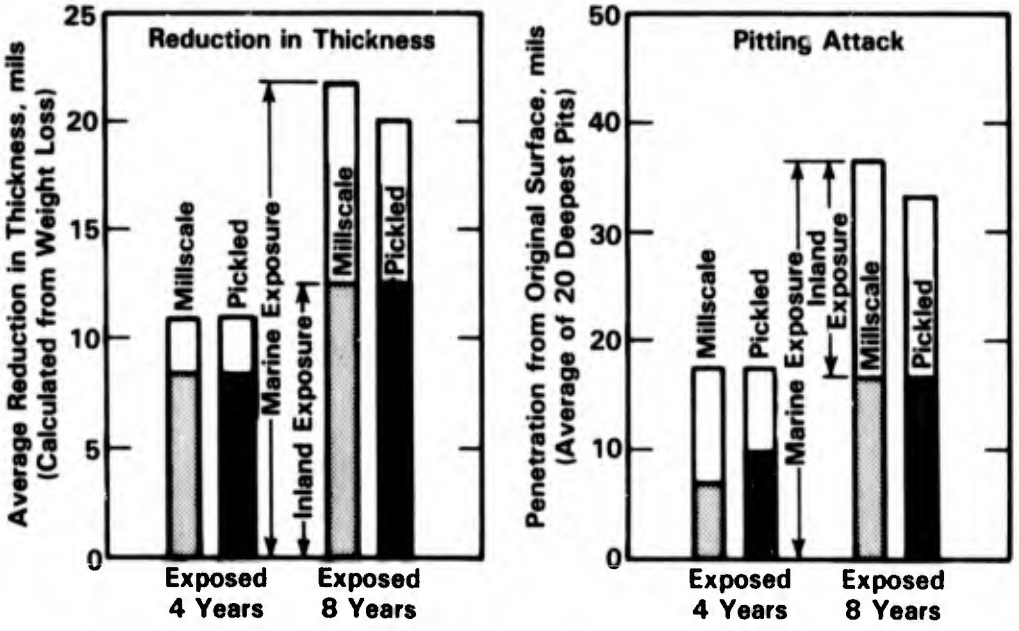

FIGURE 6-7. COMPARISON OF MILLSCALE AND PICKLED SURFACES IN CORROSION RESISTANCE OF UNALLOYED LOW-CARBON STEEL EXPOSED TO TROPICAL ATMOSPHERES[2]

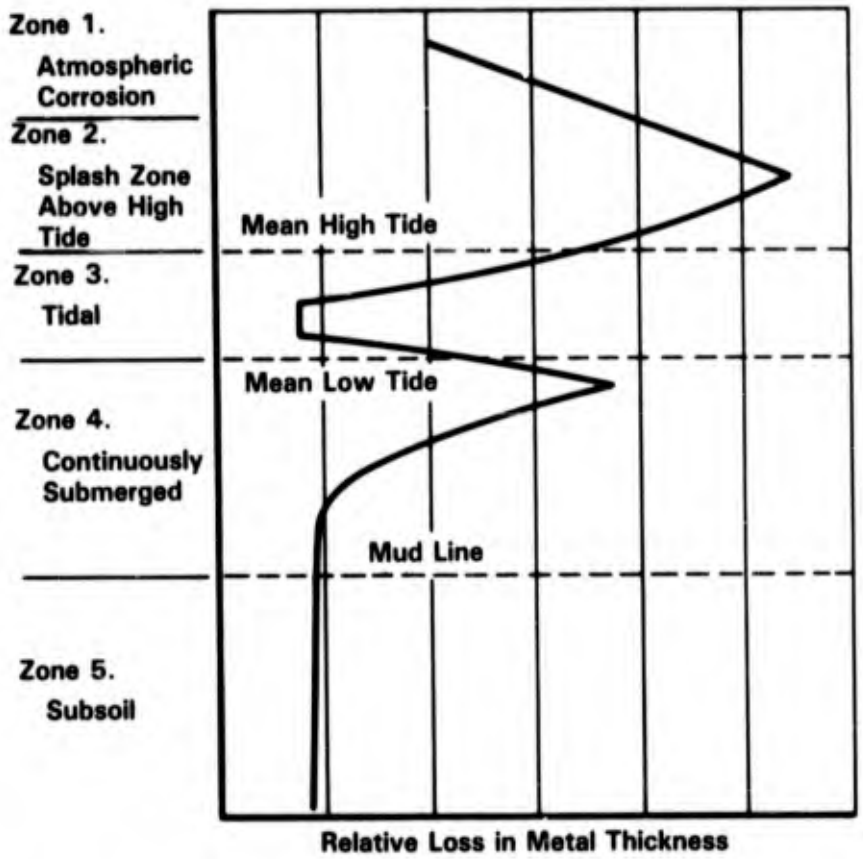

FIGURE 6-8. CORROSION PROFILE OF STEEL PILING IN 5 YEAR EXPOSURES IN SEAWATER AT KURE BEACH, NC[10]

In Zone 2, the splash zone, materials are continually exposed to seawater and there is a plentiful supply of oxygen in the thin aqueous layer on the metal surface, resulting in high corrosion rates. The high corrosion rates in the upper tidal zone (Zone 3) also are attributed to this splash zone effect. The tidal zone, Zone 3 and the upper portion of Zone 4, form a galvanic cell which is driven by differential aeration; the tidal zone which is fully aerated forms the cathode in the cell and promotes accelerated attack of the underlying region. It should be pointed out that this galvanic protection of the tidal zone is not available to the splash zone since the electrical resistance of the moisture layer on the material in the latter zone is high. Finally, rates of attack are low in Zone 5 and the lower portion of Zone 4 since the seawater is relatively deaerated in this region and the region is sufficiently far away from Zone 2 to avoid deleterious galvanic effects. Actual corrosion rate data for steel pilings for these zones are given in Figures 6-9 and 6-10. Figure 6-9 shows that these variations in corrosion rate as a function of position appear to be more pronounced in the presence of mill-scale.

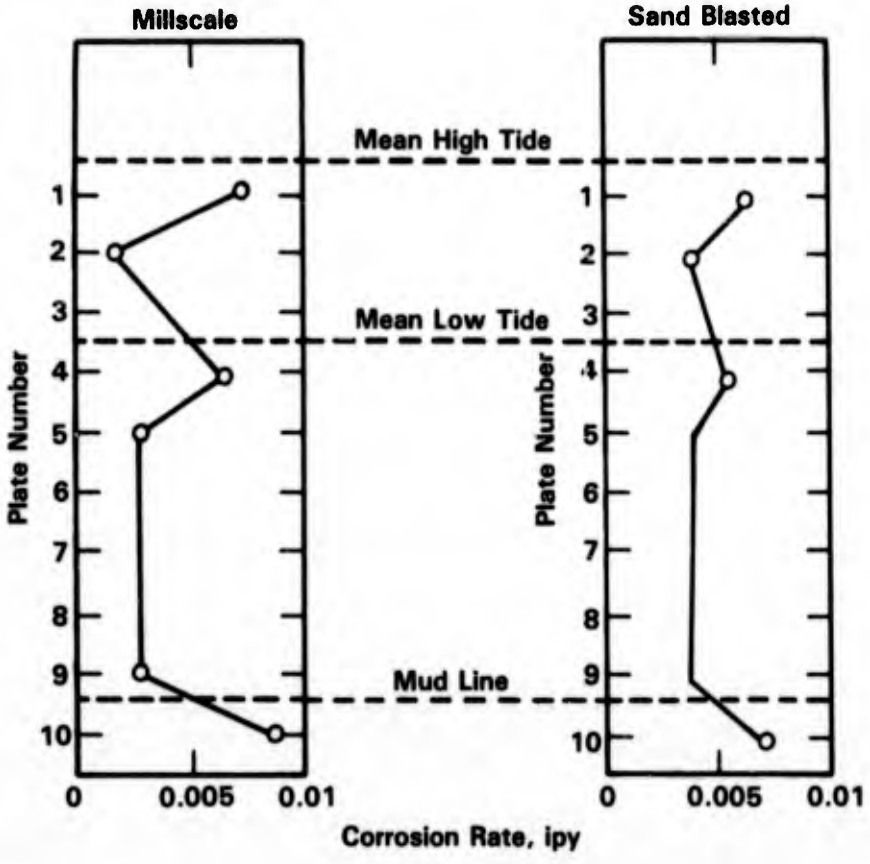

FIGURE 6-9. EFFECT OF SURFACE PREPARATION AND POSITION ON CORROSION RATE OF STEEL PILINGS IN SEAWATER FOR 291-352 DAYS[10]

Effect of Geographic Location. Corrosion rate data for pilings at various geographical locations were compiled by Kinson, et al.[12] and are shown in Table 6-7. These data show that there is considerable scatter in reported rates of attack. Although part of the scatter may be attributable to variation in the exposure time, these data do suggest that other factors also play a role in the scatter. Thus, the behavior of carbon steel in the tidal and splash zone appears to be more similar to behavior in marine atmospheres in that rates of attack probably are highly dependent upon method of exposure and local environmental conditions. This conclusion is supported by results of mean tide exposures at various locations reported by Southwell and Alexander.[13] Comparison of submerged to mean tide corrosion rates indicated ratios from 2.5 to 0.6, see Table 6-8.

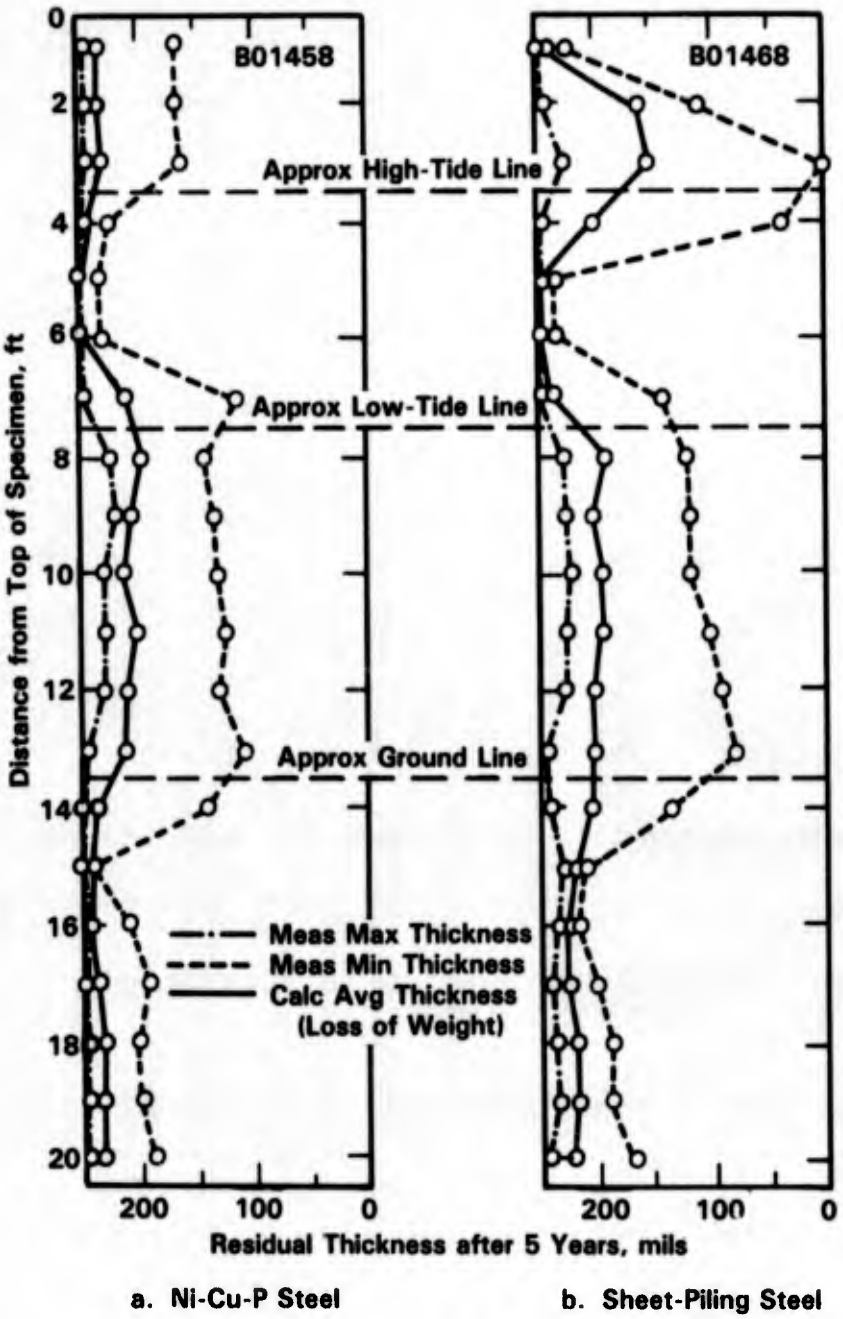

FIGURE 6-10. COMPARATIVE CORROSION ON TWO STEELS (COMPOSITIONS IN TABLE F-3, APPENDIX F) IN MARINE ENVIRONMENTS[11]

TABLE 6-7. CORROSION RATES OF CARBON STEEL PILING IN SEAWATER[12]

Location	Exposure Period, years	Maximum Corrosion Rates per Exposed Face, μm/yr			
		Buried	Submerged	Intertidal	Splash
Port Adelaide, S. Australia	52	30	50	40	70
Queenscliff, Vic., Australia	17	--	80	109	132
Wrightsville Beach, NC	8	--	110	20	300
Mayport, FL	5.5	--	160	30	580
Mobile Bay, AL	7	--	200	160	330
Dam Neck, VA (bare steel)	6	100	440	240	440
Dam Neck, VA (coated)	6	76	6	44	110
La Costa Island, Caribbean	5	46	420	320	425
Boston Harbour, MA	10	--	320	--	40
Lowestoft, U.K. (coated waterside)	20	15	40	13	15

TABLE 6-8. VARIABILITY OF MEAN-TIDE CORROSION FOR CARBON STEEL[13]

Location	Ratio of Corrosion in Seawater/ Corrosion at Mean Tide
Nova Scotia	2.5
New Zealand	2.0
Panama Pacific	1.1
England	0.8
Ceylon	0.6

Effect of Alloying. Several researchers have investigated the effect of alloy composition on corrosion performance of carbon and low-alloy steels in the splash and tide zone. Larrabee[11] studied the behavior of six steels having various combinations of nickel, copper, and phosphorus (see Table F-3 in Appendix F for compositions) at Wrightsville Beach, NC. Results of the study, which are summarized in Table 6-9, show that the nickel-copper-phosphorus alloyed steels are much more resistant than carbon steel to attack in the splash zone. On the other hand, Nose, et al.[14] found that attack below low tide was essentially independent of alloy composition (see Figure 6-11).

Nose, et al.[14] also reported on the corrosion performance of the Japanese seawater corrosion resistant steel, NK marine G, which contains 0.5 chromium, 0.25 copper, and 0.10 phosphorus (see Table F-4 in Appendix F). Results, given in Figure 6-11, show that this steel has comparable performance to that of the nickel-copper-phosphorus steel described by Larrabee.[11]

Schultze and van der Wekken[15] statistically analyzed published corrosion data for carbon and low-alloy steels under tidal exposure. A summary of the data used for the analysis is given in Table 6-10. In the analysis, a linear relationship was assumed between the corrosion rate, S, and the concentration of an element, i; C_i

$$S = S_c + \Sigma_i b_i C_i$$

where S_c is the corrosion rate of the unalloyed steel. The corrosion rate was then normalized by dividing by S_c to get a relative corrosion rate, R. This procedure enabled comparisons to be made of test results from different sites since the normalized value is expected to be site independent.

$$R = 1 + \Sigma_i r_i C_i$$

Since R is a function of exposure time, the r coefficients are time dependent. R coefficients as a function of time for the various alloying elements are given in Figure 6-12. These data show that three elements appear to measurably influence corrosion rates of low carbon steels under tidal exposure: manganese, phosphorus, and aluminum. Manganese appears to be detrimental whereas phosphorus and aluminum appear to be beneficial. It is interesting to note that nickel, copper, and chromium alone do not appear to influence corrosion behavior, which suggests that the excellent performance of the alloy steels described by Larrabee[11] and Nose, et al.[14] were solely the result of the presence of phosphorus. However, the statistical analysis did not address possible synergistic interactions of the alloying elements.

TABLE 6-9. AVERAGE DECREASE IN THICKNESS OF 20-FOOT SPECIMENS IN SEAWATER[11]* (COMPLETE COMPOSITION OF STEELS ARE GIVEN IN APPENDIX F, TABLE F-3)

Average Feet From Top	B01468 Sheet-Piling Steel			B01458 Ni-0.54% Cu-0.52% P-0.12%			B01389 Ni-0.55% Cu-0.22% P-0.17%			B01457 Ni-0.54% Cu-0.20% P-0.11%			B01459 Ni-0.55% Cu-0.20% P-0.14%			B01467 Ni-0.28% Cu-0.20% P-0.14%			B01456 Ni-0.28% Cu-0.22% P-0.17%		
	1 Yr, mils	2 Yr, mils	5 Yr, mils	1 Yr, mils	2 Yr, mils	5 Yr, mils	1 Yr, mils	2 Yr, mils	5 Yr, mils	1 Yr, mils	2 Yr, mils	5 Yr, mils	1 Yr, mils	2 Yr, mils	5 Yr, mils	1 Yr, mils	2 Yr, mils	5 Yr, mils	1 Yr, mils	2 Yr, mils	5 Yr, mils
0.5	9	7	9	3	4	11	4	7	12	5	9	9	7	7	24	4	8	9	6	13	10
1.5	9	13	87	3	7	13	3	7	16	4	9	30	6	9	18	3	7	21	5	12	21
2.5	31	46	98	8	9	17	8	7	26	8	11	54	9	9	30	7	18	45	9	19	73
Approximate High Tide Line																					
3.5	31	18	48	4	7	4	5	8	9	5	7	9	6	6	7	4	20	6	5	11	22
4.5	1	7	1	2	6	1	4	6	2	4	8	1	3	6	2	2	5	1	2	9	2
5.5	0	7	2	1	5	1	3	5	2	5	6	2	3	7	7	2	5	3	3	8	2
6.5	9	27	14	13	23	37	11	18	34	4	27	41	6	24	29	9	21	28	11	32	24
Approximate Low Tide Line																					
7.5	19	30	56	14	24	52	16	25	52	13	29	64	15	25	53	14	27	42	15	28	46
8.5	16	29	45	15	21	41	16	22	44	9	25	49	14	29	42	15	32	38	14	24	34
9.5	14	22	52	15	22	38	17	24	41	10	25	49	15	30	49	17	32	43	15	21	32
10.5	18	22	53	14	22	48	17	15	40	10	24	49	16	31	42	17	27	41	20	27	32
11.5	14	24	45	8	21	39	13	24	35	10	25	49	8	28	42	13	34	37	13	27	32
12.5	4	10	46	3	9	37	3	22	38	4	16	46	4	10	32	7	14	35	16	10	33
Approximate Ground Line																					
13.5	3	10	45	3	12	13	3	8	24	4	14	37	5	15	11	8	11	12	3	10	18
14.5	3	12	29	3	9	6	4	9	24	3	11	24	3	11	6	6	11	7	4	12	17
15.5	3	9	21	3	10	5	3	11	5	2	9	14	3	24	5	7	9	6	6	13	18
16.5	3	9	22	3	20	10	3	22	13	7	7	11	6	8	7	5	9	15	6	13	28
17.5	5	5	30	5	14	18	4	14	22	9	8	10	8	7	12	7	9	28	6	13	31
18.5	4	14	30	3	20	12	5	10	15	8	7	10	7	7	22	4	14	25	3	9	34
19.5	10	10	27	6	16	15	9	18	24	3	9	17	8	10	39	6	24	38	3	11	31

Note: Approximate mean high tide 2 to 3 feet from tops of specimens; approximate mean low tide about 6 feet from tops of specimens.
* Specimens were exposed in 1951; figures quoted were calculated from losses of weight.

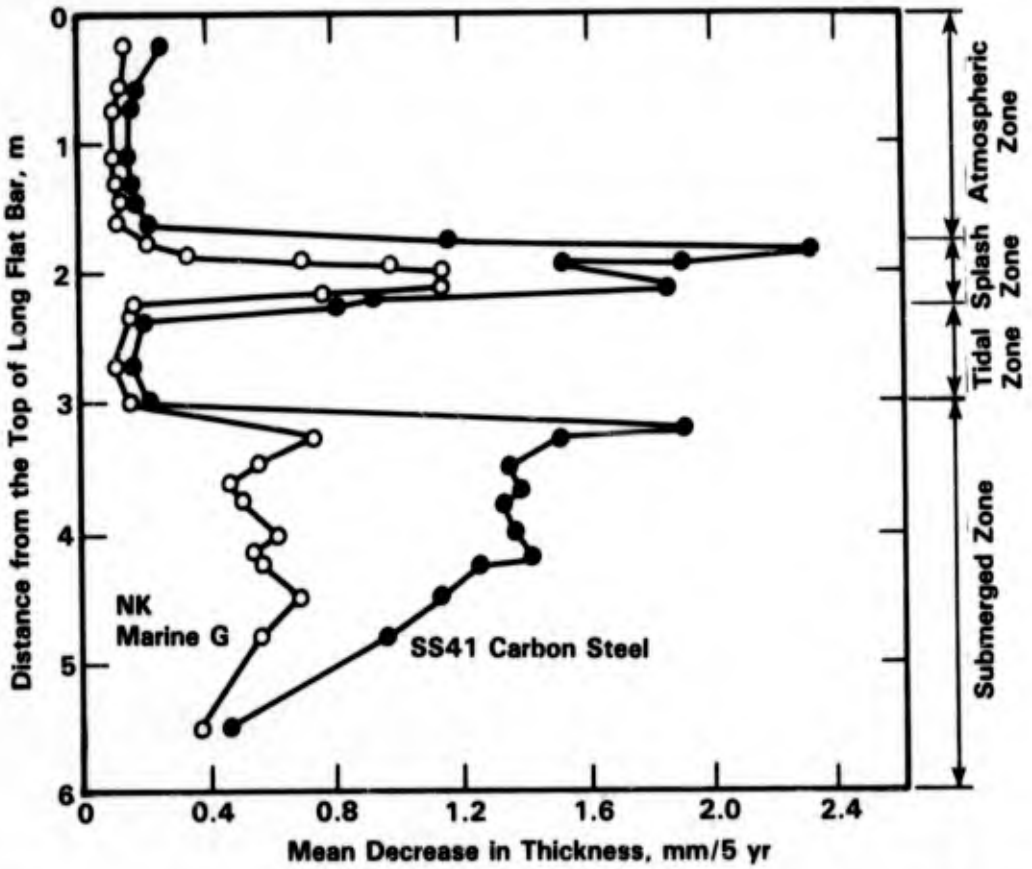

FIGURE 6-11. RESULT OF SEAWATER CORROSION TEST ON LONG FLAT BARS FOR 5 YEARS AT SHIMUZU SHIPYARD, JAPAN. THE COMPOSITION OF NK MARINE G IS GIVEN IN TABLE F-4, APPENDIX F[14]

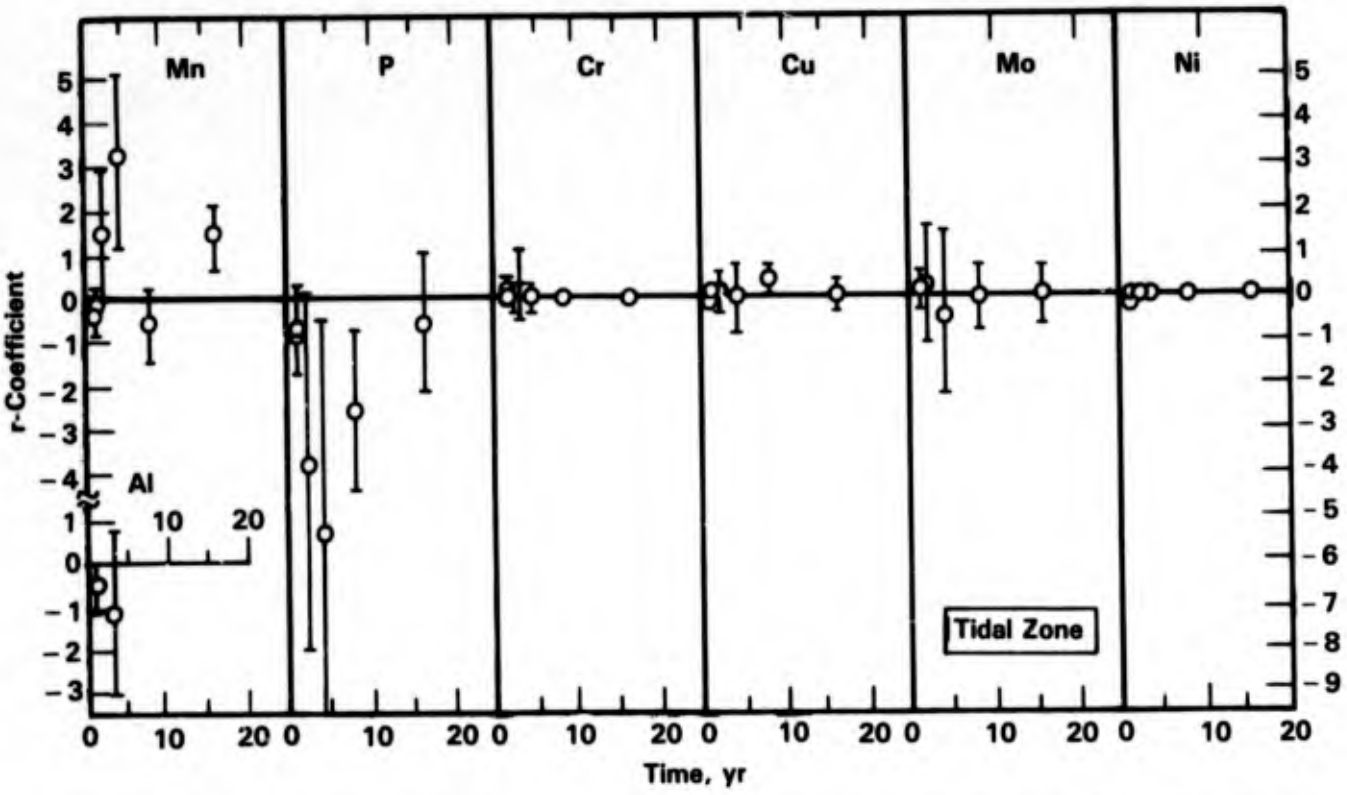

FIGURE 6-12. THE r-COEFFICIENTS OF ALLOYING ELEMENTS FOR EXPOSURE IN THE TIDAL ZONE CALCULATED FROM DATA IN TABLE 6-10[15]

TABLE 6-10. DATA USED IN STATISTIC ANALYSIS BY SCHULTZE AND VAN DER WEKKEN[15]

Investigators: Forgeson, B. W., Southwell, C. R., and Alexander, A. L., Corrosion, 16, 105t (1960)
Southwell, C. R. and Alexander, A. L., N.L.R. Report 6862 (1969)

Composition, %									Weight Loss, g/dm² Full Immersion					Weight Loss, g/dm² Tidal Zone				
C	Mn	P	S	Si	Cr	Ni	Cu	Mo	1 Yr	2 Yr	4 Yr	8 Yr	16 Yr	1 Yr	2 Yr	4 Yr	8 Yr	16 Yr
0.24	0.48	0.040	0.027	0.008	0.03	0.051	0.080	--	11.4	17.2	30.6	52.4	94.8	19.9	20.1	28.0	47.9	89
0.22	0.44	0.019	0.033	0.009	Trace	0.14	0.35	--	11.8	18.3	29.1	55.3	98.1	22.4	22.6	23.0	48.3	92.1
0.20	0.54	0.012	0.023	0.18	0.15	1.94	0.63	--	14.8	18.3	34.1	63.0	104	17.7	17.9	29.5	45.6	110
0.13	0.49	0.010	0.014	0.16	0.10	5.51	0.062	--	12.5	20.0	33.2	63.7	103	15.6	17.2	25.4	39.8	107
0.08	0.44	0.010	0.017	0.13	3.16	0.16	0.11	0.02	4.13	10.9	35.6	80.4	140	22.1	23.6	29.1	51.1	95.7
0.08	0.41	0.020	0.019	0.20	5.06	0.11	0.062	0.52	5.34	12.1	33.6	63.5	119	23.3	22.6	24.9	48.6	94.1
0.08	0.47	0.007	0.026	0.060	0.00	1.54	0.87	--	11.7	16.9	41.2	52.6	96.7	23.7	26.0	30.0	79.3	98.0
0.15	0.45	0.113	0.026	0.47	0.68	0.49	0.42	--	13.6	23.3	37.5	85.7	160	21.4	19.5	24.3	41.9	98.0
0.078	0.75	0.058	0.022	0.04	Trace	0.72	0.61	0.13	12.8	19.1	30.2	50.9	89.8	21.6	30.3	37.3	49.3	123
0.13	0.60	0.089	0.021	0.15	0.55	0.30	0.61	0.059	12.6	21.9	41.2	87.4	167	18.2	18.0	21.5	40.9	91.3

Investigators: Baudot, H. and Chaudron, G., Mem. Rev. Met., 43, 1 (1946)

C	Mn	P	S	Si	Cr	Ni	Cu	Mo	Al	Weight Loss, g/dm², After 4 Years' Immersion
0.05	0.64	0.061	0.020	0.197	--	--	0.038	--	--	56
0.106	0.34	0.013	0.029	0.126	--	--	0.105	--	0.038	50.5
0.053	0.43	0.047	0.045	--	--	--	0.529	--	--	47.5
0.096	0.39	0.016	0.029	0.042	--	--	0.480	--	0.011	57.5
0.034	0.26	0.020	0.018	--	--	--	0.480	0.075	0.009	47.5
0.034	0.26	0.020	0.018	--	--	--	0.480	0.075	0.009	45
0.218	0.710	0.025	0.031	0.122	--	--	0.048	--	0.043	52.5
0.213	0.580	0.18	0.025	0.028	--	--	0.031	--	0.030	61
0.171	0.890	0.061	0.032	0.159	0.444	--	0.558	--	--	62
0.104	0.990	0.114	0.055	0.178	0.421	--	0.654	--	--	55
0.223	0.910	0.027	0.025	0.253	0.513	--	0.478	--	0.005	63.5
0.209	0.770	0.105	0.025	0.239	0.446	--	0.414	--	0.007	56

TABLE 6-10. (Continued)

Investigator: Reinhart, F. M., U.S. Naval Civil Engineering Laboratory, Techn. Note N-1213 (1972)

Material	C	Mn	P	S	Si	Cr	Ni	Cu	Mo	Corrosion Rate, mpy (Calculated From Weight Loss) After 1 Year Immersion
Armco Iron	--	0.02	--	--	--	--	--	--	--	7.1
AISI 1010	0.12	0.50	0.004	0.23	0.060	--	--	--	--	8.2
AISI 1010	--	0.34	0.01	--	0.02	0.02	0.02	0.03	--	8.0
Copper Steel	--	0.40	0.01	--	0.02	0.03	0.01	0.28	--	6.0
ASTM A36	0.20	0.55	0.010	0.020	0.064	--	--	--	--	6.2
HSLA 2[a]	0.12	0.30	0.015	0.025	0.27	1.25	2.34	0.17	0.20	4.5
HSLA 4	--	0.36	0.08	--	0.41	0.72	0.32	0.38	--	8.0
HSLA 7	--	0.43	0.12	--	0.13	--	0.54	1.0	--	8.0
HSLA 10	--	0.63	0.01	--	--	--	0.99	1.42	--	8.0
HSLA 12	0.14	0.26	0.011	0.009	0.27	1.55	2.60	--	0.46	4.2
HS 1[b]	0.11	0.78	0.008	0.006	0.29	0.56	5.03	--	0.42	4.7
AISI Type 502	0.06	0.48	0.020	0.010	0.33	4.75	--	--	0.55	4.4
AISI Type 502	0.06	0.5	--	--	--	5.2	0.4	--	0.5	8.0

(a) HSLA = High-Strength, Low-Alloy Steel.
(b) HS = High-Strength Steel.

Investigators: Hudson, J. C. and Stan[illegible]s, J. F., J. Iron Steel Inst., 180, 271 (1955)

Composition, %										Corrosion, mils (Calculated From Weight Loss) Full Immersion	
C	Mn	P	S	Si	Cr	Ni	Cu	Mo	Al	2 Yr	5 Yr
0.08	0.65	0.027	0.047	0.18	0.01	Trace	0.014	--	--	5.5	11.1
0.12	0.62	0.028	0.040	0.17	0.01	Trace	0.015	--	--	5.6	15.9
0.29	0.76	0.027	0.043	0.17	0.03	Trace	0.014	--	--	5.4	13.3
0.51	0.78	0.026	0.031	0.18	0.01	Trace	0.016	--	--	6.0	14.7
0.18	1.82	0.033	0.047	0.11	0.01	Trace	0.014	--	--	6.0	12.6
0.17	1.71	0.032	0.045	0.12	0.01	Trace	0.52	--	--	5.2	12.6
0.04	0.48	0.057	0.052	0.21	--	--	0.061	--	--	5.6	14.2
0.20	0.52	0.057	0.053	0.22	--	--	0.52	--	--	5.0	14.0

TABLE 6-10. (Continued)

Composition, %										Corrosion, mils (Calculated From Weight Loss) Full Immersion	
C	Mn	P	S	Si	Cr	Ni	Cu	Mo	Al	2 Yr	5 Yr
0.12	0.54	0.049	0.054	0.20	1.04	--	0.059	--	--	4.1	12.7
0.23	0.55	0.049	0.053	0.22	0.96	--	0.056	--	--	4.5	13.6
0.06	0.54	0.057	0.054	0.81	--	--	0.060	--	--	5.3	10.5
0.09	0.52	0.164	0.051	0.17	--	--	0.059	--	--	5.6	11.9
0.10	0.58	0.156	0.050	0.20	--	--	0.48	--	--	5.3	11.8
0.10	0.48	0.142	0.049	0.20	0.96	--	0.059	--	--	3.8	12.4
0.11	0.54	0.055	0.054	0.20	1.02	--	0.52	--	--	3.7	13.0
0.21	0.54	0.054	0.052	0.23	0.96	--	0.51	--	--	4.0	14.5
0.10	0.59	0.058	0.049	0.83	1.04	--	0.057	--	--	3.6	11.9
0.11	0.49	0.053	0.053	0.80	--	--	0.53	--	--	4.8	14.3
0.12	0.51	0.158	0.049	0.79	1.01	--	0.51	--	--	3.6	12.0
0.11	0.46	0.057	0.053	0.26	1.5	--	0.058	--	--	3.6	10.2
0.11	0.50	0.053	0.050	0.29	2.04	--	0.054	--	--	3.0	11.0
0.12	0.52	0.056	0.051	0.23	2.47	--	0.056	--	--	2.5	11.9
0.11	0.46	0.055	0.052	0.21	1.44	--	0.49	--	--	3.8	12.8
0.10	0.48	0.054	0.053	0.29	1.95	--	0.50	--	--	3.1	11.2
0.11	0.44	0.055	0.050	0.23	2.44	--	0.48	--	--	2.7	7.8
0.13	0.69	0.048	0.043	0.27	--	--	0.017	--	--	5.4	12.1
0.11	0.45	0.046	0.050	0.17	--	--	0.075	--	1.59	3.2	13.5
0.12	0.57	0.045	0.039	0.34	2.61	--	0.014	--	--	2.2	6.7
0.13	0.66	0.049	0.043	0.31	2.63	--	0.017	--	0.14	2.4	6.2
0.10	0.55	0.050	0.036	0.78	2.79	--	0.064	--	1.44	1.9	4.9
0.11	0.50	0.048	0.040	0.23	--	3.06	0.020	--	--	4.3	12.3
0.10	0.49	0.045	0.040	0.27	--	3.11	0.49	--	--	4.3	13.2
0.12	0.52	0.052	0.038	0.11	1.00	3.05	0.015	--	--	3.2	13.3
0.12	0.50	0.049	0.046	0.25	1.13	2.98	0.45	--	--	3.1	12.6
0.11	0.65	0.046	0.038	0.24	--	1.51	1.01	--	--	4.5	10.7
0.05	0.34	0.019	0.012	0.17	0.01	--	0.010	--	--	5.6	14.6
0.12	0.44	0.021	0.011	0.15	0.05	--	0.014	--	--	5.0	11.5
0.26	0.58	0.024	0.012	0.09	--	--	0.010	--	--	5.4	13.2
0.30	0.50	0.026	0.012	0.17	0.02	--	0.016	--	--	6.4	14.8
0.10	0.38	0.022	0.011	0.11	--	--	0.016	0.55	--	5.1	13.2
0.10	0.34	0.024	0.012	0.13	--	0.21	0.54	0.55	--	4.7	10.1
0.11	0.42	0.023	0.012	0.17	0.95	--	0.020	0.54	--	3.3	10.4
0.11	0.31	0.022	0.013	0.15	0.02	1.96	0.020	0.55	--	4.3	13.3
0.12	0.39	0.023	0.026	0.13	0.76	3.0	0.018	0.51	--	3.0	14.4
0.18	0.49	0.018	0.313	0.19	3.14	0.11	0.099	0.44	--	2.2	6.6

TABLE 6-10. (Continued)

Investigators: Tamada, A., Tanimura, M., and Tenmyo, G., Proc. 5th Int. Congr. Metall. Corros., Tokyo, p. 786 (1973)

										Corrosion Loss, mm				
										Full Immersion			Tidal Zone	
C	Mn	P	S	Si	Cr	Ni	Cu	Mo	Al	1/2 Yr	1 Yr	2 Yr	1/2 Yr	3 Yr
0.14	1.18	0.016	0.015	0.41	--	--	--	--	--	0.09	0.16	0.28	0.105	0.215
0.12	0.62	0.112	0.020	0.52	0.51	0.27	0.31	--	0.16	0.04	0.10	0.19	0.21	0.31
0.06	0.56	0.029	0.016	0.24	0.81	0.81	0.89	--	--	0.07	0.11	0.22	0.21	0.35
0.03	0.76	0.130	0.014	0.37	1.07	0.03	0.05	--	0.42	0.03	0.10	0.18	0.19	0.34
0.07	0.88	0.114	0.017	0.67	1.67	0.03	0.32	--	0.74	0.04	0.10	0.17	0.08	0.21
0.10	0.88	0.134	0.020	0.53	1.94	0.28	0.38	--	1.09	0.03	0.08	0.14	0.05	0.24
0.04	0.99	0.016	0.013	0.37	1.96	0.03	0.37	--	0.74	0.04	0.08	0.13	0.13	0.23
0.11	0.90	0.035	0.021	0.59	2.04	0.02	0.38	--	1.14	0.04	0.09	0.16	0.09	0.21
0.13	0.61	0.027	0.023	0.53	3.70	0.73	0.07	--	0.62	0.03	0.07	0.12	0.08	0.19
0.06	0.31	0.161	0.018	Trace	0.05	0.58	0.40	--	--	0.09	0.15	0.21	0.12	0.19

Investigators: Takamura, A., et al., Trans. Iron Steel Inst., Japan, 11, 299 (1971)

C	Mn	P	S	Si	Cr	Ni	Cu	Weight Loss, mg/cm^2, After 1 Year in Tidal Zone
0.20	0.50	0.011	0.022	Trace	--	--	0.13	246
0.20	0.47	0.010	0.024	Trace	--	--	0.25	235
0.10	0.48	0.017	0.016	0.46	0.81	0.46	0.44	251
0.14	0.31	0.148	0.029	0.13	--	0.51	0.48	186
0.13	0.33	0.117	0.028	0.13	--	0.51	0.48	190
0.14	0.57	0.069	0.029	0.06	--	0.51	0.48	195
0.14	0.52	0.092	0.031	0.07	--	0.52	0.29	193
0.14	0.56	0.122	0.029	0.08	--	0.50	0.29	188

Immersion

General, Pitting, and Crevice Corrosion

Corrosion rates for carbon and low-alloy steels in quiescent seawater at ambient temperature, as determined from weight loss, generally are less than about 5 mpy after several years of exposure. These alloys are susceptible to pitting and crevice corrosion with pitting factors* as large as about 30. Rates of attack are not particularly sensitive to alloy composition or surface preparation, although the presence of mill-scale is deleterious. Typical data are given in Table 6-11.

Effect of Exposure Time. Reinhart[16] reported on the results of a number of studies of the effect of exposure time on the corrosion rates of low carbon steels at various geographical locations and depths. These data, given in Figure 6-13, show that rates decreased rapidly with exposure time over the first 1 to 2 years' exposure. Results of longer term exposures performed by Larrabee[3] and Southwell and Alexander[13] are qualitatively in agreement with those reported by Reinhart.[16] Larrabee[3] found that the corrosion rates of five low-alloy steels decreased with exposure time over 4.5 years' exposure at Kure Beach, NC, but the decrease over the longer periods was much more gradual than that which was observed over the first year of exposure, see Table 6-12. Similarly, Southwell and Alexander[13] found a logarithmic relationship between the average depth of penetration and exposure time for carbon steel exposed in seawater in the Panama Canal Zone as shown in Figure 6-14. The one year average rate of attack was 5.8 mpy whereas the rate calculated for the 16-year exposure was less than 3 mpy.

Rates of pitting of carbon and low-alloy steels also decrease with exposure time although pitting attack of these steels is severe even for short exposures. Data by Southwell and Alexander[13] (Table 6-11) show that depths of attack of as much as 100 mils were observed for carbon and low alloy steels within one year's exposure. The data in Table 6-11 also show that rates of pitting actually decreased more rapidly than rates of general attack; the values for the pitting factor generally decreased with exposure time. Data by Bultman, et al.[17] show the effect of exposure time on pit growth more explicitly, see Figure 6-15.

---

* Ratio of deepest pit/average penetration.

TABLE 6-11. COMPREHENSIVE TABULATION OF CORROSION DAMAGE: STRUCTURAL FERROUS METALS CONTINUOUSLY IMMERSED IN SEAWATER (PACIFIC OCEAN - PANAMA CANAL ZONE). THE COMPOSITIONS OF THE STEELS ARE GIVEN IN APPENDIX F, TABLE F-5(13)

Metals				General Corrosion										Pitting Penetration								
				Weight Loss, g/dm²					Average Penetration, mils(a)					Stabilized Corrosion Rate,(b)	Average 20 Deepest Pits,(c) mils			Deepest Pit, mils			Pitting Factor(d)		
Class	Key	Type	Surface Condition	1 Yr	2 Yr	4 Yr	8 Yr	16 Yr	1 Yr	2 Yr	4 Yr	8 Yr	16 Yr	mpy	1 Yr	8 Yr	16 Yr	1 Yr	8 Yr	16 Yr	1 Yr	8 Yr	16 Yr
	A	C steel	Pickled	11.8	16.5	31.4	50.9	90.8	5.9	8.3	16	26	46	2.5	41	66	90	62	86	155	11	3	3
	B	C steel	Machined	11.0	18.0	29.8	53.9	98.7	5.5	9.0	15	27	49	2.7	38	58	(e)	64	157	(e)	12	6	(e)
	C	C steel	Millscale	8.38	15.5	30.1	46.5	(e)	4.2	7.8	15	23	(e)	(e)	55	(e)	(e)	104	(e)	(e)	25	(e)	(e)
w	D	C steel, 0.3% Cu	Pickled	11.8	18.3	29.1	55.3	98.1	5.9	9.2	15	28	[illegible]	2.7	36	63	85	61	108	124	10	4	3
r	E	2% Ni steel	Pickled	14.8	18.3	34.1	63.0	104	7.4	9.2	17	32	52	2.7	33	94	(e)	51	179	(e)	7	6	(e)
o	F	5% Ni steel	Pickled	12.5	20.0	33.2	63.7	103	6.3	10	17	32	52	2.7	29	117	(e)	57	214	(e)	9	7	(e)
u	G	3% Cr steel	Pickled	4.13	10.9	35.6	80.4	140	2.1	5.5	18	40	70	3.8	11	65	93	20	78	109	10	2	2
g	H	5% Cr steel	Pickled	5.34	12.1	33.6	63.5	119	2.7	6.1	17	32	56	3.5	27	63	69	91	90	100	34	3	2
h	I	Low-alloy steel	Pickled	11.7	16.9	41.2	52.6	96.7	5.9	8.5	21	26	48	2.7	54	82	(e)	65	152	(e)	11	6	(e)
t	J	Low-alloy steel	Pickled	13.6	22.3	37.5	85.7	160	6.9	11	19	43	80	4.8	31	80	(e)	46	175	(e)	7	4	(e)
	K	Low-alloy steel	Pickled	12.8	19.1	30.2	50.9	89.8	6.4	9.6	15	25	45	2.5	27	56	71	47	139	110	7	5	2
	L	Low-alloy steel	Pickled	12.6	21.9	41.2	87.4	167	6.3	11	21	44	84	5.0	26	(e)	(e)	36	(e)	(e)	6	(e)	(e)
	S	Wrought iron	Machined	12.7	15.1	28.2	43.8	(f)	6.5	7.7	14	22	(f)	(f)	34	63	(f)	51	138	(f)	8	6	(f)
	T	Wrought iron	As received	12.5	18.4	29.9	51.5	86.4	6.3	9.3	15	26	44	2.5	46	(e)	127	73	(e)	200	7	(e)	3
	M	Cast steel	Machined	14.7	18.7	29.9	55.2	86.1	7.4	9.4	15	28	43	2.5	56	84	103	84	135	146	11	5	3
c	N	Cast steel	Cast (as received)	12.6	11.9	15.8	(g)	(g)	6.3	6.0	7.9	(g)	(g)	(g)	65	(g)	(g)	131	(g)	(g)	21	(g)	(g)
a	O	Gray cast iron	Machined	17.8	27.5	39.6	104	170	9.9	16	22	58	95	5.8	42	97	(g)	58	160	(g)	6	3	(g)
s	P	Gray cast iron	Cast (as received)	11.3	14.1	26.7	(g)	(g)	6.3	7.9	15	(g)	(g)	(g)	69	(g)	(g)	204	(g)	(g)	32	(g)	(g)
t	Q	Ni cast iron	Machined	5.98	8.98	14.5	27.3	41.2	3.3	5.0	8.0	15	23	1.1	<5	42	67	<5	114	116	<2	8	5
	R	Ni cast iron	Cast (as received)	4.51	4.00	(g)	(g)	(g)	2.5	2.2	(g)	(g)	(g)	(g)	<5	(g)	(g)	<5	(g)	(g)	<2	(g)	(g)

(a) $\bar{P} = 393.7\ W/AD$, where $\bar{P}$ = average penetration (mils), W = weight loss (g), A = exposed area (cm^2), and D = density (g/cc).
(b) Slope of time-corrosion curve at t = 16 yr.
(c) Five deepest on each surface of duplicate panels.
(d) Ratio: deepest pit/average penetration.
(e) Perforation of panel prevents obtaining an accurate value.
(f) No samples exposed.
(g) Not determined.

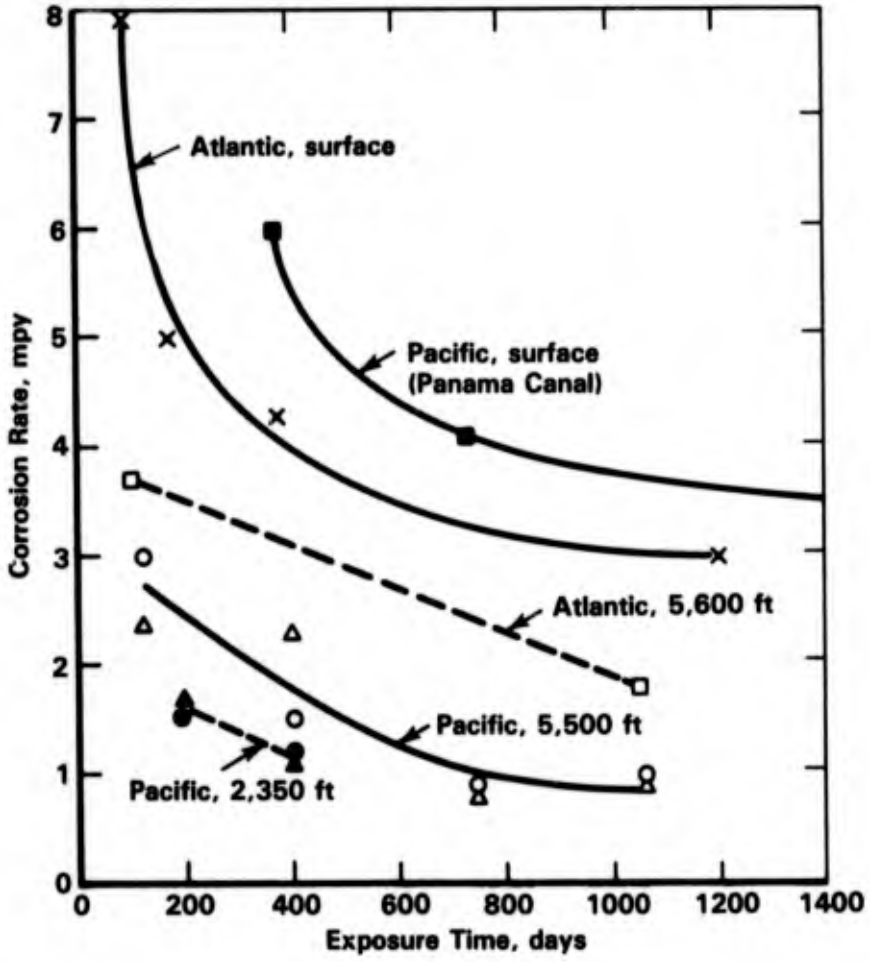

FIGURE 6-13. CORROSION RATES OF LOW CARBON STEELS AT VARIOUS LOCATIONS[16]

TABLE 6-12. CORROSION RATES AS A FUNCTION OF EXPOSURE TIME FOR STEELS SUBMERSED IN SEAWATER AT KURE BEACH, NC. (THE COMPOSITIONS ARE GIVEN IN APPENDIX F, TABLE F-6)[3]

Steel	Average Penetration, mpy		
	1.5 Yr	2.5 Yr	4.5 Yr
Cor-Ten Brand	4.2	4.3	3.8
Tri-Ten Brand	4.4	3.8	3.0
Ni-Cu	5.3	4.5	3.5
Cr-Mo	1.4	1.6	1.6
Structural Carbon	4.8	4.1	3.3

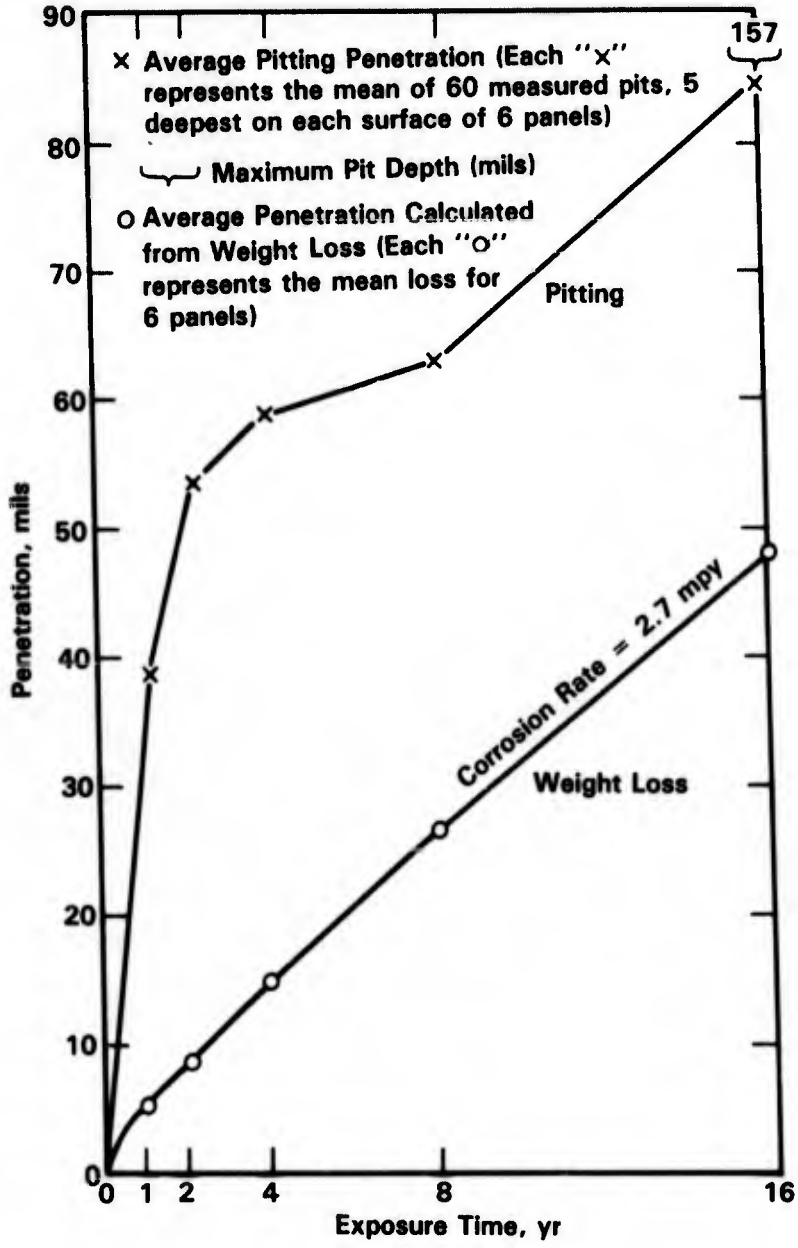

FIGURE 6-14. CORROSION OF CARBON STEEL CONTINUOUSLY IMMERSED IN SEAWATER IN THE PANAMA CANAL ZONE[13]

Effect of Alloy Composition. General corrosion rates of low-alloy steels fall between about 2.5 and 5 mpy for fully submersed conditions in seawater and are not greatly affected by alloying. Thus, the use of most low-alloy steels offers little corrosion advantage over carbon steel in submersed applications. Schultze and Van der Wekken[15] performed a statistical analysis of the published literature on the effect of alloying elements on the general corrosion

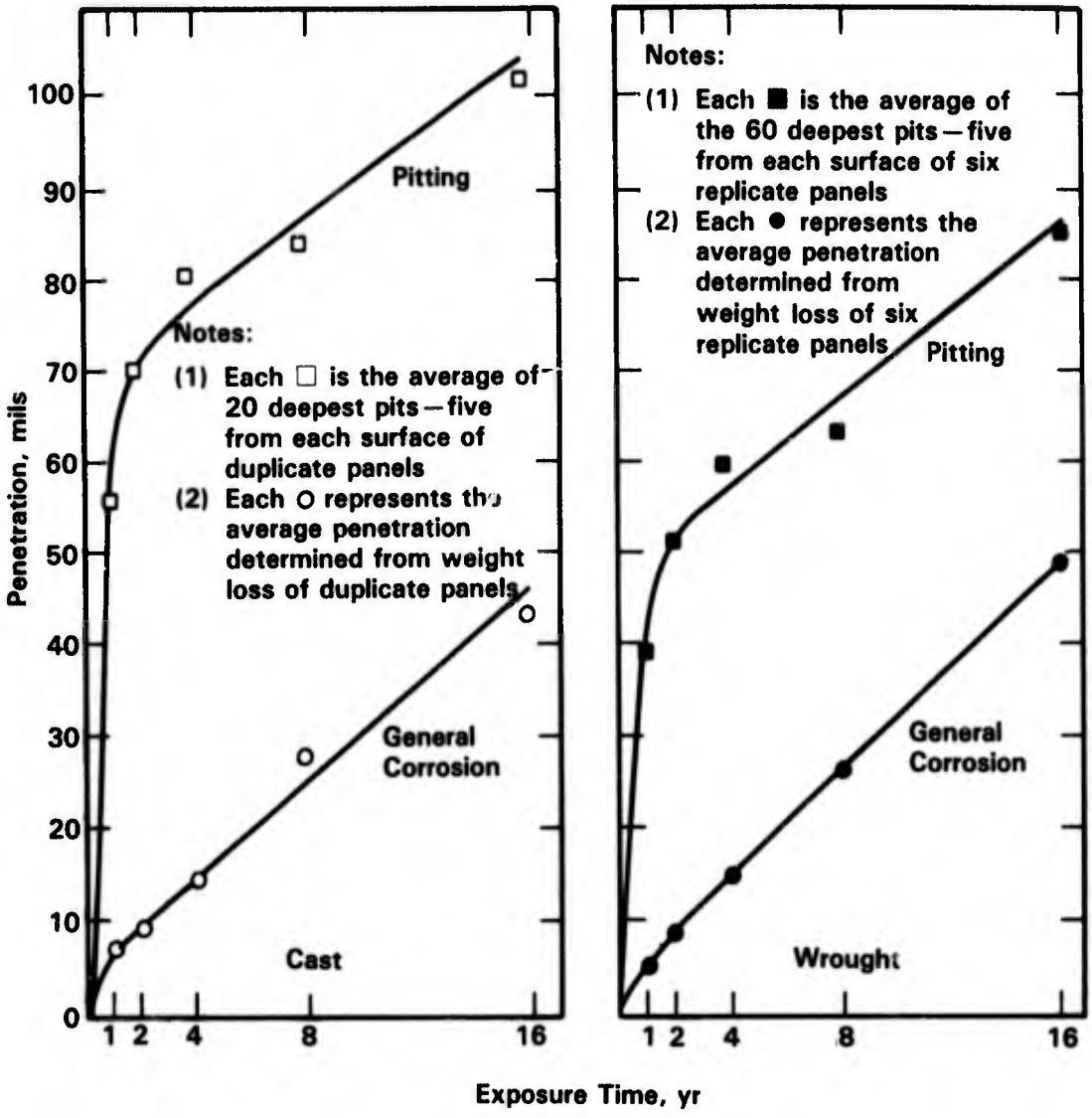

FIGURE 6-15. CURVES SHOWING WEIGHT-LOSS AND PITTING FOR (a) CAST STEEL AND (b) WROUGHT CARBON STEEL CONTINUOUSLY IMMERSED IN SEAWATER[17]

of low alloy steels under fully submersed and tidal exposure and found some systematic variation, however. A linear relationship between the corrosion rate(s) and the concentration (C_i) of an alloying element i was assumed, giving an equation of the form

$$S = S_c + \Sigma_i b_i C_i$$

where S_c is the corrosion rate of a steel not containing the elements. S was then normalized, by dividing by S_c to give a relative corrosion rate R.

$$R = S/S_c + \Sigma_i b_i/S_c C_i = 1 + \Sigma_i r_i C_i$$

Since R is a function of time, r_i values were calculated for various exposure periods: positive R values are therefore detrimental whereas negative R values are beneficial. Data for immersed conditions are given in Figure 6-16 and a summary of the effects of the various alloying elements on general corrosion is given in Table 6-13. It was concluded from the study that three alloying elements are of interest with regard to improving corrosion resistance of low-alloy steels in seawater: Cr, Mo, and Al. Cr and Mo have opposite effects which invert with time; for short times Cr is beneficial and Mo is detrimental whereas Mo is beneficial and Cr is detrimental after about 5 years' exposure. Aluminum is of interest since it is probably the only alloying element among those tested which may improve general corrosion behavior during immersion as well as tidal exposure. However, additional data on the steel-aluminum alloys are needed.

The findings from this study are generally consistent with the conclusions from the individual studies and results of other experimental studies. For example, Forgeson, et al.[18] previously had identified the time dependence of the effect of chromium on the general

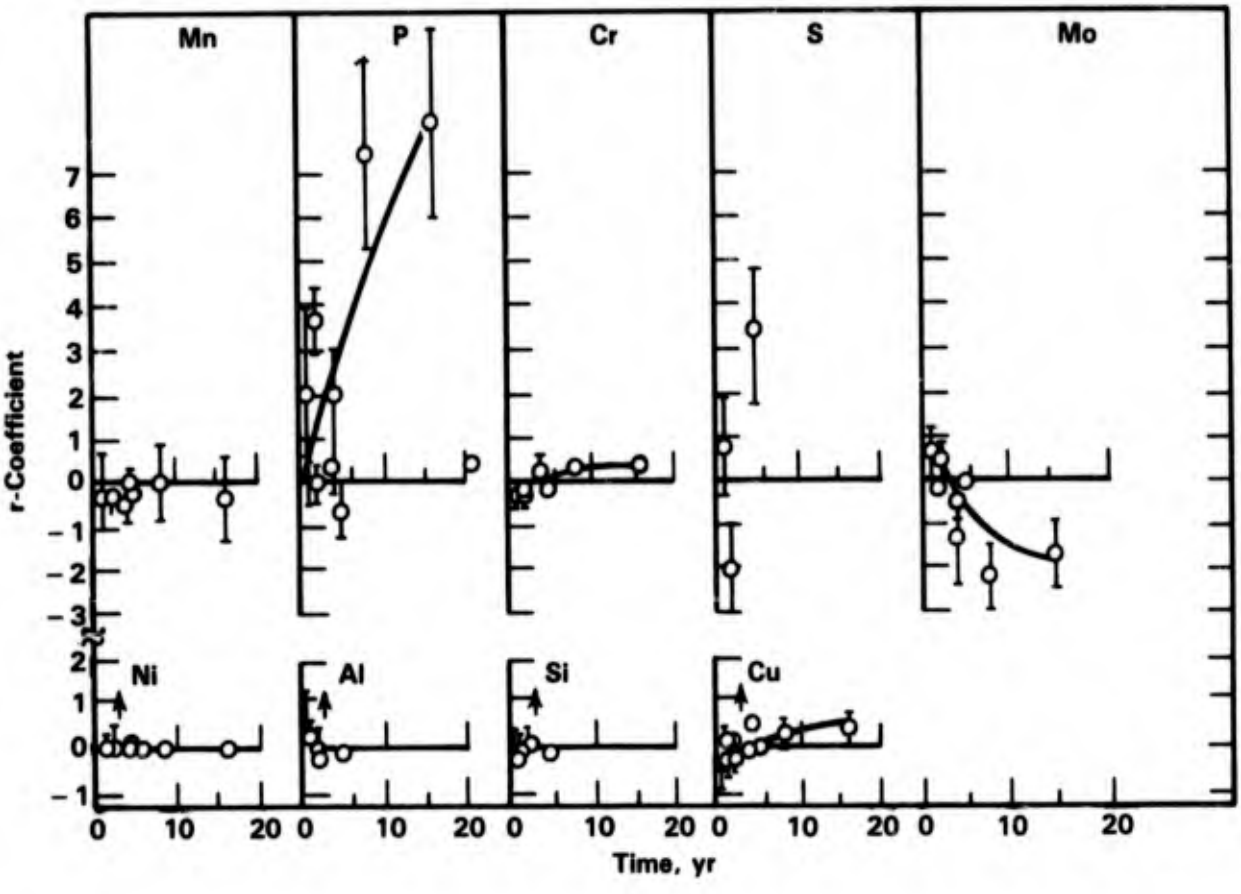

FIGURE 6-16. THE r-COEFFICIENTS OF VARIOUS ALLOYING ELEMENTS FOR FULL IMMERSION CALCULATED FROM THE DATA IN TABLE 6-10[15]

TABLE 6-13. SUMMARY OF THE EFFECTS OF VARIOUS ALLOYING ELEMENTS ON GENERAL CORROSION OF LOW-ALLOY STEELS IN SEAWATER BASED ON STATISTICAL ANALYSIS OF PUBLISHED DATA[15]

Element	Effect	
	Immersion	Tidal Zone
Manganese	Slightly beneficial	Probably detrimental
Phosphorus	Very detrimental	Beneficial
Chromium	Beneficial at short times; detrimental after >5 years	No effect
Copper	Probably detrimental after long times	No effect
Sulfur	Limited information; may be detrimental for short time	No effect
Molybdenum	Beneficial after 5 years	No effect
Nickel	Little or no effect	No effect
Aluminum	Limited information	Limited information beneficial
Silicon	Little or no effect	No effect

corrosion rate of low-alloy steels, see Figure 6-17. These conclusions also may, at first glance, seem to contradict those of Larrabee,[11] who found that Ni-Cu-P steels were highly resistant to attack for piling applications. However, Larrabee[11] reported that the beneficial influence of P on corrosion was in the splash zone above high tide; an effect also reported by Schultze and Van der Wekken.[15]

A systematic study of the effect of alloy composition on pitting and crevice corrosion of low-alloy steels was not performed by Schultze and Van der Wekken.[15] Results of long term exposures of carbon and low-alloy steels performed by Southwell and Alexander[13] do not indicate any beneficial effect of alloy addition in improving pitting and crevice corrosion resistance. In fact, their data indicate that pitting factors* for some alloy steels, such as Ni and Cr steel, frequently are higher than those for carbon steel, see Table 6-11. Thus, some alloying additions appear to be detrimental to the pitting performance of these steels.

* Ratio of deepest pit/average penetration.

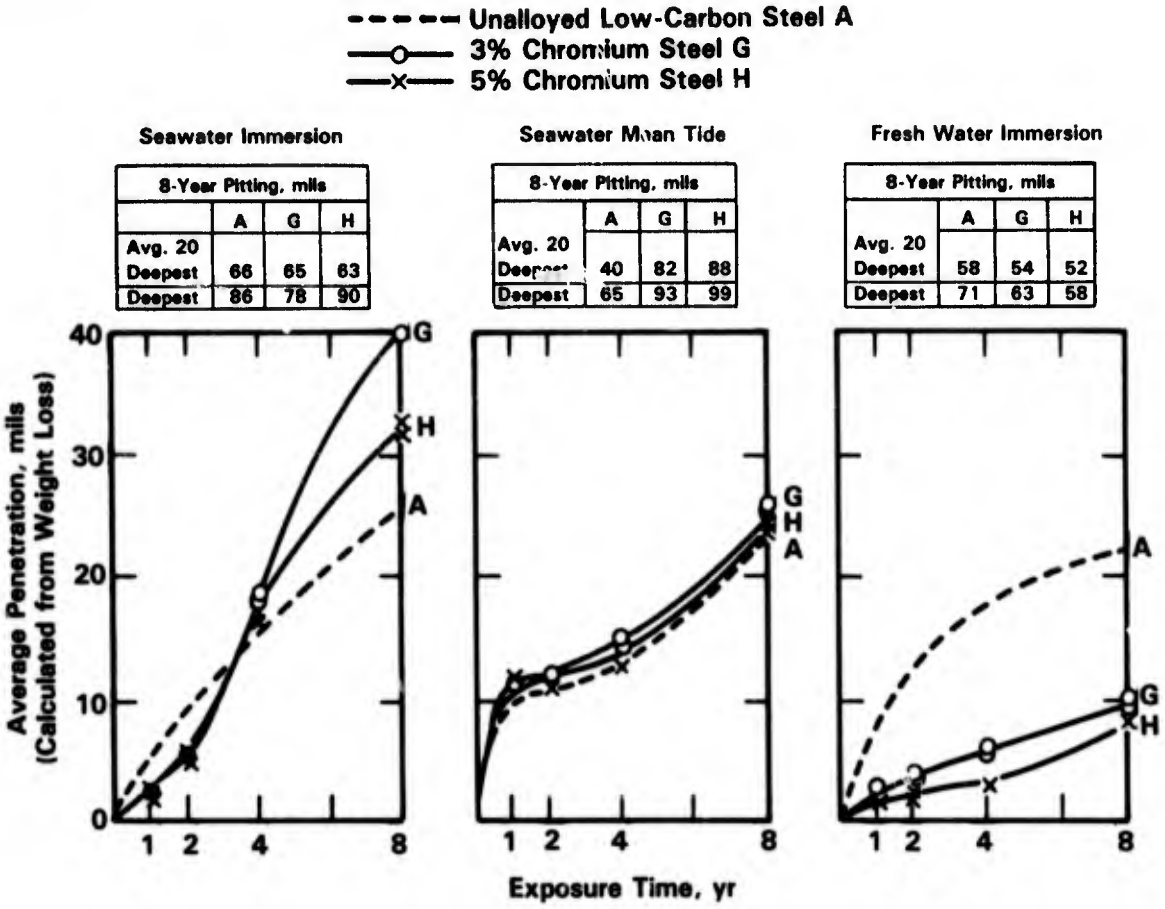

FIGURE 6-17. COMPARATIVE CORROSION OF CHROMIUM STEELS AND UNALLOYED LOW-CARBON STEEL IN THE TROPICAL WATERS OF THE PANAMA CANAL ZONE[18]

Effect of Heat Treatment and Welding. Gallagher[19] and Josefsson and Lounamaa[20] studied the effect of casting method (continuous versus ingot) on the general corrosion behavior of carbon steels in flowing seawater. No effect of casting method on corrosion behavior was observed; typical data are given in Table 6-14. However, attack of the heat affected zone (HAZ) in welded plates of both materials was observed by Gallagher.[19] The depth of attack was found to correlate with the hardness of the heat affected zone, as shown in Figure 6-18. This type of attack, which is referred to as "grooving corrosion" has been observed by other researchers,[21-23] although there appears to be some difference of opinion concerning the location of maximum attack; the HAZ or the weld metal.

A number of procedures to minimize this form of attack have been studied. Hodgkiess, et al.[21] found that post weld heat treatment, involving heating into the austenitizing temperature range reduced but did not eliminate the attack of the weld metal.

TABLE 6-14. CALCULATED AVERAGE CORROSION LOSSES OF PLATES PRODUCED FROM CONTINUOUS-CAST SLABS AND FROM INGOT CASTINGS (EXPOSED TO FLOWING SEAWATER FOR 15 MONTHS)[19]

	Calculated Average Corrosion Loss, mils				
	Plates From Continuous-Cast Slabs		Plates From Ingot Castings		Butt-Welded Plates From Continuous- and Ingot-Cast Steels
Steel	Unwelded	Bead-on-Plate-Welded	Unwelded	Bead-on-Plate-Welded	
ASTM A36	12.3	10.6	11.6	10.3	11.5
ABS A	10.3	10.0	12.5	10.3	13.0
ABS B	11.7	12.2	12.0	9.9	12.0
ABS EH	12.6	11.4	12.7	10.6	11.4

Conversion Factor: 1 mil = 0.025 mm.

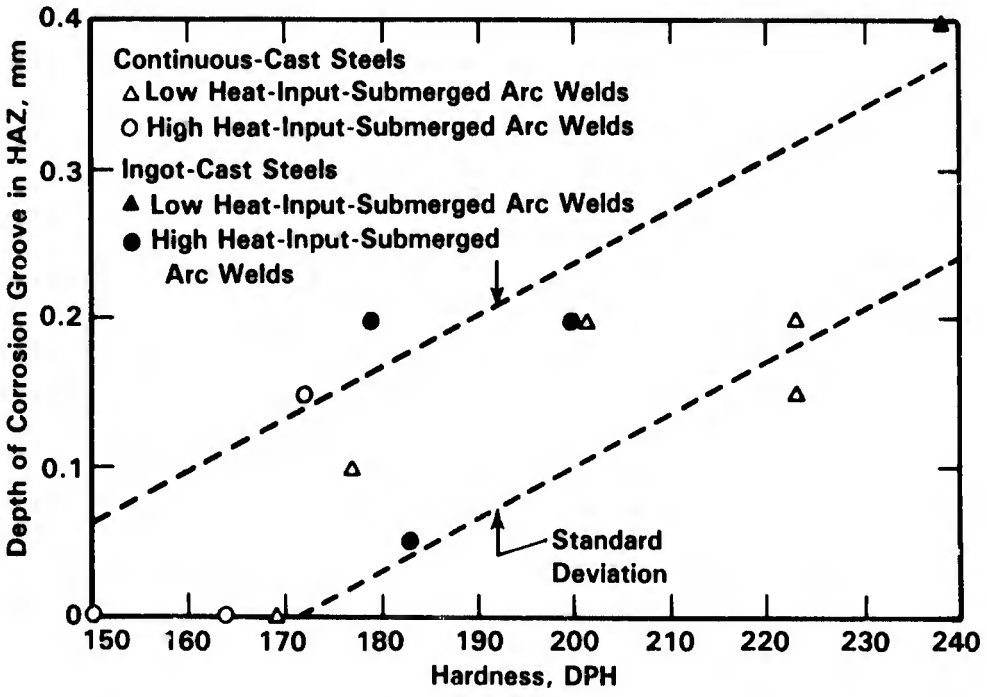

FIGURE 6-18. RELATION BETWEEN THE HARDNESS OF THE HEAT-AFFECTED ZONE IN FERRITIC STEELS AND THE DEPTH OF THE GROOVE PRODUCED BY CORROSION IN 15 MONTHS' EXPOSURE TO FLOWING SEAWATER[19]

Kato, et al.[22] reported that weld attack in electric resistance welded (ERW) steel pipe is associated with MnS inclusion while Masamura and Matsushima[23] found that low sulfur containing alloys or those containing S getters were resistant to this type of attack. They also found that heat treatment of the resistant alloys was not necessary whereas heat treatment of susceptible alloys was only effective at appropriate temperature ranges as shown in Figures 6-19 and 6-20.

Effect of Depth and Oxygen. Reinhart and Jenkins[25,26] have performed extensive studies of the corrosion of structural materials in deep ocean environments. Included in the studies were the carbon and low-alloy steels and cast irons shown in Tables F-7 and F-8 in Appendix F. These studies were performed at sites in the Pacific Ocean near Port Hueneme, CA, at depths of 1830 meters, 760 meters, and near the surface. The environments at these sites were characterized and the O_2, T, salinity, and pH were found varying as described in Figure 6-21.

It was found that the various steels exhibited similar corrosion rates at a given site over 1 year's exposure and thus the values were averaged for subsequent analysis. Data showing the relationship between corrosion rate and depth are given in Figure 6-22; superimposed upon the graph is the O_2 concentration as a function of depth. These data show that the corrosion rate appears to be a strong function of the O_2 concentration. A relationship between oxygen concentration, temperature, and corrosion rate was obtained using a linear regression analysis of the data. The derived formula:

$$\text{Corrosion Rate } (\mu m/y) = 21.3 + 25.4\ [O_2\ (ml/l)] + 0.356\ [T\ (°C)]$$

shows that the corrosion rate was much more sensitive to O_2 concentration of the seawater than to temperature and varied linearly with respect to either parameter. The actual data for the three depths are given in Figure 6-23.

A similar linear relationship between oxygen concentration and corrosion rate also was observed for the cast irons, although the dependence was much less pronounced for the gray and austenitic cast iron than for carbon steel, see Figure 6-24.

The specimens in these tests also were examined for evidence of pitting and crevice corrosion and the results are summarized in Table 6-15. Compositions of the alloys are given in Appendix F, Table F-8. These data show that, in most instances, pitting and crevice corrosion only occurred under near-surface exposure where oxygen concentrations were highest.

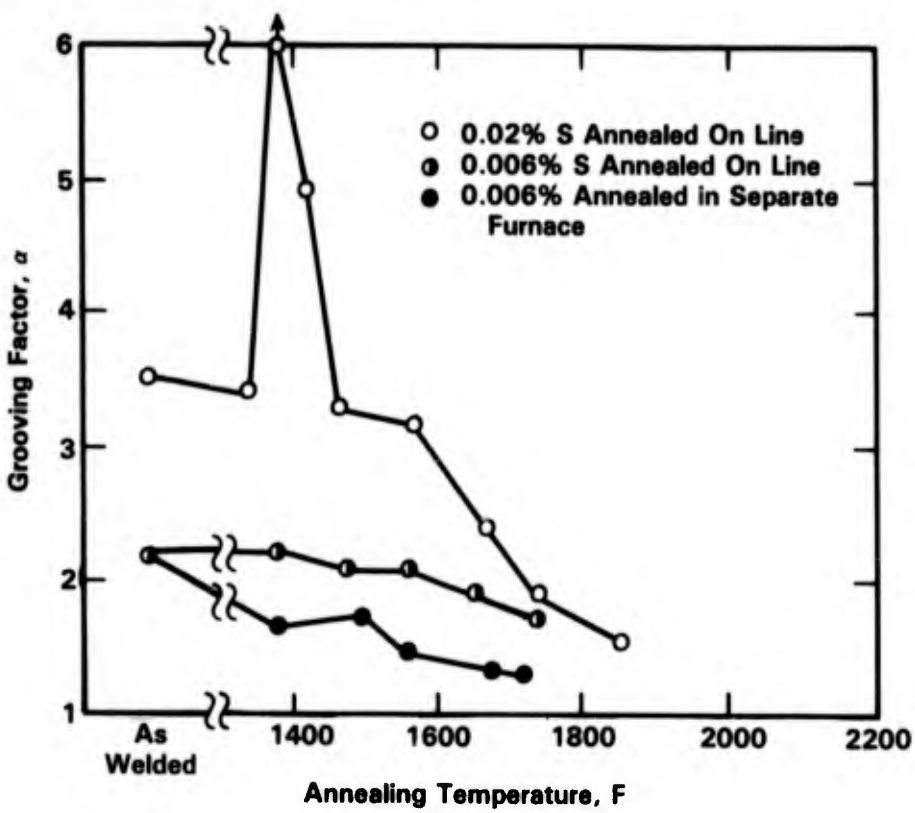

FIGURE 6-19. EFFECT OF ANNEALING TEMPERATURE, ALLOY COMPOSITION, AND HEAT TREATMENT PROCEDURE ON THE GROOVING CORROSION FACTOR FOR ERW PIPE STEELS TESTED IN AQUEOUS 3.5% NaCl AT 30 C AND -550 mV(SCE) FOR 6 DAYS[23]
α = (Rate of Weld Penetration)/(Rate of General Attack)

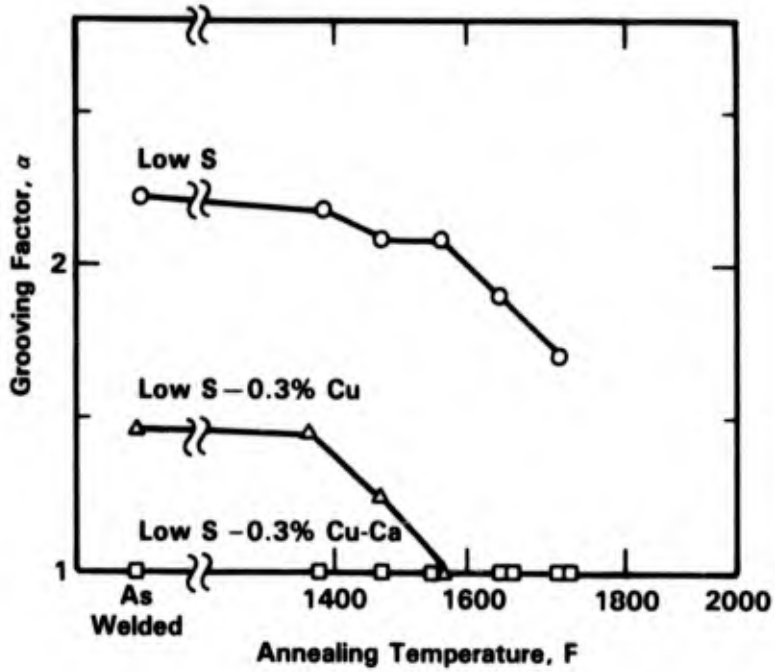

FIGURE 6-20. EFFECT OF ANNEALING TEMPERATURE AND ALLOY COMPONENTS ON THE GROOVING CORROSION FACTOR FOR ERW PIPE STEELS TESTED IN AQUEOUS 3.5% NaCl AT 30 C AND -550 mV(SCE) FOR 6 DAYS[23] α = (Rate of Weld Penetration)/(Rate of General Attack)

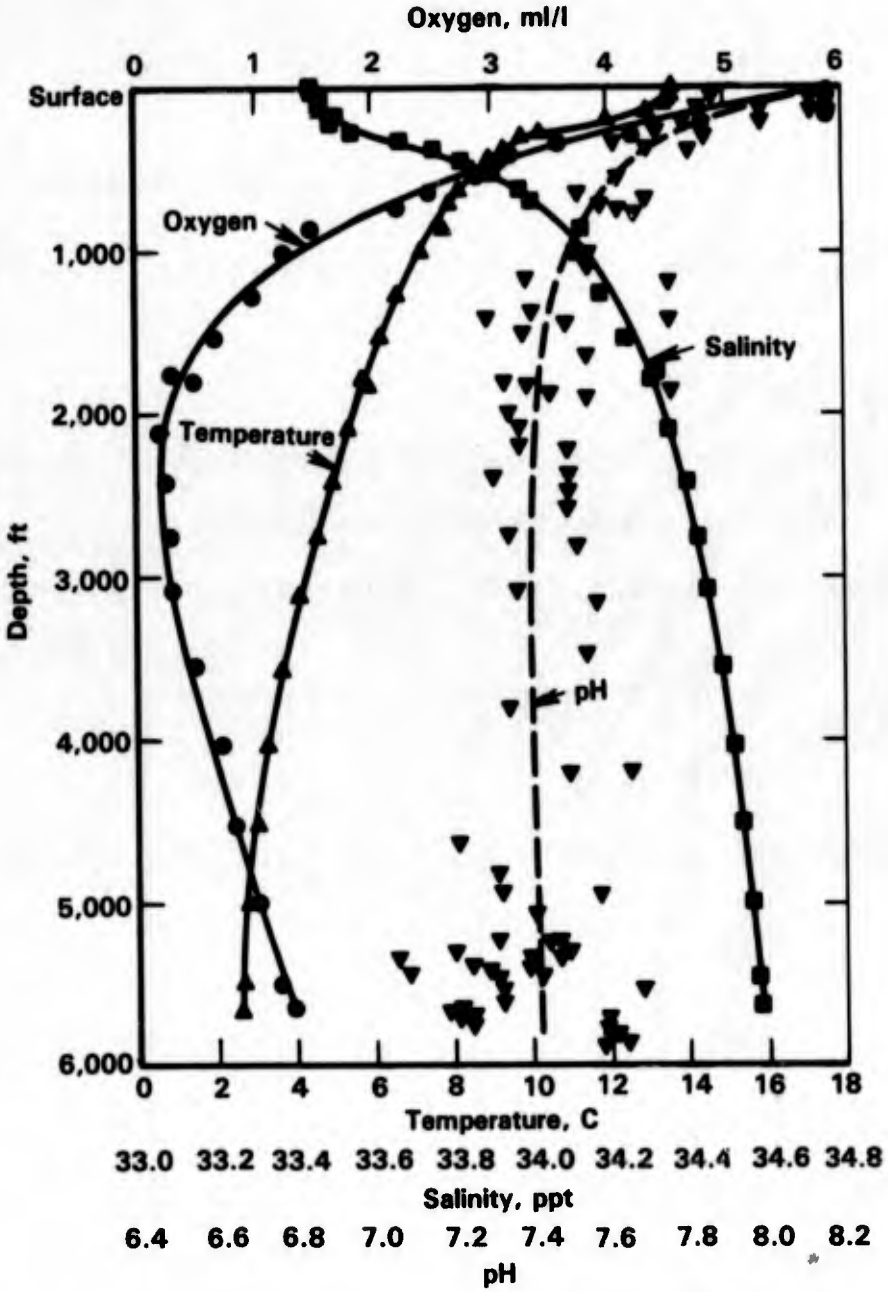

FIGURE 6-21. OCEANOGRAPHIC PARAMETERS AT EXPOSURE SITES AT VARIOUS DEPTHS NEAR PORT HUENEME, CA[25]

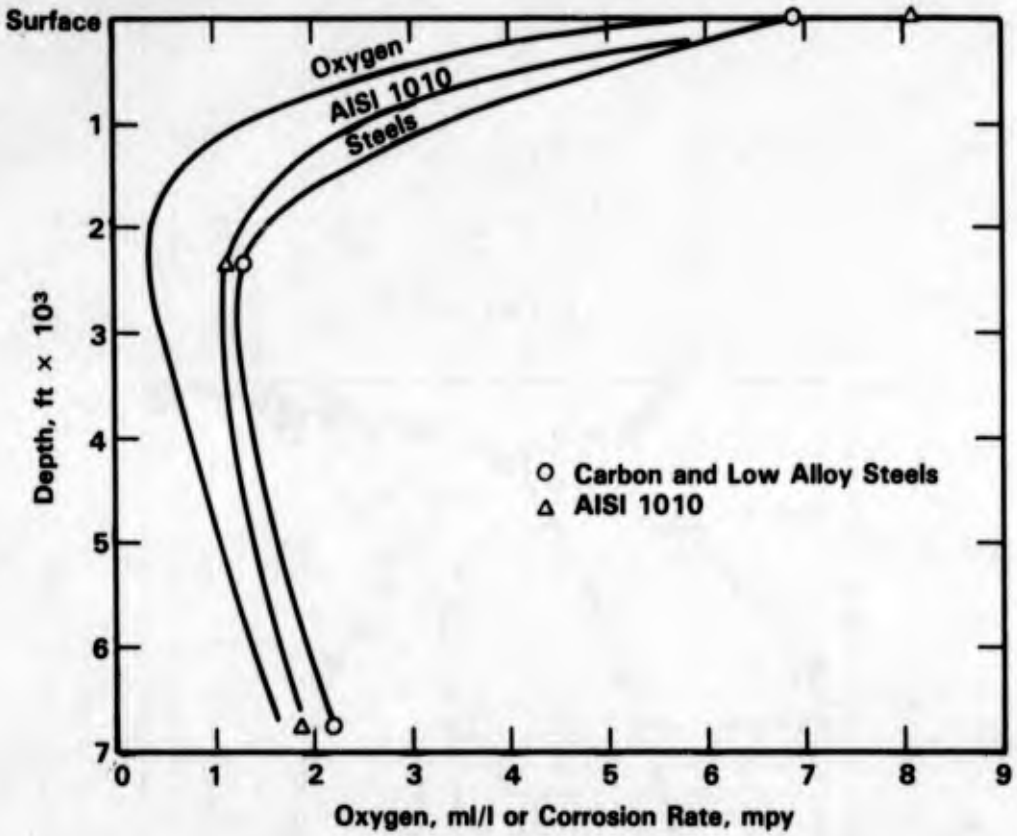

FIGURE 6-22. CORROSION OF STEELS VERSUS DEPTH AFTER 1 YEAR OF EXPOSURE[26]

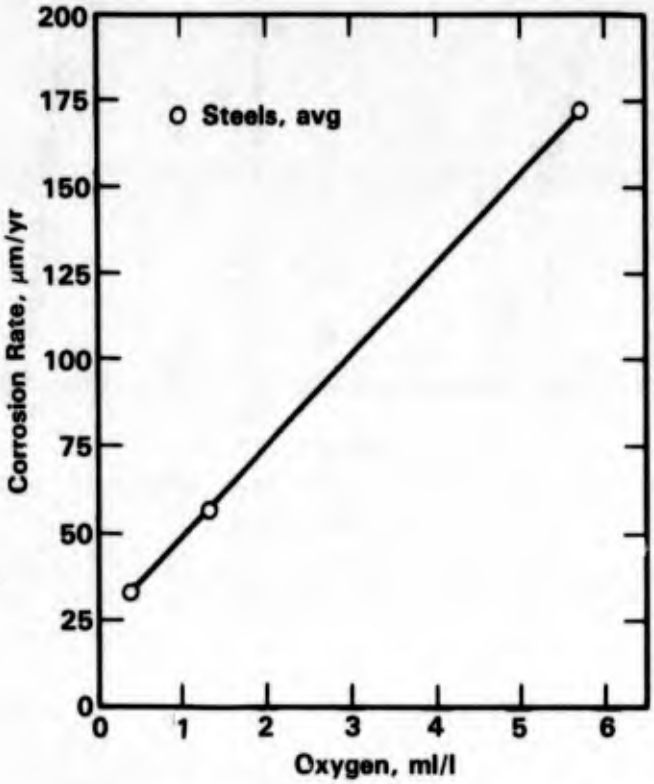

FIGURE 6-23. EFFECT OF OXYGEN CONCENTRATION OF SEAWATER ON CORROSION OF STEELS AFTER 1 YEAR OF EXPOSURE[25]

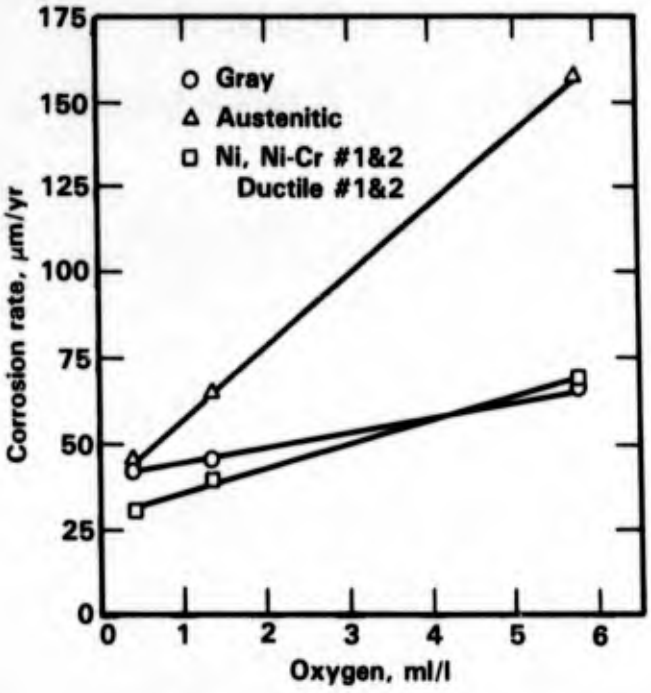

FIGURE 6-24. EFFECT OF OXYGEN CONCENTRATION OF SEAWATER ON CORROSION OF CAST IRONS AFTER 1 YEAR OF EXPOSURE[25] (COMPOSITION OF CAST IRONS ARE GIVEN IN APPENDIX F, TABLE F-7)

TABLE 6-15. CORROSION OF STEELS IN PACIFIC OCEAN SEAWATER[26] (COMPOSITION OF STEELS ARE GIVEN IN APPENDIX F, TABLE F-8)

Alloy	Exposure Days	Exposure Depth, feet	Corrosion Rate, mpy[a]	Pit Depth, mils Maximum	Pit Depth, mils Average	Crevice Corrosion Depth, mils	Corrosion, Type[b]
Armco Iron	366	5	7.1	--	--	--	G
Armco Iron	402	2370	1.4	--	--	--	G
Armco Iron	403	6780	1.5	--	--	--	U
Wrought Iron	364	5	4.8	--	--	--	G
Wrought Iron	402	2370	1.5	--	--	--	G
Wrought Iron	403	6780	1.4	--	--	--	U
Wrought Iron	723	5	4.0	--	--	--	G
Wrought Iron	763	5	4.8	--	--	--	G
AISI 1010	398	5	8.2	24	18.8	0	U, P
AISI 1010	366	5	8.0	--	--	--	G
AISI 1010	402	2370	1.2	--	--	--	U
AISI 1010	402	2370	1.1	--	--	--	G

TABLE 6-15. (Continued)

Alloy	Exposure Days	Exposure Depth, feet	Corrosion Rate, mpy[a]	Pit Depth, mils Maximum	Pit Depth, mils Average	Crevice Corrosion Depth, mils	Corrosion, Type[b]
AISI 1010	403	6780	1.5	--	--	--	U
AISI 1010	403	6780	2.3	--	--	--	G
AISI 1010	588	5	8.9	23	15	15	C, P
Copper Steel	366	5	6.0	--	--	--	G
Copper Steel	402	2370	1.1	--	--	--	G
Copper Steel	403	6780	2.1	--	--	--	G
ASTM A36	398	5	6.2	39	19.9	1	P, IC
ASTM A36	402	2370	1.3	--	--	--	U
ASTM A36	403	6780	1.5	--	--	--	U
ASTM A36	540	5	6.3	21	17	0	G, P
ASTM A36	588	5	5.8	21	17	0	G, P
HSLA Number 1[a]	398	5	5.2	42	25	0	G, C, P
HSLA Number 1	402	2370	1.0	--	--	--	U
HSLA Number 1	403	6780	2.0	--	--	--	U
HSLA Number 1	588	5	4.7	36	27	21	G, C, P
HSLA Number 2	398	5	4.5	17	15	1	U, IC, P
HSLA Number 2	402	2370	1.3	--	--	--	U
HSLA Number 2	403	6780	2.1	--	--	--	U
HSLA Number 2	540	5	4.4	28	23.4	0	G, P
HSLA Number 4	366	5	8.0	--	--	--	G
HSLA Number 4	402	2370	1.1	--	--	--	G
HSLA Number 4	402	2370	1.3	--	--	--	G
HSLA Number 4	403	6780	3.3	--	--	--	U
HSLA Number 4	403	6780	2.1	--	--	--	C
HSLA Number 5	398	5	6.0	26	14.4	1	G, IC, P
HSLA Number 5	366	5	8.0	--	--	--	G
HSLA Number 5	402	2370	1.1	--	--	--	U
HSLA Number 5	402	2370	1.4	--	--	--	G
HSLA Number 5	403	6780	2.7	--	--	2.6	U, C
HSLA Number 5	403	6780	7.4	3.0	--	--	P, SE
HSLA Number 5	540	5	5.4	17	14.1	0	G, P, E
HSLA Number 7	366	5	8.0	--	--	--	G
HSLA Number 7	402	2370	1.4	--	--	--	G
HSLA Number 7	403	6780	1.5	--	--	--	G
HSLA Number 10	366	5	8.0	--	--	--	G
HSLA Number 10	402	2370	1.5	--	--	--	G
HSLA Number 10	403	6780	1.8	--	--	--	G

TABLE 6-15. (Continued)

Alloy	Exposure Days	Exposure Depth, feet	Corrosion Rate, mpy[a]	Pit Depth, mils Maximum	Pit Depth, mils Average	Crevice Corrosion Depth, mils	Corrosion, Type[b]
HSLA Number 12	398	5	4.2	23	17.6	0	G, P
HSLA Number 12	540	5	4.9	29	23.4	0	G, P, E
HSLA Number 12	588	5	4.3	26	23.0	--	G, P, E
HS Number 1[a]	398	5	4.7	42	25	0	G, P
HS Number 1	540	5	4.5	15	10.6	0	G, P
HS Number 1	588	5	4.2	15	10.7	0	G, C, P
HS Number 2	398	5	3.5	30	28.9	0	C, P
HS Number 2	588	5	3.3	42	36.9	0	G, P
HS Number 3	398	5	5.0	15	12.6	0	U, P
HS Number 3	540	5	3.8	15	9.7	0	G, P
HS Number 3	588	5	4.6	18	12.7	0	G, P
18% Mi, Maraging	366	5	7.0	--	--	--	P
18% Mi, Maraging	398	5	3.0	10	6.2	0	U, P
18% Mi, Maraging	402	2370	1.2	--	--	--	G
18% Mi, Maraging	402	2370	0.8	0	0	0	G
18% Mi, Maraging	588	5	3.1	12	8.8	9.0	G, C, P
18% Mi, Maraging[c]	364	5	4.0	10	6.8	0	P, G
18% Mi, Maraging	402	2370	3.5	0	0	0	G
18% Mi, Maraging	723	5	3.5	10	7.7	0	P, G
18% Mi, Maraging	763	5	4.1	0	0	0	G
18% Mi, Maraging[d]	364	5	4.0	10	7.2	0	P, WB (G)
18% Mi, Maraging	402	2370	2.8	0	0	0	G
18% Mi, Maraging	723	5	3.3	10	0	0	G, P[e]
18% Mi, Maraging	763	5	3.9	0	0	0	G
1.5 Ni Steel	366	5	8.0	--	--	--	G
1.5 Ni Steel	402	2370	1.5	--	--	--	U
1.5 Ni Steel	403	6780	1.7	--	--	--	U
3 Ni Steel	366	5	8.0	--	--	--	G
3 Ni Steel	402	2370	1.3	--	--	--	G
3 Ni Steel	403	6780	1.9	--	--	2.0	C, G

(a) Calculated from weight loss.
(b) Types of corrosion: C - crevice; E - edge; G - general; I - incipient; S - severe; U - uniform; WB - weld bead; P - pitting.
(c) Aged 900 F, 3 hours and air cooled.
(d) Welded after heat treatment (3).
(e) HAZ grooving.

Effect of Temperature. General corrosion rates of carbon steel have been shown to increase with increasing temperature in laboratory studies in which deaerated aqueous chloride solutions have been used.[27,28] Typical data for concentrated synthetic or natural seawater are given in Figure 6-25 where it can be seen that weight loss followed Arrhenius behavior. In natural environments, the effect of temperature on general corrosion rates of carbon steel is complicated by the changes in oxygen solubility and biological activity which accompany changes in temperature. Data[29] showing the seasonal variation in these parameters and in the corrosion rate for carbon steel in polluted and unpolluted seawater are given in Figure 6-26. These data show that, in unpolluted seawater, the corrosion rate was

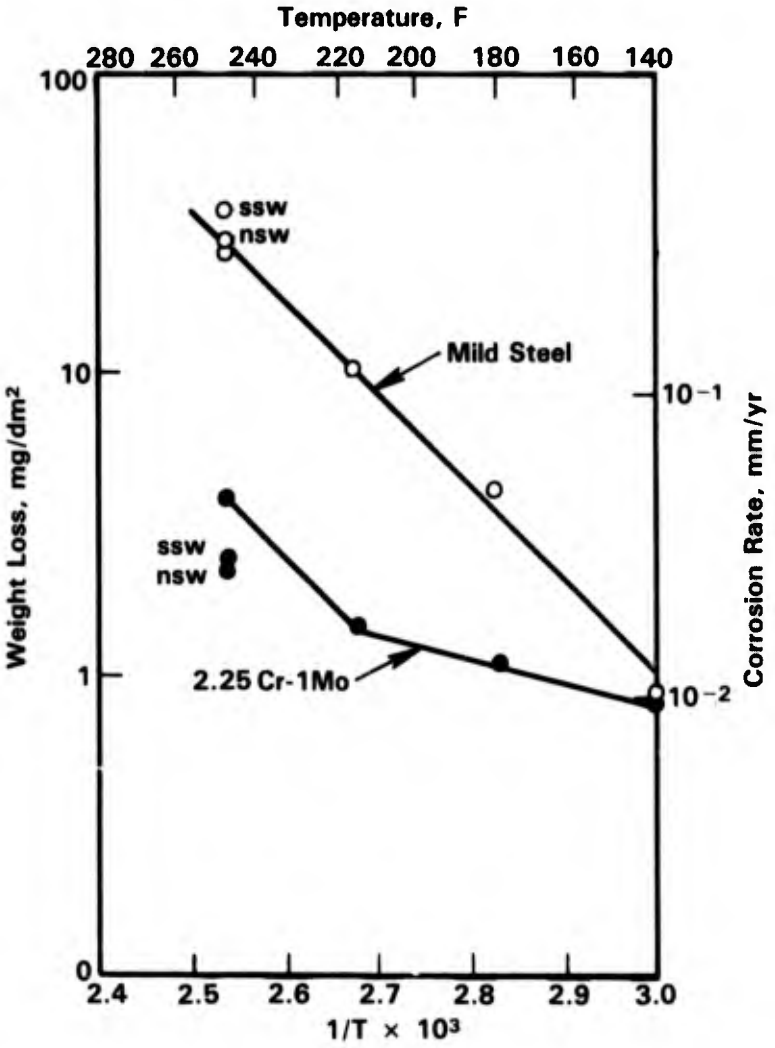

FIGURE 6-25. EFFECT OF TEMPERATURE ON CORROSION RATES IN 6% NaCl + 0.1M $MgCl_2$, 2 M/SEC, SOLUTION AT DISSOLVED OXYGEN CONCENTRATION <1 ppb AND pH 7.5 FOR 4 DAYS (ssw = synthetic seawater, and nsw = natural seawater)[28]

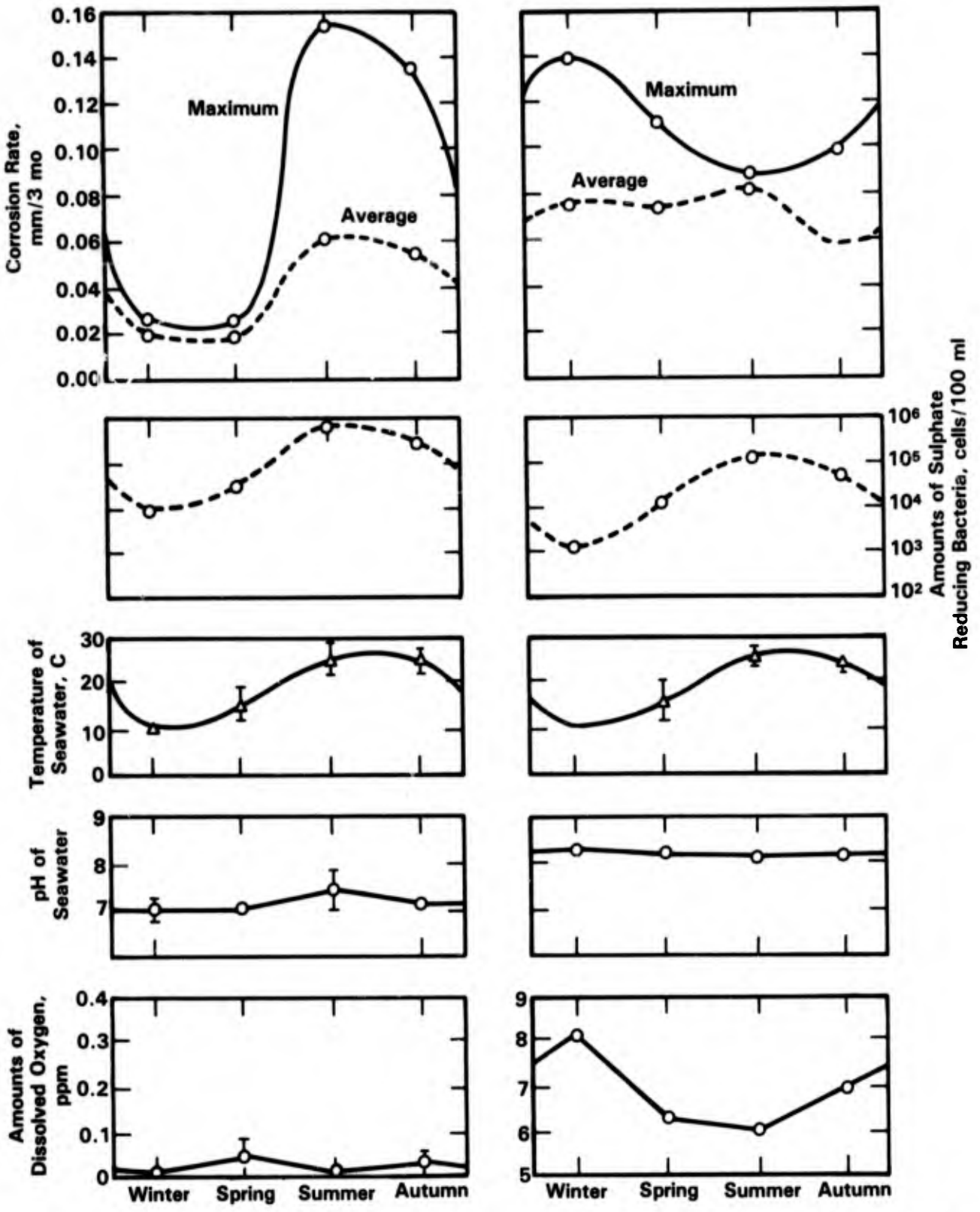

a. The polluted sea area "Okudokai Harbor"

b. The pollution free sea area "Kammon Strait"

FIGURE 6-26. SEASONAL FACTORS INFLUENCING THE CORROSION BEHAVIOR OF NORMAL CARBON STEEL IN TWO SEA AREAS[29]

proportional to the oxygen concentration of the water, which was highest during the winter when temperature and biological activity were a minimum. On the other hand, fluctuation in corrosion rates were proportional to temperature fluctuations in polluted seawater, where the oxygen concentration was low.

As discussed above, Reinhart and Jenkins[25] examined the relationship between the corrosion rate of steels in seawater and the temperature and oxygen concentration of seawater in their studies of the effect of depth on materials performances and found that O_2 concentration had a much larger effect on corrosion of steels in unpolluted seawater than did temperature.

Effect of Fouling. Efird[30] and Chandler[31] described the fouling characteristics of a variety of materials in ambient temperature seawater. For carbon and low-alloy steels, classified as highly corrodable alloys, the fouling was characterized by the periodic growth and sloughing of marine growth.

Boyd and Fink[32] speculated that biofouling layers which develop on steels in ambient temperature seawater play a role in the decreasing corrosion rate with time observed for carbon and low-alloy steels. However, the limited experimental data available do not support this contention. Traverso, et al.[33] performed immersion tests of three years' duration on carbon steel in filtered natural seawater from Genoa Harbor, Italy. Although macrofouling did not occur on the specimens, the typical decrease in corrosion rate with increasing time was observed and rates of attack after 3 years were comparable with those observed in unfiltered seawater, 2.5 to 3 mpy. Traverso, et al.[33] also reported similar pit depths in carbon steel for filtered seawater (~50 mils in 3 years) with those reported by Southwell and Alexander[13] for unfiltered seawater, see Table 6-11. On the other hand, microfouling may have played a role in the decreasing corrosion with time rate observed by Traverso, et al.[33]

Effect of Pollution. The primary effect of pollution on the seawater chemistry is to decrease the oxygen content and increase the sulfide content. pH values also are lower in polluted seawater. Typical data comparing the composition of polluted and unpolluted seawater are given in Table 6-16. It is well known that the presence of sulfide is detrimental to the corrosion behavior of steels and its effect has been studied in some detail.[34,35] On the other hand, oxygen also is detrimental to the corrosion performance of carbon and low-alloy steels in seawater and thus one might speculate that O_2 and $S^=$ would have counter-balancing effects in polluted seawater. Results of long term exposures seem to support this

TABLE 6-16. A COMPARISON OF THE CHARACTERISTICS OF THE SEAWATER AT THE UNPOLLUTED AREA (KAMMON STRAITS) WITH THAT OF THE SEAWATER AT THE POLLUTED AREA (OKUDOKAI HARBOR)[29]

Item	12/1/1969-12/1/1970 Kammon Ichigase Buoy (Strait)	12/1/1969-12/1/1970 Okudokai No. 13 Buoy (Harbor)
Temperature, F	50-81	52-84
pH value	8.0-8.3	6.6-7.9
Dissolved oxygen content, ppm	4.44-8.13	trace-0.09
NH_4^+, ppm	0.4-3.6	14.7-135.5
Sulfide-S, ppm	trace-0.01	0.03-0.39
Chemical oxygen demand Content $KMnO_4$, ppm	1.7-4.4	6.8-15.9
Number of sulphate-reducing bacteria, cells/100 ml	240-110,000	3,300-2,400,000
Muddiness, degree	trace-3	23-87
Tidal current	rapid (maximum 0.6 m/sec)	quiescent

contention. Typical data from Japanese[29] and American studies,[36,37] Figures 6-26 and 6-27 and Table 6-17, show that general corrosion rates for polluted and unpolluted seawater were comparable, although rates of attack quoted for the Japanese study were somewhat higher than those in the American study.

Although average general corrosion rates for carbon steel in polluted and unpolluted seawater appear to be comparable for long exposures, the seasonal variation in the corrosion rate for polluted and unpolluted seawater is quite different. Shimada, et al.[29] have found that the corrosion rate of carbon steel in polluted seawater is proportional to the temperature which in turn is proportional to the concentration of sulfate reducing bacteria in the seawater. On the other hand, the general corrosion rate of carbon steel in unpolluted seawater is proportional to the oxygen concentration of the seawater and inversely porportional to the temperature; corrosion rates were highest in the winter months when the temperature was the

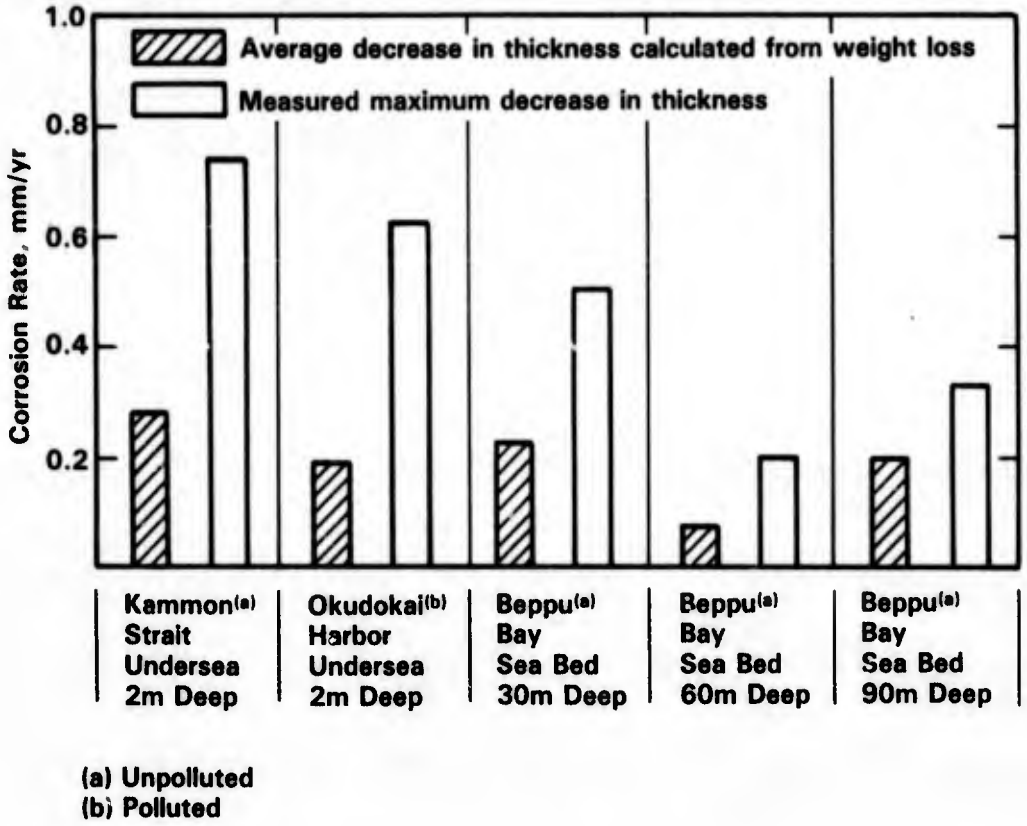

FIGURE 6-27. THE CORROSION BEHAVIOR OF NORMAL CARBON STEEL IN VARIOUS OCEAN ENVIRONMENTS (TEST PERIOD; 2 to 3.3 YEARS)[29]

TABLE 6-17. CORROSION BEHAVIOR OF MILD CARBON STEEL IMMERSED IN SEAWATER AT VARIOUS SITES[13,36-38]

Site	Exposure Time, years	Penetration Rate, mpy
Harbor Island, NC	3.3	2.1
Kure Beach, NC	7.5	4.0
	8	2.2
Santa Barbara, CA	23.6	1.25-1.75
Panama Canal (Pacific Ocean)	16	2.7
San Diego, CA (polluted seawater)	1.5	2.2

lowest and the oxygen concentrations were highest, see Figure 6-26. Of course, these seasonal effects on corrosion of carbon steel are probably location dependent and may be significantly different at other latitudes.

The relationship between pollution and localized corrosion of carbon steel appeared to be qualitatively similar to that between pollution and general corrosion. Thus, Shimada, et al.[29] observed similar maximum rates of localized attack in polluted and unpolluted seawater. It can be speculated, however, that polluted seawater is potentially very aggressive where oxygen is introduced periodically.

Effect of AC Currents. Several laboratory studies of the effect of AC currents on corrosion of mild steel in synthetic seawater and NaCl solutions have been performed[39-42] and significant effects on general corrosion have been observed under some laboratory conditions. Data by Radeka, et al.[41] showing the effect of AC current frequency on corrosion rate are given in Figure 6-28. The rates of attack correspond to 4.5 to 17.5 percent of the corrosion taking place at the equivalent direct current. Jones[40] reported an acceleration factor of 4 to 6 in the general corrosion of carbon steel in deaerated 0.1 N NaCl when an alternating current density of 30 mA/cm^2 at 60 cps was applied. However, in the latter study, no effect of AC on corrosion was observed under aerated conditions; the degree of aeration in the study by Radeka, et al.[41] was not indicated in the paper. Results of long term field studies of AC effects on corrosion of carbon and low-alloy steels in actual seawater were not found and thus it cannot be conclusively stated whether a significant effect exists.

Stress-Corrosion Cracking and Hydrogen Embrittlement

A summary of SCC data for some precracked high strength steels in actual and simulated marine environments was compiled by Sandoz[43] and is given in Table 6-18.

Although there is considerable scatter in these data as a result of variation in test technique and exposure condition, these data do show a trend of increasing susceptibility to SCC with increase in alloy yield strength. A similar trend in the data is apparent for precracked specimens of the high strength steels in marine environments and Sandoz[43] has summarized these data in Figure 6-29. Thus, steels having yield strength less than about 100 ksi are not normally considered to be susceptible to SCC in marine environments.

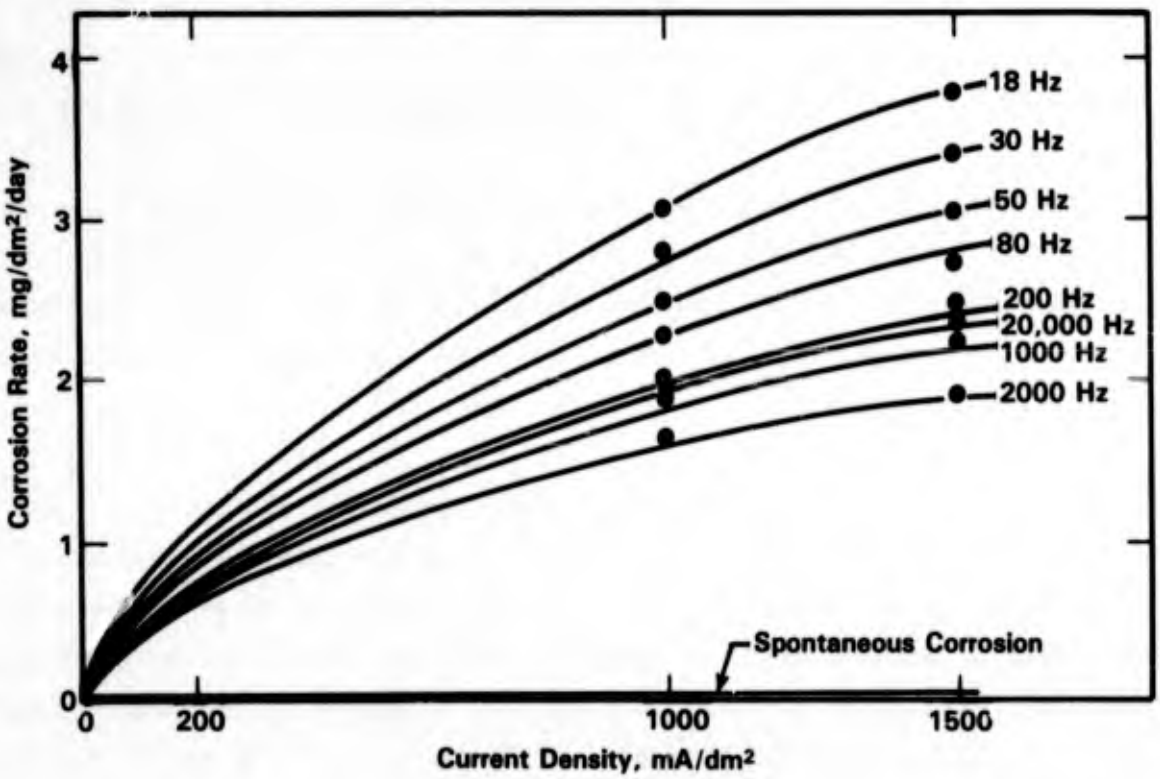

FIGURE 6-28. EFFECT OF AC CURRENT FREQUENCY ON THE GENERAL CORROSION RATE OF CARBON STEEL IN SYNTHETIC SEAWATER AT ROOM TEMPERATURE[41]

TABLE 6-18. SUSCEPTIBILITY TO SCC OF HIGH STRENGTH STEELS IN SALINE ENVIRONMENTS AS MEASURED BY NONPRECRACKED SPECIMENS AT 70 PERCENT OF THE YIELD STRESS OR HIGHER. (ALLOY COMPOSITIONS ARE GIVEN IN APPENDIX F, TABLE F-9)[43]

Type	Yield Strength Range, ksi	Environment[a]	Susceptibility[a] (70-90% YS or U-Bend)
Precipitation-Hardening Stainless			
PH-13-8-Mo	220	Salt air	Fail
PH-13-8-Mo	210-217	3-1/2% NaCl	OK
PH-14-8-Mo	220-240	Salt air	Fail
PH-14-8-Mo	190-230	3-1/2% NaCl	OK
15-5-PH	155-175	3-1/2% NaCl	OK
PH-15-7-Mo	200	1M NaCl	Fail
17-4-PH	140	5% NaCl + H_2S	Fail
	150-210	Deep sea	OK
17-7-PH	191-220	3-1/2% NaCl	Fail
	192	Deep sea	OK
AM-350	140-210	3-1/2% NaCl	Fail
AM-355	170-230	3-1/2% NaCl	Fail

TABLE 6-18. (Continued)

Type	Yield Strength Range, ksi	Environment[a]	Susceptibility[a] (70-90% YS or U-Bend)
AFC-260	205	3-1/2% NaCl	Fail
AFC-77	190-205	3-1/2% NaCl	Fail
AFC-77	200	Salt air	Fail
Martensitic Stainless			
410	160	3-1/2% NaCl	OK
410	125	4% HCl + 3% NaCl + As	Fail
12Mo-V	260 (UTS)	3-1/2% NaCl	Fail
13Cr	200-220	3% NaCl	Fail
Martensitic			
AISI 4340	200-260	5% NaCl	Fail
		3-1/2% NaCl	Fail
		Deep sea	Fail
		Salt air	Fail
AISI 4340	150-190	Deep sea	OK
AISI 4330	220	3-1/2% NaCl	Fail
AISI 4330M	217	3-1/2% NaCl	Fail
300M	210-275	3-1/2% NaCl	Fail
H-11	190-250	3-1/2% NaCl	Fail
D6AC	197-250	3-1/2% NaCl	Fail
HY130	130	Sea	OK
High Alloy Martensitic			
HP-9-4-20	197	Sea	Fail
HP-9-4-25	180	3-1/2% NaCl	OK
HP-9-4-30	200-240	3-1/2% NaCl	OK
HP-9-4-40	260	3-1/2% NaCl	Fail
HP-9-4-45 (Q&T)	235-260	3-1/2% NaCl	Fail
HP-9-4-45 (Bainite)	220-280	3-1/2% NaCl	OK
Maraging			
12Ni-5Cr-3Mo	140-205	Sea	Fail
18Ni	180-350	3-1/2% NaCl	Fail
	190	5% NaCl + H_2S	Fail
	200	Sea	OK
	200-300	Sea	Fail
	200-272	Sea	Fail
	250	Salt spray	OK
	240	Deep sea	Fail (weld)
	250-255	3-1/2% NaCl	OK
	210-286	Sea	Fail
	220-250	3% NaCl	Fail

TABLE 6-18. (Continued)

Type	Yield Strength Range, ksi	Environment[a]	Susceptibility[a] (70-90% YS or U-Bend)
	250-286	Sea	Fail
	250-270	3-1/2% NaCl	Fail
	249-354	Dist H_2O	Fail
	300	Water	Fail
	300	5% NaCl	Fail
	300	Salt spray	Fail
	260	5% NaCl	Fail
	260	3-1/2% NaCl	Fail
	280-350	3% NaCl	Fail
Maraging Stainless			
Almar 362	182-227	10% NaCl + HAc	Fail
Almar 362	115-182	10% NaCl + HAc	Fail
Almar 362	161	3-1/2% NaCl	OK

(a) Environmental variables such as alternate immersion, or degree of aeration, and the details of specimen type, geometry, and surface perforation are omitted in order to get an overall view. Specific results may be misleading unless the references are examined in detail.

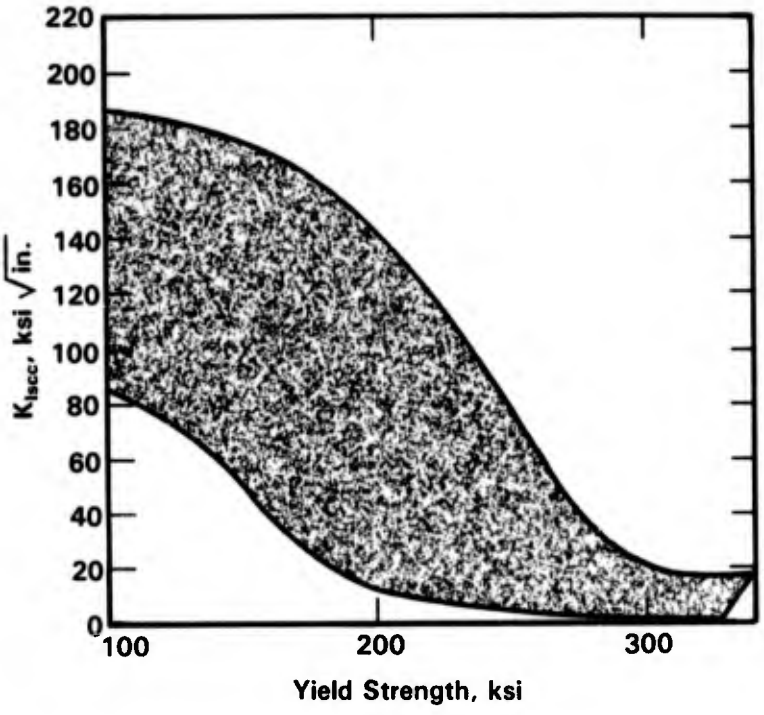

FIGURE 6-29. COMPOSITES OF THE K_{Iscc} ENVELOPES FOR HIGH STRENGTH STEELS IN SEAWATER, SALT WATER, AND DISTILLED WATER[43]

Effect of Alloy Composition. The effect of alloying elements on SCC of low-alloy steels are confounded, in most instances, by the influence these elements have on the yield strength of the materials. Nevertheless, a few experimental studies have been performed in which the SCC susceptibility of alloys of similar yield strengths, but varying compositions, were assessed. Sandoz[43,44] studied the effects of Mn and C in a base 4340 steel alloy on K_{Iscc} in seawater and in 3-1/2 percent NaCl at two yield strength levels. Results, summarized in Figures 6-30 and 6-31, show that Mn is detrimental, up to a 3.0 percent level, as is C up to approximately 0.40 percent C; a slight improvement in K_{Iscc} values was observed at 0.5 percent C.

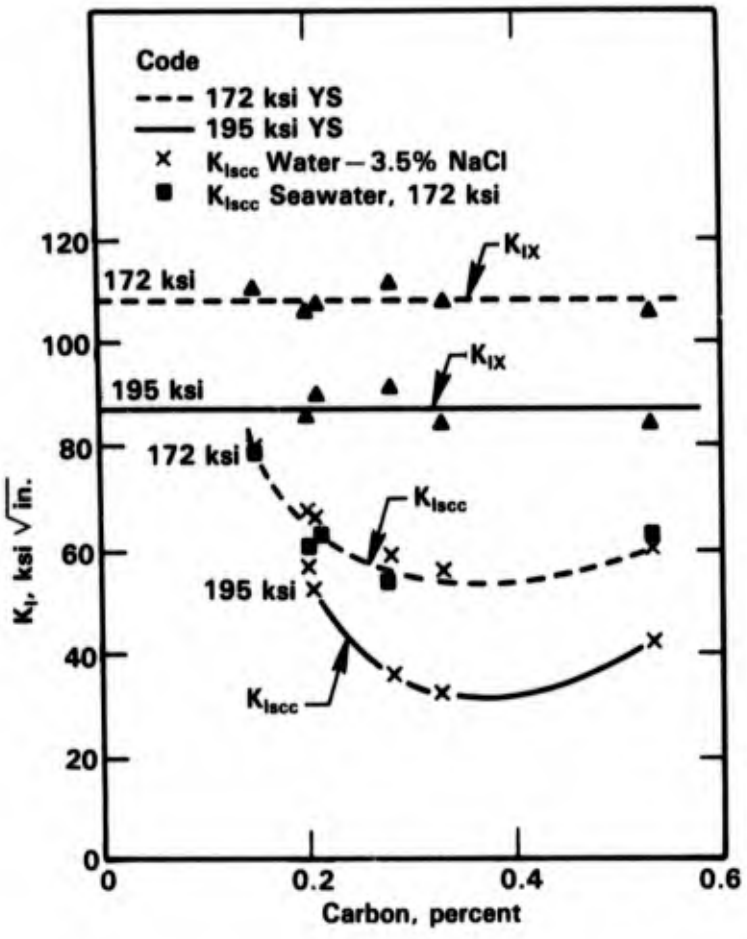

FIGURE 6-30. THE EFFECTS OF CARBON ON THE STRESS-CORROSION CRACKING OF AISI 4340-TYPE STEELS QUENCHED AND TEMPERED TO EITHER 172- OR 195-KSI YIELD STRENGTH[43]

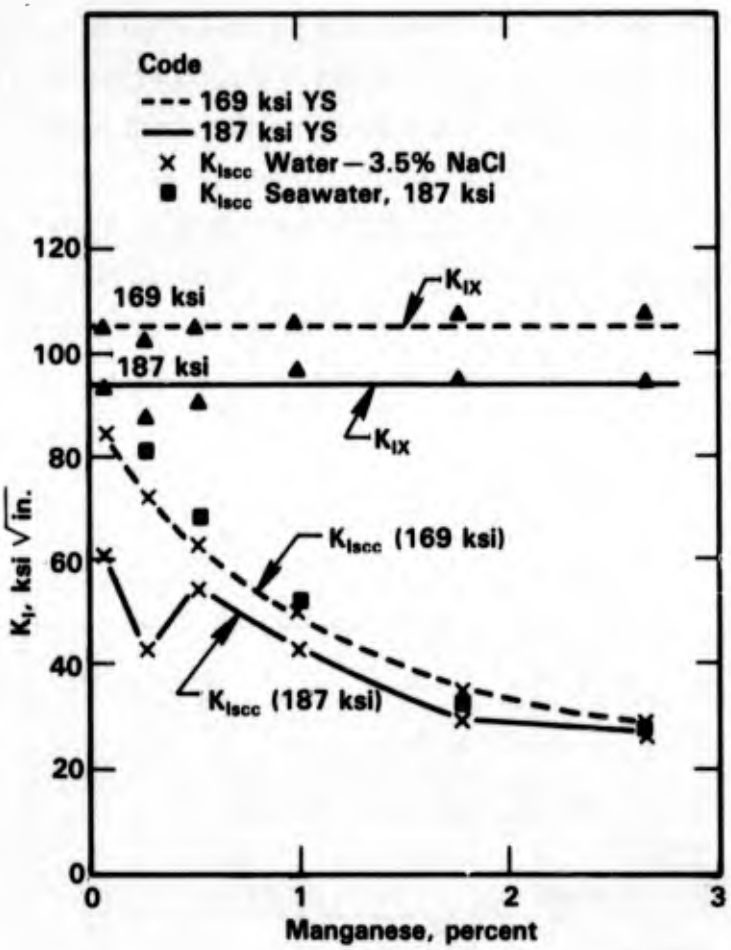

FIGURE 6-31. THE EFFECTS OF MANGANESE ON THE STRESS-CORROSION CRACKING RESISTANCE OF AISI 4340-TYPE STEELS QUENCHED AND TEMPERED TO 169- AND 187-KSI YIELD STRENGTH[43]

Results of studies of the effect of other alloying elements on SCC of low-alloy steels are summarized in Table 6-19. These data show that, with the exception of C and Mn, the alloy additions did not significantly alter K_{Iscc} values. There are a number of caveats however; first of all, synergistic interactions of the alloying elements were not considered in the studies reported above. Moreover, some of the alloying elements which had a negligible affect on K_{Iscc}, such as silicon, altered cracking velocities above K_{Iscc}.[46] Finally, the alloying elements may affect cracking where local (crevice or pit) chemistry conditions control susceptibility. Such conditions are common in the stainless steels.[46,47]

Melting practice has been shown to influence SCC susceptibility of steels having yield strength in the ranges of 180 to 200 ksi.[46,48,49] Vacuum melted steels in this strength range apparently have higher resistance to cracking (higher K_{Iscc} values) in aqueous environments

TABLE 6-19. EFFECTS OF ALLOYING ELEMENTS ON K_{Iscc} SUSCEPTIBILITY OF LOW-ALLOY HIGH STRENGTH STEELS IN ACTUAL OR SIMULATED MARINE ENVIRONMENTS

Element	Composition Range, %	Base Composition	Yield Strength, ksi	Effect on SCC	Reference
C	0-0.6	4340	172 and 195	Detrimental - Maximum suscept between 0.3-0.4% C	44
Mn	0-3	4340	169 and 187	Detrimental	44
P	0-0.03	4340	185 and 210	Negligible	43
S	0-0.03	4340	185 and 210	Negligible	43
Cr	0-2.1	4340	182 and 203	Negligible	43
Mo	0-1.2	4340	183 and 206	Negligible	43
Co	0-3.0	4340	185 and 210	Negligible	43
Ni	3-9	0.3 C steel	195	Slightly detrimental above 6%	45
Si	0-2.1	4340	193-216 and 200-240	Negligible	46

than similar air melted steels. Carter[46] attributed the improved performance of vacuum melted 4340 to lower impurity levels of sulfur and phosphorus; a conclusion which appears to contradict the previously reported studies of the effect of alloying additions on cracking susceptibility. The beneficial effect of melting practice on K_{Iscc} diminishes with increasing yield strength; steels above the 200 ksi yield strength range all tend to show low values of K_{Iscc}.[43]

Effect of Heat Treatment. The overriding effect of heat treatment on SCC susceptibility of low-alloy steels is through its influence on yield strength.[43] Thus, the general trend is for SCC resistance to increase with increasing tempering or aging temperature.[50-53] Some intermediate temperatures do produce maximum susceptibility. For example, Davis, et al.[54] found that the maximum SCC of H11 and 4340 steels in 3.5 percent NaCl occurred at the "500 F embrittlement condition" where the impact energy was a minimum. Typical data are given in Figure 6-32.

Effect of Electrochemical Potential. Electrochemical potential can have a dramatic effect on stress-corrosion susceptibility of high strength steels in aqueous environments. Data by Raymond, Figure 6-33, show that time to failure of precracked specimens of D6AC, H-11, and PH13-8Mo steels in 3.5 percent NaCl decreased with decreasing potential from the free-corrosion potentials. Shorter lives also were observed at potentials more noble than the free-corrosion potential. Similar decreases in life were observed where the steels were galvanically coupled to more active materials such as Al.[55] Increased susceptibility to cracking in 3.5 percent NaCl at active potentials is also reflected in results of slow strain rate tests. Data by Kanao, et al., Figure 6-34, show that the percent reduction in area of SM50B and HT80 decreased dramatically with decreasing potential.

Results of crack propagation studies also show a dramatic effect of potential on crack velocity, see Figure 6-35. On the other hand, potential does not appear to have a significant influence on threshold stress intensity values for crack initiation, see Figure 6-36. Thus, Sandoz[43] has speculated that cathodic protection may in fact reduce the likelihood of crack initiation by preventing pitting; pits frequently act as sites of crack initiation.

Effect of Environmental Variables. With the exception of a few deleterious species such as H_2S, the stress-corrosion cracking of high strength low-alloy steels in neutral aqueous environments is not particularly sensitive to the composition of that environment. Thus, K_{Iscc} values of 4340 steels in distilled water, 2 to 4 percent NaCl or seawater are similar at a given strength level.[43,57-59]

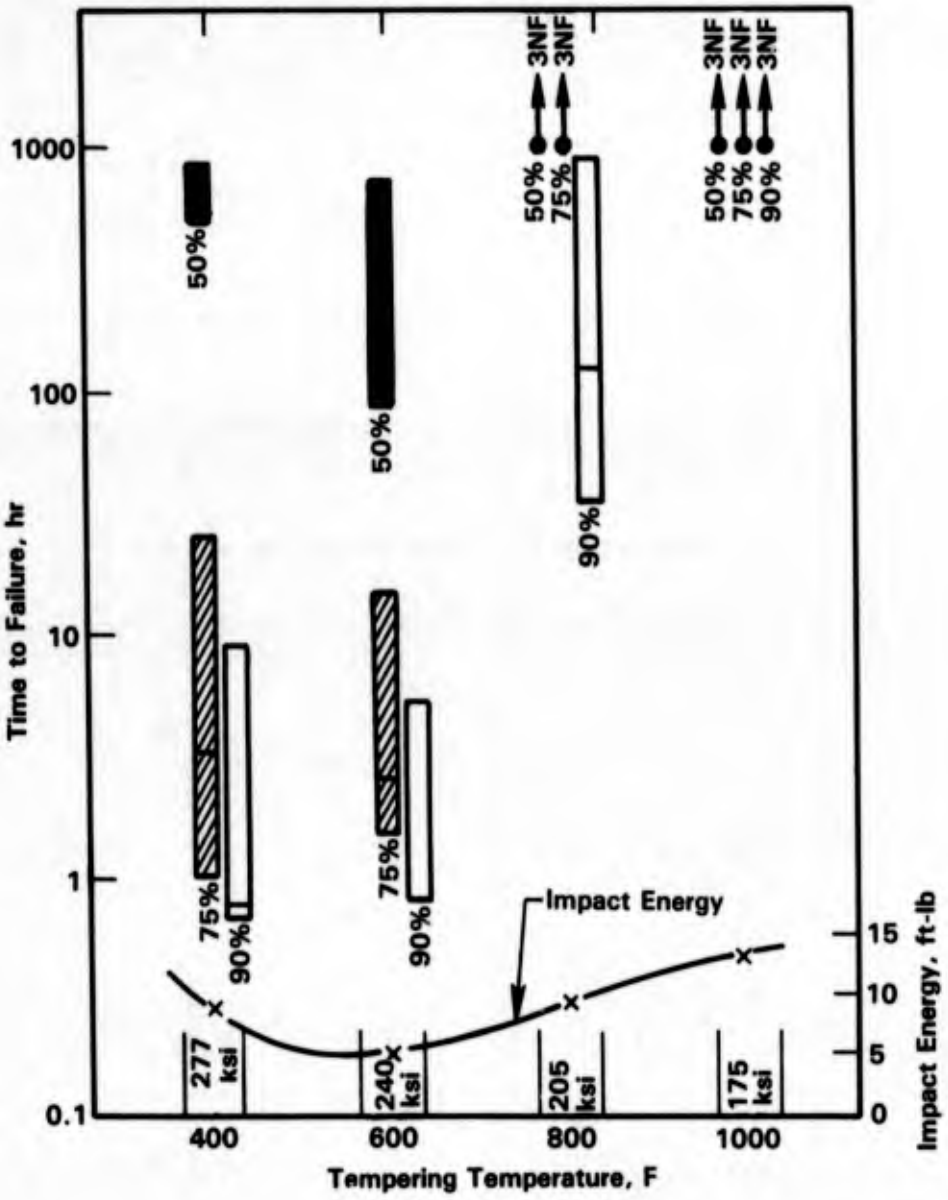

FIGURE 6-32. TIME TO FAILURE VERSUS TEMPERING TEMPERATURE FOR 4340 STEEL (OIL QUENCH) AT STRESS LEVELS OF 50, 75, AND 90 PERCENT OF F_{TY} (0.2% YIELD STRESS) IN A 3.5% AQUEOUS NaCl SOLUTION AT AMBIENT TEMPERATURE[54]

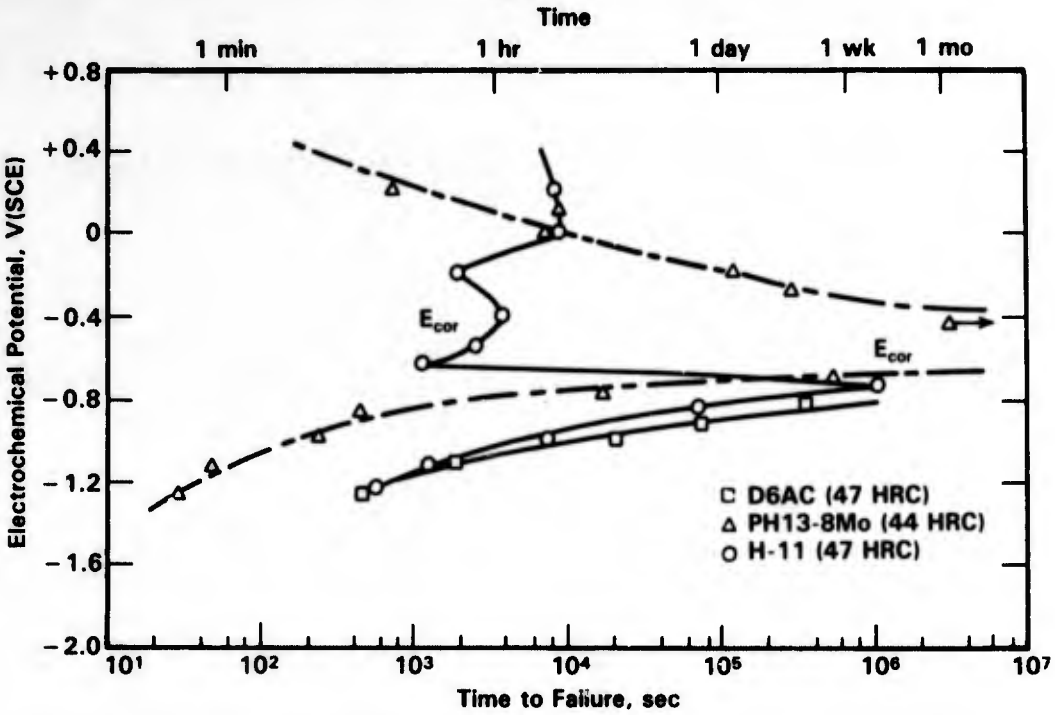

FIGURE 6-33. EFFECT OF POTENTIAL ON TIME TO FAILURE OF HIGH STRENGTH STEELS IN 3.5% NaCl (pH = 6.0)[55]

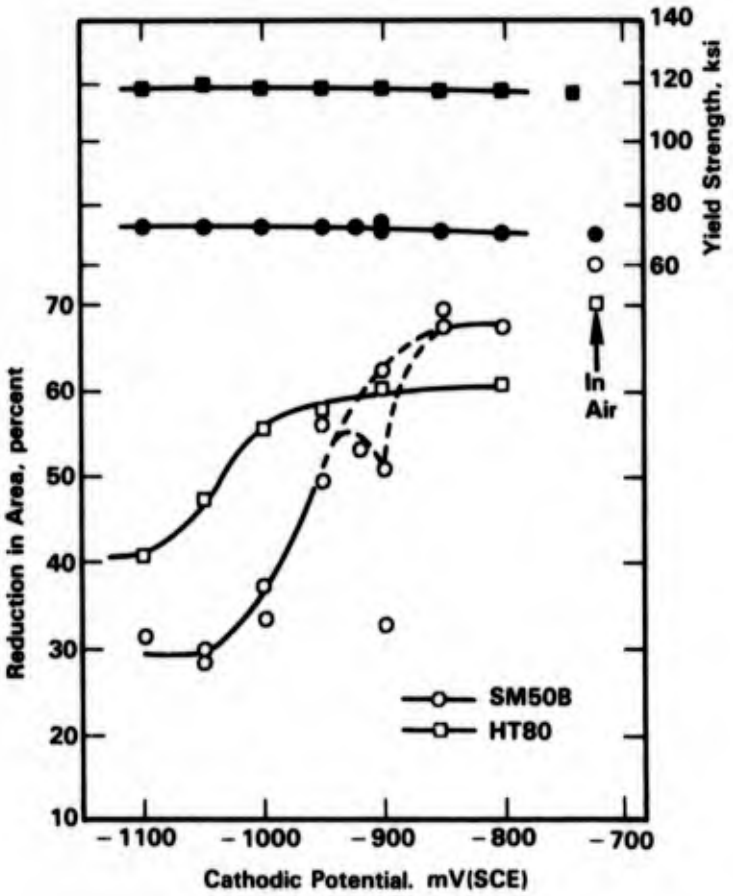

FIGURE 6-34. EFFECT OF CATHODIC POTENTIAL ON THE REDUCTION IN AREA OF STEELS WHICH WERE SLOW STRAIN RATE TESTED IN 3.5% NaCl AT 25 C[56]

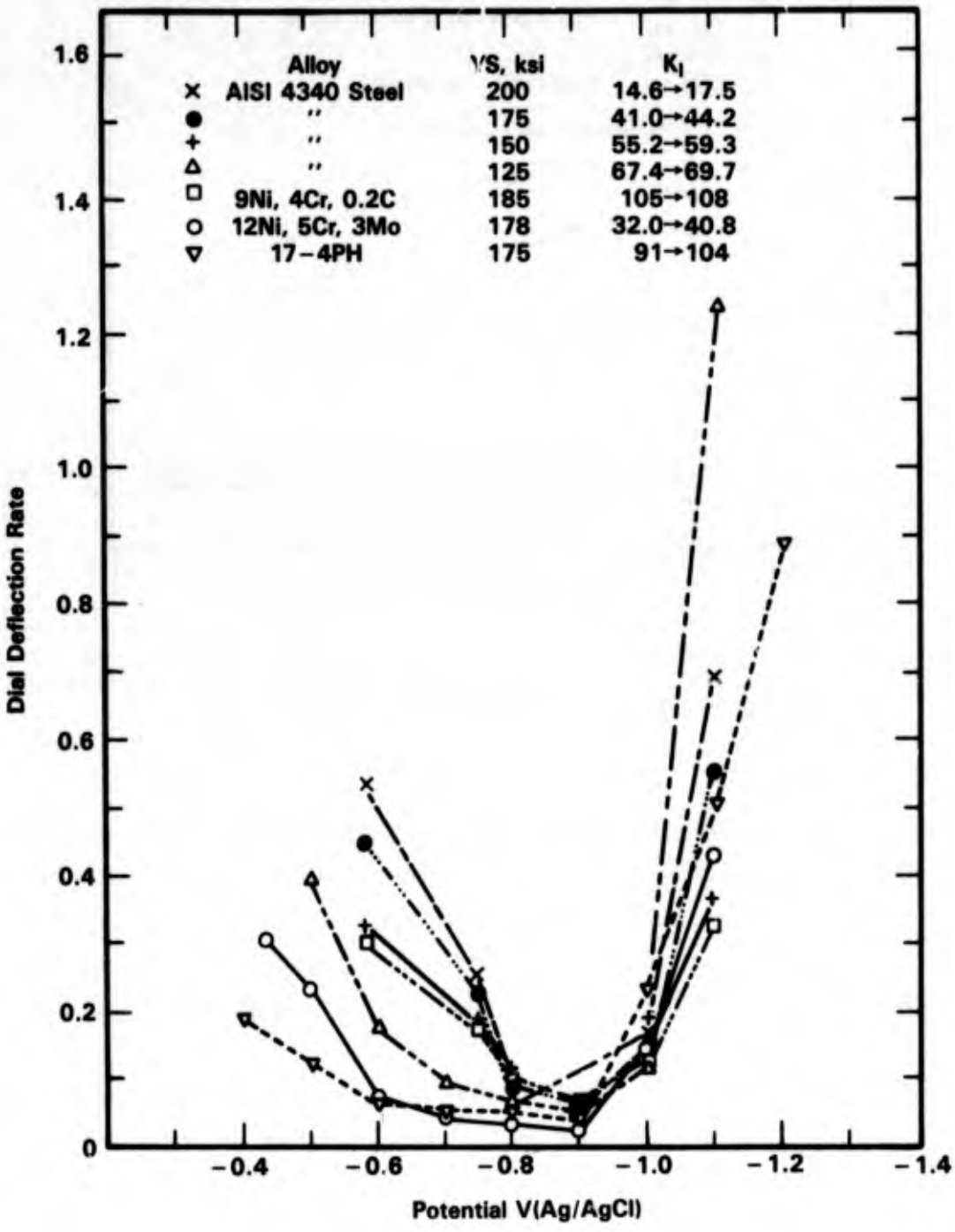

FIGURE 6-35. EFFECT OF (IMPRESSED) POTENTIAL ON CRACKING RATES FOR HIGH STRENGTH STEELS[43]

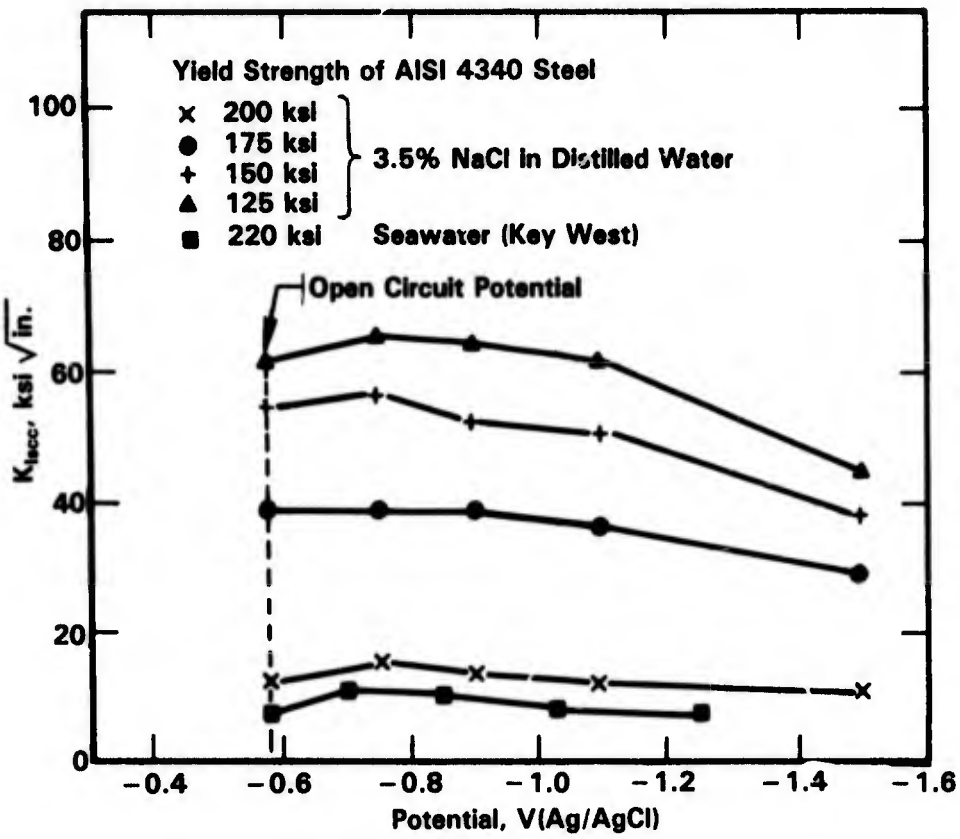

FIGURE 6-36. EFFECT OF (IMPRESSED) POTENTIAL ON CRACKING THRESHOLD STRESS INTENSITY OF AISI 4340 STEEL[43]

Cracking susceptibility of these steels is influenced by solution pH, but the effect is not pronounced. Highly acidic conditions promote cracking whereas highly basic conditions retard cracking but there is little change in SCC susceptibility over the pH range of 3 to 10.[43,60-64] Sandoz[43] speculated that the absence of a large bulk solution pH effect is the result of the fact that the pH within a growing crack is invariably about 3.7 regardless of bulk solution pH.

The temperature dependence of SCC of high strength steels has been studied in some detail.[64-67] Van Der Sluys[64] and Simmons, et al.[65] reported that cracking velocities in 4340 steel in distilled water followed Arrhenius behavior. Data by Simmons, et al. are given in Figure 6-37. Similarly, Johnson and Willner[66] reported that H-11 steel exhibited Arrhenius crack growth behavior in distilled water and 100 percent relative humidity water vapor. On the other hand, Bala and Tromans[67] observed a nonsystematic effect of temperature on crack velocity of HY-180M steel in 3.5 percent NaCl, see Figure 6-38. The latter steel was much more resistant to SCC propagation than the 4340 or H-11, as indicated by the cracking

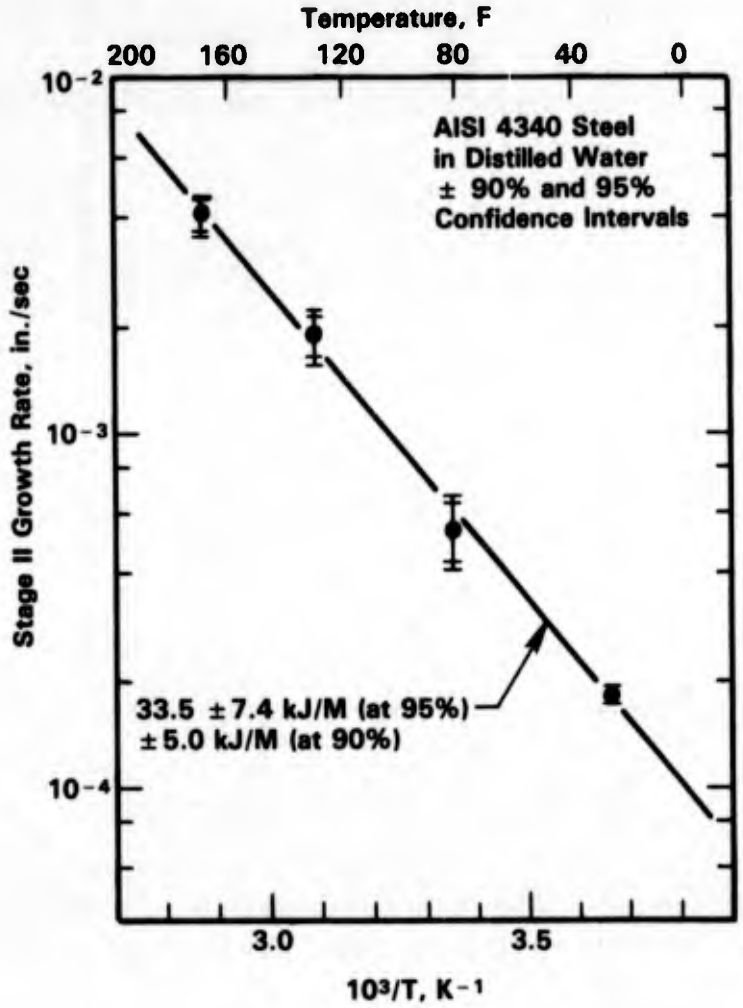

FIGURE 6-37. EFFECT OF TEMPERATURE ON THE RATE OF STAGE II (RATE LIMITED) CRACK GROWTH IN AISI 4340 STEEL (TEMPERED AT 399 F) IN DISTILLED WATER (0.2% OFFSET YIELD STRENGTH 195 KSI)[65]

velocities reported. Thus, it appears that Arrhenius cracking behavior may only be followed by low-alloy steels under conditions where they are inherently highly susceptible to SCC.

Effect of Sulfur Species. The SCC susceptibility of high strength steels in aqueous environments is greatly increased by the presence of sulfides or other reduced sulfur species.[60]

Thus, Uhlig[68] studied the effect of H_2S and $Na_2S_2O_3$ concentration on time to failure of a high strength (210 ksi tensile strength) carbon steel in acidified seawater and 3 percent NaCl and found that failure times dropped dramatically with the addition of 2 ppm S added as $S^=$ or $S_2O_3^=$, see Figure 6-39. Cracking in the presence of H_2S is generally considered to occur by a hydrogen embrittlement mechanism.[60]

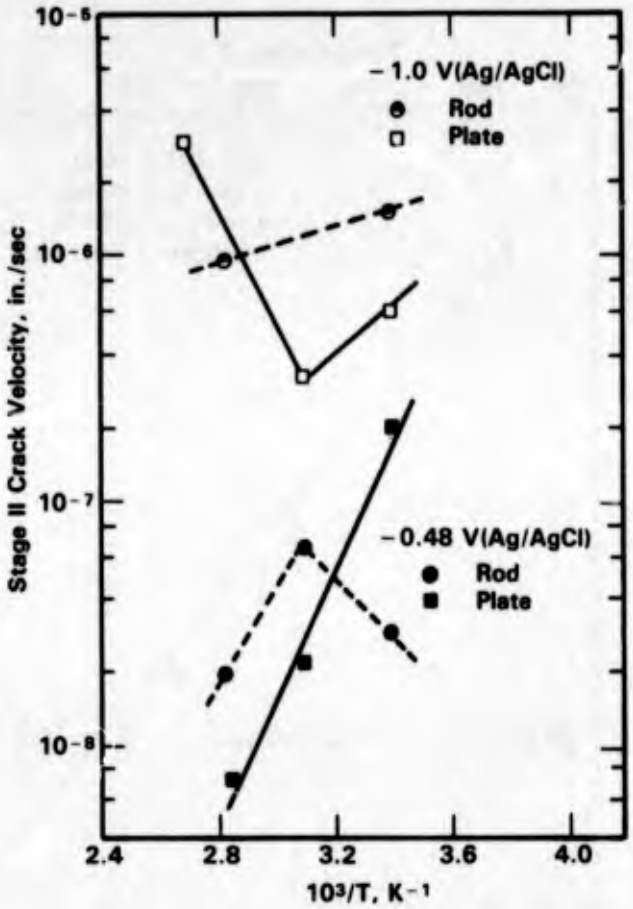

FIGURE 6-38. EFFECT OF TEMPERATURE ON STAGE II CRACK VELOCITIES OF 148-190M STEEL (226 KSI YIELD STRENGTH) IN 3.5% NaCl[67]

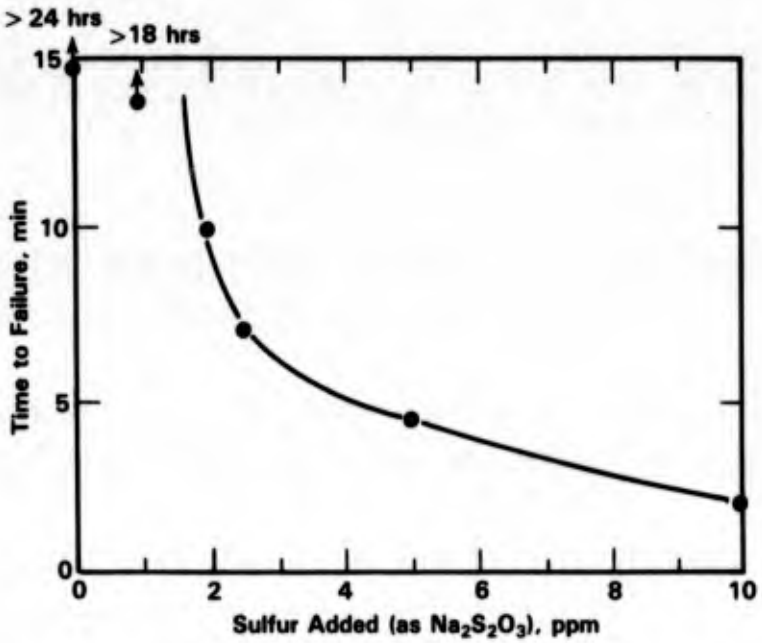

FIGURE 6-39. EFFECT OF SULFUR CONCENTRATION IN SEAWATER ON TIME TO FAILURE OF A HIGH STRENGTH STEEL WITHOUT APPLIED CURRENT, pH 0.7 to 0.8, 25 KSI AT 72 F[68]

The presence of H_2S also promotes hydrogen related failures of carbon and low-alloy steels with low yield strengths[69,70] where both internal cracking and blistering are reported. The internal cracks may be either parallel to the rolled surface of the material or perpendicular to the applied stress.[69]

Galvanic Corrosion

Carbon and low-alloy steels are quite active in seawater and thus are susceptible to galvanic attack when coupled with more noble materials. A galvanic series for metals in flowing seawater is given in Figure 6-40. These data show that, of the common metals, only aluminum, zinc, cadmium, and magnesium are more active in seawater than carbon steel. In a comprehensive study of the galvanic corrosion of metals in tropical seawater, Southwell, et al.[72] demonstrated the detrimental effect on carbon steel of coupling to most other common metals. A summary of data for up to 16 years' exposure is given in Table 6-20. In fact, Southwell, et al.[72] stated that carbon steel was a highly effective sacrificial anode for protecting the more noble materials such as the stainless steels and copper-base alloys.

Most of the couples in the work of Southwell, et al.[72] were made of metals with large potential differences, but even where the free-corrosion potentials were similar, large galvanic effects were observed in some instances. For example, the 2 percent Ni steel increased the corrosion rate of carbon steel by about 25 percent when coupled to carbon steel at a surface area ratio of about 4:1. Similarly, other researchers[71] have shown that the carbon steel-titanium couple is not as severe as the carbon steel-copper couple even though steel and titanium are much further apart on the galvanic series. Thus, the relative position of the members of the couple in the galvanic series is not always a good indication of the potential for galvanic attack; although, metals which are close together in the series are more likely to be compatible. This is because the corrosion rates of the members of the couple are a function of their polarizability as well as the values of their free-corrosion potentials.

Geometrical Effects. The relative surface areas of the two coupled materials can have a significant influence on the corrosion rate of the more active member of the couple. In an early study, Wesley[73] examined the influence of surface area ratio between copper and iron on the corrosion rate of iron in an aerated 3 percent NaCl solution. Results, summarized in Figure 6-41, show that the corrosion rate increased in a linear fashion, with increase in surface area of the copper. This effect is sometimes referred to as the catchment area principle after Evans[74] and appears to be valid where oxygen reduction at the cathode (noble metal) limits the rate of attack of the anode (active metal).

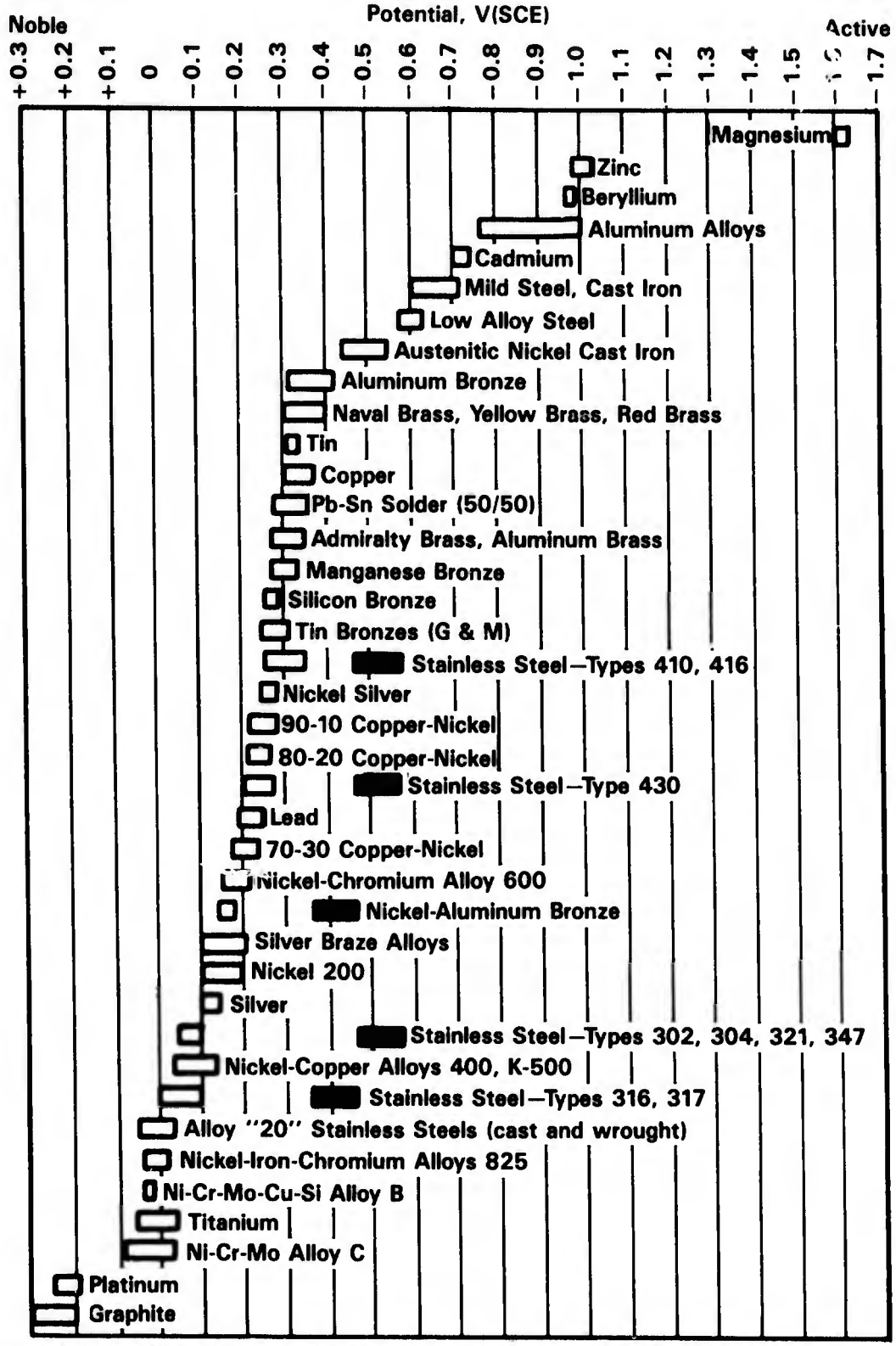

Alloys are listed in the order of the potential they exhibit in flowing seawater. Certain alloys indicated by the symbol: ■ in low-velocity or poorly aerated water, and at shielded area, may become active and exhibit a potential near −0.5 volts.

FIGURE 6-40. GALVANIC SERIES IN SEAWATER[71]

TABLE 6-20. CORROSION DAMAGE DATA FOR METALS EXPOSED AS BIMETALLIC COUPLES IN AQUEOUS ENVIRONMENTS[72]

Couple		Strip Metal Average Penetration, mils[a]									Plate Metal Average Penetration, mils[a]								
		Sea Water			Mean Tide			Fresh Water			Sea Water			Mean Tide			Fresh Water		
Strip, 2 x 9 x 14 in.	Plate, 9 x 9 x 1/4 in.	1 Yr	5 Yr	15 Yr	1 Yr	5 Yr	15 Yr	1 Yr	5 Yr	15 Yr	1 Yr	5 Yr	15 Yr	1 Yr	5 Yr	15 Yr	1 Yr	5 Yr	15 Yr
316 Stainless steel (18-13 + Mo)	Carbon steel[b] (0.24% C)	0.0	0.0	0.1 2.0*[c]	0.1	0.0 0.2*	0.1	0.0	0.0 0.0*	0.0	7.9	28.3 48.1*	49.5	12.2	24.7 45.2*	43.7	8.0	25.1 26.0*	32.4
316 Stainless steel (18-13 + Mo)	Naval brass (39Zn-1Sn)	0.0	0.0	0.0 2.0*	0.0	0.0	0.0 0.2*	0.0	0.0	0.0 0.0*	3.9	9.3	16.2 12.4*	1.0	4.7	7.7 6.0*	0.4	2.0	2.5 1.9*
316 Stainless steel (18-13 + Mo)	Phosphor bronze (4Sn-0.25P)	0.0	0.0	0.0 2.0*	0.0	0.0	0.0 0.2*	0.0	0.0	0.0 0.0*	1.6	6.0	9.4 5.5*	0.7	3.4	6.1 3.5*	0.2	0.7	0.7 0.7*
316 Stainless steel (18-13 + Mo)	316 Stainless steel (18-13 + Mo)	0.0	0.3	3.1 2.0*	0.0	0.1	0.1 0.2*	0.0	0.0	0.0 0.0*	0.0	0.6	1.3 2.0*	0.0	0.0	0.1 0.2*	0.0	0.0	0.0 0.0*
302 Stainless steel (18Cr-8Ni)	Carbon steel (0.24% C)	0.0	0.0	0.2 9.3*	0.1	0.0	0.1 1.6*	0.0	0.0	0.0 0.0*	7.5	27.3	50.6 48.1*	11.7	23.0	47.2 45.2*	8.1	25.0	31.7 26.0*
302 Stainless steel (18Cr-8Ni)	302 Stainless steel (18Cr-8Ni)	0.1	5.7	8.2 9.3*	0.2	0.5	1.3 1.6*	0.0	0.1	0.1 0.0*	0.3	4.5	7.6 2.0*	0.1	0.7	1.2 0.2*	0.0	0.0	0.0 0.0*
Nickel (99% Ni)	Carbon ste (0.24% C	0.0	0.0	0.1 19.3*	0.0	0.0	0.1 4.4*	0.0	0.0	0.0 0.0*	7.7	29.9	50.8 48.1*	12.0	21.4	42.3 45.2*	7.7	23.7	29.1 26.0*
Nickel-copper (Monel: 70Ni-30Cu, cold rolled)	Carbon ste (0.24% C)	0.0	0.0	0.1 8.7*	0.0	0.0	0.1 2.7*	0.0	0.0	0.0 0.6*	8.0	27.8	51.9 48.1*	10.5	23.0	42.8 45.2*	7.9	23.3	26.6 26.0*
Nickel-copper (Monel: 70Ni-30Cu, cold rolled)	Nickel-copper (Monel: 70Ni-30Cu, cold rolled)	3.6	6.9	17.2 8.7*	0.1	2.3	4.3 8.7*	0.2	1.3	1.3 0.6*	1.4	6.9	9.7 8.7*	0.1	1.3	2.7 2.7*	0.0	0.1	0.4 0.6*
Copper-nickel (70Cu-30Ni)	Carbon steel (0.24% C)	0.0	0.0	0.1 2.3*	0.0	0.0	0.1 0.8*	0.0	0.0	0.1 1.3*	7.6	29.8	50.4 48.1*	12.3	21.0	53.0 45.2*	7.9	22.8	29.8 26.0*
Phosphor bronze (4Sn-0.25P)	Aluminum (AA1100: 99% Al)	0.2	0.3	0.7 5.5*	0.1	0.2	0.4 3.5*	0.0	0.0	0.1 0.7*	1.7	3.6	6.5 1.0*	1.3	2.3	6.0 0.5*	1.5	6.6	12.4 5.0*
Phosphor bronze (4Sn-0.25P)	Galvanized steel	0.0 4.0*	0.1	(d)	0.1 2.1*	0.1	(d)	0.0 0.5*	0.0	(d)									
Phosphor bronze (4Sn-0.25P)	Carbon steel (0.24% C)	0.1	0.2	0.4 5.5*	0.2	0.1	0.4 3.5*	0.1	0.1	0.1 0.7*	7.5	29.6	55.1 48.1*	11.3	22.3	46.4 45.2*	8.7	24.5	28.9 26.0*
Phosphor bronze (4Sn-0.25P)	0.3% Cu steel	0.2	0.2 4.0*	(d)	0.1	0.2 2.1*	(d)	0.1	0.2 0.5*	(d)	7.8	32.6 49.3*	(d)	14.2	25.8 46.2*	(d)	8.0	23.0 28.7*	(d)
Phosphor bronze (4Sn-0.25P)	Low-alloy steel (Cu-Ni)	0.1	0.1	0.5 5.5*	0.1	0.1	0.4 3.5*	0.0	0.1	0.1 0.7*	7.4	28.8	53.3 48.4*	13.1	34.5	56.0 49.1*	6.7	18.0	23.0 22.0*
Phosphor bronze (4Sn-0.25P)	Low-alloy steel (Cu-Cr-Si)	0.2	0.3	0.5 5.5*	0.1	0.1	0.3 3.5*	0.1	0.1	0.2 0.7*	8.1	43.9	78.5 80.7*	10.8	25.9	59.8 49.3*	6.2	18.1	24.1 24.4*
Phosphor bronze (4Sn-0.25P)	Low-alloy steel (Cu-Ni-Mn-Mo)	0.1	0.2	0.6 5.5*	0.1	0.2	0.4 3.5*	0.1	0.1	0.1 0.7*	7.4	26.6	48.3 45.1*	11.2	21.2	56.3 61.0*	7.6	22.7	31.8 31.2*
Phosphor bronze (4Sn-0.25P)	Low-alloy steel (Cr-Ni-Mn)	0.1	0.2	0.5 5.5*	0.1	0.1	0.3 3.5*	0.1	0.1	0.1 0.7*	8.3	45.0	99.6 84.1*	9.9	24.3	65.2 45.8*	6.0	16.4	25.5 26.8*

TABLE 6-20. (Continued)

Couple		Strip Metal Average Penetration, mils[a]									Plate Metal Average Penetration, mils[a]								
		Sea Water			Mean Tide			Fresh Water			Sea Water			Mean Tide			Fresh Water		
Strip, 2 x 9 x 14 in.	Plate, 9 x 9 x 1/4 in.	1 Yr	8 Yr	16 Yr	1 Yr	8 Yr	16 Yr	1 Yr	8 Yr	16 Yr	1 Yr	8 Yr	16 Yr	1 Yr	8 Yr	16 Yr	1 Yr	8 Yr	16 Yr
Phosphor bronze (4Sn-0.25P)	Nickel steel (2% Ni)	0.1	0.2	0.5 5.5*	0.1	0.1	0.4 3.5*	0.0	0.1	0.2 0.7*	7.9	31.9	60.8 52.0*	8.6	23.5	55.9 55.0*	8.2	21.7	24.6 21.1*
Phosphor bronze (4Sn-0.25P)	Chromium steel (3% Cr)	0.2	0.3	0.6 5.5*	0.2	0.3	0.4 3.5*	0.1	0.1	0.2 0.7*	2.2	43.4	86.5 70.4*	10.9	29.7	57.2 48.1*	3.0	11.2	16.2 14.7*
Phosphor bronze (4Sn-0.25P)	Cast steel (0.27% C)	0.1	0.2	0.2 5.5*	0.1	0.1	0.3 3.5*	0.1	0.2	0.1 0.7*	9.3	29.8	51.6 43.3*	10.0	22.6	48.5 49.1*	8.2	18.2	30.1 26.3*
Phosphor bronze (4Sn-0.25P)	Gray cast iron (3.2% C)	0.1	0.2	0.3 5.5*	0.0	0.2	0.3 3.5*	0.0	0.2	0.1 0.7*	10.0	59.4	104.7 94.0*	19.4	51.8	76.2 87.1*	5.2	23.5	33.3 32.9*
Phosphor bronze (4Sn-0.25P)	Austenitic cast iron (18% Ni)	0.1	0.1	0.3 5.5*	0.1	0.1	0.2 3.5*	0.6	0.2	0.0 0.7*	4.2	15.1	27.3 22.8*	1.9	5.0	10.2 7.3*	1.3	7.0	13.3 8.0*
Phosphor bronze (4Sn-0.25P)	Copper-nickel (70Cu-30Ni)	1.6	3.3	4.6 5.5*	0.7	1.3	1.6 3.5*	0.1	0.4	0.5 0.7*	0.6	2.0	3.8 2.3*	0.1	0.6	1.0 0.8*	0.2	1.0	1.3 1.3*
Phosphor bronze (4Sn-0.25P)	Nickel-copper (Monel: 70Ni-30Cu, cold rolled)	2.7	66.3	71.8 5.5*	1.7	14.9	19.0 3.5*	1.6	8.8	14.1 0.7*	0.3	2.0	7.0 8.7*	0.1	1.0	2.2 2.7*	0.6	0.4	0.8 0.6*
Phosphor bronze (4Sn-0.25P)	410 Stainless steel (13% Cr)	0.5	0.4	0.7 5.5*	0.4	0.6	0.7 3.5*	0.2	0.7	0.9 0.7*	3.5	14.7	24.7 23.9*	0.6	4.2	8.8 6.4*	0.1	1.4	3.3 0.9*
Phosphor bronze (4Sn-0.25P)	302 Stainless steel (18Cr-8Ni)	7.8	16.3	21.9 5.5*	1.1	8.5	13.7 3.5*	0.5	4.1	3.8 0.7*	0.0	3.8	6.3 9.3*	0.1	0.4	1.0 1.1*	0.0	0.0	0.0 0.0*
Phosphor bronze (4Sn-0.25P)	316 Stainless steel (18-13 + Mo)	22.8	37.4	41.3 5.5*	3.2	21.9	29.8 3.5*	0.3	1.7	1.8 0.7*	0.0	0.2	0.2 2.0*	0.0	0.0	0.0 0.2*	0.0	0.0	0.0 0.0*
Aluminum bronze (5% Al)	Carbon steel (0.24% C)	0.1	0.1	0.4 1.3*	0.1	0.1	0.4 0.6*	0.0	0.1	0.2 0.4*	7.4	28.6	57.6 48.1*	10.6	23.7	46.1 45.2*	8.5	23.1	28.0 26.0*
Low brass (80Cu-20Zn)	Carbon steel (0.24% C)	0.1	0.1	0.4 3.7*	0.1	0.1	0.5 0.7*	0.1	0.2	0.2 1.7*	7.4	29.2	54.4 48.1*	12.0	20.0	44.3 45.2*	8.6	24.9	29.4 26.0*
Naval brass (39Zn-1Sn)	Carbon steel (0.24% C)	0.1	0.1	0.2 12.4*	0.2	0.1	0.3 6.0*	0.1	0.1	0.2 1.9*	7.2	29.7	54.4 48.1*	13.4	22.8	45.1 45.2*	8.6	23.8	28.0 26.0*
Copper (99.9% Cu)	Carbon steel (0.24% C)	2.0	3.0	7.0 6.0*	2.0	3.0	6.0 1.3*	0.0	1.0	3.0 1.0*	7.6	29.5	54.9 48.1*	11.9	23.0	42.7 45.2*	7.8	23.9	30.6 26.0*
Lead (99.9% Pb)	Carbon steel (0.24% C)	0.7	0.6	1.1 14.0*	0.6	1.5	3.9 8.3*	0.2	1.4	2.4 3.3*	7.2	28.9	48.5 48.1*	11.5	23.7	43.8 45.2*	8.0	23.3	30.7 26.0*
Nickel steel (5% Ni)	Carbon steel (0.24% C)	3.7	9.2	27.1 51.6*	3.9	7.8	26.5 54.0*	4.5	12.9	16.3 29.8*	6.9	27.8	47.3 48.1*	11.4	20.8	46.6 45.2*	8.8	21.2	26.9 26.0*
Carbon steel (0.24% C)	Aluminum (AA1100: 99% Al)	0.5	0.5	0.6 48.1*	0.7	0.8	2.3 45.2*	8.7	13.3	15.9 26.0*	1.5	5.1	7.1 1.0*	1.0	2.5	6.6 0.5*	0.4	5.2	11.5 5.0*
Carbon steel (0.24% C)	Aluminum (6061T)	0.5	0.8	1.6 48.1*	0.7	1.2	2.5 45.2*	9.1	15.9	17.0 26.0*	1.8	7.1	7.8 0.9*	1.0	2.3	5.5 0.3*	0.2	4.3	9.4 1.5*

TABLE 6-20. (Continued)

Couple		Strip Metal Average Penetration, mils[a]									Plate Metal Average Penetration, mils[a]								
		Sea Water			Mean Tide			Fresh Water			Sea Water			Mean Tide			Fresh Water		
Strip, 2 x 9 x 14 in.	Plate, 9 x 9 x 1/4 in.	1 Yr	8 Yr	16 Yr	1 Yr	8 Yr	16 Yr	1 Yr	8 Yr	16 Yr	1 Yr	8 Yr	16 Yr	1 Yr	8 Yr	16 Yr	1 Yr	8 Yr	16 Yr
Carbon steel (0.24% C)	Galvanized steel	0.3	10.2 25.5*	(d)	1.3	7.3 23.2*	(d)	3.6	10.9 21.9*	(d)									
Carbon steel (0.24% C)	Wrought iron (Aston process)	5.3	17.1 25.5*	(d)	8.0	17.2 23.2*	(d)	8.0	18.4 21.9*	(d)	7.4	24.7 22.2*	(d)	7.0	18.1 16.4*	(d)	8.4	19.8 14.6*	(d)
Carbon steel (0.25% C)	Carbon steel (0.24% C)	7.5	26.4 25.5*	50.0 48.1*	7.8	15.7	47.2 45.2*	8.5	20.1	25.9 26.0*	6.8	24.0	44.0 48.1*	9.8	17.9	42.2 45.2*	8.4	20.5	26.4 26.0*
Carbon steel (0.24% C)	0.3% Copper steel	8.0	22.9 25.5*	40.7 48.1*	9.8	16.6	34.1 45.2*	7.3	20.7	23.7 26.0*	6.5	25.8	41.9 49.3*	10.5	23.6	45.3 46.2*	7.5	20.8	25.1 28.7*
Carbon steel (0.24% C)	Nickel steel (2% Ni)	10.7	33.2 25.5*	63.1 48.1*	10.8	23.2	49.9 45.2*	9.8	28.7	33.9 26.0*	5.5	24.8	48.2 52.0*	7.0	20.4	47.0 55.3*	7.6	16.6	19.1 22.6*
Carbon steel (0.24% C)	Cast bronze (Ounce metal)	36.9	153.4 25.5*	M[e]	24.4	103.4 23.2*	M	15.0	58.7	77.3 26.0*	0.0	0.1	3.1 4.1*	0.1	0.2	0.3 1.2*	0.0	0.1	0.3 0.4*
Carbon steel (0.24% C)	Cast bronze (Valve metal)	36.0	185.0 25.5*	M	19.9	81.1 23.2*	M	14.9	56.7	69.0 26.0*	0.1	0.1	1.9 2.2*	0.1	0.1	0.1 1.4*	0.0	0.1	0.2 0.4*
Carbon steel (0.24% C)	Cast tin bronze (9% Sn)	35.2	164.0 25.5*	M	21.0	87.0 23.2*	M	15.1	52.0	61.0 26.0*	0.1	0.1	2.5 5.4*	0.1	0.2	0.2 1.4*	0.0	0.1	0.2 0.3*
Carbon steel (0.24% C)	Cast nickel-tin bronze (6Ni-3Sn)	36.4	180.8 25.5*	M	21.0	97.3 23.2*	M	14.6	49.1	59.8 26.0*	0.0	0.1	1.6 6.0*	0.0	0.1	0.2 1.2*	0.0	0.2	0.3 0.5*
Carbon steel (0.24% C)	Muntz brass (40Zn-0.25As)	37.2	161.8 25.5*	M	36.3	128.8 23.2*	M	14.6	61.4	77.4 26.0*	0.1	0.1	5.2 8.2*	0.2	0.3	0.9 5.7*	0.2	1.0	1.5 3.5*
Carbon steel (0.24% C)	Manganese brass (41Zn + Sn + Fe)	34.8	158.7 25.5*	M	32.7	106.2 23.2*	M	13.7	45.9	66.4 26.0*	0.1	0.1	7.9 17.2*	0.2	0.3	1.5 7.5*	0.1	0.3	0.4 0.9*
Carbon steel (0.24% C)	Naval brass (39Zn-1Sn)	35.2	176.5 25.5*	M	34.6	116.9 23.2*	M	13.9	47.7	64.3 26.0*	0.1	0.1	7.4 12.4*	0.3	0.3	0.7 6.0*	0.1	0.5	0.8 1.9*
Carbon steel (0.24% C)	Cartridge brass (30% Zn)	36.1	162.3 25.5*	M	38.4	116.8 23.2*	M	14.9	57.0	79.6 26.0*	0.0	0.0	3.1 3.6*	0.1	0.1	0.3 0.9*	0.1	0.3	0.4 1.8*
Carbon steel (0.24% C)	Low brass (20% Zn)	38.8	152.0 25.5*	M	28.2	104.6 23.2*	M	15.5	50.8	63.4 26.0*	0.1	0.1	2.4 3.7*	0.1	0.1	0.3 0.7*	0.1	0.2	0.3 1.7*
Carbon steel (0.24% C)	Commercial bronze (10% Zn)	37.9	155.6 25.5*	M	21.3	93.9 23.2*	M	14.1	50.9	67.7 26.0*	0.1	0.1	3.1 4.9*	0.0	0.1	0.2 1.0*	0.0	0.2	0.2 1.3*
Carbon steel (0.24% C)	Aluminum bronze (5% Al)	34.9	169.9 25.5*	M	24.0	102.7 23.2*	M	14.6	56.9	70.8 26.0*	0.0	0.0	4.0 1.3*	0.0	0.1	0.2 0.6*	0.0	0.1	0.2 0.4*
Carbon steel (0.24% C)	Phosphor bronze (4Sn-0.25P)	35.1	172.1 25.5*	M	25.2	96.2 23.2*	M	14.3	45.6	65.5 26.0*	0.1	0.1	1.9 5.5*	0.1	0.2	0.2 3.5*	0.1	0.2	0.3 0.7*
Carbon steel (0.24% C)	Silicon bronze (2.5% Si)	35.6	177.6 25.5*	M	21.5	96.3 23.2*	M	15.4	57.3	72.9 26.0*	0.1	0.2	2.7 5.9*	0.1	0.2	0.3 2.0*	0.1	0.2	0.3 1.2*

TABLE 6-20. (Continued)

Couple		Strip Metal Average Penetration, mils[a]									Plate Metal Average Penetration, mils[a]								
		Sea Water			Mean Tide			Fresh Water			Sea Water			Mean Tide			Fresh Water		
Strip, 2 x 9 x 14 in.	Plate, 9 x 9 x 1/4 in.	1 Yr	8 Yr	16 Yr	1 Yr	8 Yr	16 Yr	1 Yr	8 Yr	16 Yr	1 Yr	8 Yr	16 Yr	1 Yr	8 Yr	16 Yr	1 Yr	8 Yr	16 Yr
Carbon steel (0.24% C)	Copper (99.9% Cu)	36.5	191.5 25.5*	M	17.6	84.2 23.2*	M	14.2	56.3	77.7 26.0*	0.1	0.1	2.9 6.0*	0.1	0.1	0.5 1.3*	0.1	0.1	0.2 1.0*
Carbon steel (0.24% C)	Copper-nickel (70Cu-30Ni)	37.5	168.8 25.5*	M	23.2	96.7 23.2*	M	13.9	50.0	68.8 26.0*	0.0	0.1	1.6 2.3*	0.0	0.1	0.1 0.8*	0.0	0.2	0.3 1.3*
Carbon steel (0.24% C)	Nickel-copper (Monel: 70Ni-30Cu, cold rolled)	34.2	157.7 25.5*	M	23.3	92.2	191.5 45.2*	12.7	40.0	60.9 26.0*	0.0	0.1	2.4 8.7*	0.0	0.1	0.1 2.7*	0.0	0.0	0.0 0.6*
Carbon steel (0.24% C)	Nickel (99% Ni)	39.5	175.1 25.5*	M	20.3	86.4	184.8 45.2*	11.8	48.0	71.3 26.0*	0.0	0.0	4.8 19.0*	0.0	0.1	0.3 4.4*	0.0	0.0	0.2 0.0*
Carbon steel (0.24% C)	410 Stainless steel (13% Cr)	29.8	159.9 25.5*	M	22.2	73.7	178.4 45.2*	11.8	45.2	56.4 26.0*	0.2	0.1	9.2 23.9*	0.1	0.1	0.5 8.4*	0.0	0.0	0.0 0.9*
Carbon steel (0.24% C)	302 Stainless steel (18Cr-8Ni)	34.7	146.4 25.5*	M	22.7	88.9	175.6 45.2*	11.8	41.1	52.7 26.0*	0.0	0.0	0.8 9.5*	0.0	0.0	0.0 1.6*	0.0	0.0	0.0 0.0*
Carbon steel (0.24% C)	316 Stainless steel (18-13 + Mo)	34.7	140.6 25.5*	M	22.6	81.9	175.4 45.2*	10.5	33.3	44.4 26.0*	0.0	0.0	0.0 2.0*	0.0	0.0	0.0 0.1*	0.0	0.0	0.0 0.0*
Wrought iron (Aston process)	Carbon steel (0.24% C)	11.8	40.2 22.2*	72.5 (d)	9.2	17.4 16.4*	44.3 (d)	7.9	23.0 14.6*	30.0 (d)	6.2	21.9	37.0 48.1*	10.0	19.7	43.0 45.2*			
Zinc (99.5% Zn)	Carbon steel (0.24% C)	31.5	148.1	195.6 14.9*	37.3	102.5	194.2 13.2*	2.7	24.2	43.1 7.9*	0.7	0.9	15.5 48.1*	1.1	0.9	2.0 45.2*	7.0	17.8	19.9 26.0*
Zinc (99.5% Zn)	0.3% Copper steel	31.9	157.5 9.1*	(d)	37.3	91.4 8.2*	(d)	2.9	22.6 5.6*	(d)	0.4	3.8 49.3*	(d)	1.0	0.7 46.2*	(d)	8.5	18.7 28.7*	(d)
Zinc (99.5% Zn)	Nickel steel (2% Ni)	30.3	138.3 9.1*	M	52.5	83.8	191.5 13.2*	2.9	24.8	36.6 7.9*	0.4	0.3	14.9 52.0*	1.7	0.9	2.6 55.3*	6.7	15.0	17.4 22.8*
Zinc (99.5% Zn)	Cast steel (0.2% C)	30.7	145.4 9.1*	197.5	52.1	110.7	194.0 13.2*	2.7	22.9	45.6 7.9*	0.4	0.4	11.4 43.3*	1.5	1.0	5.1 49.1*	7.4	16.6	21.9 26.3*
Zinc (99.5% Zn)	Austenitic cast iron (18% Ni)	37.3	119.3 9.1*	M	19.3	101.8	126.3 13.2*	5.0	13.9	23.7 7.9*	0.0	0.0	0.1 22.8*	0.0	0.0	0.0 7.3*	0.7	3.9	7.7 8.0*
Aluminum (AA1100: 99% Al)	Carbon steel (0.24% C)	26.7	131.1 1.0*	M	23.9	83.6 0.5*	M	0.4	10.7	28.9 5.0*	0.7	0.6	16.9 48.1*	0.8	1.3	2.4 45.2*	7.4	18.6	21.7 26.0*

(a) Mils x 0.0254 = mm. Values calculated from weight losses.
(b) A couple consisting of a strip of 316 stainless steel (metal No. 58) with an exposed area of 21.9 in.^{2} attached to a plate of carbon steel (metal No. 35) with an exposed area of 151.4 in.^{2} (area ratio = 1:6.9).
(c) Values marked with an asterisk (*) show the normal uncoupled corrosion loss.
(d) Value not determined.
(e) M indicates that strips were missing—probably completely corroded away.

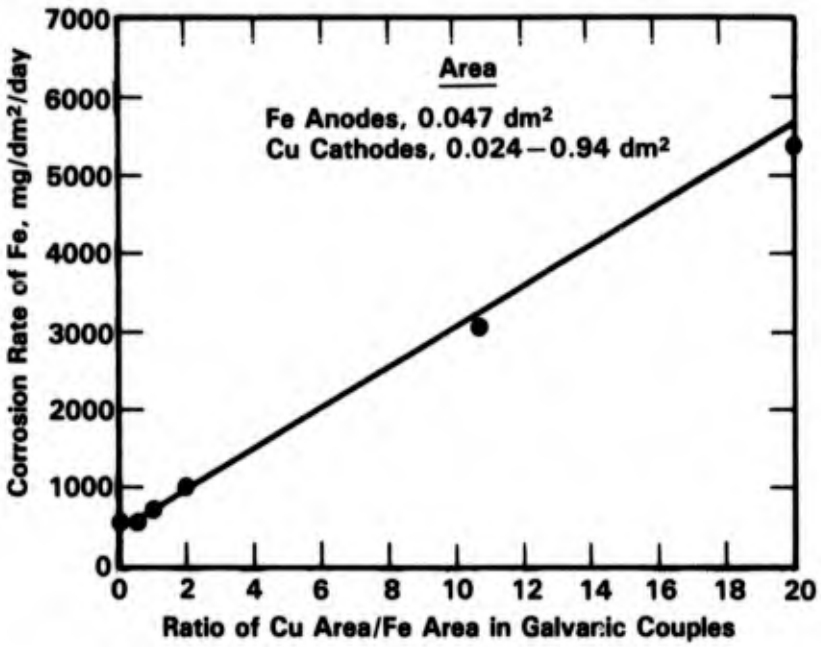

FIGURE 6-41. EFFECT OF RELATIVE AREA OF CATHODE ON EXTENT OF GALVANIC CORROSION[73]

These area ratio effects were demonstrated recently in studies of the corrosion of fasteners of various structural materials in seawater. Hack[75] exposed 1/4" x 4" x 12" panels for 6 months in quiescent seawater at Wrightsville Beach, NC. Each panel contained a single 1/4" bolt. The composition of the fasteners and panel alloys are shown in Appendix F, Table F-10. A summary of the results of the exposures is given in Table 6-21. These data show that intense galvanic corrosion of steel bolts occurred where attached to more noble metal plates. On the other hand, the low-alloy steel plate underwent only mild attack when coupled to a more noble alloy bolt.

The electrical resistance of the galvanic circuit can have a significant influence on the corrosion rate of the anode. The resistance may be either the solution resistance or the electrical resistance in the metallic portion of the circuit. Thus, Wesley[73] studied the effect of the resistance between Cu and iron on galvanic corrosion of iron in aqueous 3 percent NaCl by measuring the current flow between metal electrodes as a function of the value of an external resistor. Results, given in Figure 6-42, show that the galvanic current drops rapidly with increasing resistance. Thus, even relatively poor insulators installed between carbon steel and noble metals can reduce galvanic effects.

TABLE 6-21. SUMMARY OF RESULTS OF EXPOSURES OF 1/4" x 4" x 12" PANELS CONTAINING 1/4" BOLTS FOR 6 MONTHS IN QUIESCENT SEAWATER AT WRIGHTSVILLE BEACH, NC[75] (COMPOSITIONS OF ALLOYS ARE GIVEN IN APPENDIX F, TABLE F-10)

	Panel									
	Fiberglass Type G-10		Aluminum 5456		HY-130 Steel		Titanium 6Al-4V		17-4PH Stainless	
	Bolt	Panel	Bolt	Panel	Bolt	Panel	Bolt	Panel	Bolt	Panel
Aluminum 2024-T4										
Without sealant	Pits in crev; pits in bolt end	No attack	No attack	Mild pits & edge corr; very int galv corr	Mild galv corr head	Very mild galv corr; general corr	Very int galv corr	No attack	Very int galv corr	Very int crev corr & tunneling; mild pits & tunneling
With sealant	Pits on entire bolt	No attack	Corr exposed threads	Very mild pits & edge corr; very int galv corr	Galv corr exposed surfaces	General corr	Very int galv corr	No attack	Galv corr	Very int tunneling
Anodized Steel										
Without sealant	Mild corr exposed threads	No attack	No attack	No attack	Int galv corr; exposed surfaces	General corr	Missing; prob very int galv corr	No attack	Missing; prob very int galv corr	Int tunneling
With sealant	Mild corr exposed threads	No attack	No attack	Very mild pits & edge corr; int galv corr	Int galv corr; exposed surfaces	General corr	Missing; prob very int galv corr	No attack	Missing; prob very int galv corr	Int galv corr under sealant; mild pits & very int tunneling
304 Stainless Steel										
Without sealant	Mild crev corr	No attack	No attack	Mild pits & edge corr; galv corr	No attack	Very mild galv corr; general corr	Very int galv corr; very int pits & tunneling on threads	No attack	Mild crev corr	Very int crev corr & tunneling; tunneling
With sealant	Mild crev corr	No attack	No attack	Very mild edge corr; galv corr	No attack	General corr	Int crev corr; very int pits on threads	No attack	Very int crev corr	Very int crev corr & tunneling; tunneling & mild pits
316 Stainless Steel										
Without sealant	Very mild crev corr	No attack	No attack	Mild pits & edge corr; galv corr	No attack	Very mild galv corr; general corr	Crev corr	No attack	No attack	Very mild galv corr & tunneling; tunneling & mild pits
With sealant	No attack	No attack	No attack	Mild pits & edge corr; very int galv corr	No attack	Very mild galv corr; general corr	Crev corr; pits on threads	No attack	No attack	Very int tunneling & mild pits

TABLE 6-21. (Continued)

	Panel									
	Fiberglass Type G-10		Aluminum 5456		HY-130 Steel		Titanium 6Al-4V		17-4PH Stainless	
	Bolt	Panel	Bolt	Panel	Bolt	Panel	Bolt	Panel	Bolt	Panel
A286										
Without sealant	Very mild crev corr	No attack	No attack	Galv corr; mild edge corr	No attack	General corr	Int crev corr; pits on exposed surfaces	No attack	No attack	Very int crev corr & tunneling
With sealant	No attack	No attack	No attack	Mild pits; mild edge corr	No attack	General corr	Int crev corr; int pits on exposed threads	No attack	No attack	Very int tunneling
MP35N										
Without sealant	No attack	No attack	No attack	Pits & edge corr; int galv corr	No attack	Very mild galv corr; general corr	No attack	No attack	No attack	Very int galv corr & tunneling; mild tunneling
With sealant	No attack	No attack	No attack	Very mild pits & edge corr	No attack	Very mild galv corr; general corr	No attack	No attack	Missing; prob no attack	Very int crev corr & tunneling; mild tunneling
Titanium										
Without sealant	No attack	No attack	No attack	Very mild pits & edge corr; int galv corr	No attack	General corr	No attack	No attack	No attack	Very int crev corr & tunneling; mild tunneling
With sealant	No attack	No attack	No attack	Very mild pits & edge corr; int galv corr	No attack	Very mild galv corr; general corr	No attack	No attack	No attack	Very int crev corr & tunneling; mild tunneling

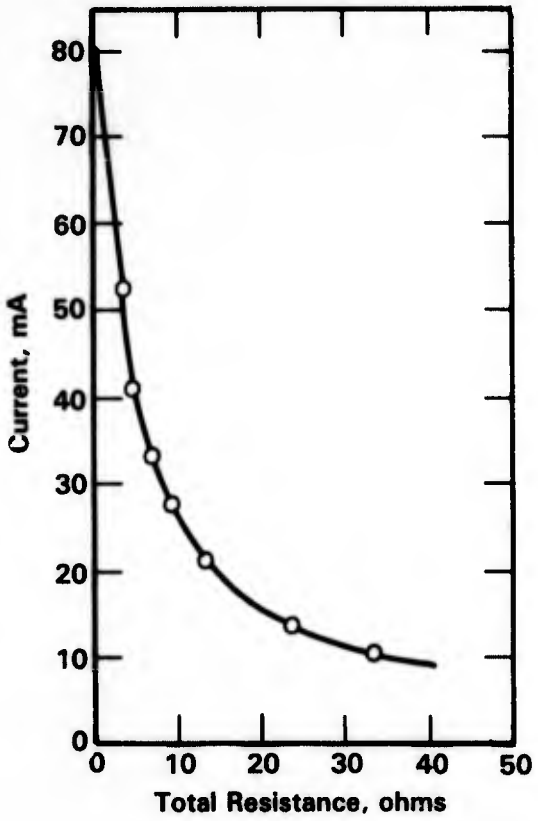

FIGURE 6-42. EFFECT OF RESISTANCE ON GALVANIC CORROSION[73]

Distance of separation of the members of the couple also influences galvanic attack of carbon steel. LaQue[71] reported on a study of the effect of distance along a carbon steel pipe on corrosion in seawater when coupled to a copper screen at an area ratio of Cu:Fe of 8:1. Results given in Figure 6-43 show that the depth of attack did decrease somewhat with distance, but the effect was not pronounced.

Environmental Effects. The severity of galvanic attack of carbon steel generally increases with increasing solution velocity in seawater. Data by Perkins, et al.[76] for carbon steel-K Monel and carbon steel-copper 30 nickel (1:1 area ratios) coupled in synthetic seawater are given in Figure 6-44. These data show that the corrosion rate of carbon steel increased rapidly with increasing velocity up to about 1.5 m/s but increased only gradually with further increase in velocity up to 3 m/s.

Electrolyte composition also influences galvanic attack of carbon steel. Results of the study by Southwell, et al.[72] show that galvanic attack of carbon steel was lower in fresh water than in seawater over 16 years' exposure, see Table 6-20. Nevertheless, corrosion of the carbon steel was significantly accelerated by galvanic coupling in fresh water.

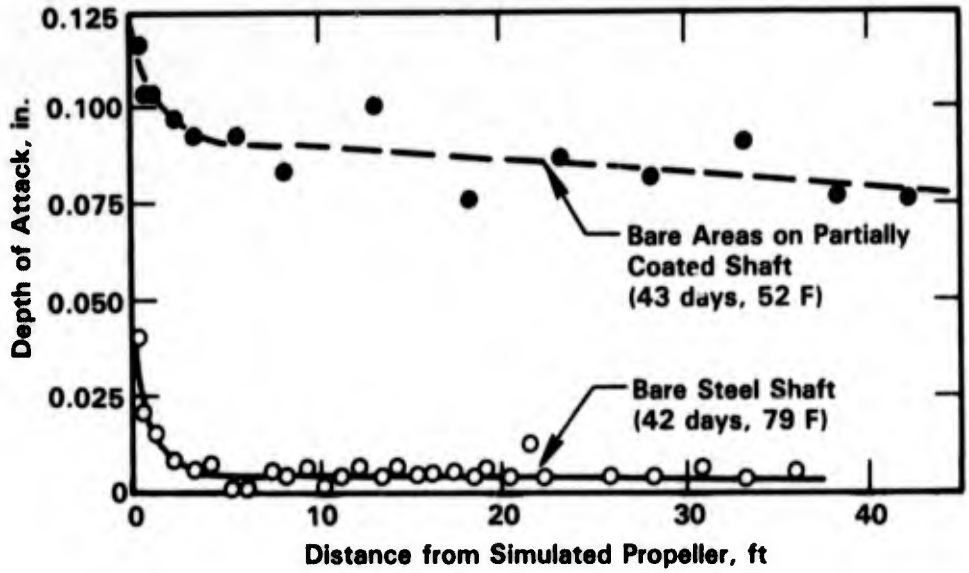

FIGURE 6-43. EFFECT OF DISTANCE ON CORROSION OF BARE AND PARTIALLY COATED STEEL SHAFT WITH SIMULATED COPPER ALLOY PROPELLER[71]

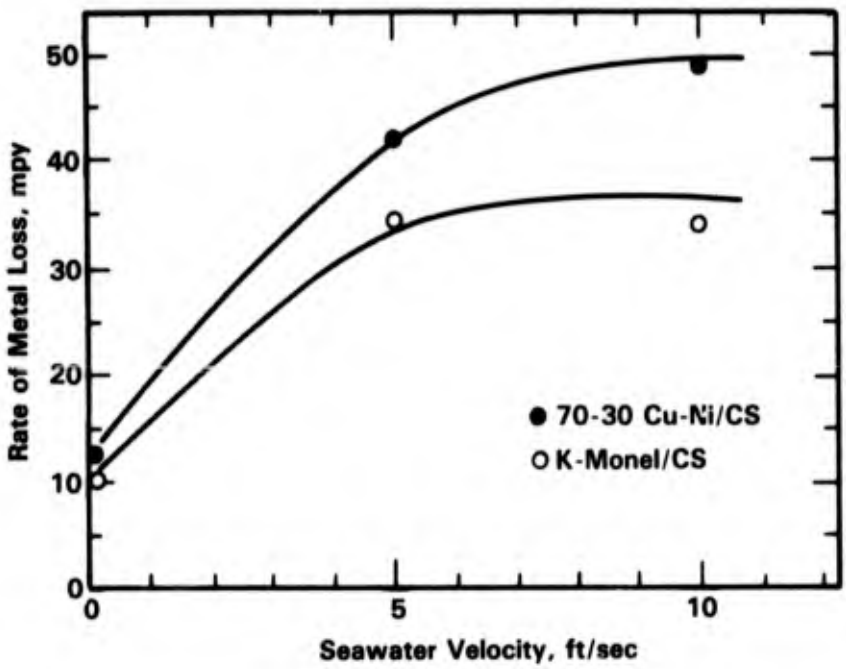

FIGURE 6-44. AVERAGE CORROSION RATE (IN 24-HOUR PERIOD) AS A FUNCTION OF VELOCITY FOR 70-30 CUPRONICKEL/CARBON STEEL (CS) AND K-MONEL/CARBON STEEL COUPLES IN SYNTHETIC SEAWATER (1:1 AREA RATIOS)[76]

Mud

Several researchers[11,12,77] have studied the corrosion behavior of carbon and low-alloy steel pipes below the mud line. Typical results by Larrabee[11] for exposures at Wrightsville Beach, NC are given in Figure 6-10 and show that rates of general and pitting attack in the mud are lower than those observed in the submerged zone and are comparable for the carbon steel and the corrosion resistant low-alloy steel B01458 (0.54 nickel, 0.52 copper, 0.12 phosphorus). Similar results were reported by Escalante and Iverson.[77]

Kinson, et al.[12] reported corrosion data for carbon steel pilings at various geographical locations throughout the world. These data, given in Table 6-7, show that corrosion rates for mud exposure varied considerably from one location to the next, as did corrosion rates under submerged, intertidal, and splash exposure, but were consistently lower than rates of attack in the other regions of the piling.

Reinhart[16] studied the effect of exposure time and alloy composition on the corrosion rate of carbon and low-alloy steels in bottom sediment under deep exposure (2,350 and 5,500 feet). Results of this study, given in Figure 6-45, show that rates of attack decreased with increasing exposure time and were comparable for all of the steels examined.

Although the above results indicate that mud exposure generally is less severe than submerged, tidal, or splash exposure, it has been suggested[32] that the presence of sulfate reducing bacteria may exacerbate attack in the mud zone. Results of limited studies by Mor, et al.[78] do suggest that the presence of anaerobic bacterial activity can accelerate corrosion of carbon steels. Specimens of carbon steel were exposed under natural anaerobic conditions in the sediment of Genoa Harbor, Italy, where significant biological activity was present. Results of the study, which are summarized in Figure 6-46, show that rates of pitting and general corrosion accelerated after about 90 weeks' exposure and were somewhat higher than most of those data reported above. Mor, et al.[78] attributed the increase in rates of attack with exposure time to break down of protective films on the metal surfaces as a result of biological activity.

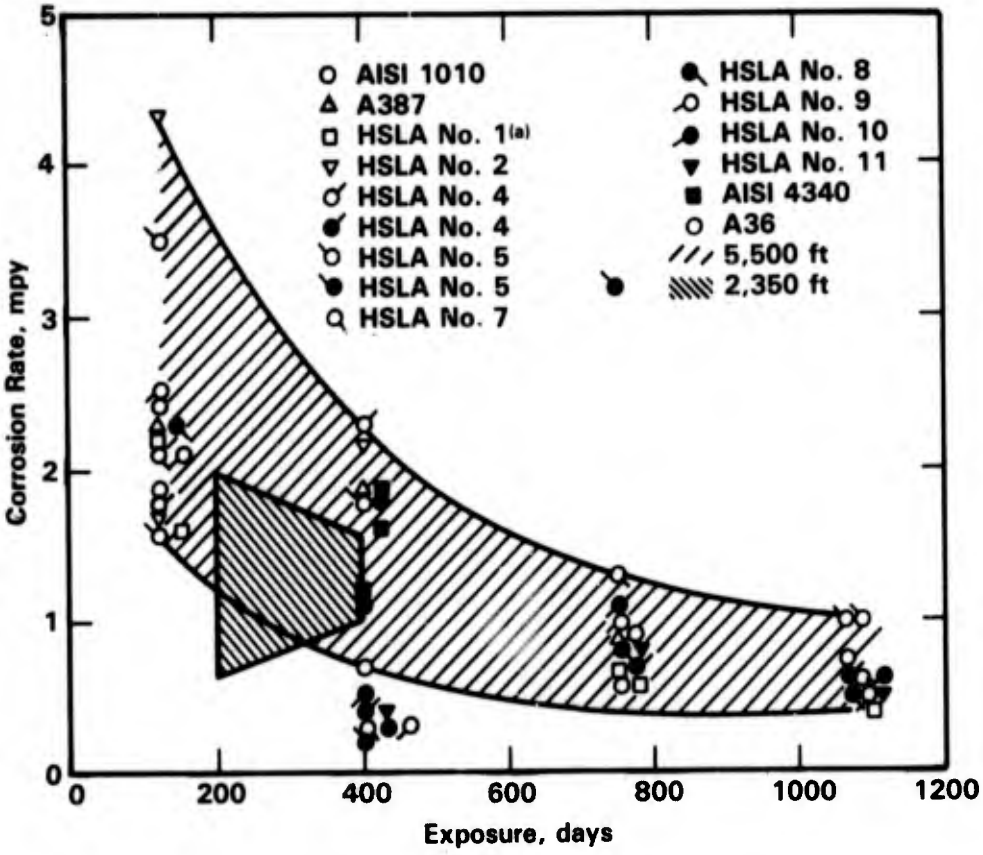

FIGURE 6-45. EFFECT OF ALLOY COMPOSITION AND EXPOSURE TIME ON CORROSION RATE OF STEELS IN THE PACIFIC OCEAN.(16)
(ALLOY COMPOSITIONS ARE GIVEN IN APPENDIX F, TABLE F-11)
(a) HSLA = High Strength Low-Alloy

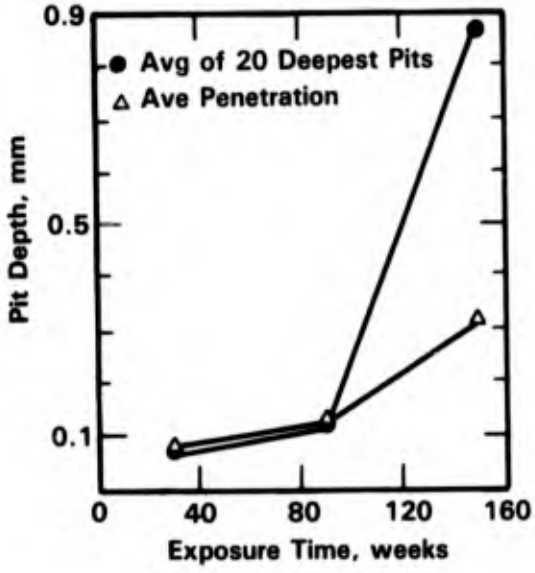

FIGURE 6-46. EFFECT OF EXPOSURE TIME ON GENERAL OR PITTING CORROSION OF CARBON STEEL EXPOSED TO SEDIMENT IN GENOA HARBOR, ITALY(78)

REFERENCES FOR CHAPTER 6

1. Copson, H. R., "Long-Time Atmospheric Corrosion Tests on Low-Alloy Steels", ASTM Proceedings, 60, pp 650-665 (1960).

2. Southwell, C. R., et al., "Corrosion of Metals in Tropical Environments. Part 2. Atmospheric Corrosion of Ten Structural Steels", Corrosion, 16 (11), pp 435t-439t (September, 1958).

3. Larrabee, C. P., "Corrosion Resistance of High-Strength Low-Alloy Steels as Influenced by Composition and Environment", Corrosion, 9 (8), pp 259-271 (August, 1953).

4. Ambler, H. R. and Bain, A.A.J., "Corrosion of Metals in the Tropics", Journal of Applied Chemistry, 5, pp 437-467 (September, 1955).

5. Southwell, C. R. and Bultman, J. D., "Atmospheric Corrosion Testing in the Tropics", Atmospheric Corrosion, pp 943-967 (October, 1980).

6. Fyfe, D., et al., "Atmospheric Corrosion of Fe-Cu Alloys and Cu-Containing Steels", Corrosion Science, 10 (11), p 821 (November, 1970).

7. Buck, D. M., "The Influence of Very Low Percentages of Copper in Retarding the Corrosion of Steel", ASTM Proceedings, 19 (2), p 224 (1919).

8. Copson, H. R., "Atmospheric Corrosion of Low-Alloy Steels", ASTM Proceedings, 52, p 1005 (1952).

9. Larrabee, C. P. and Coburn, S. K., "The Atmospheric Corrosion of Steels as Influenced by Changes in Chemical Composition", Proc. First International Congress on Metallic Corrosion, Butterworth, London, p 276 (1967).

10. Humble, A. A., "The Cathodic Protection of Steel Piling in Seawater", Corrosion, 5 (9), pp 292-302 (September, 1949).

11. Larrabee, C. P., "Corrosion Resistant Experimental Steels for Marine Applications", Corrosion, 14 (11), pp 501t-504t (November, 1958).

12. Kinson, K., et al., "Steel Piling in Materials", BHP Technical Bulletin, 25 (2), pp 8-15 (November, 1981).

13. Southwell, C. R. and Alexander, A. L., "Corrosion of Metals in Tropical Environments. Part 9. Structural Ferrous Metals - Sixteen Years' Exposure to Sea and Fresh Water", Naval Research Laboratory Report NRL-6862, 28 pp (April, 1969).

14. Nose, J., et al., "The Characteristic Properties of NK Marine G: Seawater Corrosion Resistant Steel for Pipe Piles and Sheet Piles", Nippon Kokan Technical Report (26), pp 1-9 (March, 1979).

15. Schultze, W. A. and Van der Wekken, C. J., "Influence of Alloying Elements on the Marine Corrosion of Low-Alloy Steels Determined by Statistical Analysis of Published Literature Data", British Corrosion Journal, 11 (1), pp 18-24 (1976).

REFERENCES FOR CHAPTER 6
(Continued)

16. Reinhart, F. M., "Corrosion of Materials in Hydrospace. Part I. Irons, Steels, Cast Irons, and Steel Products", U.S. Naval Civil Eng. Lab. Tech. Note N-900, 71 pp (July, 1967).

17. Bultman, J. D., et al., "Biocorrosion of Structural Steels in Seawater", Revue of Coatings and Corrosion, 2 (2-3), pp 187-214 (1977).

18. Forgeson, B. W., et al., "Corrosion of Metals in Tropical Environments", Corrosion, 16 (3), p 105t (1960).

19. Gallagher, W. P., "The Corrosion Behavior of Ship-Steel Plates Rolled From Continuous-Cast Slabs", Journal of Metals, 30 (5), pp 5-9 (May, 1978).

20. Josefsson, A. and Lounamaa, K., "Comparative Corrosion Tests on Steel Plates Rolled From Continuously Cast Slabs and Rolled From Mold Cast Ingots", Corrosion, 37 (5), pp 279-284 (May, 1981).

21. Hodgkiess, T., et al., "Corrosion of Welds in Seawater", Desalination, 27 (2), pp 129-136 (November, 1978).

22. Kato, C., et al., "Grooving Corrosion in Electric Resistance Welded Steel Pipe in Seawater", Corrosion Science, 18 (1), pp 61-74 (1978).

23. Masamura, K. and Matsushima, I., "Grooving Corrosion of Electric Resistance Welded Steel Pipe in Water: Case Histories and Effects of Alloying Elements", Corrosion '81, Toronto, Ontario, Canada, (75), 11 pp (April, 1981).

24. Litvin, D. A. and Hill, B., "Effect of pH on Seawater Stress-Corrosion Cracking Behavior of the Ti-7Al-2Cb-1Ta Alloy", Corrosion, 26 (3), pp 89-94 (March, 1970).

25. Reinhart, F. M. and Jenkins, J. F., "The Relationship Between the Concentration of Oxygen in Seawater and the Corrosion of Metals", U.S. Naval Civil Eng. Lab. Report, pp 562-577 (1971).

26. Reinhart, F. M. and Jenkins, J. F., "Corrosion of Materials in Surface Seawater After 12 and 18 Months of Exposure", Final Report NCEL-TN-1213, 106 pp (January, 1972).

27. Dosey, P. A. and Palko, A. A., "Corrosivity of Carbon Steel in Concentrated Chloride Solution", Corrosion, 35 (1), pp 38-43 (January, 1979).

28. Togano, H., et al., "Corrosion Behavior of Mild Steel and Low Alloy Steel in Deaerated Hot Sodium Chloride Solution", 5th International Congress on Metallic Corrosion, pp 807-811 (May, 1972).

29. Shimada, H., et al., "Corrosion Behavior of Steels in Various Marine Environments (A Joint Study with Maritime Safety Agency)", Nippon Steel Technical Report (8), pp 31-42 (May, 1976).

30. Efird, K. D., "Inter-Relation of Corrosion and Fouling for Metals in Seawater", Materials Performance, 15 (4), pp 16-25 (April, 1976).

REFERENCES FOR CHAPTER 6
(Continued)

31. Chandler, H. E., "Corrosion-Biofouling Relationship of Metals in Seawater", Metal Progress, 115 (6), pp 47-49, 54 (June, 1979).

32. Boyd, W. K. and Fink, F. W., "Corrosion of Metals in Marine Environments", Battelle Columbus Laboratories Report MCIC-78-37, 103 pp (March, 1978).

33. Traverso, E., et al., "Effects of Rolling Direction and Tensile Stress on the Corrosion of Naval Carbon Steel in Natural Marine Environments - I: Natural Seawater", British Corrosion Journal, 14 (2), pp 97-102 (1979).

34. Sasaki, H., et al., "Corrosion Behavior of Mild Steel in Artificial Seawater Containing Hydrogen Sulfide", Corrosion Engineering (Tokyo), 26 (5), pp 229-236 (1977).

35. Sasaki, H., et al., "Possibility of the Hydrogen Depolarization Phenomenon of Mild Steel by Sulfate-Reducing Bacteria", Corrosion Engineering (Tokyo), 26 (3), pp 125-132 (1977).

36. Larrabee, C. P., "Steel Has Low Corrosion Rate During Long Seawater Exposure", Materials Protection, 1 (12), pp 95-96 (December, 1962).

37. Larrabee, C. P., "Corrosion of Steels in Marine Atmospheres and in Seawater", Transactions of the Electrochemical Society, 87, pp 171-182 (1945).

38. Peterson, M. H. and Waldron, L. J., "An Investigation of the Corrosion Rate of Mild Steel in San Diego Harbor", Preprint NACE 16th Annual Conference, Dallas, TX (March, 1960).

39. Kruger, S. and Bird, C. E., "Corrosion of Metals by Applied Alternating Currents", British Corrosion Journal, 13 (4), pp 163-166 (1978).

40. Jones, D. A., "Effect of Alternating Current on Corrosion of Low-Alloy and Carbon Steels", Corrosion, 34 (12), pp 428-433 (December, 1978).

41. Radeka, R., et al., "Influence of Frequency of Alternating Current on Corrosion of Steel in Seawater", Anti-Corrosion, 27 (4), pp 13-15 (April, 1980).

42. Radeka, R., et al., "Corrosion of Steel in Seawater Due to Alternating Current at 50 Hz", Anti-Corrosion, 24 (9), p 5 (September, 1977).

43. Sandoz, G., "High Strength Steels", Stress-Corrosion Cracking in High Strength Steel and in Titanium and Aluminum Alloys, Ed. B. F. Brown, NRL, Washington, DC (1972).

44. Sandoz, G., "ARPA Coupling Program on Stress-Corrosion Cracking", Quarterly Report 13, NRL-MR-2101, 68 pp (March, 1970).

45. Sandoz, G., "The Effects of Alloying Elements on the Susceptibility to SCC of Martensitic Steels in Salt Water", Metallurgical Transactions, 2, p 1055 (1971).

46. Carter, C. S., "The Effect of Silicon on the Stress-Corrosion Resistance of Low-Alloy High Strength Steels", Corrosion, 25 (10), p 423 (October, 1969).

REFERENCES FOR CHAPTER 6
(Continued)

47. Benjamin, W. D. and Steigerwald, E. A., "Environmentally Induced Delayed Fractures in Martensitic High-Strength Steels", Air Force Materials Laboratory Technical Report AFML-TR-68-80 (April, 1968).

48. Puzak, P. P. and Lange, E. A., "Fracture Toughness Characteristics of the New Weldable Steels of 180- to 210-ksi Yield Strengths", Naval Research Laboratory Report NRL-6951 (September 18, 1969).

49. Gross, J. H., "The New Development of Steel Weldments", 1968 Adams Lecture, Welding Journal, 47, p 241s (June, 1968).

50. Webster, D., "The Stress-Corrosion Resistance and Fatigue Crack Growth Rate of a High Strength Martensitic Stainless Steel, AFC 77", Boeing Document D6-23973, The Boeing Company (June, 1969).

51. Kennedy, J. W. and Whittaker, J. A., "Stress-Corrosion Cracking of High-Strength Steels", Corrosion Science, 8 (6), p 359 (June, 1968).

52. Tiner, N. A. and Gilpin, C. B., "Microprocesses in Stress-Corrosion of Martensitic Steels", Corrosion, 22 p 271 (October, 1966).

53. Slunder, C. J. and Boyd, W. K., "Environmental and Metallurgical Factors of Stress-Corrosion Cracking in High Strength Steels", Battelle Memorial Institute, DMIC Report 151 (April 14, 1961).

54. Davis, R. A., et al., "Stress-Corrosion Cracking Study of Several High Strength Steels", Corrosion, 20 (3), p 93t (March, 1964).

55. Raymond, L., "Effect of Aqueous Environments on Crack Nucleation and Growth in High-Strength Steels", 3rd Tewksbury Symposium on Fracture, pp 156-169 (June, 1974).

56. Kanao, M., et al., "Fracture of Cathodically Protected High Tensile Structural Steels", Hydrogen in Metals, pp 465-468 (November, 1979).

57. Benjamin, W. D. and Steigerwald, E. A., "Stress-Corrosion Cracking Mechanisms in Martensitic High Strength Steels", Air Force Materials Laboratory Technical Report AFML-TR-67-98 (April, 1967).

58. Taniguchi, N. and Troiano, A. R., "Stress-Corrosion Cracking of 4340 Steel in Different Environments", Transactions of the Iron Steel Institute of Japan, 9 (4), p 306 (1969).

59. Sandoz, G. and Newbegin, R. L., "A Comparison of Laboratory Salt Water and Flowing Natural Seawater as an Environment for Tests of Stress-Corrosion Cracking Susceptibility", Naval Research Laboratory Progress Report, p 29 (May, 1969).

60. Phelps, E. H., "A Review of the Stress-Corrosion Behavior of Steels with High Yield Strength", Proceedings of Conference on Fundamental Aspects of SCC, Ed. R. W. Staehle, NACE, p 398 (1969).

REFERENCES FOR CHAPTER 6
(Continued)

61. Kennedy, J. W. and Whittaker, J. A., "Stress-Corrosion Cracking of High Strength Steels", Corrosion Science, 8 (6), p 359 (June, 1968).

62. Leckie, H. P., "Effects of Environments on Stress Induced Failure of High Strength Maraging Steels", Proceedings of Conference on Fundamental Aspects of Stress-Corrosion Cracking, NACE, Houston, TX, p 411 (1969).

63. Logan, H. L., "The Stress-Corrosion Cracking of Metals", Metals Engineering Quarterly, 5 (2), p 32 (May, 1965).

64. Van Der Sluys, W. A., "Mechanisms of Environment Induced Subcritical Flaw Growth in AISI 4340 Steel", Engineering Fracture Mechanics, 1, p 447 (1969).

65. Simmons, G. W., et al., "Fracture Mechanics and Surface Chemistry Studies of Subcritical Crack Growth in AISI 4340 Steel", Metallurgical Transactions, 9A, p 1147 (August, 1978).

66. Johnson, H. H. and Wilner, A. M., "Moisture and Stable Crack Growth in High Strength Steel", Applied Materials Research, 4, p 34 (1965).

67. Bala, S. R. and Tromans, D., "Effect of Temperature Upon Stress-Corrosion Cracking of HY-180M Steel in 3.5 Percent NaCl", Metallurgical Transactions, 11A (7), pp 1161-1165 (July, 1980).

68. Uhlig, H. H., "Effect of Aqueous Sulfides and Their Oxidation Products on Hydrogen Cracking of Steel", Materials Performance, 16 (1), pp 22-25 (January, 1977).

69. Herbsleb, G., et al., "Occurrence and Prevention of Hydrogen Induced Stepwise Cracking and Stress-Corrosion Cracking of Low-Alloy Pipeline Steels", Corrosion, 37 (5), pp 246-256 (1981).

70. Moore, E. M. and Warga, J. J., "Factors Influencing the Hydrogen Cracking Sensitivity of Pipeline Steels", Materials Performance, 15 (6), p 17 (June, 1976).

71. LaQue, F. L., Marine Corrosion, Causes and Prevention, Wiley & Sons, New York, p 179 (1975).

72. Southwell, C. R., et al., "Corrosion of Metals in Tropical Environments - Final Report of 16-Year Exposures", Materials Performance, 15 (7), pp 9-25 (July, 1976).

73. Wesley, W. A., "Controlling Factors in Galvanic Corrosion", ASTM Proceedings, 40, p 690 (1940).

74. Evans, U. R., Metallic Corrosion, Passivity and Protection, Edward Arnold and Company, London (1938).

75. Hack, H. P., "Seawater Corrosion of Fasteners in Various Structural Materials", Naval Ship R&D Center Report DTNSRDC-76-0034, 34 pp (April, 1976).

REFERENCES FOR CHAPTER 6
(Continued)

76. Perkins, J., et al., "Flow Effects on Corrosion of Galvanic Couples in Seawater", Corrosion, 35 (1), pp 23-33 (January, 1979).

77. Escalante, E. and Iverson, W. P., "Protection of Steel Piles by Nonmetallic Coatings in Seawater", Materials Performance, 17 (10), pp 9-15 (October, 1978).

78. Mor, E. D., et al., "Effects of Rolling Direction and Tensile Stress on the Corrosion of Naval Carbon Steel in Natural Marine Environments - II. Harbour Anaerobic Sediment", British Corrosion Journal, 14 (2), pp 103-108 (1979).

CHAPTER 7
TABLE OF CONTENTS

CHAPTER 7
LIST OF TABLES

CHAPTER 7
LIST OF FIGURES

CHAPTER 7

MAGNESIUM

Magnesium alloys exhibit poor corrosion resistance in marine environments and are rarely used for immersed exposure. In marine atmospheric exposures, extensive protection systems are required such as anodizing treatments in conjunction with organic coatings. The poor corrosion behavior of Mg alloys is attributable to the highly active nature of magnesium and the presence of impurities, such as iron, in the alloys.

Atmospheric Exposure

Southwell, et al.[1] exposed specimens of two magnesium alloys, AZ31X and AZ61X, at two atmospheric sites, one marine and one inland, in the Panama Canal Zone for up to 16 years. The marine site was located 55 feet above sea level and 300 feet from the Caribbean. The compositions of the magnesium alloys are given in Table G-1 in Appendix G. A summary of the results of the exposure is given in Table 7-1. These data show that the magnesium alloys corroded at a rate of approximately 1 mpy but were susceptible to pitting attack. The weight-loss data, plotted as a function of exposure time (Figure 7-1) show that the two alloys exhibited linear weight loss-time behavior. Based on either weight loss or pitting, the AZ61X alloy performed somewhat better than the AZ31X alloy. On the other hand, the tensile properties of the AZ31X alloy were somewhat better than those of the AZ61X alloy, following exposure, suggesting that the latter alloy had undergone some internal metal deterioration, such as intergranular attack.

Frost, et al.[2] studied the atmospheric corrosion behavior of several high strength magnesium-lithium alloys, as well as AZ31A in 32 month atmospheric corrosion tests at Battelle's exposure station near Daytona Beach, Florida. The site is approximately 500 feet inland from mean high tide and the specimens were inclined 30 degrees from the horizontal and faced south. A summary of the results of the exposure is given in Figures 7-2 and 7-3. These data show that none of the Mg-Li alloys performed as well as AZ31A but the former alloys exhibited decreasing corrosion rates with increasing test time. Rates of attack for AZ31A were comparable with those reported by Southwell, et al.[1] for AZ31X, and were approximately constant with time after several months of exposure. All of the panels exhibited pitting, which was most severe on the undersides and for the experimental alloys; actual pit depths were not reported.

TABLE 7-1. CORROSION DAMAGE OF LIGHT METALS EXPOSED IN FIVE TROPICAL ENVIRONMENTS IN THE PANAMA CANAL ZONE[1]

Metal	Exposure	Weight Loss, g/dm²					Average Penetration, mils[a]					Depth of Pitting, mils[b]										Tensile Strength Loss (%), 8 Yr[c]	Type of Corrosion Attack[d], 16 Yr
												Average 20 Deepest Pits					Deepest Pit						
		1 Yr	2 Yr	4 Yr	8 Yr	16 Yr	1 Yr	2 Yr	4 Yr	8 Yr	16 Yr	1 Yr	2 Yr	4 Yr	8 Yr	16 Yr	1 Yr	2 Yr	4 Yr	8 Yr	16 Yr		
Aluminum 1100	Immersion																						
	Seawater	0.19	0.27	0.45	0.42	0.67	0.28	0.39	0.66	0.61	0.97	9(13)	3(17)	7	11	17	15	8	15	19	33	2	J
	Mean Tide	0.24	0.08	0.17	0.22	0.37	0.06	0.11	0.25	0.31	0.53	11(9)	10	26	14	39	29	25	46	37	67	1	J, Q
	Fresh Water	0.28	0.65	0.95	1.61	3.47	0.41	0.95	1.37	2.34	5.04	24	29	38	61	98	38	37	67	92	109	4	Q, K
	Atmospheric																						
	Marine	0.006	0.024	0.008	0.013	0.075	0.01	0.04	0.01	0.02	0.11	N	N	N	N	N	N	N	N	N	N	0	A
	Inland	0.002	0.017	0.000	0.024	0.052	0.00	0.03	0.00	0.03	0.08	N	N	N	N	N	N	N	N	N	N	0	A, K
Aluminum 6061-T	Immersion																						
	Seawater	0.19	0.33	0.39	0.50	0.63	0.29	0.48	0.56	0.73	0.91	N	N	11(10)	23	14	N	N	30	49	79	0	J
	Mean Tide	0.03	0.05	0.07	0.09	0.20	0.04	0.07	0.10	0.13	0.29	N	N	N	N	17	N	N	N	N	41	0	J
	Fresh Water	0.06	0.16	0.31	0.53	1.03	0.08	0.23	0.45	0.77	1.50	14	21	33	59	96	18	29	41	64	107	1	Q, K
	Atmospheric																						
	Marine	0.021	0.037	0.051	0.018	0.077	0.03	0.06	0.08	0.03	0.11	N	N	N	N	N	N	N	N	N	N	1	A
	Inland	0.010	0.028	0.007	0.008	0.059	0.02	0.04	0.01	0.01	0.09	N	N	N	N	N	N	N	N	N	N	1	A, K
Alumina 2024-T	Atmospheric																						
	Marine	0.017	0.028	0.009	0.012	0.090	0.03	0.04	0.02	0.14	—	N	N	N	N	N	N	N	N	N	N	1	K, A
	Inland	0.009	0.009	0.000	0.002	0.050	0.02	0.02	0.00	0.07	—	N	N	N	N	N	N	N	N	N	N	2	K, A
Magnesium AZ31X[e]	Immersion																						
	Seawater	3.24	8.69	6.84	13.77	—[g]	7.21	19.32	15.21	30.62	—	193(7)	233	184	253(p)	—	253(p)	253(p)	252(p)	253(p)	—	—[h]	—
	Mean Tide	6.04	8.90	17.55	17.60	—	13.44	19.78	39.03	39.14	—	102	143	196	251(p)	—	153	254(p)	252(p)	251(p)	—	—	—
	Fresh Water	1.73	2.45	3.44	5.48	—	3.84	5.45	7.64	12.81	—	N	N	35(1)	24	—	N	N	35	35	—	12	—
	Atmospheric																						
	Marine	0.48	0.95	1.62	3.54	6.77	1.06	1.89	3.60	7.88	15.47	13(11)	11(10)	18(10)	20	22	19	14	22	29	34	25	A, E
	Inland	0.27	0.54	0.70	2.05	4.23	0.61	1.20	1.56	4.55	9.40	N	N	N	5(10)	15	N	N	N	14	20	16	A
Magnesium AZ61X[f]	Atmospheric																						
	Marine	0.22	0.59	0.16	2.84	5.35	0.48	1.27	0.35	6.19	11.66	12(12)	14(10)	N	11	16	19	19	N	21	20	28	A
	Inland	0.17	0.39	0.07	1.48	3.52	0.36	0.86	0.15	3.24	7.68	N	N	N	3(4)	11	N	N	N	6	14	18	A

(a) Calculated from weight loss and specific gravity.
(b) Represents depth of penetration from original surface: N = measurable pits; numbers in parentheses gives number of measurable pits when less than 20; and (p) denotes perforation.
(c) Percent change in tensile strength calculated on basis of 1/4 inch thick metal and average of four tests for underwater specimens, and 1/16 inch thick metal and average of three tests for atmospheric specimens.
(d) A - uniform attack, B - granular reaction, E - localized attack (uniform), H - concentration cell, J - marine fouling contact, K - no visible attack, Q - pitting attack (random), and R - localized attack (random).
(e) Former ASTM designation - 18X.
(f) Former ASTM designation - 8X.
(g) Because of high rate of corrosion, magnesium panels were exposed for only eight years in these environments.
(h) Panels too badly corroded to test.

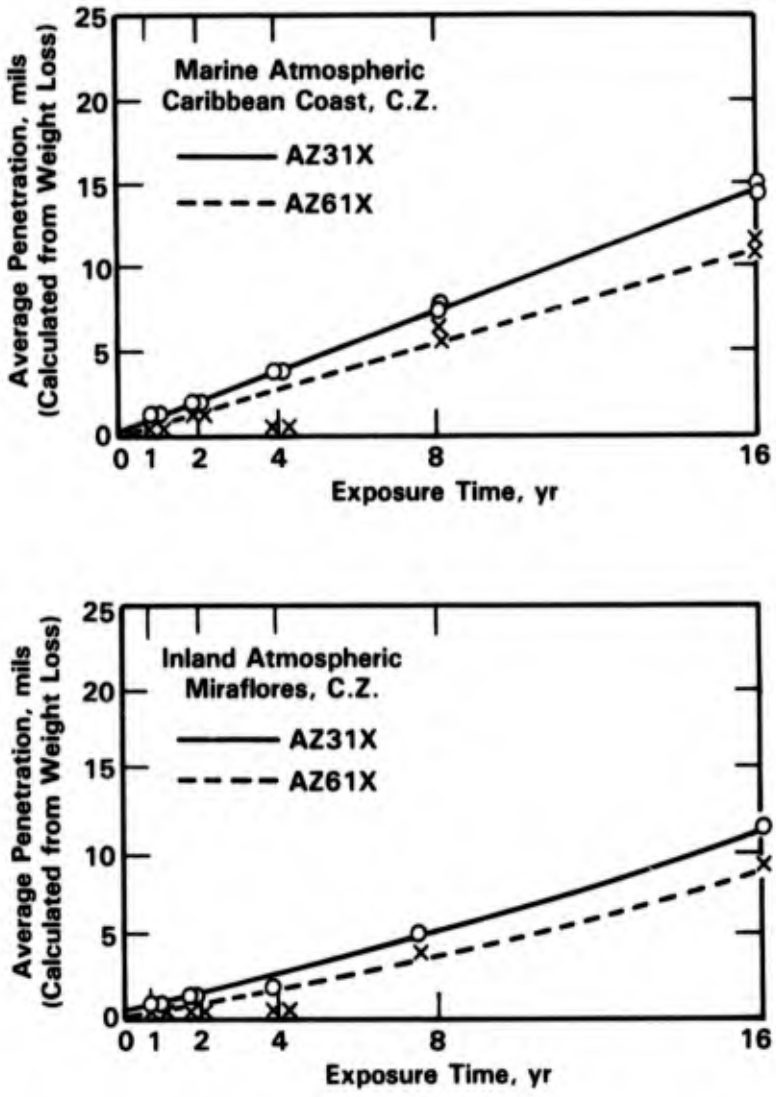

FIGURE 7-1. CORROSION RATES OF MAGNESIUM AZ61X AND AZ31X AFTER 16 YEARS' EXPOSURE TO DIFFERENT TROPICAL ATMOSPHERES[1]

Johnson and Masteller[3] reported on the corrosion behavior of several Mg-Zn-Mn alloys (ZM41 alloys) and AZ31B in salt spray and alternate immersion tests. The salt spray tests were performed at 100 F with a 20 percent NaCl solution while the alternate immersion tests were performed in 3 percent NaCl with a 30 second immersion time for a 2.5 minute cycle. The ZM41 alloys performed much better than AZ31B in these tests, see Table 7-2, but the latter alloy contained 0.01 percent Fe, which is above the specification limit. The ZM41 alloys also contained 0.01 percent Fe and thus, it was concluded that the ZM41 alloys are more tolerant of Fe impurities. More recently, Dow has developed a new high purity magnesium

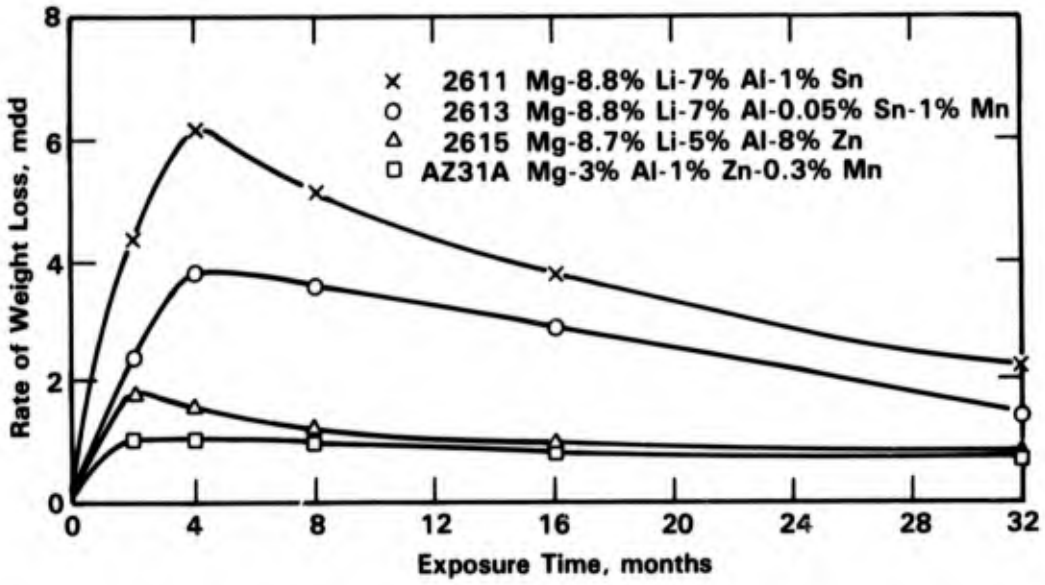

FIGURE 7-2. CORROSION RATE, EXPRESSED AS WEIGHT LOSS, OF EXPERIMENTAL MAGNESIUM-LITHIUM-BASE ALLOYS COMPARED WITH COMMERCIAL AZ31A ALLOY[2]

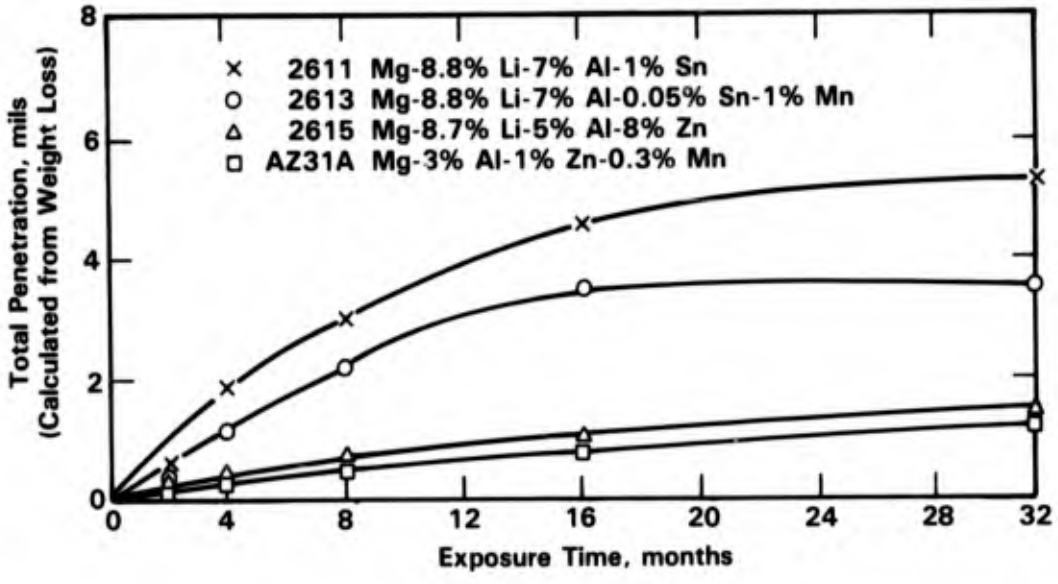

FIGURE 7-3. TOTAL PENETRATION, CALCULATED FROM WEIGHT LOSS, IN EXPERIMENTAL MAGNESIUM-LITHIUM-BASE ALLOYS COMPARED WITH COMMERCIAL AZ31A ALLOY[2]

TABLE 7-2. CORROSION RESULTS OF SOME ZM41 + M. M. ALLOYS AND AZ31B[3]

Melt Number	Alloy Actual Composition, %				Salt Spray Test Specimens		Alternate Immersion Test Specimens	
	Zn	M. M.*	Mn	Mg	Average Weight Loss, mg/in.^{2}	Standard Deviation	Average Weight Loss, mg/in.^{2}	Standard Deviation
10015	4.5	0.59	2.10	Balance	68.9	38.69	26.7	1.88
10027	4.0	0.60	1.04	Balance	43.2	7.60	24.0	1.63
10028	3.7	0.57	1.43	Balance	58.9	19.99	21.2	2.82
10084	4.06	0.38	0.63	Balance	36.8	6.6	28.1	0.667
10085	4.03	0.37	1.24	Balance	41.1	11.72	26.6	4.24
10040 (AZ31B)	Mg + 1.4 Zn + 0.47 Mn + 3.2 Al				276.4	16.1	28.8	1.87

* Misch Metal - complex combination of rare earth elements.

alloy AZ91C/HP which has the same metallurgical content as AZ91C, 9 percent Al, 1 percent Zn, and 0.13 percent Mn, but lower levels of Fe, Ni and Cu, e.g., 0.005 Fe. The alloy reportedly has lower rates of attack in the salt spray test (ASTM B117) than cold rolled steel or die cast 380 aluminum.[4]

Sato[5] performed an extensive survey of the literature on the influence of alloying elements on the corrosion behavior of Mg alloys. A summary of the findings, Table 7-3, shows that several elements are consistently harmful, such as Fe, whereas the effect of the vast majority of elements was dependent upon the specific test conditions and compositional range examined.

Mukhina, et al.[6] studied the influence between major alloy additions, such as Al and Mn, and impurity Fe on corrosion behavior in an aqueous chloride solution. It was found that the marked reduction in the corrosion resistance of Mg-Al alloys with trace additions of impurity Fe is due to the formation of Fe-Al phases which act as effective cathodes; Mn additions are beneficial because they suppress Fe-Al phase formation.

Ebihara[7] performed galvanic corrosion tests on AZ31, coupled to aluminum and other structural materials and exposed in the atmosphere at the Panama Canal Zone, U.S. Army Tropical Test Station. Equal area couples were exposed for 36 months. The orientation of the specimens or other details of the exposure were not discussed. A summary of the results is given in Table 7-4. These data show that the AZ31 alloy exhibited linear corrosion rates with time when coupled to itself or to the aluminum alloys. On the other hand, the corrosion rates for the other Mg couples were initially higher but decreased with time.

Very limited data were found on the SCC behavior of Mg alloys. Fairman and Bray[8,9] performed dead-weight load stress-corrosion tests on AZ61, AZ80, and two high purity alloys of similar nominal composition in a solution of 40 g/l NaCl + 40 g/l Na_2CrO_4. The specimens were tested in two heat treatments; one that produced grain boundary precipitates and one that did not. In the presence of the precipitates, the cracking was intergranular and AZ80 was somewhat more resistant than AZ61, see Figure 7-4. The pure equivalents of AZ61 and AZ80 exhibited similar behavior, indicating that minor constituents such as Fe and Zn did not affect intergranular SCC.

In the absence of precipitates, the cracking was transgranular and AZ80 was more susceptible than AZ61, see Figure 7-5. In fact, the change in heat treatment did not affect the threshold stress of AZ61 whereas the threshold stress for AZ80 dropped in going from the two phase to the single phase microstructure. Figure 7-5 also shows that susceptibility increased with increasing Al composition; the effect of other alloying elements on SCC, including Fe, was minimal.

TABLE 7-3. INFLUENCES OF VARIOUS ALLOYING ELEMENTS ON THE CORROSION RESISTANCE OF MAGNESIUM[5]

Alloying Element	Maximum Solid Solubility	Authors	Reported In	Range of Contents of the Element	Test Solution	Results (Corrosion Rate)
Al	12.7	Endo, Morioka	1932	1-8	0.1 N NaCl aq	Harmful; 3 times at 8% Al (material: Fe 0.019%)
		Igarashi	1936	0-6.4	0.1 N NaCl aq	Harmful; 20 times at 6.4% Al
		Ichikawa*	1957	0.02-0.05	0.3% NaCl aq	Harmful; 2.5% times at 0.05% Al (material: Fe 0.003%)
		Asada*	1958	0.01-6	3% NaCl aq	Good (Al <4%) harmful; 4.5 times at 6% Al
		Kutaitseva	1960	0-9	Industrial atmosphere	Harmful (Al >4%)
		Hummer	1965		Tropical atmosphere	Good at 6.86% Al in the Alloys AZ31X, AZ61X
		Lorant	1966		NaCl aq	Increase stress-corrosion cracking (Al <6.5%)
Zn	8.4	Endo, Morioka	1932	1-8	0.1 N NaCl aq	Good; 3-4% Zn
		Igarashi	1936	0-2.19	0.1 N NaCl aq	Good; 1/25 times at 2% Zn
		Asada*	1958	0.1-4	3% NaCl aq	Good; 1/2 times at 2% Zn, but 1 time at 4% Zn
		Kutaititseva	1960	0-1.5	Industrial atmosphere	Harmful; Zn >0.2%
		Wolkenberg	1964	0-90		Good; 1/500 times at 60-80% Zn
		Marshakov	1965	0-72	2 N NaCl aq	Harmful; extremely (0-65% Zn) intercrystalline cracking (65-72%)
Mn	1.55	Kronig-Powlow	1934	0.08-4.10	Synthesized seawater	Good; (<1.36% Mn)
		Igarashi	1936	0.34-1.34	0.1 N NaCl aq	Good; 1/10 times at 0.6% Al
		Mikejima	1937	0.23-4.54	0.1 N NaCl aq	Good (<2.5% Mn); 1/10 times at 2.5%, harmful (3.7% Mn)
		Goto	1937	0-0.4	NaCl aq	Good; (0.1-0.4% Mn)
		Belyaev	1957		Atmosphere	No difference was observed between the materials with 0.042% Fe and 0.004% Fe (Mn <1.48%)
		Asada*	1958	0.006-0.65	3% NaCl aq	No influence
		Shigeno	1960	0.2	Synthesized seawater	Good; 0.2% Mn addition eliminates the bad influence of Fe
		Romanov	1965		NaCl aq	Corrosion crack did not occur within solid solubility
		Ichikawa*	1957	0.048-0.010	3% NaCl aq	Harmful; 3 times at 0.010% Mn
Fe	-0.001	Goto	1937	0.072-0.132	NaCl aq	Not so harmful
		Hanawalt*	1942	0.0005-0.033	NaCl aq	Harmful; (Fe >0.016%)
		Ichikawa*	1957	0.072	0.3% NaCl aq	Harmful; 9 times at 0.003% Fe
		Asaka*	1958	0.0004-0.0032	3% NaCl aq	Harmful; (Fe >0.0011%)
		Emley*	1960		Seawater	Harmful; Fe >0.017% for pure Mg and Fe >0.002% for 8% Al Mg
		Rozov	1960		Atmosphere	Not so harmful; useful for practice
Ni	<0.1	Endo, Morioka	1932	1-8	NaCl aq (spray)	Harmful (after 25 days)
		Endo, Morioka	1932	0.91-8	0.1 N NaCl aq	Harmful
		Igarashi	1934	0-5.8	0.1 N NaCl aq	Harmful (at 0.54% Ni)

TABLE 7-3. (Continued)

Alloying Element	Maximum Solid Solubility	Authors	Reported In	Range of Contents of the Element	Test Solution	Results (Corrosion Rate)
		Hanawalt*	1942	0.0005-0.018	NaCl aq	Harmful; (Ni 0.0005%)
		Belyaev	1957			Harmful; (at 0.15% Ni in Mg-Mn alloy)
		Nelson	1958		3.5% NaCl aq	Harmful; in AZ 92, AZ63
		Emley*	1960		Seawater	Harmful; (Ni >0.001%)
		Emley	1960		Atmosphere	Better; (against atmospheric corrosion)
		Rozov	1960		Atmosphere	Not so harmful; useful for practice
Si	0.003	Igarashi	1935	0-1.4	0.1 N NaCl aq	Good (0.4-0.8% Si); 1/10 times at 0.5%
		Goto	1937	0-0.95	NaCl aq	Good slightly
		Igarashi	1936	0-1.4	0.1 N NaCl aq	Good; 1/a times at 0.75%, harmful (Si 0.75%)
		Ichikawa*	1957	0.007-0.028	0.3% NaCl aq	Harmful; 2 times at 0.028% Si
		Nevzorova	1964	3.5	Water in organic solution	No influence; 0.5Ni-0.1N Ti-3.5Si-0.25Fe alloy
Zr	0.7	Morioka	1939	0.13	0.1 N NaCl aq	Good; (6Al-3Zn-0.3Mn-0.1Cr alloy)
		Tanaka	1957		3% NaCl aq	Good; within solid solubility
		Ichikawa*	1957	0.5-4	0.3% NaCl aq	Good; 1/3 times at 4% Zr, as a result of elimination of Fe, Mn, Si, Al
		Emley	1966		3% NaCl aq	Good; increase the tolerance limit of Ni (0.003% Ni at 0.6% Zr)
Ca	0.95	Endo, Morioka	1932	1.2-3.06	0.1 N NaCl aq	Good (<1.2%; 2/3 times at 1.2%), harmful (>1.2%); 14 times at 3% Ca
		Obinata, Hayashi	1939	0-1.20	2.5% NaCl aq	Good; at 0.2-0.8% Ca
		Obinata, Hayashi	1940	0-0.36	2.5% NaCl	Good; (0.5-2% Ca); 1/10 times at 0.2% Ca in 0.2% Mn-Mg alloy
		Romanov	1965	0.4-1.0	35 g/l NaCl aq	No corrosion crack (under solid solubility)
Cu	0.03	Endo, Morioka	1932	1.05-7.33	0.1 N NaCl aq	Harmful
		Igarashi	1935	0-4.7	0.1 N NaCl aq	Harmful (Cu >0.48%)
		Belyaev	1957			Harmful; Cu >0.006% in Mg-Mn alloy
		Emley	1960		Seawater	Harmful (Cu >0.005%)
		Marshakov	1965	0-99.9	0.5 N NaCl aq	Harmful (Cu >35%), no influence (87-97% Cu)
		Ichikawa*	1957	0.011-0.024	0.3% NaCl aq	Harmful; 3 times at 0.024%
Cd	100	Endo, Morioka	1932	1-8	0.1 N NaCl aq	Good; 1/3 times at 1% Cd
		Igarashi	1936	0-10.88	0.1 N NaCl aq	Good; 1/50 times at 3% Cd
		Goto	1937	0-100	0.1 N NaCl aq	Harmful
		Obinata, Hayashi	1939	0-8	2.5% NaCl aq	Good; (3-5% Cd)
		Romanov	1965	0.5-6.0	35 g/l NaCl aq	No corrosion cracking (under solid solubility)

TABLE 7-3. (Continued)

Alloying Element	Maximum Solid Solubility	Authors	Reported In	Range of Contents of the Element	Test Solution	Results (Corrosion Rate)
Pb	41.7	Endo, Morioka	1932	1-8	0.1 N NaCl aq	Good (1-5% Pb); 1/4 times at 3% Pb
		Igarashi	1936	0-11.94	0.1 N NaCl aq	Good; 1/20 times at 8% Pb
		Romanov	1965	0.2-0.5	35 g/l NaCl aq	Corrosion cracking
Sn	14.85	Endo, Morioka	1932	1.18-8.44	0.1 N NaCl aq	Good; (1-8% Sn); 1/3 times at 8% Sn
		Igarashi	1936	0-3.09	0.1 N NaCl aq	Good; 1/17 times at 2% Sn
		Romanov	1965	0.2-3.0	35 g/l NaCl aq	Corrosion cracking
		Marshakov	1965	70 (Mg_2Sn)	Wet air	Breaked to fine pieces, naturally
Li	5.5	Igarashi	1936	0-0.5	0.1 N NaCl aq	Good (Li <0.2%) in Al-Mn (1.5%) -Mg alloy
		Frost	1956	11, 9	3% NaCl aq	11% Li-Al-Zn-Mg is better than 9% Li-Al-Zn-Mg alloy
		Frost	1956	11, 9	Sea-side atmosphere	9% Li-5Al-8Zn-Mg is better than 1.26% Mn-Mg alloy
		Cole	1956	~12	3% NaCl aq	No influence (Li <10%), harmful (Li >12%)
Bi	8.85	Endo, Morioka	1932	0.9-7.62	0.1 N NaCl aq	No influence (Bi <0.9%), harmful (Bi >1%); 10 times at 2.8% Bi
		Obinata, Hayashi	1940	0-0.97	2.5% NaCl aq	No influence in 0.5-2% Mn-Mg alloy
		Igarashi	1936	0-4.83	0.1 N NaCl aq	Good; 1/50 times at 2% Bi
		Romanov	1965	0.5-5.0	35 g/l NaCl aq	Corrosion cracking
Se		Morioka	1939	<0.00	0.1 N NaCl aq	Good (Se <0.01%) in 6Al-3Zn-0.3Mn-0.1Cr-Mg alloy
		Obinata, Hayashi	1940	0-0.03	2.5% NaCl aq	Good; 1/3 times at 0.02% Se in Mn (0.5-2%) -Mg alloys
Sb	<0.2	Endo, Morioka	1932	0.34-4.65	0.1 N NaCl aq	Good; 1/2 times at 0.34% Sb, harmful (Sb >0.49%)
		Igarashi	1936	0-1.99	0.1 N NaCl aq	Good; 1/10 times at 0.7% Sb, harmful (Sb >0.8%)
		Obinata, Hayashi	1940	0-0.90	2.5% NaCl aq	Good; 1/4 times at 0.5% Sb, harmful (Sb >0.6%)
Ag	15.5	Igarashi	1935	0-6	0.1 N NaCl aq	Good; 1/10 times at 1-2% Ag, harmful (Ag <1%, or 2-6% Ag)
		Igarashi	1936	0-6.03	0.1 N NaCl aq	Good; 1/4 times at 0.5% Ag, harmful (Ag >0.6%)
Te	~0	Obinata, Hayashi	1940	0-0.14	2.5% NaCl aq	Good; 1/10 times in Mn (0.5-2%) Mg alloy
Tl	60	Endo, Morioka	1932	1.35-5.26	0.1 N NaCl aq	Harmful; 20 times at 1.35%
Hg	3	Obinata, Hayashi	1940	0-1.24	2.5% NaCl aq	Good; 1/10 times at 0.5% Hg in 2 Mn-Mg alloy
As	~0	Obinata, Hayashi	1940	0-0.29	2.5% NaCl aq	Good; 1/4 times at 0.15% As in 2 Mn-Mg alloy
In	53.2	Emley	1966		NaCl aq	Good; in ZT1, ZTM, ZREI alloy
Ce	1.6	Nevzorova	1964	0.7-1.3	Organic solution	Intercrystalline cracking
Na		Asada*	1958	0.0006-0.027	3% NaCl aq	No influence

* These data were obtained by experiments with extremely pure Mg.

TABLE 7-4. ATMOSPHERIC EXPOSURE CORROSION RATES* CALCULATED FROM WEIGHT LOSS FOR GALVANIC COUPLE (1:1 AREA RATIO)[7]

Alloy	Exposure Time, months	Corrosion Rate, mm/yr							
		AZ31 Magnesium	Type 316 Stainless Steel	4340 Steel	6061-A1	7075-A1	360 Brass	400 Monel	Titanium 6Al-4V
AZ31 Magnesium	2	0.031	0.076	0.096	0.047	0.047	0.074	0.092	0.063
	4	0.037	0.079	0.089	0.050	0.040	0.066	0.077	0.059
	8	0.034	0.057	0.064	0.048	0.048	0.064	0.059	0.055
	15	0.025	0.045	0.049	0.036	0.037	0.048	0.052	0.044
	24	0.028	0.060	0.076	0.040	0.039	0.051	0.049	0.045
	36	0.030	0.046	0.049	0.039	0.041	0.051	0.050	0.045
4340 Steel	2	0.033	0.071	0.069	0.069	0.061	0.068	0.074	0.072
	4	0.018	0.050	0.055	0.055	0.050	0.050	0.050	0.057
	8	0.014	0.036	0.037	0.038	0.036	0.036	0.036	0.037
	15	0.013	0.047	0.046	0.030	0.031	0.038	0.044	0.049
	24	0.011	0.049	0.048	0.026	0.025	0.037	0.049	0.047
	36	0.012	0.061	0.048	0.025	0.030	0.040	0.047	0.057
6061-Tl Aluminum	2	0.002	0.006	0.005	0.002	0.002	0.006	0.005	0.005
	4	0.001	0.002	0.006	0.002	0	0.004	0.002	0.002
	8	0.001	0.001	0.004	0.001	0.001	0.002	0.001	0.002
	15	0	0.002	0.006	0.001	0.001	0.003	0.003	0.003
	24	0	0.003	0.007	0.001	0.001	0.007	0.003	0.003
	36	0	0.002	0.007	0.001	0.001	0.004	0.004	0.002
7075-T6 Aluminum	2	0.003	0.007	0.009	0.005	0.003	0.010	0.007	0.007
	4	0.002	0.005	0.005	0.002	0.003	0.004	0.003	0.004
	8	0.001	0.003	0.004	0.001	0.001	0.003	0.003	0.003
	15	0	0.003	0.016	0.002	0.001	0.005	0.003	0.003
	24	0	0.003	0.012	0.002	0.001	0.010	0.003	0.004
	36	0.001	0.003	0.007	0.001	0.003	0.005	0.003	0.003
360 Brass	2	0.003	0.009	0.006	0.005	0.005	0.007	0.008	0.008
	4	0.001	0.004	0.003	0.002	0.002	0.003	0.004	0.003
	8	0.001	0.002	0.002	0.001	0.001	0.001	0.002	0.002
	15	0.001	0.002	0.002	0.001	0.001	0.001	0.001	0.001
	24	0	0 002	0.002	0.001	0.001	0.001	0.001	0.001
	36	0.001	0.001	0.002	0.001	0.001	0.001	0.001	0.001

* Essentially zero corrosion rate for the 316 stainless steel, 400 Monel, and Titanium 6Al-4V specimens.

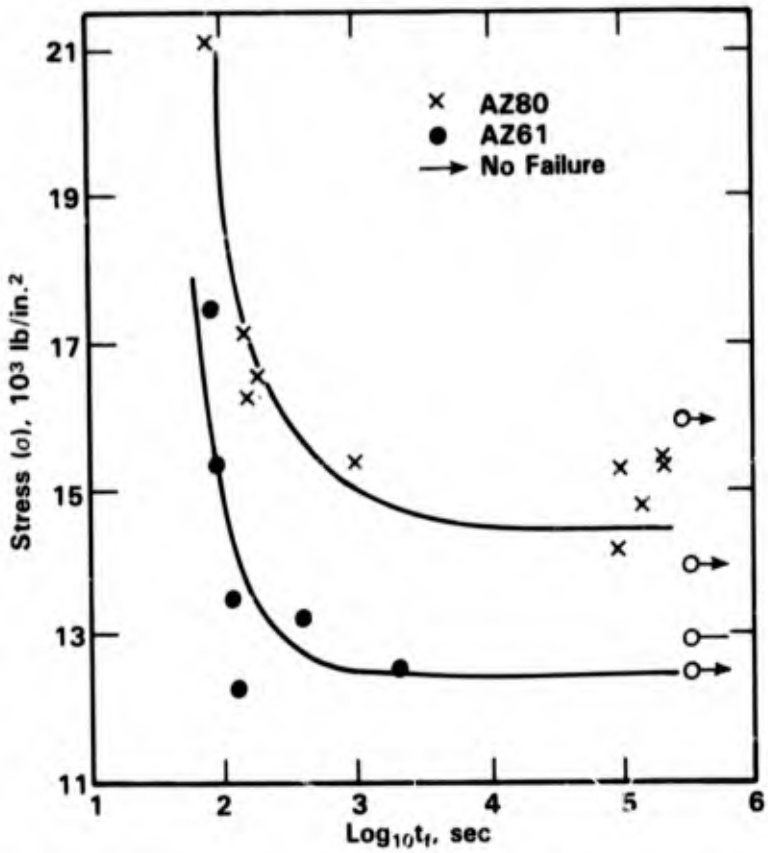

FIGURE 7-4. STRESS (σ) VERSUS TIME TO FAILURE (t_f) FOR THE TWO-PHASE ALLOYS AZ80 AND AZ61 IN AQUEOUS 40 g/l NaCl + 40 g/l Na_2CrO_4[8]

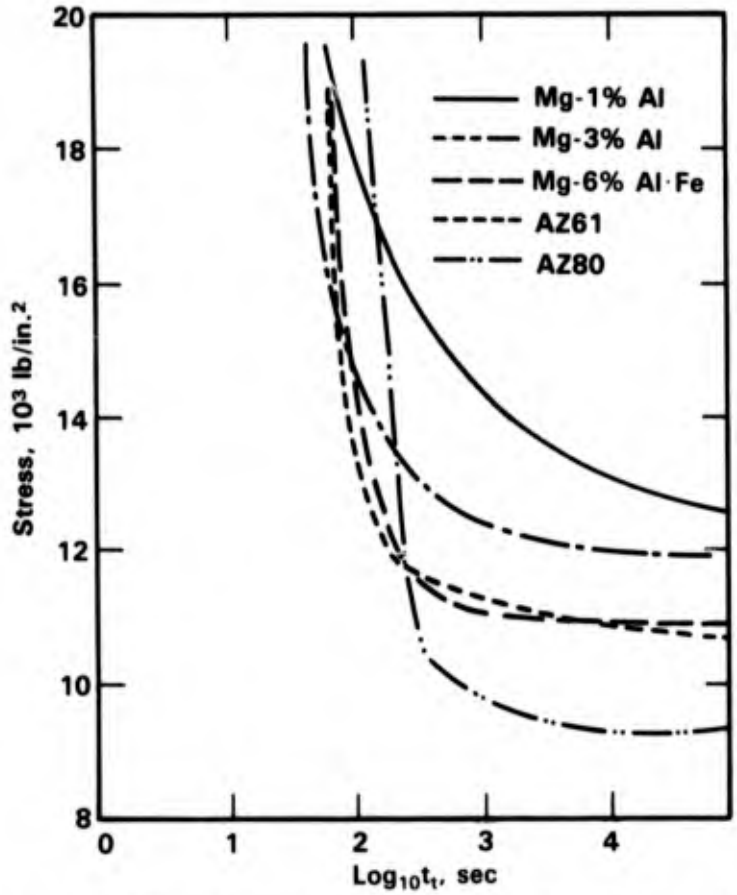

FIGURE 7-5. STRESS VERSUS TIME TO FAILURE (t_f) FOR Mg-Al ALLOYS IN AQUEOUS 40 g/l NaCl + 40 g/l Na_2CrO_4[9]

Tide and Immersed Exposure

Magnesium alloys exhibit very poor corrosion performance in tide and immersed exposure. Results of 8 year exposures by Southwell, et al.[1] in the Panama Canal Zone are summarized in Table 7-1 and Figure 7-6. These data show that the Mg alloy AZ31X corrodes at rates of about 5-10 mpy, which is not excessive, but pits at much higher rates; pits in excess of 100 mils were detected within approximately 1 year. In fact, Southwell, et al.[1] terminated the exposures of AZ31X after 8 years because of the presence of numerous perforations.

The high corrosion rates of Mg alloys in seawater and the active nature of Mg are exploited in marine applications. Mg is commonly used as a sacrificial anode in cathodic protection systems, see section on Cathodic Protection. Recently, supercorroding magnesium alloys have been developed for use in destructive links, and for generation of hydrogen.[10]

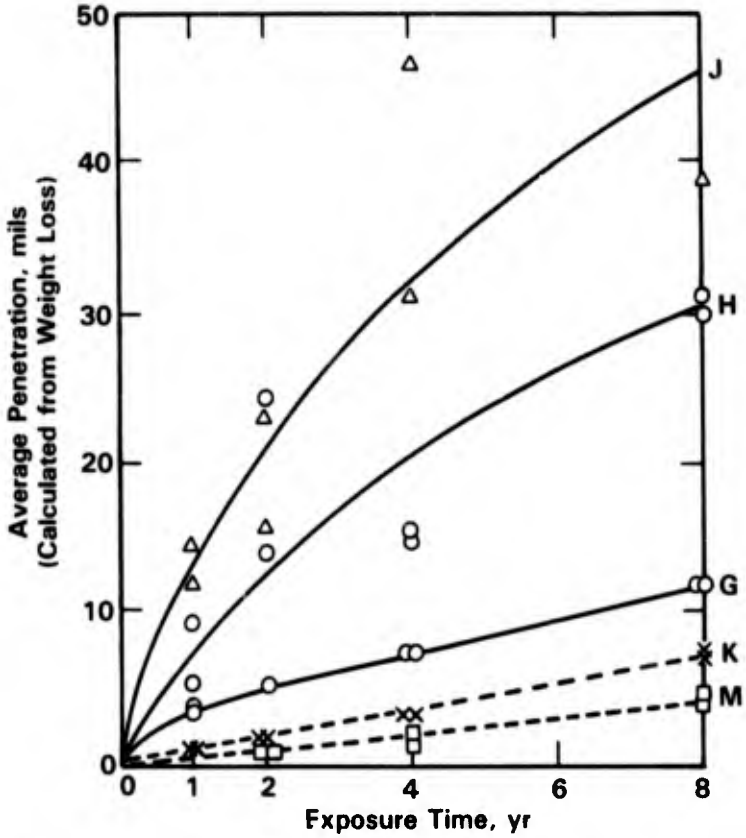

FIGURE 7-6. CORROSION OF MAGNESIUM AZ31X AFTER EIGHT YEARS' EXPOSURE IN THE CANAL ZONE[1]

H = Continuous immersion in seawater;
J = Immersion in seawater at mean tide;
G = Continuous immersion in fresh water;
K = Exposure to marine atmosphere; and
M = Exposure to inland atmosphere

REFERENCES FOR CHAPTER 7

1. Southwell, C. R., et al., "Corrosion of Metals in Tropical Environments - Aluminum and Magnesium", Materials Protection, 4 (12), p 30 (December, 1965).

2. Frost, P. D., et al., "Results of Some Marine-Atmosphere Corrosion Tests on Magnesium-Lithium Alloys", Journal Electrochemical Society, 102, p 215 (1955).

3. Johnson, H. A. and Masteller, R. D., "Development of ZM41 Magnesium Sheet Alloy", Aeronautical Systems Division WPAFB Report ASD-TR-56-415, 24 pp (September, 1957).

4. Crisafulli, T., "Anti-Corrosion Magnesium Alloys Bows", American Metal Market (December 5, 1984).

5. Sato, M., et al., "Effects of Alloying Elements of Groups II, III, and IV on Corrosion Resistance of 99.97 Percent Mg in 3 Percent NaCl Aqueous Solution", Journal Japan Institute of Light Metals, 20 (8), pp 398-409 (August, 1970).

6. Mukhina, I. Y., et al., "Influence of the Phase Composition on the Corrosion Resistance of Magnesium Alloys", Russian Metallurgy, (6), pp 123-126 (1973).

7. Ebihara, W. T., "Tropical Exposure of Galvanically Coupled Metal Systems", Army Armament R&D Report ARSCD-TR-79004, 18 pp (June, 1979).

8. Fairman, L. and Bray, H. J., "Intergranular Stress-Corrosion Crack Propagation in Magnesium Aluminum Alloys", British Corrosion Journal, 6 (4), pp 170-174 (July, 1971).

9. Fairman, L. and Bray, H. J., "Transgranular SCC in Mg-Al Alloys", Corrosion Science, 11 (7), pp 533-541 (July, 1971).

10. Black, S. A., "Development of Supercorroding Alloys for Use as Time Releases for Ocean Engineering Applications", Civil Engineering Laboratory, Port Hueneme, CA, CEL-TH-1550 MCIC 108057 (March, 1979).

CHAPTER 8
TABLE OF CONTENTS

CHAPTER 8
LIST OF TABLES

CHAPTER 8
LIST OF TABLES
(Continued)

CHAPTER 8
LIST OF FIGURES

CHAPTER 8
LIST OF FIGURES
(Continued)

CHAPTER 8
LIST OF FIGURES
(Continued)

CHAPTER 8
LIST OF FIGURES
(Continued)

CHAPTER 8

COPPER AND COPPER-BASE ALLOYS

ATMOSPHERIC CORROSION

Copper and copper alloys exhibit low rates of attack in marine atmospheres. Typical exposure data for both temperate and tropical marine exposures are presented in Tables 8-1 and 8-2. These data show some differences in the rates of attack between exposure sites and between various alloys. For example, corrosion rates were somewhat higher in the tropical zones than those in temperate exposures. However, these differences are small and in general have little or no practical significance. On the basis of weight-loss measurements, corrosion rates over periods of up to 20 years are 0.01 to 0.17 mpy.

The low corrosion rates of copper and its alloys are the result, in part, of the formation of protective corrosion product films. Soon after installation, the bright copper surface takes on a dull tan color (tarnish) which, after a few years, gradually changes to dark brown or black. At a later stage, depending on the level of sulfur contaminants in the air, the copper corrosion products turn green, which is referred to as a patina. The corrosion reactions involved in the formation of the green patina usually are more rapid on bodly exposed surfaces facing south (northern hemisphere) or in the direction of the prevailing wind (where the air is carrying pollutants) than they are for other orientations.

In a marine atmosphere containing low sulfur dioxide concentrations, the green patina may be largely basic copper chloride $CuCl_2 \cdot 3Cu(OH)_2$.[3] It corresponds to "atacamite". Basic sulfates are also present. If the atmosphere is at all contaminated, the sulfate will be the major constituent. Osborn[4], for example, has established that the patina on the bronze statue of Liberty is predominantly basic copper sulfate, even though it is surrounded by the seawater in New York harbor.

From the standpoint of alloy additions, slightly beneficial trends are indicated for aluminum, nickel, and zinc, whereas those alloys containing silicon and tin tend to be somewhat less resistant than copper alone, see Tables 8-1, 8-2, and 8-3. As previously pointed out, these trends are, in general, not so significant as to dictate the use of one alloy over another except for an extremely critical application.

TABLE 8-1. COMPREHENSIVE EVALUATION OF CORROSION DAMAGE FOR COPPER AND COPPER ALLOYS IN FIVE TROPICAL ENVIRONMENTS AT CRISTOBAL, PANAMA CANAL ZONE[1]

Metal	Exposure	Weight Loss, g/dm²					Average Penetration, mils					Depth of Pitting, mils										Tensile Strength Loss, %[b]		Type Corrosion Attack[c]
												Average 20 Deepest Pits[a]					Deepest Pit							
		1 Yr	2 Yr	4 Yr	8 Yr	16 Yr	1 Yr	2 Yr	4 Yr	8 Yr	16 Yr	1 Yr	2 Yr	4 Yr	8 Yr	16 Yr	1 Yr	2 Yr	4 Yr	8 Yr	16 Yr	8 Yr	16 Yr	16 Yr
Copper	Immersion																							
	Sea Water	2.74	5.03	5.95	12.06	13.61	1.21	2.22	2.62	5.58	6.02	27 (15)	36 (17)	16 (11)	28	31	46	75	21	53	57	1.7	5.2	E, R
	Mean Tide	1.47	1.85	4.30	2.45	2.99	0.65	0.82	1.90	1.08	1.32	9 (2)	(0)	7 (2)	10	(0)	11	(0)	8	23	(0)	1.7	1.0	E, R
	Fresh Water	0.50	0.81	1.29	1.86	2.33	0.22	0.36	0.57	0.82	1.03	(0)	(0)	(0)	(0)	(0)	(0)	(0)	(0)	(0)	(0)	2.0	2.6	A
	Atmospheric																							
	Marine	0.37	0.52	0.86	1.29	1.73	0.17	0.23	0.38	0.57	0.77	(0)	(0)	(0)	(0)	(0)	(0)	(0)	(0)	(0)	(0)	3.7	4.5	A
	Inland	0.18	0.26	0.34	0.43	0.60	0.08	0.12	0.15	0.19	0.27	(0)	(0)	(0)	(0)	(0)	(0)	(0)	(0)	(0)	(0)	1.8	0.1	A
Silicon Bronze	Immersion																							
	Sea Water	5.17	3.43	7.56	13.30	12.75	2.38	1.58	3.47	6.10	5.85	15 (18)	40 (14)	19	21	21 (17)	37	80	51	[illegible]	36	1.9	3.5	E, R
	Mean Tide	1.61	2.09	2.61	3.35	4.45	0.74	0.96	1.20	1.53	2.04	(0)	(0)	24 (7)	14	41 (7)	(0)	(0)	38	42	65	1.3	0.2	R
	Fresh Water	0.71	1.10	1.56	2.20	2.44	0.33	0.51	0.72	1.01	1.12	(0)	(0)	(0)	(0)	9 (2)	(0)	(0)	(0)	(0)	9	1.2	1.6	A, R
	Atmospheric																							
	Marine	0.67	0.87	1.41	2.36	4.06	0.31	0.40	0.65	1.09	1.86	(0)	(0)	(0)	(0)	(0)	(0)	(0)	(0)	(0)	(0)	0.0	3.9	B, A
	Inland	0.35	0.44	0.64	0.82	1.33	0.16	0.20	0.30	0.38	0.61	(0)	(0)	(0)	(0)	(0)	(0)	(0)	(0)	(0)	(0)	1.4	1.5	B, A
Phosphor Bronze	Immersion																							
	Sea Water	2.42	3.40	4.88	9.07	12.38	1.07	1.51	2.16	4.01	5.48	4 (6)	15 (16)	14	13 (10)	2 (18)	9	35	22	22	29	1.1	7.0	E
	Mean Tide	1.09	1.70	2.90	4.63	7.85	0.48	0.75	1.28	2.05	3.47	(0)	(0)	(0)	(0)	11 (2)	(0)	(0)	(0)	(0)	11	3.6	2.4	E
	Fresh Water	0.26	0.56	0.71	1.04	1.63	0.12	0.24	0.31	0.45	0.72	(0)	(0)	(0)	(0)	(0)	(0)	(0)	(0)	(0)	(0)	0.1	1.9	A
	Atmospheric																							
	Marine	0.44	0.64	0.91	1.37	2.16	0.20	0.29	0.40	0.61	0.96	(0)	(0)	(0)	(0)	(0)	(0)	(0)	(0)	(0)	(0)	6.6	2.4	K, A
	Inland	0.13	0.24	0.36	0.56	0.81	0.06	0.11	0.16	0.25	0.36	(0)	(0)	(0)	(0)	(0)	(0)	(0)	(0)	(0)	(0)	2.0	0.0	K, A
Aluminum Bronze	Immersion																							
	Sea Water	0.39	0.75	1.25	1.58	2.62	0.18	0.36	0.60	0.76	1.26	(0)	(0)	(0)	14 (3)	(0)	(0)	(0)	(0)	21	(0)	1.9	3.2	J
	Mean Tide	0.20	0.35	0.58	0.77	1.19	0.09	0.17	0.28	0.37	0.56	(0)	(0)	(0)	(0)	(0)	(0)	(0)	(0)	(0)	(0)	1.8	1.7	K
	Fresh Water	0.13	0.20	0.31	0.57	0.87	0.06	0.10	0.15	0.27	0.42	(0)	(0)	(0)	(0)	(0)	(0)	(0)	(0)	(0)	(0)	1.7	2.3	K
	Atmospheric																							
	Marine	0.18	0.23	0.31	0.47	0.84	0.08	0.11	0.15	0.23	0.39	(0)	(0)	(0)	(0)	(0)	(0)	(0)	(0)	(0)	(0)	1.5	2.4	K, A
	Inland	0.10	0.15	0.20	0.28	0.52	0.05	0.07	0.10	0.13	0.25	(0)	(0)	(0)	(0)	(0)	(0)	(0)	(0)	(0)	(0)	0.5	0.4	K, A
Commercial Bronze	Immersion																							
	Sea Water	2.01	4.67	5.33	10.63	11.01	0.90	2.08	2.39	4.75	4.93	72	65 (16)	28 (19)	25	33 (20)	158	174	54	44	51	2.6	5.1	R, O, J
	Mean Tide	0.88	1.02	1.26	1.62	2.33	0.40	0.46	0.56	0.72	1.04	6 (10)	(0)	(0)	8 (4)	(0)	10	(0)	(0)	11	(0)	1.4	1.8	C
	Fresh Water	0.50	0.88	1.39	2.23	2.98	0.22	0.40	0.62	0.99	0.34	(0)	(0)	(0)	(0)	(0)	(0)	(0)	(0)	(0)	(0)	1.6	1.8	C
	Atmospheric																							
	Marine	0.25	0.32	0.50	0.67	1.10	0.12	0.14	0.22	0.30	0.49	(0)	(0)	(0)	(0)	(0)	(0)	(0)	(0)	(0)	(0)	2.3	3.3	A, K
	Inland	0.11	0.18	0.31	0.42	0.71	0.05	0.08	0.14	0.19	0.32	(0)	(0)	(0)	(0)	(0)	(0)	(0)	(0)	(0)	(0)	0.6	0.0	A, K
Low Brass	Immersion																							
	Sea Water	1.43	2.75	4.09	6.54	8.18	0.66	1.25	1.86	2.97	3.73	8 (9)	53 (16)	18 (12)	33	22	22	130	23	53	46	1.7	3.3	O, C, Q
	Mean Tide	0.70	0.69	0.76	1.09	1.44	0.32	0.31	0.35	0.50	0.66	(0)	(0)	(0)	(0)	(0)	(0)	(0)	(0)	(0)	(0)	0.7	2.0	O
	Fresh Water	0.61	1.06	1.64	2.52	3.62	0.28	0.48	0.74	1.15	1.66	(0)	(0)	(0)	(0)	(0)	(0)	(0)	(0)	(0)	(0)	1.6	3.0	C
	Atmospheric																							
	Marine	0.18	0.23	0.35	0.49	0.81	0.08	0.11	0.16	0.23	0.37	(0)	(0)	(0)	(0)	(0)	(0)	(0)	(0)	(0)	(0)	4.8	3.2	A
	Inland	0.08	0.15	0.24	0.35	0.65	0.04	0.07	0.11	0.16	0.30	(0)	(0)	(0)	(0)	(0)	(0)	(0)	(0)	(0)	(0)	0.7	0.0	A
Cartridge Brass	Immersion																							
	Sea Water	1.01	2.17	3.39	5.28	8.45	0.47	1.00	1.56	2.43	3.90	(0)	(0)	(0)	(0)	(0)	(0)	(0)	(0)	(0)	(0)	13.7	20.0	O, C
	Mean Tide	0.37	0.34	0.55	0.82	1.93	0.17	0.16	0.25	0.37	0.89	(0)	(0)	(0)	(0)	(0)	(0)	(0)	(0)	(0)	(0)	1.3	4.2	O, K
	Fresh Water	0.75	1.30	1.87	2.84	3.87	0.34	[illegible]	0.86	1.31	1.79	(0)	(0)	(0)	(0)	(0)	(0)	(0)	(0)	(0)	(0)	0.6	2.7	O, A
	Atmospheric																							
	Marine	0.11	0.15	0.24	0.39	0.72	0.05	0.07	0.11	0.18	0.33	(0)	(0)	(0)	(0)	(0)	(0)	(0)	(0)	(0)	(0)	5.3	3.6	A, R
	Inland	0.05	0.10	0.17	0.26	0.54	0.03	0.05	0.08	0.12	0.25	(0)	(0)	(0)	(0)	(0)	(0)	(0)	(0)	(0)	(0)	0.6	0.0	A, R

TABLE 8-1. (Continued)

Metal	Exposure	Weight Loss, g/dm²					Average Penetration, mils					Depth of Pitting, mils										Tensile Strength Loss, %(b)		Type Corrosion Attack(c)
												Average 20 Deepest Pits(a)					Deepest Pit							
		1 Yr	2 Yr	4 Yr	8 Yr	16 Yr	1 Yr	2 Yr	4 Yr	8 Yr	16 Yr	1 Yr	2 Yr	4 Yr	8 Yr	16 Yr	1 Yr	2 Yr	4 Yr	8 Yr	16 Yr	8 Yr	16 Yr	16 Yr
Naval Brass	Immersion																							
	Sea Water	6.26	8.51	12.71	15.01	26.52	2.94	3.99	5.97	7.04	12.44	(0)	(0)	(0)	(0)	(0)	(0)	(0)	(0)	(0)	(0)	34.6	57.6	C
	Mean Tide	2.05	3.45	4.43	8.60	12.70	0.96	1.62	2.08	4.03	5.96	(0)	(0)	(0)	7	(0)	(0)	(0)	(0)	7	(0)	18.2	21.7	C
	Fresh Water	0.68	1.48	1.89	3.29	3.96	0.32	0.70	0.88	1.55	1.86	(0)	(0)	(0)	(0)	8 (6)	(0)	(0)	(0)	(0)	11	13.8	12.0	C
	Atmospheric																							
	Marine	0.13	0.16	0.28	0.44	0.81	0.06	0.08	0.13	0.21	0.39	(0)	(0)	(0)	(0)	(0)	(0)	(0)	(0)	(0)	(0)	2.7	6.8	K, A
	Inland	0.07	0.10	0.18	0.30	0.41	0.03	0.05	0.09	0.14	0.29	(0)	(0)	(0)	(0)	(0)	(0)	(0)	(0)	(0)	(0)	0.4	1.4	K, A
Muntz Metal	Immersion																							
	Sea Water	2.40	3.27	5.68	9.12	17.33	1.13	1.53	2.67	4.30	8.16	(0)	(0)	(0)	(0)	(0)	(0)	(0)	(0)	(0)	(0)	32.7	45.5	C, B
	Mean Tide	1.73	2.84	4.02	7.73	12.00	0.81	1.33	1.89	3.63	5.65	4 (4)	(0)	(0)	(0)	(0)	6	(0)	(0)	(0)	(0)	31.8	36.2	C, B
	Fresh Water	1.15	2.30	3.51	5.01	7.36	0.54	1.08	1.64	2.35	3.47	3 (9)	(0)	(0)	(0)	11 (15)	6	(0)	(0)	(0)	13	7.7	10.5	O
	Atmospheric																							
	Marine	0.14	0.18	0.30	0.48	0.97	0.07	0.09	0.14	0.23	0.45	(0)	(0)	(0)	(0)	(0)	(0)	(0)	(0)	(0)	(0)	4.3	8.4	K
	Inland	0.09	0.13	0.21	0.34	0.68	0.04	0.06	0.11	0.16	0.32	(0)	(0)	(0)	(0)	(0)	(0)	(0)	(0)	(0)	(0)	1.3	3.5	K
Manganese Bronze	Immersion																							
	Sea Water	6.45	7.53	12.32	25.00	36.56	3.03	3.54	5.79	11.75	[illegible]	22 (2)	(0)	(0)	12	21 (13)	27 (13)	(0)	(0)	20	36	33.1	45.8	O, C
	Mean Tide	2.10	2.81	4.83	8.18	16.03	0.99	1.32	2.27	3.84	7.5[illegible]	(0)	(0)	(0)	(0)	12 (1)	(0)	(0)	(0)	(0)	12	6.3	13.8	O, C
	Fresh Water	0.38	0.57	0.85	1.25	1.98	0.19	0.26	0.40	0.59	0.93	(0)	(0)	(0)	(0)	(0)	(0)	(0)	(0)	(0)	(0)	0.0	0.2	C
	Atmospheric																							
	Marine	0.38	0.40	0.63	0.70	1.26	0.18	0.19	0.30	0.33	0.60	(0)	(0)	(0)	(0)	(0)	(0)	(0)	(0)	(0)	(0)	6.0	8.0	K, A
	Inland	0.33	0.32	0.44	0.45	1.07	0.15	0.15	0.20	0.21	0.50	(0)	(0)	(0)	(0)	(0)	(0)	(0)	(0)	(0)	(0)	0.8	1.2	K, A

(a) Numbers in parenthesis indicate number of measurable pits when less than 20 - a measurable pit is one >5 mils.
(b) Percent losses are for samples of 1/4 inch thickness for immersion exposure and 1/16 inch thickness for atmospheric exposure.
(c) A - uniform attack, B - granular reaction, C - uniform dezincification, O - random dezincification, E - local attack (uniformly distributed), R - local attack (randomly located), J - fouling contact, and K - no visible attack.

TABLE 8-2. MARINE ATMOSPHERIC RESULTS FOR COPPER ALLOYS AFTER 2 AND 7 YEARS[2]

CDA No.[a]	Commercial Designation or Composition	Penetration, mpy (Calculated From Weight Loss) 2 Yr A[b]	2 Yr C[c]	7 Yr A	7 Yr C	Appearance After 7 Years at Kure Beach, NC
110	Tough pitch Cu	0.072	0.065	0.065	0.025	Brown film, smooth, slight patina near edges
			Tin			
505	Phos. bronze, 1.25% Sn	0.083	0.042	0.069	0.017	"Mink brown", slight patina
510	Phos. bronze, 5% Sn	0.150	0.088	0.099	--	Maroon film, heavy etch
			Aluminum			
637	Alum. bronze	0.017	0.009	0.013	--	Light tan film, smooth
			Nickel			
--	1.85 Ni, 0.03 Fe	0.134	0.145	0.044	0.036	Dark brown, mottled with green at edges
704	6.34 Ni, 0.01 Fe	0.069	0.052	0.033	--	Dark brown, plus patina streaks on panel face
707	9.16 Ni, 0.18 Fe	0.052	0.039	0.038	--	Uniform maroon with patina at edges
711	22.76 Ni, 0.04 Fe	0.036	0.024	0.031	--	Greenish brown, green near edges, slight etch
--	42.75 Ni, 0.30 Fe	0.018	0.012	0.019	0.005	Greenish brown, slight green near edges
			Zinc			
420	Tin brass	0.058	0.042	0.024	--	Dark maroon, smooth
230	Red brass	0.051	0.038	0.033	0.026	Brown-maroon film, smooth
260	Cartridge brass	0.034	0.023	0.030	0.017	Brown-maroon film, smooth, very slight patina
			Nickel-Zinc			
745	10% nickel-silver	0.030	0.020	0.024	0.010	Brown with slight patina film in center, green near edges, smooth
752	18% nickel-silver	0.030	0.020	0.021	--	Brown film in center, green near edges, smooth

(a) Copper Development Association number; see Appendix H for nominal alloy compositions.
(b) A = 80-foot lot, Kure Beach, NC.
(c) C = Point Reyes, CA.

TABLE 8-1. (Continued)

Metal	Exposure	Weight Loss, g/dm²					Average Penetration, mils					Depth of Pitting, mils: Average 20 Deepest Pits[a]					Depth of Pitting, mils: Deepest					Tensile Strength Loss, %[b]		Type Corrosion Attack[c]
		1 Yr	2 Yr	4 Yr	8 Yr	16 Yr	1 Yr	2 Yr	4 Yr	8 Yr	16 Yr	1 Yr	2 Yr	4 Yr	8 Yr	16 Yr	1 Yr	2 Yr	4 Yr	8 Yr	16 Yr	8 Yr	16 Yr	16 Yr
Naval Brass	Immersion																							
	Sea Water	6.26	8.51	12.71	15.01	26.52	2.94	3.99	5.97	7.04	12.44	(0)	(0)	(0)	(0)	(0)	(0)	(0)	(0)	(0)	(0)	34.6	57.6	C
	Mean Tide	2.05	3.45	4.43	8.60	12.70	0.96	1.62	2.06	4.03	5.96	(0)	(0)	(0)	7	(0)	(0)	(0)	(0)	7	(0)	18.2	21.7	C
	Fresh Water	0.68	1.48	1.89	3.29	3.96	0.32	0.70	0.88	1.55	1.86	(0)	(0)	(0)	(0)	8 (6)	(0)	(0)	(0)	(0)	11	13.8	12.0	C
	Atmospheric																							
	Marine	0.13	0.16	0.28	0.44	0.81	0.06	0.08	0.13	0.21	0.39	(0)	(0)	(0)	(0)	(0)	(0)	(0)	(0)	(0)	(0)	2.7	6.8	K, A
	Inland	0.07	0.10	0.18	0.30	0.61	0.03	0.05	0.09	0.14	0.29	(0)	(0)	(0)	(0)	(0)	(0)	(0)	(0)	(0)	(0)	0.4	1.4	K, A
Muntz Metal	Immersion																							
	Sea Water	2.40	3.27	5.68	9.12	17.33	1.13	1.53	2.67	4.30	8.16	(0)	(0)	(0)	(0)	(0)	(0)	(0)	(0)	(0)	(0)	32.7	45.5	C, B
	Mean Tide	1.73	2.84	4.02	7.73	12.00	0.81	1.33	1.89	3.63	5.65	4 (4)	(0)	(0)	(0)	(0)	6	(0)	(0)	(0)	(0)	31.8	36.2	C, B
	Fresh Water	1.15	2.30	3.51	5.01	7.36	0.54	1.08	1.64	2.35	3.47	3 (9)	(0)	(0)	(0)	11 (15)	6	(0)	(0)	(0)	13	7.7	10.5	O
	Atmospheric																							
	Marine	0.14	0.18	0.30	0.48	0.97	0.07	0.09	0.14	0.23	0.45	(0)	(0)	(0)	(0)	(0)	(0)	(0)	(0)	(0)	(0)	4.3	8.4	K
	Inland	0.09	0.13	0.21	0.34	0.68	0.04	0.06	0.11	0.16	0.32	(0)	(0)	(0)	(0)	(0)	(0)	(0)	(0)	(0)	(0)	1.3	3.5	K
Manganese Bronze	Immersion																							
	Sea Water	6.45	7.53	12.32	25.00	36.56	3.03	3.54	5.79	11.75	17.19	22 (2)	(0)	(0)	12	21 (13)	27 (13)	(0)	(0)	20	36	33.1	45.8	O, C
	Mean Tide	2.10	2.81	4.83	8.18	16.03	0.99	1.32	2.27	3.84	7.53	(0)	(0)	(0)	(0)	12 (1)	(0)	(0)	(0)	(0)	12	6.3	13.8	O, C
	Fresh Water	0.38	0.57	0.85	1.25	1.98	0.19	0.26	0.40	0.59	0.93	(0)	(0)	(0)	(0)	(0)	(0)	(0)	(0)	(0)	(0)	0.0	0.2	C
	Atmospheric																							
	Marine	0.38	0.40	0.63	0.70	1.26	0.18	0.19	0.30	0.33	0.60	(0)	(0)	(0)	(0)	(0)	(0)	(0)	(0)	(0)	(0)	6.0	8.0	K, A
	Inland	0.33	0.32	0.44	0.45	1.07	0.15	0.15	0.20	0.21	0.50	(0)	(0)	(0)	(0)	(0)	(0)	(0)	(0)	(0)	(0)	0.8	1.2	K, A

(a) Numbers in parenthesis indicate number of measurable pits when less than 20 - a measurable pit is one >5 mils.
(b) Percent losses are for samples of 1/4 inch thickness for immersion exposure and 1/16 inch thickness for atmospheric exposure.
(c) A - uniform attack, B - granular reaction, C - uniform dezincification, O - random dezincification, E - local attack (uniformly distributed), R - local attack (randomly located), J - fouling contact, and K - no visible attack.

TABLE 8-2. MARINE ATMOSPHERIC RESULTS FOR COPPER ALLOYS AFTER 2 AND 7 YEARS[2]

CDA No.[a]	Commercial Designation or Composition	Penetration, mpy (Calculated From Weight Loss) 2 Yr A[b]	2 Yr C[c]	7 Yr A	7 Yr C	Appearance After 7 Years at Kure Beach, NC
110	Tough pitch Cu	0.072	0.065	0.065	0.025	Brown film, smooth, slight patina near edges
			Tin			
505	Phos. bronze, 1.25% Sn	0.083	0.042	0.069	0.017	"Mink brown", slight patina
510	Phos. bronze, 5% Sn	0.150	0.088	0.099	--	Maroon film, heavy etch
			Aluminum			
637	Alum. bronze	0.017	0.009	0.013	--	Light tan film, smooth
			Nickel			
--	1.85 Ni, 0.03 Fe	0.134	0.145	0.044	0.036	Dark brown, mottled with green at edges
704	6.34 Ni, 0.01 Fe	0.069	0.052	0.033	--	Dark brown, plus patina streaks on panel face
707	9.16 Ni, 0.18 Fe	0.052	0.039	0.038	--	Uniform maroon with patina at edges
711	22.76 Ni, 0.04 Fe	0.036	0.024	0.031	--	Greenish brown, green near edges, slight etch
--	42.75 Ni, 0.30 Fe	0.018	0.012	0.019	0.005	Greenish brown, slight green near edges
			Zinc			
420	Tin brass	0.058	0.042	0.024	--	Dark maroon, smooth
230	Red brass	0.051	0.038	0.033	0.026	Brown-maroon film, smooth
260	Cartridge brass	0.034	0.023	0.030	0.017	Brown-maroon film, smooth, very slight patina
			Nickel-Zinc			
745	10% nickel-silver	0.030	0.020	0.024	0.010	Brown with slight patina film in center, green near edges, smooth
752	18% nickel-silver	0.030	0.020	0.021	--	Brown film in center, green near edges, smooth

(a) Copper Development Association number; see Appendix H for nominal alloy compositions.
(b) A = 80-foot lot, Kure Beach, NC.
(c) C = Point Reyes, CA.

TABLE 8-3. CORROSION RATES OF COPPER AND COPPER ALLOYS IN MARINE ATMOSPHERES BASED ON LOSS IN WEIGHT AFTER 10 AND 20 YEARS' EXPOSURE[5]

CDA No.[a]	Alloy	Corrosion Rate, mpy					
		Sandy Hook, NJ		La Jolla, CA		Key West, FL	
		10 Yr	20 Yr	10 Yr	20 Yr	10 Yr	20 Yr
110	Electrolytic tough pitch copper	0.028	--[b]	0.056	0.050	0.022	0.025
122	Phosphorized copper	0.028	--	0.046	0.055	0.021	0.020
655	Silicon bronze, 3.1% Si, 1.1% Mn	0.045	--	0.078	0.053	0.040	--
521	Phosphor bronze, 8% Sn, 0.1% P	0.050	--	0.089	0.092	0.031	0.028
614	Aluminum bronze, 8% Al	0.056	0.047	0.008	0.006	0.012	0.002
	High-tensile brass, 20-24% Zn, 2.5-5% Mn, 3-7% Al, 2-4% Fe	0.113	0.178	0.078	0.089	0.068	0.078
230	Red brass, 15% Zn	0.047	--	0.023	0.011	0.020	0.017
260	70-30 brass, 30% Zn	0.039	--	0.011	0.006	0.015	0.009
442	Admiralty metal, 29% Zn, 1% Sn	0.039	--	0.011	0.006	0.015	0.009
732	Copper-nickel-zinc, 75% Cu, 20% Ni, 5% Zn	0.042	--	0.013	0.016	0.012	0.010
	Copper-nickel-tin, 70% Cu, 29% Ni, 1% Sn	0.045	--	0.011	0.014	0.014	0.011

(a) See Appendix H, Table H-1, for nominal alloy compositions.
(b) Dash denotes 20-year specimens lost.

The high-zinc brasses (naval brass, Muntz metal, and manganese brass), although exhibiting low rates of penetration on the basis of weight loss, were found in studies by Hummer[1] to have lost considerably more strength than other alloys in the series (see Table 8-3). Although not indicated by Hummer, et al.[1] these materials may have exhibited dezincification as a result of exposure to the marine environment. Indeed Landegren and Mattsson[6] reported significant dezincification of Cu-37Zn deep-drawn cups following exposure for 121 months at a marine test site in Sweden, see Table 8-4. For single-phase brasses, the attack can be controlled by small additions of arsenic, antimony, or phosphorus.

TABLE 8-4. MAXIMUM DEZINCIFICATION DEPTH FOUND ON METALLOGRAPHIC EXAMINATION OF EXPOSED DEEP-DRAWN CUP SAMPLES OF Cu-37Zn FOLLOWING EXPOSURE AT THE TEST SITES INDICATED IN SWEDEN[6]

Specimen Characteristics				Maximum Dezincification Depth, μm					
				Cylindrical Part		Sloping Part		Bottom	
Annealing Temperature, C	Exposure Site	Rain Shelter	Time of Exposure, months	Outside	Inside	Outside	Inside	Outside	Inside
275	Arboga	*	121	0	0	0	0	0	0
275	Karlstad	*	121	0	0	0	0	0	0
275	Bohus Malmön	Yes	121	170	70	70	40	40	55
275	Bohus Malmön	No	121	55	40	40	40	55	55
275	Erken	Yes	121	140	40	40	0	40	70
275	Erken	No	121	40	30	0	15	0	15
275	Vanadis	Yes	121	270	185	100	55	100	130
275	Vanadis	No	121	85	40	30	30	0	55
--	Bohus Malmön	Yes	85	140	140	40	30	30	40
--	Bohus Malmön	No	121	55	40	70	55	55	55
200	Bohus Malmön	Yes	121	230	70	55	40	40	70
200	Bohus Malmön	No	121	100	55	70	40	55	40
325	Bohus Malmön	No	121	55	40	40	40	40	40

* Indoor heated facilities.

Test Site	Mean Annual Temperature, C	Precipitation, mm/year	Contaminants				pH Value of Precipitation
			In Air, $\mu g/m^3$		In Precipitation, $mg/m^2 \cdot month$		
			S	Cl	S	Cl	
Rural (Erken)	5.8	550	8	2	50	20	4.9
Marine (Bohus Malmön)	6.5	720	10	50	100	800	5.1
Urban (Vanadis)	6.6	550	70	4	180	60	4.7

About 0.02 percent arsenic is very effective. Note that in the study by Hummer,[1] Muntz metal, which contained 0.19 percent arsenic, showed significant loss of strength; in this two-phase alloy, the inhibitor apparently is not effective in preventing dezincification.

Copper-zinc alloys also are susceptible to stress-corrosion cracking in marine atmospheric environments. Landegren and Mattsson[6] exposed highly stressed specimens (deep drawn cups) of copper 37 zinc to indoor, urban, rural, and marine environments for up to 121 months. Results of the exposures given in Table 8-5 indicated that 95 percent of the unannealed specimens failed within about 120 months when exposed without shelter in a marine atmosphere. The sheltered marine atmosphere was more aggressive with 100 percent failures within 87 months. In general, the rural and urban environments were much more aggressive than the marine environments with 100 percent failures within a few months. For all environments, annealing was beneficial, presumably because the residual stresses within the cups were reduced, although the change in microstructure as a result of the heat treatment may also have affected the cracking susceptibility.

SPLASH AND TIDE

The corrosion behavior of copper alloys in the splash zone more nearly follows their performance in the atmosphere than in immersed conditions. As a general rule, any copper alloy that has good resistance to a severe marine atmosphere, such as Cristobal, Panama Canal Zone, will also do well in the splash zone.

Alloys exposed at mean tide show corrosion rates ranging from about 20 to 60 percent of those observed for alloys under fully immersed conditions. Thus, the behavior under fully immersed conditions can be used as a guide for the selection of a resistant alloy in a half-tide application. The resistance of an isolated* panel of copper in the tide zone is superior to that in the fully immersed condition, and is in marked contrast to the relatively poor behavior of an isolated steel panel at the half-tide level. Weight-loss curves for the half-tide performance of copper alloys after 16 years are given in Figure 8-1 and Table 8-1.

---

* Isolated in this context refers to a specimen exposed in one particular zone as opposed to a piling which passes through several zones.

TABLE 8-5. RESULTS OF FIELD TESTS OF DEEP-DRAWN CUPS OF Cu-37Zn; FIGURES GIVE THE PERCENTAGE OF CRACKED SPECIMENS OUT OF 20 REPLICATES AFTER THE INDICATED TIME OF EXPOSURE[6]

Specimen Variant	Inspection Without Pickling — Exposure Time, months														Inspection After Pickling
	1.5	3	5	9	12	17	25	36	52	61	78	87	101	121	121
Storehouse With Heating Facilities (Arboga)															
Without annealing	0	0	0	0	0	5	5	5	5	5	5	5	10	10	Pickling not required
Annealing 2 hr at temperature 200 C	0	0	0	0	0	0	0	0	0	0	0	0	0	0	
225 C	0	0	0	0	0	0	0	0	0	0	0	0	0	0	
250 C	0	0	0	0	0	0	0	0	0	0	0	0	0	0	
275 C	0	0	0	0	0	0	0	0	0	0	0	0	0	0	
300 C	0	0	0	0	0	0	0	0	0	0	0	0	0	0	
325 C	0	0	0	0	0	0	0	0	0	0	0	0	0	0	
Storehouse Without Heating Facilities (Karlstad)															
Without annealing	0	0	0	5	5	10	10	15	90	95	95	100	—	—	Pickling not required
Annealing 2 hr at temperature 200 C	0	0	0	0	0	0	0	0	0	0	0	0	0	50	
225 C	0	0	0	0	0	0	0	0	0	0	0	0	0	5	
250 C	0	0	0	0	0	0	0	0	0	0	0	0	0	0	
275 C	0	0	0	0	0	0	0	0	0	0	0	0	0	0	
300 C	0	0	0	0	0	0	0	0	0	0	0	0	0	0	
325 C	0	0	0	0	0	0	0	0	0	0	0	0	0	0	
Rural Atmosphere (Erken) Without Rain Shelter															
Without annealing	95	100	—	—	—	—	—	—	—	—	—	—	—	—	—
Annealing 2 hr at temperature 200 C	0	0	0	100	—	—	—	—	—	—	—	—	—	—	—
225 C	0	0	0	50	80	85	85	90	90	90	90	90	90	90	90
250 C	0	0	0	0	5	5	5	5	5	5	5	5	5	5	5
275 C	0	0	0	0	0	0	0	0	0	0	0	0	0	0	0
300 C	0	0	0	0	0	0	0	0	0	0	0	0	0	0	0
325 C	0	0	0	0	0	0	0	0	0	0	0	0	0	0	0

Table 8-5. (Continued)

Specimen Variant	Inspection Without Pickling — Exposure Time, months														Inspection After Pickling
	1.5	3	5	9	12	17	25	36	52	61	78	87	101	121	121
Rural Atmosphere (Erken) With Rain Shelter															
Without annealing	35	100	—	—	—	—	—	—	—	—	—	—	—	—	—
Annealing 2 hr at temperature 200 C	0	25	100	—	—	—	—	—	—	—	—	—	—	—	—
225 C	0	5	70	100	—	—	—	—	—	—	—	—	—	—	—
250 C	0	0	0	65	75	75	75	75	75	75	75	75	75	75	75
275 C	0	0	0	0	10	10	10	10	10	10	10	10	10	10	10
300 C	0	0	0	0	0	0	0	0	0	0	0	0	0	0	0
325 C	0	0	0	0	0	0	0	0	0	0	0	0	0	0	0
Urban Atmosphere (Vanadis) Without Rain Shelter															
Without annealing	100	—	—	—	—	—	—	—	—	—	—	—	—	—	—
Annealing 2 hr at temperature 200 C	5	70	100	—	—	—	—	—	—	—	—	—	—	—	—
225 C	0	10	100	—	—	—	—	—	—	—	—	—	—	—	—
250 C	0	0	20	100	—	—	—	—	—	—	—	—	—	—	—
275 C	0	0	0	0	0	0	10	10	10	10	10	10	10	10	10
300 C	0	0	0	0	0	0	0	0	0	0	0	0	0	0	0
325 C	0	0	0	0	0	0	0	0	0	0	0	0	0	0	0
Urban Atmosphere (Vanadis) With Rain Shelter															
Without annealing	100	—	—	—	—	—	—	—	—	—	—	—	—	—	—
Annealing 2 hr at temperature 200 C	100	—	—	—	—	—	—	—	—	—	—	—	—	—	—
225 C	85	90	90	100	—	—	—	—	—	—	—	—	—	—	—
250 C	0	20	45	95	95	95	100	—	—	—	—	—	—	—	—
275 C	0	0	0	10	30	30	75	85	90	95	95	95	95	95	95
300 C	0	0	0	0	0	0	0	0	0	0	0	0	0	0	0
325 C	0	0	0	0	0	0	0	0	0	0	0	0	0	0	0

Table 8-5. (Continued)

Specimen Variant	Inspection Without Pickling — Exposure Time, months														Inspection After Pickling
	1.5	3	5	9	12	17	25	36	52	61	78	87	101	121	121
Marine Atmosphere (Bohus Malmön) Without Rain Shelter															
Without annealing	0	0	0	60	60	60	60	70	70	70	75	85	85	95	95
Annealing 2 hr at temperature 200 C	0	0	0	0	0	0	0	0	0	0	0	0	0	0	5
225 C	0	0	0	0	0	0	0	0	0	0	0	0	0	0	0
250 C	0	0	0	0	0	0	0	0	0	0	0	0	0	0	0
275 C	0	0	0	0	0	0	0	0	0	0	0	0	0	0	0
300 C	0	0	0	0	0	0	0	0	0	0	0	0	0	0	0
325 C	0	0	0	0	0	0	0	0	0	0	0	0	0	0	0
Marine Atmosphere (Bohus Malmön) With Rain Shelter															
Without annealing	5	15	30	30	35	35	55	80	85	90	95	100	--	--	--
Annealing 2 hr at temperature 200 C	0	0	0	0	0	0	0	25	25	25	25	25	25	40	75
225 C	0	0	0	0	0	0	0	0	0	0	15	15	15	25	50
250 C	0	0	0	0	0	0	0	0	0	0	0	0	0	0	0
275 C	0	0	0	0	0	0	0	0	0	0	0	0	0	0	0
300 C	0	0	0	0	0	0	0	0	0	0	0	0	0	0	0
325 C	0	0	0	0	0	0	0	0	0	0	0	0	0	0	0

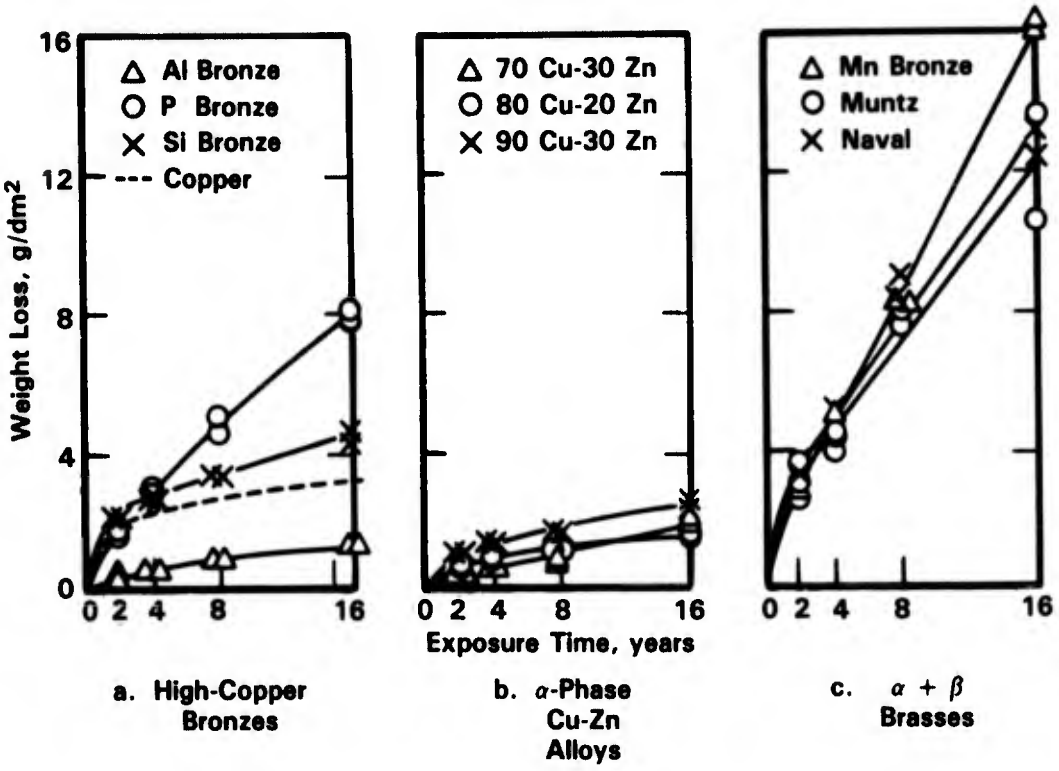

FIGURE 8-1. CORROSION WEIGHT LOSS AS A FUNCTION OF TIME FOR COPPER ALLOYS EXPOSED AT MEAN-TIDE ELEVATION IN TROPICAL SEAWATER[1]

IMMERSION

General and Pitting Corrosion

Effect of Alloy Composition

Typical general corrosion data for copper-base alloys in seawater are given in Table 8-1 and Figure 8-2 by Hummer, et al.[1] as well as Figures 8-3 to 8-9 from studies by Reinhart.[7] These data show that the corrosion rates calculated from weight loss for the copper-base alloys decrease with time and are generally less than 1 mill per year. For the brasses, depths of attack associated with dezincification are generally much greater (see section on dealloying).

The low and decreasing corrosion rates are attributed to the formation of protective films on the metal surfaces. These films are composed of copper oxides as well as oxychlorides of copper, copper carbonate, and calcareous material.[1]

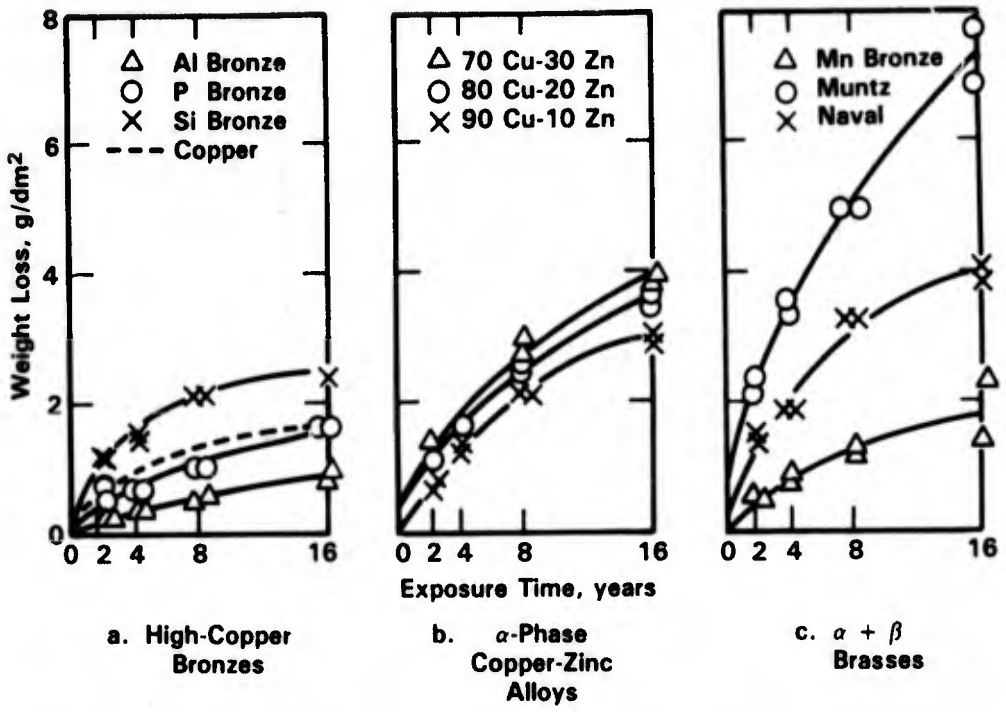

FIGURE 8-2. CORROSION WEIGHT LOSS AS A FUNCTION OF TIME FOR COPPER ALLOYS CONTINUOUSLY IMMERSED IN TROPICAL SEAWATER[1]

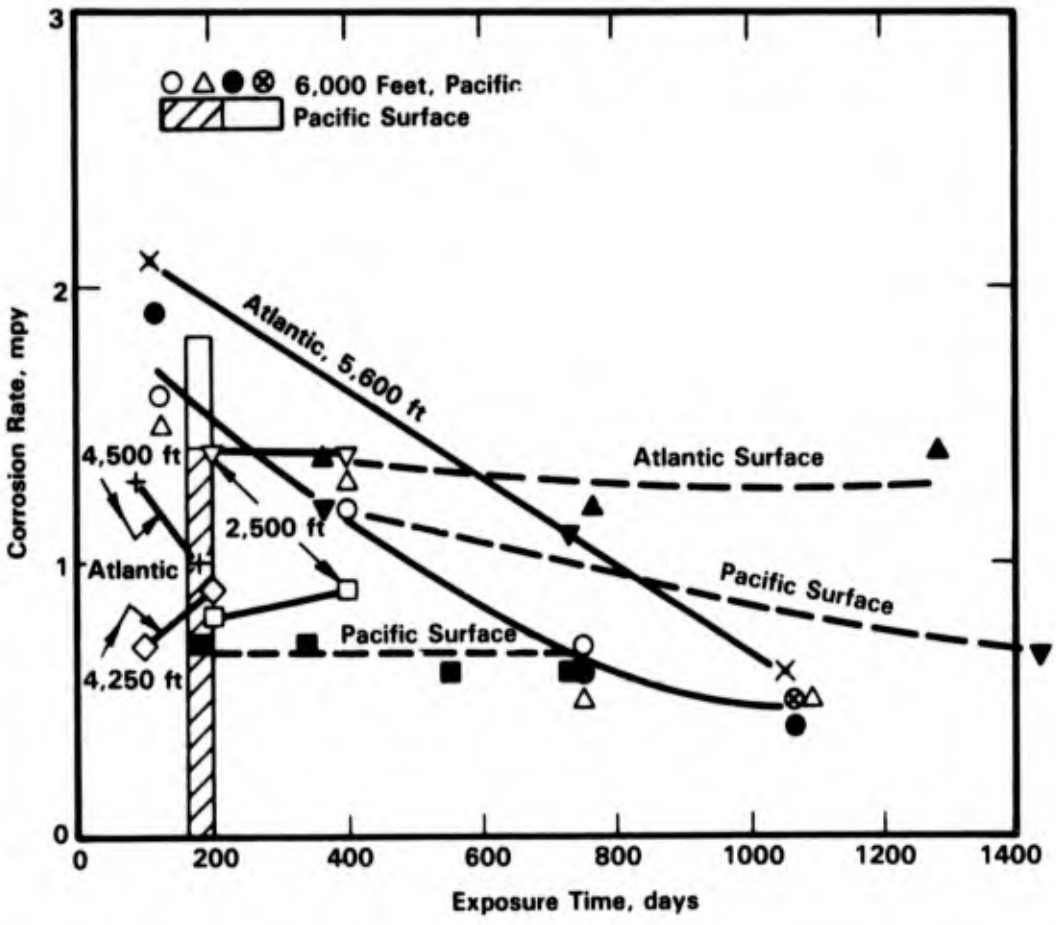

FIGURE 8-3. CORROSION RATES OF COPPER IN SEAWATER[7]

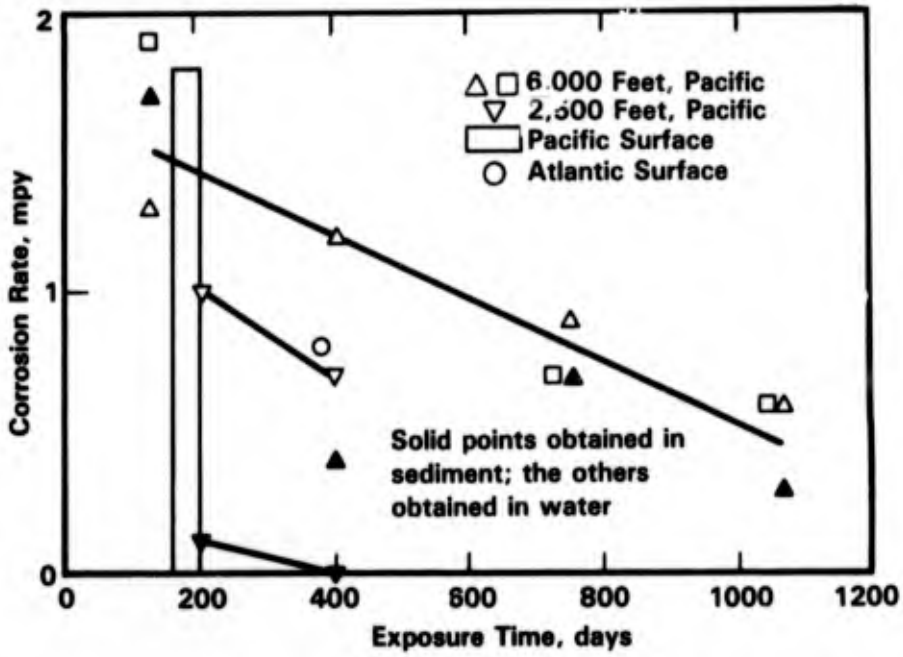

FIGURE 8-4. CORROSION RATES OF RED BRASS[7]

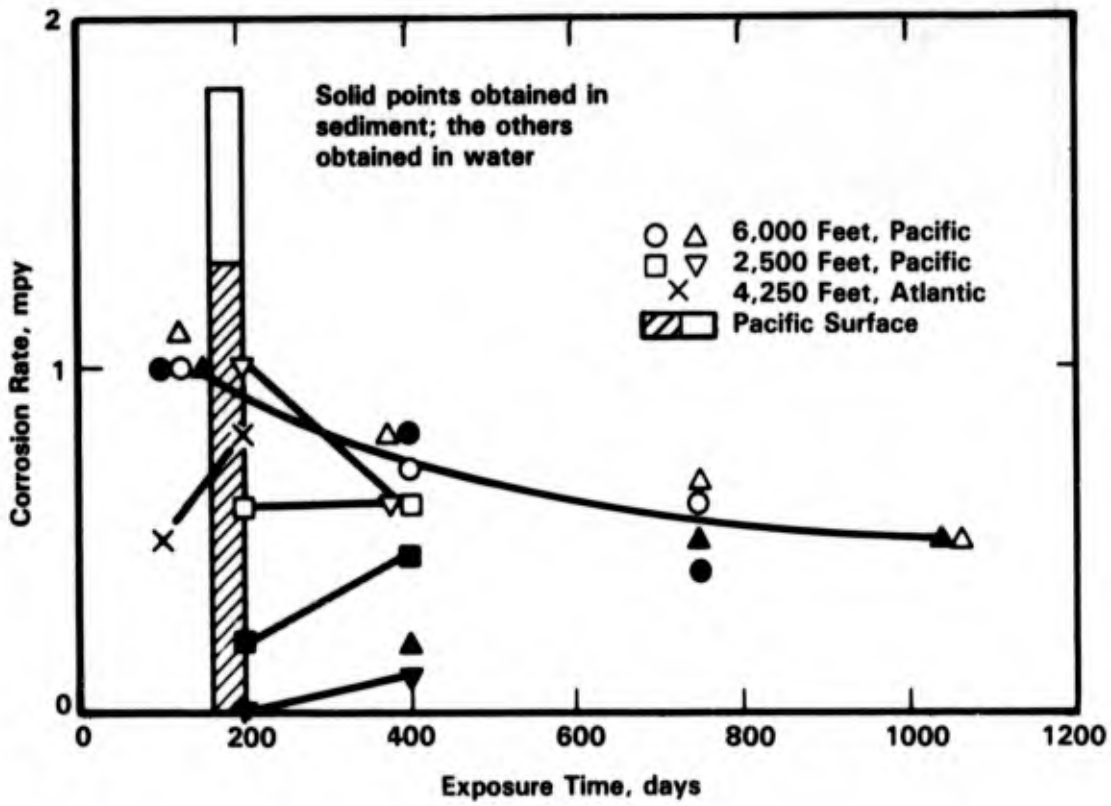

FIGURE 8-5. CORROSION RATES OF ARSENICAL ADMIRALTY BRASS[7]

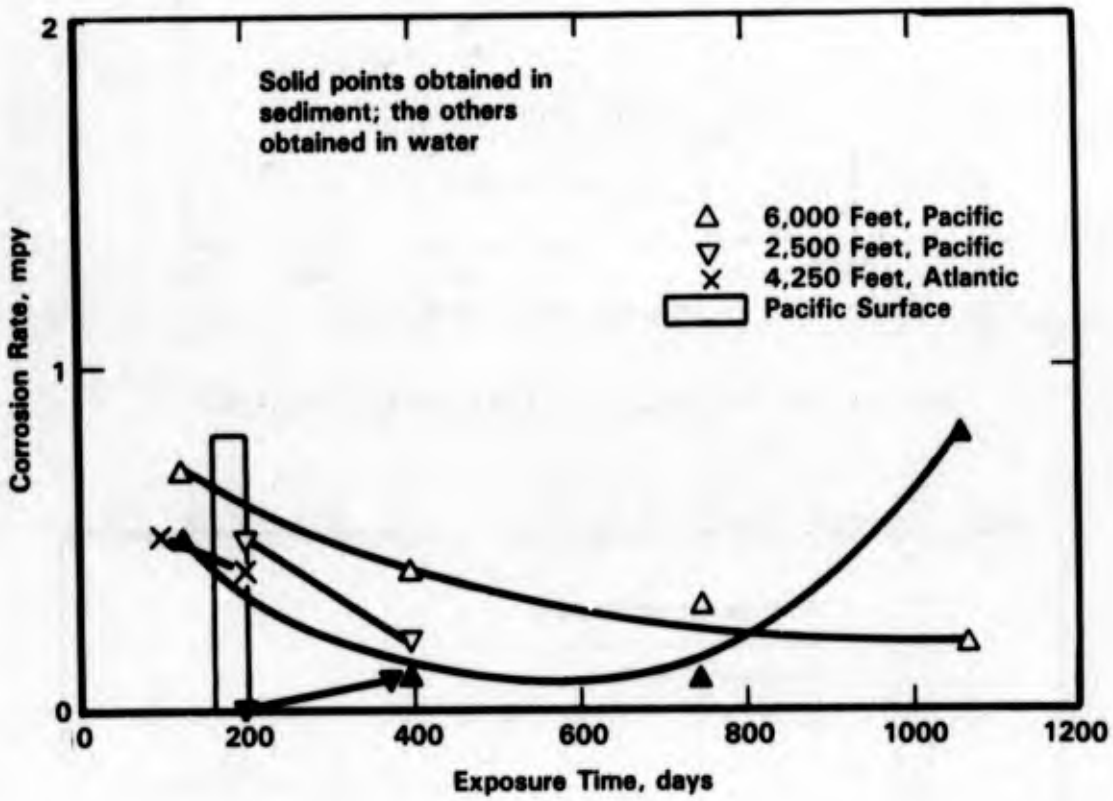

FIGURE 8-6. CORROSION RATES OF ALUMINUM BRASS[7]

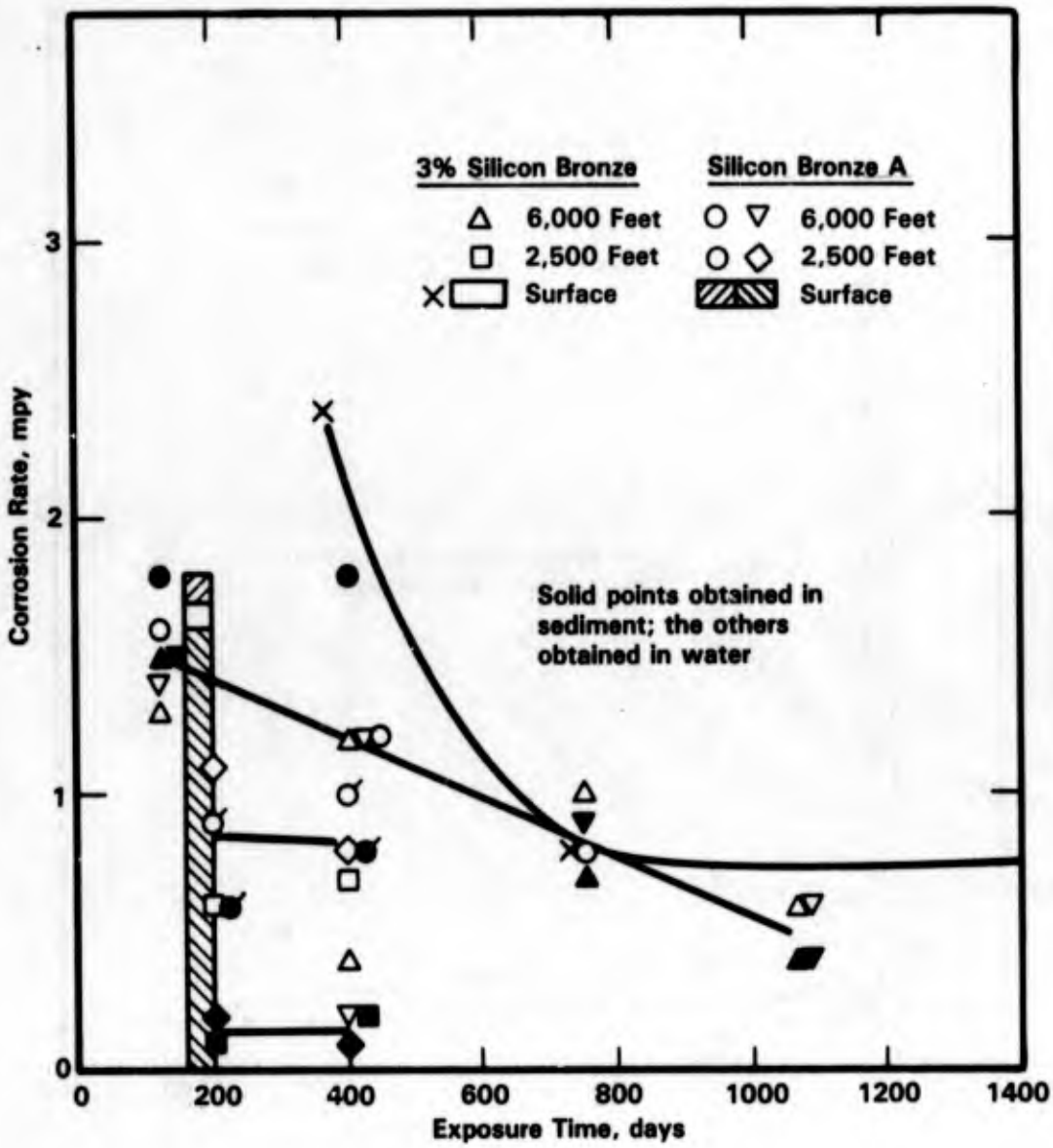

FIGURE 8-7. CORROSION RATES OF SILICON BRONZES IN THE PACIFIC OCEAN[7]

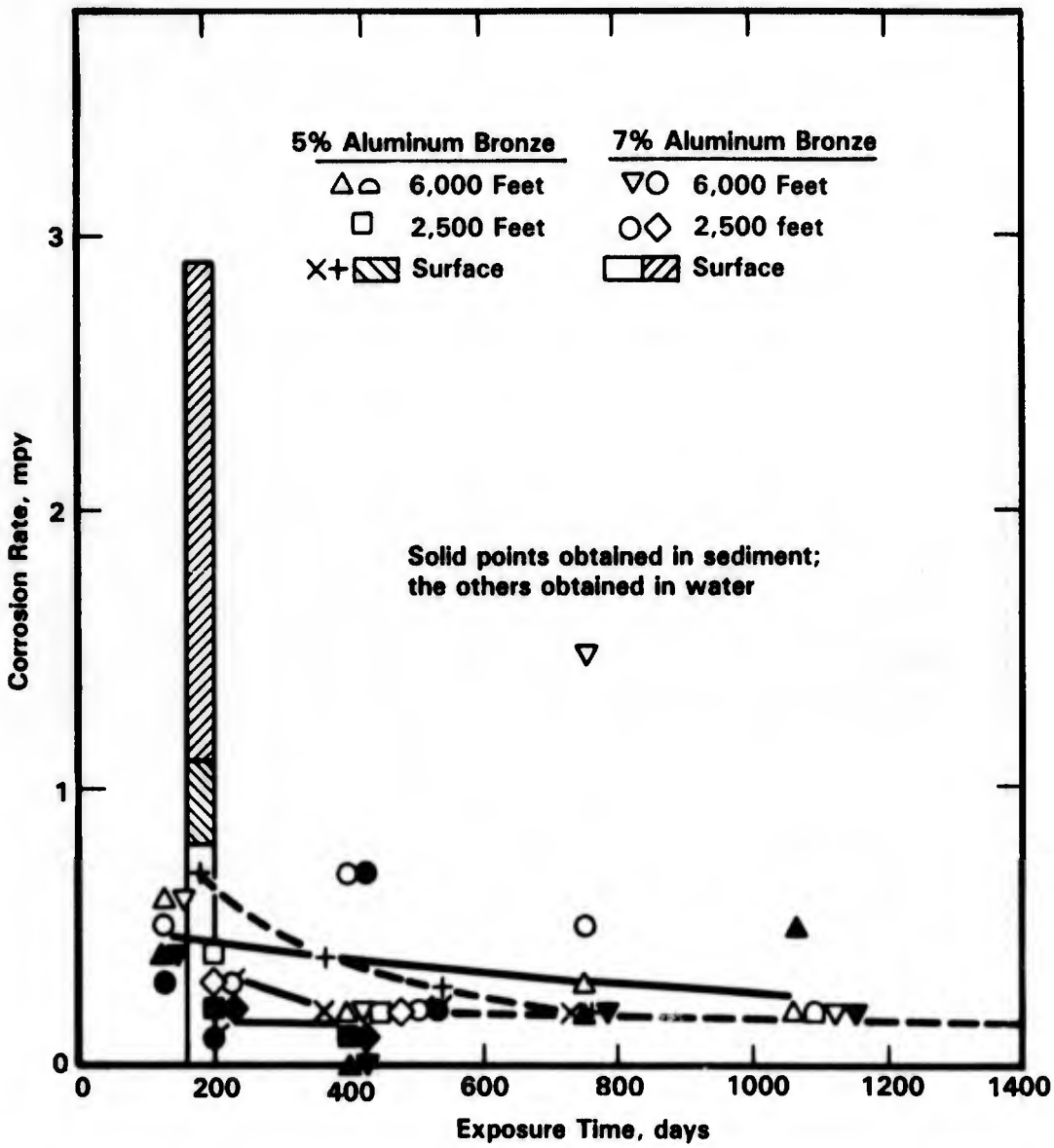

FIGURE 8-8. CORROSION RATES OF WROUGHT ALUMINUM BRONZES IN THE PACIFIC OCEAN[7]

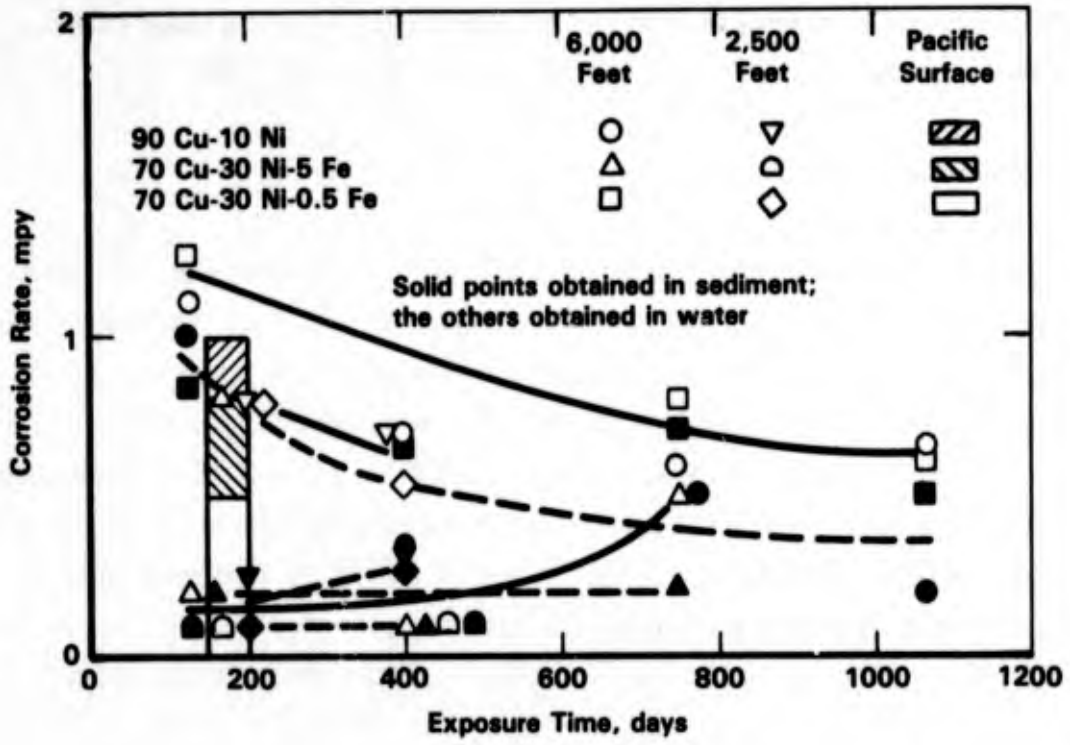

FIGURE 8-9. CORROSION RATES OF COPPER-NICKEL ALLOYS IN THE PACIFIC OCEAN[7]

The copper-base alloys also are susceptible to pitting under immersed conditions, as shown by the data in Table 8-1. However, few pitting failures of copper base alloys have been reported in heat exchanger application in nonpolluted seawater (EPRI NP-1468)[8] suggesting that pitting of copper-base alloys is not a serious problem for most fresh seawater applications.

Effect of Temperature

The corrosion rates for copper alloys usually increase, other factors being the same, as the temperature is raised. Pump impellers, condenser tubes, valves, etc., tend to corrode at higher rates in seawater at summer temperatures at Wrightsville Beach, NC, than at winter temperatures.[9] Copper alloys also show higher rates of attack in the warm waters of the Pacific Ocean near the Panama Canal Zone as compared with those obtained in waters off the coast of California. However, when the seawater is heated above ambient, corrosion rates of copper-base alloys may decrease as a result of the decrease in the oxygen concentration and the retrograde solubility of mineral scales. Data showing the effect of temperature on the

corrosion rate of several copper-base alloys in seawater over a temperature range of 130 to 250 F, are given in Figure 8-10.

Effect of Depth and Aeration

A comparison of corrosion rates for copper and copper-based alloys in the Pacific Ocean at 3 depths (surface, 2,340 feet, and 5,640 feet) is given in Figure 8-11. These data show that the corrosion rates of these alloys were generally a minimum at the 2,340 foot depth. These minimums in corrosion rate correspond to a minimum in the oxygen concentration-depth curve; the oxygen concentration was less than 0.5 ppm at 2,500 feet, about 1 ppm at 5,500 feet, and about 6 ppm at the surface. A similar correlation between oxygen content of seawater and corrosion of copper alloys was reported by Schreiber, et al.[12] for studies of heat exchanger tube materials in flowing seawater at elevated temperatures, see Figure 8-12.

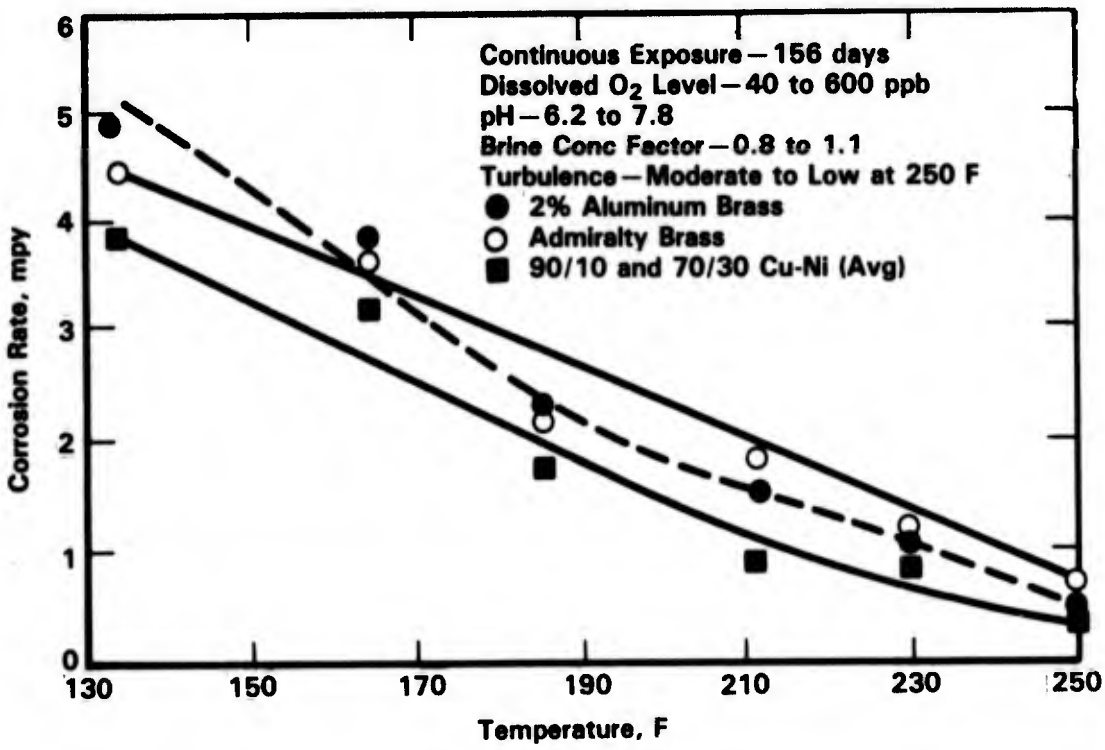

FIGURE 8-10. EFFECT OF TEMPERATURE ON CORROSION RATE OF COPPER-BASE HEAT-EXCHANGER TUBE MATERIALS IN DEAERATED SEAWATER AT FREEPORT PLANT[10]

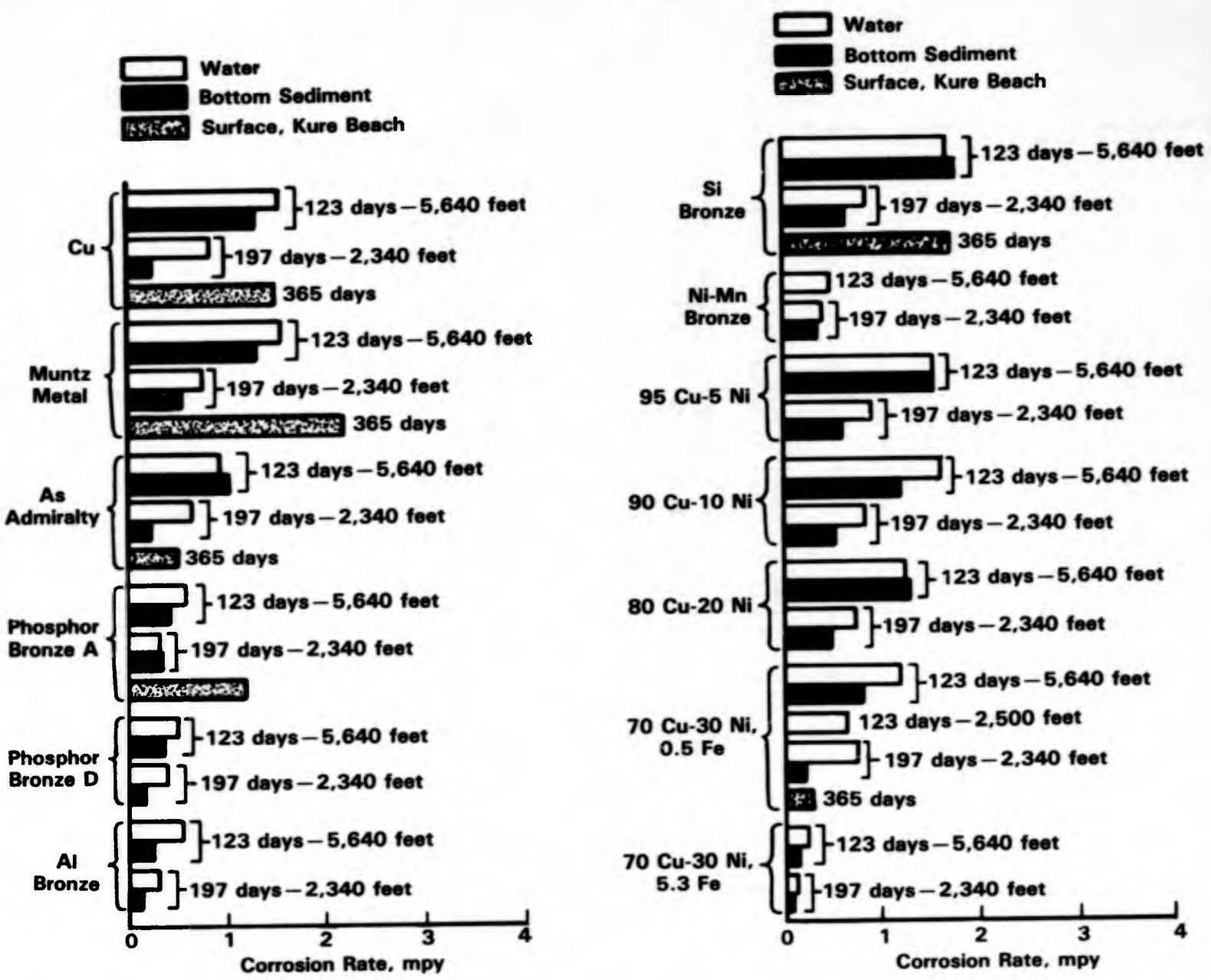

FIGURE 8-11. CORROSION OF COPPER ALLOYS FOR VARIOUS DEPTHS AND EXPOSURE TIMES NEAR PORT HUENEME, CA, IN THE PACIFIC OCEAN(11)

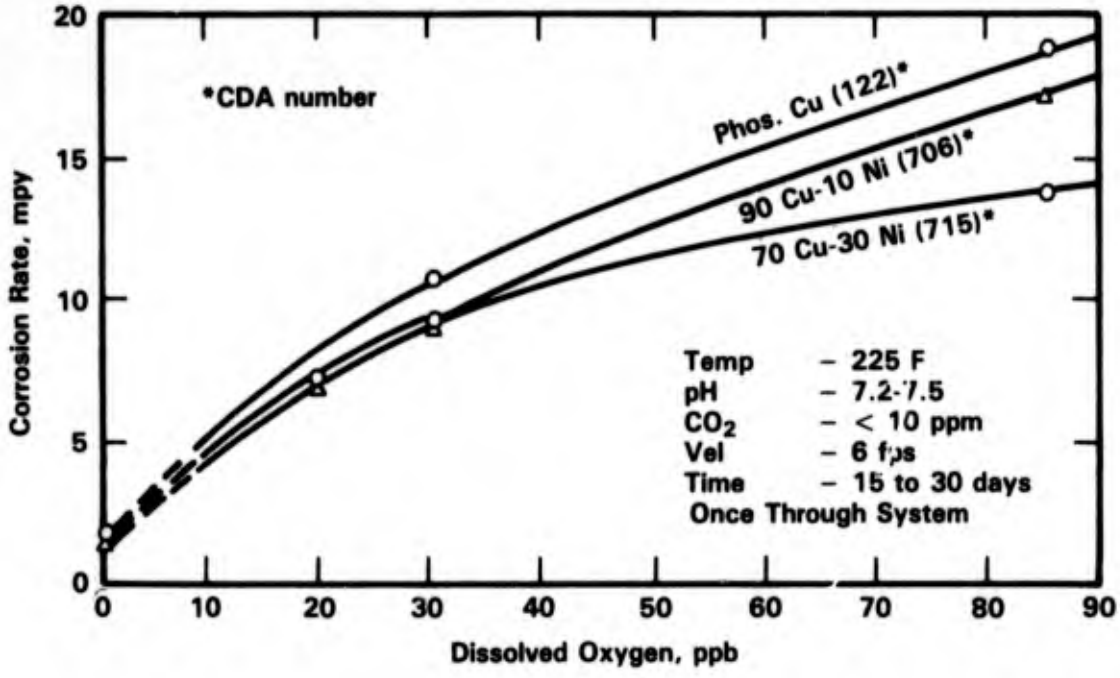

FIGURE 8-12. EFFECT OF DISSOLVED OXYGEN IN SEAWATER ON THE CORROSION RATE OF COPPER ALLOYS[12]

Effect of Velocity

Copper and its alloys are highly sensitive to velocity effects in seawater. According to Kershul,[13] tube inlet corrosion from high velocity or turbulent seawater is one of the main causes of copper alloy tube leakage in condensers of power plants. For additional information, see section on Erosion-Corrosion.

Effect of Biological Fouling

It is well established that the byproducts generated by fouling organisms or their decay products will promote the localized attack of copper-base alloys. Rogers[14] evaluated the effect of a variety of microorganisms and of their byproducts, such as cystine on the corrosion of copper-base alloys and found, in all cases, that localized attack was promoted. However, the attack only occurs if the organisms are able to attach and grow on the metal surface. LaQue and Clapp[15] found that pitting of copper-nickel alloys occurred in quiescent seawater under macroorganisms, following their death. The severity of fouling and of pitting increased with increasing nickel content of the alloys. Pitting only occurred in alloys containing 40 percent or more nickel; whereas, no fouling occurred on copper and on copper-20 nickel and

only incipient fouling occurred on copper-30 nickel. The alloys that fouled showed increases in corrosion rates with exposure time; whereas the opposite was true of the alloys that did not foul. The relationship between fouling, pitting, and the nickel content of the alloys was associated with the general corrosion rate which provided sufficient copper in solution to poison the organisms and prevent their attachment to the metal surface. On alloys of low nickel content where the general corrosion rate was greater, fouling and resulting pitting did not occur.

In flowing seawater, fouling and pitting, that is associated with fouling is less severe. A discussion of the influence of water velocity on fouling is given by Clapp[16] where it is stated that the minimum velocity required to prevent macrofouling is between about 1 to 2 m/s.

Effect of Pollution

The corrosion performance of copper-base alloys is greatly affected by seawater pollution. The presence of sulfide in the polluted seawater has a pronounced adverse effect. At low concentration, the sulfide promotes pitting; whereas, at higher concentration, high rates of general attack are observed. Data showing the corrosion rates of several copper alloys in polluted and unpolluted seawater are given in Tables 8-6 and 8-7. These data

TABLE 8-6. CORROSION OF CONDENSER TUBES IN POLLUTED AND CLEAN SEAWATER[17]

Velocity, 7.5 fps
Duration, 64 days

Alloy	Copper Development Association (CDA) No.[a]	Corrosion Rate, mpy	
		Clean Seawater	Polluted Seawater (3 pm H_2S)
90Cu-10Ni[b]	706	3	34
70Cu-30Ni[b]	715	5	26
2% Al brass	687	3	22
6% Al brass	608	5	21
As Admiralty brass	443	13	35
Phosphor copper	122	14	105

(a) See Appendix H, Table H-1, for nominal alloy compositions.

(b) Of the two alloys, 70Cu-30Ni alloy is usually preferred for more extreme conditions because of its superior corrosion resistance. However, in stagnant seawater, it has a greater tendency to pit than does the 90Cu-10Ni alloy.

TABLE 8-7. RESULTS OF SULFIDE SEAWATER EXPOSURES[18]

Alloy Compositions are Given in Appendix H, Table H-2

Alloy	Sulfide Concentration for 30-Days Exposure							
	0.0 mg/l		0.01 mg/l		0.05 mg/l		0.2 mg/l	
	Corrosion Rate, μm/yr	Depth of Attack, mm	Corrosion Rate, μm/yr	Depth of Attack, mm	Corrosion Rate, μm/yr	Depth of Attack, mm	Corrosion Rate, μm/yr	Depth of Attack, mm
Ni-Al-Bronze (Wrought)	157.8	0.11	122.5	0.09	572.6	0.42	1668.1	0.96
Ni-Al-Bronze (Cast)	158.0	0.10					1654.0	1.27
Mn-Ni-Al-Bronze (Cast)	41.0	0.09	76.3	0.24	251.2	0.27	484.1	0.20
Mn Bronze	140.6	0.31	195.5	0.32	445.4	0.30	803.9	0.26
Bronze Comp M	129.8	0.13	253.2	0.22	291.8	0.40	1037.0	1.01
Bronze Comp G	95.9	0.07	196.5	0.21	375.2	0.47	1694.2	0.50
90-10	95.9	0.09	170.1	0.18	231.3	0.25	664.0	0.58
90-10 + Sn	74.9	0.05					558.8	0.29
70-30	207.9	0.12	214.5	0.38	467.0	0.78	836.9	1.02
70-30 + Cr (CA719)	84.9	0.06	175.6	0.36	587.5	0.41	1480.3	0.53
Monel 411 (Cast)	6.7	0.07	257.0	0.22	865.5	0.39	1362.5	0.27
Monel 400 (Wrought)	2.5	0.04	14.4	0.05	10.6	0.15	59.7	0.18
K-Monel	1.7	0.07	3.3	0.16	3.4	0.20	41.2	0.29
316 Stainless Steel	0	0	0	0	0.2	0	0.7	0
Al-Bronze D	184.3	0.09	181.4	0.28	300.2	0.46	1314.2	1.13
Ph-Bronze + 5% Sn	70.6	0.08	286.6	0.15	415.5	0.23	629.5	0.41
PH-Bronze + 10% Sn	75.5	0.06	279.1	0.17	265.7	0.28	409.0	0.30

TABLE 8-7. (Continued)

Alloy	Sulfide Concentration for 60-Days Exposure						Sulfide Concentration for 120-Days Exposure					
	0.0 mg/l		0.01 mg/l		0.05 mg/l		0.0 mg/l		0.01 mg/l		0.05 mg/l	
	Corrosion Rate, µm/yr	Depth of Attack, mm	Corrosion Rate, µm/yr	Depth of Attack, mm	Corrosion Rate, µm/yr	Depth of Attack, mm	Corrosion Rate, µm/yr	Depth of Attack, mm	Corrosion Rate, µm/yr	Depth of Attack, mm	Corrosion Rate, µm/yr	Depth of Attack, mm
Ni-Al-Bronze (Wrought)	130.4	0.10	241.2	0.49	602.4	1.23	106.3	0.24	202.3	1.27	517.1	1.17
Ni-Al-Bronze (Cast)							101.0	0.51	223.4	1.12	381.1	1.39
Mn-Ni-Al-Bronze (Cast)	16.9	0.09	53.6	0.15	179.4	0.42	18.1	0.08 (0.94)	27.7	0.10	84.1	0.37
Mn Bronze	144.6	0.63	119.2	0.56	483.2	0.82	87.6	1.06	91.7	0.67	301.9	0.64
Bronze Comp M	152.0	0.20	212.2	0.69	363.1	0.76	160.6	0.49	185.2	0.66	351.6	1.18
Bronze Comp G	95.4	0.13	230.5	0.36	436.4	0.79	124.1	0.52	205.2	Perf	474.7	Perf
90-10	96.5	0.14	174.4	0.39	221.2	0.50	91.9	0.24	126.6	0.56	268.7	1.20
90-10 + Sn							79.0	0.12	143.8	0.39	220.2	0.86
70-30	209.9	0.22	245.2	0.80	517.7	1.25	190.0	0.39	137.9	0.55	569.2	1.49
70-30 + Cr (CA719)	68.8	0.06	258.5	0.45	640.6	0.68	53.1	0.28	302.2	0.87	610.7	1.74
Monel 411 (Cast)	11.3	0.19	298.3	0.55	678.1	0.67	10.0	0.52	344.5	1.08	839.8	Perf
Monel 400 (Wrought)	3.4	0.10	14.1	0.21	23.1	0.28	2.8	0.40	25.9	0.49	44.7	0.44
K-Monel	3.4	0.38	14.7	0.40	51.5	0.35	3.3	0.48	22.5	0.84	40.5	0.88
316 Stainless Steel	0.2	0	0.3	0	0.5	0	0	0	0.5	0.12	0.1	0

indicate that even the normally corrosion resistant Cu-Ni alloys are highly susceptible to accelerated attack in the presence of H_2S.

Gudas and Hack[19] performed a parametic study of the effect of sulfide concentration, seawater velocity, and duration of sulfide exposure on corrosion of Cu-10Ni and Cu-30Ni. All exposures were conducted in fresh seawater, with the sulfide concentration varying from 0.007 to 0.25 mg/l, seawater velocity after sulfide exposure of 0.5 to 5.3 m/s, and sulfide exposure times of 1 to 90 days. Results of exposures carried out at 0.01 to 0.25 mg/l sulfide concentration are summarized in Tables 8-8 and 8-9. These data show that the sensitivity to attack increased with increasing sulfide concentration over the range studied; subsequent tests at lower concentrations, down to 0.007 mg/l, indicated significant localized attack of both alloys, although Cu-30Ni was more resistant in long term exposures to low concentrations of sulfide. These data also show that where sulfide exposure conditions were sufficient to initiate attack, the seawater velocity dependence was minimal over the range of 0.5 to 5.3 m/s. Finally, exposure time to sulfide and sulfide concentration were found to be interrelated. For sulfide concentrations of 0.01 mg/l or less, 30 day exposures were required to promote subsequent accelerated attack in fresh seawater; whereas short term exposures of 1 to 5 days at high sulfide concentrations promoted accelerated attack; greater than 1 mg/l.

Subsequent studies by Hack and Gudas[20] were carried out to determine the effectiveness of the ferrous ion in inhibiting sulfide induced attack of the copper-nickel alloys. A summary of the matrix of experiments is given in Table 8-10 and results of the 90 day exposures with no preexposure to sulfide are given in Figures 8-13 and 8-14. These data show that 0.2 mg/l Fe^{++} was effective in reducing attack, although the effect of sulfide was not completely mitigated. Similarly, in tests where the specimens were pre-exposed to sulfide, with no ferrous ions, the subsequent accelerated attack was reduced but not eliminated by the ferrous ions. A number of researchers have investigated the mechanism of accelerated attack of copper-base alloys by sulfide.[21-27] Although details of mechanisms proposed by the different researchers vary, the general picture which emerges is that the sulfide interferes with the formation of the protective films on the surface of the copper-base alloys and, in addition, catalyzes the oxygen reduction reaction. The morphology of the attack is dependent upon the concentration and distribution of the sulfide which, in turn, is dependent upon the concentration of the sulfide in the seawater and the prior history of the specimen.

TABLE 8-8. RESULTS OF EXPOSURES OF Cu-10Ni TO SULFIDE-CONTAINING SEAWATER FOR A TOTAL EXPOSURE PERIOD OF 90 DAYS[19]

Sulfide Concentration, mg/l	Velocity, m/s	Exposure to Sulfide-Containing Seawater, days																					
		0				1				3				5				10				25			
		Rate, μm/yr		Depth, mm		Rate, μm/yr		Depth, mm		Rate, μm/yr		Depth, mm		Rate, μm/yr		Depth, mm		Rate, μm/yr		Depth, mm		Rate, μm/yr		Depth, mm	
0.01	2	30	29	0	0.02	23	23	0.02	0.02	29	30	0.08	0.02	37	38	0.02	0.05	61	64	0.11	0.09	116	101	0	0.02
	5	55	70	0.13	0.23	31	35	0.19	0.18	44	40	0.18	0.15	43	48	0.03	0.13	64	69	0.16	0.21	93	96	0.07	0.21
	7	100	80	0.46	0.38	56	67	0.38	0.69	62	64	0.36	0.46	73	78	0.19	0.25	62	72	0.36	0.28	94	95	0.14	0.12
	11	178	192	0.25	0.48	55	73	0.48	0.61	133	135	0.46	0.43	84	105	0.51	0.56	69	80	0.53	0.56	93	93	0.14	0.08
	14	219	221	0.25	0.30	113	106	0.36	0.46	112	119	0.46	0.43	126	125	0.38	0.43	78	106	0.48	0.48	96	95	0.14	0.12
0.03	2	24	24	0.01	0	24	24	0.04	0.05	21	21	0.01	0	20	23	0.07	0.07	72	74	0.04	0.06	89	99	0.05	0.09
	5	34	37	0.15	0.50	32	32	0.09	0.10	35	34	0.13	0.15	22	21	0.01	0.01	68	71	0.15	0.11	84	90	0.15	0.50
	7	59	49	0.22	0.32	65	68	0.18	0.27	55	56	0.32	0.36	22	28	0.02	0.09	65	72	0.37	0.24	66	72	0.08	0.16
	11	107	102	0.33	0.37	67	82	0.29	0.38	104	111	0.23	0.18	31	35	0.32	0.49	70	57	0.28	0.22	80	77	0.20	0.17
	14	144	129	0.30	0.31	165	165	0.17	0.15	94	86	0.18	0.24	22	26	0.21	0.22	64	68	0.26	0.39	89	79	0.29	0.33
0.05	2	24	24	0.01	0	30	30	0.03	0.06	37	31	0.04	0.02	65	69	0.10	0.08	103	136	0.21	0.46	252	213	0.60	0.81
	5	34	37	0.11	0.07	43	40	0.08	0.12	45	46	0.26	0.26	58	56	0.31	0.16	94	103	0.50	0.34	337	177	0.47	0.29
	7	59	49	0.22	0.32	69	77	0.17	0.25	93	69	0.33	0.31	93	67	0.33	0.57	127	112	0.42	0.35	155	149	0.34	0.50
	11	107	103	0.33	0.47	112	109	0.27	0.33	110	115	0.32	0.48	146	127	0.26	0.27	101	94	0.55	0.56	262	240	0.47	0.39
	14	144	129	0.30	0.31	94	104	0.23	0.28	123	107	0.21	0.23	112	126	0.23	0.23	91	85	0.26	0.51	171	176	0.40	0.33
0.10	2	30	29	0	0.02	42	41	0.04	0.07	65	64	0.09	0.05	69	81	0.04	0.11	110	168	0.66	0.69	276	192	1.26	0.24
	5	55	70	0.13	0.24	48	53	0.16	0.09	76	73	0.21	0.14	83	65	0.09	0.09	136	144	0.10	0.12	394	302	0.60	0.26
	7	100	80	0.46	0.39	59	62	0.15	0.30	125	128	0.31	0.47	80	87	0.12	0.11	149	197	0.50	0.68	320	411	0.30	0.49
	11	178	193	0.25	0.47	73	78	0.37	0.43	142	123	0.47	0.50	118	90	0.16	0.17	101	167	0.42	0.41	559	297	0.46	0.33
	14	219	221	0.25	0.31	99	103	0.49	0.55	167	177	0.47	0.44	127	134	0.13	0.51	125	122	0.38	0.25	225	135	0.47	0.08
0.25	2	24	24	0	0	57	62	0.15	0.11	125	117	0.16	0.09	245	240	0.45	0.46	759	607	1.30	1.29	353	455	0.76	0.73
	5	40	40	0	0	59	58	0.13	0.30	122	121	0.21	0.18	250	289	0.55	0.70	488	437	1.31	0.95	594	417	0.63	0.68
	7	48	50	0.12	0.06	59	65	0.40	0.19	161	184	0.92	0.87	195	229	0.58	0.71	551	579	1.30	1.29	782	767	1.29	1.28
	11	104	105	0.27	0.30	58	62	0.28	0.33	145	155	0.99	0.89	105	223	0.83	0.87	471	450	1.36	1.29	491	312	0.96	0.35
	14	287	306	0.34	0.50	183	203	0.78	0.88	111	128	1.30	1.30	209	187	0.87	1.16	277	450	0.76	0.84	356	279	0.47	0.76

TABLE 8-9. RESULTS OF EXPOSURES OF Cu-30Ni TO SULFIDE-CONTAINING SEAWATER FOR A TOTAL EXPOSURE PERIOD OF 90 DAYS[19]

Sulfide Concentration, mg/l	Velocity, m/s	Exposure to Sulfide-Containing Seawater, days																							
		0				1				3				5				10				25			
		Rate, μm/yr		Depth, mm		Rate, μm/yr		Depth, mm		Rate, μm/yr		Depth, mm		Rate, μm/yr		Depth, mm		Rate, μm/yr		Depth, mm		Rate, μm/yr		Depth, mm	
0.01	2	24	21	0.02	0.03	22	24	0.02	0.02	32	29	0.01	0.01	42	42	0.04	0.03	52	62	0.05	0.02	224	194	0.10	0.13
	5	55	42	0.05	0.05	39	40	0.10	0.11	41	35	0.05	0.02	41	42	0.03	0.06	57	54	0.03	0.03	209	219	0.36	0.40
	7	46	44	0.02	0	72	70	0.26	0.28	83	55	0.27	0.18	50	46	0.11	0.19	46	41	0.25	0.03	218	126	0.04	0.04
	11	110	94	0.05	0.03	161	214	0.45	0.33	185	112	0.40	0.38	59	64	0.32	0.43	46	37	0.05	0.05	185	203	0.28	0.13
	14	287	208	0.26	0.22	169	166	0.26	0.26	191	185	0.35	0.41	210	140	0.40	0.36	49	46	0.04	0.04	219	163	0.44	0.34
0.03	2	21	23	0	0	16	16	0.01	0.02	9	9	0.03	0	23	22	0.02	0.02	149	145	0.23	0.10	176	158	0.45	0.22
	5	56	54	0.09	0.09	23	14	0.02	0.02	11	11	0	0.03	20	20	0.01	0.01	299	231	0.26	0.28	209	151	0.52	0.20
	7	76	81	0.13	0.13	25	29	0.20	0.03	13	11	0.07	0.03	25	24	0.02	0.02	202	216	0.67	0.32	204	228	0.35	0.38
	11	122	146	0.40	0.12	33	29	0.11	0.07	9	13	0.07	0.08	23	27	0.08	0.10	105	175	0.24	0.28	250	257	0.44	0.30
	14	224	234	0.33	0.30	30	20	0.01	0.01	14	14	0.24	0.18	27	24	0.09	0.10	198	72	0.20	0.08	191	162	0.52	0.37
0.05	2	21	23	0	0	13	16	0.04	0.03	70	83	0.03	0.06	72	94	0.22	0.04	181	166	0.21	0.20	259	330	0.51	0.33
	5	56	54	0.09	0.09	26	20	0.03	0.05	127	91	0.21	0.04	114	125	0.15	0.45	346	356	0.74	0.26	340	307	0.53	0.56
	7	76	81	0.13	0.13	21	21	0.05	0.04	79	61	0.18	0.03	201	158	0.25	0.35	301	300	0.95	0.38	414	414	0.51	0.69
	11	122	146	0.40	0.12	46	52	0.28	0.18	71	102	0.25	0.37	64	114	0.32	0.28	248	316	0.53	0.52	320	335	0.55	0.80
	14	224	234	0.33	0.30	49	40	0.23	0.29	43	27	0.41	0.12	50	47	0.25	0.14	197	190	0.66	0.39	310	310	0.48	0.60
0.10	2	24	21	0.02	0.03	274	234	0.24	0.11	363	277	0.25	0.19	295	356	0.27	0.38	345	312	0.54	0.29	300	315	0.50	0.34
	5	55	47	0.05	0.06	257	257	0.11	0.30	378	391	0.66	0.44	381	457	0.33	0.35	318	380	0.41	0.38	351	302	0.28	0.28
	7	46	43	0.02	0	254	207	0.13	0.69	328	321	0.64	0.97	307	254	0.12	0.08	432	434	0.79	0.25	345	384	0.38	0.33
	11	110	94	0.05	0.03	182	164	0.28	0.05	321	343	0.73	0.66	253	236	0.46	0.13	368	373	0.50	0.41	396	429	0.37	0.51
	14	287	226	0.26	0.22	46	100	0.05	0.30	175	238	0.52	0.68	146	178	0.37	0.13	343	292	0.30	0.21	366	366	0.18	0.20
0.25	2	25	22	0	0	109	99	0.16	0.21	259	279	0.41	0.42	300	351	0.30	0.35	394	640	0.24	0.26	318	300	0.40	0.34
	5	48	41	0.05	0.03	78	68	0.19	0.25	378	340	0.64	0.68	691	940	0.69	0.94	643	770	0.35	0.43	305	599	0.43	0.90
	7	60	63	0.11	0.10	116	96	0.60	0.26	523	498	0.30	0.28	450	361	0.70	0.36	701	749	0.70	0.74	511	511	0.50	0.43
	11	93	91	0.07	0.06	95	99	0.16	0.53	483	465	0.50	0.42	650	739	0.65	0.74	897	864	1.31	0.94	353	424	0.38	0.43
	14	404	422	0.48	0.42	35	40	0.29	0.13	437	406	1.17	1.05	201	650	0.42	0.65	559	630	0.78	1.19	508	488	1.39	0.61

TABLE 8-10. EXPOSURE MATRIX FOR STUDY BY HACK AND GUDAS[20]

Sulfide Ions, mg/l	Ferrous Ions, mg/l*			
	0	0.01	0.05	0.2
0	N, P	N	N	N
0.01	N	N, P	N, P	N, P
0.05	N	N	N	N
2.4 m/s 30, 60, 90 days				

* P - preexposure 0.2 mg/l sulfide for 5 days without ferrous ions, and N - no preexposure.

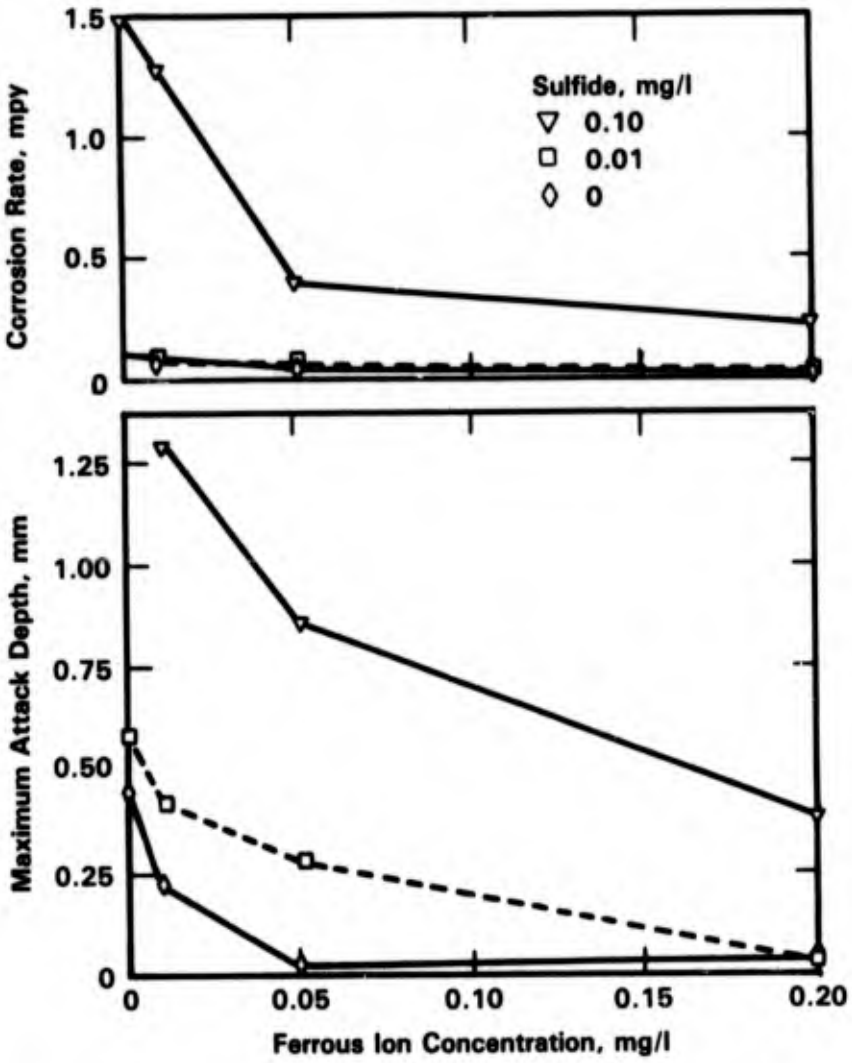

FIGURE 8-13. EFFECT OF IRON IONS ON CORROSION OF Cu-10Ni IN SULFIDE CONTAINING SEAWATER; 90 DAYS EXPOSURE[20]

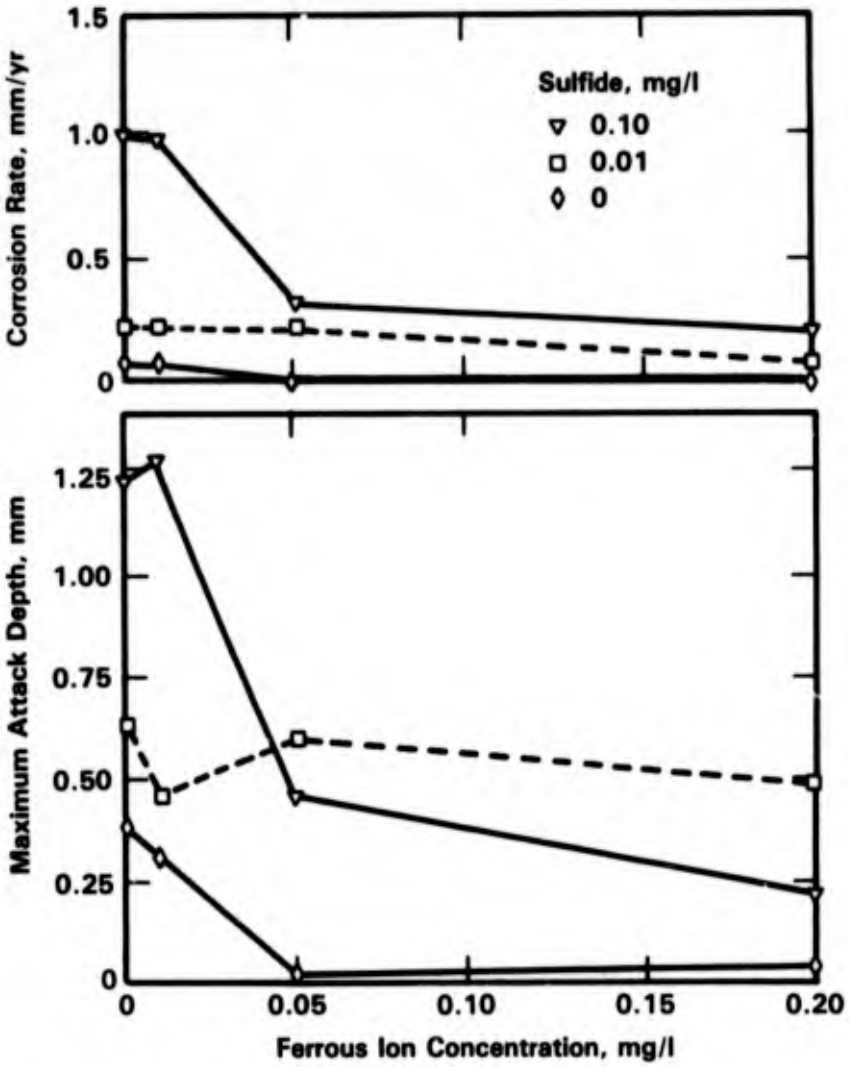

FIGURE 8-14. EFFECT OF IRON IONS ON CORROSION OF Cu-30Ni IN SULFIDE CONTAINING SEAWATER; 90 DAYS EXPOSURE[20]

Effect of Carbon

Pitting failures of copper-nickel alloys have been attributed to the presence of carbonaceous deposits or tube surfaces. This form of attack is most commonly thought to occur as a result of improper cleaning of heat exchanger tubes following drawing, but prior to heat treatment. The oily residues on the tubes break down during heat treatment to produce the carbon deposits. These carbon deposits then act as local cathodes, promoting localized attack. Difficulty in identifying this mechanism of attack in the field arises because the carbon deposits frequently cannot be detected following severe attack.

Erosion-Corrosion

Effect of Alloy Composition

Extensive research has been done on the effect of alloying elements on the resistance of copper-base alloys (particularly of copper-nickel alloys) to erosion/corrosion. Freeman and Tracy[28] investigated the performance of eight copper-base alloys, including bronzes and brasses, for their resistance to erosion-corrosion in a model condenser using water at 3.6 m/s. They ranked the alloys in order of decreasing resistance to impingement attack:

Copper-30 nickel (0.45 percent iron)
Copper-30 nickel (0.03 percent iron)
Copper-10 nickel (0.08 percent iron)
8 percent Phosphor Bronze
Aluminum Brass (Ambraloy 927)
Aluminum Bronze (Ambraloy 901)
Arsenical Admiralty
Uninhibited Admiralty.

Note that the copper-nickel alloys were found to have greater resistance to impingement attack than the brasses and bronzes.

The relative erosion-corrosion resistance of seven candidate copper alloys--noninhibited Admiralty brass, arsenical Admiralty brass, aluminum brass, Albrac*, copper-10 nickel, copper-30 nickel, and aluminum bronze--was investigated using a model condenser which operated as an auxiliary unit of the main condenser at Meiko Power Station.[29] In total, 470 tubes of the different alloys were installed in the auxiliary condenser, and the auxiliary unit was operated for over 6,000 hours. Admiralty brass tubes, both noninhibited and arsenical, suffered the worst erosion-corrosion damage. Extensive impingement attack occurred at the inlet end, outlet end, and in other parts near deposits. Impingement attack at the inlet end occurred in the upper part of the tubes, probably because of release of entrained air bubbles. Impingement attack on the other alloys was not reported.

Contrary to the findings of Otsu and Sato,[29] Pruvot[30] reported extensive erosion-corrosion in aluminum brass tubes in a model condenser that operated for about 6,000 hours at Dunkerque. The difference in performance of aluminum brass at the two locations may be the result of the difference in operating conditions on the quality of seawater at Dunkerque and Japan. In agreement with the Japanese authors, however, Pruvot found no attack on copper-30 nickel.

Results of testing of experimental copper-nickel alloys containing 0 to 30 percent nickel with varying amounts of iron and manganese showed that the addition of iron to tne alloys

improved resistance against erosion-corrosion.[31] The amount of iron needed in copper-nickel alloys for the optimum resistance increased with decreasing nickel content of the alloy as follows: 0.5 percent iron was required for copper-30 nickel, 0.6 percent iron for copper-20 nickel. Addition of 0.75 percent iron for copper-2 nickel improved the performance of the alloy only marginally, and showed no improvement in pure copper. No critical relationship was found between the iron and manganese contents of the alloys and their resistance to erosion-corrosion.

LaQue, et al.[32,33] used rotating spindle and jet impingement tests to study the erosion corrosion resistance of copper-30 nickel and copper-10 nickel, along with some brasses in seawater. It was found that the performance of copper-30 nickel improved with increasing (from 0.03 to 0.49 percent) iron content of the alloy. Similarly, for copper-10 nickel, weight loss dropped with increasing (up to 2 percent) iron (Figure 8-15). The copper-10 nickel alloys with 0.7 percent or 2 percent iron performed as well as or better than copper-30 nickel with 0.47 percent iron and Admiralty brass, and much better than aluminum brass and low iron copper-30 nickel (see Table 8-11).

However, a few specific cases are reported in which the addition of iron to copper-nickel alloys reduced the overall performance of copper-nickel alloys.[33] In one test at 7.5 m/s water velocity, copper-30 nickel with 0.6 percent iron suffered worse attack than the same alloy with 0.06 percent iron. At velocities above 7.6 m/s, however, the 0.6 percent iron alloy

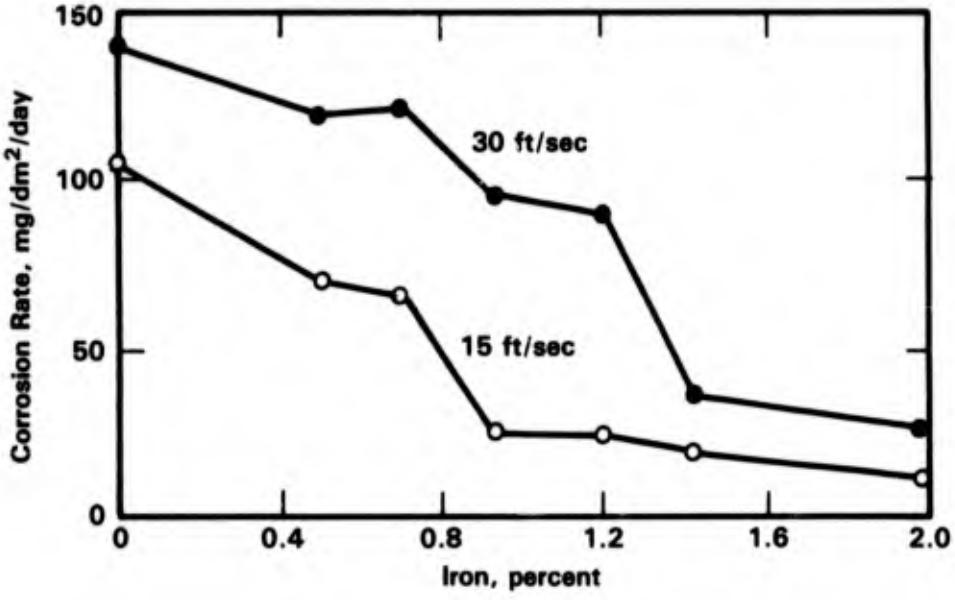

FIGURE 8-15. EFFECT OF IRON CONTENT AND SEAWATER VELOCITY ON EROSION-CORROSION RESISTANCE OF COPPER-10 NICKEL[33]

TABLE 8-11. RESULTS OF IMPINGEMENT TESTS WITH JET TEST APPARATUS (VOLUME OF AIR ADMITTED: 3 PERCENT; AVERAGE TEMPERATURE: 20 C; DURATION OF TEST: 28 DAYS; PEAK VELOCITY: 12 FT/SECOND)[32]

Material	Composition, percent							Average Weight Loss, mg per day	Maximum Depth of Impingement Attack, in. per month
	Cu	Ni	Fe	Mn	Al	Zn	Sn		
Copper-10 Nickel - 0.7 Iron	89.06	9.8	0.71	0.19	--	0.20	--	9	0.001
Copper-10 Nickel - 2 Iron	87.18	10.25	2.07	0.46	--	0.04	--	7	0.002
Admiralty Brass	71.11	--	--	--	--	27.87	0.98	30	0.025
Aluminum Brass	76.55	--	--	--	2.18	21.25	--	7	0.004
Copper-30 Nickel - Low Iron	69.05	30.26	0.06	0.48	--	0.15	--	20	0.004
Copper-30 Nickel - High Iron	68.92	30.16	0.47	0.45	--	--	--	6	0.003

showed better resistance than the 0.06 percent iron alloy. In another test, addition of more than 1 percent iron increased the susceptibility of the copper-30 nickel alloy to local pitting.[34] Similarly, in a comparison test of aluminum brass and copper-30 nickel containing 2 percent iron, the latter perforated completely at 10 m/s jet velocity, but the aluminum brass was less severely attacked.[35] Thus, the role of iron in copper-30 nickel alloy appears to be ambiguous and somewhat velocity dependent in a few specific cases.

Chromium modified copper-nickel alloys have been investigated for their resistance to erosion-corrosion at high water velocities (up to 40 m/s).[36] Addition of 0.5 to 3 percent chromium to copper-nickel alloys reduced remarkably the depth of attack in seawater jet impingement tests. Results (Figure 8-16) for copper-15 to 18 nickel and copper-30 nickel alloys as a function of chromium content of the alloys show that, at about 0.5 percent chromium, the impingement attack becomes almost negligible at 7.5 m/s water velocity.[35] Results for velocities from 3 to 18 m/s for different copper-nickel alloys (Table 8-12) were obtained in a multi-velocity parallel flow apparatus rather than in a jet impingement apparatus.[36] The data show that copper-30 nickel-3 chromium has superior erosion-corrosion resistance to that of the copper-nickel iron alloys (CA-706 and CA-715), and copper-15 nickel-0.5 chromium (IN-838) has about the same resistance as CA-715.

Effect of Velocity

The effect of water velocity on the erosion-corrosion of copper alloys has been investigated by several authors.[28,33,36-46] Davis, et al.[47] conducted a general review of the literature pertaining to copper alloys. Syrett[34] and Beavers and Boyd[48] directed reviews specifically towards copper-nickel alloys.

The corrosion rate of copper alloys generally increases with increasing velocity until a critical or breakaway velocity is reached, beyond which the rate increases rapidly up to a certain value and then it starts to taper off with further increases in velocity. According to Efird[45] the accelerated corrosion, due to high water velocity, occurs when the surface shear stress on the protective passive film of the alloy exceeds the bonding strength of the film to the alloy substrate. Similar explanations for the erosion-corrosion have been given by several authors previously.

Steward and LaQue[33] studied the effect of velocity on the corrosion of several copper alloys using a number of test techniques. Results from their rotating spindle erosion-corrosion tests (Figure 8-17) show the critical breakaway velocity in seawater for the different alloys appears to be in the range 4.5 to 6 m/s.

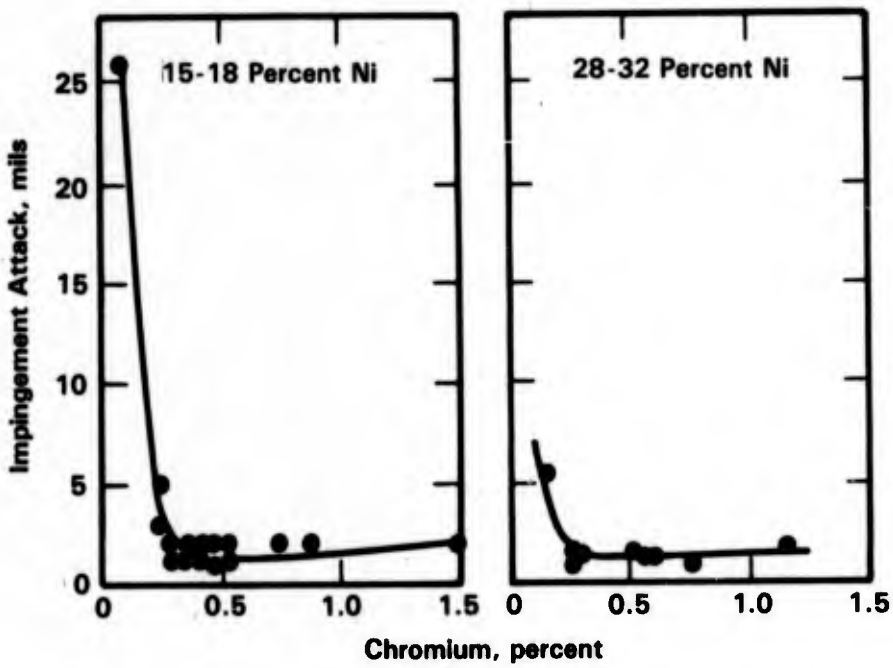

FIGURE 8-16. EFFECT OF CHROMIUM ADDITIONS ON SEAWATER IMPINGEMENT--CORROSION RESISTANCE OF COPPER-NICKEL ALLOYS. 36-DAY TEST WITH 7.5 M/S JET VELOCITY, SEAWATER TEMPERATURE: 27 C[36]

TABLE 8-12. EFFECT OF WATER VELOCITY OF EROSION-CORROSION OF VARIOUS ALLOYS FOR 30 DAYS' EXPOSURE[36]

Alloy	Average Seawater Temperature	Localized Attack, mm			
		3 m/s	6 m/s	11 m/s	15 m/s
CA-706	10 C	0.10	0.10	0.08	0.08
CA-715	10 C	0.03	0.03	0.08	0.13
IN-838	20 C	<0.03	0.03	0.10	0.13
Cu-Ni-3Cr	10 C	<0.03	<0.03	<0.03	<0.03

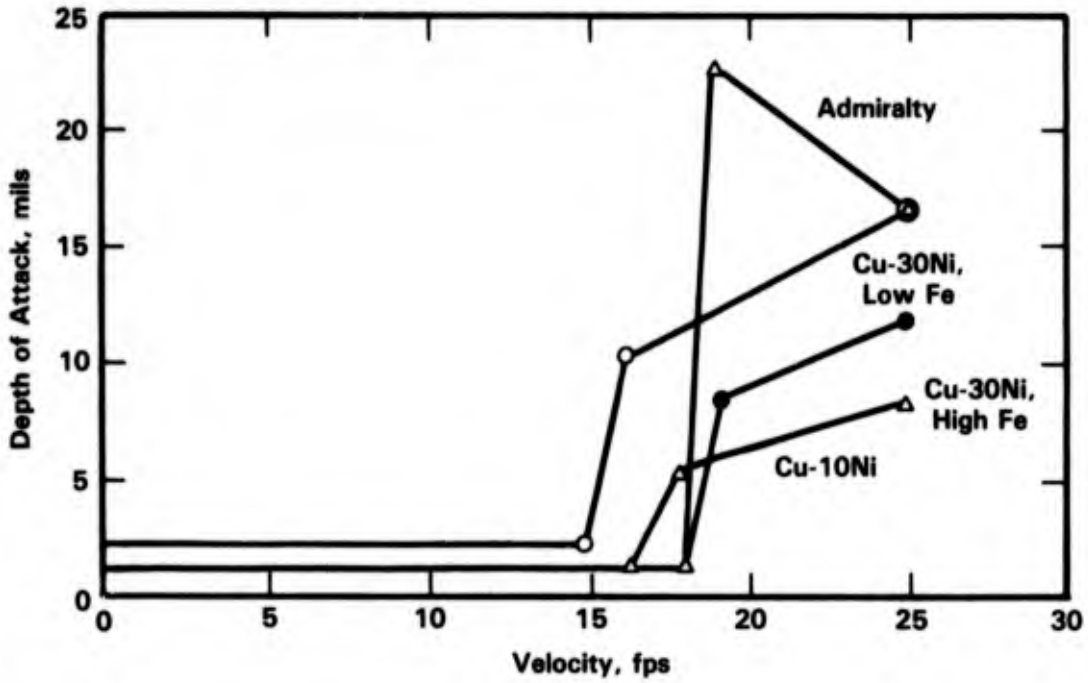

FIGURE 8-17. EFFECT OF VELOCITY ON DEPTH OF ATTACK IN SEAWATER AT KURE BEACH, NC, FOR 60 DAYS[33]

Syrett[34] compiled the results of several studies for copper-10 nickel and copper-30 nickel alloys. Figures 8-18 and 8-19 show the corrosion rate in seawater as a function of velocity for copper-10 nickel and copper-30 nickel, respectively. Considerable scatter in the data makes a meaningful assessment of the critical velocities difficult. The scatter in the data are attributed to the use of different test techniques by different authors, but variations in water chemistry and iron content of the alloys are also contributing factors. Syrett[34] suggested that all the alloys may not have well defined critical breakaway velocities, and therefore it is more reasonable to evaluate alloys according to an acceptable rate of erosion-corrosion.

Ferrara and Gudas[46] used a variety of test techniques to determine the effect of seawater velocity, up to 36 m/s, on eight different copper alloys. Results of multivelocity and high velocity jet tests are given in Figure 8-20. Solution annealed alloy CA-716 (64 copper--29.6 nickel--5.3 iron) showed excellent resistance to erosion-corrosion over the entire range of velocities tested; no breakaway velocity was found. Other alloys did show some indication of transition from low corrosion rate to accelerated corrosion with increasing velocity.

Symbol	% Fe	Test Method	Testing Time, days	Temperature, C
		Low Iron		
△	0.06	Jet Impingement	60	Ambient
○	0.06	Rotating Disc	60	Ambient
·····	0.06	Multivelocity Jet	30	Ambient
□	0.06	Rotating Spindle	60	Ambient
—·—	0.04	Rotating Spindle	60	26
▽	0.02	Unspecified	365	2-30
		Medium Iron		
◇	0.4-1.0	Simulated Service (Flow Through Tubes)	208	15
▬	0.42	Unspecified	365	2-30
▲	0.6	Jet Impingement	60	Ambient
●	0.6	Rotating Disc	60	Ambient
●	0.5	Rotating Disc	60	15
——	0.6	Multivelocity Jet	30	Ambient
■	0.6	Rotating Spindle	60	Ambient
— — —	0.47	Rotating Spindle	60	26
//////	0.5	Unspecified	--	Ambient
		High Iron		
— — —	5	Unspecified	--	Ambient
▲	5.38	Jet Impingement	60	Ambient
●	5.38	Rotating Disc	60	Ambient
—— — —	5.38	Multivelocity Jet	30	Ambient
■	5.38	Rotating Spindle	60	Ambient

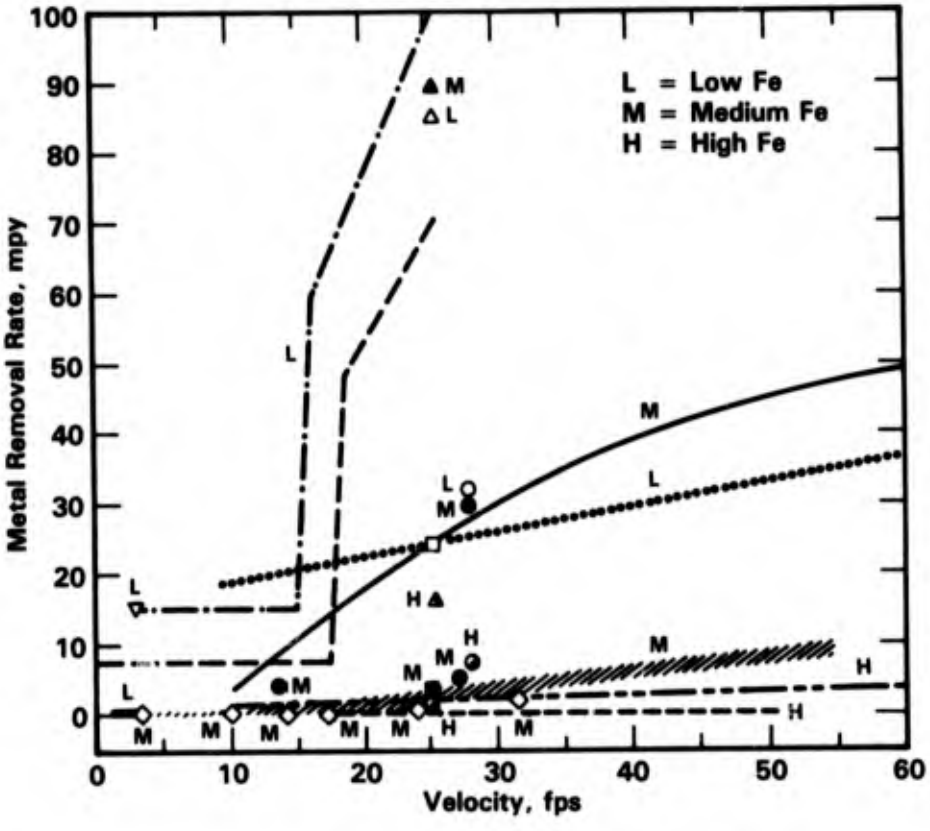

FIGURE 8-18. THE EFFECT OF VELOCITY OF THE EROSION-CORROSION RATE OF COPPER-30 NICKEL IN SEAWATER[34]

Symbol	% Fe	Test Method	Testing Time, days	Temperature, C
		Low Iron		
○	0.7	Rotating Disc	60	15
◇	0.7	Simulated Service (Flow Through Tubes)	120	Ambient
●	0.7	Rotating Disc	55	23
		Medium Iron		
◆	1.2	Simulated Service (Flow Through Tubes)	120	Ambient
		High Iron		
////	1.5	Unspecified	--	Ambient
▲	1.45	Jet Impingement	60	Ambient
◕	1.45	Rotating Disc	60	Ambient
—	1.45	Multivelocity Jet	30	Ambient
■	1.45	Rotating Spindle	60	Ambient
●	1.4	Rotating Disc	55	23

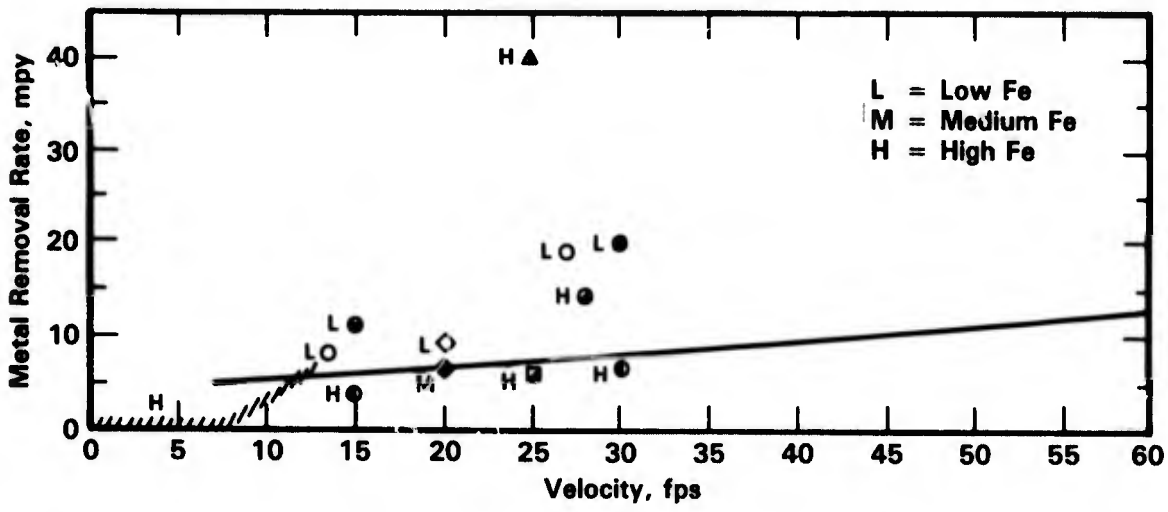

FIGURE 8-19. THE EFFECT OF VELOCITY OF THE EROSION-CORROSION RATE OF COPPER-10 NICKEL IN SEAWATER[34]

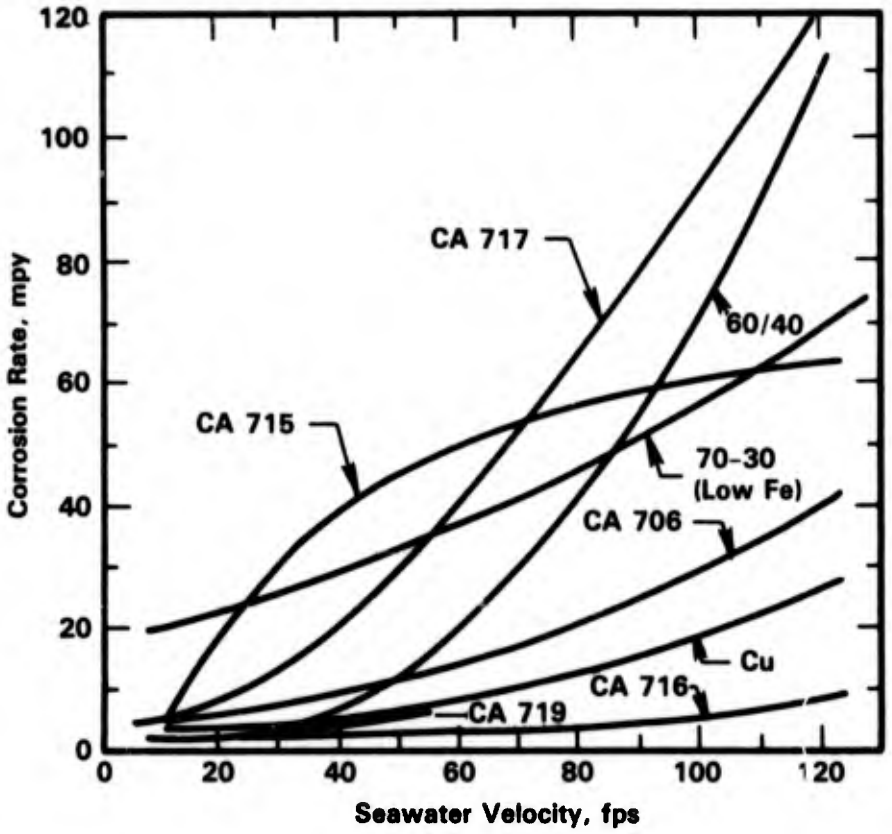

FIGURE 8-20. EFFECT OF SEAWATER VELOCITY ON THE EROSION-CORROSION RATE OF VARIOUS COPPER-BASE ALLOYS IN SEAWATER[46]

The critical velocity for five copper alloys measured by a parallel flow apparatus, and their critical shear stresses are given in Table 8-13. The critical shear stress was calculated using the critical velocity and the fluid properties of the seawater under test conditions. The critical shear stress takes into account the numerous environmental variables which are not reflected in the critical velocity alone, and can be used to determine critical velocities for the copper alloys in other systems having different geometries.[45] As seen in Table 8-13, both the critical velocity and the critical shear stress are quite different for different alloys.

Sato[37] found that the wall shear stress in the entry region of a tube can be twice as high as at other parts of the tube for a given velocity (Figure 8-21). This implies that in order to avoid inlet impingement attack, the normal flow velocity should be one-half or less that of the critical velocity for the alloy under the fully developed flow conditions. Sato[37] has also showed that the lodgement of foreign bodies, such as mussels, in tubing or piping can increase the local velocity at restrictions to several times the normal flow velocity (Figure 8-22).

TABLE 8-13. CRITICAL VELOCITY AND SHEAR STRESS FOR COPPER-BASE ALLOYS IN SEAWATER[45]

Alloy	Critical Velocity, m/s	Temperature, C	Critical Shear Stress, N/m^2
CA-122	1.3	17	9.6
CA-687	2.2	12	19.2
CA-706	4.5	27	43.1
CA-715	4.1	12	47.9
CA-722	12.0	27	296.9

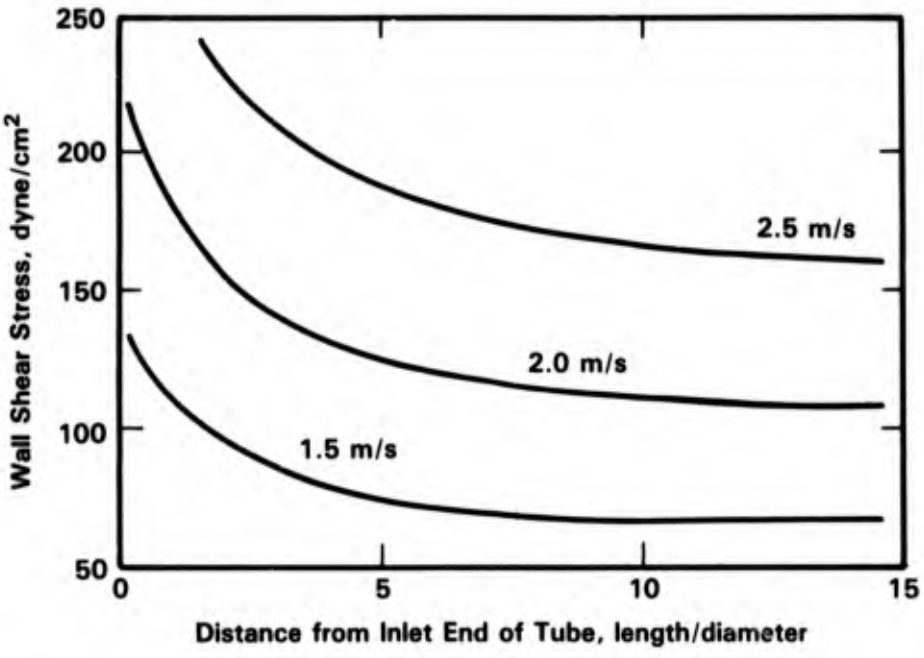

FIGURE 8-21. WALL SHEAR STRESS AS A FUNCTION OF DISTANCE FROM INLET END OF TUBE FOR VARIOUS FLOW VELOCITIES[37]

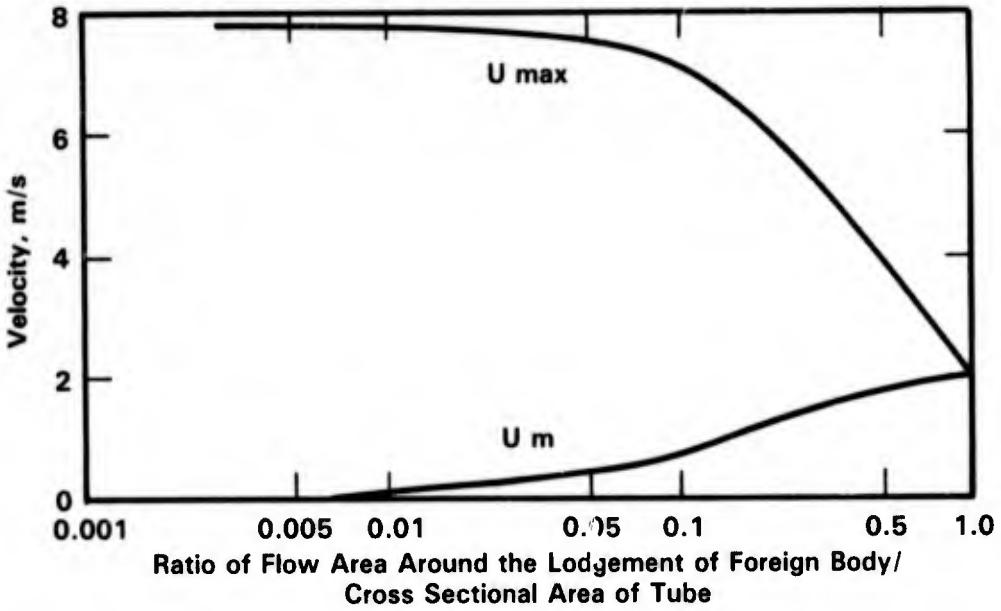

FIGURE 8-22. EFFECT OF THE LODGEMENT OF FOREIGN BODIES ON THE VELOCITY AT NORMAL PORTION (Um) AND AROUND THE LODGEMENT (Umax)[37]

Thus, if the designed normal flow velocity is kept substantially lower than the highest acceptable velocity, or by selecting a material with high surface shear stress tolerance, the erosion-corrosion of tubes can be avoided.

Effect of Water Temperature

Results of a study of the effect of water temperature on the erosion-corrosion of copper-30 nickel containing two different iron contents[31] are given in Table 8-14. The weight loss of the high-iron (0.48 to 0.69 percent) alloy at 30 C was about one-half of that at 15 C, whereas the reverse was the case for the low iron (0.03 to 0.04 percent) alloy. According to the authors, the drop in weight loss of the high-iron alloy was due to an improvement in the quality of the protective film at the higher temperatures.

A series of studies of copper alloys in model condensers concluded that the erosion-corrosion in deaerated seawater decreases with an increase in temperature.[49] The findings are summarized in Figure 8-23. In zone A, representing lower temperatures and higher velocities, impingement attack of copper alloys is severe; in zone B, a transition zone develops where impingement attack can occur, but generally to a less significant extent; and in zone C, corrosion attack of all types is minimal.

TABLE 8-14. INFLUENCE OF SEAWATER TEMPERATURE ON CORROSION AND EROSION OF COPPER-30 NICKEL[32]

Duration of test: 60 days
Velocity: 3 m/s for tubes; 4.5 m/s for bars

Material and Form	Weight Loss, mg/dm^2/day		Maximum Depth of Attack, inch	
	A, 50 F	B, 86 F	A	B
70-30 cupro-nickel, low iron (0.03 percent) bars	159	247	0.006	0.006
70-30 cupro-nickel, high-iron (0.48 percent) bars	63	25	0.002	0.000
70-30 cupro-nickel, low-iron (0.04 percent) tubes	92	275	0.008	0.000
70-30 cupro-nickel, high-iron (0.49 percent) bars	39	22	0.000	0.000

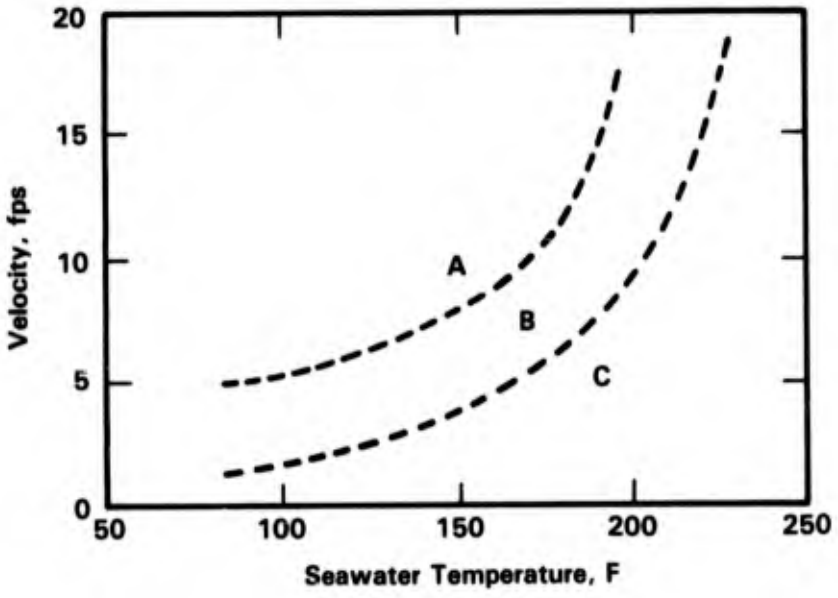

FIGURE 8-23. CORROSION OF COPPER ALLOYS IN HOT, DEAERATED (25-40 ppb OXYGEN) SEAWATER, ZONE A--SEVERE IMPINGEMENT OF LESS CORROSION RESISTANT ALLOYS; ZONE B--MORE GENERAL CORROSION, SOME IMPINGEMENT; ZONE C--MINIMUM CORROSION, NO IMPINGEMENT ON MANY ALLOYS[49]

Data compiled from several studies on the erosion-corrosion of copper alloys at different temperatures, show a mixed trend with regard to the effect of temperature on the erosion-corrosion rate.[34] The rate increased in some cases, decreased in others, and changed little with temperature in still others. The lack of a trend in the data in Table 8-15 was attributed to the differences in the oxygen content of the waters used by different authors.

Efird[45] calculated the surface shear stress as a function of seawater velocity for different temperatures. Results (Figure 8-24) show that the shear stress drops for a given velocity with an increase in temperature. The drop is due to the changes in the physical properties of the water, e.g., viscosity, density. Since high shear stress may be responsible for the erosion-corrosion, a drop in its value due to an increase in temperature, should lower the erosion-corrosion rate. These findings are in agreement with the observations of Anderson.[49] Thus, the drop in shear stress with temperature may be a contributing factor in lowering the erosion-corrosion rate of copper alloys, but an improvement in the protective quality of the surface film at the higher temperature is also an important factor.

Effect of pH

Erosion-corrosion of copper alloys has been studied mainly in surface seawater. As such, little attempt has been made to quantitatively define the effect of pH on the erosion-corrosion. A recent theoretical study of horseshoe type erosion-corrosion indicated that pH is the critical factor in causing the attack in seawater.[50] Thermodynamically, lower pH values favor the corrosion of copper since the protective Cu_2O film becomes less stable at the lower pH's. Therefore, it is to be expected that lowering of pH will also increase the erosion-corrosion of copper alloys. Syrett,[34] in fact, noted that lowering the pH of either fresh water or seawater increased the rate of erosion-corrosion.

Effect of Aeration

According to Syrett,[34] "It is generally agreed that when air or other gases are present as bubbles in flowing water, the erosion-corrosion properties of copper alloys are adversely affected." Anderson[49] recommended, on the basis of a pilot plant study, that for long life of copper-10 nickel in hot seawater service the water should be deaerated because the presence of dissolved air accelerates the corrosion rate.

Evidence to the contrary has been presented by Stewart and LaQue,[34] and Danek[39] for copper-nickel alloys. These authors have observed a reduction in erosion-corrosion rate in seawater when air was present in the test media. Their observations are based on tests using

TABLE 8-15. THE EFFECT OF TEMPERATURE ON THE EROSION-CORROSION RATE OF COPPER ALLOYS IN FLOWING FRESH WATER OR SALT WATER[34]

Aerated or Deaerated	Type of Water	Test Temperatures, C	Alloy	Effect on Corrosion Rate of Increasing Temperature	Velocity, m/s
A	Seawater	20, 49	90-10 Cu-Ni	Little change	3.0
A	Seawater	20, 49	70-30 Cu-Ni	Little change	3.0
A	Seasalt brine (11% salt content)	24, 96, 121	90-10 Cu-Ni	Decreases	2.6
A	Seasalt brine (11% salt content)	24, 96, 121	70-30 Cu-Ni	Maximum at 96 C	2.6
A	NaCl solution (Same salinity as seawater)	20-80	Cu, Cu alloys	Increases	--
A	Fresh	30, 65, 90	Cu	Increases	11.9
A	Fresh	30, 65, 90	Cu	Maximum at 65 C	6.1
D	Seawater	82, 107, 121	90-10 Cu-Ni	Little change	1.5
D	Seawater	82, 107, 121	70-30 Cu-Ni	Little change	1.5
D	Seawater	35-107	Cu alloys	Decreases	--

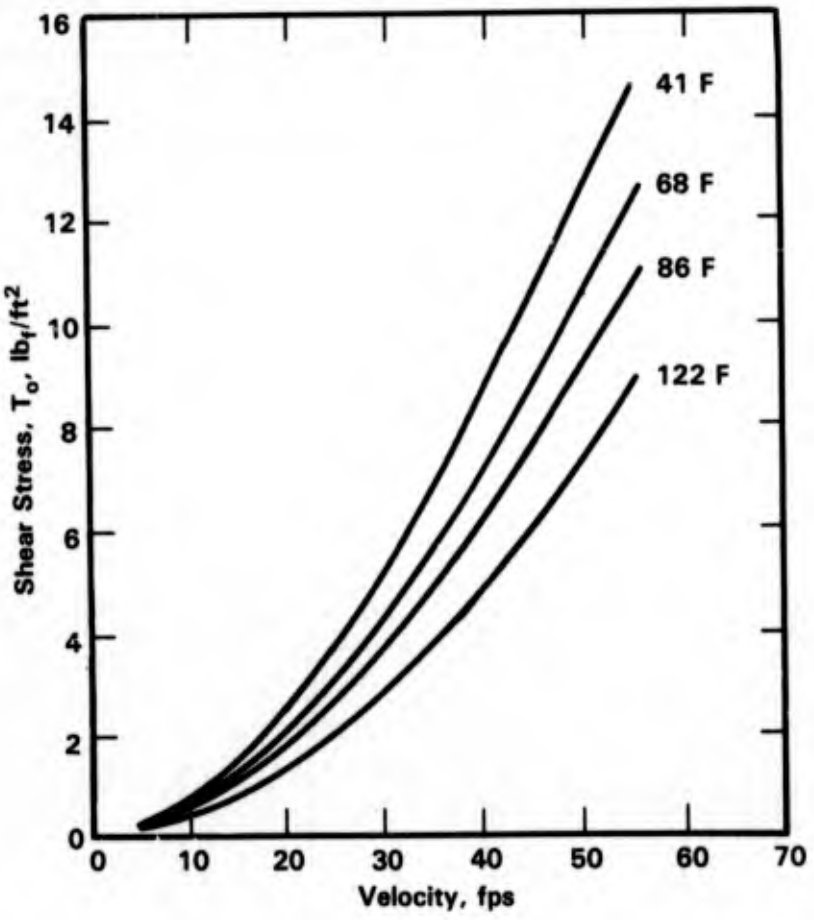

FIGURE 8-24. THE SURFACE SHEAR STRESS AS A FUNCTION OF VELOCITY FOR VARYING SEAWATER TEMPERATURES[45]

either a rotating spindle or disc apparatus. Syrett[34] is of the view that the discrepancy between these observations and those of others is due to the test techniques employed by the latter authors. With rotating spindle or disc method any air bubbles present in the water do not strike the surface of the test alloy directly, but the bubbles are held back by the boundary layer. As a result, the surface of the sample is not damaged when the bubbles break; on the contrary, the increased oxygen supply promotes film growth and reduces the corrosion rate.

Results from two jet impingement studies demonstrated that when either air bubbles or nitrogen bubbles were present in water, the severity of impingement attack increased over that of plain water.[34] In cavitation erosion, the rapid breaking of vapor bubbles can create shock waves with pressures as high as 415 MN/m^2.[51] Forces this high are sufficient to cause damage to many metal surfaces.

Effect of Chlorination

The effect of chlorination on the erosion-corrosion of copper alloys was studied using model condensers and jet impingement tests.[52] In the model condenser study, chlorinated seawater at a velocity of 2 m/s was used. Chlorination promoted corrosion, but attack was not serious up to 1 ppm chlorine. In a study[32] of the effect of chlorination on the corrosion of copper-30 nickel in seawater from 0.15 to 3 m/s velocity, no adverse effects of chlorination were reported. However, under erosion-corrosion conditions, such as with jet impingement tests, chlorination exacerbated the attack. The depth of attack on all of the copper alloys tested increased with increasing chlorine concentration in tests[52] performed at 5 m/s with 3 percent NaCl containing 5 volume percent air (Figure 8-25).

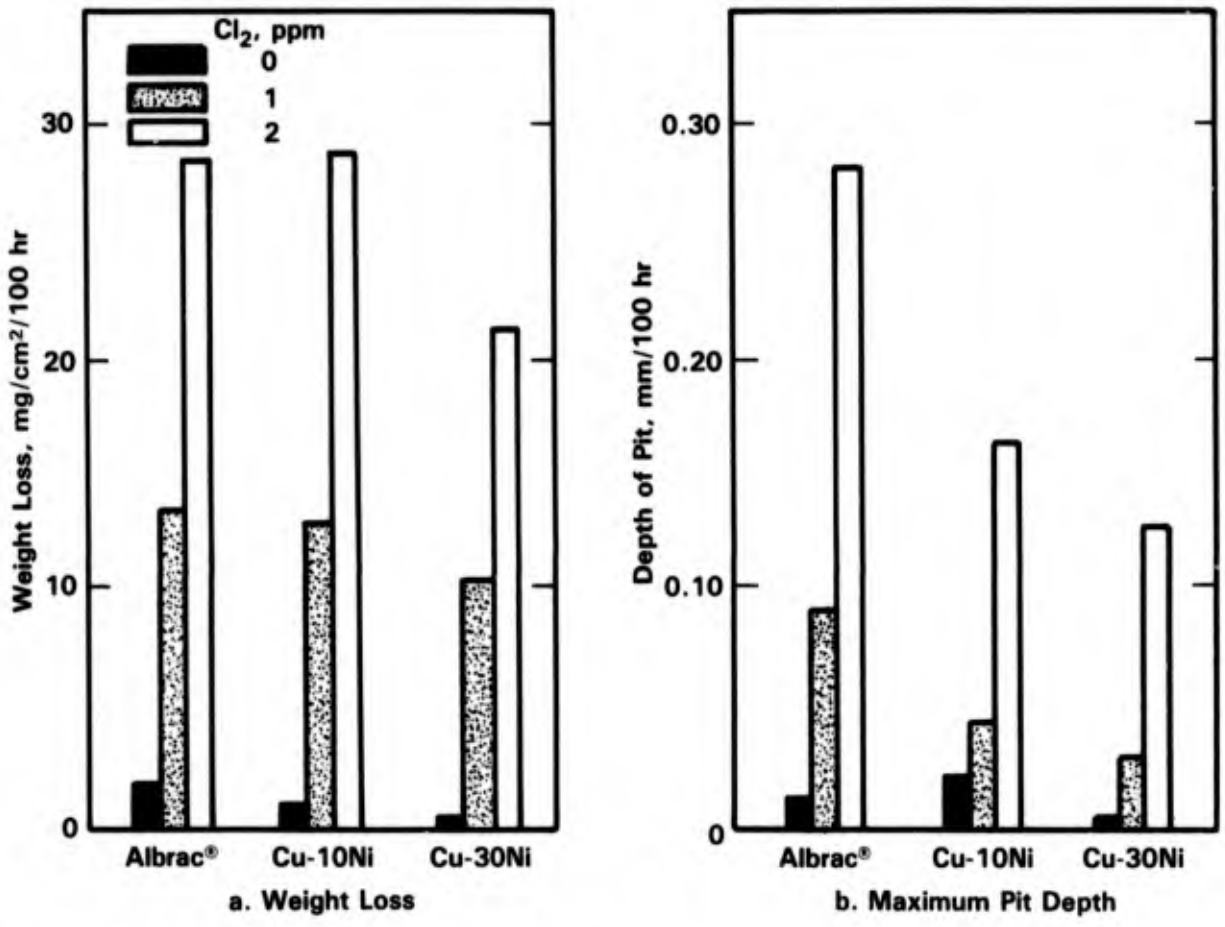

FIGURE 8-25. EFFECT OF CHLORINATION ON EROSION-CORROSION RESISTANCE OF COPPER-BASE ALLOYS IN 3 PERCENT NaCl AT AMBIENT TEMPERATURES[52]

Effect of Particulates

Tanabe[53,54] and Sato[37,55] studied the effect of sand particles on the erosion-corrosion of aluminum brass. A rotating spindle apparatus was used to study the erosion-corrosion of Albrac* in tap water and in 3 percent NaCl solution. The erosion-corrosion rate of aluminum brass was higher in 3 percent NaCl solution than in tap water under identical test conditions. As shown in Figure 8-26 at 2 m/s water velocity, the corrosion rate increased

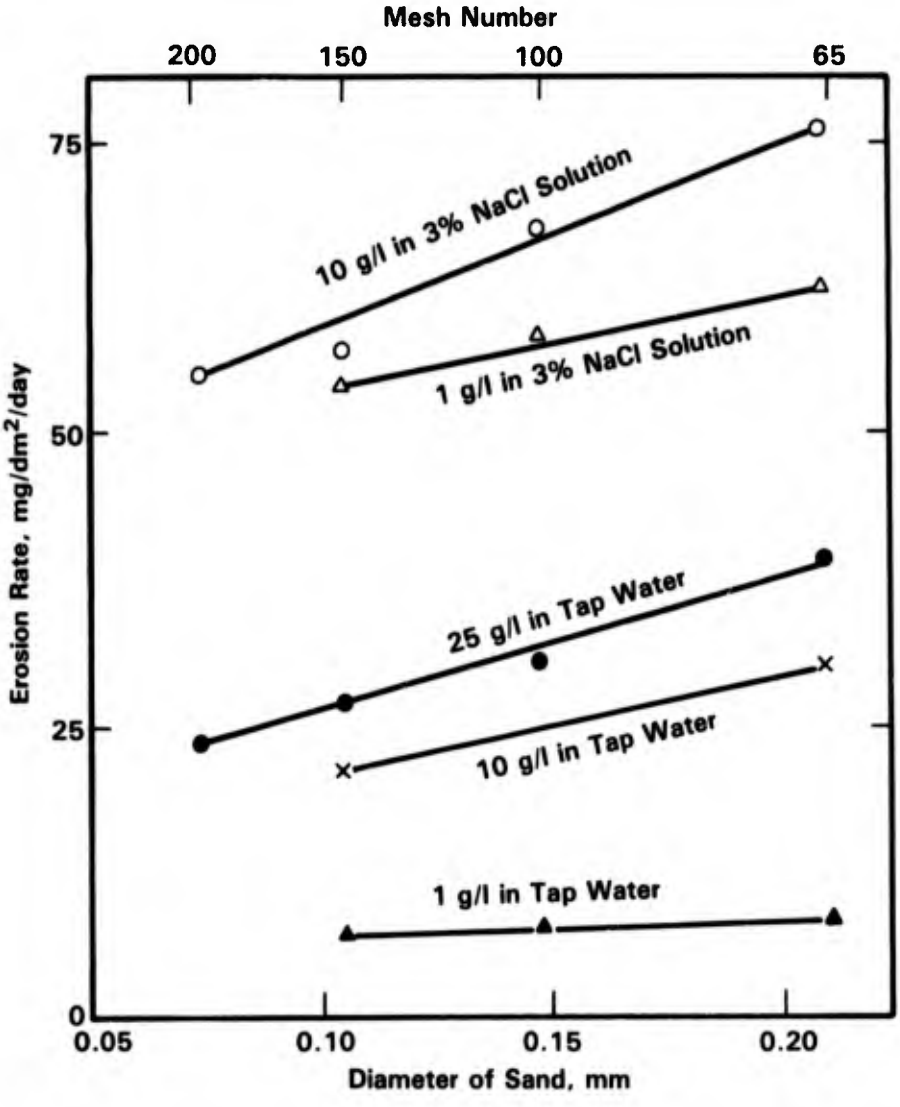

FIGURE 8-26. EFFECT OF PARTICLE DIAMETER ON THE SAND EROSION-CORROSION OF ALBRAC* (VELOCITY 2 m/s)[53]

linearly with the increasing grain size of the sand for both the tap water and the 3 percent NaCl solution. The increase in sand content of the media also resulted in increased corrosion rates. Moreover, when the rotation speed was increased at a fixed sand content, the rates increased almost logarithmically with speed.

Sato, et al.[55] investigated the sand erosion-corrosion in seawater of aluminum brass, copper-30 nickel and titanium tubes using a model condenser. The study included effects of grain size, sand content, ferrous ion injection, surface pretreatment and cathodic protection. The behavior of aluminum brass is shown in Figure 8-27. Increasing the sand content and the grain size increased the erosion-corrosion rate. Cathodic protection with or without Fe^{++} injection was effective in lowering the rate when the grain size was 50 μm but not when the grain size was 250 μm. The latter behavior probably indicates that the damage at the larger grain size is primarily mechanical in nature. The erosion-corrosion rate of copper-30 nickel was about twice that of aluminum brass under identical conditions of testing. Titanium was found to be immune to erosion-corrosion. Polluted seawater containing sand was less aggressive than nonpolluted seawater on aluminum brass. This effect was attributed to the formation of an adherent sulfide film in polluted seawater.

In a later study of sand erosion-corrosion, Sato[37] has shown that the rate of attack progresses in four stages with increasing content of sand. Figure 8-28 shows a typical example. Most virulent attack occurs when the sand content of the water is more than 300 ppm.

Effect of Protection Methods

The effect of various protection methods on erosion-corrosion of copper alloys is discussed below.

Inhibitors. The primary inhibitor used for the protection of erosion-corrosion of copper alloys is ferrous sulfate. In 1955, excessive tube failures (863 out of 6370 tubes) at the city of Jacksonville, Florida, power plants prompted the use of $FeSO_4$ injection in cooling waters from the St. John River.[56] Ferrous ion injection on one unit resulted in dramatic change in the failure rate of the tubes (Figure 8-29).

Similar success with $FeSO_4$ injection was reported at a 760 MW power plant in Kincardine, Scotland.[57] Before the $FeSO_4$ treatment, condensers tubed with aluminum brass suffered severe horseshoe impingement attack at the inlet end and deep pitting at the outlet end. A $FeSO_4$ injection of 1 ppm (Fe^{++}) for 30 minutes every 12 hours mitigated the problem

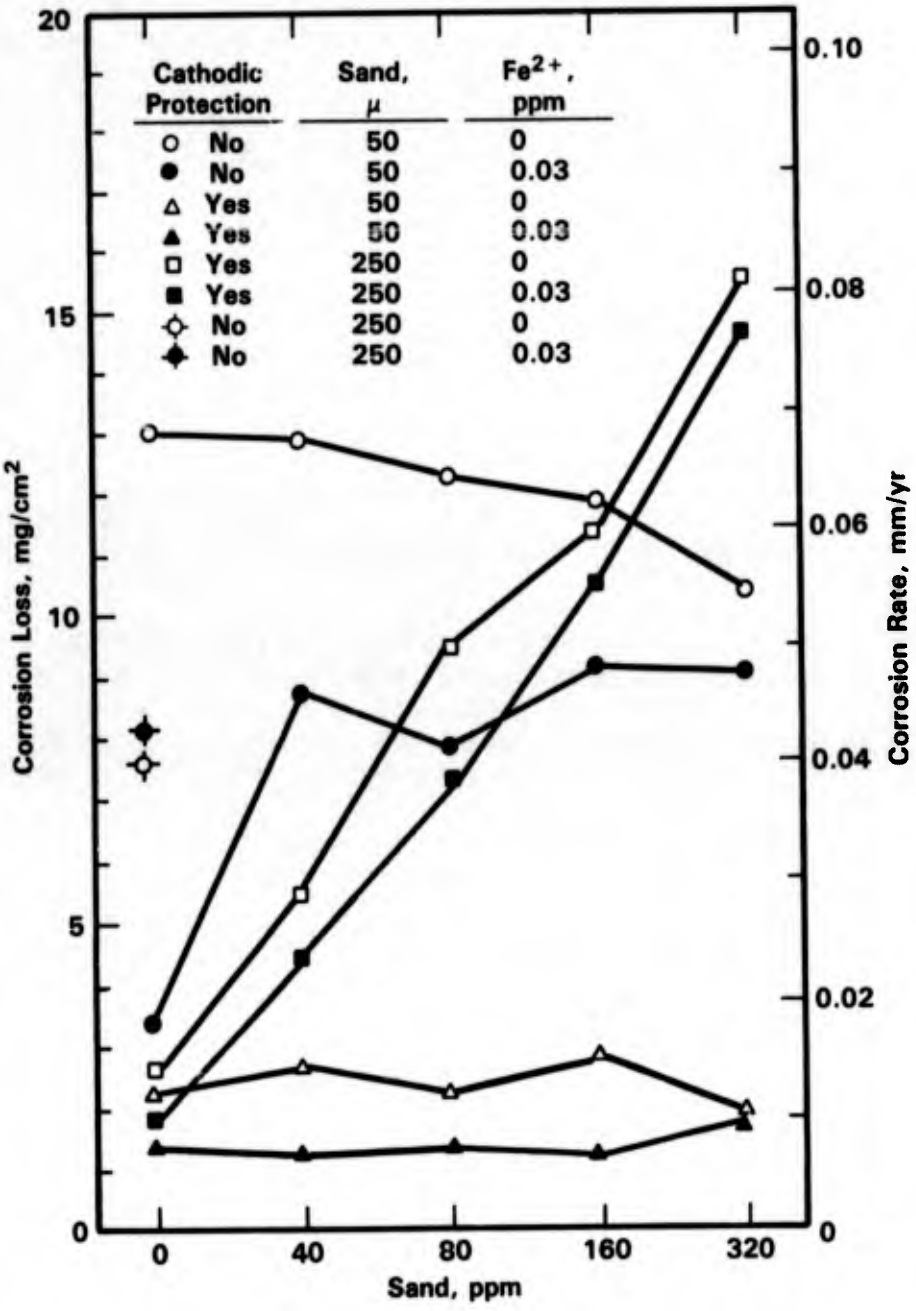

FIGURE 8-27. EFFECT OF SAND CONTENT, CATHODIC PROTECTION, AND FERROUS ION INJECTION ON INLET EROSION-CORROSION OF ALUMINUM BRASS[55]

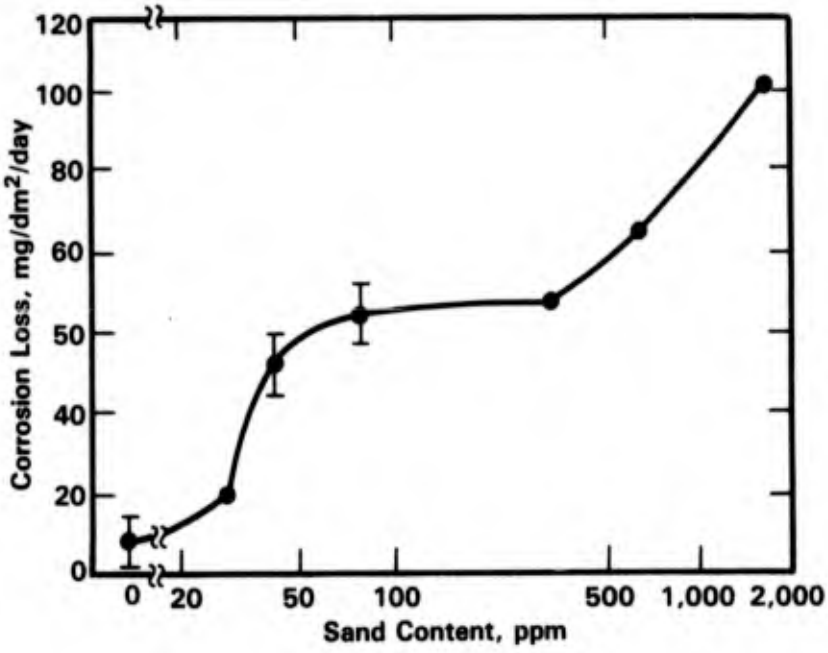

FIGURE 8-28. EFFECT OF THE SAND CONTENT ON THE CORROSION OF ALUMINUM BRASS CONDENSER TUBES. TEST WAS MADE AT CHITA MARINE LABORATORY ON TUBULAR SPECIMENS AT A FLOW RATE OF 2.0 M/S FOR ONE MONTH USING CIRCULATED SANDS LESS THAN 0.1 MM IN DIAMETER[37]

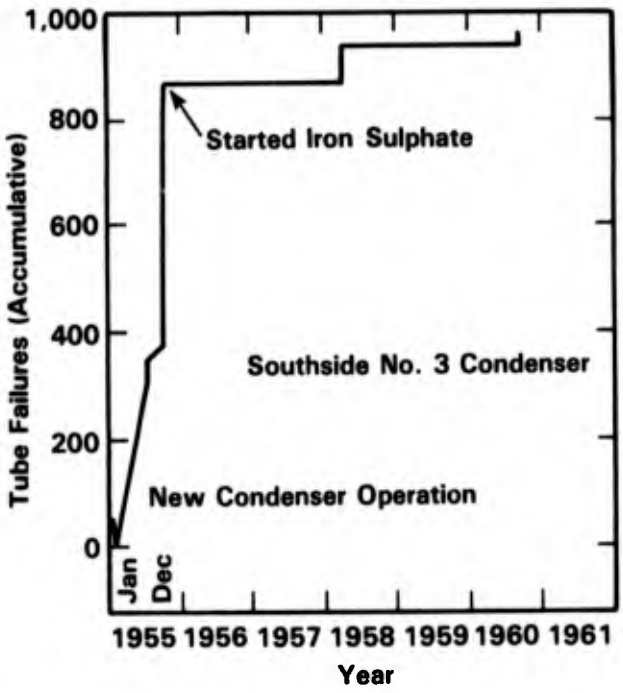

FIGURE 8-29. THE INFLUENCE OF FERROUS SULFATE INJECTION ON CUMULATIVE FAILURES AT A JACKSONVILLE, FLORIDA, POWER PLANT[56]

(Figure 8-30). Impingement attack on aluminum brass condenser tubes of super tankers has also been successfully suppressed by the use of $FeSO_4$ injection.[58]

Using model condensers for testing, Sato, et al.[43] investigated the beneficial effects of ferrous ion injection on the impingement attack of aluminum brass. As little as 0.01 ppm of Fe^{++} ion injection in the cooling seawater was found to be sufficient to reduce the erosion-corrosion rate by at least a factor of ten in the velocity range of 2 to 3.5 m/s (Figure 8-31). Results also imply that if Fe^{++} ion injection is used in the cooling water, a condenser can be operated at higher water velocities without erosion-corrosion attack.

Continuous use of Fe^{++} ion injection is more beneficial than an intermittent one.[40] A 0.01 ppm continuous injection was significantly more beneficial than a 0.25 ppm injection for 1 hour per day, even though the total daily addition of Fe^{++} ion in solution was the same for the two cases, see Figure 8-32.

Ferrous ion injection not only offers protection from the high water velocity impingement attack, but also protects tubing from sand erosion-corrosion. The beneficial effect of Fe^{++} ion injection on sand erosion-corrosion of aluminum brass is shown in Figure 8-27. The corrosion rate dropped substantially when 0.03 ppm Fe^{++} ions were present in the cooling water containing 50 μm sand. However, if the sand size was 250 μm, Fe^{++} ions offered little protection. Similar results for copper-30 nickel are shown in Figure 8-33.

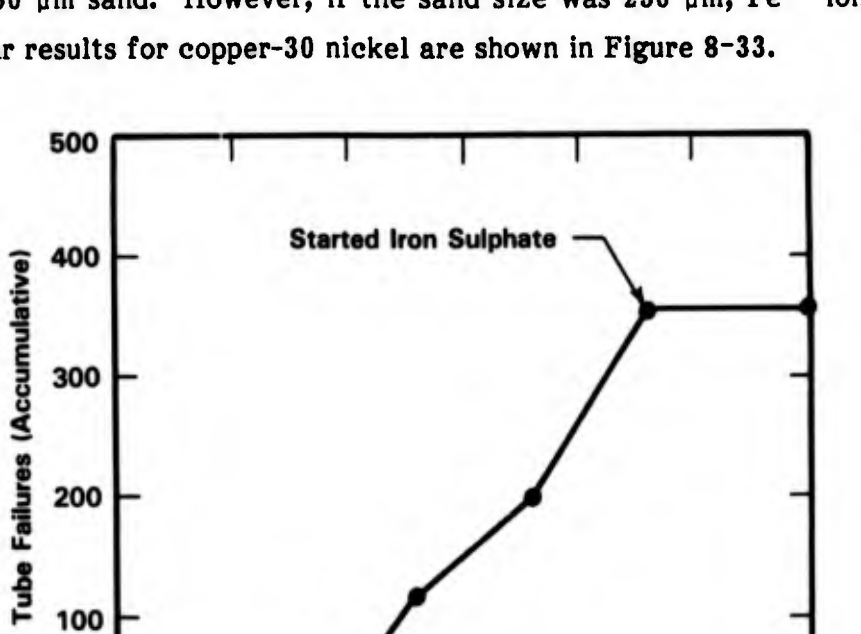

FIGURE 8-30. THE INFLUENCE OF FERROUS SULFATE INJECTION ON CUMULATIVE FAILURES AT A KINCARDINE, SCOTLAND, POWER PLANT[57]

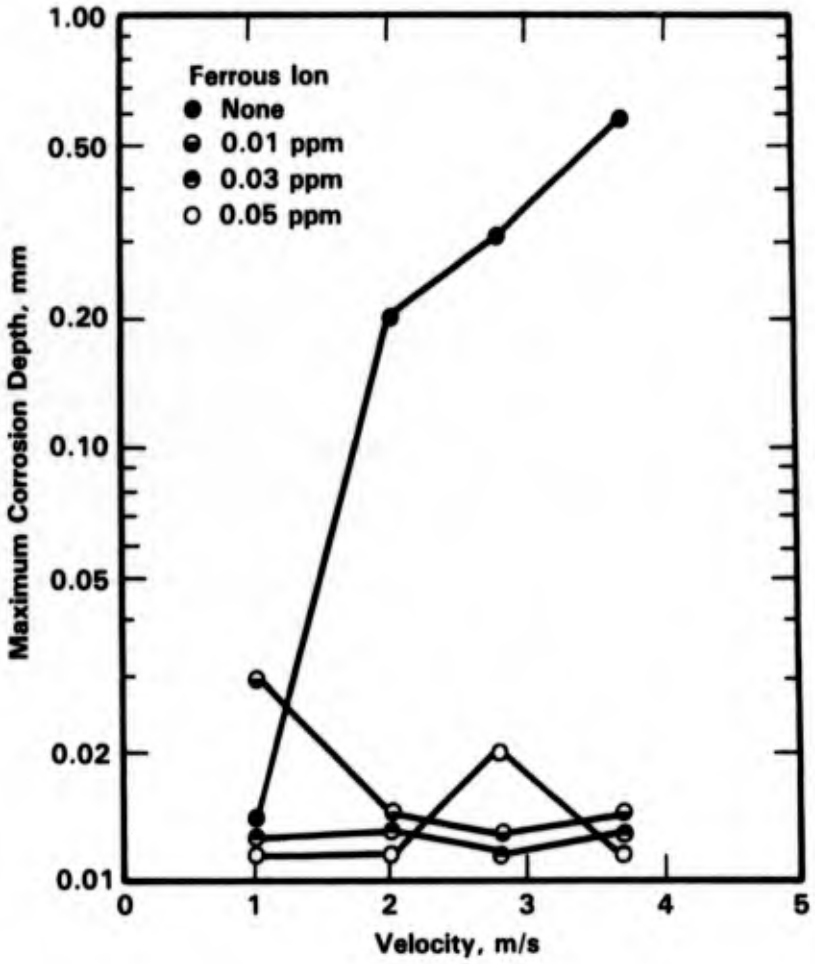

FIGURE 8-31. EFFECTS OF FERROUS ION AND VELOCITY ON CORROSION RATE OF ALUMINUM BRASS[43]

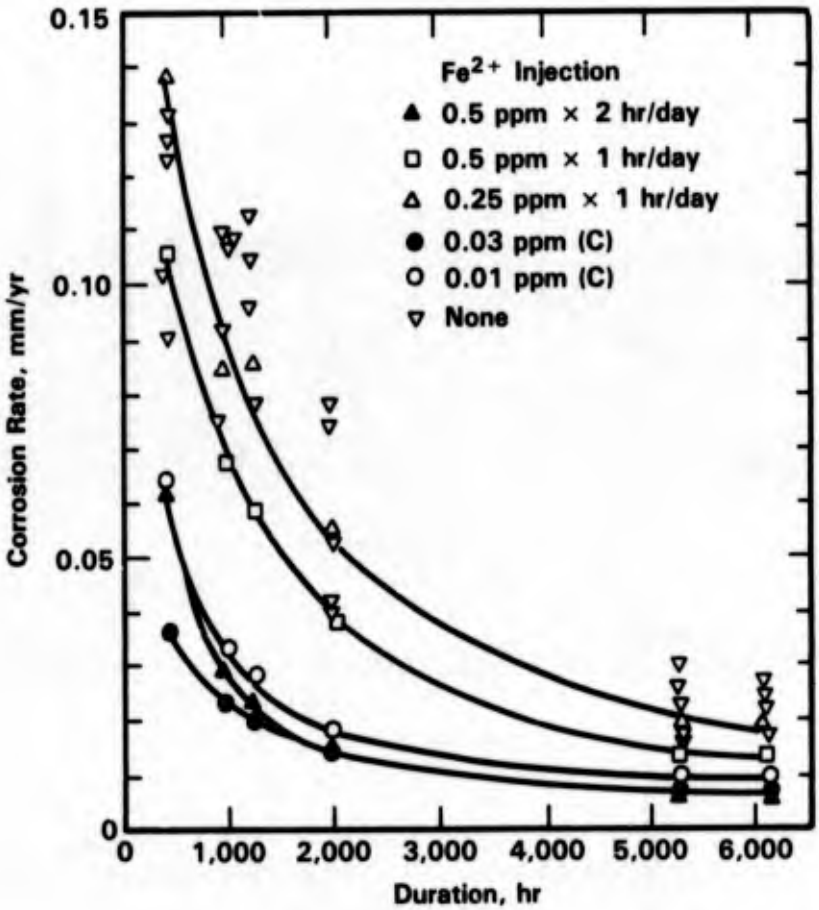

FIGURE 8-32. EROSION-CORROSION RATES OF ALUMINUM BRASS AS A FUNCTION OF TEST DURATION FOR INTERMITTENT AND CONTINUOUS (C) INJECTION OF FERROUS SULFATE[40]

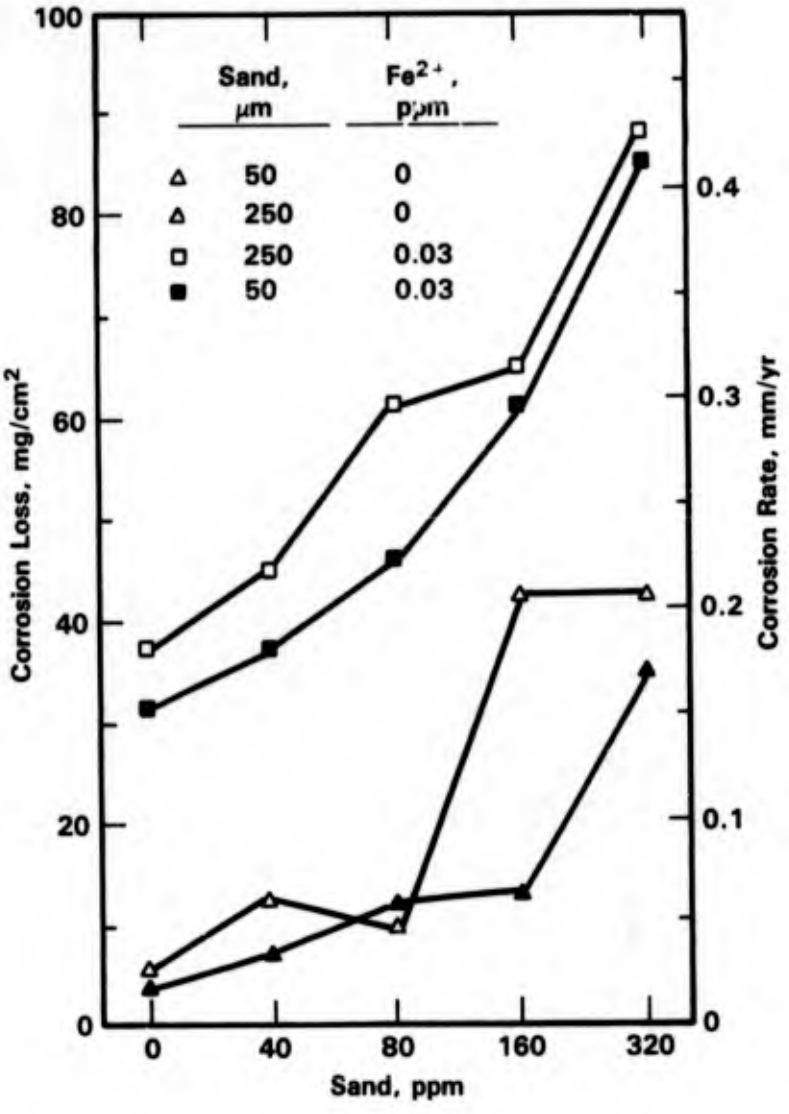

FIGURE 8-33. EFFECT OF SAND SIZE AND CONCENTRATION, AND FERROUS ION INJECTION ON EROSION-CORROSION RATE OF COPPER-30 NICKEL TUBES IN SEAWATER[55]

Cathodic Protection. Sata and Nagata[37] argued that, since erosion-corrosion is an electrochemical process, cathodic protection should be effective against inlet impingement attack. They presented an equation for calculating the resulting potential, E, at a distance Z from the inlet end of the tube, when a cathodic current Io is applied to the tube:

$$E = Io \cosh \left\{ \frac{\sqrt{2P}}{\gamma R} (L-Z) \right\} \Big/ \sinh \frac{\sqrt{2P}}{\gamma R} L$$

In the above equation, L is the length of the tube, γ is the inside tube radius, R is the polarization resistance of the tube, and P is the resistivity of seawater. Conversely, if the tube length to be protected at a desired potential is known, the needed cathodic current can be calculated.

Cathodic protection against sand erosion-corrosion of an aluminum brass (Albrac®) has been studied[54] using a rotating spindle type apparatus. Experimental results in tap water and in 3 percent NaCl solution, containing 25 g/l sand of 65 mesh grain size, are shown in Figure 8-34. For the case of 2 m/s relative velocity, the protection efficiency for the aluminum brass improved with increasing cathodic current, and the efficiency reached almost 100 percent at 100 $\mu A/cm^2$. On the other hand, at 4 m/s relative velocity, the protection efficiency remained low, 20 percent, irrespective of the current density applied.

Erosion-corrosion rates for cathodically protected and unprotected aluminum brass in tap water at 2 m/s, as a function of sand content of the water, are shown in Figure 8-35 for three different mesh size grains. The rates for the cathodically protected samples are less than one-half those of the unprotected samples.

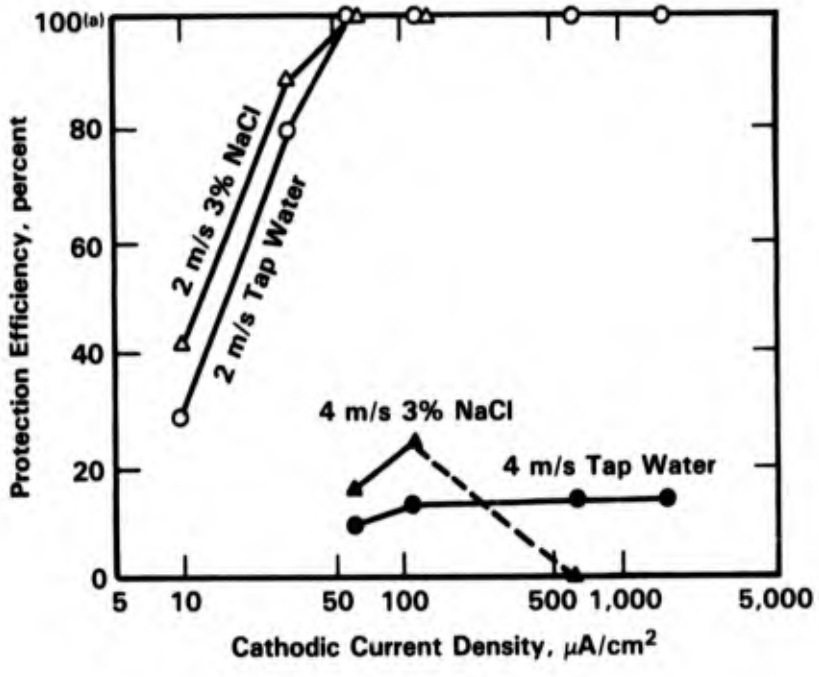

FIGURE 8-34. RELATION BETWEEN CATHODIC PROTECTION EFFICIENCY AND CURRENT DENSITY (SAND CONTENT 25 GRAMS/LITER, SAND GRAIN 65 MESH) FOR ALUMINUM BRASS[54]

(a) 100 percent efficiency = negligible weight loss

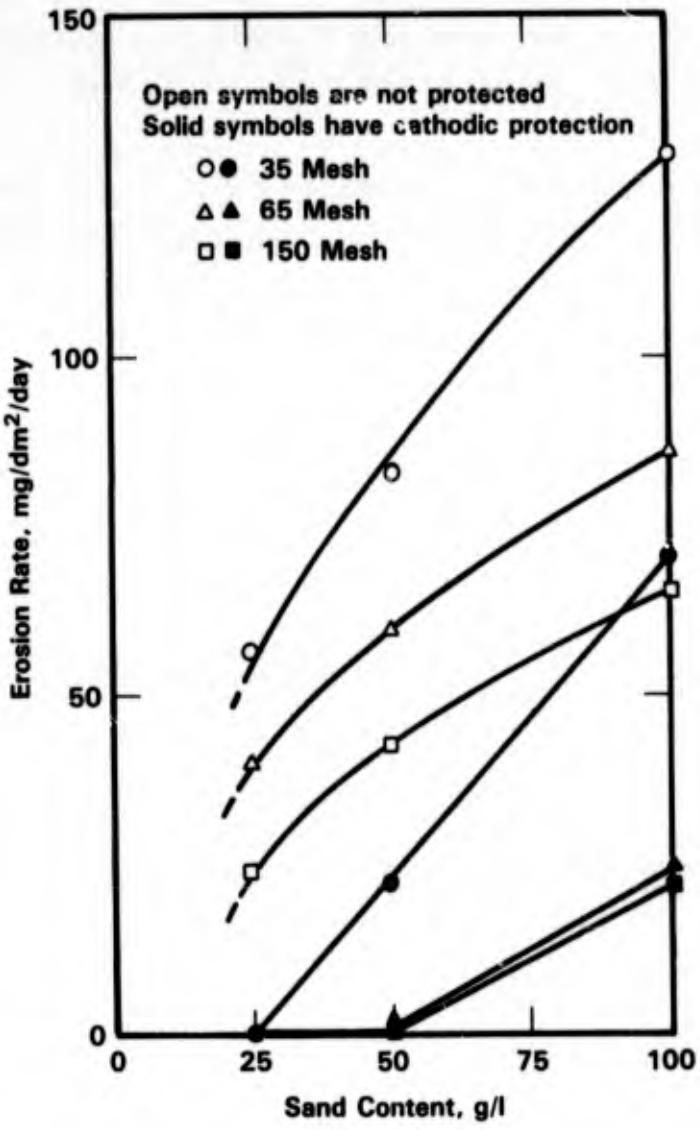

FIGURE 8-35. EFFECT OF CATHODIC PROTECTION ON SAND EROSION IN 2 M/S TAP WATER(53)

Galvanic Corrosion

A galvanic series for commercial alloys and metals in seawater is shown in Table 8-16 where it can be seen that the copper-base alloys are noble to common construction materials such as steel cast iron and aluminum but active to the noble metals and passive stainless steels and nickel-base alloys. Results of long term galvanic corrosion tests, given in Table 8-17 are consistent with the galvanic series. The copper-base alloys were galvanically protected by coupling to active metals such as carbon steel; whereas they experienced accelerated

TABLE 8-16. GALVANIC SERIES OF SOME COMMERCIAL METALS AND ALLOYS IN SEAWATER[51]

Noble or cathodic ↑	Platinum
	Gold
	Graphite
	Titanium
	Silver
	Chlorimet 3 (62 Ni, 18 Cr, 18 Mo)
	Hastelloy C (62 Ni, 17 Cr, 15 Mo)
	18-8 Mo stainless steel (passive)
	18-8 stainless steel (passive)
	Chromium stainless steel 11-30% Cr (passive)
	Inconel® (passive) (80 Ni, 13 Cr, 7 Fe)
	Nickel (passive)
	Silver solder
	Monel® (70 Ni, 30 Cu)
	Cupronickels (60-90 Cu, 40-10 Ni)
	Bronzes (Cu-Sn)
	Copper
	Brasses (Cu-Zn)
	Chlorimet 2® (66 Ni, 32 Mo, 1 Fe)
	Hastelloy B® (60 Ni, 30 Mo, 6 Fe, 1 Mn)
	Inconel® (active)
	Nickel (active)
	Tin
	Lead
	Lead-tin solders
	18-8 Mo stainless steel (active)
	18-8 stainless steel (active)
	Ni-Resist (high Ni cast iron)
	Chromium stainless steel, 13% Cr (active)
	Cast iron
	Steel or iron
	2024 aluminum (4.5 Cu, 1.5 Mg, 0.6 Mn)
Active or anodic ↓	Cadmium
	Commercially pure aluminum (1100)
	Zinc
	Magnesium and magnesium alloys

corrosion as a result of coupling to the stainless steels and the nickel-base alloy Monel. In general, the copper-base alloys were found to be galvanically compatible, but galvanic corrosion occurred under some circumstances. The Monel 400-phosphorus bronze couple was surprisingly aggressive, producing more severe galvanic corrosion of phosphorus bronze than any other couple. The corrosion rate of the phosphorus bronze increased from 0.3 to 4.5 mpy as a result of the couple.

TABLE 8-17. CORROSION DAMAGE DATA FOR BIMETALLIC COUPLES OF COPPER-BASE ALLOYS IN AQUEOUS ENVIRONMENTS[59]

Couple		Strip Metal Average Penetration, mils[a]									Plate Metal Average Penetration, mils[a]								
		Sea Water			Mean Tide			Fresh Water			Sea Water			Mean Tide			Fresh Water		
Strip, 2 x 9 x 14 in.	Plate, 9 x 9 x 1/4 in.	1 Yr	8 Yr	16 Yr	1 Yr	8 Yr	16 Yr	1 Yr	8 Yr	16 Yr	1 Yr	8 Yr	16 Yr	1 Yr	8 Yr	16 Yr	1 Yr	8 Yr	16 Yr
316 Stainless steel (18-13 + Mo)	Naval brass (39Zn-1Sn)	0.0	0.0	0.0 2.0*[c]	0.0	0.0	0.0 0.2*	0.0	0.0	0.0 0.0*	3.9	9.3	16.2 12.4*	1.0	4.7	7.7 6.0*	0.4	2.0	2.5 1.9*
316 Stainless steel (18-13 + Mo)	Phosphor bronze (4Sn-0.25P)	0.0	0.0	0.0 2.0*	0.0	0.0	0.0 0.2*	0.0	0.0	0.0 0.0*	1.6	6.0	9.4 5.5*	0.7	3.4	6.1 3.5*	0.2	0.7	0.7 0.7*
316 Stainless steel (18-13 + Mo)	316 Stainless steel (18-13 + Mo)	0.0	0.3	3.1 2.0*	0.0	0.1	0.1 0.2*	0.0	0.0	0.0 0.0*	0.0	0.6	1.3 2.0*	0.0	0.0	0.1 0.2*	0.0	0.0	0.0 0.0*
302 Stainless steel (18Cr-8Ni)	302 Stainless steel (18Cr-8Ni)	0.1	5.7	8.2 9.3*	0.2	0.5	1.3 1.6*	0.0	0.1	0.1 0.0*	0.3	4.5	7.6 2.0*	0.1	0.7	1.2 0.2*	0.0	0.0	0.0 0.0*
Nickel-copper (Monel: 70Ni-30Cu, cold rolled)	Carbon steel (0.24% C)	0.0	0.0	0.1 8.7*	0.0	0.0	0.1 2.7*	0.0	0.0	0.0 0.6*	8.0	27.8	51.2 48.1*	10.5	23.0	42.8 45.2*	7.9	23.3	26.6 26.0*
Nickel-copper (Monel: 70Ni-30Cu, cold rolled)	Nickel-copper (Monel: 70Ni-30Cu, cold rolled)	1.6	6.9	17.2 8.7*	0.1	2.3	4.3 8.7*	0.2	1.3	1.3 0.6*	1.4	6.9	9.7 8.7*	0.1	1.3	2.7 2.7*	0.0	0.1	0.4 0.6*
Copper-nickel (70Cu-30Ni)	Carbon steel (0.24% C)	0.0	0.0	0.1 2.3*	0.0	0.0	0.1 0.8*	0.0	0.0	0.1 1.3*	7.6	29.8	50.4 48.1*	12.3	21.0	53.0 45.2*	7.9	22.8	29.8 26.0*
Phosphor bronze (4Sn-0.25P)	Aluminum (AA1100: 99% Al)	0.2	0.3	0.7 5.5*	0.1	0.2	0.4 3.5*	0.0	0.0	0.1 0.7*	1.7	3.6	6.5 1.0*	1.3	2.3	6.0 0.5*	1.5	6.6	12.4 5.0*
Phosphor bronze (4Sn-0.25P)	Galvanized steel	0.0	0.1 4.0*	(d)	0.1	0.1 2.1*	(d)	0.0	0.0 0.5*	(d)									
Phosphor bronze (4Sn-0.25P)	Carbon steel (0.24% C)	0.1	0.2	0.4 5.5*	0.2	0.1	0.4 3.5*	0.1	0.1	0.1 0.7*	7.5	29.6	55.1 48.1*	11.3	22.3	46.4 45.2*	8.7	24.5	28.9 26.0*
Phosphor bronze (4Sn-0.25P)	0.3% Cu steel	0.2	0.2 4.0*	(d)	0.1	0.2 2.1*	(d)	0.1	0.2 0.5*	(d)	7.8	32.6 49.3*	(d)	14.2	25.8 46.2*	(d)	8.0	23.0 28.7*	(d)
Phosphor bronze (4Sn-0.25P)	Low-alloy steel (Cu-Ni)	0.1	0.1	0.5 5.5*	0.1	0.1	0.4 3.5*	0.0	0.1	0.1 0.7*	7.4	28.8	53. 48.4*	13.1	34.5	56.0 49.1*	6.7	18.0	23.0 22.0*
Phosphor bronze (4Sn-0.25P)	Low-alloy steel (Cu-Cr-Si)	0.2	0.3	0.5 5.5*	0.1	0.1	0.3 3.5*	0.1	0.1	0.2 0.7*	8.1	43.9	78.5 80.7*	10.8	25.9	59.8 49.3*	6.2	18.1	24.1 24.4*
Phosphor bronze (4Sn-0.25P)	Low-alloy steel (Cu-Ni-Mn-Mo)	0.1	0.2	0.6 5.5*	0.1	0.2	0.4 3.5*	0.1	0.1	0.1 0.7*	7.4	26.6	48.3 45.1*	11.2	21.2	56.3 61.0*	7.6	22.7	31.8 31.2*
Phosphor bronze (4Sn-0.25P)	Low-alloy steel (Cr-Ni-Mn)	0.1	0.2	0.5 5.5*	0.1	0.1	0.3 3.5*	0.1	0.1	0.1 0.7*	8.0	45.0	99.6 84.1*	9.9	24.3	65.2 45.8*	6.0	16.4	25.5 26.8*
Phosphor bronze (4Sn-0.25P)	Nickel steel (2% Ni)	0.1	0.2	0.5 5.5*	0.1	0.1	0.4 3.5*	0.0	0.1	0.2 0.7*	7.9	31.9	60.8 52.0*	8.6	23.5	55.9 55.0*	8.2	21.7	24.6 21.1*

Table 8-17. (Continued)

Couple		Strip Metal Average Penetration, mils[a]									Plate Metal Average Penetration, mils[a]								
		Sea Water			Mean Tide			Fresh Water			Sea Water			Mean Tide			Fresh Water		
Strip, 2 x 9 x 14 in.	Plate, 9 x 9 x 1/4 in.	1 Yr	8 Yr	16 Yr	1 Yr	8 Yr	16 Yr	1 Yr	8 Yr	16 Yr	1 Yr	8 Yr	16 Yr	1 Yr	8 Yr	16 Yr	1 Yr	8 Yr	16 Yr
Phosphor bronze (4Sn-0.25P)	Chromium steel (3% Cr)	0.2	0.3	0.6 5.5*	0.2	0.3	0.4 3.5*	0.1	0.1	0.2 0.7*	2.2	43.4	86.5 70.4*	10.9	29.7	57.2 48.1*	3.0	11.2	16.2 14.7*
Phosphor bronze (4Sn-0.25P)	Cast steel (0.27% C)	0.1	0.2	0.2 5.5*	0.1	0.1	0.3 3.5*	0.1	0.2	0.1 0.7*	8.3	29.8	51.6 43.3*	10.0	22.6	48.5 49.1*	8.2	18.2	30.1 26.3*
Phosphor bronze (4Sn-0.25P)	Gray cast iron (3.2% C)	0.1	0.2	0.3 5.5*	0.0	0.2	0.3 3.5*	0.0	0.2	0.1 0.7*	10.0	59.4	104.7 94.6*	19.4	51.8	76.2 87.1*	5.2	23.5	33.3 32.9*
Phosphor bronze (4Sn-0.25P)	Austenitic cast iron (18% Ni)	0.1	0.1	0.3 5.5*	0.1	0.1	0.2 3.5*	0.6	0.2	0.0 0.7*	4.2	15.1	27.3 22.8*	1.9	5.0	10.2 7.3*	1.3	7.0	13.3 8.0*
Phosphor bronze (4Sn-0.25P)	-nickel 10Ni)	1.8	3.3	4.6 5.5*	0.7	1.3	1.6 3.5*	0.1	0.4	0.5 0.7*	0.6	2.0	3.8 2.3*	0.1	0.6	1.0 0.8*	0.2	1.0	1.3 1.3*
Phosphor bronze (4Sn-0.25P)	N opper (Monel: 70Ni-30Cu, cold rolled)	2.7	66.3	71.8 5.5*	1.7	14.9	19.0 3.5*	1.6	8.8	14.1 0.7*	0.3	2.0	7.0 8.7*	0.1	1.0	2.2 2.7*	0.0	0.4	0.8 0.6*
Phosphor bronze (4Sn-0.25P)	410 Stainless steel (13% Cr)	0.5	0.4	0.7 5.5*	0.4	0.6	0.7 3.5*	0.2	0.7	0.9 0.7*	3.5	14.7	24.7 23.9*	0.6	4.2	8.8 6.4*	0.1	1.4	3.3 0.9*
Phosphor bronze (4Sn-0.25P)	302 Stainless steel (18Cr-8Ni)	7.8	16.3	21.9 5.5*	1.1	8.5	13.7 3.5*	0.5	4.1	3.8 0.7*	0.0	3.8	6.3 9.3*	0.1	0.4	1.0 1.1*	0.0	0.0	0.0 0.0*
Phosphor bronze (4Sn-0.25P)	316 Stainless steel (18-13 + Mo)	22 8	37.4	41.3 5.5*	3.2	21.9	29.8 3.5*	0.3	1.7	1.8 0.7*	0.0	0.2	0.2 2.0*	0.0	0.0	0.0 0.2*	0.0	0.0	0.0 0.0*
Aluminum bronze (5% Al)	Carbon steel (0.24% C)	0.1	0.1	0.4 1.3*	0.1	0.1	0.4 0.6*	0.0	0.1	0.2 0.4*	7.4	28.6	57.6 48.1*	10.6	23.7	46.1 45.2*	8.5	23.1	28.0 26.0*
Low brass (80Cu-20Zn)	Carbon steel (0.24% C)	0.1	0.1	0.4 3.7*	0.1	0.1	0.5 0.7*	0.1	0.2	0.2 1.7*	7.4	29.2	54.4 48.1*	12.0	20.0	44.3 45.2*	8.6	24.9	29.4 26.0*
Naval brass (39Zn-1Sn)	Carbon steel (0.24% C)	0.1	0.1	0.2 12.4*	0.2	0.1	0.3 6.0*	0.1	0.1	0.2 1.9*	7.2	29.7	54.4 48.1*	13.4	22.8	45.1 45.2*	8.6	23.8	28.0 26.0*
Copper (99.9% Cu)	Carbon steel (0.24% C)	2.0	3.0	7.0 6.0*	2.0	3.0	6.0 1.3*	0.0	1.0	3.0 1.0*	7.6	29.5	54.9 48.1*	11.9	23.0	42.7 45.2*	7.8	23.9	30.6 26.0*
Carbon steel (0.25% C)	Carbon steel (0.24% C)	7.5	26.4 25.5*	50.0 48.1*	7.8	15.7	47.2 45.2*	8.5	20.1	25.9 26.0*	6.8	24.0	44.0 48.1*	9.8	17.9	42.2 45.2*	8.4	20.5	26.4 26.0*
Carbon steel (0.24% C)	Cast bronze (Ounce metal)	36.9	153.4 25.5*	M[e]	24.4	103.4 23.2*	M	15.0	58.7	77.3 26.0*	0.0	0.1	3.1 4.1*	0.1	0.2	0.3 1.2*	0.0	0.1	0.3 0.4*
Carbon steel (0.24% C)	Cast bronze (Valve metal)	36.0	185.0 25.5*	M	19.9	81.1 23.2*	M	14.9	56.7	69.0 26.0*	0.1	0.1	1.9 2.2*	0.1	0.1	0.1 1.4*	0.0	0.1	0.2 0.4*

Table 8-17. (Continued)

Couple		Strip Metal Average Penetration, mils[a]									Plate Metal Average Penetration, mils[a]								
		Sea Water			Mean Tide			Fresh Water			Sea Water			Mean Tide			Fresh Water		
Strip, 2 x 9 x 14 in.	Plate, 9 x 9 x 1/4 in.	1 Yr	8 Yr	16 Yr	1 Yr	8 Yr	16 Yr	1 Yr	8 Yr	16 Yr	1 Yr	8 Yr	16 Yr	1 Yr	8 Yr	16 Yr	1 Yr	8 Yr	16 Yr
Carbon steel (0.24% C)	Cast tin bronze (9% Sn)	35.2	164.0 25.5*	M	21.0	87.0 23.2*	M	15.1	52.0	61.0 26.0*	0.1	0.1	2.5 5.4*	0.1	0.2	0.2 1.4*	0.0	0.1	0.2 0.3*
Carbon steel (0.24% C)	Cast nickel-tin bronze (6Ni-3Sn)	36.4	180.8 25.5*	M	21.0	97.3 23.2*	M	14.6	49.1	59.8 26.0*	0.0	0.1	1.6 6.0*	0.0	0.1	0.2 1.2*	0.0	0.2	0.3 0.5*
Carbon steel (0.24% C)	Muntz brass (40Zn-0.25As)	37.2	161.8 25.5*	M	36.3	128.8 23.2*	M	14.6	61.4	77.4 26.0*	0.1	0.1	5.2 8.2*	0.2	0.3	0.9 5.7*	0.2	1.0	1.5 3.5*
Carbon steel (0.24% C)	Manganese brass (41Zn + Sn + Fe)	34.8	158.7 25.5*	M	32.7	106.2 23.2*	M	13.7	45.9	66.4 26.0*	0.1	0.1	7.9 17.2*	0.2	0.3	1.5 7.5*	0.1	0.3	0.4 0.9*
Carbon steel (0.24% C)	Naval brass (39Zn-1Sn)	35.2	176.5 25.5*	M	34.6	116.9 23.2*	M	13.9	47.7	64.3 26.0*	0.1	0.1	7.4 12.4*	0.3	0.3	0.7 6.0*	0.1	0.5	0.8 1.9*
Carbon steel (0.24% C)	Cartridge brass (30% Zn)	36.1	162.3 25.5*	M	38.4	116.8 23.2*	M	14.9	57.0	79.6 26.0*	0.0	0.0	3.1 3.6*	0.1	0.1	0.3 0.9*	0.1	0.3	0.4 1.8*
Carbon steel (0.24% C)	Low brass (20% Zn)	38.8	152.0 25.5*	M	28.2	104.6 23.2*	M	15.5	50.8	63.4 26.0*	0.1	0.1	2.4 3.7*	0.1	0.1	0.3 0.7*	0.1	0.2	0.3 1.7*
Carbon steel (0.24% C)	Commercial bronze (10% Zn)	37.9	155.6 25.5*	M	21.3	93.9 23.2*	M	14.1	50.9	67.7 26.0*	0.1	0.1	3.1 4.9*	0.0	0.1	0.2 1.0*	0.0	0.2	0.2 1.3*
Carbon steel (0.24% C)	Aluminum bronze (5% Al)	34.9	169.9 25.5*	M	24.0	102.7 23.2*	M	14.6	56.9	70.8 26.0*	0.0	0.0	4.0 1.3*	0.0	0.1	0.2 0.6*	0.0	0.1	0.2 0.4*
Carbon steel (0.24% C)	Phosphor bronze (4Sn-0.25P)	35.1	172.1 25.5*	M	25.2	96.2 23.2*	M	14.3	45.6	65.5 26.0*	0.1	0.1	1.9 5.5*	0.1	0.2	0.2 3.5*	0.1	0.2	0.3 0.7*
Carbon steel (0.24% C)	Silicon bronze (2.5% Si)	35.6	177.6 25.5*	M	21.5	96.3 23.2*	M	15.4	57.3	72.9 26.0*	0.1	0.2	2.7 5.9*	0.1	0.2	0.3 2.0*	0.1	0.2	0.3 1.2*
Carbon steel (0.24% C)	Copper (99.9% Cu)	36.5	191.5 25.5*	M	17.6	84.2 23.2*	M	14.2	56.3	77.7 26.0*	0.1	0.1	2.9 6.0*	0.1	0.1	0.5 1.3*	0.1	0.1	0.2 1.0*
Carbon steel (0.24% C)	Copper-nickel (70Cu-30Ni)	37.5	168.8 25.5*	M	23.2	96.7 23.2*	M	13.9	50.0	68.6 26.0*	0.0	0.1	1.6 2.3*	0.0	0.1	0.1 0.8*	0.0	0.2	0.3 1.3*
Carbon steel (0.24% C)	Nickel-copper (Monel: 70Ni-30Cu, cold rolled)	34.2	157.7 25.5*	M	23.3	92.2	191.5 45.2*	12.7	40.0	60.9 26.0*	0.0	0.1	2.4 8.7*	0.0	0.1	0.1 2.7*	0.0	0.0	0.0 0.6*

(a) Mils × 0.0254 = mm. Values calculated from weight losses.
(b) A couple consisting of a strip of 316 stainless steel (metal No. 58) with an exposed area of 21.9 in.^{2} attached to a plate of carbon steel (metal No. 35) with an exposed area of 151.4 in.^{2} (area ratio = 1:6.9).
(c) Values marked with an asterisk (*) show the normal uncoupled corrosion loss.
(d) Value not determined.
(e) M indicates that strips were missing—probably completely corroded away.

More recently, Scully and Hack[60] studied the galvanic corrosion of a number of couples, including three-metal couples, in seawater. A listing of the couples studied is given in Table 8-18 and the compositions of these alloys are given in Appendix H, Table H-2. Weight losses for the couples are given in Tables 8-19 and 8-20. These data show that the corrosion of the copper-base alloys is significantly accelerated by coupling to the more noble metals such as Inconel Alloy 625 and titanium. In this study, Scully and Hack[60] also reported that electrochemical techniques such as potentiostatic and potentiodynamic polarization were capable of predicting the observed galvanic corrosion behavior, even for the multi-metal couples. Data demonstrating this predictive capability for copper-base alloys are given in Table 8-21.

TABLE 8-18. LISTING OF COUPLES STUDIED BY SCULLY AND HACK[60] (ALLOY COMPOSITIONS ARE GIVEN IN APPENDIX H, TABLE H-2)

BI-METAL GALVANIC COUPLE COMBINATIONS
HY-80 coupled to Zinc
Ni-Al-Bronze coupled to Zinc
90-10 Copper-Nickel to Zinc
Titanium 50 to Monel
Titanium 50 coupled to 70-30 Copper Nickel
Monel coupled to 70-30 Copper Nickel
Inconel 625 coupled to 70-30 Copper Nickel
Inconel 625 coupled to Ni-Al-Bronze
M-Bronze coupled to 70-30 Copper Nickel
M-Bronze coupled to 90-10 Copper Nickel
MULTIMETAL (3) GALVANIC COUPLE COMBINATIONS
HY-80 coupled to Ni-Al-Bronze coupled to Zinc
Ti-50 coupled to Inconel 625 coupled to 70-30 Copper Nickel
Ti-50 coupled to 70-30 Copper Nickel coupled to Zinc
Monel coupled to 90-10 Copper Nickel coupled to Zinc
Inconel 625 coupled to Ni-Al-Bronze coupled to Zinc
Inconel 625 coupled to Monel coupled to 70-30 Copper Nickel
Monel coupled to Ti-50 coupled to Ni-Al-Bronze
Inconel 625 coupled to Ni-Al-Bronze coupled to 70-30 Copper Nickel
FREELY CORRODING COUPONS (CONTROLS)
HY-80
Ni-Al-Bronze
M-Bronze
90-10 Copper Nickel
Inconel 625
Monel
Anode Zinc
70-30 Copper Nickel
Titanium 50

TABLE 8-19. WEIGHT LOSS FOR BI-METAL GALVANIC COUPLE SPECIMENS IN SEAWATER, AREA RATIO 1:1[60]

Material		Exposure	Anode Weight	Control Weight
Cathode	Anode	Duration, days	Loss, g	Loss, g
HY-80	Zinc	30	0.1802	0.2581
		60	0.4459	0.3929
		120	0.7091	0.2082
Ni-Al-Bronze	Zinc	30	0.1935	0.2581
		60	0.4453	0.3929
		120	0.7153	0.2082
90-10 Cu-Ni	Zinc	30	0.1730	0.2581
		60	0.4883	0.3929
		120	0.8322	0.2082
Titanium 50	Monel 400	30	0.1043	0.0988
		60	0.1002	0.0949
		120	0.1978	0.0384
Monel 400	70-30 Cu-Ni	30	0.0574	0.0245
		60	0.0887	0.0275
		120	0.2910	0.0316
Inconel 625	70-30 Cu-Ni	30	0.0836	0.0245
		60	0.2291	0.0275
		120	0.5135	0.0316
Inconel 625	Ni-Al-Bronze	30	0.2446	0.2446
		60	0.1948	0.1948
		120	0.2773	0.2773
90-10 Cu-Ni	M-Bronze	30	0.0764	0.0820
		60	0.1174	0.1118
		120	0.1577	0.1658
Titanium 50	70-30 Cu-Ni	30	0.0742	0.0245
		60	0.0949	0.0275
		120	0.2090	0.0316

TABLE 8-20. WEIGHT LOSS FOR MULTI-METAL GALVANIC COUPLE SPECIMENS IN SEAWATER, AREA RATIO 1:1[60]

Materials	Cathode Materials	Anode Materials	Exposure Duration, days	Anode Weight Loss, g	Control Weight Loss, g (Anode Material)
Ni-Al-Bronze	Ni-Al-Bronze		30	0.5322	0.2581
HY-80 Steel	HY-80 Steel		60	0.7844	0.3929
Anode Zinc		Anode Zinc	120	1.1355	0.2082
Titanium 50	Titanium 50		30	0.1300	0.0245
Inconel 625	Inconel 625		60	0.3588	0.0275
70-30 Cu-Ni		70-30 Cu-Ni	120	0.6125	0.0316
Titanium 50	Titanium 50		30	0.3762	0.2581
70-30 Cu-Ni	70-30 Cu-Ni		60	0.6506	0.3929
Anode Zinc		Anode Zinc	120	1.3211	0.2082
Monel 400	Monel 400		30	0.2923	0.2581
90-10 Cu-Ni	90-10 Cu-Ni		60	0.3147	0.3929
Anode Zinc		Anode Zinc	120	0.5711	0.2082
Inconel 625	Inconel 625		30	0.4460	0.2581
Ni-Al-Bronze	Ni-Al-Bronze		60	0.8821	0.3929
Anode Zinc		Anode Zinc	120	1.7652	0.2082
Inconel 625	Inconel 625		30	0.1980	0.0245
Monel 400	Monel 400		60	0.2602	0.0275
Ni-Al-Bronze		70-30 Cu-Ni	120	0.5712	0.0316
Titanium 50	Titanium 50		30	0.0404	0.0460
Monel 400	Monel 400		60	0.1123	0.0291
Ni-Al-Bronze		Ni-Al-Bronze	120	0.5284	0.1009
			30	0.0568	0.0460
Inconel 625	Inconel 625	Ni-Al-Bronze	60	0.1453	0.0291
Ni-Al-Bronze			120	0.4849	0.1009
70-30 Cu-Ni		70-30 Cu-Ni	30	0.0225	0.0245
			60	0.0306	0.0275
			120	0.0311	0.0316

TABLE 8-21. COMPARISON OF PREDICTED AND ACTUAL GALVANIC COUPLE PARAMETERS FROM LONG-TERM POTENTIOSTATIC DATA, AREA RATIO 1:1[60]

Material		Exposure Duration, days	Current Density, μA/cm²		Couple Potential, mV versus Ag/AgCl		Anode Corrosion Rate, mm/yr	
Cathode	Anode		Predicted	Actual*	Predicted	Actual	Predicted	Actual
HY-80	Zinc	30	11.0	7.1	-1025	-1035	.43	.160
		60	9.0	9.4	-1025	-1032	.43	.198
		120	6.0	2.4	-1024	-1030	.43	.157
Ni-Al-Bronze	Zinc	30	10.5	4.3	-1025	-1021	.43	.172
		60	6.5	5.9	-1024	-1032	.43	.198
		120	2.0	5.1	-1023	-1036	.43	.159
90-10 Cu-Ni	Zinc	30	15.0	5.0	-1024	-1031	.43	.154
		60	10.0	10.1	-1023	-1031	.43	.217
		120	9.0	5.5	-1022	-1031	.43	.185
Titanium 50	Monel 400	30	1.8	1.4	-70	-55	.045	.075
		60	0.3	1.2	-90	-130	.022	.036
		120	<0.2	<0.1	-130	-95	--	.035
Monel 400	70-30 Cu-Ni	30	3.0	1.1	-100	-125	.180	.041
		60	2.5	0.4	-102	-130	.095	.031
		120	4.2	1.7	-110	-110	.070	.052
Inconel 625	70-30 Cu-Ni	30	1.3	2.2	-101	-106	.180	.059
		60	1.9	1.0	-120	-62	.045	.051
		120	2.0	3.5	-160	-50	.0085	.127
Inconel 625	Ni-Al-Bronze	30	5.5	4.0	-145	-145	.180	.202
		60	4.5	3.5	-155	-250	.180	.081
		120	--	3.9	--	--	--	.057
90-10 Cu-Ni	M-Bronze	30	0.3	0.2	-173	-116	.150	.057
		60	0.4	<0.1	-171	-115	.170	<.044
		120	--	0.2	--	-145	--	.060
Titanium 50	70-30 Cu-Ni	30	2.1	1.0	-110	-121	.150	.053
		60	1.2	0.4	-120	-105	.045	.034
		120	0.5	1.1	-170	-70	.0080	.037

* Based on coulombs of anodic charge passed during first 30, second 30, and final 60 days of experiments.

Seawater velocity can have a dramatic effect on the galvanic corrosion behavior of copper-base alloys. For instance, where a copper alloy is coupled to a more noble metal, the galvanic attack of the copper is greatly accelerated with increase in seawater velocity. Typical data showing this effect for several copper alloys coupled to titanium are given in Figure 8-36. This effect is responsible for the severe attack reported for copper-base alloy tube sheets in surface condensers where stainless steel or titanium tubes or tube inserts have been installed.(62)

The severe galvanic attack observed in condensers also appears to be highly temperature dependent. In recent condenser studies by Gehring and Maurer,(63) the rate of galvanic attack of Muntz metal, when coupled to titanium doubled for every 10 C rise in temperature, see Figure 8-37.

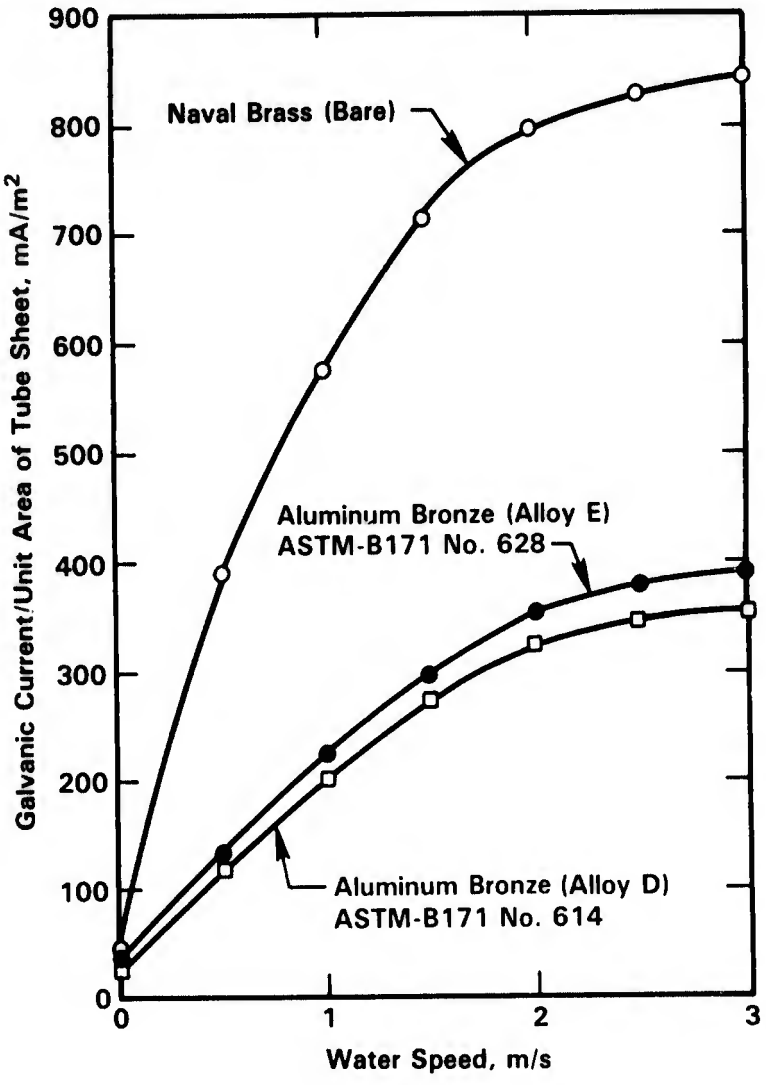

FIGURE 8-36. EFFECT OF WATER VELOCITY ON THE GALVANIC CURRENT BETWEEN TITANIUM TUBES AND TUBE SHEETS IN SEAWATER(61)

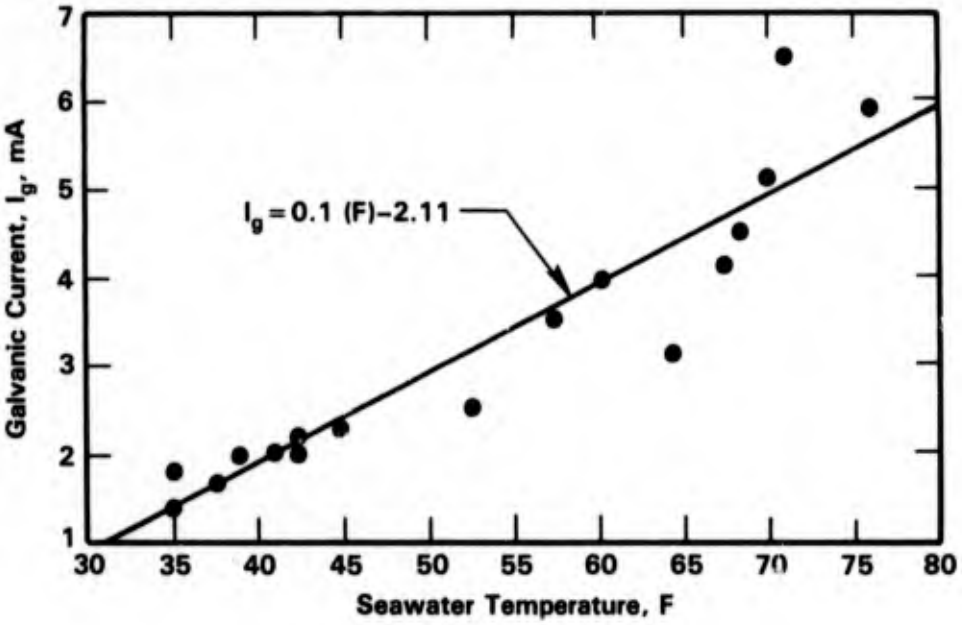

FIGURE 8-37. GALVANIC CORROSION VERSUS SEAWATER TEMPERATURE (MUNTZ/Ti-50A, INLET END)[63]

Galvanic corrosion of copper-base alloys also appears to be promoted by the presence of sulfides. Hack[64] performed galvanic corrosion tests on two piping alloys Cu-30Ni and Cu-10Ni and four fitting materials, bronze (composition M), cast Monel, wrought nickel-aluminum bronze, and cast Cu-30Ni. The experiments were performed at an area ratio of 3:1 (piping material/fitting material) in seawater at 2.4 m/s and three sulfide concentrations; 0.0, 0.01, or 0.05 mg/l. Results of the experiments, summarized in Figures 8-38 to 8-43 show that significant galvanic effects occurred in the presence of sulfide with alloys that are compatible in unpolluted seawater.

Stress-Corrosion Cracking

In general, the copper-base alloys are highly resistant to stress-corrosion cracking under submersed exposure in seawater. For example, Reinhart[11] exposed a series of stressed copper-base alloy specimens at a depth of about 2,000 feet in the Pacific Ocean and observed no stress-corrosion cracking failures in 197 days, see Table 8-22.

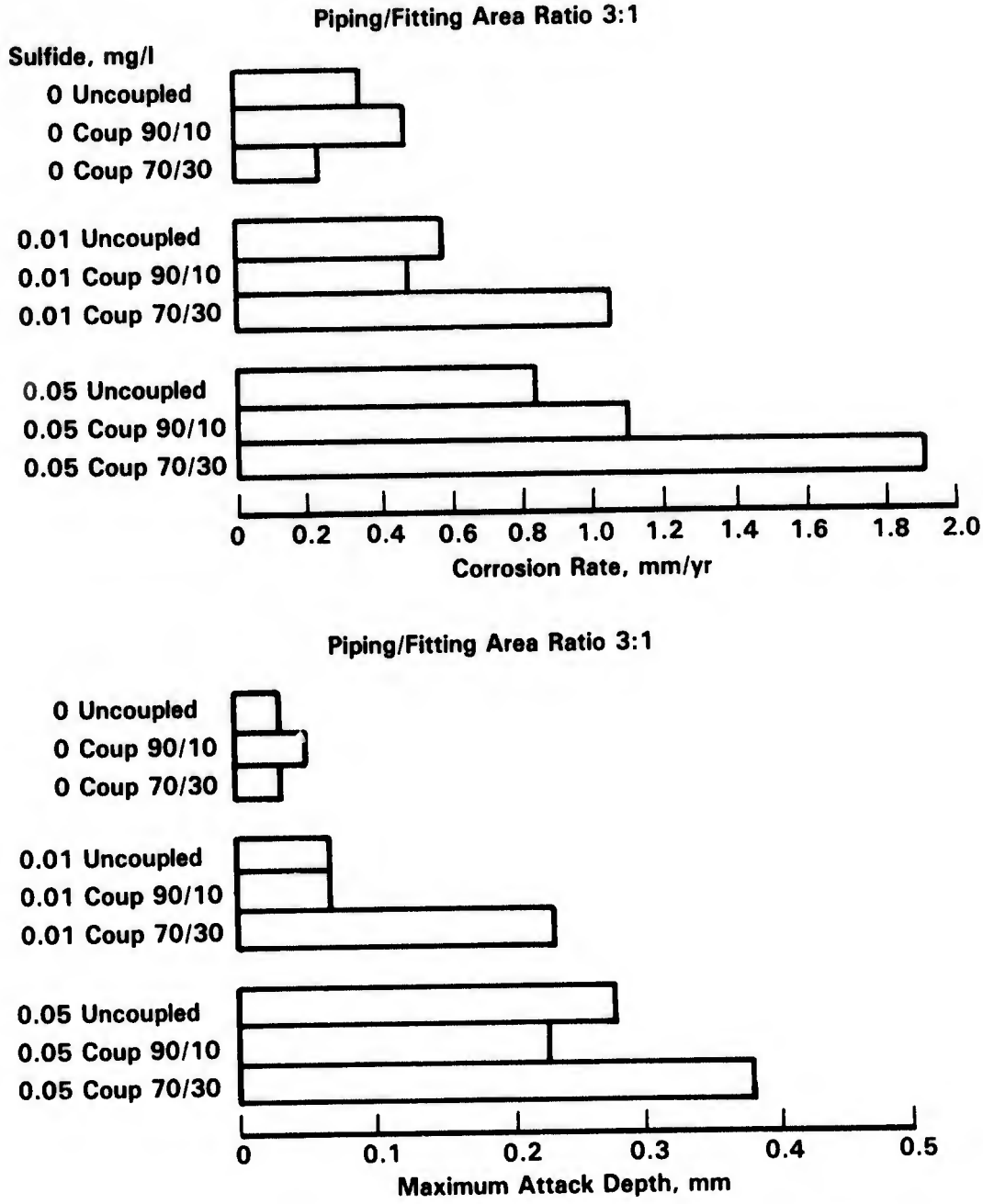

FIGURE 8-38. CORROSION OF M-BRONZE COUPLED TO PIPING MATERIALS IN SULFIDE CONTAINING SEAWATER AT 2.4 M/S[64]

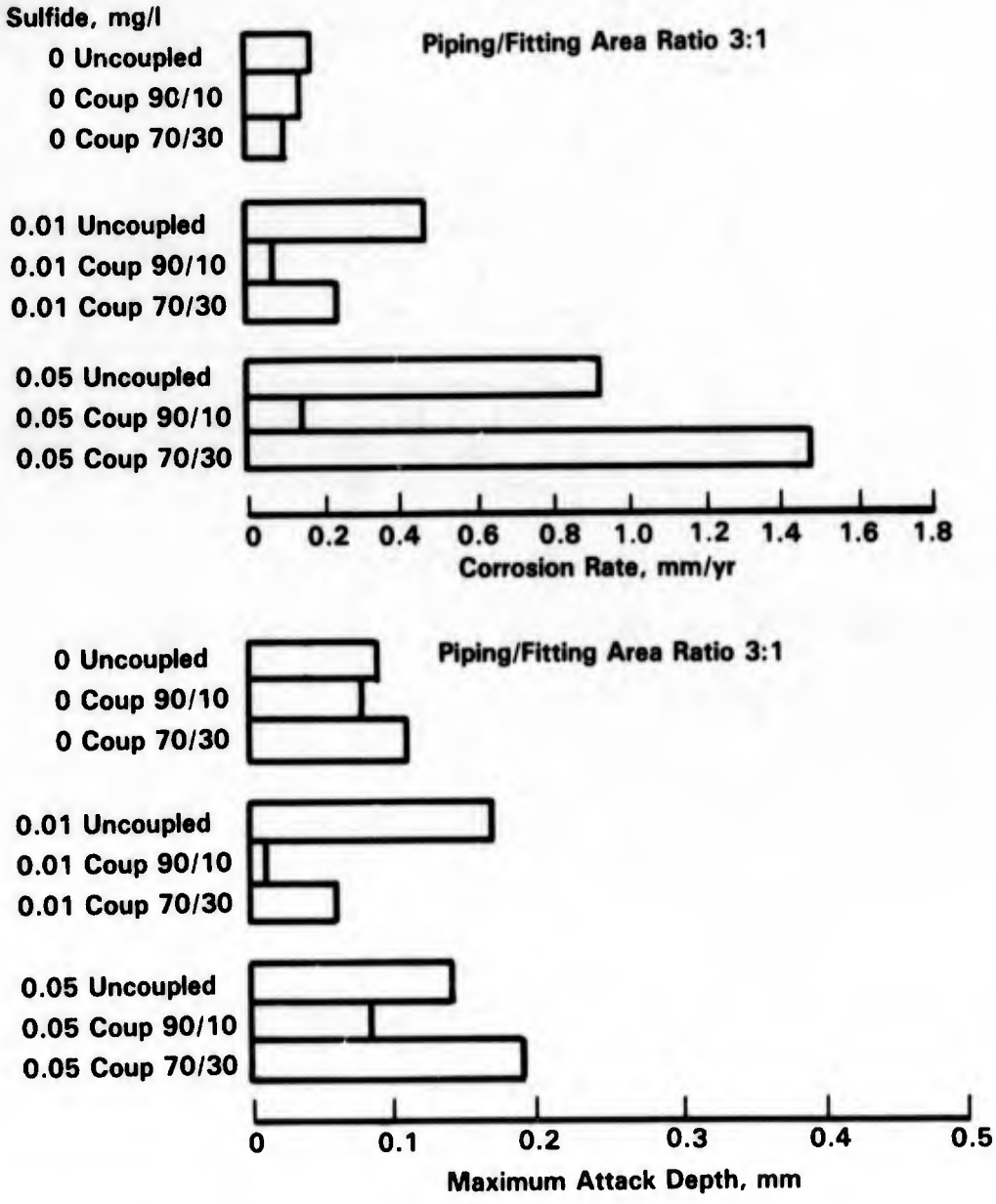

FIGURE 8-39. CORROSION OF MONEL COUPLED TO PIPING MATERIALS IN SULFIDE CONTAINING SEAWATER AT 2.4 M/S[64]

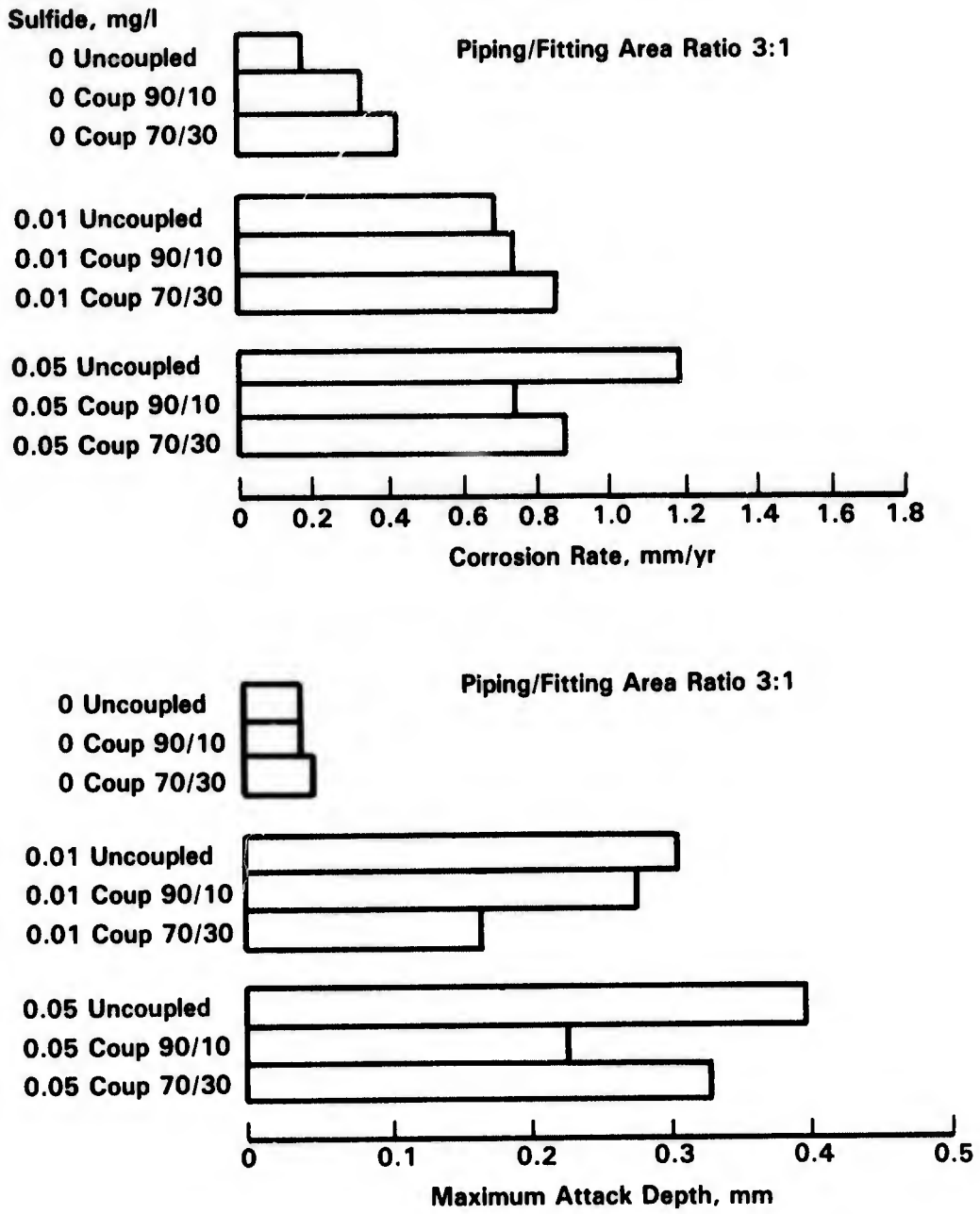

FIGURE 8-40. CORROSION OF Ni-Al-BRONZE COUPLED TO PIPING MATERIALS IN SULFIDE CONTAINING SEAWATER AT 2.4 M/S[64]

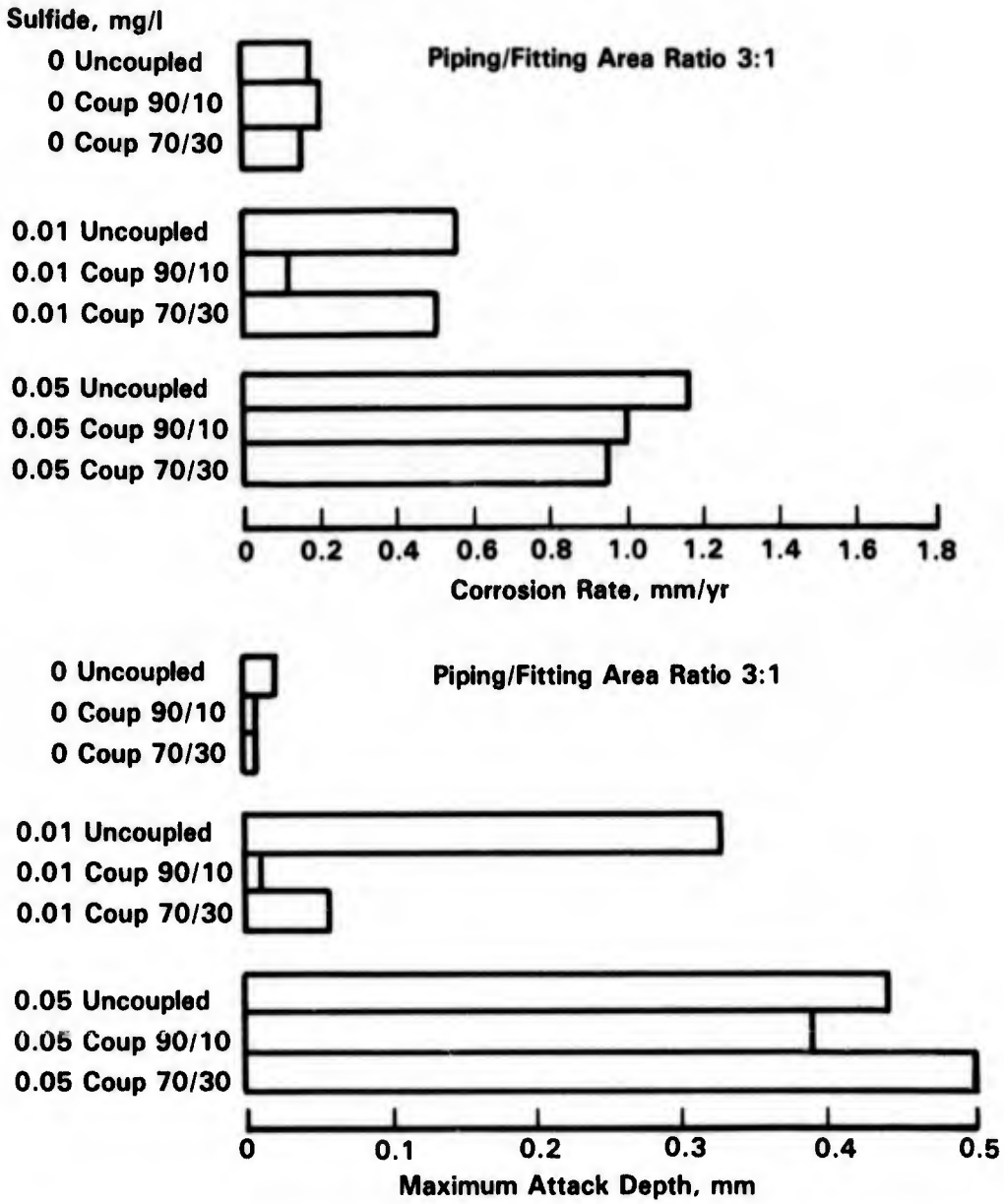

FIGURE 8-41. CORROSION OF CAST 70-30 Cu-Ni COUPLED TO PIPING MATERIALS IN SULFIDE CONTAINING SEAWATER AT 2.4 M/S[64]

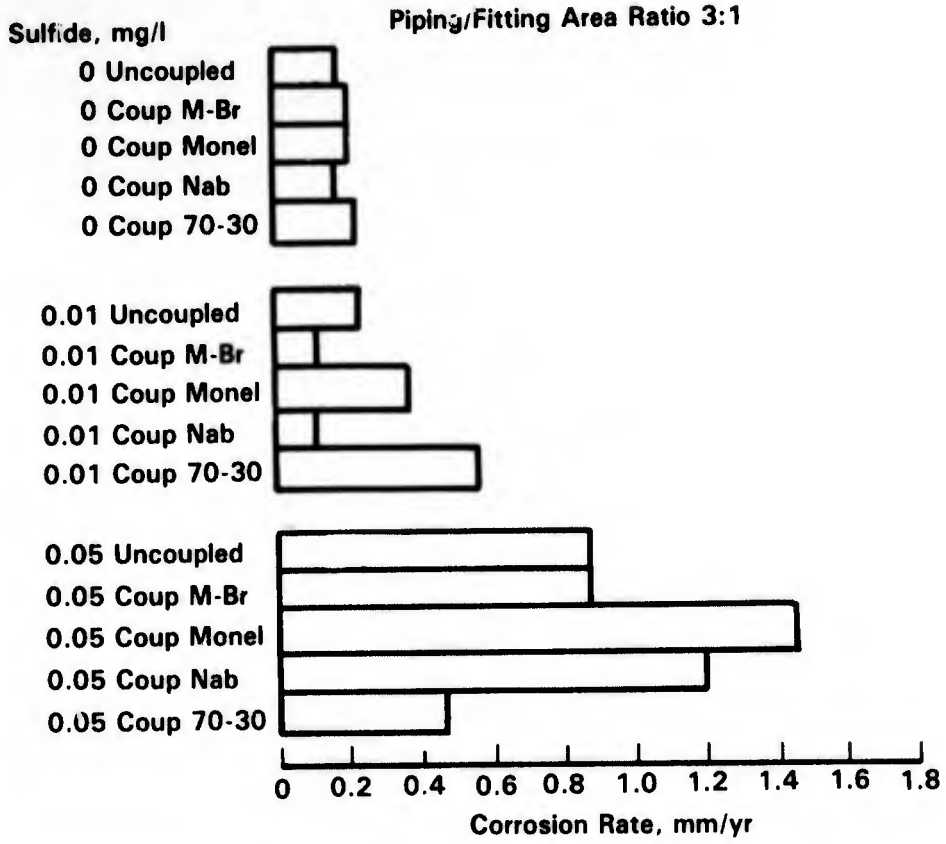

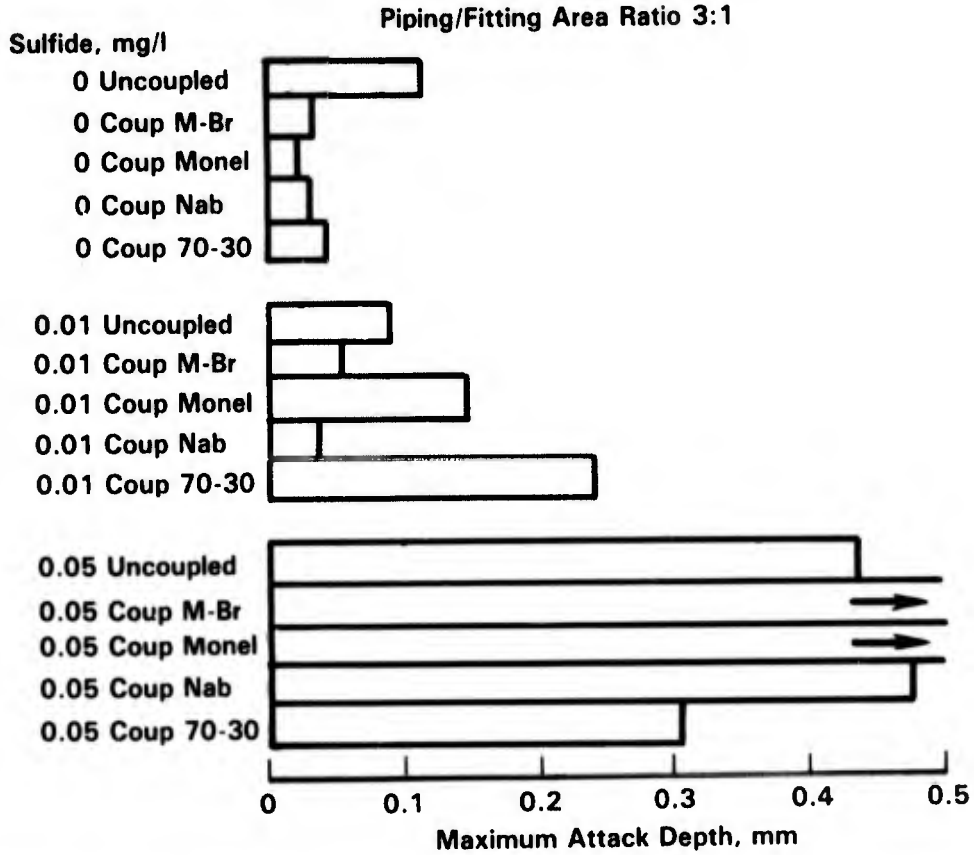

FIGURE 8-42. CORROSION OF 90-10 Cu-Ni COUPLED TO FITTING MATERIALS IN SULFIDE CONTAINING SEAWATER AT 2.4 M/S[64]

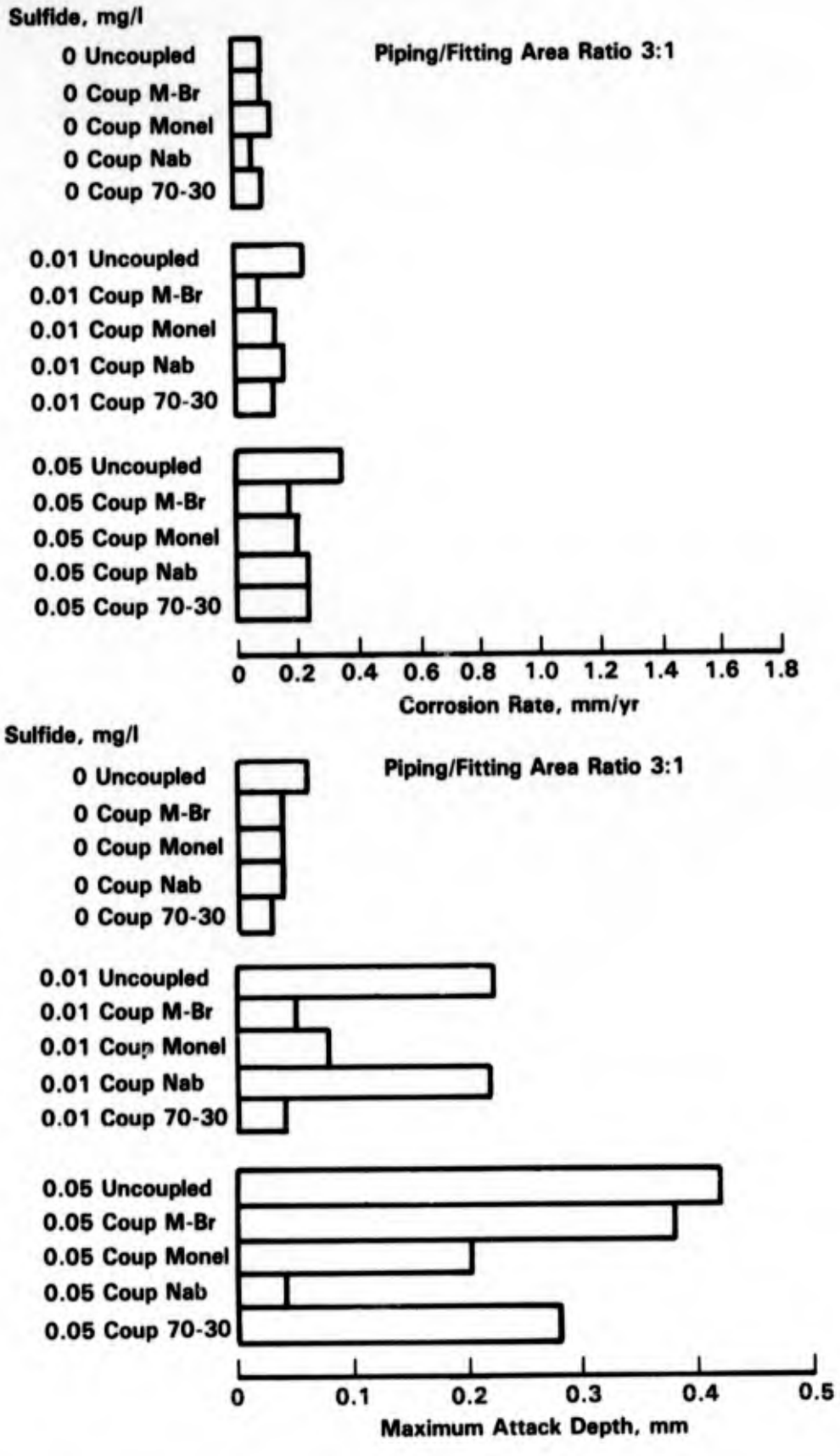

FIGURE 8-43. CORROSION OF 70-30 Cu-Ni COUPLED TO FITTING MATERIALS IN SULFIDE CONTAINING SEAWATER AT 2.4 M/S[64]

TABLE 8-22. RESULTS OF STRESS-CORROSION TESTS OF COPPER ALLOYS IN THE PACIFIC OCEAN[11]

Alloy	Stress, ksi	Percent of Yield Strength	Exposure, days	Depth, feet	Number of Specimens	Number Failed
Cu	10.7	75	197	2,340	3	0
Muntz metal	27.8	50	197	2,340	3	0
Muntz metal	41.6	75	197	2,340	3	0
As Admiralty	25.5	50	197	2,340	3	0
As Admiralty	38.2	75	197	2,340	3	0
Phosphor bronze A	25.7	50	197	2,340	3	0
Phosphor bronze A	38.5	75	197	2,340	3	0
Phosphor bronze D	22.4	35	197	2,340	3	0
Phosphor bronze D	32.0	50	197	2,340	3	0
Phosphor bronze D	47.9	75	197	2,340	3	0
Al bronze	29.6	35	197	2,340	3	0
Al bronze	42.3	50	197	2,340	3	0
Al bronze	63.5	75	197	2,340	3	0
Si bronze	22.5	35	197	2,340	3	0
Si bronze	32.2	50	197	2,340	3	0
Si bronze	48.3	75	197	2,340	3	0
Cu-Ni, 95-5	23.8	50	197	2,340	3	0
Cu-Ni, 95-5	35.7	75	197	2,340	3	0
Cu-Ni, 80-20	36.8	75	197	2,340	3	0
Cu-Ni, 70-30, 0.5 Fe	29.2	50	197	2,340	3	0
Cu-Ni, 70-30, 0.5 Fe	43.7	75	197	2,340	3	0
Cu-Ni, 70-30, 5.3 Fe	27.4	35	197	2,340	3	0
Cu-Ni, 70-30, 5.3 Fe	39.2	50	197	2,340	3	0
Cu-Ni, 70-30, 5.3 Fe	58.7	75	197	2,340	3	0

Isolated cases of SCC failures of copper-base alloys in seawater have been reported. Bulow[5] reported SCC of manganese bronze propellers having high residual stresses while Beavers, et al.[48] reported SCC of admirality brass condenser tubes which were exposed to brackish river water. In the latter failure, the cracking was attributed to nitrite, which formed as a result of decay of organic matter, in conjunction with high residual stresses from the tube rolling operation.

Most all the SCC failures of copper-base alloys in service have been attributed to ammonia or other nitrogen compounds such as nitrates and amines. These species may form beneath deposits in seawater, as discussed above. In these environments, copper-zinc alloys are highly susceptible to SCC, whereas the copper nickel alloys are resistant. A summary of the relative susceptibilities of the copper-base alloys to SCC is given in Table 8-23. The effects of nickel and zinc in copper on SCC in ammoniacal environments are shown more explicably in Figures 8-44 and 8-45.

TABLE 8-23. RANKING OF COPPER-BASE ALLOYS ACCORDING TO THEIR RESISTANCE TO SCC IN CONCENTRATED AMMONIA ENVIRONMENT(65)

- Highly susceptible to ammonia-SCC

  brass with 10% zinc and more
  aluminum bronze with 1 to 8% aluminum
  silicon bronze with 0.8 to 1.2% silicon
  all copper alloys with more than 20% zinc

- Moderately susceptible to ammonia-SCC

  beryllium copper, alloys 170, 172
  brass with less than 10% zinc
  aluminum bronze with 9% or more aluminum
  copper-nickel with less than 10% nickel
  phosphorus deoxidized copper, alloy 122

- Resistant to ammonia-SCC

  pure copper, e.g., alloys 101 through 113
  copper-iron, alloy 194
  copper-nickel-iron with 10% and more nickel
  copper-tin alloys with 2% and more tin

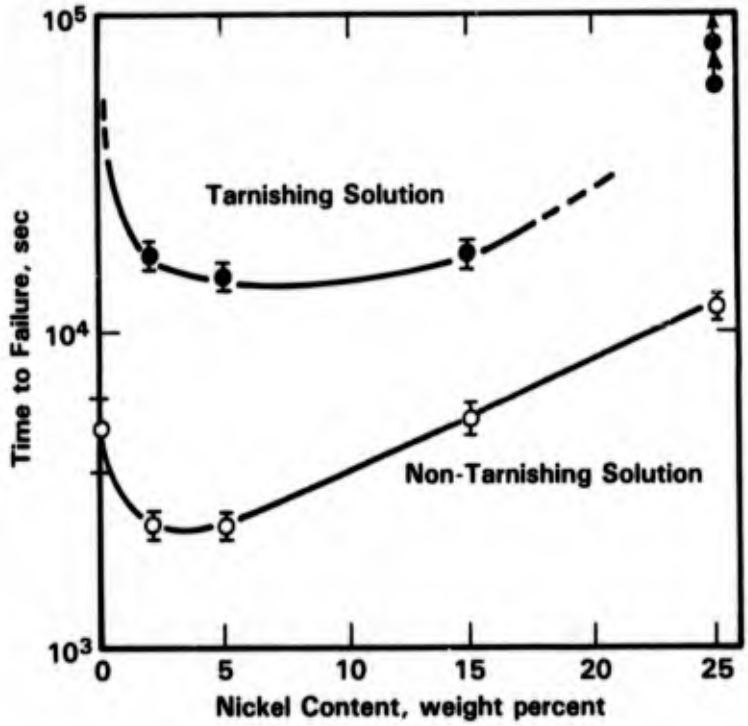

FIGURE 8-44. EFFECT OF NICKEL CONTENT ON TIME TO FAILURE OF COPPER-NICKEL ALLOYS TESTED IN TARNISHING AND NONTARNISHING 15 N AQUEOUS AMMONIA[66]

MUD

Corrosion rates for copper-base alloys in bottom sediments at two depths in the Pacific Ocean are given in Figure 8-11. These data show that the corrosion rates in the sediments were lower than those in the seawater, at the same depth, for most of the alloys studied. These data also show that the corrosion rates in the sediment were lower at a depth of 2,340 feet than at a depth of 5,630, as were the corrosion rates in the seawater. As discussed in the section (Depth and Aeration under general and pitting corrosion) this behavior was the result of the lower oxygen concentration of the seawater at the 2,340 foot depth. Similarly, the lower corrosion rate in the sediment than in the seawater, at a given depth, was also probably attributable to the lower concentration of oxygen in the sediment. However, it must be cautioned that the high sensitivity of copper-base alloys to sulfide must be considered when they are used in sediments in polluted seawater or where sulfate reducing bacteria are present.

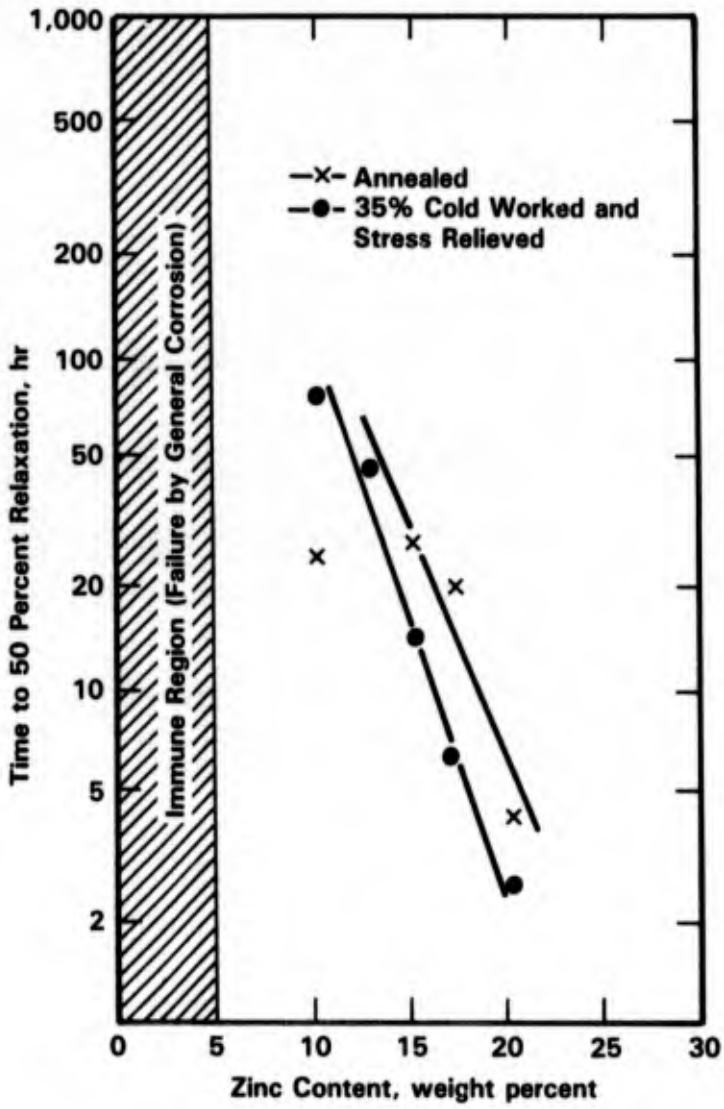

FIGURE 8-45. THE EFFECT OF ZINC CONTENT ON THE RESISTANCE OF COPPER-10 NICKEL-ZINC ALLOYS TO STRESS-CORROSION[67]

REFERENCES FOR CHAPTER 8

1. Hummer, C. W., Southwell, C. R., and Alexander, A. L., "Corrosion of Metals in Tropical Environments-Copper and Wrought Copper Alloys", Materials Protection, 7 (1), pp 41-47 (1968).

2. Copson, H. R. (Chairman), "Atmospheric Exposure of Nonferrous Metals and Alloys", ASTM Subcommittee VI, 1957 Test Program, Reprint from American Society for Testing Materials Proceedings 59, 61, 62, and 66 (1959, 1961, 1962, and 1966).

3. May, T. P., Holmberg, E. G., and Hinde, J., "Seawater Corrosion and Elevated Temperatures", Deckema-Monographian Bank, 47, pp 253-274 (Inco Reprint) (1962).

4. Newton, E. H. and Birkett, J. D., "Survey of Materials Behavior in Multi-Stage Flash Distillation Plants", Report C68373 on Contract No. 14-01-0001-956 from A. D. Little, Inc., to the Office of Saline Water (August, 1968).

5. Bulow, C. L., "Use of Copper-Base Alloys in Marine Services", Naval Engineers Journal, 77 (3), pp 470-482 (1965).

6. Landegren, W. and Mattsson, E., "Stress-Corrosion of Brass: Field Tests in Different Types of Atmosphere", British Corrosion Journal, II (21), p 291 (1976).

7. Reinhart, F. M., "Corrosion of Materials in Hydrospace, Part IV, Copper and Copper Alloys", Naval Civil Engineering Laboratory, Technical Note N-961 (April, 1968).

8. Beavers, J. A., Agrawal, A. K., and Berry, W. E., "Corrosion-Related Failures in Power Plant Condensers", EPRI NP-1468 (August, 1980).

9. Kato, C., Otoguro, Y., and Kado, S., "Grooving Corrosion Resistance of Electric Resistance Welded Low-Alloy Steel Pipes in Seawater", Tetsu to Hagane, 63 (1), pp 130-138 (January, 1977).

10. Mattson, M. E. and Fuller, R. M., "A Study of Materials of Construction in Distillation Plants", Joint Report by Office of Saline Water and the International Nickel Company, Inc., R&D Progress Report No. 163 (October, 1965).

11. Reinhart, F. M., "Corrosion of Materials in Hydrospace", U.S. Naval Civil Engineering Laboratory, R504, 118 pp (December, 1966).

12. Schreiber, C. F., Osborn, O., and Coley, F. H., "Corrosion of Metals in Desalination Environments", Materials Protection, 7 (10), pp 20-25 (October, 1968).

13. Kershul, W. L., "Condenser Tube Failures in Light-Water Reactors", Transactions of the American Nuclear Society, 26, pp 57-58 (August, 1977).

14. Rogers, T. H., "The Promotion and Acceleration of Metallic Corrosion by Micro-Organisms", Journal of the Institute of Metals, 75, pp 19-38 (1948-1949).

15. LaQue, F. L. and Clapp, W. F., "Relationships Between Corrosion and Fouling of Copper-Nickel Alloys in Seawater", Transactions of the Electrochemical Society, 87, pp 103-125 (1945).

REFERENCES FOR CHAPTER 8
(Continued)

16. Clapp, W. F., "Micro-Organisms in Seawater and Their Effect on Corrosion", Corrosion Handbook, Edited by H.H.S. Uhlig, Wiley and Sons, p 443 (1948).

17. May, T. P. and Weldon, B. A., "Copper-Nickel Alloys for Service in Seawater", Congress International de la Corrosion Marine et des Salissures, Cannes, France, pp 141-156 (June, 1964).

18. Hack, H. P., "Susceptibility of 17 Machinery Alloys to Sulfide-Induced Corrosion in Seawater", Naval Ship R&D Center, Annapolis, MD, ADB041334L, SME-79/56, 62 pp (September, 1979).

19. Gudas, J. P. and Hack, H. P., "Parametric Evaluation of Susceptibility of Copper-Nickel Alloys to Sulfide Induced Corrosion in Seawater", Corrosion, 35 (6), pp 259-264 (June, 1979).

20. Hack, H. P. and Gudas, J. P., "Inhibition of Sulfide Induced Corrosion With a Stimulated Iron Anode", Materials Performance, 19 (4), pp 49-54 (April, 1980).

21. Syrett, B. C., "The Mechanism of Accelerated Corrosion of Copper-Nickel Alloys in Sulfide-Polluted Seawater", Corrosion Science, 21 (3), pp 187-209 (1981).

22. Syrett, B. C. and Wing, S. S., "Effect of Flow on Corrosion of Copper-Nickel Alloys in Aerated Seawater and in Sulfide-Polluted Seawater", Corrosion, 36 (2), pp 73-85 (February, 1980).

23. Syrett, B. C., MacDonald, D. D., and Wing, S. S., "Corrosion of Copper-Nickel Alloys in Seawater Polluted With Sulfide and Sulfide Oxidation Products", Corrosion, 35 (9), pp 409-422 (September, 1979).

24. Eiselstein, L. E., Syrett, B. C., Wing, S. S., and Caligiuri, R. D., "The Accelerated Corrosion of Copper-Nickel Alloys in Sulfide-Polluted Seawater: Mechanism No. 2", Corrosion Science, 23 (3), pp 223-239 (March, 1983).

25. Eiselstein, L. E., Caligiuri, R. D., Wing, S. S., and Syrett, B. C., "Mechanisms of Corrosion of Copper-Nickel Alloys in Sulfide-Polluted Seawater", SRI Int., Menlo Park, CA, ADA096865, Final, N00014-77C0046, 71 pp (February, 1981).

26. Schrader, M. E., "Mechanism of Sulfide-Accelerated Corrosion of Copper-Nickel (90-10) Alloys in Seawater", Naval Ship R&D Center, Bethesda, MD, DTNSRDC-80-127, ADA093951, 27 pp (December, 1980).

27. Sanchez, S. R. and Schiffrin, D. J., "The Flow Corrosion Mechanism of Copper-Base Alloys in Seawater in the Presence of Sulfide Contamination", Corrosion Science, 22 (6), p 585 (1982).

28. Freeman, J. R., Jr. and Tracy, A. W., "Comparative Corrosion Resistance of Some Copper Alloy Condenser Tubes", Corrosion, 5 (8), pp 245-248 (August, 1949).

REFERENCES FOR CHAPTER 8
(Continued)

29. Otsu, T. and Sato, S., "Comparative Corrosion Test of Condenser Tube Materials by Model Condenser at Meiko Power Station", Sumitomo Light Metal Technical Reports, 2 (4), pp 299-322 (October, 1961).

30. Pruvot, C., "Service Life of Condenser Tubes at the Dunkerque Station", Rev. Generale de Thermique, 174-175, pp 505-519 (June-July, 1976).

31. Tracy, A. W. and Hungerford, R. L., "The Effect of the Iron Content of Cupro-Nickel on its Corrosion Resistance in Seawater", Proceedings of the American Society of Testing and Materials, 45, p 591 (1945).

32. LaQue, F. L. and Mason, J. F., Jr., "The Behavior of Iron Modified 70-30 Cupro-Nickel Alloy in Salt Water and in Some Petroleum-Industry Environments", Paper presented to the 15th Mid-Year Meeting of the American Petroleum Institute's Division of Refining, Cleveland, OH, 3M (3) (May, 1950).

33. Stewart, W. C. and LaQue, F. L., "Corrosion Resisting Characteristics of Iron Modified 90:10 Cupro Nickel Alloy", Corrosion, 8 (8), pp 259-277 (August, 1952).

34. Syrett, B. C., "Erosion Corrosion of Copper-Nickel Alloys in Seawater and Other Aqueous Environments--A Literature Review", Corrosion, 32 (6), pp 242-252 (June, 1976).

35. Heaton, W. E., "Impingement Corrosion of Condenser Tubes", Chemistry and Industry, (13), pp 29-36 (July 2, 1977).

36. Anderson, D. B. and Badia, F. A., "Chromium Modified Copper-Nickel Alloys for Improved Seawater Impingement Resistance", Transactions of the ASME, Series A, Journal of Engineering for Power, 95 (2), pp 132-135 (April, 1973).

37. Sato, S. and Nagata, K., "Factors Affecting Corrosion and Fouling of Condenser Tubes of Copper Alloys and Titanium", Sumitomo Light Metal Technical Reports, 19 (3-4), pp 83-94 (July, 1978).

38. Michels, H. T., Kirk, W. W., and Tuthill, A. H., "The Influence of Corrosion and Fouling on Steam Condenser Performance", Paper presented at the 16th INCO Power Conference, Wrightsville Beach, NC, p 54 (August 15-17, 1978).

39. Danek, G. J., Jr., "The Effect of Seawater Velocity on the Corrosion Behavior of Metals", Naval Engineers Journal, 78 (5), pp 763-769 (October, 1966).

40. Nosetani, T., Sato, S., Onda, K., Yamaguchi, Y., and Ando, S., "Comparative Corrosion Test on the Protection of Aluminum Brass Condenser Tubes by Continuous and Intermittent Injection of Ferrous Ion", Sumitomo Light Metal Technical Reports, 15 (1), pp 11-18 (January, 1974).

41. Anderson, G. A. and Cox, B. T., "Manufacture and Service Experience of High Frequency Induction Welded Copper Alloy Condenser and Heat Exchanger Tube", Paper presented at the CDA-ASM Conference on Copper, Cleveland, OH, p 9 (October 16-19, 1972).

REFERENCES FOR CHAPTER 8
(Continued)

42. Efird, K. D. and Anderson, B. D., "Seawater Corrosion of 90-10 and 70-30 Cu-Ni: 14 Year Exposures", Materials Performance, 14 (11), pp 37-40 (November, 1975).

43. Sato, S. and Nosetani, T., "Allowable Water Velocity and Cleanliness Factor of Aluminum Brass Condenser Tube With Ferrous Ion Addition into Seawater", Sumitomo Light Metal Technical Reports, 11 (4), pp 271-280 (October, 1970).

44. Anderson, D. B. and Efird, K. D., "The Influence of Chromium on the Corrosion Behavior of Copper-Nickel Alloys in Seawater", Proceedings of the 3rd International Congress on Marine Corrosion and Fouling, pp 264-276 (1973).

45. Efird, K. D., "Effect of Fluid Dynamics on the Corrosion of Copper-Base Alloys in Seawater", Corrosion, 33 (1), pp 3-8 (January, 1977).

46. Ferrara, R. J. and Gudas, J. P., "Corrosion Behavior of Copper-Base Alloys with Respect to Seawater Velocity", Proceedings of the 3rd International Congress on Marine Corrosion and Fouling, pp 285-298.

47. Davis, J. A., "Review of High Velocity Seawater Corrosion: NACE T-7C-5 Task Group Report", Corrosion/77, San Francisco, CA (March 14-18, 1977).

48. Beavers, J. A. and Boyd, W. K., "Evaluation of Copper-Nickel Alloys for OTEC Application", Final Report to Battelle's Pacific Northwest Laboratories, Battelle's Columbus Laboratories (December, 1977).

49. Anderson, D. B., "In Desalination Service Copper Alloys Provide Optimum Corrosion Resistance at Temperatures Above 200 F", Materials Performance, 10 (11), p 26 (1971).

50. Bianchi, G., Fiori, G., Longhi, P., and Mazza, F., "'Horseshoe' Corrosion of Copper Alloys in Flowing Seawater: Mechanism, and Possibility of Cathodic Protection of Condenser Tubes in Power Stations", Corrosion, 34 (11), pp 396-406 (November, 1978).

51. Fontanna, M. G. and Greene, N. D., Corrosion Engineering, McGraw-Hill (1978).

52. Sato, S., "Effect of Chlorination of Seawater on the Corrosion of Condenser Tubes", Sumitomo Light Metal Technical Reports, 3 (3), pp 106-116 (July, 1962).

53. Tanabe, Z. I., "On the Erosion of Condenser Tube Alloys by Sand in Water", Sumitomo Light Metal Technical Reports, 9 (3), pp 169-175 (July, 1968).

54. Tanabe, Z. I., "On the Sand Erosion of Aluminum Brass", Journal of the Japan Institute of Metals, 33 (4), pp 476-480 (1969).

55. Sato, S., Nosetani, T., Yamaguchi, Y., and Onda, K., "Factors Affecting the Sand Erosion of Aluminum Brass Condenser Tubes", Sumitomo Light Metal Technical Reports, 16 (1-2), pp 23-37 (January, 1975).

56. Bostwick, T. W., "Reducing Corrosion of Power Plant Condenser Tubing with Ferrous Sulfate", Corrosion, 17 (8), pp 12-16, 18-19 (August, 1961).

REFERENCES FOR CHAPTER 8
(Continued)

57. Lockhart, A. M., "Curing Condenser Tube Corrosion at Kincardine Power Station", The Engineer, 219, pp 499-500 (March 19, 1965).

58. Bethon, H. E., "Performance of Steam Condensers Aboard U.S. Naval Vessels", Corrosion, 4 (10), pp 457-462 (October, 1948).

59. Southwell, C. R., Bultman, J. D., and Alexander, A. L., "Corrosion of Metals in Tropical Environments - Final Report of 10 Year Exposures", Materials Performance, p 9 (July, 1976).

60. Scully, J. R. and Hack, H. P., "Galvanic Corrosion Prediction Using Long Term and Short Term Polarization Curves", Corrosion/84, Paper 34.

61. Nosetani, T., Shimono, M., Tanabe, Z., Sato, S., and Hirose, H., "Service Experience of Welded Titanium Tubes in Air Cooling Zone of Surface Condensers", Sumitomo Light Metal Technical Reports, 15 (3), pp 163-173 (July, 1974).

62. Private Communication, Peteris Skulte (July, 1978).

63. Gehring, G. A., Jr. and Maurer, J. R., "Galvanic Corrosion of Selected Tubesheet/Tube Couples Under Simulated Seawater Condenser Conditions", Corrosion/81, Paper 202.

64. Hack, H. P., "Galvanic Corrosion of Piping and Fitting Alloys in Sulfide-Modified Seawater", Naval Ship R&D Center, Annapolis, MD, DTNSRDC/SME-79-31, ADA070677, 31 pp (May, 1979).

65. Speidel, M. O., "ARPA Handbook on Stress-Corrosion Cracking", to be published.

66. Pugh, E. N., Craig, J. V., and Sedriks, A. J., "The Stress-Corrosion Cracking of Copper, Silver, and Gold Alloys", Proceedings on Fundamental Aspects of Stress-Corrosion Cracking, pp 118-158 (August, 1969).

67. Helliwell, B. J. and Williams, K. J., "The Effect of Composition on the Susceptibility to Stress-Corrosion of Some Wrought Copper-Base Alloys", Metallurgia, pp 131-135 (April, 1970).

CHAPTER 9
TABLE OF CONTENTS

CHAPTER 9
LIST OF TABLES

CHAPTER 9
LIST OF FIGURES

CHAPTER 9

COBALT AND COBALT-BASE ALLOYS

Cobalt and cobalt-base alloys generally are resistant to corrosion in the marine atmosphere. Miska[1] reported that cobalt corroded at a rate of less than 0.2 mpy over 3 years at the 800-ft lot at Kure Beach, NC. Similar corrosion rates were reported at the 80-ft lot.[2]

Cobalt and cobalt-base alloys also are resistant to ambient temperature seawater. Vreeland[3] exposed several cobalt-base alloys to natural seawater at a velocity of 2 ft/sec at Wrightsville Beach, NC. The nominal compositions of the alloys are given in Appendix I, Table I-1. The corrosion rates of freely corroding specimens and specimens which were coupled to Monel (Monel:Co area ratio of 4:1) were measured by weight loss for a 353 day exposure. Results of the tests are summarized in Table 9-1 where it can be seen that most of the cobalt alloys corroded at rates less than 0.1 mpy and were unaffected by coupling to Monel. The reason for the poorer performance of several of the cobalt alloys was not discussed by the author. Following exposure, the specimens were metallographically examined and no evidence of localized attack of the cobalt alloys was found.

Tuthill and Schillmoller[4] reported that the cobalt-base hard facing alloys are also highly resistant to erosion-corrosion and cavitation in marine environments. A table which summarizes the resistance of marine materials to cavitation damage is given in Table 9-2.

Reinhart and Jenkins[5] exposed wire rope samples of a cobalt alloy (40.5 Co, 15 Ni, 14.6 Fe, 20 Cr, 7 Mo) as well as many other steels and stainless steels in seawater at 5,900 feet for 189 days in the Pacific Ocean southwest of Port Hueneme, California. A summary of the exposure results is given in Table 9-3. These data show that there was no visible indication of corrosion or stress-corrosion cracking of the Co alloy, whereas many of the stainless steels underwent pitting, crevice corrosion, and cracking.

The relationship between alloy composition and corrosion behavior of cobalt-base alloys has not been studied extensively. Calhoon and Cheung[6] did study the effect of molybdenum additions to Co-25 Cr-Mo alloys on electrochemical behavior in a 0.17M saline solution at room temperature. It was found that the values of the protection potential increased with increasing Mo and were equal to the pitting potential above about 3.5 percent Mo in the alloy, see Figure 9-1. Thus, the pitting behavior of Co-Cr-Mo alloys appear to be similar to that of the Ni-Cr-Mo alloys in aqueous chloride solutions in that Mo is beneficial with regard to pitting resistance.

TABLE 9-1. RESULTS OF CORROSION TESTS BY VREELAND[3]

Material	Corrosion Rate of Test Metal, mpy		Rate Ratio
	Coupled to Monel	Uncoupled	Coupled/Uncoupled
Tantung G	<0.1	--	--
Cobenium	<0.1	0.5	~0.2
Stellite 6K	<0.1	<0.1	~1
Stellite 6B	<0.1	<0.1	~1
Stellite 98M2	<0.1	<0.1	~1
Stellite 3	3.4	1.5	2.3
Stellite Star J	1.2	<0.1	12
Kennametal K162B	1.9	--	--
Kennametal K82	6.6	--	--
Kennametal K96	2.7	3.5	0.8
Kennametal K601	<0.1	1.2	0.1
Kennametal K701	4.6	2.6	1.8
Kennametal K801	3.6	2.8	1.3
Bearium Metal	18.1	2.4	7.5

TABLE 9-2. MATERIALS RESISTANCE TO CAVITATION DAMAGE IN SEAWATER[4]

Resistance to Cavitation Damage Rating	Metals
Group I - Most resistant. Little or no damage. Useful under highly cavitating conditions.	Cobalt-base hardfacing alloys Titanium alloys Austenitic (series 300) and precipitation hardening stainless steels Nickel-chromium alloys such as Alloy 718 Nickel-chromium-molybdenum alloys such as Alloys 625 and C-276
Group II - These metals are commonly utilized where a high degree of resistance to cavitation damage is required but where some metal loss under the most severe conditions of cavitation is acceptable.	Nickel-copper-aluminum Alloy K-500 Nickel-copper Alloy 400 Nickel-aluminum bronze Nickel-aluminum-manganese bronze
Group III - These metals have some degree of cavitation resistance but are generally limited to low speed applications.	70/30 copper-nickel alloy Manganese bronze G Bronze and M Bronze Austenitic nickel cast irons
Group IV - These metals are normally not used in applications where cavitation damage may occur.	Carbon and low-alloy steels Cast irons Aluminum and aluminum alloys

TABLE 9-3. CORROSION OF WIRE ROPES IN SEAWATER, 189 DAYS AT 5,900 FEET[5]

Alloy	Location	Diameter, inch	Construction	Coating	Remarks
Plow Steel[a][b]	Water	0.250	3 x 19	Zn, 0.50 oz/ft^2	Light uniform rust, heavy in some grooves, zinc completely gone.
Plow Steel[a]	Water	0.500	3 x 19	Zn, 0.50 oz/ft^2	Yellow with few areas of heavy rust in grooves, some zinc remaining.
Plow Steel[a]	Water	0.500	3 x 7	Zn, 0.50 oz/ft^2	Gray-yellow, few areas of white corrosion products, few areas of yellow corrosion products in grooves, zinc not completely gone in many areas.
Plow Steel[a]	Water	0.500	3 x 19	Zn, 0.50 oz/ft^2, polyurethane, transparent	No breaks in coating, some white corrosion products on wires, otherwise gray in color, seawater escaped under pressure when polyurethane was punctured, terminals on ends leaked slightly.
Plow Steel[a]	Water	0.500	3 x 19	Zn, 0.50 oz/ft^2, polyethylene, black	No breaks in coating, seawater escaped under pressure when polyethylene was punctured, terminals on ends leaked, zinc gone near ends and wires rusted, white corrosion products on wires away from terminals.
Plow Steel[a]	Water	0.500	3 x 19	Zn, 0.50 oz/ft^2, polyethylene, black, punctured	No rust at punctures, some white corrosion products in holes, seawater escaped under pressure when polyethylene was punctured, terminals on ends leaked, zinc gone near ends and wires rusted, white corrosion products on wires away from ends.
AISI Type 304 SS	Water	0.187	3 x 19	None	Cleaned - many broken wires, tunneling, pitting and crevice corrosion worse on internal wires.
AISI Type 304 SS[b]	Water	0.187	3 x 19	None	Cleaned - numerous broken wires, tunneling, pitting and crevice corrosion worse on internal wires.
AISI Type 304 SS	Water	0.187	3 x 7	None	Cleaned - some broken wires, pitting, tunneling and crevice corrosion worse on internal wires.
AISI Type 304 SS[b]	Water	0.187	3 x 7	None	Cleaned - no broken wires, pitting, tunneling and crevice corrosion worse on internal wires.
Fe-Cr-Ni-Si SS	Water	0.125	1 x 7	None	Cleaned - many shallow pits and many areas of slight crevice corrosion.
Fe-Cr-Ni-Mo-Cu SS	Water	0.125	1 x 7	None	Cleaned - incipient crevice corrosion.

TABLE 9-3. (Continued)

Alloy	Location	Diameter, inch	Construction	Coating	Remarks
Fe-Cr-Ni-Mo-Si-N SS	Water	0.125	1 x 7	None	Cleaned - no visible corrosion.
Fe-Cr-Ni-V-N SS	Water	0.125	1 x 7	None	Only ends recovered, failed by crevice corrosion inside potting compound.
Ni-Cr-Mo 103	Water	0.250	7 x 19	None	No visible corrosion, original metallic sheen still present.
Ni-Cr-Mo 103	Sediment	0.250	7 x 19	None	Same as seawater exposure.
Ni-Cr-Mo 625	Water	0.250	7 x 19	None	No visible corrosion, original metallic sheen still present.
Ni-Cr-Mo 625	Sediment	0.250	7 x 19	None	Same as seawater exposure.
Ni-Mo-Cr "C"	Water	0.062	1 x 7	None	No visible corrosion, original metallic sheen still present.
Ni-Co-Cr-Mo	Water	0.062	1 x 7	None	No visible corrosion, original metallic sheen still present.
Co-Cr-Ni-Fe-Mo	Water	0.187	3 x 19	None	No visible corrosion, original blue tarnish gone leaving bright metallic sheen.
Co-Cr-Ni-Fe-Mo	Water	0.187	3 x 19	None	Stressed at 1,600 lb (original breaking strength 3,980 lb) prior to exposure. After exposure, no failure, no visible corrosion, original blue tarnish gone leaving bright metallic sheen.
Fiberglass	Water	0.123	Monofilament	None	Original breaking strength, 3,000 lb - after exposure, dull and brittle.
Fiberglass	Water	0.094	Monofilament	None	Original breaking strength, 1,600 lb - after exposure, dull and brittle.
Fiberglass	Water	0.072	Monofilament	None	Original breaking strength, 1,100 lb - after exposure, dull and brittle.
Fiberglass	Water	0.046	Monofilament	None	Original breaking strength, 440 lb - after exposure, dull and brittle.
Fiberglass	Water	0.031	Monofilament	None	Original breaking strength, 220 lb - after exposure, dull and brittle.

(a) Extra improved plow steel, high strength.
(b) Stress relieved.

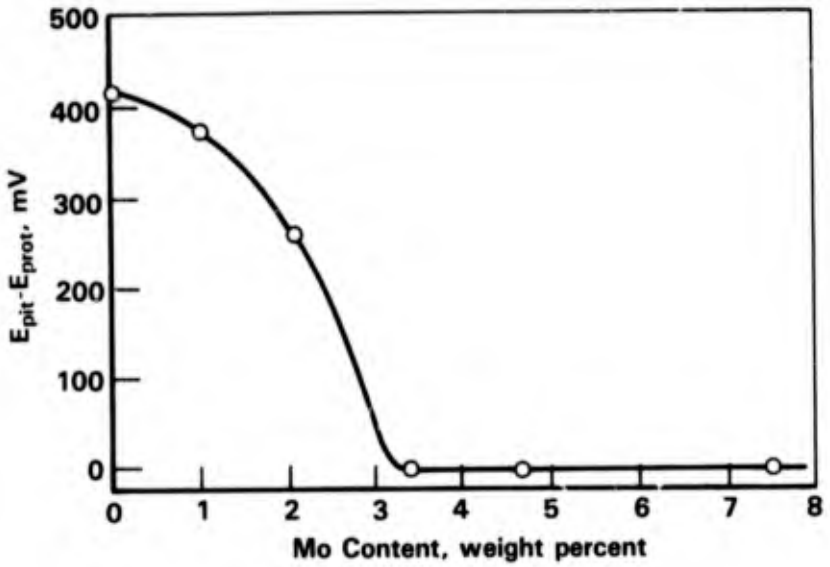

FIGURE 9-1. EFFECT OF Mo CONTENT ON THE DIFFERENCE BETWEEN THE PITTING POTENTIAL E_{pit} AND THE PROTECTION POTENTIAL E_{prot} OF Co-25 PERCENT Cr-Mo ALLOYS[6]

Several other studies of the corrosion and stress-corrosion performance of cobalt-base alloys have been performed. Davis[7] performed alternate immersion tests on two cobalt-base alloys (Haynes 188 and L605*) as well as several other high temperature alloys. The tests were performed in a simulated seawater for 60 days, as specified in ASTM-D114-152. A listing of alloys included in the tests and weight change data for unstressed specimens which were also included are given in Table 9-4. Metallographic examination of the stressed and unstressed specimens did not reveal any evidence of general, pitting, or SCC as a result of the exposure.

Cobalt-base alloys are susceptible to SCC in aqueous chloride environments under severe exposure conditions. For example, Kane, et al.[8] performed stress-corrosion tests on C-ring specimens of Haynes Alloy 188 (48 percent cold reduced) and MP35N as well as several nickel-base alloys** in 5-25 percent NaCl, 0.5 percent acetic acid, 1 gm/l S and H_2S at 350-500 F. Results, given in Table 9-5, show that all of the alloys failed by SCC under sufficiently aggressive conditions. Haynes Alloy 188 was considerably more susceptible to SCC than the nickel-base alloys tested while MP35N was somewhat less susceptible to SCC than several of the nickel-base alloys.

---

* Essentially Haynes 188 without Lanthanum.

** Alloy compositions are given in Table I-2 in Appendix I.

TABLE 9-4. WEIGHT CHANGE (ACCORDING TO ASTM D114-152) OF COUPONS EXPOSED TO ALTERNATE IMMERSION STRESS-CORROSION TEST[7]

Alloy	Specimen Number	Weight Before Exposure, g	Weight After 15 Days Exposure, g	Weight Change After 15 Days, mg	Weight After 30 Days Exposure, g	Weight Change After 30 Days, mg	Weight After 45 Days Exposure, g	Weight Change After 45 Days, mg	Weight After 60 Days Exposure, g	Net Weight Change, mg
Rene' 41	R95	2.7616	2.7612	-0.4	2.7611	-0.5	2.7611	-0.5	2.7613	-0.3
	R104	2.7236	--	--	--	--	--	--	2.7234	-0.2
Inconel 718	A77	4.5323	4.5327	+0.4	4.5327	+0.4	4.5323	0	4.5330	+0.7
	A79	4.5040	--	--	--	--	--	--	4.5050	+1.0
TDNiCr	T62	3.4220	3.4217	-0.3	3.4215	-0.5	3.4219	-0.1	3.4220	0
	T89	3.4869	--	--	--	--	--	--	3.4871	+0.2
L605[a]	L78	3.1670	3.1650	-2.0	3.1647	-2.3	3.1645	-2.5	3.1645	-2.5
	L97	3.2439	--	--	--	--	--	--	3.2423	-1.6
L605[b]	L95	3.3501	3.3500	-0.1	3.3502	+0.1	3.3502	+0.1	3.3506	+0.5
	L100	3.2739	--	--	--	--	--	--	3.2735	-0.4
Haynes 188	H63	3.1199	3.1200	+0.1	3.1199	0	3.1201	+0.2	3.1202	+0.3
	H97	3.0780	--	--	--	--	--	--	3.0787	+0.7
Hastelloy X	X64	2.6891	2.6887	-0.4	2.6889	-0.2	2.6889	-0.2	2.6890	-0.1
	X102	2.6945	--	--	--	--	--	--	2.6943	-0.2
FS-85/R512E	F83	5.0212	5.0219	+0.7	5.0269	+5.7	5.0228	+1.6		
	F84	5.0158	5.0164	+0.6	5.0215	+5.7	5.0179	+2.1		

(a) This specimen was heat oxidized (1950 F to 1975 F for 30 minutes in air).
(b) This specimen was tested in the "as received" condition.

TABLE 9-5. RESULTS OF SCC TESTS OF C-RING SPECIMENS IN NaCl-H_2S-S ENVIRONMENT[8]

Material	Test Environment (Test Temperature)									
	5% NaCl (350 F)		25% NaCl (350 F)		25% NaCl (400 F)		25% NaCl* (450 F)	25% NaCl (550 F)	
	Stress, percent of Trans YS		Stress, percent of Trans YS		Stress, percent of Trans YS		Stress, percent of Trans YS	Stress, percent of Trans YS	
	70	90	70	90	70	90	100	70	90
Hastelloy Alloy C-276 (37% Cr)	(>200)O	(>200)O	(>150)O	(124)X	(80-134)X	(80-134)X		(12-20)X	(5-18)X
Haynes dev. Alloy 8675 (59% Cr)	(>200)O	(>200)O			(>200)O	(59-80)X		(11-50)X	(4-18)X
Hastelloy Alloy C-276 (48% Cr)	(>200)O	(>200)O			(134)X	(134)X		(8-21)X	(5-18)X
MP35N (59% Cr)			(102)X	(47)X	(77)X	(46-60)X		(12-18)X	(8-57)X
Hastelloy Alloy C-276 (59% Cr)	(>200)O	(>200)O						(7)X	(7)X
Haynes dev. Alloy 8700 (59% Cr)	(>200)O	(>200)O			(13)X	(27)X			
Hastelloy Alloy G (59% Cr)	(>200)O	(164)X			(27)X	(27)X			
Haynes Alloy 188 (48% Cr)	(<2)X	(<2)X							
Inconel Alloy 625 (59% Cr)							(<6)X		
Inconel Alloy 718 (0% Cr)							(66)X		
Hastelloy Alloy X (59% Cr)							(<12)X		
Snapealloy (?% Cr)							(20)X		

Environment - 5-25% NaCl (as indicated), 0.5% acetic acid, 1 gm/l sulfur, H_2S.

( ) - Exposure time, days.
O - No failure.
X - Failure.
* - No sulfur.

REFERENCES FOR CHAPTER 9

1. Miska, K. H., "Most Nonferrous Metals and Alloys Weather Well", Materials Engineering, 79 (4), pp 64-66 (April, 1974).

2. Boyd, W. K. and Fink, F. W., "Corrosion of Metals in Marine Environments", Battelle Columbus Laboratories MCIC-78-37, 103 pp (March, 1978).

3. Vreeland, D. C., "Galvanic Corrosion Behavior of Wear-Resistant Materials for Mechanical Shaft Seals", Navy Marine Engineering Laboratory, Annapolis, MD, MEL-242/66, 13 pp (July, 1966).

4. Tuthill, A. H. and Schillmoller, C. M., "Guidelines for Selection of Marine Materials", The Ocean Science and Ocean Engineering Conference - Marine Technology Society, Washington, DC (June 14-17, 1965).

5. Reinhart, F. M. and Jenkins, J. F., "Corrosion of Alloys in Hydrospace - 189 Days at 5,900 Feet", Final Report NCEL-TN-1224, 41 pp (April, 1972).

6. Cahoon, J. R. and Cheung, C.T.F., "The Susceptibility of Metallic Surgical Implant Materials to Crevice Corrosion", Canadian Metallurgical Quarterly, 21 (3), pp 289-292 (September, 1982).

7. Davis, J. W., "Corrosion and Stress-Corrosion Susceptibility of Several High Temperature Materials", McDonnell Douglas, St. Louis, MO, 3rd Quarterly, NAS8-27270, 34 pp (1972).

8. Kane, R. D., et al., "Stress-Corrosion Cracking of Nickel- and Cobalt-Base Alloys in Chloride-Containing Environments", Corrosion '79, Atlanta, GA, Paper 174, 21 pp (March, 1979).

CHAPTER 10
TABLE OF CONTENTS

CHAPTER 10
LIST OF TABLES

CHAPTER 10
LIST OF FIGURES

CHAPTER 10

BERYLLIUM

Atmosphere

Beryllium has excellent resistance to corrosion in humid air. However, it is susceptible to pitting in marine atmosphere and in seawater. Figure 10-1 indicates that in synthetic seawater the pitting rate is highest during the first 2 months. Pitting becomes more widespread with time, and pits up to 4 mils deep have been observed. As presented in Table 10-1, similar pitting behavior was observed in natural seawater at 59 F. Seawater at warmer temperatures would be expected to have more fouling activity. Thus, beryllium in tropical waters would typically be covered with marine organisms which would induce a rate of pitting higher than those reported in Table 10-1.

Immersion

The stress-corrosion cracking behavior of beryllium in aqueous NaCl solutions has been studied by several investigators.[1-4] The results to date have not indicated any susceptibility of commercial-purity beryllium to stress-corrosion cracking in artificial or actual seawater. However, severe pitting was found to drastically lower the load-carrying ability of the material. There is some evidence to suggest that with stress, certain pits become more active and penetrate the metal rapidly.

Some method of controlling the corrosion is required if beryllium is to be used in marine environments. Anodized coatings sealed with sodium silicate have shown improved stability in saline solutions. A ceramically bonded aluminum coating (Serme Tel W) is also used on beryllium. The best results are obtained by applying a double coat to a grit-blasted surface, drying at 175 F, and curing at 650 F.[3] In marine atmospheres, this coating can be used at temperatures above 400 F, whereas the anodized coatings cannot be used at these temperatures because they become unstable.

Since information on behavior of beryllium in marine environments is very limited and the composition of commercial beryllium varies considerably, any consideration of its use should be preceded by an intensive study of the corrosion behavior in the actual environment involved.

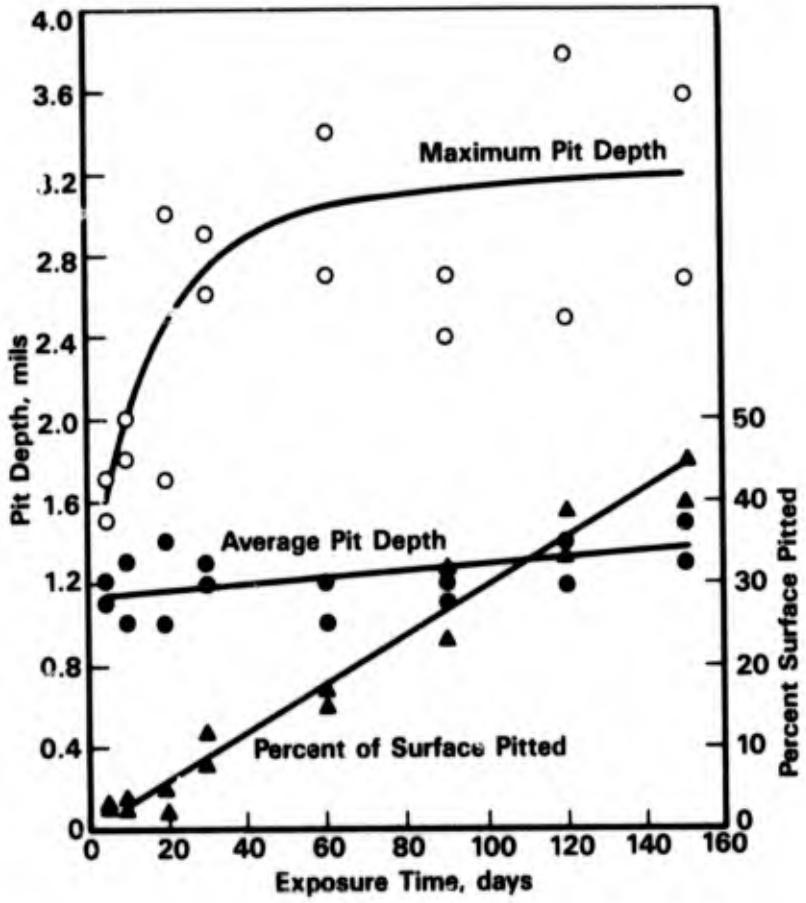

FIGURE 10-1. PITTING ATTACK OF UNSTRESSED, PICKLED BERYLLIUM SHEET MATERIAL EXPOSED TO SYNTHETIC SEAWATER AT 77 F[1]

TABLE 10-1. PITTING OF PICKLED BERYLLIUM (CONTINUOUS TOTAL IMMERSION IN 59 F NATURAL SEAWATER)[2]

Exposure Time, days	Pit Depth, mils		Percent of Surface Pitted
	Average	Maximum	
0	Negligible	0.2[a]	Negligible
2	Negligible	1.5	Negligible
3	1.3	1.9	Negligible
5	1.0	1.6	1
10	1.2	1.8	2
14	1.4	2.0	3
20	1.4	3.0	5
30	1.2	3.0	12
40	1.0	2.5	15
60	1.2	3.0	20

(a) Resulted from pickling.

REFERENCES FOR CHAPTER 10

1. Miller, R. A., Myers, J. R., and Saxer, R. K., "Stress-Corrosion of Beryllium in Synthetic Seawater", Corrosion, 23 (1), pp 11-14 (1967).

2. Prochko, R. J., Myers, J. R., and Saxer, R. K., "Corrosion of Beryllium by Salt Water(s)", Materials Protection, 5 (12), pp 39-42 (1966).

3. Gilpin, C. B. and Mackay, T. L., "Corrosion Research Studies on Forged Beryllium", AFML-TR-66-294, Contract AF 33(615)-2242, AD-646508 (January, 1967).

4. Miller, P. D. and Boyd, W. K., "Corrosion of Beryllium", DMIC Report 242 (December 11, 1967).

CHAPTER 11
TABLE OF CONTENTS

CHAPTER 11
LIST OF TABLES

CHAPTER 11

REFRACTORY METALS

The refractory metals covered here include tantalum, zirconium, niobium, molybdenum, tungsten, vanadium, hafnium, and chromium. Relatively little information is available on the corrosion behavior of these metals in marine environments. As a group, however, these metals show excellent resistance to attack by a variety of corrosive environments. The chemical properties of these metals have several points in common. Foremost among these is the fact that they all form a tight, thin, passive oxide film on their surface. This feature is related to their good-to-excellent corrosion behavior in saline environments. All of these metals are fouled by marine organisms in ocean waters. However, most of them are sufficiently passive to perform well even in the presence of deposits and fouling.

Tantalum

Of the refractory metals, tantalum is the most corrosion resistant to a wide spectrum of corrosive environments. This corrosion resistance is caused by the presence of a passive film of Ta_2O_5. As shown in Table 11-1, the corrosion rate for tantalum was only 0.0017 mpy after exposure to a 3 percent aqueous NaCl solution at room temperature for 84 days. In seawater, with a pH of 8, tantalum rivals titanium in corrosion resistance. After 181 days' exposure in shallow seawater, no measurable corrosion was observed.(2) An alloy of 90Ta-10W also has been found to be completely resistant to ambient seawater.

As shown in Table 11-1, the corrosion rate of tantalum in a 3 percent NaCl solution is an order of magnitude higher at 212 F than at 68 F. Thus in hot seawater, an acceleration in the attack would also be expected. Also, crevice corrosion in tantalum may become a factor in hot seawater.

Tantalum is also used as an impressed-current anode in ambient seawater. The tantalum surface, in this application, is normally platinized.

When coupled to such structural metals as steel or aluminum, tantalum may develop nascent hydrogen on its cathodic surface. In acid solutions, this leads to embrittlement of the tantalum.(1) However, in seawater there appears to be less danger of this action taking place. The same rules apply for coupling tantalum as for coupling other metals, such as titanium, to common structural metals.

TABLE 11-1. CORROSION RATES OF REFRACTORY METALS IN 3 PERCENT NaCl[1]

Temperature, F	Test Period, days	Corrosion Rate, mpy (Calculated From Weight Loss)								
		Ti	Zr	Hf	V	Nb	Ta	Cr	Mo	W
68	7[a]	0	0	0	0.07	0	0	0	0.013	0.015
68	84	0	0.011	0	0.57	0.0069	0.0017	0	0.011	0.0031
212	2	0	0.067	0.022	0.7	0.05	0.03	0	0.04	0.28

(a) Alternate-immersion; the other two tests are for continuous-immersion.

Zirconium

Zirconium has good resistance to corrosion in a wide spectrum of solutions. For example, no corrosion was observed in $CaCl_2$ solutions up to boiling temperatures and, as shown in Table 11-1, its corrosion rate in 3 percent NaCl is 0.011 mpy at 68 F and 0.067 mpy at the boiling point. In synthetic ocean water, zirconium is fully resistant up to the boiling point. The Navy has reported the seawater behavior of zirconium to resemble that of titanium.[3] However, seawater with free chlorine present attacks zirconium.

Zirconium, from the evidence at hand, can be expected to be completely resistant to corrosion in seawater, as well as in marine atmosphere, at ambient temperatures.

Niobium

Niobium is similar to tantalum and zirconium in its corrosion properties, in that it will resist acids and salt solutions. Niobium, as indicated in Table 11-1, showed the same order of corrosion resistance in 3 percent NaCl as did zirconium[1]. Further, niobium showed no measurable attack after 181 days of exposure in seawater.[2]

Molybdenum

Pure molybdenum oxidizes slowly in the marine atmosphere, developing a series of interference colors. ASTM tests have shown corrosion rates of 0.1 mpy after 7 years for

specimens at the 80- and 800-foot lots at Kure Beach, NC.[4] The maximum pit depth was 2.4 mils.

There is some attack under submerged conditions, particularly when the solutions are aerated. In the German work reported in Table 11-1, the corrosion rate obtained for molybdenum in aerated 3 percent NaCl was only 0.011,[1] as compared with a rate of 0.4 mpy reported in a study by the Bureau of Mines.[5] It can be speculated that this difference is due to a difference in the aeration of the different solutions with the more effective aeration in the Bureau of Mines' experiment. At 95 F, corrosion rates of 0.4 mpy in 3 percent NaCl and 0.3 mpy in synthetic seawater have been obtained.[6] At still higher temperatures of the synthetic seawater, the rate of attack was found to increase, e.g., up to 2.1 mpy at 140 F and 3.5 mpy at 212 F.

In seawater at Port Hueneme, CA, molybdenum showed uniform corrosion, with a rate of only 0.1 mpy after 181 days.[2] Thus, molybdenum is very resistant in ambient seawater, but at elevated temperatures, some attack may be expected.

TZM is a dilute molybdenum-base alloy containing about 0.45 percent titanium and 0.10 percent zirconium. Mo30W contains 30 percent tungsten. These two alloys were compared with molybdenum in substitute seawater as a liquid and as a spray[5]. In the substitute seawater test at 140 F, the corrosion rates for molybdenum, TZM, and Mo30W were 2.1, 1.7, and 1.4 mpy, respectively. In the spray test, the rates, in the same order, were 0.4, 1.1, and 0.5 mpy. All specimens developed a thin black deposit with very slight corrosion.[5] These results suggested that the two alloys have marine resistance of the same order as that for unalloyed molybdenum.

Tungsten

Tungsten, like molybdenum, resists attack in marine atmospheres (see Table 11-1). In synthetic seawater, corrosion rates of 0.2 mpy (95 F), 0.3 (140 F), and 0.7 mpy (212 F) are reported.[6] In actual seawater, a corrosion rate of 0.3 mpy after 181 days was obtained.[2] These results are similar to those for molybdenum.

Vanadium

Vanadium shows good resistance to aqueous NaCl solutions (see Table 11-1) and to synthetic seawater.[7] In air-saturated NaCl solutions at 95 F, corrosion rates of 0.4 mpy were obtained.[1] In actual seawater, vanadium was found to corrode at 3 mpy.[7] From this

evidence, one would expect vanadium to be less resistant to marine environment than are titanium and tantalum, but to have a resistance similar to that of molybdenum.

Hafnium

Hafnium, for which no marine data were found, would be expected to resemble zirconium in resistance to marine corrosion. In stagnant 20 percent NaCl solution at 95 F, hafnium showed corrosion rates of 0.08 mpy.[8] (See also Table 11-1.)

Chromium

Chromium, as a metal sheet, is not attacked by NaCl solution (see Table 11-1) at temperatures up to the boiling point.[1] In this environment it was as resistant as titanium. In seawater, the strong passive film should be resistant, and local attack should be less likely than in the case of the stainless steels.

Chromium, as an electroplate over a nickel coating confers good resistance to the basic metal, e.g., steel, brass, or zinc-base die castings, in marine atmospheres.[7]

REFERENCES FOR CHAPTER 11

1. Kiefer, R., Bach, H., Binder, F., and Kurka, F., "Contribution to the Corrosion Behavior of the IVA, VA, and VI A Metals" (In German), Werkstoffe und Korrosion, 19 (4), pp 312-316 (1968).

2. Reinhart, F. M., "Corrosion of Materials in Surface Seawater After 6 Months' Exposure", Naval Civil Engineering Laboratory, Port Hueneme, CA, Technical Note N-1023 (March, 1969).

3. The Metallurgy of Zirconium, Edited by B. Lustman and F. Kerze, First Edition, McGraw Hill, New York, NY, p 647 (1955).

4. Copson, H. R., "Long-Time Atmospheric Corrosion Tests on Low-Alloy Steels", ASTM Proceedings, 60, pp 650-665 (1960).

5. Acherman, W. L., Carter, J. P., and Schlain, D., "Corrosion Properties of the TZM and Molybdenum-30 Tungsten Alloys", Bureau of Mines, Boulder, CO, Report of Investigations 7169 (August, 1968).

6. Acherman, W. L., Carter, J. P., Kenahan, C. B., and Schlain, D., "Corrosion Properties of Molybdenum, Tungsten, Vanadium, and Some Vanadium Alloys", Bureau of Mines, Boulder, CO, Report of Investigations 6715 (1966).

7. Corrosion Resistance of Metals and Alloys, Edited by F. L. LaQue and H. R. Copson, Second Edition, Reinhold Publishing Company, New York, NY (1963).

8. Rare Metals Handbook, Edited by C. A. Hampel, Reinhold Publishing Company, New York, NY (1961).

CHAPTER 12
TABLE OF CONTENTS

CHAPTER 12

NOBLE METALS

The group of noble metals that is highly resistant to corrosion in marine environments consists of platinum, palladium, gold, and silver.

Platinum

Platinum is completely resistant to marine atmospheres and to seawater. In the latter, its main application is as impressed-current anodes. Platinum is more often used with another metal as a backing, such as platinized titanium or tantalum. It also is an essential part of the lead-platinum anode system. All types of platinum impressed-current anodes have been highly successful. On titanium or tantalum, for example, a platinum coating 100 microinches thick will provide for impressed currents as high as 100 amp/ft^2. The oxidation loss of platinum in seawater anode applications is taken as 6 mg/amp-yr.(1)

Palladium

Palladium resembles platinum in marine resistance. In seawater as an anode, palladium also is resistant, but less so than platinum.

Gold

Gold is completely resistant to the marine atmosphere and to seawater. It has been used to protect electrical contacts from tarnishing and corrosion in a marine atmosphere. Gold also has been used as a coating to protect a magnetic diaphragm exposed directly to seawater.

Silver

Silver has good corrosion resistance to marine environments, but will tarnish in a marine atmosphere, especially if sulfur components are present. After 2.6 years at Kure Beach, NC, the corrosion rate of silver in seawater was 0.5 mpy.(2) Silver's main use in the marine field is in electrical and electronic equipment such as radar waveguides.(3) On electrical contacts, a thin coating of palladium or gold is sometimes used to retard tarnishing. Lead-silver alloys are used for impressed-current anodes.(4)

REFERENCES FOR CHAPTER 12

1. "Platinized Titanium Anodes for Cathodic Protection", Englehard Industries Publication EI 6425 (May 16, 1966).

2. Corrosion Resistance of Metals and Alloys, Edited by F. L. LaQue and H. R. Copson, Second Edition, Reinhold Publishing Company, New York, NY (1963).

3. Rogers, T. H., The Marine Corrosion Handbook, McGraw Hill Company of Canada, New York and Toronto (1960).

4. Morgan, J. H., Cathodic Protection, Leonard Hill, London (1959).

CHAPTER 13
TABLE OF CONTENTS

CHAPTER 13
LIST OF TABLES

CHAPTER 13
LIST OF FIGURES

CHAPTER 13

LEAD, ZINC, CADMIUM, AND TIN

Lead

Atmosphere

Lead is resistant to corrosion in marine atmospheres. At Cristobal, Canal Zone, corrosion rates of 0.1 mpy were recorded for an 8-year exposure.[1] The corrosion was uniform and, as shown in Figure 13-1, is proportional with time. Even lower rates were found at La Jolla, CA, namely, 0.016 mpy after 10 years. Although lead is noble to steel, it does provide protection as a metal coating. For thicker coatings of about 1 mil or more, lead corrosion products tend to fill damaged areas such as at a scratch. Protection is actually improved if the marine atmosphere is polluted.

Immersion

The corrosion of lead is 0.3 mpy after 16 years in the Pacific Ocean.[2] A comparison of lead with other metals (Figure 13-2) indicates that its corrosion rate stabilizes at about the

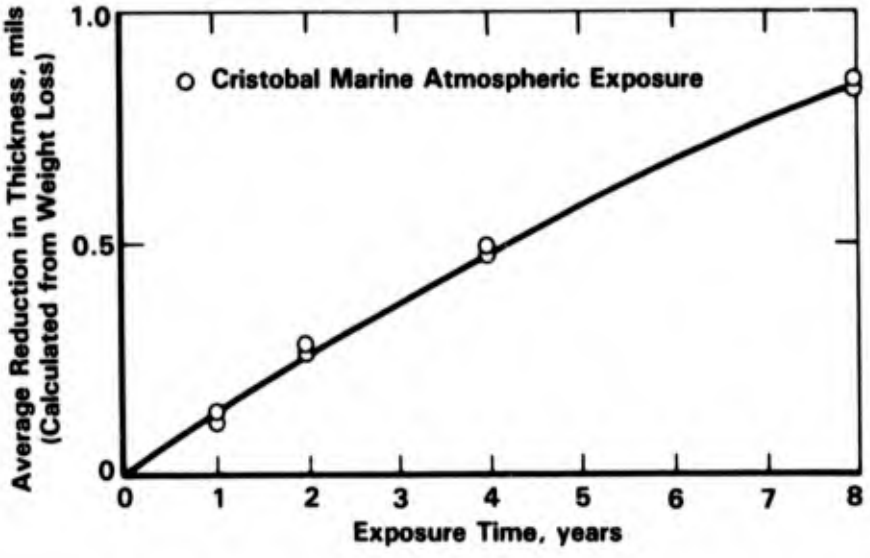

FIGURE 13-1. RELATION BETWEEN CORROSION AND EXPOSURE TIME FOR LEAD EXPOSED TO MARINE ATMOSPHERE IN PANAMA CANAL ZONE[2]

TABLE 13-1. CORROSION OF LEAD IN SEAWATER[4]

Specimen	Form	Exposure Time, years	Corrosion Rate mdd[a]	Corrosion Rate mpy	Location
99.96% Pb	Bar	4	4.0	0.5	Weston super Mare
1.6% Pb	Bar	4	3.0	0.4	Weston super Mare
Chemical lead	Sheet	0.5	3.1	0.4	San Francisco Harbor
Lead	Plate	1.7	4.7	0.6	Kure Beach

(a) mdd = $mg/dm^2/day$.

TABLE 13-2. CORROSION OF LEAD, SOLDER, TIN, AND ZINC IN SEAWATER[5]

Metal	Days	Depth, feet	Weight Loss, mpy	Pit Depth, mils	Remarks
Chemical lead[a]	181	5	1.2	--	Uniform attack
	197	2,340	0.3	--	Uniform attack
	123	5,640	0.8	--	Uniform attack
Tellurium lead[b]	181	5	1.0	--	Uniform attack
	197	2,340	0.3	--	Uniform attack
	123	5,640	1.1	--	Uniform attack
Antimonial lead[c]	181	5	1.2	--	Uniform attack
	197	2,340	0.3	--	Uniform attack
	123	5,640	0.8	--	Uniform attack
Solder[d]	181	5	3.7	--	Uniform attack
	197	2,340	0.5	--	Uniform attack
	123	5,640	0.5	--	Uniform attack
Tin[e]	181	5	8.3	30	Perforated
	197	2,340	1.8	2	Crevice attack
	123	5,640	0.5	--	General attack
Zinc[f]	181	5	4.5	5	Pitting
	197	2,340	2.3	2	Pitting
	123	5,640	6.7	13	Pitting

(a) 99.9 Pb.
(b) 99+ Pb, 0.04 Te.
(c) 94.0 Pb, 6.0 Sb.
(d) 67 Pb - 33 Sn.
(e) 99.9 Sn.
(f) 0.01 Fe, 0.09 Pb.

TABLE 13-3. ASTM DATA ON CORROSION RATES OF ZINC AT VARIOUS GEOGRAPHIC LOCATIONS[6]

Location	Penetration Rate, mpy	
	10 Yr	20 Yr
Key West	0.019	0.022
Sandy Hook	0.059	0.073
La Jolla	0.068	0.069
State College	0.040	0.044

TABLE 13-4. CORROSION RATES OF IRON-CONTAINING ROLLED ZINC EXPOSED TO MARINE ENVIRONMENTS AT KURE BEACH[6]

Iron, percent	Penetration Rate, mpy			
	80-ft Rack		800-ft Rack	
	6 Months	1 Yr	6 Months	1 Yr
0.0003	0.4	0.4	0.3	0.2
0.0008	0.45	0.3	0.3	0.2
0.0014	0.5	0.4	0.3	0.2
0.0021	0.5	0.4	0.3	0.2
0.006	0.45	0.4	0.3	0.2
0.011	0.45	0.6[a]	0.3	0.2

(a) 0.2 and 1 mpy on duplicate panels.

ranging from 1.5 to 2.6 oz/ft^2) coated on both sides have gone more than 32 years without any rust appearing. At the present rate of attack, it is estimated that the 2-ounce coating (3.5 mils thick) will last 79 years.(6) However, higher corrosion rates would be expected where actual seawater splash strikes the galvanized surface.

Immersion

In seawater, the corrosion rate of sheet zinc is usually 1 to 2 mpy,(6) although more recent data indicate higher rates. After 3 years' exposure at Eastport, ME, a rate of 1.0 mpy was observed. Similar rates are reported for zinc exposure in the Pacific Ocean off the Panama Canal Zone. Corrosion rates in flowing seawater at Kure Beach for special high-grade zinc are given below.(6)

Exposure Time, year	Corrosion Rate, mpy
0.5	1.9
4	0.8

Corrosion rates for zinc specimens containing 0.01 percent iron and 0.09 percent lead exposed in Pacific waters were found to range from 2.3 to 6.7 mpy.(5) These data are presented in Table 13-2. Pits as deep as 13 mils were reported. On the other hand, in experiments conducted at Harbor Island, NC, zinc with as much as 0.011 percent iron showed a rate of only 1.4 mpy.(6) These data are listed in Table 13-5 along with tidal and low-velocity data. Note the good behavior of zinc in the tide zone and the increase in attack with a seawater velocity of only 2 fps.

Even though zinc usually corrodes at a rate lower than that of iron, it is not recommended as a metal for service in seawater. There has been little actual use of metallic zinc in seawater, partly because of poor physical properties and partly because of its susceptibility to localized attack.(7) Zinc's major contribution is as a sacrificial anode in seawater, as discussed elsewhere. Zinc is also used as a galvanic coating on steel. Galvanized-steel piping is used on board ship to handle seawater lines used for fire fighting. The limited oxygen present in the stagnant seawater inside the pipe no doubt is a factor in the low rate of corrosion observed.

TABLE 13-5. SEAWATER CORROSION OF IRON-CONTAINING ZINC[6]

Iron, percent	Corrosion Rate,[a] mpy		
	Total Immersion	Tidal Zone	2 fps Flow
0.0003	1.4	0.8	3.0
0.0008	0.8	0.8	2.0
0.0014	0.8	0.9	2.0
0.0021	0.8	0.9	2.0
0.006	0.8	0.8	2.0
0.011	1.4	0.9	2.0

(a) Average of two 1 x 4 x 1/2-inch specimens exposed 1 year.

Cadmium

Cadmium is used as a metal coating over steel in marine applications. In the marine atmosphere, zinc is usually preferred, but if the local conditions are very corrosive, cadmium may be better by a substantial margin, as illustrated by Figure 13-3.

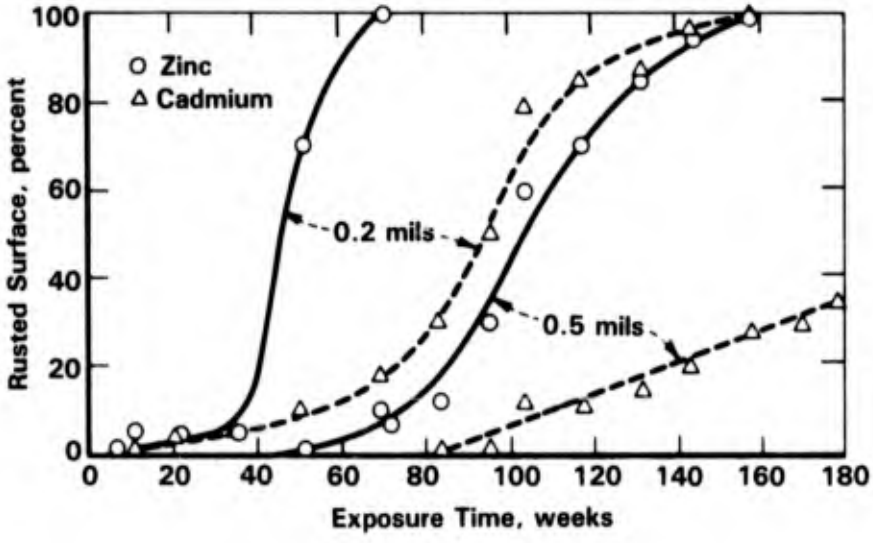

FIGURE 13-3. COMPARISON OF PROGRESSIVE DEVELOPMENT OF RUST ON ZINC- AND CADMIUM-PLATED STEEL PANELS AT 80-FOOT LOT, KURE BEACH, NC[8]

Coating thicknesses 0.2 and 0.5 mils.

Tin

Tin is resistant to marine atmospheres and could be used in some special applications. After 10 years at a marine location, tin showed a weight gain of 0.11 mg/dm^2/day.[9] When the deposit was removed, the penetration (calculated from the weight loss) was found to be 0.089 mpy.

More recent results for tin in seawater are given in Table 13-2. Weight-loss penetrations of 1.8 and 0.5 mpy were obtained for two deep-ocean exposures. The 30-mil-thick sample in the surface exposure perforated in 181 days, and the correspondingly high penetration figure based on weight loss is only approximate.[5] Although the older results suggested that tin was resistant to seawater, the newer information does not bear this out. The tendency of tin to pit as well as its susceptibility to crevice attack and to local corrosion under biofouling and deposits would predicate against using tin in seawater.

REFERENCES FOR CHAPTER 13

1. Southwell, C. R., Forgeson, B. W., and Alexander, A. L., "Corrosion of Metals in Tropical Environments, Part 3 - Underwater Corrosion of Ten Structural Steels", Corrosion, 16 (3), pp 105t-118t (1960).

2. Southwell, C. R., Forgeson, B. W., and Alexander, A. L., "Corrosion of Metals in Tropical Environments, Part 1 - Five Non-Ferrous Metals and a Structural Steel", Corrosion, 14 (2), pp 73t-81t (1958).

3. Southwell, C. R. and Alexander, A. L., "Marine Corrosion of Cast and Wrought Non-Ferrous Metals - Results of Sixteen Years' Exposure in the Tropics", preprint of Paper No. 63 presented at the National Association of Corrosion Engineers, Houston, TX (1969).

4. Von Franhofer, J. A., "Lead Corrosion in Seawater", Anti-Corrosion, 16 (5), pp 21-26 (1969).

5. Reinhart, F. M., "Corrosion of Materials in Surface Seawater After 6 Months' Exposure", Naval Civil Engineering Laboratory, Port Hueneme, CA, Technical Note N-1023 (March, 1969).

6. Anderson, E. A., "Zinc in Marine Environments", Corrosion, 15 (8), pp 409t-412t (1958).

7. Corrosion Resistance of Metals and Alloys, Edited by F. L. LaQue and H. R. Copson, Second Edition, Reinhold Publishing Company, New York, NY (1963).

8. Protective Coatings for Metals, Edited by R. M. Burns and W. W. Bradley, Second Edition, Reinhold Publishing Company, New York, NY (1955).

9. The Corrosion Handbook, Edited by H. H. Uhlig, John Wiley and Sons, New York, NY (1948).

CHAPTER 14
TABLE OF CONTENTS

CHAPTER 14
LIST OF TABLES

CHAPTER 14
LIST OF FIGURES

CHAPTER 14

CATHODIC PROTECTION

Cathodic protection is an electrochemical technique that is often used to reduce the corrosion rate of buried or submerged metallic structures. It may be applied to completely bare metal structures, but most often is applied in combination with a painted or coated surface. When properly designed, installed, maintained, and monitored, cathodic protection is perhaps the most important method of reducing the corrosion rate of submerged structures in marine environments.

This chapter consists of a discussion of the fundamentals of cathodic protection, followed by sections on various criteria that are presently used to apply cathodic protection in marine environments. Finally, the various types of cathodic protection systems and materials used are presented. Because of the engineering importance of ferrous materials, the discussion focuses on immersed steel structures.

Fundamentals of Cathodic Protection

There are several different ways of describing the cathodic protection process. One way is to view the corroding metallic surface as being made up of local anodes and cathodes that develop when the metal is first immersed in an electrolyte, like seawater. The local anodes and cathodes arise because of compositional or other variations on the metallic surface or in the electrolyte. The corrosion reaction takes place at the anode sites resulting in the oxidation of the metal to form metal ions. At the cathodes, simultaneous reactions must occur in order to maintain a balanced electrical charge. Generally, when oxygen is present in the water, it diffuses to the metal surface where it is reduced to produce hydroxide (OH^-) ions or the direct reduction of water may occur, which produces hydrogen gas (H_2) and hydroxide ions. Because of the relatively complex nature of marine environments, these reactions taking place at the steel surface can be combined with other reactions involving the corrosion products to form scales and other types of deposits on the metal surface. Under some conditions, the rate of the cathodic reaction (and the current required for protection) may be controlled by transport (e.g., diffusion) of reactants (e.g., oxygen) to the metal surface through the surface deposits.

When cathodic protection is applied, a net cathodic direct current (DC) is applied to the metal surface. As the metal surface begins to polarize (that is, change in potential), the

anodic current corresponding to the corrosion rate decreases in a proportion to the applied net cathodic current. When the cathodic current is made sufficiently large, the anodic reaction or corrosion rate is reduced to a negligible value. In general, the quantity of current, specifically, the current density, to achieve protection will depend upon the metal, the environment, and various factors that can affect the polarization of the metal in the particular environment, and will influence the type of cathodic protection system that is actually used to achieve protection.

Protection Criteria

The effectiveness of a cathodic protection system in any environment will depend upon maintaining a predetermined adequate level of protection throughout the expected life of the structure. To this end, criteria have been developed through research and practical experience that suggest the required or minimum levels of current density for protection.

The current requirements for protection of steels in various marine environments will generally vary with the geographic location as illustrated in Table 14-1. The data in this table have evolved primarily from practical experience and, thus, reflect a variety of different environmental conditions suggested by the range of current densities for each environment.

The design of cathodic protection systems is largely based upon current densities, but the actual monitoring of cathodic protection level is assessed by measurement of the potential of the structure in the environment with respect to a reference electrode. Most often, a silver/silver chloride/seawater reference electrode is used. Based partly upon experience with on-shore buried structures and pipelines, it is generally accepted that a potential of at least -0.80 V(Ag/AgCl) at the steel/seawater interface is sufficient for complete protection.[1-3] However, because of the complex and varied nature of marine environments, variances from this -0.80 V criterion and current density requirements have been recognized. The following complicating factors are important: (1) temperature, (2) water velocity, (3) oxygen level, (4) calcareous deposits, (5) anaerobic bacteria, and (6) time. In general, these factors are interrelated.

Effect of Temperature

The effect of temperature on the current density requirements is complex. With increasing temperature, oxygen solubility decreases but the rate of transport of oxygen (by diffusion) to the steel surface increases. These trends should have counterbalancing effects, but the overall effect appears to be an increase in the current requirement with increasing

TABLE 14-1. CURRENT DENSITIES FOR OFFSHORE CATHODIC PROTECTION[1]

	Current Density, mA/m^2
Location	
Gulf of Mexico	65-85
Nigeria	85
Cook Inlet, Alaska	250
Arabian Gulf	80-150
North Sea	90-150
Mud Zone, all locations	20-30
Harbor Piling	
Tidal Harbors	80
Nontidal Harbors	30-40
Mobile Drilling Rigs	
External Hull (Bare Steel)	100-150
Ballast Tanks (Bare Steel)	108
Ballast Tanks (Bitumastic coating)	54

For impressed current systems the above values may require increasing by up to 25 percent depending upon current distribution.

temperature. For example, at a surface temperature of 125 F (52 C), a current density of 260 to 336 mA/cm^2 (24 to 34 mA/ft^2) is required for protection[4] which is considerably higher than values given in Table 14-1 for ambient temperature seawater.

Temperature also can affect the minimum potential for cathodic protection. Experiments have shown that, over the range from approximately 4 C to 54 C, the polarized potential for protection increases in magnitude at a rate of approximately 2 mV/C from a value of approximately -0.80 V at 4 C.[4] Some of the apparent change in the protective potential is due to changes in the free-corrosion (unpolarized) potential of bare steel, which becomes more negative as the temperature of the surface increases.

Effect of Velocity

Velocity effects on the current requirements for cathodic protection are as complex as the flow conditions that may exist in marine environments. Water currents may be tidal, wind driven, or caused by density differences as a result of salinity and temperature gradients. Wave action can be important also. In general, the current density requirements increase with increasing velocity. When the current is controlled by diffusion of the reactants (e.g., oxygen) to the metal surface, the limiting current density, i_L, that is obtainable under flowing conditions is usually described as

$$i_L = C \cdot v^m \qquad (1)$$

when C and m are constants and v is the local flow rate. For bare steel, theoretical values for m of 0.5 for laminar flow and 0.8 to 0.9 for turbulent flow have been observed experimentally.(5)

An increase in the velocity of the seawater causes the products of the cathodic reaction to be removed more rapidly and the amount of oxygen arriving at the cathodic surface per unit of time to increase. Therefore, the combined effects will be to increase the current density needed to maintain the polarization, and hence, cathodic protection. For example, as shown in Figure 14-1, increasing the velocity of the seawater from a stagnant condition to one of approximately 13 ft/sec would increase the current density required to maintain the polarization on bare steel in seawater by tenfold. One factor, however, that can reduce the effect of velocity is the formation of calcareous deposits on the steel surface.

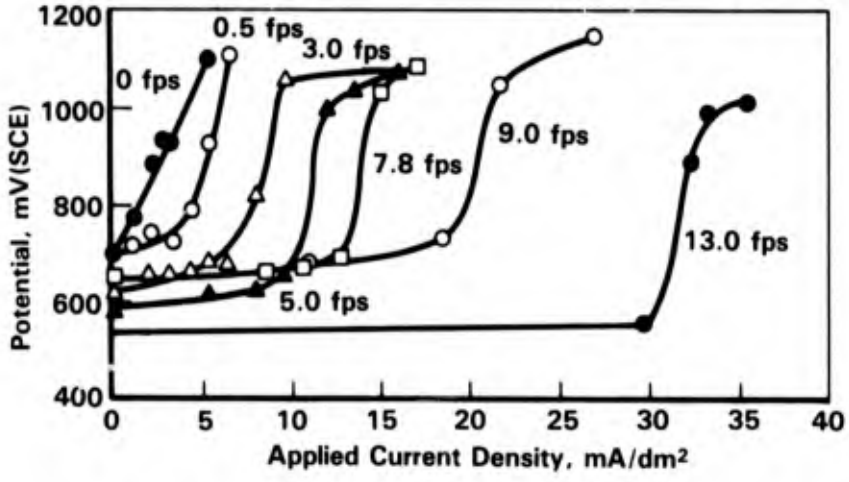

FIGURE 14-1. CATHODIC POLARIZATION OF MILD STEEL IN SEAWATER FLOWING AT DIFFERENT VELOCITIES AT 26 C(6)

The films and scales that form on marine structures generally reduce the current density required for protection, but, under some circumstances, seawater velocity can alter this. Vibrations, caused by vortex shedding on the tubular members of marine structures, can break down the scales and increase the current required for protection.[5] Also, erosion, promoted by sand from the seabed, can cause scale removal near the bottom of marine structures, and, hence, increased current requirements.[5]

Effect of Oxygen

The oxygen content of seawater is related to several factors, such as temperature, biological activity, salinity, and velocity. In surface waters, the oxygen content is generally close to the saturation level at normal atmospheric pressure. However, production of oxygen from photosynthesis and, to some extent, the entrainment of air bubbles due to wave action in marine environments may cause oxygen supersaturation in the upper layers. At greater depths, oxygen consumption due to biochemical oxidation of organic matter reduces the oxygen content and may ultimately cause anaerobic conditions.

Oxygen reduction is one of the principle reduction reactions on metal surfaces in seawater. An increase in the oxygen content generally will promote greater cathodic currents and a corresponding increase in the current required to maintain protection.

Effect of Calcareous Deposits

The formation of calcareous deposits on steel surfaces in marine environments generally results in a decrease in the current density required to cathodically protect the steel surface over the long term. Factors such as the current density, temperature, seawater flow velocity, and the seawater composition can all affect the composition, thickness, and morphology of these calcareous deposits.

During the application of cathodic protection, oxygen or water is reduced with an accompanying increase in pH (alkalinity) near the metal surface. Depending upon various conditions, protective calcareous deposits begin to form when the solubility of calcium and magnesium ions is exceeded. The deposits that form are mainly $CaCO_3$, $MgCO_3$, and $Mg(OH)_2$, and they form at pH levels between about 8 and 10. The primary reason that the calcareous deposits are effective in reducing the current density for protection is that the deposit is an effective barrier to oxygen diffusion to the steel surface.

The effectiveness of these deposits as an oxygen barrier will depend, in part, upon the current density and time. Experiments have indicated that the calcareous coatings formed with equal parts of $CaCO_3$ and $Mg(OH)_2$ at current densities between 500 to 3,000 mA/m^2 were the most effective barriers to oxygen diffusion and had the best mechanical properties.[7] This range of current densities is higher than normally encountered in practice. Therefore, a relatively high current density may be applied initially to achieve more desirable deposits. Table 14-2 illustrates the current density-time requirements for the formation of calcareous deposits that result in low current requirements for protection.[7] DiGregorio and Fraser[8] found the best deposits formed in the Mexican Gulf waters at current densities of about 60 mA/m^2. Spalling occurred at current densities of about 88 mA/m^2.

Deposition of calcareous films from seawater generally increases with increasing temperature because of the retrograde solubility of many calcium compounds. In addition, there are indications that the quality and rate of deposition of the calcareous deposits decrease with decreasing temperature.[5,9]

Pressure, or equivalently depth, can have an effect on the formation of calcareous deposits, but the behavior pattern is not clear as the properties of the deposits are expected to vary from one location to the next. One suggestion is that a higher current density may be needed to form a given amount of calcareous deposit at depth than near the surface.[9]

TABLE 14-2. POLARIZATION OF BARE STEEL IN SEAWATER[12]

Initial Current Density, mA/ft^2	Exposure Time	Film	Current Density Required for Continued Protection, mA/ft^2
200	1 day	Soft, with high magnesium content	2-3
100	2-3 days	Fairly hard	2-3
50	5-6 days	Hard, mainly calcareous	2-3
20	20-30 days	Medium thickness, hard	3-4
10	2-3 months	Medium thickness, hard	4
6	Up to 6 months if at all	Light, hard	4-5

Calcareous deposits formed under conditions of flowing seawater may have better (more protective) properties than those formed under quiescent conditions.[9] However, increasing flow velocity tends to decrease the deposit thickness. Once formed, the deposits strongly reduce the sensitivity of the current required for protection to flow velocity.[5]

Effect of Anaerobic Bacteria

As was shown in Table 14-1, the current density requirements for cathodic protection in the seabottom or mud zones are typically lower than in the seawater environment itself. This is usually due to a reduced oxygen content in these zones as well as a reduced effect of seawater flow velocity. However, for cathodic protection of steel buried in saline muds, it is usually considered necessary to increase the absolute value of the protective potential to about -0.90 V(Ag/AgCl) or -0.95 V ($Cu/CuSO_4$) in order to avoid corrosion by sulfate-reducing (anaerobic) bacteria.[10,11] The effect of temperature is generally to increase the current density requirements in the presence of anaerobic bacteria. For example, for a temperature increase from 5 C to 30 C, the corrosion rate will increase the equivalent of 15 mA/m^2 to 44 mA/m^2, respectively, in an anaerobic saline mud. Experimentation has shown that the current densities for protection in the presence of an anaerobic mud will vary with time, but they will be 45 mA/m^2 and 120 mA/m^2 at 5C and 30 C, respectively.[10] Thus, as a guide, the current density for protection will be 2.7 to 3.3 times the equivalent corrosion rate.

While it is recognized that it is necessary to reduce the protective potential to at least -0.90 V(Ag/AgCl) to avoid corrosion from sulfate-reducing bacteria, overprotection is to be avoided. Overprotection can result in the evolution of atomic hydrogen and can increase the risk of hydrogen-induced cracking for some materials. It has been recommended that the protection potential should not be more negative than -0.95 V(Ag/AgCl) for steels with yield strengths greater than 700 N/mm^2, or more negative than -1.05 V(Ag/AgCl) for steels with yield strengths less than 700 N/mm^2.[3]

The presence of anaerobic bacteria can impact upon two other areas associated with cathodic protection of buried or submerged pipelines in seabottom muds. The first effect impacts the performance of the sacrificial anodes. The activity of the sulfate-reducing bacteria produces a sulfide-containing environment. Depending upon the chemical composition of the particular sediment, it is possible for conditions to be produced which can lead to either corrosion or passivation of the anodes. Experiments have shown that it is possible to obtain a reduction of approximately 16 percent in the efficiency of a sacrificial anode in the presence of approximately 500 parts per million H_2S.[12]

The second area upon which the sulfate-reducing bacteria can impact performance in seawater concerns the metal structure itself. Some materials are known to be susceptible to sulfide stress cracking. Therefore, the environment generated by the products of reaction involving the sulfate-reducing bacteria could ultimately lead to material failure problems associated with environmental cracking (see section on stress-corrosion cracking of carbon and high-strength, low-carbon steels).

Effect of Time

Time plays an important role in establishing complete protection of a submerged structure. Figure 14-2 illustrates the time required to achieve adequate protection (that is, for the steel to polarize to at least -0.80 V) as a function of the applied current density. In this figure, the time to polarize to -0.80 V increases gradually as the current densities are reduced. In addition, once protection has been obtained and calcareous deposits begin to form, the current density required to maintain a polarized potential of -0.80 V will decrease further.

Time can also affect the current density for protection on a seasonal basis. Off-shore measurements in the North Sea have indicated a seasonal effect on the current density to maintain a minimum potential of -0.80 V.[5] In this case, a direct correlation was found between the current requirements and the wave height distribution throughout the year for the upper levels of the sea. The correlation has been explained by a relationship between the

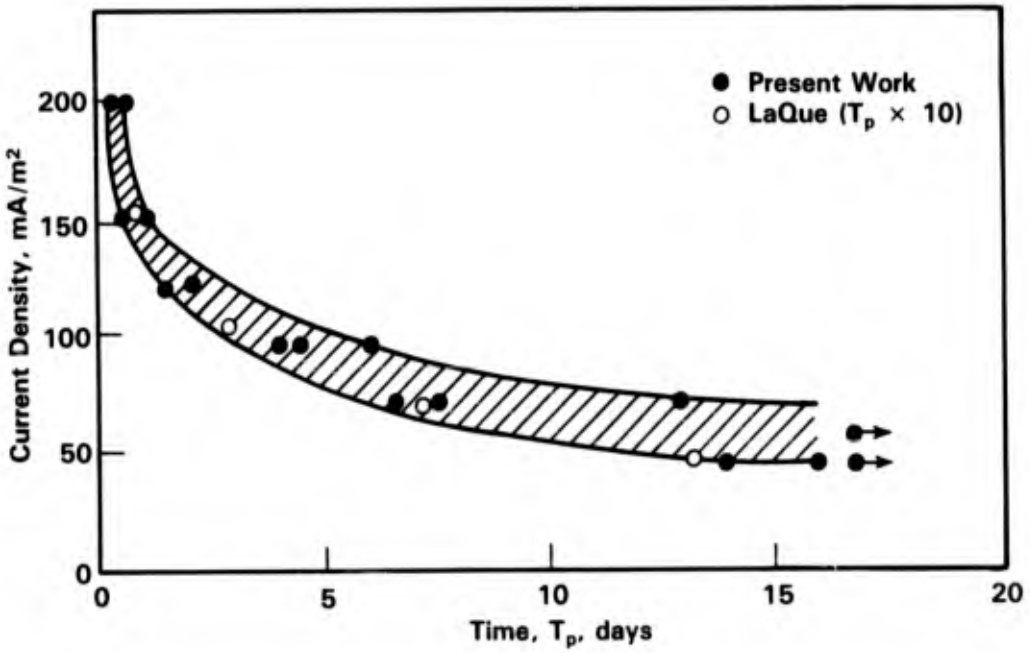

FIGURE 14-2. THE TIME (T_p) REQUIRED TO POLARIZE THE SPECIMENS TO -800 mV(Ag/AgCl) FOR VARIOUS CURRENT DENSITIES[5]

water velocity, which is higher near the upper levels of the sea, and the descaling tendency created by the wave activity.

Monitoring Methods

In the present context, monitoring refers to assessing the effectiveness of the level of cathodic protection. This may be done by visual inspection of the physical structure itself or by the use of monitoring methods to assess the electrochemical potential at the steel surface.

Examination of the external surfaces of marine structures is based upon visual examination of the appearance of the metal surface and measurements of the remaining wall thickness. Photographs or TV cameras are sometimes used to obtain an accurate documentation of corrosion or areas suspected of corrosion. Thickness measurements are usually carried out by ultrasonic techniques. For great depths, remotely controlled or manned submersibles are used.

Monitoring of the cathodic protection system is carried out to establish that the structure has been polarized to at least the minimum required level. Silver-silver chloride or zinc reference electrodes are often used for these measurements. The potential difference between the reference electrode and the structure is measured using a high resistance voltmeter. The potential measurements are carried out either by a diver or by means of remotely controlled or manned underwater vehicles. Potential measurements are also sometimes performed by immersing the reference electrode at the sea surface and measuring the average potential, which includes an IR drop in the seawater.

For off-shore pipelines, there are particular problems associated with monitoring the level of cathodic protection. On buried pipeline sections, potential measurements close to the steel surface are not possible. Various methods have been devised to monitor the cathodic protection systems. These include (1) the use of a reference electrode that is trailed over the pipeline section to be monitored, as the potential difference between the pipe and the reference electrode is measured, (2) the use of a remote electrode and one carried along and very close to (1 to 3 m) the pipe by means of an underwater vehicle to assess the relatively local variations in the potential profile next to the pipe, and (3) the use of electric field gradient surveys to estimate the current output from individual anodes.[13,14]

Cathodic-Protection Systems

There are two types of cathodic-protection systems used to protect metals in marine environments; these are sacrificial-anode and impressed-current systems. With

sacrificial-anode systems, a more active metal is electrically connected to the metal or structure to be protected. Because of the electrochemical potential difference between the two metals, the more active metal corrodes thereby driving a cathodic DC current onto the structure. As discussed previously in this chapter, when the cathodic current density (see Table 14-1, for example) or the polarized potential is sufficiently negative, corrosion of the protected structure will be reduced to a tolerable level. In this type of cathodic-protection system, the more active metal is consumed or sacrificed at the expense of the protected structure. Zinc, aluminum, or magnesium are typical sacrificial-anode materials.

With an impressed-current system, an external source drives a direct current from nearby inert anodes through the electrolyte to the structure to be protected. The power source is generally a transformer-rectifier, which converts AC to DC. Normally, only one type of cathodic-protection system is employed to protect a given structure. However, in more recent times, so-called hybrid systems utilize both types of protection systems to protect the same structure.

The decision to use one type of system over the other is not a straightforward process. There are advantages and limitations to both types of systems. Tables 14-3 and 14-4 list some of the advantages and limitations of these two types of protection systems. Often, the decision to use one type of system over the other appears to be arbitrary, but it is usually based on economic, technical, and application factors. However, when properly designed, either type of system can be effective in reducing the corrosion rate on the structure to be protected. Such designs are often quite conservative.[16] For example, examination of twelve case histories of structures in the Gulf of Mexico show that the actual average current obtained on a structure was approximately 50 to 75 percent of the design current, but all structure potentials were of the order of -1.0 V(Ag/AgCl), which would be considered protective based upon a -0.85 V criterion.

Sacrificial-Anode Systems

The design of a sacrificial-anode, cathodic-protection system is usually based upon the current density required to protect the structure, that is, to achieve a protective level of the polarized potential. Data such as those in Table 14-1 are often used as a guide to establish the current density requirements in a particular application. From the estimated area of metal to be protected, the total current needed for protection can be determined, with an allowance (for example, 10 to 20 percent) for contingent needs. The total weight of sacrificial-anode material required to provide the necessary current for the required design life of the structure is calculated on the basis of the current capacity of the anode material (in units of

TABLE 14-3. ADVANTAGES AND LIMITATIONS OF SACRIFICIAL-ANODE SYSTEMS

Advantages	Limitations
1. Low maintenance	1. High initial cost
2. Immediate protection	2. Significant total anode weight in some cases
3. High equipment reliability	3. Limited driving voltage
4. Even current distrit ution	4. Impractical retrofit in deep waters
5. Avoids overprotection	5. Critical weld region of anode attachment

TABLE 14-4. ADVANTAGES AND LIMITATIONS OF IMPRESSED-CURRENT SYSTEMS

Advantages	Limitations
1. Flexible range of driving voltages, impressed current	1. Equipment susceptible to damage in rough environments
2. No weight penalty	2. No protection until system in place and energized
3. Automatic potential control available	3. Current distribution may be uneven
4. Protection level can be increased as needed	4. Overprotection possible

ampere-hour/kg). The distribution of the required weight of anode material is then assessed by calculation or experience based on the ability of a given anode material to throw current a certain distance in a given environment. This then results in the number and distribution of anodes to be applied to the structure for protection. In some cases, the design is then modified to meet other requirements, such as the initial current to polarize the structure to an acceptable level, or the current to maintain an acceptable level of polarization during the final years of the design life of the structure, when the anodes are largely consumed and have their minimum capability to produce current.

Of the active metals, aluminum, zinc, and magnesium normally are used with sacrificial-anode, cathodic-protection systems; zinc and aluminum are by far the most commonly used in marine applications. Tables 14-5, 14-6, and 14-7 illustrate some compositions and properties of aluminum, zinc, and magnesium alloys used in sacrificial-anode, cathodic-protection systems in marine environments. Aluminum-alloy, sacrificial anodes have the greatest current capacity, expressed in ampere-hours/kg of alloy consumed, of the three types of sacrificial-anode materials.

The actual current capacity of sacrificial anodes is generally less than the theoretical amount that would be calculated based upon the Faraday consumption of the alloy materials. This difference is generally attributed to local galvanic-corrosion activity on the anode surface, which does not result in current flow from the anode. The difference between the theoretical and actual current capacity is expressed as an efficiency which can change substantially from alloy system to alloy system and from environment to environment. Aluminum-alloy, sacrificial anodes have current-capacity efficiencies typically in the range of 80 to 90 percent whereas those for zinc-alloy, sacrificial anodes are in the range of 90 to 95 percent typically. The efficiency for magnesium alloy sacrificial anodes is in the range of 55 to 65 percent.

The efficiency and capacity of each alloy anode can be altered by the environment and the temperature in which the anode operates. For example, an aluminum-zinc-indium-silicon anode can have a current capacity of 1984 to 2161 ampere-hour/kg in ambient saline mud. At 80 C (176 F), the capacity will be 40 percent of that observed in ambient mud.[13] In perhaps

TABLE 14-5. COMPOSITION AND PROPERTIES OF SOME ALUMINUM SACRIFICIAL ANODES[1,17,18]

Alloy	Composition, weight percent					
	Zn	Hg	Sn	In	Si	Al
No. 1	0.45	0.045	--	--	0.11	Remainder
No. 2	4.5	--	0.10	--	--	Remainder
No. 3	3.0	--	--	0.02	0.16	Remainder

Open-Circuit Potential = -1.05 to -1.10 V(Ag/AgCl).
Capacity = 2400-2700 A-hr/kg.
Efficiency = 80-90 percent.

TABLE 14-6. COMPOSITION AND PROPERTIES OF SOME ZINC SACRIFICIAL ANODES[1,17,19]

Alloy	Composition, weight percent			
	Al	Cd	Si	Zn
No. 1	0.1-0.5	0.025	0.125	Remainder
No. 2	0.1-0.4	0.03-0.10	--	Remainder
No. 3	--	--	--	Remainder

Open-Circuit Potential = -1.05 to -1.10 V(Ag/AgCl).
Capacity = 780-810 A-hr/kg.
Efficiency = 90-95 percent.

TABLE 14-7. COMPOSITION AND PROPERTIES OF SOME MAGNESIUM SACRIFICIAL ANODES[1,18]

Alloy	Composition, weight percent				
	Al	Zn	Mn	Si	Mg
No. 1	5.3-6.7	2.5-3.5	0.15	0.3	Remainder
No. 2	2.7-3.5	0.7-1.3	0.2	0.03	Remainder
No. 3	0.01	--	0.5-1.3	--	Remainder

Open-Circuit Potential = -1.5 to -1.7 V(Ag/AgCl).
Capacity = ~1230 A-hr/kg.
Efficiency = 55-65 percent.

more extreme cases, the efficiency and capacity of the anodes can be significantly reduced by premature failure. For example, a zinc-aluminum-indium anode alloy has been shown to exhibit intergranular attack resulting in premature failure of the anodes in North Sea muds.[19]

Whether to use aluminum-alloy, sacrificial anodes or zinc-alloy, sacrificial anodes will depend upon the application. Aluminum alloys are often used to protect large areas of bare metal on off-shore structures where weight reduction is beneficial. In those cases, the low

weight, high-current capacity, and high efficiency, are highly desirable. In other cases, such as coated and buried or submerged off-shore pipelines, zinc anodes are more desirable because of their high efficiency and the weight that they provide to keep the pipeline submerged or buried.

Impressed-Current Systems

Although cathodic protection by sacrificial anodes is still the most common technique for protection of some structures, impressed-current systems have been gaining steadily in popularity. The design of impressed-current, cathodic-protection systems for off-shore marine structures follows a pattern that is similar to that for a sacrificial-anode design. The total current requirement is determined based upon the estimated area to be protected and the current density for protection. The selection of the anode material and the number and distribution of the anodes over the structure are interrelated. The selection process at this stage of the design is often difficult to define, and therefore, decisions are perhaps somewhat intuitive and based upon experience. Typical alternatives may include a decision to use (1) a small number of high-current output anodes fitted to the structure, (2) a large number of low-current output anodes attached to the structure, (3) replaceable anodes, or (4) a single or small number of very high-current output anodes placed remote from the structure.

There are now available a number of materials for impressed current anodes. Normally, the anodes should be effectively inert with very low consumption rates as compared with the sacrificial-anode systems. Table 14-8 illustrates some of the types of impressed-current anodes and their properties in marine environments. Of the anode materials listed in Table 14-8, the use of platinized titanium, columbium, and tantalum anodes has grown steadily and is the subject of much research. More recently, there has been interest in the magnetite anodes. Also, investigations have explored the use of ceramic-coated anodes for cathodic protection in marine environments. This type of anode employs a lithium-ferrite-ceramic plasma-spray coated on a metal substrate (e.g., titanium), which reportedly has the desirable features of low consumption rates and high current density output.[20]

Aside from the anode material, the most critical component of an impressed-current system is the power source. The source is usually a transformer-rectifier which may be either manually or automatically controlled. When automatically controlled, the potential between the structure and a permanently fixed reference electrode (e.g., pure zinc) is maintained within fixed limits by the rectifier.

TABLE 14-8. IMPRESSED-CURRENT ANODE PROPERTIES FOR MARINE ENVIRONMENTS[1,18,20]

Anode Material	Recommended Current Density, A/m^2	Maximum Voltage, V	Consumption Rate, g/A-yr	Comments
Scrap Steel	Varies	None	200-9,000	Life prediction difficult.
Graphite	10	None	30-450	Very brittle.
Silicon-Chromium-Cast Iron	10-100	None	90-250	Very brittle.
Lead-Silver	250-500	None	30-90	Heavy and poor mechanical properties. Susceptible to damage from excessive AC ripple.
Lead-Platinum	100	--	2-60	
Magnetite	10-500	--	40	Very brittle.
Platinized Titanium	250-700	9 V(SCE)	0.01	5 μm thick platinum film. 10 year life obtainable. Susceptible to failure from <100 Hz AC.
Platinized Tantalum	500-1000	>100 V(SCE)	0.01	Same as above for platinized titanium.
Platinized Columbium	500-1000	>100 V(SCE)	0.01	Same as above for platinized titanium.
Lithium-Ferrite Ceramic	15-2000	9.7	1-2	Lightweight, but tough.

Hybrid Systems

There is a growing use of hybrid systems which employ both types of cathodic-protection systems. Hybrid systems have been used for several reasons: (1) weight limitations may eliminate a system consisting entirely of sacrificial anodes, (2) an impressed-current system may not be operative for as long as a year after a structure has been in place, (3) no protection will be available during periods when the impressed current must be turned off for maintenance or because of divers working in the area, or (4) an initial design employing sacrificial anodes may be insufficient and upgrading of the system is needed. The Murchison platform in the North Sea is an example of where a hybrid cathodic-protection system has been employed using aluminum anodes and an impressed-current system with platinized titanium anodes.(21)

Economic Factors

Economics play a very important role in the decision to use one type of cathodic-protection system over another. Each situation will dictate which type of cathodic-protection system should be used. For example, Figure 14-3 compares the cost of protecting a large off-shore structure in the North Sea at a current density of about 108 mA/m^2.(16) The comparison in Figure 14-3 includes the cost of the initial investment, and interest at a rate of 8 percent compounded over the total system life. In this case, a sacrificial-anode system is clearly more costly. Table 14-9 illustrates the relative cost of cathodically protecting a steel structure in a marine environment with driven pile foundations. The analysis compares the alternatives for a bare structure, a coated structure, a sacrificial-anode, cathodic-protection system, and a combined sacrificial-anode and impressed-current, cathodic-protection system. The analyses were based upon a 30-year design life. This table shows that, when compared to a purely sacrificial anode (aluminum) cathodic-protection system on a bare structure, a coated structure with a purely sacrificial-anode, cathodic-protection system is the lowest cost option, with a coated and hybrid system being the second least expensive option and a bare structure with a hybrid system being the third least expensive option.(22)

Although there are technical and economic advantages that will dictate one type of cathodic-protection system over the other, the cost of the system is very low when compared with the total cost and investment in the structure to be protected. For example, in one case of an off-shore structure, the cathodic-protection system cost, including mounting, is less than 0.5 percent of the total cost of the structure.(23) Hence, cathodic protection is inexpensive, and vitally important to the life of the structure. When properly designed and maintained, cathodic protection is an effective means of corrosion control.

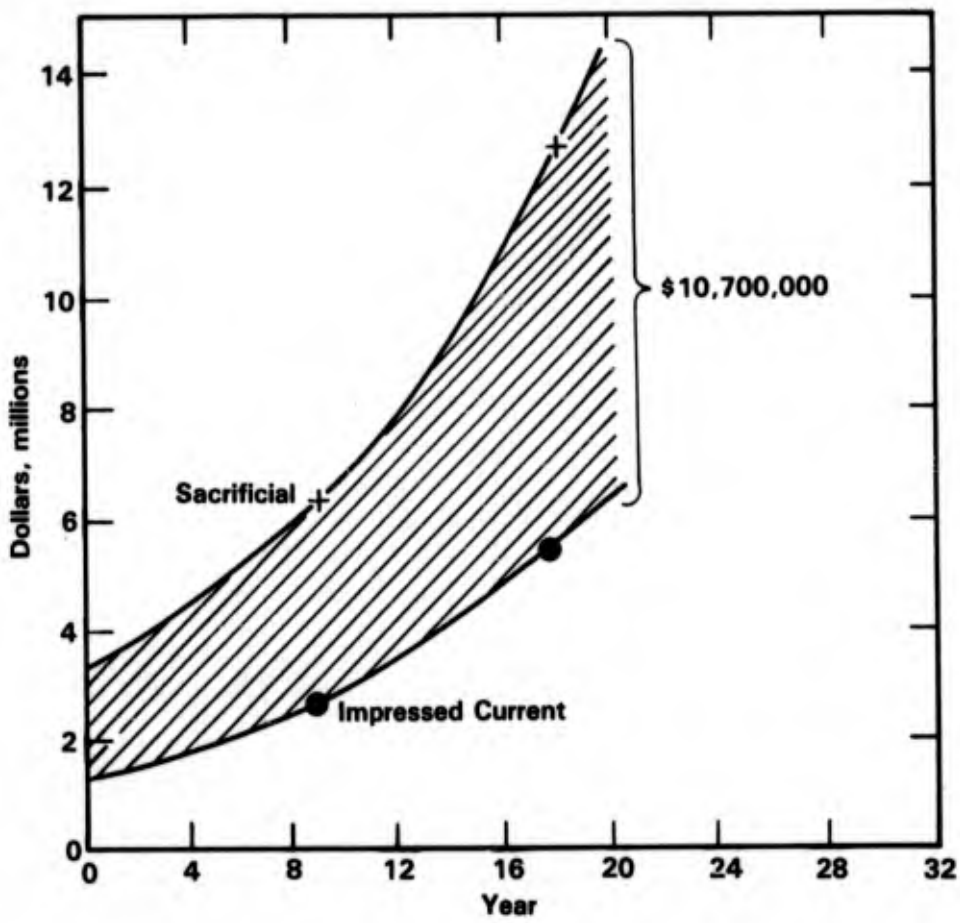

FIGURE 14-3. COST OF ALUMINUM ANODE SYSTEM COMPARED TO IMPRESSED CURRENT OVER A PROJECTED 20 YEAR SYSTEM LIFE[16]

TABLE 14-9. RELATIVE COST OF CATHODIC-PROTECTION SYSTEMS ON AN OFFSHORE STRUCTURE[22]

	Option[a]	Relative Cost
1.	Bare structure; aluminum anode cathodic-protection system	1.0
2.	Bare structure; combined aluminum anode and impressed-current cathodic-protection system	0.60
3.	Coated structure; combined aluminum anode and impressed-current cathodic-protection system	0.50
4.	Coated structure; aluminum anode cathodic-protection system	0.46

(a) Includes design and material supply including monitoring system, 30-year design life.

REFERENCES FOR CHAPTER 14

1. Wyatt, D. S., "Cathodic Protection of Offshore Structures, Part 1", Anticorrosion Methods and Materials, 24 (4), pp 5-10 (April, 1977).

2. "Corrosion Control on Steel, Fixed Offshore Platforms Associated with Petroleum Production", NACE Standard RP-01-76.

3. "Cathodic Protection Evaluation for Fixed Offshore Installations", Technical Note: TNA 703, Detnorske Veritas, Oslo, Norway (1981).

4. Vernnett, R. M., "Cathodic Protection at a Hot Riser in Cold Seawater", Corrosion '79, Atlanta, GA, Paper 251, 13 pp (March, 1979).

5. Gartland, P. O., Strommen, R., and Bardal, E., "Current Density Requirements for Cathodic Protection of Steel Structures in the North Sea", Materials Performance, 22 (6), pp 40-48 (June, 1983).

6. LaQue, F. L. and May, T. P., "Experiments Relating to the Mechanism of Cathodic Protection of Steel in Seawater", The Second International Congress on Metallic Corrosion, NACE, pp 789-794 (1966).

7. Humble, R. A., "Cathodic Protection of Steel in Seawater With Magnesium Anodes", Corrosion, 4, (17), p 358 (1948).

8. DiGregario, J. S. and Fraser, J. P., "Corrosion Tests in the Gulf Floor", ASTM, STP 558, p 185, Philadelphia, PA (1974).

9. Hart, W. H., Culberson, C. H., and Smith, S. W., "Calcareous Deposits on Metal Surfaces in Seawater - A Critical Review", Corrosion '83, Anaheim, CA, Paper 244 (March, 1980).

10. Fischer, K. P., "Cathodic Protection Criteria for Saline Mud Contining SRB at Ambient Temperature", Corrosion '81, Toronto, Ontario, Canada, Paper 110, 17 pp (April, 1981).

11. King, R. A., "Prediction of Corrosiveness of Sea Bed Sediments", Corrosion '79, Atlanta, GA, Paper 228 (March, 1979).

12. Doremus, E. P. and Doremus, G. L., "Cathodic Protection of Fourteen Offshore Drilling Platforms", Corrosion, 6 (7), pp 216-224 (1950).

13. Schrieber, C. F. and Murray, R. W., "Supplemental Studies of the Galvalum III Anode - Hot Saline Mud and Brine Environments", Corrosion '79, Atlanta, GA, Paper 252 (March, 1979).

14. Scorer, M., "Computerized Subsea Pipeline Protection Survey System", Anticorrosion Methods and Materials, 29 (9), pp 13-16 (September, 1982).

15. Steensland, O., Andersen, T., and Sydberger, T., "Corrosion and Corrosion Protection in Offshore Engineering", 8th International Congress on Metallic Corrosion, Mainz, West Germany, 3, pp 2227-2240 (September, 1981).

REFERENCES FOR CHAPTER 14
(Continued)

16. Gleason, J. D., "Impressed Current Cathodic Protection for Large Offshore Platforms", Materials Performance, 17 (2), pp 9-12 (July, 1978).

17. Houghton, C. J. and Ashworth, V., "The Performance of Commercially Available Zinc and Aluminum Anodes in Seabed Mud at Elevated Temperatures", Corrosion '81, Toronto, Ontario, Canada, Paper 112 (April, 1981).

18. Handbook of Cathodic Protection, by W. v. Baeckmann and W. Schwenk, Portcullis Press Ltd., Redhill Surrey, England, Chapter XIV: "Ships and Steel Marine Structures", pp 260-303 (1975).

19. Jensen, F. O., Rygg, A., and Setre, O., "Testing of Zinc Anodes for Offshore Buried Pipelines at Elevated Temperature", Materials Performance, 17 (9), pp 9-15 (September, 1978).

20. Segan, E. G. and Kumar, A., "Preliminary Investigation of Ceramic-Coated Anodes for Cathodic Protection", National Technical Information Service, Springfield, VA 22161, Report CERL-TR-M-33, pp 1-15 (August, 1983).

21. Vennett, R. M., Seager, R. W., and Warne, M. A., "Design of the Cathodic Protection System for Conoco's North Sea Murchison Platform", Materials Performance, 22 (2), pp 22-30 (February, 1983).

22. Wyatt, B. S., "Cathodic Protection of Offshore Structures, Part 2", Anticorrosion Methods and Materials, 24 (5), pp 9-12, 15 (May, 1977).

23. Saetre, O. and Jensen, F., "Developments in Protection of Offshore Concrete Structures", Corrosion '81, Toronto, Ontario, Canada, Paper 43 (April, 1981).

APPENDICES

APPENDIX A

GLOSSARY

LIST OF SYMBOLS

BCC = body centered cubic
βSTA = Beta solution treated and aged (titanium alloys)
CCR = crevice corrosion resistance
CCS = critical crevice solution
CCT = critical crevice temperature
CP = cathodic protection
cps = cycles per second
da/dt = crack velocity
DCB = double cantilever beam
DO = dissolved oxygen concentration
DPH = Diamond Pyramid Hardness
EAS = environmentally assisted cracking
E_{cor} = corrosion potential
Eg = galvanic potential
E_{pit} = pitting potential
EPR = electrochemical potentiokinetic reactivation
E_{prot} = protection potential
ERW = electric resistance welded
fps = feet per second
Ftu = ultimate tensile stress
GECM = graphic epoxy composite materials
HAZ = heat affected zone
HCP = hexagonal close packed
HSLA = high-strength, low-alloy
i_{cor} = current density at E_{cor}
I_g = galvanic current
i_g = galvanic current density
IGA = intergranular attack
IGSCC = intergranular SCC
i_L = limiting current density
i_{max} = maximum current density
i_{pass} = passive current density
ipy = inch per year

K_I = mode I stress intensity factor

K_{Ic} = mode I threshold stress intensity factor for rapid fracture, plane strain fracture toughness

K_{Iscc} = mode I threshold stress intensity factory for stress-corrosion cracking

K_{Ix} = first approximation of K_{Ic}

ksi = 1,000 pounds per square inch

L = longitudinal orientation

LT = long transverse orientation

mdd = milligrams per square decameter per day

mil = 0.001 inch

mpy = mils per year

NHE = natural hydrogen electrode

OTEC = ocean thermal energy conversion

PM = power metallurgy

ppb = parts per billion

ppm = parts per million

psi = pounds per square inch

r_A = galvanic dissolution rate

SCC = stress-corrosion cracking

SCE = saturated calomel electrode

SHE = standard hydrogen electrode

SMA = shielded metal arc

SSR = slow strain rate

ST = short transverse orientation

TIG = tungsten inert gas

TS = tensile stress

TTF = time-to-failure

WQ = water quenched

YS = yield stress

ZRA = zero resistance ammeter

APPENDIX B

ALUMINUM ALLOYS

TABLE B-1. COMPOSITIONS OF TEST METALS

Alloy	Values in Weight Percent									
	Al	Cu	Fe	Si	Mn	Mg	Zn	Cr	Ti	Ni
1199-H14	(a)	<0.001	0.001	0.001	<0.001	0.001	<0.001	<0.001	<0.001	<0.001
2014-T3	(a)	4.35	0.48	0.90	0.81	0.37	--	--	--	--
3005	(a)	0.14	0.52	0.20	1.11	0.26	0.02	0.02	0.01	--
5052-H34	(a)	--	0.30	0.13	--	2.31	--	0.22	--	--
5086-H32	(a)	0.05	0.25	0.15	0.32	3.75	0.12	0.12	0.01	--
5456-H321	(a)	0.13	0.25	0.14	0.80	5.49	0.07	0.14	0.03	0.01
Al-7Mg-O	(a)	0.02	0.18	0.10	0.26	7.25	--	--	--	--
6061-T6	(a)	0.33	0.41	0.68	--	0.90	--	0.20	--	--
Alclad 6061-T6										
Core	(a)	0.32	0.42	0.63	--	0.84	--	0.25	--	--
Cladding	(a)	0.03	0.22	0.11	<0.01	0.04	1.15	--	--	--
6062-T5	(a)	0.32	0.21	0.66	0.02	0.99	0.04	0.09	0.01	0.02
7075-T6	(a)	1.58	0.40	0.18	--	2.61	5.74	0.21	--	--

(a) Remainder.

TABLE B-2. COMPOSITION OF THE Al ALLOYS

Alloy		Alloying Elements, percent by weight
Al99.5	Wrought alloys	--
AlMn1		Mn1.2
AlSi1Mg		Si1.0, Mg0.8, Mn0.7
AlCu4Mg1		Cu4.5, Mg1.6, Mn0.7
AlMg2.5		Mg2.5, Cr0.25
AlSi12	Cast alloys	Si11-13.5
AlSi5Cu3		Si5, Cu3, Mn0.5
Cu99.5		
Mild Steel (Fe)		Mn1.2, C0.17 (AISI C 1117)
Stainless Steel (SS)		Cr.18, Ni9.5 (AISI 304)
Zn99.99		

TABLE B-3. CHEMICAL COMPOSITION OF TEST ALLOYS

Alloy	Identity[a]	Weight Percent							
		Si	Fe	Cu	Mn	Mg	Cr	Zn	Ti
2024-T351	10.0 cm (MS)	0.16	0.39	4.4	0.58	1.6	0.02	0.15	0.04
2024-T851	6.4 cm (KA)	0.11	0.37	4.1	0.61	1.6	0.02	0.18	0.04
2124-T851	5.0 cm (RM)	0.06	0.12	3.6[b]	0.68	1.5	0.05	0.07	0.02
2124-T851	6.4 cm (KA)	0.07	0.17	3.8	0.63	1.4	0.01	0.06	0.03
2124-T851	10.0 cm (KA)	0.05	0.15	4.3	0.61	1.4	0.01	0.02	0.02
2048-T851	5.0 cm (RM)	0.05	0.12	3.6	0.52	1.4	--	--	--
2219-T87	5.0 cm (MS)	--	0.20	6.0	0.30	0	0	0	0.08
7049-T7351	7.6 cm (KA)	0.06	0.10	1.6	--	2.5	0.14	7.7	0.02
7050-T73651	5.0 cm (AC)	0.06	0.07	2.1	0.01	2.3	--	6.1	0.03
7050-T73651	7.6 cm (KA)	0.06	0.11	2.2	--	2.2	0	6.2	0.02
7075-T651	6.4 cm (MS)	--	0.30	1.5	0.07	2.2	0.30	5.6	--
7075-T7351	6.4 cm (AC)	0.11	0.27	1.7	0.08	2.6	0.19	5.8	0.04
7075-T7351	7.6 cm (KA)	0.14	0.16	1.4	--	2.4	0.20	5.7	0.03
7475-T7351	5.0 cm (AC)	0.06	0.12	1.3	0.02	2.1	0.19	5.3	0.02
7475-T7351	7.6 cm (KA)	0.06	0.10	1.5	--	2.2	0.20	6.0	0.02

(a) Source and plate thickness: AC - Alcoa, KA - Kaiser, MS - MSFC, and RM - Reynolds.
(b) Below minimum.

TABLE B-4. COMPOSITION OF ALUMINUM-MAGNESIUM ALLOYS

Alloy	Alloying Element, percent					
	Mg	Mn	Ti	Be	Cr	Zr
AMg6	5.96	0.6	0.05	0.005	--	--
AMg6 + Ti	6.1	0.6	0.3	0.006	--	--
AMg6 + Cr	5.92	0.55	0.04	0.007	0.3	--
AMg6 + Cr	5.78	0.59	0.053	0.005	--	0.3

TABLE B-5. CHROMIUM, MANGANESE, AND ANTIMONY CONTENTS OF THE ALLOYS STUDIED

Alloy	Percent		
	Cr	Mn	Sb
Al-2.7 Mg-Cr	0-0.47	<0.01	--
Al-2.7 Mg-Mn	<0.003	0-0.94	--
Al-2.7 Mg-0.14 Cr-Mn	0.14	0-1.0	--
Al-2.7 Mg-0.43 Mn-Cr	0-0.31	0.43	--
Al-4.7 Mg-Cr-Mn	0.13	0.78	--
Al-5.1 Mg-Sb	--	<0.01	0.1, 0.3
2S-1/2H	--	0.006	--
Super pure Al	--	--	--

MAXIMUM IMPURITY CONTENTS OF THE ALLOYS STUDIED

Element	Si	Fe	Cu	Zn	Ti
Percent	0.06	0.15	0.016	0.052	0.018

TABLE B-6. CHEMICAL COMPOSITION LIMITS OF Al ALLOYS STUDIED (WEIGHT PERCENT)

Alloy	Si	Fe	Cu	Mn	Mg	Cr	Zn	Ti	Al[a]
1100	1.0 (Si + Fe)		0.05-0.20	0.05			0.10		R
2024	0.5	0.5	3.8-4.9	0.30-0.9	1.2-1.8	0.10	0.25		R
2219	0.20	0.30	5.8-6.8	0.20-0.40	0.02		0.10	0.02-0.10	R
6061	0.40-0.8	0.7	0.15-0.40	0.15	0.8-1.2	0.04-0.35	0.25	0.15	R
7075	0.40	0.50	1.2-2.0	0.30	2.1-2.9	0.18-0.35	5.1-6.1	0.20	R

(a) R - remainder.

TABLE B-7. NOMINAL COMPOSITION OF SEVERAL ESTABLISHED AND EXPERIMENTAL ALUMINUM ALLOYS

Alloy	Weight Percent of Alloying Elements								
	Si	Cu	Mn	Mg	Cr	Zn	Zr	Fe	Other
2014	0.8	4.4	0.8	0.50	0.10*			0.70*	
2219	0.20*	6.3	0.30	0.02*			0.18		V 0.10
2024	0.50*	4.4	0.6	1.5	0.10*			0.50*	
2124	0.20*	4.4	0.6	1.5	0.10*	0.25*		0.30*	Total 0.15*
2048	0.15*	3.3	0.4	1.5		0.25*		0.20*	Total 0.15*
Avior	0.05	4.6		0.4		1.4		0.05*	Ag 0.8
7039			0.27	2.8	0.20	4.0			
7075	0.40*	1.6		2.5	0.30	5.6		0.50*	
7178	0.40*	2.0		2.7	0.30	6.8		0.50*	
7079	0.30*	0.6	0.20	3.3	0.20	4.3		0.50*	
7049	0.25*	1.5	0.20*	2.5	0.15	7.6		0.35*	
7050	0.12*	2.4	0.10*	2.3	0.04*	6.3	0.12	0.15*	Ti 0.06*
7175	0.15*	1.6	0.10*	2.5	0.24	5.6			
RX 720	0.10*	1.2	0.10*	2.5	0.30	6.75	0.12	0.12*	
RR 58	0.19	2.4	0.06	1.6		0.10	--	1.0	Ni 1.0
5050	0.10	1.3	0.2	2.5	0.1	5.9	--	0.3	Ni 0.01*
5020	0.7	4.3	0.7	0.4		--	--	0.3	Ni 0.03
X 3067	0.1	1.5		2.5		6.0	0.15	0.1	Ag 0.35
X 3066	0.1	1.5		2.5		6.0	0.15	0.1	
Zergal 4	0.20*	0.8	0.20	2.3	0.05*	6.0	0.18	0.25*	
AZ 74	0.40	0.7-1.0	0.10	2.3	0.2	6.0		0.50	Ag 0.4
P/M K		1.0		2.5	0.1	8.0	--	3.25	Ni 5.0

* Maximum values.

APPENDIX C

TITANIUM ALLOYS

TABLE C-1. TITANIUM ALLOYS INCLUDED IN CHAPTER 3

Ti-50A (99.5 CPTi)
Ti-75A (99.0 CPTi Powder)
Ti-Grade 7 (Ti + 0.25 Pd)
Ti-Grade 12 (Ti + 0.8Ni + 0.3Mo)
Ti-8Mn
Ti with 0 >0.3 weight percent
Ti with 0 >0.32 weight percent
Ti-0.15Pd
Ti-Pd
Ti-2Al-4Mo-4Zr
Ti-2.5Al-1Mo-11Sn-5Zr-0.2Si
Ti-3Al-11Cr-13V
Ti-4Al-4Mn
Ti-4Al-3Mo-1V
Ti-4Al-4Mo-2Sn-0.5Si
Ti-5Al-2Sn
Ti-5Al-2.5Sn
Ti-5Al-2Sn-2Mo-2V
Ti-5Al-2Sn-3Mo-1V
Ti-5Al-2.75Cr-1.25Fe
Ti-5Al-5Sn-5Zn
Ti-5Al-5Sn-5Zr-1Mo-1V
Ti-6Al-2Mo
Ti-6Al-2.5Sn
Ti-6Al-4V
Ti-6Al-3Cb-2Sn
Ti-6Al-3V-1Mo
Ti-6Al-4V-2Mo
Ti-6Al-4V-1Sn
Ti-6Al-4V-2Co
Ti-6Al-4V-2Sn
Ti-6Al-4Sn-1V
Ti-6Al-4Zr-2Mo
Ti-6Al-6Zr-1Mo
Ti-6Al-6V-2Sn
Ti-6Al-6V-2.5Sn
Ti-6Al-2Nb-Ta-0.8Mo
Ti-6Al-2Cb-1Ta-1Mo
Ti-6Al-2Sn-1Mo-1V
Ti-6Al-2Sn-1Mo-3V
Ti-6Al-2Sn-2Mo-2V
Ti-6Al-5Zr-0.5Mo-0.2Si
Ti-6Al-4Zr-2Sn-0.5Mo-0.5V
Ti-6Al-6V-2Sn-0.7Cu-0.7Fe
Ti-6Al-6V-2Sn-1Cu-0.5Fe
Ti-6.5Al-4V
Ti-7Al-2.5Mo (as received and beta annealed + WQ + 1100 F age for 2 hours)
Ti-7Al-3Cb (as received and beta annealed)

TABLE C-1. (Continued)

Ti-7Al-3Mo
Ti-7Al-4Mo
Ti-7Al-12Zn
Ti-7Al-12Zr
Ti-7Al-1Mo-1V
Ti-7Al-2Mo-1V
Ti-7Al-2Cb-1Ta
Ti-7Al-2Cr-1Ta
Ti-7Al-3Cb-2Sn
Ti-7Al-6V-2Sn
Ti-8Al-1Mo-1V
Ti-8Al-2Cl-1Ta
Ti-8Al-3Cb-2Sn
Ti-1.5Mo-5V
Ti-8Mo-8V-3M-2Fe
Ti-10Mo-5.4Sn
Ti-11.5Mo-6Zr-3.4Sn
Ti-11.5Mo-6Zr-4.5Sn

TABLE C-2. CHEMICAL COMPOSITION OF TITANIUM ALLOYS*

	Composition, weight percent			
Element	Ti-50A[a] (ASTM Gr. 2)	Ti-6Al-4V[a] (ASTM Gr. 5)	Ti-Pd[a] (ASTM Gr. 7)	TiCode-12[a] (ASTM Gr. 12)
Nitrogen, Max	0.03	0.05	0.03	0.03
Carbon, Max	0.10	0.10	0.10	0.08
Hydrogen, Max	0.015	0.015	0.015	0.015
Iron, Max	0.30	0.40	0.30	0.30
Oxygen, Max	0.25	0.20	0.25	0.25
Aluminum	--	5.5/6.75	--	--
Vanadium	--	3.5/4.5	--	--
Palladium	--	--	0.12/0.25	--
Molybdenum	--	--	--	0.2/0.4
Nickel	--	--	--	0.6/0.9
Titanium	remainder	remainder	remainder	remainder

(a) TIMET® designation.

* Source: Franson, I. A. and Covington, L. C., "Titanium and the OTEC Environment", Ocean Thermal Energy Conversion (OTEC) Biofouling and Corrosion Symposium, Seattle, WA, pp 293-304 (October 10-12, 1977).

APPENDIX D

STAINLESS STEELS

TABLE D-1. COMPOSITIONS OF STAINLESS STEELS

Alloy	Element, weight percent										
	C	Cr	Ni	Mo	Fe	Ti	Cb	Cu	Mn	Si	Other
201	0.08	17	4	--	Balance	--	--	--	7	--	--
202	0.15 Max	18	5	--	Balance	--	--	--	8.7	--	0.25N Max
216	0.08 Max	20	5	2.5	Balance	--	--	--	8.5	--	0.3N
301	0.11	17	7	--	Balance	--	--	--	--	--	--
302	0.08	18	9	--	Balance	--	--	--	--	--	--
303	0.15	18	9	--	Balance	--	--	--	--	--	--
304	0.08 Max	18.5	9.5	--	Balance	--	--	--	--	--	--
304L	0.03 Max	18	10	--	Balance	--	--	--	--	--	--
305	0.12	18	12	--	Balance	--	--	--	--	--	--
308	0.08 Max	20	11	--	Balance	--	--	--	--	--	--
309	0.20	23	13.5	--	Balance	--	--	--	--	--	--
310	0.05	25	20	--	Balance	--	--	--	--	--	--
316	0.08 Max	17	12	2.5	Balance	--	--	--	--	--	--
316L	0.03 Max	18	14	2.5	Balance	--	--	--	--	--	--
317	0.08 Max	19	13	3.5	Balance	--	--	--	--	--	--
317L	0.03 Max	19	14	3.5	Balance	--	--	--	--	--	--
321	0.08 Max	18	11	--	Balance	5 x C	--	--	--	--	--
325	0.03	24	9	--	Balance	--	--	--	--	--	--
329	0.03	26	5	1.5	Balance	--	--	--	--	--	--
330	0.20	15	35	--	Balance	--	--	--	--	--	--
347	0.08 Max	19	11	--	Balance	--	10 x C	--	--	--	--
403	0.04	13	--	--	Balance	--	--	--	--	--	--
405	0.05	13	--	--	Balance	--	--	--	--	--	0.25Al
409	0.05 Max	12	--	--	Balance	0.4	--	--	--	--	--
410	0.15	12.5	--	--	Balance	--	--	--	--	--	--
416	0.15	13	--	0.6	Balance	--	--	--	--	--	--
422	0.23	12	0.8	1	Balance	--	--	--	--	--	1.0W, 0.25V
430	0.06	17	0.3	--	Balance	--	--	--	--	--	--

TABLE D-1. (Continued)

Alloy	Element, weight percent										
	C	Cr	Ni	Mo	Fe	Ti	Cb	Cu	Mn	Si	Other
431	0.15	16	2	--	Balance	--	--	--	--	--	--
434	0.12	17	--	1	Balance	--	--	--	--	--	--
439	--	18	--	--	Balance	?	--	--	--	--	--
440C	1.1	17	0.75	0.55	Balance	--	--	--	--	--	--
444	0.025	18	1	2	Balance	0.5Ti + Cb Max		--	--	--	--
446	0.12	26	--	--	Balance	--	--	--	--	--	--
630	0.03	15	4	--	Balance	--	0.25	3	--	--	--
631	0.07	17	7	--	Balance	--	--	--	--	--	1.2Al
632	0.07	15	7	2	Balance	--	--	--	--	--	1.1Al
633	?	17	4	3	Balance	--	--	--	--	--	--
635	0.05	17	7	--	Balance	0.8	--	--	--	--	--
700	0.02	20	25	4.5	Balance	--	0.3	1.5	--	--	--
800	0.04	21	32	--	Balance	--	--	--	--	--	--
825	0.05 Max	20	30	3	Balance	1	--	2	--	--	--
904L	0.02	20	25	4.5	Balance	--	--	1.5	--	--	--
17-4PH	0.07	16.5	4	--	Balance	--	0.3	0.4	--	--	--
17-7PH	0.09	17	7	--	Balance	--	--	--	--	--	1.1Al
PH13-8Mo	0.05	13	8	2.25	Balance	--	--	--	--	--	--
PH14-8Mo	0.05	14	8	2.5	Balance	--	--	--	--	--	1.1Al
PH15-7Mo	0.09	15	7	2.5	Balance	--	--	--	--	--	1.1Al
15-5PH	0.07	15	5	--	Balance	--	0.3	0.35	--	--	--
15-7PH	--	--	--	--		--	--	--	--	--	--
AM-350	0.10	16.5	4.5	2.9	Balance	--	--	--	--	--	0.1N
AM-355	0.12	15.5	4.5	2.9	Balance	--	--	--	--	--	0.1N
Alamar 362	0.03	14.5	16.5	--	Balance	0.8	--	--	--	--	--
Custom 455	0.05	12	8.5	0.5	Balance	1.1	0.3	2	--	--	--

TABLE D-1. (Continued)

Alloy	Element, weight percent										
	C	Cr	Ni	Mo	Fe	Ti	Cb	Cu	Mn	Si	Other
A286	0.05	15	25	1.3	Balance	2.15	--	--	--	--	0.15Al, 0.3V
Al-6X	0.03	20	24	6	Balance	--	--	--	--	--	--
E-Brite 26-1	0.005 Max	26	--	1	Balance	--	--	--	--	--	--
Sanicro 28	0.02 Max	27	31	3.5	Balance	--	--	1.0	2 Max	1 Max	--
Sandvik 2RK65	0.02 Max	19.5	25	4.5	Balance	--	--	1.5	1.8	0.5	--
Crucible SC 1	0.01	75	2	3	Balance	0.4	--	--	--	--	--
Sea-Cure	0.01	26	--	3	Balance	0.3	--	--	--	--	--
Sandvik 3RE60	0.02	18	5	2.5	Balance	--	--	--	1.5	1.5	--
iN-748	--	20	28	8	Balance	--	0.5	--	--	--	--
IN-862	0.07 Max	20	24	5	Balance	--	--	--	--	--	--
AFC-77	0.15	14	--	5	Balance	--	--	--	--	--	13Co, 0.4V
Illium-PD	0.04	25	5.5	2.5	Balance	--	--	--	--	1.0	6Co
Monit	0.01	25	4	4	Balance	--	--	--	--	--	--
254 SMO	0.02 Max	20	18	6	Balance	--	--	0.7	--	--	0.2N
20Cb3	0.03	20	33	2	Balance	--	0.8	3	--	--	--
Ferralium 255	0.04	26	5.5	--	Balance	--	--	1.7	--	--	0.17N
Unitemp 212	0.08	16	25	--	Balance	4	0.5	--	--	--	0.15Al
Haynes 20	0.03	22	26	4	Balance	0.35	--	--	--	--	--
USS 100	0.06	12	--	--	Balance	--	--	--	--	--	--
CF8M	0.04	19	10	2.5	Balance	--	--	--	1	0.8	--
CN7M	0.04	20	28	2.5	Balance	--	--	3	0.2	0.75	--
CN7MS	0.05	19	22	3	Balance	--	--	1.5	1	3	--
CD4MCu	0.04 Max	26	5.4	2	Balance	--	--	3	1	1	--
CA6NM	0.04	13	4	0.5	Balance	--	--	--	--	1	--

APPENDIX E

NICKEL-BASE ALLOYS

TABLE E-1. COMPOSITION OF NICKEL ALLOYS

Alloy	Element, weight percent											
	Ni	C	Cr	Fe	Mo	Al	Ti	Cu	Cb	Ta	Mn	Other
Ni 200	99.5	0.06	--	0.15	--	--	--	--	--	--	0.25	--
Ni 201	99.5	0.01	--	0.15	--	--	--	--	--	--	0.20	--
Ni 301	Balance	0.15	--	0.15	--	4.5	0.5	--	--	--	0.25	0.5Si
Ni-Cu Alloy 400	Balance	0.12	--	1.35	--	--	--	31.5	--	--	0.9	--
Ni-Cu Alloy 402	58.0	--	--	1.0	--	--	--	40.0	--	--	0.9	--
Ni-Cu Alloy 406	84.0	--	--	1.4	--	--	--	13.0	--	--	0.9	--
Ni-Cu Alloy 410	66.0	0.15	--	1.0	--	--	--	30.5	--	--	0.8	4.6Si
Ni-Cu Alloy K500	Balance	0.15	--	1.0	--	2.8	0.5	29.5	--	--	0.6	--
Ni-Cu Alloy K505	64.0	--	--	2.0	--	--	--	29.0	--	--	0.8	4.0Si
NiSnZn 23	79.0	--	--	--	--	--	--	--	--	--	2.0	8.0Sn, 7.0Zn, 4.0Pb
NiCrFe Alloy 600	Balance	0.04	16.0	7.0	--	--	--	0.10	--	--	0.20	--
NiCrFe Alloy 610	71.0	--	16.0	9.0	--	--	--	--	--	--	--	2.0Si
NiCrFe Alloy 617	54.0	0.07	22.0	--	9.0	1.0	--	--	--	--	--	12.5Co
NiCrFe Alloy 625	62.0	0.05	22.0	3.0	9.0	0.4 Max	0.4 Max	--	3.5Cb + Ta		--	0.5Si Max
NiCrFe Alloy 700	46.0	--	15.0	1.0	4.0	3.0	3.5	--	--	--	--	28.5Co
NiCrFe Alloy 702	Balance	0.01	16.0	0.3	--	3.0	0.5	--	--	--	--	--
NiCrFe Alloy 706	Balance	0.03	16.0	36.0	--	0.25	1.5	--	3.0Cb + Ta		--	--
NiCrFe Alloy 710	Balance	0.07	18.0	0.14	3.0	2.5	5.0	--	--	--	--	15.0Co, 1.5W
NiCrFe Alloy 718	52	0.04	20.0	18.0	3.0	0.6	1.0	--	5.0Cb + Ta		--	--
NiCrFe Alloy X750	Balance	0.04	15.0	7.0	--	0.8	2.5	--	0.85	--	0.70	--
NiCrFe Alloy 88	71.0	--	10.0	7.0	--	--	--	--	--	--	--	5.0Sn, 3.0Bi
NiCrFe Alloy 800	32.0	0.04	21.0	Balance	--	0.40	0.40	--	--	--	--	--
NiCrFe Alloy 804	43.0	--	29.0	25.0	--	--	--	--	--	--	--	--
NiCrFe Alloy 825	42.0	0.05 Max	20.0	30.0	3.0	0.2 Max	1.0	2.0	--	--	--	--

TABLE E-1. (Continued)

Alloy	Element, weight percent											
	Ni	C	Cr	Fe	Mo	Al	Ti	Cu	Cb	Ta	Mn	Other
NiCrFe Alloy 901	43.0	--	14.0	34.0	--	--	--	--	--	--	--	--
NiCrFe Alloy 902	42.0	0.02	5.4	48.5	--	0.65	2.40	--	--	--	0.40	--
NiCrFe Alloy 904L	25.0	0.02	20.0	Balance	4.5	--	--	1.5	--	--	--	--
NiCrFe Electrode 135	38.0	0.05	19.0	31.0	5.5	--	--	1.8	1.0	--	0.50	--
NiCrFe Alloy 20Cb3	33.0	0.03	20.0	Balance	2.0	--	--	3.0	0.8Cb + Ta		--	--
NiCrFe 304SS	9.5	0.08 Max	18.5	Balance	--	--	--	--	--	--	--	--
NiCrFe 316SS	12.0	0.08 Max	17.0	Balance	2.0 to 3.0	--	--	--	--	--	--	--
Alloy B	Balance	--	--	5.0	28.0	--	--	--	--	--	--	0.3V
Alloy C	Balance	0.06	15.0	5.0	16.0	--	--	--	--	--	--	4.0W
Alloy C276	Balance	0.01	15.5	5.5	16.0	--	--	--	--	--	--	4.0W
Alloy F	Balance	--	22.0	21.0	7.0	--	--	--	--	--	--	--
Alloy G	Balance	0.05 Max	22.0	19.5	6.5	--	--	2.0	2.0Cb + Ta		--	2.5Co Max
Alloy G3	Balance	0.015 Max	22.0	19.5	7.0	--	--	2.0	2.0Cb + Ta		--	5.0Co Max
Alloy X	Balance	0.10	22.0	18.5	9.0	--	--	--	--	--	--	1.0Co, 0.6W
Chlorimet-3	60.0	0.07 Max	18.0	3.0 Max	18.0	--	--	--	--	--	--	1.0Si Max
Elgiloy	15.0	--	20.0	15.0	7.0	--	--	--	--	--	2.0	40.0Co, 0.05Be
Rene' 41	56.0	--	19.0	--	10.0	--	3.1	--	--	--	--	11.0Co
MP35N	35.0	--	20.0	--	10.0	--	--	--	--	--	--	35.0Co
Haynes 188	22.0	0.08	22.0	1.5	--	--	--	--	--	--	0.75	14.0W, Balance Co
Illium B	Balance	0.05	28.0	3.0	8.5	--	--	5.5	--	--	1.25	4.5Si, 0.30B
Illium R	68.0	--	21.0	--	5.0	--	--	3.0	--	--	--	--
TDNiCr	Balance	0.04	20.0	--	--	--	--	--	--	--	--	2.0ThO_2

APPENDIX F

CARBON AND LOW-ALLOY STEELS

TABLE F-1. COMPOSITION OF STRUCTURAL STEELS EXPOSED IN TROPICAL AND TEMPERATE CLIMATES BY SOUTHWELL, ET AL. AND PRESENTED IN TABLE 6-1*

Steel	Type	Specification	Composition, percent								
			C	Mn	P	S	Si	Cr	Ni	Cu	Mo
A	Unalloyed low-carbon	QQ-S-741, Type II Grade A, Class 1	0.25	0.46	0.083	0.014	0.004	0.025	0.035	0.020	--
B(a)	Unalloyed low-carbon		0.16	0.42	0.013	0.021	0.01	0.01	0.02	0.02	--
C	Low-alloy	Proprietary Cu-Ni	0.13	0.41	0.007	0.026	0.048	--	1.70	0.90	--
D	Low-alloy	Proprietary Cu-Cr-Si	0.12	0.41	0.084	0.026	0.50	0.60	0.63	0.43	--
E	Low-alloy	Proprietary Cu-Ni-Mn-Mo	0.087	0.73	0.65	0.018	0.067	0.03	0.82	0.59	0.19
F	Low-alloy	Proprietary Cr-Ni-Mn	0.11	0.54	0.086	0.029	0.18	0.50	0.40	0.57	--
G(a)	Low-alloy		0.09	0.24	0.15	0.024	0.80	1.1	0.05	0.43	--
H(a)	Low-alloy		0.06	0.48	0.11	0.030	0.54	1.0	0.51	0.41	--
I(a)	Low-alloy		0.05	0.36	0.05	0.016	0.008	0.01	2.0	1.1	--
J(a)	Low-alloy		0.11	0.55	0.08	0.026	0.06	0.31	0.28	0.55	--
K_1(a)	Low-alloy		0.16	1.4	0.013	0.021	0.18	0.03	0.50	0.30	--
K_2(a)	Copper-bearing		0.27	0.48	0.024	0.036	0.009	0.12	0.01	0.21	--
L	Copper-bearing	QQ-S-741 Class 2	0.22	0.41	0.004	0.030	0.008	0.015	0.10	0.24	--
M	Nickel (2%)	RR-SPECS-3-A	0.18	0.52	0.036	0.024	0.19	0.14	2.06	0.61	--
N	Nickel (5%)	SAE-2515 5% Ni Steel	0.10	0.50	0.01	0.21	0.20	0.07	4.55	0.054	0.074
O	Chromium (3%)	Maximum 0.10% C Hot Rolled	0.07	0.54	0.008	0.016	0.14	3.24	0.13	0.11	0.032
P	Chromium (5%)	Co 1% AISI Type 501D	0.12	0.58	0.020	0.014	0.32	5.20	0.060	0.036	0.41

(a) Exposed by Larrabee in temperature climates.

* Source: Southwell, C. R., Forgeson, B. W., and Alexander, A. L., "Corrosion of Metals in Tropical Environments. Part 2: Atmospheric Corrosion of Ten Structural Steels", Corrosion, 14 (9), pp 435t-439t (1958).

TABLE F-2. COMPOSITIONS OF ALLOYS STUDIED BY LARRABEE AND PRESENTED IN FIGURE 6-3*

Steel	Composition, percent							
	C	Mn	P	S	Si	Cu	Ni	Cr
A(a)	0.09	0.24	0.15	0.024	0.80	0.43	0.05	1.1
M(a)	0.06	0.48	0.11	0.030	0.54	0.41	0.51	1.0
P(a)	0.05	0.36	0.05	0.016	0.008	1.1	2.0	0.01
N(a)	0.11	0.55	0.08	0.026	0.06	0.55	0.28	0.31
O(a)	0.16	1.4	0.013	0.021	0.18	0.30	0.50	0.03
p(a)	0.23	1.5	0.018	0.021	0.19	0.29	0.04	0.08
J(b)	0.19	0.52	0.008	0.039	0.01	0.29	0.05	0.05
L(b)	0.16	0.42	0.013	0.021	0.01	0.02	0.02	0.01

(a) High-strength low-alloy steels.
(b) Structural carbon and structural copper steels.

* Source: Larrabee, C. P., "Corrosion Resistance of High-Strength Low-Alloy Steels as Influenced by Composition and Environment", Corrosion, 9 (8), pp 259-271 (1953).

TABLE F-3. COMPOSITIONS OF MATERIALS STUDIED AND PRESENTED IN TABLE 6-9*

Exposure	Material Number	Type	Composition, percent							
			C	Mn	P	S	Si	Cu	Ni	Cr
SW-MA(a)	BO1458	0.5Ni, 0.5Cu, 0.1P	0.14	0.44	0.12	0.023	0.044	0.52	0.54	0.009
SW-MA	BO1389	0.5Ni, 0.2Cu, 0.2P	0.13	0.38	0.17	0.023	0.026	0.22	0.55	0.009
SW-MA	BO1457	0.5Ni, 0.2Cu, 0.1P	0.12	0.40	0.11	0.021	0.044	0.20	0.54	0.02
SW-MA	BO1459	0.5Ni, 0.2Cu, 0.1P	0.14	0.42	0.14	0.024	0.042	0.20	0.55	0.02
SW-MA	BO1467	0.3Ni, 0.2Cu, 0.1P	0.16	0.41	0.14	0.023	0.038	0.20	0.28	0.02
SW-MA	BO1456	0.3Ni, 0.2Cu, 0.2P	0.12	0.36	0.17	0.025	0.05	0.22	0.28	0.01
SW-MA	BO1468	Sheet-Steel Piling	0.27	0.53	0.011	0.036	0.007	0.06	0.09	0.04
MA(b)	D367	Structural Carbon Steel	0.18	0.51	0.010	0.032	0.07	0.05	0.03	0.09
MA	D368	Structural Copper Steel	0.19	0.61	0.013	0.042	0.029	0.23	0.04	0.05

(a) Seawater and marine atmosphere.
(b) Marine atmosphere.

* Source: Larrabee, C. P., "Corrosion-Resistant Experimental Steels for Marine Applications", Corrosion, 14 (11), pp 501t-504t (1958).

TABLE F-4. CHEMICAL COMPOSITION OF STEEL NK MARINE G PRESENTED IN FIGURE 6-11*

Analysis	Chemical Composition								Ceq(a)
	C	Si	Mn	P	S	Cu	Cr	Ni	
Ladle	0.14	0.20	0.77	0.107	0.006	0.25	0.53	--	0.38
Check	0.15	0.23	0.76	0.105	0.004	0.25	0.55	0.10	0.39

(a) Ceq = C + 1/24 Si + 1/6 Mn + 1/5 Cr + 1/40 Ni + 1/4 Mo + 1/14 V (%).

* Source: Nose, J., et al., "The Characteristic Properties of NK Marine G: Seawater Corrosion Resistant Steel for Pipe Piles and Sheet Piles", Nippon Kokan Technical Report, (26), pp 1-9 (1979).

TABLE F-5. COMPOSITION OF STRUCTURAL FERROUS METALS STUDIED BY SOUTHWELL AND ALEXANDER AND PRESENTED IN TABLE 6-11*

Key	Metals	Initial Surface Condition	Specification	Composition, percent								
				C	Mn	P	S	Si	Cr	Ni	Cu	Mo
A	C steel	Pickled	QQ-S-741, IIA1	0.24	0.48	0.040	0.027	0.008	0.03	0.051	0.080	--
B	C steel	Machined										
C	C steel	Millscale										
D	C steel - 0.3% Cu	Pickled	QQ-S-741, IIA2	0.22	0.44	0.019	0.033	0.009	Trace	0.14	0.35	--
E	2% Ni steel	Pickled	RR-3A	0.20	0.54	0.012	0.023	0.18	0.15	1.94	0.63	--
F	5% Ni steel	Pickled	SAE 2515	0.13	0.49	0.010	0.014	0.16	0.10	5.51	0.062	--
G	3% Cr steel	Pickled	Proprietary	0.08	0.44	0.010	0.017	0.13	3.16	0.16	0.11	0.02
H	5% Cr steel	Pickled	AISI Type 501D	0.08	0.41	0.020	0.019	0.20	5.06	0.11	0.062	0.52
I	Low-alloy steel	Pickled	Proprietary	0.08	0.47	0.007	0.026	0.060	0.00	1.54	0.87	--
J	Low-alloy steel	Pickled	Proprietary	0.15	0.45	0.113	0.026	0.47	0.68	0.49	0.42	--
K	Low-alloy steel	Pickled	Proprietary	0.078	0.75	0.058	0.022	0.04	Trace	0.72	0.61	0.13
L	Low-alloy steel	Pickled	Proprietary	0.13	0.60	0.089	0.021	0.15	0.55	0.30	0.61	0.059
M	Cast steel	Machined	QQ-S-6816, 1	0.27	0.68	0.028	0.028	0.41	0.12	0.22	0.10	--
N	Cast steel	As received										
O	Gray cast iron	Machined	QQ-I-652, 30	3.18	0.80	0.162	0.103	1.98	0.57	0.31	0.08	--
P	Gray cast iron	As received										
Q	Austenitic cast iron	Machined	INCO 18-22 Ni	2.66	0.94	0.24	0.104	3.17	2.29	17.9	0.80	--
R	Austenitic cast iron	As received										
S	Wrought iron	Machined	Aston Process ASTM A42-39	0.04	0.038	0.141	0.018	0.098	Trace	0.006	0.020	--
T	Wrought iron	As received										

* Source: Southwell, C. R. and Alexander, A. L., "Corrosion of Metals in Tropical Environments. Part 9: Structural Ferrous Metals - Sixteen Years' Exposure to Sea and Fresh Water", Naval Research Laboratory Report NRL-6862, 28 pp (April, 1969).

TABLE F-6. COMPOSITIONS OF ALLOYS REPORTED IN SURVEY BY LARRABEE AND PRESENTED IN TABLE 6-12*

Steel	Compositions, percent								
	C	Mn	P	S	Si	Cu	Ni	Cr	Mo
Cor-Ten Brand	0.08	0.36	0.08	0.026	0.31	0.41	0.49	0.73	--
Tri-Ten Brand	0.17	1.2	0.026	0.025	0.18	0.31	0.53	0.07	--
Ni-Cu	0.19	0.44	0.030	0.032	0.025	0.81	1.8	0.22	--
Cr-Mo	0.07	0.39	0.014	0.020	0.09	0.020	0.04	2.6	0.52
Structural Carbon	0.25	0.42	0.020	0.032	0.025	0.012	0.02	0.06	--

* Source: Larrabee, C. P., "Corrosion Resistance of High-Strength Low-Alloy Steels as Influenced by Composition and Environment", Corrosion, 9 (8), pp 259-271 (1953).

TABLE F-7. CHEMICAL COMPOSITION OF CAST IRONS TESTED BY REINHART AND JENKINS AND PRESENTED IN FIGURE 6-24*

Material	C	Mn	Si	Ni	Cr	Mo	Cu
Nickel	--	0.68	2.47	1.56	--	--	--
Ni-Cr #1	--	0.73	1.64	1.66	0.60	--	--
Ni-Cr #2	--	0.86	1.99	3.22	0.98	--	--
Ductile #1	--	0.35	2.50	0.91	--	--	--
Ductile #2	--	0.34	2.24	--	--	--	--
Silicon	--	--	14.5	--	--	--	--
Si-Mo	--	--	14.0	--	--	3.0	--
Austenitic, Type 1	--	1.4	2.05	15.8	1.79	--	6.71
Austenitic, Type 2	--	1.01	2.29	18.2	2.04	--	--
Austenitic, Type 3	--	0.6	1.15	28.4	2.87	--	--
Austenitic, Type 4	--	0.56	5.34	29.7	4.97	--	--
Austenitic, Type 4	2.13	0.79	5.60	29.98	5.02	--	0.16
Austenitic, Type D-2	--	0.94	3.0	21.4	2.26	--	--
Austenitic, Type D-2b	--	0.96	2.0	20.8	31.9	--	--
Austenitic, Type D-2c	2.45	2.12	2.38	22.34	0.08	--	--
Austenitic, Type D-3	--	0.5	1.83	29.8	2.70	--	--
Austenitic, Hardenable	not recorded						

* Source: Reinhart, F. M. and Jenkins, J. F., "The Relationship Between the Concentration of Oxygen in Seawater and the Corrosion of Metals", U.S. Naval Civil Engineering Laboratory Report, pp 562-577 (1971).

TABLE F-8. CHEMICAL COMPOSITIONS OF IRONS AND STEELS TESTED BY REINHART AND JENKINS AND PRESENTED IN TABLE 6-15*

Material	C	Mn	P	S	Si	Ni	Cr	Mo	V	Cu	Other
Armco Iron	--	0.02	--	--	--	--	--	--	--	--	--
Wrought Iron	0.02	0.06	0.13	0.01	0.13	--	--	--	--	--	2.5 Slag
AISI 1010	0.12	0.50	0.004	0.23	0.060	--	--	--	--	--	--
AISI 1010	--	0.34	0.01	--	0.02	0.02	0.02	--	--	0.03	--
Copper Steel	--	0.40	0.01	--	0.02	0.01	0.03	--	--	0.28	--
ASTM A36	0.20	0.55	0.010	0.020	0.064	--	--	--	--	--	--
HSLA #1[a]	0.18	0.86	0.014	0.023	0.28	0.05	0.64	0.18	0.047	--	B-0.1028 Ti-0.020
HSLA #2	0.12	0.30	0.015	0.025	0.27	2.34	1.25	0.20	--	0.17	--
HSLA #4	--	0.36	0.08	--	0.41	0.32	0.72	--	--	0.38	--
HSLA #5	0.14	0.78	0.020	0.025	0.23	0.74	0.56	0.42	0.36	0.22	B-0.0041
HSLA #5	With mill scale										
HSLA #7	--	0.43	0.12	--	0.13	0.54	--	--	--	1.0	--
HSLA #10	--	0.63	0.01	--	--	0.99	--	--	--	1.42	--
HSLA #12	0.14	0.26	0.011	0.009	0.27	2.60	1.55	0.46	0.02	--	--
HS #1[b]	0.11	0.78	0.008	0.006	0.29	5.0	0.56	0.42	0.05	--	--
HS #2	0.002	0.018	0.004	0.005	0.05	12.20	5.07	3.12	--	--	Ti-0.21 Al-0.25
HS #3	0.28	0.29	0.005	0.005	0.10	8.26	0.53	0.47	--	--	Co-3.82 V-0.15
18% Ni-Maraging	0.02	0.10	0.005	0.007	0.14	17.92	--	4.78	--	--	Co-8.75 B-0.003 Ti-0.94 Al-0.17
1.5% Ni	Not recorded										
3.0% Ni	Not recorded										
5.0% Ni	Not recorded										
9.0% Ni	Not recorded										
AISI Type 502	0.06	0.48	0.020	0.010	0.33	--	4.75	0.55	--	--	--
AISI Type 502	0.06	0.5	--	--	--	0.4	5.2	0.5	--	--	--

(a) High-strength low-alloy steel.
(b) High-strength steel.

* Source: Reinhart, F. M. and Jenkins, J. F., "Corrosion of Materials in Surface Seawater After 12 and 18 Months of Exposure", Final Report NCEL-TN-1213, 106 pp (1972).

TABLE F-9. TYPICAL COMPOSITIONS OF HIGH STRENGTH STEELS WHICH WERE REPORTED IN STUDY BY SANDOZ AND PRESENTED IN TABLE 6-18*

Type or Designation	C	Cr	Ni	Mo	Mn	Co	Cu	Al	Ti	Si	V	Other	Range of Nominal Tensile and Yield Strength, ksi TS	YS
Low-Alloy Martensitic														
HY-130	0.12	0.6	5.0	—	0.9	--	--	--	--	0.2	--	--	145-155	130-145
4130	0.30	1.0	--	0.2	0.5	--	--	--	--	0.3	--	--	200-300	180-250
4340	0.40	0.8	1.9	0.25	0.7	--	--	--	--	0.6	--	--		
D6AC	0.45	1.15	0.55	1.0	0.8	--	--	--	--	0.25	0.05	--		
H-11	0.40	5.0	--	1.3	0.3	--	--	--	--	0.90	0.50	--		
High-Alloy Martensitic														
HP 9-4-45	0.45	0.3	8.5	0.20	0.10	3.75	--	--	--	0.10	0.10	--	185-250	170-220
HP 9-4-25	0.25	0.50	8.5	0.50	0.10	3.75	--	--	--	0.10	0.10	--		
HP 9-4-20	0.20	0.80	9.0	1.0	0.3	4.5	--	--	--	0.10	0.10	--		
10Ni-2Cr-1Mo-8Co	0.11	2.20	10.0	1.0	0.06	8.0	--	--	--	0.1	--	--		
Martensitic Stainless														
410	0.12	12.0	--	--	0.5	--	--	--	--	0.35	--	--	120-200	100-150
431	0.15	16.0	2.0	--	0.5	--	--	--	--	0.35	0.25	--		
12Mo-V	0.26	12.3	0.75	1.0	0.5	--	--	--	--	0.3	0.29	--	60-220	130-210
Precipitation-Hardening Stainless														
AM-364 (M)[a]	0.011	11.1	11.2	--	0.05	--	--	0.61	0.22	0.05	--	--	180-270	175-220
Custom 455 (M)[a]	0.014	11.8	8.5	--	0.03	--	2.2	--	1.3	0.15	--	0.26Cb		
PH13-8-Mo (M)[a]	0.04	13.0	8.0	2.0	0.10	--	--	1.0	--	<0.10	--	--		
PH14-8-Mo (SA)[a]	0.035	14.5	8.5	2.2	0.85	--	--	1.2	--	0.05	--	--		
PH15-7-Mo (SA)[a]	0.07	15.0	7.0	2.2	0.60	--	--	1.0	--	0.30	--	--		
15-5-PH (M)[a]	0.06	15.0	4.6	--	0.25	--	3.3	--	--	0.40	--	0.25Cb		
17-4-PH (M)[a]	0.04	16.0	4.0	--	0.25	--	3.3	--	--	0.30	--	0.25Cb		
17-7-PH (SA)[a]	0.07	17.0	7.0	--	0.50	--	--	1.0	--	0.30	--	--		
AM-350 (SA)[a]	0.10	16.5	4.3	2.7	0.75	--	--	--	--	0.30	--	0.10N		
AM-355 (SA)[a]	0.13	15.5	4.3	2.7	0.75	--	--	--	--	0.30	--	0.12N		
AFC-260 (SA)[a]	0.07	15.0	1.8	4.5	--	13.0	--	--	--	0.13	0.25	0.15Cb		
AFC-77 (M)[a]	0.16	14.0	0.2	5.0	0.2	13.0	--	--	--	--	--	--		

TABLE F-9. (Continued)

Type or Designation	C	Cr	Ni	Mo	Mn	Co	Cu	Al	Ti	Si	V	Other	Range of Nominal Tensile and Yield Strength, ksi TS	YS
Maraging														
12-5-3	0.03 Max.	5.0	12.0	3.0	--	--	--	0.4	0.2	--	--	--	175-200	160-190
18Ni-200	0.03 Max.	--	18.0	3.2	--	8.0	--	0.1	0.2	--	--	--	215-245	200-235
18Ni-250	0.03 Max.	--	18.0	4.8	--	8.0	--	0.1	0.4	--	--	--	245-270	230-260
18Ni-300	0.03 Max.	--	18.0	5.0	--	9.0	--	0.1	0.6	--	--	--	275-310	260-300
18Ni-350	0.004	--	18.5	4.6	--	11.9	--	0.1	1.5	--	--	--	265-360	250-350
Maraging Stainless														
Almar 362	0.03	14.5	6.5	0.08	0.30	--	0.1	0.6	0.80	0.2	--	--	180-200	170-185
Marvac 736	0.02	10.2	9.5	2.0	0.15	--	--	0.30	0.25	0.15	--	--		

(a) Semiaustenitic (SA) or martensitic (M).

* Source: Sandoz, G., "High Strength Steels", Stress-Corrosion Cracking in High Strength Steel and in Titanium and Aluminum Alloys, Ed. B. F. Brown, NRL, Washington, DC (1972).

TABLE F-10. NOMINAL COMPOSITIONS OF ALLOYS STUDIED BY HACK AND PRESENTED IN TABLE 6-21*

Alloys	Nominal Compositions
	Fasteners
Aluminum	
A12024	4.5Cu, 1.5Mg, 0.5Mn
Stainless steels	
Type 304	18Ni, 8Cr
Type 316	18Ni, 12Cr, 2.5Mo
A286	26Ni, 15Cr, 1.75Mo, 2.0Ti
Titanium	
Ti6-4	6Al, 4V
Multiphase	
MP35N	35Ni, 35Co, 20Cr, 10Mo
Steel	Medium-carbon anodized steel
	Panels
Aluminum	
A15456	5Mg, 0.8Mn, 0.1Cr
Low-alloy steel	
HY-130	5Ni, 0.6Cr, 0.4Mo
Stainless steel	
17-4PH	17Cr, 4Ni, 4Cu, 0.3 (Nb + Ta)
Titanium	
Ti6-4	6Al, 4V

* Source: Hack, H. P., "Seawater Corrosion of Fasteners in Various Structural Materials", R&D Report DTNSRDC-76-0034, 34 pp (1976).

TABLE F-11. CHEMICAL COMPOSITION OF STEELS AND IRONS IN STUDY BY REINHART AND PRESENTED IN FIGURE 6-45*

Material	Percent by Weight										Other
	C	Mn	P	S	Si	Ni	Cr	Mo	Cu	Co	
Wrought Iron	0.02	0.06	0.13	0.01	0.13	--	--	--	--	--	2.5 Slag
AISI 1010	0.12	0.50	0.004	0.023	0.060	--	--	--	--	--	--
AISI 1010	0.11	0.52	0.016	0.024	0.048	--	--	--	--	--	--
AISI 1010	--	0.34	0.01	--	0.02	0.04	0.02	--	0.03	--	--
Copper Steel	--	0.40	0.01	--	0.02	0.01	0.03	--	0.28	--	--
ASTM-A36	0.24	0.70	0.011	0.027	0.055	--	--	--	--	--	--
ASTM-A36	0.20	0.55	0.010	0.020	0.064	--	--	--	--	--	--
ASTM-A387, D	0.06	0.49	0.013	0.021	0.24	--	2.20	1.02	--	--	--
HSLA #1[(a)]	0.18	0.86	0.014	0.023	0.28	0.05	0.64	0.18	--	--	V-0.047 B-0.0028 Ti-0.020
HSLA #2	0.12	0.30	0.015	0.025	0.27	2.34	1.25	0.20	0.17	--	--
HSLA #3	0.17	0.28	0.020	0.018	0.20	2.96	1.76	0.40	--	--	--
HSLA #3	0.10	0.28	0.014	0.010	0.25	2.91	1.59	0.52	--	--	--
HSLA #4	0.07	0.38	0.11	0.025	0.54	0.31	0.88	--	0.28	--	--
HSLA #4	--	0.36	0.08	--	0.41	0.32	0.72	--	0.38	--	--
HSLA #5	0.14	0.78	0.020	0.025	0.23	0.74	0.56	0.42	0.22	--	V-0.36 B-0.0041
HSLA #5	With mill scale										
HSLA #6	0.26	0.13	0.007	0.008	0.01	3.07	1.43	0.97	--	--	Cb-0.07
HSLA #7	--	0.43	0.12	--	0.13	0.54	--	--	1.0	--	--
HSLA #8	--	0.24	0.03	--	0.004	0.47	0.51	--	0.51	--	--
HSLA #9	--	0.75	0.12	--	0.55	1.00	0.70	--	0.50	--	--
HSLA #10	--	0.63	0.01	--	--	0.99	--	--	1.42	--	--
HSLA #11	--	0.69	0.08	--	--	0.50	0.26	--	0.30	--	--
Ni-Co	0.28	0.29	0.005	0.005	0.10	8.26	0.53	0.47	--	3.82	V-0.15
18% Ni-Maraging	0.02	0.10	0.005	0.007	0.14	17.92	--	4.78	--	8.75	B-0.003 Ti-0.94 Al-0.17

(a) High-strength low-alloy constructional steel.

* Source: Reinhart, F. M., "Corrosion of Materials in Hydrospace. Part 1: Irons, Steels, Cast Irons, and Steel Products", U.S. Naval Civil Engineering Laboratory Technical Note N-900, 71 pp (1967).

APPENDIX G

MAGNESIUM

TABLE H-1. COMPOSITIONS OF TEST MATERIALS, WEIGHT PERCENT

	Wrought Ni-Al Bronze	Cast Ni-Al Bronze	Mn Ni-Al Bronze	Mn Bronze	Bronze Comp M	Bronze Comp G	90-10 Cu-Ni	90-10 Cu-Ni + Sn	70-Cu Cu-Ni	70-30 Cu-Ni + Cr	Wrought Monel	Cast Monel	Monel K-500	316 SS	Al Bronze D	Phos Bronze +5% Sn	Phos Bronze +10% Sn
Cu	80.0	81.8	72.8	55.4	87.5	86.5	88.6	82.7	68.5	58.7	30.8	26.2	28.0	--	90.6	95.6	Balance
Fe	3.90	3.74	2.83	0.86	0.09	0.04	1.06	0.04	0.50	0.05	1.47	0.77	1.01	Balance	2.77	0.01	0.01
Mn	1.50	1.09	13.3	0.82	--	--	0.37	0.08	0.74	0.89	0.83	0.93	0.71	1.75	0.06	--	--
Ni	4.81	4.73	2.18	--	0.53	0.49	9.63	9.30	30.07	29.95	66.7	54.3	65.2	12.9	--	--	--
P	--	--	--	--	0.008	0.010	0.011	0.000	0.009	0.026	--	--	--	--	0.000	0.048	0.112
Pb	0.00	0.00	0.00	0.33	--	0.21	0.01	0.01	0.01	0.01	--	--	--	--	0.00	0.01	0.01
S	--	--	--	--	--	--	0.007	0.007	0.014	0.007	0.02	0.002	0.00	0.02	--	--	--
Sn	--	--	--	0.7	5.86	8.2	--	7.7	--	--	--	--	--	--	--	4.2	9.71
Zn	--	--	--	40.9	3.32	4.47	0.33	0.91	0.02	--	--	--	--	--	0.05	0.05	0.16
Al	9.06	8.72	7.94	0.78	--	--	--	--	--	--	--	--	--	--	6.62	--	--
C	--	--	--	--	--	--	--	--	--	0.013	0.10	0.13	0.18	0.05	--	--	--
Si	0.08	0.00	0.04	--	--	--	--	--	--	0.06	0.07	1.49	0.00	0.71	--	--	--
Ti	--	--	--	--	--	--	--	--	--	0.02	--	--	--	--	--	--	--
Zr	--	--	--	--	--	--	--	--	--	0.16	--	--	--	--	--	--	--
Cr	--	--	--	--	--	--	--	--	--	2.85	--	--	--	17.8	--	--	--
Others	--	--	--	--	--	--	--	--	--	--	--	1.7Cb	1.6Cb	2.8Mo	--	--	--

TABLE H-2. SPECIFICATIONS AND NOMINAL COMPOSITION OF MATERIALS TESTED BY SCULLY AND HACK*

Material	SAE/ASTM UNS Number	Purchase Specification	Cu	Ni	Fe	C	Mn	P	S	Al	Zn	Ti	Sn	Pb	Mo	Si	Others
90-10 Cu-Ni	C70600	MIL-C-15726E	88.04	10.2	1.45		0.10	<0.02	<0.02		0.13			<0.2			
Monel 400	N04400	QQ-N-281D	31.43	65.55	1.63	0.11	1.08		0.006	0.020						0.17	
Inconel 625	N06625	ASTM-B443-75		62.15	3.46	0.02	0.16	0.013		0.16		0.26			8.41	.25	21.46Cr 3.66Cb &Ta
M-Bronze	C92200	MIL-B-16541	86.91	0.45	0.09						4.74		6.05	1.7			0.06
Ni-Al-Bronze	C95800	MIL-B-21230A	79.85	4.88	4.24		1.49			9.36	0.07		0.04	.02			
HY-80 Steel	--	MIL-S-16216H	0.046	2.83	Balance	0.15	0.23	0.012	0.020			0.001			0.47	.27	<0.001V 1.61Cr
Titanium 50	R50400	MIL-T-7993		0.1	0.3	0.10						Balance					0.250
70-30 Cu-Ni	CA71500		68.02	30.34	.60	<.03	.77	.01	.006		.09			.01			
Anode Grade Zinc	--	MIL-STD-18001	0.05 max		0.05 max					0.1-0.5	Balance			0.06 max		0.125 max	0.025Cd

* Source: Scully, J. R. and Hack, H. P., "Galvanic Corrosion Prediction Using Long Term and Short Term Polarization Curves", Corrosion '84, Paper 34.

APPENDIX I

COBALT AND COBALT-BASE ALLOYS

TABLE I-1. NOMINAL COMPOSITION MATERIALS TESTED BY VREELAND*, WEIGHT PERCENT

Material	Trade Name	MEL Material Code	C	Mn	Mo	Cr	Co	Fe	W	Si	Ni	Cu	Pb	Sn	Others
Co-Cr-W alloy	Tantung G	ECA	3	2		29.5	47.5	3.5	16.5						0.2B, 4.5Ta + Cb
Co-Cr-Ni-Mo alloy	Cobenium	AMK	0.15	2	7	20	40.0	~15			15				0.4Be
Co-Cr-W-Ni-Mo alloy	Stellite 6K	ECB	1.6	2.0(a)	1.5(a)	31	~51	3.0(a)	4.5	2.0(a)	3.0(a)				
Co-Cr-W-Ni-Mo alloy	Stellite 6B	ECC	1.1	2.0(a)	1.5(a)	30	~53	3.0(a)	4.5	2.0(a)	3.0(a)				
Co-Cr-W-V-Ni-Mo alloy	Stellite 98M2	ECD	2.0	1.0(a)	0.8(a)	30	~37	2.5(a)	18.5	1.0(a)	3.5(a)				4.0V
Co-Cr-W-Ni-V alloy	Stellite 3	ECE	2.45	1.0(a)		30.5	~44	3.0(a)	12.5	1.0(a)	3.0(a)				2.0V
Co-Cr-W-Ni-V alloy	Star J	ECF	2.5	1.0(a)		32	~39	3.0(a)	17.0	1.0(a)	2.5(a)				2.0V
Cu-Pb-Sn alloy	Bearium Metal	DVI										70	20	10	
Ni-Cu alloy	Monel	ECM	0.12	0.9				1.4			66	31			
Titanium carbide with Ni-Mo binder	Kennametal K162B	ECC													25Ni + Mo, balance TiC
Tungsten-titanium carbide with Co binder	Kennametal K82	ECH					13								Balance WC-TiC
Tungsten carbide with Co binder	Kennametal K96	ECI					6								Balance WC
Tungsten-tantalum carbides, no binder	Kennametal K601	ECJ													WC-TaC (no binder)
Tungsten carbide with Cr-Co binder	Kennametal K701	ECK													10Cr + Co, balance WC
Tungsten carbide with Ni binder	Kennametal K801	ECL									6				Balance WC

(a) Maximum.

* Source: Vreeland, D. C., "Galvanic Corrosion Behavior of Wear-Resistant Materials for Mechanical Shaft Seals", Navy Marine Engineering Laboratory Report MEL-242/66, 13 pp (July, 1966).

TABLE I-2. NOMINAL COMPOSITION OF ALLOYS USED IN SCC TESTS*
(percent by weight)

Alloy	Ni	Fe	Co	Cr	Mo	W	C	Others
Hastelloy Alloy C-276	Balance	5	2.5(a)	16	16	4	0.02(a)	V-0.35(a)
Hastelloy Alloy X	Balance	19	2.5(a)	22	9	0.56	0.1	
Hastelloy Alloy G	Balance	19.5	2.5(a)	22	6.5	1(a)	0.05	Cb + Ta-2 Cu-2
Haynes Alloy 718	53	Balance	0.23	18	3	--	0.04	Cb + Ta-5 Ti-1 Al-0.5
Haynes Alloy 188	22	3(a)	Balance	22	--	14	0.1	La-0.04
Haynes dev. Alloy 8700	Balance	20	1.7	22	9	0.61	0.018	
Haynes dev. Alloy 8675	Balance	15	0.6	16	16	3.5	0.006	V-0.2
Inconel Alloy 625	Balance	5(a)	1(a)	21.5	9	--	0.1(a)	Cb + Ta-3.5 Al-0.4(a) Ti-0.4(a)
Inconel Alloy 718	53	Balance	1(a)	19	3	--	0.08(a)	Cb + Ta-5 Ti-1 Al-0.6
Snapealloy	Balance	25	20	20	8.5	--	0.01	Al-0.1
MP35N	35	--	35	20	10	--	0.007	Ti-0.7

(a) Maximum concentration allowable.

* Source: Kane, R. D., et al., "Stress-Corrosion Cracking of Nickel and Cobalt-Base Alloys in Chloride-Containing Environments", Corrosion '79, Atlanta, GA, Paper 174, 21 pp (March, 1979).